CHARACTERIZATION OF GASTRIC ATPase VESICLE TRANSPORT

George Sachs

D.Sc. Degree; University of Edinburgh; Edinburgh, Scotland
Submitted 1978.

This work is dedicated to my co-workers: Drs. Shah, Spenney, Chang, Rabon, Schackmann, Sarau, Lewin, Goodall and Saccomani who have remained friends in spite of it all.

TABLE OF CONTENTS:

Paper IX — Pronase Method for Isolation of Viable Cells From Necturus Gastric Mucosa. Gastroenterology 61: 189-200, 1971.

Paper X — Specific Effect of Acetylsalicylic Acid on Cation Transport of Isolated Gastric Mucosal Cells. Am. J. Physiol. 235: E16-E21, 1978.

Paper XI — Studies on Adenyl Cyclase in Necturus Gastric Mucosa. Arch. Biochem. Biophys. 143: 123-126, 1971.

Paper XII — Adenyl and Guanyl Cyclase in Rabbit Gastric Mucosa. Am. J. Physiol. 225: 1359-1363, 1973.

Paper XIII — Action of Cholinergic Drugs on Necturus Gastric Mucosa. Am. J. Physiol. 210: 1056-1060, 1970.

Paper XIV — Action of Burimamide, a Histamine Antagonist, on Acid Secretion in Vitro. Am. J. Physiol. 226: 898-902, 1974.

Paper XV — Effects of Sodium Removal on Acid Secretion by the Frog Gastric Mucosa. Proc. Soc. Exptl. Biol. Med. 123: 47-52, 1966.

Paper XVI — Ion Transport by Amphibian Antrum in Vitro. I. General Characteristics. Am. J. Physiol. 228: 1188-1198, 1975.

Paper XVII — Quantitation of Conductance Pathways in Antral Gastric Mucosa. J. Gen. Physiology 65: 645-662, 1975.

Paper XVIII — Properties of Gastric Antrum. III. Selectivity and modification of shunt conductance. Gastroenterology 72: 72-77, 1977.

Paper XIX A Molecular Approach to Epithelial Conductance: Gastric Mucosa. Alred Benzon Symp. V. Transport Mechanisms in Epithelia, Munksgaard, Copenhagen, pp. 257-274, 1973.

Paper XX Conductance Pathways in Epithelial Tissues. Exp. Eye Res. 16: 241-249, 1973.

Paper XXI Electrical Properties of Isolated Cells of Necturus Gastric Mucosa. Biochim. Biophys. Acta 241: 261-272, 1971.

Paper XXII Microelectrode Studies of Gastric Mucosa and Isolated Gastric Cells. Symp. Med. Hoechst. IN: Electrophysiology of Epithelial Cells, p. 257-279, 1971.

Paper XXIII Microelectrode Studies of Fundic Gastric Mucosa: Cellular Coupling and Shunt Conductance. J. Membr. Biol. 19: 105-128, 1974.

Paper XXIV The Action of Amytal on Frog Gastric Mucosa. Biochim. Biophys. Acta 143: 522-531, 1967.

Paper XXV Metabolism of Dog Gastric Mucosa. I. Nucleotide Levels in Parietal Cells. J. Biol. Chem. 250: 8321-8329, 1975.

Paper XXVI Metabolism of Dog Gastric Mucosa. Levels of glycolytic citric acid cycle and other intermediates. J. Biol. Chem. 252: 8572-8581, 1977.

Paper XXVII — Redox Involvement in Acid Secretion in the Amphibian Gastric Mucosa. J. Membr. Biol. 35: 189-204, 1977.

Ppaer XXVIII — REVIEW: H^+ Transport by a Non-electrogenic Gastric ATPase as a Model for Acid Secretion. Rev. Physiol. Biochem. Pharmac. 79: 133-167, 1977.

Paper XXIX — Characterization of Gastric Mucosal Membranes. VIII. Localization of peptides by iodination and phosphorylation. J. Biol. Chem. 250: 4802-2809, 1975.

Paper XXX — Characterization of Gastric Mucosal Membranes. IX. Fractionation and Purification of K^+-ATPase containing vesicles by zonal centrifugation and free flow electrophoresis technique. Biochim. Biophys. Acta. 465: 311-330, 1977.

Paper XXXI — A Non-electrogenic H^+ Pump in Plasma Membranes of Hog Stomach. J. Biol. Chem. 251: 7690-7698, 1976.

Paper XXXII — Proton Transport by Gastric Membrane Vesicles. Biochim. Biophys. Acta 464: 313-327, 1977.

Paper XXXIII — Cation Transport by Gastric $H^+ + K^+$ ATPase. J. Membr. Biol. 32: 361-381, 1977.

Paper XXXIV — Use of 1-anilino-8-naphthalene sulfonate as a Probe of Gastric Vesicle Transport. J. Membr. Biol. 32: 301-318, 1977.

Paper XXXV — Reconstitution of a Proton Pump from Gastric Mucosa. J. Membr. Biol. 35: 285-301, 1977.

Paper XXXVI — Metabolic and Membrane Aspects of Gastric H^+ Transport. Gastroenterology 73: 931-940, 1977.

Paper XXXVII — Tissue and Cell Localization of Hog Gastric Plasma Membrane by Antibody Technique. Proc. Symp. Gastric. Ion Transport, Special Suppl. Acta Physiol. Scand (Obrink, K.J. and Flemstrom, G., eds) p. 293-305, 1978.

Paper XXXVIII — Transport Parameters of Gastric Vesicles. Proc. Symp. Gastric Ion Transport, Special Suppl. Acta Physiol. Scand. (Obrink, K.J. and Flemstrom, G., eds) p. 409-426, 1978.

Paper XL — Enzymic Modification of Gastric Transport ATPase. IN: Frontiers of Biological Energetics (Dutton, P.L., Leigh, J., Scarpa, A., eds) Academic Press, New York, Vol. 1, p. 545-554, 1978.

Paper XLI — Transport Characteristics of Frog Gastric Membranes Biochim. Biophys. Acta 551: 432-447, 1979.

Paper XLII — Quantitation of Hydrogen Ion and Potential Gradients in Gastric Plasma Membrane Vesicles. Biochemistry 17: 3345-3353, 1978.

ABSTRACT

The microsomal fraction of both dog and hog gastric mucosa contains a K^+ activated ATPase. ATP phosphorylates a peptide of $\bar{c}$ 100,000 M_r in both species, and dephosphorylation is stimulated by K^+. By a combination of differential and zonal density gradient centrifugation a membrane fraction is produced containing almost exclusively this peptide region. These vesicles, upon the addition of ATP, take up H^+ and extrude K^+. The action of ionophores such as nigericin or valinomycin and the uptake of lipid permeable anions such as thiocyanate or anilino-naphthosulfonic acid indicate the lack of a potential difference during transport. Reconstitution of this material into a planar bilayer indicates that ATP activates a K^+ conductance and hence, in the presence of K^+, also a low potential difference is observed. These data suggest that this H^+ pump is non-electrogenic as prepared in the vesicular form. Using an antibody obtained from rabbits immunized with the highly purified membrane fractions, it was demonstrated that this membrane was derived uniquely from gastric parietal cells. Hence, based on the ability of this ATPase to actively transport H^+, its cellular origin and on the well known K^+ requirement for acid secretion in amphibia and mammals, it is concluded that this ATPase is a component of the HCl secretory mechanism of gastric mucosa.

Secretion by in Vitro Amphibian Gastric Mucosa

G. SACHS & B. I. HIRSCHOWITZ

Division of Gastroenterology, Department of Medicine, University of Alabama, Medical Center, Birmingham, Alabama, U.S.A.

Abstract: SACHS, G. & HIRSCHOWITZ, B. I. Secretion by in Vitro Amphibian Gastric Mucosa. *The Physiology of Gastric Secretion*, 186-202, 1968. Universitetsforlaget, Oslo. The growth in knowledge related to the gastric mucosa resulting from the in vitro technique has been quite considerable. However, our picture of the transport process is far from complete. One drawback has been the virtually exclusive attention that has been paid to frog mucosa. In this species there is very little Na^+ transport, and little ouabain sensitivity. Necturus, in contrast, shows considerable ouabain sensitivity. Mammalian species may also have a potent Na^+ transport mechanism. Furthermore, secretory rates in vitro are much lower than in vivo, hence the critical metabolic changes expected with onset, or cessation, of secretion will be less drastic in vitro, hence more difficult to detect.

From this review, we would draw the following conclusions: (1) The mechanism for H^+ secretion is electrogenic only under certain conditions, and in standard Cl^- solutions may be essentially non-electrogenic. (2) The passive resistance of the mucosa, primarily to K^+ and Cl^- is probably the most important component involved in resistive changes resulting from addition of inhibitors etc. (3) Both Na^+ and K^+ are essential for Cl^- or H^+ secretion respectively, but forced exchange does not occur. 4) H secretion is dependent on mitochondrially generated ATP present in the cytoplasm, and cannot utilize any of the intermediates of phosphorylation. (5) Non-acidic Cl^- transport is also ATP dependent, but may also be driven by anaerobically generated ATP from glycolysis, and this may occur in the surface cell.

In conclusion, we should like to predict what new departures future research will take. The area of gastric mucosal intermediary metabolism remains virtually unexplored, and it is clear that our understanding of this tissue will be related to our knowledge of its metabolism. The work on the electrical phenomena related to transport will also require new approaches. One probable avenue of approach will be the use of microelectrodes, as has been done in other tissues. One of the problems in this area has been the inherent motility of the muscularis mucosa, and since we have shown that various nucleotides are potent inhibitors of motility, but not secretion, this technical problem now appears surmountable. Probably the most important area of current and future investigation is the nature and properties of the ATPase. This enzyme has recently been solubilized; with retention of its SCN^- sensitivity and with further purification it is hoped that the enzymic mechanism of H^+ and Cl^- transport will become clearer.

Key-words: Amphibia; electrolytes; enzymes; enzyme inhibitors; gastric juice; gastrin; gastrointestinal hormones; pepsin; stomach

The fundamental problems in gastric secretion may be conveniently classified into three major areas: (1) central control, (2) peripheral or end organ secretory stimulatory mechanisms, and (3) parietal or tubular cell transport properties. Central control evidently exists only in the intact preparation, and in vitro methods are not relevant to this area. Until recently, secretagogue action in vitro was not accessible to investigation, but with the finding that *Necturus* gastric mucosa, in contrast to *Rana pipiens* or *Catesbiana*, is obtained generally in the resting state (Shoemaker, Hirschowitz & Sachs 1967), the stimulation of gastric secretion by histamine, acetyl choline, and gastrin has become amenable to in vitro experimentation. It is essentially in the third area of gastric secretion,

This work was supported by grant Nos. AM-08541, AM-09260 and TI AM-5296 from the US PHS and GB-3511 from the National Science Foundation.

Biochemistry of Gastric Mucosa

Praesidium: K. HARTIALA (Turku)

CONTENTS

a nsport mechanisms of the tubular cell, that o methods have proved most useful. In fact, the range of experimental and chemical ulations in the intact animal is limited, and s obtained may be related to other properties preparation, such as blood flow, in vitro ds offer the only available approach to ar physiology of gastric secretion.

st of the observations in the field have been on amphibian mucosa, since mammalian sa has only recently been prepared in the ing state (Shoemaker, Sachs & Hirschowitz . An advantage of amphibian preparations ir long term viability and the absence of cells from the gastric mucosa in the frog, ich these cells are limited to the esophagus. the application of the pH stat technique z & Durbin 1959), it became possible to re H ion transport, easily, accurately, and uously. This is probably one of the major ntages of the use of gastric mucosa for trans- studies in vitro, since a quantitative precise rement of the unidirectional (i.e. net) move- of a transported ion is possible. Additionally, he development of the in vitro preparation cturus gastric mucosa, changes related to of secretion occurring over short time als (2 to 15 minutes) have become exper- ally observable. Accordingly, this prepara- as become of more general interest in the port field.

interest in the chambered frog mucosa has d to 4 main areas: (1) the electrophysiological omena related to secretion of ions, (2) the determinants of the potential difference and ion, (3) the energy source for transport, and ie enzymic mechanisms of transport. This will attempt to cover only part of these, o present perhaps a less cautious viewpoint velopment in this area than has been cus- ry in the field. It is to be hoped that the ntation of results in this way will lead to r experiments proving or disproving the presented.

g gastric mucosa has been shown to trans- both H^+ and Cl^- against electrochemical ents (Rehm 1957, Hogben 1951). Most of the work in the field has been concerned, however, with H^+ secretion and little attention has been paid to the mechanisms of Cl^- transport. The transport of other ions, such as Na^+ or K^+ in either R. pipiens or catesbiana is of a relatively minor nature, whereas in Necturus Na^+ transport contributes about 50 per cent of the resting P.D. (Shoemaker et al. 1967). To account for uphill movement of molecules through a biological membrane, some cyclic changes in the forces of attraction between those molecules and a site in the membrane appears the only reasonable mechanism. The P.D. across the gastric mucosa is oriented with the lumen-ve, and thus cannot account for Cl^- movement. Furthermore, a 30 mv gradient is insufficient to account for H^+ transport; thus, H and Cl are actively transported across the mucosa. The major questions in the transport field are the driving force for transport, and the nature of the cyclic changes occurring during transport.

METHODS

The technique used for in vitro frog gastric mucosa is essentially a modification of the Ussing flux chamber. Fig. 1 shows the details of a closed chamber specifically constructed to determine O_2 consumption in addition to H^+ rate, potential difference (P.D.), resistance, and short circuit current (I_{SC}). The chamber is constructed of Kel F, since this plastic, like glass, is impermeable to oxygen in contrast to lucite or teflon for example. Magnetic stirring is used, and the solutions are equilibrated with 95% O_2, 5% CO_2 prior to use. Oxygen consumption is measured via a pair of membrane- covered Pt electrodes, H^+ rate by the pH stat method, P.D. by a pair of matched calomel electrodes with renewable KCl junctions; resistance is calculated from the change in P.D. obtained by sending 20 μa of current in either direction through end-on agar electrodes for 10 sec., and I_{SC} defined as the current required to maintain the P.D. at zero after 30 sec. Fig. 2 shows a diagram of the apparatus used.

In the standard open reservoir system, lucite is

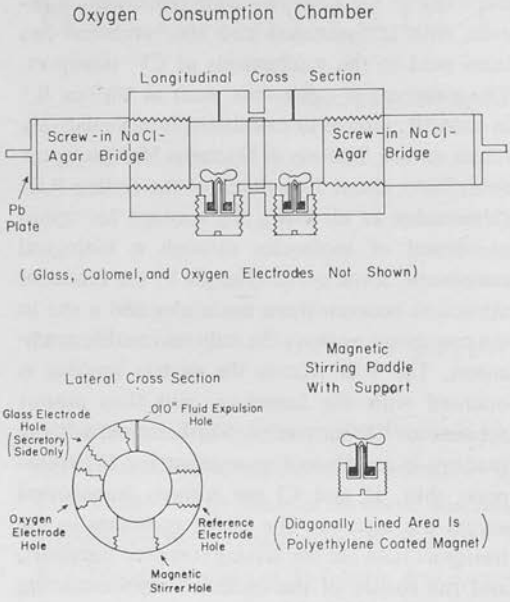

Fig. 1. Diagram of chamber used for measurement of H^+ rate, potential difference, resistance, short circuit current, and O_2 consumption of in vitro mucosa.

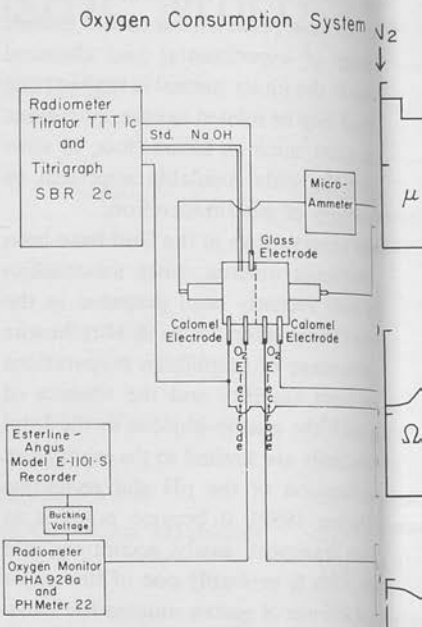

Fig. 2. Diagram of equipment arrangement O_2 consumption chamber.

used as construction material, and a 95% O_2, 5% CO_2 gas lift system is used for stirring.

In addition a chamber with no agar electrodes and clear end windows has been used to determine the steady state of the redox components using an Aminco Chance dual beam spectrophotometer.

Studies on subcellular components have utilized standard methods of cell fractionation and enzyme assay (Sachs, Mitch & Hirschowitz 1965).

In this paper the cell plasma membrane of the acid-secreting cell will be referred to as nutrient or secretory membranes respectively, while the intact tissue will be referred to as mucosa or gastric mucosa.

ELECTROPHYSIOLOGY OF SECRETION

This section is concerned with the changes related to onset or inhibition of secretion occurring in the electric parameters of the amphibian mucosa and their implications. There are three ways in which H^+ ion can be visualized as moving across the secretory membrane of the cell. Mec (Fig. 3) can be distinguished from 2 that changes of P.D. resulting from the of models 2 and 3 are due to alteratio gradients. Accordingly, mechanism 1 to as electrogenic and mechanisms 2 non-electrogenic, in which 2 may be as a forced exchange model, and 3 as mechanism. Rehm (1964), has presented review of the concepts in this field.

In frog mucosa, the P.D. is normally

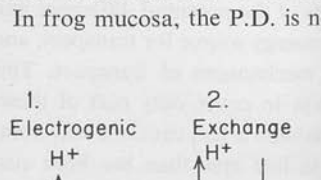

Fig. 3. Models of H ion transport acr mucosa.

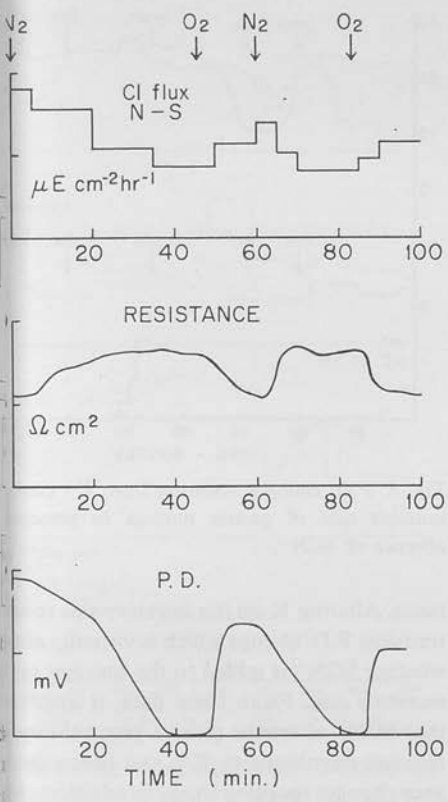

Effect of cycles of anoxia on amytal-inhibited gastric mucosa.

lumen-ve in Cl^- solutions. In Necturus, a ar orientation is obtained, whether acid ion is present or not. Accordingly, transport from nutrient (N) to secretory solutions (S) ot account for this P.D. In fact it has been nstrated that Cl^- transport is responsible for .D. in frog, since it has been shown that for circuited mucosa, $Cl^-net = H^+ + I_{SC}$ (Hogben

cordingly, in frog gastric mucosa, the P.D. either as a result of electrogenic Cl^- trans- or as a result of a Cl^- diffusion potential or y both. Various inhibitors may be used to e the P.D. of the frog mucosa. Anoxia for ple generally reduces the P.D. to values very to zero after about 40 minutes. Fig. 4 shows the effect of anoxia on a mucosa where acid secretion has been abolished by 2 mM amytal. When O_2 is readmitted in such a preparation, there is a rapid rise of P.D. to about 50 per cent of the original value. It would appear that the time required for the establishment of ion gradients would be considerably longer. A further cycle of anoxia reduces the P.D. to zero in about 20 minutes. One interpretation of this finding is therefore that, under standard steady state conditions, half the P.D. can be accounted for by diffusion potential and half by electrogenic Cl^- transport.

The electrogenicity of a mechanism involves an asymmetry in the site or rate of accompanying charge transport. The distinction with respect to H^+ secretion then involves the question of whether this occurs at a site in the membrane separate from Cl^- (i.e. electrogenic), or whether Cl^- diffuses or is transported through an identical region in the membrane (unitary), or whether there is a cation exchange mechanism (also non-electrogenic). This does not exclude the possibility that there are two distinct mechanisms in the stomach, a unitary HCl pump and a separate Cl^- transport system. In fact, work in the field has concentrated perhaps too hard on trying to explain acid secretion without due regard to the basal transport function of the mucosa, which is Cl^- transport.

The evidence for electrogenicity of H^+ secretion rests essentially on three lines of evidence: (1) effect of SCN^- and other inhibitors on resistance of gastric mucosa, (2) the relationship between resistance and secretory rate, and (3) the effect of

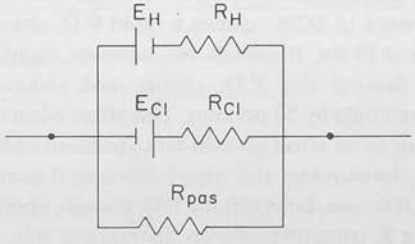

Fig. 5. Simplified circuit diagram of in vitro frog mucosa.

SO_4'' solutions. The interpretation of these experiments has been essentially an electrogenic one, and we shall attempt to show that these observations may be explained also on a unitary or forced exchange basis. On the basis of an electrogenic mechanism, inhibition of the EMF of the H^+ mechanism alone would be predicted to have an effect on the P.D. but not the resistance. A simplified circuit diagram, as shown in Fig. 5, for a separate site electrogenic mechanism, illustrates what would be most simply predicted. A sudden decrease in E_H would lead to a P.D. transient, but no overall resistance change would be predicted. That this does occur has led to the assumption that changes in EMF of the hydrogen or chloride batteries alters their internal resistance i.e. R_H or R_{Cl}. On this basis, therefore, the effect of inhibitors in altering the P.D. and resistance has been used as evidence for electrogenic mechanism of H^+ ion secretion. A similar argument holds for the relationship between H^+ rate and resistance. At high H^+ rates there is an approximate inverse relationship between H^+ transport and resistance. If one assumes that increase of E_H results in a decrease of R_H, one may use this as evidence for an H^+ battery in the gastric mucosa. In the equivalent circuit illustrated above (Fig. 5), however, two other components of resistance are involved, viz. R_{Cl}, the resistance of the Cl^- limb, and R_{pas}, the resistance of the mucosa to passive diffusion of ions such as Na^+, K^+, HCO_3, etc.

If inhibitors altered either R_{Cl} or R_{pas}, then their actions on the gastric mucosa would not be evidence for or against an electrogenic mechanism. Fig. 6 shows that changing the K^+ concentration on the nutrient side from 4 to 20 mM in the absence of SCN^- causes a rapid P.D. change of about 15 mv. 10 mM SCN^-, however, significantly delayed this P.D. change and reduced its magnitude by 50 per cent. This effect occurs even prior to an effect on acid rate. Addition of SCN^- on the secretory side also inhibits acid secretion. In this case, however, the P.D. change, upon altering K concentrations on the nutrient side, is the same as before the addition of SCN^-, although characteristic changes have occurred in the resis-

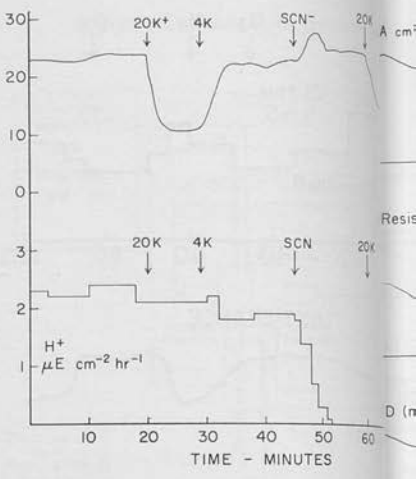

Fig. 6. P.D. changes resulting from K^+ ch nutrient side of gastric mucosa in pres absence of SCN^-.

tance. Altering K on the secretory side re transient P.D. change which is virtually whether SCN^- is added to the nutrient secretory site. From these data, it appe that SCN^- alters the passive permeabili nutrient membrane to K^+, and hence t ance changes resulting from the addition may be interpreted in this way rather being due to changes in the resistance limb. Since, however, SCN on the secre does not immediately affect K-indu changes, resistance changes also oc result of SCN action on the secretory per se, and indeed K^+ effects resulting changes on the secretory side are abo SCN added to either side of the fro mucosa.

Another line of evidence which sho resistance changes should be cautious preted is the effect of dimethyl sulfoxide (DMSO) on the secretory side. As can from Fig. 7, with 5% DMSO, it is po induce marked changes in resistance effect on secretory rate. Accordingly, tance of the H limb is not the sole det of observable resistance changes.

When Cl^- is removed from the bathi

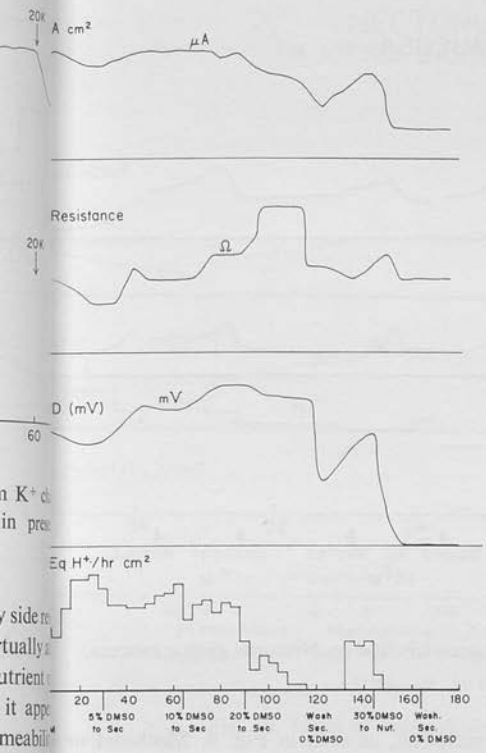

7. Effect of dimethylsulfoxide (DMSO) on ory side of frog gastric mucosa.

placed by a non-transported anion such as the P.D. inverts and is linearly related to H^+ rate (Rehm & Lefevre 1965). This is reted as being evidence for electrogenicity H^+ mechanism. It has been demonstrated SO_4'' is not transported by frog gastric sa (Hogben 1965) and presumably, there- whatever mechanism is chosen, there is no ovement of SO_4'', either through the H^+ Cl^- mechanism. This raises the unsettled ion of what accompanies the H^+ ion under circumstances. What are the consequences predicted on the basis of a normally unitary anism or on a forced exchange model? The would predict a fall in P.D. to around zero Cl^- transport stops) but certainly not an sion, unless the forced exchange were Cl^- dent and was no longer an exchange mechanism in the absence of Cl^-. On the basis of an obligatory unitary mechanism, the P.D. and H^+ rate would fall to zero.

In simple electrogenic theory there would be an inversion of the P.D. with maintained H rate, and furthermore there would be a linear relationship between P.D. and H rate, as has been found. However, the H^+ rate is reduced by about 60 per cent in the absence of Cl^-. This has been explained on the basis of biochemical coupling between Cl^- and H^+ transport. There is no evidence for this, and no convincing biochemical mechanism has been advanced for this finding.

Accordingly, there is very good evidence for the electrogenicity of the H^+ mechanism in SO_4'' conditions and the evidence in Cl^- solutions rests on resistive changes in the mucosa with changes in acid rate. Two alternate mechanisms, unitary or forced exchange remain to be considered.

Removal of Na^+ or K^+ from the secretory solutions of frog, guinea pig, or Necturus in vitro mucosa, has no effect on the secretory rate. Maintenance of Na^+ on the secretory side with removal from the nutrient side drastically alters secretory rate. Measurements of Na^{22} or K^{42} flux also show that these are much lower than would be found if a forced exchange model was

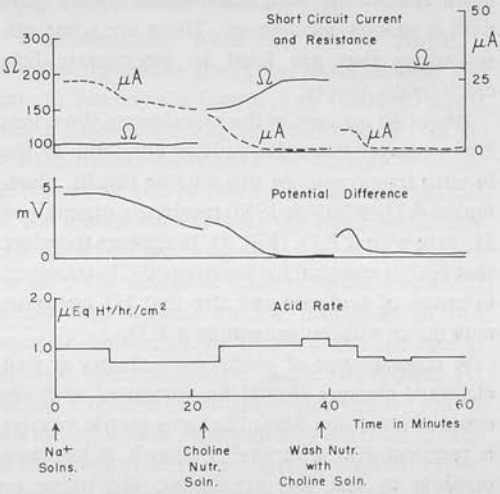

Fig. 8. Effect of choline substitution for Na^+ on nutrient side of frog gastric mucosa.

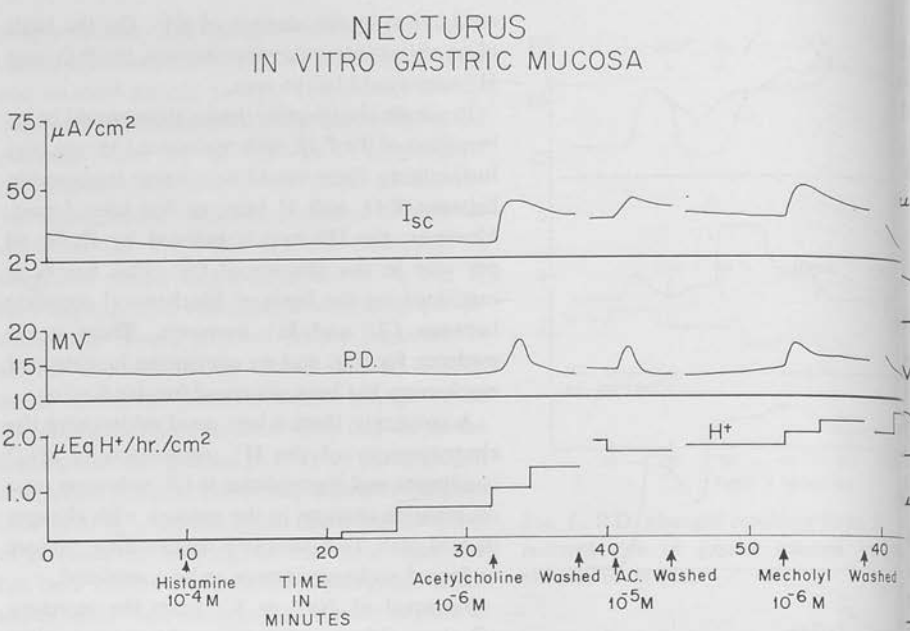

Fig. 9. Effect of histamine and subsequently acetylcholine on Necturus gastric mucosa

correct. On the basis of these data, we can exclude a forced exchange model as being reasonable for the in vitro frog mucosa.

We have discussed some of the observations more compatible with electrogenic theory than with a unitary mechanism. There are some observations that are hard to incorporate into electrogenic theory.

About 40 per cent of the experiments show that Na^+ removal from the bathing solutions of the in vitro frog or guinea pig mucosa (Sachs, Shoemaker & Hirschowitz 1966) results in a maintained H^+ rate with 0 P.D. (Fig. 8). It appears therefore that Na^+ is essential for maintained Cl^- transport in excess of acid rate and also that H^+ transport may occur without generating a P.D.

A consequence of electrogenic theory is that electrical changes should be associated with the onset of secretion. Since Necturus gastric mucosa is responsive to a variety of stimuli, it has been possible to test this prediction. Histamine or gastrin results in very little change in any of the electrical parameters related to the onset of acid secretion, as seen in Fig. 9. Mecholyl choline results in a sharp spike in th shown in Figs. 9, 10. This spike is ab atropine, occurs without the onset o or at least precedes it, is not affected b and is abolished by Cl^- removal and SC ment. Accordingly, this is due to stim Cl^- movement, not H^+ transport, wh lower the P.D. ATP also stimulat Necturus at 10^{-4}M concentration. with this, as seen in Fig. 11, is a ri and I_{SC} with a fall in resistance. Ouab this P.D. effect, which is thus presuma to $Na^+ + K^+$ movement. Of further i this regard is the extremely short lat observed (<2 min. in terms of H^+ rat in terms of P.D., etc.). Changes with t secretion in Necturus, therefore, do support to an electrogenic mechanism.

Perhaps the most cogent reason for c an exclusively electrogenic mechanism that for a pH gradient of 5 units, potential drop would be predicted to oc

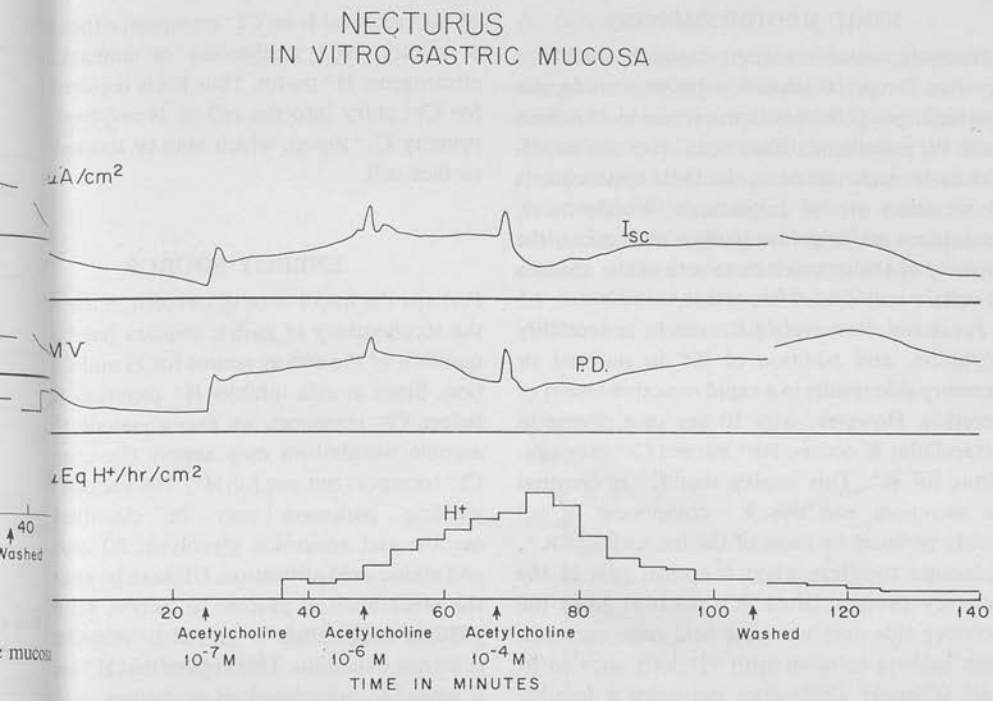

Fig. 10. Effect of acetylcholine on Necturus gastric mucosa.

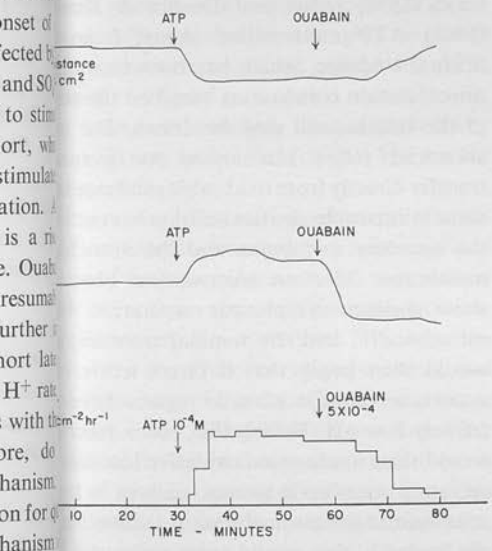

Effect of ATP and ouabain on Necturus gastric

the gastric mucosa, and this evidently does not occur.

Fundamentally, what one has to decide is whether the carrier for H ion has a cationic and anionic binding site (unitary), or whether there is only a cationic binding site (electrogenic). In the unitary mechanism H and Cl would both be bound to the carrier and be released on the luminal side of the membrane, whereas the electrogenic concept would demand a separate system or exit point for Cl^-. The degree of observable electrogenicity would then depend on the properties of this separate system, i.e. its location and the rate at which it operates relative to the electrogenic H^+ carrier. Conversely the observable unitary nature of a system will be determined by the relative rates of dissociation of H and anion from the carrier. Therefore, although there is a conceptual distinction between the two processes, it will be hard to devise a conclusive experiment.

IONIC REQUIREMENTS

Ultimately, since transport through the tissue involves forces of attraction between molecules that undergo cyclic variation, enzyme mechanisms must be postulated. Since ions may act as co-factors in such reactions, the ionic requirements of secretion are of importance. Furthermore, because an exchange mechanism may occur, the capacity of the stomach to secrete in the absence of certain ions is also important.

Potassium. Removal of K^+ results in secretory inhibition, and addition of K^+ to nutrient or secretory side results in a rapid reestablishment of secretion. However, only 10 per cent change in intracellular K occurs. Rb^+ but not Cs^+ may substitute for K^+. This implies that K^+ is essential for secretion, and this K^+ component is not readily replaced by most of the intracellular K^+. Potassium therefore plays a critical role in the secretory process. Since K^+ removal from the secretory side does not alter acid rate, exchange from bathing solution with H^+ ions such as in yeast (Conway 1953) does not seem a feasible mechanism. Further evidence against an exchange mechanism is that flux of K^{42} S → N is an order of magnitude smaller than the H^+ rate. A possibility, by analogy with the Na^+ ATPase system is that K is involved in the ATP mechanism in the gastric mucosa, and this will be discussed in more detail later.

Sodium. As has been discussed above, complete removal of Na^+ from the bathing solutions of frog gastric mucosa results in inhibition of both Cl^- and H^+ transporting mechanisms. With both Na^+ and K^+, alterations of these concentrations in the ECF will lead to a redistribution of these cations within the cell. Accordingly, observed effects may be due to this latter effect, rather than a simple depletion of the removed ion from an essential site. The role of Na^+, therefore, in the secretory process is obscure. Since Na removal from the secretory solution has little effect on H^+ secretion, whereas maintained Na^+ in the secretory with Na^+ absent from the nutrient solution results in transport inhibition, an Na^+:H^+ exchange mechanism is unlikely. It appears, in frog, Necturus, and guinea pig, that the primary effect of Na^+ removal is on Cl^- transport, ei a unitary HCl mechanism or un electrogenic H^+ pump. Thus Na is req for Cl^- entry into the cell or is invo primary Cl^- pump, which may be lo surface cell.

esiston
, cm²

ENERGY SOURCE

Perhaps the major area of concern in the biochemistry of gastric mucosa h question of the energy source for H an tion. Since anoxia inhibits H^+ secret before Cl^- transport, we may conclu aerobic metabolism may supply the Cl^- transport but not for H^+. The var yielding pathways may be class aerobic and anaerobic glycolysis, fat and amino-acid utilization. Ultimately, the breakdown of glucose to lactate, yielding metabolism is geared to mit substrate oxidation. This implies that H is geared to mitochondrial oxidations

H^+
E cm
IC

g. 12.

We must then decide what aspect of drial energy is utilized. This crystalli essentially opposing views on this ques way's (1953) redox and Durbin & (1965) ATP mechanisms. Apart fr imental evidence, which has been es direct, certain conclusions based on th of the tubular cell may be drawn. Fo chondrial redox mechanism to op transfer directly from oxidizable subst some intimate physical association to the secretory membrane and the mit membrane. Electron microscopic ob show distinct cytoplasmic separatio mitochondria and the luminal mem would then imply that if direct red occurs, certain cytoplasmic regions h tremely low pH. Failing this, redox would then imply some oxidative rea secretory membrane system, such as microsomal fractions of several tissue the stomach, that would come under heading of mixed function oxidases 1965). It is, however, clear that these

itive
ay is
nce
re fo
d AT
ansp
estiga
id o
use
ecifi
s. H
ble f
of th
H^+ rat
to
on o
ratio
dis
, a
d in

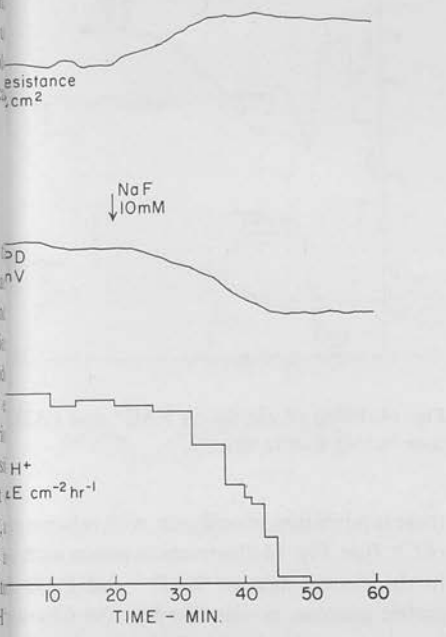

g. 12. Effect of NaF on frog gastric mucosa.

itive to most of the classical mitochondrial
in & ltors, whereas acid secretion is sensitive.
part fr e in cell metabolism the glucose-lactate
een es ay is the sole anaerobic source for ATP,
d on th nce Cl^- may be transported anaerobically,
awn. F e forced to conclude that glycolytically
to o d ATP may be utilized for Cl^-, but not for
substr ansport.
on to e stigation of the problem of energy sources
he mit id or chloride secretion has been confined
opic o use of inhibitors. As inhibitors may well be
parati ecific, such an approach has many possible
memb s. However, if a variety of inhibitors are
ect red ble for a given reaction amongst others, and
gions h of them have the same effect on the tissue
redox m $^+$ rate), then it is likely that the common effect
ive reac to inhibition in this region, since there is
ch as on of overlap in terms of known action. This
tissues rationale for the use of multiple inhibitors.
under discussing some of the theory behind the
dases (S, a brief description of the action of certain
these d inhibitors will be given.

A. *Glycolytic Inhibitors*

a) *Sodium fluoride.* At 10 mM concentration on the nutrient side, as shown in Fig. 12, after a period of 30 min. acid rate and P.D. are inhibited. The effect on P.D. occurs slightly before the effect on acid rate. Addition on the secretory side results in a rapid fall of secretory rate to a new steady state. Since F^- acts by virtue of its metal complexing ability, a tentative explanation would be interference with ATP utilization via an $ATP^- - Mg^{2+} - F^-$ complex.

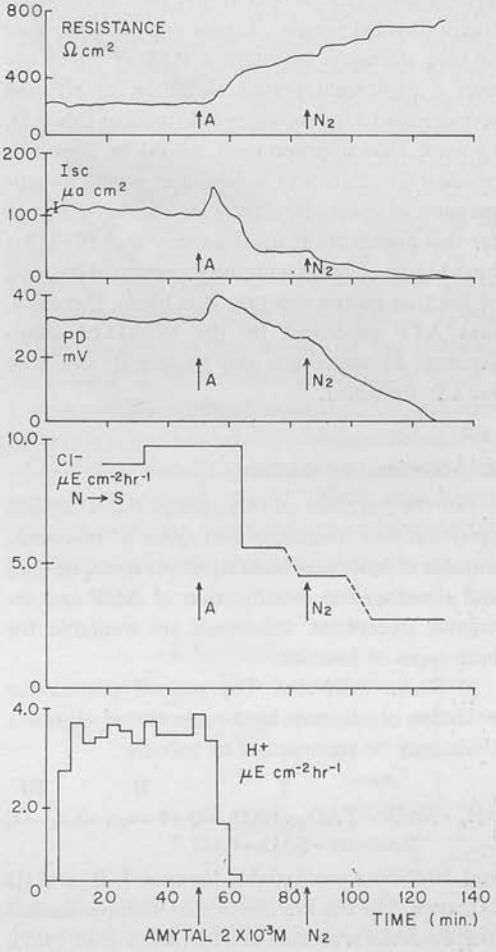

Fig. 13. Effect of amytal on frog gastric mucosa.

b) 2 *deoxyglucose*. This substance inhibits acid secretion in vitro at 20 mM concentration, while the P.D. and I_{SC} are relatively insensitive to its action. Although 2-DG is a glycolytic inhibitor, acid secretion is relatively independent of externally added glucose, since frog gastric mucosa metabolizes endogenous triglycerides (Alonso, Nigon, Dorr & Harris 1967), as well as glycogen. Accordingly, since there is an irreversible formation of 2-deoxyglucose-6-phosphate, depletion of ATP would appear to be the most likely explanation.

c) *Iodoacetate*. The phosphoglyceraldehyde dehydrogenase system (PGAD) is very sensitive to this sulfhydryl reagent. Under anoxia, a number of frog stomachs maintain a P.D. of 12-15 mv over a prolonged period. Addition of 10 mM iodoacetate to the secretory side reduces this P.D. to zero. One interpretation would be that this residual Cl^- transport is inhibited, owing to suppression of anaerobic glycolysis. Further evidence for this possibility is the discovery that PGAD is found in association with the microsomal fraction of the frog gastric mucosa. It is likely, therefore, that ATP generated by the PGAD-phosphoglycerate kinase couple may be directly available for Cl^- transport.

B. *Mitochondrial Inhibitors*

For the purposes of this review, mitochondria carry out two interdependent types of reactions, transfer of hydrogen from substrate to O_2 (redox) and simultaneous esterification of ADP and inorganic phosphate. Inhibitors are available for both types of reaction.

a) *Redox inhibitors*. The general scheme for oxidation of substrate by the mitochondrial redox chain may be summarized as follows:

$$\begin{array}{lccc} & \text{I} & \text{II} & \text{III} \\ \text{AH}_2 \rightarrow \text{NAD}^+ \rightarrow \text{FAD}_1 \rightarrow \text{FAD}_2 \rightarrow \text{Q} \rightarrow \text{b} \rightarrow \text{c,c}_1 \rightarrow \text{a,a}_3 \rightarrow \text{O}_2 & & & \\ \text{Succinate} \rightarrow \text{FAD} \rightarrow \text{FAD} \nearrow & & & \end{array}$$

and inhibitors are avilable for sites I, II, and III as shown. The site I inhibitor that we have studied in some detail is sodium amytal (Sachs et al. 1967). Its action is illustrated in Fig. 13, where at 2 mM,

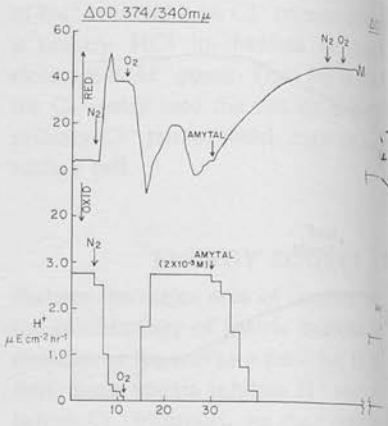

Fig. 14. Effect of amytal on NAD⁺ and f
state in frog gastric mucosa.

there is inhibition of acid rate, with relat
of Cl^- flux. Fig. 14 illustrates its action w
to the steady state of NAD⁺ and FA
gastric mucosa, as visualized in the Ch
beam spectrophotometer. It can be seen
is reduction of NAD⁺ and oxidation of
would be predicted from a block in elec
between these compounds. However,
coupled heart mitochondria, the cross
is on the O_2 side of FAD, explain
locus of action as shown. Another
interest is the non-correlation betwee
of reduction of NAD⁺ and the acid rate
neously with the transport effects of am
is a drop in tissue ATP and O_2 con
Figs. 15 (a) and (b) illustrate this findi
interest that the greatest percentage d
at 0.2 mM amytal, which is without m
effect on transport.

Antimycin A inhibits electron flow
cytochromes b and c (site II) and its e
qualitatively similar to those of amyta
CN^-, at high concentrations relativ
required for mammalian mitochondri
mM), acting at site III, inhibits acid
P.D. with reduction of cytochrome a_3. S
ly on occasions, both the inhibition a
reduction are reversible.

Accordingly, redox inhibition inhibits

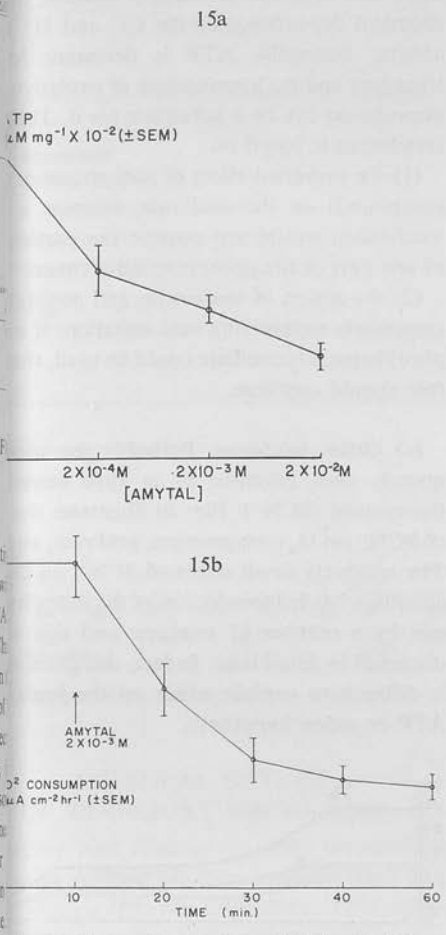

5 a, b. Effect of amytal on ATP levels (a) and nsumption (b) of frog mucosa.

relative sparing of net Cl^- movement, but mitochondrial ATP synthesis is simultasly blocked, these inhibitors do not distinbetween redox or ATP dependent secretion. ever, if a redox mechanism is operating, it to be of the mitochondrial, rather than osomal type.

Phosphorylative uncouplers and inhibitors. A ntly formulated scheme for this sequence of ions is illustrated in Fig. 16. Here C is a ratory carrier that undergoes oxidation or reduction and as a result combines with a compound I (this occurs at 3 sites in the respiratory chain). As a result X~I is formed, which undergoes phosphorylysis to form X~P, which then transfers the P to ADP forming intramitochondrial ATP. An enzyme system in the mitochondrial membrane allows phosphorylation of extramitochondrial ADP by this ATP. There are inhibitors available for the reactions marked (1) and (2) (uncouplers), and (3) and (4) (inhibitors), and we will discuss them in this order.

(i) *Phosphorylative uncouplers.* The best known of this group acting at (1), resulting in hydrolysis of the intermediate C′~I to C′+I is 2, 4 dinitrophenol. Accordingly, ATP synthesis is blocked, and in fact there is an induction of an ATPase. Corresponding to this there is no change or a rise in O_2 consumption in intact mitochondria. We have used a series of these, pentachlorophenol 1, 3, tricyanoamino propene, and m-chlorocyano carbonyl phenyl hydrazone (CCCP). All of these have qualitatively similar actions, in inhibiting acid and sparing P.D. or I_{SC}. Fig. 17 illustrates the effect of CCCP on the gastric mucosa. Surprisingly there is inhibition of O_2 rate, which emphasizes the danger of extrapolating from work in cell fractions to the intact tissue.

Arsenate is considered to act at (2) in the scheme shown. Again, there is inhibition (somewhat slow) of acid rate, with Cl^- transport maintained for a considerable period. ASO_4'' also acts as an uncoupler, with the arsenolysis of an intermediate being the postulated mode of action.

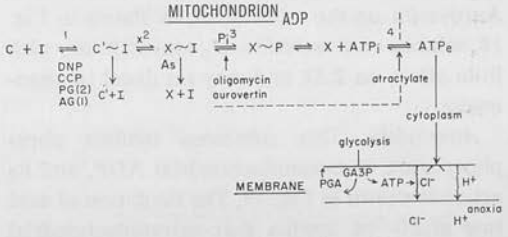

Fig. 16. Simplified scheme for phosphorylation in mitochondria and possible coupling of Cl^- transport to glycolysis.

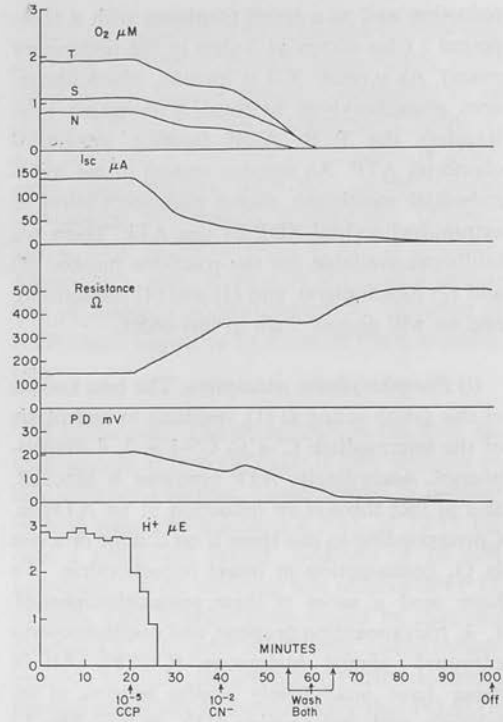

Fig. 17. Effect of m-chlorocyano carbonyl phenylhydrazone on frog mucosa.

(ii) *Phosphorylative Inhibitors.* Application of this group of compounds to a study of the mode of acid secretion is of interest from several points of view. The alkyl guaniames and phenethyl biguanide inhibit at site I or II and also inhibit O_2 consumption and acid rate. The other inhibitors act at site (3) by blocking the entry of Pi into the phosphorylating sequence. Oligomycin, the best known of this group, was found to have no effect on transport or O_2 consumption of frog mucosa. Aurovertin on the other hand, as shown in Fig. 18, inhibits acid secretion, O_2 consumption, with little effect on P.D, and may act distal to oligomycin.

Atractylate. This substance inhibits phosphorylation of extramitochondrial ADP, and its action is shown in Fig. 19. The inhibition of acid rate at 10^{-3}M implies that extramitochondrial ATP is a necessary condition for acid secretion.

Conclusions: From the data discussed above, we feel that two conclusions can be drawn. Firstly, there is a clearcut distinction betwe chemical dependence of the Cl^- and anisms. Secondly, ATP is necessar transport and no intermediate of oxid phorylation can be a substitute for it. conclusion is based on:

(1) the universal effect of anti-phos compounds on the acid rate, where mechanism would not require the p of any part of the phosphorylative cha

(2) the action of aurovertin and atr completely suppressing acid secretion phorylative intermediate could be used rate should continue.

(c) *Other Inhibitors.* Probably the quently used inhibitor of in vitro st thiocyanate (SCN^-). Fig. 20 illustrates of SCN^- on O_2 consumption, acid rate The relatively small effect of SCN^- o sumption has led to rejection of the red esis by a number of workers, and th discussed in detail later. In fact, this phe is difficult to explain either on the ba ATP or redox hypothesis.

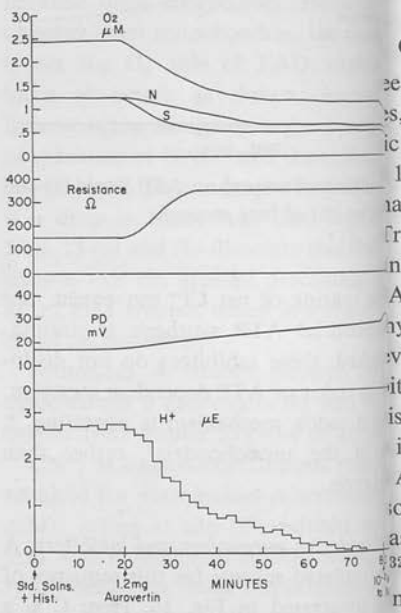

Fig. 18. Effect of aurovertin on frog muc

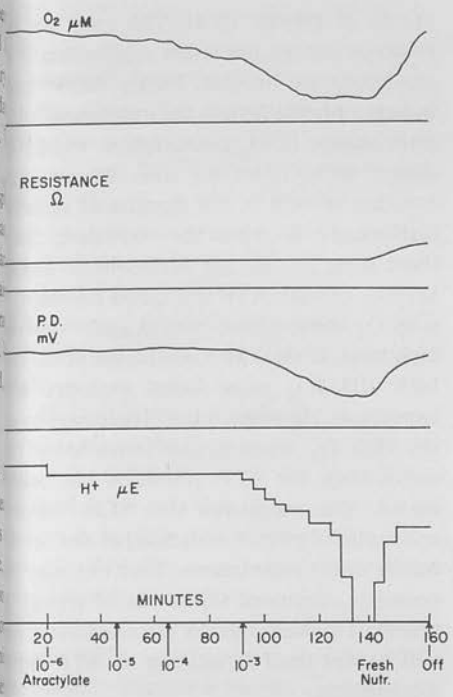

9. Effect of atractylate on frog mucosa.

CHEMICAL NATURE OF TRANSPORT MECHANISM

eeping with findings in other transporting s, an ATPase has been isolated from frog ic mucosa (Durbin & Kasbekar 1965; Sachs 1965). It occurs in the microsomal fraction as no detectable Na, K, or ouabain sensitiv- Treatment with deoxycholate does not alter nsensitivity. Although its highest activity is ATP, the other nucleoside triphosphates are ydrolysed. The property which is of interest, ver, is its SCN^- sensitivity. Since SCN^- its gastric H^+ secretion, the tempting conclu- is that this SCN^- sensitive ATPase is some- involved in H^+ transport. Unfortunately ATPases show a SCN^- sensitivity, although omewhat lesser degree than the frog mucosal ase. Attempts to label this enzyme with ^{32} have shown extremely variable results, no conclusive evidence for any intermediate. encouraging line of evidence has been the irreversible inhibition by diisopropyl fluorophosphate (DFP) of gastric secretion and ATPase. The latter action can also be shown to occur in the intact tissue (Sachs and Hirschowitz 1965).

Another approach has been to analyse potential partial reactions of this system. A K^+-stimulated acetyl phosphatase has been found in the gastric microsomes, inhibited by ATP or ADP, but not sensitive to ouabain. On this basis and on the basis of the DFP data, it may be postulated that the active site of the gastric ATPase contains a sequence --R-ser--- $\overset{\text{asp}}{\underset{\textbf{glu}}{}}$ ----- where serine is the DFP site and glutamyl or aspartyl is the phosphorylation site. The dephosphorylation is then K^+ dependent. Neither the involvement of this ATPase in transport nor the nature of the phosphorylating mechanism is at present known.

BIOCHEMICAL MODELS

From the equation

$$\Delta G \pm = n\ RT \log a_1/a_2^{\pm}\ nFE$$

where $\Delta G \pm$ is the free energy change, n the number of moles transported, R the gas constant,

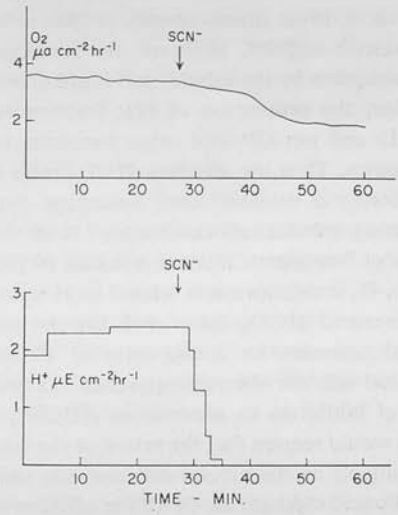

Fig. 20. Effect of SCN on acid rate and O_2 consumption of frog mucosa.

T the absolute temperature, a_1 and a_2 the ionic activities, F the faraday, and E the potential difference, it is possible to calculate the minimal free energy for H^+ ion transport across the frog mucosa. Assuming a pH gradient of 5, this is approximately 6,300 cals per mole hydrogen ion. Alternatively, a potential of 300 mv is required for establishing the given pH gradient. From time to time it has been suggested that the net P.D. across the mucosa is the energy source for H^+ ion transport, but since this is maximally 60 mv, evidently it cannot account for the transport. In a discussion of possible mechanisms of H secretion, one hypothesis, the redox model, remains extremely well known in spite of much evidence against it, and virtually no evidence in its support. Originally this concept was formulated by Rehm and Conway independently. A mechanism of the following type is considered to operate

$$AH_2+C \rightarrow C''+2H^+ \qquad \text{lumen}$$
$$O_2+C'' \rightarrow C+1/2\ O_2^{2-} \qquad \text{cell}$$

Accordingly, there is direct transfer of protons from substrate to the gastric lumen,and ultimately passage of the electrons to O_2. Several consequences arise from this type of model. The best known is that the maximal H^+/O_2 ratio obtainable is 4. Most measurements of this ratio fall between 1 and 2.5. However, the fractional O_2 consumption by the tubular cell is unknown, and further, the proportion of that fraction related to H^+ and not Cl^- and other functions is also unknown. Thus the absolute H^+/O_2 ratio is undoubtedly a minimal one. Assuming that the secreting tubular cell constitutes 1/4 of the cell mass of frog gastric mucosa and that 60 per cent of its O_2 consumption is related to H transport, a measured H^+/O_2 ratio of 2 for the mucosa could represent an actual ratio of 10 for the parietal cell. An alternate approach has been the use of inhibitors to measure as $\Delta H/\Delta O_2$ ratio. This would require that the action of the inhibitor is uniquely on the tubular cell, and also uniquely on the acid mechanism. Of all the inhibitors used, only SCN^- may approach this specificity, and in fact $\Delta H/\Delta O_2$ values of 5 to 12 have been obtained (Forte & Davies 1964). This may ATP DI evidence against the redox mechanis ally the conditions are fulfilled. Firstly, SCN y source induce a proton leak in the membran is the little change in O_2 consumption wo een sho dicted. SCN^- does not alter the port in titration of acid in the chambered m ham 19 furthermore it raises the resistance ved in there must not be any homeostatic us mod keeping cellular ATP utilization cons ase mec wise O_2 consumption would again re The sin high level. If these two conditions hol depen high $\Delta H/\Delta O_2$ ratio found exclude lysis hypothesis. However, it is still necessar H_2O the high O_2 consumption levels fou would major route for ATP utilization has ase in t inated. The suggestion that SCN^- ratio of uncoupler of phosphorylation has not anism out by direct experiments. Thus one ree of postulate continued utilization of ene mediate transport system under SCN^- condition An a will be discussed in relation to ATP er mo mechanisms. format

Since the redox pumps must be loc that secretory membrane, the action of ph les bac tive uncouplers and inhibitors and mi otein redox inhibitors cannot be explained ence o redox theory. It may be possible to sure of or other on the basis of non-specific rmally all of them taken together. Another co of the redox theory is that a 300 mv s A redox chain is being utilized to form gradient, not an intermediate in phosph Since the action of uncouplers does O_2 consumption, and is on an inter the t phosphorylation, uncouplers would ly 6,3 affect H^+ secretion. Since a large num lysis couplers do inhibit acid, we must con 0 cals an intermediate of phosphorylation is is 2, acid secretion, which then implies Acco energy is not utilized directly, i.e. that type mechanism is operating. osed f

To summarize, it is our view that presen theory is no longer tenable in its unmod se in and modification to allow for an in l well ATP or redox mechanism occurring n fo neously results in a biologically unlikely y, Ga

may
chanis
', SCN
mbran
on wo
the r
ered m
stance
static
n cons
gain r
ons ho
xclude
cessar
ls fo
n has
CN⁻
as not
one m
of ene
nditio
ATP
be loc
of ph
nd mi
ined b
e to e
ecific
her co
) mv s
form
hosph
does
inter
uld n
e num
st con
on is
olies t
that
that
nmod
an in
urring
likely

ATP DEPENDENT MECHANISMS

ally the only alternative to redox as an
y source is 'high energy' phosphate. Since
is the major high energy phosphate, and
een shown to be the energy source for Na
port in red blood cells and squid axon
ham 1957), it is presumed that ATP is
ved in transport in the gastric mucosa.
us models are possible, and only two simple
ase mechanisms will be discussed.

The simplest possible ATP dependent mech-
n depends on the release of H ion upon ATP
olysis

$$H_2O+ATP \rightarrow ADP+Pi+H^+$$

would require the presence of an anisotropic
ase in the secretory membrane. Assuming a
ratio of 3, the maximal H^+/O_2 ratio by this
anism is 6. This anisotropic model would
ee of other cation requirements, and no
mediate would be detected.

An alternate mechanism would involve
er molecule which would undergo cyclic
formation—namely a carrier. This does not
that the carrier is a small molecule that
les back and forth. It could equally well be
otein that alters conformation as a con-
nce of phosphorylation resulting in cyclic
sure of binding sites to the luminal fluid.
rmally, this mechanism could be represented

$$ATP+XH_n \rightarrow P\sim XH_n+ADP$$
$$P\sim XH_n \rightarrow P-X^{n-}+nH^+$$
$$P-X^{n-} \rightarrow X^{n-}+Pi$$
$$X^{n-}+nH \rightarrow XH_n \quad \text{cell}$$

the transport of H^+ ion requires approx-
ly 6,300 cal/mole, and the free energy of
olysis of ATP intracellularly approximates
0 cals, the maximal thermodynamic ratio of
is 2, and with a P/O of 3 the H^+/O_2 ratio
Accordingly n in the above model equals 2.
type of model is generally similar to models
osed for Na^+ transport. Since we have shown
presence of a K^+ stimulated acetyl phos-
ase in the gastric mucosa, the $P\sim XH_2$ complex
l well be a carboxyl phosphate as has been
n for brain $Na^+ + K^+$ ATPase (Hokin,
y, Galsworthy & Yoda 1965). The hydrolysis would be K^+ dependent, and this hypothesis would provide a role for K in H transport.

(3) It is conceivable that some form of oxidation reduction reaction does occur during H^+ secretion. A model which would be feasible is

$$XH_2+ATP \rightarrow P\sim XH_2+ADP$$
$$P\sim XH_2+C \rightarrow P\sim X+C''+2H^+ \quad \text{lumen}$$
$$P\sim X \rightarrow X+Pi$$
$$X+C''+2H^+ \rightarrow XH_2+C \quad \text{cell}$$

Here phosphorylation of XH_2 results in reaction with an oxidation-reduction (O-R) carrier C, with expulsion of H^+ ions. P~X is hydrolysed and its redox potential is altered, thus allowing C'' to donate the electrons. This is then an ATP-driven redox reaction—analogous to ATP-induced reversed electron transport. Again with a P.O ratio of 3, the maximal H^+/O_2 would be 12.

Unfortunately the models presented above are too general for specific testing.

THE EFFECT OF THIOCYANATE (SCN)

The effect of SCN^- on transport and the ATPase mechanism, as discussed above, is an important finding which must be incorporated into any scheme of acid secretion. One possibility is that, since SCN^- is a pseudohalide, it interacts with an anion site in acid secretion. The most likely type is a Cl^- binding site. To account for continued ATP utilization, this SCN^- carrier complex must be capable of being phosphorylated and dephosphorylated, but remains non-dissociable

$$X+HCl \rightarrow X-HCl \rightarrow P\sim XHCl \rightarrow P\pm X+HCl$$
$$X+HSCN \rightarrow X-HSCN \rightarrow P\sim XHSCN \rightarrow X\text{-}HSCN+Pi$$

Accordingly, ATP utilization by transport mechanism will be only minimally depressed, and O_2 utilization will remain high. As the SCN^- concentration increases, however, inhibition of the enzyme ATPase activity occurs (as happens in subcellular fractions) and it has been found that O_2 consumption decreases.

ACKNOWLEDGEMENTS

We gratefully acknowledge the expert technical assistance of Dr. Richard L. Shoemaker and Mr. Richard H. Collier.

REFERENCES

ALONSO, D., NIGON, K., DORR, I. & HARRIS, J. B. (1967) Energy sources of gastric secretion. *Amer. J. Physiol.* **292,** 992-1000.

CONWAY, E. J. (1953) *Biochemistry of Acid Secretion.* Charles C. Thomas, Springfield, Ill., U.S.A.

DUNHAM, E. T. (1957) Abstract. *Physiologist* **1,** 23.

DURBIN, R. P. & KASBEKAR, D. K. (1965) Adenosine triphosphate and active transport by the stomach. *Fed. Proc.* **24,** 1377-1381.

FORTE, J. G. & DAVIES, R. E. (1964) Relation between hydrogen ion secretion and oxygen uptake by gastric mucosa. *Amer. J. Physiol.* **206,** 218-222.

HOGBEN, C. A. M. (1951) The chloride transport system of the gastric mucosa. *Proc. nat. Acad. Sci. (Wash.)* **37,** 393-398.

HOGBEN, C. A. M. (1965) Natural history of isolated bullfrog gastric mucosa. *Fed. Proc.* **24,** 1353-1359.

HOKIN, L. E., SASTRY, P. S., GALSWORTHY, P. R. & YODA, A. (1965) Evidence that a phosphorylated intermediate in a brain transport adenosine triphosphatase is an acyl phosphate. *Proc. nat. Acad. Sci. (Wash.)* **54,** 177-184.

REHM, W. S. (1964) Gastric potentials and ion transport. pp. 64-91 in *Transcellular Membrane Potentials and Ion Fluxes.* F.M. Snell, ed. GORDON & BREACH.

REHM, W. S. & LEFEVRE, M. E. (196
dinitrophenol on potential resistance and
frog stomach. *Amer. J. Physiol.* **208,** 922-

SACHS, G. & HIRSCHOWITZ, B. I. (1965
diisopropyl fluorophosphate on gastric se
gastric ATPase. *Proc. Soc. exp. Biol.*
702-704.

SACHS, G., MITCH, W. E. & HIRSCHOWITZ,
Frog gastric mucosa ATPase. *Proc. Soc.*
(N.Y.) **119,** 1023-1027.

SACHS, G., SHOEMAKER, R. L. & HIRSCHO
(1966) Effect of Na^+ removal on in vitro fr
Proc. Soc. exp. Biol. (N.Y.) **123,** 47-52.

SACHS, G., SHOEMAKER, R. L. & HIRSCHO
(1967) Effect of amytal on in vitro fro
Biochim. Biophys. Acta (Amst.) **143,** 522-

SACHS, G., HIRSCHOWITZ, B. I. & SHOEMA
Unpublished observations.

SHOEMAKER, R. L., SACHS, G. & HIRSCHO
(1966) Secretion by guinea pig gastric muco
Proc. Soc. exp. Biol. (N.Y.) **123,** 826-827.

SHOEMAKER, R. L., HIRSCHOWITZ, B. I. &
(1967) Hormonal stimulation of Necto
mucosa in vitro. *Amer. J. Physiol.* **212,** 1

STRITTMATTER, P. (1965) Protein and coen
actions in the NADH-Cytochrome b
system. *Fed. Proc.* **24,** 1156-1163.

G. SACHS, M.D.
Division of Gastroenterology
Department of Medicine
University of Alabama Medical Center
Birmingham, Alabama 35233, U.S.A.

Reprinted from PROCEEDINGS OF THE SOCIETY FOR EXPERIMENTAL BIOLOGY AND MEDICINE,
1965, v119, 1023-1027

Frog Gastric Mucosal ATPase.* (30366)

G. SACHS, W. E. MITCH† AND B. I. HIRSCHOWITZ
Department of Medicine, Division of Gastroenterology, University of Alabama Medical Center, Birmingham, Alabama

In recent years interest in extramitochondrial ATPases has centered in large part on 'transport' ATPases. These enzymes have been prepared from a variety of tissue—such as crab nerve(1), red blood cells(2), kidney (3), rat brain(4), and other tissues(5). They share a certain number of features in common, namely a stimulation by Na^+ and K^+ and at least partial inhibition by ouabain. Furthermore, in the standard cellular fractionation methods, the ouabain-inhibitable Na^+ and K^+ sensitive component occurs in the microsomal fraction which is considered to contain a large proportion of fragmented membrane. Further evidence for the involvement of the microsomal fraction in transport involves (a) ATP-dependent Na^+ binding to the protein of brain microsomes(4); (b) P^{32} labelling of protein derived from ATP^{32} in r.b.c. membranes(6) and (c) the reduction of labelled phosphoserine from kidney ATPase preparations incubated with DFP^{32} in the presence of ATP and a possible identity of this ATPase and diglyceride kinase(7).

The gastric mucosa under normal conditions apparently contains at least 2 electrogenic pumps acting on Cl^- and H^+ respectively(8). The specificity of the pumps in the gastric mucosa may make it extremely difficult to characterize a 'pump' ATPase in the same manner as has been done for those described above. Thus the chloride mechanism has been shown to transport several univalent anions in the mucosa and to have some action on sulfate(9). Therefore the anion pump may be regarded as relatively nonspecific. The hydrogen ion pump is apparently specific for H^+. A demonstration of H^+ activation is naturally complicated by the pH activity curves obtained for enzymic reactions. The evidence therefore for a hydrogen ion pump must at present rest on the action of specific inhibitors.

In this connection Kasbekar and Durbin (10) have recently described a SCN^- sensitive ATPase in the microsomal fraction of the gastric mucosa, and in view of the possible importance of this observation in relation to H^+ ion secretion mechanism, which is inhibited by SCN^-, some of the properties of the mucosal ATPases have been investigated with particular reference to the action of SCN^-.

Methods-materials. All chemicals were reagent grade. Nucleotides were purchased from Sigma Chemical Co., labelled nucleotides from Schwarz Bioresearch, P^{32} from Abbott Laboratories, DEAE-cellulose from Gallard-Schlesinger.

Enzyme preparation. Starved *Rana pipiens* were decapitated and the stomach removed. The mucosal cells were scraped into ice cold 0.25 sucrose containing 0.1 M tris pH 7.4 and homogenized with a teflon homogenizer. The homogenate was fractionated into a nuclear, mitochondrial, microsomal and supernatant fraction by the Schneider-Hogeboom procedure(11). The microsomal fraction was used for these studies unless otherwise noted.

In some experiments further fractionation was carried out by layering an aliquot of the microsomal fraction or microsomal fraction containing 0.1% Triton X-100, on a linear gradient of sucrose from 0.7 to 2.5 M. After centrifuging for 2 hours at 39,000 r.p.m. in an SW39 rotor, fractions were collected *via* a tube-piercing device and assayed for protein and enzymatic activity.

ATPase studies. The standard incubation mixture contained 3 mM $MgCl_2$ 3 mM ATP 20 mM tris buffer pH 8.4, 0.5 mg protein in a final volume of 1 ml. Incubation was carried out in a water bath at 37° for 20 minutes. The reaction was stopped by addition

* This work was supported by U.S.P.H.S. grants 2A-5286 and 08541.

† Trainee USPHS Grant 2A 5286.

of an equal volume of ice-cold 10% chloracetic acid, and the phosphate released was determined by the Fiske-Subbarow(12) procedure. For kinetic studies the Mg^{++}/ATP ratio was 1/1 throughout. Blanks were run with each determination and all assays were run in duplicate.

ATP-ADP exchange enzyme. The basic system contained 5 mM ATP, 5 mM $MgCl_2$, 1 mM ADP with c 20,000 cpm C^{14} ADP, 20 mM tris buffer pH 7.4 and c 0.5 mg enzyme in final volume of 1 ml. Incubation was carried out for 30 minutes at room temperature. The reaction was stopped by immersing tubes in boiling water for 4 minutes; control tubes showed there was no significant hydrolysis of the polyphosphates by this procedure. Control tubes containing boiled enzyme were run with each determination. After clarification by centrifugation, 10 μl were spotted on a DEAE-cellulose plate and developed for 30 minutes with 0.02 N HCl as solvent. The spots were located by U.V. light and eluted using 0.25 M NaCl pH 7.4. An aliquot was assayed for nucleotide content in a Beckman DU spectrophotometer at 260 mμ and another aliquot counted in a Nuclear Chicago scintillation spectrometer using a solvent system containing 70 g/l napthalene, 7 g/l PPO and 0.05 g/l POPOP in dioxane (spectroquality). Data were calculated from the average concentration of labelled precursor and average specific activity during incubation period(13).

ATP-Pi exchange. In this assay various concentrations of the reactants were used in an attempt to demonstrate activity. Thus Pi was added in a final concentration ranging from 1-10 mM, containing 5×10^5 cpm of P^{32} 20 mM tris pH 7.4-8.0, ADP 0-3 mM, ATP 5-10 mM, $MgCl_2$ 0-10 mM. SCN^- was also used to a final concentration of 3 mM. Assay was as in ATP-ADP exchange system.

Adenylate kinase. This activity was assayed by formation of ADP formed from labelled AMP (c 15,000 cpm) and ATP. The test system contained 5 mM ATP, 5 mM AMP, 5 mM $MgCl_2$, 20 mM tris pH 7.4, 0.5 mg enzyme and assay was performed as before with addition of carrier ADP prior to chromatography.

Nucleoside diphosphokinases. The reacti was estimated by the formation of C^{14} G from C^{14} GDP and ATP. The incubati mixture contained 3 mM ATP, 3 mM G containing 20,000 cpm, 3 mM $MgCl_2$, mM tris pH 7.4 and 0.5 mg enzyme. In bation was carried out for 30 minutes room temperature and assay was perform as before. Protein was assayed by the Low method(14).

Results. ATPase activity. ATPases we found to be distributed in all the fractions the gastric mucosa. 3 mM SCN^- inhibit all the fractions to approximately the sa extent (Table I), and thus acted non-spe fically with respect to the frog gastric m cosal ATPases. Further studies were carri out with the ATPase of the 'microsom fraction.

Metal ion specificity. A divalent me cation was essential for activity and t greatest activity was obtained with Mg^+ (100%). However, both Mn^{++} (93%) a Ca^{++} (97%) could substitute for Mg^{+} Various concentrations of Na^+ and K^+ (100 mM) were without effect on the ATP activity. The optimal Mg/ATP ratio w found to be 1 in most preparations, while 2 of 10 experiments the ratio was close to

pH studies. The pH optimum curve of t enzyme showed a minor peak at pH 7.75 a a larger peak at 8.4. SCN^- eliminated t smaller peak and reduced the height of t peak at 8.4.

Specificity of ATPase. The highest acti ity was found with GTP (2.0 μM min^{-1} mg^{-1}) and ATP (1.8 μM min^{-1} mg^{-1} and activity was about 50% lower towa CTP (1.3 μM) and UTP (1.2 μM). The was little hydrolysis of ADP (<0.25 μM SCN^- was found to have an inhibitory a tion on the CTPase activity as well as t ATPase.

Inhibition of ATPase. Dinitrophenol, N ethylmaleimide (NEM), cyanide, and ou bain were found to be without effect on t ATPase at 3×10^3 M. In contrast oligom cin, sodium nitrate, ammonium ion, cyanog iodide and sodium thiocyanate were all fou to have an inhibitory action (Table II $HgCl_2$ was also found to be strongly inhib tory. Thus the -SH groups of the enzym

TABLE I. SCN^- Sensitivity of ATPase in Subcellular Fractions μm Pi min^{-1} mg^{-1} Protein.

Nuclear	2.4
SCN^-	1.5
Mitochondrial	3.6
SCN^-	1.7
Microsomal	3.2
SCN^-	1.8
Supernatant	1.7
SCN^-	1.1

Assay performed with 3 mM ATP, 3 mM $MgCl_2$, 20 mM Tris pH 8.4 and 3 mM SCN^-, c 0.5 mg protein, 30 min, 37°.

were reactive to mercurials but not NEM, but H^+ secretion is sensitive to both.

Na^+ and K^+ and ouabain insensitivity. Various concentrations of Na^+ and K^+, varying Na^+ from 0-100 mM and K^+ from 0-80 mM were without effect on enzyme activity. Ouabain at a concentration of 10^{-3} to 10^{-8} M was also without effect on the system. The exchange enzyme was similarly insensitive. Ouabain is without effect on the secretion of the *in vitro* frog mucosa.

Histamine effects. In 6 of 15 preparations, a variable degree of histamine sensitivity of the enzyme was found (about 30% stimulation), at concentrations of 10^{-3} to 10^{-4} M histamine. Various treatments such as Triton X-100, deoxycholate, diamine oxidase neither increased the sensitivity of the enzyme to such pharmacological doses, nor converted an insensitive preparation to a sensitive one.

Kinetic studies. 1/S *versus* 1/V plots with 3×10^{-3} M thiocyanate show apparently a non-competitive mechanism of inhibition, with a calculated K_M for ATP of 5×10^{-4} M and a K_i of 12 mM for thiocyanate (Fig. 1). Similar studies for CNl showed that CNl also inhibited, apparently uncompetitively, but more potently with a K_i of 4 mM.

Exchange studies. A potent ATP-ADP exchange enzyme was found to be present in the microsomal fraction of the frog gastric mucosa. The pH optimum was 7.4 and the average exchange rate was 350 mμM mg^{-1} min^{-1} (Table III). Thiocyanate, cyanogen iodide and oligomycin were found without effect on the exchange activity. No evidence could be found for an ATP-Pi exchange activity and the adenylic kinase and nucleoside diphosphokinases account for less than 10% of the exchange activity observed.

Gradient fractionation. Two peaks of ATPase activity were found, with the major peak of ATPase activity corresponding to the peak of ATP-ADP exchange activity. The density at which the enzyme activity fractionates corresponds to the region at which larger membrane fragments would fractionate. Triton X-100 apparently solubilized both enzyme activities (Fig. 2).

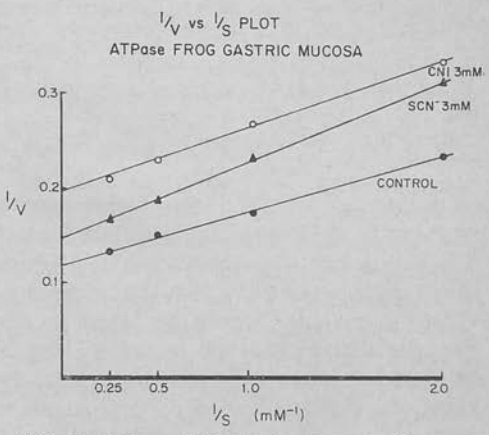

FIG. 1. 1/S *vs* 1/V plot for frog gastric mucosae microsomal ATPase, with SCN^-, CNl at 3 mM and ATP/mg ratio of 1, pH 8.4.

Discussion. ATPases were found in all fractions of the frog gastric mucosa. No very active inhibitor was found for the microsomal fraction apart from oligomycin and the mercurials. The SCN^- sensitivity of the microsomal ATPase was found to hold also for the other ATPases. The mechanism of inhibition of the microsomal ATPase with SCN^- appeared to be non-competitive. However, the high K_i found suggests that SCN^- is not a potent inhibitor of this system. A similar

TABLE II. Frog Gastric Mucosa Inhibition of Microsomal ATPase.

	% Inhibition
DNP, NEM, CN^- Ouabain	0
NO_2^-, NH_3	30
CNS^-	40
Oligomycin (10^{-5} M)	45
CNl	50
$HgCl_2$	100

Assayed as in Table I, with 3 mM inhibitor, except oligomycin as noted.

TABLE III. Frog Gastric Mucosa ATP-ADP, ATP-Pi Exchange mμmoles mg^{-1} min^{-1}.

(a)	ATP-ADP	350
	ATP-ADP + SCN^-	341
	Control boiled enzyme	<5
(b)	ATP-Pi	<15
(c, d)	Kinases (GDP, ATP, AMP)	<30

(a) ATP-ADP exchange assayed with 5 mM ATP, 5 mM $MgCl_2$, 1 mM C^{14} ADP, 20 mM Tris buffer pH 7.4, room temperature 30 min.

(b) ATP-Pi assayed with Pi^{32} 1-10 mM, ADP 0-3 mM, ATP 5-10 mM, $MgCl_2$ 0-10 mM, room temperature 30 min.

(c) GDP kinase assayed with C^{14} GDP 3 mM, ATP 3 mM, $MgCl_2$ 3 mM, 20 mM Tris pH 7.4, room temperature 30 min.

(d) Adenylate kinase with 5 mM ATP, 5 mM C^{14} AMP, 5 mM $MgCl_2$, 20 mM Tris pH 7.4, room temperature 30 min.

Nucleotides were separated by the thin layer chromatography.

mechanism of inhibition was found for the brush border ATPase of the hamster intestine (15) and the rat liver mitochondrial ATPase. Thus the action of SCN^- on the microsomal ATPase apparently cannot be taken as evidence for the participation of the ATPase in hydrogen ion transport, and may rather be related to displacement of Cl^- from anion binding sites. The other inhibitors found, namely nitrite, ammonia(16), cynogen iodide (15), have also been found to inhibit gastric secretion *in vitro*. In the case of CNl, the mechanism of inhibition of the ATPase has been found to be uncompetitive. The lack of sensitivity to ouabain and to $Na^+ + K^+$ distinguished this ATPase from other 'transport' ATPases. It is not clear therefore from these experiments whether this ATPase is associated with transport and if so whether with hydrogen ion or anion transport, or with some other type of reaction.

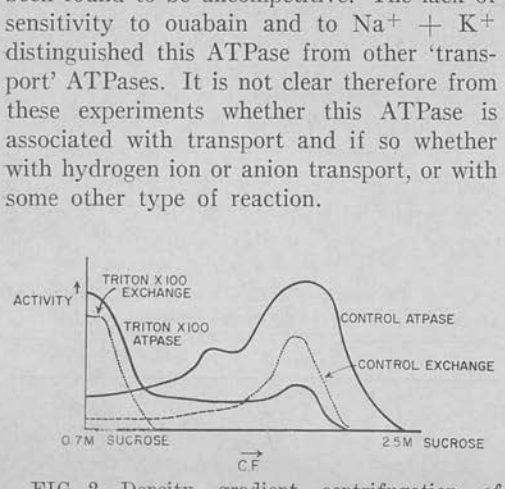

FIG. 2. Density gradient centrifugation of frog gastric mucosa microsomal ATPase, and ATP-ADP exchange enzyme between 0.7 M and 2.5 M sucrose, with and without Triton X-100.

The exchange enzyme demonstrated in microsomal fraction shows similar prope to the other transport ATPases in tha though ATP-ADP exchange activity is ent, no ATP-Pi exchange activity was onstrated(17). The exchange activity wa associated with adenylate kinase or NDI nase. Since the ATPase inhibitors tested no effect on the exchange enzyme their a must be confined to the second stage o following scheme:

$$ATP + X \rightleftarrows P \sim X + ADP$$
$$P \sim X + H_2O \rightarrow Pi + X$$

Since no phosphate stimulation of the A ADP exchange reaction was found, the a scheme is the simplest compatible with data.

We acknowledge with thanks the technical he Mrs. Jerri Taylor and Miss Elvira Finley.

1. Skou, J. C., Biochim. Biophys. Acta, 1957, 394.

2. Post, R. L., Fed. Proc., 1959, v18, 121.

3. Skou, J. C., Biochim. Biophys. Acta, 1962, 314.

4. Jarnefelt, J., von Stedingk, L. V., Acta Ph Scand., 1963, v57, 328.

5. Bonting, S. L., Simon, K. A., Hawkins, N Arch. Biochem. Biophys., 1961, v95, 416.

6. Charnock, J. S., Post, R. L., Nature, 1963, 910.

7. Hokin, L. E., Yoda, A., Proc. Nat. Acad 1964, v52, 454.

8. Rehm, W. S., The Cellular Functions of M brane Transport, Prentice-Hall, Englewood C N. J., 1963, p231.

9. Hogben, C. A. M., Fed. Proc., 1957, v20, 1

10. Kasbekar, D. K., Durbin, R. P., Biophy Meeting, 1964.

11. Schneider, W. C., Hogeboom, J. Biol. C 1950, v183, 123.

12. Fiske, C. H., Subbarow. Y., ibid., 1925, v66

13. Chiga, M., Plaut, W. E., ibid., 1959, v234,

14. Lowry, O. H., Rosebrough, N. J., Farr, A Randall, R. J., ibid., 1951, v193, 265.

15. Sachs, G., unpublished observations.

16. LeFevre, M. E., Gohmann, E. J., Jr., B W. S., Am. J. Physiol., 1964, v207, 613.

17. Skou, J. C., Biochim. Biophys. Acta, 1960, 6.

Received April 30, 1965. P.S.E.B.M., 1965,

Reprinted from PROC. SOC. EXPTL. BIOL. AND MED. Volume 133, Number 2 February 1970
 Printed in U.S.A.

PROCEEDINGS OF THE SOCIETY FOR EXPERIMENTAL BIOLOGY AND MEDICINE, 133, 456–459 (1970)

Action of SCN^- on Rat Liver Mitochondria[1] (34496)

G. SACHS, R. H. COLLIER,[2] AND B. I. HIRSCHOWITZ

Department of Medicine, University of Alabama Medical Center, Birmingham, Alabama 35233

Thiocyanate has been shown to inhibit the following functions in liver mitochondria: Succinate and β-hydroxybutyrate oxidation, P/O ratio, ATP binding, P_i–ATP exchange, and valinomycin-induced K^+ uptake. This inhibition can be overcome by increased ADP or substrate concentrations, and is presumably due to interaction of SCN^- with anion-binding sites in the mitochondrial membrane.

It has been shown (1) that the action of SCN^- on the gastric mucosa is not limited to inhibition of HCl secretion, but appears to extend to effects on K^+ permeability and on metabolism since there is alteration in O_2 consumption (2) and inhibition of microsomal and mitochondrial ATPase (3).

By measurements of the action of SCN^- on: (1) P/O ratio of mitochondrial preparations with a variety of substrates; (2) oxidation rate of various substrates; (3) ion transport of mitochondria; and (4) binding of nucleotides by mitochondria, it was shown that SCN^- had significant effects on various aspects of mitochondrial metabolism. These results have been presented in preliminary form (4).

Methods. Rat liver mitochondria were prepared by differential centrifugation using standard techniques with three additional washings (5), and the purity of the preparation was routinely checked by phase-contrast microscopy. The medium was 0.25 *M* sucrose, 0.001 *M* Tris, pH 7.4, and 0.001 *M* EDTA. The mitochondria were either used fresh, aged for 24 hr at 4°, sonicated for 30 sec at 0°, or treated with digitonin (6). For measurement of oxidative phosphorylation, either the Chance-Williams technique (7), or the glucose-hexokinase method were used. The medium contained 50 m*M* Tris HCl, pH 7.4, 5 m*M* $MgNO_3$, 2.5 m*M* K_2HPO_4, 0.5 m*M* EDTA, 2.5 mg/ml albumin, and 55 m*M* KCl. Rate of oxidation of various substrates at 10 m*M* was measured using either the Clark electrode or the Warburg apparatus. NADH-cytochrome *c* reductase was measured spectrophotometrically (8), as was cytochrome *c* oxidase (9) and succinate:Fe $(CN)_6^{3-}$ oxidoreductase (10). K^+ release and uptake by mitochondria was monitored by a system consisting of three electrodes specific for H^+, Na^+, and K^+. Binding of nucleotides was assayed by adding the labeled di- or triphosphopo-nucleotide (0.2 m*M*) to a medium at 0° containing 2 mg mitochondrial protein, 100 m*M* Tris-Cl, pH 7.4, and 5 m*M* $MgCl_2$, spinning at 37,000*g*, and counting the precipitated mitochondria. Controls were run by comparing counts obtained with tracer only to counts obtained with excess cold nucleotide in addition to the same amount of tracer. Results were corrected by the latter amount. P_i–ATP exchange was measured according to Conover *et al.* (11). Protein was measured by the Lowry method (12).

Results. Mitochondria obtained in this study showed respiratory control ratios of better than 8.0 with β-OH butyrate, malate, or succinate. Addition of SCN^- to mitochondria in state 3 inhibits O_2 consumption by 25% at 10 m*M*, and 45% at 30 m*M* when β-OH butyrate is used as substrate. When the mitochondria are uncoupled by using dinitrophenol or carbonyl cyanide *m*-chlorophenylhydrazone the action of SCN^- is quantitatively similar.

Measurement of P/O ratios, using the O_2 consumption increment obtained upon the addition of ADP to state 4 mitochondria,

[1] Supported by N.I.H. Grants AM 08541 and 09260 and NSF Grant GB-3511.

[2] Trainee of U.S.P.H.S. Grant 2A-5286.

TABLE I. Effect of 10 and 30 m*M* SCN^- on P/O Ratios of Rat Liver Mitochondria (Five Experiments in Each Group) Using the ADP Addition (O_2) or Hexokinase Method.

	P/O ratio					
	Control		10 m*M* SCN^-		30 m*M* SCN^-	
	O_2	Hexokinase	O_2	Hexokinase	O_2	Hexokinase
Succinate	1.8	1.48	1.1	1.11	0.85	0.84
β-OH Butyrate	2.5	2.21	1.9	1.76	1.41	1.14

showed that in the preparations a ratio of 1.6 was obtained with succinate as substrate and 2.5 with β-OH butyrate. Addition of SCN^- resulted in a slower rate of ADP-dependent O_2 consumption, as did addition of atractylate of fluoride. The P/O ratios, however, calculated from the total O_2 uptake declined slightly. Similar results were obtained using the hexokinase method (Table I). Increasing the ADP/SCN ratio gradually restored the oxidation rate, which would suggest competitive effects, particularly since similar data are obtained with atractylate. Since previous work used high ADP/SCN ratios, these effects were not observed (13).

Sonicated mitochondria have a much reduced sensitivity to SCN^-, with succinate as substrate, whereas digitonin-treated mitochondria appear identical to intact mitochondria in terms of their response to SCN^-, data similar to those for atractylate (14).

SCN^- had no effect on ferrocytochrome *c* oxidation but succinate:$Fe(CN)^3_6$ oxidoreductase was inhibited 45%.

Table II summarizes data on the effect of SCN^- and atractylate on binding of ADP and ATP to intact mitrochondria. Whereas atractylate reduces binding of ADP by about 90%, SCN^- reduces nucleotide binding, ATP more than ADP, by about 40%. Additionally P_i–ATP exchange is inhibited by 30 m*M* SCN^- as effectively as by oligomycin.

With the demonstration that K^+ flux is inhibited in the gastric mucosa, measurements of K^+ movement in intact mitochondria using cation-specific electrodes showed that SCN^- significantly slows the uptake of K^+ induced by valinomycin, but is without effect on subsequent nigericin-induced K^+ efflux (Fig. 1).

Discussion. Thiocyanate ion (SCN^-) appears to inhibit coupled or uncoupled mitochondrial respiration. Although no effect was observed distal to cytochrome *c*, inhibition of NADH-cytochrome *c* oxidoreductase and succinate:$Fe(CN)^3_6$ oxidoreductase was demonstrated, and the degree of inhibition could account for the respiratory inhibition observed in uncoupled mitochondria. A slight reduction in P/O ratios was observed, and the respiration rate was slowed, which could be overcome by increasing the ADP/SCN^- ratio, similar data being observed for atractylate (15).

TABLE II. Binding and Exchange Activity of Rat Liver Mitochondria.

	Binding (mμ*M* mg^{-1} protein)		ATP-P_i exchange (mμ*M* P_i incorporated mg^{-1} protein)
	H^3ATP	H^3ADP	
Control	2.4	2.5	23
Atractylate (10^{-6} *M*)	.7	0.8	—
Oligomycin (0.05 mg/ml)	2.3	2.4	2.8 (0.1 mg/ml)
SCN^- (30 m*M*)	1.4	2.0	1.7
Oligomycin + atractylate	1.3	0.5	—
Oligomycin + SCN^-	1.3	1.4	—

Means of 3 experiments.

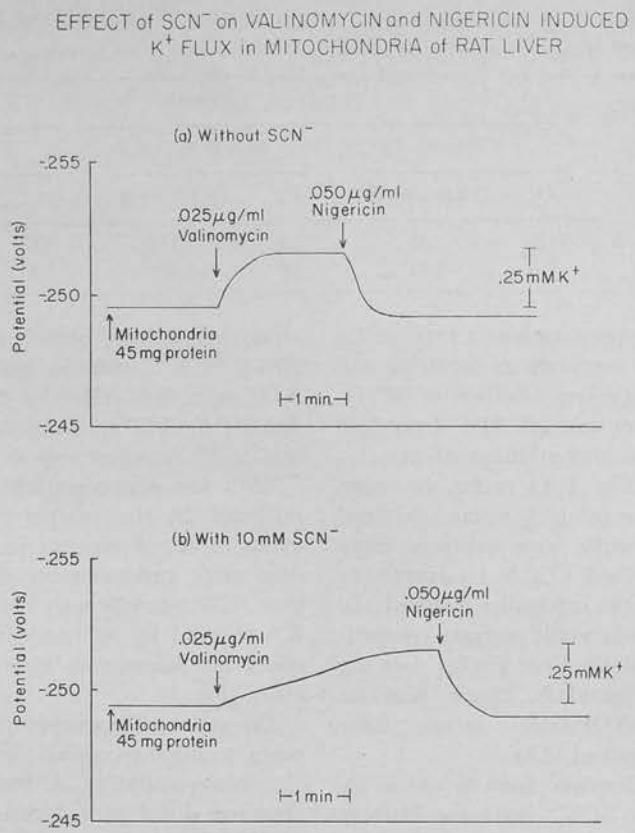

FIG. 1. Effect of SCN^- on K uptake and efflux in rat liver mitochondria induced by valinomycin and nigericin.

Since sonication, but not digitonin treatment, reduced SCN^- effectiveness, there would appear also to be a structural requirement for the action of SCN^--inhibited binding of labeled ATP or ADP by mitochondria. These effects were less than those observed with atractylate and were greater for ATP than for ADP. Since nucleotide binding is required for P_i–ATP exchange, the inhibitory action of SCN^- on this reaction confirmed the action of SCN^- on nucleotide binding.

From these data, and those reported for the gastric mucosa (1), it would appear that SCN^- interferes with both cation- and anion-transport processes across membranes, presumably by binding at anion sites and altering the electrostatic properties of those membranes.

1. Sachs, G., Collier, R. H., Pacifico, A., Shoe
R. L., Zweig, R. A., and Hirschowitz, B. I., Bi
Biophys. Acta. **173**, 509 (1969).

2. Forte, J. G., and Davies, R. E., Am
Physiol. **204**, 812 (1963).

3. Sachs, G., Mitch, W. E., and Hirschowitz
Proc. Soc. Exp. Biol. Med. **119**, 1023 (1965).

4. Collier, R. H., and Sachs, G., Biophys. J.
(1968).

5. Johnson, D., and Lardy, H. A., *in* "Meth
Enzymology" (R. W. Estabrook, and M. E. Pu
eds.), Vol. X, p. 9A. Academic Press, New
(1967).

6. Haas, D. W. and Elliott, W. B., J. Biol.
238, 1132 (1963).

7. Chance, B., and Williams, G. R., Nature
(1955).

8. Lehman, I. R., and Nabor, A., J. Biol.
222, 497 (1956).

9. Smith, L., and Stotz, E., J. Biol. Chem.
(1956).

10. Singer, T. P. and Kearney, E. B., Methods Biochem. Anal. **4**, 307 (1957).

11. Conover, T. E., Prarie, R. L., and Racker, E. J. Biol. Chem. **238**, 2831 (1963).

12. Lowry, O. H., Roxborough, N. J., Fort, A. L., and Randall, R. J., J. Biol. Chem. **193**, 265 (1951).

13. Forte, J. G., Forte, G. M., Gerard, R., and Saltsman, P., Biochem. Biophys. Res. Commun. **28**, 215 (1967).

14. Winkler, H. H., and Lehninger, A. L., J. Biol. Chem. **243**, 3000 (1968).

15. Bruni, A., Contessa, A. R., and Scalella, P., Nature **201**, 1219 (1964).

Received June 26, 1969. P.S.E.B.M., 1970, Vol. 133.

Reprinted from
Biochimica et Biophysica Acta
Elsevier Publishing Company
Amsterdam
Printed in The Netherlands

BBA 75264

ACTION OF THIOCYANATE ON GASTRIC MUCOSA *IN VITRO*

G. SACHS, R. H. COLLIER, A. PACIFICO, R. L. SHOEMAKER, R. A. ZWEIG AND B. I. HIRSCHOWITZ

Departments of Medicine and Surgery, University of Alabama, Medical Center, Birmingham, Ala. (U.S.A.)

(Received November 18th, 1968)

SUMMARY

Thiocyanate in addition to its well-known action in inhibiting HCl secretion by the amphibian gastric mucosa has been shown to inhibit ^{42}K flux and the potential difference change due to K^+ or Rb^+ concentration changes in the bathing solutions. Cs^+ does not substitute for K^+ in the stomach. Other secretory inhibitors have similar effects. These data may be interpreted by regarding the mucosa as consisting of two parallel circuits residing in the parietal and surface cells, with the parietal cell being responsible for the major fraction of the ^{42}K movement through the mucosa, which is associated with HCl secretion, and the surface cell possessing the K^+ perm-selective membrane.

INTRODUCTION

Thiocyanate has been intensively studied as an inhibitor specifically of acid secretion by the gastric mucosa[1]. At one time it was thought that its action could be explained by an effect on carbonic anhydrase[2], but since that time it has been shown repeatedly[3] that inhibition of this enzyme affects the Cl^- rather than the H^+ transport mechanism in the secreting mucosa. More recently, an ATPase which has been isolated from various species shows sensitivity to SCN^-, occurs in the microsomal fraction obtained from gastric mucosal homogenates and thus by inference has been implicated in the acid transporting mechanism[4,5].

In addition to its gastric actions, SCN^- has multiple other effects including effects on iodide transport in the thyroid, central nervous system disturbances and generalized effects on histochemical reactivity of membrane enzymes[6].

In efforts to obtain some insight into SCN^- action, O_2 consumption studies of gastric mucosa either in an Ussing chamber, or in the Warburg respirometer have shown that SCN^-, while completely inhibiting acid secretion, has only a gradual effect on O_2 consumption reaching a level of about 10–15 % inhibition at 10 mM and about 40 % at 30 mM final concentration[7]. This observation has raised serious difficulties for any simple redox theory of acid secretion, since ratios of changes in acid secretion rate to changes in O_2 consumption are obtained which greatly exceed the maximum $\Delta H/\Delta O_2$ ratio of 4 predicted by redox theory. However, if one considers that SCN^-

Abbreviation: PD, potential difference.

acts by inhibition of an acid transport ATP-dependent system in the tissue by inhibiting ATP breakdown[4,5], the lack of an effect on O_2 consumption is not explained by SCN presence possible explanation is that along with inhibition of membrane ATPase, the but still mitochondrial uncoupling. That this is not the case is suggested by the finding diffusio mitochondrial ATPase may also be inhibited by this ion[5], and in direct mitochon studies no such uncoupling was observed[8]. Since SCN^- not only does not inhibit flux in gastric mucosa (*i.e.*, short circuit chloride) but in fact may be transported the Cl^- or anion pump[9], we must localize its action to the H^+ transport mecha distal to the energy-consuming reaction. This action is equivalent in part to action of uncouplers in mitochondrial systems whereby the substrate-consu reactions are uncoupled from the energy utilization pathway of phosphorylation.

The action of SCN^- on the apparent passive permeability of the gastric mu to K^+ demonstrated in this paper is reflected in a like action on mitochondria movement which is discussed in a subsequent paper.

METHODS

Rana pipiens or Necturus gastric fundic or esophageal mucosa were mou in an Ussing flux chamber modified as previously described[10]. In a lucite cham measurements were routinely made of potential difference (PD), resistance, sh circuit current (I_{sc}) and acid secretion rate using the pH stat technique[11].

When O_2 consumption studies were to be performed, a Kel-F chamber was u with Clark O_2 electrodes and Radiometer amplifiers either with direct recordin by an oxystat method[12]. Solution compositions (frog Ringer nutrient, isotonic l secretory) were varied by K^+ substitution for Na^+, SO_4^{2-} or SCN^- substitution Cl^- and choline substitution for Na^+. In some experiments Rb^+ or Cs^+ replaced Flux measurements were carried out by standard techniques using ^{42}K (high spe activity) ^{22}Na or ^{36}Cl, and counting was performed in a liquid scintillation counte

RESULTS

Fig. 1 illustrates the general action of SCN^- on the gastric mucosa. Thus t is a rapid fall of the H^+ rate to zero, at 10 mM SCN^-. With the fall in acid secre rate there is a maintained rise in resistance and a rise in the PD which may be maint ed or may be transient. O_2 consumption falls with the onset of secretory inhibi by about 20 % in this particular experiment. Although it has been previously repo that addition of SCN^- results in oxidation of cytochrome *c*, in a system where CO was used to eliminate possible interference by hemoglobin[13], this observation c not be confirmed with any consistency in well-perfused gastric mucosae when CO not used.

Table I summarizes the results of 20 experiments where H^+ rate, PD and were measured. Additionally Table I summarizes the data obtained for $^{36}Cl^-$ measurements in 20 experiments (10 in either direction) and $S^{14}CN^-$ flux measments (N→S) in 10 experiments. It can be seen that the effect of SCN^- is to re the H^+ rate and Cl^- rate by an equivalent amount, leaving the short-circuit chlo unaffected. In addition the exchange diffusion component is also uninfluenced by presence of thiocyanate. The flux of SCN^- is only a small fraction of the Cl^- flux in

presence of chloride. When Cl^- is omitted from the bathing solutions and is replaced by SCN^-, there is a marked reduction in I_{sc}, and the flux of SCN^- is much increased, but still falls short of the Cl^- flux under Cl^- conditions. This suggests that the exchange diffusion component (or Cl^- carrier) handles SCN^- much less efficiently than Cl^-.

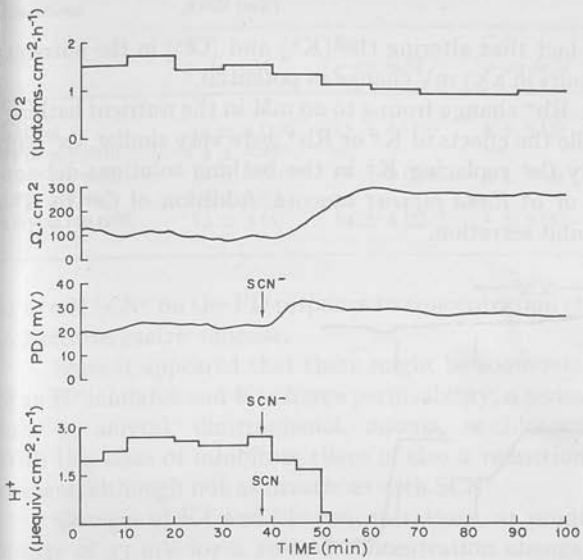

Fig. 1. Effect of 10 mM SCN^- on nutrient side of frog gastric mucosa on H^+, PD, resistance and O_2 consumption.

TABLE I

EFFECT OF SCN^- ON VARIOUS PROPERTIES OF GASTRIC MUCOSA

Values are ± S.E. and except where noted expressed as μequiv. $cm^{-2} \cdot h^{-1}$.

	Control	*10 mM SCN⁻*	*109 mM SCN⁻*
H^+	3.12 ± 0.28	0	0
I_{sc}	2.51 ± 0.19	2.11 ± 0.13	1.43 ± 0.20
$^{36}Cl^-$ N→S	10.43 ± 0.41	7.10 ± 0.39	—
$^{36}Cl^-$ S→N	5.51 ± 0.29	5.77 ± 0.27	—
$S^{14}CN^-$ N→S	—	0.24 ± 0.03	2.14 ± 0.33
PD (mV)	32 ± 3	41 ± 5	21 ± 2

The change in PD and resistance has been explained as being due to the inhibition of the H^+ transport mechanism. In fact, these changes have been regarded as strong evidence for the electrogenicity of H^+ transport[14].

However, since some workers have regarded the gastric PD as being a result of K^+ and/or Cl^- gradients transmucosally[15], it is also possible that SCN^- had some action on Cl^- or K^+ permeability, measured either chemically or by the PD change resulting from concentration changes in the bathing solutions. In Cl^- solutions it

appears that for Nectures or for *Rana pipiens* the charge permeability of the mu membrane can be described by the equation

$$E = \frac{RT}{nF} \ln \frac{[K_I^+] + r\,[Cl_0^-]}{[K_0^+] + r\,[Cl_I^-]}$$

where $r = P_K/P_{Cl}$ (ref. 15).

This is confirmed by the fact that altering the $[K^+]$ and $[Cl^-]$ in the nu solutions, product constant, results in a 53 mV change in potential.

The effect of a K^+ and a Rb^+ change from 4 to 20 mM in the nutrient b solution is shown in Fig. 2. While the effects of K^+ or Rb^+ were very similar, C little if any effect. Additionally Cs^+ replacing K^+ in the bathing solutions d support secretion of Necturus or of *Rana pipiens* mucosa. Addition of Cs^+ t containing solutions did not inhibit secretion.

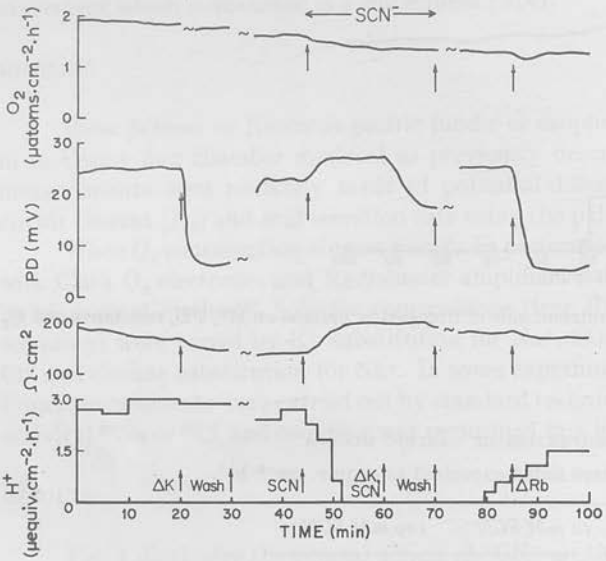

Fig. 2. Effect of changes of K^+ and Rb^+ on the PD, resistance and O_2 consumption of the ga mucosa and the effect of 10 mM SCN^- on the K^+ induced PD changes.

With SCN^- there appears to be a drastic reduction in both the rate and ma tude of the PD changes. Addition of 10 mM SCN^- on the secretory side has a m lesser effect on the PD change induced by K^+ changes on the nutrient side of mucosa, which would localize the PD effect to the nutrient membrane of the cel the gastric mucosa, although the acid mechanism is located on the secretory side.

Since 10 mM SCN^- abolishes the acid secretion rate within 10 min, an atte was made to distinguish between the effects of SCN^- on K^+ and on H^+ either using only 1 mM SCN^-, or by K^+ change induced within 1 min of 10 mM S addition. It was found that even 1 mM SCN^- induced profound changes in the response to K^+ addition (30 % suppression).

When Cl^- changes were carried out under similar conditions again there w significant reduction in the PD response. Table II summarizes the effects of addi

TABLE II

EFFECT OF 5-FOLD CONCENTRATION CHANGES OF K^+ AND 4.5-FOLD CHANGES OF Cl^- ON THE PD OF NECTURUS GASTRIC MUCOSA

Values are mean ± S.E. (number of determinations).

Conditions	ΔPD (mV)			
	K^+ 4–20 mM	Rb^+ 4–20 mM	Cs^+ 4–20 mM	Cl^- 20–89 mM
Control	23 ± 4 (10)	25 ± 2 (10)	3 ± 3 (5)	16 ± 3 (5)
ΔPD, mV/min	1.3 ± 0.20	—	—	—
SCN^- (10 mM)	12 ± 2 (10)	11 ± 2 (10)	4 ± 2 (5)	7 ± 4 (5)
ΔPD, mV/min	0.6 ± 0.22	—	—	—
Amytal (10 mM)	15 ± 3 (5)	14 ± 4 (5)	1 ± 3 (5)	—

of 10 mM SCN^- on the PD response to concentration changes of K^+, Rb^+, Cs^+ and Cl^- in Necturus gastric mucosa.

Since it appeared that there might be some relationship between the presence of an H^+ inhibitor and K^+ charge permeability, a series of other inhibitors was tested, such as amytal, dinitrophenol, anoxia, *m*-chlorocyanocarbonylphenylhydrazone. With this class of inhibitors there is also a reduction in the magnitude of the PD changes, although not as drastic as with SCN^-.

Changes of K^+ and Cl^- concentrations, at product constant, result in a mean change of 53 mV for a 10-fold concentration change. In the presence of SCN^- or amytal, for example, significant differences in rate and/or magnitude of PD change are found, with values ranging from 33 to 45 mV.

To amplify the above observations, measurement of K^+ flux across the *Rana pipiens* gastric mucosa was performed using ^{42}K. The conditions chosen were with K^+ gradients across the mucosa of 4–0 mM, 20–0 mM or 89–0 mM K^+, N→S, since it was found that the presence of K^+ on the secretory side had little effect on the K^+ flux.

Table III summarizes the findings on the N→S movement of K^+ under a variety of conditions. Increasing the K^+ gradient results in a marked increase in K^+ flux, as might be expected. Under these conditions simultaneous measurement of N→S $^{36}Cl^-$ flux showed little change, but after 1 h there was an increase in the S→N $^{36}Cl^-$ flux.

TABLE III

N→S MOVEMENT OF K^+

Values are mean K^+ fluxes ± S.E. (number of experiments).

Conditions	ΔK^+, N→S ($\mu equiv \cdot cm^{-2} \cdot h^{-1}$) $[K^+]$ nutrient (mM):		
	4	20	80
Control	0.203 ± 0.046 (8)	0.471 ± 0.055 (6)	1.43 ± 0.17 (5)
SCN^-	0.031 ± 0.022 (6)	0.083 ± 0.06 (4)	0.21 ± 0.22 (6)
Amytal	0.094 ± 0.041 (4)	—	0.50 ± 0.38 (4)
Control*	0.100 ± 0.050 (4)*	—	—

* ΔK^+, S→N.

Also included in the table are measurements of the effect of SCN^- at the differe... concentrations, and the effect of amytal at the 4 and 80 mM K^+ levels.

Accordingly SCN^- reduces the N→S flux of K^+ almost to zero under al... ditions. Amytal and other inhibitors also reduce K^+ flux but not as significan... SCN^-. An interesting relationship between resistance, inhibitor and K^+ flux m... seen in Fig. 3, which shows the effect of 10^{-6} M *m*-chlorocyanocarbonylph... hydrazone on the standard parameters of the gastric mucosa, and additiona... N→S K^+ flux. In the phase of increased mucosal resistance, there is diminuti... K^+ flux, whereas when the resistance starts to fall, K^+ flux increases.

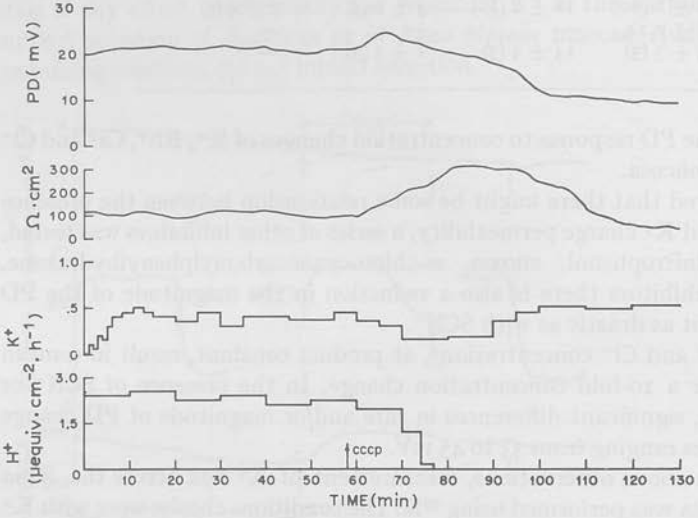

Fig. 3. Effect of *m*-chlorocyanocarbonylphenylhydrazone (CCCP) on H^+, PD, resistance an... flux N→S of gastric mucosa.

Although the above data appear to substantiate a relationship between m... tance and K^+ flux, this is not invariably the case, as is illustrated in experim... carried out in collaboration with Dr. W. S. Rehm. It had been previously shown ... addition of Ba^{2+} (1 mM) increased resistance approx. 2-fold[16]. This occurs in ... absence of any significant change in the H^+ rate, and may be reversed by incr... of nutrient K^+ concentration. In spite of this, addition of Ba^{2+} has no effect ... measured K^+ flux, although there is reduction of the PD changes in K^+ concentrat...

DISCUSSION

The inhibition of HCl transport in the gastric mucosa by SCN^-, as well as ... rise of resistance and lack of change of I_{sc} in the chambered preparation, has been ... documented[7].

From the data in Table I, there is no significant change in I_{sc}, which ref... nonacidic Cl^- transport, confirmed by measurements of net Cl^- flux. It must ... concluded, therefore, that the action of SCN^- is specifically on the HCl compon... of transport in this tissue, and that SCN^- is without effect on the nonacidic ...

component. Although net SCN^- transport does occur, it is only a small fraction of the Cl^- transport. When Cl^- was omitted from the bathing solutions, and completely replaced by SCN^-, transport of SCN^- increased, but remained at less than 20% of the unidirectional Cl^- movement, showing that both the "active" Cl^- mechanism and the "carrier" presumably responsible for the high calculated Cl^- conductance[17] have relatively low affinity for SCN^-.

Since, therefore, with inhibition of HCl secretion SCN^- does not alter the current produced at zero external potential difference the action of SCN^- does not appear to result in any change in the electrogenicity of gastric mucosal transport. This conclusion, however, does not take into account the transients involved in reaching the final steady state, namely an increase in PD and resistance. One interpretation of this finding has been that these changes are due to inhibition of a primary electrogenic H^+ transport mechanism, but, according to the data presented, this does not contribute to current flow in the secretory steady state. An alternative interpretation is based on the possibility that the potential gradient across the gastric mucosa is due to K^+ and/or Cl^- gradients established across the nutrient surface of the gastric cells. According to this view, alterations in the passive permeability characteristics of the cell membrane to either of these ions would result in a lowering of the tissue conductance, or a rise in the resistance.

Measurement of alterations of PD when appropriate bathing solution concentrations are changed is the simplest method of determining the relative permeability of a membrane to the various ions. This, however, does not give information as to the relative chemical flux rates, since it may not involve passage of charged species across the serosal or mucosal boundary. When K^+ or Cl^- induced potential difference changes were measured in the presence or absence of SCN^-, significant differences were observed. Thus, in particular, the response to K^+ substitution for Na^+ was much reduced, suggesting that the selectivity of the membrane to K^+ with respect to Na^+ had been altered by SCN^-. Measurements of the $^{42}K^+$ flux showed that SCN^-, while inhibiting H^+, also inhibited $^{41}K^+$ flux in the gastric mucosa in the open-circuit condition. Thus SCN^- reduces both "chemical" and "charge" permeability of the gastric mucosa to potassium. This is in contrast to conclusions reached by others using chemical methods to measure K^+ flux[18].

The relationship between the degree of inhibition of acid secretion and K^+ flux was also striking, and the use of other inhibitors of acid secretion, such as amytal, also concomitantly reduced H^+ and K^+ flux. This confirms what has been found in the intact mammalian stomach, namely that there is an association between acid and K^+ secretion[19]. Hence the larger fraction of N→S K^+ movement observed in frog mucosa *in vitro* is associated with parietal cell function. *Necturus esophagus*, which is readily mounted in the Ussing chamber and generates an I_{sc} of between 10 and 25 μA, shows a PD response to change of K^+ which is similar to that observed in the fundus, which contains both surface and parietal cells[20]. Thus at least part of the potential response to K^+ changes is probably a function of the surface epithelial cell.

Accordingly it should be possible to dissociate the K^+ transport properties of the mucosa by selective inhibition of one or the other of the cell types. Ba^{2+}, which has been shown to increase transmucosal resistance, and decrease the K^+ response[16], does not alter the $^{42}K^+$ flux transmucosally. Thus this ion may be affecting primarily the surface cell properties whereas amytal and other metabolic inhibitors affect primarily

the parietal cell. SCN^- would then be unique, since it drastically inhibits both PD response and $^{42}K^+$ movement, and would thus affect the relative permeability characteristics of both cell types. This is further brought out by the inhibitory effect of low (non-acid inhibitory) concentrations of SCN^- on K^+ potential response when added to the nutrient side.

An alternative interpretation of PD changes due to alterations of K^+ concentrations has been advanced by HOGBEN[21]. He showed that 45 min following a change in K^+ concentration, the S→N Cl^- flux was significantly increased. However, since SO_4^{2-} solutions K^+ changes also alter the PD, the short-term potential and current changes across the mucosa resulting from changes in K^+ concentration are due to alterations in K^+ transport, not Cl^-. Over longer periods, however, it appears that Cl^- back flux is increased. The current across the tissue, therefore, in the presence of a K^+ gradient is carried by Cl^- and K^+, as our flux data showed.

REHM[16] has shown by the use of equivalent circuits, that alteration of resistance across the secretory membrane would be predicted to alter the PD response to change in the nutrient membrane electromotive force, hence alteration in PD response to K^+ changes does not necessarily reflect the passive charge permeability of the gastric mucosa. However, measurements of $^{42}K^+$ movement in the case of SCN amytal show that it is reduced. To reconcile these data, it is only necessary to postulate two pathways for K^+ movement across the mucosa, the surface cell and the parietal cell[22]. The surface cell pathway has a high resistance relative to the parietal cell. Alterations of K^+ affect the PD across the nutrient membrane of the surface and the PD change would be given by

$$\Delta \text{ PD} = \frac{-R_{SEC}}{R_{PC} + R_{SEC}} \cdot \Delta E_{SEC}$$

where R_{SEC} is resistance through surface cell, R_{PC} is parietal cell resistance, Δ is actual change in surface cell nutrient membrane PD due to K^+ changes and Δ is transmucosal PD change. If R_{PC} is altered by SCN^- or amytal and is then of same order of magnitude as R_{SEC}, evidently Δ PD will decrease, for a given Δ. Thus agents which alter the electrical resistance of the parietal cell would be expected to alter the PD change across the mucosa in response to K^+ changes. Amytal would be such an agent, and significantly depresses K^+ flux as well as the PD response. SCN^- depresses the K^+ flux even more dramatically and may therefore also affect surface cell membrane and hence ΔE_{SEC} directly.

From these observations, the resistance changes due to SCN^- action may be due to a more general action of SCN^- on biological membranes, whereby the selective permeability properties are altered. This is likely to be due to the chemical property of SCN^- of being able to participate in halide reactions. Thus if there are anion binding sites on the nutrient and secretory surfaces of the gastric mucosa such as in Cl^- solutions they normally bind Cl^-, yet have a high affinity for SCN^-, the membrane lattice will be significantly modified by the presence of SCN^-.

ACKNOWLEDGMENTS

This work was supported by the National Institutes of Health, Grants 08541 and 09260 and the National Science Foundation, Grant GB-3511.

One of us (R.H.C.) is a trainee of the U.S. Public Health Service and has received Grant No. 2A-5286.

REFERENCES

1 W. S. REHM AND A. J. ENELOW, *Am. J. Physiol.*, 144 (1945) 701.
2 H. W. DAVENPORT, *Gastroenterology*, 7 (1946) 374.
3 R. P. DURBIN AND E. HEINZ, *J. Gen. Physiol.*, 41 (1958) 1035.
4 R. P. DURBIN AND D. K. KASBEKAR, *Federation Proc.*, 24 (1966) 1377.
5 G. SACHS, W. E. MITCH AND B. I. HIRSCHOWITZ, *Proc. Soc. Exptl. Biol. Med.*, 120 (1965) 702.
6 M. WOLMAN, J. J. BUBIS AND H. WIENER, *Histochemie*, 9 (1967) 1.
7 J. G. FORTE AND R. E. DAVIES, *Am. J. Physiol.*, 206 (1964) 218.
8 J. G. FORTE, G. M. FORTE, R. GOE AND P. SALTMAN, *Biochem. Biophys. Res. Commun.*, 28 (1967) 215.
9 C. A. M. HOGBEN AND N. D. GREEN, *Federation Proc.*, 17 (1958) 72.
10 G. SACHS, R. L. SHOEMAKER AND B. I. HIRSCHOWITZ, *Am. J. Physiol.*, 209 (1965) 461.
11 E. HEINZ AND R. P. DURBIN, *Biochim. Biophys. Acta*, 31 (1959) 746.
12 L. C. CLARK AND G. SACHS, *Ann. N.Y. Acad. Sci.*, 148 (1908) 133.
13 G. W. KIDDER, P. F. CURRAN AND W. S. REHM, *Am. J. Physiol.*, 211 (1966) 513.
14 W. S. REHM, *Am. J. Physiol.*, 203 (1962) 63.
15 J. B. HARRIS AND I. S. EDELMAN, *Am. J. Physiol.*, 206 (1964) 769.
16 W. S. REHM, *J. Gen. Physiol.*, 51 (1968) 2505.
17 C. A. M. HOGBEN, *Federation Proc.*, 24 (1966) 1353.
18 J. B. HARRIS AND I. S. EDELMAN, *Am. J. Physiol.*, 196 (1959) 1266.
19 B. I. HIRSCHOWITZ AND G. SACHS, *Am. J. Physiol.*, 213 (1967) 1401.
20 G. SACHS AND R. L. SHOEMAKER, in preparation.
21 C. A. M. HOGBEN, *J. Gen. Physiol.*, 51 (1968) 240.
22 G. SACHS AND G. M. MAKHLOUF, *Nature*, submitted for publication.

Reprinted from:
GASTRIC SECRETION

Academic Press, Inc., New York and London

ROLE OF ATP AND ATPase IN GASTRIC ACID SECRETION

G. Sachs, V. D. Wiebelhaus, A. L. Blum and B. I. Hirschowitz

Much of our fascination with acid secretion and its mechanism is due to the very high concentration gradient of hydrogen ion that can be achieved by the adult mammalian mucosa. In contrast, most of our knowledge of its mechanism derives from studies of in vitro mucosa with much lower transport capacity. It is perhaps a result of this that we have only fragmentary knowledge of the biochemical pathways involved in acid secretion and that, after many years, it has not been possible to decide with certainty between a redox dependent or an ATP dependent process.

A redox dependent acid secretion system is based on the vectorial organization of a dehydrogenase on one side of a membrane and an electron acceptor on the other. Thus with oxidation of substrate, protons may be released from one side of the membrane and the electrons transferred to the other side ultimately to O_2. Therefore in this scheme there is no participation of ATP.

An ATP dependent model can be constructed in many different ways, but ultimately the energy available from the hydrolysis of ATP is transferred to a proton carrier which as a result moves protons against an electrochemical gradient.

It seems to us that a logical approach to the biochemical mechanism of acid secretion would include the following steps:

a. Proof that ATP is required for acid secretion;
b. Isolation of the acid secreting cell from the mucosa and isolation of that subcellular component ultimately responsible for the process. It can be presumed to be in the vesicular or microtubular structures present in the luminal surface of that cell;
c. Demonstration that an ATPase, stimulated by HCO_3^- and inhibited by SCN^- is present in these vesicles;
d. A study of the properties of the ATPase, showing

that these properties can be readily related to proton transport mechanism;

e. A reconstitution of an acid transporting system using the vesicular preparation.

A. Energy Source for Acid Secretion

Several years ago we decided that, from the indirect methods available, the use of inhibitors should furnish the best estimate of the probability that ATP is required for acid secretion. The use of inhibitors is open to objection because of non-specificity and complex cellular reactions to metabolic alterations. The use of a large number of inhibitors for a given chemical reaction perhaps overcomes the problem of non-specificity since, if all the inhibitors give an identical result, it would be unlikely that this could be explained on the basis of a similar non-specificity. It would be more likely that the single reaction known to be inhibited, would provide the explanation. As will be emphasized in this section, however, there are anomalies in some of the effects of the inhibitors to be discussed, and these may be on occasion extremely significant. The chart (on the following page) shows a scheme of the inhibitors used.

1. Metabolic Inhibitors: 2-deoxyglucose has been investigated in this laboratory (1). In the presence of hexokinase and ATP, 2-deoxyglucose-6-PO_4 is formed, and cannot be further metabolized. Thus if 2-DG is the primary sugar present, phosphate and ATP are depleted and glycolysis is inhibited in each cell (2). Although it was a reasonably effective inhibitor of acid secretion we could not show any significant alteration of cellular levels of ATP (1). This finding has been confirmed (3). However, there was an increased production of $C^{14}O_2$ from glucose-1-C^{14} and reduction in $C^{14}O_2$ from glucose-6-C^{14} as would be expected from glycolytic inhibition. We were forced to conclude that: (a) There may be a compartment of ATP which is selectively depleted; and (b) A key intermediate in glycolysis is depleted. To date, however, investigation of intermediary metabolism of the gastric mucosa has been superficial, and the relationship of metabolic intermediates to acid secretion rate is unknown. This is clearly necessary in this area, since it should be possible on this basis alone, to

Succinate

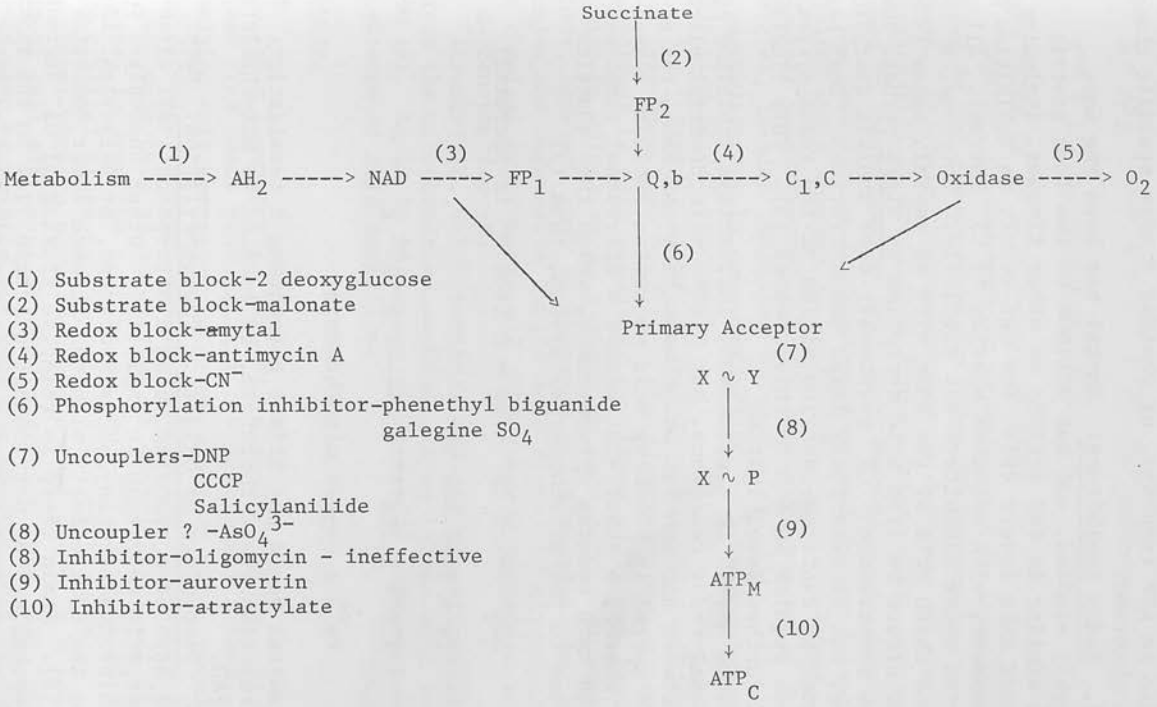
Succinate
(2)
FP_2
(1)
(3)
(4)
(5)
Metabolism -----> AH_2 -----> NAD -----> FP_1 -----> Q,b -----> C_1,C -----> Oxidase -----> O_2
(6)
Primary Acceptor
(7)
X ~ Y
(8)
X ~ P
(9)
ATP_M
(10)
ATP_C
(1) Substrate block-2 deoxyglucose
(2) Substrate block-malonate
(3) Redox block-amytal
(4) Redox block-antimycin A
(5) Redox block-CN^-
(6) Phosphorylation inhibitor-phenethyl biguanide
galegine SO_4
(7) Uncouplers-DNP
CCCP
Salicylanilide
(8) Uncoupler ? -AsO_4^{3-}
(8) Inhibitor-oligomycin - ineffective
(9) Inhibitor-aurovertin
(10) Inhibitor-atractylate

Chart

determine whether metabolic changes are consistent with would increase in ATP turnover, or whether a more specific ch can be observed.

2. Redox Inhibitors: Amytal has been the most thoroughly studied, and has actions on the frog gastric mucosa similar to its actions on other tissues, includi increased NADH levels (4). The net result is inhibitio H^+ transport, with relative sparing of Cl^- current. Al effective redox inhibitors act similarly. Rotenone, a compound which acts at the same site as amytal, seems t without effect on frog acid secretion *in vitro* perhaps to slow penetration. CN^- eventually does inhibit secre in frog, but at relatively large concentrations. Dual spectroscopy confirms that inhibition of the redox syst CN^- does require 10^{-2} M in this species (5). This find merits further investigation.

Since amytal is a relatively ineffective inhibitor microsomal redox reactions, but blocks mitochondrial el flow between NAD and FAD or between FAD_1 and FAD_2, the fect of amytal in blocking acid secretion excludes a hy thesis whereby a substrate reduces a microsomal compone which in turn reduces cytochrome c, which then shuttles electrons to the mitochondrial system, thus (7)

$$AH_2 \text{ -----> } 2H^+ + 2e + A \text{ (the } H^+ \text{ is secreted)}$$

$$2e + X \text{ -----> } X^{--}$$

$$X^{--} + X\ 2Fe^{+++}\ c \text{ -----> } 2\ Fe^{++}\ c$$

$$Fe^{++}\ c \text{ -----> mitochondria}$$

since amytal would not affect cytochrome c reoxidation. redox reaction must, therefore, be coupled to mitochond above FAD.

3. Uncouplers of Oxidative Phosphorylation: Many studies have been reported using dinitrophenol, all agre ing that acid secretion is inhibited. Other uncouplers as m-chlorocyanocarbonylphenylhydrazone, or salicylanili produce the same effect, although at much lower concentr tions (8). Again there is relative sparing of Cl^- curre Since uncouplers do not inhibit electron flow in the re system, and in fact increase it in tightly coupled mito chondria with high ATP/ADP ratios, a simple redox hypot

would at first sight seem to be untenable, i.e. (9)

$$X + AH_2 \text{ -----> } A + X^{--} + 2H^+ \ (H^+ \text{ secreted})$$

$$X^{--} + 1/2\ O_2 \text{ -----> } O^{--} + X$$

since there is no involvement of ATP.

However, O_2 consumption measurements in frog gastric mucosa do not always show the expected O_2 consumption increase. Secondly, uncouplers act as inducers of proton translocation in artificial lipid systems (10), and several groups of investigators feel that uncoupling is dependent on this capacity to increase proton conductance in membranes. A system which appears to be clearly redox dependent, the D-lactate dehydrogenase coupled transport system of E. coli vesicles, is also inhibited by uncouplers (11). The action of uncouplers can be explained by mechanisms not requiring inhibition of ATP synthesis.

4. Phosphorylative Inhibitors: Various inhibitors of this type have been studied. The classical one, oligomycin, in contrast to data published by others (12), was found to be without effect on R. pipiens O_2 consumption or secretion. Others, however, such as galegine sulfate, phenethyl biguanide and aurovertin (which acts distal to oligomycin in the chemical hypothesis) all inhibit acid secretion as well as O_2 consumption (8).

Atractylate, which inhibits ATP-ADP translocation across the mitochondrial membrane, also blocks acid secretion (8). Again in all cases studied, Cl^- current remains, in absence of acid secretion.

SUMMARY:

Table I summarizes the data discussed above. It would appear from these results that a simple redox scheme, involving only secretory membrane electron flow, requires many secondary assumptions to explain the inhibitory actions of compounds such as aurovertin or atractylate. It is more rational to draw the conclusion that ATP is required at some critical stage in the acid secretory process.

Other workers have also shown that there is a relationship of cell ATP level to acid secretion rate (13), and it should also be pointed out that the oxyntic cell is extremely rich in mitochondria, which presumably have some function in acid secretion!

B. Isolation of Secretory System

Having decided that an ATP utilizing system is prob involved in acid secretion by the gastric mucosa, we tur our attention to the HCO_3^--stimulated, SCN^--inhibited AT ase present in the mucosa. This enzyme is present in to homogenate of gastric mucosa (14), and was further local ized mainly to the microsomal fraction of this tissue (1 Additionally it was shown that an SCN^--sensitive ATPase present in other tissues such as rat liver. Thus it bec necessary to further localize this ATPase (since oxyntic cells account for only 1/3 of the mucosa), and explain i presence elsewhere.

1. Isolation of Oxyntic Cells: After trying a var of methods to produce an oxyntic cell suspension, we fou that the use of controlled pronase digestion of amphibia gastric mucosa produced cell suspensions progressively richer in oxyntic cells reaching as high as 90% (16). F 1 illustrates such a cell suspension. These cells were viable by a variety of criteria, but for the purposes of this paper we were interested in isolation of the vesicu system at the lumenal surface of the oxyntic cell (17), localizing the SCN^--inhibited ATPase in that structure.

2. ATPase Localization: First, we showed that the SCN^- inhibited ATPase was indeed enriched in the oxyntic cell fraction, along with the mitochondrial marker, succinic dehydrogenase (Fig. 2)(18). Simultaneously, we fo a dramatic increase in the sensitivity of this enzyme to HCO_3^-. We feel that SCN^- inhibition or HCO_3^- stimulatio are interchangeable properties of this enzyme. This wor extended previous observations of the ontogenetic develo ment of the ATPase to the adult mucosa (19).

The next stage was isolation and purification of th subcellular fraction containing this ATPase. This was achieved as shown in Table II and Fig. 3 by differential density gradient centrifugation of the oxyntic cell homogenates.

When this approach was extended to mammalian mucosa similar results were obtained. Thus at least part of th SCN^--inhibited HCO_3^--stimulated ATPase is located in a smooth surfaced vesicular fraction presumably derived fr the secretory surface of the oxyntic cell. This then co firms histochemical observations of others (20). Furthe work established that this HCO_3^- ATPase was distinct fro the ATPase found in association with mitochondrial enzym

markers (Figs. 4,5,6)(21). Therefore, with this technique we have been able to isolate a particle which is probably derived from the vesicles found at the luminal surface of the acid secreting cell. Associated with it, is a HCO_3^--stimulated SCN^--inhibited ATPase. 5'AMP is absent from this fraction, which is, therefore, not contaminated with plasma membrane.

C. Properties of ATPase

Further purification of this enzyme was achieved using zonal rotor purification from dog gastric mucosa (Fig. 7), followed by triton X-100 solubilization, passage over Sephadex G-200 and centrifugation through a 2-22% sucrose gradient. This is shown in the following flow sheet:

Homogenate (0.25 M sucrose)
↓
6×10^6 g min fraction
↓
B14 zonal rotor, 5 hrs, 30 K
Interface 24-34% sucrose
↓
Triton X-100 solubilization
↓
Initial peak from Sephadex G-200
↓
Sucrose gradient 2-22%, 16 hrs, 22K
(usually 2 peaks of activity)
final purification x 100

With this procedure preparations with activities as high as 300 μmoles Pi $mg^{-1}hr^{-1}$ have been obtained. Solubilization produced an ATPase which was stimulated several fold by CO_3^-, and on occasion, actually dependent on the presence of HCO_3^- for activity (Table II).

Of the various properties of this soluble ATPase perhaps the most interesting was the capacity of various oxyanions to stimulate the ATPase activity as a function of their pK. This Brønsted relationship (Fig. 8) implies that proton transfer step is involved in the activation. These arguments have been presented in detail elsewhere (22). It is the activation by base that is mainly blocked by SCN^- and other inhibitors.

An excellent correlation has also been found betw
inhibition of the ATPase and inhibition of acid secreti
(Table III).

The finding that mitochondrial ATPase is also sti
lated by HCO_3^- (23) and other oxybases such as arsenat
chromate, etc. (24) suggests that there may well be at
a mechanistic similarity between mitochondrial ATPase
the gastric vesicular ATPase.

Table IV lists some similarities and differences b
tween these two enzymes. The similarity to the mitoch
drial ATPase suggests that careful study of a tissue is
required to establish that a non-mitochondrial HCO_3^- A
is functioning in that tissue, and may explain the wide
spread distribution of this enzyme.

Another striking property of this vesicular fracti
is the capacity to undergo a conformational change in t
presence of ATP. In collaboration with Drs. L. Masotti
D. W. Urry, we have studied the effect of ATP on the C
spectrum of the suspension. Fig. 9 shows that in the
sence of ATP there is an apparent marked decrease of th
ellipticity at 224, 208 and 192 nm. Much of this alter
may be due to changes in optical artifacts. When this
corrected for at 224 nm, by the use of the equation

$$\theta_{corr} = \frac{\theta_{susp}}{Q^2_A Q_\sigma} \qquad (25)$$

the molar ellipticity θ in the absence of ATP is -0.89
and in the presence of ATP, -0.55×10^4. This shows th
probably, in addition to scattering changes, there are
formational changes produced by ATP. These effects are
reproduced by MgAMP.

D. Function of the ATPase

The localization of this enzyme, the stimulation b
HCO_3^-, correlated with the well-known requirement of C
for maximal acid rates, and the inhibition of acid secr
by inhibitors of this enzyme, all suggest that this AT
should be included in any hypothesis of acid secretion.

Two hypotheses may be considered here. One, that
ATPase is alone responsible for acid secretion as in A
Fig. 10. Here the ATPase I mechanism of Mitchell is us
(26), but modified to allow the transport of HCO_3^-.

Alternatively, a combined redox and ATP hypothesis, as in b of Fig. 9 may be suggested. O^{--}, produced from a redox reaction, combines with CO_2 forming CO_3^{--}, which is then transported away from the secretory surface by the action of the ATPase. The vectorial characteristics of this system are thus the responsibility of the ATPase system, and both hypotheses allow for the general base stimulation. In this scheme SCN^- or similar inhibitors would destroy the vectorial characteristics of the system without inhibiting the O_2 utilization in the membrane. In this regard, it has been shown that oxygenation of the secretory surface of the mucosa produces a PD transient which precedes any observable change in the mitochondrial redox components (27).

In searching for an ATPase involved in proton transport by the gastric mucosa, SCN^- has been important as an inhibitor of acid secretion, and of ATPase action. At first glance, however, the effect of SCN^- on gastric mucosa cannot be explained by inhibition of the ATPase since O_2 consumption is reduced by only 20% (28). SCN^- has other complex actions on the gastric mucosa, and on mitochondria. Thus the K^+ permeability and K^+ flux is reduced by SCN^- in both systems, and in addition SCN^- inhibits ATP binding to the mitochondrial membrane (29,30).

Again we have a similarity between the properties of the gastric mucosa, and the properties of the mitochondrial membrane system, as explained in Table IV.

To account for the lack of effect of SCN^- a combined ATPase and redox hypothesis may be necessary. SCN^-, by inhibiting the ATPase would not reduce O_2 consumption at the secretory site, but no driving force would be available for removal of OH^- or O^{--}. Recombination of protons with these would occur, and H^+ secretion would stop.

Another aspect of gastric secretion which is not explained by the ATPase hypothesis is the requirement for K^+ (31) for acid secretion. However, K^+/H^+ exchange occurs in mitochondria and in yeast. Perhaps as H^+ secretion by the gastric vesicles is examined, a K^+ requirement will be uncovered in this subcellular system.

SUMMARY:

A vesicular system has been isolated in relatively pure form from gastric mucosa. An ATPase stimulated by a variety of anions has been isolated from this vesicular

system, and shown to have properties quite similar to t
of mitochondrial ATPase. Conformational changes can be
detected in this system which may relate to the changes
that occur with onset of secretion by the stomach in th
cell canaliculi. Considering the evidence as a whole, t
possible mechanisms are suggested for the involvement o
ATPase in acid secretion.

The work reported in this paper was supported in p
by Public Health Service, National Institutes of Health
Grants TIAM05286 and AM08541, and by National Science
Foundation Grant GB25364.

1. Sa
Ph
2. To
3. Mi
4. Sa
(1
5. Re
6. Er
Ce
7. Ki
8. Sa
Hi
16
9. Co
TH
10. CH
ch
11. Ba
24
12. Ba
13. Fo
Bi
14. Ka
Bi
15. Sa
Pr
16. Bl
F.
er
17. He
18. Wi
G.
ph
19. Fo
J.
20. Ko
Cy
21. Sa
Su
22. Bl
Su
Bi

References

1. Sachs, G. and Hirschowitz, B. I. (1965). Amer. J. Physiol. 209:461.
2. Tower, D. B. (1958). J. Neurochem. 3:185.
3. Michelangeli, F. and Durbin, R. P. This volume.
4. Sachs, G., Shoemaker, R. L. and Hirschowitz, B. I. (1967). Biochim. Biophys. Acta 143:522.
5. Rehm, W. S. and Sachs, G. Unpublished observations.
6. Eraster, L., Low, H. and Lindberg, O. (1955). Exp. Cell Res. 3:124.
7. Kidder, G. W. (1971). Amer. J. Physiol. 221:421.
8. Sachs, G., Collier, R. H., Shoemaker, R. L. and Hirschowitz, B. I. (1968). Biochim. Biophys. Acta 162:210.
9. Conway, E. J. (1953). Biochemistry of Acid Secretion, Thomas, Springfield, Ill.
10. Chappell, J. B. and Haarhoff, K. N. (1967). In Biochemistry of Mitochondria, Academic Press, New York.
11. Barnes, E. H. and Kaback, H. R. (1971). J. Biol. Chem. 246:5519.
12. Bannister, W. H. (1965). J. Physiol. 177:440.
13. Forte, J. G., Adams, P. H. and Davies, R. E. (1965). Biochim. Biophys. Acta 104:25.
14. Kasbekar, D. K. and Durbin, R. P. (1965). Biochim. Biophys. Acta 105:478.
15. Sachs, G., Mitch, W. E. and Hirschowitz, B. I. (1965). Proc. Soc. Exptl. Biol. 119:1023.
16. Blum, A. L., Shah, G. T., Wiebelhaus, V. D., Brennan, F., Helander, H. F. and Sachs, G. (1971). Gastroenterology 61:189.
17. Helander, H. F. (1962). J. Ultra. Res., Suppl. 4:1.
18. Wiebelhaus, V. D., Sung, C. P., Helander, H. F., Shah, G., Blum, A. L. and Sachs, G. (1971). Biochim. Biophys. Acta 241:49.
19. Forte, G. M., Limlomwongse, L. and Forte, J. G. (1969). J. Cell Sci. 4:709.
20. Koenig, C. S. and Vial, J. D. C. (1970). J. Histochem. Cytochem. 18:340.
21. Sachs, G., Shah, G., Strych, A. and Hirschowitz, B. I. Submitted to Biochim. Biophys. Acta.
22. Blum, A. L., Shah, G., St. Pierre, T., Helander, H. F., Sung, C. P., Wiebelhaus, V. D. and Sachs, G. (1971). Biochim. Biophys. Acta 249:101.

23. Racker, E. (1962). Fed. Proc. 21:54A.
24. Mitchell, P. and Moyle, J. (1971). Bioenergetics
25. Urry, D. W. Biochim. Biophys. Acta, Res. Biol. Me
In press.
26. Mitchell, P. (1970). In Membranes and Ion Transp
Wiley, New York.
27. Rehm, W. S., Sanders, S. and Sachs, G. (1966). Pr
Int. Cong. Biophys., Vienna.
28. Moody, F. G. (1971). Amer. J. Physiol. 220:467.
29. Sachs, G., Collier, R. H., Pacifico, A., Shoemaker
R. L., Zweig, R. A. and Hirschowitz, B. I. (1969).
Biochim. Biophys. Acta 173:509.
30. Sachs, G., Collier, R. H. and Hirschowitz, B. I. (
Proc. Soc. Exptl. Biol. 133:456.
31. Harris, J. B. and Edelman, I. S. (1959). Amer. J.
Physiol. 196:1266.

TABLE I

COMPOUNDS TESTED IN GASTRIC MUCOSA

Given are minimal effective concentrations (mM) at 15 min following addition. (-) no effect.

Substrate level inhibition	Redox inhibitors	Redox acceptors	Phosphorylative uncouplers	Phosphorylative inhibitors
Malonate (-) Oxamate (-) 2 Deoxyglucose (10)	Amytal (2) Rotenone (-) Antimycin A (0.05) Thenoyl trifluoro-acetophenone (0.1) Azide (1) Cyanide (1)	Phenazine metho-sulfate Methylene blue Tetramethyl-*p*-phenylene diamine Ferricyanide (ineffective in supporting anoxia secretion)	Dinitrophenol (0.05) Pentachlorophenol (0.03) Arsenate (2) *m*-Chlorocyanocarbonyl phenyl hydrazone (0.001) 1,1,3-Tricyano-2-amino-1-propene (0.01)	Oligomycin (-) Rutamycin (-) Aurovertin* Atractyloside (0.01) Galegine sulfate (1) Phenethyl biguanide (0.1)

TABLE II

DISTRIBUTION AND SOLUBILIZATION OF ATPase

	μmoles Pi mg^{-1} hr^{-1}	
	Mg^{++}	Mg^{++} HCO_3^-
Total homogenate	6.7	7.2
6 x 10^6 g min fraction	17.2	25.4
1.12 sucrose band	18.5	29.9
Solubilized enzyme	13.2	44.6

TABLE III

INHIBITORS OF ATPase AND EFFECT ON H^+ SECRETION

Compound (10 mM)	% ATPase Inhibition	% Secretory Inhibition
SCN^-	75	100
CNO^-	88	100
N_3^-	63	90
NO_2^-	70	70
NH_2NH_2	60	50

TABLE IV

COMPARISON OF

SOLUBLE GASTRIC AND MITOCHONDRIAL ATPase

Gastric	Mitochondrial
1.12 sucrose density	1.18 sucrose density
DNP no effect	DNP stimulates
HCO_3^- activates 3-5x	HCO_3^- activates < 2x
AsO_3^-, AsO_4^{3-} activates	Both activate
BO_3^- activates	BO_3^- inhibits
SCN^-, CNO^- inhibit	SCN^-, CNO^- inhibit
Cold stable	Cold labile
N_3^- inhibits	N_3^- inhibits
Activation inhibited by ionic strength	?
SCN blocks K^+ flux	SCN blocks K^+ flux

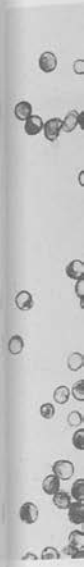

Fig. la
gastri
dark s

ig. 1b
tainin

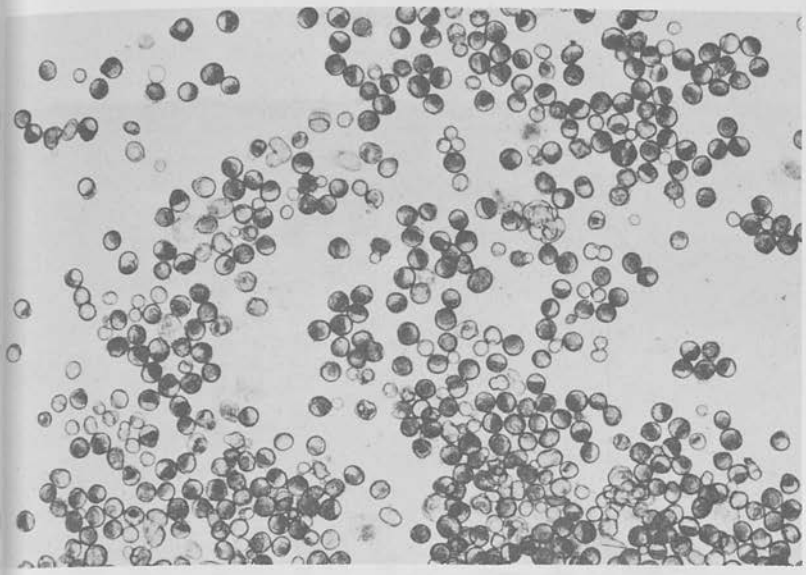

Fig. 1a: Micrograph of isolated cell suspension of Necturus gastric cells containing mostly oxyntic cells which are dark staining.

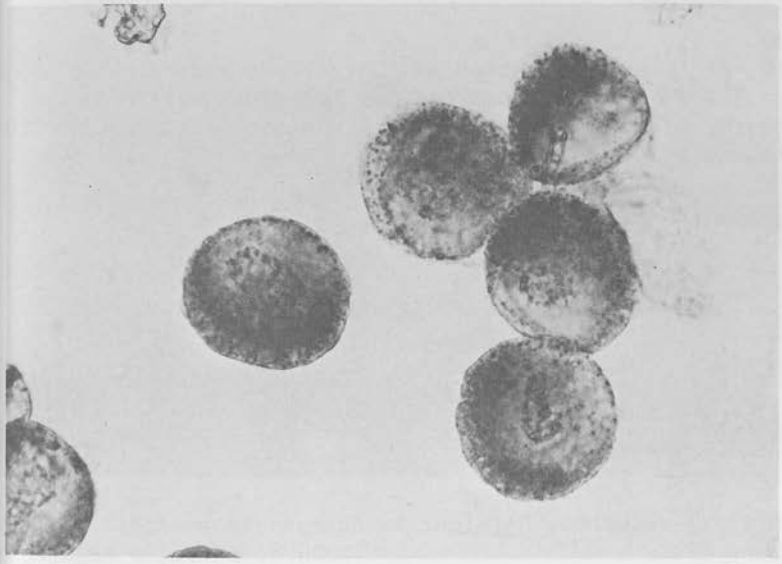

ig. 1b: Enlarged view of above, showing the stippling due to taining for SDH.

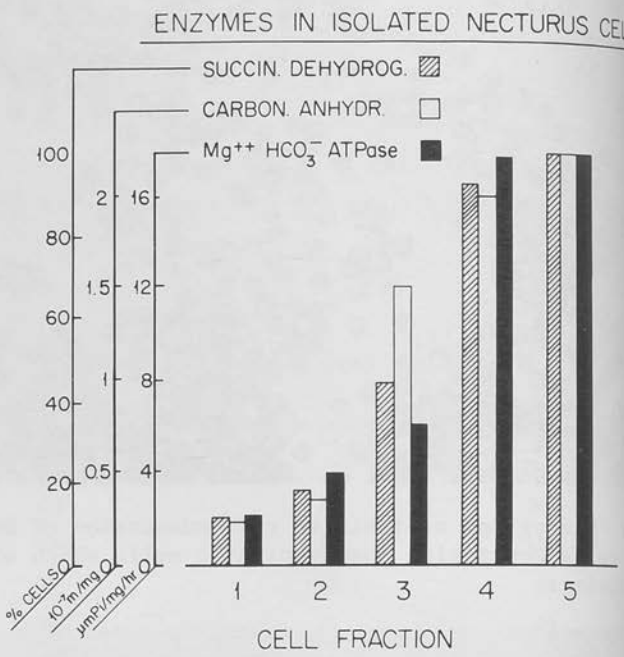

Fig. 2: The distribution of SDH, ATPase and carbonic a
in cell suspensions derived from Necturus gastric mucos
showing increasing activity of these enzymes in the fra
rich in acid secreting cells.

Fig. 3
of oxy

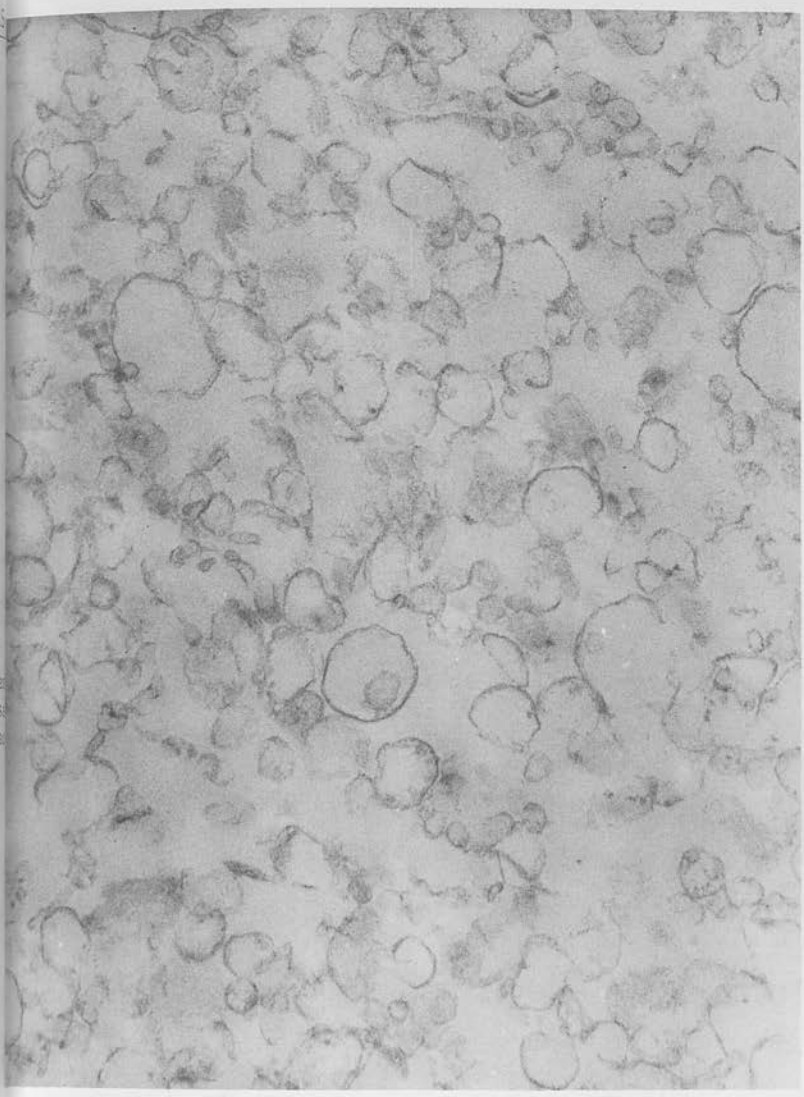

Fig. 3: Electron micrograph of isolated vesicular fraction of oxyntic cell. x 56,000.

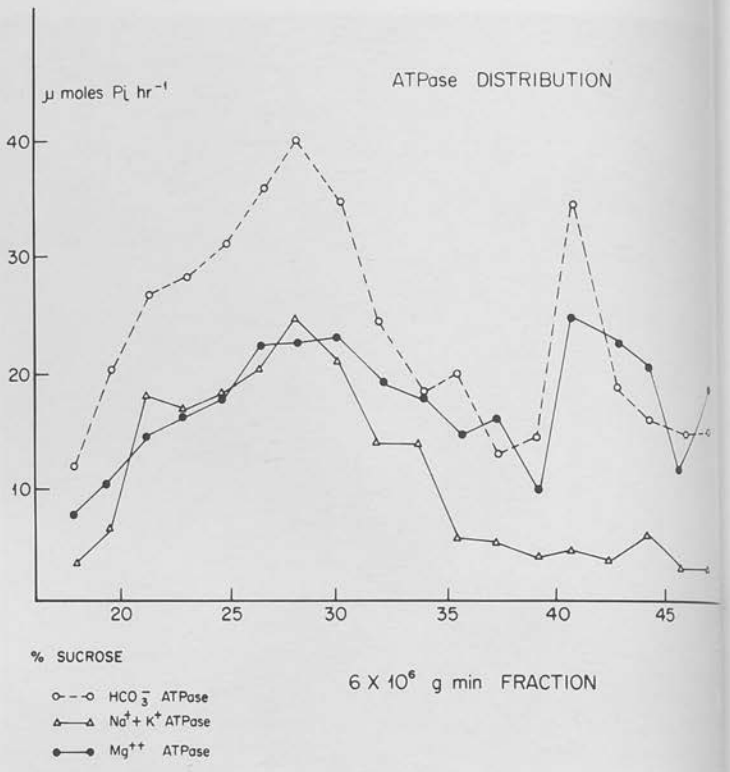

Fig. 4: Density gradient distribution of the 6 x 10^6 g min fraction (microsomal fraction) of HCO_3^-, $Na^+ + K^+$ and Mg^{++} ATPase (16 hrs, SW25 rotor, 22,000 rpm).

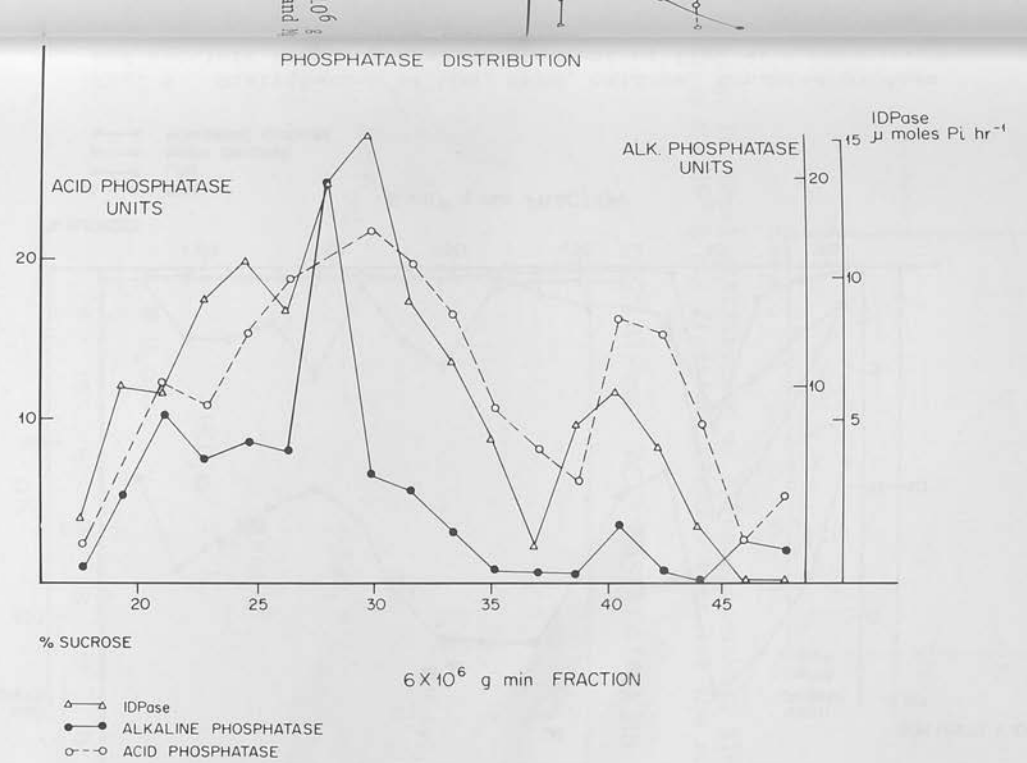

Fig. 5: Distribution of IDPase and acid and alkaline phosphatase in the gradient of Fig. 4.

Fig.
from

Fig. 8:
for dog
log k_{ca}

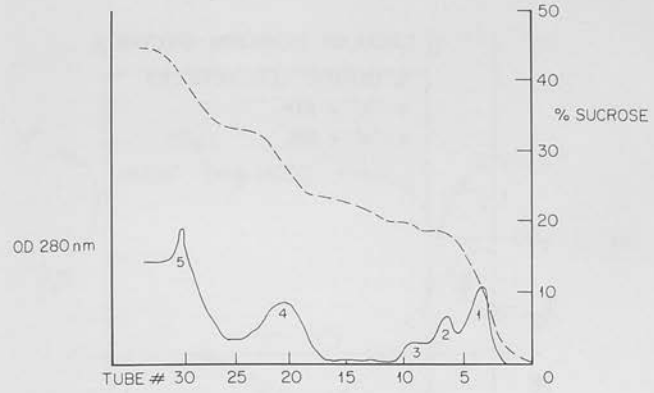

Fig. 7: Zonal distribution of ATPase in Beckman B14 rotor from 6 x 10^6 g min fraction. Peak 4 contains the activity.

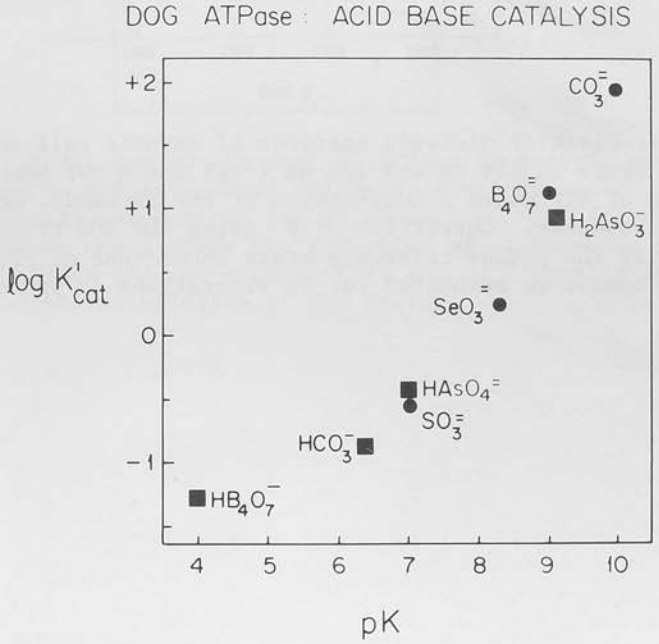

Fig. 8: Plot of log k'_{cat} vs pK of different activating bases for dog gastric ATPase showing a Brønsted relationship log $k_{cat} = \alpha + \beta(pK)$.

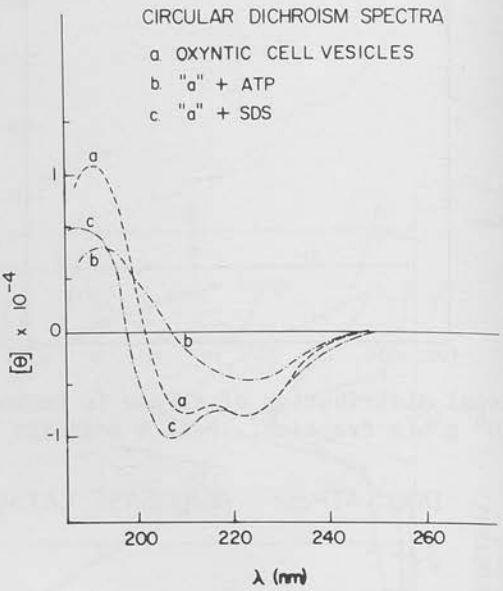

Fig. 9: Circular dichroic spectrum of oxyntic cell vesi showing peaks at 224 nm and 208 nm (-ve) and a +ve peak a Addition of ATP shows a suppression of the CD bands, and of the crossover. Correction of Θ using the SDS treated pension as the pseudo reference state shows that at 224 n changes cannot be accounted for by alterations in optical facts.

Fig. 1
(a) Sh
is ult
redox-
and th
vecto

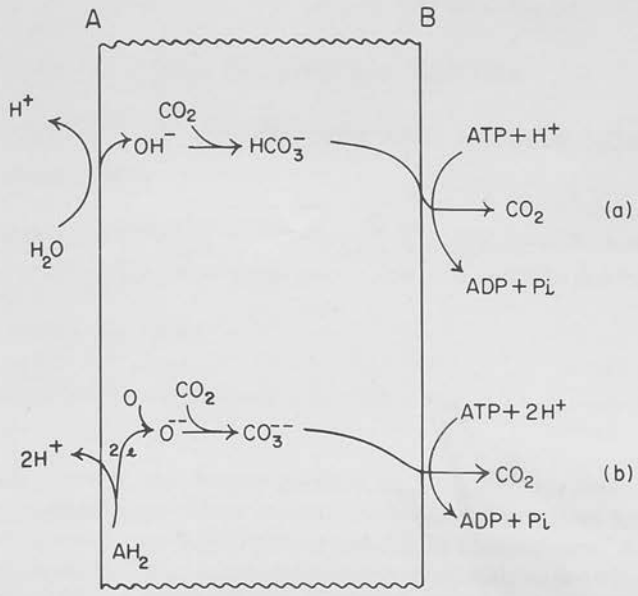

Fig. 10: Model for involvement of ATPase in gastric secretion. (a) Shows an ATPase such as ATPase I, where transport of HCO_3^- is ultimately responsible for H^+ secretion. (b) A combined redox-ATPase model where the reduction of O_2 provides proton, and the ATPase induced transport of the O_2^{--} results in the vectorial characteristics of the system.

Reprinted from

Biochimica et Biophysica Acta, 311 (1973) 545–564

BBA 76369

PROPERTIES OF ATPase OF GASTRIC MUCOSA

V. PREPARATION OF MEMBRANES AND MITOCHONDRIA BY ZONAL CENTRIFUGATION

J. G. SPENNEY[a], A. STRYCH[a], A. H. PRICE[a], H. F. HELANDER[b] and G. SACHS[a,*]

[a] *University of Alabama in Birmingham, Birmingham, Ala. (U.S.A.) and* [b] *University of Umeå, Umeå (Sweden)*

(Received February 9th, 1973)

SUMMARY

Using zonal sucrose density gradient centrifugation methods to fractionate the subcellular components in gastric mucosal homogenates have been developed. Methods are described which give high yield or rapidity in fractionation. A procedure is described which enables large-scale preparations of smooth walled vesicular membranes containing HCO_3^--ATPase activity free from mitochondrial contamination as assessed by electron microscopic morphology and undetectable succinic dehydrogenase or monoamine oxidase activity. A method to purify gastric mitochondria is also described.

An HCO_3^--stimulated ATPase present in gastric mucosal homogenates has been implicated in proton transport by this epithelium[1,2]. The complexity of this tissue and the resulting homogenate necessitated isolation of the oxyntic (acid secreting) cells to confirm localization of HCO_3^--ATPase to these cells[3]. Further, the enzyme was localized in the oxyntic cell microsomes by differential centrifugation[3]. By sucrose density gradient centrifugation a fraction appearing as smooth walled vesicular membranes was also isolated from dog gastric mucosa[4]. These membranes contained no detectable glucose-6-phosphatase, succinic dehydrogenase, or monoamine oxidase activity[5]. A similar enzyme can be found in pancreas[6].

Further biochemical characterization necessitated large scale preparation in zonal rotors. This report describes preparative techniques utilizing zonal sucrose density gradient centrifugation to provide either rapid separation, high total yield, or high purity separation of gastric vesicular membranes or mitochondria. Our major concern has been with high purity separation of these particles.

METHODS

The stomach is removed from a fasted dog and immediately opened along the greater curvature, washed with water, and cooled in ice. After 3–5 min any remaining

* To whom correspondence should be sent.

esophagus and antrum is cut away. The stomach is layed flat on a cooled pyrex and with a microscope slide the mucosa is scraped as a sheet from the underl muscular layer. The mucosa, suspended in 700 ml of buffer, is chopped into s fragments in a Waring blender with a dulled blade at medium speed. In a "bomb" it is allowed to equilibrate with magnetic stirring for 20 min under lb/inch^2 nitrogen. The mucosal fragments are disrupted on decompression. A 10 min standing at 0 °C the floating mucus layer is aspirated and discarded. remaining homogenate is filtered through 4 layers of cheese cloth and subjected differential and/or zonal sucrose density gradient centrifugation.

The buffer used in each instance is 40 mM Tris–HCl, pH 7.4, with suc In methods designed for intact mitochondria 0.44 M sucrose is used while 0.2 sucrose is used when gastric membranes are prepared. The addition of 3 mM Mg or EDTA or 1 mM dithiothreitol seemed to have no effect either on the level activity obtained or on the separations achieved, hence were omitted at later st

(1) Fractionation of the tissue by centrifugation

To ascertain the best methods of preparation of subcellular componen gastric mucosa we have studied zonal sucrose density fractionation of the total ho genate and at various stages of purification using differential centrifugation.

(A) Differential centrifugation (Fig. 1). The total homogenate in 40 mM T HCl–0.25 M sucrose is centrifuged at $1000 \times g$ for 30 min in a Sorvall RC-2 trifuge. The pellet is washed once with the same buffer and the washing and ori supernate are combined. This suspension is centrifuged at $8000 \times g$ for 30 min the pellet washed once. Washing and supernate are sedimented at $20000 \times g$ 30 min. The pellet is washed once and the supernate and washing are centrifug

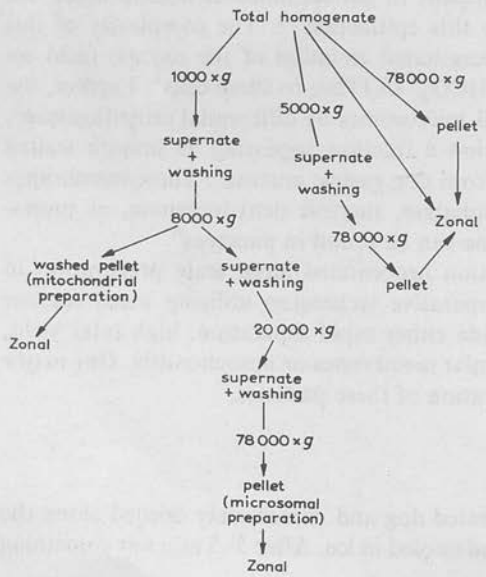

Fig. 1. Preparative steps in purification of material prior to zonal density gradient centrifug

78000×g* for 60 min in a No. 30 rotor in a Beckman L-2 preparative ultracentrifuge. The final 78000×g pellet is not washed. In preparations of gastric mitochondria 0.44 M sucrose is substituted for the 0.25 M sucrose.

(*B*) *Zonal centrifugation.* Three types of runs have been used: (1) Step gradients using 20, 24, 34, and 47% sucrose; (2) rate zonal centrifugation utilizing a 5–35% linear gradient; and (3) isopycnic density gradient centrifugation using 20–45 or 50% linear sucrose gradient.

Fractionation of the total homogenate presents a special problem since the volume of the sample approaches the volume of the rotor. When fractionating the total homogenate on a sucrose density gradient it is divided and dry sucrose added to raise the sucrose content to 20% and 50%, respectively, and the total volume of each to 325 ml. Total homogenate volume and volume to be raised to 20% sucrose (w/w) and 50% sucrose (w/w) can be estimated with sufficient accuracy that material is not wasted by the following formula:

$$V_I = V_F \cdot \frac{(1-S_F)}{(1-S_I)}$$

where V_I, starting volume; V_F, volume of homogenate to be used in forming gradient (usually 300–325 ml); D_F, density of final solution assuming it is a sucrose and water (w/w) solution; D_I, density of starting solution with same assumption; S_F, final desired % sucrose (w/w); S_I, % sucrose (w/w) of starting solution.

The sucrose to be added is estimated from:

$$V_F \cdot D_F - V_I \cdot D_I$$

The sucrose is dissolved by magnetic stirring in an ice water bath. After dissolution accuracy is checked on an Abbe refractometer. For zonal fractionation of all other material the gradient is formed from sucrose of the desired concentration dissolved in 40 mM Tris–HCl, pH 7.4.

(*C*) *Formation of the gradient.* Gradients are formed in a Beckman Ti-14 zonal rotor spinning at 3000 rev./min in a Beckman L-2 ultracentrifuge.

(1) Step gradients are formed using 100 ml 20% sucrose, 200 ml 24% sucrose, 150 ml 34% sucrose and 150 ml 47% sucrose. The solutions are sequentially pumped into the zonal rotor beginning with the 20% sucrose. The sample is added last, usually at the center of the rotor.

(2) Continuous gradients are formed from 5 and 35% sucrose or from 20 and 45 or 50% sucrose using a Beckman gradient maker calibrated to deliver a 600 ml gradient which is linear with volume delivered from the pump.

(*D*) *Preparation of the sample.* Preparation of the total homogenate is given above. All other samples are obtained in pellet form during centrifugation. The pellet may be prepared for injection at the periphery of the rotor by suspending it in the most dense sucrose solution. When the sample is injected into the center of the rotor it is suspended in 0.25 M sucrose for isopycnic runs and in 5% sucrose for rate zonal centrifugation. We most commonly use central injection. We examined the efficacy of injection into the center of the gradient. In this instance 200–350 ml of the gradient is allowed to form. The pump is stopped and 10–20 ml of gradient is pumped from

* g value at R_{max} = 105500.

the side arm of the delivery tube. The pellet is resuspended in this solution and injected into the rotor *via* the side arm of the delivery tube. The remainder of gradient is then formed.

(*E*) *Zonal fractionation.* After loading, the rotor is closed and brought 47000 rev./min. For rate zonal and step gradient separations the run is termin after 30 min and 2–3 h, respectively. Isopycnic centrifugation, our usual prac is allowed to continue for 6–8 h. The gradient is unloaded at 3000 rev./min by cen displacement by 60% sucrose pumped into the periphery of the rotor. 33 20 fractions are collected for assays and further biochemical characterization.

(*2*) *Assays*

Sucrose concentration was measured with an Abbe refractometer. Mg^{2+} HCO_3^--ATPase and 5′-nucleotidase were measured as previously described[5]. S cinate dehydrogenase activity was measured by the method of King and How and monoamine oxidase according to the method of Tabor *et al.*[8]. Lactate dehyd genase was measured as described by Reeves and Fimognari[9].

(*3*) *Electron microscopy*

A 1–3 ml portion of one of the fractions is diluted to 8.6% sucrose with 40 m Tris–HCl, pH 7.4, placed in centrifuge tubes in which a flat agar cushion had b formed. The material is centrifuged at 39000 rev./min in a Beckman SW-39 ro for 60 min. Supernate is decanted and buffered 1% osmium tetroxide is layered the agar base for 12 h. The material is subsequently dehydrated, embedded Vestopal W. Thin sections contrasted with lead hydroxide and uranyl acetate, w studied in a Phillips EM 200 and EM 300 electron microscope at 80 kV.

RESULTS

The total homogenate was fractionated in two ways. Firstly (Fig. 2) the gradi was actually formed from the total homogenate as described above. By this techni protein distribution on the gradient is a reflection of the soluble protein concentrat as well as the very heavy components which usually sediment out at low *g* force differential centrifugation. The Mg^{2+}-ATPase activity is a low broad plateau fr 23% sucrose to 46% sucrose while the HCO_3^--ATPase is clearly bimodal in dis bution. The upper peak is not associated with a discernible protein peak. Even w the large protein load the lower HCO_3^--ATPase closely reflects that of protein succinic dehydrogenase. Table I gives the relative enrichment of these peaks.

To avert the soluble protein accompanying the total homogenate, the t homogenate in a volume of 325 ml was layered on a linear 20–50% sucrose gradi in the other 325 ml of the rotor. Protein, Mg^{2+}-ATPase and HCO_3^--ATPase dis bution were bimodal. The lower peak of Mg^{2+}- and HCO_3^--ATPase coincided w the lower protein peak. The upper peak of Mg^{2+}- and HCO_3^--ATPase at 31% sucr was not associated with a clear cut peak of protein. The peaks of Mg^{2+}- and HCO ATPase activity are very close and undoubtedly overlap considerably.

We further examined fractionation of all particulates in the total homoge by collecting the $78000 \times g$ for 60 min sediment of the total homogenate. This p was fractionated on a 20–50% linear sucrose gradient, Fig. 3. The protein is di

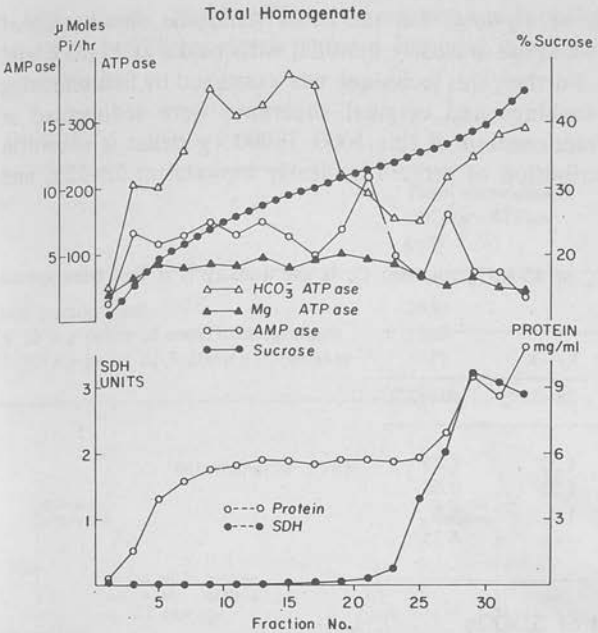

Fig. 2. Fractionation of protein and enzymes obtained from the total homogenate on a 20–45% linear sucrose gradient. SDH, succinate dehydrogenase.

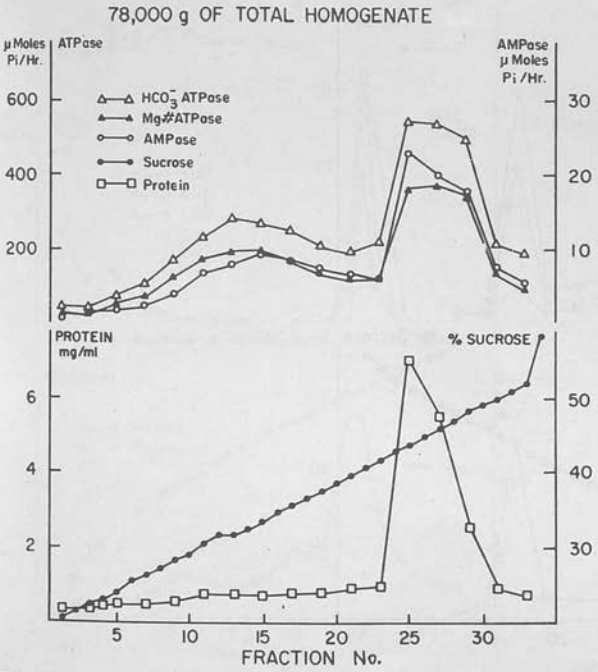

Fig. 3. Fractionation of the 78000 × *g* pellet from the total homogenate. A 20–50% sucrose gradient is used.

buted largely as a collection at 41–48%. On the other hand the distribution
AMPase, Mg^{2+}- and HCO_3^--ATPase is clearly bimodal with peaks at 29–33% a
43–48% sucrose, respectively. Further, this technique was examined by first removi
the $5000 \times g$ sediment. Its washings and original supernate were sedimented
$78000 \times g$ for 60 min. The fractionation of this $5000–78000 \times g$ pellet is shown
Fig. 4. By this technique distribution of protein is clearly bimodal at 28–32% a

TABLE I

C is the peak activity at 28–32% or 40–45% sucrose. C_0 is the activity if it had been spre
evenly over the entire gradient.

	C/C_0	
	28–32%	*40–45%*
HCO_3^--ATPase	1.52	1.23
Mg^{2+}-ATPase	1.35	0.68
AMPase	1.3	1.5
Succinate dehydrogenase	—	4.25

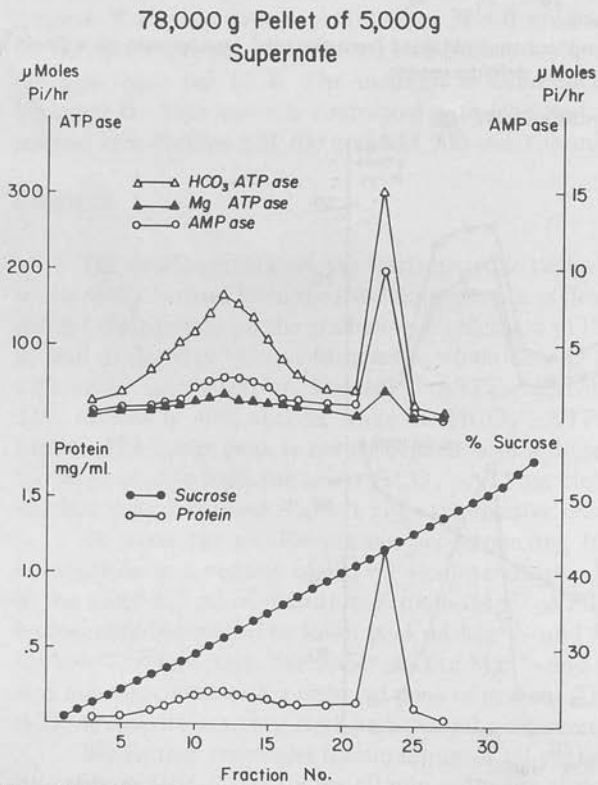

Fig. 4. Fractionation of the $78000 \times g$ pellet from the post $5000 \times g$ supernate. A 20–50% line
sucrose gradient is used.

41–45% sucrose. Mg^{2+}-ATPase shows two small peaks of activity while AMPase and HCO_3^--ATPase clearly show a bimodal distribution corresponding with the protein peaks.

TABLE II

	Total membrane HCO_3^--ATPase ($\mu M\ P_i/h$)
Total homogenate	3050
$7.8 \cdot 10^4 \times g$ pellet of total homogenates	1560
$7.8 \cdot 10^4 \times g$ pellet of $5 \cdot 10^3 \times g$ supernate	919

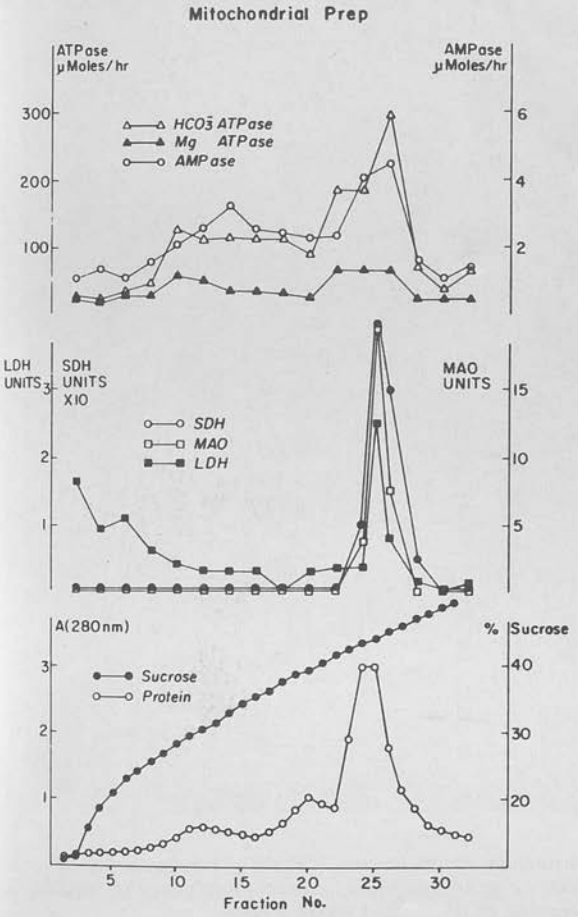

Fig. 5. Fractionation of the washed $8000 \times g$ pellet on a 20–50% linear sucrose gradient. MAO, monoamine oxidase; SDH, succinate dehydrogenase; LDH, lactate dehydrogenase.

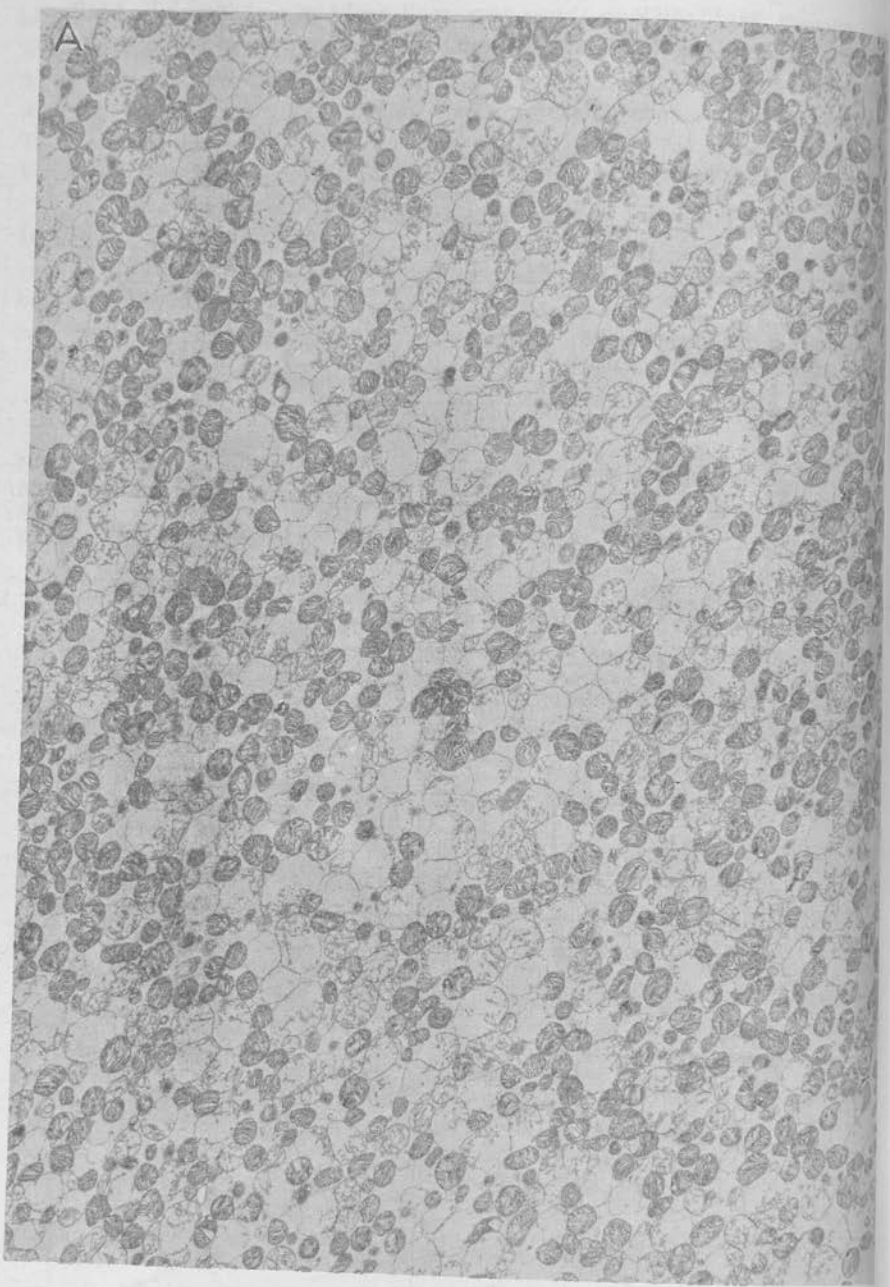

Fig. 6. (A) Electron microscopic morphology (magnification $\times 3100$) of the fraction at 41–45% sucrose obtained from the washed $8000 \times g$ pellet. (B) Mitochondrial morphology (magnification $\times 31000$) from the 41–45% sucrose fraction of the washed $8000 \times g$ pellet.

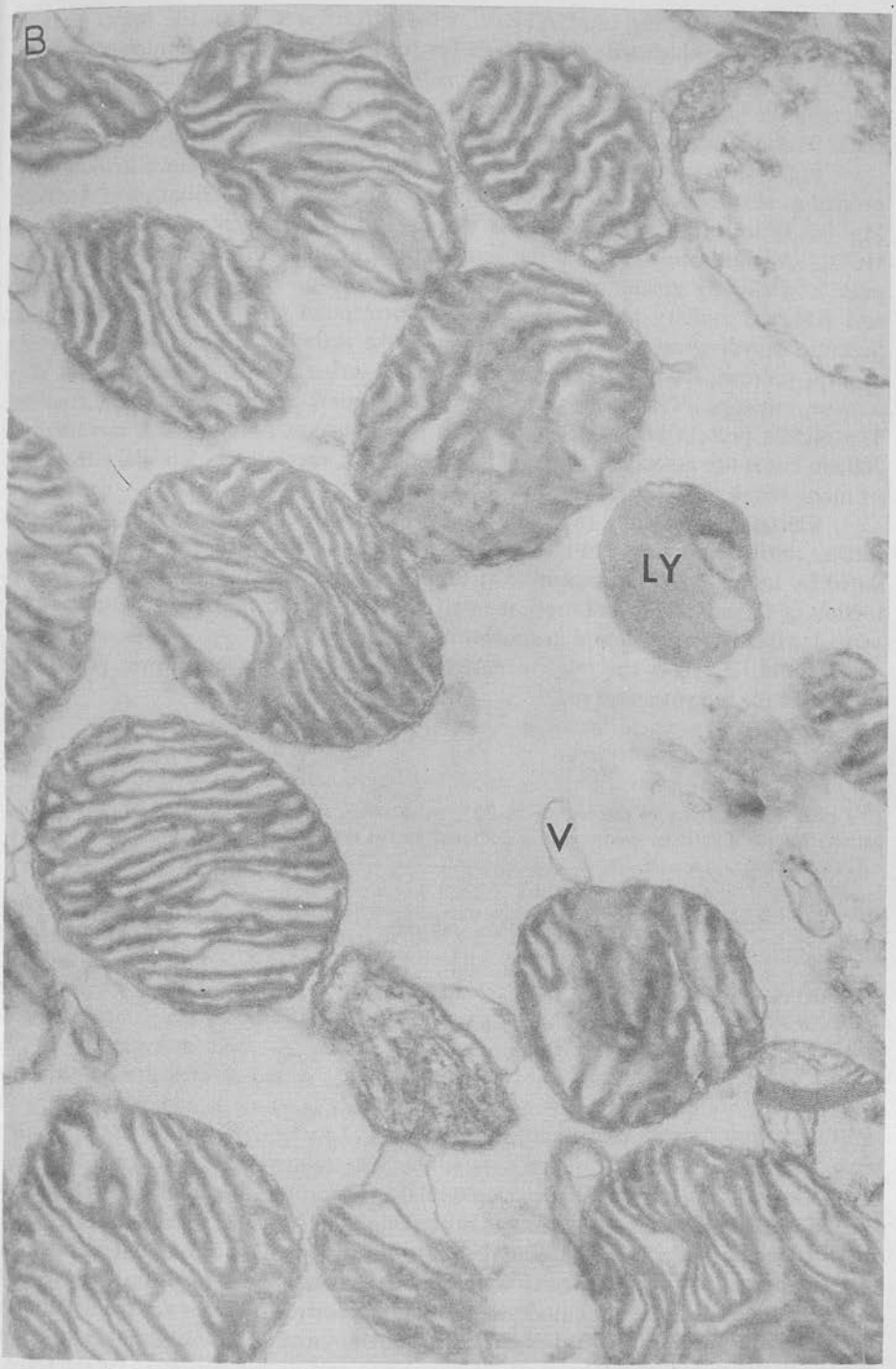
B
LY
V

Table II gives the total ATPase activity recovered from the upper peak HCO_3^--ATPase which would be usable for further biochemical characterization.

To further examine the losses of ATPase activity during differential centrifugation, we have subjected the washed $8000 \times g$ pellet of the $1000 \times g$ supernate zonal fractionation.

Fig. 5 shows the analysis of a representative gradient. Protein distribution pressed as absorbance at 280 nm is clearly trimodal while the distribution of AMP Mg^{2+}-ATPase, and HCO_3^--ATPase is bimodal. The upper peak of Mg^{2+}- HCO_3^--ATPase coincides with the protein peak at 30% sucrose while the AMP peak is at slightly greater sucrose concentration, 33%. The lower peak of ATP and AMPase activity at 42–45% sucrose correspond to the third protein pe Succinic dehydrogenase and monoamine oxidase activity are uni-modal with pe at 44% sucrose. Lactate dehydrogenase on the other hand has one peak at 4 sucrose, but appears to have a second peak at the point of application to the gradi The middle protein peak at 39% sucrose is a constant finding when measured 280 nm but is not associated with ATPase, AMPase, succinic or lactic dehydroge or monoamine oxidase activity.

Electron microscopy (Fig. 6) of the peak at 41–45% sucrose was obtained further clarify the presence of the HCO_3^--ATPase and AMPase. The picture is do nated by intact gastric mitochondria; some, however, are burst or have some d tortion of the cristae. In addition, a small number of lysosomes and smooth wal vesicular membrane structure are seen.

Table III shows the relative enrichment of the upper and lower peaks w respect to the enzymes assayed.

TABLE III

C is peak total activity in the region 28–32% or 40–44% sucrose. C_0 is the hypothetical to activity/sample if activity were evenly distributed on the gradient.

	C/C_0	
	28–32%	*40–44%*
Mg^{2+}-ATPase	1.6	2.0
HCO_3^--ATPase	1.2	2.8
AMPase	1.5	2.1
Succinate dehydrogenase	—	5.0
Monoamine oxidase	—	7.7

Lastly, fractionation of the microsomal preparation, the $78000 \times g$ pellet fro the $20000 \times g$ supernate, was assessed. In the example (Fig. 7) the sample was inject into the center of the rotor but in other runs the sample was injected at about 30 in the gradient. By this preparative technique a protein peak (280 nm absorban at 28–31% sucrose is about equal to a peak at the periphery of the rotor. In additio a peak usually appears at 36–39% sucrose. HCO_3^-- and Mg^{2+}-ATPase distributio is trimodal with major peaks at 28–31% sucrose and at the periphery of the roto

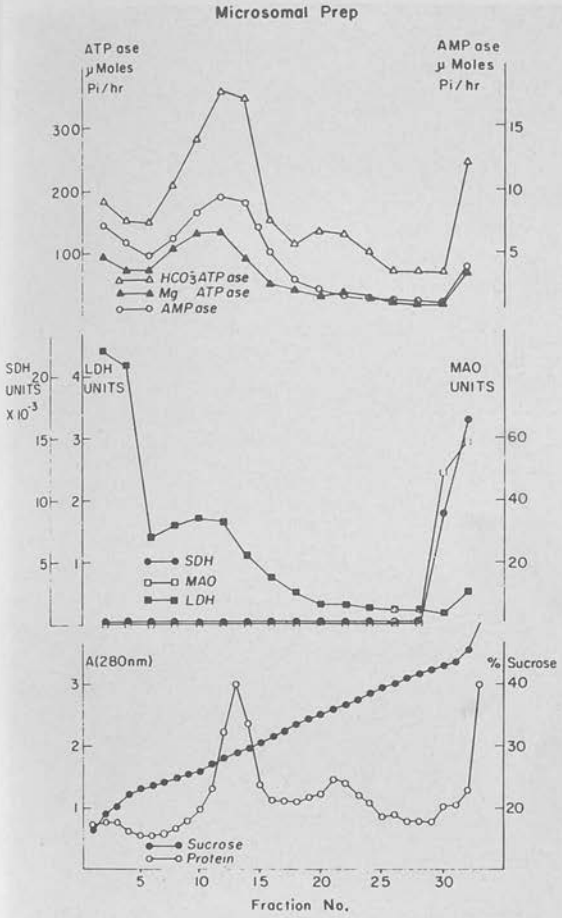

Fig. 7. Fractionation of the microsomal fraction on a 20–45% sucrose gradient. MAO, monoamine oxidase; LDH, lactate dehydrogenase; SDH, succinate dehydrogenase.

A small tertiary peak occurs at 35–38% sucrose. AMPase activity is bimodal coinciding with the two major ATPase peaks. Succinic dehydrogenase and monoamine oxidase are undetectable below 41.5% and peak at the periphery of the rotor. Lactic dehydrogenase is most active at the site of sample application, but a peak coincides with the lighter density HCO_3^--ATPase and a lesser peak at the periphery of the rotor.

Table IV shows the enrichment of the two major protein peaks with respect to these enzymes.

Electron microscopic morphology of the material recovered at 28–32% sucrose is shown (Fig. 8). In five experiments the fractions at 28–32% sucrose displayed smooth surfaced vesicular membrane structures of very high purity.

We further examined the feasibility of performing fractionation of this fraction on step gradients and by rate zonal centrifugation to achieve more rapid separation of particles. Fig. 9 shows fractionation achieved by rate zonal fractionation. There

ATPase

Fig.
sucr
bran
sucr

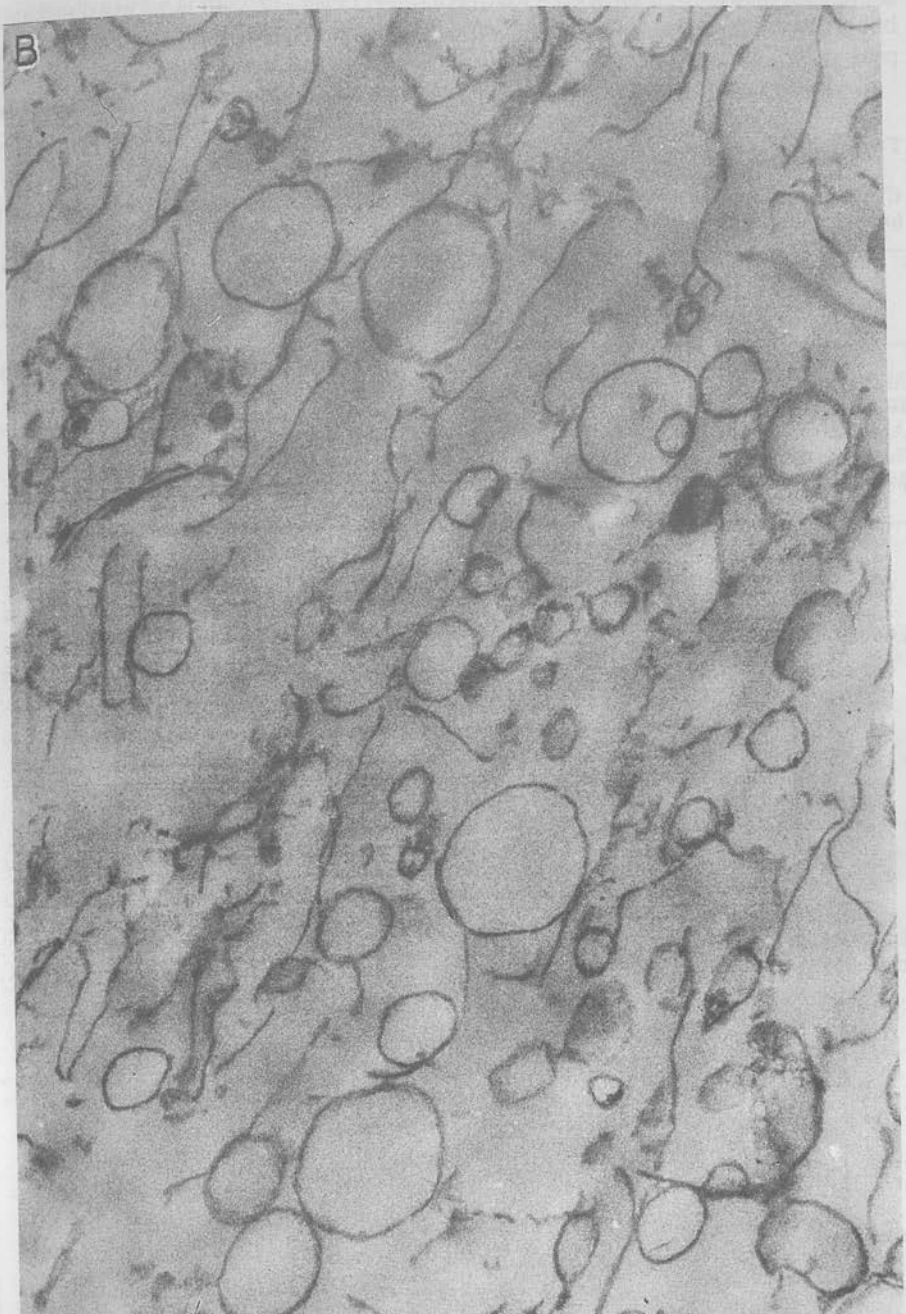

Fig. 8. (A) Electron microscopic morphology (magnification ×3100) of the material at 28–32% sucrose obtained from fractionation of the microsomal fraction. (B) Morphology of the membrane structures (magnification ×31000) isolated from the microsomal preparation at 28–32% sucrose on linear gradients.

is bimodal distribution of Mg^{2+}- and HCO_3^--ATPase. Protein is widely distribu but greatest near entry into the gradients. Mg^{2+}- and HCO_3^--ATPase and AMP peak at 10% sucrose and again at 24–26%; the activity is, however, widely distribu

Step gradient fractionation of the gastric mucosa has been investigated. Fig

TABLE IV

C is the peak total activity in the region 28–32% or 40–44% sucrose. C_0 is the hypothe total activity/sample if activity were evenly distributed on the gradient.

	C/C_0	
	28–32%	*40–44%*
Mg^{2+}-ATPase	2.2	1.1
HCO_3^--ATPase	2.1	1.4
AMPase	2.2	0.9
Succinate dehydrogenase	—	8.5
Monoamine oxidase	—	11.0

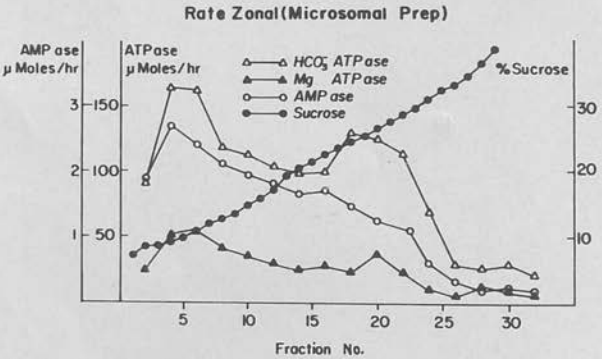

Fig. 9. Fractionation of the microsomal pellet by rate zonal centrifugation on 10–35% sucro gradient.

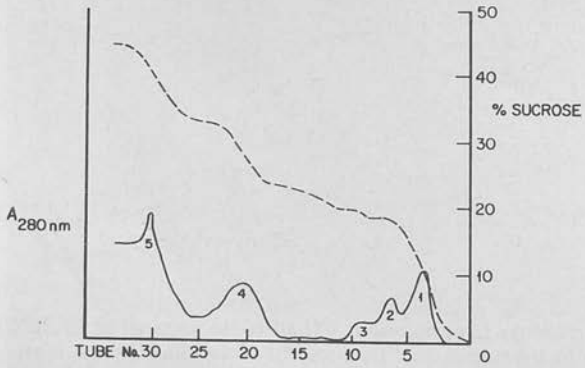

Fig. 10. Fractionation of the microsomal pellet on a sucrose step gradient.

shows the protein fractionation and Table V the ATPase activities obtained in these protein peaks. Protein is accumulated at each step in the gradient, and HCO_3^--ATPase preferentially in the fourth protein peak at about 28% sucrose. Succinic dehydrogenase and monoamine oxidase activity were not assessed in either the rate zonal or the step gradient.

On many linear sucrose gradients of the microsomal fraction there appeared to be a separation of one or two tubes between the peak HCO_3^--ATPase and AMPase activities. Gradients consisting of 7.5% Ficoll–0.25 M sucrose to 0% Ficoll–37.5% sucrose were utilized to separate the ATPase and AMPase activities. Fig. 11 shows

TABLE V

ACTIVITY OF BANDS FROM ZONAL ROTOR

Band	*HCO_3^--ATPase specific activity (μmoles $P_i \cdot mg^{-1}$)*
Total homogenate	3.20
1	0.25
2	3.73
3	4.50
4	26.55
5	11.91

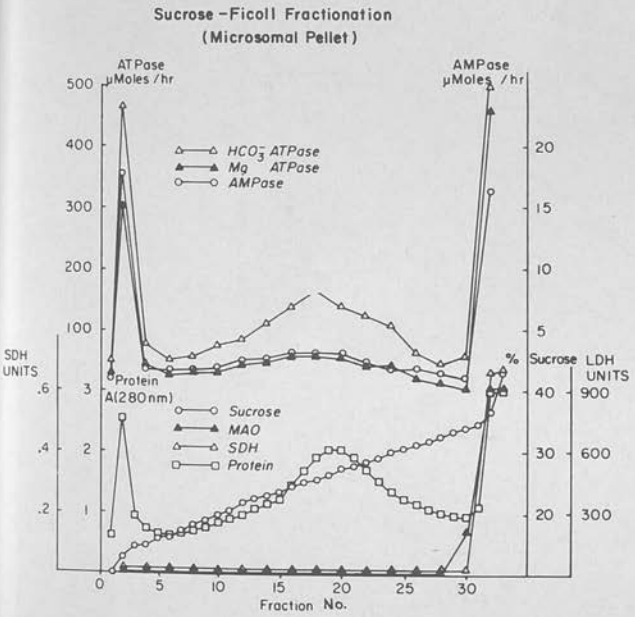

Fig. 11. Fractionation of the microsomal preparation on a linear Ficoll–sucrose gradient. Refraction index expressed as percent sucrose. MAO, monoamine oxidase; SDH, succinate dehydrogenase; LDH, lactate dehydrogenase

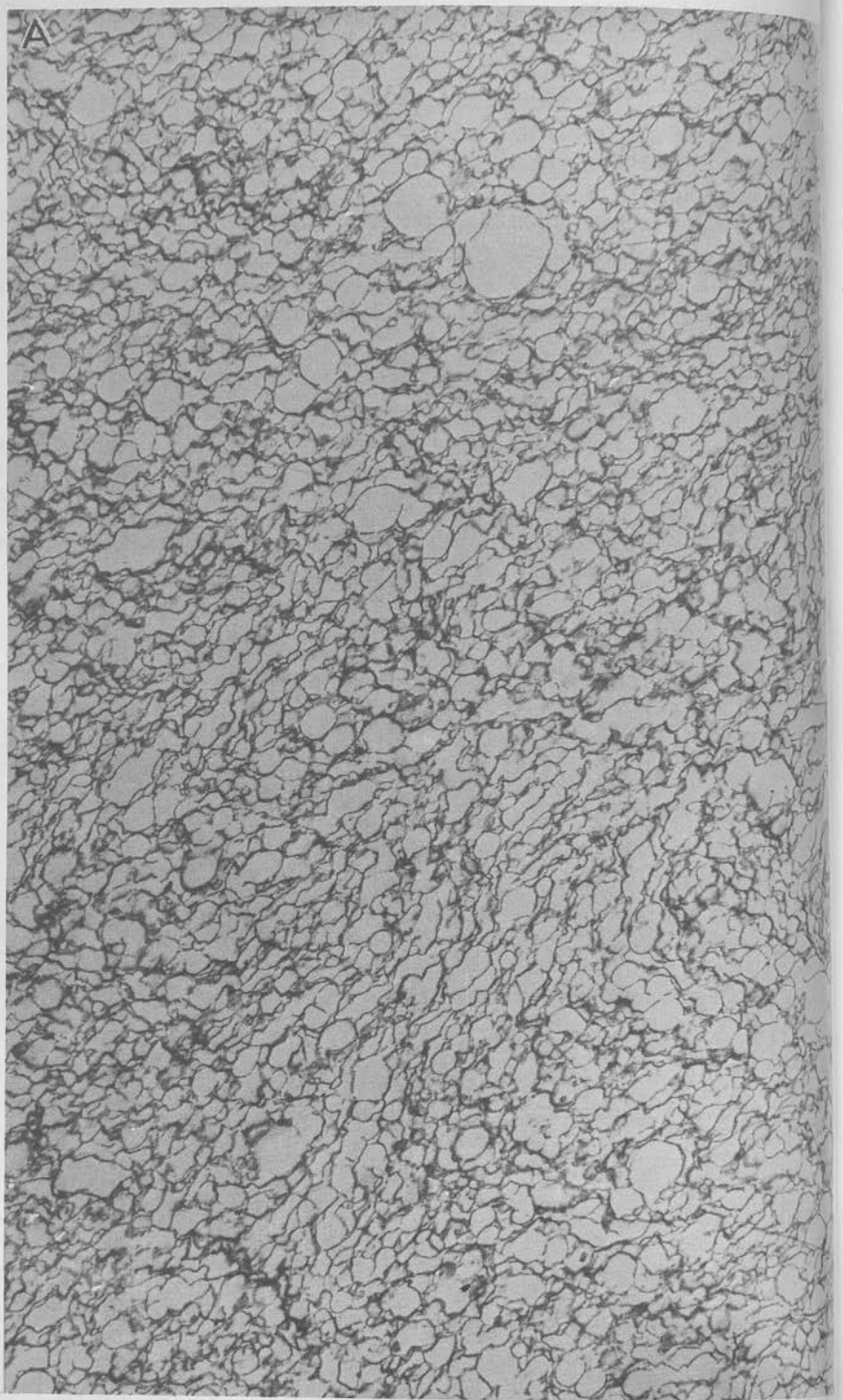

Fig. 12. (A) Morphology (magnification ×8500) of the fraction at 13% on the Ficoll-sucr gradient.

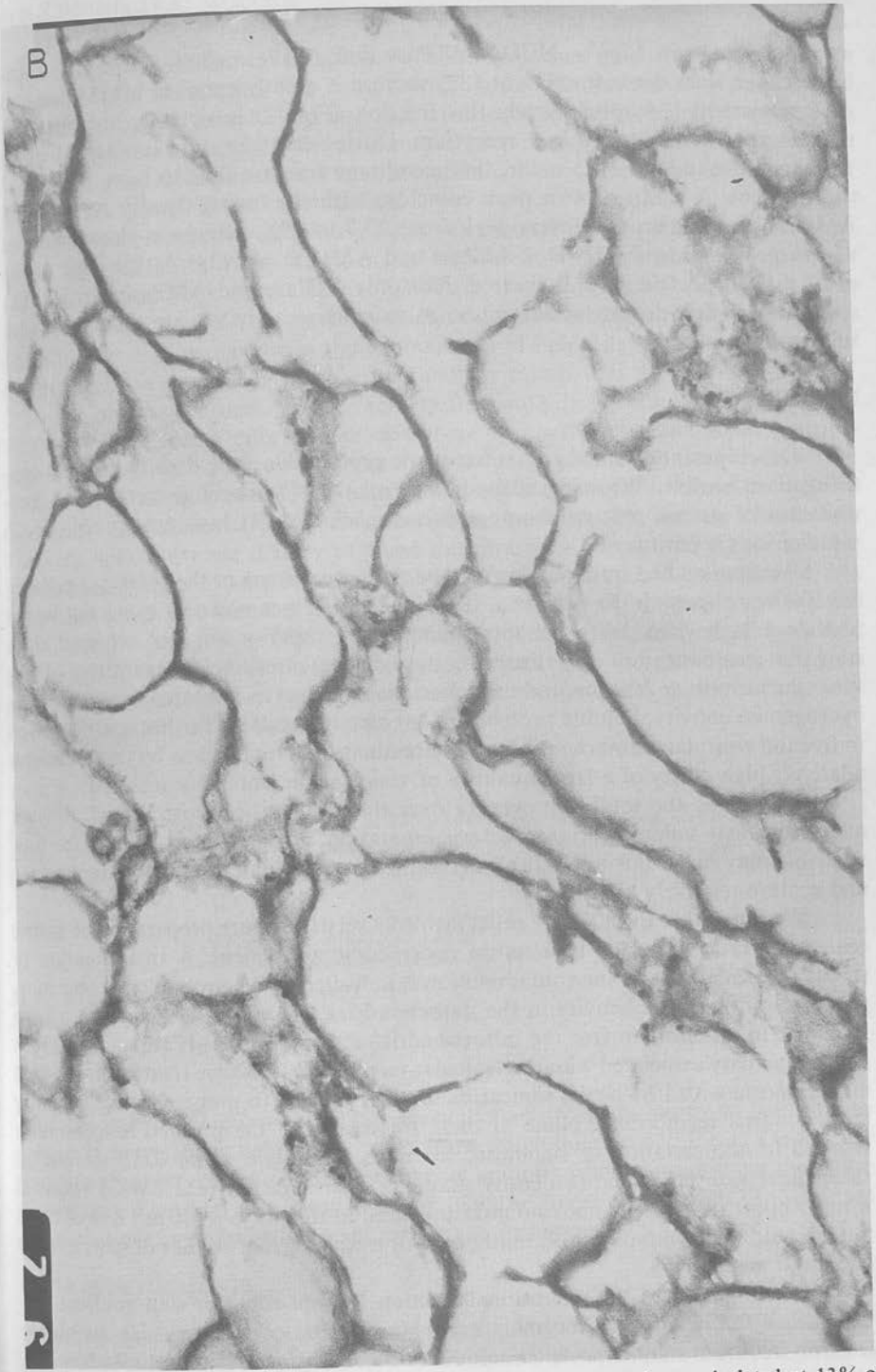

Fig. 12. **(B) Detailed structure (magnification $\times 68\,200$) of the membranes isolated at 13% on** the Ficoll–sucrose gradient.

one such gradient. Mg^{2+}-, HCO_3^--ATPase and AMPase show a trimodal distribution. The least dense fraction at 13% sucrose is greatly enriched in AMPase ATPase activity. Morphologically this fraction (Fig. 12) is virtually homogeneous membranes interconnected in a syncytium. During centrifugation lasting as long 18 h in a Beckman SW-25 rotor, this membrane fraction fails to leave the top the gradient. A sharp protein peak coincides with the lowest density ATPase AMPase peak. A broad protein peak from 23.5 to 29% sucrose is also associated with a peak of Mg^{2+}-, HCO_3^--ATPase and AMPase activity. At the edge of rotor a third protein peak is located. Not only ATPase and AMPase activity also succinic dehydrogenase and monoamine oxidase activities are associated this protein peak.

DISCUSSION

Development of zonal rotors has made preparative scale density gradient centrifugation feasible. We have utilized this technique to develop methods of fractionation of gastric mucosal homogenates to achieve: (1) high total yield, or rapidity, or (3) purity.

We first studied fractionation of the total homogenate or the 78000 $\times g$ pellet the 5000 $\times g$ supernate to achieve a technique which was not only rapid but would provide a high yield. With the total homogenate rapidity was not achieved since isopycnic centrifugation was necessary to achieve satisfactory separation of vesicular membrane fraction and mitochondrial fraction as indicated by succinic hydrogenase activity. Soluble protein present also necessitates further centrifugation to free the vesicular membranes of this contamination. Nonetheless by this technique relatively high purity of a large quantity of vesicular membrane is achieved.

Overlaying the total homogenate over the gradient, each in 325 ml, did not allow sufficient volume for satisfactory separation. Larger rotors which are now available may make this a practical method to avoid soluble protein contamination and achieve relatively high purity.

We found that the 8000 $\times g$ pellet yielded a relatively pure preparation of gastric mitochondria as indicated by electron microscopic assessment. A small amount of smooth vesicular membrane contamination is indicated by electron microscopic morphology and AMPase activity in the mitochondrial region, 40–44% sucrose, of the gradient. In an effort to free the mitochondrial region from AMPase and HCO_3^- ATPase activity associated with the vesicular membranes, we have treated the purified mitochondria with 1 M NaCl, sonication, and techniques to prepare inner and outer mitochondrial membranes. None of these treatments of the purified mitochondria resulted in accumulation of significant amounts of protein at 28–32% sucrose on subsequent isopycnic sucrose density gradient centrifugation in a SW-25 rotor. It would appear that gastric mitochondria prepared in this way, while not free of enzymes, are sufficiently pure to enable further studies of gastric mitochondrial metabolism.

Fractionation of the microsomal fraction by rate zonal or step gradient centrifugation has resulted in the most rapid purification of the vesicular membrane fraction free from soluble protein contamination. Our greatest interest has, however, been in the greater purity of the smooth vesicular membrane fraction obtained

isopycnic density gradient centrifugation of the microsomal preparation. Membranes prepared in this manner are free from mitochondrial contamination as assessed by electron microscopic morphology and lack of detectable succinate dehydrogenase or monoamine oxidase activity. We do, however, routinely use SDH to monitor the freedom of these membranes from mitochondrial contamination since mitochondrial ATPase also shows HCO_3^- stimulation.

It is this preparative technique which we routinely use to prepare gastric membranes for solubilization with Triton X-100 and further characterization of transport properties. In addition to the HCO_3^--ATPase these solubilized membranes have yielded at least 3 proteins, separable by analytical polyacrylamide gel electrophoresis, which induce step increments in the conductance of lipid bilayers. Characterization of this effect has shown one to be anion, another cation, and the last non-selective.

The observation that AMPase activity frequently peaks one to two tubes after HCO_3^--ATPase led to efforts to resolve these two activities. Rate zonal centrifugation, however, failed to resolve these into two peaks of activity. On Ficoll-sucrose gradients a third peak of ATPase activity was resolved, while AMPase activity accompanies each peak there is enrichment in the peak at 13% sucrose (Table VI). The very light isopycnic density of these membranes is certainly not expected for plasma membranes. In long runs high frictional resistance should be overcome, but these membranes are found at the same density after 6- or 10-h zonal runs or after 18 h of centrifugation in an SW-25 rotor. We have felt that osmotic intactness would best explain the failure of these membranes to sediment. It is consistent that on sucrose gradients this very light peak is non existent or quite small and is greatly increased when Ficoll is used in the gradient.

TABLE VI

C is the peak total activity in the regions of 13%, 26–27% or 35% sucrose. C_0 is the hypothetical total activity/sample if activity were evenly distributed on the gradient.

	C/C_0		
	13%	*26–27%*	*35%*
Mg^{2+}-ATPase	3.8	0.73	5.8
HCO_3^--ATPase	3.3	1.1	3.4
AMPase	4.7	0.72	4.2

Using hypotonic lysis of isolated oxyntic cells from Necturus we are able to prepare large vesicular "ghost-like" structures which float on 5% Ficoll. On sucrose gradients these structures are reduced to tiny granules when viewed under the phase microscope. Thus the possibility remains that the upper peak of HCO_3^--ATPase activity resides in osmotically intact membrane structures.

ACKNOWLEDGEMENTS

This work was supported by NIH Grants AM08541 and AM15878 and NSF Grant GB31075. A.S. is a trainee on NIH Grant TIAM05286. Credit is given to Project No. 8059-01, VA Hospital in Birmingham, Ala.

REFERENCES

1 Kasbekar, D. K. and Durbin, R. P. (1965) *Biochim. Biophys. Acta* 105, 472–482
2 Sachs, G., Mitch, W. E. and Hirschowitz, B. I. (1965) *Proc. Soc. Exp. Biol. Med.* 119, 10
3 Wiebelhaus, V. D., Sung, C. P., Helander, H. F., Shah, G., Blum, A. L. and Sachs, G. *Biochim. Biophys. Acta* 241, 49–56
4 Blum, A. L., Shah, G., St. Pierre, T., Sung, C. P., Wiebelhaus, V. D. and Sachs, G. *Biochim. Biophys. Acta* 249, 101–113
5 Sachs, G., Shah, G., Strych, A., Cline, G. and Hirschowitz, B. I. (1972) *Biochim. Biophys.* 266, 625–638
6 Simon, B., Kinne, R. and Sachs, G. (1972) *Biochim. Biophys. Acta* 282, 293–300
7 King, T. E. and Howard, R. L. (1967) *Methods in Enzymology*, Vol. 10, pp. 275–294, Acad Press, New York
8 Tabor, C. W., Tabor, H. and Rosenthal, S. M. (1954) *J. Biol. Chem.* 208, 645–661
9 Reeves, W. J. and Fimognari, G. M. (1966) *Methods in Enzymology*, Vol. 9, pp. 28 Academic Press, New York

Reprinted from

Biochimica et Biophysica Acta, 332 (1974) 233–247

BBA 76535

CHARACTERIZATION OF GASTRIC MUCOSAL MEMBRANES

VI. THE PRESENCE OF CHANNEL-FORMING SUBSTANCES

G. SACHS*, J. G. SPENNEY, G. SACCOMANI and M. C. GOODALL

Division of Gastroenterology and Department of Physiology and Biophysics University of Alabama in Birmingham, Birmingham, Ala. 35294 (U.S.A.)

(Received October 1st, 1973)

SUMMARY

Highly purified gastric membranes were extracted by ionic or non-ionic detergents. Further fractionation was carried out on acrylamide gel electrophoresis. Some defined bands, incorporated into artificial bilayer membranes, produced discrete conductance changes characteristic of channel activity. A low molecular weight peak, purified through two cycles of electrophoresis was characterized as an anion-selective, positively voltage dependent channel, and a model to account for the action of the transport ATPase incorporating this channel concept is suggested.

INTRODUCTION

Conductance across epithelia may be described as the sum of the conductances of the cellular and paracellular route [1]. The relative magnitude of these conductances varies from tissue to tissue, and in the case of the gastric mucosa, the paracellular conductance is at most 20% of the cellular conductance [2]. It, therefore, follows that conductance measurements on the intact tissue, whether in vivo, or in vitro, determine the conductance of the cell membranes of the mucosa. The cell membrane presumably contains structures, be they channels or carriers, responsible for the conductance patterns observed in the intact tissue. Such molecules exist in abundance in unicellular organisms. Valinomycin [3], enniatins A, B, C, [4], the actins [5], nigericin [6] are just some examples of carriers produced by various bacteria or fungi. These cyclic compounds have as a common structural feature in hydrophobic environments, a central polar region and a peripheral hydrophobic shell. All of these compounds induce specific conductances in artificial bilayers up to $10^{-2}\,\Omega^{-1}\cdot cm^{-2}$.

Other molecules such as amphotericin [7] and Nystatin [8] are capable of inducing channels in bilayers. In this case it has been proposed that a relatively large (5 Å) pore is formed by cylindrical stacking of rod-like structures. There is a lipid

* To whom correspondence should be addressed.

specificity here in the form of a cholesterol requirement. Dehydration of solv... ions probably plays no role in selectivity with these compounds.

Linear peptides such as gramicidins [9–11] or *N*-formyl(Ala–Ala–Gly)$_4$-O... [12,13] also form channels across bilayers characterized by quantal increments... conductance of the order 10^{-11}–10^{-10} Ω^{-1}. To account for these properties... helical structure has been proposed such that there is a central polar and periph... hydrophobic region, as for the cyclic compounds. This novel $\beta^6{}_{3,3}$ helix also sh... a common mechanism for ion complexation with the cyclic carriers, consisting... competition between polar oxygen groups and the hydration shell for cation bindi... Excitability inducing material [14], also of bacterial origin, forms voltage depend... channels of the same order of magnitude ($3 \cdot 10^{-10}$ Ω^{-1}) and appears to be a prote...

Information about ionophores derived from mammalian tissues is considera... more sparse. High ionic strength extracts of rat brain microsomes or frozen dr... electroplax produced channel activity in bilayers. These were Na^+ selective or K... selective and voltage dependent [15]. Crude mitochondrial fraction from electrop... was separated on density gradients in a zonal rotor. Incorporation of the (Na^++K... ATPase rich fraction in the presence of ATP was accompanied by an increase in z... current voltage which decayed in a stepwise fashion, suggesting a channel mechani... for voltage shunting [16]. In the same paper the authors showed that the low dens... fraction of the same gradient induced step changes in conductance. More recently t... supernatant of trichloroacetic acid precipitated trypsin digest of electroplax me... branes, when added to an oxidized cholesterol bilayers, lowered the conductan... only in the presence of Na^+, and the conductance was cation selective [17]. Cholin... terase preparations have been shown to contain channels which require acetylchol... for activity [18].

In this work we showed that: (a) channel-active material can be extract... from highly purified gastric membranes by non-ionic detergents; (b) that there a... various types of channel activity in the crude extract; (c) that these activities can b... separated by polyacrylamide gel electrophoresis; and (d) that an anion channel ha... been obtained in a high degree of purity.

In relation to this, some of the conductance properties of gastric mucosa hav... been well defined. Importantly this tissue secretes HCl such that the secretion o... H^+ is electrogenic, and we would, therefore, expect a fair quantity of anion selectiv... channel material to be present in the cell membrane. Moreover, from experiment... in the intact tissue, the $SO_4{}^{2-}$ conductance is considerably less than that of Cl^-... a property which we would predict to be shared by the anion selective channel shown... to be present in the tissue extract.

METHODS

Bilayer technique

Electrical considerations. In order to be able to resolve individual channe... events down to 10^{-12} Ω^{-1}, a bilayer with a background conductance of 10^{-9} Ω^{-1}... cm^{-2} is required with a corresponding low noise level. Fig. 1 shows the technique... we use to monitor the electrical characteristics. A voltage source or signal generator... and a current amplifier are connected through the bilayer, with the signal and am...

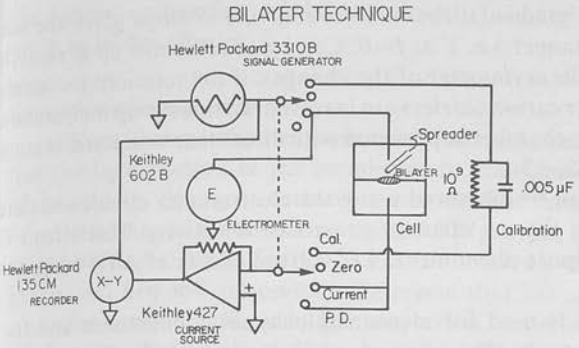

Fig. 1. Diagrammatic representation of the bilayer technique. A voltage generator (Hewlett-Packard 3310B) and a current amplifier (Keithley 427) are connected across a bilayer formed from soybean lecithin in decane and their output to an X–Y recorder. A switching mechanism is provided to connect an electrometer for measuring zero current voltage, and for capacitance and conductance calibration.

plifier output respectively to an X–Y recorder. The generator is used in two modes: a triangular sweep with $|dV/dt|$ constant, or as a piecewise constant voltage source (square wave). In the sweep mode, the curve obtained is shown in Fig. 2. The X-axis is the voltage and the Y-axis the current. The slope is the conductance, and the separation between the two sweep directions is due to the capacitance of the bilayer. This occurs because dV/dt changes sign at the extremes of voltage. Both channel and carrier incorporation can be detected. Channels are manifested as discrete conductance steps, and the size (conductance Δg) of the individual channel can be determined as the change in slope of the $I-V$ plots. If the studies are carried out in asymmetric

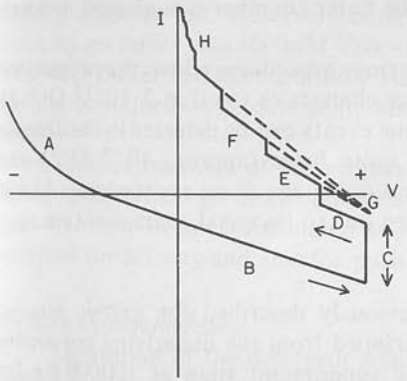

Fig. 2. Diagrammatic representation of type of result observed in sweep mode (triangular wave). A, effect of carrier incorporation showing smooth conductance changes even at very high sensitivity. B, background conductance. C, capacitance of bilayer, since dV/dt changes sign at extremes of plot, and is constant in between. D, E, F, successive single channel events in the bilayer, the change in slope giving Δg, the channel size or conductance. G, the point of intersection of the slope increments, giving the zero current voltage of the individual channels, i.e. their selectivity in asymmetric solutions. H, increase in conductance due to "unresolved" channels.

solutions (e.g. a $10 \times X^+Y^-$ gradient), the intersection of the slope gives the selectivity of the individual channel, i.e. V at $I=0$. Carrier effects show up as small conductance increments, and the asymmetry of the changes, if the solutions are asymmetric, shows whether anion or cation carriers are involved. In this set-up temperature effects can be studied since the chamber is provided with direct thermoelectric heating or cooling (Thermoelectrics SK-12).

Zero current voltage can be measured using the electrometer circuit and in asymmetric solutions gives the net channel or carrier selectivity. This circuit used for studying active transport phenomena, i.e. voltage effects of ATP additions to ATPase preparations.

The square wave mode is used for measuring channel conductance and frequency distribution of conductance after some idea of selectivity and voltage dependence has been obtained on the sweep mode. A check on selectivity can be obtained in asymmetric solutions by determining the numbers of channels obtained with + or −ve current applied across the bilayer. One artifact must be considered in this context in that incorporation into the bilayer of a charged particle would also be voltage dependent, and this could not be distinguished from selectivity in this mode of operation.

Lipids. Various precautions have to be taken with the type of lipid used in order to reduce background conductance. The method we use as a routine is to dissolve soybean lecithin (Sigma, Type 11A) which contains some triglyceride, to 30 mg/ml in decane, and pass the solution over a neutral alumina (Bio Rad AG7) column immediately before use. All glassware is preheated to 400 °C to remove contaminating films.

Solutions. All solutions are made up in glass distilled water, and salts when necessary calcined to remove organic and bacterial contamination.

Cleaning procedures. The polyethylene inner chamber is disposable and only reused after an extensive cycle of cleaning and testing of a sample batch. The spreader and electrode tips are not reused. The outer chamber is sonicated in detergent with prolonged water rinses.

Conclusion. The combination of these various procedures allows the production of a bilayer in which we can detect conductance changes as small as $2 \cdot 10^{-12}\ \Omega^{-1}$. In spite of all precautions, sometimes spontaneous events can be detected in the absence of any known additions. Usually they are quite large (approx. $10^{-9}\ \Omega^{-1}$) and hence can be distinguished from most of the natural channels we are studying. In our experience these spurious events are most often due to bacterial contamination.

Membrane preparation

The techniques we use have been previously described for gastric mucosa [19,20]. Briefly, the dog gastric mucosa is stripped from the underlying connective tissue, homogenized, and the post $20000 \times g$ supernatant spun at $100000 \times g$ for 60 min.

The precipitate is then distributed through a linear ficoll–sucrose gradient in a Beckman Ti XIV zonal rotor (47000 rev./min, 5–7 h) and two peaks of membrane are obtained, as well as a peak of mitochondrial activity. By both biochemical and morphological techniques the membrane fractions are not contaminated by other cell constituents. Membrane peak 2 is enriched in HCO_3^--ATPase, a marker for

the luminal cell surface of the oxyntic cell [21] and has been used for most of the work to be described.

Extraction of membranes

Since the membrane presumably contains proteins or peptides oriented so that the lipid portion of the membrane is associated with the hydrophobic portion of the protein, detergent extraction was the first method used. Since it was successful no other has as yet been investigated. Three types of detergents were used: sodium dodecylsulfate (SDS), Triton X-100, a non-ionic detergent containing a phenyl group, and Brij 36T, a non-ionic detergent that has no 280-nm absorption.

For sodium dodecylsulfate extraction, sodium dodecylsulfate was added at 1% final concentration, and the protein solubilized for 4 h at room temperature. Complete solubilization was achieved. For both Brij 36T and Triton X-100 extraction a 3:1 detergent/protein ratio was determined to be the most successful in solubilizing the HCO_3^--ATPase in active form. Solubilization was carried out by stirring at 0 °C for 1 h using conditions as previously described [22], i.e. approx. 1 mg/ml protein, 3 mg/ml detergent, 50 mM HEPES buffer (pH 7.4), 10 mM NaCl at 0 °C for 1 h. Following all three procedures the suspension was centrifuged at $100000 \times g$ for 60 min and the supernatant used for all further experimentation.

Characterization of extract

Although most of our recent experiments have been carried out with the Brij extract, the first active preparation was obtained with Triton X-100. All the detergent solubilized material was characterized on 7% analytical acrylamide gels. The positions of the peaks were determined on a Gilford gel scanner, following Coomassie Blue staining. Parallel gels were serially sectioned and fractions tested for activity in the bilayer.

Preparative gel fraction of the Brij extract was carried out on 7% gels using a 3.5% stacking gel. Reservoir buffer was 0.19 M glycine–Tris buffer (pH 8.6), stacking gel buffer was 100 mM Tris –HCl (pH 6.8), separating gel buffer was 0.4 M Tris–HCl buffer (pH 8.6) and flow buffer was as for the separating gel. All buffers usually contained 0.1% detergent. Similar conditions were used for analytical gel work.

Various fractions of the preparative run were tested in the bilayer, and subjected to analytical gel electrophoresis in 7 and 15% gels. The fastest moving active peak was then further fractionated on 15% preparative gel electrophoresis, the bands analyzed for activity and also for purity on 15% analytical gels.

Column chromatography

Separation of the detergent solubilized extracts was carried out on Sephadex columns of varying porosities. Elution was carried out using buffers containing 0.1% detergent to reduce precipitation of protein in the gels.

Bilayer experiments

Two types of solution were used in the bilayer chambers. When symmetric solutions were used, both inner and outer chambers contained 30 mM NaCl and

120 mM KCl at pH 7.4. For asymmetric solutions, the inner solution was the sa... as above, the external solution was 10-fold diluted.

The membrane extract was added in 10-μl quantities as a 400-fold dilu... to the inner chamber, following a period during which the background had be... shown to be satisfactory. The final protein concentration was usually about 1·10... g/ml in the inner chamber. Usually both the sweep and constant voltage mode we... used to scan the bilayer with the membrane extract incorporated.

RESULTS

Acrylamide gel characterization

Sodium dodecylsulfate gels. The gel pattern was similar whether 1 or 4... sodium dodecylsulfate extraction was carried out. Fig. 3 shows the pattern obtain... There is clearly a major heterogeneous protein peak and several minor ones tot... ling about 25. Since sodium dodecylsulfate is charged, several artifacts were possi... in our bilayer analyses, and relatively few experiments were carried out. More par... cularly, the negative charge on sodium dodecylsulfate would lead us to expect pe... haps an artifactual cation selectivity on incorporation into the bilayer. Alternatively... better incorporation may be obtained with the negatively charged sodium dodec... sulfate being driven into the bilayer by the applied voltage.

The sodium dodecylsulfate was fractionated into two peaks on Sephad... G-50 columns. Two peaks were obtained and the included peak checked for activi... in the bilayer.

Triton X-100 gels. Since membrane fragmentation by Brij 36T extracti... seemed better than that of Triton X-100, coupled with the ease of determining...

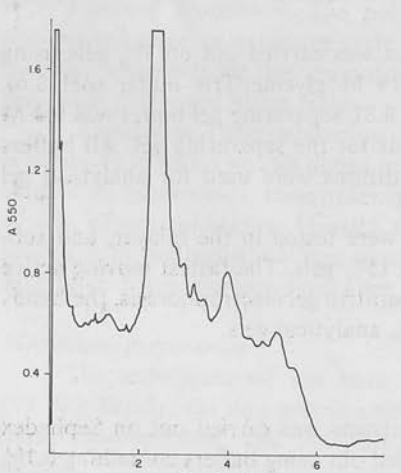

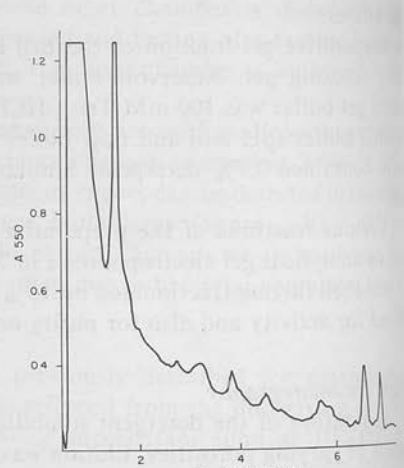

Fig. 3. Scan of protein bands present in 7% acrylamide gels following sodium dodecylsulfa... solubilization of Peak 2 of gastric membrane fraction. The major peak which is heterogeneo... has a mol. wt of 84000.

Fig. 4. Scan of protein bands present in 7% acrylamide gel following Triton X-100 solubilizati... The highest R_F peak is a buffer front artifact. The second highest R_F peak has channel activ...

protein spectroscopically with Brij 36T, most of the work with Triton X-100 was confined to analysis of the total extract. The scan of a Triton X-100 gel is shown in Fig. 4. The fastest moving protein band has channel activity as will be discussed.

Sephadex G-100 chromatography using 8 mM HEPES buffer (pH 7.4) for

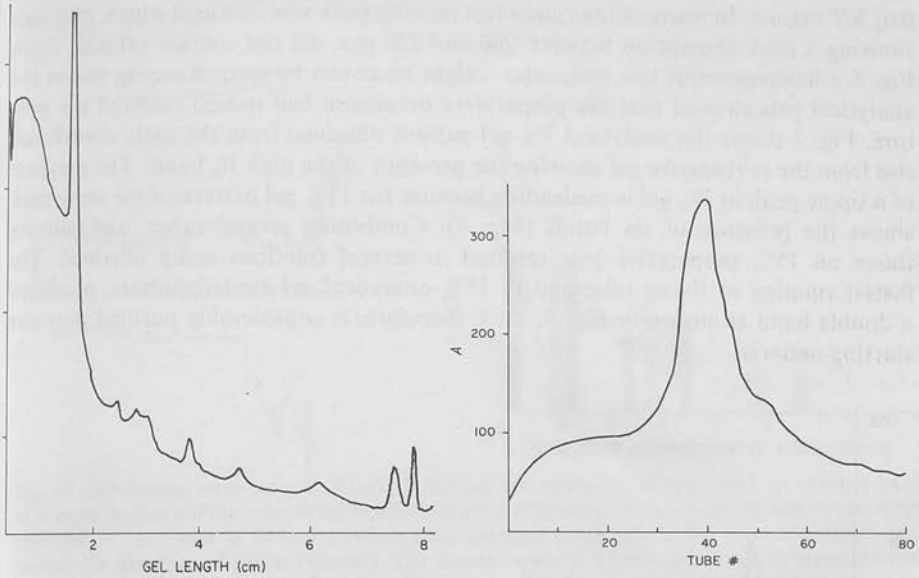

Fig. 5. Scan of protein bands present in 7% acrylamide gel following Brij 36T solubilization. The similarity of the pattern to Triton X-100 should be noted, especially the penultimate band.

Fig. 6. Profile of the low molecular weight band obtained from 7% preparative gel electrophoresis of a Brij 36T extract of gastric membranes. The initial major peak was studied further.

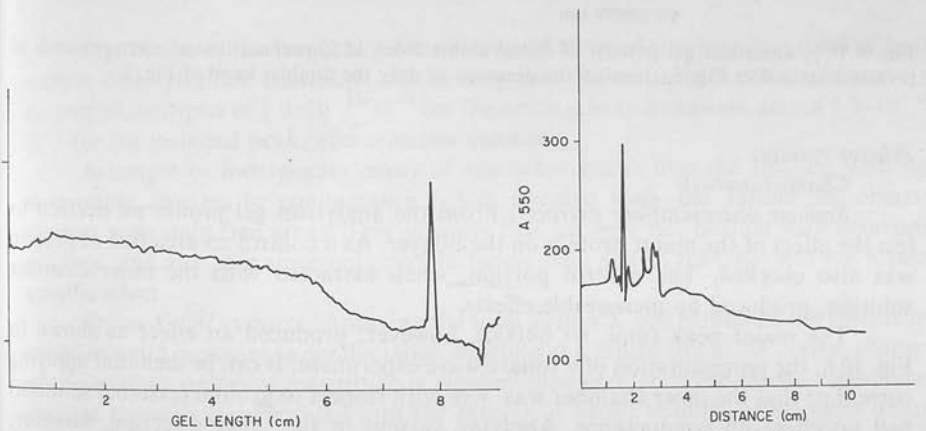

Fig. 7. 7% acrylamide gel pattern of peak obtained from preparative gel electrophoresis, showing the presence of a single protein band, corresponding to a mol. wt of about 8000.

Fig. 8. 15% analytical gel pattern of same preparative gel band as shown in Figs 6 and 7, showing the presence of six peaks at this resolution.

elution fractionated the Triton X-100 extract into two peaks. The included p contained the majority of the channel activity.

Brij 36T gels. Fig. 5 shows a scan of a Brij 36T extract run in 7% acrylam The similarity of the faster moving bands in the Brij 36T and Triton X-100 r should be noted. Fig. 6 shows the elution profile of a preparative gel run on the Brij 36T extract. In many of the runs a fast moving peak was obtained which, altho showing a peak absorption between 260 and 280 nm, did not contain protein. F Fig. 6 a heterogeneous low molecular weight band can be seen. Running this in analytical gels showed that the preparative procedure had indeed resolved the m ture. Fig. 7 shows the analytical 7% gel pattern obtained from the early absorb rise from the preparative gel showing the presence of the high R_F band. The pres of a single peak in 7% gel is misleading because the 15% gel pattern of the same p shows the presence of six bands (Fig. 8). Combining several tubes, and run those on 15% preparative gels resulted in several fractions being obtained. T fastest running of these, subjected to 15% analytical gel electrophoresis, produ a double band as shown in Fig. 9. This, therefore, is considerably purified over starting material.

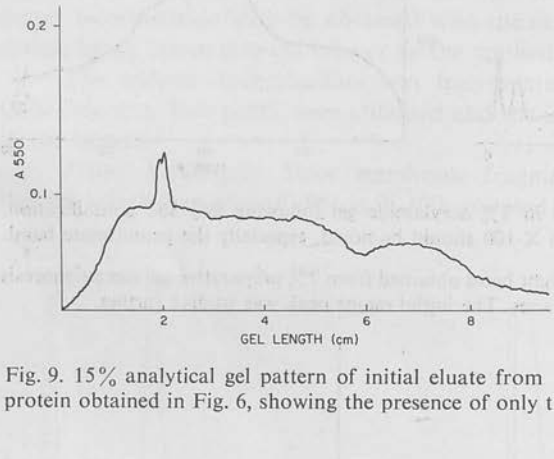

Fig. 9. 15% analytical gel pattern of initial eluate from 15% preparative gel electrophores protein obtained in Fig. 6, showing the presence of only the doublet band of Fig. 8.

Bilayer results

Channel activity

Sodium dodecylsulfate extracts. From the analytical gel profile we decided test the effect of the major protein on the bilayer. As a control an area free of pro was also checked. The control portion, when extracted with the inner cham solution, produced no measurable effects.

The major peak (mol. wt 84000), however, produced an effect as shown Fig. 10A, the representation of a square wave experiment. It can be seen that appl current so that the inner chamber was +ve with respect to ground (external solut had no effect on conductance. Applying current in the other direction, howe produced a large number of channel events. Since in this experiment, asymm solutions were present, one may be tempted to conclude that anion selectivity been demonstrated. However, sodium dodecylsulfate is negatively charged an may be that the applied voltage is facilitating incorporation into the bilayer. Ag

this argument, experiments which tested the Sephadex G-50 included peak of the sodium dodecylsulfate extract produced no evidence of selectivity in the square wave mode. Thus Fig. 10B shows that the sign of the applied voltage had no effect on channel appearance.

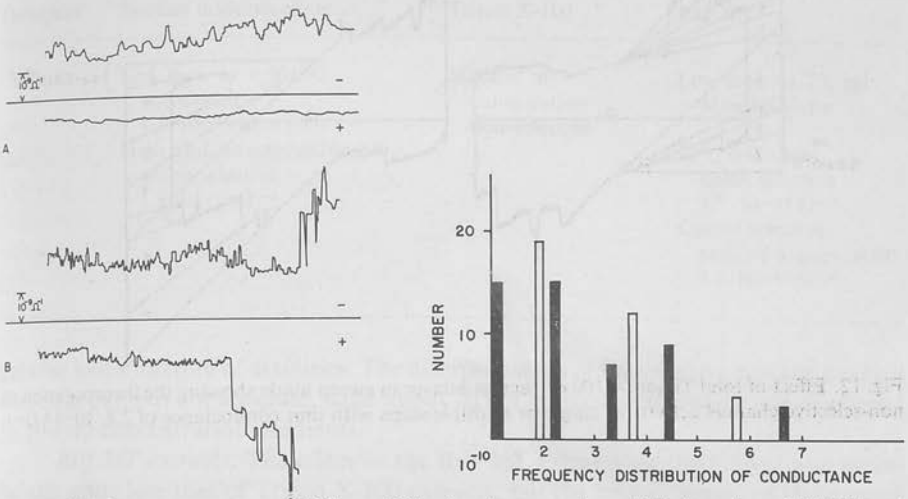

Fig. 10. (A) Square wave scan of bilayer following incorporation of high mol. wt (84000) band of sodium dodecylsulfate solubilized extract, showing channel activity essentially only when inner chamber is –ve, with a 10-fold concentration gradient (high salt in the inner chamber), suggesting the presence of anion channels. (B) Similar scan of bilayer following incorporation of material from included area of a Sephadex G-50 eluate showing channel activity that is presumably non-selective.

Fig. 11. Frequency distribution of channel events following incorporation of sodium dodecylsulfate of high mol. wt and low mol. wt material into the bilayer. The anion channel occurs as a multiple of $1.9 \cdot 10^{-10}\ \Omega^{-1}$ (clear bar), the non selective channel as a multiple of $1.1 \cdot 10^{-10}\ \Omega^{-1}$.

Fig. 11 shows the frequency distribituon of channel size (conductance) of both sodium dodecylsulfate studies. It can be seen that channel size varies quantitatively, as integral multiples of $1.9 \cdot 10^{-10}\ \Omega^{-1}$ for the anion selective channel, and of $1.1 \cdot 10^{-10}\ \Omega^{-1}$ for the included peak, non-selective channel.

Attempts to incorporate many of the other peaks into the bilayer, with demonstrable changes in conductance failed, coupled with the failure to observe changes with stain free areas. This suggests that we were not dealing with detergent artifacts, and also that since only certain bands were active, that this was not a non-specific effect.

Triton X-100 extracts. Applying the total Triton X-100 extract to the bilayer resulted in rapid increases in conductance. Starting at a sensitivity of 10^9, often changes of two or more orders of magnitude in conductance were observed. More often, however, as channels incorporated into the bilayer, it broke readily, hence most observations were carried out at a sensitivity of 10^9 only. Three types of channel activity were observed. Fig. 12 shows the sweep appearance following incorporation of a nonselective channel, which appeared to be the major activity. In addition anion and cation selective channels were observed. The fastest moving band on the Triton X-100

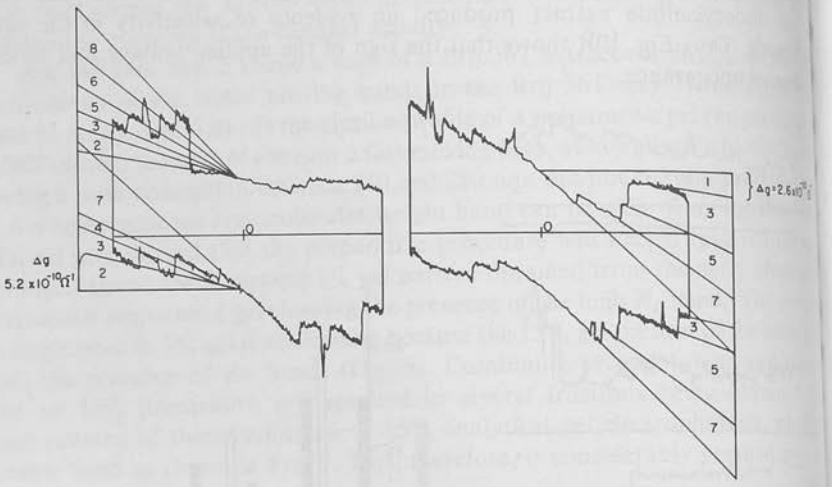

Fig. 12. Effect of total Triton X-100 extract on bilayer in sweep mode showing the incorporation of non-selective channel activity as single or multiple steps with unit conductance of $2.6 \cdot 10^{-10}\ \Omega^{-1}$.

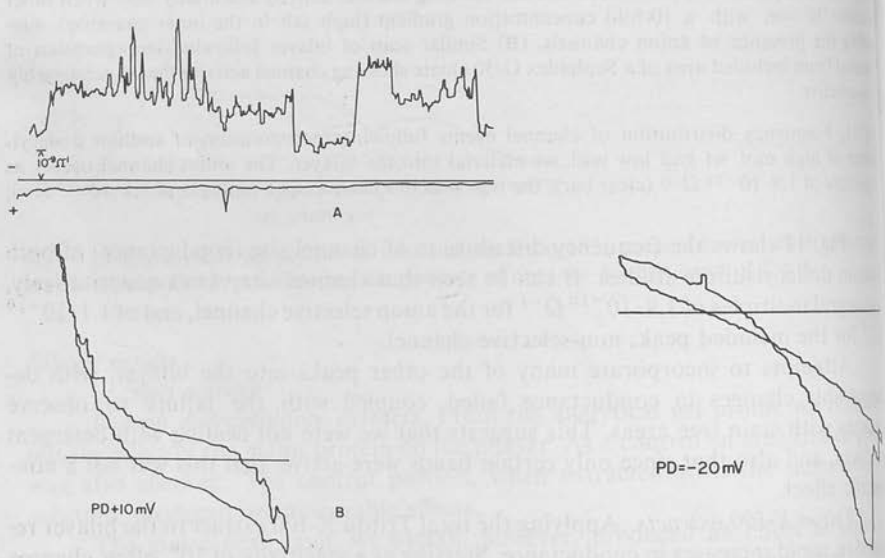

Fig. 13. Effect on bilayer of incorporation of purified low mol. wt material as shown in Fig. 9 in square wave A and sweep mode B. Zero current voltage was +10 mV, confirming weak anion selectivity of channel, as suggested by both sweep and square wave pattern. The +ve voltage dependence of activity should also be noted.

Fig. 14. Appearance of bilayer in sweep mode following incorporation of low R_F band of Fig. 8, showing the presence of "unresolved" cation selective channels generating a PD of −20 mV across the bilayer.

TABLE I

SUMMARY OF CHANNELS FOUND

Electrolyte concentration 120 mM NaCl.

Detergent	Sodium dodecylsulfate	Triton X-100	Brij 36T
	Low mol. wt < 50000 non-selective $1.1 \cdot 10^{-10}\ \Omega^{-1}$	Mixture of anion cation non-selective	Low mol. wt 7% gel Mixed activity
	High mol. wt approx. 84000 anion selective $1.9 \cdot 10^{-10}\ \Omega^{-1}$		15% resolved anion selective $1.7 \cdot 10^{-10}\ \Omega^{-1}$
			Cation selective mol. wt approx. 8000 $3.5 \cdot 10^{-10}\ \Omega^{-1}$

gel also had a mixture of activities. The discrimination of the selective types of channel was clear cut, but not absolute, since about 20 mV zero current voltage was developed in 10-fold concentration gradients.

Brij 36T extracts. The effect of the Brij 36T extracts on the bilayer was superficially quite like that of Triton X-100 extracts, but the bilayer appeared to be much more stable than with Triton X-100. Since both the sodium dodecylsulfate and Triton X-100 experiments had established the presence of channels, our Brij 36T experiments were carried out with the major purpose of separating and characterizing channel activity. Fig. 13 shows the data obtained when the material corresponding to the analytical gel of Fig. 9 is added to the bilayer. Based on the sweep, square wave and zero current voltage data (i.e. the potential developed across the whole membrane), this material is anion selective. Less than 0.1 μg of protein (based on absorbance at 280 nm) produces easily detectable activity. Based on molecular weight calibration of the gel, molecular weight of the channel is about 8000 or less [2]. The slowest moving peak of Fig. 8 when incorporated into the bilayer produced a sweep characteristic as in Fig. 14. Square wave, sweep and voltage analysis showed this to be a cation selective channel. Again, as with the Triton X-100, the selectivity ratio was usually less than 5, anion/cation for the "anion" channel and cation/anion for the "cation" channel. In the case of the frequency distribution for the anion channel, this showed that channel size is a multiple of $1.7 \cdot 10^{-10}\ \Omega^{-1}$, close to the sodium dodecylsulfate size.

DISCUSSION

The purpose of this work was to devise techniques wich could allow the study of natural ionophores occuring in animal cell membranes.

We selected gastric mucosa for this purpose since we know that conductance of this tissue is mainly cellular, hence the electrical properties of the epithelium in the Ussing chamber reflect the properties of the cell membrane. Hence structures responsible for anion conductance will show $P_{Cl^-} > P_{SO_4^{2-}}$, and if the electrogenic proton pump hypothesis is correct, will also show positive voltage dependence.

Another reason for the use of this tissue was that we had available a supply of highly purified membrane fractions from the zonal rotor, hence we could be fairly confident that the material extracted was membrane derived.

Examining the data presented we have the following facts: (a) The starting material is a highly purified plasma membrane suspension. (b) Direct addition of this material shows no activity in the bilayer, hence the active materials are not water soluble, or are tightly bound to the membrane. (c) Detergent extraction produces a highly active preparation which shows channel rather than carrier properties. Presumably, then, with adequate structural characterization, the mammalian analog to compounds such as digramicidin malonamide will be identified. (d) Several of the protein bands show no activity in the bilayer. Thus the property of channel induction is confined to only some of the proteins extractable from the membrane and this serves as a satisfactory control. (e) Ion selective channel activity is found in a relatively low molecular weight peptide band, corresponding to a molecular weight of about 8000 present in both Brij 36T and Triton X-100 extracts on 7% analytical gels. This band seems to have mixed anion and cation selectivities. (f) Preparative gel fractionation results in purification of this band which is further subfractionated on 15% gels (preparative and analytical) into six bands. The highest mobility band was anion selective. The cation selective compound appeared to be subject to aggregation and was of low mobility on 15% gels. The intermediate bands had no activity. (g) There was anion and cation discrimination of about 5:1. (h) The anion channel showed positive voltage dependence in that bilayer conductance increased with voltage. This could be due to alteration in channel incorporation or a voltage effect on the channel itself. (i) Several channel sizes were observed. The larger channels could be accounted for as multiples of a single channel event, suggesting associativity between channels. (j) Channel activity was heat labile, perhaps due to denaturation, or aggregation of the channels into an inactive form. (k) The conductance concentration curves for the channels were different for the anion and cation selective types. Although not conclusive, the simplest interpretation of the curves would be that the anion channel was charged, and the cation channel neutral. (l) In other regions of the gel, non-selective channels were found. The 84 000 mol. wt protein

Fig. 15. Frequency distribution of channel events following incorporation of partially purified anion channel into the bilayer, showing that conductance increments occur as multiples of a unit conductance of $1.7 \cdot 10^{-10}\ \Omega^{-1}$.

found on sodium dodecylsulfate gels was anion selective, and the crude sodium dodecylsulfate fractions from Sephadex columns were non selective. (m) The anion channel we obtain shows considerable Cl^-/SO_4^{2-} discrimination, as we would predict from intact tissue studies. The positive voltage dependence was also an interesting property, since this could be one way of linking Cl^- flux to the activity of an electrogenic H^+ pump.

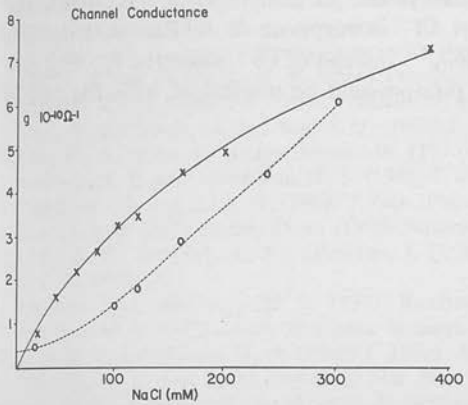

Fig. 16. Channel conductance as a function of NaCl concentration, showing, in the upper curve, the effect of ionic strength on the cation selective channel (×—×), and on anion selective channel (○---○).

This work thus provides the first evidence for channel activity in epithelial membranes. Their physiological significance has not as yet been defined, but it is encouraging that one of these channel activities is of low molecular weight, and relatively easily separated from the rest of the membrane material. It is hoped that controlled proteolysis will be able to reduce the molecular weight by about half without loss of activity so that studies can be initiated on its conformation.

With the application of any novel approach, one is cognisant of several possible artifacts. Many of these have been excluded by our work. Thus the effect of several detergents on bilayers has been well documented [22]. Control experiments showed that detergents at concentrations used had no effect on the bilayer (<3 μg/ml) and at much higher concentrations smooth conductance changes were observed which did not correspond to the changes we observed. Since the majority of the separable bands on acrylamide gel were also without detectable bilayer activity, it would appear that the property of inducing conductance changes is confined to only a few of the membrane constituents. This increases our confidence that the conductance changes are physiologically relevant.

The use of Brij 36T or Triton X-100 was initially based on their capacity to solubilize the ATPase activity of the membrane. The finding of channel activity raises the possibility that channels were an integral part of this enzyme, as has been suggested for the $(Na^+ + K^+)$-ATPase [17]. Clearly we can separate channel activity from ATPase activity which is located on top of the gel in the case of Triton X-100 extracts, and at about 1 cm for the Brij 36T preparation. We have not, however,

shown that purified ATPase is devoid of channel activity. As mentioned in the introduction, the PD obtained by the addition of ATP to ATPase preparations for $(Na^+ + K^+)$-ATPase decayed in stepwise fashion. Similar data were obtained in these preparations, and it was shown that this stepwise decay was due to the induction of channels by the bilayer voltage. This type of observation led us to postulate a function for the anion voltage dependent channel in the gastric mucosa. Thus the ATPase in Fig. 17 is visualized as an electrogenic pump, responsible for increased OH^- (HCO_3^-) translocation. The anion channel is the parallel limb of the circuit, and being voltage dependent would transport Cl^- in response to ATPase activity. The net result would be HCl secretion. With SO_4^{2-} instead of Cl^-, since the $P_{Cl^-}/P_{SO_4^{2-}} = 6$, the electrogenic nature of the proton pump would be unmasked, as is the case in SO_4^{2-} solutions [23].

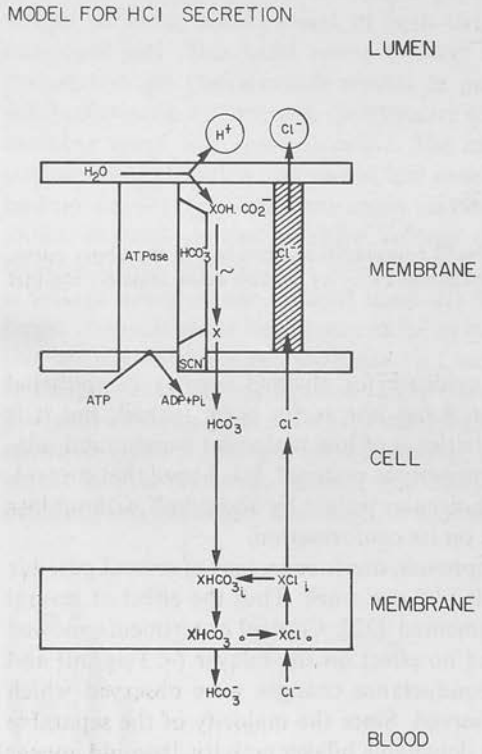

Fig. 17. Hypothetical model for acid secretion incorporating a voltage dependent Cl^- selective channel in parallel to an electrogenic ATPase pump of the Mitchell Type I, responsible for H^+ production. The net effect of these two systems is the secretion of HCl, and the intracellular production of HCO_3^-, which is dissipated by a $Cl^- - HCO_3^-$ forced exchange mechanism in the basal membrane.

ACKNOWLEDGEMENT

Thanks are due to J. Monti for expert technical assistance.
This study was supported by N.I.H Grants AM08541, AM18578 and GM18721;

N.S.F. Grant GB31075; Grant in Aid, Smith Kline and French Laboratories; and Veterans Administration Hospital, Birmingham, Alabama. Credit is given to Project No. 8059-01, VA Hospital.

REFERENCES

1 Diamond, J. M., Barry, P. H. and Wright, E. M. (1970) in Electrophysiology of Epithelial Cells (Biebisch, G., ed.), pp. 23–39, Schattauer
2 Sachs, G., Shoemaker, R. L., Spenney, J. G. and Goodall, M. C. (1973) in Alfred Benzon Symposium V: Transport Mechanisms in Epithelia, 257–275
3 Lev, A. A. and Bushinski, E. P. (1964) Tsitologiya 9, 102–106
4 Stefanac, Z. and Simon, W. (1966) Chimia 20, 436–441
5 Ciani, S., Eisenman, G. and Szabo, G. (1969) J. Membrane Biol. 1, 1–36
6 Lutz, W. K., Wipt, H. K. and Simon, W. (1970) Helv. Chim. Acta 53, 1741–1946
7 Andreoli, T. E. and Monahan, M. S. (1968) J. Gen. Physiol. 52, 300–325
8 Finkelstein, A. and Cass, A. (1968) J. Gen. Physiol. 52, 145–173S
9 Hladky, S. B. and Haydon, D. A. (1970) Nature 225, 451–453
10 Urry, D. W., Goodall, M. C., Glickson, J. D. and Mayers, D. (1971) Proc. Natl. Acad. Sci. U.S. 68, 1907–1911
12 Goodall, M. C. and Urry, D. W. (1973) Biochim. Biophys. Acta 291, 317–320
13 Goodall, M. C. (1973) Arch. Biochem. Biophys. 157, 514–519
14 Mueller, P. and Rudin, D. O. (1968) J. Theor. Biol. 18, 222–258
15 Goodall, M. C. and Sachs, G. (1972) Nat. New Biol. 237, 252–253
16 Jain, M. K., White, F. P., Strickholm, A., Williams, E. and Cordes, E. H. (1972) J. Membrane Biol. 8, 363–388
17 Shamoo, A. E. and Albers, R. W. (1973) Proc. Natl. Acad. Sci. U.S. 70, 1191–1194
18 Jain, M. K., Mehl, L. E. and Cordes, E. H. (1973) Biochem. Biophys. Res. Commun. 51, 192–197
19 Sachs, G., Shah, G., Strych, A., Cline, G. and Hirschowitz, B. I. (1972) Biochim. Biophys. Acta 266, 625–638
20 Spenney, J. G., Price, A., Strych, A. and Sachs, G. (1973) Biochim. Biophys. Acta 311, 545–564
21 Konig, G. S. and Vial, J. P. C. (1970) J. Histoch. Cytochem. 18, 340–347
22 Van Zutphen, H., Merola, A. J., Brierley, G. P. and Cornwell, D. G. (1972) Arch. Biochem. Biophys. 152, 755–766
23 Durbin, R. P. and Heinz, E. (1958) J. Gen. Physiol. 41, 1035–1047

ARCHIVES OF BIOCHEMISTRY AND BIOPHYSICS 161, 456–471 (1974)

Characterization of Gastric Mucosal Membranes

Composition of Gastric Cell Membranes and Polypeptide Fractionation using Ionic and Nonionic Detergents[1, 2]

J. G. SPENNEY, G. SACCOMANI, H. L. SPITZER, M. TOMANA, AND G. SACHS[3]

University of Alabama in Birmingham and Veterans Administration Hospital Birmingham, Alabama 35294

Received September 28, 1973

Lipid, carbohydrate, amino acid, and polypeptide composition of 2 fractions of cell membranes obtained by sucrose–Ficoll zonal density gradient fractionation of gastric mucosal homogenates has been studied. The membranes with density = 1.04 contain 0.7 μmole lipid P and 0.54 μmole cholesterol/mg protein, while the membranes of density 1.10 contain only 0.25 μmole lipid P and 0.28 μmole cholesterol/mg protein. Phosphatidylcholine and phosphatidylethanolamine are the most abundant phospholipids. Free fatty acids were present. Carbohydrates were most abundant in the proteins of the Peak II membranes (density = 1.10). One polypeptide band was dominant on sodium dodecyl sulfate, Triton X-100, and Brij 36T gels, and the adenosine triphosphatase activity in Brij 36T gels was found to have a relative mobility of 0.14 and 0.19 in the two fractions.

One means of approaching an understanding of membrane function is to carry out a detailed analysis of the constituents of the membranes. Tissues which have been studied in this way include liver (1), erythroycytes (2), and ameba (3) among many others (4). From such studies certain generalizations can be made. For example, a few proteins account for the majority of all the protein and a multitude of proteins—each contributing only a few percent—account for the remainder. Except for a few membrane proteins best exemplified by Na-K ATPase, the majority have not been ascribed a role in membrane function. A large proportion of the dry weight is also accounted for by lipid with a relatively high cholesterol/phospholipid ratio (5). Carbohydrates which are present are in general similar to those which occur in soluble glycoproteins.

The tissue of interest to us in this study is the gastric mucosa. This is a tissue containing several cell types usually identified as surface, mucous neck, parietal, and peptic. Recently we have been able to separate plasma membrane of these cells into two fractions using zonal rotors and Ficoll-sucrose density gradients (6).

In some future time it may be possible to understand the unique function of the gastric mucosa, the capacity to generate and maintain a 10^6-fold concentration gradient of H^+, in terms of the composition and function of the membranes of the constituent cells. A first step is definition of amino acid, lipid, and carbohydrate composition and solubilization and fractionation of its constituent parts. This report characterizes gastric cell

[1] This is paper VII in the series. Paper VI will appear in *BBA Biomembranes* (in press).

[2] Supported by NIH Grants AM08541, AM15878, CA13158 and AM03555; PHS Grant HE13129, and Grant-in-Aid from Smith Kline & French Laboratories of Philadelphia, Pennsylvania. Credit is given to Project No. 8059-01, V. A. Hospital, Birmingham, Alabama.

[3] To whom reprint requests should be addressed.

membranes in terms of amino acid and protein, lipid and carbohydrate composition of the whole membrane and Triton X-100, Brij 36T, and sodium dodecyl sulfate solubilized membranes.

MATERIALS AND METHODS

Preparation of Gastric Membranes

Canine stomachs were obtained from Pel-Freeze Biologicals Inc. (P. O. Box 68, Rogers, AR 72756) or fresh in our own laboratory. The fresh stomachs were removed immediately on sacrifice of the animals. Contents were washed with tap water, and the stomach was immediately frozen on dry ice; they were stored at −20°C until use. Gastric membranes were prepared by homogenization of the mucosa in 0.25 M sucrose, 40 mM Tris–HCl (pH 7.4), differential centrifugation, and zonal centrifugation using a continuous density gradient made from 7.5% Ficoll/0.25 M sucrose and 37% sucrose as described (6). Membranes collected at 11.5% sucrose (Peak I) and 23% sucrose (Peak II) were then diluted with 40 mM Tris–HCl (pH 7.4) to less than 10% sucrose and centrifuged at 78,000*g* for 60 min to obtain purified gastric cell membrane pellets from either Peak I or Peak II. Absorbance at 280 nm was used to estimate protein peaks in gradient fractions, while the method of Lowry (7), using bovine serum albumin as standard, was used in all other instances.

Analysis of Amino Acids

Samples of membranes from Peak I and Peak II are suspended in 6 N HCl in closed ampules under vacuum and incubated at 106°C for 22 hr. After hydrolysis amino acid composition is determined using a Beckman Model 116 amino acid analyzer and quantitated by standard amino acids subjected to identical hydrolysis and column chromatography (8). Results are expressed as moles % (residue/100).

Determination of Carbohydrate Content of Membranes

The purified membranes (Peak I or Peak II) are extracted three times with a mixture of acetone–H_2O (3:1) or chloroform–methanol (3:1). After each extraction the membranes are centrifuged for 15 min at 2,500 rpm, 4°C (International Centrifuge, Model PR-2). The extracted membranes are suspended in water, dialyzed for 48–72 hr against distilled water with frequent changes of water, and lyophilized. The protein is stored overnight in a desiccator. The dry preparation is weighed and suspended in 0.01 M HCl and digested at 37°C for 16 hr with pepsin (Worthington Biochemical Co., Freehold, NJ) at an enzyme to substrate ratio of 1:200. After digestion material extracted with acetone–H_2O still contains insoluble particles whereas that extracted with chloroform–methanol is clear. Results reported, therefore, were derived from the chloroform–methanol extracted membranes.

Determination of sialic acid. The pepsin digest is analyzed for sialic acid by the method of Warren (9) following hydrolysis for 45 min in 0.038 M H_2SO_4. The presence of unextracted fatty acids necessitates use of anion exchange chromatography AG1-X8 (Bio Rad) on columns 7 × 48 mm on which the recovery of sialic acid is 85–92%. The column is eluted with H_2O until all protein is eluted (12 ml); sialic acid is then eluted with 0.3 M formic acid. Both fractions are lyophilized. Sialic acid is measured (9) and is compared to sialic acid standards exposed to the same hydrolysis and chromatography.

Determination of fucose, hexoses, and hexosamines. The pepsin digested membranes are pipetted into 3 acylation tubes (Regis Chemical Co., Rockford, IL), each containing about 3 mg of protein. HCl is added so that final concentration is 1 M in the total volume of 5 ml. The tubes are sealed and hydrolyzed for 1, 4, and 10 hr at 100°C. One-hour hydrolysate is used for determination of fucose, 4-hr hydrolysate for mannose and galactose, and 10-hr. hydrolysate for hexosamines.

After hydrolysis the internal standard solution containing 0.125 μmole of arabinose (Calbiochem) and 0.25 μmole of mannosamine–HCl (Pfanstiehl Labs., Inc., Waukegan, IL) is added to all samples. The hydrochloric acid is removed by anion exchange chromatography (AG1-X8 resin in bicarbonate form), and sugars are reduced overnight with sodium borohydride (0.1 mg/ml) at 4°C. The excess of borohydride is then destroyed by addition of HCl, and the solution is lyophilized to dryness. Borates are removed as the methyl borates by 6× repeated evaporation with 2 ml of methanol. The mixture of alditols is converted to alditol acetates by heating with 0.2 ml acetic acid anhydride–pyridine (1:1) in sealed tubes at 100°C for 15 min (10). The neutral sugars are chromatographed on 6 ft × ¼ in. glass columns packed with 0.2% polyethylene glycol succinate, 0.2% polyethylene glycol adipate, and 0.4% silicone XF-1150 on 100/120 mesh Gas Chrom P (Applied Science Laboratories, State College, PA). From the initial 140°C, the temperature is increased at the rate of 5°C/min. Hexosamines are chromatographed in the same glass columns packed with 3% Poly A103 (Applied Science Laboratories). The starting temperature of 160°C

is programmed to 260°C at a rate of 5°/min. An F & M Model 402 dual column gas chromatograph with flame ionization detectors (Hewlett Packard Corp., Avondale, PA) and an Infotronics Model CRS 104 electronic integrator (Infotronics Inc., Houston, TX) is used.

Analysis of Lipids

Membranes designated Peak I and Peak II and mitochondrial fraction (Peak III) are diluted to 8.6% sucrose with 40 mM Tris–HCl (pH 7.4) and pelleted in a Beckman No. 30 rotor at 78,000*g* for 1 hr. The pellets are resuspended in distilled water. Each peak is treated individually.

Extraction of lipids is carried out as follows: To 5 ml of suspended membrane (10–15 mg protein) 100 ml of chloroform–methanol (2:1, v/v) are added. After overnight extraction the protein residue is filtered and rinsed with 20 ml of chloroform–methanol. The total extract is partitioned against an equal volume of 0.15 M NaCl. The lower phase is collected, dried over Na_2SO_4, filtered, and evaporated to dryness in a vacuum. The lipid is then diluted with chloroform to a known volume for analysis. Cholesterol is determined by the method of Zak (11) and lipid phosphorus by the method of Bartlett (12).

Thin-layer chromatography is carried out on silica gel plates (Quanta Industries). For neutral lipids the solvent is petroleum ether (30–60°C)/ethyl ether/acetic acid (146:43:2). For phospholipids three solvent systems are used: chloroform/methanol/water (65:25:4) for the separation of cardiolipin and phosphatidic acid; chloroform/methanol/58% ammonium hydroxide (65:25:4) for the separation of phosphatidylserine and phosphatidylinositol, and chloroform/methanol/acetic acid/water (100:50:16:8) for the separation of lysolecithin, sphingomyelin, lecithin, and phosphatidylethanolamine. For quantitation the methods of Skipski are used (13). All samples are compared to mixtures of known standards. Iodine vapor, ninhydrin, and H_2SO_4 plus charring are used for detection. Gas chromatography is performed as previously described (14).

Solubilization of Membranes

Triton X-100 or Brij 36T. Peak I or II membranes obtained as described above are resuspended in 8 mM Hepes, 4 mM NaCl (pH 7.4) to a concentration of approximately 2 mg/ml. An equal volume of 8 mM Hepes, 4 mM NaCl (pH 7.4) containing 6 mg/ml of Triton X-100 or Brij 36T (3:1 detergent to protein ratio) is added. Thus final concentrations are 1 mg/ml protein, 3 mg/ml Triton X-100 or Brij 36T, 8 mM Hepes, 4 mM NaCl (pH 7.4).

The membrane suspension is incubated for 60 min with magnetic stirring at 0°C. The suspension is then centrifuged at 100,000*g* × 60 min. The supernate represents the solubilized membrane protein and is clear to slightly opalescent. Adenosine triphosphatase and adenosine monophosphatase activity rises during the first 24–48 hr and then remains stable for at least 2 weeks when stored at 4°C.

SDS[4] *solubilization.* Membranes are resuspended in 40 mM Tris–HCl or Hepes (pH 7.4) in a concentration of approximately 1 mg/ml. Six percent SDS is added to a final concentration of 1% SDS, and the suspension is incubated at 37°C for 2 hr.

Alternatively we have incubated for 3, 5, and 10 min with and without 2-mercaptoethanol in a boiling water bath followed by 2 hr at 37°C. Boiling immediately after addition of SDS does not change the subsequent number or mobility of protein bands. 2-Mercaptoethanol in the incubation mixture causes a decrease in only one band. Hence we have used 1% SDS final concentration and omitted 2-mercaptoethanol. The membranes are completely solubilized by this treatment, and ATPase and AMPase activity is reduced to nondetectable levels.

Polyacrylamide Gel Electrophoresis

Solubilized membranes are fractionated on polyacrylamide gels 5 mm × 90 mm. A 3.5% stacking gel is prepared in 100 mM Tris–HCl (pH 6.8) by polymerization using dimethylaminopropionitrile and ammonium persulfate. Separating gels are 7% acrylamide prepared in 0.4 Tris–HCl (pH 8.6). In each gel 2.5% of the acrylamide is *N*,*N*-methylenebisacrylamide. Reservoir buffer is 0.75 M glycine adjusted to pH 8.6 with solid Tris base. Samples applied are usually 50–100 μl (50–100 μg), and the volume of the stacking gel is adjusted to equal the sample volume. Electrophoresis is done at 2 mA/tube. Gel and reservoir buffers contained 1% sodium dodecyl sulfate, or 0.1% Triton X-100, or 0.1% Brij 36T.

Staining of Gels

Gels are stained for proteins, carbohydrates, and lipids. Gels for protein are stained 18 hr in 0.25% Coomassie Blue in 9% acetic acid, 50% methanol, and destained for 48 hr in a solution containing 7.5% acetic acid, 5.0% methanol.

Gels for lipids are stained in Oil Red O prepared from a saturated solution in methanol

[4] Abbreviations used: SDS, sodium dodecyl sulfate; Hepes, *N*-2-hydroxyethylpiperazine-*N*′-2-ethanesulfonic acid; TCA, trichloroacetic acid.

diluted with an equal volume of 12.5% trichloroacetic acid (TCA) at the time of use. After 24 hr gels were placed in 50% methanol/6.25% TCA. Each 12 hr the solution is changed, and each new solution contained ½ the methanol concentration of the previous solution. In this way the gels which shrank greatly during staining progressively rehydrate and return to original size.

To confirm that Oil Red O staining was dependent on lipid content and not upon protein–SDS complexes we used native bovine serum albumin and fat-free bovine serum albumin. The former after electrophoresis in 1% SDS stained positively for lipid, while the latter did not stain with Oil Red O.

Gels for carbohydrates are fixed in 12.5% TCA for 60 min, briefly washed in water, and placed in a solution of 1% periodic acid in 3% acetic acid for 2 hr. The gel is then washed in 200 ml deionized H_2O for 18 hr. Thereafter it is placed in a Schiff reagent prepared according to Korn (3). After 18 hr the gel is placed in 1.5% sodium metabisulfite. During the first 60 min in the Schiff reagent bands appeared. Sodium dodecyl sulfate gels become progressively stained over several hours. With continued incubation in the sodium metabisulfite the gels destain except for the bands which were originally seen. In gels containing Triton X-100 or Brij 36T bands appear but the gels do not become totally stained. Suspecting some nonspecific periodic acid Schiff (PAS) staining, we used a 24-hr wash (100 ml/gel, changed 3 times) in 7% acetic acid to remove the detergent. After subsequent reaction with PAS, washing, and reacting with Schiff reagent, there was no difference in the number of bands or the position on the gels. Therefore we have avoided the prolonged initial wash in these studies.

ATPase and AMPase Assays on Soluble Enzymes and Enzymes in Suspension

Mg^{2+}- and HCO_3^--stimulated ATPase activity and AMPase activity are assayed by methods previously described (6, 15), and P_i released is measured by the method of Yoda and Hokin (16).

ATPase Assays on Gels

After electrophoresis the gel is incubated for 2 hr at 37°C in a solution containing 3 mM ATP, 3 mM Mg^{2+}, 20 mM $NaHCO_3$, 40 mM Tris–HCl (pH 7.4). After completion of incubation the gel is washed 3 times with water and placed in staining solution based on the Fisk–Subbarow method (17). The solution contains H_2O, 10% TCA, 4.5% ammonium molybdate, 1,2,4-aminonaphthalsulfonic acid solution (50:30:10:4). The band of ATPase activity develops a blue color over a period of ½–2 hr; after many hours the entire gel gradually develops a deep blue color.

AMPase Assay on Gels

AMPase activity in the polyacrylamide gel is demonstrated by incubating the gel in 40 mM Hepes (pH 7.4) containing 3 mM AMP and 3 mM $MgCl_2$. Incubation at 37°C is continued for 3–5 hr. Phosphate released is demonstrated as described above for ATPase activity in gels.

Scanning of Gels

Absorbance of the gels is measured on a Gilford 2400 spectrophotometer equipped with a gel scanner and connected to a graphic recorder. Coomassie Blue is scanned at 550 nm, Oil Red O at 525 nm, and periodic acid Schiff at 560 nm. Gels stained for ATPase and AMPase activity are scanned at 660 nm.

RESULTS

Preparation of Membranes

Figure 1 shows the distribution of Mg^{2+}- and HCO_3^--ATPase, AMPase, succinic dehydrogenase, lactic dehydrogenase; protein is estimated by the absorbance at 280 nm, and the density of the Ficoll–sucrose gradient is expressed as percent sucrose. The region of 11.5% sucrose contains a prominent peak of protein, ATPase activity, and particularly AMPase activity. This region is designated Peak I hereafter. The protein peak at 23% sucrose is enriched with Mg^{2+}- and HCO_3^--ATPase to a greater extent than AMPase. This region is hereafter designated Peak II. It is important that Peak I and Peak II are free of contamination by mitochondria as assessed by absence of enzyme markers (succinic dehydrogenase and monoamine oxidase) and by electron microscopic morphology (6). Previous studies (6, 15) have shown these membranes to be free of detectable contamination by nuclear membrane or endoplasmic reticulum. The morphology is that of membranous structures, either vesicles, sheets, or syncytial configuration. Peak III at 37% sucrose is enriched with ATPase and AMPase probably reflecting the presence of some membranes. More important, this region of the gradient is the site of mitochondrial marker enzymes: succinic dehydrogenase and monoamine oxidase.

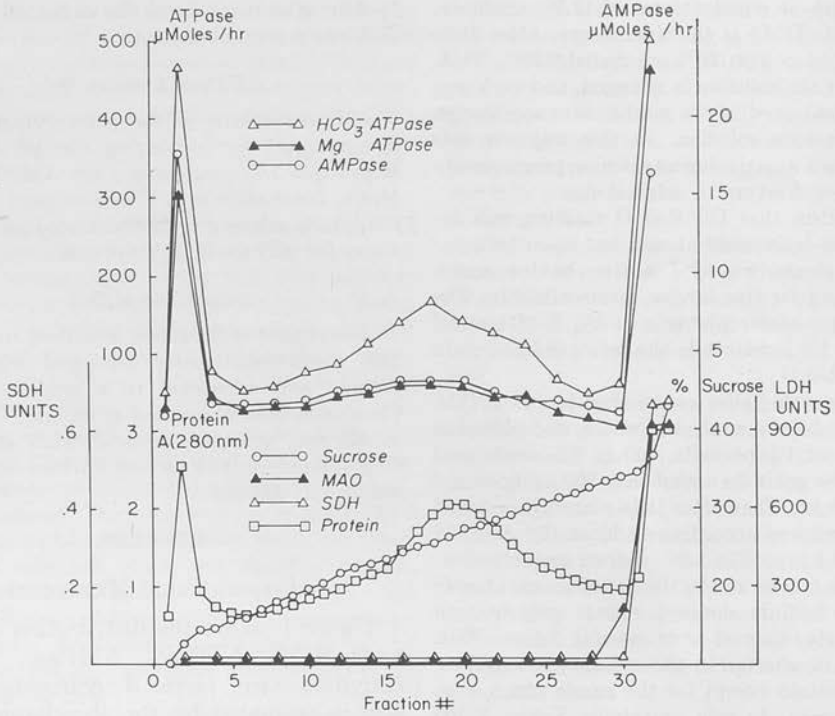

FIG. 1. Fractionation of gastric cell membranes (microsomal pellet) by isopycnic zonal centrifugation on a density gradient prepared from 7.5% Ficoll in 0.25 M sucrose and 37% sucrose. The protein peak at 11.5% sucrose is designated Peak I, the protein peak at 23% sucrose is called Peak II, and the peak at 37% sucrose containing succinic dehydrogenase and monoamine oxidase activities is designated the mitochondrial peak or Peak III.

Amino Acid Composition

The amino acid composition (Table I) is very similar in Peak I and Peak II. Glutamic acid is the most plentiful amino acid in both membrane fractions. There is as well no difference in the content of basic amino acids. Serine is slightly more abundant in the membrane of Peak I than Peak II.

Lipid Composition

The lipid composition of membrane Peaks I and II and the mitochondrial peak is summarized in Table II. Free cholesterol and free fatty acids are the only neutral lipids in each fraction. No glycerides are detectable on thin-layer chromatography. Peaks I and II contain phosphatidylethanolamine, phosphatidylcholine, and sphingomyelin as the principal phospholipids. Trace amounts of phosphatidyl serine and phosphatidylinositol are present as well. Distribution of the phospholipids of Peaks I and II are given in Table III. Peak III differs in that the major phospholipids were cardiolipin, phosphatidylethanolamine, and phosphatidylcholine, with the others present in only small amounts.

Peak I contains more phospholipid and cholesterol (Table IV) than either Peak II or the mitochondrial peak (III), and the percent of total lipid as phospholipid is slightly greater than the more dense Peak II membrane whose isopycnic density is about 1.095.

Analysis of the fatty acid composition reveals that saturated fatty acids compose 42.5% in Peak I and 39.9% in Peak II. The predominant fatty acids in both membrane fractions are palmitic, followed by oleic and then linoleic acids. We have not, as yet, quantitatively examined the lipid composition of detergent solubilized protein fractions from these membranes.

TABLE I

AMINO ACID COMPOSITION OF GASTRIC MEMBRANES[a]

	Peak I (*mole %*)	Peak II (*mole %*)
Lys	7.01	7.55
His	2.18	2.18
Arg	4.86	5.04
Asp	9.24	9.72
Glu	10.5	11.3
Thr	5.57	5.67
Ser	9.51	8.07
Pro	5.15	5.10
Gly	9.51	7.90
Ala	7.31	7.60
½Cys	0.77	1.07
Val	5.70	6.01
Met	1.40	1.65
Ile	4.50	4.44
Leu	9.53	9.84
Tyr	2.63	2.79
Phe	4.64	4.09

[a] Peak I or Peak II membranes are suspended in 6 N HCl and hydrolyzed for 22 hr at 106°C in closed ampules under vacuum. Amino acid analysis is performed on a Beckman Model 116 amino acid analyzer.

Carbohydrate Composition

Mucus, a complex glycoprotein, represents a potential contaminant which could be adsorbed. The use of the "Parr bomb" for disruption of the tissue enables much mucus to be removed before fractionation by differential centrifugation. Pellets obtained subsequently are not mucoid in character. The carbohydrate composition of the membranes from Peaks I and II are given in Table V. Membranes isolated at 23% sucrose contain approximately twice the carbohydrate/mg protein of Peak I. The single exception is glucose.

Initial efforts to quantitate sialic acid resulted in an interfering yellow color probably arising from unsaturated fatty acids. This requires anion exchange chromatography prior to colorimetric analysis.

The repeated analysis of different membrane preparations gives reproducible results for all the carbohydrates except galactose and glucose. The galactose:mannose ratio in Peak I after extraction with acetone–H_2O is 2.89, while after extraction with chloroform–

TABLE II

SUMMARY OF LIPID COMPOSITION OF GASTRIC MEMBRANES AND MITOCHONDRIA[a]

	Fraction[b]		
	I	II	III
Cholesterol			
free	++	++	++
esterified	trace	trace	ND
Glycerides			
mono	ND	ND	ND
di	ND	ND	ND
tri	ND	ND	ND
Free fatty acids	+	+	+
Phosphatidic acid	ND	ND	ND
Cardiolipins	ND	ND	++
Phosphatidylethanolamine	+++	+++	+++
Phosphatidylserine	trace	trace	trace
Phosphatidylinositol	trace	trace	trace
Phosphatidylcholine	++++	++++	++++
Sphingomyelin	+	+	+
Lysolecithin	ND	ND	ND

[a] ND, not detected. Phosphatidylserine and phosphatidylinositol were not sufficiently separated for identification. Values are arbitrary and based on the darkness of the spot after H_2SO_4 plus charring.

[b] I refers to membranes isolated at 11.5% sucrose, II to membranes isolated at 23% sucrose, and III to the mitochondrial fraction at 37% sucrose.

TABLE III

DISTRIBUTION OF PHOSPHOLIPIDS IN MEMBRANE FRACTIONS[a]

	% Distribution			
	PE	PC	Sphingo	Other
Fraction 1	32.8	55.8	7.4	3.9
Fraction 2	30.4	57.4	7.6	4.6

[a] Phospholipids are extracted from each membrane fraction with chloroform–methanol (2:1) as described under Methods. The various phospholipids are fractionated by thin layer chromatography and quantitated by the methods of Skipski (13). PE refers to phosphatidylethanolamine, PC to phosphatidylcholine, sphingo to sphingomyelin, and Other to the total of phosphatidylserine, phosphatidylinositol, lysolecithin, and all other areas of the plate not containing identified compounds.

TABLE IV

PHOSPHOLIPID AND CHOLESTEROL CONTENT OF GASTRIC MEMBRANES AND MITOCHONDRIA[a]

	A (μmole lipid P/mg protein)	B (μmole cholesterol/ mg protein)	B/A
Fraction 1	0.70	0.54	.77
Fraction 2	0.25	0.28	1.12
Mitochondria	0.18	0.13	.72

[a] Lipids are extracted with chloroform–methanol (2:1) as described in Methods. Lipid phosphorous is determined by the method of Bartlett (12) and cholesterol by the method of Zak (11). B/A indicates the cholesterol:phospholipid ratio.

TABLE V

CARBOHYDRATE COMPOSITION OF GASTRIC CELL MEMBRANE PROTEINS[a]

	Carbohydrate composition	
	Peak I (nmoles/mg protein)	Peak II
Fucose	16.4	31.1
Mannose	47.8	92.4
Galactose	94.0	189
Glucosamine	63.6	138
Sialic acid	13.9	24.2
Glucose	231	306

[a] Carbohydrates are determined as indicated in methods on the chloroform–methanol (3:1) extracted membranes. Peak I refers to the membranes isolated at 11.5% sucrose and Peak II to those isolated at 23% sucrose.

methanol it drops to 1.96. The same galactose:mannose ratio (1.96) is found after the acetone–water extracted membranes are subjected to anion exchange chromatography before hydrolysis. This suggests that lipids adsorbed to the anion exchange resin contain a carbohydrate moiety rich in galactose. The glucose content of different membrane preparations varies irreproducibly, indicating that at least in part glucose may be derived from the sucrose used in the density gradient. The absence of fructose is expected even if sucrose had been incompletely removed, since during conversion of the hexoses to alditols the glucose and fructose will become identical.

Polypeptide Composition

SDS solubilization. Sodium dodecyl sulfate proved to be the best detergent in terms of disaggregation of the membrane polypeptides of both Peaks I and II. Complete solbuilization can be achieved as defined by optical clarity and absence of any visible pellet following centrifugation in an SW-39 rotor (g_{max} 134,000) for 60 min. In contrast, Triton X-100 or Brij 36T in a 3:1 detergent to protein ratio would solubilize only about 50% of the membrane protein. Figures 2 and 3 show the spectrophotometric scans of

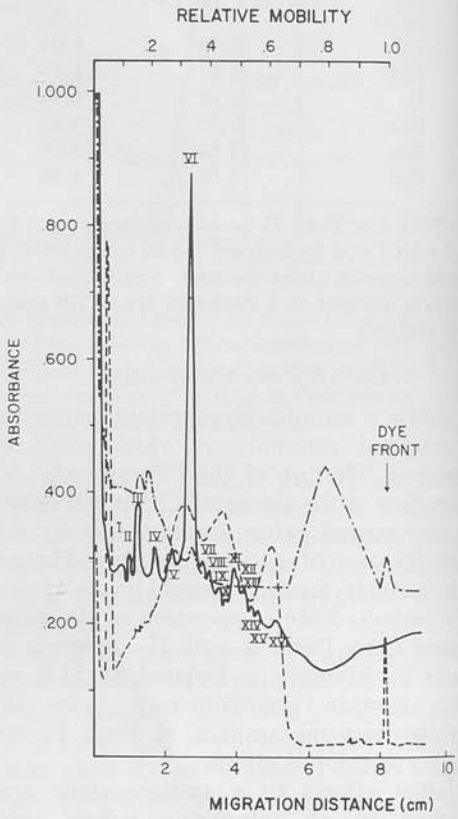

FIG. 2. Scan of 7.0% acrylamide gels used to fractionate Peak I membranes solubilized by 1% sodium dodecyl sulfate. Protein, carbohydrate, and lipid fractionation is on separate gels, and the length has been normalized for inclusion on one graph. Protein was scanned at 550 nm, carbohydrate 560 nm, and lipid at 525 nm. Relative mobility is shown for estimation of molecular weight. Protein (——), carbohydrate (– – –), lipid (-·-·-).

7% acrylamide gel fractionation of SDS solubilized Peaks I and II membrane (Fig. 4), respectively. Gels are stained for protein, lipid, and carbohydrate. The vast majority of protein penetrates the 7% gels, and one polypeptide band predominates. No less than 18 other minor bands can be seen visually or by scanning using a 0.05-mm slit. Figure 5 shows the standard proteins used to estimate molecular weight, and Table VI identifies the molecular weights of the identifiable bands. The predominant band corresponds to a molecular weight of 87,000 daltons in Peak I and 78,000 in Peak II. Of the many other bands none can be considered a major protein, although there is a variation in content. Of particular interest are the lipid and carbohydrate content of these membrane proteins. The carbohydrate staining is quite dissimilar in Peak I and Peak II membranes. Peak I membranes contain a sharp slow-moving band and three bands of intermediate mobility corresponding to molecular weights of 92,000, 46,000, and 22,000; these should be considered maximal molecular weights, since variation in SDS complexing by glycoprotein (4) may reduce mobility and hence overestimate molecular weight (18). An addition band moves at the buffer front. Lipids in Peak I membranes travel in 5 bands also. The largest travels behind the buffer front and is quite broad. There is little evidence of protein or carbohydrate associated with this band. A band travels at the buffer front as well.

In Peak II membranes a doublet band of carbohydrate is present with the major protein band. The most prominent band travelling just behind the buffer front is also the most prominent lipid band. A small protein Peak XVIII appears to be associated. There are two or three additional faint broad lipid bands, one of which corresponds to the major protein band. The poor Coomassie Blue staining properties of some glycoproteins (4) may explain the failure to detect prominent protein peaks with the lipid and carbohydrate. Alternatively, this may represent glycolipid dissociated from protein by the SDS.

Enzymes assays on these gels was not possible, since SDS inactivates the gastric Mg^{2+}- and HCO_3^--ATPase.

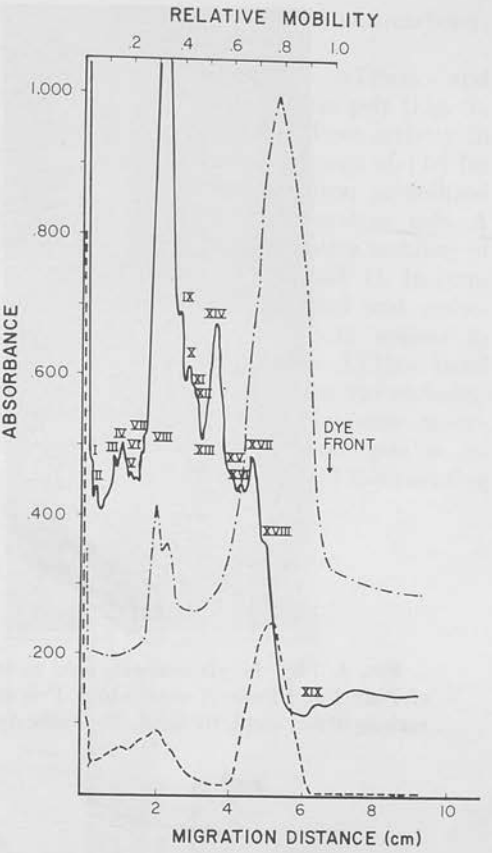

FIG. 3. Scan of 7.0% acrylamide gels used to fractionate Peak II membranes solubilized in 1% sodium dodecyl sulfate. Protein, carbohydrate, and lipid fraction is done on separate gels, and the length has been normalized for inclusion in one graph. Relative mobility is indicated. Protein (——), carbohydrate (– – –), lipid (–·–).

Triton solubilized membranes. Membranes solubilized by nonionic detergents, Triton X-100, and Brij 36T, are of interest since Mg^{2+}- and HCO_3^--ATPase and AMPase retain activity and appear in the 100,000*g* supernate.

Figures 6 and 7 show the scans for protein, lipid, and carbohydrate from 0.1% Triton X-100 gels of Peak I and Peak II membranes (Fig. 8), respectively. The majority of material is located in the upper portion of the gel or at the surface of the separating gel. Most likely, poor disaggregation and high

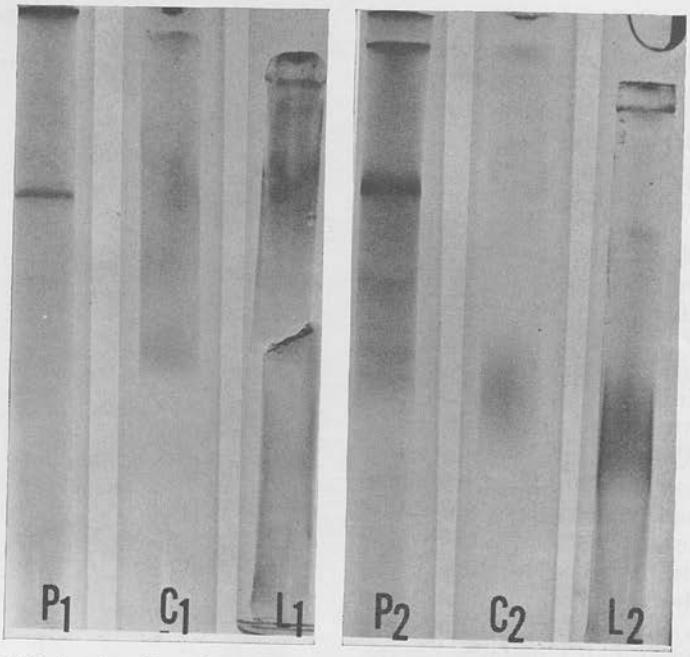

FIG. 4. 7.0% Acrylamide gels used to fractionate the protein, carbohydrate, and lipid of Peak I and Peak II membranes. P is stained for protein with Coomassie Blue, C for carbohydrate, and L for lipid. The subscript refers to Peak I or Peak II membranes.

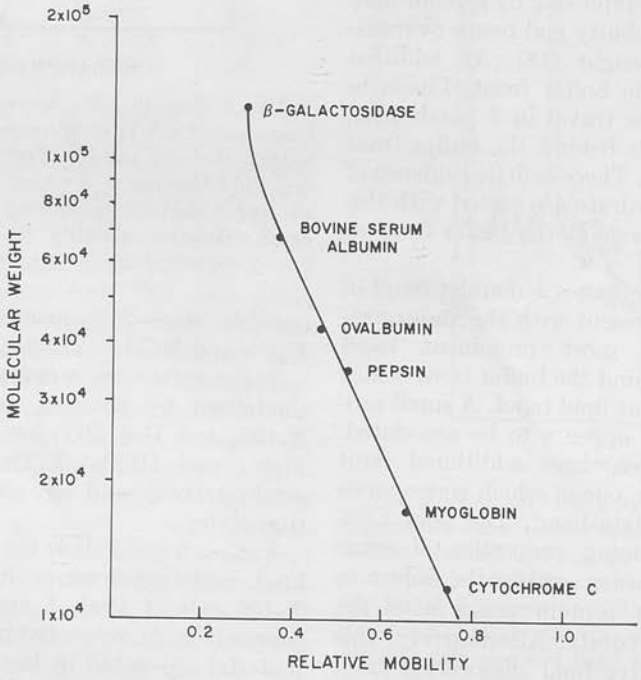

FIG. 5. Standards and their relative mobility on 7.0% acrylamide gels in 1% sodium dodecyl sulfate used to estimate molecular weight of polypeptide bands of 1% SDS solubilized membranes from Peak I and Peak II.

TABLE VI

MOLECULAR WEIGHTS OF COMPONENT PROTEINS

Protein band	Peak I	% Composition	Peak II	% Composition
I	↓	5.9	↓	1.9
II	↓	5.3	↓	3.0
III	>130,000	5.6	>130,000	5.9
IV	↓	4.6	↓	5.2
V	↓	10.5	↓	2.9
VI	87,000[b]	29.6	↓	3.1
VII	70,000	5.9	↓	1.5
VIII	60,750	5.0	78,000[b]	29.0
IX	53,000	3.7	62,000	5.0
X	46,750	3.0	52,500	4.1
XI	40,500	6.0	49,000	4.7
XII	38,600	3.0	46,250	3.4
XIII	35,250	3.4	38,000	11.1
XIV	30,000	2.6	31,250	4.1
XV	28,000	2.2	23,500	3.6
XVI	20,250	3.7	19,250	4.6
XVII			16,000	2.2
XVIII			14,000	4.2
XIX			11,000	0.4

[a] Gastric membranes are solubilized in 1% SDS and fractionated on 7.0% acrylamide gels. Relative mobility of a protein is used to compare its molecular weight with that of standard proteins (Fig. 6) of known molecular weight.

[b] The major peak on each gel.

molecular weight explains this finding but small negative charge is possible. As in the SDS gels one protein peak clearly predominates and would again appear to differ in molecular weight or charge in the two fractions. In addition, there are several rapidly moving bands, one of which migrates at or just in back of the buffer front. The band is not an electrophoretic artifact since gels run without sample show no such band.

The lipid and carbohydrate bands are more prominent and fewer in number when nonionic detergents are used for solubilization. Some material is present atop the gel, but in addition 2 bands which enter the gel coincide for both carbohydrate and lipid staining.

The major band would appear to be of high molecular weight (relative mobility = 0.15 and 0.11, Peak I and Peak II, respectively), but as in the SDS gels is not associated with a clearly defined protein band. The protein band travelling at the buffer front stains as well for lipid and carbohydrate.

The characteristics of ATPase and AMPase were studied on these gels (Fig. 9). There are two bands of ATPase activity in Peak I and Peak II gels. The first and by far the most prominent in Triton solubilized membranes is atop the separating gels. A second, minor band has a relative mobility of 0.13 in Peak I and 0.17 in Peak II. In comparing ATPase gels with lipid and carbohydrate gels the bands would appear to migrate together, though the ATPase band is considerably narrower than the carbohydrate and lipid bands. Adenosine monophosphatase activity on these gels is restricted to the very top of the 7% separating

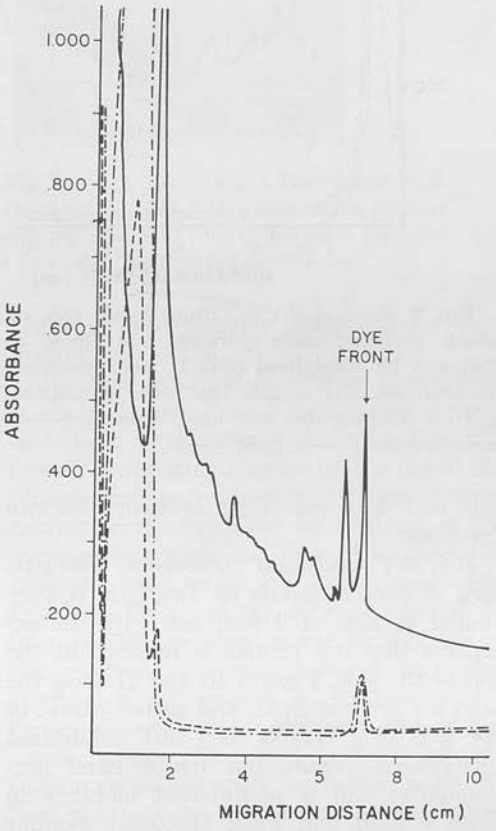

FIG. 6. Scan of 0.1% Triton X-100 gels on which proteins, carbohydrates, and lipids in Triton X-100 solubilized Peak I membranes are fractionated. Gel length has been normalized and no tracking dye was used. Protein (——), carbohydrate (– – –), lipid (–·–).

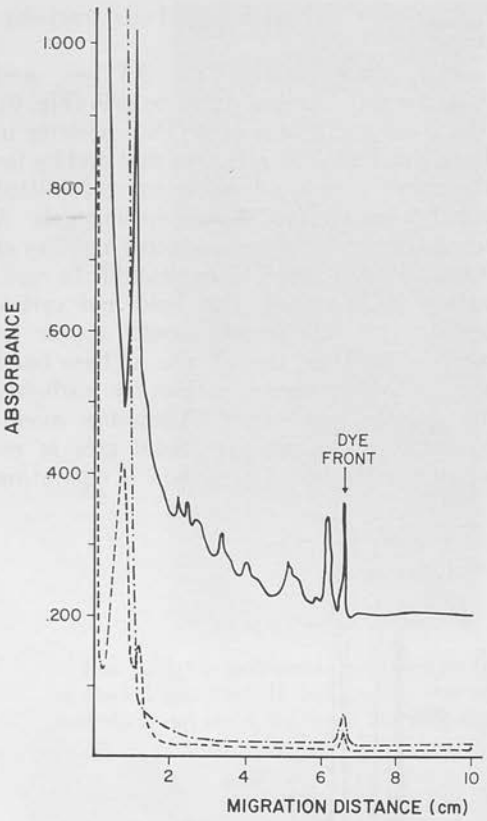

FIG. 7. Scan of 0.1% Triton X-100 gels on which proteins, carbohydrates, and lipids in Triton X-100 solubilized Peak II membranes are fractionated. Gel length has been normalized, and no tracking dye was used. Protein (——), carbohydrate (– – –), lipid (-·-).

gels and does not differ between the two fractions.

Brij 36T solubilized membranes. The pattern of protein bands on Brij gels is very similar to that of Triton gels with the exception that less protein is retained at the top of the gels. Figures 10 and 11 show the scan for protein, lipid, and carbohydrate of the gels (Fig. 12) of Brij 36T solubilized membranes. Again, one major band predominates and is of different mobility in Peak I (0.5) and Peak II (0.25). Similar bands travel at and just in back of the buffer front. The major peaks of lipid and carbohydrate coincide and are of lesser mobility than the major protein peak. There is a protein peak which coincides with the lipid and carbohydrate, but on protein gels this is not well separated from the material atop the gels. A second quite minor peak is present and a third is at the buffer front.

Analysis of ATPase and AMPase activity on these gels gave results quite different from that on the Triton X-100 gels. On Brij gels AMPase activity was located atop the separating gels (Figure 13) in both Peak I and Peak II, showing that the AMPase is of high molecular weight. No ATPase activity was found atop the gels. The bands of ATPase activity were of differing mobilities in Peak I (0.19) and Peak II (0.14). The band in Peak II is broader than that of Peak I, indicating perhaps more heterogeneity of Peak II ATPase.

In none of our gels does the ATPase travel as a discrete band. This, however, may be due to the method of detection. It seems reasonable to assume that the diffusion of liberated PO_4 is equal in all directions, and the central portion is the ATPase band. In Figs. 10 and 11 the arrow indicates the protein bands corresponding to the central region of ATPase staining.

DISCUSSION

Principal questions which have been posed by study of membranes are (a) the presence of structural polypeptides common to membranes in general in a variety of cells, (b) the nature and function of the lipid and carbohydrate associated with these polypeptides, and (c) the role of functional units and the general occurrence of these functional units in membranes. We have approached some of these questions in the gastric mucosa where we can achieve some separation of membranes based on relative enrichment with HCO_3^--ATPase or AMPase. Electron microscopic studies have shown HCO_3^--ATPase to be localized at the luminal surface of the acid-secreting cell. On a functional basis the luminal and basal membranes must be quite different. The luminal membrane must be able to generate and withstand an H^+ concentration as great as 0.1 M and a concentration gradient of 10^6; this is not the case for the basal membrane. We would assume its composition would in some way reflect this property. In this study

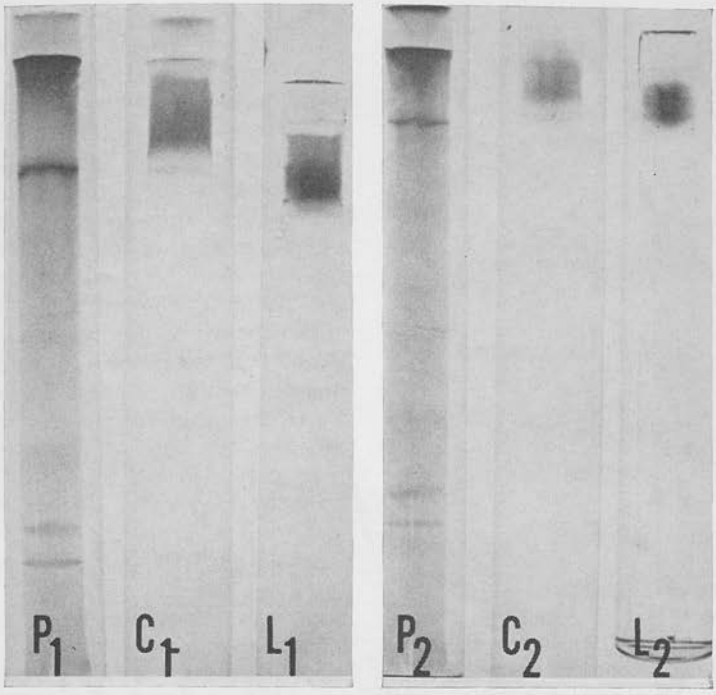

FIG. 8. 7.0% Acrylamide gels containing 0.1% Triton X-100 on which Peak I and Peak II Triton X-100 solubilized membranes were fractionated. Gel P was stained for protein with Comassie Blue, gel C for carbohydrate with periodic acid Schiff, and gel L for lipid with Oil Red O. The subscript refers to Peak I or Peak II solubilized membranes.

we have shown differential composition of two membrane fractions isolated from dog gastric mucosa.

This differential composition was first shown fractionating the protein bands by SDS gel electrophoresis. Particularly, the molecular weight of the principal protein band is different in the two membrane fractions. The number of bands present in membranes of Peak II is significantly greater than that of Peak I. Also, inspection of the spectrum of molecular weights estimated by mobility on the SDS gels shows few that are identical in the two membranes. Each membrane has a single polypeptide which is predominant, but of clearly differing molecular weights.

The amino acid composition is very similar to that reported for erythrocyte (20), liver (19), and Ehrlich ascites cell (21) membranes. The most abundant amino acid is glutamic acid, and there is no increase in the basic amino acid which could give the membrane a fixed positive charge and reduce proton permeation.

The lipid composition of these membranes is also different. Peak I membranes contain more lipid by a factor of about 2.5. This difference is accounted for by both a rise in the phospholipid and cholesterol; the membranes cannot be distinguished by analysis of the various phospholipids. Table VII gives the percent composition of both membrane fractions. Origin of the ATPase of Peak II from plasma membranes has been based on the electron microscopic morphology and absence of the mitochondrial marker enzymes: succinic dehydrogenase and monoamine oxidase. The lipid analyses confirm these conclusions, since cardiolipin is absent from this fraction and the cholesterol/phospholipid ratio is greater than that generally reported for mitochondria. The lipid composition of gastric membranes differs markedly from that reported for liver cell membranes (22, 23) in that gastric cell

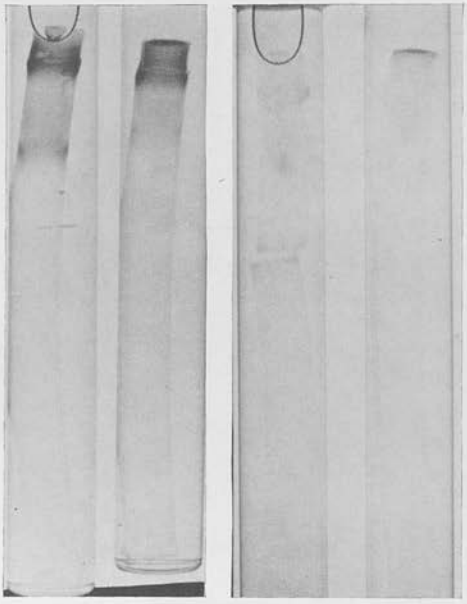

FIG. 9. Migration of ATPase (left) and AMPase (right) activities on 7.0% acrylamide gels in 0.1% Triton X-100. Sample applied was Triton X-100 solubilized membrane protein from Peak I (the left one of each set) or Peak II (the right one of each set).

membranes have high concentrations of phosphatidylethanolamine and phosphatidylcholine and low concentrations of phosphatidylserine, phosphatidylinositol, and sphingomyelin. The fatty acid composition—40% are saturated—also differs from that reported for liver plasma membranes which are highly saturated (22, 23).

The high cholesterol content of our mitochondrial material is best explained by contamination by cell membranes. The presence of AMPase in this region of the density gradients is in support of this interpretation.

On the basis of the electrophoresis studies in Triton X-100 or Brij 36T the vast majority of lipid would appear to be associated with the same proteins which contain carbohydrate. They would appear to be large molecular weight species. Whether the largest band is one or a variety of proteins is not clear, but no discrete bands can be visualized on gels stained for lipid.

The possibility remains that the majority of carbohydrate and lipid is associated with a single protein based on the Triton X-100 and Brij 36T gels. In contrast, SDS gels of Peak I and Peak II show 6 and 3 lipid peaks and 5 and 4 carbohydrate peaks, respectively, a pattern much more complex than the nonionic detergent gels. The number of proteins from which these bands are derived is undefined, since several proteins of similar molecular weights and charges could produce the pattern of lipid and carbohydrate seen on the Triton X-100 and Brij 36T gels.

In contrast to the lipid composition where Peak I membranes are richest, Peak II membranes are richest in carbohydrates. Forte (24), studying the electron microscopic

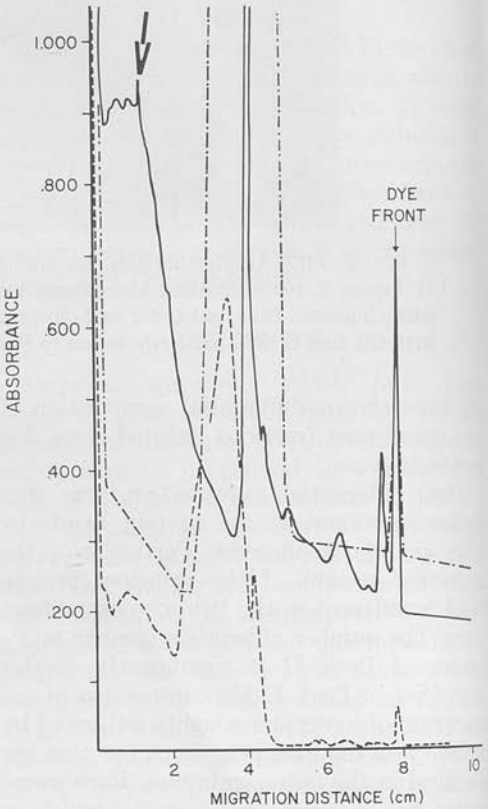

FIG. 10. Scan of 7.0% acrylamide gels in 0.1% Brij 36T used to fractionate protein, carbohydrate, and lipid solubilized by treatment of Peak I membranes with Brij 36T at a Brij:protein ratio of 3 to 1. Gel length has been normalized. No tracking dye was used. The arrow indicates the protein peak corresponding in mobility to the central portion of ATPase staining. Protein (——), carbohydrate (– – –), lipid (–·–).

histochemistry of the frog gastric mucosa, found that the outer aspect of the apical cell membranes and the inner surface of the intracellular canaliculi or vesicles stained intensely for carbohydrate, while the lateral and basal cell membranes were virtually unstained. It is relevant that the Peak II membrane is also relatively enriched with HCO_3^--ATPase, which by electron microscopic histochemistry is also located at the lumenal cell surface. The role of carbohydrate is unclear; the mechanism whereby carbohydrate would protect the membrane from denaturation by acid and digestion is also unclear.

It is particularly interesting that on gels stained for carbohydrate there are at most 3 bands, one of which is clearly major. In each case, lipid and carbohydrate are associated. The major band probably has a high carbohydrate content based on its poor Coomassie Blue staining properties. To date it is not clear that this is a single glycolipoprotein or whether it is a complex mixture of very similar molecular weight and charge. Glossman and Neville (25) studying various cell membranes from the rat found more heterogeneity of carbohydrate distribution. Still in their study a few bands represented the majority of carbohydrate; they found as well 3 glycopeptides common (based on similar molecular weight) to the liver, erythrocyte, and renal brush border membranes. Between the two membrane fractions isolated from the stomach, the band at the buffer front is the only glycopeptide in common. Glossman (25) found a similar band in cell membranes from several rat tissues; Lenard (26), studying erythrocyte membranes, confirmed that this band was a glycolipid, but found little associated protein.

The ATPase of the gastric membranes has different mobilities in Peaks I and II. The ATPase is in that region of the gel which stains intensely for lipid and carbohydrate, but the lipid and carbohydrate content of the ATPase remains unknown. Additionally, it would appear that the ATPase represents a small fraction of protein which is solubilized by Brij 36T. Solubilization by Triton X-100 results in an ATPase of quite large molecular weight which penetrates only a few millimeters of gel. Using either nonionic deterent, AMPase remains of large molecular weight and essentially does not enter the 7% gels.

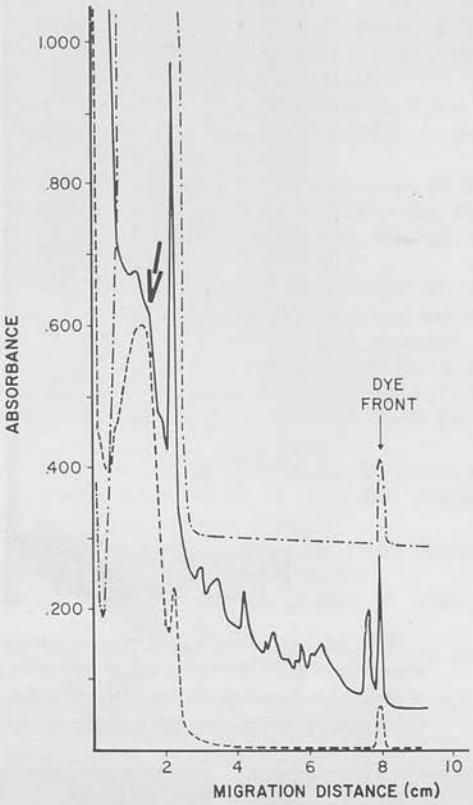

FIG. 11. Scan of 7.0% acrylamide gels in 0.1% Brij 36T used to fractionate protein, carbohydrate, and lipid solubilized by treatment of Peak II membranes with Brij 36T at a Brij:protein ratio of 3 to 1. Gel length has been normalized. No tracking dye was used. The arrow indicates the protein peak corresponding in mobility to the central portion of ATPase staining. Protein (——), carbohydrate (– – –), lipid (–·–).

The two membrane peaks obtained from gastric mucosa thus differ significantly in a number of properties. Peak I has an isopycnic density of 1.04, whereas Peak II has a density of 1.095. The peptide composition of the two peaks is also dissimilar based on SDS gel electrophoresis, although the amino acid composition is not significantly different. The carbohydrate content of Peak II is twice that of Peak I, whereas the

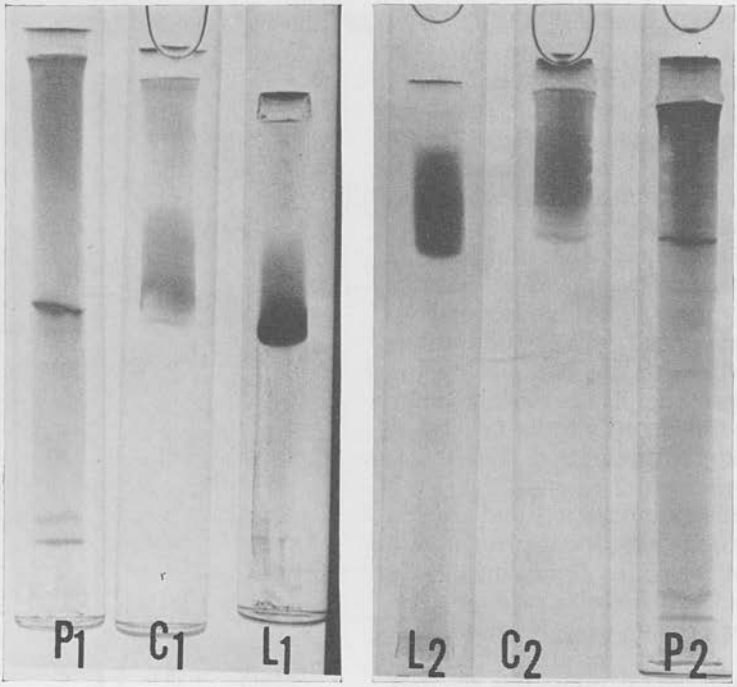

FIG. 12. 7.0% Acrylamide gels containing 0.1% Brij 36T on which the Brij 36T solubilized membranes were fractionated. P indicates gels stained for protein with Commassie Blue, C is stained for carbohydrate with periodic acid Schiff and L for lipid with Oil Red O. The subscript indicates the origin of the protein from Peak I or Peak II membranes.

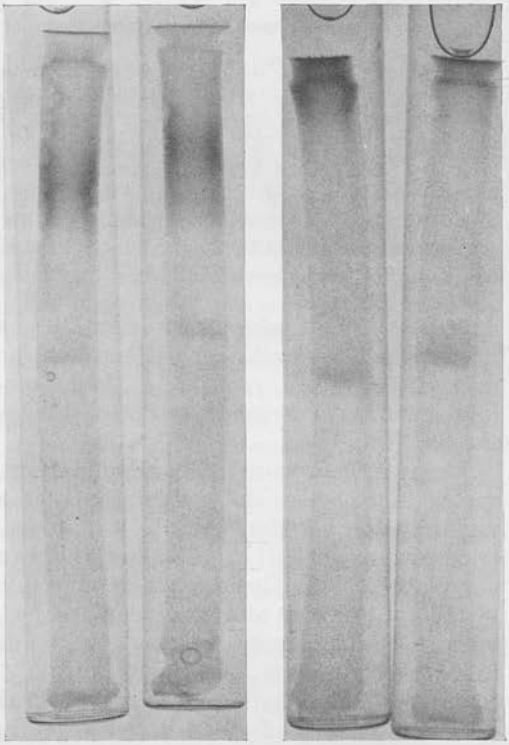

TABLE VII

PERCENT COMPOSITION OF GASTRIC CELL MEMBRANES

	Protein	Lipid	Carbohydrate
Peak I	54.9	42.6	2.5
Peak II	71.3	22.2	6.5

FIG. 13. Mobility of ATPase (left pair) and AMPase (right pair) activities on 7.0% acrylamide gels containing 0.1% Brij 36T. The sample applied in each case was Brij 36T solubilized membranes from Peak I (left one of each pair) or Peak II (right one of each pair). The faint staining area in the mid portion of each gel is yellowish in color and represents protein precipitated by trichloroacetic acid used to stop the reaction.

opposite holds true for lipid. Associated with Peak II is a high ATPase and low AMPase activity, while Peak I is more enriched with AMPase. The mobility of the ATPase from the two peaks appears to be different when Brij 36T solubilization is carried out.

The origin of these membranes remains unanswered. Studies on necturus fundic mucosa (27) has localized the HCO_3^--ATPase to the acid-secreting (oxyntic) cell; hence Peak II membranes may represent membranes from oxyntic cells. The carbohydrate content would tend to localize them to the luminal membrane of these cells (24). Whether Peak I membranes represent basal membranes of oxyntic cells or membranes from another cell type remains unanswered. We have found explanations not considering two types of membranes (such as one membrane in an isolated and aggregated form) to fail to explain the vastly different lipid, carbohydrate, and enzyme composition of these membrane fractions.

ACKNOWLEDGMENT

We are indebted to Dr. Barry Starcher whose laboratory we utilized to define the amino acid composition of the native membranes.

REFERENCES

1. Neville, D. M., and Glossman, H. (1971) *J. Biol. Chem.* **246,** 6335.
2. Trayer, H. R., Nozaki, Y., Reynolds, J. A., and Tanford, A. (1971) *J. Biol. Chem.* **246,** 4485.
3. Korn, E. D., and Wright, P. L. (1973) *J. Biol. Chem.* **248,** 439.
4. Guidotti, G. (1972) *Annu. Rev. Biochem.* **41,** 731.
5. Ferber, E., Resch, K., Wallach, D. F. H., and Imm, W. (1973) *Biochim. Biophys. Acta* **266,** 494.
6. Spenney, J. G., Strych, A., Price, A. H., Helander, H. F., and Sachs, G. (1973) *Biochim. Biophys. Acta* **311,** 545.
7. Lowry, O. H., Rosebrough, N. J., Farr, A. L., and Randall, R. J. (1951) *J. Biol. Chem.* **193,** 265.
8. Starcher, B. C. (1968) *J. Chromatogr.* **38,** 293.
9. Warren, L. J. (1959) *J. Biol. Chem.* **234,** 1971.
10. Niedermyer, W. (1971) *Anal. Biochem.* **40,** 465.
11. Zak, B. (1957) *Amer. J. Clin. Pathol.* **27,** 583.
12. Bartlett, G. R. (1959) *J. Biol. Chem.* **234,** 466.
13. Skipski, V. P., Peterson, R. F., Sanders, J., and Barclay, M. (1963) *J. Lipid Res.* **4,** 227.
14. Balint, J. A., Beeler, D. A., Treble, D. H., and Spitzer, H. L. (1967) *J. Lipid Res.* **8,** 486.
15. Sachs, G., Shah, G., Strych, A., Cline, G., and Hirschowitz, B. I. (1972) *Biochim. Biophys. Acta* **266,** 625.
16. Yoda, A., and Hokin, L. E. (1970) *Biochem. Biophys. Res. Commun.* **40,** 880.
17. Fiske, C. H., and Subbarow, Y. (1925) *J. Biol. Chem.* **66,** 375.
18. Bretscher, M. S. (1971) *Nature New Biol.* **231,** 229.
19. Rosenberg, S. A., and Guidotti, G. J. (1968) *J. Biol. Chem.* **243,** 1985.
20. Evans, W. H. (1970) *Biochem. J.* **166,** 833.
21. Wallach, D. F. H., and Zahler, P. H. (1968) *Biochim. Biophys. Acta* **150,** 186.
22. Colbeau, A., Nachbauer, J., and Vignais, P. M. (1971) *Biochim. Biophys. Acta* **249,** 462.
23. Skipski, V. P., Barclay, M., Archibald, E. M., Terebus-Kekich, O., Reichman, E. S., and Good, J. J. (1965) *Life. Sci.* **4,** 1673.
24. Forte, J. G., Forte, T. M., and Ray, T. K. (1972) *in* Gastric Secretion (Sachs, G., Heinz, E., and Ullrich, K. J., eds.), pp. 37–67, Academic Press, New York.
25. Glossman, H., and Veville, D. (1971) *J. Biol. Chem.* **246,** 6339.
26. Lenard, J. (1970) *Biochemistry* **9,** 1129.
27. Wiebelhaus, V. D., Sung, C. P., Helander, H. F., Shah, G., Blum, A. L., and Sachs, G. (1971) *Biochim. Biophys. Acta* **241,** 49–56.

GASTROENTEROLOGY

Vol. 61, No. 2
Printed in U.S.A.

PRONASE METHOD FOR ISOLATION OF VIABLE CELLS FROM NECTURUS GASTRIC MUCOSA

ANDRE L. BLUM, GING T. SHAH, VIRGIL D. WIEBELHAUS, FRANK T. BRENNAN, H. F. HELANDER, R. CEBALLOS, AND GEORGE SACHS

Division of Gastroenterology, Department of Medicine, University of Alabama in Birmingham, School of Medicine, Veterans Administration Hospital, Birmingham, Alabama, and Smith, Kline and French Laboratories, Philadelphia, Pennsylvania

Isolated cells of Necturus gastric mucosa were prepared with a simple method using pronase digestion and shaking. In dye exclusion tests cell suspensions containing more than 80% of oxyntic cells were more than 90% viable. Isolated cells had respiration rates of 0.411 ± 0.043 microatom O_2 per mg of protein per hr (mean ± SE). Na and K concentrations in cell water were 44.2 ± 1.8 mEq per liter, and 66.7 ± 2.2 mEq per liter respectively. The transmembranal potential of isolated cells was 44 ± 3 mv, similar to that obtained for intact mucosa.

Attempts to study the properties of one particular cell type in the gastric mucosa have relied on techniques such as histochemistry,[1, 2, 3] electron microscopy,[1, 4] and observations during embryological development.[5] In this study, a more direct approach was chosen: the preparation of isolated cell suspensions which consist mainly of one cell type. Similar approaches have previously been described in composite tissues such as fat pad,[6] kidney,[7] small intestine,[8, 9] and also in the stomach.[10-12] Since, however, many techniques which separate cells may also lead to damage of the cell membrane, cell isolation procedures are not in wide use. In this paper, a simple method is described which yields a homogeneous yet viable suspension of gastric mucosal cells. Viability was shown in dye exclusion tests and by the ability of cells to maintain functions of intact tissue such as respiration, electrical potential, and ionic concentration gradients across the cell membrane.

Received November 3, 1970. Accepted March 15, 1971.

Address requests for reprints to: Dr. George Sachs, Department of Medicine, University of Alabama Medical Center, 1919 Seventh Avenue, South, Birmingham, Alabama 35233.

This work was supported by NSF Grant GB-8351, National Institutes of Health Grants 2A-5286 and AM09260 and Veterans Administration Hospital in Birmingham, Alabama, Research Funds, and by the Swedish Medical Research Council Grant B-71-12R-3297.

The authors acknowledge valuable technical assistance by Mr. James Pickett and Miss Karen McKoy.

Method of Cell Isolation

Necturus fundic mucosa was stripped off the external muscle layer, stretched, and pinned surface upwards on the bottom of a lucite dish. A thin layer of oxygenated standard amphibian Ringer's solution containing 0.175% pronase was added. The lucite dish was covered with a lid, gassed with 95% O_2 and 5% CO_2, and incubated in a shaking water bath (30 C, 60 to 100 cycles per min). Cells were collected at 60 min (fraction 1), 75 min (fraction 2), 90 min (fraction 3), and 120 min (fraction 4) of the incubation. A final collection (fraction 5) was obtained by removing the pins and shaking the mucosa with a forceps. The yield of cells in fractions 1 and 2 was small, compared to the yield of fractions 3, 4, and 5. Cell suspensions were centrifuged for 5 min at 50 *g* and resuspended in amphibian Ringer's solution. Centrifugation and resuspension were repeated and final suspensions were refrigerated until 30 min prior to use.

Figure 1*A* is a paraffin section of Necturus gastric mucosa. This shows the surface epithelial cell as a tall columnar cell with mucus present

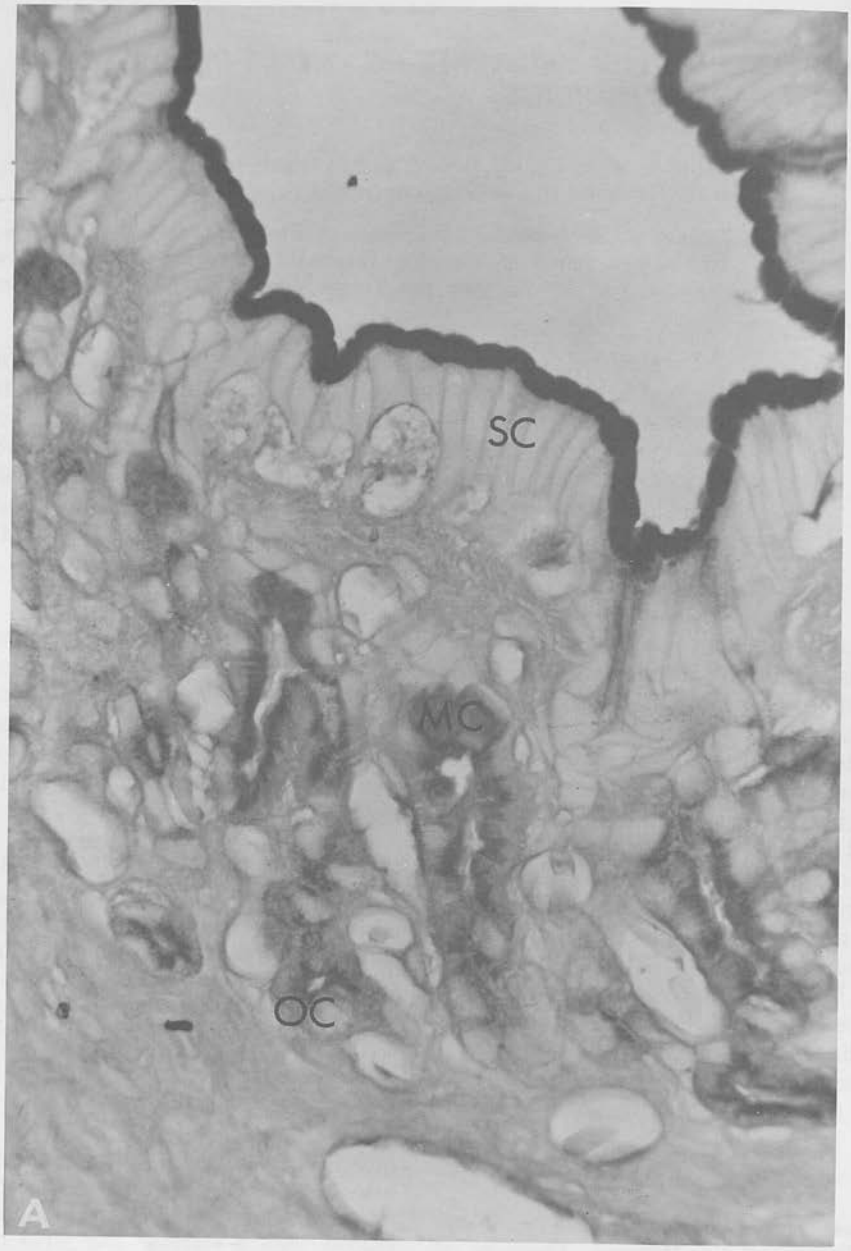

FIG. 1A. Alcian blue-PAS stain of paraffin section of Necturus gastric gastric mucosa showing the surface epithelial cells (*SC*), mucus neck cells (*MC*), and oxyntic cells (*OC*) (× 125).

in the apical portion of the cytoplasm, the neck cells [containing two different types of mucus (dark and lighter stain)], and the deeper cells which are oxyntic cells secreting both acid and zymogen in this species.

Figure 1*B* is a section from the same mucosa following 70 min of incubation in the pronase solution. It can be seen that the surface epithelial cell has been removed, leaving the gastric tubule loosely inserted in the connective tissue framework. At this stage of the incubation violent shaking produces a preparation of iso-

lated tubules. Further smooth shaking in the presence of pronase gradually produces a suspension of virtually pure oxyntic cells.

Of several pronase preparations tested, satisfactory results were only obtained with pronase Merck (A. G. Merck, Darmstadt, Germany, 70,000 protease units per mg). Pronase was superior to hyaluronidase, collagenase, Ca removal, EDTA, trypsin, scraping, and hydrostatic pressure used either on their own or combined with other methods, presumably due to its mucolytic and proteolytic activity.

Occasionally results of isolation procedures were unsatisfactory because of mucus production which led to clumping of isolated cells in mucus plugs. This difficulty could partly be overcome by suspending cells in large volumes of solution before centrifugation. When only experiments on deep cells were planned, the mucosa was heavily and repeatedly blotted against hard filter paper before starting pronase incubation.

Identification of Cells

Figure 2 shows a low power magnification of a fundic cell suspension, fraction 2. The contrast in this unstained preparation between the dark oxyntic cell and the other cell types can be clearly seen.

Intact isolated cells were round, oval, or pear-shaped. A few cells maintained their original polygonal shape or had an irregular surface. Irregular cells were nonviable in viability tests. In phase contrast at higher magnification (× 400) at least four cell types could be recognized: (1) large cells with a diameter of 35 to 70 μ, dark cytoplasm, and small granula; (2) cells with similar diameter but translucent cytoplasm and both large and small granula; (3) small cells with a diameter of 20 to 40 μ, translucent cytoplasm, and sparse granula; and (4) cells of similar shape which had on their surface rows of beating cilia.

Electron microscopic studies were carried out on sections of 1% OsO_4-fixed preparations of isolated cells embedded in Epon or Vestopal. Figures 3*A* and 3*B* show the appearance of an isolated surface cell and an isolated oxyntic cell. It can be seen

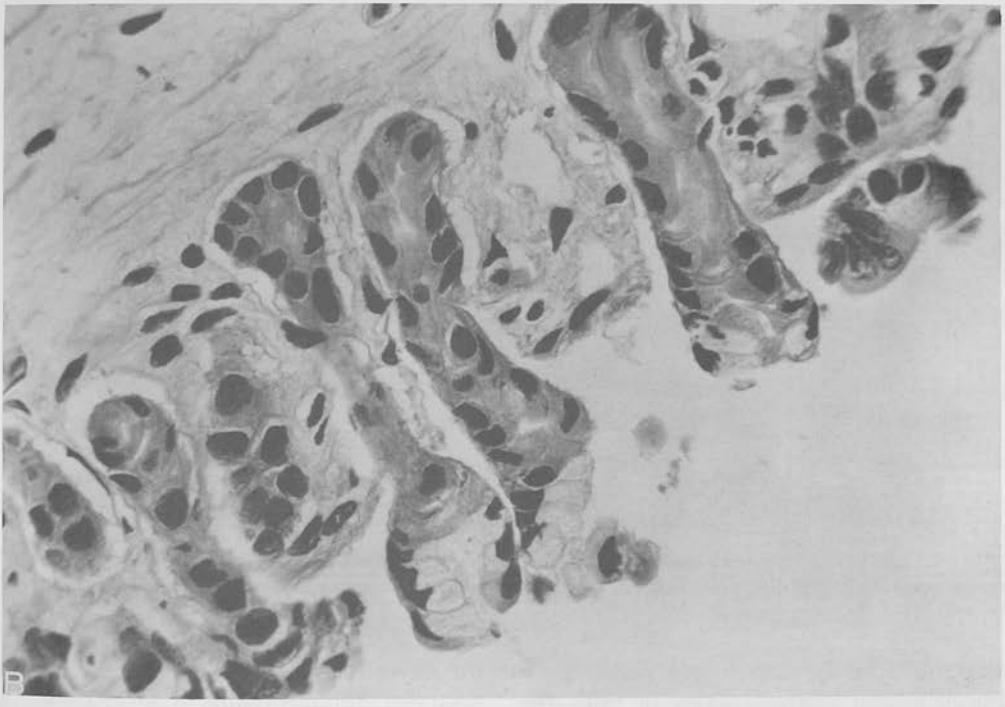

FIG. 1*B*. Section of Necturus gastric mucosa following 70-min incubation in pronase solution showing absence of surface epithelial cells and presence of tubules in the connective tissue framework (Hematoxylin and eosin, × 125).

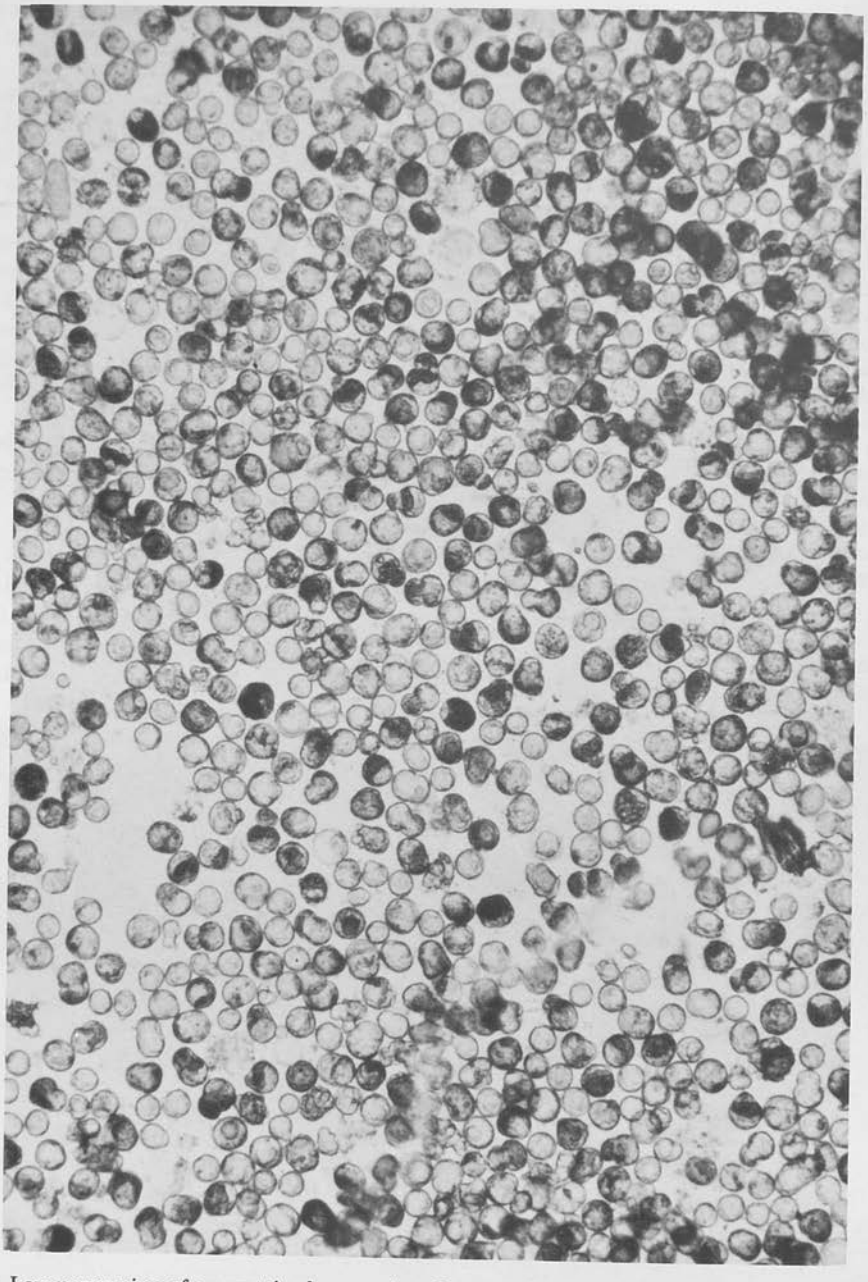

FIG. 2. Low power view of an unstained suspension of intact cells obtained at 75 min from Necturus gastric mucosa showing largely light-rounded cells (surface epithelial cells) and a few larger dark cells (oxyntic cells) (× 125).

that the cells are intact and retain good morphological characteristics of both the plasma membrane and the mitochondria. There is a high content of mitochondria in the oxyntic cell, and there are also several zymogen granules visible in the section.

The presence of ciliated cells was at first surprising. In serial sections of esoph-

agus and fundus, however, a gradient of ciliated cells could be demonstrated. In some parts of the esophagus, the majority of surface cells was ciliated while in the fundus ciliated cells were interspersed between nonciliated surface cells (fig. 4*A*). Figure 4*B* shows an isolated ciliated cell.

For further identification of oxyntic cells succinic dehydrogenase stains were performed using a modification of the method described by Myren et al.[3] Cell suspensions were spread on glass slides and covered with a thin layer of agar. The slides were incubated for 30 to 60 min at 37 C in amphibian Ringer's solution containing 50 mM Na succinate and 1 mg per ml nitro-

FIG. 3*A*. Electron micrograph of isolated surface epithelial cell. This cell is sectioned so that none of the mucous secretory granules are visible. However, such granules (*G*) may be seen in another surface epithelial cell in the *lower right corner*. A characteristic component of many of these cells is the large lipid droplets (*L*). Compared with the oxyntic cells there are few mitochondria (*M*), and the surface of the cell is smoother. Golgi apparatus (*GA*); cell nucleus (*N*) (× 6700).

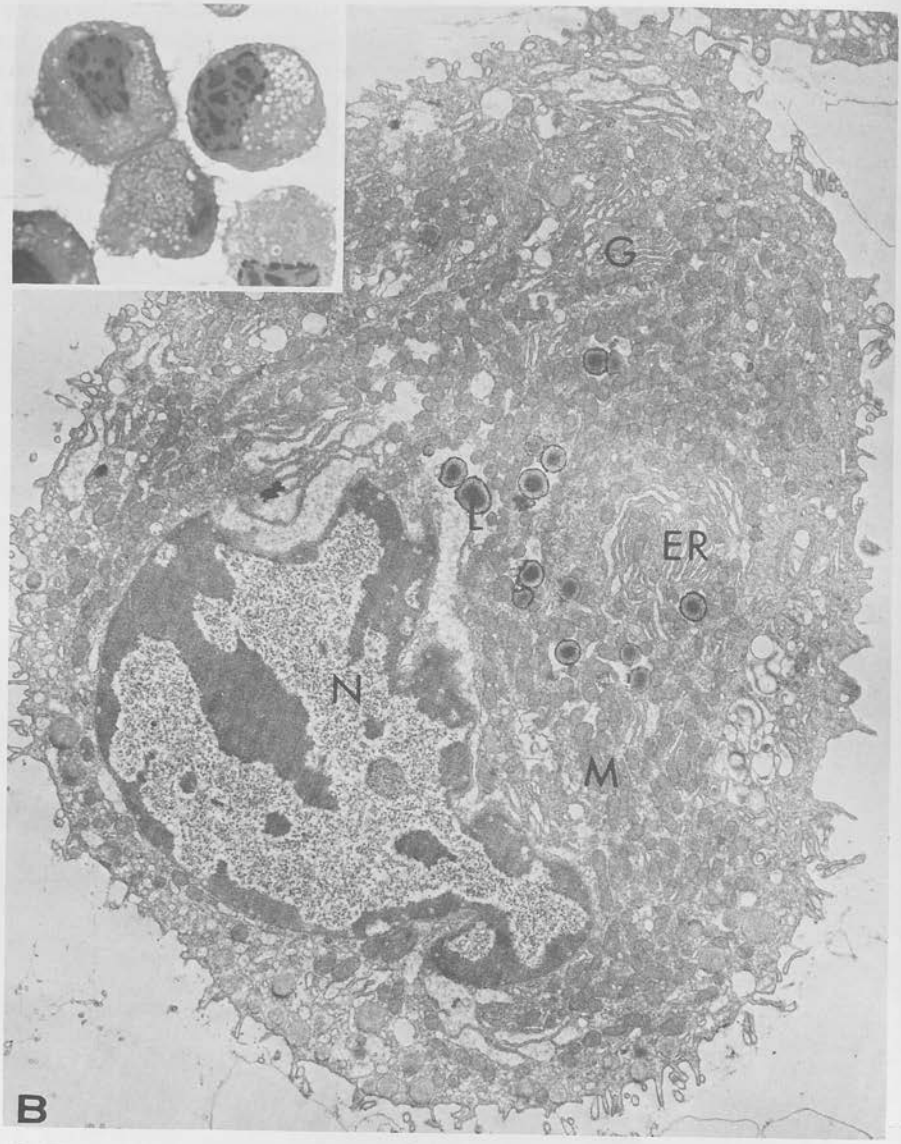

FIG. 3*B*. Electron micrograph of isolated oxyntic cell, showing numerous microvilli projecting from the cell surface. The cytoplasm contains a large number of mitochondria (*M*) and a well developed endoplasmic reticulum (*ER*). The general appearance of this cell suggests good viability. *L*, lipid droplets; *N*, cell nucleus (× 3300). *Inset* shows light micrograph of a few isolated oxyntic cells, as they appear in toluidine blue-stained 1-μ thick Epon sections (× 700).

tetrazolium blue. In control experiments cryostat sections of intact mucosa were treated similarly. Cells with a positive stain were densely packed with dark purplish brown granules. These cells were located in the deeper part of glandular tubules. Counts of isolated cells were performed in four experiments by 2 independent observers with excellent agreement. In each experiment cells were prepared from four stomachs. Results of cell counts are given in table 1. Cells with a positive succinic dehydrogenase stain were rare in early cell collections but represented more than 80% of

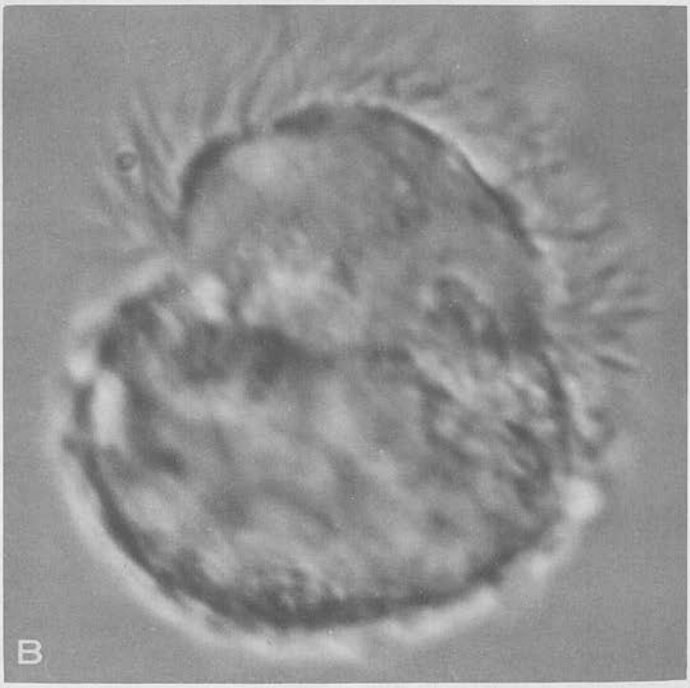

FIG 4A. Section of Necturus gastric mucosa stained with hematoxylin and eosin showing the presence of intercalated ciliated cells (*CC*) in the surface epithelium (× 320).

FIG. 4B. A high power view of an isolated ciliated cell (× 960).

TABLE 1. *Percentage of cells with positive stain for succinic dehydrogenase in suspensions of isolated cells from Necturus stomach*[a]

Cell fraction	Incubation time	Percentage of cells with positive stain (mean ± SE)
	min	
1	0–60	15 ± 1.3
2	60–75	17 ± 1.4
3	75–90	55 ± 5.4
4	90–120	80 ± 5.0
5	>120	84 ± 2.7

[a] Incubation time is measured from start of pronase incubation to time of cell collection ($N = 5$).

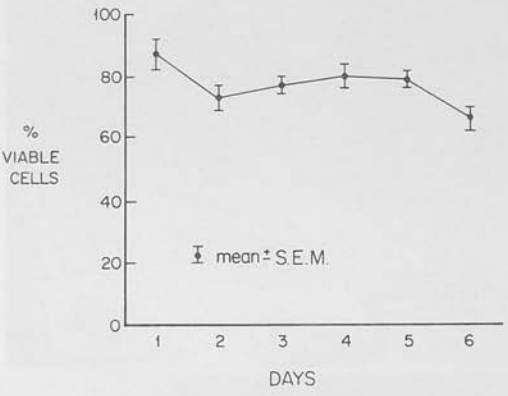

FIG. 5. Uptake of eosin by a suspension of Necturus oxyntic cells over 6 days of refrigeration.

the cell population in late collections. The diameter of cells with a positive stain was relatively large (30 to 50 μ) while negative cells had diameters ranging from 20 to 40 μ, the majority of the latter being in the range of 20 to 30 μ.

Viability Tests

Dye exclusion test with eosin. Equal volumes of cell suspension and of amphibian Ringer's solution containing 0.05% eosin were incubated for 1 min. Cells were counted in a hemocytometer. "White" cells whose membranes exclude the dye are considered to be viable and "pink" cells with leaky membranes are considered to be nonviable.

In 21 counts of fraction 1, 2, and 3 "viability" was 68.7 ± 8.3% (mean ± SE), and in 19 counts of fraction 4 and 5 it was 91.8 ± 2.1%. The difference between the two means is statistically significant ($P <$ 0.001). In nine of 21 collections of fraction 4 and 5 "viability" was higher than 95%.

In 4 experiments, cells of fraction 4 and 5 were refrigerated and samples were counted daily for 6 days. Results are given in figure 5 and table 2. There was a general tendency for decrease in "viability" but even after 6 days two-thirds of the cells still excluded eosin. The number of cells did not especially decrease.

It would appear that this method results in reasonably long term viability for these amphibian cells. However it should be emphasized that this method was designed to produce cells which displayed good short-term viability, and no attempt was

TABLE 2. *"Viability" of isolated gastric mucosal cells as determined by a dye exclusion technique with eosin*[a]

Day	No. of cells per mm³ (millions, mean ± SE)	Percentage of "viable" cells (mean ± SE)
1	0.38 ± 0.07	87 ± 5
2	0.44 ± 0.10	73 ± 4
3	0.32 ± 0.11	77 ± 3
4	0.40 ± 0.12	80 ± 4
5	0.35 ± 0.09	79 ± 3
6	0.32 ± 0.07	66 ± 4

[a] Cell suspensions (fraction 4 and 5) were refrigerated after collection. Total cell counts and differential counts for pink and white cells were performed daily.

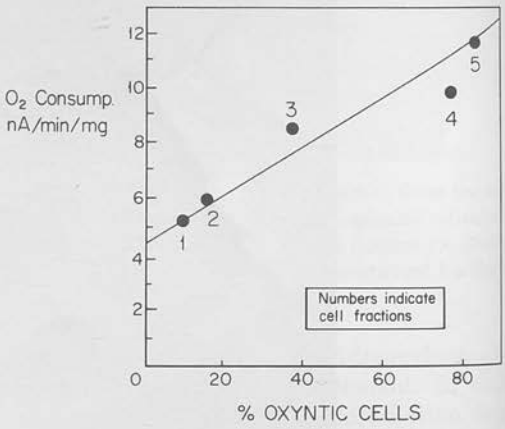

FIG. 6. O_2 consumption of the cell fractions obtained from Necturus plotted against percentage oxyntic cells (succinic dehydrogenase stain).

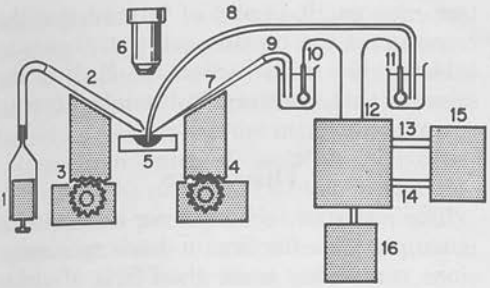

FIG. 7. Experimental arrangement for micropuncture of isolated Necturus gastric cells: (1) Oil-filled syringe; (2) Oil-filled suction micropipette; (3, 4) Micromanipulators; (5) Agar-filled microculture slide; (6) Stereomicroscope; (7) Microelectrode; (8, 9) 3 M KCl-agar bridge; (10, 11) Calomel electrode; (12) Amplifier; (13, 14) Recorder connections; (15) Recorder or CRO: (16) Current source.

made to establish long term viability beyond the eosin uptake test described above.

Cells with beating cilia always excluded eosin. While most ciliated cells were still beating at the time of collection, only occasional cells continued to beat after 24 hr of refrigeration. After 48 hr of refrigeration no cilial movement was observed and ciliated cells started to stain pink with eosin.

O_2 *consumption.* A 1.7-ml stirred Kel F chamber with a Clark type O_2 electrode was connected to amplifier and current source (Radiometer, Copenhagen) and an Esterline Angus recorder. The protein content of samples was determined by the Lowry method.

O_2 consumption of stripped Necturus fundic mucosa was 0.207 ± 0.019 microatom per mg of protein per hr (mean ± SE, $n = 15$). O_2 consumption of cell suspensions, fraction 4 and 5, was 0.411 ± 0.043 microatom per mg of protein per hr ($n = 15$). The difference between the two rates is statistically significant ($P < 0.01$).

Dinitrophenol (DNP, 10^{-4} M) increased respiration rate of intact mucosa to 182 ± 16% (mean ± SE, $n = 6$), and respiration rate of isolated cells to 406 ± 20% ($n = 6$) of control value. The difference between the two values is statistically significant ($P < 0.001$).

Amytal (2.10^3 M) abolished respiration both of intact mucosa and isolated cells.

When O_2 consumption was measured over a period of 4 hr on aliquots of cell suspension, it was found that the consumption remained constant over the period of observation. Figure 6 shows the O_2 consumption of the various cell fractions obtained. By extrapolation the O_2 consumption of pure oxyntic cells is 5 times that of non-oxyntic cells of the tissue.

Ionic composition of isolated oxyntic cells. Cells of fraction 4 and 5 incubated for 5 min in amphibian Ringer's solution containing 1.1 μCi of C^{14} inulin per ml. Suspensions were centrifuged for 5 min at 500 *g*. The cell pellet was weighed before and after drying for 16 hr at 140 C. The dried pellet was dissolved in 3 ml of 3 M Li OH and the solution was titrated to *p*H 7 with 10 M H_2SO_4. An aliquot was counted in a liquid scintillation counter. Na and K analyses were performed in an Eppendorf flame photometer. This procedure allowed calculation of Na^+ and K^+ concentration

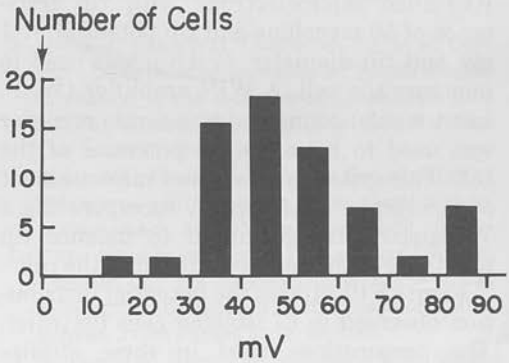

FIG. 8. The distribution of potential in a group of 67 cells, with a mean of 44 ± 3 mv.

TABLE 3. *Intracellular potentials*

	Isolated surface epithelial cells	Isolated oxyntic cells		Surface epithelial cells in intact mucosa
K^+ concentration	4 K^+	4 K^+	18.5 mM K^+	4 K^+
Potential[a]	36 ± 11	48 ± 6	31 ± 5	43 ± 8
No.	12	22	11	15

[a] mv ± SE. The cell interior is negative with respect to the external solution.

in cell water. In nine experiments the water content of isolated cells was 80.2 ± 0.7% (mean ± SE) of their wet weight. Na and K concentrations in cell water were 44.2 ± 1.8 mM and 66.7 ± 2.2 mM respectively.

Electrical potential of isolated cells. The maintenance of ionic gradients across the cell membrane is necessary for continued cell function. Measurement of cell potentials provide additional evidence for normal ionic gradients and qualitative integrity of the plasma membrane.

Figure 7 illustrates the experimental arrangement used. Briefly, a suspension of cells was placed on an agar-filled microculture slide and a cell was trapped by a suction micropipette, care being taken to use minimal suction. Experiments carried out before a suction device was used gave similar values for the cell potential, but allowed successful puncture of only a few of the cells attempted. Hence the results described are confined to the measurements made using the micropipette.

When the cell was immobilized, a 3 M KCl-filled microelectrode with tip resistance of 50 megohms and tip potential < 1 mv and tip diameter < 0.5 μ was used to puncture the cell. A WP4 amplifier (W. P. Instruments) connected to a Grass recorder was used to measure the potential of the cell. This system also allowed measurement of membrane resistance by incorporating a Wheatstone bridge circuit to balance tip resistance with the electrode out of the cell.

Figure 8 illustrates the potential distribution observed in 67 isolated cells (oxyntic). The preparations used in these studies showed better than 95% eosin exclusion. The low potentials seen in the figure may well signify damaged cell membranes, although these cells excluded eosin.

Table 3 shows the value of the potential obtained in surface cells, oxyntic cells, oxyntic cells in high K^+, and in intact mucosa. The latter values were obtained from small pieces of intact mucosae which were placed on the slide and punctured in the same way as the isolated cell.

It can be seen that there is no significant difference between the potential of the isolated cell (surface or oxyntic), and the intact mucosa. It is also of interest that the response of the oxyntic cell to a change in external K^+ (substitution for Na^+) is the same as that observed in the intact Necturus mucosa.[13]

Discussion

The reported technique for cell isolation is simple yet effective: it leads to suspensions containing more than 90% of viable cells. Isolated cells were not permeable to large dye molecules and maintained high rates of respiration, Na and K contents similar to estimates for intact mucosa, and a high transmembranal potential.

A significant finding was the presence of a transmembranal potential similar to the cell-to-lumen potential of intact mucosa.[13] Micropuncture methods, however, did not give information on the average viability of cell suspensions since approximately 50% of the attempts to puncture isolated cells were unsuccessful. The cause for this failure was in some cases the inability to immobilize cells with the cell-holding device. In other cases trapped cells disintegrated before they could be punctured. It cannot be excluded that these properties were related to cell viability.

The concentration of Na and K in cell water was determined after incubation of isolated oxyntic cells in solution with ionic composition similar to that of frog plasma. The Na content in isolated cells was 44 mEq per liter of cell water and corresponded closely to an estimate for intact frog mucosa, while the K content was lower than the estimate for intact frog mucosa (67 and 87 mEq per liter of cell water respectively). This difference might be accounted for by loss of viability and leakiness of isolated cells. However a more likely explanation is the high proportion of oxyntic cells in cell suspensions, assuming that K concentration is lower in oxyntic cells than in surface cells. In fact, this has been considered to be the case[14] in that the amphibian mucosa is thought to have a high Na, relatively low K cell (oxyntic cell), and a high K, low Na cell (surface cell). Our data would support this view. In this regard it would be of interest to determine the elec-

trolyte content of isolated surface cell suspensions. With the present technique only 70% of isolated surface cells were viable and, therefore, determination of their electrolyte content was not attempted.

Respiration rate of isolated Necturus cells was in the range of 0.4 microatoms per mg of protein per hr. This value is slightly higher than rates found for isolated toad bladder[15] and lower than values for isolated cells of mammalian stomach[11] and liver.[16] Respiration rate of isolated cells was significantly higher than the rate in intact stomach. Similar differences have previously been reported for isolated cells and intact tissue of toad bladder.[14]

High respiration rates are often used as evidence against cell damage.[7, 9, 11, 14, 15] It is, however, conceivable that cell damage may partially uncouple mitochondrial phosphorylation and hence increase respiration rate. In this case, an uncoupler of respiration such as dinitrophenol would be less effective on isolated cells than on intact tissue. In this study, dinitrophenol increased respiration rate of isolated cells more than the rate of intact tissue. A likely explanation for this observation is the high proportion of oxyntic cells and the absence of metabolically inactive connective tissue from cell suspensions. The high proportion of oxyntic cells and their high mitochondrial content would also explain the high rate of respiration observed in cell suspensions as compared to intact tissue. This effect might be so pronounced that it could mask reduction of the respiratory rate by cell damage.

By far the simplest viability test was the dye exclusion technique with eosin. Although this test only measures passive property of the cell membrane which might persist after cell damage, it is a reliable screening procedure and allows immediate assessment of the quality of a cell preparation.

While no one property is sufficient evidence for viability of isolated cells, the results obtained in multiple viability tests measuring both properties of the cell membrane and metabolic activity of the cytoplasm indicate that the pronase method is adequate for isolation of viable gastric mucosal cells. Moreover, this method leads to suspensions with a high proportion of oxyntic cells. The use of Necturus gastric mucosa allows easy cell identification and manipulation of individual cells for direct experimentation. The data obtained for Necturus were sufficiently encouraging that similar methods were attempted in other species. In preliminary experiments equally good results were obtained with frog (*Rana pipiens* and *catesbeiana*), and promising results have been obtained with rat and guinea pig. The various tests applied to this cell suspension show that with a multiplicity of tests, excellent short-term viability was obtained, which was the essential requirement for the studies planned with these cells.

REFERENCES

1. Helander HF: Ultrastructure of fundus glands of the mouse gastric mucosa. J Ultrastruct Res (suppl 4):1–123, 1962
2. Koenig CS, Vial JDC: A histochemical study of adenosine triphosphatase in the toad (Bufo spinulosus) gastric mucosa. J Histochem Cytochem 18:340–353, 1970
3. Myren J, Unhjem O, Gheruldsen ST, et al: Oxygen consumption of unstimulated gastric mucosa in relation to the secretion of hydrochloric acid and the number of parietal cells. Scand J Clin Lab Invest 17:31–38, 1965
4. Sedar AW, Friedman MH: The fine structure of the oxyntic cell in relation to functional activity of the stomach. Ann NY Acad Sci 99:9–29, 1969
5. Forte JG, Limlomwongse L, Kasbekar DK: Ion transport and the development of hydrogen ion secretion in the stomach of the metamorphosing tadpole. J Gen Physiol 54:76–95, 1969
6. Butcher RW, Baird CE, Sutherland EW: Effects of lipolytic and antilipolytic substance on adenosine 3′ -5′ monophosphate levels of isolated fat cells. J Biol Chem 243:1705–1712, 1968
7. Burg MB, Orloff T: Oxygen consumption and active transport in separated renal tubules. Amer J Physiol 203:327–330, 1962
8. Harrison DD, Webster HL: The preparation of isolated intestinal crypt cells. Exp Cell Res 55: 257–260, 1969
9. Stern BK, Jensen WE: Active transport of glucose by suspensions of isolated rat intestinal epithelial cells. Nature 209:789–790, 1966
10. BreMiller RA: Attempt to separate cells of gastric mucosa. Gastroenterology 40:798–802, 1961
11. Croft DN, Ingelfinger FT: Isolated gastric parietal

cells: oxygen consumption electrolyte content and intracellular pH. Clin Sci 37:491–501, 1969
12. Walder AL, Lunseth JB: A technic for separation of cells of the gastric mucosa. Proc Soc Exp Biol Med 112:494–496, 1963
13. Sachs G, Shoemaker RL, Blum AL, et al: Electrical properties of necturus gastric mucosa. Symp Medica Hoechst (in press)
14. Davenport HW: Sodium space and acid secretion in frog gastric mucosa. Amer J Physiol 204:213–216, 1963
15. Gatzy JT, Berndt WO: Isolated epithelial cells of the toad bladder: their preparation oxygen consumption and electrolyte content. J Gen Physiol 51:770–784, 1968
16. Howard RB, Pesch LA: Respiratory activity of intact isolated parenchymal cells from rat liver. J Biol Chem 243:3105–3109, 1968

Specific effect of acetylsalicylic acid on cation transport of isolated gastric mucosal cells

HANS R. KOELZ, JAN A. FISCHER, GEORGE SACHS, AND ANDRÉ L. BLUM
Calcium Research Laboratory, University Hospital for Orthopedics, and Department of Medicine, Triemli Hospital, Zurich, Switzerland

KOELZ, HANS R., JAN A. FISCHER, GEORGE SACHS, AND ANDRÉ L. BLUM. *Specific effect of acetylsalicylic acid on cation transport of isolated gastric mucosal cells*. Am. J. Physiol. 235(1): E16–E21, 1978 or Am. J. Physiol.: Endocrinol. Metab. Gastrointest. Physiol. 4(1): E16–E21, 1978. —To investigate whether isolated cells from rat antral and fundic mucosa show active ion transport, the cellular uptake and efflux of Na^+, K^+, and Rb^+ was measured. The effects of ouabain (OUA) and 2,4-dinitrophenol (DNP) were compared to the effect of acetylsalicylic acid (ASA), another inhibitor of active ion transport in vivo. OUA, DNP, and also ASA inhibited the uptake of K^+ and Rb^+. ASA plus OUA together were more effective than either agent given alone at a maximally effective concentration. ASA but not OUA was more effective at low pH than at neutral pH. The effect of ASA was not prevented by giving ASA together with prostaglandins of the E series (PGE_1, PGE_2, and 16,16-dimethyl-PGE_2). ASA, OUA, and DNP had no effect on efflux of K^+ and Rb^+ from the cells. OUA and DNP stimulated influx and inhibited efflux of Na^+, whereas ASA had no effect on Na^+ transport of the cells. Antral and fundic cells reacted similarly in all aspects of cation transport. We concluded that: *1*) isolated mammalian gastric cells show active ion transport across their plasma membrane. The effects of OUA and DNP can be explained by inhibition of the Na^+–K^+ pump that regulates cellular Na^+ and K^+ content. *2*) The ASA-induced inhibition of K^+ uptake is not related to the Na^+–K^+ pump, and it is probably not due to inhibition of a prostaglandin synthetase. ASA entry into the cells may be necessary for its action.

aspirin; ouabain; 2,4-dinitrophenol; indomethacin; prostaglandins; Na^+ transport; K^+ transport; Rb^+ transport; rat gastric mucosa

STUDIES ON ION FLUXES in intact epithelia are complicated by the presence of both paracellular and cellular pathways. Isolated cell preparations allow direct cellular effect to be tested. In addition, active ion transport across the cell membrane appears to be a good index of cellular integrity. The tests that so far have been used to assess viability of isolated cells have shortcomings. For example, O_2 consumption and hormone sensitivity may be observed in cell fragments, and potential difference can only be determined in a few selected cells (3, 4).

In the present study, cation transport into and out of isolated gastric mucosal cells has been measured. This model lends itself to studying the effects of inhibitors of ion transport such as ouabain (OUA) and 2,4-dinitrophenol (DNP). OUA (7, 11, 35) and DNP (30, 39) have been shown to inhibit gastric acid secretion. OUA inhibits active Na^+ and K^+ transport by rabbit antral mucosa (18). DNP increases the permeability of the intact gastric mucosa for protons, Na^+ and K^+ (30).

In addition, it is of particular interest to investigate the cellular effects of agents known to disrupt the gastric mucosa (9). The most important of these agents is acetylsalicylic acid (ASA), which produces epithelial defects and ulcers in man (12) and animals (14) although under certain circumstances it may also protect the gastric mucosa (31). ASA inhibits gastric acid secretion (13, 20, 23, 24, 26), changes electrical resistance (26) and leads to electrical uncoupling of mucosal cells (32). It also increases cation permeability of the gastric mucosa (6, 8). In most of these instances, distinction was not made between effects on the plasma membrane and on paracellular pathways.

MATERIALS

Reagents were obtained from the following sources: pronase E (70,000 PUK/g), HEPES buffer, and choline chloride from Merck, Darmstadt, Germany; 2,4-dinitrophenol (DNP, grade II), ouabain (OUA) and indomethacin from Sigma, St. Louis, Mo.; acetylsalicylic acid (ASA) from Siegfried, Buchs, Switzerland; antifoam (SE-2) from Wacker Chemie GmbH, München, Germany. The radionuclides were purchased from Amersham, Buckinghamshire, England. The prostaglandins were a generous gift from Dr. A. Robert, The Upjohn Company, Kalamazoo, Michigan.

METHODS

Solutions. The incubation media were prepared on the day of the experiment. They were kept at a pH of 7.4 (5.0 in some experiments indicated in the text) and continuously gassed with O_2/CO_2 95/5 in siliconized vessels. All solutions contained, in millimoles per liter: NaH_2PO_4, 0.5; Na_2HPO_4, 1.0; $NaCO_3$, 20; NaCl, 70; KCl, 5.0 or RbCl, 5.0; glucose, 80; and HEPES, 50. Media buffered by HEPES proved to be superior in terms of cell survival (trypan blue test) to other media, such as Eagle's minimal essential medium and Krebs-Ringer bicarbonate solution. In addition to the above mentioned substances, *medium A* contained 2 mM EDTA, 2% bovine serum albumin, and 1% antifoam. *Medium*

B contained $CaCl_2$, 1 mM; MgCl, 1.5 mM; and 1% bovine serum albumin. Pronase solution contained *medium A* plus pronase 1,000 PUK/ml.

Cell isolation procedure. A method modified from Lewin et al. (27) was used. In each experiment 10 rats of either sex weighing 150–250 g were killed by a blow on the head. The stomach was removed, and its contents were flushed off with deionized water. Everted sacs were produced by setting ligatures at the pylorus, at the antral border, and at the proximal end of the corpus. Pronase solution was injected into the sacs, which were incubated in *medium A* at 37°C for 30 min. The medium was discarded, and the sacs were incubated in fresh *medium A* at 37°C for another 30 min. The medium now containing isolated cells was filtered through nylon stocking. The filtrate was washed twice in *medium B* without albumin. The resuspended cells were kept on ice. The sacs were then placed into an Erlenmeyer flask at room temperature. They were gently moved by a magnetic stirrer for 15 min. The medium was then processed as above. Fresh *medium B* was added to the sacs, which were incubated for two additional 30-min periods; the isolated cells were washed as above.

Assessment of cell viability. Samples of each individual batch were examined microscopically after adding trypan blue solution (Table 1) (1% in Krebs-Ringer bicarbonate buffer). The percentage of cells excluding the dye was determined. Only batches containing less than 10% of colored cells were used for the experiments. Trypan blue exclusion was seen in more than 80% of the cells after a 60-min exposure to the various agents used.

Identification of parietal cells. Succinic dehydrogenase in parietal cells was identified as follows (4). A sample of isolated cells was smeared over a slide. Dried cells were covered with warm (45°C) liquid casein agar. After cooling, the slide was transferred into a staining cuvette containing *medium B* with 1 mg/ml *p*-nitrotetrazolium blue, 20 mM NaCl, and 50 mM sodium succinate. Incubation at 37°C lasted for 30 min. Parietal cells were identified by dark blue granules representing mitochondria.

Measurement of ion uptake. Ion uptake was measured according to a technique described by Kondo et al. (25). A sample of the cell suspension (0.5 ml, corresponding to about 5×10^6 cells) was pipetted into a 50-ml Erlenmeyer flask that contained 4.5 ml of incubation *medium B* and the agent(s) to be tested. In ASA experiments, the pH was previously adjusted to 7.4 (using NaOH 0.1 N) or 5.0 (using HCl 0.1 N). The flasks were agitated at 80 oscillations/min. Then the radioactive tracer (2 μCi/5 ml) was added. At different time intervals, samples (0.5 ml) of the cell suspension were removed and squirted into a conical glass centrifugation tube containing 20 ml of ice cold choline chloride solution adjusted to pH 7.4. The tubes were immediately centrifuged at $100 \times g$ for 45 s. The supernatant was rapidly decanted, and the tubes were inverted for further drainage. Cells were mixed with 10 ml of Bray solution. The radioactivity was measured using a beta-scintillation spectrometer (Unilux II, Nuclear Chicago). The specific activity of the probe ion was calculated by dividing the radioactivity in 0.1 ml incubation medium by the amount of the probe ion in that volume. The number of cells per volume incubation medium was determined using a Neubauer chamber for blood cell counting. Ion uptake into the cells was expressed in nanomoles per 10^6 cells.

Measurement of ion efflux. The cell suspension was loaded with radioactive tracer (2 μCi/ml) for 30 min at 37°C. The suspension was centrifuged at $1,000 \times g$ for 45 s. The sediment was washed twice by resuspending and centrifugation in 20 ml of incubation medium without tracer. A sample (0.5 ml) of the suspension containing preloaded cells was pipetted into an Erlenmeyer flask containing 4.5 ml of incubation media with the agent(s) to be tested. Additional procedures were the same as in ion uptake experiments.

TABLE 1. *Trypan blue exclusion before and after 60-min exposure to ASA, OUA, or DNP at pH 7.4*

Procedure	Unstained Cells	
	Antrum	Corpus
Before exposure	94.3 ± 2.5	93.7 ± 6.3
After exposure		
Without additions	90.5 ± 7.9	89.2 ± 8.8
ASA	88.2 ± 4.0	88.1 ± 7.6
OUA	89.0 ± 4.3	89.6 ± 13.8
DNP	84.5 ± 12.6	80.3 ± 15.9*

Values are means ± SD% of 200 cells counted. Cell debris was counted as a cell stained by trypan blue. ASA, acetylsalicylic acid (10^{-2} M); OUA, ouabain (10^{-3} M); DNP, 2,4-dinitrophenol (10^{-3} M). *$P < 0.005$ compared with values before exposure. Other differences are not significant ($P > 0.05$).

RESULTS

Morphology of isolated cells. Ten rat stomachs yielded 86.4 ± 47.2 SD $\times 10^6$ isolated antrum cells and 278 ± 61 $\times 10^6$ corpus cells. Antrum cell preparations contained 10.2 ± 5.3% SD, and corpus cell preparations contained 29.5 ± 3.7% parietal cells, respectively.

Potassium uptake. ASA (10^{-2} M), OUA (10^{-3} M), and DNP (10^{-3} M) inhibited K^+ uptake (Fig. 1). The effect was significant within 1–5 min after exposure to these agents. The effect of these compounds appeared to be on the K^+ content of the cells and not on the half-time of uptake. The concentrations of the three agents used in these experiments were shown to be more effective than tenfold smaller concentrations, but not less effective than tenfold larger concentrations, respectively.

Potassium efflux. ASA (10^{-2} M), OUA (10^{-3} M), and DNP (10^{-3} M) did not affect $^{42}K^+$ efflux (Fig. 2). The effect of these compounds in reducing the size of the exchangeable K^+ compartment is due to inhibition of uptake in the face of a constant efflux.

Rubidium uptake. ASA (10^{-2} M), OUA (10^{-3} M), and DNP (10^{-3} M) inhibited Rb^+ uptake (Fig. 3). ASA (10^{-2}) and OUA (10^{-3}) together were more effective than either agent alone (Fig. 4). The equilibrium value of Rb^+ uptake was the same as that for K^+ and the effect of each individual inhibitor was similar.

Lowering the pH of the incubation medium from 7.4 to 5.0 enhanced the effect of acetylsalicylic acid (10^{-2} M) on corpus cells (Fig. 5). OUA did not share the increased

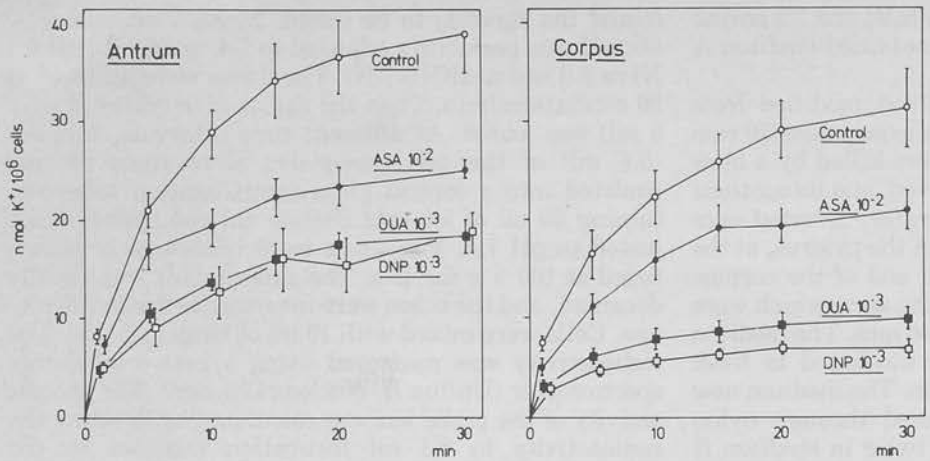

FIG. 1. Inhibition of K uptake into isolated rat antrum and corpus cells by acetylsalicylic acid (10^{-2} M) (ASA), ouabain (10^{-3} M) (OUA), and dinitrophenol (10^{-3} M) (DNP), respectively. pH of medium was adjusted to 7.4. Each point represents mean ± SE of 5 independent experiments. All values are significantly different from controls ($P < 0.05$ to < 0.001) except ASA at 1 min.

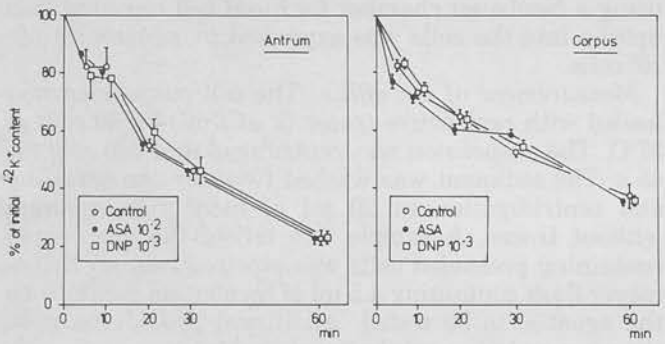

FIG. 2. Effect of acetylsalicylic acid (10^{-2} M) (ASA), ouabain (10^{-3} M) (OUA), and dinitrophenol (10^{-3} M) (DNP) on ^{42}K efflux from isolated antrum and corpus cells. Each point represents mean ± SE of 3 experiments. There is no significant difference between control values and values in presence of ASA, OUA, or DNP.

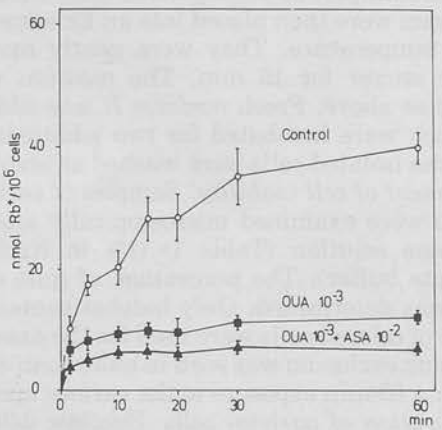

FIG. 4. Effect of ouabain (10^{-3} M) (OUA) and ouabain (10^{-3} M) together with acetylsalicylic acid (10^{-2} M) (ASA) on Rb uptake in isolated corpus cells. Each point represents mean ± SE of 2 experiments.

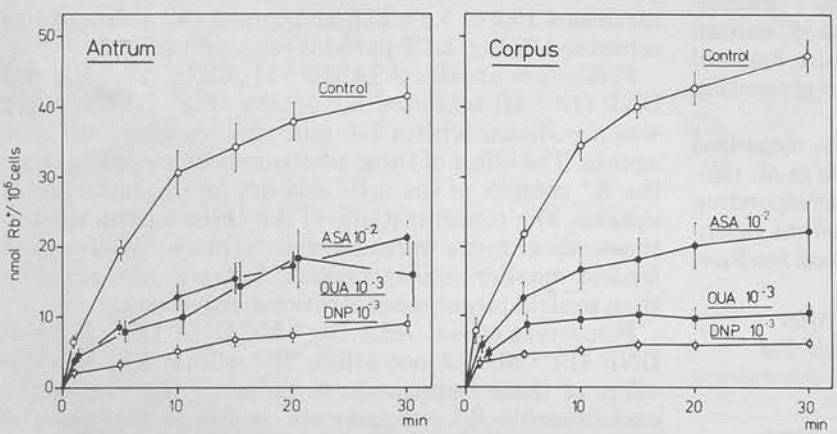

FIG. 3. Inhibition of Rb uptake into isolated antrum and corpus cells at pH 7.4 by acetylsalicylic acid (10^{-2} M) (ASA), ouabain (10^{-3} M) (OUA), and dinitrophenol (10^{-3} M) (DNP), respectively. Each point represents mean ± SE of 5 experiments. Differences from controls are significant ($P < 0.05$ to < 0.001) for all points except 1-min value of antrum cells in presence of ouabain.

inhibitory effect of ASA observed at a lower pH. This result suggests that at the lower pH, the probably increased intracellular ASA concentration results in additional actions of the drug. The prostaglandins [PGE_1 (1 μg/ml), PGE_2 (1–100 μg/ml) and 16,16-dimethyl-PGE_2 (0.1–10 μg/ml)] did not affect Rb^+ uptake both in the absence and in the presence of ASA (Fig. 6). Indomethacin (0.8, 8, and 80 μg/ml, respectively) had no effect ($P = 0.5$) on Rb^+ uptake into corpus cells. This is evidence that inhibition of prostaglandin synthesis does not account for the ASA effect on Rb^+ uptake.

Rubidium efflux. ASA, OUA, and DNP did not affect Rb^+ efflux from antrum and corpus cells previously loaded with $^{86}Rb^+$ (Fig. 7).

Sodium uptake. In both antrum and corpus cells sodium uptake (Fig. 8) was increased in the presence of OUA (10^{-3} M) or DNP (10^{-3} M). ASA did not affect sodium uptake ($P > 0.1$).

Sodium efflux. Sodium efflux (Fig. 9) was not influenced by ASA (10^{-2} M), whereas OUA (10^{-3} M) and

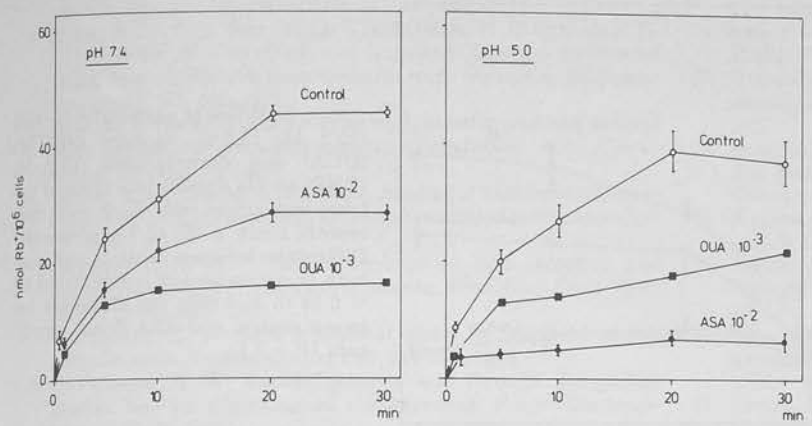

FIG. 5. Effect of acetylsalicylic acid (10^{-2} M) (ASA) on Rb uptake into isolated corpus cells at pH 7.4 and 5.0, respectively. Results of control experiments and aspirin experiments are represented as mean ± SE (3 experiments). Differences between aspirin at pH 7.4 and 5.0 are significant ($P < 0.05$ to < 0.005). In addition, figure shows result of 1 experiment with ouabain (10^{-3} M) (OUA) at pH 7.4 and 5.0.

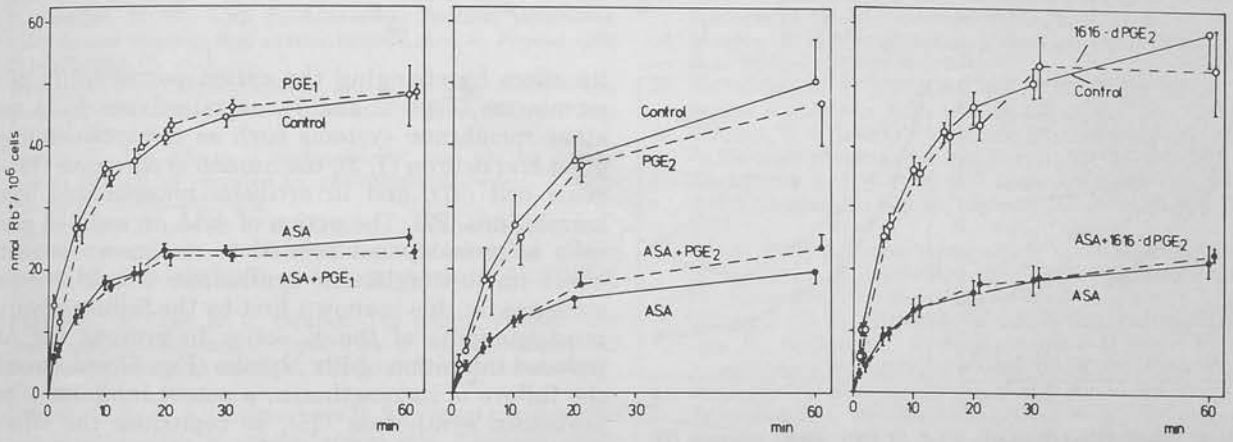

FIG. 6. Effect of prostaglandins on Rb uptake into isolated corpus cells. Prostaglandins were given alone or together with acetylsalicylic acid (10^{-2} M) (ASA). Each point represents mean ± SE of 3 experiments. PGE_1, prostaglandin E_1 (1 μg/ml); PGE_2, prostaglandin E_2 (10 μg/ml); 16,16-$dPGE_2$, 16,16-dimethyl prostaglandin E_2 (1 μg/ml).

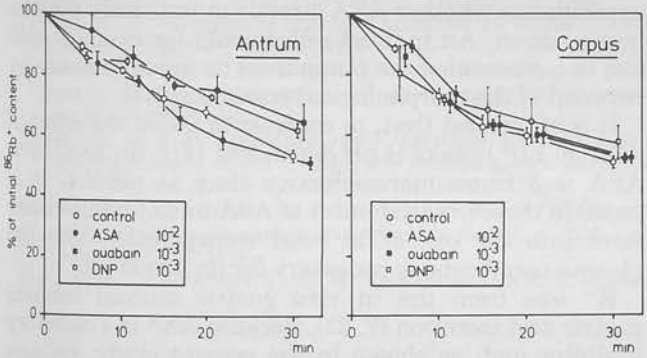

FIG. 7. Effect of acetylsalicylic acid (10^{-2} M) (ASA), ouabain (10^{-3} M) (OUA), and dinitrophenol (10^{-3} M) (DNP) on ^{86}Rb efflux from isolated antrum and corpus cells. Each point represents mean ± SE of 3-4 experiments. There is no significant difference between controls and values in presence of ASA, OUA, or DNP.

DNP (10^{-3} M) reduced the $^{22}Na^+$ efflux ($P < 0.025$ and < 0.005, respectively).

DISCUSSION

In the present study, cation transport of isolated gastric mucosal cells was measured. In contrast to the intact mucosa, this preparation allows a direct assessment of ion movement across the plasma membrane because paracellular transport is excluded. The cations chosen were Na^+, K^+, and Rb^+. The similarity of the gastric mucosal handling of K^+ and Rb^+ (22) was again confirmed (Figs. 1–3 and 7).

Antrum and corpus were examined because the intact mucosa of these two tissues shows different handling of ions and a different response to compounds such as salicylates that affect ion permeability (17, 18, 24). In the present study, isolated cells from antrum and corpus were markedly similar with respect to ion transport (Figures 1–3, 5, and 7–9).

ASA, DNP, and OUA have qualitatively similar actions on K^+ and Rb^+ movements in isolated gastric cells but qualitatively different actions on Na^+. K^+ and Rb^+ uptake into isolated gastric cells are inhibited by ASA, DNP, and OUA (Figs. 1 and 3), whereas K^+ and Rb^+ efflux are not affected by any one of these agents (Figs. 2 and 7). ASA does not affect Na^+ transport across the plasma membrane. The effect of OUA and DNP on Na^+ efflux can be explained by direct inhibition of the Na^+ pump or by reduction of the energy supply, respectively. The onset of the action is evident already at the first sampling time, i.e., after 5 min of exposure. These data suggest that the Na^+-K^+-ATPase is the major mechanism for Na^+ and K^+ regulation in the gastric mucosa. OUA or DNP may have an additional effect to their inhibition of the Na^+ pump because Na^+ efflux is more affected by DNP than by OUA, whereas the rise of Na^+ uptake is higher in the presence of OUA.

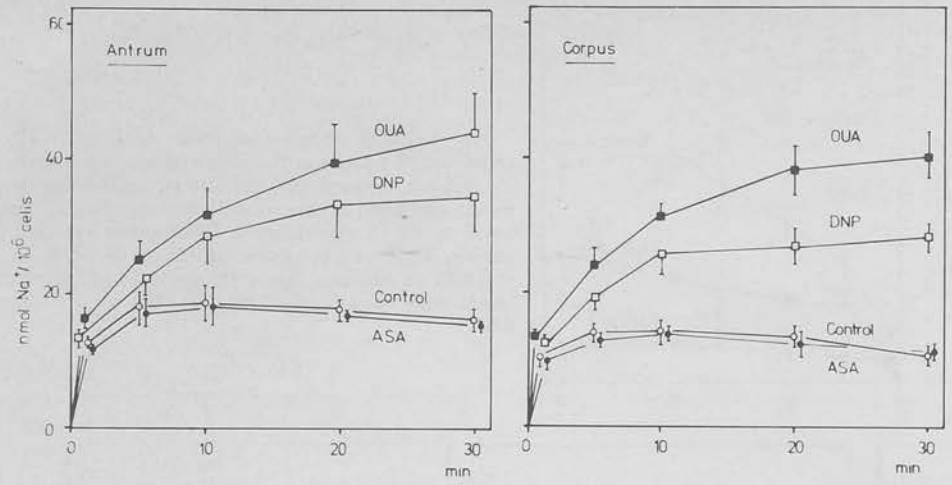

FIG. 8. Effect of acetylsalicylic acid (10^{-2} M) (ASA), ouabain (10^{-3} M) (OUA) and dinitrophenol (10^{-3} M) (DNP) on Na uptake into isolated antrum and corpus cells. Each point represents mean ± SE of 4 experiments. Difference between controls and ouabain or dinitrophenol is significant ($P < 0.05$ to < 0.005); the difference between control and ASA is not significant ($P > 0.1$).

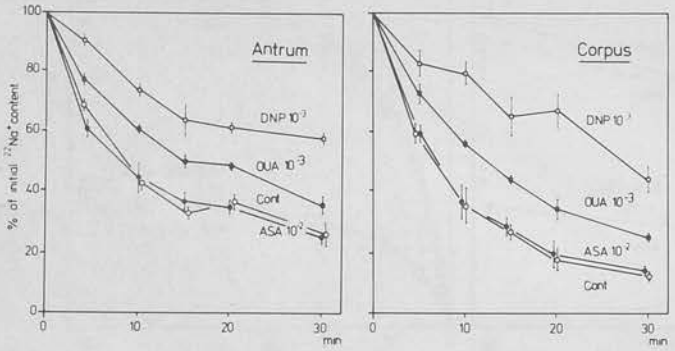

FIG. 9. Effect of acetylsalicylic acid (10^{-2} M) (ASA), ouabain (10^{-3} M) (OUA), and dinitrophenol (10^{-3} M) (DNP) on ^{22}Na efflux from isolated antrum and corpus cells. Each point represents mean ± SE of 3–5 experiments. Effect of OUA and DNP is significant ($P < 0.05$ to < 0.005) for each value. ASA values are not different from controls ($P = 0.05$).

The isotopic equilibrium in Na^+ uptake experiments exceeds the control values by about 4 times with OUA and by 2 times with DNP due to similar expansions of the exchangeable cellular Na^+ compartment. This indicates that isolated cells are able to maintain ion regulation. The relatively small amount of expansion is compatible with the previous observation that the gastric mucosa has a relatively high Na^+ content (4, 7, 10).

The uptake of K^+ and Rb^+ is strongly inhibited by OUA, DNP, and also by ASA. As in Na^+ experiments, the effect of OUA and DNP can be explained by direct and indirect inhibition of the Na^+-K^+-ATPase. The effect of ASA appears to be due to a different mechanism. Although ASA, like DNP, is known to uncouple oxidative phosphorylation (5, 21), this mechanism of action is unlikely in isolated gastric cells because ASA does not share the effect of DNP and OUA on Na^+ transport. Furthermore, the effect of ASA is additive to the effect of OUA when both agents are given at maximally effective concentrations (Fig. 4). Because ASA does not affect K^+ and Rb^+ efflux, it does not exert its effect by changing the cation permeability of the membrane (Figs. 2 and 7), as salicylates do in many other membrane systems such as the molluscan ganglion and neuron (1, 2), the human erythrocyte (40), the yeast cell (37), and in artificial phospholipid bilayer membranes (29). The action of ASA on isolated gastric cells is probably not related to its known inhibitory effect on prostaglandin synthetase (36, 38). Indirect evidence for this is shown first by the failure of various prostaglandins of the E series to prevent the ASA-induced inhibition of Rb^+ uptake (Fig. 6) and second by the failure of indomethacin, a potent inhibitor of prostaglandin synthetase (15), to reproduce the effect of ASA. ASA may inhibit a Na^+-independent K^+ pump. Such a pump is indeed present in parietal cells of the stomach (16, 33). It exchanges K^+ for H^+ and is driven by ATP. It cannot be determined from the present experiments whether ASA directly or indirectly inhibits pump action. An indirect effect could for example consist in a removal of the pump from its membrane site by reversal of the morphological transition (34).

It is of interest that, in contrast to OUA, the effect of ASA on Rb^+ uptake is pH dependent (Fig. 5). At pH 5.0, ASA is 5 times more effective than at pH 7.4. It is possible therefore that entry of ASA in its undissociated form into the cell or at least incorporation into the plasma membrane is necessary for its action (28).

K^+ loss from the in vivo gastric mucosa inhibits gastric acid secretion (7, 22). Because ASA is a secretory inhibitor and, as shown in the present study, reduces the K^+ uptake of gastric cells, it is speculated that the secretory inhibition of ASA in vivo may be due to direct action on the K^+-H^+ pump or to another Na^+-K^+-ATPase-independent K^+ depletion.

The expert technical assistance of Mrs. M. Lukachich is gratefully acknowledged.

This study was supported by Swiss National Science Foundation Grant 3.398.74.

Received 26 July 1977; accepted in final form 10 March 1978.

REFERENCES

1. BARKER, J. L., AND H. LEVITAN. The antagonism between salicylate-induced and pH-induced changes in the membrane of molluscan neurons. *Biochim. Biophys. Acta* 274: 638–643, 1972.
2. BARKER, J. L., AND H. LEVITAN. Studies on mechanism underlying non-narcotic analgesia. In: *Advan. Neurol.* 4: 503–511, 1974.
3. BLUM, A. L., B. I. HIRSCHOWITZ, H. F. HELANDER, AND G. SACHS. Electrical properties of isolated cells of necturus gastric

mucosa. *Biochim. Biophys. Acta* 241: 261–272, 1971.
4. BLUM, A. L., G. T. SHA, V. D. WIEBELHAUS, F. T. BRENNAN, H. F. HELANDER, R. CEBALLOS, AND G. SACHS. Pronase method for isolation of viable cells from necturus gastric mucosa. *Gastroenterology* 61: 189–200, 1971.
5. BOSUND, I. The effects of salicylic acid, benzoic acid and some of their derivatives on oxidative phosphorylation. *Acta Chem. Scand.* 11: 541–544, 1957.
6. COOKE, A. R., AND M. G. KIENZLE. Studies of anti-inflammatory drugs and aliphatic alcohols on antral mucosa. *Gastroenterology* 66: 56–62, 1974.
7. DAVENPORT, H. W. Effect of ouabain on acid secretion and electrolyte content of frog gastric mucosa. *Proc. Soc. Exptl. Biol. Med.* 110: 613–615, 1962.
8. DAVENPORT, H. W. Gastric mucosal injury by fatty and acetylsalicylic acids. *Gastroenterology* 46: 245–253, 1964.
9. DAVENPORT, H. W. Backdiffusion of acid through the gastric mucosa and its physiological consequences. *Progr. Gastroenterol.* 2: 42–56, 1970.
10. DAVENPORT, H. W., AND F. ALZAMORA. Sodium, potassium, chloride and water in frog gastric mucosa. *Am. J. Physiol.* 202: 711–715, 1962.
11. DURBIN, R. P., F. MICHELANGELI, AND A. MICHEL. Active transport and ATP in frog gastric mucosa. *Biochim. Biophys. Acta* 367: 177–189, 1974.
12. EDMAR, D. The effects of acetylsalicylic acid on the human gastric mucosa as revealed by gastrocamera. *Scand. J. Gastroenterol.* 10: 495–499, 1975.
13. FLEMSTROM, G., AND N. V. B. MARSDEN. Dextran permeability, electrical properties, and H secretion in isolated frog gastric mucosa after acetylsalicylic acid. *Gastroenterology* 64: 278–284, 1973.
14. FRENNING, B., AND K. J. OBRINK. The effects of acetic and acetylsalicylic acid on the appearance of the gastric mucosal surface epithelium in the SEM. *Scand. J. Gastroenterol.* 6: 605–612, 1971.
15. FLOWER, R. J., H. S. CHEUNG, AND D. W. CUSHMAN. Quantitative determination of prostaglandins and malondialdehyde formed by the arachidonate (prostaglandin synthetase) system of bovine seminal vesicle. *Prostaglandins* 4: 325–340, 1973.
16. FORTE, J. G., A. L. GANSER, AND A. S. TANISAWA. The K-stimulated ATPase system of microsomal membranes from gastric oxyntic cells. *Ann. N.Y. Acad. Sci.* 242: 255–267, 1974.
17. FROMM, D. Ion selective effects of salicylate on antral mucosa. *Gastroenterology* 71: 743–749, 1976.
18. FROMM, D., AND R. ROBERTSON. Effects of alcohol on ion transport by isolated gastric and esophageal mucosa. *Gastroenterology* 70: 220–225, 1976.
19. FROMM, D., J. H. SCHWARTZ, AND R. QUIJANO. Effects of salicylate and bile salt on ion transport by isolated gastric mucosa of the rabbit. *Am. J. Physiol.* 230: 319–326, 1976.
20. GLARBORG JORGENSEN, T., E. L. KAPLAN, AND G. W. PESKIN. Salicylate effects on gastric acid secretion. *Scand. J. Clin. Lab. Invest.* 33: 31–38, 1974.
21. GLARBORG JORGENSEN, T., U. S. WEIS-FOGH, AND H. P. OLESEN. The influence of acetylsalicylic acid (aspirin) on gastric mucosal content of energy-rich phosphate bonds. *Scand. J. Clin. Lab. Invest.* 36: 771–777, 1976.
22. HIRSCHOWITZ, B. I., AND G. SACHS. Insulin inhibition of gastric secretion: reversal by rubidium. *Am. J. Physiol.* 213: 1401–1405, 1967.
23. IMAMURA, A. In vitro effects of uncouplers on ionic fluxes across frog gastric mucosa. In: *Gastric Secretion*, edited by G. Sachs, E. Heinz, and K. Ullrich. New York: Academic, 1972, p. 181–188.
24. KASBEKAR, D. K. Effects of salicylate and related compounds on gastric HCl secretion. *Am. J. Physiol.* 225: 521–527, 1973.
25. KONDO, S., AND I. SCHULZ. Ca uptake in isolated pancreas cells induced by secretagogues. *Biochim. Biophys. Acta* 419: 76–92, 1976.
26. KUO, Y. J., AND L. L. SHANBOUR. Mechanisms of action of aspirin on canine gastric mucosa. *Am. J. Physiol.* 230: 762–767, 1976.
27. LEWIN, M., A. M. CHERET, A. SOUMARMON, AND J. GIRODET. Methode pour l'isolement et le tri des cellules de la muqueuse fundique de rat. *Biol. Gastroenterol., Paris* 7: 139–144, 1974.
28. MARTIN, B. K. Accumulation of drug anions in gastric mucosal cells. *Nature* 198: 896–897, 1963.
29. MCLAUGHLIN, S. Salicylate and phospholipid bilayer membranes. *Nature New Biol.* 243: 234–236, 1973.
30. RITCHIE, W. P., AND R. P. FISCHER. Effect of metabolic inhibitors on the gastric mucosal barrier. *Surgery* 73: 614–622, 1973.
31. ROBERT, A., A. J. HANCHAR, C. LANCASTER, AND J. E. NEZAMIS. Antiulcer effects of aspirin (Abstract). *Gastroenterology* 72: 1120, 1977.
32. SACHS, G., B. I. HIRSCHOWITZ, AND R. L. SHOEMAKER. Microelectrode studies of aspirin damage to gastric mucosa (Abstract). *Gastroenterology* 62: 804, 1972.
33. SACHS, G., H. H. CHANG, E. RABON, R. SCHACKMAN, M. LEWIN, AND G. SACCOMANI. A nonelectrogenic H pump in plasma membranes of hog stomach. *J. Biol. Chem.* 251: 7690–7698, 1976.
34. SEDA, A. W. Fine structures of the stimulated oxyntic cell. *Federation Proc.* 24: 1360–1367, 1965.
35. SERNKA, T. J., AND C. A. M. HOGBEN. Active ion transport by isolated gastric mucosa of rat and guinea pig. *Am. J. Physiol.* 217: 1419–1424, 1969.
36. SMITH, J. B., AND WILLIS, A. L. Aspirin selectively inhibits prostaglandin production in human platelets. *Nature New Biol.* 231: 235–237, 1971.
37. SCHARFF, T. G., AND A. C. PERRY. The effects of salicylic acid on metabolism and potassium content in yeast. *Proc. Soc. Exptl. Med.* 151: 72–77, 1976.
38. VANE, J. R. Inhibition of prostaglandin synthesis as a mechanism of action for aspirin-like drugs. *Nature New Biol.* 231: 232–235, 1971.
39. VIAL, J. D., AND H. ORREGO. Action of 2,4-dinitrophenol and iodoacetate on the ultrastructure of the oxyntic cells. *Exptl. Cell Res.* 30: 232–235, 1971.
40. WIETH, J. O. Paradoxical temperature dependence of sodium and potassium in human red cells. *J. Physiol., London* 207: 563–580, 1970.

Reprinted from ARCHIVES OF BIOCHEMISTRY AND BIOPHYSICS, Volume 143, No. 1, March 1971

Printed in U.S.A.

ARCHIVES OF BIOCHEMISTRY AND BIOPHYSICS **143**, 123–126 (1971)

Studies on Adenyl Cyclase in *Necturus* Gastric Mucosa[1]

SUMIO NAKAJIMA, BASIL I. HIRSCHOWITZ, AND GEORGE SACHS

Division of Gastroenterology, Department of Medicine, University of Alabama School of Medicine, Birmingham, Alabama 35233

Received September 21, 1970; accepted December 23, 1970

Adenyl cyclase activity of *Necturus* gastric mucosa was determined by measuring the amount of radioactive adenosine 3′,5′-cyclic monophosphate formed from ^{3}H-labeled adenosine triphosphate. Histamine, pentagastrin, and fluoride added *in vitro* significantly increased fundic adenyl cyclase activity. The dose response curves show that the affinity of pentagastrin for adenyl cyclase is greater than that of histamine, whereas the peak response to pentagastrin is less than that to histamine. Additive stimulation was not obtained when maximal doses of pentagastrin and histamine were combined. These findings suggest that gastric mucosa contains a single adenyl cyclase unit which is coupled to distinctive selectivity sites for gastrin and histamine. *N*-Benzyl-3-pyrrolidyl acetate methobromide (AHR-602), the muscarinic compound, caused a significant reduction in adenyl cyclase activity, indicating a different mechanism of stimulation of gastric acid secretion for cholinergic muscarinic compounds.

Adenosine 3′,5′-cyclic monophosphate (cyclic 3′,5′-AMP) provokes acid secretion in isolated amphibian gastric mucosa (1, 2). Cyclic 3′,5′-AMP is formed from ATP in the reaction catalyzed by adenyl cyclase, and recent investigations (1, 2) indicate that methylxanthine derivatives such as theophylline stimulate gastric acid secretion by inhibiting phosphodiesterase which catalyzes hydrolysis of the 3′- bond of cyclic 3′,5′-AMP. The basic question arises as to whether the effects of other gastric secretagogues are mediated via cyclic 3′,5′-AMP. The objective of the present work was to determine the effect of a variety of gastric secretagogues and fluoride on adenyl cyclase activity in *Necturus* gastric mucosa.

MATERIALS AND METHODS

The gastric mucosae from *Necturus maculosus* (common name: mudpuppy) were stripped of outer muscularis mucosa and the fundic mucosal membranes were minced and homogenized with a motor-driven Teflon pestle (A. H. Thomas) in cold 0.2 M sucrose (10:1, v/w). The crude homogenate was centrifuged at 3,000 *g* for 10 min. The supernatant was then centrifuged at 10,000 *g* for 20 min to obtain a crude mitochondrial fraction and the supernatant decanted; the particles were suspended in distilled water and protein concentration determined by the procedure of Lowry *et al.* (3). The crude mitochondrial fractions of many tissues have been shown to contain significant adenyl cyclase activity (4–6). These results do not imply, however, that adenyl cyclase is mitochondrial, since the mitochondrial fractions may well contain membrane fragments (7).

The amount of ^{3}H-labeled cyclic 3′,5′-AMP formed was measured by a modification of the method of Krishna *et al.* (4). One-fifth milliliter aliquots of the particular fraction were incubated at 37° for various times in a total volume of 0.6 ml with Tris–HCl buffer, pH 7.4 (3×10^{-2} M); $MgSO_4$ (3×10^{-3} M); theophylline (10^{-2} M); ATP (1.6×10^{-3} M); ^{3}H-ATP (New England Nuclear, 1.8×10^{-6} M). The final specific activity of ^{3}H-ATP was 16 μCi/μmole. Additions of histamine, pentagastrin, *N*-benzyl-3-pyrrolidyl acetate methobromide (AHR-602), and NaF were as indicated. The reactions were terminated by the addition of 0.1 ml (0.5 mg) of unlabeled cyclic 3′,5′-AMP, and by placing the tubes in boiling water for 3 min. After

[1] This study was supported by the National Institutes of Health, Grants AM-08541, AM-09260 and TIAM-5286, and the National Science Foundation, Grant GB-8351.

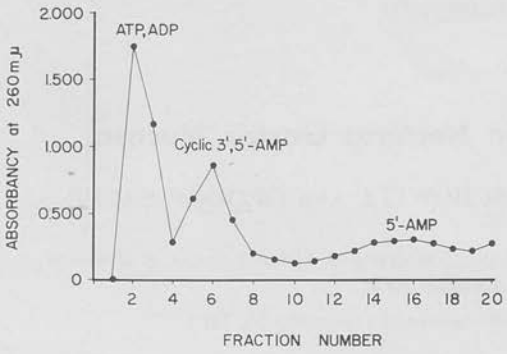

FIG. 1. Chromatographic separation of ATP, ADP, cyclic 3′,5′-AMP, and 5′-AMP on Dowex 50-H^+ (50W–X2, 200–400 mesh) columns (1.6 × 2.0 cm). Each compound (0.5 mg) was added to the incubation medium for adenyl cyclase assay which consisted of Tris–HCl, pH 7.4 (3×10^{-2} M), $MgSO_4$ (3×10^{-3} M), and theophylline (10^{-2} M). Columns were eluted with distilled water and 2-ml fractions were collected. The absorbance at 260 mμ was determined.

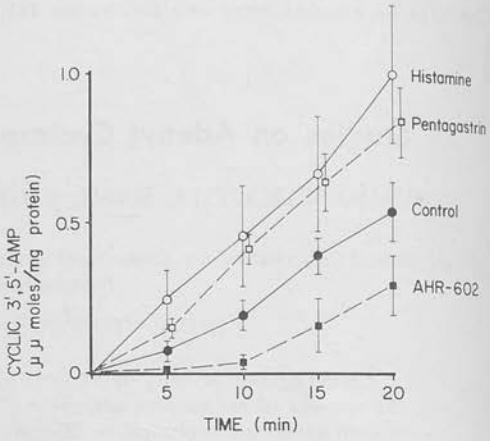

FIG. 2. The effect of 10^{-3} M histamine, 5.0×10^{-6} M pentagastrin, and 1.6×10^{-4} M AHR-602 on the formation of cyclic 3′,5′-AMP by adenyl cyclase in *Necturus* gastric mucosa. Each point represents the mean of five experiments. Vertical bars indicate SE of the mean.

centrifugation to remove the precipitate, the entire supernatant from each tube was chromatographed on Dowex 50-H^+ (J. T. Baker Chemical Co.; 50W–X2, 200–400 mesh) columns (1.6 × 2.0 cm), prepared by pipetting 4 ml of a 50% (w/v) suspension of the resin into columns and washing with water. The column was eluted with water and 2-ml fractions were collected. Approximately 45% of cyclic 3′,5′-AMP was recovered in the sixth fraction (Fig. 1). Nucleotides other than cyclic 3′,5′-AMP were precipitated twice with 0.2 ml each of 0.25 M $ZnSO_4$ and 0.25 M $Ba(OH)_2$ as described by Krishna *et al.* (4). The supernatant solution (0.5 ml) was added to 15 ml of a 1,4-dioxane medium containg 70 g/l. naphthalene, 7 g/l. 2,5-diphenyloxazole (PPO), and 0.05 g/l. POPOP-1,4-bis-2-(5-phenyloxazolyl)-benzene, and then counted for ^3H-labeled cyclic 3′,5′-AMP in a Beckman liquid scintillation counter. The results were expressed as pmoles cyclic 3′,5′-AMP produced per milligram protein. The statistical significance of results was evaluated by application of *t* test for paired samples.

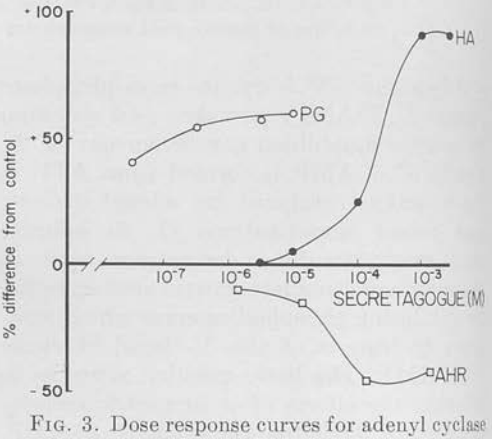

FIG. 3. Dose response curves for adenyl cyclase activity in response to pentagastrin (PG), histamine (HA), and AHR-602. Incubations were carried out at 37° for 20 min. Each point represents the mean of three to five experiments.

RESULTS

Figure 2 illustrates the effect of duration of incubation on the formation of cyclic 3′,5′-AMP by crude mitochondrial fraction from *Necturus* gastric mucosa with or without gastric secretagogues. The amount of cyclic 3′,5′-AMP measured progressively increased with the time of incubation for 5–20 min.

As can be seen from Fig. 2, adenyl cyclase activity was significantly increased by 10^{-3} M histamine ($p < 0.05$ when compared with control at 20 min), and to a lesser extent by 5.0×10^{-6} M pentagastrin ($p < 0.05$ compared with control at 15 and 20 min). The amounts of cyclic 3′,5′-AMP formed at 15 and 20 min with 1.6×10^{-4} M AHR-602 were

TABLE I

THE COMBINED EFFECTS OF MAXIMAL DOSES OF PENTAGASTRIN AND HISTAMINE ON ADENYL CYCLASE ACTIVITY IN *Necturus* GASTRIC MUCOSA

Secretagogue	Adenyl cyclase activity[a] (% increase from control)
Pentagastrin (10^{-5} M)	60.8 ± 14.0
Histamine (10^{-3} M)	93.4 ± 18.8
Pentagastrin (10^{-5} M) + Histamin (10^{-3} M)	94.5 ± 18.9

[a] Values are mean ± SEM for five separate analyses. Incubations were carried out at 37° for 20 min.

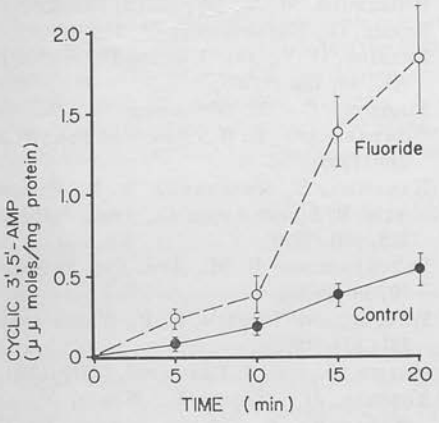

FIG. 4. The effect of 10^{-2} M sodium fluoride on the formation of cyclic 3′,5′-AMP by adenyl cyclase in *Necturus* gastric mucosa. Each point represents the mean of five experiments. Vertical bars indicate SE of the mean.

significantly less than those without AHR-602 ($p < 0.05$).

Figure 3 shows dose response curves for pentagastrin, histamine, and AHR-602. The peak responses were obtained with concentrations of about 1.0×10^{-5} M pentagastrin, 1.0×10^{-3} M histamine, and 1.6×10^{-4} M AHR-602. The cyclase activation by combinations of maximal doses of pentagastrin and histamine was not significantly different from that by maximal doses of histamine given singly (Table I, $p > 0.05$).

As shown in Fig. 4, 10^{-2} M NaF had a marked stimulatory effect on adenyl cyclase activity during incubation periods varying from 15 to 20 min ($p < 0.05$ when compared with control).

DISCUSSION

Recently Perrier and Laster (8) have reported that histamine and its analogs, betazole and aminoethyltriazole, and prostaglandins stimulate adenyl cyclase in guinea pig gastric mucosa three- to four-fold, and that choline esters and gastrin have no effect. They concluded that their observations might support the hypothesis that histamine is, or is related to, the final common stimulus for gastric acid secretion. The results of the present study, however, show that, in *Necturus* gastric mucosa, fundic adenyl cyclase is activated by histamine, pentagastrin and fluoride, and inhibited by AHR-602, the cholinergic muscarinic compound. Since many peptide hormones do not appear to affect phosphodiesterase (9), the results presented suggest that both histamine and pentagastrin may increase the intracellular level of cyclic 3′,5′-AMP. However, in previous studies *in vitro*, some differences were observed between the effects of pentagastrin and theophyline (2). Furthermore, resting *Necturus* gastric mucosa is relatively refractory to a large amount of histamine—requiring 10^{-3} M for maximal acid response of approximately 0.6 μEq/hr·cm^2—a response which is significantly less than that to pentagastrin (10). Since combinations of maximal doses of pentagastrin and histamine do not produce additive effects on adenyl cyclase activity, it is tentatively concluded that gastric mucosa contains a single adenyl cyclase unit which is coupled to distinctive selectivity sites for pentagastrin and histamine.

While fluoride was the most potent stimulant of adenyl cyclase activity in gastric mucosa, as also reported in other tissues (11), it failed to evoke acid secretion in *Necturus* gastric mucosa *in vitro*, possibly because of its cytotoxic effect. Similarly, prostaglandin, which stimulates gastric adenyl cyclase (8), apparently inhibits gastric acid secretion *in vitro* (12). Fluoride has also been shown to inhibit ($Na^+ + K^+$)-ATPase activity from stomach and heart (13), brain (14), and erythrocytes (15). Schramm and Naim (16)

postulate that fluoride and Mg^{2+} form a complex with the specific inhibitors of adenyl cyclase so that the inhibition is largely abolished. It should also be noted that fluoride does not increase cyclic 3′,5′-AMP concentrations in thyroid slices despite the fact that it enhances thyroid adenyl cyclase activity (17).

It is of special interest that AHR-602 caused a significant inhibition of adenyl cyclase activity in *Necturus* gastric mucosa. The muscarinic compounds, therefore, stimulate acid secretion *in vitro* (10) by a mechanism which is unrelated to activation of adenyl cyclase, and is highly susceptible to atropine. Similar effects of cholinergic compounds have been observed by Murad *et al.* (18) who demonstrated that acetylcholine, carbachol and acetyl-β-methylcholine inhibit cardiac adenyl cyclase and that atropine prevents the inhibitory effect of carbachol. If acid secretion is mediated by cyclic 3′,5′-AMP, then the gastric secretagogues will either stimulate adenyl cyclase or inhibit phosphodiesterase. The effect of muscarinic compounds on phosphodiesterase activity remains to be established. It has been shown, however, that carbachol does not increase the concentrations of cyclic 3′,5′-AMP in thyroid slices (17) and that acetylcholine, which stimulates glucose oxidation, phospholipid synthesis, and phosphorylase activity (19, 20), does not activate adenyl cyclase in thyroid (21). Thus it seems probable that the muscarinic compounds may exert similar metabolic effects on gastric mucosa by a mechanism unrelated to concentrations of cyclic 3′,5′-AMP. In the light of these findings, it appears reasonable to question whether the effects of all gastric secretagogues are mediated solely by the adenyl cyclase–cyclic 3′,5′-AMP system.

ACKNOWLEDGMENTS

The authors are grateful to Dr. T. Robitscher of Ayerst Research Laboratories, New York, New York, for pentagastrin AY-6608 (I.C.I. 50,123) and to Dr. J. W. Ward of Robins Research Laboratories, Richmond, Virginia, for AHR-602.

REFERENCES

1. Harris, J. B., Nigon, K., and Alonso, D., *Gastroenterology* **57**, 377 (1969).
2. Nakajima, S., Shoemaker, R. L., Hirschowitz, B. I., and Sachs, G., *Amer. J. Physiol.* **219**, 1259 (1970).
3. Lowry, O. H., Rosebrough, N. J., Farr, A. L., and Randall, R. J., *J. Biol. Chem.* **193**, 265 (1951).
4. Krishna, G., Weiss, B., and Brodie, B. B., *J. Pharmacol. Exp. Ther.* **163**, 379 (1968).
5. Sutherland, E. W., Øye, I., and Butcher, R. W., *Recent Progr. Horm. Res.* **21**, 623 (1965).
6. Hollinger, M. A., *Life Sci.* **9**, 533 (1970).
7. Burke, G., *Endocrinology* **86**, 346 (1970)
8. Perrier, C. V., and Laster, L., *J. Clin. Invest.* **49**, 73a (1970).
9. Robison, G. A., Butcher, R. W., and Sutherland, E. W., *Ann. Rev. Biochem.* **37**, 149 (1968).
10. Nakajima, S., Shoemaker, R. L., Hirschowitz, B. I., and Sachs, G., *Amer. J. Physiol.* **218**, 990 (1970).
11. Breckenridge, B. M., *Ann. Rev. Pharmacol.* **10**, 19 (1970).
12. Way, L., and Durbin, R. P., *Nature London* **221**, 874 (1969).
13. Mozsik, G., *Eur. J. Pharmacol.* **7**, 319 (1969).
14. Yoshida, H., Nagai, K., Kamei, M., and Nakagawa, Y., *Biochim. Biophys. Acta* **150**, 162 (1968).
15. Farias, R. N., Goldemberg, A. L., and Trucco, R. E., *Arch. Biochem. Biophys.* **139**, 38 (1970).
16. Schramm, M., and Naim, E., *J. Biol. Chem.* **245**, 3225 (1970).
17. Kaneko, T., Zor, U., and Field, J. B., *Science* **163**, 1062 (1969).
18. Murad, F., Chi, Y. M., Rall, T. W., and Sutherland, E. W., *J. Biol. Chem.* **237**, 1233 (1962).
19. Altman, M., Oka, H., and Field, J. B., *Biochim. Biophys. Acta* **116**, 586 (1966).
20. Butcher, F. R., and Serif, G. S., *Biochim. Biophys. Acta* **156**, 59 (1968).
21. Pastan, I., and Katzen, R., *Biochem. Biophys. Res. Commun.* **29**, 792 (1967).

AMERICAN JOURNAL OF PHYSIOLOGY
Vol. 225, No. 6, December 1973. *Printed in U.S.A.*

Adenyl and guanyl cyclase in rabbit gastric mucosa

C. P. SUNG, B. C. JENKINS, L. RACEY BURNS, V. HACKNEY, J. G. SPENNEY, G. SACHS, AND V. D. WIEBELHAUS
Smith Kline & French Laboratories, Philadelphia, Pennsylvania 19101; and University of Alabama, Birmingham, Alabama 35294

SUNG, C. P., B. C. JENKINS, L. RACEY BURNS, V. HACKNEY, J. G. SPENNEY, G. SACHS, AND V. D. WIEBELHAUS. *Adenyl and guanyl cyclase in rabbit gastric mucosa.* Am. J. Physiol. 225(6): 1359–1363. 1973.—The adenyl cyclase present in rabbit gastric mucosa is stimulated by histamine and fluoride when derived from the fundic area, but from the antral area histamine does not affect the activity of the enzyme. Burimamide inhibits the histamine-stimulated component, as does Mn^{++}. Of the various histamine analogs tested, those which stimulate adenyl cyclase also stimulate secretion. Guanyl cyclase activity is not affected by any of the hormones tested, and antrum has a higher specific activity than fundus.

cyclic AMP; gastric secretion; cyclic GMP; histamine; antihistamine; burimamide

IN RECENT YEARS controversy has surrounded the role of 3′,5′-cyclic AMP in the stimulation of acid secretion. In Amphibia, acid secretion is stimulated by cAMP and phosphodiesterase inhibitors (4, 11). In support of this observation an adenyl cyclase stimulated by histamine has been described in amphibian gastric mucosa (10). Gastric mucosal cAMP levels are, however, not increased during histamine-stimulated acid secretion (unpublished observation). With this latter exception the evidence warrants the conclusion that in Amphibia cAMP plays the role of second messenger in the acid secretory response.

Since the gastric stimulatory hormones are not species specific the role of cAMP in gastric secretory activity would be anticipated to be general. Accordingly, in both dog and man, cAMP levels in both gastric mucosa and gastric juice increase prior to the onset of acid secretion (1). In man the methyl xanthines stimulate acid secretion, but in dog neither the methyl xanthines nor injection of cAMP are effective (6). While it has been claimed that guinea pig gastric mucosa contains a histamine-sensitive adenyl cyclase, the presence of histamine-sensitive enzyme in the dog has been denied. Thus while evidence for involvement of cAMP in amphibian gastric secretion is compelling, the conclusion that cAMP is involved in mammalian gastric secretion is not widely accepted.

To further investigate the role of cAMP in mammalian gastric secretion we have studied an adenyl cylase in rabbit gastric mucosa. This enzyme was found to be stimulated by histamine and a variety of its analogues which also stimulate gastric secretion. Guanyl cyclase, while present in the tissue, was insensitive to any of the hormones tested.

METHODS

Preparation of Homogenate

We have used only fresh mucosae obtained from rabbits killed by cervical dislocation. The stomach was immediately removed and washed with ice-cold buffer. The mucosa was scraped off after blotting, and the scrapings homogenized in 5 volumes of ice-cold 50 mM Tris-Cl pH 7.6 containing 10 mM EDTA. The homogenate was centrifuged at 2,000 *g* for 15 min and the pellet washed once and resuspended in 15–18 ml of medium, giving a protein concentration of 20–25 mg/ml. This suspension was used immediately.

Adenyl Cyclase Assay

Of this suspension, 20 μl were incubated in the presence of 50 mM Tris-Cl buffer, pH 7.8, 10 mM phosphoenol pyruvate, 1.75 μg pyruvate kinase, 5 mM $MgCl_2$, 0.02 mg bovine serum albumin, 10 mM theophylline, 2 mM cAMP, 1 mM ATP containing 1 μc ATP-^{14}C, 40 mM KCl ± 10 mM NaF, ± 1 mM histamine or other additive where noted, in a final volume of 100 μl. The incubation temperature was 37 C and the time of incubation was for 10 min.

Boiled controls were obtained by heating for 5 min at 100 C prior to the addition of isotope.

The reaction was stopped either by heating to 100 C for 5 min or by the addition of an equal volume of ice-cold 10% TCA. In the instances where TCA was used, the samples were centrifuged and the supernatants were extracted twice in 3 ml ether to remove TCA. Residual ether was removed by blowing a gentle stream or air of N_2 over the samples.

The samples were placed on an ice bath and 10 μl of 0.3 N $Ba(OH)_2$ and 10 μl of 0.3 N $ZnSO_4$ added to each. After standing for 15 min the samples were centrifuged 5 min in a Beckman microfuge. A further addition of 10 μl $Ba(OH)_2$ and 10 μl $ZnSO_4$ was followed by a second centrifugation; 20 μl of the supernatant were spotted on Eastman Kodak no. 6065 thin-layer chromatography sheets.

The system was developed in a solvent consisting of 100 ml *n*-butanol, 50 ml acetone, 20 ml glacial acetic acid, 30 ml 5% NH_4OH, and 20 ml H_2O.

After 2 hr the chromatogram was removed, dried, and the spots corresponding to 3′,5′-cAMP cut out, put in Aquasol scintillation fluid, and counted in a Beckman SC100 liquid scintillation counter. The recovery of cAMP, checked by measuring the OD at 260 nm and by recovery of labeled cAMP, was in excess of 90%.

Guanyl Cyclase Assay

This was measured by a technique similar to adenyl cyclase. The 100,000 $g \times 60$ min supernatant was used, Mn^{++} substituted for Mg^{++} and GTP for ATP in the incubation. No Ba^{++}/Zn^{++} precipitation was carried out since this removes cGMP.

Results are expressed as mμmoles cAMP or cGMP formed mg^{-1} hr^{-1}. The protein was measured by the Lowry method (8).

RESULTS

Validation of Technique

Constancy of ATP level. One of the potential problems in this type of assay is depletion of ATP due to activity of a variety of ATPases. Accordingly, ATP was measured by a microfluorimetric procedure (7) at various incubation times. ATP levels were maintained for a 10-min period; hence this was the incubation time chosen (Table 1). The effect of F^- and a regenerating system in maintaining ATP levels was noteworthy.

Thin-layer chromatography. A potential source of error with this technique results from count contamination from adjacent spots. AMP is well separated from cyclic AMP. A spot with an R_F slightly more than cAMP was noted; the counts in this spot were significantly decreased by the presence of F^-. Care had to be taken, therefore, to run the chromatogram to within 1 cm of the top to allow separation of this spot. The spot was cut out and identified as inosine by UV spectroscopy and cochromatography with authentic inosine in two other solvent systems. Inosine production has also been established in toad bladder (3). To verify the adequacy of our separation technique autoradiograms of the chromatography sheets were carried out. Figure 1 shows the effect of Ba^{++}/Zn^{++} precipitation, as well as the effect of F^-. The lack of contamination of the cAMP spot is quite evident.

TABLE 1. *ATP level during incubation in adenyl cyclase activity assay*

Incubation Time, min	Total ATP Remaining in Incubation Medium, mM				
	Boiled enzyme (blank)	Control level	Histamine level	NaF level	Nonregenerating system
0	0.81	0.91	0.76	0.78	0.75
2	0.72	0.58	0.68	0.83	0.33
4	0.49	0.54	0.64	0.69	0.21
6	0.72	0.93	0.71	0.83	0.09
8	0.65	0.83	0.76	0.93	0.05
10	0.97	1.15	1.12	0.99	0.04
15	1.09	0.40	0.51	1.09	0.02
20	0.84	0.16	0.13	0.77	0.04
30	0.45	0.14	0.15	0.46	0.04

The general adenyl cyclase assay as mentioned in METHODS was used except that no radioactivity was present in 1 mM ATP. 10-μl samples were taken at different incubation times and boiled to terminate the reaction. ATP level was then assayed using the following reaction by measuring TPNH formation (7):

$$\text{ATP} + \text{glucose} \xrightarrow{\text{hexose kinase}} \text{ADP} + \text{G-6-}P;$$

$$\text{and G-6-}P + \text{TPN}^+ \xrightarrow{\text{G-6-}P\text{-dehydrogenase}} 6\text{-}P\text{-gluconolactone} + \text{TPNH} + \text{H}^+.$$

Effect of time of incubation, protein concentration. The production of cAMP or cGMP was linear with time up to 10 min of incubation, and was linear with protein concentration up to a value of 4 mg/ml final concentration (Fig. 2).

Effect of F^-

Fluoride appears to be an almost universal stimulant of adenyl cyclase activity (13). The adenyl cyclase of rabbit gastric mucosa is no exception. Table 2 shows that the presence of F^- activates the adenyl cyclase of both fundic and antral mucosa between 5- to 10-fold.

Effect of Histamine

The addition of 1 mM histamine to the incubation medium results in a two- to fivefold stimulation of adenyl cyclase

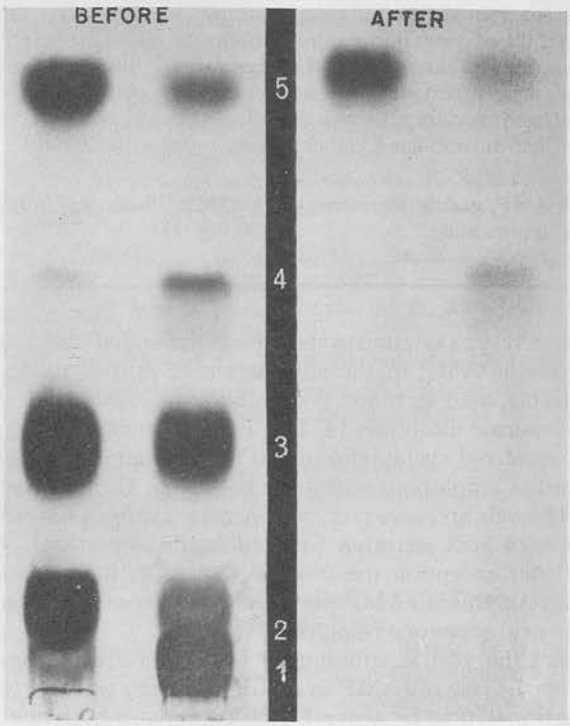

FIG. 1. Autoradiogram of TLC plate showing separation of nucleotides in a control and fluoride-stimulated sample before and after Ba^{++}/Zn^{++} precipitation. Increased cAMP formed in presence of F^- is clearly evident as is removal of other nucleotides by Ba^{++}/Zn^{++} precipitation. Diminution in cAMP spot following precipitation is due to dilution of sample with the $Ba(OH)_2$ and $Zn(OH)_2$. Spots visualized are: 1, ATP; 2, ADP; 3, AMP; 4, cAMP; and 5, adenosine.

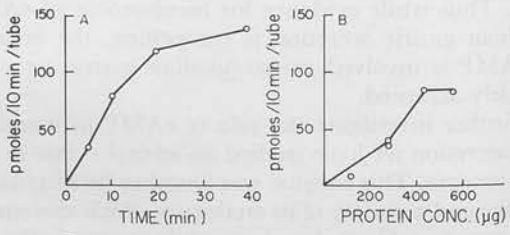

FIG. 2. *A:* effect of time of incubation on cAMP formation (382 μg protein). *B:* effect of protein concentration (μg/100 μl) on cAMP formation.

activity. This stimulation occurs in fundic mucosa, but not antral mucosa (Table 2). Moreover, the effect is dose responsive, as shown in Fig. 3. At very high histamine (10^{-1} M) there is an inhibition showing only 60% of control activity.

Effect of pH

Studies of adenyl cyclase activity at various pHs revealed an optimum for both basal and histamine-stimulated activity at pH 7.8 (Fig. 4). The peaks of basal and histamine-stimulated activity are broad, but the increment due to histamine stimulation is clearly greater at pH 7.8 than at pH 5 or 9 (100 versus 35 and 65 pmoles/tube per 10 min, respectively).

TABLE 2. *Adenyl cyclase levels in tissue (mucosa)*

	Fundic	Antral
	mμmoles mg⁻¹ hr⁻¹	
Control	0.73 ± 0.21	0.41 ± 0.18
Histamine, 10^{-3} M	2.04 + 0.33	0.36 ± 0.14
Fluoride, 10^{-2} M	3.55 ± 0.31	1.20 ± 0.35
Fluoride + histamine	3.44 ± .40	1.16 ± 0.29

For fundic mucosa each value is the mean of 10 experiments ± SD, and from antrum each value is the mean of 3 experiments ± SD.

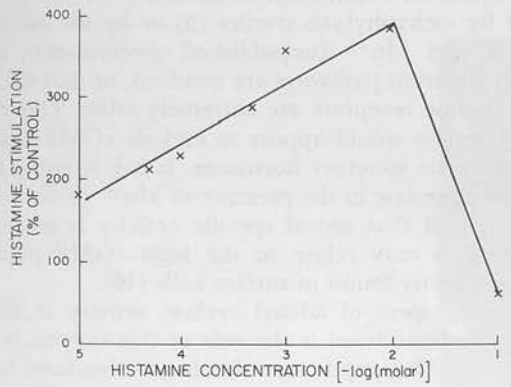

FIG. 3. Effect of varying concentrations of histamine (−log M) on adenyl cyclase activity (expressed as percent control).

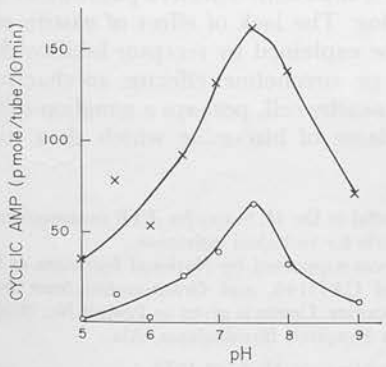

FIG. 4. pH optimum of adenyl cyclase activity. Assays were performed using 50 mM HEPES (*N*-2-hydroxyethyl piperazine *N'*-2-ethanesulfonic acid) adjusted to the stated pH with NaOH. ○——○ indicates basal activity and ×——× indicates activity in presence of 10^{-3} M histamine. 434 μg protein were used in each assay tube.

Effect of Histamine Analogues

A variety of analogues of histamine were used to establish a correlation between gastric secretroy activity and adenyl cyclase activation. These data are summarized in Table 3. It can be seen that there is a very good correlation between effect in this assay and effect on gastric acid secretion. A dose-response curve for *N*-methyl and *N,N'*-dimethyl histamine was also run and the K_m's for *N*-methyl and *N,N'*-dimethyl histamine were not significantly different from the K_m for histamine.

Effect of Antihistamines

Two analogues of histamine were chosen for this aspect of the work, an anti H_1 and an anti H_2 compound. H_1-type histamine receptors are responsible, for example, for blood vessel responses, ileal contraction, etc., whereas H_2-type receptors are responsible for myometrial contraction of gastric secretion. Butyl methyl thioureaimidazole (burimamide) is the prototype anti H_2 compound (2) and diphenylhydramine and mepyramine maleate were used as anti H_1 compounds.

Both compounds inhibited the histamine stimulation of adenyl cyclase activity (Table 4) but diphenylhydramine also blocked F^- stimulation, whereas burimamide and mepyramine did not. The action of H_1 and H_2 compounds thus overlapped.

Effect of Mn^{++}

Mn^{++} has been used to inhibit spontaneous acid secretion in frog gastric mucosa (15). As shown in Table 4, Mn^{++}

TABLE 3. *Effect of histamine analogs on adenyl cyclase*

Compound	Gastric Secretion	Adenyl Cyclase, % of Control
Control	None	100
Histamine	+++	342
N-methyl histamine	+++	288
N,N-dimethyl histamine	+++	253
4-methyl histamine	+++	301
2-methyl histamine	++	230
3-(2'-aminoethyl)-1,2,4-triazole	++	234
3-(2'-aminoethyl)-pyrazole*	++	142
2-amino-4-aminoethyl thiazole	++	192
2-aminoethyl pyridine	+	137
N-tert-butyl histamine	+	115
3-methyl histamine	+	85
N-acetyl histamine*	+	123
4-(2 methyl-2-amino propionyl)- imidazole		89
Histidine		103
Imidazole 4-acetic acid*		93
2-methyl-4-amino methyl imidazole		105
4-chloroethyl imidazole		102
4-hydroxyethyl imidazole		102
4-thioamido ethyl imidazole		74
4-(2'-aminoethyl)-1,2,3-triazole		102

The compounds were tested at a final concentration of 10^{-3} M in the standard adenyl cyclase system. The adenyl cyclase data are means of two experiments, expressed as percent of control. Gastric secretion data were obtained in the Shay rat or the conscious dog. +++ 10–100% of histamine output (on a molar basis); ++ 1–10% of histamine output; + 0.1–1% of histamine output; − < 0.1% of histamine output. * Values taken from the literature (14).

inhibited the histamine stimulation at 5 mM. Interestingly, Mn^{++} increased the F^- activation.

Effect of Gastrin and Urecholine

Whereas under the described conditions the action of F^- and histamine in stimulating adenyl cyclase activity was quite consistent, the action of pentagastrin was quite variable. In some instances, at a final concentration of 0.03 mg/ml there was a 20–50% stimulation, on others there was no effect. In the case of urecholine the same variability was found.

Guanyl Cyclase

Measurements of this activity were carried out both in fundus and antrum. Most of the activity was found in the supernatant fraction of the homogenate in both tissues. This enzyme was not stimulated by either histamine or fluoride (Table 5).

DISCUSSION

The adenyl cyclase of rabbit gastric mucosa has several properties which make it of interest with respect to acid secretion.

a) It is dose responsive to histamine (three- to fivefold stimulation at 10^{-3} M) when the enzyme is derived from fundic mucosa. Antral mucosal cyclase is not sensitive to histamine. We may conclude that the histamine-sensitive adenyl cyclase is a property of the tubular cell system (i.e., parietal or peptic cells).

b) The comparison of the action of histamine agonists on adenyl cyclase and acid secretion shows a distinct correlation between stimulation of the adenyl cyclase and stimulation of secretion. A similar correlation exists with brain adenyl cyclase (14).

c) Mn^{++}, which inhibits basal acid secretion in Amphibia (15), also inhibits histamine stimulation of adenyl cyclase. In addition, Mn^{++} increases the F^- stimulation of the enzyme. This may be due to the formation of Mn^{++}-F-ATP complex which is an effective substrate for adenyl cyclase but not for the two types of catabolic enzymes present in the homogenate, the hydrolases (ATPases), and deaminases (inosine pathway). The Mg^{++} complex may be more readily attacked by those enzymes.

On the other hand, some of the data obtained raise doubts as to the role of this enzyme. Thus, confirming the data of others (9), we were unable to detect any hormonal sensitivity in dog mucosa. Moreover, our adenyl cyclase test systems did not distinguish between H_1 and H_2 antagonists even using dose-response curves, whereas the intact system does so (2; unpublished observations). This may be used as an argument against the role of adenyl cyclase or as an argument against any real distinction between histamine receptors. The selectivity of burimamide and inactivity of antihistamines in acid secretion may reflect location of the receptor rather than two separate molecular systems.

The work reported here also does not help elucidate the mechanisms of gastrin or urecholine stimulation. It may be that sequential stimulation is involved, as has been suggested by tachyphylaxis studies (5) or by the use of burimamide and Mn^{++} (unpublished observations), or that entirely different pathways are involved, or that the gastrin or urecholine receptors are extremely labile. Our data on guanyl cyclase would appear to exclude cGMP as a mediator of gastric secretory hormones. It is interesting that F^- does not stimulate in the presence of Mn^{++} (it does if Mg^{++} is used), and that antral specific activity is greater than fundic. This may relate to the high cGMP phosphodiesterase activity found in surface cells (16).

Another aspect of adenyl cyclase activity as described here to be considered is the role of this enzyme in peptic stimulation. Dog peptic secretion is not stimulated by histamine, in contrast to many other species. A possible explanation for the effects of histamine on rabbit or guinea pig (12) adenyl cyclase is that cAMP mediates pepsin secretion and is formed by a histamine-sensitive pathway in these species, but not in dog. The lack of effect of gastrin or urecholine could then be explained by receptor lability. Alternatively, the gastrin or urecholine effector mechanism could be located in a nearby cell, perhaps a ganglion cell, and act by the local release of histamine which then stimulates the oxyntic cell.

TABLE 4. *Effect of histamine on basal and stimulated adenyl cyclase activity*

Assay Condition	None	Antagonists: Burimamide, 10^{-3} M	Diphenylhydramine, 10^{-2} M	Mepyramine maleate, 10^{-3} M	Mn^{++}, 5×10^{-3} M
Control	100	96	47	51	98
Histamine, 10^{-3} M	175	94	45	45	75
Fluoride, 10^{-2} M	245	251	104	185	470

Results are expressed as percent of control with no antagonist addition.

TABLE 5. *Measurements of guanyl cyclase*

	Fundus	Antrum
	$m\mu moles\ mg^{-1}\ hr^{-1}$	
Control	1.62	5.73
Histamine, 10^{-3} M	1.62	6.70
Pentagastrin, 10^{-4} M	1.36	4.94
Fluoride, 10^{-2} M	1.52	5.79

Each value is the mean of two experiments and is in the presence of Mn^{++} only.

We are grateful to Dr. H. Sarau for ATP measurements and to Mrs. M. A. Mackenzie for technical assistance.

This study was supported by National Institutes of Health Grants AMO8541 and CA13148, and Grant-in-Aid from Smith Kline & French Laboratories. Credit is given to Project No. 8059-01, Veterans Administration Hospital, Birmingham, Ala.

Received for publication 15 April 1973.

REFERENCES

1. Bieck, P. R. Role of cyclic AMP in the regulation of gastric secretion in dogs and humans. In: *Advance in Cyclic Nucleotide Research*. New York: Raven, 1972, vol. 1, p. 149–161.

2. Black, J. W., W. A. M. Duncan, C. J. Durant, C. R. Ganellin, and E. M. Parsons. Definition and antagonism of histamine H_2-receptors. *Nature* 236: 385–390, 1972.

3. FERGUSON, D. R., AND R. H. PRICE. The actions of cyclic nucleotides on the toad bladder. In: *Advance in Cyclic Nucleotide Research.* New York: Raven, 1972, vol. 1, p. 113–119.
4. HARRIS, J. B., AND D. ALONSO. Stimulation of the gastric mucosa by adenosine-3′,5′-monophosphate. *Federation Proc.* 24: 1368–1376, 1965.
5. KASBEKAR, D. K. Secretagogue-induced tachyphylaxis of gastric H^+ secretion and its reversal. *Am. J. Physiol.* 223: 294–299, 1972.
6. LEVINE, R. A., AND D. E. WILSON. The role of cyclic AMP in gastric secretion. *Ann. N. Y. Acad. Sci.* 185: 363–375, 1971.
7. LOWRY, O. H., AND J. V. PASSONNEAU. *A Flexible System of Enzymatic Analysis.* New York: Academic, 1972, p. 151.
8. LOWRY, O. H., N. J. ROSEBROUGH, A. L. FARR, AND R. J. RANDALL. Protein measurement with the Folin phenol reagent. *J. Biol. Chem.* 193: 265–275, 1951.
9. MAO, C. C., L. L. SHANBOUR, D. S. HODGINS, AND E. D. JACOBSON. Adenosine-3′,5′-monophosphate (cyclic AMP) and secretion in the canine stomach. *Gastroenterology* 63: 427–438, 1972.
10. NAKAJIMA, S., B. I. HIRSCHOWITZ, AND G. SACHS. Studies on adenyl cyclase in *Necturus* gastric mucosa. *Arch. Biochem. Biophys.* 143: 123–126, 1971.
11. NAKAJIMA, S., R. L. SHOEMAKER, B. I. HIRSCHOWITZ, AND G. SACHS. Comparison of actions of aminophylline and pentagastrin on *Necturus* gastric mucosa. *Am. J. Physiol.* 219: 1259–1262, 1970.
12. PERRIER, C. V., AND L. LASTER. Adenyl cyclase activity of guinea pig gastric mucosa: stimulation by histamine and prostaglandins. *J. Clin. Invest.* 49: 73a, 1970.
13. ROBISON, G. A., R. W. BUTCHER, AND E. W. SUTHERLAND. *Cyclic AMP.* New York: Academic, 1971.
14. SHIMIZU, H., C. R. CREVELING, AND J. W. DALY. The effect of histamine and other compounds on the formation of adenosine 3′,5′-monophosphate in slices from cerebral cortex. *J. Neurochem.* 17: 441, 1970.
15. SHOEMAKER, R. L. Inhibition of acid secretion by manganese in the *in vitro* frog gastric mucosa. *Alabama J. Med. Sci.* 8: 424–430, 1971.

AMERICAN JOURNAL OF PHYSIOLOGY
Vol. 210, No. 4, October 1970. *Printed in U.S.A.*

Action of cholinergic drugs on *Necturus* gastric mucosa

R. L. SHOEMAKER, G. M. MAKHLOUF, AND G. SACHS
Departments of Medicine, Physiology and Biophysics, University of Alabama Medical Center, Birmingham, Alabama 35233

SHOEMAKER, R. L., G. M. MAKHLOUF, AND G. SACHS. *Action of cholinergic drugs on Necturus gastric mucosa.* Am. J. Physiol. 219(4): 1056–1060. 1970.—Acetylcholine or mecholyl has been shown to stimulate acid secretion in *Necturus* gastric mucosa. In addition, there is a transient increase in transmembrane potential (PD) dependent on the presence of Cl^- in the serosal solution. Microelectrode punctures of the surface epithelial cell indicate that this cell has at least one electromotive force and that cholinergic drugs increase the potential across the serosal membrane and decrease the potential across the mucosal membrane. This can be explained by assuming permeability changes at the serosal border and changes in Cl^- transport across the mucosal side of the surface cell.

potential difference; microelectrode; O_2 consumption; H^+ secretion; Cl^- transport

---

THE ISOLATED GASTRIC MUCOSA of the *Necturus* is normally obtained in the resting state but maintains its capacity to secrete acid in response to stimulation by histamine, gastrin, and cholinergic compounds (13). This property permits the study of metabolic, secretory, and electrical changes that accompany the transition from the resting to the secreting state. In addition, the surface cells of the gastrointestinal tract in this species are large (ca. 80 μ in length) and thus accessible to exploration with microelectrodes. This study describes the characteristic changes in the fundus which follow stimulation with cholinergic compounds.

METHODS

Necturus gastric mucosa was mounted in an Ussing type chamber as previously described (11, 13). The following parameters were measured: acid secretion using a pH-stat, potential difference (PD), resistance and short circuit current (I_{sc}). In some experiments O_2 consumption was also measured in a Kel-F chamber by Clark oxygen electrodes (2).

Standard serosal solutions contained, in millimoles per liter: Na^+ 100, K^+ 4, Mg^{++} 0.9, Ca^{++} 1.6, Cl^- 90, $HPO_4^=$ 1, HCO_3^- 18, glucose 5, and mucosal solutions contained Na^+ 105, K^+ 4, Cl^- 109. For Cl^--free solutions, $SO_4^=$ was substituted for Cl^-, and the osmotic deficit was made up by mannitol. For Na^+-free solutions, choline was substituted for Na^+. The drugs used were added at the required concentrations to the serosal solutions. All reagents were the highest purity available, dissolved in double-glass distilled water.

Microelectrodes were pulled from cleaned glass capillary tubing 1.2 mm od using a Nastuk type puller (1, 8). They were filled by vacuum distillation in methanol and then equilibrated with water and then 3 M KCl. Tip diameter was less than 1 μ, and tip resistance was between 5 and 20 megohms.

The electrical connection between the microelectrode and the measuring calomel electrode was by a 3 M KCl-agar bridge. In addition a saturated KCl bridge-calomel electrode was placed in the serosal and mucosal solutions. The three calomel electrodes were connected to a Keithley 200B voltmeters, and the output of the voltmeters was recorded on a multichannel recorder. The three channels recorded the potentials from: *1*) microelectrode (ME)-serosal solution calomel electrode; *2*) microelectrode-mucosal calomel electrode; *3*) transmembrane (mucosal-serosal). A current-sending device was placed in series with the microelectrode lead so that the ME tip resistance could be estimated before, during, and after cell puncture; current (10 μamps/cm^2) was sent transmucosally by a current source connected to Ag/AgCl electrodes mounted in the mucosal and serosal sides of the chamber. The resistance from the microelectrode to calomel electrode was expressed as relative resistance (5), i.e. (ME-serosa) + (ME-mucosa) = 100%.

After withdrawal of the microelectrode, if the ME tip resistance had changed 20% or the tip potential recorded from ME-serosa had changed 10% compared to the reading before the cell was punctured, that reading was not used and a new microelectrode was obtained.

For an experiment using microelectrodes, the external muscle layers were stripped from the *Necturus* mucosa, and the mucosa was stretched on top of a tantalum screen separating the two halves of the chamber. Motion of the mucosa was reduced by maintaining the mucosal reservoir level about 5 cm higher than the serosal. Spontaneous motility was only rarely observed and could be readily suppressed by addition of adenine nucleotides. The mucosa was mounted in a chamber with the mucosal surface exposed and the microelectrode placed in the mucosal solution. Circulation on both sides was by a gas-lift system using 95% O_2 and 5% CO_2.

After the potential of the calomel electrodes was nulled to zero by use of a balancing voltage, one electrode was placed in the mucosal and the other electrode was placed in the serosal solution. The microelectrode tip was lowered, by use of a micromanipulator, into the mucosal fluid, and the tip

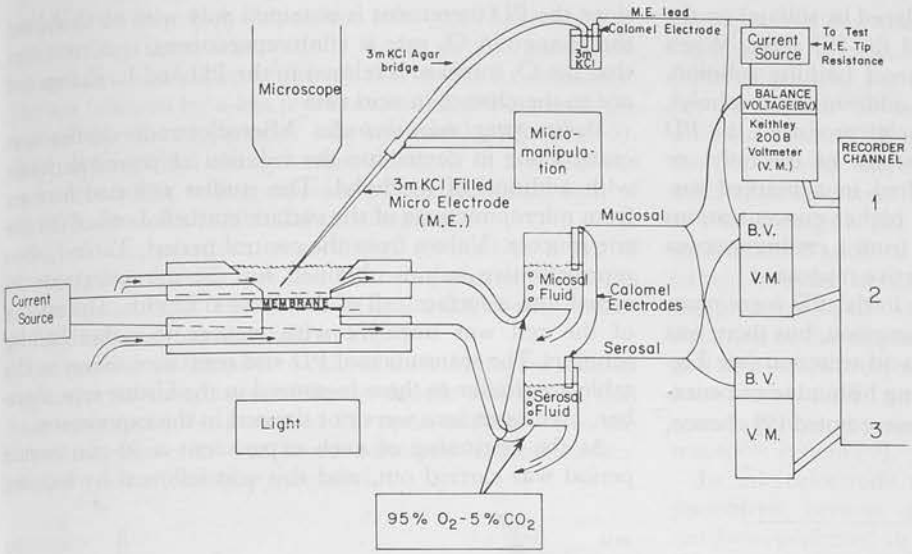

FIG. 1. Experimental arrangement for microelectrode potential and resistance measurements for surface epithelial cell of *Necturus* gastric mucosa. Plexiglas chamber contained 2 cm² active area.

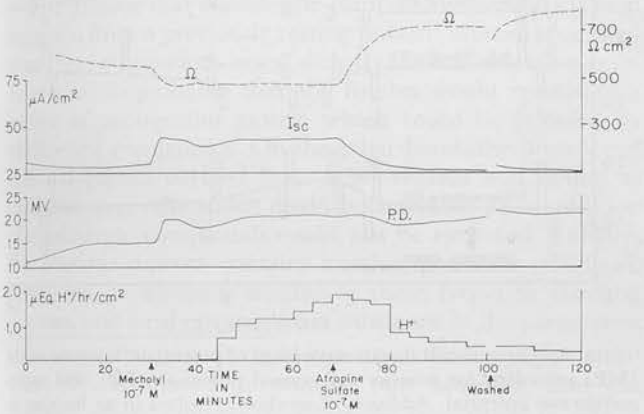

FIG. 2. Effects of addition of 10^{-7} M mecholyl and equimolar atropine sulfate to serosal side of *Necturus* gastric mucosa in an Ussing type chamber. Serosal side of membrane is positive to mucosal. Short circuit denoted as I_{sc}.

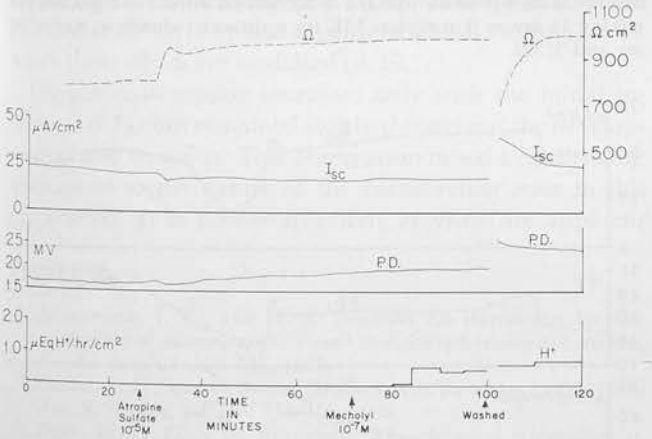

FIG. 3. Effect of pretreatment of *Necturus* gastric mucosa by atropine sulfate and effect of adding mecholyl.

potentials between the microelectrode and calomel electrodes were nulled by balancing voltages. Then the tip of the microelectrode was lowered to the surface of the mucosa. Insertion of the microelectrode into the cell was under direct microscopic observation using a Zeiss stereoscope, ×100 magnification (9) (see Fig. 1). The criteria for determining when a cell was punctured were: visualization of the mucosal cell dimpling, sharp spike in potential, and a shift in relative resistance (increase in ME-mucosal relative resistance and a decrease in ME-serosal relative resistance).

Several superficial and deep punctures were made and current sent to measure transmucosal resistance and the relative resistance of the mucosal and serosal membranes (5). In some experiments a microelectrode was inserted into a cell, and while maintained in the cell, acetylcholine or β-methylacetylcholine (mecholyl), 10^{-7} M, was added to the nutrient solution. Thus the PD and the resistance changes recorded from one cell could be monitored continuously. The stability of the system which made it possible to use the above-mentioned technique was due in part to the positive pressure arrangement of the circulating fluids and also the cell size of the *Necturus* gastric mucosa and its lack of inherent motility.

RESULTS

Studies using Ussing type chamber. Addition of 10^{-7} M mecholyl to a previously resting mucosa resulted in a rapid transient increment of the transmembrane potential with a fall in the transmembrane resistance within 2 min from addition of the compound (see Fig. 2). Acid secretion was only detected 10–15 min later. Atropine (10^{-7} M) reduced the acid rate and I_{sc}; it also resulted in a marked increase in the resistance. As noted in Fig. 2, removing atropine from the bathing solution did not reduce the resistance to the level before atropine was added. Also note the small change in the PD after adding atropine. Pretreatment of the mucosa with 10^{-7} M atropine blocked the mecholyl-PD increment. When the atropine concentration was increased to 10^{-5} M (Fig. 3), there was still acid secretion and also there was a very sharp increase in the transmembrane resistance that persisted even after the bathing solution was changed to those not containing atropine.

To test which ions might be involved in the PD change, a series of experiments was carried out. In the Ussing type

chamber when Cl^- was removed (replaced by sulfate) on the mucosal side, mecholyl still produced the PD spike. When Cl^- was removed only from the serosal bathing solution, there was no PD change with the addition of mecholyl. Concentrations of 10^{-7}–10^{-6} M mecholyl produced the PD spike; addition of higher concentrations of mecholyl or acetylcholine (10^{-5} or 10^{-4} M) resulted in a marked sustained suppression of PD (5). These higher concentrations also failed to stimulate acid secretion from a resting mucosa or an interrupted secretion from an active mucosa.

Oxygen consumption. Relative to the initial PD increment, there was an increase in oxygen consumption, but there was no further increase with the onset of acid secretion (see Fig. 4), using mecholyl as a stimulant. Using histamine or pentagastrin, no O_2 consumption changes were noted (2); hence, since the PD increment is obtained only with mecholyl and the change in O_2 rate is contemporaneous, it is concluded that the O_2 increase is related to the PD and I_{sc} change and not to the change in acid rate.

Studies using microelectrodes. Microelectrode studies were carried out to determine the location of potential change with addition of mecholyl. The studies reported here are from micropunctures of the surface epithelial cell of the gastric mucosa. Values from the control period, Table 1, show representative values obtained for the microelectrode inserted into a surface cell of the *Necturus* fundus. The interior of the cell was negative with respect to either bathing solution. The transmucosal PD and resistance shown on this table are similar to those measured in the Ussing type chamber. Hydrogen ions were not titrated in the experiments.

At the beginning of each experiment a 30-min control period was carried out, and this was followed by four test

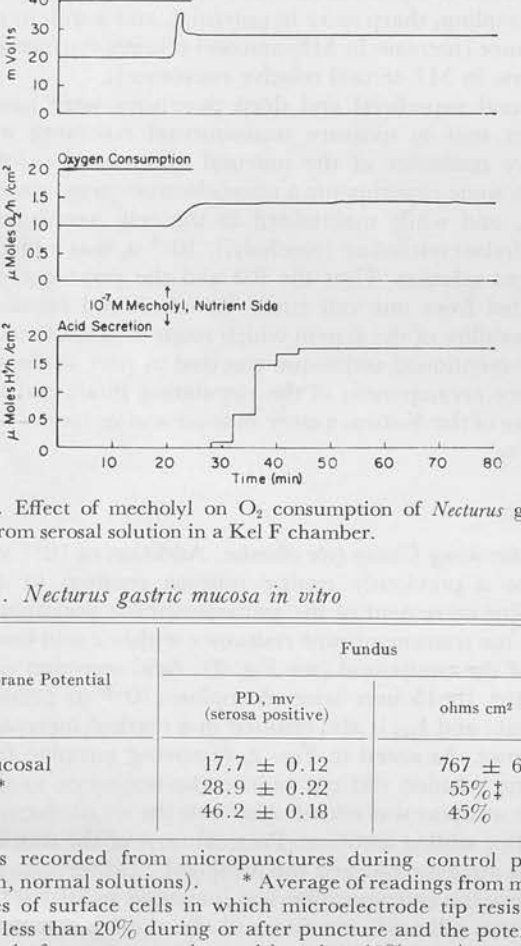

FIG. 4. Effect of mecholyl on O_2 consumption of *Necturus* gastric mucosa from serosal solution in a Kel F chamber.

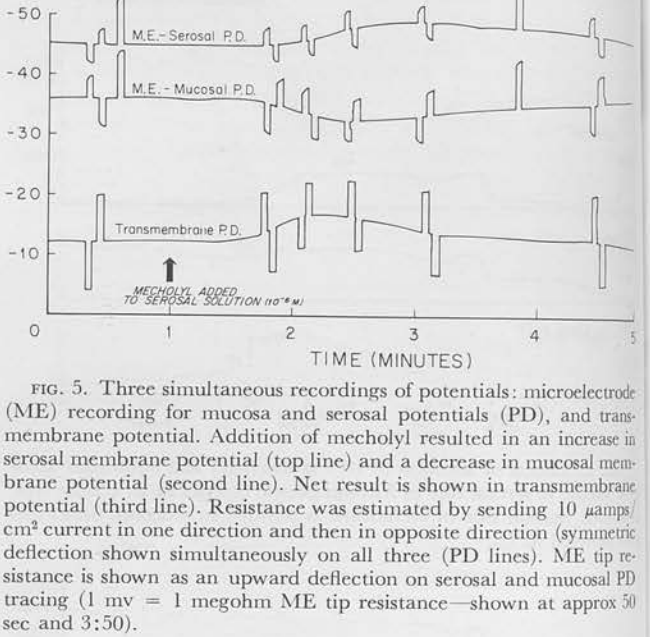

FIG. 5. Three simultaneous recordings of potentials: microelectrode (ME) recording for mucosa and serosal potentials (PD), and transmembrane potential. Addition of mecholyl resulted in an increase in serosal membrane potential (top line) and a decrease in mucosal membrane potential (second line). Net result is shown in transmembrane potential (third line). Resistance was estimated by sending 10 μamps/cm² current in one direction and then in opposite direction (symmetric deflection shown simultaneously on all three (PD lines). ME tip resistance is shown as an upward deflection on serosal and mucosal PD tracing (1 mv = 1 megohm ME tip resistance—shown at approx 50 sec and 3:50).

TABLE 1. *Necturus gastric mucosa in vitro*

Membrane Potential	Fundus	
	PD, mv (serosa positive)	ohms cm²
Transmucosal	17.7 ± 0.12	767 ± 6†
Mucosal*	28.9 ± 0.22	55%‡
Serosal*	46.2 ± 0.18	45%

Values recorded from micropunctures during control period (0–30 min, normal solutions). * Average of readings from micropunctures of surface cells in which microelectrode tip resistance changed less than 20% during or after puncture and the potentials before and after puncture changed less than 10%. † A pulse of 10 μamps/cm² of current, 1-sec duration was passed through the membrane by use of Ag:AgCl electrodes. The resistance was calculated by using Ohm's law from the ΔPD with the known current pulse. ‡ The relative resistance expressed as % (5).

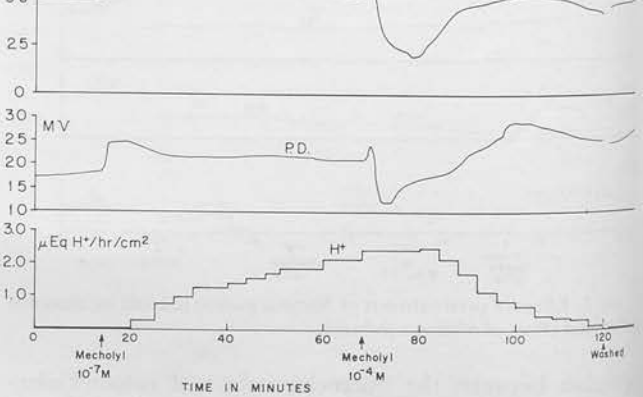

FIG. 6. Effect of 10^{-7} M mecholyl and 10^{-4} M mecholyl on *Necturus* gastric mucosa.

periods of 30 min each. Upon the addition of mecholyl or acetylcholine, there was initially a rise in PD across the mucosal (interior more negative) and a fall in resistance. This was followed by a less pronounced fall of PD across the mucosal membrane (interior side negative) (12) (Fig. 5). These asymmetrical changes were reflected in a rise of the transmucosal PD, which represented the algebraic sum of the PD's across the individual membranes.

Higher concentrations of mecholyl resulted in a fall of PD across both membranes, the fall being greater across the mucosal membrane. The net result was a fall in transmucosal PD similar to that observed in Fig. 6.

The response of the surface cells of the esophageal mucosa was similar to that observed in the fundic mucosa in that there was a rapid rise in serosal PD upon addition of mecholyl which, however, was more sustained. Antral surface cells were not affected by mecholyl.

DISCUSSION

The finding that cholinergic compounds could elicit acid secretion from a previously resting isolated mucosa suggested that these compounds acted directly on acid-secreting cells. It seemed improbable that the fundus would constitute a source of endogenous gastrin which could be released by cholinergic compounds. On the other hand, the presence of residual gastrin derived from other regions and bound to acid-secreting cells which could be activated upon addition of cholinergic compounds could not be excluded. Further, the *Necturus* mucosa contains another potential stimulant, histamine, in amounts similar to those found in the frog mucosa, and local release of this substance in the presence of cholinergic compounds could constitute the significant stimulant (7). It should be pointed out, however, that the *Necturus* gastric mucosa is relatively insensitive to added histamine, requiring about 10^{-4} M for stimulation of acid secretion.

The inhibitory effects on acid secretion of atropine (10) and of high concentrations of acetylcholine or mecholyl recall similar effects in vivo and point to a local mechanism by which these effects are mediated (3, 6).

Oxygen consumption increased only with the initial increment of PD but remained steady throughout the development of acid secretion. This observation raised a challenging question as to the nature of the nonsecreting state in this preparation. It is conceivable that in vitro the apparent resting state is due to the uncoupling of acid production from metabolism. It is also possible that the acid rates obtained (about 2 μEq/hr per cm^2 and equivalent to 1 μatom of O_2 per hr per cm^2 of tissue) could result from a mechanism utilizing basal ATP production. A final possibility is that the PD-related increment in O_2 consumption could be utilized for acid secretion when this is initiated.

The transient PD rise was obtained repeatedly with acetylcholine addition followed by washing and was accompanied by a fall in resistance. This effect was dependent on the presence of Cl^- in the serosal solution. The effect was obtained in the esophagus and fundus, but not the antrum, and it is noteworthy that the former two regions appear to have mainly a Cl^- transport mechanism from serosa to mucosa, whereas the antrum has an inwardly directed Na^+ transport system (9).

In microelectrode studies the fundic surface cells were punctured, because a microelectrophoretic technique has not been perfected to positively identify the oxyntic cells in this preparation. The surface cells had a negative interior (punctured from mucosal side), but the microelectrode was also negative to the calomel electrode in the serosal solution. On this basis there must be at least one independent electromotive force in this cell. With the addition of acetylcholine or mecholyl there was a rise in the serosal potential, with a decrease in the percentage resistance across this surface. This was followed by a fall in potential across the mucosal membrane, with little change in resistance. This may be interpreted as follows: the serosal membrane of the mucosa is sensitive to acetylcholine, and the drug produces an increase of relative permeability to Cl^-. This permeability increase results in an increased Cl^- entry and lowered resistance. A higher intracellular Cl^- stimulates chloride movement across the mucosal surface, hence lowering the PD across this interface.

The changes observed in the surface epithelial cell therefore show that cholinergic drugs affect at least the electrical parameters of this cell, independently of an effect on the oxyntic cell. This argues against the view that the surface cell acts simply as a passive resistance (14).

This work was supported by National Science Foundation Grants GB6840 and 8351, and National Institutes of Health Grant 08541.

Address requests for reprints to: Dr. George Sachs, Dept. of Medicine, University of Alabama Medical Center, 1919 7th Avenue South, Birmingham, Ala. 35233.

Received for publication 24 October 1969.

REFERENCES

1. ALEXANDER, J. T., AND W. L. NASTUK. An instrument for the production of microelectrodes used in electrophysiological studies. *Rev. Sci. Instr.* 24: 528–531, 1953.
2. CLARK, L. C., AND G. SACHS. Bioelectrodes for tissue metabolism. *Ann. N. Y. Acad. Sci.* 148: 133–153, 1968.
3. DALE, H. W., AND W. FELDBERG. The chemical transmitter o vagus effects to the stomach. *J. Physiol., London* 81: 320–334, 1934.
4. FORTE, J. C., L. LIMLOMWONGSE, AND D. K. KASBEKAR. Ion transport in the development of hydrogen ion secretion in the stomach of the metamorphosing bullfrog tadpole. *J. Gen. Physiol.* 54: 76, 1969.
5. FRAZER, H. S. The electrical potential profile of the isolated toad bladder. *J. Gen. Physiol.* 45: 515–528, 1962.
6. GRAY, J. S., AND A. C. IVY. The effects of mecholyl on gastric secretion. *Am. J. Physiol.* 120: 705–711, 1937.
7. KASBEKAR, D. K., AND J. G. FORTE. Evidence for histamine as an intermediate in stimulation of gastric acid secretion by pentagastrin and acetyl choline (Abstract). *Federation Proc.* 27: 580, 1968.
8. LING, G., AND R. W. GERARD. The normal membrane potential of frog sartorius fibers. *J. Cellular Comp. Physiol.* 34: 383–396, 1949.
9. MAKHLOUF, G. M., R. L. SHOEMAKER, AND G. SACHS. Effects of ion changes on intracellular PD in Necturus gastric mucosa. *Intern. Biophysics Congr., 3rd, 1969.*
10. NAKAJIMA, S., R. L. SHOEMAKER, B. I. HIRSCHOWITZ, AND G. SACHS. Influence of atropine on resistance, potential and H^+ se-

cretion in isolated gastric mucosa. *Am. J. Physiol.* 218: 990–994, 1970.
11. SHOEMAKER, R. L., B. I. HIRSCHOWITZ, AND G. SACHS. Hormonal stimulation of Necturus mucosa in vitro. *Am. J. Physiol.* 212: 1013–1016, 1968.
12. SHOEMAKER, R. L., G. M. MAKHLOUF, AND G. SACHS. Intracellular potentials of in vitro Necturus gastric mucosa (Abstract). *Biophys. J.* 9: A263, 1969.
13. SHOEMAKER, R. L., G. SACHS, AND B. I. HIRSCHOWITZ. Properties of Necturus gastric mucosa (Abstract). *Physiologist* 9: 285, 1966.
14. VILLEGAS, L. Cellular location of the electrical potential difference in frog gastric mucosa. *Biochim. Biophys. Acta* 64: 359–367, 1962.

AMERICAN JOURNAL OF PHYSIOLOGY
Vol. 226, No. 4, April 1974. *Printed in U.S.A.*

Action of Burimamide, a histamine antagonist, on acid secretion in vitro

R. L. SHOEMAKER, ELLEN BUCKNER, J. G. SPENNEY, AND G. SACHS
Departments of Physiology and Medicine, University of Alabama, and Veterans Administration Hospital, Birmingham, Alabama 35294

SHOEMAKER, R. L., ELLEN BUCKNER, J. G. SPENNEY, AND G. SACHS. *Action of burimamide, a histamine antagonist, on acid secretion in vitro.* Am. J. Physiol. 226(4): 898–902. 1974.—Burimamide, a histamine antagonist (5-butylmethylthiourea, an anti H_2), is used to inhibit spontaneous acid secretion in the *Rana pipiens* gastric mucosa in vitro. By removing the compound from the solution, the acid rate remains at zero so a nonsecreting mucosa is obtained by this method. Mucosae treated in this manner are still sensitive to the commonly used stimuli. Burimamide (10^{-3} M) inhibits acid secretion stimulated by histamine (10^{-5} M), mecholyl (10^{-5} M), or pentagastrin (10^{-5} M). Theophylline prevents this inhibition, and only histamine and cAMP reverse inhibition in the presence of Burimamide. The data are interpreted as supporting a sequential model for acid secretion involving an adenyl cyclase as a critical step.

H_2 antagonist; potential difference; stimulatory pathway; pentagastrin stimulation; DB-cAMP; frog gastric mucosa

GASTRIC ACID SECRETION is subject to control by at least three types of stimuli: histamine, gastrin, and acetylcholine. One of the problems which remains unsolved is the interaction, if any, between the three groups of stimuli. However, the difficulty of obtained resting mucosae in vitro and also of obtaining dose-response curves has impeded progress in this area.

Harris and Alonso (1) and subsequently our laboratory (7, 8) have provided fairly substantial support for the role of 3′,5′-cAMP as a "second messenger" for acid secretion in amphibian mucosa. This has been supported by studies in the dog in some laboratories (2) but not in others (6). Resting amphibian mucosa, both frog and *Necturus*, have provided some information as to the role of the three groups of stimuli in amphibians under in vitro conditions.

There are at least two obvious approaches one can take: The first approach, taken by Kasbekar (5), using the bullfrog, was to study tachyphylaxis. With these studies he provided evidence that a sequence such as

$$\text{cholinergic} \rightarrow \text{gastrin} \rightarrow \text{histamine} \rightarrow \text{cAMP}$$

would explain the data he obtained. An alternate approach is to use specific inhibitors for each type of stimulus and to define the overlap of effects. For example, if an antigastrin inhibits either gastrin or methacholine-induced secretion but not histamine-induced secretion, it would be natural to conclude that histamine is beyond the convergence point of the two inhibited stimuli.

The gastric mucosa, myocardium, and uterine tissue are histamine-responsive tissues that were found previously to be insensitive to antihistamine suppression. Recently, Burimamide (5-butylmethylthiourea) imidazole has been synthesized (Fig. 1) and shown to be an antagonist of this second set of histamine receptor sites called H_2 receptors (3).

A rational explanation for this segregation of receptors may be found in results obtained with calculations designed to establish the most probable histamine conformation. Two such conformations appear possible, an open form and a closed form, where the amine closely approaches the imidazole ring. Burimamide is able to mimic the closed but not the open form.

Burimamide is found to inhibit histamine-stimulated gastric secretion in rat, dog, and man and produces effects which overlap into gastrin but not cholinergic stimulation of the species studied. The availability of this type of compound could make it a useful tool for the analysis of stimulation in vitro as well. This paper reports some of our observations of its effects on the chambered amphibian mucosa.

METHODS

Tissue preparation and acid secretion measurement. Rana pipiens are used in the experiments. After pithing the frog, the stomach is removed and opened along the lesser curvature. The external muscle layers are removed, and the gastric mucosa is placed as a sheet between two halves of a Lucite chamber (11). The active area of the chamber is 1.23 cm^2. The acid rate is estimated by titration with 5 mM NaOH by the pH stat method (4) at a luminal pH of 4.8. The transmucosal potential difference (PD) is recorded by a calomel electrode attached to a potentiometric strip-chart recorder. The transmucosal resistance is calculated from the ΔPD response to a 0.1-s electrical pulse of 20 $\mu A/cm^2$ (9). The bathing fluids are oxygenated and circulated by use of a 95% O_2-5% CO_2 gas-air lift system. The experiments are conducted at room temperature.

Solution and chemicals. All solutions are prepared from the highest grade chemicals available. The composition of the isotonic mucosal bathing fluid (secretory solution) and serosal bathing fluid (nutrient solution) has been described previously (10, 11). All test compounds are added to the

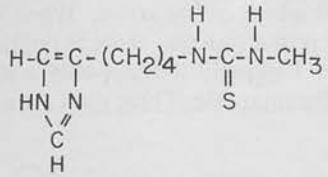

FIG. 1. Structure of Burimamide.

serosal solution, and the results are expressed as final concentration in moles per liter. A compound is washed from the chamber by draining the solution from the chamber and replacing the fluid with serosal solution not containing the test compound. This procedure is repeated at least 3 times during a 5-min period.

Burimamide is a gift of Smith, Kline & French Laboratories, and histamine (free base),dibutyryl adenosine 3′,5′-cyclic monophosphate (DB-cAMP), and 3′,5′-cAMP are obtained from Sigma Chemical Co. Pentagastrin, Peptavlon, is a gift from Ayerst Laboratories. Mecholyl (acetyl beta-methyl choline chloride) is obtained from Nutritional Biochemical Corp. All solutions are stored in the refrigerator when not in use, and all peptide compounds are stored in powder form at −20°C until they are prepared for each experiment.

RESULTS

Spontaneous secretion. The general experience of several laboratories using *R. pipiens* gastric mucosa has been that spontaneous secretion is usually present, and a large increase in acid rate in response to secretagogue addition is often quite difficult to obtain.

As shown in Fig. 2, and in Table 1*A*, Burimamide at 10^{-3} M completely inhibits spontaneous secretion. Along with inhibition of H^+ rate, there is a rise in resistance and a fall of PD, hence a decrease in calculated short circuit current, I_{sc}. Removal of Burimamide does not result in restoration of secretion (3).

Interaction of burimamide with histamine. Three types of experiments to investigate this aspect of Burimamide action are described: when histamine is added prior to the addition of Burimamide, as shown in Fig. 3 and Table 1*B*, Burimamide is effective in abolishing acid rate and decreasing calculated I_{sc}, but approximately a 100-fold excess of Burimamide is required.

Following inhibition, either Burimamide is removed and histamine is added subsequently, or histamine is added in the continuing presence of Burimamide. Figure 2 shows that following Burimamide removal, histamine is again effective in restoring secretion; there is also an increase in I_{sc}. However, the effects on PD and resistance vary somewhat from experiment to experiment. Figure 3 shows an experiment of the latter type. Secretion is restored by 1/100 M ratio of histamine to Burimamide and is further stimulated by a 10-fold increase of histamine.

In both protocols there is a typical 10-min lag before secretory onset.

Interaction with pentagastrin or mecholyl. Addition of Burimamide to a mecholyl- or pentagastrin-stimulated mucosa also results in secretory inhibition. Figure 4 shows an experiment

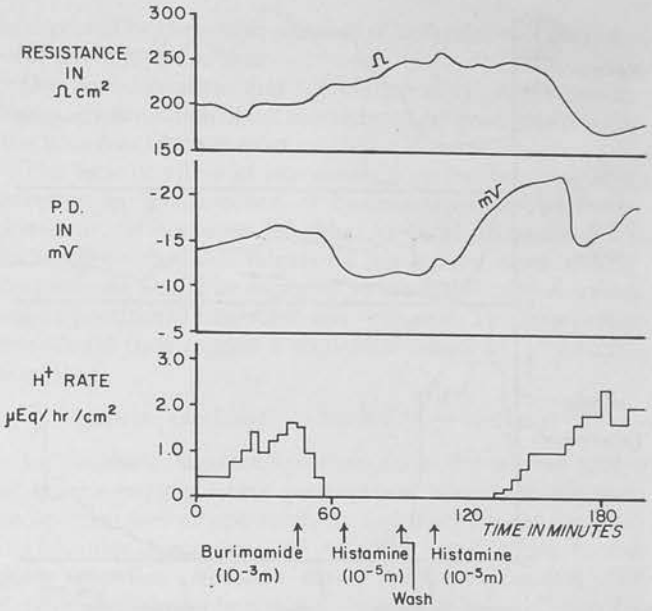

FIG. 2. Effect of 10^{-3} M Burimamide is shown on spontaneous acid secretion in *Rana pipiens*. Histamine does not restore acid rate until Burimamide is washed out of the chamber. Burimamide decreases the PD, and this effect is also reversed by histamine.

TABLE 1. *Effect of burimamide on Rana pipiens gastric mucosa in vitro*

	H^+ Rate, μeq/h (per cm²)	PD, mV	Resistance, Ωcm²
A) Control	2.09 ± .26	17.6 ± 1.3	153 ± 47
Burimamide (10^{-3} M)*	0	16.0 ± 1.9	226 ± 14
B) Control†	1.68 ± .34	19.9 ± 1.7	161 ± 16
Histamine (10^{-5} M)	3.26 ± .25	16.4 ± 0.9	145 ± 11
Burimamide (10^{-3} M)	0	14.2 ± 1.4	242 ± 23
C) Control‡	1.70 ± .30	21.7 ± 1.0	160 ± 19
Mecholyl (10^{-6} M)	1.86 ± .28	20.6 ± 1.2	153 ± 14
Burimamide (10^{-3} M)	0	20.0 ± 0.8	240 ± 24
Burimamide (10^{-3} M) + Mecholyl (10^{-3} M)	0	16.0 ± 1.2	270 ± 31

Values are average values ± SEM. Number of experiments = 14. *Values taken 30 min after Burimamide was added. †*A* and *B* were separate sets of experiments. There are 10 experiments in *group B*. Similar results were obtained when pentagastrin (5×10^{-5} M) was used instead of histamine. ‡In *group C* two types of experiments were performed, Mecholyl followed by Burimamide and Burimamide followed by Mecholyl ($n = 3$).

in which Burimamide inhibits pentagastrin-stimulated secretion. Associated with this there is the typical fall in I_{sc}, in this case associated with a fall of PD and increase of resistance. Similar results were obtained when mecholyl was added (see Table I).

Figure 5 shows that following removal of Burimamide pentagastrin is capable of restoring secretion and I_{sc} to control values. It is our experience, however, that this type of result is somewhat more difficult to obtain than with histamine in that on occasion neither pentagastrin nor

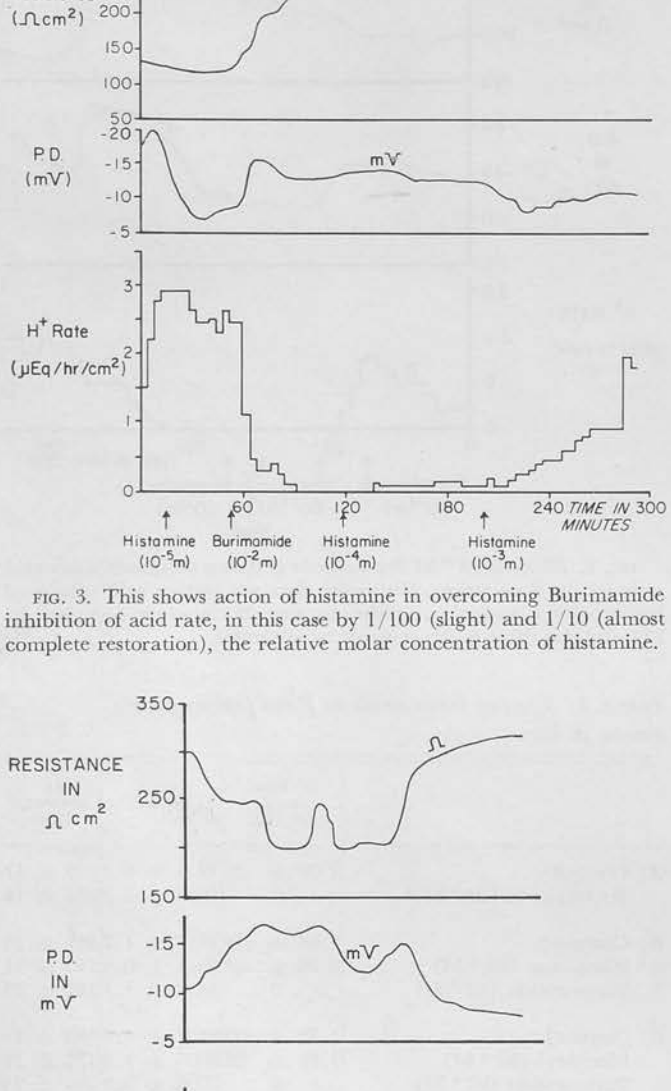

FIG. 3. This shows action of histamine in overcoming Burimamide inhibition of acid rate, in this case by 1/100 (slight) and 1/10 (almost complete restoration), the relative molar concentration of histamine.

FIG. 4. This shows that 10^{-3} M Burimamide inhibits acid rate, decreases PD and I_{sc}, and increases resistance in presence of 6.5×10^{-5} M pentagastrin.

mecholyl is capable of stimulation, but in the same experiment, histamine is effective, as usual.

In the presence of Burimamide, neither pentagastrin nor mecholyl, even at large doses for an in vitro system, is capable of restoring secretion, in contrast to the data obtained with histamine. This is shown in the initial part of the experiment in Fig. 6. It must be emphasized that for gastrin, a 10^{-5}- M dose is a very large one for this tissue.

Interaction with adenyl cyclase system. When theophylline is added to the secreting mucosa, there is typically a doubling of the acid rate. Uniquely there is only a slight reduction in acid rate by Burimamide. These data are shown in Fig. 7.

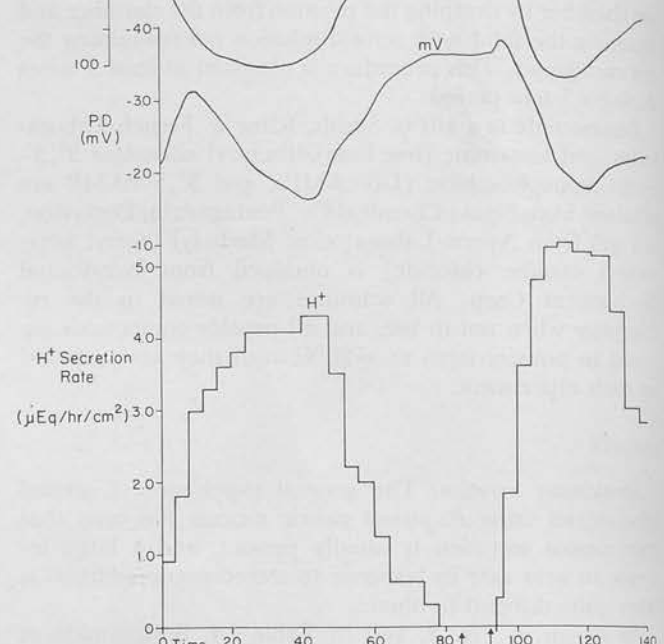

FIG. 5. This shows reversal of Burimamide inhibition by 3.3 X 10^{-5} M pentagastrin on H^+ rate, PD, and resistance.

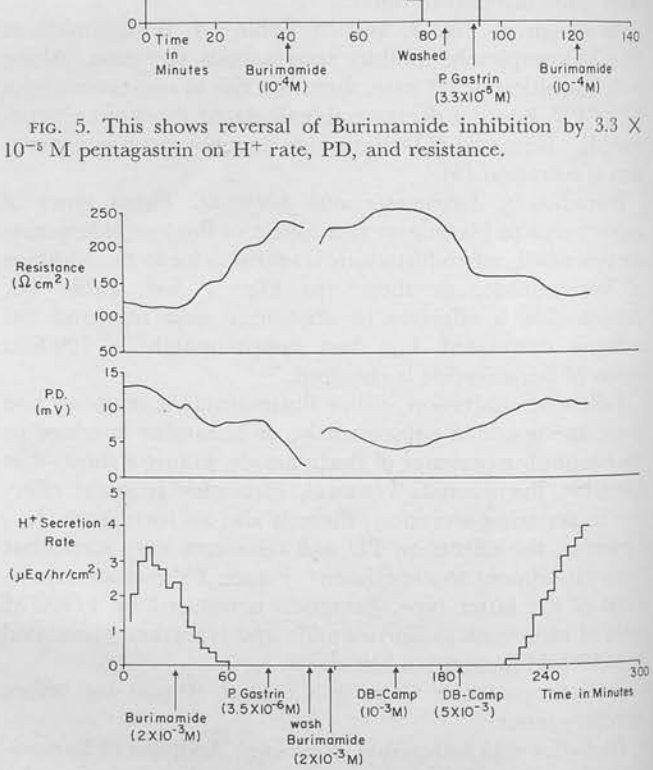

FIG. 6. Spontaneous acid rate is inhibited by Burimamide, and this is not reversed by pentagastrin. Second half of experiment shows that DB-cAMP is capable of counteracting Burimamide.

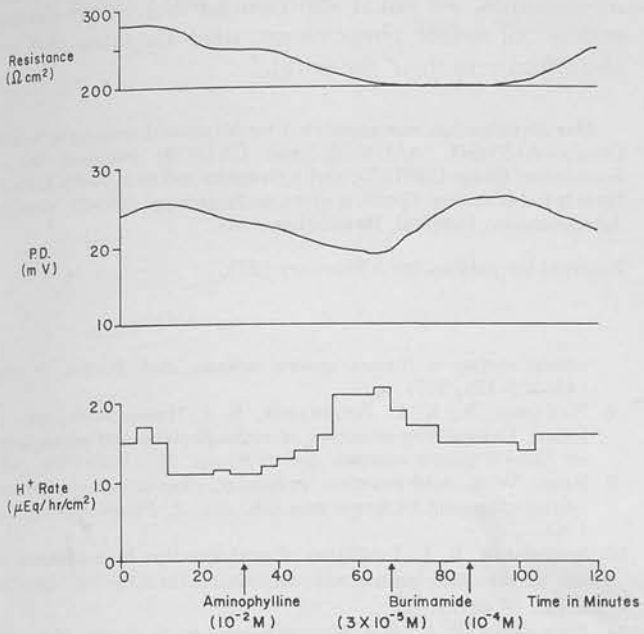

FIG. 7. Theophylline doubles spontaneous acid rate, and under these conditions Burimamide does not inhibit H^+ secretion.

In Fig. 6 the effect of cAMP is shown. Thus, in the presence of Burimamide, cAMP is capable of restoring acid secretion to its control level. The high dose level of cAMP necessary may be due to poor penetration. In work presented elsewhere (12) we show that Burimamide is capable of abolishing histamine stimulation of adenyl cyclase from rabbit fundus.

DISCUSSION

The data described in this paper may be related to the following problems: *1*) effects of Burimamide on spontaneous secretion, *2*) the role of histamine in acid secretion, *3*) the role of the adenyl cyclase system in this process, and *4*) the distinction between H_1 and H_2 receptors.

Spontaneous secretion. Our data clearly show that Burimamide (and preliminary data with Metiamide, a "second generation" H_2 antagonist, are qualitatively identical) is capable of producing a "resting" mucosa in the sense that secretion is inhibited until a secretagogue is added. Histamine is invariably effective in restoring secretion, and whereas pentagastrin or mecholyl is also usually effective, in a few experiments no reversal was obtained. These compounds then provide a particularly useful tool for studying the effects of stimuli on a nonsecreting in vitro mucosa.

Role of histamine. The data shown here provide information on the interaction of stimuli with the gastric mucosa. Three stimuli are capable of antagonizing the action of Burimamide directly: histamine, theophylline, and cAMP. These data are most readily interpreted as if Burimamide antagonizes the action of histamine on an adenyl cyclase system critical for acid secretion. An additional finding is that the action of Burimamide is not that of a metabolic inhibitor such as amytal or 2-deoxyglucose, since no reversal would be expected by the simple addition of histamine to a Burimamide-containing mucosa.

Our data also show that stimulation of H^+ secretion also results in stimulation of the short-circuit current, presumably due to active Cl^- transport.

The lack of effect of pentagastrin or mecholyl on acid secretion in the presence of Burimamide may be interpreted in various ways. If either of these drugs mediates their effects by the release of histamine, then clearly Burimamide would be expected to block their action unless huge quantities of histamine were released. This interpretation would then suggest a sequential model for acid secretion, thus:

(gastrin, mecholyl) → histamine → secretion

Equivalently, the receptor situation in the mucosa might be quite complex, where pentagastrin and histamine may occupy two sites on one receptor, and blocking one site with Burimamide inactivates the receptor with respect to the other stimulus. A fairly strong argument against this hypothesis is the finding that at least for rabbit (12), gastrin does not stimulate adenyl cyclase. On the other hand, *Necturus* (7) or frog gastric adenyl cyclase (Ray and Forte, unpublished observations) does show gastrin sensitivity. If a common receptor were the case, then if histamine were capable of stimulating adenyl cyclase, gastrin would also be effective. Thus, this may be the case in amphibians, in contrast to mammals.

Alternatively, two independent receptors may be involved. In this case, the interaction of Burimamide with the gastrin or mecholyl receptor would simply reflect nonspecificity of this inhibitor. Apart from its strong structural similarity to the closed conformation of histamine, it would be expected that either type of stimulus could then overcome the effect of Burimamide. Since neither mecholyl nor pentagastrin is able to counteract 10^{-3} M Burimamide, but histamine is able to do so, this last interpretation is also somewhat unlikely. Moreover, the action of Mn^{++} in being able to inhibit gastrin or mecholyl stimulation but not that of histamine would also argue for a sequential stimulation (10) as had been suggested by Kasbekar (5).

Adenyl cyclase system. Since Burimamide does not inhibit acid secretion in the presence of theophylline and cAMP is able to stimulate secretion up to control values in the presence of Burimamide, we may conclude that acid secretion in amphibian mucosa is adenyl cyclase mediated. Our data showing adenyl cyclase stimulation by histamine and its active analogs (12), and inhibition of this adenyl cyclase by Burimamide in rabbit fundic mucosa, and also our data on *Necturus* adenyl cyclase (7) further substantiate this view.

Moreover, since cAMP can overcome an H_2 antagonist, this means that not only is cAMP production a necessary condition for acid secretion, it is also a sufficient condition. This rules out the possibility that cAMP effects occur prior to histamine release. The sequence then reads

(acetylcholine, gastrin) → histamine →
cAMP → acid secretion

as being most likely. However, clear-cut evidence for a histamine requirement for other primary hormones has not as yet been obtained.

Since H_1 antagonists such as diphenhydramine do not inhibit in vitro secretion and Burimamide (and a more recent analog, Metiamide) does, it seems reasonable to suggest that two types of receptors do indeed occur. Moreover, since most adenyl cyclases are membrane-bound enzymes, the receptor is likely to be at the cell surface. The unlikely possibility does remain that we are dealing with, in the case of the oxyntic cell, an intracellular membrane system to which H_1 antagonists do not have access. When other tissue data are considered, however, such as heart or myometrium, we would also contend that we are dealing with a cell-surface phenomenon, since H_2 antagonists are also effective in these tissues (3).

This investigation was supported by National Institutes of Health Grants AM08541, AM18578, and CA13158; National Science Foundation Grant GB31075; and a Grant-in-Aid from Smith Kline & French Laboratories. Credit is given to Project no. 8059-01, Veterans Administration Hospital, Birmingham, Ala.

Received for publication 5 February 1973.

REFERENCES

1. Alonso, D., and J. B. Harris. Effect of xanthines and histamine on ion transport and respiration by frog gastric mucosa. *Am. J. Physiol.* 208: 18–23, 1965.
2. Bieck, P. B. Role of cyclic AMP in the regulation of gastric secretion in dogs and humans. In: *Advances in Cyclic Nucleotide Research*, edited by P. Greengard, G. Robinson, and R. Paoletti. New York: Raven, 1972, vol. 1, p. 149–162.
3. Black, J. R., W. A. M. Duncan, L. J. Durant, O. R. Ganellin, and E. M. Parsons. Definition and antagonism of histamine H_2-receptors. *Nature* 236: 385–390, 1972.
4. Durbin, R., and E. Heinz. Electromotive chloride transport and gastric acid secretion in the frog. *J. Gen. Physiol.* 41: 1035–1047, 1958.
5. Kasbekar, D. K. Secretagogue induced tachyphylaxis of gastric H^+ secretion and its reversal. *Am. J. Physiol.* 223: 294–299, 1972.
6. Mao, C. C., L. L. Shanbour, D. S. Hodgins, and E. D. Jacobson. Adenosine 3′,5′-monophosphate (cyclic AMP) and secretion in the canine stomach. *Gastroenterology* 53: 427–438, 1972.
7. Nakajima, S., B. I. Hirschowitz, and G. Sachs. Studies on adenyl cyclase in *Necturus* gastric mucosa. *Arch. Biochem. Biophys.* 143: 123–126, 1971.
8. Nakajima, S., R. L. Shoemaker, B. I. Hirschowitz, and G. Sachs. Comparison of action of aminophylline and pentagastrin on *Necturus* gastric mucosa. *Am. J. Physiol.* 219: 1259–1262, 1970.
9. Rehm, W. S. Acid secretion, resistance, short-circuit current and voltage-clamping in frog's stomach. *Am. J. Physiol.* 203: 63–72, 1962.
10. Shoemaker, R. L. Inhibition of acid secretion by manganese in the in vitro frog gastric mucosa. *Ala. J. Med. Sci.* 8: 424–430, 1971.
11. Shoemaker, R. L., B. I. Hirschowitz, and G. Sachs. Hormonal stimulation of Necturus mucosa in vitro. *Am. J. Physiol.* 212: 1013–1016, 1968.
12. Sung, C. P., B. C. Jenkins, L. R. Burns, V. Hackney, J. G. Spenney, G. Sachs, and V. D. Wiebelhaus. Adenyl and guanyl cyclase in rabbit gastric mucosa. *Am. J. Physiol.* 225: 1359–1363, 1973.

Reprinted from PROCEEDINGS OF THE SOCIETY FOR EXPERIMENTAL BIOLOGY AND MEDICINE
1966, v123, 47-52

Effects of Sodium Removal on Acid Secretion by the Frog Gastric Mucosa.* (31398)

GEORGE SACHS, RICHARD L. SHOEMAKER,† AND BASIL L. HIRSCHOWITZ
Department of Medicine, Division of Gastroenterology, University of Alabama Medical Center, Birmingham

In various studies of ionic requirements of the bathing solutions for H^+ and Cl^- transport in the frog gastric mucosa, K^+ and Ca^{++} have both been shown to be essential for acid secretion(1,2) while Na^+ free solutions have been claimed to support normal secretion in the mucosa(3) and 75% substitution of Na^+ by choline was shown to be without effect(4). The results presented here show that when the intracellular Na^+ concentration is reduced to very low levels, there is significant inhibition of acid and chloride secretion which is reversed by readmission of Na^+ to the nutrient but not to the secretory side.

Methods. *Rana pipiens* gastric mucosa was mounted between 2 lucite chambers as described previously(5). The potential difference (PD) was measured with a pair of calomel electrodes with renewable KCl junctions. Resistance was calculated from the change in PD obtained by sending 10 microamps of current in either direction and short circuit current was determined as the current necessary to reduce the PD to 0 within 30 seconds. Acid secretion was determined using the pH stat method(6) and Cl^{36} tracer fluxes were measured using the Nuclear Chicago liquid scintillation counter in which quench correction was performed using the channels ratio method. The bathing solutions were of the following composition: Nutrient: Na^+ 118 mM, K^+ 4 mM, Ca^{++} 1.7 mM, Mg^{++} 0.8 mM, Cl^- 109 mM, HCO_3^- 18 mM, glucose 10 mM; secretory: Na^+ 105 mM, K^+ 4 mM, Cl^- 109 mM. In the Na^+ free experiments choline was substituted for Na^+ and in the Na^+ and Cl^- free experiments SO_4^{--} was additionally substituted for Cl^-. In all the substitution experiments the membrane was washed 4 times over a period of 5 minutes with the appropriate solutions. The substitutions were carried out either on both sides simultaneously or one side followed by the other. In the experiments where the Na^+ was readmitted, aliquots of the choline nutrient or secretory solutions were withdrawn and replaced with aliquots of the Na^+

* Supported by USPHS grants AM-08541, AM-09260 and 2A-5286 and NSF grant GB3511.

† Predoctoral trainee, gastroenterology training grant 2A-5286.

TABLE I. Summary Table of Effects of Na^+ Removal on *in vitro* Frog Gastric Mucosa. (Cl^- fluxes 15 in either direction. Too few in individual groups for adequate statistics.)

Solution		No. exp	H^+, μEq hr^{-1} cm^{-2}	PD, mv	Resistance, Ω cm^2	Short circuit current, μa cm^{-2}	Cl^- flux, μEq hr^{-1} cm^{-2} N→S	S→N
Na^+			3.10	26.7	223	115.8	—	—
Na^+-free	(a)	7	1.21 ± .34	8.4 ± 3.5	348 ± 41	26.9 ± 5.3	—	—
(± SEM)	(b)	8	1.12 ± .44	0	437 ± 93	0	—	—
	(c)	15	0	0	625 ± 48	0	—	—
All Na-free			0.55	3.2	499	9.8	2.59 ± .54	1.78 ± .31
Change			—2.55*	—23.5*	+276*	—106.0*		

* $P < .01$ by t test.

nutrient or secretory solution until virtually all of the choline had been replaced. Na^+ and K^+ analyses were performed on membranes treated in various ways. In some experiments the membranes were exposed after 3 washings to Na^+ free solutions in small beakers and gassed with 95% O_2-5% CO_2 for 30 minutes. In other experiments the membranes were set up in the standard secretory chamber and washed as usual with Na^+ free solutions. Secretory values were recorded and the membranes removed from the chamber for analysis. The Na^+ and K^+ analyses were performed by digestion according to Davenport's method(3), using internal standard flame photometry for Na^+ and K^+ analysis.

Results. Secretion: The parameters obtained with the standard NaCl solutions are shown in the first row of Table I. Previous solutions used in this and other laboratories have generally contained inorganic phosphate. It appears from these data that omission of phosphate has little effect on the secretory parameters of the frog gastric mucosa. When choline solutions were substituted for the Na^+ solutions on the secretory side only slight changes were observed. These changes could be accounted for by the presence of a Na^+ gradient in the direction nutrient to secretory (Fig. 1). The removal of Na^+ from the nutrient side produced a marked reduction of the short circuit current, potential difference and secretory rate, accompanied by a rise in resistance (Fig. 1).

It appeared that the results fell into 3 groups (Table I). In one group (7/30 exp.) although there was a marked reduction in PD, this did not fall to 0, and there was residual finite acid rate, short circuit and the usual rise in resistance. In the second group, (8/30 exp.) in spite of the absence of both PD and short circuit current, there was a residual finite acid rate (Fig. 2), sensitive to SCN^-. In the experiments described above with PD = 0 and a finite acid rate, the acid rate fell to 0 within 3 to 5 minutes when the tissue was made anoxic by bubbling 95% nitrogen and 5% CO_2. During this fall there was no observed change of the PD. When oxygen was readmitted acid secretion was re-established. At no time could any change in the PD be noted. The third and largest (15/30 exp.) group showed neither PD nor acid secretion. There appeared to be a progressive rise in resistance from Group 1 to Group 3. The mean net chloride flux corresponded closely to the sum of the mean residual H^+ rate and residual short circuit current. It appears then that there was little transport of chloride other than that associated with HCl or Cl^- secretion, for instance in the form of choline chloride.

Na^+ readmission: When Na^+ was readmitted on the secretory side there was no significant reversal of the inhibitory effects. However, when Na^+ was readmitted to the nutrient side, the effects were reversed as shown in Fig. 3. Degree of reversal was related to degree of Na^+ re-substitution on the nutrient side. Small amounts of Na^+ (up to 6 mM) on the nutrient side did not reverse the effects on H^+ secretion. However, there was partial reestablishment of the PD, and a fall in resistance. At 12 mM Na^+, acid secretion was initiated. Further addition of Na^+ resulted in progressive increase in H^+ rate and PD with a fall in resistance. At 45 mM Na^+, the H^+ rate and the PD had

reverted to normal, but resistance was 400 Ω cm^2 compared to the 200 Ω cm^2 in Na^+ solutions initially. Readmission of Na^+ on the secretory side further lowered the resistance, and with a return to normal

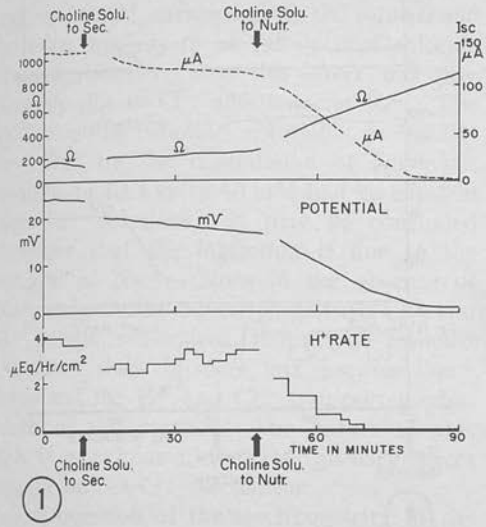

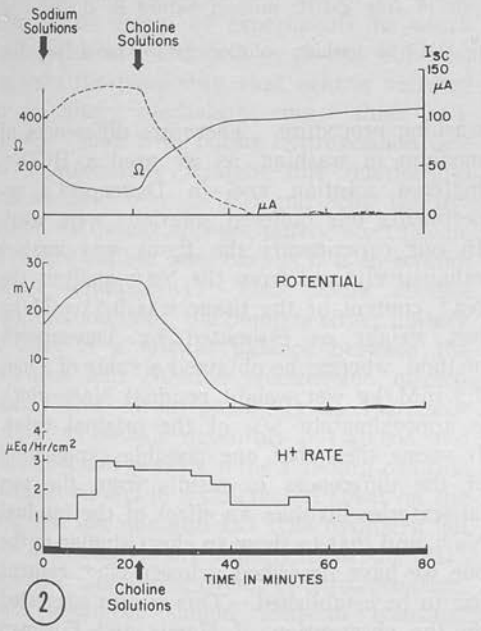

FIG. 1. Effect of choline substitution for Na^+ on secretory and nutrient side of *in vitro* frog gastric mucosa.

FIG. 2. A typical experiment where choline replacement of Na^+ resulted in a finite acid rate with a zero PD (group b, Table I)—see text.

TABLE II. Na^+ and K^+ Levels of Control and Choline Washed Tissues (± SEM).

Membrane taken from:	No. of membranes	mEq/kg wet wt Na^+	mEq/kg wet wt K^+
Sodium solutions	6	48.7 ± 3.6	47.3 ± 3.5
Choline "	10	.33 ± .31	48.5 ± 1.8

Na^+ conditions, the resistance fell to the original value. Addition of K^+ up to 40 mM did not reverse the choline effects.

Na^+ levels: The data obtained by the Na^+ and K^+ analyses of the membrane showed that the technique of washing reduced the sodium concentration to less than 1% of control. There was no significant effect, however, on potassium concentration (Table II).

Na^+ and Cl^- substitution: The choline sulfate experiments were of 2 types. In the first type (6 exp.) the membrane was initially exposed to Na^+ = containing solutions and then choline chloride was substituted for sodium chloride on both sides. In this set of experiments when SO_4^{--} was additionally substituted for Cl^- there was maintained secretion with an inversion of PD. This secretion rate was maintained through a period of 13.6 ± 3.0 minutes then fell off progressively and reached 0 after 25.8 ± 3.4 minutes (mean of 6 exp. ± SEM) (Fig. 4). During the decline of H rate to 0 there was an approximately ($r = .729$, $n = 21$) linear relationship between the PD and the secretory rate. These data confirm Rehm's observations of a direct relationship between the PD and the hydrogen ion rate in sulfate(8) using dinitrophenol.

In the second type, both Cl^- and Na^+ were replaced by sulfate and choline simultaneously following exposure to $NaCl^-$ containing solutions. In this group, the choline sulfate data initially were virtually indistinguishable from results obtained with sodium sulfate-containing solutions. There was a rise in resistance, an inversion of the PD and a reduction of the H^+ secretory rate (which eventually fell to 0), as in the experiments above. The resistance obtained in the choline sulfate experiments was extremely high, in some experiments reaching as high as 1,800

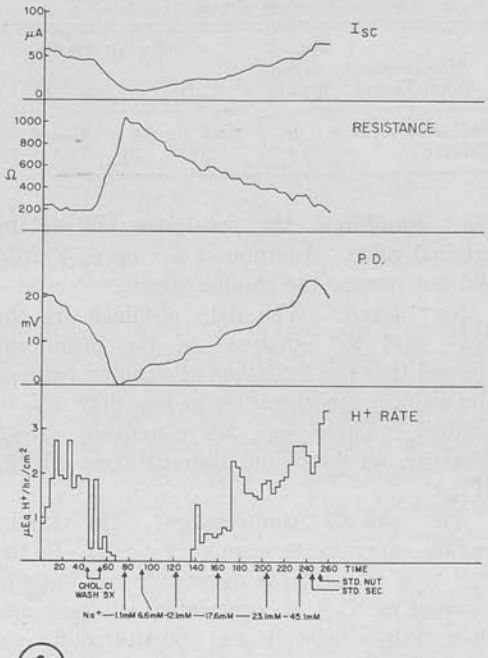

3

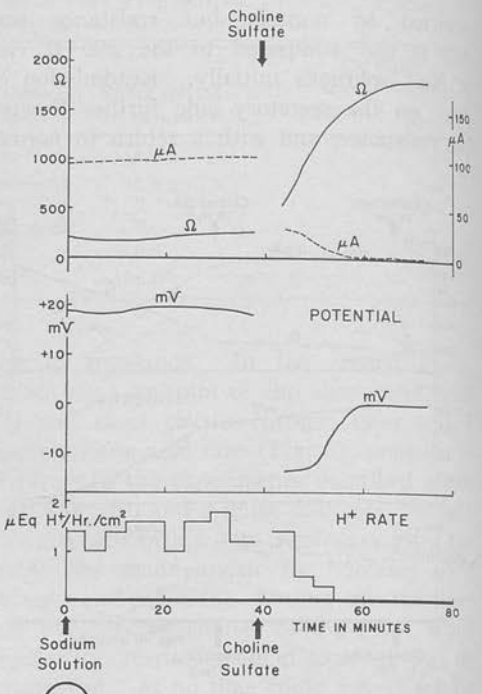

4

FIG. 3. Effect of Na^+ readmission on nutrient side of frog gastric mucosa bathed in choline solutions.

FIG. 4. Effect of choline sulfate substitution for NaCl in bathing solutions of *in vitro* frog gastric mucosa.

Ω cm^2. The acid secreted under choline sulfate conditions was inhibited by 10 mM SCN^-.

Discussion. It has become clear that there is an interdependence between K^+ concentration in the medium and H^+ secretion in the frog gastric mucosa(2). Davenport(3) has published an analysis of the various spaces of the gastric mucosa with reference to Na^+, K^+ and inulin, for example, and has demonstrated, using a tied-off sac of mucosa, that there is relatively little effect of choline substitution for Na^+ on acid secretion. These results are in contrast to the effects of K^+ removal on acid secretion where acid secretion is inhibited in the absence of K^+(2). With the sac technique none of the electrical parameters are measured and it is not clear why the data obtained with this method should differ from those obtained in the flux chamber. There are, however, various other points of difference, such as medium and washing procedure. There are differences of medium in washing, as we used a HCO_3^- buffered solution and in Davenport's experiments tris buffered solutions were used. In our experiments the tissue was washed exhaustively and from the Na^+ analysis the Na^+ content of the tissue was 0.33 mM/kg wet weight as estimated by Davenport's method, whereas he obtained a value of about 2.5 mM/kg wet weight residual Na^+ which is approximately 5% of the original value. It seems then that one possible explanation of the differences in results from the two laboratories involves an effect of the residual Na^+, and that to show an effect similar to the one we have described a lower Na^+ content has to be established. This is also suggested by the observation of Harris and Edelman and confirmed by us, that choline substitution up to 75% was virtually without effect on the mucosal parameters(4). That the effect is due to Na^+ removal rather than to a direct

action of choline, is also borne by the above observations. With respect to the reversal by KCl addition rather than NaCl addition (3) those experiments were performed in low Cl^- (*i.e.*, tris-mannitol) media and the optimal potassium concentration found, namely 36 mM, corresponds to the value found by other workers to be the optimal chloride concentration(7); thus this effect was presumably due to Cl^- addition, not K^+. The inhibition by choline solutions is readily reversible by the readmission of Na^+ but addition of KCl up to 40 mM had no effect in high Cl^- solutions. It may be concluded therefore that the inhibition is due to the removal of Na^+. Since in the absence of Na^+ a significant inhibition of both Cl^- and H^+ pumps is observed, it must be assumed then that there is some link between Na^+ levels and the H^+ and Cl^- transport mechanisms of the mucosa. The nature of this link is not known, but the primary effect may be on the Cl^- mechanism.

The question of the electrogenicity of the hydrogen ion pump is also raised by these data. The group of experiments in which finite acid rate with PD = 0 was obtained suggests the possibility that acid is secreted by a unitary mechanism under these conditions. Since with falling hydrogen ion rate an approximately straight line relationship was obtained between PD and acid, the hydrogen ion pump appears purely electrogenic in choline sulfate solutions, as it is in sodium sulfate solutions(8). Thus under choline chloride conditions, the pump is either unitary or there is a critical balance between the hydrogen and chloride electrogenic mechanism. This latter possibility is extremely difficult to exclude rigorously but anoxia and readmission of oxygen in the standard chloride solutions results in a differential effect on the hydrogen ion rate and PD (the hydrogen ion rate is reduced more rapidly than the PD) even after successive cycles of deoxygenation. Such treatment should lead to transient changes in PD in choline solutions, but, since no transient changes were observed, the simplest explanation of the data would be that the H^+ pump may have a unitary mechanism under these conditions (*i.e.*, low Na^+). In NaCl solutions, it is clear that the hydrogen ion mechanism acts as if it is at least partially electrogenic (from the fall in resistance on stimulation of hydrogen ion secretion and the PD changes with various inhibitors such as thiocyanate and amytal). Hogben has suggested that in the dogfish stomach the hydrogen ion mechanism is essentially nonelectrogenic(9), but in the frog stomach the hydrogen ion transport system may appear to be unitary, or partially electrogenic or purely electrogenic, depending on bathing solution composition.

The existence of 3 groups of data following Na^+ removal is a puzzling one. As far as possible the conditions of exposure of the membrane to choline solutions were kept consistent. The most reasonable explanation for these findings would be a variation in the amount of Na^+ retained in the different groups. Na^+ analyses however did not provide evidence for this hypothesis, but it should be pointed out that there are uncertainties in analytical procedures for Na^+ levels low in relation to K^+, and difficulty also in determining the extracellular water in frog gastric mucosa. These sources of error might mask critical variation in Na^+ levels which in any case are less than 1 mEq/kg wet weight of tissue.

The basic observation in this paper, namely, the inhibitory effect of sodium removal on Cl^- and H^+ transport, adds to the known cation requirements for gastric secretion. Thus Na^+, K^+, and Ca^{++} in the nutrient solutions all appear to be essential for acid and Cl^- secretion by the *in vitro* frog stomach. These ions, particularly Na^+ and Ca^{++}, may be acting essentially as activators of the H^+ and Cl^- transport system.

Summary. Removal of sodium from the frog gastric mucosa results in an inhibition of H^+ secretion and PD, short circuit current, Cl^- flux with a rise in the resistance. Choline sulfate experiments show an inverted PD with low hydrogen ion rates or 0 PD with 0 hydrogen ion rates. In some experiments in choline chloride acid secretion occurred in the presence of a 0 PD and this secretion appears likely to be by a unitary mechanism.

1. Forte, J. G., Nauss, A. H., Am. J. Physiol., 1963, v205, 631.

2. Davis, T. L., Rutledge, J. R., Rehm, W. S., Physiologist, 1963, v6, 164.

3. Davenport, H. W., Am. J. Physiol., 1963, v204, 213.

4. Harris, J. B., Edelman, I. S., ibid., 1964, v206, 769.

5. Sachs, G., Shoemaker, R. L., Hirschowitz, B. I., ibid., 1965, v20, 461.

6. Durbin, R. P., Heinz, E., J. Gen. Physiol., 1958, v41, 1035.

7. Heinz, E., Durbin, R. P., Biochem. Biophys. Acta, 1959, v31, 206.

8. Rehm, W. S., Le Fevre, M. E., Am. J. Physiol., 1965, v208, 922.

9. Hogben, C. A. M., Clifton, J. A., Fed. Proc., 1965, v24, 407.

Received April 22, 1966. P.S.E.B.M., 1966, v123.

AMERICAN JOURNAL OF PHYSIOLOGY
Vol. 228, No. 4, April 1975. *Printed in U.S.A.*

Ion transport by amphibian antrum in vitro. I. General characteristics

GUNNAR FLEMSTRÖM AND GEORGE SACHS
Laboratory of Membrane Biology and Department of Physiology and Biophysics, University of Alabama, Birmingham, Alabama 35294

FLEMSTRÖM, GUNNAR, AND GEORGE SACHS. *Ion transport by amphibian antrum in vitro. I. General characteristics.* Am. J. Physiol. 228(4): 1188–1198. 1975.—Both *Necturus* and bullfrog antrum show stable PD, resistance, and short-circuit current (I_{sc}) when mounted in an Ussing chamber. Measurements of Na^+ and Cl^- flux showed that both ions are actively transported across *Necturus* antrum, Na^+ from secretory to nutrient, Cl^- from nutrient to secretory (both net fluxes being $\sim$ 0.30 μeq cm^{-2} h^{-1}). Only the Na^+ transport contributed to the I_{sc} and PD as evidenced by *a*) Na^+ removal, *b*) the effects of amiloride on the secretory surface, *c*) the effects of ouabain on the nutrient side. Microelectrode experiments confirm the Na^+ conductance of the secretory cell membrane, a HCO_3^- conductance of both cell membranes, and a KCl conductance across the nutrient cell membrane. In addition, antrum apparently secretes alkali ($\sim$0.35 μeq cm^{-2} h^{-1}), which secretion is sensitive to metabolic inhibitors and Diamox. Nutrient-side HCO_3^- increased the rate of alkaline secretion and a transmucosal HCO_3^- gradient could contribute to I_{sc} and PD. A model is proposed to account for the electrical properties of the tissue.

Necturus antrum; Na^+ flux; Cl^- flux; microelectrodes; amiloride; ouabain; HCO_3^-; alkali secretion

---

ANTRAL MUCOSAL PROPERTIES are of considerable clinical and physiological significance. It is this region of the stomach which undergoes peptic ulcer damage, and, also, it provides an epithelium which separates the secretory epithelium of the fundus from the absorptive epithelium of the small intestine. The permeability properties of this tissue in relation to control of gastric secretion are also an area of interest (1, 4).

Studies in dog (5) and man (2) have shown that, like the fundus, the antrum generates a transmucosal electric potential difference (PD, lumen negative), albeit somewhat lower than the PD across the fundic mucosa. More recently, it has been shown that, in *Necturus*, the fundic mucosa exhibits little, if any, paracellular or shunt conductance (19), whereas the antrum has a shunt/cell conductance ratio of about 3 (18).

Since details of transport by the antrum are unknown, this paper describes mainly properties of *Necturus* antrum in the Ussing chamber and also some of the properties of bullfrog antrum. Here we deal with the ions transported transepithelially, the effect of inhibitors on transport, and the origin of the antral PD. Some of these data have been presented in a preliminary form (7, 18).

MATERIALS AND METHODS

Animals. Necturus and *Rana catesbeiana*, which had been caught wild, were purchased from a local dealer. Both species were kept in tap water at room temperature until used. The *Necturus* were fed with minnows, while no food was given to the frogs. The latter were, however, used within 10 days after purchase and had, until then, been fed with crickets. No *Necturus* were used during the months June–September when the animals were mostly in poor condition. No *Rana catesbeiana* were used during the mating period (March to June).

Ussing chamber experiments. The animals were killed by section of the spinal cord, the abdomen was then opened, and the stomach was removed. The mucosa was separated from the rest of the stomach wall by blunt dissection in an oxygenated frog-Ringer solution, and then mounted as a membrane between the two halves of a Perspex chamber. The exposed mucosal surface was 1.1 cm^2.

The *Necturus* antrum could be readily distinguished from fundic mucosa by an absence of folds and of surface pigmentation. The demarcation was less distinct in the bullfrog: although the antral mucosa was of paler appearance than the fundic, the dividing line was convoluted. The absence of any measurable acid secretion following a challenge with histamine (10^{-5} M) was also used as a criterion to determine that we were dealing with antrum rather than fundus and was used regularly with bullfrog antrum.

On each side of the mucosa there were 7 ml of solution (Table 1) which was changed 3–4 times during a 20-min period before the experiments were started. A gas lift (O_2-CO_2, 95:5, vol/vol or 100% O_2) was used for circulation of the solutions. In some experiments O_2 was replaced with N_2 to produce anoxic conditions. All experiments were performed at 23°C. The pH on the nutrient (submucosal) side of the mucosa was always kept at 7.20 with a buffered solution. The pH on the secretory (luminal) side was kept at 7.30 when an unbuffered solution was used on this side, HCl (5×10^{-3} M) being infused under automatic control from a pH-stat instrument (Radiometer, Copenhagen). In some experiments a buffered solution (pH 7.20) was used also in this side. An alkaline-secretion rate could be calculated from the amount of HCl infused. Alkali secretion was recorded only when 100% O_2 or N_2 was used on the secretory side—the gas was prewashed in $Ba(OH)_2$ to exclude contamination with CO_2.

The transmucosal PD was measured via two calomel

electrodes (K4112, Radiometer, Copenhagen) and recorded with a high-input impedance voltmeter. Short-circuit current (I_{sc}) was applied to the mucosa through two end-on agar bridges. The current was adjusted manually and calculated from the voltage drop over a precision resistor. The electrical resistance (R) was determined from the voltage drop caused by sending a fixed current (20 $\mu A/cm^2$) through the tissue in both directions, and was always corrected for the resistance of the solutions. The time for the current pulse was made shorter than 0.1 s to avoid polarization phenomena (13).

Flux isotope measurement. Either ^{22}Na or ^{36}Cl was used in these measurements. We added 20 μCi of ^{22}Na or 7 μCi of ^{36}Cl to the solution on either side of the mucosa. Samples (0.2 ml) were taken from the *trans* side every 45 min and transferred to 10-ml of a scintillation solution (Aquasol). The samples were counted in a liquid scintillation counter (Beckman LS-133). The number of counts counted in the sample with the lowest activity was more than 3,000 above background. The equipment was tested with ^{22}Na and gave a linear response in the range used (up to 3×10^6 cpm).

Microelectrode experiments. These experiments were performed only with mucosas from *Necturus* due to the convenience of the large cell size. The secretory surface was mounted upward and the upper half-chamber had an open top to permit the use of microelectrodes. The secretory-side solution was circulated with a gas lift or by perfusion at 10 ml/min from Marriott bottles containing the appropriate solutions bubbled with gas, as was the nutrient side. The composition of the gases used was the same as in the Ussing-chamber experiments. The transmucosal PD was recorded in the same way as in the Ussing-chamber experiments, while current for resistance determination in these experiments was applied through Ag/AgCl circular wires mounted at the periphery of the half-chambers. The nutrient solution was used as reference for the intracellular PD, and the cell-secretory PD was then calculated from the difference between the cell-nutrient PD and the transepithelial PD.

Microelectrodes were pulled on a Nastuk puller, filled with methanol in vacuum, and with distilled water and 3 M KCl, respectively, by diffusion. The tip potential of the microelectrodes was less than 5 mV and the tip resistance 5–30 MΩ. A micropuncture was considered stable when the value of the intracellular potential and the ratio between the secretory- and the nutrient-side membrane resistances remained essentially unchanged for more than 3 min. The resistance ratio (calculated from the changes in the secretory and nutrient membrane PD when current was sent transmucosally) would appear to be the most reliable index of stability of the puncture, in that a shift of the ratio was seen often before a shift in the PD. In experiments in which one of the solutions was changed, the results were used only when the subsequent control period gave similar values (resistance ratio and cell-reference PD) to the control period preceding the change. For these experiments, therefore, a 3-way stopcock arrangement was used so that solution changes could be carried out without pressure alterations. When the effect of adding amiloride was studied, this was done only after a stable microelectrode potential had been recorded for 10 min, since amiloride removal with maintained puncture was not achieved.

RESULTS

A) General characteristics. In amphibia, the antrum is a relatively unfolded tissue with an absence of the complex tubular system of the fundus (Fig. 1). The secretory cells appear to be similar to the surface epithelial cells of the fundic area in that they are columnar with a mucous bar at the luminal surface. Occasional pits are found which contain cells presumably responsible for the endocrine function of this tissue.

As mounted in an Ussing chamber, with basal nutrient solutions (Table 1, 17.8 mM HCO_3^-), *Necturus* antrum generates a PD smaller than that of the fundus, with a higher transepithelial resistance and a lower measured I_{sc}. Bullfrog antrum generated a somewhat higher PD and I_{sc}, although the resistance was similar to that recorded in *Necturus* antrum (Table 2).

B) Effects of ion replacement. The effects of $SO_4^=$, glucuronate, and isethionate substitution of Cl^- in the case of *Necturus* antum are shown in Table 3.

In these experiments, buffered solutions were used on both sides of the mucosa (HCO_3^-, 17.8 mM; pH 7.20). $SO_4^=$ substitution for Cl^- had an insignificant effect on PD and resistance ($P < 0.05$ for both) of antral mucosa. With both isethionate and glucuronate there was a significant increase in both PD ($0.01 < P < 0.02$ and $P < 0.01$) and resistance ($0.01 < P < 0.02$ and $P < 0.01$), whereas there was an insignificant change in I_{sc}.

In contrast, removal of Na^+ with choline substitution

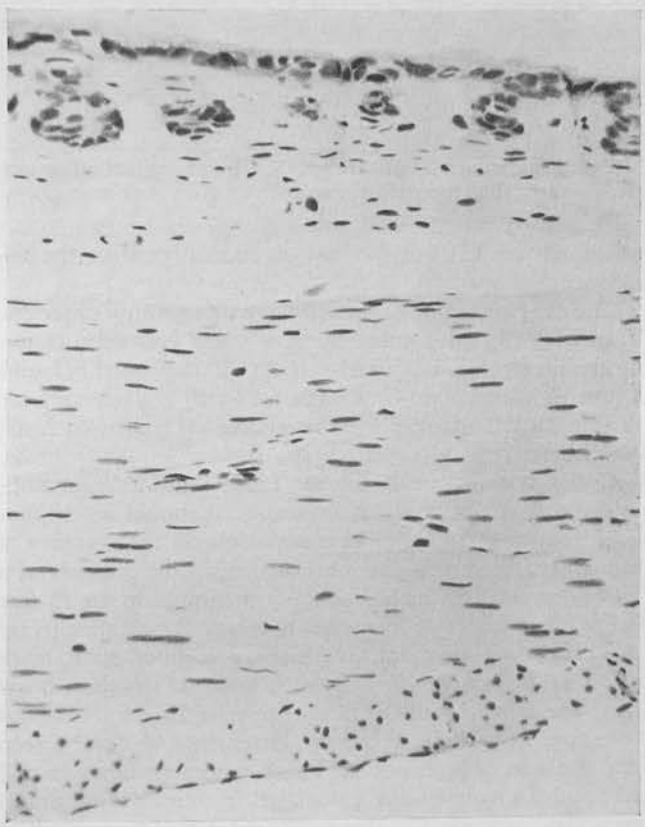

FIG. 1. Micrograph of full-thickness section of *Necturus* antrum showing relative absence of pits and uniformity of cell type. (Magnification × 250).

TABLE 1. *Composition of solutions*

	Nutrient					Secretory			
				K^+Cl^- exp				K^+Cl^- exp	
	Basal	HEPES	Na^+ = 20.5	K^+ = 4	K^+ = 40	Basal	Na^+ = 20.5	K = 4^+	K = 40^+
Na^+	102.4	102.4	20.5	66.4	66.4	102.4	20.5	66.4	66.4
K^+	4.0	4.0	4.0	4.0	40.0	4.0	4.0	4.0	40.0
Ca^{++}	1.8	1.8	1.8	1.8	1.8	1.8	1.8	1.8	1.8
Mg^{++}	0.8	0.8	0.8	0.8	0.8	0.8	0.8	0.8	0.8
$Choline^+$			81.9	36.0			81.9	36.0	
Cl^-	91.4	91.4	91.4	91.4	9.2	91.4	91.4	91.4	9.2
$SO_4^=$	0.8	7.2	0.8	0.8	41.9	10.1	10.1	10.1	51.2
HCO_3^-	17.8		17.8	17.8	17.8				
$H_2PO_4^-$	0.8	0.8	0.8	0.8	0.8				
$HEPES^-$		5.0							
Mannitol		6.4				11.3	11.3	11.3	11.3
Glucose	2.0	2.0	2.0	2.0	2.0				

All concentrations are given in mM. pH in the nutrient side solution was always adjusted to 7.20 with H_2PO_4 in the gas to be used.

TABLE 2. *Electric properties of Necturus and bullfrog antrum in symmetric (17.8 mM HCO_3^-) solutions*

	PD, mV	I_{sc}, μeq cm^{-2} h^{-1}	Resistance, Ω-cm^2	*n*
Necturus	5.5 ± 0.4	0.25 ± 0.03	828 ± 46	(20)
Bullfrog	14.4 ± 2.1	0.65 ± 0.12	828 ± 115	(7)

The mean values ± SE are given. The presented values are steady-state values recorded 45 min after the start of an experiment.

abolished the PD but did not significantly affect the resistance.

The data for bullfrog mucosas were significantly different. Thus both Cl^- substitution by $SO_4^=$, and Na^+ substitution by choline significantly ($0.01 < P$ for all) depressed PD, and I_{sc}, with a significant ($P < 0.01$ for both) rise in resistance (Table 3). All changes were reversible on return to NaCl conditions.

C) Ion fluxes in Necturus antrum. Table 4 shows the data obtained during ion flux measurements. It should be emphasized that these measurements were done in the presence of unbuffered, secretory-side solution, i.e., in the presence of a HCO_3^- gradient, which probably contributes to the I_{sc} (see below), but this made it possible to record the alkaline secretion. It can be seen that, in the short-circuited state, there was a net flux of Na^+ from S → N, and that simultaneously there was a net flux of Cl^- in the opposite direction of about the same magnitude. From the latter data, it can be seen that the sum of both net ion fluxes exceeded the measured I_{sc}, and the conductance calculated from individual unidirectional Na^+ and Cl^- fluxes (2.5×10^{-3} Ω^{-1} cm^{-2}) also exceeded tissue conductance (1.2×10^{-3} Ω^{-1} cm^{-2}).

D) Inhibitors of Na^+ transport. In an initial series of experiments 10^{-5} M ouabain was added to either the secretory

TABLE 3. *Effects of replacement of Cl^- and Na^+ on electric properties of Necturus and bullfrog antrum*

	PD, mV	Resistance, Ω-cm^2	I_{sc}, μeq cm^{-2} h^{-1}	*n*
		Necturus		
NaCl	3.5±0.5	997± 64	0.13±0.03	(5)
Na_2SO_4	3.4±0.3	1087±139	0.12±0.02	
NaCl	4.4±1.2	987±114	0.17±0.03	
NaCl	6.8±0.9	790±142	0.32±0.06	(4)
Na-isethionate	8.1±0.8	1010±193	0.30±0.06	
NaCl	5.5±0.9	817±150	0.25±0.05	
NaCl	7.9±1.2	747± 82	0.39±0.08	(6)
Na-glucuronate	10.8±1.5	1206±147	0.33±0.07	
NaCl	6.5±1.3	829±143	0.29±0.08	
NaCl	3.6±0.8	785± 83	0.17±0.03	(5)
Choline-Cl	0	760± 67	0	
NaCl	3.8±1.1	685± 60	0.21±0.04	
		Bullfrog		
NaCl	13.3±1.6	742± 65	0.67±0.08	(4)
Na_2SO_4	3.5±0.5	1038± 92	0.13±0.02	
NaCl	14.1±2.0	735± 61	0.72±0.12	
NaCl	12.1±1.3	679± 55	0.66±0.10	(4)
Choline-Cl	1.5±0.2	985± 92	0.06±0.02	
NaCl	13.1±1.7	723± 64	0.68±0.11	

The mean values ± SE of the PD, transepithelial electric resistance, and I_{sc} during the last 15 min of each period are presented. The experiments were performed during three consecutive 60-min periods. Buffered (pH 7.20) solutions with 17.8 mM HCO_3^- and gassed with O_2-CO_2, 95:5 (vol/vol) were used on both sides of the mucosa. The experiments were performed during open-circuit conditions; the I_{sc} was calculated from the PD and the resistance.

TABLE 4. *Na^+ and Cl^- fluxes across short-circuited necturus antrum*

$J^{Na}_{S\to N}$	$J^{Na}_{N\to S}$	$J^{Cl}_{S\to N}$	$J^{Cl}_{N\to S}$
Unidirectional ion fluxes, μeq cm^{-2} h^{-1}			
0.74 ± 0.06 (n = 10)	0.47 ± 0.13 (n = 10)	0.52 ± 0.06 (n = 8)	0.78 ± 0.14 (n = 8)

PD, mV	Resistance, Ω-cm^2	I_{sc}, μeq cm^{-2} h^{-1}	OH^-, μeq cm^{-2} h^{-1}
Electrical properties and OH^- secretion (n = 36)			
9.5 ± 0.7	867 ± 62	0.41 ± 0.03	0.33 ± 0.02

The mean values ± SE are given. An unbuffered solution and 100% O_2 were used on the secretory side in these experiments to allow recording of the alkaline secretion while there was 17.8 mM HCO_3^- and O_2-CO_2, 95:5 (vol/vol) on the nutrient side. The experiments were performed during 90-min periods.

or nutrient side of *Necturus* antral mucosa. When placed on the nutrient side, there was a significant ($P < 0.01$ for both after 45 min) inhibition of PD and I_{sc}, and there was a concomitant and significant ($0.01 < P < 0.02$) reduction of $J^{Na}_{S\to N}$ (but not $J^{Na}_{N\to S}$, Fig. 2). Ouabain in the same concentration did not affect the electrical or flux parameters when added to the secretory side (n = 4). Amiloride, 10^{-6} M, achieved essentially the same result, however, when added to the secretory side. In this case the fall in I_{sc} was larger than the fall ($P < 0.01$) in J_{Na}, but the rise in I_{sc} following removal of amiloride exactly corresponded to the increase in J_{Na} (Fig. 3). Amiloride did not affect the electrical parameters if added to the nutrient side, although the higher concentration of 10^{-4} M was tried (n = 3). Both amiloride and

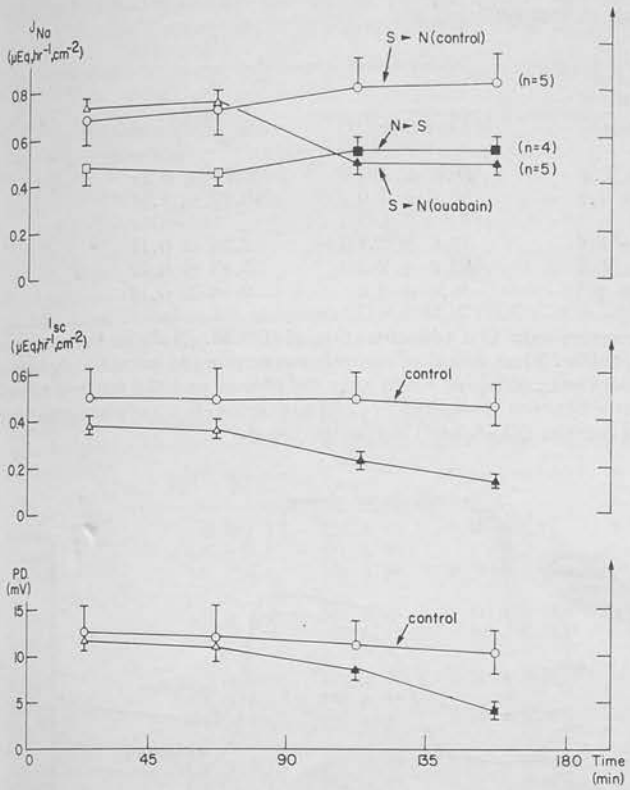

FIG. 2. Effect of 10^{-5} M ouabain addition on nutrient side of mucosa on Na^+ flux (J_{Na}), short-circuit current (I_{sc}) and PD. Presence of drug is indicated by solid symbols. Mean values ± SE (n = 4) during 4 consecutive 45-min periods show that there are no significant changes in control experiments, and that ouabain reduces I_{sc} and $J^{Na}_{S\to N}$ equivalently. Unbuffered secretory solution was used.

ouabain abolished the I_{sc} and PD if added in the absence of a HCO_3^- gradient (see below).

Neither ouabain nor amiloride significantly ($P < 0.05$) changed the rate of alkali secretion or the conductance of the tissue (Table 5).

E) Microelectrode studies with amiloride. Since the effect of amiloride was confined to the secretory side, and in other tissues, a reduction in Na^+ conductance would appear to be a reasonable explanation for the mode of action of this compound (3), microelectrode experiments were performed to confirm the site of action. Figure 4 shows that there is a rapid decline of transmucosal PD with a hyperpolarization of the secretory membrane and a lesser hyperpolarization of the nutrient membrane of the cell. Although there is only a slight rise of transmucosal resistance, the ratio of secretory/

TABLE 5. *Effects of ouabain and amiloride on alkaline secretion and electrical resistance of Necturus antrum*

	OH^-, μeq cm^{-2} h^{-1}	Resistance, Ω-cm^2	PD, mV	n
Control	0.31 ± 0.05	925 ± 104	10.5 ± 1.3	(9)
Ouabain	0.31 ± 0.04	920 ± 104	8.8 ± 1.3	
Ouabain	0.33 ± 0.03	934 ± 107	4.7 ± 0.8	
Control	0.38 ± 0.11	1104 ± 130	7.6 ± 2.2	(4)
Amiloride	0.43 ± 0.13	1136 ± 164	2.0 ± 0.7	

The mean values ± SE during the last 15 min in each experimental period are given. The experiments were performed during three or two consecutive 45-min periods, the first being a control without any drug added. Ouabain (10^{-5} M) was added to the nutrient side and amiloride (10^{-6} M) was added to the secretory side at the beginning of the second 45-min period. The effects on the rate of alkaline (OH^-) secretion, resistance, and PD are shown.

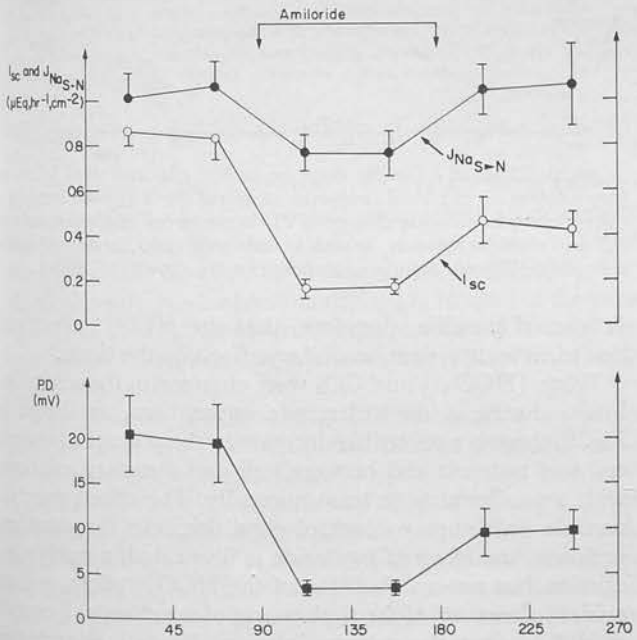

FIG. 3. Effect of 10^{-6} M amiloride on secretory side of *Necturus* antrum on $J^{Na}_{S\to N}$, I_{sc} and PD with 6 consecutive 45-min periods, in which amiloride was present during 3rd and 4th period showing reversible inhibition of measured parameters (mean values ±SE, n = 4). Unbuffered secretory solution was used.

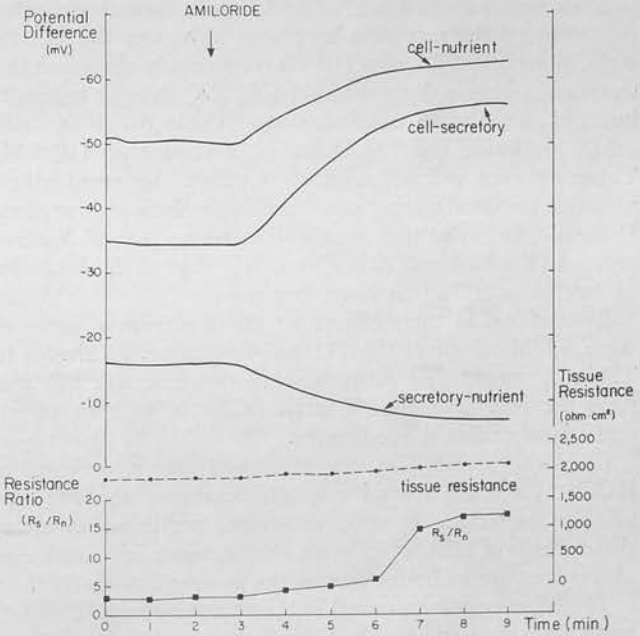

FIG. 4. A microelectrode experiment showing effect of amiloride on PD between cell and nutrient, and cell and secretory solutions, and transepithelial PD (secretory-nutrient). Also shown is effect on transepithelial resistance and membrane resistance ratio R_S/R_N. Unbuffered secretory solution was used.

TABLE 6. *Effect of amiloride and a fivefold secretory-side [Na^+] decrease on transepithelial and cell membrane potentials of Necturus antrum*

	PD, mV			R_S/R_N	n
	Secr-Nutr	Cell-Secr	Cell-Nutr		
Control	11.2 ± 2.3	36.4 ± 1.4	47.8 ± 2.0	2.77 ± 0.23	(5)
Amiloride	3.2 ± 0.8	56.0 ± 1.2	59.2 ± 1.0	10.77 ± 1.81	
Control	10.2 ± 0.6	28.4 ± 1.6	38.6 ± 2.1	2.36 ± 0.17	(5)
Na^+ decrease, secretory side	3.3 ± 0.2	49.3 ± 0.2	52.6 ± 2.5	5.43 ± 0.72	
Control	10.8 ± 0.8	25.8 ± 1.5	36.6 ± 2.0	2.46 ± 0.18	

The mean values ± SE are given. Amiloride was added to the secretory side to a concentration of 10^{-5} M. [Na^+] on the secretory side was decreased from 102.4 to 20.5 mM, Na^+ being replaced with choline. The preceding controls were recorded immediately before the addition of amiloride or change in Na^+ concentration. The test values were obtained 4 min after the change and the controls following the Na^+ decrease 4 min after return to control conditions. The ratio between the secretory- and nutrient-side membrane resistance (R_S/R_N) was calculated from the voltage change obtained on sending current (20 $\mu A/cm^2$) across the tissue.

nutrient membrane resistance (R_S/R_N) rises considerably—more than fourfold as shown in Table 6).

A fivefold decrease in Na^+ concentration on the secretory side (from 102.4 to 20.5 mM, Na^+ replaced with choline; Table 1) also produced an effect similar to that obtained with secretory-side amiloride (Table 6 and Fig. 5), although the increase of the cell membrane-resistance ratio was somewhat smaller. A very high resistance ratio was obtained in Na-free solutions (Table 7); under this condition secretory-side amiloride was without effect on the membrane potentials and the resistance ratio ($n = 3$).

F) Alkali secretion. When pH-stat experiments were run with unbuffered mucosal solution and use of 100% O_2 instead of O_2-CO_2, 95:5 (vol/vol), it was found that there was a significant alkalinization of the antral secretory surface. A variety of experiments was carried out to elucidate the nature of this alkali secretion.

Thus, removal of HCO_3^- and CO_2 from the nutrient solution reduced the secretion by about 50%, but the PD by 40%. Anoxia and Diamox (10 mM) reversibly abolished the secretion, whereas dinitrophenol (10^{-4} M) sharply reduced, but did not abolish alkalinization (Table 8). SCN^- (20 mM), amiloride (10^{-6} M, Table 5), and ouabain (10^{-5} M, Table 5) were without significant effect. Apparent alkali secretion persisted during short-circuiting of the preparation. It should be noted that the alkali secretion rate of *Necturus* antrum (Tables 4 and 8) is about 20% that of the acid rate of the fundus (17) of the same species.

In addition to their effects on alkali secretion, some of these inhibitors affect the PD and resistance. As shown in Table 8, anoxia and dinitrophenol decrease the PD and raise the resistance significantly. SCN^- is without effect, and Diamox raises the resistance.

G) HCO_3^- permeability. As mentioned above, removal of HCO_3^- from the serosal solution decreased the PD and alkaline secretion. It was, therefore, pertinent to study these effects of HCO_3^- in some detail, since identical manipulations are without effect on the in vitro fundus (16).

The effect on transmucosal PD by changing both [HCO_3^-] and CO_2 is shown in Fig. 6. The effects were due, mainly, to the changes in [HCO_3^-]; changes in CO_2 alone had only minimal effects (Fig. 7). The changes observed with HCO_3^- changes are relatively slow in comparison to effects of nutrient-side K^+Cl^- changes (Fig. 8), in the same tissue.

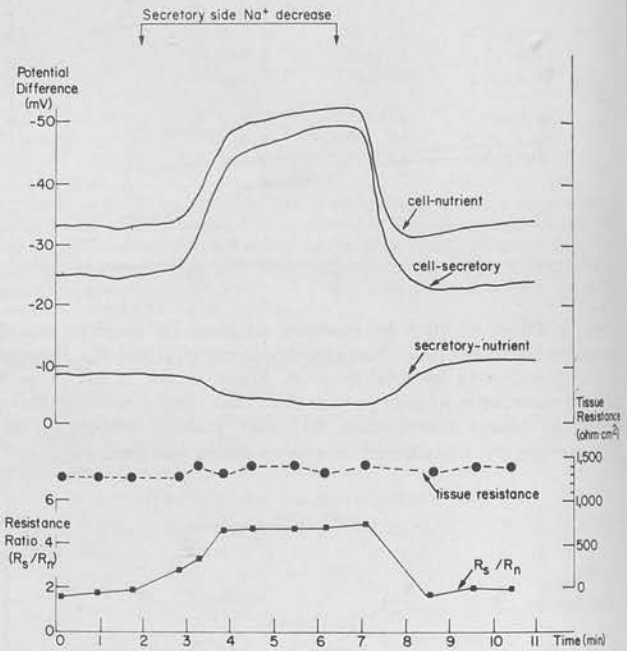

FIG. 5. Effect of a fivefold decrease in Na^+ concentration in secretory solution on electrical properties of antral tissue as monitored by a microelectrode, showing change in PD between cell and secretory and cell and nutrient solution, as well as resistance ratio R_S/R_N and transmucosal resistance. Solution compositions are shown in Table 1.

It seemed possible, therefore, that the HCO_3^- effect was due to, at least in part, secondary effects on the tissue.

When [HCO_3^-] and CO_2 were changed in the serosal solution during a microelectrode experiment, as shown in Fig. 9, there is a reversible decrease in the potential between cell and nutrient and between cell and secretory solutions, with a smaller change transmucosally. The effects were reversible on return to control conditions. In the same experiment the effect of amiloride is illustrated, namely a reduction but not an abolition of the HCO_3^- effect, and no evident alteration of the time course of the change. Removal of HCO_3^- from the nutrient solution also slightly decreased ($P < 0.01$) the ratio between the secretory and nutrient membrane resistances (Table 7).

Ouabain inhibition of Na^+ transport, on the other hand, alters the time course of the HCO_3^- change so that now the

TABLE 7. *Effect of nutrient-side HCO_3^- removal in Na^+ and choline solutions in microelectrode experiments*

	Nutrient Buffer	PD, mV			R_S/R_N
		Secr-Nutr	Cell-Secr	Cell-Nutr	
Na solutions ($n = 6$)	$HCO_3^- + CO_2$	11.2 ± 3.3	27.7 ± 3.3	39.0 ± 2.4	1.86 ± 0.35
	HEPES	7.6 ± 3.1	18.6 ± 2.4	26.2 ± 2.4	1.46 ± 0.40
	$HCO_3^- + CO_2$	11.7 ± 2.8	29.2 ± 3.6	40.8 ± 2.8	1.88 ± 0.88
Choline solutions ($n = 4$)	$HCO_3^- + CO_2$	0	35.3 ± 3.8	35.3 ± 3.8	14.51 ± 2.11
	HEPES	0.3 ± 0.2	35.2 ± 3.4	35.5 ± 3.4	16.54 ± 2.30
	$HCO_3^- + CO_2$	0.3 ± 0.2	33.5 ± 3.5	33.8 ± 3.8	15.30 ± 1.66

The mean values ± SE are given. 17.8 mM of HCO_3^- was replaced with 5 mM of HEPES. Concomitantly the nutrient-side gas was changed from O_2-CO_2, 95:5 (vol/vol) to 100% O_2. The potentials were recorded immediately before and 12 min after changes in HCO_3^- concentration. On the secretory side, 100% O_2 and an unbuffered solution were used.

TABLE 8. *Alkaline secretion of Necturus antrum*

	PD, mV	Resistance, Ω-cm²	OH^-, μeq cm⁻² h⁻¹	n
Control	8.8 ± 1.8	747 ± 63	0.40 ± 0.10	(6)
Anoxia	3.0 ± 0.7	891 ± 56	0	
Control	7.0 ± 1.1	835 ± 50	0.32 ± 0.05	(4)
Control	11.9 ± 1.4	685 ± 54	0.41 ± 0.14	(4)
DNP, 10^{-4} M	7.8 ± 1.0	798 ± 75	0.20 ± 0.07	
Control	10.3 ± 3.3	835 ± 54	0.38 ± 0.12	
Diamox, 10 mM	10.7 ± 3.3	940 ± 44	0	
Control	9.3 ± 3.6	922 ± 46	0.24 ± 0.07	
Control	8.9 ± 2.1	694 ± 40	0.35 ± 0.06	(5)
HEPES	5.8 ± 1.2	784 ± 57	0.17 ± 0.06	
Control	9.4 ± 1.8	742 ± 35	0.28 ± 0.08	
Control	8.3 ± 2.0	752 ± 62	0.35 ± 0.08	(4)
SCN, 20 mM	8.6 ± 2.1	730 ± 74	0.38 ± 0.09	

The mean values ± SE of PD, resistance, and rate of alkaline secretion are given. Anoxia was produced by replacement of O_2 in the gas with N_2. All drugs were added only to the nutrient side of the mucosa. The control values were obtained immediately before or 30 min after the test period. All test values were obtained 30 min after change to anoxic conditions or addition of a drug. In those experiments 17.8 mM of HCO_3^- were replaced with 5 mM of HEPES buffer; concomitantly, the nutrient-side gas was changed from O_2-CO_2, 95:5 (vol/vol) to 100% O_2. An unbuffered solution and 100% O_2 was always used on the secretory side.

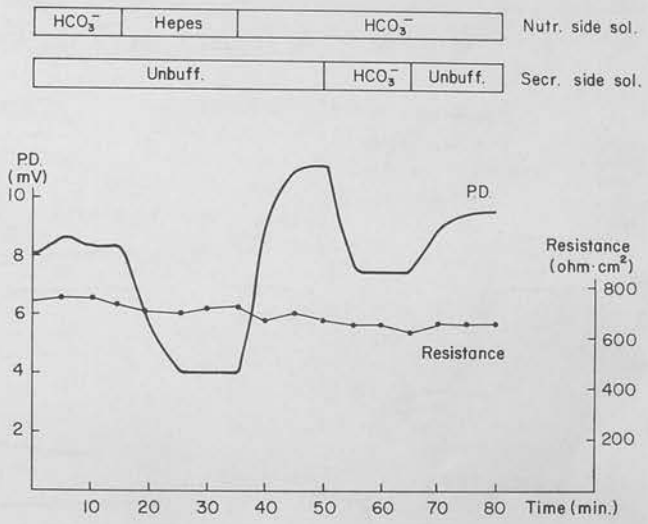

FIG. 6. PD and resistance of the *Necturus* antrum with variations of HCO_3^- and CO_2 in bathing solutions. HCO_3^- in nutrient-side solution (17.8 mM) was replaced with HEPES (Table 1) and unbuffered secretory-side solution was replaced with nutrient-side solution (17.8 mM HCO_3^-) as indicated. Together with unbuffered and HEPES solutions 100% O_2 was used, while HCO_3^--buffered nutrient-side solution was gassed with O_2-CO_2, 95:5 (vol/vol).

effects are as rapid as the effects of nutrient-side K^+Cl^- changes (Fig. 10).

This suggested that there might be a relationship between Na^+ transport and HCO_3^- conductance, hence experiments were carried out in which HCO_3^- changes were made in the absence of Na^+ (i.e., in choline solutions, Table 8). Na^+ removal results in an abolition of the PD in spite of the presence of a HCO_3^- gradient. Subsequent HCO_3^- changes were without effect on cell or transmucosal potential (Table 7, and Fig. 11).

It is, however, obvious (Fig. 11) that return of Na^+ to only the secretory side reinduced HCO_3^- conductance in the nutrient-side cell membrane.

H) Asymmetry of membranes. The effect of changes in ion concentrations of the cell membrane potentials were made to evaluate the nature of the diffusion potentials across the membranes. Figure 8 shows the response to secretory and nutrient-side 10-fold changes in K^+ and Cl^- concentrations. The Na^+ and HCO_3^- concentrations were kept constant, K^+ replacing choline and $SO_4^=$ replacing Cl^- (Table 1). It is clear that the K^+ and Cl^- change produced a significant effect only when made on the nutrient side. No effects greater than 4 mV were obtained on the secretory-side change. The effect of a nutrient-side K^+ and Cl^- change are largest in the nutrient-side cell membrane, but there is also a depolarization of the secretory membrane potential and the secretory-nutrient (transmucosal) potential.

The effect of nutrient and secretory-side fivefold Na^+ changes is illustrated in Figs. 5 and 12 and in Table 6. The effect of a Na^+ change shows an asymmetry opposite to that obtained with K^+Cl^- changes, although both the cell membranes are sensitive. A secretory-side Na^+ decrease hyperpolarizes both cell membranes, the greater effect being obtained across the secretory-side membrane. There is a concomitant decrease of the transmucosal PD. A nutrient-side Na^+ decrease also hyperpolarizes both cell membranes; in this case there is a greater change across the nutrient membrane, and there is an accompanying small increase in the transmucosal potential. The time course of the change obtained with a secretory-side Na^+ change is similar to that obtained with a nutrient-side K^+Cl^- change. The time course of the PD obtained with a nutrient-side Na^+ change is, however, different. In all experiments ($n = 8$) there was a two-phase response, consisting of an immediate smaller

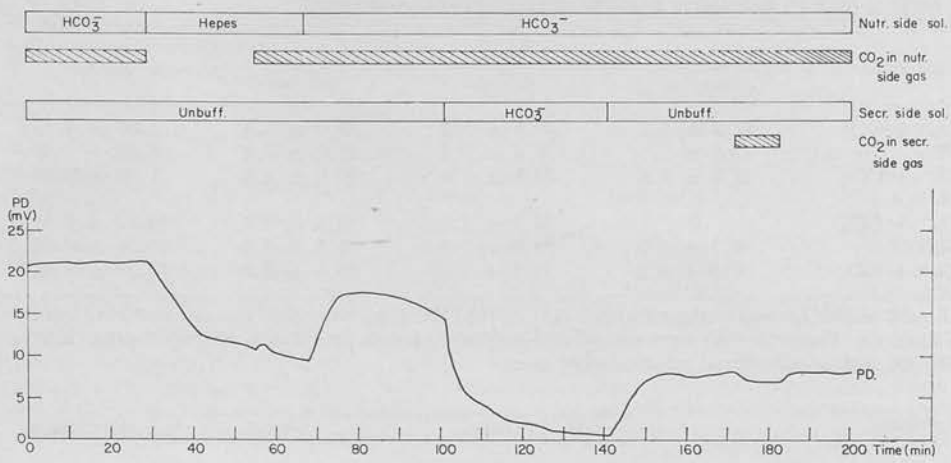

FIG. 7. This experiment illustrates that CO_2 alone on nutrient side cannot restore effect of PD on removal of HCO_3^- from that side. Effect of secretory-side CO_2 alone is very small compared to that of secretory-side HCO_3^-. Unless indicated, O_2-CO_2, 95:5 (vol/vol) was used, otherwise gas was 100% O_2.

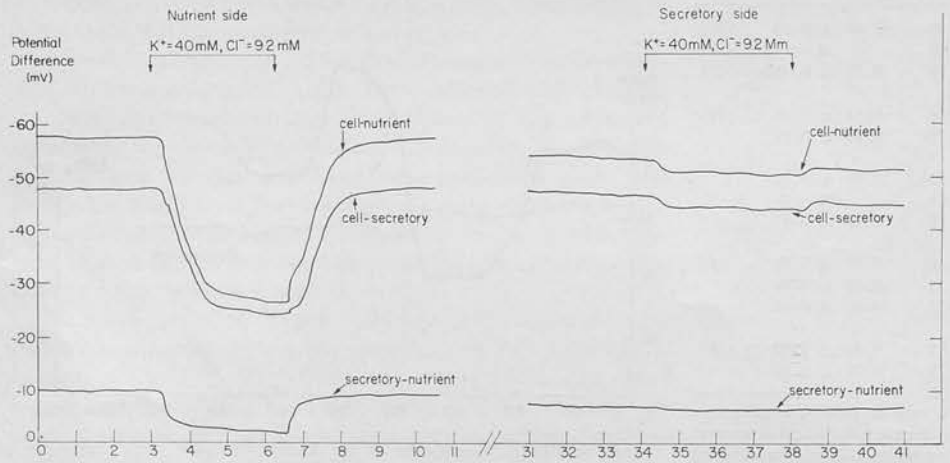

FIG. 8. Results of 2 microelectrode experiments, in same mucosa, in which a constant product change in K^+ (4–40 mM) and Cl^- (91.4–9.2 mM) was made on nutrient and secretory side of *Necturus* antrum. Both Na^+ and HCO_3^- concentrations were unchanged in this experiment and secretory solution was unbuffered.

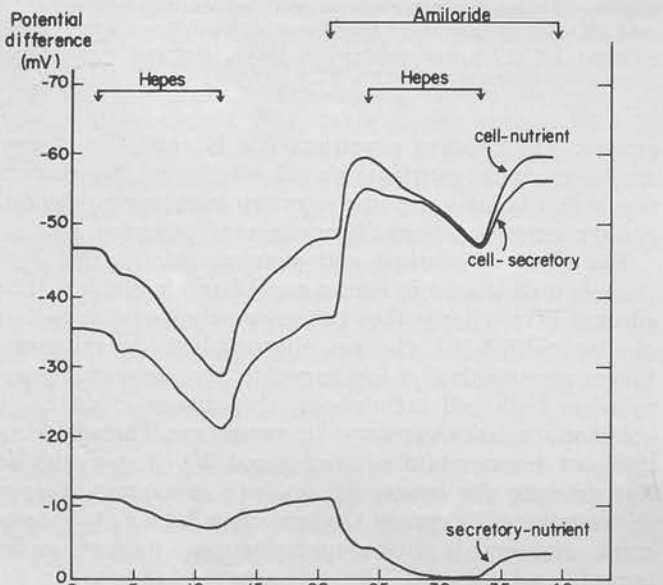

FIG. 9. A microelectrode recording of effect of HCO_3^- removal and replacement on cell and transmucosal PD's before and after amiloride treatment of *Necturus* antrum. Combination of HCO_3^- removal and amiloride addition abolishes PD (and I_{sc}), whereas either of these alone do not. Unbuffered secretory-side solution was used.

hyperpolarization and a later greater hyperpolarization. The latter appeared 1–3 min after the immediate change. This might indicate that the nature of the Na^+ conductance in the nutrient-side cell membrane is different from that in the secretory-side membrane.

Finally, results from Ussing-chamber experiments (Figs. 6 and 7) showed that the transmucosal PD changed with variation in HCO_3^- concentration in the solutions on both sides. This made it interesting to examine with microelectrodes whether the secretory-side membrane was well as the nutrient-side membrane (see above) showed a HCO_3^- conductance. Figure 13 shows the result of a typical experiment. Adding HCO_3^- (basal nutrient solution, 100% O_2) to the secretory side results in a slow hyperpolarization of the secretory-side membrane, similar to that obtained across the nutrient-side membrane (Fig. 9) with a HCO_3^- change on that side. There is a smaller hyperpolarization of the nutrient membrane and a decrease of the transmucosal PD. The effect of a HCO_3^- change on either side of the mucosa is thus mainly exerted across the cell membranes, rather than across the shunt pathway.

DISCUSSION

It has previously been established that the gastric fundus of *Necturus* actively transports H^+ and Cl^- luminally and Na^+ serosally (17). The antrum of this species demonstrated

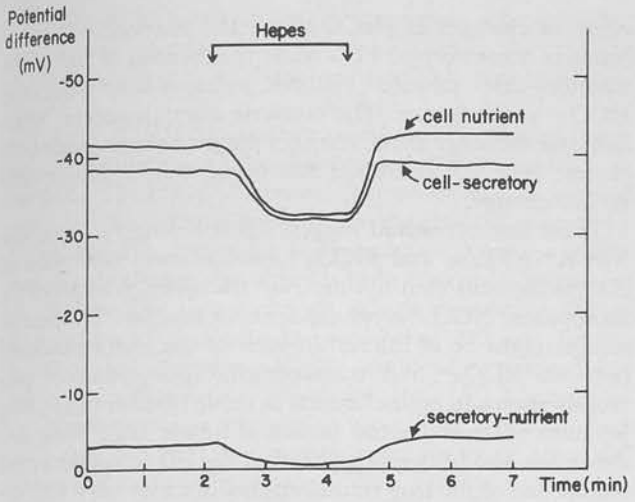

FIG. 10. Effect of HCO_3^- and CO_2 removal from nutrient solution on electrical properties of *Necturus* antrum as visualized in a microelectrode experiment, following ouabain pretreatment (10^{-5} M, nutrient side) for 45 min. An unbuffered secretory-side solution was used.

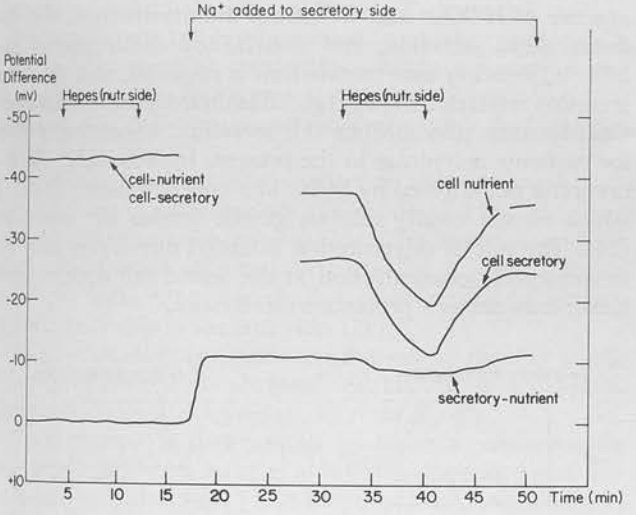

FIG. 11. Effect of a HCO_3^- change in choline (Na^+ free) solutions and after readdition of Na^+ (102.4 mM) to secretory solutions, showing that secretory Na^+ is adequate for restoring HCO_3^- conductance to nutrient surface of tissue.

some notable differences. Thus acid secretion is clearly absent, the PD and I_{sc} generated are significantly lower, and the tissue resistance is higher. In assessing the details of transport by this tissue various types of studies provide considerable information as to which ions are transported, and across which membrane of the cell.

Ion-substitution experiments, with either Na^+ or Cl^- removal, provide some insight as to which transport system is responsible for the PD and I_{sc}. Cl^- removal, with $SO_4^=$ substitution, does not affect the transmucosal PD, resistance, or I_{sc}. Glucuronate or isethionate, however, produce increased tissue resistance and PD. From this, one would be tempted to conclude that Cl^- transport does not contribute to the electrical characteristics of the tissue.

Based on the fact that conductance of the antrum appears

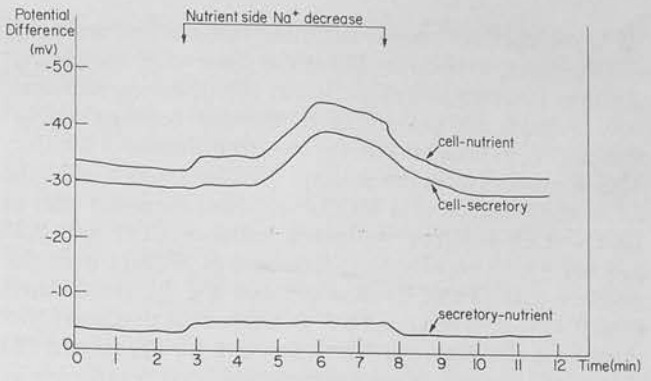

FIG. 12. Effect of decreasing Na^+ 5-fold on nutrient surface of *Necturus* antrum showing that nutrient membrane has a significant Na^+ conductance, but that there is a 2-phase response. Composition of solutions are given in Table 1.

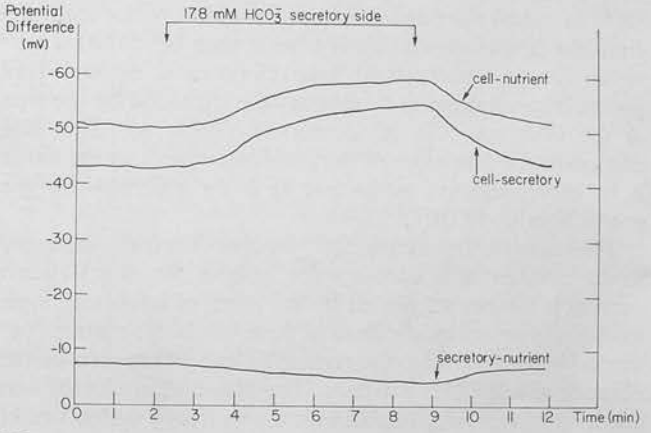

FIG. 13. Effect of HCO_3^- addition to secretory solution of *Necturus* antrum showing that secretory surface of tissue also has a HCO_3^- conductance.

to be mainly due to extracellular passage of ions (18), it would seem that this pathway does not discriminate between sulfate and chloride, but is restrictive to the movement of anions having a larger molecular weight such as glucuronate or isethionate.

In contrast to the above findings for *Necturus*, the bullfrog antrum responds to Cl^- removal with a decrease in PD an increase in resistance, and with a 50% fall in I_{sc}, showing that in this species in vitro Cl^- transport probably does contribute to the electrical properties of antrum.

However, when radioisotope flux measurements were carried in *Necturus* antrum there was a net flux of Cl^- from serosa to mucosa in the short-circuited preparations in the absence of a transmucosal chemical gradient for Cl^-. This demonstrates that there probably is active Cl^- transport in this species, but this is electrically silent, presumably a neutral mechanism, as has recently been demonstrated in the intestine (12).

In the case of Na^+ substitution, removal of Na^+ with choline as the substituting cation results in abolition of the PD and I_{sc}, with no significant change in resistance. Flux measurements in the presence of a transmucosal HCO_3^- gradient showed that the I_{sc} (0.41 μeq cm^{-2} h^{-1}) exceeded the net Na^+ flux (0.27 μeq cm^{-2} h^{-1}) as well as the decrease in $J_{S\to N}^{NA}$ obtained on amiloride (0.32 μeq cm^{-2} h^{-1}) or ouabain

(0.30 μeq cm^{-2} h^{-1}) treatment. Both ouabain and amiloride did, however, abolish the PD of the tissue when the HCO_3^- gradient was removed (Figs. 9 and 10). It seems, therefore, very probable that the measured difference between net Na^+ flux and I_{sc} represents current due to diffusion of HCO_3^-. This is supported by the findings (Tables 2 and 3) that the I_{sc} in the presence of a HCO_3^- gradient exceeded that in HCO_3^--CO_2–buffered symmetric solutions (0.41 and 0.25 μeq cm^{-2} h^{-1}, respectively). Removal of HCO_3^- from the nutrient side (Table 8) also reduced the I_{sc} (calculated) from 0.47 to 0.28 μeq cm^{-2} h^{-1}. It seems clear that a net Na^+ absorption (0.30 μeq cm^{-2} h^{-1}) accounts for the I_{sc} and PD measured in symmetrical solutions and that a diffusion of HCO_3^- along a transmucosal gradient can contribute to the I_{sc} and PD.

No measurements of the K^+ flux were made in the present study; the results of in vivo studies indicate, however, that $[K^+]$ in antral secretion is higher than that in the secretion from the fundic pouch (6). It cannot then be excluded that some K^+ transport could take place as a neutral KCl pump. The total tissue conductance is exceeded by the sum of the Na^+ and Cl^- conductances (Table 4). This also demonstrates that some of the ionic movement in the tissue is by nonconductive pathways, as is the case also for the gastric fundus (8, 10).

The concept that active Na^+ transport from the secretory to the nutrient side accounts for most of the short-circuit current is further supported by the effect of inhibitors, such as ouabain or amiloride. Both of these inhibitors reduce Na^+ flux S $\rightarrow$ N selectively, and reduce I_{sc} and PD to zero in the absence of a HCO_3^- gradient. The action of amiloride was on the secretory side, ouabain on the nutrient, which would be compatible with a cell containing a secretory surface with passive Na^+ conductance, and a basal surface with Na^+-K^+-ATPase.

Amiloride sharply increased the ratio of the resistances between the secretory and the nutrient-side cell membranes. Similar increases in the ratio were obtained on removal of sodium from the solutions and on a decrease of only secretory-side $[Na^+]$. Therefore, it can be concluded that amiloride in this tissue acted by decreasing Na^+ conductance in the secretory-side cell membrane, and that Na^+ conductance is a major contributor to the conductance of this membrane.

The role of a HCO_3^- gradient in maintaining a PD across *Necturus* antrum is demonstrated by *a*) the reduction in PD with the removal of HCO_3^- from the serosal solution, *b*) the increase in PD when HCO_3^- is removed from the secretory solution. In a tissue with high paracellular conductance it is necessary to establish that these effects are due to changes across the cell membrane, rather than across the shunt path, which was done with microelectrodes.

The situation is somewhat more complicated, due to an interaction between Na^+ transport and HCO_3^- conductance. One line of evidence pointing to a complex interaction between the tissue and HCO_3^- concentration is the time course of the PD change occurring with change in $[HCO_3^-]$, which is significantly slower than a PD change occurring when the K^+ and Cl^- concentrations are changed (compare Figs. 8 and 9) showing that the time shift is probably not due to diffusion limitation. Amiloride reduces the magnitude of the HCO_3^- effect, but does not alter the time course. Removal of Na^+ from the bathing solutions abolishes any effect of changes in $[HCO_3^-]$ on the nutrient cell membrane of transmucosal PD's while readmission of Na^+ to the secretory-side solution restores nutrient-side membrane HCO_3^- conductance. The converse may also occur. Ouabain, on the other hand, changes the time course so that the change (Fig. 10) resembles that found with a nutrient-side K^+Cl^- change.

These findings would suggest a link between a functional Na^+-K^+-ATPase and HCO_3^- conductance. Admission of Na^+ to the cells (but not net Na^+ transport) is required for an apparent HCO_3^- conductance to be manifest. The present results might be of interest in view of the interdependence between HCO_3^- and transepithelial Na^+ transport previously shown in epithelia such as turtle bladder (9), human jejunum (21), and renal proximal tubule (22). Some evidence has also been given (20) that the PD across the apical membrane of the frog retinal epithelium may vary with external HCO_3^- concentration.

Alkali secretion may also be relevant to the problem of the HCO_3^- effect on the tissue. *Necturus* antrum secretes base into (or absorbs protons from) the luminal solution under in vitro conditions. The maximum rate observed was about 20 % of the maximal acid rate found for *Necturus* fundus. The absence of HCO_3^- and CO_2 from the nutrient solution reduces alkali secretion, and anoxia and dinitrophenol inhibit it, showing that metabolism is required, and that the secretion is not due to HCO_3^- diffusion from the serosal solution. Diamox also inhibits this secretion, suggesting a role for carbonic anhydrase in the process. Interestingly, the secretion is not affected by SCN^- at a concentration (20 mM) which almost totally inhibits gastric fundus H^+ secretion (14). The role of this secretion in antral physiology may be to reduce H^+ concentration at the antral cell surface, and hence may act as a protective mechanism.

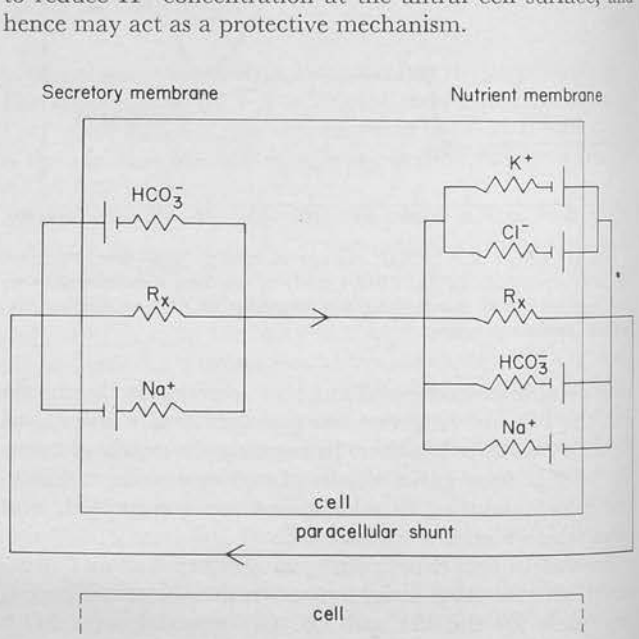

FIG. 14. A representational equivalent circuit for *Necturus* antrum consisting of a K^+, Cl^-, HCO_3^-, and Na^+ conductance in nutrient membrane, and a Na^+ and HCO_3^- conductance in secretory membrane. Orientation of diffusion potentials is based on assumption that cellular ionic concentrations are "usual" and that symmetric solutions (17.8 mM HCO_3^-) bathe tissue. It should be noted that no evidence was presented suggesting electrogenicity of Na^+ pump located on nutrient surface.

Further delineation of antral properties was achieved using microelectrodes, *Necturus* antrum being particularly advantageous due to its large cell size and anatomic simplicity.

Changes of K^+Cl^- concentrations in the nutrient and secretory bathing solutions have quite different effects in this tissue. The effect of a constant product change applied to the nutrient surface is greater than the effect of a secretory change. The PD across both cell membranes changes with a nutrient-side change, but there is little effect of a secretory-side change. The larger change in cell membrane PD as compared to a change in transepithelial PD can be explained by the presence of a higher conductance paracellular pathway of different ion selectivity (18, 19). Changes of $[Na^+]$ produce effects opposite to those with K^+Cl^- in that in this case the secretory surface responds more than the nutrient surface to a change in the $[Na^+]$ in the appropriate bathing solutions.

The concept that Na^+ conductance across the secretory membrane is highly significant is substantiated by the action of amiloride. The presence of this drug on the secretory side results in hyperpolarization of the secretory membrane, due to reduction of Na^+ conductance, and there is also, as expected, a significant increase of the R_S/R_N ratio.

From these data it can be seen that whether amiloride is used to alter the Na^+ conductance of the secretory membrane, or secretory Na^+ concentration is decreased, or Na^+ is removed, the cell membrane resistance ratio R_S/R_N shows a large increase.

Amiloride, however, has no effect on the nutrient surface and this surface also responds differently to a Na^+ decrease in the bathing solution on that side. The Na^+ conductance mechanisms across each cell surface are thus most probably different. Different types of Na^+ conductance have been shown previously in the frog skin (11).

HCO_3^- changes in either solution affect the PD of the tissue or of the cell membranes, and HCO_3^- removal from the nutrient side also increases the ratio R_S/R_N.

From these data it is possible to derive a model for the antral cell. This consists of *a*) a nutrient-side membrane significantly sensitive to K^+ and Cl^- gradients, with constant product change, also containing HCO_3^- and small Na^+ conductances (amiloride insensitive); *b*) a secretory-side membrane relatively permeable to Na^+. This membrane also displays a HCO_3^- conductance, but under in vivo conditions HCO_3^- would be absent from the secretory bathing solutions. The model is illustrated in Fig. 14.

The paracellular pathway is presumably less ion-selective than the cell membranes, and since most of the transepithelial conductance is paracellular (18), this pathway may play an important role in determining the electrical properties of the tissue. Whenever the PD across one of the cell membranes was changed by a change in external ion concentrations (Kg^+Cl^-, Na^+, or HCO_3^-) or by the use of amiloride, there was also a concomitant change of the PD across the other cell membrane. The sign of these *trans* changes were always as postulated (15) for a tissue in which there is a coupling between the surface potentials through a paracellular leak pathway and the *trans* changes are most probably due to changes in the ion current flow across that membrane generated by the change in the *cis* membrane PD. The results thus further support the existence of a paracellular shunt pathway in the antral mucosae.

Since the resistance of the secretory membrane is greater than that of the nutrient membrane, the PD generated by an *IR* drop across this membrane will be greater than that across the nutrient membrane.

Transport by this tissue may be visualized then as being due to the Na^+ conductance of the secretory membrane in series with a Na^+ pump, the ouabain-sensitive Na^+-K^+-ATPase. This pump activity, however, may not contribute significantly to the PD across the nutrient membrane in that ouabain did not have rapid effects on the tissue potential or resistance. However, the Na^+ conductance of the nutrient membrane which is amiloride insensitive might indeed be related to the Na^+ pump mechanism.

This study was supported by National Institutes of Health Grants AM-15878 and CA-13158, and by a Grant-In-Aid from Smith Kline & French Laboratories, Philadelphia, Pa.

G. Flemström was an International Postdoctoral Fellow under National Institutes of Health Grant T-W02083. His present address: Dept. of Physiology and Medical Biophysics, University of Uppsala, S-75123 Uppsala 1, Sweden.

Reprint requests should be sent to G. Sachs.

Received for publication 28 June 1974.

REFERENCES

1. Andersson, S., and C. E. Elwin. Relationship between antral acidity and gastrin releasing potency of chemical stimulants. *Acta Physiol. Scand.* 83: 437–445, 1971.
2. Andersson, S., and M. I. Grossman. Profile of pH, pressure and potential difference at gastroduodenal junction in man. *Gastroenterology* 49: 364–371, 1965.
3. Bently, P. J. A potent inhibitor of sodium transport across the toad bladder. *J. Physiol., London* 195: 317–330, 1968.
4. Berkowitz, J. M., G. Buetow, M. Walden, and M. Praissman. Molecular factors in antral permeation: their proposed role in gastrin release. *Am. J. Physiol.* 221: 259–265, 1971.
5. Dennis, W. H., C. Canosa, and W. S. Rehm. Potential difference across the pyloric antrum. *Am. J. Physiol.* 197: 19–21, 1959.
6. Dyck, W. P., J. L. Werther, J. Rudick, and H. D. Janowitz. Electrolyte movement across canine antral and fundic mucosa. *Gastroenterology* 56: 488–495, 1969.
7. Flemström, G., and G. Sachs. Properties of isolated antral mucosa (Abstract). *Federation Proc.* 33: 208, 1974.
8. Forte, J. G. Three components of Cl^- flux across the isolated bullfrog gastric mucosa. *Am. J. Physiol.* 216: 167–174, 1969.
9. Gonzales, C. F., Y. E. Shamoo, and W. A. Brodsky. The accelerating effect of serosal bicarbonate on sodium transport in short circuited turtle bladder. *Biochim. Biophys. Acta* 193: 403–418, 1969.
10. Hogben, C. Q. M. Active transport of chloride by isolated frog gastric epithelium. Origin of the gastric mucosal potential. *Am. J. Physiol.* 180: 641–649, 1955.
11. Lindeman, B. Electrical excitation of the outer resistive membrane in frog skin epithelium. In: *Electrophysiology of Epithelial Cells*, edited by G. Giebisch. Stuttgart: Schattauer, 1971, p. 53–88.
12. Munck, B. G., and S. G. Schultz. Properties of the passive conductance pathway across in vitro rat jejunum. *J. Membrane Biol.* 16: 163–174, 1974.
13. Noyes, D. H., and W. S. Rehm. Voltage response of the frog gastric mucosa to direct current. *Am. J. Physiol.* 219: 184–192, 1970.
14. Rehm, W. S. Some aspects of the problem of gastric hydrochloric acid secretion. *Arch. Internal. Med.* 129: 270–278, 1972.
15. Rehm, W. S., J. O'Callaghan, S. S. Sanders, and R. L. Shoemaker. Anomalous response of intercellular potentials to

change in K^+ in presence of Ba^{++} (Abstract). *Physiologist* 16: 431, 1973.

16. SANDERS, S. S., J. O'CALLAGHAN, C. F. BUTLER, AND W. S. REHM. Conductance of submucosal-facing membrane of frog gastric mucosa. *Am. J. Physiol.* 222: 1348–1354, 1972.
17. SHOEMAKER, R. L. *Characteristics of the Necturus in Vitro Gastric Mucosa* (PhD Thesis). Birmingham: Univ. of Alabama, 1967.
18. SPENNEY, J. G., G. FLEMSTRÖM, R. L. SHOEMAKER, AND G. SACHS. The antral "barrier" (Abstract). *Gastroenterology* 66: 681, 1974.
19. SPENNEY, J. G., R. L. SHOEMAKER, AND G. SACHS. Conductance properties of gastric fundic mucosa. *J. Membrane Biol.* 19: 105–128, 1974.
20. STEINBERG, R. H., AND S. MILLER. Aspects of electrolyte transport in frog pigment epithelium. *Exptl. Eye Res.* 16: 335–372, 1973.
21. TURNBERG, L. A., J. S. FORDTRAN, N. W. CARTER, AND F. C. RECTOR. Mechanism of bicarbonate absorption and its relationship to sodium transport in the human jejunum. *J. Clin. Invest.* 49: 548–556, 1970.
22. ULRICH, K. J., H. W. RADTKE, AND G. RUMRICH. The role of bicarbonate and other buffers on isotonic fluid absorption in the proximal convolution of the rat kidney. *Pfluegers Arch.* 330: 149–161, 1971.

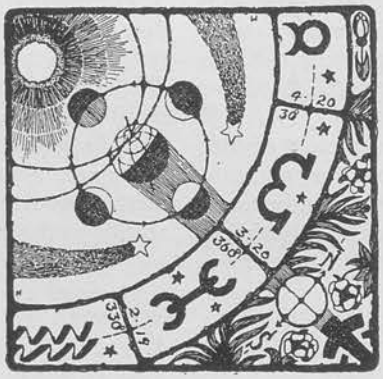

Quantitation of Conductance Pathways in Antral Gastric Mucosa

J. G. SPENNEY, G. FLEMSTROM, R. L. SHOEMAKER, and G. SACHS

From the V. A. Hospital, Birmingham, Alabama 35233 and the University of Alabama in Birmingham, Birmingham, Alabama 35294. Dr. Flemstrom's present address is the University of Uppsala, Uppsala, Sweden.

ABSTRACT The magnitude of cellular and shunt conductance of *Necturus* gastric antral mucosa was studied by (*a*) comparing the cellular PD response to transepithelial PD response during changes of ionic activity in the serosal bathing solution and (*b*) by measurement of current spread within the epithelial sheet. Using constant product KCl changes cellular resistance was 6,788 Ωcm^2 and shunt resistance was 1,803 Ωcm^2. Deletion of HCO_3^- from the serosal solution produced similar but quantitatively smaller changes in PD. Using HCO_3^- deletion cellular resistance was 7,338 Ωcm^2 and shunt resistance was 1,973 Ωcm^2. Measurement of current spread within the mucosa avoids changing ionic gradients yet gave very similar results; cellular resistance was 8,967 Ωcm^2 and shunt resistance was 2,947 Ωcm^2. The shunt contribution to transepithelial conductance ranged from 75.2 to 79.0%. Shunt selectivity was assessed using KCl dilution potentials, where mucosal dilution gave a small change in tissue PD compatible with an anion/cation selectivity ratio of 1.16 across the shunt, whereas serosal dilution effect was dominated by a PD change across the serosal membrane of the cell.

The magnitude of the cellular and transepithelial shunt conductance of a variety of epithelia has been quantitated. The proximal tubule (Windhager et al., 1966; Hoshi and Sakai, 1967), gall bladder (Diamond et al., 1971; Frömter, 1972), and intestine (Clarkson, 1967; Frizzell and Schultz, 1972) can be classified as "leaky" tissues with the cell:shunt conductance ratio being 1:10–20. These epithelia demonstrate low transepithelial potential difference (PD), symmetry of PD response to changes in ionic activity, low transepithelial resistance, and failure to support large concentration gradients. In contrast, frog skin, toad bladder, and fundic gastric mucosa develop large concentration gradients, have a high PD, high transepithelial resistance, and have an asymmetric response to changes in ionic activity. These epithelia have cell to shunt conductance ratios >1 (Mandel and Curran, 1972; Reuss and Finn, 1974; Spenney et al., 1974).

Necturus antrum develops only a low PD dependent on mucosal to serosal Na^+ transport, but has a relatively high resistance (Flemstrom and Sachs, 1974). Therefore quantitation of antral cellular and shunt conductance is of particular interest since antral mucosa is directly exposed to the large (10^6) proton gradients generated by the adjacent fundic mucosa, a "tight" epithelium. We have quantitated these pathways using two techniques: (*a*) The cellular PD response is compared to transepithelial PD response after either a 10-fold constant product change in KCl or a change in $[HCO_3^-]$ in the serosal solution. (*b*) Analysis of current spread within the epithelium using a two-microelectrode technique.

EXPERIMENTAL METHODS

Adult *Necturus* were kept in an aquarium and fed minnows. Animals were killed by severing the spinal cord in the neck. The abdomen was quickly opened and the stomach removed and opened and placed in amphibian Ringer's solution bubbled with 95% O_2–5% CO_2 at 23°C. The muscularis was stripped from the mucosa which was then stretched and mounted (mucosal surface upward) between two Lucite half chambers; the upper half had an open top to allow use of microelectrodes. The chambers were filled with mucosal and serosal solution (Table I) which were circulated from external reservoirs at 23°C by using 95% O_2–5% CO_2 as an airlift system. Alternately the mucosa was perfused (15 ml/min) from Marriot bottles bubbled with 95% O_2–5% CO_2. Fig. 1 shows the electrical arrangement for two microelectrodes. In the single-microelectrode experiments the current-sending electrode, manipulator, current source, and recording connections were deleted from

TABLE I

COMPOSITION OF SOLUTIONS

	Constant product KCl experiments			HCO_3 experiments		
	Serosal control	ΔKCl	Mucosal control	Serosal control	HCO_3^- deletion	Mucosal control
	mM	*mM*	*mM*	*mM*	*mM*	*mM*
Na^+	91	46	91	102.4	102.4	102.4
K^+	5	50	5	4.0	4.0	4.0
Cl^-	80	8	80	91.4	91.4	91.4
$SO_4^=$		36	8	0.8	7.2	10.1
Mg^{++}	1.0	1.0	—	0.8	0.8	0.8
Ca^{++}	1.5	1.5	—	1.8	1.8	1.8
HCO_3^-	20	20	0	17.8	—	—
$H_2PO_4^-$	1.0	1.0	—	0.8	0.8	—
HEPES	—	—	—	—	5.0	—
Glucose	5	5	5	2.0	2.0	—
Sucrose	—	36	15.5	—	—	—
Mannitol	—	—	—	—	6.4	11.3

Composition of solutions (mM) used in the constant product KCl and $\Delta(HCO_3^-)$ experiments. Composition of solutions used for determination of dilution potential is given in Table V.

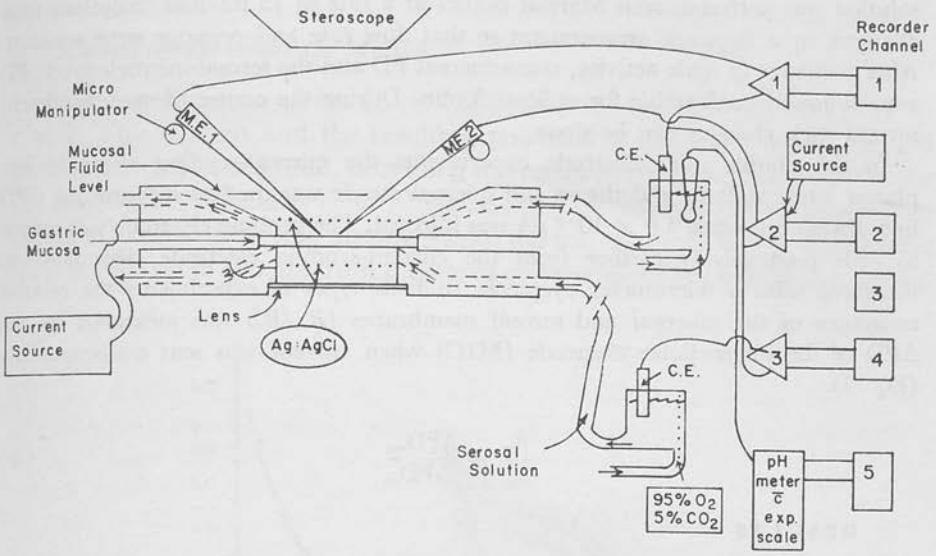

FIGURE 1. The design of the microelectrode chamber and electrical connections used in the dual microelectrode experiments. ME1 is used as the probing electrode while ME2 is used for current injection. Bathing solutions are circulated from external reservoirs; orifices at the edge of the chamber jet circulating fluid across the mucosal and serosal surfaces.

the circuit. Either the mucosal or serosal solution can be used as reference; we usually referenced the serosal solution.

Tissue resistance and the ratio of mucosal:serosal membrane resistance (R_m/R_s) were measured by sending 10 μA/cm^2 through Ag-AgCl wires mounted around the edge of the chamber. The transepithelial PD was measured by a pair of saturated KCl-calomel electrodes (Radiometer K 4112, Radiometer, Copenhagen, Denmark) while the PD across the serosal cell membrane was measured between an intracellular electrode and one of the calomel electrodes. All resistances were corrected for the resistance of solutions. Current sending through the microelectrode or transepithelially was limited to less than 100 ms to minimize polarization effects.

Microelectrodes were prepared using a commercially available two-stage micropipette puller and microforge. Microelectrodes were examined under a microscope, filled with methanol in a vacuum, transferred to distilled water, and subsequently filled with 3 M KCl by diffusion during storage in 3 M KCl at 4°C for 24 h before use. Microelectrodes prepared in this manner were used within 72 h when the tip potential was less than 5 mV and the tip resistance was 5–40 MΩ.

CONDUCT OF EXPERIMENTS

The tissue mounted in the microelectrode chamber was bathed initially in mucosal solution and serosal solution (Table I). In the two-microelectrode experiments these solutions alone were used. In experiments with changes of ionic activity, the serosal

solution was perfused from Marriot bottles at a rate of 15 ml/min. Solutions were changed by a stopcock arrangement so that flow rate and pressure were constant. After a change in ionic activity, transmucosal PD and the serosal-microelectrode PD were followed until stable for at least 3 min. During the course of one experiment several such changes can be done.

In the double microelectrode experiments the current-sending electrode was placed intracellularly and the second microelectrode was used to measure the ΔPD in a distant cell when 5.9×10^{-9} μA was injected. The probing electrode was moved to cells progressively further from the current-sending electrode. Distance was measured with a micrometer eyepiece. In both types of experiments the relative resistance of the mucosal and serosal membranes (R_m/R_s) was measured by the ΔPD of the intracellular electrode (MIC) when current was sent transmucosally (Eq. 1).

$$\frac{R_m}{R_s} = \frac{\Delta PD_{mc}}{\Delta PD_{sc}}. \tag{1}$$

RESULTS

Intracellular PD

Micropuncture of antral epithelial cells was considered good if (*a*) there was a rapid negative change of PD which (*b*) was stable for at least 20 s and (*c*) the PD returned to the base line upon withdrawal of the microelectrode, (*d*) there was no change in tip resistance during or after the puncture. Fig. 2 displays the results of micropuncture of 85 cells in seven different *Necturus* antra. The PD across the serosal membrane was −41.2 ± 7.13 mV (cell-solution) and the PD across the mucosal membrane was −34.6 ± 7.43 mV (cell-solution). The mean transmucosal PD (mucosal-serosal) in these experiments was −6.6 mV.

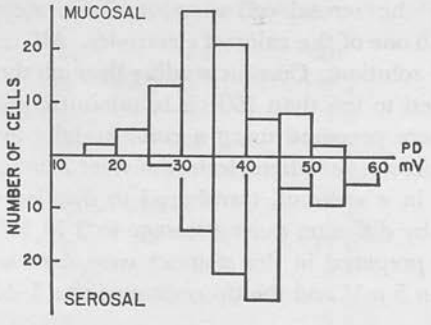

FIGURE 2. The frequency distribution of intracellular PD's is shown. The upper half of the figure shows the cell-mucosal PD while the lower half shows the cell-serosal PD. In this group of 85 micropunctures the mean transepithelial PD was −6.6 mV (mucosal-serosal).

Current Spread within the Mucosa

In these experiments current ($I_o = 5.9 \times 10^{-9}$ A) was injected into a cell at $r = 0$. This current and the resulting potential is dissipated across the cell membrane of that cell, and, providing intercellular coupling exists, across the cell membranes of nearby cells. A second microelectrode was used to measure the ΔPD in cells at varying distances from the cell of injection. Fig. 3 shows the ΔPD in cells up to 500 μm from the site of current injection; electrical coupling

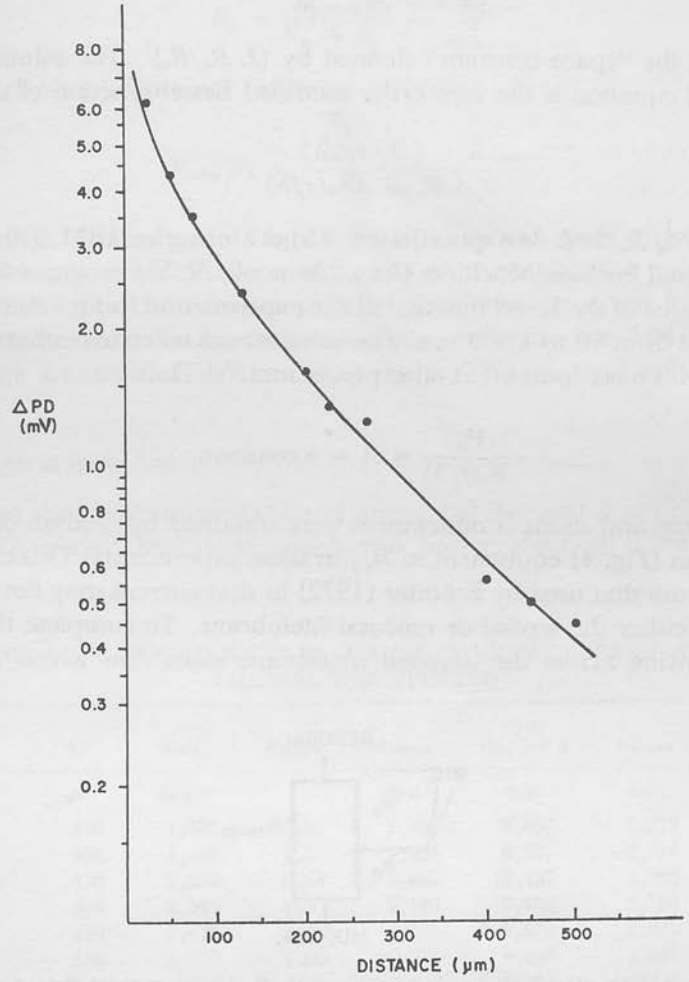

FIGURE 3. The PD is recorded in cells 25–500 μm from the cell at $r = 0$ into which 5.9×10^{-9} A was injected. The curve drawn is the Bessel function $V_r = AK_o(r/\lambda)$ generated from the experimentally derived parameters A and λ.

between cells of *Necturus* antral epithelium is indicated. Coupling was radial inasmuch as very similar ΔPD's were recorded around a circle of any given radium from the cell of injection.

To further analyze the data we used the methods developed by Frömter (1972) for the gall bladder. In this model the mucosa is visualized as a flat sheet of thickness L which is limited by membranes with resistivity, R_z. The resistivity to spread of current within the sheet is R_c. The spread of current is then described by the differential equation:

$$\frac{d^2V}{dr^2} + \frac{1}{r}\frac{dV}{dr} - \frac{1}{\lambda^2}V = 0, \tag{2}$$

where λ is the "space constant" defined by $(L\,R_z/R_c)^{\frac{1}{2}}$. The solution of the differential equation is the zero order modified Bessel function of the second kind:

$$V_r = A\mathrm{K}_0(r/\lambda)$$

where $A = I_o\,R_c/2\pi L$. We quantitated A and λ using an IBM 370 computer (International Business Machines Corp., Armonk, N. Y.) programmed to generate the value of the Bessel function at the experimental r's for values of λ that are iterated from 10 to 1,000 μm. The solution was taken to be that value of λ for which A is most constant at all experimental r's. Thus

$$\frac{V_{(r)}}{\mathrm{K}_0(r/\lambda)} = A = \text{a constant.} \tag{3}$$

Membrane and shunt conductances were obtained by analysis of the electrical circuit (Fig. 4) equivalent to R_z, in these experiments. This circuit was modified from that used by Frömter (1972) in that current may flow from the cell across either the serosal or mucosal membrane. To complete the circuit, current flowing across the mucosal membrane must flow across the trans-

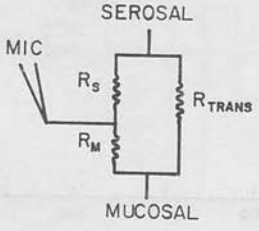

FIGURE 4. An electrical circuit equivalent to R_Z in the current spread experiments. R_S is the resistivity of the serosal cell membranes and R_M is the resistance of mucosal cell membranes. R_{trans} is the transepithelial resistance. MIC represents the microelectrode used to inject current ($I_o = 5.9 \times 10^{-9}$ A).

epithelial resistance to the serosal (reference) side. R_s is the positive solution of the quadratic equation:

$$-(R_m/R_s)R_s^2 + [R_z + (R_m/R_s)R_z - R_{trans}]R_s + R_z R_{trans} = 0, \quad (4)$$

while the mucosal membrane resistance was obtained from the ratio R_m/R_s:

$$R_m = (R_m/R_s)R_s. \quad (5)$$

The shunt resistance was obtained from:

$$R_L = \frac{R_{trans}(R_m + R_s)}{R_m + R_s - R_{trans}}. \quad (6)$$

And the cell/shunt resistance ratio was given by:

$$R_{cell}/R_L = \frac{(R_m + R_s) - R_{trans}}{R_{trans}}. \quad (7)$$

Table II gives the results of six experiments. The mean space constant, λ, was 359 ± 53.3 μm. The cellular component of transepithelial resistance was 8,967 ± 2,017 Ωcm² while transepithelial shunt resistance was 2,947 ± 492 Ωcm². Thus the ratio of cell resistance to shunt resistance was 3.04. In *Necturus* antrum the transepithelial shunt contributes 75% to total epithelial conductance.

Changes in Ionic Activity

To confirm the above quantitation of antral cellular and shunt conductance we chose a second technique which was independent of tissue geometry,

TABLE II

RESULTS OF FIVE EXPERIMENTS IN WHICH CURRENT SPREAD WITHIN THE MUCOSA WAS STUDIED

	λ	R_c/L	R_m/R_s	R_{trans}	$\frac{R_{cell}}{(R_m + R_s)}$	R_{shunt}	$R_{cell}R_{shunt}$
	μm	KΩcm⁻²		Ωcm²	Ωcm²	Ωcm²	
	410	1,576	0.66	1,951	8,650	2,519	3.43
	400	1,193	1.5	1,951	6,937	2,714	2.56
	410	2,236	0.65	2,887	12,157	3,786	3.21
	316	2,545	1.5	2,149	9,423	2,784	3.38
	310	2,428	1.0	2,121	7,672	2,931	2.62
$\bar{X}$±SD	359	1,995	1.06	2,211	8,967	2,947	3.04
	±53.3	±584.5	±0.42	±388.6	±2,017	±492.0	±0.42

Methods of determination of R_{trans} and R_m/R_s are given in the text and calculation of R_m, R_s, and R_{shunt} used Eqs. 5, 4, and 6, respectivelv.

and depended on a different set of assumptions for quantitative analysis. In this way agreement between the two techniques substantiated the assumptions inherent in each analytical model.

Changing the $[K^+]$ and $[Cl^-]$ in the serosal bathing fluid caused a change in both the transepithelial PD, $\Delta\psi_{ms}$, and the PD across the serosal, $\Delta\psi_{sc}$, and mucosal membrane, $\Delta\psi_{mc}$. Table I gives the solutions used and Fig. 5 shows the change in transepithelial PD, $\Delta\psi_{ms}$, and the change across the serosal membrane, $\Delta\psi_{sc}$, in a typical experiment. Table III gives the results of four mucosae subjected to a constant product KCl[1] change in the serosal bathing fluid. In these experiments the $\Delta\psi_{ms}$ was 9.20 ± 0.89 mV and $\Delta\psi_{sc}$ was 28.9 ± 3.00 mV.

The mean transepithelial resistance was 1,424 Ωcm^2 and did not change during the experiments. The resistance of the serosal and mucosal membrane was monitored by the ratio R_m/R_s which was 1.32 ± 0.60 before and 2.02 ± 0.77 during the constant product change and returned to 1.39 ± 0.60 on replacing the original solutions. The return of the ratio as well as ψ_{sc}, indicates that there was satisfactory stability of the midpuncture within the time periods used.

To further analyze these data we used an electrical circuit (Fig. 6) equivalent to *Necturus* antral mucosa, composed largely of one cell type. This cell was given a lumped emf on the serosal (E_s) and mucosal (E_m) membrane. The resistances of the serosal and mucosal membranes were R_s and R_m, respectively. A transepithelial shunt was given a resistance R_L and an emf (E_L). Rose and Schultz (1971) used a similar circuit to examine the PD response of intestinal epithelial cells to transport of sugars and amino acids across the mucosal membrane. We included their shunt resistance at the serosal and mucosal membranes in the lumped emf and resistance of those membranes. The emf's are absolute values and in a particular solution the sign as well as magnitude must be inserted.

According to this model the transepithelial PD (ψ_{ms}) is:

$$\psi_{ms} = \frac{R_L(E_s + E_m) + E_L(R_s + R_m)}{R_s + R_m + R_L}, \tag{8}$$

and the PD (ψ_{sc}) across the serosal cell membrane is given by:

$$\psi_{sc} = \frac{E_s(R_m + R_L) + R_s(E_m + E_L)}{R_s + R_m + R_L}. \tag{9}$$

In these experiments we assumed that the ΔPD resulted from a change in emf

[1] In these experiments a constant product KCl change means a change in $[K^+]$ and $[Cl^-]$ such that the product $[K^+] \times [Cl^-] = 400\ mM^2$ at all times.

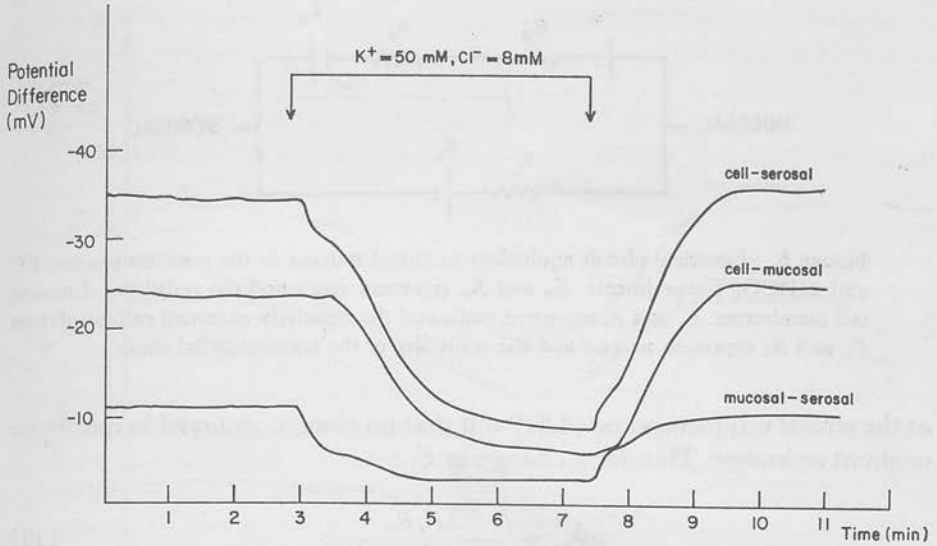

FIGURE 5. ψ_{sc}, ψ_{mc}, ψ_{ms} were recorded during a constant product KCl change in the serosal solution. Large changes in ψ_{sc} and ψ_{ms} are recorded while ψ_{ms} changes much less. Analysis of these changes is given in the text.

TABLE III

RESULTS OF CONSTANT PRODUCT KCl CHANGES IN FOUR MUCOSAE

	ψ_{sc}		$-\psi_{ms}$			R_m/R_s		
	$K^+ = 5$	$\Delta\psi_{sc}$	$K^+ = 5$	$\Delta\psi_{ms}$	$\Delta\psi_{sc}/\Delta\psi_{ms}$	$K^+ = 5$	$K^+ = 50$	R_{trans}
	mV		*mV*					Ωcm^2
	62.2±3.5	32.2	14.9	10.3	3.21	1.41	2.14	1,538
		3.7	2.4	0.6	0.39	0.73	0.96	38
	48.0±4.4	29.7	9.1	8.7	3.41	1.88	1.90	1,869
		2.7	0.7	0.5	0.41	0.81	0.85	68
	34.1±1.9	25.1	8.9	8.3	2.97	1.52	2.94	850
		2.2	2.5	2.0	0.27	0.33	0.97	16
	33.0±11.0	28.4	9.3	9.5	2.98	0.47	1.08	1,438
		1.5	2.9	0.6	0.24	0.53	1.18	23
Mean ±SD		28.9		9.2	3.14	1.32	2.02	1,424
		3.0		0.89	0.21	0.60	0.77	25

In one column, the intracellular and transmucosal potentials before the constant product KCl change are given and then the change in PD after the change is in the adjacent column. After the changes the potential returns to its control value. Further analysis of $\Delta\psi_{sc}/\Delta\psi_{ms}$ is given in the text.

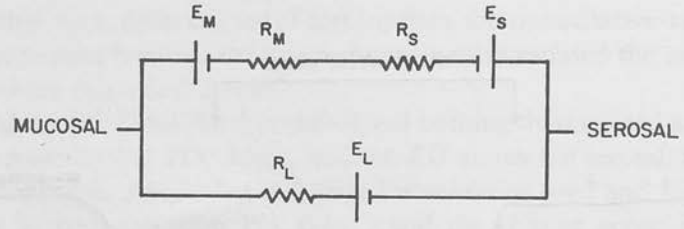

FIGURE 6. Electrical circuit equivalent to antral mucosa in the constant product KCl and $\Delta[HCO_3^-]$ experiments. E_m and R_m represent emf's and the resistivity of mucosal cell membranes. E_s and R_s represent emf's and the resistivity of serosal cell membranes. E_L and R_L represent an emf and the resistivity of the transepithelial shunt.

at the serosal cell membrane (ΔE_s) and that no change occurred in membrane or shunt resistance. Thus for a change in E_s :

$$\Delta\psi_{ms} = \frac{\Delta E_s R_L}{R_s + R_m + R_L}. \quad (10)$$

$$\Delta\psi_{sc} = \frac{\Delta E_s(R_m + R_L)}{R_s + R_m + R_L}. \quad (11)$$

$$\Delta\psi_{sc}/\Delta\psi_{ms} = 1 + R_m/R_L. \quad (12)$$

From Table III the ratio $\Delta\psi_{sc}/\Delta\psi_{ms} = 3.14$; hence $R_m/R_L = 2.14$. From this relationship and $R_m/R_s = 1.32$ (Table III), the serosal and mucosal membrane resistances and the transepithelial shunt resistance can be obtained by substitution into

$$R_{trans} = \frac{(R_m + R_s)R_L}{R_m + R_s + R_L}. \quad (13)$$

The transepithelial shunt resistance was 1,803 Ωcm^2 while the serosal and mucosal membrane resistances were 2,931 and 3,857 Ωcm^2, respectively. Thus the cellular resistance was 6,788 Ωcm^2 and the cell/shunt resistance ratio was 3.77.

Identical experiments were also performed using deletion of HCO_3^- from the serosal bathing solution; thus the $\Delta(HCO_3^-)$ was 17.8 mM. Fig. 7 shows typical PD changes which were recorded and Table IV gives the results of five experiments. The mean $\Delta\psi_{sc}$ was 12.9 ± 6.6 mV while the mean $\Delta\psi_{ms}$ was 3.9 ± 2.1 mV. The ratio $\Delta\psi_{sc}/\Delta\psi_{ms}$ was 3.31 ± 0.18 which was very close to that recorded using the constant product KCl changes. With the exception of the first experiment the potentials returned to basal level when HCO_3^- was returned to the serosal solution. The transmucosal resistance did not change significantly during the course of the ion changes.

Applying the same equations to this perturbation gave a ratio R_m/R_L =

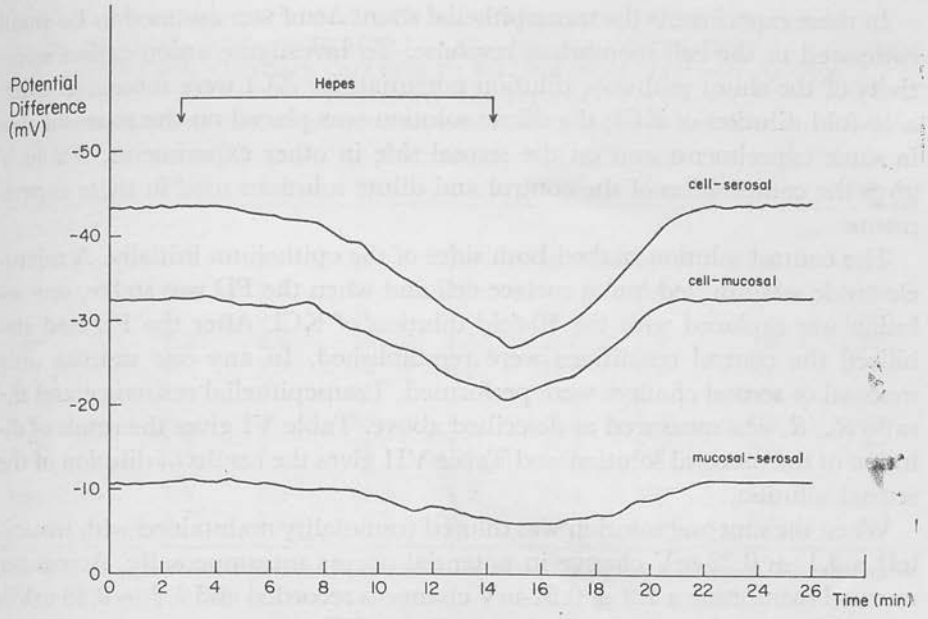

FIGURE 7. ψ_{sc}, ψ_{ms}, and ψ_{mc} were recorded when HCO_3^- was deleted from the serosal solution (originally 17.8 mM). Changes recorded were similar to changes shown in Fig. 6. ψ_{sc}/ψ_{ms} was 3.31.

TABLE IV

RESULTS OF HCO_3^- DELETION IN FIVE *NECTURUS* ANTRA

	ψ_{sc}		$-\psi_{ms}$			R_m/R_s		
	HCO_3^-	$\Delta\psi_{sc}$	HCO_3^-	$\Delta\psi_{ms}$	$\Delta\psi_{sc}/\Delta\psi_{ms}$	HCO_3^-	HEPES $SO_4^=$	R_{trans}
	mV		*mV*					Ωcm^2
	37	22.2	9	7	3.21	1.79	1.08	861
	44	17	11	5	3.40	1.04	0.55	1,014
	36	6.5	24	2	3.25	1.31	0.91	1,867
	40	9.5	10	3	3.17	1.18	0.79	2,200
	30	9	2	2.5	3.60	3.04	2.85	1,830
Mean ±SD	37.4	12.9	11.2	3.9	3.31	1.65	1.23	1,554
	5.2	6.6	8.0	2.1	0.18	0.83	0.92	584

Intracellular and transmucosal potentials are given for the period before HCO_3^- deletion and the change in PD after HCO_3^- deletion is in the adjacent column. R_{trans} does not change. Further analysis of $\Delta\psi_{sc}/\Delta\psi_{ms}$ is given in the text.

2.31. Mucosal membrane resistance was 4,558 Ωcm^2 and serosal membrane resistance was 2,780 Ωcm^2. Thus cellular resistance ($R_m + R_s$) was 7,338 Ωcm^2 while transepithelial shunt resistance was 1,973 Ωcm^2. The cell to shunt resistance ratio was 3.71 or the shunt contributed 79% of total epithelial conductance.

In these experiments the transepithelial shunt Δemf was assumed to be small compared to the cell membrane response. To investigate anion-cation selectivity of the shunt pathway, dilution potentials for KCl were measured using a 10-fold dilution of KCl; the dilute solution was placed on the mucosal side in some experiments and on the serosal side in other experiments. Table V gives the composition of the control and dilute solutions used in these experiments.

The control solution bathed both sides of the epithelium initially. A microelectrode was inserted into a surface cell and when the PD was stable, one solution was replaced with the 10-fold dilution of KCl. After the PD had stabilized the control conditions were reestablished. In any one mucosa only mucosal or serosal changes were performed. Transepithelial resistance and the ratio R_m/R_s was measured as described above. Table VI gives the resuls of dilution of the mucosal solution and Table VII gives the results of dilution of the serosal solution.

When the mucosal solution was diluted (osmolality maintained with mannitol) a 3.1 ± 0.22-mV change in potential occurs transmucosally. Across the mucosal membrane a 1.9 ± 0.52-mV change is recorded and 1.2 ± 0.39 mV is recorded across the serosal membrane (Table VI).

The ratio $\Delta\psi_{mc}/\Delta\psi_{ms}$ is 0.61 which was very different from the ratios obtained with the constant product KCl and (HCO_3^-) changes in the serosal solution. According to equations developed for a ΔE_M

$$\frac{\Delta\psi_{mc}}{\Delta\psi_{ms}} = 1 + \frac{R_s}{R_L}, \tag{14}$$

a value of 0.61 was incompatible with a ΔE_M being the origin of the ΔPD. Solution of the equations for a ΔE_L revealed that:

$$\frac{\Delta\psi_{mc}}{\Delta\psi_{ms}} = \frac{R_m}{R_m + R_s} = \frac{1}{1 + \dfrac{R_s}{R_m}}. \tag{15}$$

TABLE V

COMPOSITION OF SOLUTIONS USED FOR MEASUREMENT OF KCl DILUTION POTENTIAL

	Control solution	10-fold KCl dilution
	mM	*mM*
K^+	95	9.5
Cl^-	80	8.0
Mg^{++}	1.5	1.5
Ca^{++}	1.0	1.0
HCO_3^-	19	19
$H_2PO_4^-$	1.0	1.0
Choline	—	13.5
Mannitol	—	146.5

TABLE VI

TRANSMUCOSAL AND INTRACELLULAR PD IN SYMMETRICAL CONTROL SOLUTION AND THE CHANGE IN PD DURING DILUTION OF THE MUCOSAL SOLUTION

	$-\psi_{ms}$		ψ_{sc}		ψ_{mc}		R_{trans}	
	Control	$\Delta\psi_{ms}$	Control	$\Delta\psi_{sc}$	Control	$\Delta\psi_{mc}$	Control	Dilution
							Ωcm^2	
	7	3	27	2	20	1	1,400	2,150
	6	3.5	30	1	24	2.5	1,525	2,250
	8	3	31	1	23	2	650	1,050
	7.5	2.8	30	1.5	22.5	1.3	700	1,200
	7	3.3	32	0.8	25	2.5	700	1,250
	7	3	26	1	19	2	850	1,250
	8	3	26	1	18	2.0	850	1,250
	8.5	3	26	1	17.5	2.0	900	1,325
Mean ±SD	7.4	3.1	28.5	1.2	21.1	1.9	946	1,465
	0.79	0.22	2.5	0.39	2.9	0.52	332	461

Changes in R_{trans} are recorded in the two columns at the right. Return to control conditions reestablishes the prior PD.

TABLE VII

TRANSMUCOSAL AND INTRACELLULAR PD IN SYMMETRICAL CONTROL SOLUTIONS, AND THE CHANGE IN PD DURING DILUTION OF THE SEROSAL SOLUTION

	$-\psi_{ms}$		ψ_{sc}		ψ_{mc}		R_{trans}	
	Control	$\Delta\psi_{ms}$	Control	$\Delta\psi_{ms}$	Control	$\Delta\psi_{ms}$	Control	Dilution
	mV		mV		mV		Ωcm^2	
	4	4	23	12	19	8.0	1,350	1,900
	4	4	23	10	19	6	1,450	1,850
	3	4	30	10	27	6	1,500	1,900
	5	5	32	10.5	27	5.5	1,300	1,725
Mean ±SD	4	4.3	27.0	10.6	23.0	6.4	1,400	1,844
	0.8	0.5	4.7	0.95	4.6	1.1	91.3	82.6

Return to control conditions reestablishes prior PD. Changes in R_{trans} are recorded in the two columns at the right.

$$\frac{\Delta\psi_{sc}}{\Delta\psi_{ms}} = \frac{R_s}{R_m + R_s}. \tag{16}$$

$$\frac{\Delta\psi_{mc}}{\Delta\psi_{sc}} = \frac{R_m}{R_s}. \tag{17}$$

Thus the ratio $\Delta\psi_{mc}/\Delta\psi_{sc}$ should be very close to the voltage divider ratio, R_m/R_s . $\Delta\psi_{mc}/\Delta\psi_{sc}$ was 1.58 and the ratio R_m/R_s in these experiments was 1.55.

Upon dilution of the serosal solution very different results were obtained

(Table VII). In this case the transepithelial ΔPD was 4.3 ± 0.5 mV while the ΔPD across the serosal cell membrane was 10.6 mV. The ratio $\Delta\psi_{sc}/\Delta\psi_{ms}$ was 2.44 which is somewhat less than the same ratio obtained with constant product KCl (3.14) or $\Delta(HCO_3^-)$ (3.31). The ratio $\Delta\psi_{mc}/\Delta\psi_{sc}$ was 0.60 which was very different from the voltage divider ratio 1.55 and likewise $\Delta\psi_{sc}/\Delta\psi_{ms}$ is very different from $R_s/(R_m + R_s)$ and was not compatible with a ΔPD caused solely by a ΔE_L.

DISCUSSION

The gastric antrum has not received the interest that has been focused on the gastric fundus. Recently the electrophysiologic properties of *Necturus* gastric antrum have been studied by Flemstrom and Sachs (1974). They found that *Necturus* antrum developed a small potential difference, 4–10 mV lumen negative. In symmetrical solutions the short circuit current could be attributed to a mucosal to serosal Na^+ flux. Ouabain abolished PD when added to the serosal solution; amiloride, in the mucosal solution abolished the PD in the absence of a HCO_3^- gradient. The effect of amiloride was reversible.

Previously the PD of antrum has been studied in vivo in humans (Andersson and Grossman, 1965) and dogs (Dennis et al., 1959). Dyke et al. (1969) used H^+, Na^+, K^+, and H_2O flux into fundic or antral pouches to assess permeability. In those experiments where surface area was measured Na^+ and H^+ flux was 7–15 times greater in antral pouches than in fundic pouches. Himal et al. (1970) found that Na^+ and H^+ flux was less in canine antral than in duodenal mucosa by a ratio of ½ to ⅓. No in vitro studies have attempted quantitation of the cellular and transepithelial shunt conductance in antral mucosa.

In this study we have quantitated the cellular and transepithelial shunt resistance in antral mucosa by two different techniques. Table VIII summarizes the results obtained by each technique.

In these experiments the mean cellular resistance was 7,697 Ωcm², while the

TABLE VIII

SUMMARY OF RESULTS OF THE THREE TYPES OF EXPERIMENTS USED TO QUANTITATE CELLULAR AND TRANSEPITHELIAL SHUNT RESISTANCE

	Trans resistance	Cellular resistance	Shunt resistance	Shunt contribution to epithelial conductance
	Ωcm²	Ωcm²	Ωcm²	%
Constant product KCl	1,424	6,788	1,803	79.0
$\Delta[HCO_3^-]$	1,554	7,338	1,973	78.8
Current spread	2,211	8,967	2,947	75.2
Mean	1,730	7,697	2,241	77.7

Note the very close agreement of percent contribution of the shunt in the three types of experiments.

mean shunt resistance was 2,241 Ωcm^2. The mean cell/shunt resistance ratio was 3.43. The cellular pathway accounted for 22.3% and the shunt pathway accounted for 77.7% of tissue conductance. The mean transepithelial resistance was 1,730 Ωcm^2.

Not only is the magnitude of the shunt conductance important, but so is the selectivity. This can be deduced from the KCl and HCO_3^- experiments or can be measured directly using dilution potentials. In the case of KCl dilution under our conditions, the maximum potential which should develop due to differing mobilities of K^+ and Cl^- is less than 1 mV. We have also argued that the shunt should be symmetric, i.e. an equal potential should be obtained regardless of which side is diluted, and the obtained selectivities should be the same.

In the case of mucosal dilution of KCl, there was a 3.1 $\pm$ 0.22 mV increase in transepithelial potential. This per se is not sufficient evidence that the shunt was the source of the ΔPD. However, Eq. 15 predicts that the $\Delta\psi_{mc}/\Delta\psi_{sc}$ will be in the ratio of R_m/R_s if current flow is altered by a change in shunt emf. Since this in fact happened (Table VI) it is legitimate to conclude that the shunt selectivity for Cl^- over K^+ was 1.16, i.e. the shunt is weakly anion selective.

Serosal dilution of KCl gave a PD change of 4.3 $\pm$ 0.5 mV (Table VII). But since $\Delta\psi_{sc}/\Delta\psi_{ms} = 2.47$ and the predicted ratio R_s/R_m was 0.65, this change was largely due to a change in cell potential, in contrast to what is obtained with mucosal dilution. These considerations demonstrate that it is important to determine the suitability of a given ion for dilution potential assessment of shunt selectivity.

The constant product KCl experiments or the ΔHCO_3^- experiments also allow assessment of the change in shunt emf under these conditions (ΔE_L). Thus if the ΔPD arises only from ΔE_L, from Eqs. 2 and 3 we have

$$\Delta\psi_{sc}/\Delta\psi_{ms} = \frac{R_s}{R_m + R_s} = \frac{1}{R_m/R_s + 1},$$

and for the ΔKCl the predicted value was 0.43, the value obtained was 3.14, and for ΔHCO_3^- the predicted value was 0.38 and the value obtained was 3.31; hence ΔE_L was small as would be predicted from the dilution potentials.

If the change in potential is due to both a ΔE_s and a ΔE_L then again from Eqs. 2 and 3 we have

$$\Delta\psi_{sc}/\Delta\psi_{ms} = \frac{\Delta E_s(R_m + R_L) + \Delta E_L R_s}{\Delta E_s R_L + \Delta E_L(R_s + R_m)},$$

and using either the mean resistance from all experiments or the resistance from the current spread experiments, it is possible to calculate ΔE_L, deriving ΔE_s from $\Delta\psi_{sc} + \Delta IR_s$. Table IX shows that in the case of the KCl experi-

TABLE IX

SUMMARY OF CALCULATED VALUES FOR *IR* DROPS AND ΔE_s ENABLING CALCULATION OF THE MAGNITUDE OF ΔE_L

Experiment	ΔIR_m	ΔIR_s	ΔE_s	$\Delta E_L{}^1$	$\Delta E_L{}^2$
	mV	*mV*	*mV*	*mV*	*mV*
Constant Product KCl	19.7	14.9	43.8	−0.81	−3.1
$\Delta(HCO_3^-)$	9.0	5.45	18.4	−0.64	−1.58

$\Delta E_L{}^1$ is the value calculated using the mean resistance values for all experiments. $\Delta E_L{}^2$ is the value calculated using resistance values from only the current spread experiments since those experiments are not dependent on ionic gradients.

ment the ΔE_L was only 7.1% of ΔE_s, and in the case of the ΔHCO_3^- experiment 8.6% of ΔE_s. Hence all three approaches signify a low shunt selectivity in *Necturus* gastric antrum, both with respect to intracationic selectivity (Na^+ versus K^+) and anion-cation selectivity (K^+ versus Cl^-) data which are in contrast with for example gall bladder (Diamond, 1971) where there is considerable anion-cation discrimination, or small intestine (Frizzell and Schultz, 1972).

Flemstrom and Sachs (1971) demonstrated that the serosal membrane conductance was largely due to K^+ or Cl^- conductance, which explains the asymmetry of the dilution potentials. Since dilution of the serosal solution results in a $\Delta\psi_{sc}$ of 10.6 mV with the cell interior becoming more negative, the K^+ conductance of the serosal membrane is greater than that for Cl^-.

The two techniques used for evaluation of the shunt conductance depend on quite different assumptions. The current spread technique requires a flat epithelial sheet of uniform cell type for analysis. This is approximately true for *Necturus* antrum, in contrast to *Necturus* fundus. From R_c/L, we can calculate R_c to be 59.9 Ω/cm which approximates the resistance of the intracellular fluid hence coupling in the antrum is comparable to coupling in several other epithelia such as gall bladder (Frömter, 1972).

The use of ionic changes also rests on several explicit assumptions. The assumption of low shunt selectivity compared to membrane selectivity has been dealt with above. It is also assumed that the changes in emf occur only across one membrane. This follows in the antrum from consideration of the ΔI_{sc} in the ΔKCl and ΔHCO_3^- experiments which is 6.46 and 2.51 μA, respectively. This allows prediction of the $\Delta\psi_{mc}$ due to current flow alone, being 24.9 and 11.4 mV in the two cases, which compare well to the measured values of 19.7 and 9.0 mV. Finally, constancy of resistance parameters is assumed in utilizing the equations developed. Transmucosal resistance did not change during the experiments, whereas membrane resistance ratio R_m/R_s increased by 53% ($t = 2.43$, $P < 0.05$) during the KCl change and fell by 25% ($t = 5.19$, $P < 0.005$) during HCO_3^- deletion. However, there is close agreement between the two

ionic change conditions, and between those and the current spread technique (Table VIII).

We can therefore conclude that in antral mucosa cellular conductance contributes 22.3% of tissue conductance whereas in fundic mucosa cellular conductance accounts for at least 80% of tissue conductance. Antral conductance is relatively anion selective at neutral pH, and progressively becomes more anion selective with fall in pH (Bajaj and Sachs, unpublished). The antrum is exposed to the same proton gradient as the fundus, with a shunt conductance about four times greater than the fundus. The physiologic significance of this finding is not established; it may be of importance in control of gastrin release by antral "G" cells (Berkowitz et al., 1971; Andersson and Elwin, 1971). The distribution of shunt conductance however correlates well with the known distribution of ulcer in man.

Credit is given to Projects 8059-01, 02, V. A. Hospital, Birmingham, Ala. and to NIH Grants AM 17315, AM 15878, and CA13158 and to NSF Grant GB31075.
Dr. Flemstrom is a recipient of the NIH Fogarty International Fellowship.

Received for publication 21 September 1974.

REFERENCES

ANDERSSON, S., and C. E. ELWIN. 1971. Relationship between antral acidit and gastrin releasing potency of chemical stimulants. *Acta Physiol. Scand.* **83**:473.

ANDERSSON, S., and M. I. GROSSMAN. 1965. M. I. profile of pH, pressure, and potential difference at gastroduodenal junction in man. *Gastroenterology.* **49**:364.

BERKOWITZ, J. M., G. BUETOW, M. WALDEN, and M. PRAISSMAN. 1971. Molecular factors in antral permeation: their proposed role in gastrin release. *Am. J. Physiol.* **221**:259.

CLARKSON, T. W. 1967. The transport of salt and water across isolated rat ileum. Evidence for at least two distinct pathways. *J. Gen. Physiol.* **50**:695.

DENNIS, W. H., C. CANOSA, and W. C. REHM. 1959. Potential difference across the pyloric antrum. *Am. J. Physiol.* **97**:19.

DIAMOND, J. M., P. H. BARRY, and E. M. WRIGHT. 1971. Route of transepithelial ion permeation in the gall bladder. *In* Electrophysiology of Epithelial Cells G. Giebisch, Editor. Friedrich-Karl Schattauer-Verlag, Stuttgart, Germany.

DYCK, W. P., J. L. WERTHER, and J. RUDICK. 1969. Electrolyte movement across canine antral and fundic mucosa. *Gastroenterology.* **56**:488.

FLEMSTROM, G., and G. SACHS. 1974. Properties of isolated antral mucosa. I. General characteristics. *Am. J. Physiol.* In press.

FRIZZELL, R. A., and S. G. SCHULTZ. 1972. Ionic conductances of extracellular shunt pathway in rabbit ileum. Influence of shunt on transmucosal Na^+ transport and electrical potential differences. *J. Gen. Physiol.* **29**:318.

FRÖMTER, E. 1972. Route of passive ion movement through the epithelium of *Necturus* gall bladder. *J. Membr. Biol.* **8**:259.

HIMAL, H. S., S. B. YOUNG, J. RUDICK, J. L. Werther, and H. D. Janowitz. 1970. Ionic flux across the duodenal mucosa: effects of varying concentrations of acid. *Gastroenterology.* **58**:959.

HOSHI, T., and F. SAKAI. 1967. Comparison of electrical resistance of surface cell membrane and cellular wall in proximal tubule of Newt kidney. *Jap. J. Physiol.* **17**:627.

MANDEL, L. J., and P. F. CURRAN. 1972. Response of frog skin to steady state voltage clamping. I. The shunt pathway. *J. Gen. Physiol.* **59**:503.

REUSS, L., and A. L. FINN. 1974. Passive electrical properties of toad urinary bladder epithelium.

Intercellular electrical coupling and transepithelial cellular and shunt conductances. *J. Gen. Physiol.* **64**:1.

ROSE, RICHARD C., and STANLEY G. SCHULTZ. 1971. Studies on the electrical potential profile across rabbit ileum: the effect of sugars and amino acids on transmural and transmucosal electrical potential differences. *J. Gen. Physiol.* **57**:639.

SPENNEY, J. G., R. L. SHOEMAKER, and G. SACHS. 1974. Microelectrode studies of fundic gastric mucosa: cellular coupling and shunt conductance. *J. Membr. Biol.* **19**:105–128.

WINDHAGER, E. E., E. L. BOULPAEP, and G. GIEBISCH. 1966. Electrophysiological studies on single nephrons. *Proc. Int. Congr. Nephrol.* **1**:35.

GASTROENTEROLOGY 72:72-77, 1977

Vol. 72, No. 1
Printed in U.S.A.

PROPERTIES OF GASTRIC ANTRUM

III. Selectivity and modification of shunt conductance

S. C. BAJAJ, J. G. SPENNEY, AND G. SACHS

Laboratory of Membrane Biology, University of Alabama in Birmingham, Birmingham, Alabama

The permselectivity of the paracellular pathway of amphibian (Necturus and bullfrog) antrum was investigated with respect to intracationic selectivity and the K^+ and Cl^- permeability ratio as a function of mucosal *p*H. The intracationic selectivity sequence was $Rb^+ > K^+ > Cs^+ > Na^+ > Li^+$. Both antra showed weak cationic selectivity at *p*H 7.4, and at *p*H 4.4 for bullfrog and *p*H 3.0 for Necturus, the ratio P_{K^+}/P_{Cl^-} was unity. At lower mucosal *p*H the tissues were anion selective. Treatment of the tissue with a water-soluble carbodiimide enhanced anion selectivity at higher *p*H; carbenoxolone, a weak acid, resulted in maintained cation selectivity at lower *p*H. These data sugest that carboxyl groups play a role in determining shunt selectivity; the increase in anion selectivity below *p*H 2.0 suggests that phosphate or sulfate groups could also be involved.

The mammalian stomach consists of 2 main regions, the fundus and the antrum. The fundus secretes acid and pepsinogen, and the antrum is responsible for the secretion of gastrin. The difficulty of maintaining function in mammalian mucosa, with the exception of the piglet,[2] has made it necessary to study amphibian properties in vitro. Recent studies on the electrical and transport properties of the amphibian antrum have shown that Necturus and bullfrog antrum differ in that although both absorb Na^+ and secrete Cl^- actively, in Necturus Cl^- transport is electrically silent.[3] The antrum of both species is geometrically much simpler in structure than the fundus, consisting essentially of a flat sheet of cells, with few tubules. This has allowed quantitation of the relative importance of the cellular and paracellular resistance. Measurements have shown that about 80% of tissue conductance can be accounted for by the paracellular pathway.[4] Similar estimates for the fundus showed at most 20% of conductance as being due to the paracellular route.[5]

Clinically, most gastric ulcers occur in the antral area, or the fundic-antral junction,[6] hence the properties of the antrum are significant in understanding the pathogenesis of this disease. Although the relative paracellular conductance of antrum was considerably greater than fundus, cell membrane resistance was about the same, therefore, the paracellular path may be of considerable importance in explaining the occurrence of ulcer in this region. This paper describes selectivity properties of this path, and means of modifying the selectivity.

Received April 26, 1976. Accepted July 8, 1976.

A preliminary report of this work has been presented and is published in abstract form.[1]

Address requests for reprints to: G. Sachs, Laboratory of Membrane Biology, University of Alabama, Birmingham, Alabama 35294.

This work was supported by Grants AM15878, AM17315, and CA 16722 from the National Institutes of Health; a grant-in-aid from Smith Kline & French; and Projects 8059-01 and 0.2 from the Veterans Administration.

The authors are grateful to Biorex, Ltd., for donating the carbenoxolone.

Materials and Methods

Necturus or bullfrog antrum was obtained fresh from a decapitated animal and mounted in an Ussing chamber as previously described.[3] Paracellular or shunt selectivity was measured in two ways. Intracationic selectivity was measured by fixing the concentration of the anion and varying the nature of cation (cation substituting for choline) in the mucosal solution, with a constant choline-containing serosal solutions and measuring the change in tissue potential difference. Cation-anion selectivity was measured by the method of dilution potentials with KCl initially on both sides of the tissue in identical solutions, and diluting the mucosal solution 10-fold with respect to KCl only. After each change, normal solution is placed on the mucosal side to ensure that no mucosal damage has occurred. Solution composition is presented in table 1 for each type of experiment.

The cation-anion selectivity ratio was also measured, (1) under varying conditions of *p*H by adjusting the *p*H of the mucosal solution by addition of H_3PO_4; (2) following chemical treatment of the mucosa by 1-ethyl-3-(3-dimethylaminopropyl) carbodiimide (EDCD); (3) following treatment by carbenoxolone (chemical name, 3β-hydroxyl-11-oxoolean-12-en-30-oic acid hydrogen succinate), an antiulcer agent; and (4) neuraminidase treatment.

In any of these techniques it is necessary to show that the potential changes are due to changes in the shunt emf, and not in the cell membrane emf. This was previously confirmed by microelectrode experiments[4] and is detailed in the results. If the antrum is considered to be presented by the simple equivalent circuit of figure 1, then a change in shunt emf will also change the measured membrane potentials, but these changes, $\Delta V_M/\Delta V_S$, will be equal to the voltage divider ratio obtained by sending current transepithelially. A change in membrane

emf will, however, produce changes in membrane potential difference (PD) and the ratio of change between serosal and mucosal membranes will not equal the voltage divider ratio.

Results

The PD across the isolated amphibian antrum bathed in amphibian Ringer's solution ranges from 5 to 15 mv, mucosal side negative, and the tissue resistance from 900 to 1200 ohms cm^2. Cation substitution in the mucosal solution produces changes of PD as a function of the nature of the cation as shown in table 2, giving the selectivity sequence Rb > K > Cs > Na > Li for bullfrog. This sequence is similar to the Eisenman sequence III[7] and different from free solution mobility. This would suggest large diameter pores (about 10 A) with negative charges. The intracationic selectivity of the paracellular path is considerably less than that of the serosal surface.[3]

Flemstrom and Sachs[3] previously found a much larger PD when Na^+ in the mucosal solution was partially replaced with choline. The experimental design was different from that reported here. Flemstrom initially bathed both surfaces with Amphibia Ringer's solution before replacement of ions in the mucosal solution.

TABLE 1. *Composition of solutions*[a]

Solution composition	Cation changes		Solution composition	Dilution changes	
	Serosal	Mucosal		Serosal/ mucosal	Mucosal
Choline Cl	70	Cation[b] Cl 70	KCl	74.0	5.0
$MgCl_2$	5	5	$MgCl_2$	1.5	1.5
$CaCl_2$	1.5	1.5	$CaCl_2$	1.0	1.0
Choline HCO_3	20	20	$KHCO_3$	20.0	3.5
KH_2PO_4	1.0	1.0	KH_2PO_4	1.0	1.0
Glucose	5	5	Glucose	5.0	5
			Mannitol		140
			Choline HCO_3		16.5

[a] The composition of the solutions used in A: the determination of intracationic selectivity by successively substituting alkali metal cation for choline chloride in the mucosal solution. Choline chloride mucosal solution is used to wash the tissue between each substitution. B: the determination of K^+ and Cl^- selectivity of the antrum obtained by a 10-fold KCl dilution in the mucosal solution, all other ions being maintained constant. The *p*H was varied by addition of H_3PO_4. All concentrations are millimolar.

[b] Cation Rb^+, Cs^+, Li^+, Na^+, K^+, choline.

TABLE 2. *Changes of potential difference (PD) (millivolts) with ion substitution*[a]

Cation	PD
Li^+	−0.33 ± 0.08
Na^+	−1.6 ± 0.3
K^+	−2.6 ± 0.43
Rb^+	−3.1 ± 0.56
Cs^+	−2.0 ± 0.44

[a] The intracationic selectivity was measured by substituting alkali metal cation for choline chloride in the mucosal solution. Between each substitution choline chloride mucosal solution was used to wash the mucosal surface of the tissue. The sign of the PD refers to the change in the mucosal solution, i.e., all of these cations were more permeable than choline.

Hence, serosal solution contained a normal complement of ions. In the experiments reported here, choline serosal solution was used and K^+ was only 1 mM. Thus the altered ion composition may account for the differences between our experiments and those of Flemstrom and Sachs, in that the low K^+ used here may reduce the activity of the Na^+K^+ adenosine triphosphatase.

Ten-fold dilution of KCl in the mucosal solutions at *p*H 7.4 produces a transepithelial change of PD due to a cation selectivity of the shunt in both species. Varying the *p*H, as shown in figures 2 and 3 produces a gradual change in shunt selectivity until at *p*H 3 for Necturus and at *p*H 4.4 for bullfrog, the direction of change of PD inverts and subsequently changes of PD correspond to relative anion selectivity. Control experiments in which only *p*H of the mucosal solution was changed caused changes of PD no more than 10% of those observed with KCl diluted at the same *p*H. Transmucosal resistance was 1400 ohms cm^2 in the control solution and increased slightly to 1800 ohms cm^2 during dilution. The resistances were not found to *p*H dependent.

Three means were used to modify shunt selectivity. The carboxyl reagent, EDCD was added at a concentration of 10 mM for 30 min, after a dilution experiment at different *p*H values. The reagent was removed by two washes and the dilution series was repeated at varying *p*H values. This gave the data presented in figure 2, showing that the selectivity, even at *p*H 7.4 was characteristic of anion selectivity after EDCD treatment. This treatment therefore, modified the paracellular pathway toward anion selectivity. It should also be noted that the shape of the two curves is different. In the case of control mucosa there was a sharp transition at *p*H 3, with increasing anion selectivity until *p*H 1.0. In the case of the EDCD-treated mucosa there was only a gradual increase in anion selectivity, with an increase occurring more rapidly beyond *p*H 2.0, at which *p*H the selectivity of control and treated mucosa were about equal. This suggests the presence of a second type of group with a *p*K′ less than 2.0 which is not modified by EDCD treatment.

Addition of carbenoxolone (10 mM) to the mucosal or serosal surface of the tissue after a *p*H selectivity experiment had been performed, followed by a second dilution sequence gave the data shown in figures 3 and 4

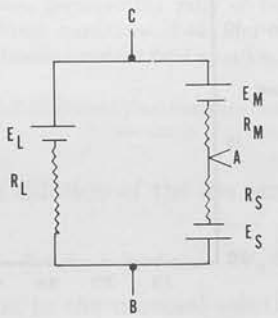

FIG. 1. A simple equivalent circuit of antrum in which E_S, R_S are emf and resistance of serosal membrane, E_M, R_M that of mucosal membrane, and E_L, R_L that of shunt. A change in E_L will be reflected in $\Delta V_{AC}/\Delta V_{AB}$ similar to that produced by external current flow.

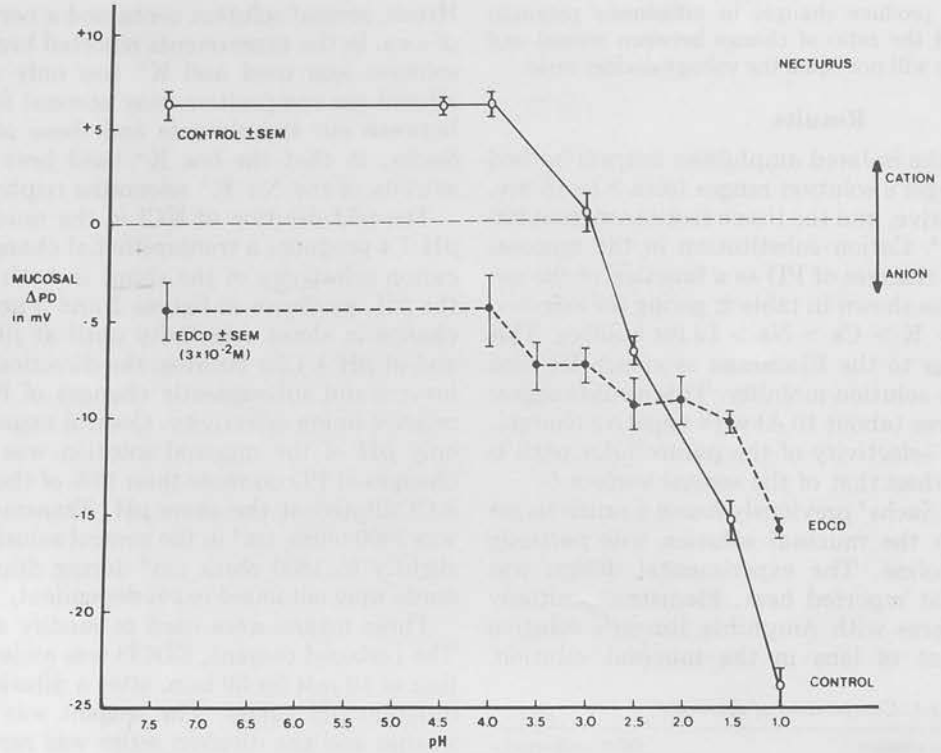

FIG. 2. A plot of the change in potential difference (PD) in response to a 10-fold dilution of KCl in the mucosal solution under control conditions with the mucosal *p*H varying from 7.5 to 1.0 in Necturus antrum (○——○); ●——● shows a similar plot after treatment of the antrum with 1-ethyl-3-(3-dimethylaminopropyl)carbodiimide (*EDCD*). All *points* are means ± SEM of four experiments.

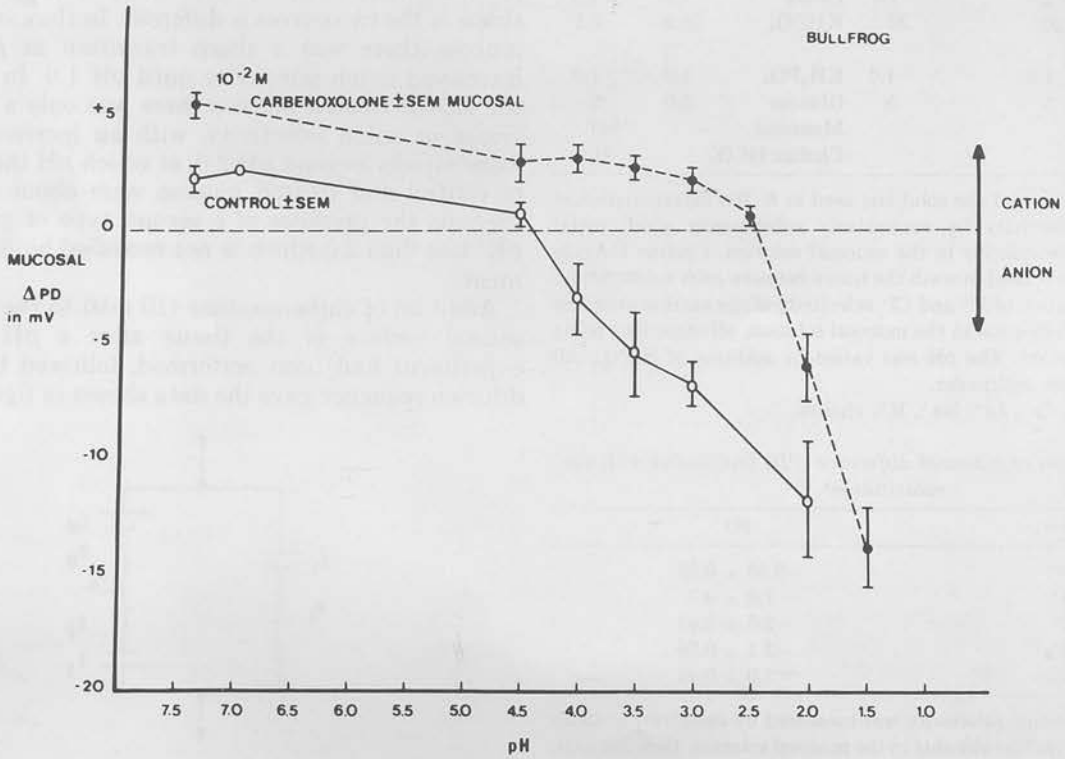

FIG. 3. A Plot of the change in potential difference (PD) in response to a 10-fold dilution if KCl in the mucosal solution of bullfrog antrum in the absence and presence of carbenoxolone in the mucosal solution as a function of mucosal *p*H. All points were the mean ± SEM of

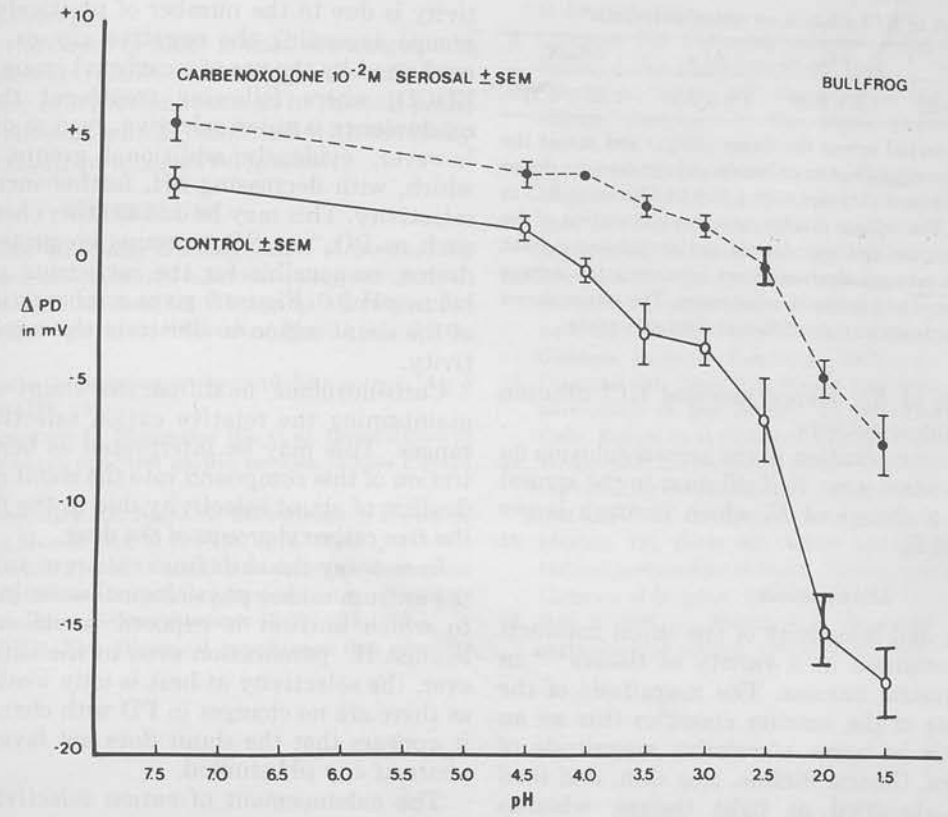

FIG. 4. A plot as in figure 3 in bullfrog antrum of the change in potential difference (PD) in response to a 10-fold KCl mucosal dilution showing the effect of serosal carbenoxolone.

obtained in bullfrog antrum. This showed that cation selectivity was maintained until a mucosal *p*H of 2.5, compared to 4.0 and 4.5 for control, hence this reagent also results in an apparent shift of the *p*K′ of the groups responsible for the cation-anion selectivity ratio, but now enhancing the cation selectivity. This was independent of which surface was treated by the drug.

Incubation of the tissue with 1 mg per ml of neuraminidase (Sigma Chemical Co., St. Louis, Mo.) for 45 min, followed by washing, reduced the cation-anion selectivity ratio at *p*H 7.4 and 4.0 in Necturus, suggesting that carbohydrates may be involved in the shunt pathway.

By substitution in the Goldman constant field equation[8] it is possible to calculate the permeability ratio of K^+ to Cl^- under the above conditions. The results of these calculations are presented in table 3.

It should be noted that a change of *p*H in itself resulted in no change of transepithelial PD under any of the circumstances discussed above.

Justification of shunt analysis. The antral mucosa is composed largely of one cell type and can be represented by the equivalent circuit in figure 1. It can be shown[4] that if dilution of an ion in the mucosal solution changes E_M, i.e., cell membrane emf, then the ratio of

$$\Delta V_M/\Delta V_{MS} = 1 + (R_S/R_L)$$

This must always be a value greater than 1.

TABLE 3. *Cation-anion permeability ratio*[a]

Species and conditions	*p*H	P_K/P_{Cl^-}
Bullfrog		
Control	7.4	1.05
Control	2.0	0.48
Carbenoxolone	7.4	1.34
Carbenoxolone	2.0	0.82
Necturus		
Control	7.4	1.40
Control	2.0	0.48
EDCD	7.4	0.75
EDCD	2.0	0.52

[a] The cation/anion permeability ratio of bullfrog and Necturus antrum under different conditions of *p*H and drug treatment calculated from the Goldmand constant field equation, assuming an activity coefficient of 0.9.

[b] EDCD, 1-ethyl-3-(3-dimethylaminopropyl)carbodiimide.

In contrast if dilution of the ion generates a new E_L then

$$\Delta V_S/\Delta V_{MS} = R_S/(R_M + R_S) \quad \text{and} \quad \Delta V_M/\Delta V_S = R_M/R_S$$

For KCl dilution in the mucosal solution the results of table 4 were obtained.

The ratio $\Delta V_M/\Delta V_S = 1.58$ and the ratio R_M/R_S was 1.55. The ratio $\Delta V_M/\Delta V_{MS} = 0.61$ is incompatible with changing E_M whereas the former ratios are very consist-

TABLE 4. *Effect of KCl dilution on antral potentials*[a]

	ΔV_{MS}	ΔV_S	ΔV_M	$\Delta R_M/R_S$
Mean ± SD	3.1 ± 0.22	1.2 ± 0.39	1.9 ± 0.52	1.55 ± 0.21

[a] The change in potential across the tissue (ΔV_{MS}) and across the serosal (ΔV_S) and mucosal (ΔV_M) membranes determined by direct microelectrode measurement obtained with a 10-fold dilution of KCl in the mucosal solution. The voltage divider ratio was indpendent of the mucosal KCl concentration and was determined by passing current across the tissue from external electrodes and measuring the voltage deflection and the serosal and mucosal membranes. The values shown are the mean of experiments in eight different Necturus antra.

ent with a change of E_L. Hence mucosal KCl dilution effects reflect shunt selectivity.

Changes of ion concentration in the serosal solution do not behave in the same way; KCl dilution in the serosal solution leads to a change of E_S which is much larger than the change of E_L.

Discussion

The magnitude and selectivity of the shunt conductance has been measured in a variety of tissues[5-12] in addition to the gastric mucosa. The magnitude of the shunt conductance of the antrum classifies this an an intermediate tissue in terms of relative magnitude of shunt conductance. Gastric fundus, frog skin, and toad bladder can be classified as tight tissues, whereas gallbladder, small intestine, and proximal tubule of the kidney are classified as very leaky tissues. Perhaps the most detailed investigation of shunt properties has been carried out on gallbladder,[13] and modification of the shunt permselectivity in this tissue was carried out by techniques similar to those used here.[14] However, the physiological significance of *p*H modification of the shunt conductance in gallbladder is doubtful because the *p*H of bile remains fairly constant. In the antrum on the other hand, which is exposed to gastric contents, the *p*H of the mucosal solution varies from neutrality or even slightly alkaline (due to antral secretion)[3] to a *p*H as low as 0.8.

At a *p*H of neutrality the shunt intracation selectivity is similar to that of sequence III for glasses of low field strenght.[7] This implies that the ions permeating the shunt do so under conditions of partial hydration, and that the selectivity is due to widely spaced negative charges.

Inasmuch as at neutral *p*H, cation is favored over anion, it is possible to speculate that this selectivity is due in part to negatively charged groups such as carboxyl groups, or due to polar groups such as the carbonyl group. Altering the *p*H of the mucosal solutions results in the change from cation to anion selectivity, with equal selectivity in case of Necturus at *p*H 3.5, and bullfrog at *p*H 4.0, and increasing anion selectivity below this *p*H. Similar data have been obtained for the piglet fundus[15] Na^+ channel. This suggests the controlling groups in the shunt pathway may well be carboxyl groups with a *p*K′ of between 3.5 and 4.0 and perhaps phosphate or sulfate groups at lower *p*H ranges. Ultimately the anion selectivity is due to the number of positively charged NH_3^+ groups exceeding the negative groups. This is further confirmed by the use of a carboxyl group reagent such as EDCD, where following treatment the tissue shunt conductance is anion selective, even at *p*H 7.4. There are however, evidently additional groups protonation of which, with decreasing *p*H, further increases the anion selectivity. This may be due to other chemical structures such as PO_4^- or SO_4^- groups on proteins or carbohydrates, responsible for the increasing anion selectivity below *p*H 2.0. Figure 5 gives a schematic representation of the shunt region to illustrate the mechanism of selectivity.

Carbenoxolone modified the shunt conductance by maintaining the relative cation selectivity at acid *p*H ranges. This may be interpreted as being due to penetration of this compound into the shunt region and modification of shunt selectivity due to the *p*K′ (*p*K′ = 2) of the free carboxyl groups of the drug.

In one way the shift from cation to anion selectivity in the antrum makes physiological sense in that the low *p*H to which antrum is exposed would require a barrier against H^+ penetration even in the shunt region. However, the selectivity at best is only weak, and moreover, as there are no changes in PD with changes only in $[H^+]$ it appears that the shunt does not favor H^+ over phosphate at any *p*H studied.

The enhancement of cation selectivity of the shunt pathway by carbenoxolone was a surprising result in view of the reported effectiveness[16] of carbenoxolone in treatment of gastric ulcer. This finding suggests that (1) carbenoxolone is ineffective in reducing cation back diffusion; (2) altering shunt selectivity is the major therapeutic effect; or (3) the permeable paracellular pathway plays a minor role in initiation of ulcer. A large increase in this path, with a leak of HCl to the basal surface of the cells, can clearly be pathogenic, but based on the above this would be a massive nonselective leak. The unmodified conductance however, may contribute but cannot per se be the cause of ulceration of the tissue.

In these experiments 10 mM carbenoxolone was applied to the mucosal surface. The concentration is in the range achieved in the gastric lumen after a dose of 100 mg in approximately 100 ml of fluid. The concentration used here is much higher than blood concentration achieved during therapy. To our knowledge there are no

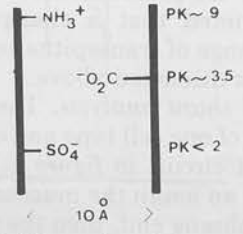

FIG. 5. A schematic illustration of the possible chemical groups determining tight junction selectivity. As illustrated at neutral *p*H, negative charges would be in excess producing relative cation selectivity. A decrease in *p*H would progressively exclude the negative charges resulting in anion selectivity.

studies as to the importance of oral versus intravenous exposure during therapy.

What may be the cause of ulcer is that the magnitude of the shunt pathway results in a marginally effective barrier so that any other lesion, such as in the cell path, produces the conditions, which, combined with the leaky shunt pathway, result in ulcer development.

REFERENCES

1. Bajaj SC, Spenney JG, Sachs G: Modification of permeability properties of gastric antrum (abstr) Gastroenterology 68:978, 1975
2. Forte JG, Forte TM, Machen TE: Histamine stimulated H^+ secretion by in vitro tight gastric mucosa. J Physiol (Lond) 244: 15–31, 1975
3. Flemstrom G, Sachs G: Ion transport by amphibian antrum. Am J Physiol 228:1188–1198, 1975
4. Spenney JG, Flemstrom G, Shoemaker RL, et al: Quantitation of conductance pathways in antral gastric mucosa. J Gen Physiol 65:645–662, 1975
5. Spenney JG, Shoemaker RL, Sachs G: Microelectrode studies of fundic mucosa. J Membr Biol 19:105–128, 1974
6. Oi M, Yoji I, Kumagai F, et al: A possible dual control mechanism in the origin of peptic ulcer: a study on ulcer location as affected by mucosa and musculature. Gastroenterology 57:280–293, 1969
7. Diamon JM, Wright EM: Biological membranes: the physical basis of ion and non-electrolyte selectivity. Ann Rev Physiol 31:581–646, 1969
8. Goldman DE: Potential, impedance and rectification in membranes. J Gen Physiol 27:37–60, 1943
9. Mandel L, Curran PF: Responses of frog skin to steady state voltage clamping. I. The shunt pathway. J Gen Physiol 59:503–518, 1972
10. Fromter E, Diamond JM: Routes of passive ion permeation in gall bladder. Nature 235:9–12, 1972
11. Rose RC, Schultz SG: Studies on the electrical potential profile across rabbit ileum. J Gen Physiol 57:639–663, 1971
12. Bonlpalp EL: Electrophysiological properties of the proximal tubules: the importance of cellular and intercellular transport pathways. *In* Electrophysiology of Epithelial Cells. Edited by G Giebisch. Stuttgart, Schattauer, 1971, p 99–119
13. Diamond JM, Barry PH, Wright EM: Route of transepithelial ion permeation in gall bladder. *In* Electrophysiology of Epithelial Cells. Edited by G Giebisch. Stuttgart, Schattauer, 1971, p 23–33
14. Wright EM, Diamond JM: Effects of pH and polyvalent cations on the selective permeability of gall bladder epithelium to monovalent ions. Biochim Biophys Acta 163:57–74, 1968
15. Machen TE, Forte JG: Active and passive Na^+ transport by isolated mammalian stomach. Presented at the Fifth International Congress of Biophys. 15a, 1975
16. Doll R, Hill ID, Hutton CF: Treatment of gastric ulcer with carbenoxolone sodium. Gut 6:19–23, 1965

A Molecular Approach to Epithelial Conductance: Gastric Mucosa

G. Sachs, J. G. Spenney, R. L. Shoemaker & M. C. Goodall

INTRODUCTION

Transport across epithelial tissues can be divided into active and passive components. Biochemically an Na-K (Skou 1957), Ca^{++} (Martonosi 1971), and HCO_3^- ATPase (Tanisawa & Forte 1971) have been extensively studied and implicated in active transport function of various epithelia. The similarities in the hydrolytic site of these membrane bound ATPases – an acyl group, a serine, and an imidazole residue – leads to the conclusion that their functional differences may result from associated subunits. Most recently, conformational change in a part (or whole) of the molecule (Jardetzky 1966) has been suggested as the transport mechanism. In the case of Na-K ATPase assessment of intrinsic or extrinsic fluorescence (Mayer & Avi-Dor 1970), or circular dichroism (Long *et al.* In preparation) have revealed no evidence of conformational change. An alternative is the presence of a carrier or channel subunit whose mobility or structure is a function of ATPase activity. What is even more likely is that a specialized structure is present in the membrane for the passive movement of ions accompanying the actively transported species, for example, the Cl ion which accompanies the secreted H ion. Indeed, in epithelia such as frog skin or toad bladder, there also has to be a route with passive conductance properties for ion transport across the cell membrane.

Clear definition of molecular functions such as these has been possible only since the advent of artificial bilayers as a model system in which they could be studied (Mueller & Rudin 1963). The classical carrier prototype is

---

Departments of Physiology and Biophysics, Medicine and Division of Neurosciences, University of Alabama in Birmingham, Birmingham, Alabama 35294.

Supported by NIH AM08541, Cancer and Cardiovascular Training and Research Grants; NSF Grant GB31075; and Veterans Administration Hospital, Birmingham, Alabama 35294, and Grant by Smith Kline & French Laboratories.

»Transport Mechanisms in Epithelia«, Munksgaard, Copenhagen.

valinomycin (Lev *et al.* 1966), and channel prototype gramicidin (Hladky & Haydon 1970). It is pertinent to inquire whether this type of molecule exists in epithelial tissues and whether it can be isolated and incorporated in an active form into artificial bilayers. In this context, the intact tissue is a useful starting point for a study of the nature of the conductance pathways present.

Epithelial tissues may be classified firstly as to whether conductance is largely cellular or paracellular (Diamond *et al.* 1971). If conductance is paracellular, we would be tempted to conclude that the properties of this conductance pathway would reflect the anatomic apposition of adjacent cells, rather than the presence of isolatable entities such as channels. Tissues, however, which are tight, a reflection perhaps of the density of Ca^{++} sites on the opposing junctional membrane surfaces, will have electrical properties which are those of the cell membranes rather than those of the junctional regions.

With many assumptions, it is possible then to study the electrical properties of tight tissues in a simple Ussing chamber, and to obtain some idea of the types of molecules contributing to the electrical structure of the tissue. We can classify the types of molecules reponsible for charge transport across membranes as mobile or carrier type and fixed or channel type. In turn, these can be either neutral, such as valinomycin or gramicidin, or have formal charges such as those associated with amine or carboxyl groups. There can be anion or cation selectivity or no charge discrimination. The selectivity series can also give useful information for relating the isolated channels to the channels in the intact tissue.

Thus it is possible to establish the predominant route – cellular vs. paracellular – as well as the nature – mobile vs. fixed and charged vs. neutral – of the sites of ion permeation in the intact tissue. Extraction of the tissue, assessment of activity in artificial bilayers, and purification of activity will enable passive permeability characteristics to achieve the same molecular basis as active transport.

METHODS

A. Paracellular vs. Cellular Conductance:

As a model tight tissue, gastric mucosa would appear to be an appropriate choice, because of high resistance, high P D and extremely high H^+ concentration gradients developed, of the order of 10^4–10^6 depending on species

However, a more quantitative definition of tightness would be desirable, and this can be done in several ways.

1. Comparison of isolated cell conductance and tissue conductance: This approach depends on the capability of isolation of viable cells from a given tissue and of making electrical measurements on these isolated cells. In the case of *Necturus* gastric mucosa, this has proved possible (Blum *et al.* 1971). Fig. 1 shows a current-voltage plot for isolated cells compared to intact tissue. The 100-fold difference in slope is readily explained by intercellular coupling in this tissue.

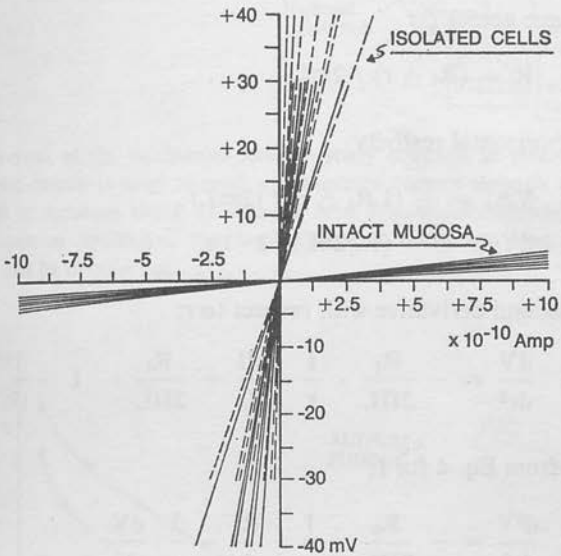

Fig. 1. Current voltage plots obtained by current sending through a microelectrode implanted either in an isolated cell, where no junctional conductance exists, or in similar cells where intercellular junctional conductance is present. This accounts for the differences in slope observed.

Since we can measure the conductance of the isolated cell in Ω^{-1} cm^{-2}, and the tissue conductance in similar units, then the shunt conductance is simply derived as $g_{shunt} = g_{tissue} - g_{cells}$.

Using this approach for *Necturus* gastric mucosa, the shunt conductance would appear to be about equal to cellular conductance. This is to be contrasted with a tissue such as gall bladder epithelium, where the ratio is about 20.

2. Direct Measurement in Intact Tissue: An alternate approach to th problem is the use of a 2-electrode system for measuring voltage decay w distance from a current sending electrode. The apparatus used for gas mucosa is illustrated in Fig. 2. Data derived from this type of experim are illustrated in Fig. 3 for *Necturus* antral and fundic mucosa.

Considering a disc of tissue of thickness L and radius r with the curr source inserted in the center of the disc, then voltage change across a dista $\triangle r$ is:

$$(1) \quad V_r = V_{(r+\triangle r)} - V_{(r)} = - IR$$

R is the resistance across $\triangle r$

$$(2) \quad R = (R_t \triangle r) / 2\pi rL$$

R_t = specific horizontal restivity

$$(3) \quad V\triangle_r = - (I R_t \triangle r) / (2\pi rL)$$

$$(4) \quad dV/dr = - (R_t/2\pi L) \cdot I \cdot 1/r$$

Taking the second derivative with respect to r:

$$(5) \quad \frac{dV}{dr^2} = - \frac{R_t}{2\Pi L} \cdot \frac{1}{r} \cdot \frac{dI}{dr} + \frac{R_t}{2\Pi L} \cdot I \cdot \frac{1}{r^2}$$

Substituting from Eq. 4 for I:

$$(6) \quad \frac{d^2V}{dr^2} = - \frac{R_t}{2\Pi L} \cdot \frac{1}{r} \cdot \frac{dI}{dr} - \frac{1}{r} \frac{dV}{dr}$$

Finding an expression for dI/dr: $\triangle$ I, the current loss vertically is pr portional to the surface area subject to loss and inversely proportional t the resistance of this surfaze (R_Z = vertical specific resistivity).

$$(7) \quad \triangle I = - (V/R_Z) \cdot 2\pi r \triangle r$$

$$(8) \quad dI/dr = - (2\pi rV) / R_Z$$

and substituting into Eq. 6:

$$(9) \quad \frac{d^2V}{dr^2} = \frac{VR_t}{LR_Z} - \frac{1}{r} \frac{dV}{dr}$$

Fig. 2. A One half the other ment of luminal f

Fig. 3. fundus fundus,

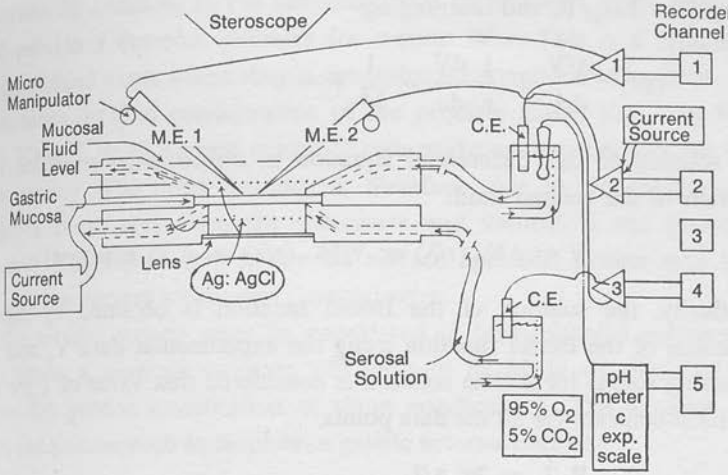

Fig. 2. A diagram of the equipment used to study coupling in intact gastric mucosa. One half of the circuit is used to send and measure current through a microelectrode, the other half to measure the P D changes in a distant cell. Simultaneous measurement of trans-tissue resistance, the luminal/serosal resistance ratio, and pH in the luminal fluid can be carried out.

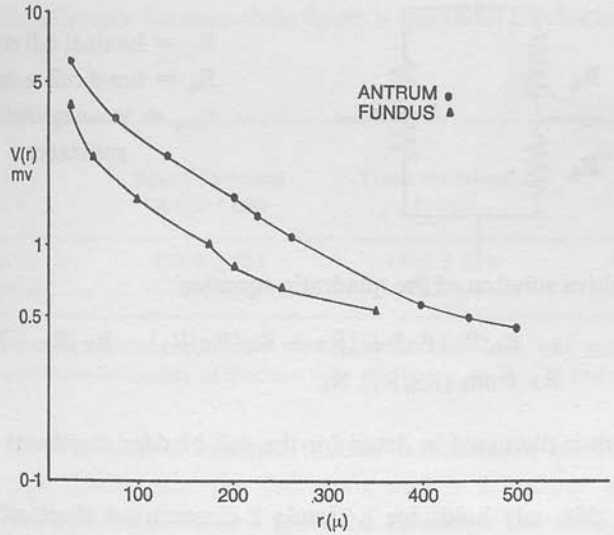

Fig. 3. The decay of voltage with distance from a current-sending microelectrode for fundus and antrum of *Necturus* gastric mucosa. Note the break in the curve for the fundus, due to the presence of a tubule.

letting $\lambda^2 = LR_Z/R_t$ and rearranging:

$$(10) \quad \frac{d^2V}{dr^2} + \frac{1}{r}\frac{dV}{dr} - \frac{1}{\lambda^2}V = 0$$

The solution to this differential equation is a zero order modified Bes function of the second kind:

$$V = AK_o\,(r/\lambda) \text{ or } V/IK_o\,(r/\lambda) = A \text{ (a constant)}$$

Practically, the solution of the Bessel function is obtained by repetit expansion of the Bessel function using the experimental data V_r and r a increasing values for λ. The solution is considered that value of λ for whi A is most constant for all the data points.

and

$$R_t/L = 2\pi\,A/I_o$$
$$R_Z = \lambda^2\,(R_t/L) = (\lambda^2 2\pi A)\,/\,I_o$$

I_o is the current injected.

The membrane resistances are derived from consideration of an equivale electrical circuit:

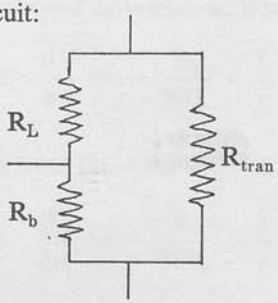

R_L = luminal cell membra
R_b = basal cell membrane
r_{tran} = trans epithelial resistance

R_L is the positive solution of the quadratic equation:

$$(-R_b/R_L)\,R_L^2 + [R_Z + R_Z\,(R_B/R_L) - R_T\,]R_L + R_Z R_T =$$
R_B from $(R_B/R_L)\,R_L$

This approach is discussed in detail for the gall bladder membrane (Fröm 1973).

However, this only holds for a simple 2-dimensional sheet such as g bladder or antrum. The fundic mucosa is riddled with a series of indent tions (i. e. tubules) which will result in an area correction term for t transepithelial resistance (2.7 fold for *Necturus*, 13 fold for dog gast

mucosa). In addition, in the microelectrode experiments, these indentations will provide a complex pathway for current flow. This is a separate case from infolded tissue where simple dimensional corrections will suffice.

A more detailed consideration of the problem shows that only between 1 in 10 or 1 in 20 surface epithelial cells make connection with the tubular indentations. The error introduced, therefore, due to the tubular parallel resistive shunt with both the transverse and vertical R can probably be ignored. The values derived for the surface epithelial system may then be regarded as correct within experimental error.

The tubular system must be considered in transepithelial measurements, and hence a separate estimate will have to be made on this part of the tissue for precise quantitation of shunt conductance. The equation, therefore, for a tissue such as amphibian gastric mucosa becomes:

$$g_{tissue} = g_{SEC} + g_{tub} + g_{shunt} \therefore g_{shunt} = g_{tissue} - g_{SEC} - g_{tub}$$

g tissue is obtained from transepithelial measurements and surface area correction for this value from histological sections, g_{SEC}, the surface epithelial conductance from microelectrode measurements on intact tissue, g_{tubule} from measurements on isolated tubules and area correction again from histological data. The difference between these terms is the shunt conductance.

Table I.

	Space Constant λ (10^{-4} cm)	Trans Resistance Ω cm^2	Cell Membrane Resistance Ω cm^2
Fundus	352.9 ± 211	1882 ± 534	6433 ± 4119
Antrum	511	2254	8,130

Values for space constant, corrected transepithelial resistance, and sum of luminal and serosal membrane resistance of surface cells of fundus (n = 17) and antrum (n = 3).

For *Necturus* gastric mucosa, tubular conductance is at least equal to surface cell conductance per unit area, and is 1.7 times greater because of the area difference. Table I gives the values for the different conductive parameters of the surface epithelial cells and using these data we have:

$$g_{shunt} = 5.31 \times 10^{-4}\Omega^{-1} - 4.2 \times 10^{-4}\Omega^{-1} = 1.11 \times 10^{-4}\Omega^{-1}\text{cm}^{-2}$$

a very low shunt value relative to loose epithelia, being 1/5 of cellular conductance.

In the case of the antrum, a region of the stomach, largely devoid of indentations, the problem is comparable to that of gall bladder. Table 1 summarizes our findings for this tissue. Here, therefore:

$$g_{shunt} = 4.9 \times 10^{-4}\Omega^{-1}cm^{-2} - 1.2 \times 10^{-4}\Omega^{-1}cm^{-2} = 3.7 \times 10^{-4}\Omega^{-1}cm^{-2}$$

still a low value, but higher than that of fundic mucosa. Since this is about thrice that of the cellular conductance, there could therefore be some significant back leak of acid through the junctional region, with effects such as inhibition of gastric secretion.

To amplify these comments, the antrum is the site of release of gastrin. This hormone is situated deep in the tissue and its release is inhibited by acidification of antral contents. Evidently, a possible route for H^+ back diffusion is through the junctional region. An unlikely route is through the cell, since the cell pH would have to fall to low values. This may therefore be a justification for the leakiness of the antral junctions compared to the fundic junctions.

3. Intracellular $\triangle$ P D Measurements: A third approach to the problem of paracellular conductance also uses microelectrodes. A constant product KCl change in the serosal bathing solution of *Necturus* gastric mucosa results in a P D change across the whole tissue, and also across the serosal membrane of the cells. If a shunt conductance is present, then:

$$\triangle \text{P D tissue} = \triangle \text{P D cell.} \frac{(\quad g_{cell} \quad)}{(g_{cell} + g_{shunt})}$$

so that if the shunt and cell conductance were equal the tissue P D change would only be half that of the cell. From Fig. 4, it can be seen that the cellular and tissue P D changes are almost equal. This results in one of two conclusions: that either there is a low shunt conductance or else the permeability properties of the shunt region are the same as that of the cell membrane. If the latter were so, then altering the ionic concentration on the other side of the tissue should have the same effects, i. e. the tissue should be symmetric. This is not the case in the gastric mucosa, hence again there is little shunt conductance in *Necturus* gastric mucosa.

Summarizing our findings, therefore, the shunt conductance of *Necturus*

Fig. 9.
Dr. H. F

Fig. 10.
the zona
Dr. H.

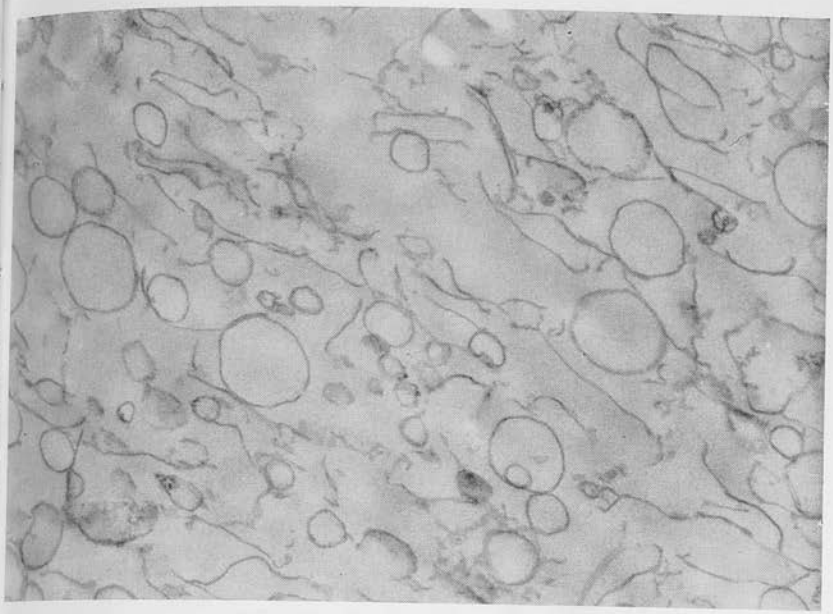

Fig. 9. Electron micrograph of membrane fraction used for channel work. (Courtesy Dr. H. F. Helander). (× 75,000)

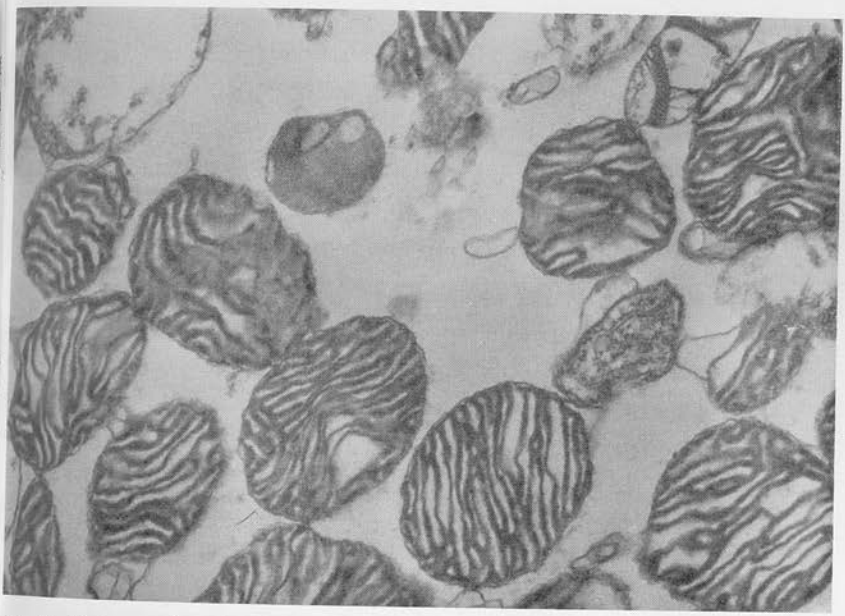

Fig. 10. Electron micrograph of mitochondrial fraction obtained at 40+% sucrose in the zonal rotor, from which channels were not extracted by Triton X-100. (Courtesy Dr. H. F. Helander). (× 75,000)

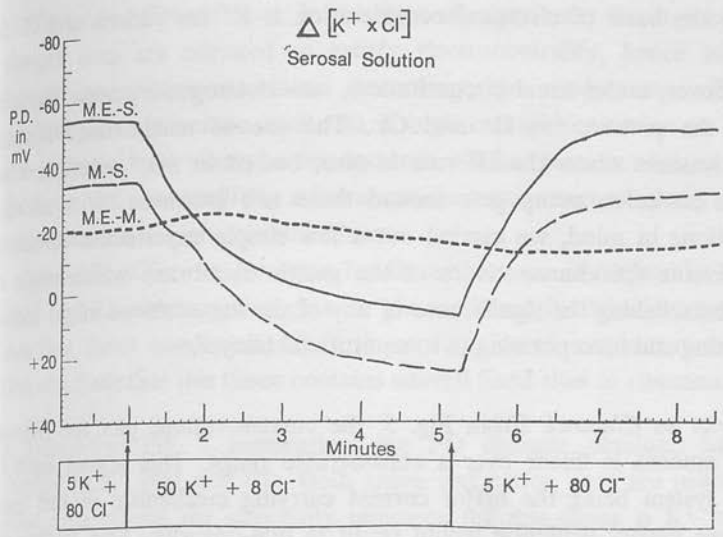

Fig. 4. The effect of a constant product KCl change on the serosal surface of *Necturus* gastric mucosa, on the trans-tissue P D, the P D from cell to serosal bathing solution, and the P D from cell to mucosal solution.

gastric fundic mucosa is almost two orders of magnitude less than that of *Necturus* gall bladder or proximal tubule. In studying the electrical properties of this tissue, therefore, in a simple Ussing chamber, we are dealing with the properties of the cell membranes.

B. Channels and Carriers, Charged and Uncharged:

It has been shown due to the work of Eisenman and his collaborators (Conti & Eisenman 1966; Eisenman *et al.* 1968) that one can distinguish the mechanism whereby ions permeate artificial membranes. Many of these considerations have been applied to the gall bladder in a series of three papers (Barry & Diamond 1971, Wright *et al.* 1971, Barry *et al.* 1971).

The advantage of the gall bladder in these studies is that permeation is controlled by the junctional region, i. e. a single membrane. This is not the case in the gastric mucosa where permeation is controlled by the luminal and basal membranes of a heterogeneous cell population. It is questionable, therefore, whether a simplistic approach can yield any useful information about any ion permeation mechanism other than the dominant one, which on the basis of chemical flux studies is Na^+ for cations, and Cl^- for anions,

and on the basis of electrical consideration is K^+ for cations and Cl^- for anions.

Moreover, under usual circumstances, two electrogenic pumps may complicate the picture, for H^+ and Cl^-. The use of unstimulated *Necturus* gastric mucosa where the H^+ rate is zero, bathed in SO_4'' solutions where there is no anion pump gets around these two problems. With all these reservations in mind, we carried out a few simple experiments to attempt to determine the characteristics of the gastric membrane which might aid us in ebstablishing the significance of any of the materials we might succeed in isolating and incorporating in to an artificial bilayer.

1. Carrier vs Channel: From Fig. 5, the current-voltage plot for *Necturus* gastric mucosa is linear over a considerable range. This argues against a carrier system being the major current carrying mechanism in this tissue since free carrier depletion would result in non-linearity. This finding also suggests that the rate limiting step is not at the solution-membrane interface since here too we would expect a saturation phenomenon. Thus this finding can be taken as tentative evidence that we are dealing with fixed sites or channels. It must be pointed out that carrier systems may still be present as a minor component of the conductance system.

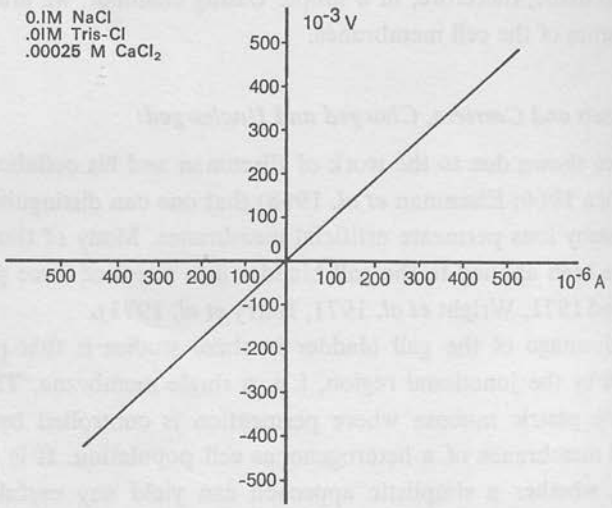

Fig. 5. Current-voltage plot obtained for *Necturus* gastric mucosa by recording voltage change obtained after 100 msec. current pulse showing linearity up to 500 mv.

2. *Charged vs Neutral Sites:* In this type of experiment the argument is that charged sites are required to satisfy electroneutrality, hence will always have the counter ion associated. Accordingly the conductance will be independent of concentration until this is high enough for co-ion to be forced into the membrane when the conductance will increase; in contrast a neutral fixed site will show initially a linear conductance concentration relationship with saturation at high concentrations.

Our findings for the *Necturus* fundic mucosa are illustrated in Fig. 6 for NaCl or LiCl, showing that gNa $>$ gLi, as found for biionic potentials and also that tissue conductance is a linear function of concentration. We can then conclude that this tissue contains neutral fixed sites or channels.

3. *Selectivity:* Fig. 7 summarizes the PD changes obtained for 10-fold changes in K^+, Na^+ and Cl^-. Both anion and cation sites are present. From other experiments the selectivity sequence for this tissue is $K^+ > Rb^+ > Na^+ > Li^+$, Cs^+ for cations and $Br^- > Cl^- > I^- > SO_4^=$ for anions, different from the free solution sequence.

Section Summary: We therefore have tentative evidence for both anion and cation selective channels present in gastric mucosa, and have some know-

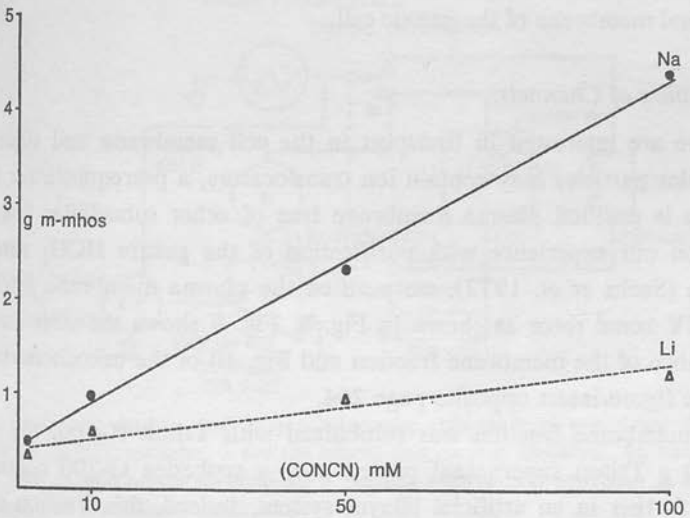

Fig. 6. A plot of the conductance of *Necturus* gastric mucosa against varying concentrations of NaCl and LiCl, showing good linearity over the concentration range studied.

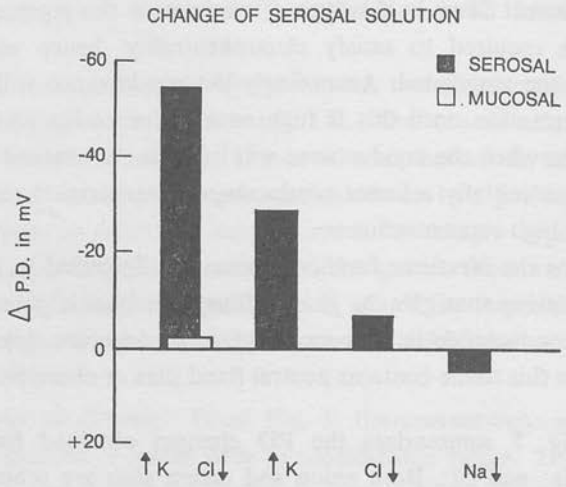

Fig. 7. A summary of the P D changes obtained across the serosal membrane of Necturus gastric mucosa in response to 10-fold changes in K^+, Cl^- and Na^+, and constant product KCl changes.

ledge of their selectivity. An additional feature of this tissue that may be of importance is the effect of acetyl choline (Shoemaker *et al.* 1970), which may be interpreted as being due to the opening of nonselective channels in the serosal membrane of the gastric cell.

C. Isolation of Channels:

Since we are interested in transport in the cell membrane and since other subcellular particles may contain ion translocators, a prerequisite for further progress is purified plasma membrane free of other subcellular fragments. Based on our experience with purification of the gastric HCO_3^- stimulated ATPase (Sachs *et al.* 1972), we purified the plasma membrane fraction in a Ti XIV zonal rotor as shown in Fig. 8. Fig. 9 shows the ultra-structural appearance of the membrane fraction and Fig. 10 of the mitochondrial fraction, see figure insert opposite page 264.

The membrane fraction was solubilized with Triton X-100, the soluble 100,000 g Triton supernatant passed over a sephadex G-200 column and studied further in an artificial bilayer system. Indeed, this fraction induced step changes in conductance; 3 types of channels initially were distinguishable on the basis of their size or charge discrimination.

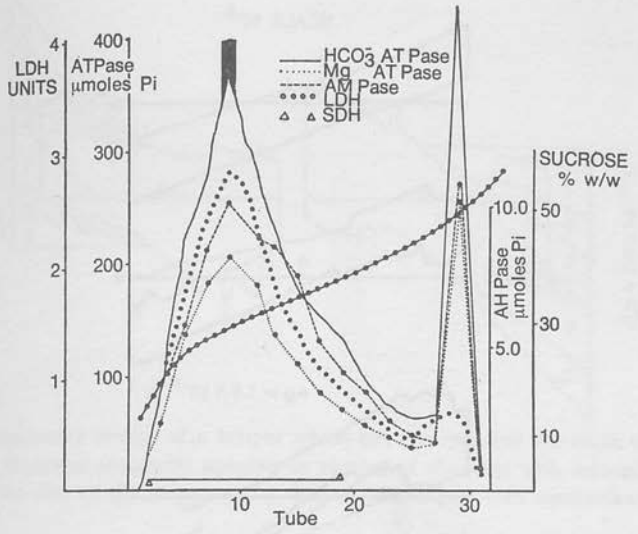

Fig. 8. Zonal pattern of 100,000g precipitate (post 5000g), showing activities of succinic dehydrogenase (SDH), lactic dehydrogenase (LDH), ATPase, HCO_3^- ATPase. The shaded area represents the tube used for the channel extraction.

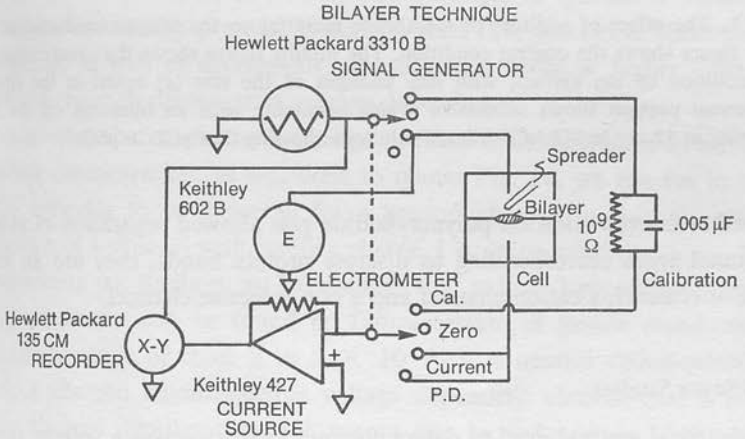

Fig. 11. Equipment used to study step conductance changes in an experimental bilayer, consisting of an X-Y recorder, a voltage source and current amplifier. An electrometer may be used in this set-up to measure 0 current voltage and provision is made for conductance and capacitance calibration.

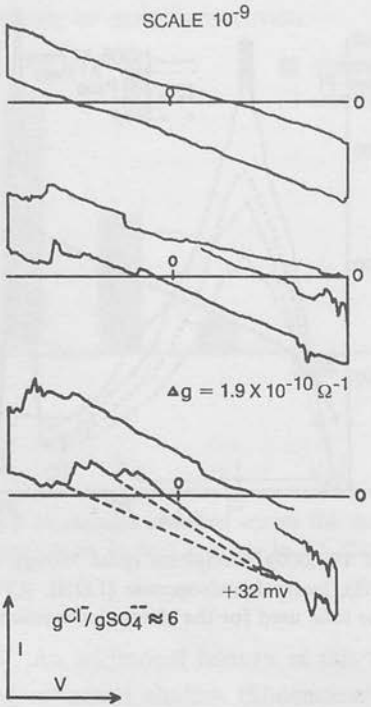

Fig. 12. The effect of addition of membrane material on the bilayer conductance. The upper figure shows the control condition. The middle figure shows the events occurring with addition of the extract, with step changes of the size (g) noted in the figures. The lowest portion shows successive events occurring with an intercept on the lines occurring at 32 mv in SO_4″:Cl^- biionic solutions showing that $gCl' > gSO_4$″.

Further fractionation on polyacrylamide gels allowed separation of at least 3 channel types corresponding to discrete protein bands; they are an anion selective channel, a cation channel and a non-selective channel.

D. Bilayer Studies:

The electrical method used to detect channel formation was a voltage current sweep across a bilayer formed from soy bean lecithin dissolved in decane as illustrated in Fig. 11.

Fig. 12 shows the events obtained when the gastric preparation was added to one side of the system. With this technique the slope change immediately gives us the size (conductance value) of the channel, and the intersection of

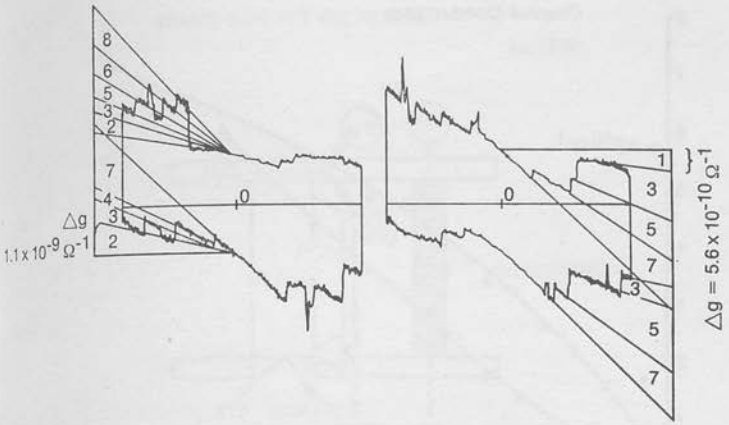

Fig. 13. Two successive sweeps of a bilayer which has incorporated the anion selective channels. This illustrates successive opening or closing of channels with increasing voltage and that the size of the steps can be related to a single unit conductance g = $5.6 \times 10^{-10}\Omega^{-1}$.

the slopes in asymmetric solutions the biionic voltage or selectivity of the channel. It can be seen that discrete step changes occur upon addition of the extract demonstrating the presence of channels.

Fig. 13 shows two successive sweeps of a bilayer in symmetric solutions with the extract already present. It can be seen that successive increments are obtained, as well as decrements. These events occur at higher voltage; hence these channels demonstrate voltage dependence.

By measuring the conductance change of these individual steps as a function of salt concentration, as was done to obtain Fig. 14, we can see in one case the behavior to be expected for a neutral channel, and in the other the behavior of a channel with positive charge, i. e. anion selective.

Summarizing our findings, we have shown that at least 3 separable channel forming substances can be found in Triton extract of gastric membranes, with a conductance of from 2 to 5 $\times$ $10^{-10}\Omega^{-1}$, a neutral cation-selective channel, a charged anion-selective voltage dependent channel and a non-selective channel. Similar types of events can be induced in bilayers by extracts of sarcoplasmic reticulum (Szabo *et al.* In press.), and perhaps by Na^+K^+ ATPase preparations from kidney (Tosteson & Skou, personal communication), and extracts of electric organ or rat brain (Goodall & Sachs 1972). These channels are absent from similar extracts of purified gastric mitochondria.

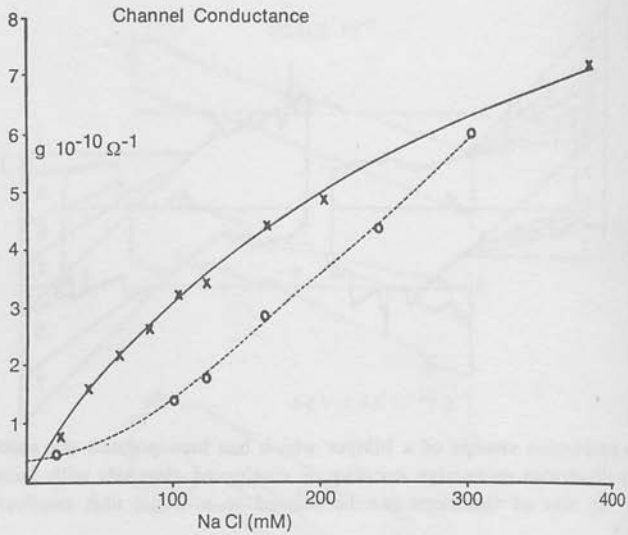

Fig. 14. The effect of varying NaCl concentration on unit channel conductance. The upper line represents the neutral cation selective channel, the lower line the smaller voltage dependent anion selective channel.

CONCLUSIONS

This work has demonstrated the feasibility of a direct approach to the passive conductance elements occuring in epithelial tissues. Thus having established the cellular pathway of gastric mucosal conductance by direct measurements and having found suggestive evidence for a mosaic of anion and cation selective channels, we have succeeded in incorporating these channels into a bilayer. We can therefore study their properties directly, a feat which would be impossible in the high conductance situation in the intact cell membrane. We have further shown that these channels can be separated and purified and may become amenable to direct chemical and biochemical investigation.

HCl Secretion Implications:

Finally, we are tempted to speculate about the significance of the voltage dependent, anion selective channel that we have found. This we do by considering the model illustrated in Fig. 15. Here the HCO_3^- ATPase is considered to act by removing OH^- or HCO_3^- from the site of proton secretion. This system is clearly electrogenic. In the absence of any other mem

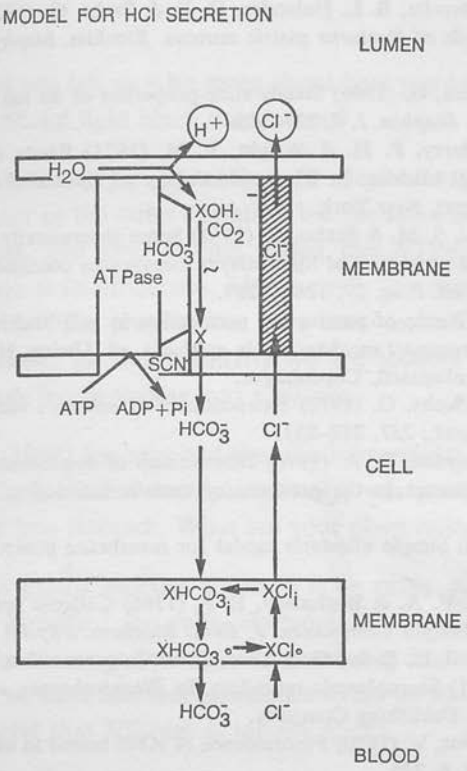

Fig. 15. A model incorporating the voltage dependent anion channel into an electrogenic HCO_3^- ATPase mechanism for H^+ secretion by the gastric mucosa.

brane conductance system a P D would build up equal to the pump EMF. In the presence of a voltage dependent Cl^- channel, in association with the ATPase site, but not necessarily part of it, the developed voltage would open the channel and Cl^- flux would occur exactly equal to the demands of the H_3^+ pump resulting in electroneutral secretion.

Similar mechanisms may be involved for other electrogenic pumps such as the Na^+K^+ ATPase.

REFERENCES

Barry, P. H. & Diamond, J. M. (1971) Theory of ion permeation through membranes with fixed neutral sites. *J. Membr. Biol. 4,* 295–330.

Barry, P. H., Diamond, J. M. & Wright, E. M. (1971) Mechanism of cation permeation in gall bladder. *J. Membr. Biol. 4,* 358–394.

Blum, A. L., Hirschowitz, B. I., Helander, H. F. & Sachs, G. (1971) Electrical properties of isolated cells of *Necturus* gastric mucosa. *Biochim. biophys. Acta (Amst.)* 241 261–272.

Conti, F. & Eisenman, G. (1966) Steady state properties of an ion exchange membrane with mobile sites. *Biophys. J. 6,* 227–246.

Diamond, J. M., Barry, P. H. & Wright, F. M. (1971) Route of transepithelial ion permeation in gall bladder. In *Electrophysiology of Epithelial Cells,* pp. 23–28, ed. Schattauer, Stuttgart, New York.

Eisenman, G., Ciani, S. M. & Szabo, G. (1968) Some theoretically expected and experimentally observed properties of lipid bilayer membranes containing neutral molecular carriers of ions. *Fed. Proc. 27,* 1289–1297.

Frömter, E. (1973) Route of passive ion permeation in gall bladder. In Alfred Benzon Symposium V: *Transport mechanisms in epithelia,* ed. Ussing, H. H. & Thorn, N. A. pp. 492–499. Munksgaard, Copenhagen.

Goodall, M. C. & Sachs, G. (1972) Extraction of K selective channels from excitable tissue. *Nature (Lond.) 237,* 252–253.

Hladky, S. B. & Haydon, D. A. (1970) Discreteness of conductance change in bimolecular lipid membranes in the presence of certain antibiotics. *Nature (Lond.)* 225 451–453.

Jardetzky, O. (1966) Simple allosteric model for membrane pump. *Nature (Lond.)* 211 969–970.

Lev, A. A., Gotlib, V. A. & Buzhnisky, E. P. (1966) Cationic specificity of model bimolecular phospholipid membranes. *J. Evol. Biochem. Physiol. (USSR) 2,* 109–117.

Long, M. M., Masotti, L., Sachs, G. & Urry, D. W. In preparation.

Martonosi, A. (1971) Sacroplasmic reticulum. In *Biomembranes,* ed. Hanson, L. A, pp. 191–224. Plenum Publishing Company.

Mayer, M. & Avi-Dor, V. (1970) Fluorescence of ANS bound to ox brain NaK ATPase. *Israel J. Med. Sci. 6,* 276.

Mueller, P. & Rudin, D. O. (1963) Induced excitability in reconstituted cell membrane structure. *J. theoret. Biol. 4,* 268–280.

Sachs, G., Shah, G. Strych, A., Cline, G. & Hirschowitz, B. I. (1972) Properties of ATPase of gastric mucosa. III. Distribution of HCO_3^- – stimulated ATPase in gastric mucosa. *Biochim. biophys. Acta (Amst.) 266,* 625–638.

Shoemaker, R. L., Makhlouf, G. M. & Sachs, G. (1970) Action of cholinergic drugs on *Necturus* gastric mucosa. *Amer. J. Physiol. 210,* 1056–1059.

Skou, J. C. (1957) Influence of cations on ATPase from peripheral nerves. *Biochim. biophys. Acta (Amst.) 23,* 394–401.

Szabo, G., Eisenman, G., Laprade, R., Ciani, S. & Krasne, S. Experimentally observed effects of carriers on the electrical properties of bilayer membranes – equilibrium domain. In *Membranes,* ed. Eisenman, G. Dekker. In press.

Tanisawa, A. S. & Forte, J. G. (1971) Phosphorylated-intermediate of microsomal ATPase from rabbit gastric mucosa. *Arch. Biochem. Biophys. 147,* 165–175.

Tosteson, M. T., Tosteson, D. C. & Skou, J. C. Personal communication.

Wright, E. M., Barry, P. H. & Diamond, J. M. (1971) Mechanism of cation permeation in gall bladder. *J. Membr. Biol. 4,* 331–357.

DISCUSSION

ZADUNAISKY: Could you tell us a bit more about how you incorporated these membranes into artificial lipid black membranes?

SACHS: You can do it simply by adding the Sephadex purified ATPase fraction into the inner or the outer chamber. We use inner chamber of an artificial bilayer setup, and after having added the ATPase you form the bilayer and then look at its properties. Alternatively you can form the bilayer first and then add ATPase preparation: Now how much incorporates, obviously we don't know. At the sensitivity we are looking at here we can detect single channels incorporating into a bilayer.

SCHULTZ: Villegas (1962) has reported that the intracellular electrical potential of parietal cells, identified iontophoretically, was positive with respect to the lumen of the frog stomach. What are your observations on this point?

SACHS: In Necturus gastric mucosa we have done many many experiments and we have also identified the cells, electrophoretically. We do not find positive potential in the oxyntic cells. We inevitably find a negative level. In amphibia where we have had less experience so far we haven't been able to find this positive level that Villegas is talking about.

ULLRICH: How pure is your enzyme preparation, did you check that?

SACHS: At the moment it looks like there are 15 bands on gel electrophoresis.

FRÖMTER: Could you please repeat for me what the resistance of the cell membrane was? I think that you mentioned a figure of 800 Ohm cm². This value would be much smaller than the values of approximately 3000 Ohm cm², which have been observed in gallbladder (this symposium p. 496) and proximal tubule (Boulpaep 1971) of the same species.

SACHS: In the fundus the calculated values were about 700–800 Ohm cm² and the trans tissue resistance in the experiments that we showed was about

---

Vilegas, L. (1962) Cellular location of the electrical potential difference in frog gastric mucosa. *Biochim. Biophys. Acta, 64,* 359–367.

Boulpaep, E. (1971) Electrophysiological properties of the proximal tubule: Importance of cellular and intercellular pathways. In *Electrophysiology of Epithelial Cells,* ed. Giebisch, G. pp. 91–112 F. K. Schattauer Verlag, Stuttgart.

a 1000 Ohm cm^2. So we sum the two and there was a small shunt conductance. But that is only assuming that we can neglect the tubules, which could account for all of the shunt conductance, obviously.

HOSHIKO: Were you classifying these channels in terms of the height of the transients?

SACHS: In terms of the change of slope.

HOSHIKO: What sort of dispersion did you get with these slopes?

SACHS: If you look at the smallest channels which you have got at the high sensitivity, that was one family. And then you have two other families of slope, one 3–5 and one 2×10^{-10} reciprocal Ohms.

HOSHIKO: They were separated by orders of magnitude?

SACHS: No.

TOSTESON: What was the speed of your ramp?

SACHS: The whole sweep takes about between 30 sec to 1 min.

TOSTESON: What is the relation between the zero frequency conductance and the concentration of the material which you get from the gradient?

SACHS: This is the bilayer system. And we incorporated some channels. And instead of doing a sweep over 30 sec we do a very slow sweep.

TOSTESON: You impose 1 voltage, measure the current . . .

SACHS: and go on very slowly, right.

TOSTESON: Have you made such measurements in the presence of different concentrations of the material from the gradient?

SACHS: Yes, we can do that.

TOSTESON: What is the maximum conductance you have under those conditions?

SACHS: For a single channel?

TOSTESON: No, for the whole bilayer in Ohm^{-1} cm^{-2}.

SACHS: If you have a lot of channels present the bilayer becomes very unstable, to this sort of slow sweep. It seems to break at extreme voltages, so if we do it within a very narrow range.

TOSTESON: Extreme means very low voltages, is that right?

SACHS: No, it was ± 100 mV across the bilayer, or 80.

HOSHIKO: I was surprised to see your voltage curve for the gastric mucosa, the voltage span going up to ½ V. What is the break-down voltage of the gastric mucosa?

SACHS: It must be larger than that.

HOGBEN: Which gastric mucosa? Around 60 mV a break-down occurs.

SACHS: And which gastric mucosa was that?

HOGBEN: *Rana temporaria* and *Bufo bufo*.

SACHS: Warren Rehm did the stuff in *Rana pipiens* up to 200–250 mV and with *Necturus* which didn't break down at 500.

HOGBEN: I presume that an alteration was not detected because the mucosa was challenged by a transient pulse.

SACHS: Oh yes, it wasn't clamping.

KEYNES: Are these channels of yours like gramicidin ones? Do they just stay open, or are there fluctuations all the time?

SACHS: You can get them staying on or sometimes switching off. We don't know why sometimes it will stay on so the conductance will climb up, and up and up.

KEYNES: But the story about gramicidin is that the channels only open for dimers. When the dimer form is present it is long enough to stretch all the way across the membrane and make a channel right through.

WHITTEMBURY: How many cell types do you have in the *Necturus* gastric mucosa, is there any difference in their profile of electrical potential, are they communicated?

SACHS: Yes, they are all communicated. The *Necturus* gastric mucosa has at least one cell type less than the guinea-pig gastric mucosa, because the oxyntic cell in the *Necturus* has both peptic or zymogen granules and acid secretory properties. In the guinea-pig where you have as many cell types as in the rat I think, you have coupling between each cell type. In the *Necturus* gastric mucosa you also have. We have not found, however, any significant difference in potential between the different cells we punctured.

GENERAL DISCUSSION

TOSTESON: Dr. Sachs, could I ask a question about these bilayers. You commented that when you add magnesium, the selectivity changes from being cation-selective to being anion-selective. You gave a number for chloride compared with sulphate but you did not cite a number for chloride as compared with cations. For instance if you put a 10-fold concentration ratio of sodium chloride across the bilayers in the presence of this material, what is the value of the zero current potential difference across the membrane?

SACHS: Before we added magnesium, if you had a 10-fold gradient for sodium chloride you get a PD of about 16–20 mV showing sodium selectivity. After you add magnesium, the PD will invert and you get a value which is the one calculated for a chloride/sodium conductance of about 3.

TOSTESON: And may I ask, if you add some other peak from the sucrose gradient to the solutions bathing the bilayer, do you observe changes in conductance?

SACHS: If we take some other peak, no we don't get these data at all. We don't see anything then, except what you call a garbage effect where you don't get thinning of the bilayer. If you take preparations from rat brain or electroplax, you get data which look like that but with different selectivities and different sizes.

KIRSCHNER: Does ATP have any effect?

SACHS: Yes, it does. But I don't know how to explain it. There is a potential development, as a function of the presence of ATP in symmetrical solutions and you require the ATP and the enzyme preparation to be present. You

don't see the potential when the bilayer goes black. But if you watch it thin and at the silvery stage of the bilayer a potential starts to develop. If you scan the bilayer at that time there is no evidence of channels. Then if you see evidence of channels occuring under a scan and then look at the PD, the PD is shorted out. Occasionally the channels will disappear as I showed on a slide and you look at the PD again it is present. The PD is in the direction which you would expect the protons to be moving. But whether you can conclude that we get an active transport system or surface charge effect or other positive effects I can't say.

SCHULTZ: Dr. Hogben, the resistance of the rat stomach that you recorded was in the order of a 100 Ohm cm^2 which places it in a rather low resistance range, and yet it maintains roughly a 10,000-fold gradient for hydrogen ion. Do you expect there is a rather large leak of hydrogen ion back from the lumen?

HOGBEN: Yes, there is a large leak. This is an abnormal situation, the low resistance or high conductance you referred to is one of the artifacts of isolating the mucosa. We cannot maintain the hydrogen concentration in the mucosal chamber at 5 mMol without continually replacing the mucosal solution.

ZADUNAISKY: Dr. Sachs. If you tried to keep the ATPase activity of your Sephadex column and then incorporated it in the inhibited membrane did you get these changes or not?

SACHS: Yes, we do. If I found that thiocyanate or cyanide inhibited the PD developed in the presence of ATP, I would have had some confidence that I might have been dealing with active transport. Since these do nothing in terms of PD that's why I would hesitate very much to assume that it has anything to do with active transport. Also, the presence of thiocyanate or cyanide does not affect the appearance of these channels.

KIRSCHNER: Let me make sure I sorted this out correctly. The thiocyanate doesn't prevent the formation of channels, but it also does not block this effective ATP, which is really what you would like to.

SACHS: That's right.

MAETZ: Has something similar been done on bilayer preparations with Na-K-dependent ATPase?

SACHS: Yes, there have been papers published by Jarni *et al.* where they look at fractions coming off a zonal rotor. I think it was a rat brain membrane preparation, and they were interested mainly in the zero potential current developed as a function of the presence of ATP, that was inhibited by ouabain. If you look at their figure they have coming off their zonal rotor a peak which they said gave step-like changes in conductance of the bilayer. Similar to what we found. They did not apparently take it any further. And they were not dealing with soluble, purified ATPase preparation.

TOSTESON: I can report that we have observed rather similar effects on the electrical properties of bilayers exposed to preparations from torpedo electric organ (in collaboration with E. Schoffeniels), and with preparations of Na-K ATPase in collaboration with J. C. Skou. The problem to be resolved is whether these effects have something to do with this specific protein or with any protein which is able to interact with bilayers.

ULLRICH: Is there a difference between the HCO_3 ATPase and Na-K ATPase with respect to solubility?

SACHS: You can solubilise both but with different detergents.

Reprinted from *Exp. Eye Res.* (1973) **16,** 241–249

Conductance Pathways in Epithelial Tissues

G. Sachs, J. G. Spenney, R. L. Shoemaker and M. C. Goodall

Department of Medicine, Department of Physiology and Biophysics, Division of Neurosciences, University of Alabama, Birmingham, Ala. 35294, U.S.A.

It has been shown that ionic conductance of the fundic area of gastric mucosa is via the cellular route, whereas in the antrum, conductance is by a shunt or paracellular pathway, using a variety of microelectrode techniques. Definition of the nature of the fundic conductance pathways has shown them to be largely neutral fixed-site (channel) ionophores of varying ion selectivity. Extraction of highly purified membrane fractions produces three separable channels—a cation, an anion and a non-selective channel, as measured after incorporation into an artificial bilayer. A model for proton transport, involving an electrogenic HCO_3^- ATPase pump shunted by a Cl^- channel, is discussed.

1. Introduction

Studies of epithelial transport may be divided into five phases:

(1) assessment of route of ionic conductance (cellular or paracellular);

(2) definition of ions transported actively or passively;

(3) definition of the properties of the elements responsible for the conductance (carrier, channel, charged or neutral);

(4) identification and isolation of components responsible for active transport;

(5) isolation and identification of components responsible for passive transport.

This paper will discuss some of these aspects.

2. Route of Transport through Epithelia

For many years it had been accepted as dogma that the major route of ion permeation through epithelia was cellular. More recently, however, it has been realized that there are two possible transport routes, cellular and paracellular (Diamond, Barry and Wright, 1971). Various techniques can be used to define the importance of each route (Diamond, Barry and Wright, 1971; Mandel and Curran, 1972). The most direct methods involve measurement of the cell membrane resistance of cells isolated from the epithelium and comparison of tissue resistances with those values. The paracellular conductance is obtained directly (Blum, Hirschowitz, Helander and Sachs, 1971). Alternatively, with the use of two microelectrodes, one to send current, the other to measure the change of p.d. in a distant cell (Frömter and Diamond, 1972), the cell membrane conductance can be calculated. Figure 1 shows the decay of voltage with distance for both Necturus fundus and Necturus antrum. Considering Necturus antrum we can readily derive values for the conductance of the cell membranes, and for the intact tissue. From the equation

$$g_{\text{shunt}} = g_{\text{tissue}} - g_{\text{cell}} \tag{1}$$

we find that the shunt conductance is about three times that of the cell conductance. Thus, most of the ionic flux upon sending current is paracellular, rather than cellular.

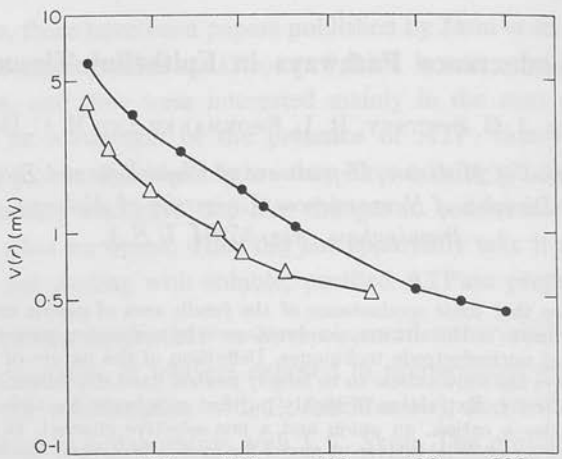

FIG. 1. The decay of voltage with distance from a current-sending microelectrode for fundus (△—△) and antrum (●—●) of Necturus gastric mucosa. Note the break in the curve for the fundus, due to the presence of a tubule.

For gastric fundus the situation is reversed, for in this case cellular conductance is about five times paracellular conductance. For this tissue, however, the analysis is more difficult since a series of indentations or tubules complicate the model of a simple two-dimensional sheet. This problem can be solved by considering the two systems separately, with the relative surface area contribution being the proportionality factor.

A third approach would compare the change of cell membrane p.d. to a change of transepithelial p.d. This can be done by sending current, or by changing the ionic content of one or other bathing solution. Figure 2 shows a typical result from Necturus fundic gastric mucosa using a

$$\Delta K^+ \times Cl^- = \text{Constant}. \qquad (2)$$

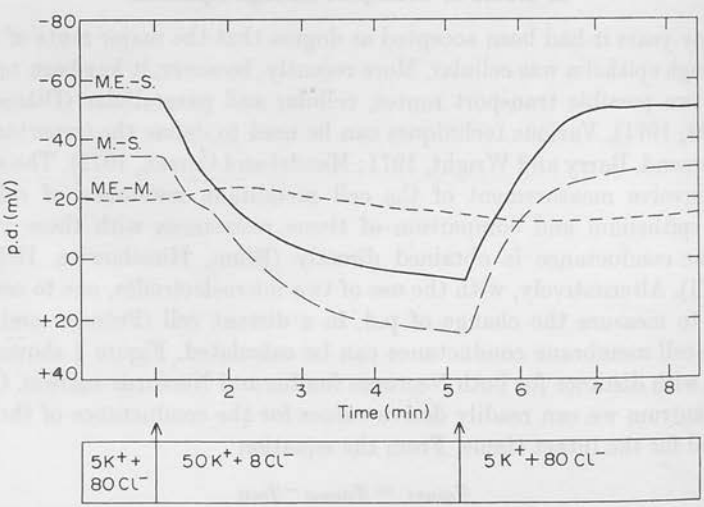

FIG. 2. The effect of a constant product KCl change on the serosal surface of Necturus gastric mucosa on the trans-tissue p.d.; the p.d. from cell to serosal bathing solution ($\Delta[K^+ \times Cl^-]$); and the p.d. from cell to mucosal solution.

Considering the equivalent circuit for a cellular conductance in parallel with a paracellular or shunt conductance

$$\Delta \text{p.d.}_{\text{tissue}} = \Delta \text{p.d.}_{\text{cell}} \cdot \frac{g_{\text{cell}}}{g_{\text{shunt}} + g_{\text{cell}}}. \quad (3)$$

From this, the greater the shunt/cell conductance ratio, the smaller will be the tissue p.d. change relative to the cell membrane change.

In gastric mucosa of Fig. 2, it can be seen that the change in the trans-tissue p.d. is almost the same as the change in the serosal membrane p.d. Hence from this line of reasoning, the shunt conductance is very low.

A fourth approach would consider the symmetry of the system to ionic concentration changes. If a paracellular route is the predominant one, we would necessarily find the tissue to have a symmetric response to ion changes. If the route were cellular, then unless the two membranes of the cell were identical, identical ion changes on either side of the tissue would give different p.d. responses. In the case of the fundic gastric mucosa, this is a highly asymmetric system, hence the paracellular contribution is minor.

In general, therefore, tissues may be classified as very leaky, such as gall bladder (Diamond, Barry and Wright, 1971), small intestine (Rosen and Schultz, 1971), proximal tubule of Necturus kidney (Boulpaep, 1971) (a shunt/cell conductance ratio of 10 × or more), moderately leaky such as gastric antral mucosa (a ratio of 5 or less), or tight, such as gastric fundic mucosa or distal tubule (a ratio of less than 1). Values such as these remain to be established for the cornea or ciliary body. The absence of anatomic tight junctions in the endothelium, and the lower than predicted Nernst potentials for ionic changes across the epithelial cell layer would argue for the cornea, at least, as being not tight. With a resistance of about 1000 Ω cm^2, we can speculate that this tissue could presumably be classified into the group of tissues such as the antrum.

3. Identification of Active Transport Components

It is relatively easy to identify the ions actively transported, by a knowledge of the p.d. and concentration gradients in vivo, or by the Ussing flux ratio test in vitro. In the case of the cornea both Na^+ and Cl^- are actively transported. The ciliary body may in addition transport HCO_3^-.

The best defined system responsible for transport in eukaryotic cells is the $Na^+ + K^+$ ATPase (Skou, 1965). Apart from the localization of the enzyme in the plasma membrane and its activation by Na + K, the best evidence for its role in Na^+ transport is the effect of ouabain. The role of this enzyme in Na^+ transport by epithelial tissues cannot depend upon its presence in the tissue because of its ubiquitous distribution (Bonting, 1970). The action of ouabain in inhibiting Na^+ flux within a few minutes is perhaps the most telling evidence available. If the action requires an hour or so, the ionic redistribution resulting from ouabain action is a more probable explanation of transport inhibition.

The other ATPase which has been implicated in ion transport by cell plasma membranes is the HCO_3^- stimulated ATPase first described in gastric mucosa (Kasbekar and Durbin, 1965) and subsequently in the pancreas (Simon, Kinne and Sachs, 1972). This enzyme probably plays a role in proton transport and for HCO_3^-/Cl^- exchange based on its localization and the action of some inhibitors.

One of the problems in assigning a role to this enzyme is its striking similarity to mitochondrial ATPase. Hence detailed cellular fractionation procedures had to be worked out, as well as methods of purifying the cell membrane. Figure 3 shows a distribution profile for various enzymes in a gastric mucosal homogenate. At 29.4% sucrose the fraction obtained contains almost exclusively smooth-surfaced membrane vesicles and fragments (Sachs, Shah, Strych, Cline and Hirschowitz, 1972). These two ATPases are so far the only ones described in the plasma membrane fraction of mammalian cells. Two other ATPases are involved in ion transport, the Ca^{2+} ATPase of sarcoplasmic reticulum (Martonosi, 1971) and the mitochondrial ATPase (Pressman, 1970).

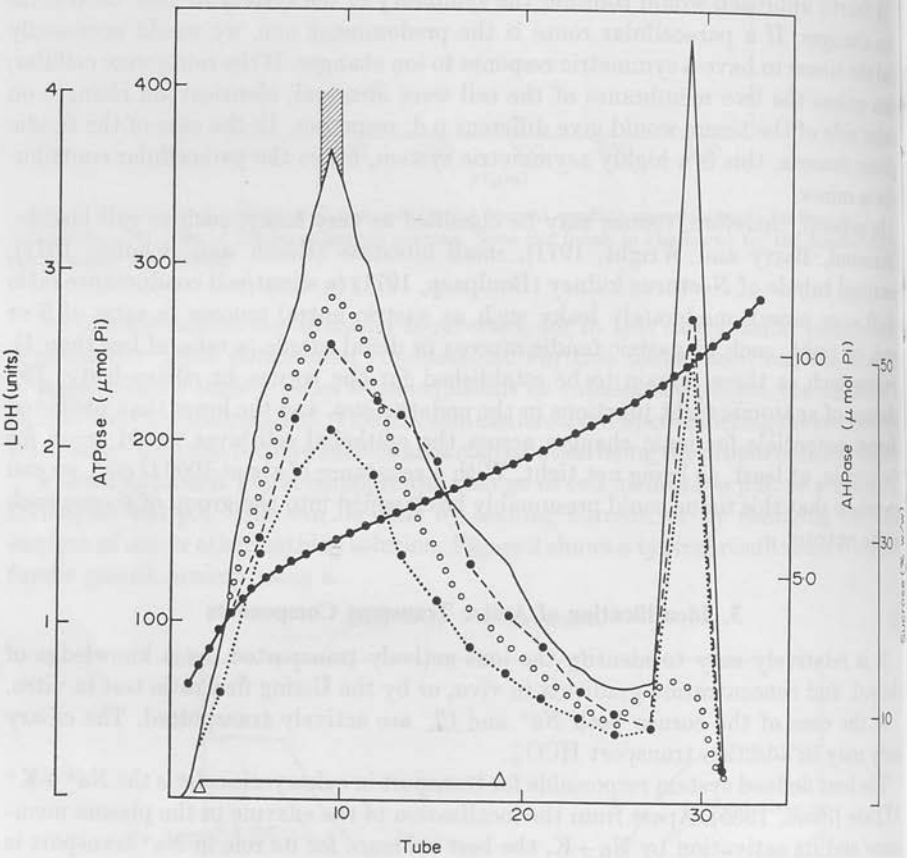

FIG. 3. Zonal pattern of 100,000 **g** precipitate (post 5000 **g**), showing activities of succinic dehydrogenase (SDH, △—△); lactic dehydrogenase (LDH), (○—○); Mg ATPase (. .); HCO_3^- ATPase (—); AMPase (- - -). The shaded area represents the tube used for the channel extraction.

Most of these enzymes appear to consist of 3–6 sub-units of unknown function, and also to involve an acyl group, a seryl group and a histidyl residue in the active center. This transport function could then depend on the action of one or more of these sub-units interacting with the ATPase site. A particularly appealing idea is that this sub-unit can act as an ionophore, i.e. induce conductance changes in artificial lipid bilayers. This type of ionophore may not only be associated with active transport, but may also be involved with the passive conductance properties of tissues. Using

purified membrane fractions as a source material, it would seem pertinent to attempt to establish whether such ionophores can be extracted in active form.

4. Eukaryotic Ionophores

Several ionophores have been extracted from bacteria, but to date, only nerve tissue or electroplax have been shown to contain such molecules (Goodall and Sachs, 1972). Epithelial tissues also, however, must contain such substances, based on direct experiments in intact tissue. For example, in the gastric mucosa we have shown, as outlined in the beginning of this paper, that the conductance pathway is cellular. This being the case, we can determine the types of molecules responsible for the conductance properties of the epithelium. Briefly we can attempt to distinguish between mobile and fixed sites (i.e. carriers and channels) charged and uncharged sites, anion, cation and non-selective sites. This approach is based on relatively simple experiments. For example, a linear current-voltage plot over a range greater than 150 V or so, would imply fixed site rather than mobile site transport. A linear relationship between ionic concentration and conductance suggests the presence of neutral ionophores such as gramicidin rather than charged ionophores, where initially one would expect a conductance independent of concentration. One can also compare relative ionic conductance by a variety of techniques such as p.d. changes under bi-ionic conditions, chemical flux studies, tissue conductance in the presence of the given ions and dilution potentials (Barry, Diamond and Wright, 1971). From all these techniques we can tentatively conclude that in the gastric mucosa, a major fraction of the conductance is accounted for by channels which are uncharged and are anion and cation selective.

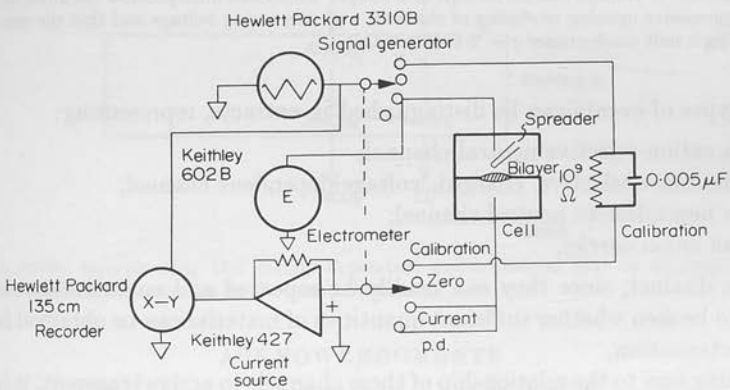

FIG. 4. Equipment used to study step conductance changes in an experimental bilayer, consisting of an X-Y recorder, a voltage source and current amplifier. An electrometer may be used in this set-up to measure zero current voltage and provision is made for conductance and capacitance calibration.

When the membrane fraction is extracted with Triton X–100, the extract at considerable dilution produces conductance changes in a bilayer composed of soybean lecithin. This system is illustrated in Fig. 4. It is designed to perform a current-voltage sweep using a voltage source and a current amplifier. Under suitable conditions, it can detect changes in conductance of about $10^{-11}\,\Omega^{-1}$. The conductance change can be determined directly by measuring the change in slope of the I–V curve. The selectivity of this change can be obtained in two ways. First, by measuring the zero

current potential in asymmetric solutions. Second, by determining the voltage at which the various slopes interesect, which has the advantage of being able to analyse single events. The effect of the membrane extract is shown in Fig. 5. Two points should be noted. One is the step nature of the slope change, suggesting the presence of channels. Second, is the fact that these changes occur at higher voltages, i.e. are voltage dependent.

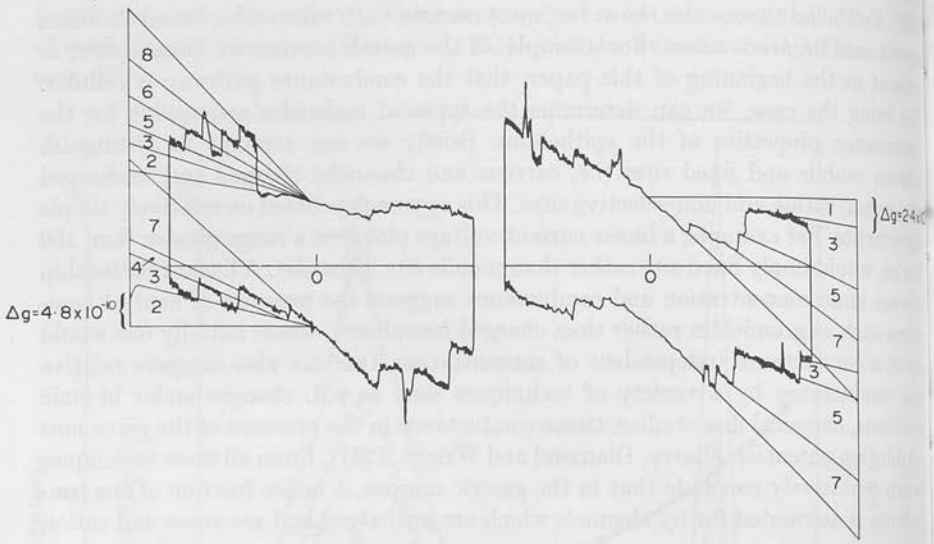

FIG. 5. Two successive voltage-current sweeps of a bilayer which has incorporated the anion selective channel. This illustrates successive opening or closing of channels with increasing voltage and that the size of the steps can be related to a single unit conductance $g = 2{\cdot}4 \times 10^{-10}\ \Omega^{-1}$.

Four types of events can be distinguished in extracts, representing:

(1) a cation-selective neutral channel;
(2) an anion-selective, charged, voltage-dependent channel;
(3) a non-selective neutral channel;
(4) an anion carrier.

These are distinct, since they can readily be repeated and considerably purified. It remains to be seen whether sufficient quantities of material can be obtained for chemical characterization.

Returning now to the relationship of these channels to active transport, it is possible to develop an hypothesis consistent with experimental data which combines the active transport characteristics of the ATPase, and the voltage-dependent anion channels.

Figure 6 illustrates such a model. In this the HCO_3^- ATPase acts as an electrogenic proton pump by removing OH^- or HCO_3^- from the secretory site. The voltage generated by this electrogenic model serves to open the anion channel, with ensuing flux of Cl^-, with a stoichiometric ratio to H^+ of one. In the absence of Cl^-, in the presence of SO_4'', where the measured $gCl^-/gSO_4'' = 6$, the flux through the channel will be considerably lower than the H^+ rate of the pump. Hence, instead of electroneutral secretion, direct evidence for the electrogenic nature of the H^+ pump may be obtained under these conditions, as has been done.

To summarize this last section, we have demonstrated not only the occurrence of ionophores in vertebrate cell membranes, but we have also succeeded in, at least, their electrical characterization and separation. This would argue well for the hope that the passive conductance properties of epithelial tissue will be described in molecular terms.

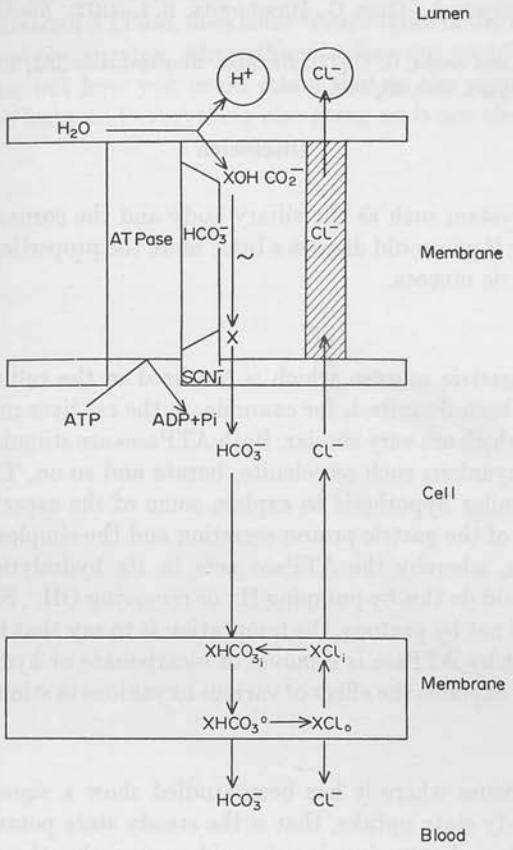

FIG. 6. A model incorporating the voltage-dependent anion channel into an electrogenic HCO_3^- ATPase mechanism for H^+ secretion by the gastric mucosa.

ACKNOWLEDGMENTS

Supported by NIH AM08541, GM18721, Cancer and Cardiovascular Training and Research Grants, NSF Grant GB31075, Veterans Administration Hospital, Birmingham, Ala., and Smith Kline and French Laboratories, Philadelphia, Pa.

REFERENCES

Barry, P. H., Diamond, J. M. and Wright, E. M. (1971). *J. Memb. Biol.* **4**, 358.

Blum, A. L., Hirschowitz, B. I., Helander, H. F. and Sachs, G. (1971). *Biochim. Biophys. Acta* **241**, 261.

Bonting, S. L. (1970). In *Membranes and Ion Transport* (Ed. Bittar, E.) Vol. 1, p. 257.

Boulpaep, E. L. (1971). In *Electrophysiology of Epithelial Cells*. p. 91. Schattauer-Verlag, Stuttgart.

Diamond, J. M., Barry, P. H. and Wright, E. M. (1971). In *Electrophysiology of Epithelial Cells*. p. 23. Schattauer-Verlag, Stuttgart.

Frömter, E. and Diamond, J. M. (1972). *Nature (London)* **235**, 9.
Goodall, M. C. and Sachs, G. (1972). *Nature (London)*, **237**, 252.
Kasbekar, D. K. and Durbin, R. P. (1965). *Biochim. Biophys. Acta* **105**, 672.
Mandel, L. J. and Curran, P. F. (1972). *J. Gen. Physiol.* **59**, 503.
Martonosi, A. (1971). In *Biomembranes* (Ed. Hanson, L. A.) p. 191.
Pressman, B. C. (1970). In *Membranes of Mitochondria and Chloroplasts* (Ed. Racker, E.) p. 213.
Rosen, R. C. and Schultz, S. G. (1971). *J. Gen. Physiol.* **57**, 639.
Sachs, G., Shah, G., Strych, A., Cline, G., Hirschowitz, B. I. (1972). *Biochim. Biophys. Acta* 266, 625.
Simon, B., Kinne, R. and Sachs, G. (1972). *Biochim. Biophys. Acta* **282**, 293.
Skou, J. C. (1965). *Physiol. Rev.* **45**, 596.

Discussion

Dr Zadunaisky

In some ocular system such as the ciliary body and the cornea there is a chloride pump and I wonder if you could discuss a little more the properties of the bicarbonate ATPase of the gastric mucosa.

Dr Sachs

The ATPase of gastric mucosa which is localized in the cell membrane and the ATPase which has been described, for example, in the rat liver mitochondria, have a class of properties which are very similar. Both ATPases are stimulated by bicarbonate and many other oxyanions such as selenite, borate and so on. The temptation is to try and make a similar hypothesis to explain some of the aspects of mitochondrial transport and that of the gastric proton secretion and the simplest hypothesis is the Mitchell hypothesis, whereby the ATPase acts in its hydrolytic sense to separate H^+ and OH^-. It could do this by pumping H^+ or removing OH^-. Since it is stimulated by bicarbonate and not by protons, the temptation is to say that the actual transport reaction carried out by ATPase is removal of bicarbonate or hydroxyl or carbonate. That being the case explains the effect of various oxyanions in stimulating the ATPase.

Dr Neville

A good many tissues where it has been studied show a sigmoid-type potassium equilibrium or steady state uptake, that is the steady state potassium concentration as a function of external potassium is a sigmoid curve rather than a Michaelis-Merten or hyperbolic function. This has been postulated to come from some kind of a co-operative potassium sodium uptake mechanism. Do you see multivalent ATPases which could account for this in the first place? And in the second, when you put the ATPases into your artificial membrane do you see any evidence of co-operativity in the transport?

Dr Sachs

Let me answer the second question first. The thing I was emphasizing today was the capacity to study, perhaps, some of the passive conductance properties of epithelia in artificial membranes. It has nothing to do with the active transport component. We are not looking at active transport. These are just the presence of ion-conducting channels.

Dr Neville

But didn't you postulate this to have come from sodium potassium ATPase?

Dr Sachs

What I said was, this was prepared from the purified gastric membrane fraction. Now it may be associated with ATPases for a certain while during purification, but after that probably it will dissociate away from it. So all it has to be is present in the same membrane. It doesn't have to be part of the molecule. Now, in answer to the first question, the only good evidence that there are, perhaps, conformational changes in sodium potassium ATPase, does come from studies of the kinetics of sodium potassium activation of the enzyme, where there is clear-cut co-operativity between sodium and potassium, but how you could relate that to the sigmoid plot of intact tissue where you have leaks and everything else going on is not clear.

Reprinted from

Biochimica et Biophysica Acta
Elsevier Publishing Company, Amsterdam - Printed in The Netherlands

BBA 75675

ELECTRICAL PROPERTIES OF ISOLATED CELLS OF NECTURUS GASTRIC MUCOSA

A. L. BLUM, B. I. HIRSCHOWITZ, H. F. HELANDER AND G. SACHS*

Division of Gastroenterology, Department of Medicine, University of Alabama, and Veterans Administration Hospital, Birmingham, Ala. (U.S.A.)

(Received February 1st, 1971)

SUMMARY

A micropuncture technique is described for isolated surface epithelial cells and oxyntic cells of Necturus gastric mucosa, and for intact isolated tubules from the same tissue. The potential obtained is similar to that found for the cells in the intact tissue, whereas the measured membrane resistance is about 100 times higher. This is explained by cell–cell coupling in the intact mucosa, and is confirmed by direct two-electrode experiments in the intact tissue or isolated tubule. The calculated tissue resistance is about twice as high as the measured resistance after allowance is made for glandular infolding, hence the possibility remains that there is a low resistance shunt across the tissue.

INTRODUCTION

A description of electrical events on the cellular level associated with transport by the gastric mucosa is complex for the following reasons: The gastric mucosa is a heterogeneous tissue composed of several cell types with different morphological and functional characteristics. Evidence has been presented that these cells contain two or more electromotive forces which may lead to different and independent changes of potential (PD) across mucosal and serosal surface of the plasma membrane[1,2]. In analogy to other epithelial tissues, cells of the same type may be electrically coupled along linear or circumferential pathways, while electrical coupling may or may not exist between different cell types[3]. It is thus apparent that results obtained by placing a microelectrode into a cell of intact mucosa may not give information on independent electrical properties of this cell[4]. Furthermore, such studies do not allow an estimate of the magnitude of intercellular conductive shunts which in analogy to gallbladder[5] and other tissues[6] might constitute major pathways of ion flux across the mucosa. An additional disadvantage of microelectrode studies in intact gastric mucosa is the visual inaccessibility of the gastric glands, which contain the oxyntic cells.

In the present paper, a new method for the study of electrical properties is described, which involved preparation and subsequent micropuncture of isolated intact cells of the gastric mucosa and isolated gastric tubules. The spread of current

Abbreviation: PD, potential difference.

* To whom correspondence should be addressed.

in oxyntic and surface cell systems is examined by simultaneous measurements in two cells. It may thus be shown that surface and oxyntic cells in intact mucosa are electrically coupled while significant intercellular conductive pathways may also be present. In addition, micropuncture studies in isolated cells may allow an assessment of the electrical properties of specific cell types under a variety of conditions.

METHODS

Isolated Necturus gastric cells were prepared by the pronase technique as previously described[7]. Stripped Necturus gastric mucosa was pinned mucosal surface upwards on the bottom of a lucite dish and shaken in HCO_3^- buffered frog Ringer containing 0.175 % pronase for 120 min. The cell suspension thus obtained was centrifuged at 50 g for 5 min, washed twice in frog Ringer and resuspended either in frog Ringer's solution or in a solution containing 18.5 mM K^+ with correspondingly lower Na^+ levels.

Isolated gastric gland tubules were prepared by a modification of the pronase technique. In this case stripped mucosa was incubated for one hour and then rapidly shaken in pronase solution. Clumps of cells and isolated tubules were readily obtained.

Fig. 1 shows the experimental arrangement used for micropuncture of isolated cells. The cell suspension was placed on the agar filled depression of a microscope culture slide. The cell types were identified under a stereomicroscope. Oxyntic (i.e. acid secreting) cells could be differentiated by their size and granular appearance from other cells such as surface cells[7].

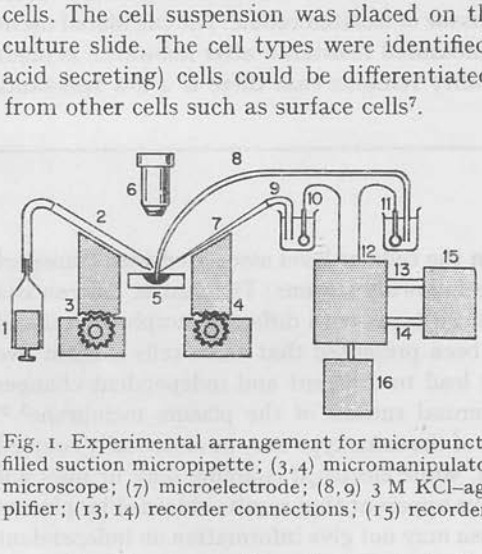

Fig. 1. Experimental arrangement for micropuncture of isolated cells: (1) oil filled syringe; (2) oil filled suction micropipette; (3, 4) micromanipulators; (5) agar filled microculture slide; (6) stereomicroscope; (7) microelectrode; (8, 9) 3 M KCl–agar bridge; (10, 11) calomel electrodes; (12) amplifier; (13, 14) recorder connections; (15) recorder or CRO; (16) current source.

For the preparation of microelectrodes, glass capillary tubing was precleaned in chromic acid and alcohol and mounted on a Nastuk electrode puller[8] (Industrial Science Associates) with a 4-mm platinum loop. Microelectrodes were examined microscopically and were filled with 3 M KCl. Their tip resistance was about 50 mΩ and their tip potential was less than 3 mV. As shown in Fig. 1, they were held by a micromanipulator and connected to a WP4 amplifier and thence to a Grass recorder. The amplifier also had provision for sending and monitoring current and a Wheatstone bridge circuit for balancing the electrode response to current before starting a cell puncture.

A micropipette with a tip diameter of approx 5 μm was used for trapping of

isolated cells and immobilizing them during micropuncture. This pipette was also pulled on a Nastuk puller from precleaned capillary tubing. The tip was then broken against the platinum wire of a de Fonbrunne microforge and fire polished. The micropipette was filled with oil from a Hamilton microsyringe and connected to a suction system, as shown in Fig. 1, care being taken to exclude air bubbles.

When isolated tubules and pieces of intact mucosa were used for obtaining cell potentials, each micromanipulator held a microelectrode. In this way potential recordings could be obtained from 2 cells simultaneously, allowing, for example, current injection into one cell, and recording potential changes in a distant cell.

Micropunctures were considered successful when the measured potential difference remained stable for at least 10 sec. Cell membrane resistance was calculated using Ohm's law from the change in potential produced by a 1–2-sec pulse of 10^{-9} A sent through the intracellular electrode. For obtaining current–voltage curves hyper- and de-polarizing current pulses of varying intensity and 0.5–1-sec duration were sent through the microelectrode, and the change in potential difference plotted against amount of current injected.

Morphological studies were performed on intact mucosae as well as on isolated cells from five animals. After fixation in an ice-cold 1 % solution of OsO_4, veronal acetate buffered to pH 7.4 (ref. 9), the tissues were embedded in Epon. 1-μ-thick sections were cut in an ultramicrotome and stained with toluidine blue, or by the periodic acid–Schiff method. In each of 4 sections from each of 5 animals, the relative surface area of the gastric gland lumina and of the mucosal surface was estimated in intact mucosae by counting the intercepts between these surfaces and the lines of a super-imposed grid (for further details on this method see WEIBEL AND ELIAS[10]).

Additional morphological information was obtained by electron microscopy on thin sections of the same tissues mentioned above. The sections were contrasted with lead hydroxide followed by uranyl acetate and examined in a Philips EM 200 electron microscope at 60 kV. The relative surface area of isolated oxyntic cells were estimated by the method described above, and compared with the surface of smooth spheres of the same diameter.

RESULTS

Potential of isolated cells

Stable PD readings were obtained in about 50 % of the punctures attempted. Failures occurred in cells which disintegrated or swelled while being held by the micropipette or upon puncture by the microelectrode. Cells which appeared swollen prior to puncture or cells with a grossly irregular surface had a PD of less than 5 mV. Further studies, therefore, were confined to cells without morphologic signs of damage such as swelling and irregular surface. Fig. 2 shows a PD recording obtained from an oxyntic cell. The duration of this recording was 20 min. Other recordings were obtained for as long as 60 min with less than 10 % decay in PD. In most cases long-term stability of the PD was not tested, and the electrode was removed from the cell after 1–5 min. In a representative batch of 67 cells the PD ranged from values of about 10 to 90 mV, with a mean ($\pm$ S.E.) of 44 $\pm$ 3 mV (Fig. 3).

In control experiments the PD was determined in surface cells of intact mucosa, and compared to the PD in isolated surface and oxyntic cells. The experimental ar-

rangement was similar to that used for isolated cells (Fig. 1). The mean (± S.E.) PD for the surface cell in the intact mucosa was 43 ± 8 mV. The effect of K^+ concentration change on the PD of isolated oxyntic cells was also measured. When K^+ was increased from 4 to 18.5 mM and Na^+ correspondingly decreased, the PD fell by 17 mV (Table I).

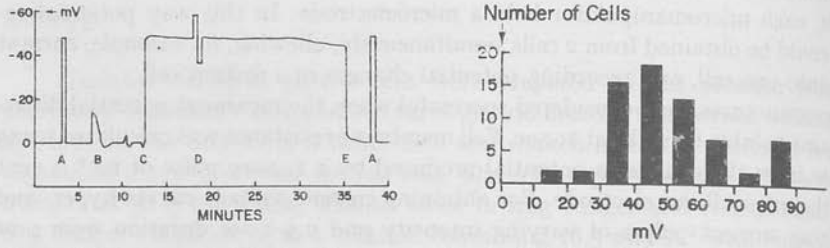

Fig. 2. Cellular potential obtained from oxyntic cell. At A tip resistance is measured, at B current is sent through the electrode and balanced out through the Wheatstone bridge, at C the cell is punctured, at D current is sent in both directions through the electrode, at E the electrode is removed from the cell, and at A tip resistance is checked.

Fig. 3. The distribution of potential difference obtained from a batch of 67 cells.

TABLE I

INTRACELLULAR POTENTIALS

Values in mV ± S.E.

Isolated surface epithelial cells 4 mM K^+	*Isolated oxyntic cells 4 mM K^+*	*Isolated oxyntic cells 18.5 mM K^+*	*Surface epithelial cells in intact mucosae 4 mM K^+*
36 ± 11	48 ± 6	31 ± 5	43 ± 8
$N = 12$	$N = 22$	$N = 11$	$N = 15$

Resistance of isolated cells

In Fig. 4 the resistance of 17 oxyntic cells is plotted against the measured cell PD. There is no simple relationship between PD and resistance. More detailed resistance studies were carried out as discussed below.

Current voltage curve

Fig. 5 shows current–voltage plots obtained from an isolated surface cell and from a surface cell in intact gastric mucosa, the slope representing the resistance of the system. There is a striking difference in slope between the two experiments. Since in this and all other experiments a uniform and statistically significant curvature ($P < 0.001$) was observed, the slope was calculated from the tangent of a curve which was defined by a cubic equation forced through the origin. The calculated tangents for isolated surface cells, isolated oxyntic cells and surface cells in intact mucosa are given in Fig. 6. Similar values were found for isolated oxyntic cells and surface cells, while the mean obtained for isolated surface cells was about 100 times greater than the mean of intact mucosa ($1.5 \pm 0.3 \cdot 10^8$ and $1.6 \pm 0.2 \cdot 10^6 \Omega$, respectively, $P < 0.0001$).

Two electrode system

When stable PD readings were obtained in two surface cells of intact gastric mucosa, a current pulse was applied to one cell and the deflections of PD in both cells were recorded. A PD deflection in the distant cell was used as expression of electrical coupling. An estimate of the type of electrical coupling was obtained by systematic circumferential puncture of surface cells around the cell which contained the current sending electrode. Electrical coupling was found in 10–20 % of the cells with a radial distance of up to 100 μm, *i.e.* about 1–10 cells away from the current sending electrode.

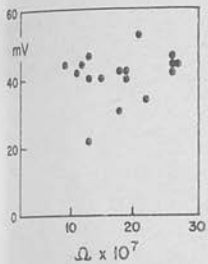

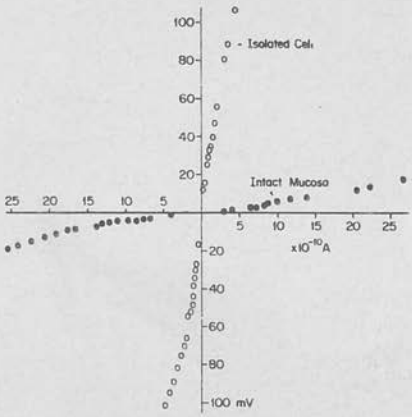

Fig. 4. Resistance of 17 oxyntic cells plotted against PD of the cells showing little correlation.

Fig. 5. Current–voltage plot for the surface epithelial cell in the intact mucosa and when isolated, showing a marked difference in slope, and non-linearity in the depolarization (downward) direction.

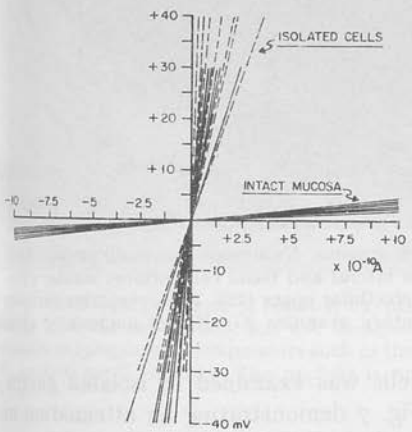

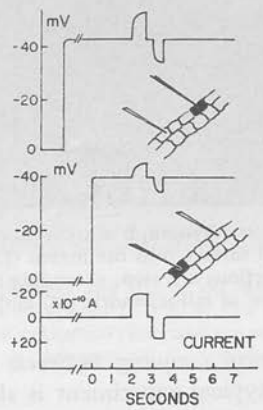

Fig. 6. Calculated tangents to the current–voltage curves obtained for intact mucosa and isolated cells. The tangents were obtained from the equation $y = ax^3 + bx^2 + cx$, solid lines are surface cells, broken lines are oxyntic cells.

Fig. 7. Experiment demonstrating coupling in isolated tubules of Necturus gastric mucosa. The upper electrode is used for recording PD and sending current, and the other electrode records PD changes in another cell. The bottom trace records the amount of current sent.

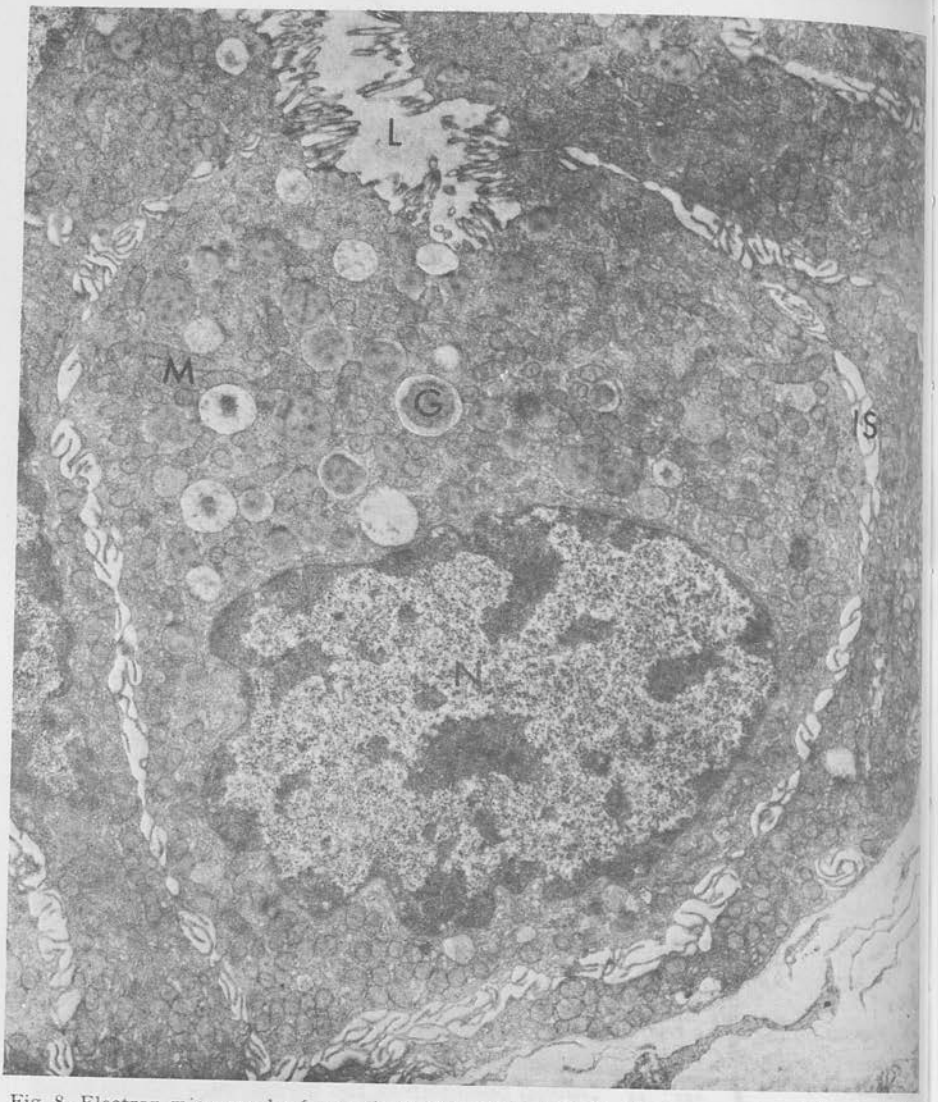

Fig. 8. Electron micrograph of oxyntic cell in gastric mucosa. Numerous microvilli project from the apical cell surface into the lumen (L). Along the lateral and basal cell surfaces similar cytoplasmic projections are seen, extending into the intercellular space (IS). The cytoplasm contains a large number of mitochondria (M) and some secretory granules (G). N, cell nucleus. × 4300.

Electrical coupling between oxyntic cells was examined in isolated gastric tubules. A typical experiment is shown in Fig. 7 demonstrating an attenuation of the current pulse of 50 % over a distance of only 3 cells. In other experiments, the distance for 50 % attenuation was 4–5 cells.

Morphologic observations

The increase in surface area of the mucosa caused by the infoldings of the gastric glands was calculated to be 2.7 ± 0.10 (S.E.) for 5 animals. In the dog the increase

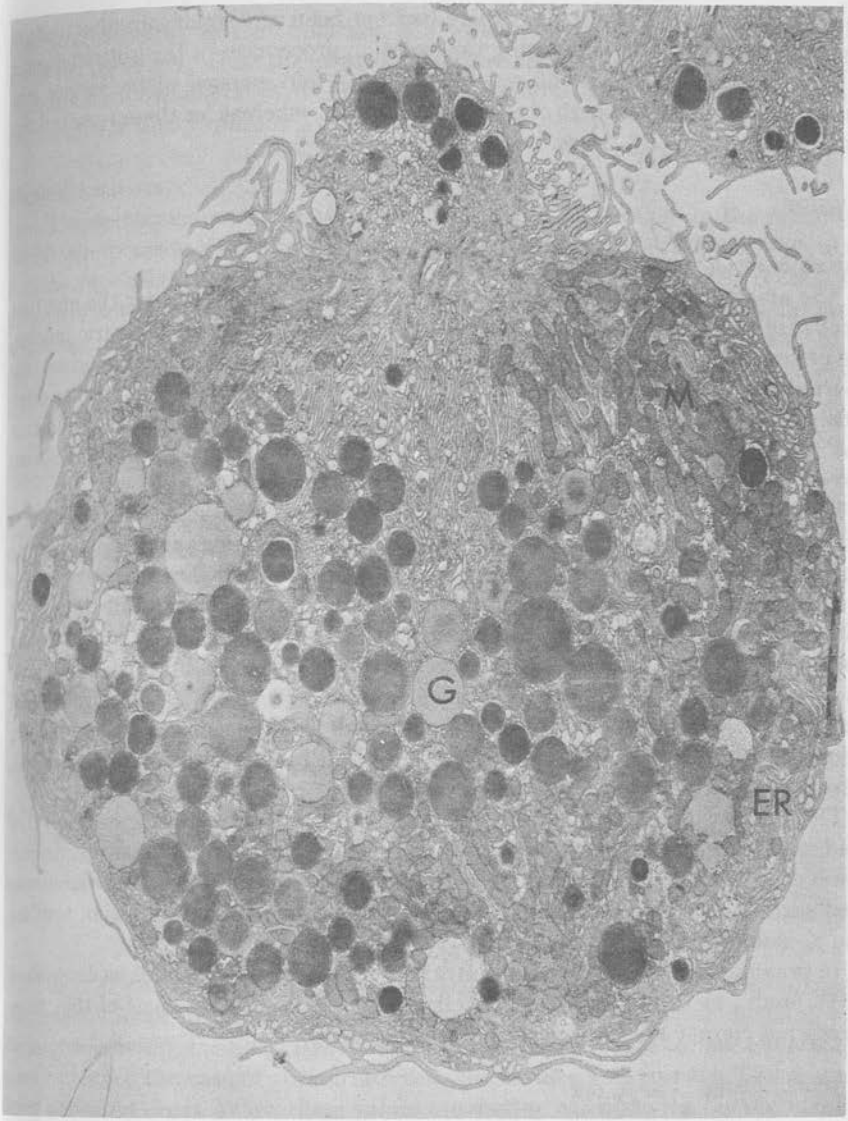

Fig. 9. Electron micrograph of isolated oxyntic cell. The number and size of the microvilli projecting from the cell surface has not changed greatly, as compared to Fig. 8. The general appearance of cytoplasmic components such as the endoplasmic reticulum (ER) and the mitochondria (M) suggest good viability. The nucleus is not included in this section. G, secretory granule. × 4300.

is 13 times (ref. 11). On this basis the mucosal surface of the tissue consists of approx. 37% surface cells and 63% oxyntic cells. These values were used for calculation of the specific resistance from values obtained from isolated cells.

Electron micrographs of oxyntic cells from intact mucosa as well as in the isolated state are shown in Figs. 8 and 9. The isolated oxyntic cells showed evidence of good

morphologic integrity and also that there had not been any significant alterations in surface infoldings or microvilli during the isolation procedure. In the isolated oxyntic cells the infoldings and microvilli resulted in a 3–5-fold increase of the surface area as compared to a smooth sphere of the same diameter, whereas for the surface cell this increase amounted to 1.5 times.

DISCUSSION

Potentials of isolated cells

The ability to perform micropunctures in isolated cells allows for the first time a direct assessment of functional properties in specific cell types of gastric mucosa. In the present study, the transmembranal PD of nonstimulated isolated mucosal cells is reported (Table I, Fig. 3). The average PD of these cells is 44 mV and is not significantly different from values obtained from pieces of intact mucosa. It would thus appear that the isolation procedure does not lead to damage of the cell membrane and/or of the mechanisms which are responsible for the PD.

This interpretation should, however, be accepted with some caution since a spuriously normal PD in cells with a damaged plasma membrane could be due to leak of KCl from the microelectrode into the cell. Such a leak would have relatively little effect on the PD of electrically coupled cells of intact mucosa, while in isolated cells its effect would be proportionately much greater. In the present study, the use of fine tip electrodes minimized the occurrence of leakage. A leak is also improbable on the basis of observations with KCl filled microelectrodes in electrically coupled and uncoupled cells of intact toad bladder. If a leak would occur in this preparation, electrical uncoupling of a punctured cell would result in an apparent increase of PD. However, no such increase is observed[3].

The PD of isolated surface cells was not significantly different from the PD of isolated oxyntic cells. Further confirmation of this observation by different techniques is, however, necessary since it has been shown in previous studies that viability of isolated surface cells is lower than of oxyntic cells which in eosin exclusion tests are 80–100 % viable[7].

In previous studies, the K^+ concentration of isolated oxyntic cells as determined by a [^{14}C]inulin method was 67 mM /l cell water (ref. 7). On the basis of this value, the predicted Nernst PD for a perfect K^+ electrode is:

$$\mathrm{PD} = \frac{RT}{nF} \ln \frac{67}{4} = 70 \text{ mV}$$

This value is considerably higher than the PD observed in oxyntic cells, suggesting that the oxyntic cell membrane is permeable to ions other than K^+, such as Cl^- or Na^+. An alternate explanation is that cell injury has occurred, either due to the isolation procedure, or due to the puncture itself. In the latter case, decay of the measured potential from some higher value would be likely to be observed, which was not generally found. Injury due to the isolation procedure is more difficult to exclude, but values of 70 mV have never been observed by us for intracellular potentials even with multiple deep punctures of intact mucosa, where penetration of oxyntic cells is highly probable.

Similar conclusions may be reached from the PD response to change of K^+

concentration in the nutrient solution. A 4.5-fold increase in K^+ leads to a reduction of the PD by 17 mV, while the expected decrease for a membrane with selective permeability for K^+ would be 38 mV. These findings closely correspond to observations in surface cells of intact mucosa[4].

Membrane resistance

The membrane resistance was calculated in all instances from the deflection of the PD in response to a standard current pulse. A more accurate estimate was obtained from the slope of current voltage plots (Figs. 5 and 6). In order to express the resistance per area of cell membrane, the surface area of isolated cells was estimated on the basis of findings in phase contrast microscopy. Thus, isolated surface cell and oxyntic cell are spheres with a radius of 10 μm and 15 μm, respectively, and their resistances are 1800 and 2730 $\Omega \cdot cm^2$, respectively (Table II).

TABLE II

The values obtained for cell dimensions, voltage current slopes and calculated membrane core resistance and space constants for the surface cell, intact mucosa, oxyntic cell and isolated tubule. The values in parentheses are those corrected for infolding of the plasma membrane of the isolated cell as measured in electron micrographs.

	Surface cell		*Oxyntic cell*	
	Intact	*Isolated*	*Tubule*	*Isolated*
Cell dimensions (μm)	30 × 10	$r = 10$	$r = 15$	$r = 15$
V_0/I_0 (Ω)	$1.6 \cdot 10^6$	$1.5 \cdot 10^8$	$7 \cdot 10^6$	$2.0 \cdot 10^8$
R_m ($\Omega \cdot cm^2$)	—	1800 (2700)	—	2730 (8190)
R_e ($\Omega \cdot cm$)	50	—	800	—
Space constant (μ)	1400	—	400	—

Since the relative surface area of isolated oxyntic cells was calculated in electron micrographs to be 3–5 times greater than estimated for a smooth surfaced sphere (lacking microvilli), the estimates for specific membrane resistance are too low by the same factor. In the case of the surface cell, the surface area increase was much less, being about 1.5 times. When these values are used to calculate the specific membrane resistance of the surface cell and oxyntic cell, the values obtained are 2700 and 8190 $\Omega \cdot cm^2$, respectively.

Since the specific membrane resistance of the resting oxyntic cell is considerably higher than that of the surface cell, the larger portion of the tissue conductance in the resting mucosa is accounted for by the conductance of the surface epithelial cell system.

Transmucosal electrical shunts

If such shunts were present, the resistive properties of intact tissue could not be predicted on the basis of findings in isolated cells. In the following section, therefore, predicted and observed resistance of intact mucosa are compared.

Since the resistance R_m of mucosal (or apical) membrane and the resistance R_s of serosal (or basal) membrane in isolated cells are electrically in parallel, the total resistance R_t is:

$$R_t = \frac{R_m \cdot R_s}{R_m + R_s}$$

In the intact mucosa R_m and R_s are electrically in series and thus resistance of the intact mucosa (R) in the Ussing chamber is:

$$R = R_m + R_s$$

If R_m and R_s are assumed to be of equal magnitude, a minimal value for R is obtained which is 4 times the R_t value.

For a mucosa such as the one shown in Fig. 8 whose surface area consists of 63 % oxyntic cell surface and of 37 % surface cell surface, the calculated resistance is approximately:

$$R = 5000\ \Omega \cdot cm^2$$

The observed value of R for intact resting Necturus gastric mucosa in an Ussing chamber is $710 \pm 47\ \Omega \cdot cm^2$ assuming the area is given by the dimensions of the chamber[12]. If the 2.7-fold increase in surface area by the tubular infoldings is taken into account, the corrected observed resistance was $2000\ \Omega \cdot cm^2$. This value can be compared to the value calculated above from isolated cell measurements since in both cases it was assumed the cells had a smooth surface.

It is apparent that the predicted resistance of Necturus gastric mucosa is about twice the observed value. On this basis, therefore, the possibility is not excluded that there are intercellular resistive shunts similar to other tissues such as the gall bladder[4] and the tubule of Necturus kidney[6].

Comparisons of this type would be misleading if the surface area of the mucosal cells would change during isolation. However, by comparing electron micrographs of isolated cells and of cells in the intact mucosae it appeared that there was no major difference in the surface area or the size of the cells under the two conditions.

Another possibility is that there is a qualitative change of the cell membrane as a result of isolation. Gross damage to the membrane is probably excluded by a number of observations such as eosin exclusion, O_2 consumption and good morphology[7]. In addition the cellular Na^+ and K^+ content appears to be the same as for intact tissue[13].

Formation of an altered surface layer, with a resultant increase of resistance is, however, not excluded by these observations. In fact, proteases including pronase have been shown to have stimulatory effects on cell division by initiating escape from contact inhibition[14]. Internal perfusion of squid axon with pronase, however, increased membrane conductance[15]. Since there was no change of surface area upon isolation, the effect of pronase would have to be on the composition of the membrane to account for the increased resistance. In this process, there can be no alteration of relative K^+ conductance since there was no alteration in the response to extracellular K^+ concentration changes.

Electrical coupling

The resistive properties of isolated surface cells and of surface cells in intact mucosa were examined in current voltage plots (Figs. 5 and 6). As shown by the 100-fold difference in slope, the resistance measured in intact mucosa is much lower than in isolated cells. This difference cannot be explained by a reduction in surface area of the cell membrane during the process of isolation. More likely is the presence of low resistance pathways between cells of intact mucosa which are not present in isolated cells. Such pathways have been described by LOEWENSTEIN AND KANNO[16] who observed electrical coupling between epithelial cells and the movement of fluorescent dyes across cell junctions. This low resistance R_c is electrically in parallel with the membrane resistance R_m with respect to an intracellular current source and is — in the present study — about 100 times smaller than R_m.

Since even in close proximity to the surface cell which receives current pulses only a small proportion of the cells show signs of electrical coupling, circumferential spread of current is very unlikely. A more likely model for the type of coupling assumes radial spread of current along a "cell cable" with a low core resistance R_c and a high resistance of the insulating membrane sheath R_m. For such a cable LOEWENSTEIN AND KANNO[16] derived the following equation:

$$R_m = \lambda c \frac{V_0}{I_0} \tanh \frac{L}{\lambda} \qquad (1)$$

where λ is the space constant and is defined by $\lambda = \sqrt{r_m/r_i}$, r_m is the resistance of unit length of the insulating membrane sheath in Ω/cm, r_i is the resistance per unit length of the core conductor in Ω/cm, c is the circumference of the "cell cable", V_0 is the value of potential difference at the current source, I_0 is the total current flowing into the core from the internal electrode, and L is the total length of the core conductor. For surface cells of intact tissue, c is $80 \cdot 10^{-4}$ Ω/cm and V_0/I_0 as obtained in a current voltage plot is $1.6 \cdot 10^6$ Ω. Since in intact tissue $L \gg \lambda$, $\tanh L/\lambda = 1$. The value of $R_m = 1800\ \Omega \cdot cm^2$ is obtained from measurements in isolated surface cells where the low core resistance is absent and therefore total observed resistance $R = R_m$. Thus, λ may be calculated from Eqn. 1 and is approx. 1400 μm. The core resistance R_c is defined by:

$$R_c = \frac{a}{\lambda} \cdot \frac{V_0}{I_0} \tanh \frac{L}{\lambda} \qquad (2)$$

where a is the crosscut area of the "cell cable". For surface cells, R_c is thus about $50\ \Omega \cdot cm$.

Calculations similar to those given for surface cells are more difficult in the case of oxyntic cells. Verifiable puncture of oxyntic cells in intact mucosa is at present technically not possible since localization of the electrode tip deep in the tissue has not been attempted. Thus the current voltage plot (Fig. 6) allows only comparison of isolated oxyntic cells with surface cells of intact mucosa. It may, however, not be permissible to compare properties of two different cell systems. Furthermore, the assumption that $L \gg \lambda$ cannot readily be made for Necturus gastric tubules. Gastric tubules are relatively short (about 0.5 mm) and electrical coupling between oxyntic cells and surface cells has not yet been demonstrated. An attempt was, therefore,

made to measure λ directly with a two-electrode system in isolated gastric tubules. A representative experiment is shown in Fig. 7. It is apparent that a 50% attenuation of the PD response occurs across a few (3–5) cells. However the measurement of cell separation assumes that there is a direct path between the two electrodes, and no branching in this pathway. With these reservations, the apparent space constant in the tubule is of the order of 150 μ, since the cell diameter is 30 μ. If true, an additional artefact has to be considered, namely, rupture of the intercellular junctions by the action of pronase used in the tubule preparation.

Alternatively, the slope of the voltage current curve for the isolated tubule ($7.0 \cdot 10^6$) can be used for the calculation of λ and R_c by the same method as for the surface cell. With this method the space constant is about 400 μ, and the core resistance is about 800 $\Omega \cdot$cm. Again, due to the pronase treatment, these values are subject to revision when techniques for definitive puncture of oxyntic cells in the intact mucosa become available.

ACKNOWLEDGEMENTS

This investigation was supported by National Institutes of Health. Grants AM09260, TIAM 2A-5286 and AM08541, and National Science Foundation Grant GB8351 and by the Swedish Medical Research Council Grant B-71-12R-3279.

REFERENCES

1 J. B. HARRIS AND I. S. EDELMAN, *Am. J. Physiol.*, 206 (1964) 769.
2 W. S. REHM, *Fed. Proc.*, 24 (1966) 1387.
3 W. R. LOEWENSTEIN, S. J. SOCOLAR, S. HIGASHINO, Y. KANNO AND N. DAVIDSON, *Science*, 141 (1965) 295.
4 G. SACHS, R. L. SHOEMAKER, A. L. BLUM, G. M. MAKHLOUF AND B. I. HIRSCHOWITZ, *Symp. Med. Hoechst*, in the press.
5 J. M. DIAMOND, *Symp. Med. Hoechst*, in the press.
6 E. M. BOULPAEP, *Symp. Med. Hoechst*, in the press.
7 A. L. BLUM, G. T. SHAH, V. D. WIEBELHAUS, F. BRENNAN, H. F. HELANDER AND G. SACHS, *Gastroenterology*, in the press.
8 J. T. ALEXANDER AND W. L. NASTUK, *Rev. Sci. Instrum.*, 24 (1953) 528.
9 H. F. HELANDER, *J. Ultrastruct. Res. Suppl.*, 4 (1962) 1.
10 G. R. WEIBEL AND H. ELIAS, *Quantitative Methods in Morphology*, Springer, Berlin, 1967.
11 C. A. CANOZA AND W. S. REHM, *Gastroenterology*, 35 (1958) 292.
12 R. L. SHOEMAKER, B. I. HIRSCHOWITZ AND G. SACHS, *Am. J. Physiol.*, 212 (1967) 1013.
13 H. W. DAVENPORT AND F. ALZAMORA, *Am. J. Physiol.*, 202 (1962) 1710.
14 M. M. BURGER, *Nature*, 227 (1970) 170.
15 E. ROJAS AND C. ARMSTRONG, *Nature*, 229 (1971) 177.
16 W. R. LOEWENSTEIN AND Y. KANNO, *J. Cell Biol.*, 22 (1966) 565.

Reprint from

Electrophysiology of Epithelial Cells

Symposium, Schloß Reinhartshausen/Rhein
October 12th/13th 1970

Chairman: **Prof. Dr. G. Giebisch**

With 132 figures
and 24 tables

F. K. SCHATTAUER VERLAG · STUTTGART—NEW YORK

Microelectrode Studies of Gastric Mucosa and Isolated Gastric Cells*

G. Sachs, R. L. Shoemaker, A. L. Blum, H. F. Helander, G. M. Makhlouf, and B. I. Hirschowitz

The description of electrical events associated with transport by the amphibian gastric mucosa has largely been confined to data obtained with extracellular electrodes and current sources. But since a more complete understanding of the phenomena can be achieved by studying the properties of the serosal and mucosal membranes directly, this paper will deal with observations on the independent properties of these membranes as measured by intracellular microelectrodes.

However, since in analogy with other tissues electrical coupling may exist between cells of the same type and different types, intracellular measurements in the intact tissue may not yield information on the independent electrical properties of the individual cell types. Thus the degree and nature of cellular coupling was assessed in the mucosa and in addition techniques were developed for measurement of electrical properties of isolated cells. Based on these studies, a model was derived which could explain many of the electrical characteristics of the mucosa.

This paper is divided into two parts, dealing with the experiments using the intact mucosa on one hand, and the isolated cells and tubules on the other.

A. Intact mucosa

It can be shown that both H^+ and Cl^- are transported against electrochemical gradients (1, 2), by analysis of the ion distribution across the tissue, and by the electrical polarization of the tissue (mucosal surface negative). The potential difference (p.d.) across the tissue could then arise as a result of these transport processes, or could be due to asymmetric permeability of the tissue to another ion. Harris and Edelman (3) using the Ussing chamber and Villegas (4) using microelectrodes concluded that the transmucosal p.d. was due to the series contribution of the serosal and mucosal surfaces of the tissue.

* Supported by NIH grants TIAM 2A-5286, AM 09260 and NSF grants GB 8351 and GB 25364.

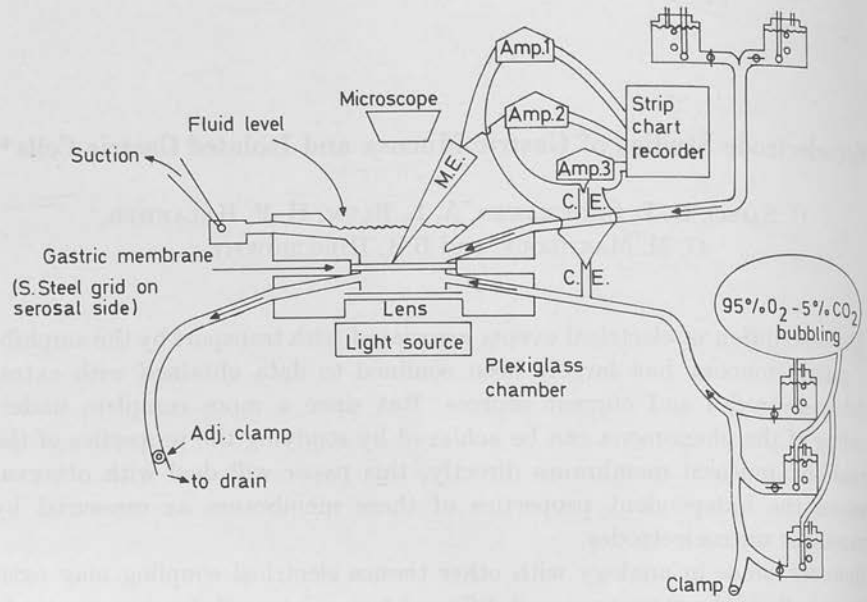

Fig. 1. Experimental setup: Gastric mucosa mounted between two halves of a Lucite chamber. M.E. = microelectrode, C.E. = calomel electrode, Amp. 1, etc. = Bioelectric Instrument Corporation amplifiers. The type of solutions was changed by opening or closing the stopcocks near the solution bottles.

This has been confirmed for the Necturus gastric mucosal surface epithelial cell (5). The question arises as to whether this asymmetry is due to a transport process across one or other of the surfaces or due to asymmetry of passive properties. To study this, ion concentration changes were carried out on each side of the tissue while the p.d. across each cell surface was continuously monitored.

Methods

The Necturus maculosus (mudpuppies) used in these experiments were housed prior to use in fiberglass tanks with constant temperature (22° C), water flowing through the tanks. The animals were fed crickets approximately 3 times per week; during the cooler months of the year shipments were received every two weeks from a commercial dealer. Animals maintained in this manner secreted acid spontaneously when the in vitro mucosa was prepared. To obtain consistently a mucosa that was not secreting acid spontaneously this animal was housed at 3° C for 3 days and fasted during this time; acid secretion could be stimulated by use of mecholyl or pentagastrin in these preparations.

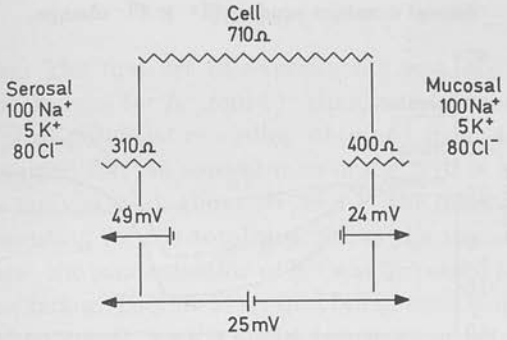

Fig. 2. Idealized diagram of a typical cell potential and resistance: Trans p.d. 25 mV, lumen negative. Trans resistance 710 ohm · cm².

For an experiment an animal was killed, the stomach removed and placed in oxygenated amphibian Ringer solution (5). The external muscle layers were removed and the remaining gastric membrane was placed, as a sheet, between two halves of a Lucite chamber, the mucosal side facing upward. The transmembrane p.d. was measured by using saturated KCl-calomel electrodes. Current was sent through the membrane by use of Ag:AgCl electrodes in the solution and the ΔV for a known current strength was used to estimate the resistance of the mucosa, by Ohm's law.

The solutions bathing the tissue were circulated by a perfusion method (Fig. 1). The serosal solution was allowed to flow through the tubes and chamber to remove the bubbles and then the reservoir bottle was lowered and the siphon effect produced a negative pressure on the membrane to stabilize the serosal side against the stainless steel grid. By use of 3-way stopcocks different types of solutions could be used with the microelectrode remaining in the same cell. The rate of flow was approximately 5 ml/min. All fluids were oxygenated by bubbling through 95% 0_2 and 5% CO_2. The serosal solution was a modified frog Ringer with 5 mEq/l K^+ and 80 mEq/l Cl^-. As the concentration of K^+ increased it replaced Na^+; as the concentration of Cl^- decreased it was replaced by $SO_4^=$ and sucrose was used to maintain isotonicity. Mucosal solutions contained 5 mM K^+, 100 mM Na^+ and 80 mM Cl^-.

Microelectrodes were pulled from 1.2 mm O.D. cleaned capillary tubes using a mechanical two-stage puller (6). The microelectrodes were filled with methanol under a negative pressure and then the methanol equilibrated with water and water with 3 M KCl. During an experiment a microelectrode was held by use of a Leitz micromanipulator and the movements observed by use of a Zeiss surgical stereoscope (40 × 25 cm working distance). The microelectrode was

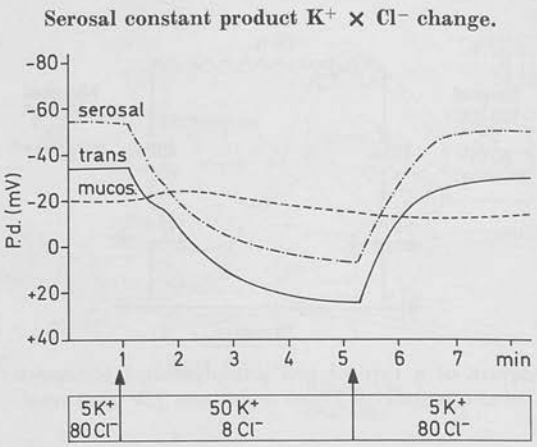

Fig. 3. Effect on p.d.'s by constant product change in serosal K^+ and Cl^-: The bar at the bottom of the figure indicates the type of the solution bathing the serosal side. The mucosal side was bathed in standard solution throughout the experiment. P.d. "serosal" indicates p.d. between microelectrode inside a surface epithelial cell and the reference electrode in the serosal solution. "Mucosal" is p.d. between microelectrode and reference electrode in the mucosal solution. "Trans" is the potential from the calomel electrode in the mucosal solution in reference to the calomel electrode in the serosal solution (negative indicates mucosal negative to serosal).

connected by a 3 M KCl-Agar bridge to 3 M KCl solution in which was also placed a calomel electrode. The reference calomel electrode and the one from the microelectrode were connected to a Bioelectric Instruments Amplifier and the output of the amplifier recorded by use of a Grass polygraph.

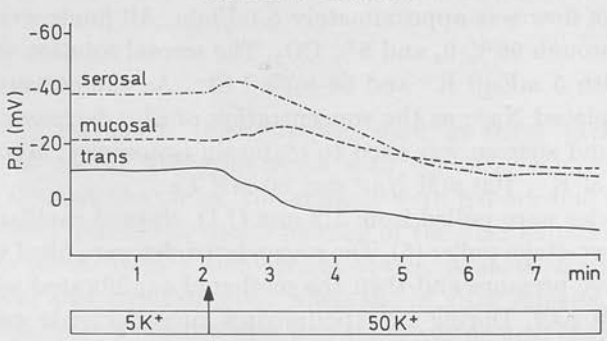

Fig. 4. Increase in serosal solution K^+ and its effect on the p.d.'s: K^+ replaced Na^+ in the serosal solution. No change in the composition of the mucosal bathing solution.

Results

Serosal membrane: The first set of experiments was carried out using the product constant technique for K^+ and Cl^- changes in the serosal solutions (7). Fig. 2 shows a typical potential recording obtained from a surface epithelial cell. The value obtained for the serosal membrane p.d. is typically about 50 to 60 mV, and the mucosal p.d. about 20–30 mV, the difference between these two potentials accounting for the total p.d. across the tissue. In Fig. 3, indicated by the first arrow, the concentration of K^+ was increased tenfold, and Cl^- decreased by the same factor. There was a rapid fall in total p.d. accounted for by a change in serosal potential, with a slight transient in mucosal potential. At the second arrow, these changes were reversed by restoring the original solution concentrations. There was a total change of 54 mV for this tenfold change. Accordingly the sum of transference numbers t_{K+} and t_{Cl-} for the serosal surface was 0.9 from this type of experiment.

Figs. 4 and 5 show typical experiments in which the concentration of K^+ and Cl^- were changed individually. Fig. 4 shows the effect of a tenfold change in K^+. There is a transient increase in serosal potential, followed by a 30 mV decrease, and a transient increase in mucosal potential followed by a slight fall. Fig. 5 shows the effect of a tenfold Cl^- decrease, with a 5 mV fall in serosal, a gradual rise in mucosal and 3–4 mV fall in total p.d.

From these two experiments, the sum of the transference numbers $t_{K+} + t_{Cl-} \approx 0.6$, significantly less than that obtained for the constant product experiments is obtained. This is explained by changes occurring in intracellular ion concentration when changes are carried out individually.

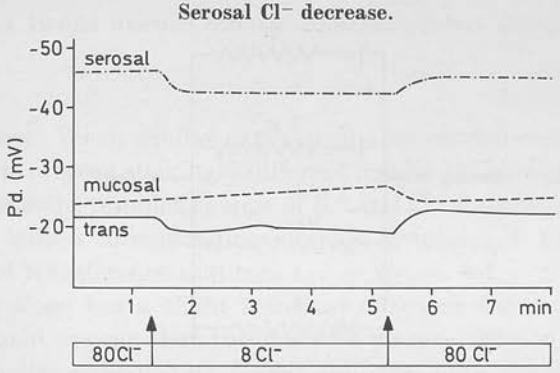

Fig. 5. Effect of serosal Cl^- concentration on the p.d.'s: The concentration of Cl^- was reduced and replaced by $SO_4^=$ and sucrose was added to maintain the same osmotic pressure. Mucosal solution was normal throughout the experiments.

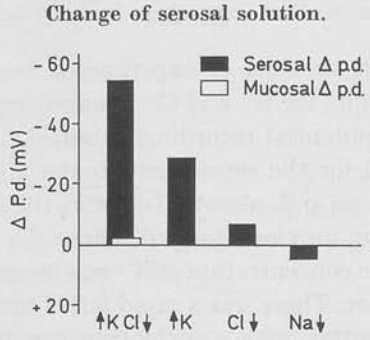

Fig. 6. Summary of changes in p.d. as K^+ and/or Cl^- was changed in the serosal solution. With a constant product change increasing K^+ tenfold and decreasing Cl^- concentration tenfold, there was an approximately 50 mV change in the serosal p.d. and 2 mV in mucosal p.d. The other bars indicate the changes due to K^+, Cl^- or Na^+ alone.

Fig. 6 summarizes the effects of tenfold changes of ion concentration in the serosal solutions. From these findings it can be concluded that the potential across the serosal membrane can be accounted for by a diffusion potential for K^+, Cl^- and Na^+. Fig. 7 thus shows an equivalent circuit for this membrane. A shunt resistance, x, has to be included in the circuit because of the finding that Cl^- changes alone have less than the predicted effect on the serosal p.d.. If the conductance G_x is high relative to G_{Cl}, this will reduce the predicted change in p.d. Since the measurements are made intracellularly, this shunt pathway exists across the serosal membrane of the surface epithelial cell.

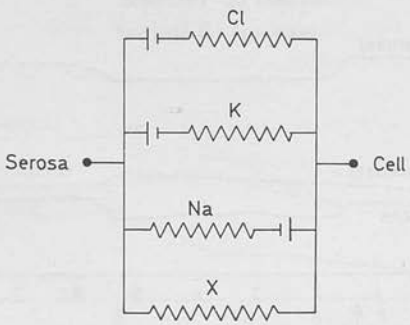

$$P.d. = E_K \frac{G_K}{G_K + G_{Cl} + G_{Na} + G_X} + E_{Cl} \frac{G_{Cl}}{G_K + G_{Cl} + G_{Na} + G_X} - E_{Na} \frac{G_{Na}}{G_K + G_{Cl} + G_{Na} + G_X}$$

Fig. 7. Schema of an equivalent circuit for the serosal membrane.

It should be pointed out that the electrical measurements are carried out with the electrode in the surface epithelial cell. If this cell system is coupled to the oxyntic cell system, events at the surface cell membrane will be essentially indistinguishable from events at the oxyntic cell surface.

If the surface epithelial cell exists as a generator in parallel to the oxyntic cell, then, since the change in the serosal membrane of the surface epithelial cell exactly reflects the total change in the p.d., the change in the oxyntic cell membrane will be exactly equal to that of the surface cell.

Finally, if the surface cell is acting only as a passive resistance, then the lack of change in the mucosal membrane is not accounted for. Accordingly we can conclude that it is likely that the oxyntic and surface cell serosal membrane display the same passive properties.

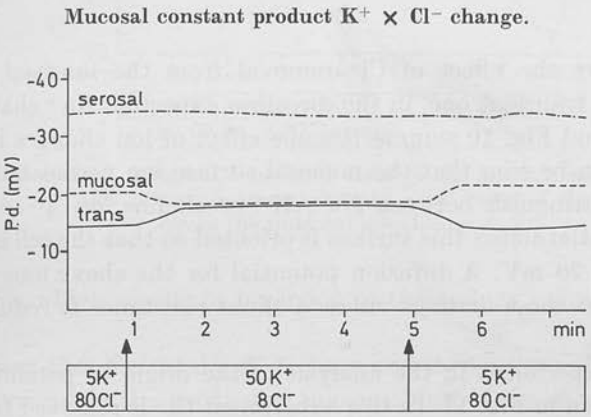

Fig. 8. Effect of a 10-fold mucosal solution constant product change of K^+ and Cl^-.

Mucosal membrane: When similar experiments are carried out on the mucosal side of the gastric mucosa strikingly different results are obtained. Fig. 8 shows the effect of a constant product change of K^+ and Cl^- showing a slight decrease in mucosal p.d. with a corresponding increase in total p.d. From this experiment the sum of transference numbers $t_{K^+} + t_{Cl^-} \approx 0.1$.

Changing K^+ alone has a slight transient effect on the mucosal potential. From this, it could appear that the mucosal permeability to Na^+ and K^+ is about equal. Choline substitution for Na followed by a change of K concentration makes little difference to the lack of effect observed. Hence the cation permeability of this membrane is low.

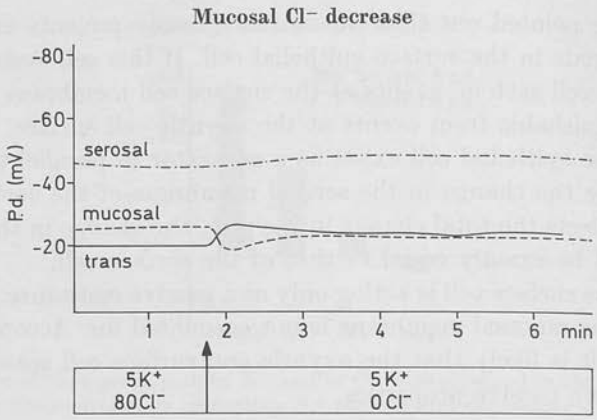

Fig. 9. The effect of removing Cl^- from the mucosal solution.

Fig. 9 shows the effect of Cl^- removal from the mucosal solution. The effect is also a transient one, in the direction expected. Na^+ changes also have small effects and Fig. 10 summarizes the effect of ion changes in the mucosal solution. It can be seen that the mucosal surface ion permeability is low, and it does not distinguish between Na^+, K^+ or choline, or Cl^- and $SO_4^=$. However, the potential across this surface is oriented so that the cell interior is negative by about 30 mV. A diffusion potential for the above ions therefore does not account for these findings unless a shunt resistance is reducing the effect of ion changes.

A critical experiment in the analysis of the origin of potentials across the mucosa is shown in Fig. 11. In this experiment Cl^- is removed from both sides

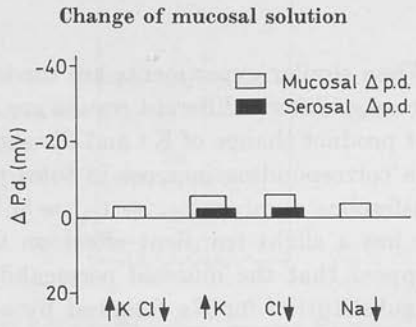

Fig. 10. Mucosal changes. The magnitude of these ionic changes were the same as in Fig. 6, but the effects on p.d. were greatly reduced.

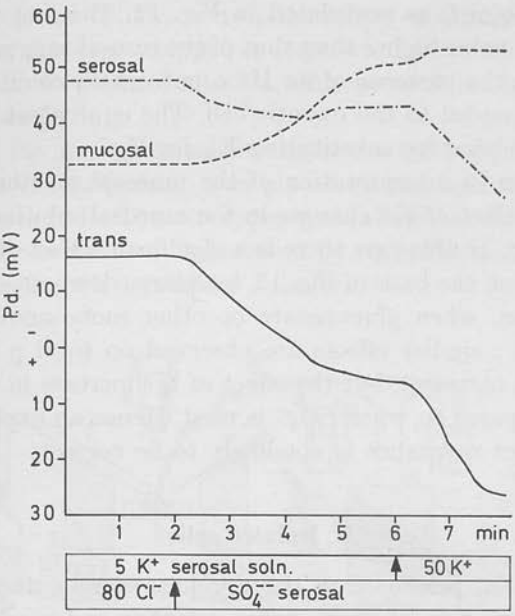

Fig. 11. The effect of Cl^- removal from both sides of the bathing solution of Necturus gastric mucosa. The p.d. across the tissue inverts, with most of the change occurring across the mucosal membrane.

of the mucosa, which results in inversion of the p.d. as a function of acid secretory rate (8).

It can be seen that the total p.d. declines and then inverts showing that acid secretion is present in this particular mucosa. Most of the change is accounted for by an increase of mucosal potential, which may be explained by abolition

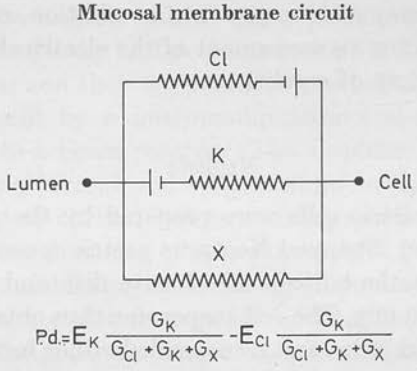

Fig. 12. Schema of an equivalent circuit for the mucosal membrane.

of the Cl^- pump e.m.f. as postulated in Fig. 12. The fact that the mucosal p.d. increases to a value higher than that of the serosal suggests that this membrane is reflecting the presence of an H^+ e.m.f. which could only occur if the surface cell was coupled to the oxyntic cell. The equivalent circuit of Fig. 12 would then be modified by substituting E_H for E_K.

Another problem in interpretation of the mucosal membrane permeability properties is the effect of K^+ changes in the mucosal solution when $SO_4^=$ was substituted for Cl^-. In this case there is a significant effect of K^+, which could be accounted for, on the basis of Fig. 12, by a large decrease in G_x by $SO_4^=$ substitution. However, when glucuronate or other mono-nonvalent anions are substituted for Cl^-, similar effects are observed on total p.d. and resistance (i.e. inversion and increase), but the effect of K^+ increase in the mucosal solution is small compared to when $SO_4^=$ is used. Hence an explanation based on alterations of shunt resistance is not likely to be correct.

B. Isolated cells

Evidence has been presented in the previous section that the surface epithelial cell contains two or more independent e.m.f.'s which lead to different and independent changes of p.d. across the mucosal and serosal surfaces of the cell. Since there may also be coupling between cells, distinguishing the electrical properties of the different cell types may be impossible.

In the present section, therefore, a new method for the study of electrical properties is described, which involves preparation and subsequent micropuncture of isolated intact mucosal cells and isolated gastric tubules. The spread of current in oxyntic and surface cell systems is examined by simultaneous measurements in two cells. It may thus be shown that surface and oxyntic cells in intact mucosa are electrically coupled while significant intercellular conductive pathways may also be present. In addition, micropuncture studies in isolated cells may allow an assessment of the electrical properties of specific cell types under a variety of conditions.

Methods

Isolated Necturus gastric cells were prepared by the pronase technique as previously described (9). Stripped Necturus gastric mucosa was pinned mucosal surface upwards on the bottom of a Lucite dish and shaken in a 0.175% pronase solution for 120 min. The cell suspension thus obtained was centrifuged at 50 g for 5 min, washed twice and resuspended either in frog Ringer's solution or in a solution containing 18.5 mM K^+ with correspondingly lower Na^+ levels.

Isolated gastric gland tubules were prepared by a modification of the pronase technique. In this case stripped mucosa was incubated for one hour and then rapidly shaken in pronase solution. Clumps of cells and isolated tubules were readily obtained.

Fig. 13 shows the experimental arrangement used for micropuncture of isolated cells. The cell suspension was placed on the agar-filled depression of a microscope culture slide. The cell types were identified under a stereomicroscope. Oxyntic cells could be differentiated by their size and granular appearance from other cells such as surface cells (9).

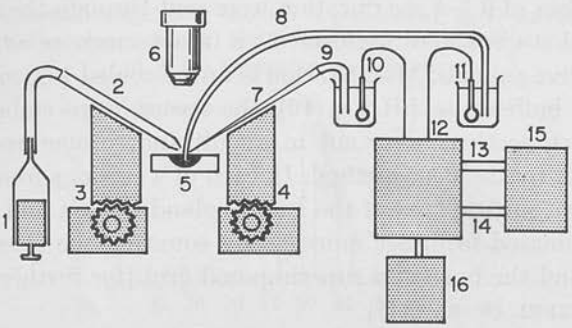

Fig. 13. Experimental arrangement for micropuncture of isolated cells: 1. Oil-filled syringe; 2. Oil-filled suction micropipette; 3., 4. Micromanipulators; 5. Agar-filled microculture slide; 6. Stereomicroscope; 7. Microelectrode; 8., 9. 3 M KCl-agar bridge; 10., 11. Calomel electrodes; 12. Amplifier; 13., 14. Recorder connections; 15. Recorder or CRO; 16. Current source.

For the preparation of microelectrodes, glass capillary tubing was precleaned in chromic acid and alcohol and mounted on a Nastuk electrode puller (6) (Industrial Science Associates) with a 4 mm platinum loop. Microelectrodes were examined microscopically and were filled with 3 M KCl. Their tip resistance was about 50 megohms and their tip potential was less than 3 mV. As shown in Fig. 13, they were held by a micromanipulator and connected to a WP4 amplifier and thence to a Grass recorder. The amplifier also had provision for sending and monitoring current and a Wheatstone bridge circuit for balancing the electrode response to current before starting a cell puncture.

A micropipette with a diameter of approximately 5 μ was used for trapping of isolated cells and immobilizing them during micropuncture. This pipette was also pulled on a Nastuk puller from precleaned capillary tubing. The tip was then broken against the platinum wire of a de Forbrunne microforge and fire-polished. The micropipette was filled with oil from a Hamilton microsyringe

and connected to a suction system, as shown in Fig. 12, care being taken to exclude air bubbles.

For micropuncture of isolated tubules and pieces of intact mucosa, the use of a micropipette was not necessary and both micromanipulators were used for holding microelectrodes. Simultaneous measurements could thus be obtained from two cells of the same tissue.

Micropunctures were considered successful when transmembranal p.d. remained stable for at least 10 sec. Membrane resistance was calculated from the deflection of p.d. observed in response to a 1–2 sec current pulse of 10^{-9} Amp. For the construction of current voltage curves, hyper- and de-polarizing current pulses of 0.5–1 sec duration were sent through the microelectrode.

Morphological studies were performed on intact mucosae as well as on isolated cells from five animals. After fixation in an ice-cooled 1% solution of OsO_4, veronal acetate buffered to pH 7.4 (10), the tissues were embedded in epon. One-micron thick sections were cut in an ultramicrotome and stained with toluidine blue, or by the PAS method. In each of 4 sections from each of 5 animals, the relative surface area of the gastric gland lumina and of the mucosal surface was estimated in intact mucosae by counting the intercepts between these surfaces and the lines of a superimposed grid [for further details on this method see WEIBEL et. al. (11)].

Additional morphological information was obtained by electron microscopy on thin sections of the same tissues mentioned above. The sections were contrasted with lead hydroxide followed by uranyl acetate and examined in a Phillips EM 200 electron microscope at 60 kv. The relative surface area of isolated oxyntic cells was estimated by the method described above and compared with that of smooth spheres of the same diameter.

Results

I. Potential of isolated cells: Stable p.d. readings were obtained in about 50% of the punctures attempted. Failures occurred in cells which disintegrated or swelled while being held by the micropipette or upon puncture by the microelectrode. Cells which appeared swollen prior to puncture or cells with a grossly irregular surface had a p.d. of less than 5 mV. Further studies, therefore, were confined to cells without morphologic signs of damage such as swelling and irregular surface. Fig. 14 shows a p.d. recording obtained from an oxyntic cell. The duration of this recording was 20 min. Other recordings were obtained for as long as 60 min with less than 10% decay in p.d. In most cases long-term stability of the p.d. was not tested and the electrode was removed from the

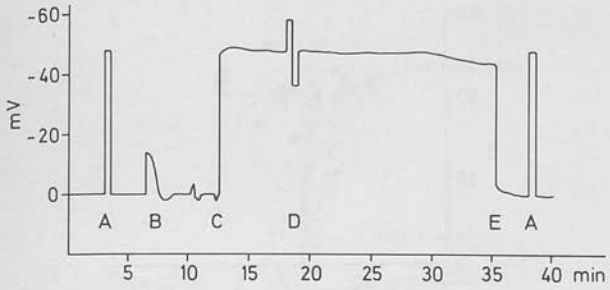

Fig. 14. Cellular potential obtained from a micropuncture of an oxyntic cell. At A tip resistance is measured, at B current is sent through the electrode and balanced out through the Wheatstone bridge, at C the cell is punctured, at D current is sent in both directions through the electrode, at E the electrode is removed from the cell, and at A tip resistance is checked.

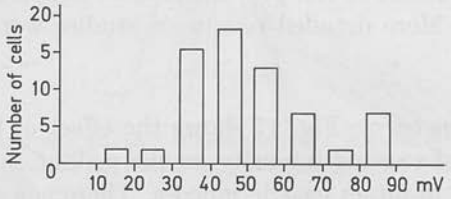

Fig. 15. The distribution of potential difference obtained from a batch of 67 cells.

cell after 1–5 min. In a representative batch of 67 cells the p.d. ranged from values of about 10 mV to 90 mV, with a mean ($\pm$ S.E.M.) of 44 $\pm$ 3 mV (Fig. 15).

In control experiments the p.d. was determined in surface cells of intact mucosa, and compared to the p.d. in isolated surface and oxyntic cells. The experimental arrangement was similar to that used for isolated cells (Fig. 13). The mean ($\pm$ S.E.M.) p.d. for the surface cell in the intact mucosa was 43 $\pm$ 8 mV. The effect of K concentration change on the p.d. of isolated oxyntic cells was also measured. When K was increased from 4 to 18.5 mM and Na correspondingly decreased, the p.d. fell by 17 mV (Table 1).

Table 1. Intracellular potentials*.

Surface epithelial cells 4 K^+	Oxyntic cells		Intact mucosa 4 K^+
	4 K^+	18.5 mM K^+	
36 $\pm$ 11 N = 12	48 $\pm$ 6 N = 22	31 $\pm$ 5 N = 11	43 $\pm$ 8 N = 15

* mV $\pm$ S.E.M.

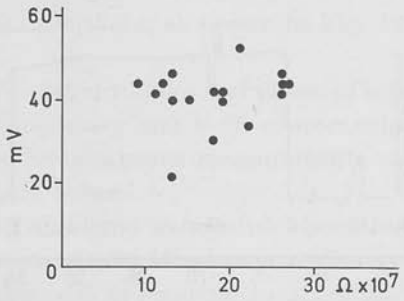

Fig. 16. Resistance of 17 oxyntic cells plotted against p.d. of the cells showing little correlation.

II. Resistance of isolated cells: In Fig. 16 the resistance of 17 oxyntic cells is plotted against the measured cell p.d. There is no simple relationship between p.d. and resistance. More detailed resistance studies were carried out as discussed below.

III. Current voltage curve: Fig. 17 shows the effect of hyper- and depolarizing current pulses of varying intensity on the p.d. of an isolated surface cell and of a surface cell in intact gastric mucosa. There is a striking difference in

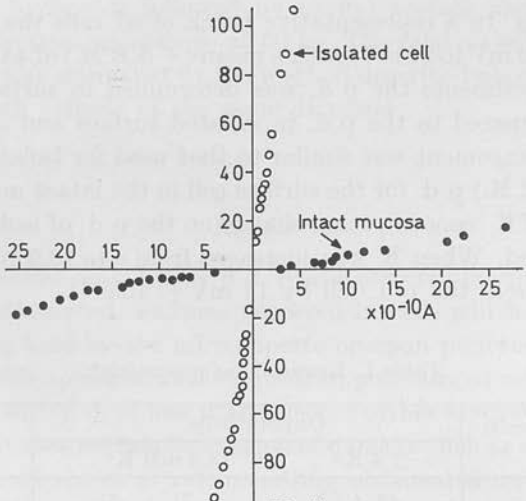

Fig. 17. Current-voltage plot for the surface epithelial cell in the intact mucosa and when isolated, showing a marked difference in slope, and non-linearity.

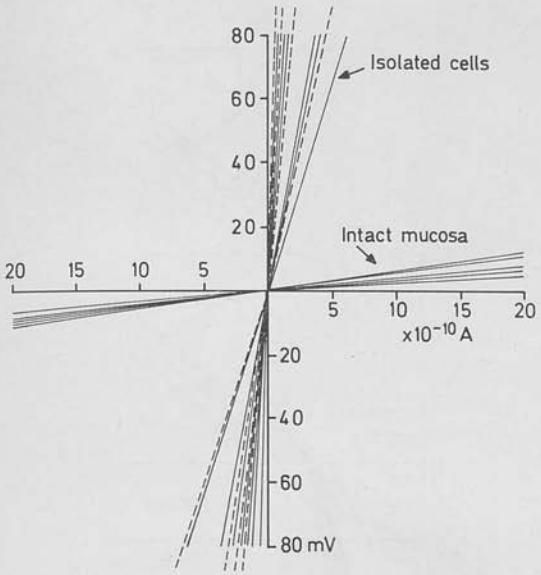

Fig. 18. Calculated tangents to the current-voltage curves ($y = ax^3 + bx^2 + cx$) obtained for intact mucosa and isolated cells.

slope between the two experiments. Since in this and all other experiments a uniform and statistically significant curvature ($p < 0.001$) was observed, the slope was calculated as the tangent of a curve which was defined by a cubic equation forced through the origin. The calculated tangent for isolated surface cells, isolated oxyntic cells and surface cells in intact mucosa are given in Fig. 18. Similar values were found for isolated oxyntic cells and surface cells while the mean obtained for isolated surface cells was about 100 times greater than the mean of intact mucosa ($1.5 \pm .3 \times 10^8$ and $1.6 \pm .2 \times 10^6$ respectively, $p < 0.0001$).

IV. Two-electrode system: When stable p.d. readings were obtained in two surface cells of intact gastric mucosa, a current pulse was applied to one cell and the deflections of p.d. in both cells were recorded. A p.d. deflection in the distant cell was used as expression of electrical coupling. An estimate of the type of electrical coupling was obtained by systematic circumferential puncture of surface cells surrounding the cell which contained the current sending electrode. Electrical coupling was found in 10–20% of the cells with a radial distance of up to 100 μ, i.e. about 10 cells away from the current sending electrode.

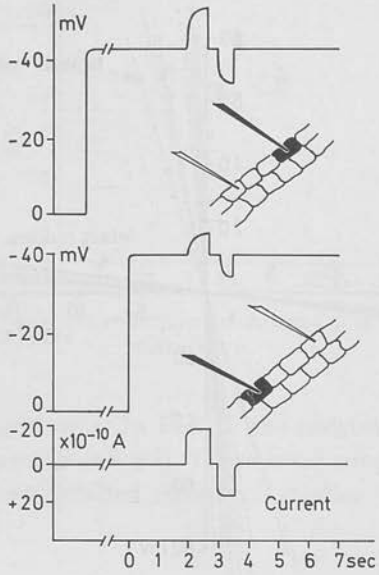

Fig. 19. Experiment demonstrating coupling in isolated tubules of Necturus gastric mucosa. The upper electrode is used for recording p.d. and sending current, and the other electrode records p.d. changes in another cell. The bottom trace records the amount of current sent.

Electrical coupling between oxyntic cells was examined in isolated gastric tubules. A typical experiment is shown in Fig. 19 demonstrating an attenuation of the current pulse of 50% over a distance of only 3 cells. In other experiments, the distance for 50% attenuation was 4–5 cells.

V. Morphologic observations: The increase in surface area of the mucosa caused by the infoldings of the gastric glands was calculated to be 2.7 $\pm$ 0.1 (S.E.M.) for 5 animals. In the dog the corresponding increase is 13 times (12). On this basis the mucosal surface of the tissue consists of approximately 37% surface cells and 63% oxyntic cells. These values were used for calculation of the specific resistance of the mucosa measured in the Ussing chamber, and for calculation of the mucosal resistance from values obtained from isolated cells.

Electron micrographs of oxyntic cells from intact mucosa as well as in the isolated state are shown in Figs. 20 and 21. The isolated oxyntic cell showed evidence of good morphologic integrity, and also that there had not been any significant alteration in surface infolding or microvilli in the isolation procedure. In the isolated oxyntic cell the infolding resulted in a three- to fivefold increase of the surface area of an oxyntic cell compared to a smooth sphere of the same diameter.

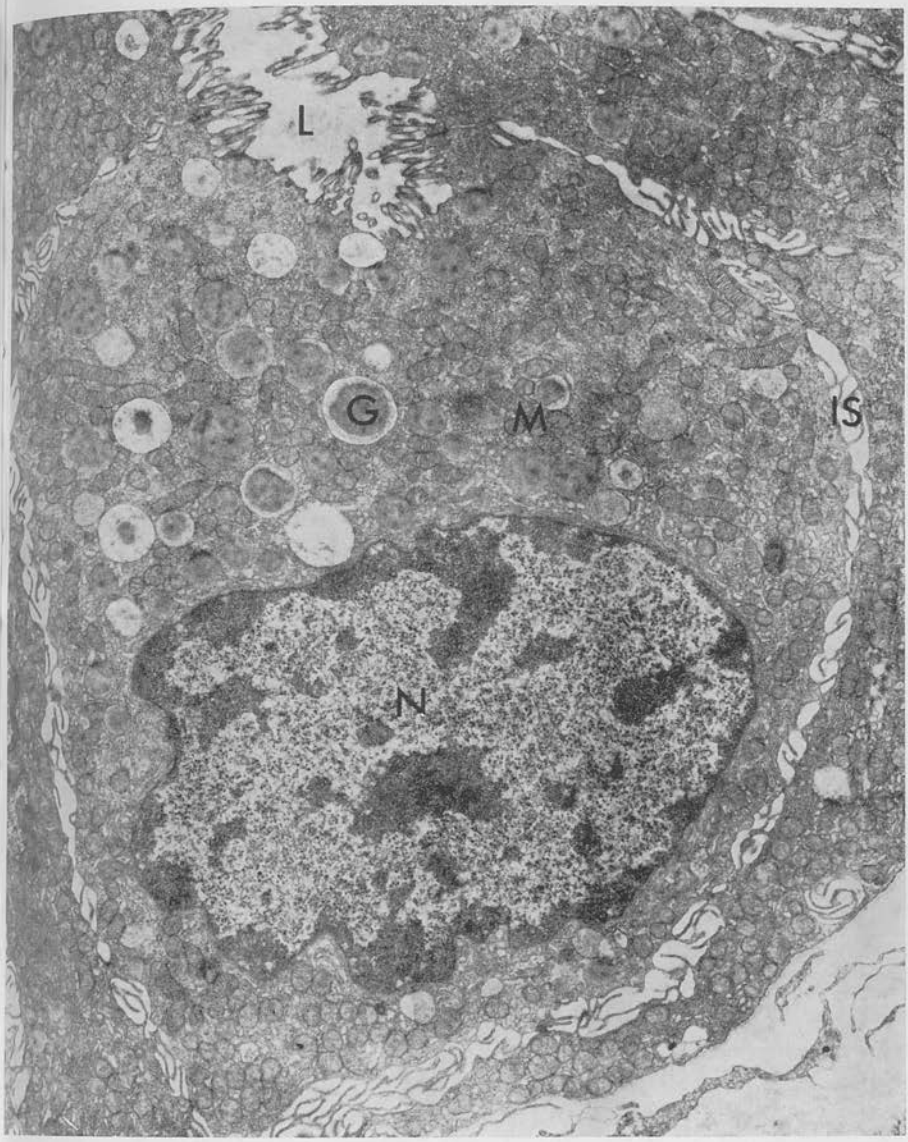

Fig. 20. Electron micrograph of oxyntic cell from intact gastric mucosa. Numerous microvilli extend into the intercellular space (IS). The cytoplasm contains a large number of secretory granules (G) and mitochondria (M). L = gland lumen; N = cell nucleus. 4,800×.

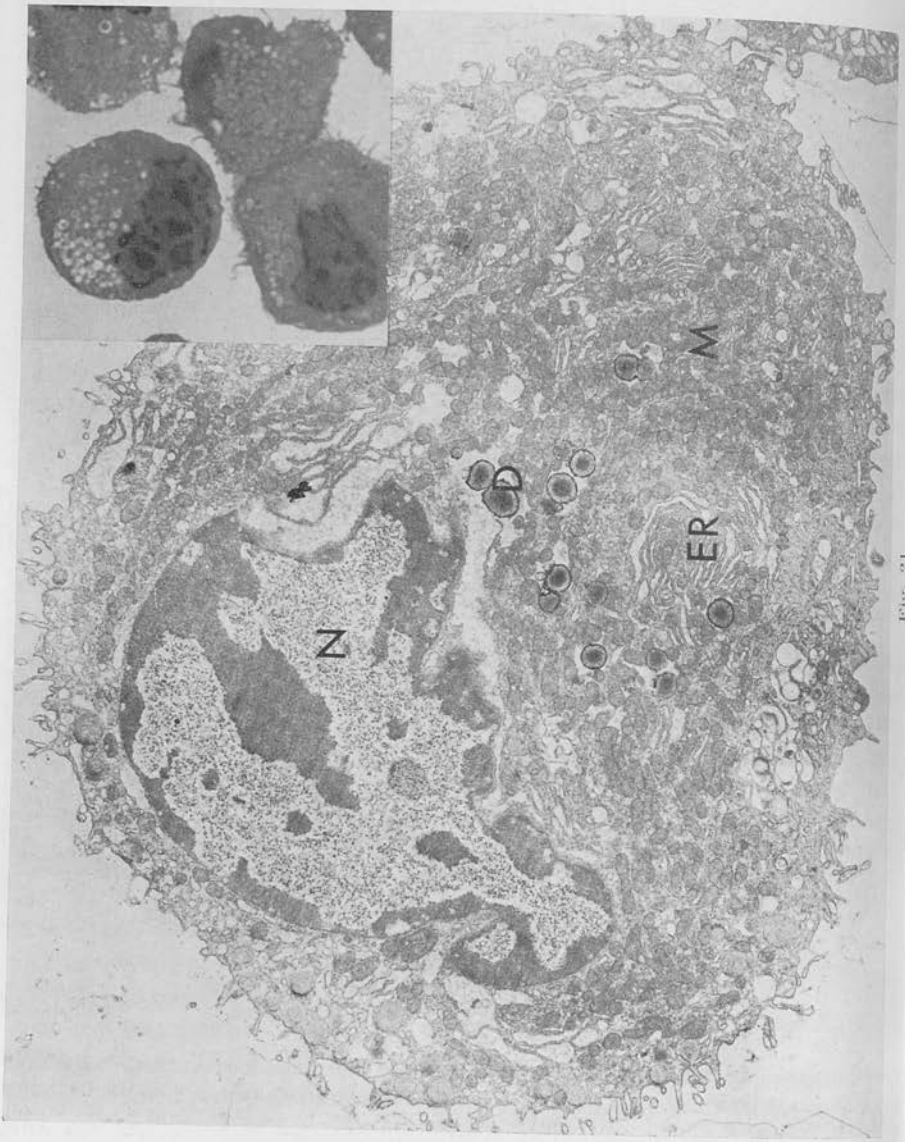
M
D
ER
N

Discussion

I. Potentials of isolated cells: The ability to perform micropunctures in isolated cells allows for the first time a direct assessment of functional properties in specific cell types of gastric mucosa. In the present study, the transmembranal p.d. of nonstimulated isolated mucosal cells is reported (Table 1, Fig. 14). The average p.d. of these cells is 44 mV and is not significantly different from values obtained from pieces of intact mucosa. It would thus appear that the isolation procedure does not lead to damage of the cell membrane and/or of the mechanisms which are responsible for the p.d.

This interpretation should, however, be accepted with some caution since a spuriously normal p.d. in cells with a damaged plasma membrane could be due to leak of KCl from the microelectrode into the cell. Such a leak would have relatively little effect on the p.d. of electrically coupled cells of intact mucosa, while in isolated cells its effect would be proportionately much greater. In the present study, the use of fine-tip electrodes minimized the occurrence of leakage. A leak is also improbable on the basis of observations with KCl-filled microelectrodes in electrically coupled and uncoupled cells of intact toad bladder. If a leak would occur in this preparation, electrical uncoupling of a punctured cell would result in an apparent increase of p.d. However, no such increase is observed (13).

The p.d. of isolated surface cells was not significantly different from the p.d. of isolated oxyntic cells. Further confirmation of this observation by different techniques is, however, necessary since it has been shown in previous studies that viability of isolated surface cells is lower than of oxyntic cells which in eosin exclusion tests are 80–100% viable (9).

In previous studies, the K concentration of isolated oxyntic cells as determined by a ^{14}C inulin method was 67 mM per liter cell water (9). On the basis of this value, the predicted Nernst p.d. for a perfect K electrode is:

$$\text{p.d.} = \frac{RT}{nF} \ln \frac{67}{4} = 70\,\text{mV}$$

This value is considerably higher than the p.d. observed in oxyntic cells, suggesting that the oxyntic cell membrane is permeable to ions other than K^+,

Fig. 21. Electron micrograph of isolated oxyntic cell. The endoplasmic reticulum (ER), and the mitochondria (M) suggest good viability of this cell at the moment of fixation. The number of microvilli projecting from the surface of the cell has not changed significantly, as compared to oxyntic cells in intact mucosae. D = lipid droplets; N = cell nucleus. ×3,300. Inset shows light micrograph of section from the same preparation of isolated oxyntic cells. ×960.

such as Cl^- or Na^+. Similar conclusions may be reached from the p.d. response to change of K concentration in the nutrient solution. A 4.5-fold increase in K^+ leads to a reduction of the p.d. by 17 mV, while the expected decrease for a membrane with selective permeability for K^+ would be 38 mV. These findings closely correspond to observations in surface cells of intact mucosa.

II. Membrane resistance: The membrane resistance was calculated in all instances from the deflection of the p.d. in response to a standard current pulse. A more accurate estimate was obtained from the slope of current voltage plots (Figs. 17 and 18). In order to express the resistance per area of cell membrane, the surface area of isolated cells was estimated on the basis of findings in phase contrast microscopy. Thus, isolated surface cell and oxyntic cell are spheres with a radius of 10 microns and 15 microns respectively, and their resistances are 1800 and 2700 Ω cm^2 respectively (Table 2).

Table 2. The values obtained for cell dimensions, voltage-current slopes and calculated membrane core resistance and space constants for the surface cell, intact mucosa, oxyntic cell and isolated tubule.

	Surface cell		Oxyntic cell	
	Intact	Isolated	Tubule	Isolated
Cell dimensions (μ)	30 × 10	r = 10	r = 15	r = 15
Slope in current-voltage plot	1.6×10^6	1.5×10^8	7×10^6	2.0×10^8
Specific resistance				
R_m (Ω cm^2)	—	1800	—	2730
R_c (Ω cm)	50	—	800	—
Space constant (μ)	1400	—	400	—

Since the relative surface area of isolated oxyntic cells was calculated in electron micrographs to be 3–5 times greater than estimated for a smooth-surfaced sphere (lacking microvilli), thus the estimates for specific membrane resistance are too low by the same factor.

III. Transmucosal electrical shunts: If such shunts were present, the resistive properties of intact tissue could not be predicted on the basis of findings in isolated cells. In the following section, therefore, predicted and observed resistance of intact mucosa are compared.

Since the resistance R_m of mucosal (or apical) membrane and the resistance R_s of serosal (or basal) membrane in isolated cells are electrically in parallel, the total resistance R_t is.

$$R_t = \frac{R_m \cdot R_s}{R_m + R_s}$$

In the intact mucosa R_m and R_s are electrically in series and thus resistance of the intact mucosa (R) in the Ussing chamber is:

$$R = R_m + R_s$$

If R_m and R_s are assumed to be of equal magnitude, a minimal value for R is obtained which is 4 times the R_t value.

For a mucosa whose surface area consists of 63% oxyntic cell surface and of 37% surface cell surface, the calculated resistance is approximately:

$$R = 5000\ \Omega\ cm^2.$$

The observed value of R for intact resting Necturus gastric mucosa in an Ussing chamber is $710 \pm 47\ \Omega\ cm^2$ assuming the area is given by the dimensions of the chamber. If the 2.7–fold increase in surface area by tubular infoldings is taken into account, the corrected observed resistance was $2000\ \Omega\ cm^2$. This value can be compared to the isolated cell value since in both cases it was assumed that the cells had a smooth surface.

It is apparent that the predicted resistance of Necturus gastric mucosa is twice the observed value. On this basis, therefore, the possibility is not excluded that there are intercellular resistive shunts similar to other tissues such as the gall-bladder (14).

Comparisons of this type would be misleading if the surface area of the mucosal cells would change during isolation. Where the surface area of isolated cells and of cells in the intact mucosa was compared in electron micrographs, it appeared that there was no difference in the surface area or the size of the cells under the two conditions.

Another possibility is that there is a qualitative change of the cell membrane as a result of isolation. This possibility has not been excluded by our current study. Other evidence suggests that there is little gross change since the cellular K^+ and Na^+ content appears to be the same as for intact tissue (15).

IV. Electrical coupling: The resistive properties of isolated surface cells and of surface cells in intact mucosa were examined in current voltage plots (Figs. 17 and 18). As shown by the 100-fold difference in slope, the resistance measured in intact mucosa is much lower than in isolated cells. This difference cannot be explained by a reduction in surface area of the cell membrane during the process of isolation. More likely is the presence of low resistance pathways between cells of intact mucosa which are not present in isolated cells. Such pathways have been described by LOEWENSTEIN and coworkers (13) who observed electrical coupling between epithelial cells and could also observe the movement of fluorescent dyes across cell junctions. This low resistance R_c is electrically in parallel with the membrane resistance R_m with respect to an

intercellular current source and is in the present study about 100 times smaller than R_m.

Since even in close proximity to the surface cell which receives current pulses only a small proportion of the cells show signs of electrical coupling, circumferential spread of current is very unlikely. A more likely model for the type of coupling assumes radial spread of current along a "cell cable" with a low core resistance R_c and a high resistance of the insulating membrane sheath R_m. For such a cable LOEWENSTEIN et al. derived the following equation (16):

$$R_m = \lambda c \frac{V_o}{I_o} \tanh \frac{L}{\lambda} \quad [1]$$

where λ is the space constant and is defined by $\lambda = \sqrt{r_m/r_i}$, r_m is the resistance of unit length of the insulating membrane sheath in Ω cm, r_i is the resistance per unit length of the core conductor in Ω cm, c is the circumference of the "cell cable", V_o is the value of potential difference at the current source, I_o is the total current flowing into the core from the internal electrode, and L is the total length of the core conductor. For surface cells of intact tissue, c is 80×10^{-4} cm and V_o/I_o as obtained in a current voltage plot is $1.6 \times 10^6 \Omega$. Since in intact tissue $L \gg \lambda$, $\tanh L/\lambda = 1$. The value of $R_m = 1800\ \Omega\ cm^2$ is obtained from measurements in isolated surface cells where the low core resistance is absent and therefore total observed resistance $R = R_m$. λ may be calculated from eq. 1 and is approximately 1400 μ. The core resistance R_c is defined by:

$$R_c = \frac{a}{\lambda} \cdot \frac{V_o}{I_o} \tanh \frac{L}{\lambda} \quad [2]$$

where a is the crosscut area of the "cell cable". For surface cells, R_c is thus about 50 Ω cm. Since, however, only a small area of the cell surface is involved, this is a considerable overestimate.

Calculations similar to those given for surface cells are more difficult in the case of oxyntic cells. Puncture of oxyntic cells in intact mucosa is at present technically not possible. Thus the current voltage plot (Fig. 18) allows only comparison of isolated oxyntic cells with surface cells of intact mucosa. It may, however, not be permissible to compare properties of two different cell systems. Furthermore, the assumption that $L \gg \lambda$ cannot readily be made for Necturus gastric mucosa. Gastric tubules are relatively short (about 0.5 mm) and electrical coupling between oxyntic cells and surface cells has not yet been demonstrated. An attempt was, therefore, made to measure λ directly with a two-electrode system in isolated gastric tubules. A representative experiment is shown in Fig. 19. It is apparent that a 50% attenuation of the p.d. response occurs across a few – 3 to 5 – cells. However, the measurement

of cell separation assumes that there is a direct path between the two electrodes, and no branching in this pathway. With these reservations, the apparent space constant in the tubule is of the order 150 μ, since the cell diameter is 30 μ. Also, an additional artefact has to be considered, namely, rupture of the intercellular junctions by the action of pronase used in the tubule preparation.

Alternatively, the slope of the voltage current curve for the isolated tubule (7.0×10^6) can be used for the calculation λ and R_c by the same method as for the surface cell. With this method the space constant is about 400 μ, and the core resistance is about 800 Ω cm. Again, due to the pronase treatment, these values are subject to revision when techniques for definitive puncture of oxyntic cells in the intact mucosa become available.

Summary

Microelectrode measurements were carried out on surface cells of intact mucosa, oxyntic cells in isolated gastric tubules, and on both cell types in isolated cell suspensions. It has been shown that the serosal membrane p.d. is due to a KCl diffusion potential, and that there are probably anion shunts across both membranes of the surface cell. Directly, using a two-electrode system, and indirectly by comparing the resistance of the isolated cell with the resistance of the cell in the tissue, the presence of electrical coupling has been demonstrated in the gastric mucosa.

References

(1) Rehm, W. S.: Amer. J. Physiol. *159:* 586 (1949).
(2) Hogben, C. A. M.: Proc. Nat. Acad. Sci. *38:* 13 (1952).
(3) Harris, J. B., I. S. Edelman: Amer. J. Physiol. *26:* 769 (1964).
(4) Villegas, L.: Biochim. biophys. Acta *64:* 359 (1962).
(5) Shoemaker, R. L., B. I. Hirschowitz, G. Sachs: Amer. J. Physiol. *212:* 1013 (1967).
(6) Alexander, J. T., W. L. Nastuk: Rev. Sci. Instr. *24:* 528 (1953).
(7) Boyle, P. J., E. J. Conway: J. Physiol. *100:* 1 (1941).
(8) Heinz, E., R. P. Durbin: Biochim. biophys. Acta *31:* 246 (1959).
(9) Blum, A. L., G. T. Shah, V. D. Wiebelhaus, F. Brennan, H. F. Helander, G. Sachs: Gastroenterology. (In press.)
(10) Helander, H. F.: J. Ultrastruct. Res., Suppl. *4:* 1 (1962).
(11) Weibel, G. R., H. Elias (eds.): Quantitative Methods in Morphology. Springer, Berlin-Heidelberg-New York 1967.
(12) Loewenstein, W. R., S. J. Socoler, S. Higashino, Y. Kanno, N. Davidson: Science *149:* 295 (1965).
(13) Canosa, C. A., W. S. Rehm: Gastroenterology *35:* 292 (1958).
(14) Diamond, J. M., P. H. Barry, E. M. Wright: This symposium, p. 23.
(15) Davenport, H. W., F. Alzamora: Amer. J. Physiol. *202:* 1710 (1962).
(16) Loewenstein, W. R., Y. Kanno: J. Cell Biol. *22:* 565 (1964).

J. Membrane Biol. 19, 105–128 (1974)

Microelectrode Studies of Fundic Gastric Mucosa: Cellular Coupling and Shunt Conductance

J. G. Spenney, R. L. Shoemaker, and G. Sachs*

Departments of Medicine and Physiology, Laboratory of Membrane Biology, University of Alabama in Birmingham and Veterans Administration Hospital, Birmingham, Alabama 35294

Received 7 March 1974; revised 24 June 1974

Summary. *Necturus* fundic gastric mucosa was studied to define the magnitude of cellular and shunt conductance. Electrotonic coupling of surface epithelial cells by a low resistance pathway was shown by analysis of current spread within the epithelial sheet. From this analysis cellular conductance was found to be $4.18 \pm 1.57 \times 10^{-4} \Omega^{-1}\,cm^{-2}$, and transepithelial shunt conductance was $1.1 \times 10^{-4} \Omega^{-1}\,cm^{-2}$. The ratio of cell-to-shunt conductance was 3.80. These results are confirmed by a second technique in which the Δp.d. across the serosal membrane of surface cells was compared to the transepithelial Δp.d. resulting from a $\Delta[K^+]$ in the serosal solution. The data were analyzed using an electrical circuit equivalent to a mucosa composed of two highly coupled cell types. By this technique cell conductance was $3.07 \times 10^{-4} \Omega^{-1}\,cm^{-2}$, and transepithelial shunt conductance was $0.830 \times 10^{-4} \Omega^{-1}\,cm^{-2}$. The cell/shunt conductance ratio was 3.70. Thus, by two independent techniques the transepithelial shunt contributes only 1/5 of the conductance of *Necturus* fundic gastric mucosa.

Definition of the pathways of ion flow across epithelial tissues has presented problems not encountered in the study of individual cells. Until a decade ago (Ussing & Windhager, 1964) tissue conductance was thought to be the sum of conductance of its cells. The region of cell contact, the tight junction, was considered impermeable. The importance of the paracellular pathway has been confirmed in gallbladder (Diamond, Barry & Wright, 1971; Frömter, 1972), small intestine (Clarkson, 1967; Frizzell & Schultz, 1972), kidney proximal tubule (Windhager, Boulpaep & Giebisch, 1966; Hoshi & Sakai, 1967) and frog skin (Mandel & Curran, 1972). Epithelial conductance is the sum of cellular and paracellular (shunt) conductance.

Some criteria which predict the magnitude of the shunt conductance have been summarized by Diamond *et al.* (1971). A high transepithelial

* To whom correspondence should be addressed.

resistance, large potential difference (p.d.), asymmetry of p.d. responses to changes in ionic activity, high ion selectivity ratios, and maintenance of large concentration gradients would imply a small paracellular conductance. Consequently, fundic gastric mucosa appears to be a "tight" or nonleaky tissue, but quantitation of the two pathways remains important.

Blum, Hirschowitz, Helander and Sachs (1971) examined the magnitude of the shunt conductance of *Necturus* gastric mucosa by comparing the electrical resistance of the intact tissue with that of isolated cells. They concluded that the shunt conductance was no larger than cellular conductance. Treatment of the cells with proteolytic enzymes, the altered geometry, and the lack of polarization in the isolated system precluded more precise quantitation.

In this report cellular and shunt conductances are quantitated. Two methods for intact tissue will be described.

(1) A Δemf of the serosal cell membranes is induced by changing ionic activities in the serosal solution. The change of potential, across the serosal cell membrane, $\Delta\psi_{sc}$, and across the tissue, $\Delta\psi_{ms}$, is measured and analyzed using an equivalent circuit.

(2) Analysis of current spread within the epithelial sheet is a second, independent technique.

Experimental Methods

Adult *Necturus* were obtained commercially and maintained in an aquarium until use. Following decapitation the stomach was excised quickly and placed in amphibian Ringer's solution bubbled with 95% O_2—5% CO_2. After stripping the muscularis, the mucosa was stretched and mounted between two Lucite half-chambers. The upper half was open to expose the mucosal surface for microelectrode studies. The serosal and mucosal solutions were circulated from external reservoirs bubbled with 95% O_2—5% CO_2.

Fig. 1*A* is a microscopic section showing the cell types present in *Necturus* fundic gastric mucosa. The surface and neck cells comprise 37% of the cells; only the surface cells are accessible on the mucosal surface. Gastric pits branch into 3 to 5 gastric glands lined by oxyntic cells (64%). Micropuncture of oxyntic cells cannot be accomplished with visual control; iontophoresis after impalement can be used to identify the cell punctured (Shoemaker & Sachs, 1972). Thus, all micropunctures in these experiments are in surface epithelial cells.

Microelectrodes were prepared with a two-stage micropipette puller. They were examined with a phasecontrast microscope, filled with methanol in a vacuum, soaked in distilled water, and filled with 3 M KCl by diffusion during storage at 4 °C for 24 hr. Microelectrodes were used within 72 hr when the tip potential was less than 5 mV and the tip resistance was 10 to 40 MΩ.

Fig. 1B is a diagrammatic representation of equipment used to assess current spread within the mucosa. In the single microelectrode experiments the current-sending electrode and its current source, and recording connections were deleted from the circuit. Tissue resistance and the ratio of mucosal/serosal membrane resistance (R_m/R_s) were measured

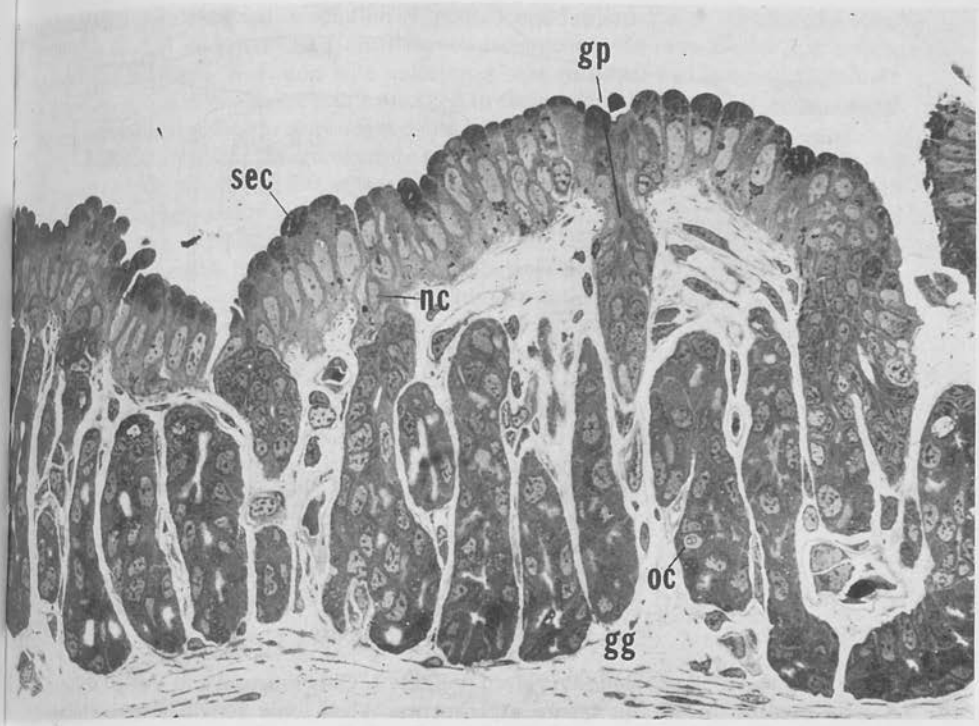

Fig. 1 (A)

Fig. 1. (*A*) A photomicrograph of *Necturus* fundic gastric mucosa showing the complex geometry of the epithelial membrane. The mucosa is composed of (1) surface epithelial cells (*sec*), the only cells which can be directly visualized, (2) neck cells (*nc*) lining the gastric pits (*gp*), and (3) oxyntic cells (oc) which line the gastric glands (*gg*) 3 to 5 of which branch from each gastric pit. The muscular layer has been stripped from the mucosa but a layer of connective tissue restricts access to gastric glands from the serosal surface. (*B*) Diagram of microelectrode equipment designed for gastric mucosa experiments. M.E. 1 is a channel for voltage recording only. M.E.2 is a channel also equipped for current sending. The microelectrode channels may be referenced to either the serosal or mucosal macroelectrode C.E. In the diagram both are referenced to the mucosal macroelectrode. Provision is also made for recording the transpotential between electrodes C.E. and sending external current through Ag/AgCl electrodes from a current source on the left-hand side of the diagram. pH changes are monitored if necessary through a battery operated pH-meter, and the solutions are circulated by a gas lift system using 95% O_2–5% CO_2 or from Marriot bottles bubbled with 95% O_2–5% CO_2. The circulating solution is jetted across the surface of the mucosa by orifices directed at the mucosa

by pulses of 10 μamp/cm^2 through Ag-AgCl circular wires mounted in the chamber. The transepithelial p.d. was measured using a pair of saturated KCl-calomel electrodes with renewable junctions. Intracellular p.d. was measured with a microelectrode referenced to the serosal solution. All resistances were corrected for resistance of the solutions in the chamber. Current pulses were limited to less than 100 msec to minimize polarization effects.

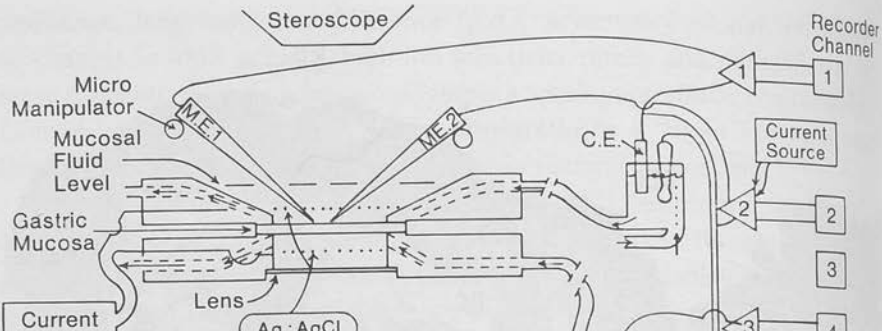

Fig. 1 (B)

Conduct of Experiments

The composition of solutions is given in Table 1. Only mucosal and serosal solutions A were used in the current spread experiments. When ionic activities were changed, Marriott bottles and a stopcock arrangement were used to perfuse the solution. When

Table 1. Composition (mM) of solutions used

	Constant product KCl experiments					Constant serosal [Cl^-] experiments	
	Serosal		Mucosal		Sulfate mucosal	5 mM K^+ Cl serosal	50 mM K^+ Cl serosal
	A	B	A	B			
Na^+	91	46	91	46	91	91	46
K^+	5	50	5	50	5	5	50
Cl^-	80	8	80	8	—	80	80
SO_4^{2-}		36	8	44	48	—	—
Mg^{++}	1.0	1.0	—	—	—	—	—
Ca^{++}	1.5	1.5	—	—	—	1.5	1.5
HCO_3^-	20	20	0	0	0	20	20
$H_2PO_4^-$	1.0	1.0	—	—	—	1	1
Glucose	5	5	5	5	5	5	5
Sucrose	—	36	15.5	51.5	55.5	—	—

Constant product KCl changes are performed with the 4 solutions at the far left. Solutions A are the starting solutions and B are the solutions giving the constant product KCl change. The remaining columns were used with $\Delta[K^+]$ while $[Cl^-] = 80$ mM. The sulfate mucosal (column 5) was used in all these experiments. Sucrose is used to maintain osmolarity.

stable p.d.'s were obtained in solution A, perfusion (15 ml/min) with the alternate solution was started and continued until the transepithelial and intracellular p.d.'s were stable (about 5 min). Perfusion with solution A was restarted and continued until the p.d.'s were stable. Usually the p.d.'s returned to their original values. During the course of one experiment several such changes could be done.

Criteria of a "good" micropuncture are: (1) an abrupt change in p.d. when the cell is punctured, (2) stable p.d. for at least 20 sec, (3) return of microelectrode potential to control level upon withdrawal from the cell, and (4) no alteration in tip resistance. While a micropuncture must have a stable p.d. for at least 20 sec to be considered "good", stability over a much longer period was routinely achieved to allow measurements of p.d. during changes in ionic activity in the bathing solution.

In the current spread experiments one microelectrode was placed intracellularly to inject current pulses ($I_0 = 5.9 \times 10^{-9}$ amps). A second microelectrode was used to measure the resulting intracellular Δp.d. in other cells as a function of distance from the source cell. Distance was measured with a micrometer eyepiece in the stereomicroscope. In both types of experiments, the relative resistance of the mucosal and serosal membranes (R_m/R_s) was measured by the Δp.d. of the intracellular electrode when current was sent transmucosally. The mucosal (m) or serosal (s) solutions were used as reference.

$$\frac{R_m}{R_s} = \frac{\Delta \text{p.d.}_{mc}}{\Delta \text{p.d.}_{sc}}. \tag{1}$$

Results

Intracellular Potential Differences

Intracellular potential of surface epithelial cells was -30 to -65 mV referenced to the serosal solution. The value varied in different mucosae but in a single epithelium the range of values was usually quite small. A transient overshoot of the potential (about 1 sec) was occasionally recorded upon impalement; thereafter the potential was stable. If a leak around the electrode was responsible for this overshoot, it was obviously only transitory since a stable potential was obtained thereafter. Fig. 2 shows the distribution of intracellular p.d.'s recorded in fundic surface cells.

Effect of Constant Product KCl Changes[1]

These changes were used to minimize ion redistribution within the mucosa; similar techniques have been applied to muscle (Hodgkin & Horowicz, 1959). The *Necturus* fundic mucosa responds asymmetrically to constant product KCl changes. A mucosal constant product KCl change (Table 2) caused a 6.55 ± 3.54 mV increase in the transmucosal p.d.; a 5.5 ± 2.07 mV change was recorded across the mucosal membrane. In contrast, serosal

1 Constant product KCl change refers to a change in (K^+) and (Cl^-) such that $(K^+) \times (Cl^-)$ is 400 mM^2 at all times.

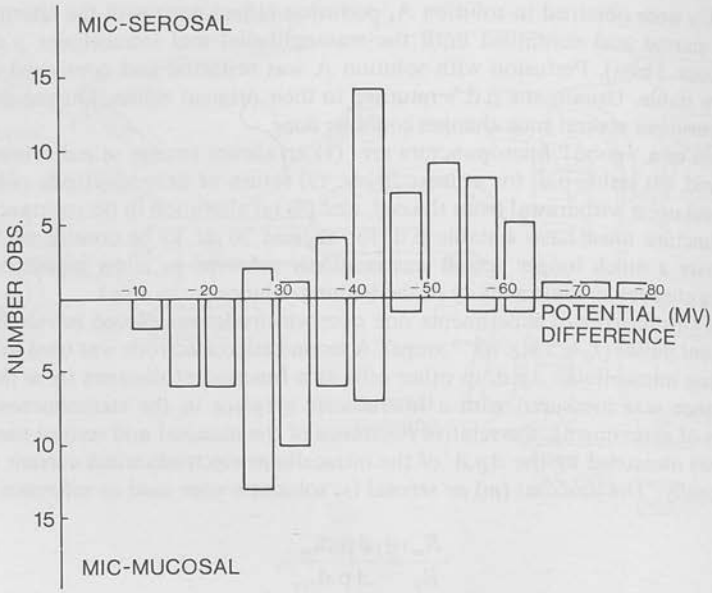

Fig. 2. The distribution of membrane potentials observed in 5 different experiments where a total of 50 cells were punctured. The upper part of the figure shows the potential measured between the microelectrode and serosal solution; the lower part is the potential between the microelectrode and mucosal solution, the difference being equal to the transtissue potential

Table 2. Changes in potentials with constant product changes in the mucosal solution

Exp. No.	$\Delta\psi_{mc}$	$\Delta\psi_{mc}/\Delta\psi_{ms}$
1	6	0.5
2	5	0.72
3	5	1.0
4	8	1.14
5	7	0.7
6	2	1.0
$\bar{X}\pm$SD	5.5±2.07	0.84±0.24

$\Delta\psi_{ms}$ designates the change in transepithelial p.d. when ionic concentration in the mucosal bathing solution is changed. $\Delta\psi_{mc}$ designates the corresponding change in p.d. across the mucosal cell membranes

constant product changes caused a transmucosal Δp.d. of 54 ± 6.2 mV. A 42 ± 9.8 mV change occurred across the serosal membrane and a 12 ± 7.2mV change was measured across the mucosal membrane of the surface epithelial cells. Fig. 3 shows a typical experiment in which the constant product change is made in the serosal solution. Table 3 summarizes the results of five experiments.

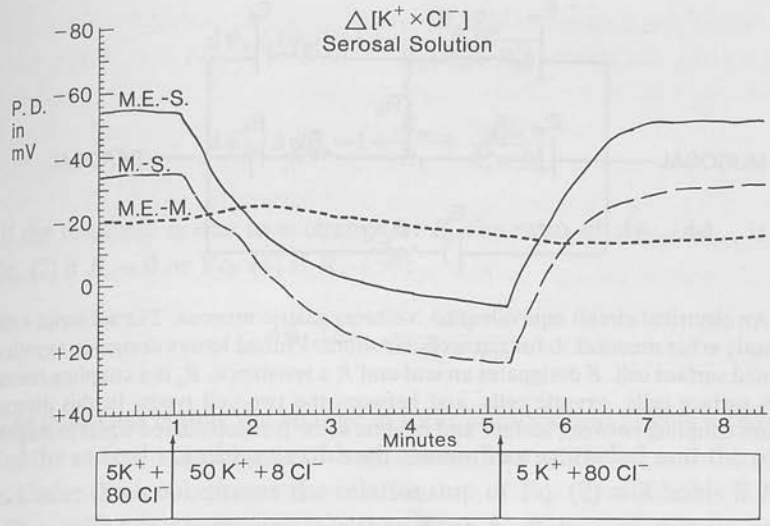

Fig. 3. The effect of a constant product KCl change (serosal solution) on the transepithelial potential and the potential across the serosal cell membrane and across the mucosal cell membrane. In the experiment shown, the Δp.d. across the serosal membrane is almost equivalent to the transepithelial Δp.d. Table 2 gives the means for all experiments

Table 3. Change in electrical parameters during constant product KCl experiments

Exp. No.	Trans resistance Sol. A	Trans resistance Sol. B	R_m/R_s Sol. A	R_m/R_s Sol. B	$\Delta\psi_{ms}$	$\Delta\psi_{sc}$	$\Delta\psi_{mc}$	$\Delta\psi_{sc}/\Delta\psi_{ms}$
1	1395	1350	0.93	0.52	59	55.5	3.5	0.94
2	2124	1844	1.47	1.47	50.75	43.25	7.5	0.85
3	1687	1485	1.2	1.0	55	32.5	22.5	0.59
4	2160	2160	1.28	1.0	60	46	14	0.77
5	1350	1215	1.0	1.11	45	32.5	12.5	0.72
Avg. ±	1743±	1610±	1.18±	1.02±	54±	42.0±	12.0±	0.77±
SD	387	386	0.22	0.34	6.2	9.8	7.2	0.13

The mucosa, initially bathed by mucosal and serosal solution A, is perturbed by changing the serosal solution to solution B. Serosal to mucosal ionic gradients (mM) are Na^+, 46:91; K^+, 50:5, Cl^-, 8:80; SO_4^{2-}, 36:8. Other ions remain in the same proportion as in solution A. Transresistance is calculated from the transepithelial Δp.d. when 10 $\mu A/cm^2$ is sent transepithelially. R_m/R_s is the Δp.d. across the mucosal cell membrane: Δp.d. across the serosal cell membrane when 10 $\mu A/cm^2$ is sent transepithelially. $\Delta\psi_{ms}$ is the change in transepithelial p.d. resulting from the change in ionic activity. $\Delta\psi_{sc}$ is the corresponding change across the serosal membrane of a surface epithelial cell.

Rose and Schultz (1971) described the analysis of a similar problem resulting from transport of sugars or amino acids across the mucosal membrane of the intestinal epithelial cell. The model could not be used directly

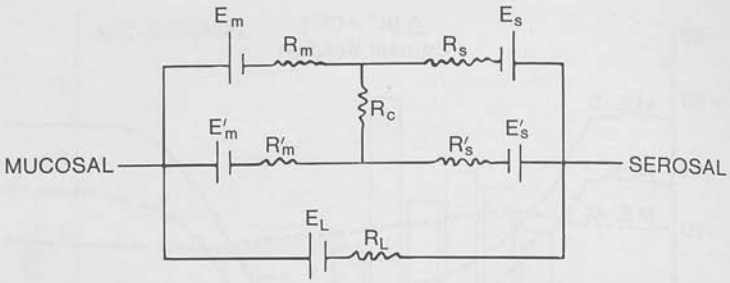

Fig. 4. An electrical circuit equivalent to *Necturus* gastric mucosa. The subscript s stands for serosal; m for mucosal, L for paracellular shunt. Primed letters designate oxyntic cell, nonprimed surface cell. E designates an emf and R a resistance. R_c is a coupling resistance between surface cells, oxyntic cells, and between the two cell types. In this diagram it designates coupling between surface and oxyntic cells. It is considered equal in magnitude within and between the two cell systems

since gastric fundic mucosa is composed of at least two cell types. We extended their model to include two cell types. Fig. 4 is the equivalent circuit for this model. E_s and E'_s represent the emf's, and R_s and R'_s represent the resistivities of the serosal membranes of surface epithelial and oxyntic cells (primed letter), respectively. E_m and E'_m are the emf's, and R_m and R'_m are the resistivities of the mucosal membranes of surface epithelial and oxyntic cells, respectively. E_L and R_L represents an emf and a resistivity of a transepithelial shunt pathway. R_c represents an intercellular coupling resistance of the type described by Loewenstein and Kanno (1964). Coupling between cells in isolated gastric tubules has been demonstrated previously (Blum *et al.*, 1971) and is quantitated for surface cells (vide infra). In the model we have assumed that the surface cell system and the oxyntic cell system of the gastric glands, as well as the two cell systems, are connected by the coupling resistance. Further, we have assumed that R_c is equal in the two cell systems. Experimentally the emf's are changed by altering ionic composition; in the analysis we have assumed that ΔE_s or $\Delta E'_s \gg \Delta E_L$. For simplicity ΔE_L is taken as 0. For validation of these assumptions please refer to the Discussion.

The equivalent circuit is used to predict the response, $\Delta\psi_{sc}$ and $\Delta\psi_{ms}$, if the Δemf arises in (1) E_s or (2) E'_s or (3) $E_s + E'_s$. In each instance the intercellular coupling resistance is either (a) zero or (b) infinite. In the first case (ΔE_s) the ratio $\Delta\psi_{sc}/\Delta\psi_{ms}$, the Δp.d. across the serosal membrane/Δp.d. across the tissue resulting from the change in ionic activity, is given in Eq. (2) if $R_c \to 0$ or Eq. (3) if $R_c \to \infty$. (For further derivation *see* Appendix.)

$$\Delta\psi_{sc}/\Delta\psi_{ms}=1+\frac{R_m R'_m}{R_L(R_m+R'_m)} \tag{2}$$

$$\Delta\psi_{sc}/\Delta\psi_{ms}=1+\frac{R_m}{R_L}+\frac{R_m}{R'_s+R'_m}. \tag{3}$$

If the response is due to a change in E'_s the ratio of $\Delta\psi_{sc}/\Delta\psi_{ms}$ is given in Eq. (2) if $R_c\to 0$ or Eq. (4) if $R_c\to\infty$:

$$\Delta\psi_{sc}/\Delta\psi_{ms}=\frac{R_s}{R_s+R_m}. \tag{4}$$

The third case is that the change in ionic composition affects a change of emf of the serosal membranes of both the surface epithelial and the oxyntic cells. Under these conditions the relationship of Eq. (2) still holds if $R_c\to 0$. Eq. (2) is valid for *any* change in either E_s or E'_s. If $R_c\to\infty$, a more complicated relationship exists:

$$\Delta\psi_{sc}/\Delta\psi_{ms}=\frac{R_m}{R_L\left[1+\frac{\Delta E'_s}{\Delta E_s}\left(\frac{R_s+R_m}{R'_s+R'_m}\right)\right]}+\frac{1+\frac{R_m+\left(\frac{\Delta E'_s}{\Delta E_s}\right)R_s}{R'_m+R'_s}}{1+\frac{\Delta E'_s}{\Delta E_s}\left(\frac{R_s+R_m}{R'_s+R'_m}\right)}. \tag{5}$$

The range of each function may be helpful in analysis of experimental results. Eqs. (2) and (3) will produce values greater than unity. In contrast, Eq. (4) will produce values from 0 to 1, but none larger. Only Eq. (5) will produce values for $\Delta\psi_{sc}/\Delta\psi_{ms}$ ranging above zero but not limited at one. Clearly, Eqs. (3) and (4) are only special cases of Eq. (5) where $\Delta E_s \gg \Delta E'_s$ and $\Delta E'_s \gg \Delta E_s$, respectively.

Necturus fundic mucosae give a spectrum of $\Delta\psi_{sc}/\Delta\psi_{ms}$ (Table 3) in response to the constant product KCl change. Values from 0.59 to 0.94 are obtained. Clearly, with these values (mean 0.77), Eqs. (2) and (3) do not apply, yet the surface cells are not responding passively to a $\Delta E'_s$. If the surface cell $\Delta\psi_{sc}$ is only a function of a $\Delta E'_s$ (Eq. 4), $\Delta\psi_{sc}/\Delta\psi_{ms}$ will be given by the voltage divider ratio:

$$\frac{\Delta\psi_{sc}}{\Delta\psi_{ms}}=\frac{R_s}{R_m+R_s}=\frac{1}{\frac{R_m}{R_s}+1}=0.46.$$

In fact, not even one mucosal response is predicted by its voltage divider ratio. Therefore, the surface cell must have a ΔE_s, and the correct analytical

model would have to include a $\Delta E_s + \Delta E'_s$ and R_c would have to be large to give a ratio < 1, hence Eq. (5). This requirement, that R_c is large, is not in agreement with intercellular coupling found in this tissue (*see below*).

Eq. (5) predicts that $\Delta\psi_{sc}/\Delta\psi_{ms}$ measured in a surface cell will be less than unity only when $\Delta E_s \ll \Delta E'_s$. ΔE_s can be quantitated if R_c is large. $\Delta\psi_{mc}$ results from a change in current flow across R_m (12.0 mV) (Table 3). From the voltage divider ratio, R_m/R_s, ΔIR_s is 10.2 mV. Thus ΔE_s, due to the constant product change, is 31.8 mV. It has not been possible to directly measure the potential changes in an oxyntic cell, but assuming even a maximum change of 58 mV (the Nernst potential) ΔE_s is not small relative to $\Delta E'_s$.

Inconsistencies, that R_c is large and that ΔE_s is small compared to $\Delta E'_s$, lead to the conclusion that E_m or E'_m may be undergoing some change – specifically an electrogenic mechanism (the Cl^- pump, a component of E'_m) is being inhibited by the low serosal $[Cl^-]$.

For a $\Delta E_s + \Delta E'_s + \Delta E'_m$, $\Delta\psi_{sc}/\Delta\psi_{ms}$ is given by Eq. (6), if $R_c \to 0$:

$$\frac{\Delta\psi_{sc}}{\Delta\psi_{ms}} = \frac{(\Delta E_s R'_s + \Delta E'_s R_s)[R_L(R_m + R'_m) + R_m R'_m] + R_s R'_s R_m \Delta E'_m}{R_L(R_m + R'_m)(\Delta E_s R'_s + \Delta E'_s R_s) + R_L R_m (R_s + R'_s)\Delta E'_m}; \quad (6)$$

If $R_c \to \infty$,

$$\frac{\Delta\psi_{sc}}{\Delta\psi_{ms}} = \frac{R_m}{R_L\left[1 + \frac{\Delta E'_m + \Delta E'_s}{\Delta E_s}\left(\frac{R_s + R_m}{R'_s + R'_m}\right)\right]} + \frac{1 + \frac{R_m + R_s\left(\frac{\Delta E'_m + \Delta E'_s}{\Delta E_s}\right)}{R'_s + R'_m}}{1 + \frac{\Delta E'_m + \Delta E'_s}{\Delta E_s}\left(\frac{R_s + R_m}{R'_s + R'_m}\right)}. \quad (7)$$

Eqs. (6) and (7) predict that inhibition of anion (Cl^-) transport ($\Delta E'_m$), and an increase in E'_s due to $\Delta[K^+]$ would be additive. ΔE_s could appear small compared to the sum $\Delta E'_s + \Delta E'_m$.

To examine the involvement of E'_m we have performed similar experiments utilizing a 10-fold change of $[K^+]$ from 5 to 50 mM; presumably, Cl^- emf is constant under these conditions. In these experiments sulfate replaces Cl^- in the mucosal solution while $[Cl^-]$ is 80 mM in the serosal solution. Table 4 summarizes the data from six experiments in which the serosal solution $[K^+]$ is changed. Fig. 5 shows similar data obtained when Cl^- is replaced by SO_4^{2-} in both serosal and mucosal solutions.

When $[Cl^-]$ is constant, $\Delta\psi_{sc}$ is 34.7 ± 5.79 mV and $\Delta\psi_{ms}$ is 30.3 ± 7.11 mV. The ratio $\Delta\psi_{sc}/\Delta\psi_{ms}$ is 1.17. All experiments (Table 4) give $\Delta\psi_{sc}/\Delta\psi_{ms} > 1$. With $[Cl^-]$ constant these results are very different from

Table 4. Change in electrical parameters with change in serosal $[K^+]$

	R_{trans} (before ΔK^+)	R_{trans} (after ΔK^+)	R_m/R_s (before ΔK^+)	R_m/R_s (after ΔK^+)	$\Delta\Psi_{ms}$	$\Delta\Psi_{sc}$	$\Delta\Psi_{mc}$	$\Delta\Psi_{sc}/\Delta\Psi_{ms}$
	2025	1822	1.62	1.58	21	32	−11	1.52
	2767	2700	1.61	1.44	39	42	− 3	1.08
	2160	1755	1.73	1.64	22.5	25	− 2.5	1.11
	2497	2430	1.72	1.5	35	38	− 3	1.09
	2835	2295	1.63	1.48	33	36	− 3	1.09
	3105	2902	1.88	1.44	31	35	− 4	1.13
$\bar{X}\pm$	2565±	2317±	1.70±	1.51±	30.3±	34.7±	− 4.42±	1.17±
SD	416	461	0.10	0.08	7.11	5.79	3.26	0.17

R_{trans} designates the transepithelial resistance determined from the transepithelial Δ p.d. when 10 μA/cm² is sent transepithelially. R_m/R_s is the Δ p.d. across the mucosal membrane: Δp.d. across the serosal membrane of a surface epithelial cell when 10 μA/cm² is sent transepithelially. $\Delta\Psi_{ms}$ is the transepithelial change in p.d. and $\Delta\Psi_{sc}$ is the change in p.d. across the serosal membrane of a surface epithelial cell resulting from the $\Delta[K^+]$ from 5 to 50 mM. All experiments are done with SO_4^{2-} replacing Cl^- in the mucosal solution while $[Cl^-] = 80$ mEquiv/liter in the serosal solution

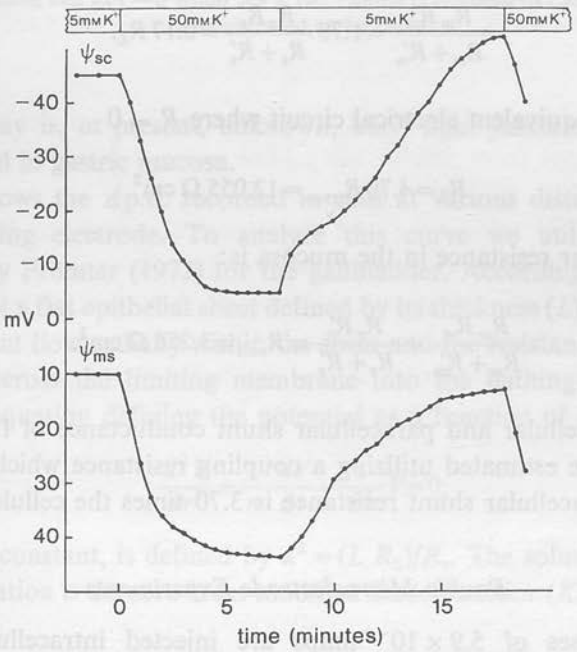

Fig. 5. This figure demonstrates the effect of a 10-fold change in $[K^+]$ in the serosal bathing solution. The transepithelial potential Ψ_{ms}, and the potential from the serosal solution to intracellular electrodes, Ψ_{sc}, are recorded. $[K^+]$ in the serosal solution is recorded at the top of the figure, and sulfate replaces Cl^- in both serosal and mucosal solutions. Note that in these experiments, in contrast to the constant product KCl changes, the $\Delta\Psi_{sc}$ is greater than the $\Delta\Psi_{ms}$

those obtained using constant product KCl changes. Constant $[Cl^-]$ seems to avoid the $\Delta E'_m$ which occurs in changing to $[Cl^-]$ serosal solution.

With the intercellular coupling demonstrated below, the equivalent circuit should include an R_c which is small and can be taken to approach zero. If $R_c \to 0$, Eq. (2) is valid for a change in E_s, E'_s, or both. Hence, Eq. (2) is used for further analysis.

$$0.17 = \frac{R_m R'_m}{R_L(R_m + R'_m)}.$$

Under the conditions that $R_c \to 0$, the voltage divider ratio R_m/R_s actually reflects the mucosal membranes in parallel and serosal membranes in parallel.

$$\text{Voltage divider ratio} = \frac{\dfrac{R_m R'_m}{R_m + R'_m}}{\dfrac{R_s R'_s}{R_s + R'_s}}.$$

Thus, from Table 4

$$\frac{R_m R'_m}{R_m + R'_m} = 1.70 \frac{R_s R'_s}{R_s + R'_s} = 0.17 R_L.$$

Utilizing the equivalent electrical circuit where $R_c \to 0$

$$R_L = 4.70 R_{\text{trans}} = 12{,}055\ \Omega\,\text{cm}^2$$

whereas cellular resistance in the mucosa is:

$$\frac{R_m R'_m}{R_m + R'_m} + \frac{R_s R'_s}{R_s + R'_s} = R_{\text{cell}} = 3{,}258\ \Omega\,\text{cm}^2.$$

Thus the cellular and paracellular shunt conductance of fundic gastric mucosa can be estimated utilizing a coupling resistance which approaches zero. The paracellular shunt resistance is 3.70 times the cellular resistance.

Double Microelectrode Experiments

When pulses of 5.9×10^{-9} amps are injected intracellularly, radial coupling can be demonstrated by measuring the resulting intracellular Δ p.d. as a function of distance from the current source. Fig. 6 shows the voltage recorded at several points 33 μ and 66 μ from the current-sending electrode. Radial coupling is shown. The site or molecular anatomy of the low resis-

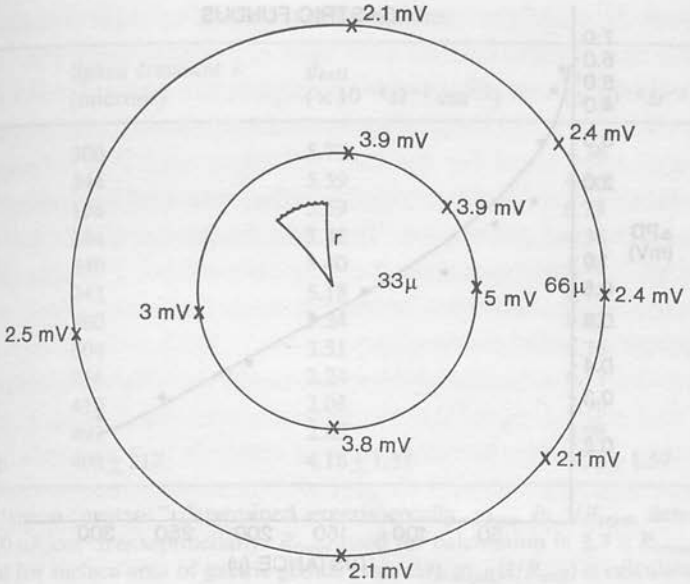

Fig. 6. This figure demonstrates the Δp.d. recorded in several cells at 33 and 66 μ from a surface epithelial cell at $r=0$ when 5.9×10^{-9} amps is injected in the cell. Coupling is demonstrated to be radial

tance pathway is, at present, unknown, but "tight junctions" have been demonstrated in gastric mucosa.

Fig. 7 shows the Δp.d. recorded in cells at various distances from the current-sending electrode. To analyze this curve we utilize the model developed by Frömter (1972) for the gallbladder. According to this model the mucosa is a flat epithelial sheet defined by its thickness (L) and resistance (R_c) to current flow radially within the sheet and the resistance (R_Z) to flow of current across the limiting membrane into the bathing solution. The differential equation defining the potential as a function of distance (r) is:

$$\frac{d^2V}{dr^2}+\frac{1}{r}\frac{dV}{dr}-\frac{1}{\lambda^2}V=0. \tag{8}$$

λ, the space constant, is defined by $\lambda^2=(L\,R_Z)/R_c$. The solution of the differential equation is the zero order modified Bessel function (K_0) of the second kind.

$$V_r=AK_0(r/\lambda) \quad \text{where } A=(I_0\,R_c)/2\pi L. \tag{9}$$

A numeric solution is obtained using an iterative technique with an IBM 370 computer. The solution is that value of λ for which A is most constant at the experimental r's.

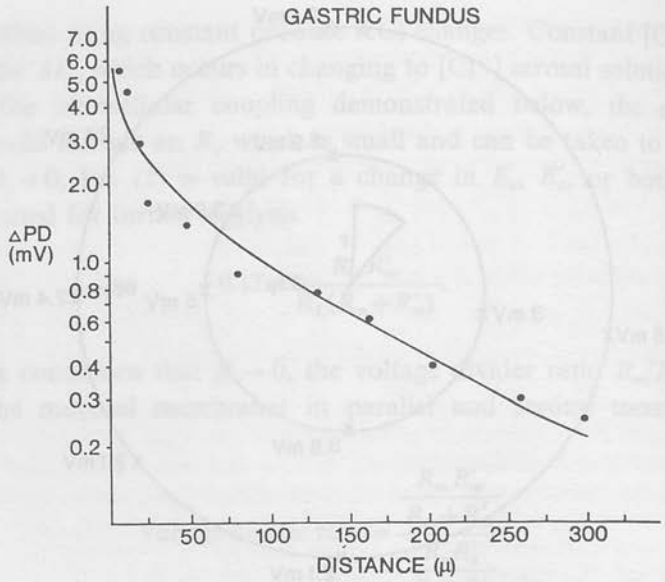

Fig. 7. The voltage recorded intracellularly at a distance r from the current-sending electrode in the gastric fundus. The curve drawn is the Bessel function, $V=AK_0(r/\lambda)$, generated from the experimentally derived parameters A and λ

The results for 11 different experiments are given in Table 5. A space constant λ ranges from 196 to 960 μ. The mean λ is 408 μ and standard deviation is 217 μ.

The computed value of λ and the electrical circuit equivalent to R_Z (Fig. 8) provide an alternate quantitation of the cellular and shunt resistance in the intact mucosa. This circuit differs from that used by Frömter (1972) in that current leaving surface cells via the mucosal membranes must return to the reference side by crossing the transepithelial resistance. Frömter (1972) used only the shunt conductance in the return limb presumably because transepithelial reistance in gallbladder is dominated by the shunt resistance.

R_s, the serosal cell membrane resistivity, is the positive solution of the quadratic equation:

$$-[R_m/R_s]R_s^2+[R_Z+(R_m/R_s)R_Z-R_{\text{trans}}]R_s+R_{\text{trans}}R_Z=0. \tag{10}$$

R_M, the mucosal cell membrane resistivity, is

$$R_M=(R_m/R_s)R_s \tag{11}$$

and the shunt resistivity R_L is

$$R_L=\frac{R_{\text{trans}}(R_m+R_s)}{(R_m+R_s)-R_{\text{trans}}} \tag{12}$$

Table 5. Gastric fundus

	Space constant λ (microns)	g_{cell} ($\times 10^{-4}\,\Omega^{-1}\,cm^{-2}$)	g_{trans} ($\times 10^{-4}\,\Omega^{-1}\,cm^{-2}$)
	300	5.72	4.36
	344	5.59	4.36
	196	5.59	6.73
	344	5.42	4.36
	340	5.40	4.36
	242	5.18	6.73
	960	3.24	8.72
	604	3.51	4.36
	256	2.24	6.17
	410	2.08	3.90
	492	2.03	3.98
Mean$\pm$SD	408$\pm$217	4.18$\pm$1.57	5.28$\pm$1.57

λ is the "space constant" determined experimentally. g_{trans} is $1/R_{trans}$ determined by sending 10 $\mu A/cm^2$ transepithelially. R_{trans} used for calculation is $2.7 \times R_{trans}$ measured to account for surface area of gastric glands (*see text*). $g_{cell}(1/R_{cell})$ is calculated as given in the text

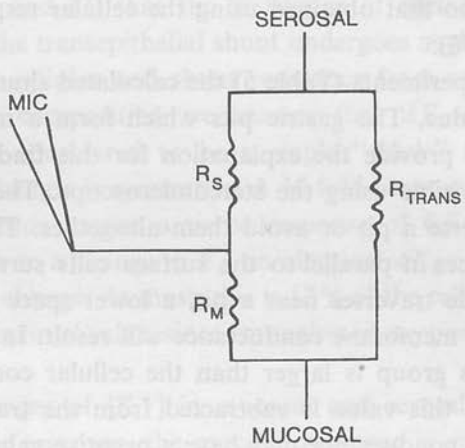

Fig. 8. A simplified circuit equivalent to R_Z as measured in the two microelectrode experiments. Current may flow across the serosal cell membrane represented by R_S or alternatively across the mucosal membrane R_M and back across the tissue, where R_{trans} is the lumped tissue resistance to transepithelial current flow

and the shunt-to-cell resistivity ratio is

$$\frac{R_L}{R_m+R_s}=\frac{R_{trans}}{(R_m+R_s)-R_{trans}}. \tag{13}$$

These equations are directly applicable to a flat tissue such as the gallbladder. In contrast, *Necturus* fundic mucosa is multiply indented with glands

which greatly increase the surface area subjected to measurements. Blum *et al.* (1971) have shown that for each cm^2 of surface area there is 1.7 cm^2 of tubular surface area. Thus, the transepithelial resistivity is calculated from the surface plus glandular surface area assuming that conductance per unit area is identical for the two cell types, and thus, transepithelial resistance is corrected for this increased surface area (2.7 × measured R_{trans}). Because some injected current must flow into the tubular glands, the distance of current spread may be greater than the measured r. λ is also altered by this glandular conductance but no model could be found which considers current spread into the gastric glands.

Table 5 shows the results of 11 experiments in which the cellular conductance and transepithelial conductance are computed. The 11 mucosae demonstrate a mean space constant λ of 408 ± 217 μ. The mean cellular conductance is $4.18 \pm 1.57 \times 10^{-4} \Omega^{-1}$ cm^{-2} and mean transepithelial conductance is $5.28 \pm 1.57 \times 10^{-4} \Omega^{-1}$ cm^{-2}. The shunt conductance is $1.10 \times 10^{-4} \Omega^{-1}$ cm^{-2}. The ratio of cell-to-shunt conductance is 3.80. In terms of resistance the ratio of shunt resistance to cell resistance is also 3.80. This value is very close to that obtained using the cellular response to changes in ionic activity (3.70).

In four of 11 experiments (Table 5) the calculated shunt conductance is a small negative value. The gastric pits which form a mosaic of surface discontinuities may provide the explanation for this finding. In *Necturus* these pits are not visible using the stereomicroscope. The probing microelectrode may traverse a pit or avoid them altogether. The gastric glands will act as resistances in parallel to the surface cells surrounding the pit. If the microelectrode traverses near a pit, a lower space constant and an overestimate of cell membrane conductance will result. In fact, the cellular conductance of this group is larger than the cellular conductance of the others. Thus, when this value is subtracted from the transepithelial conductance, the shunt conductance may have a negative value.

Discussion

Data derived from chambered gastric fundic mucosa suggest that gastric fundic mucosa is quite tight. It develops a p.d. of 30 to 40 mV, supports a 10^6-fold H^+ gradient, and reacts asymmetrically to changes in ion concentration. *In vivo* studies also suggest that fundic mucosa has conductance properties quite different from other areas of the gastrointestinal tract. Dyck, Werther and Rudick (1969) and Himal, Young, Rudick, Werther and Janowitz (1970) studied the loss of ions from the lumen of the GI tract

and found that "back flux of ions" in the antrum was 15 times, in the duodenum 45 times and in the small intestine 60 times larger than that in gastric fundus. With this supporting evidence it is essential to quantitate the magnitude of the cellular and transepithelial shunt resistance in fundic gastric mucosa.

Using two techniques we find that the shunt conductance is small compared to tissues such as intestine, gallbladder, or proximal tubule. A change of $[K^+]$ in the serosal solution causes a transepithelial Δp.d. and a Δp.d. across the serosal membrane of the surface epithelial cell. These changes result from a Δemf of the serosal membrane of both the surface and oxyntic cells. Estimation of the shunt resistance requires analysis of an electrical circuit equivalent to the gastric mucosa (Fig. 4). The analysis is greatly simplified if one or two elements can be perturbed while the others are held constant. Specifically, we assume that (1) the transepithelial shunt emf incurs no significant ΔE_L and that the diffusion potential due to change in $[K^+]$ and $[Cl^-]$ is small compared to the Δp.d. measured; (2) the changes in p.d. are a result of a change in an emf across the serosal membrane of the surface or oxyntic cells; and (3) that the resistance of surface and oxyntic cell membranes and the transepithelial shunt undergoes negligible change.

To quantitate cellular and shunt resistance from experiments utilizing changes in ionic composition we assume that $\Delta E_L \ll \Delta E_{\text{cell}}$. The shunt pathway may be considered to be a single "thick" membrane, and its response to ion changes is symmetric. A 10-fold constant product change in the mucosal solution causes a tissue response of 6.5 mV. If we assume that this is all due to a change in E_L, an identical ΔE_L occurs with a serosal constant product change. At most, this is 12% of the cell membrane change. This is clearly a maximal value, since we neglected any possible cell membrane change.

Similarly, changes of $[K^+]$ in mucosal and serosal solutions, show a highly asymmetric response; the mucosal response is only a small fraction of the serosal response (Sachs *et al.*, 1971). Thus, the shunt in gastric mucosa, like gallbladder (Diamond *et al.*, 1971), does not discriminate significantly between K^+ and Na^+.

The model allows prediction of $\Delta\psi_{sc}/\Delta\psi_{ms}$ if the Δemf occurs solely in the paracellular shunt. Eqs. (14) and (15) give the $\Delta\psi_{sc}/\Delta\psi_{ms}$ if the changes were due only to a ΔE_L while all other emf's are constant. If $R_c \to 0$

$$\frac{\Delta\psi_{sc}}{\Delta\psi_{ms}} = \frac{\dfrac{R_s R_s'}{R_s + R_s'}}{\dfrac{R_s R_s'}{R_s + R_s'} + \dfrac{R_m R_m'}{R_m + R_m'}} \tag{14}$$

while if $R_c \to \infty$

$$\frac{\Delta\psi_{sc}}{\Delta\psi_{ms}} = \frac{R_s}{R_s + R_m}. \tag{15}$$

$\Delta\psi_{sc}/\Delta\psi_{ms}$ must be less than 1 and must reflect the voltage divider ratio. From Table 4, $\Delta\psi_{sc}/\Delta\psi_{ms}$ would be 0.39 if the change were due only to ΔE_L. In contrast, $\Delta\psi_{sc}/\Delta\psi_{ms}$ was 1.17. According to this model for gastric mucosa, the Δemf in these experiments does not arise from the paracellular shunt. Comparing the predicted $\Delta\psi_{sc}/\Delta\psi_{ms}$ to the actual results, the shunt would appear to contribute minimally to the Δemf.

Further, ΔE_L can be quantitated in the $\Delta[K^+]$ experiments. Calculated ΔI_{sc} is 12 μamps cm^{-2} in these experiments. R_{trans} and R_m/R_s are the mean values from Table 4. Cell resistance and shunt resistance are taken from Table 5 because these values do not depend on ionic gradients. ΔIR is calculated for both membranes giving ΔE_L of -1.08 mV. In contrast, ΔE_s is calculated to be 37.3 mV. Thus, by this method ΔE_L is estimated to be only 2% of ΔE_s. By these three criteria we find $\Delta E_L \ll \Delta E_s$ and consider that the experimental design conforms adequately to the requirements of the model.

The origin of the Δemf within the cell is also crucial to analysis of these experiments. Based on the equivalent circuit (Fig. 4) and the assumption that the constant product KCl change affects only E_s and E'_s, a $\Delta\psi_{sc}/\Delta\psi_{ms} < 1$ can only arise if $\Delta E_s \ll \Delta E'_s$, and only if R_c is large. It can be calculated, however, that ΔE_s is 31.8 mV. The obvious explanation for this discrepancy is that another E is changing (i.e. E'_M, the electrogenic Cl^- pump emf) due to the reduction in $[Cl^-]$ from 80 to 8 mM. Thus when $[Cl^-]$ is kept constant, and only $[K^+]$ is changed from 5 to 50 mM, the ratio $\Delta\psi_{sc}/\Delta\psi_{ms}$ is invariably greater than 1. With a small coupling resistance the serosal or mucosal membrane of the surface and oxyntic cells are parallel resistances. $\Delta\psi_{mc} = -4.42$ mV is the ΔIR across $R_m R'_m/(R_m + R'_m)$. ΔIR across $R_s R'_s/(R_s + R'_s)$ is -2.60 mV and the Δemf across the serosal membranes is 37.3 mV. It is not possible to quantitate ΔE_s and $\Delta E'_s$ since the relative magnitude of R_s and R'_s remain unknown. With this information, and the low value for R_c derived from the two electrode experiments we can calculate the shunt conductance contribution to tissue conductance.

The effect of $\Delta[K^+]$ and constant product KCl changes on membrane resistance is assessed by the voltage divider ratio and by transepithelial resistance. There is a small (9.6%) but statistically significant change in transepithelial resistance ($t = 3.20$, $0.01 < p < 0.025$). The change in the ratio

R_m/R_s ($t = 3.24$, $0.01 < p < 0.025$) as a result of change in ionic activity is statistically significant, but is only 10.8%.

Identical conclusions are derived from current spread and changes of ionic activity methods, although the assumptions of the analysis are different. The ratio of shunt resistance to cell resistance is 3.70 when assessed by change in ionic activity and 3.80 when assessed by radial spread of current injected intracellularly in a surface cell.

By this latter technique, however, 4/11 mucosae gave small negative values for the shunt conductance. The remainder gave small positive values. We have felt this represents experimental error which is most manifest in mucosae with large shunt resistance (small shunt conductance);

$$g_{\text{tissue}} - g_{\text{cell}} \to 0.$$

Analysis of current spread in mucosa such as proximal tubule gallbladder, or intestine with a large tissue conductance compared to cellular conductance can tolerate small errors in cellular conductance. Mucosae where g_{tissue} approaches g_{cell} cannot. Alternatively, the model of a flat epithelial sheet does not account for tubular indentations (gastric pits) which can be considered high conductance discontinuities in the plane of the tissue. Unfortunately, a mathematical expression to describe a mucosa multiply indented by tubular glands could not be found.

It would appear from these studies that techniques independent of tissue geometry are most applicable to gastric fundic mucosa; but by using an adequately large sample of mucosae, techniques dependent on mucosal geometry can be used. Whichever technique is used, the shunt conductance of the *Necturus* fundic gastric mucosa is only 1/5 of tissue conductance.

Appendix

The fundic mucosa of *Necturus* is composed of two major cell types – the surface epithelial and oxyntic cells. A low resistance pathway has been demonstrated between cells of the same type and between the different types. The electrical circuit equivalent to a mucosa with these characteristics is shown in Fig. 4. This circuit was analyzed by first obtaining an expression for the current flow I_c across the coupling resistance:

$$I_c R_c = (E_s - E_s') + I_s R_s - I_s' R_s'$$

where the subscripts s and m refer to the serosal and mucosal membrane of the surface cell system and s' and m' refer to the same membranes of the

Table 6. Formulas

	$R_c \to 0$
Change due to ΔE_s	$1+\dfrac{R_m R'_m}{R_L(R_m+R'_m)}$
Change due to $\Delta E'_s$	$1+\dfrac{R_m R'_m}{R_L(R_m+R'_m)}$
Change due to $\Delta E_s+\Delta E'_s$	$1+\dfrac{R_m R'_m}{R_L(R_m+R'_m)}$
Change due to $\Delta E_s+\Delta E'_s+\Delta E'_m$	$\dfrac{[R_L(R_m+R'_m)+R_m R'_m](\Delta E_s R'_s+\Delta E'_s R_s)+\Delta E'_m R_m R_s R'_s}{R_L(R_m+R'_m)(\Delta E_s R'_s+\Delta E'_s R_s)+\Delta E'_m R_m R_L(R_s+R'_s)}$

Formulas relating change in p.d. across the serosal membrane of a surface cell to the change in p.d. measured transepithelially when there is a change in one or more emf in the surface, oxyntic cell, or both. To obtain these formulas the coupling resistance is

oxyntic cell system. I_s and I'_s can then be found from the expression for the p.d. drop (ψ_{ms}) transmucosally and by substitution:

$$I_s=\frac{\psi_{ms}[R'_s(R_m+R'_m)-R_c(R'_s+R'_m)]-E_s[R'_s(R_m+R'_m)+R_m R'_m-R_c(R'_s+R'_m)]+E_m[R_c(R'_s+R'_m)-R'_m R'_s]+R_m R'_m E'_s-R_m R'_s E'_m}{R_m R_s(R'_s+R'_m)+R'_m R'_s(R_s+R_m)-R_c(R_s+R_m)(R'_s+R'_m)}$$

$$I'_s=\frac{\psi_{ms}[R_s(R_m+R'_m)-R_c(R_s+R_m)]+R_m R'_m E_s-R_s R'_m E_m-E'_s[R_s(R_m+R'_m)+R_m R'_m-R_c(R_s+R_m)]+E'_m[R_c(R'_s+R'_m)-R_s R_m]}{R_m R_s(R'_s+R'_m)+R'_m R'_s(R_s+R_m)-R_c(R_s+R_m)(R'_s+R'_m)}.$$

By appling Kirchhoff's law ψ_{ms} can be found to be

$$\psi_{ms}=\frac{\begin{aligned}&E_s R_L[R'_s(R_m+R'_m)-R_c(R'_s+R'_m)]+E_m R_L[R'_m(R_s+R'_s)-R_c(R'_s+R'_m)]\\&+E'_s R_L[R_s(R_m+R'_m)-R_c(R_s+R_m)]+E'_m R_L[R_m(R_s+R'_s)-R_c(R_s+R_m)]\\&+E_L[R_m R_s(R'_m+R'_s)+R'_m R'_s(R_m+R_s)-R_c(R_s+R'_s)(R_m+R'_m)]\end{aligned}}{\begin{aligned}&R_L(R_m+R'_m)(R_s+R'_s)+R_m R_s(R'_m+R'_s)+R'_m R'_s(R_m+R_s)\\&-R_c R_L(R_m+R_s+R'_m+R'_s)-R_c(R_s+R_m)(R'_s+R'_m)\end{aligned}}$$

relating $\Delta\psi_{sc}/\Delta\psi_{ms}$
$R_c \to \infty$
$1+\dfrac{R_m}{R_L}+\dfrac{R_m}{R'_m+R'_s}$
$\dfrac{R_s}{R_m+R_s}$
$\dfrac{R_m}{R_L\left[1+\dfrac{\Delta E'_s}{\Delta E_s}\left(\dfrac{R_s+R_m}{R'_s+R'_m}\right)\right]}+\dfrac{1+\dfrac{R_m+\left(\dfrac{\Delta E'_s}{\Delta E_s}\right)R_s}{R'_m+R'_s}}{1+\dfrac{\Delta E'_s}{\Delta E_s}\left(\dfrac{R_s+R_m}{R'_s+R'_m}\right)}$
$\dfrac{R_m}{R_L\left[1+\dfrac{\Delta E'_m+\Delta E'_s}{\Delta E_s}\left(\dfrac{R_s+R_m}{R'_s+R'_m}\right)\right]}+\dfrac{1+\dfrac{R_m+R_s\left(\dfrac{\Delta E'_m+\Delta E'_s}{\Delta E_s}\right)}{R'_m+R'_s}}{1+\dfrac{\Delta E'_m+\Delta E'_s}{\Delta E_s}\left(\dfrac{R_s+R_m}{R'_s+R'_m}\right)}$

taken to be small compared to membrane resistances and is visualized to approach zero. Alternatively, R_c is visualized as large compared to membrane resistance and is visualized to approach infinite size

and ψ_{sc}, the voltage drop across the serosal membrane of the surface epithelial cell, is found by substitution into

$$\psi_{sc}=E_s+I_sR_s$$

$$\psi_{sc}=\frac{\begin{array}{l}\{R_L(R_m+R'_m)(R_s+R'_s)+R_mR_s(R'_m+R'_s)+R'_mR'_s(R_m+R_s)\\ -R_c[R_L(R_m+R_s+R'_m+R'_s)+(R_s+R_m)(R'_s+R'_m)]\}\{E_s[R_mR'_mR'_s\\ -R_cR_m(R'_m+R'_s)]+E_m[R_sR'_mR'_s-R_cR_s(R'_s+R'_m)]+E'_sR_mR_sR'_m\\ +E'_mR_mR_sR'_s\}+R_L[R_sR'_s(R_m+R'_m)-R_cR_s(R'_s+R'_m)]\{E_s[R'_s(R_m+R'_m)\\ -R_c(R'_s+R'_m)]+E_m[R_c(R'_s+R'_m)-R'_m(R_s+R'_s)]+E'_s[R_s(R_m+R'_m)\\ -R_c(R_s+R_m)]+E'_m[R_c(R_s+R_m)-R_m(R_s+R'_s)]\}+E_L[R_sR'_s(R_m+R'_m)\\ -R_cR_s(R'_s+R'_m)][R_sR_m(R'_s+R'_m)+R'_sR'_m(R_s+R_m)-R_c(R_s+R_m)(R'_s+R'_m)]\end{array}}{\begin{array}{l}[R_sR_m(R'_s+R'_m)+R'_sR'_m(R_s+R_m)-R_c(R_s+R_m)(R'_s+R'_m)][R_L(R_m+R'_m)\\ \cdot(R_s+R'_s)+R_mR_s(R'_m+R'_s)+R'_mR'_s(R_m+R_s)-R_cR_L(R_m+R_s+R'_m+R'_s)\\ -R_c(R_s+R_m)(R'_s+R'_m)]\end{array}}.$$

Using these expressions we can obtain an expression for the ratio $\Delta\psi_{sc}/\Delta\psi_{ms}$ over some increment in ΔE_s, $\Delta E'_s$ or $\Delta E_s+\Delta E'_s$. When there is only a change

ΔE_s, while E'_s remains constant

$$\frac{\Delta\psi_{sc}}{\Delta\psi_{ms}} = \frac{\begin{array}{l}\{[R_L(R_m+R'_m)(R_s+R'_s)+R_sR_m(R'_s+R'_m)+R'_sR'_m(R_s+R_m)]\\ -R_c[R_L(R_s+R_m+R'_s+R'_m)+(R_s+R_m)(R'_s+R'_m)]\}[R_mR'_sR'_m\\ -R_c(R_s+R_m))R'_s+R'_m)+R_cR_s(R'_s+R'_m)]+[R_LR_sR'_s(R_m+R'_m)\\ -R_cR_LR_s(R'_s+R'_m)][R'_s(R_m+R'_m)-R_c(R'_s+R'_m)]\end{array}}{\begin{array}{l}R_L[R_sR_m(R'_s+R'_m)+R'_sR'_m(R_s+R_m)-R_c(R_s+R_m)(R'_s+R'_m)]\\ \cdot[R'_s(R_m+R'_m)-R_c(R'_s+R'_m)]\end{array}}.$$

Alternatively for some increment in E'_s, $\Delta E'_s$, while E_s is constant, the function relating the change measured across the serosal membranes of surface epithelial cells to the transmucosal change is

$$\frac{\Delta\psi_{sc}}{\Delta\psi_{ms}} = \frac{\begin{array}{l}R_mR_sR'_m\{R_L(R_m+R'_m)(R_s+R'_s)+R_sR_m(R'_s+R'_m)+R'_sR'_m(R_s+R_m)\\ -R_c[R_L(R'_s+R'_m+R_s+R_m)+(R_s+R_m)(R'_s+R'_m)]\}+[R_LR_sR'_s(R_m+R'_m)\\ -R_cR_LR_s(R'_s+R'_m)][R_s(R_m+R'_m)-R_c(R_s+R_m)]\end{array}}{\begin{array}{l}R_L[R_sR_m(R'_s+R'_m)+R'_sR'_m(R_s+R_m)-R_c(R_s+R_m)(R'_s+R'_m)]\\ \cdot[R_s(R_m+R'_m)-R_c(R_s+R_m)]\end{array}}.$$

The change in transmucosal and intracellular p.d. could result from a change in both E_s and E'_s. Thus, the expression relating the potential drop, $\Delta\psi_{sc}$, across the serosal membrane of the surface epithelial cells to the transmucosal potential change, $\Delta\psi_{ms}$

$$\frac{\Delta\psi_{sc}}{\Delta\psi_{ms}} = \frac{\begin{array}{l}\{R_L(R_m+R'_m)(R_s+R'_s)+R_sR_m(R'_s+R'_m)+R'_sR'_m(R_s+R_m)\\ -R_c[R_L(R_s+R_m+R'_s+R'_m)+(R_s+R_m)(R'_s+R'_m)]\}\\ \cdot\left[R_mR'_m\left(R_s+\left(\frac{\Delta E'_s}{\Delta E_s}\right)R_s\right)-R_c(R_s+R_m)-R_cR_s(R'_s+R'_m)\right]\\ +[R_LR_sR'_s(R_m+R'_m)-R_cR_LR_s(R'_s+R'_m)]\\ \cdot\left\{\left(\frac{\Delta E'_s}{\Delta E_s}\right)[R_s(R_m+R'_m)-R_c(R_s+R_m)]+R'_s(R_m+R'_m)-R_c(R'_s+R'_m)\right\}\end{array}}{\begin{array}{l}R_L[R_sR_m(R'_s+R'_m)+R'_sR'_m(R_s+R_m)-R_c(R_s+R_m)(R'_s+R'_m)]\\ \cdot\left\{R'_s(R_m+R'_m)-R_c(R'_s+R'_m)+\left(\frac{\Delta E'_s}{\Delta E_s}\right)[R_s(R_m+R'_m)-R_c(R_s+R_m)]\right\}\end{array}}.$$

Lastly, the change in potential $\Delta\psi_{sc}$ and $\Delta\psi_{ms}$ could result from a change in E'_m as well as in $\Delta E_s+\Delta E'_s$. In this case the relation is still more complex.

$$\frac{\Delta\psi_{cs}}{\Delta\psi_{ms}} = \frac{\begin{array}{l}\{R_L(R_m+R'_m)(R_s+R'_s)+R_m R_s(R'_m+R'_s)+R'_m R'_s(R_m+R_s)\\ -R_c[R_L(R_m+R_s+R'_m+R'_s)+(R_s+R_m)(R'_s+R'_m)]\}\{\Delta E_s[R_m R'_m R'_s\\ -R_c R_m(R'_m+R'_s)]+\Delta E'_s R_m R_s R'_m+\Delta E'_m R_m R_s R'_s\}\\ +R_L[R_s R'_s(R_m+R'_m)-R_c R_s(R'_s+R'_m)]\{\Delta E'_s[R'_s(R_m+R'_m)-R_c(R'_s+R'_m)]\\ +\Delta E'_s[R_s(R_m+R'_m)-R_c(R_s+R_m)]+\Delta E'_m[R_c(R_s+R_m)-R_m(R_s+R'_s)]\}\end{array}}{\begin{array}{l}R_L[R_s R_m(R'_s+R'_m)+R'_s R'_m(R_s+R_m)-R_c(R_s+R_m)(R'_s+R'_m)]\\ \cdot\{\Delta E_s[R'_s(R_m+R'_m)-R_c(R'_s+R'_m)]+\Delta E'_s[R_s(R_m+R'_m)-R_c(R_s+R_m)]\\ +\Delta E'_m[R_m(R_s+R'_s)-R_c(R_s+R_m)]\}\end{array}}.$$

Since in the gastric fundic mucosa the individual membrane resistivities have not been quantitated, some further simplifications are necessary. There are two alternative assumptions: (1) that R_c is much less than all membrane resistances and can be taken to approach zero, or (2) that R_c is large compared to cell membrane resistance and can be taken to approach infinite size. Table 6 gives the formulas which result from these alternative assumptions. Application of these formulas to the gastric fundic mucosa is given in the previous pages.

This work was supported by NSF Grant No. GB31075 and NIH Grants No. AM15878 and CA13158. Credit is given to Project No. 8059-01, Veterans Administration Hospital, Birmingham, Alabama.

References

Blum, A. L., Hirschowitz, B. I., Helander, H. F., Sachs, G. 1971. Electrical properties of isolated cells of *Necturus* gastric mucosa. *Biochim. Biophys. Acta* **241**:261

Clarkson, T. W. 1967. The transport of salt and water across isolated rat ileum. Evidence for at least two distinct pathways. *J. Gen. Physiol.* **50**:695

Diamond, J. M., Barry, P. H., Wright, E. M. 1971. Route of transepithelial ion permeation in the gall bladder. *In*: Electrophysiology of Epithelial Cells. G. Giebisch, editor. p. 23. Schattauer Verlag

Dyck, W. P., Werther, J. L., Rudick, J. 1969. Electrolyte movement across canine antral and fundic mucosa. *Gastroenterology* **56**:488

Frizzell, R. A., Schultz, S. G. 1972. Ionic conductances of extracellular shunt pathway in rabbit ileum. Influence of shunt on transmucosal Na transport and electrical potential differences. *J. Gen. Physiol.* **29**:318

Frömter, E. 1972. Route of passive ion movement through the epithelium of *Necturus* gallbladder. *J. Membrane Biol.* **8**:259

Himal, H. S., Young, S. B., Rudick, J., Werther, J. L., Janowitz, H. D. 1970. Ionic flux across the duodenal mucosa: Effects of varying concentrations of acid. *Gastroenterology* **58**:959 (Abstr.)

Hodgkin, A. L., Horowicz, P. 1959. The influence of K and Cl ions on membrane potential of single muscle fibers. *J. Physiol.* **148**:127

Hoshi, T., Sakai, F. 1967. Comparison of electrical resistance of surface cell membrane and cellular wall in proximal tubule of Newt kidney. *Jap. J. Physiol.* **17**:627

Loewenstein, W. R., Kanno, Y. 1964. Studies on epithelial (gland) cell junction. *J. Cell Biol.* **22**:65

Mandel, L. J., Curran, P. F. 1972. Response of frog skin to steady state voltage clamping. I. The shunt pathway. *J. Gen. Physiol.* **59**:503

Rose, R. C., Schultz, S. G. 1971. Studies on the electrical potential profile across rabbit ileum: The effect of sugars and amino acids on transmural and transmucosal electrical potential differences. *J. Gen. Physiol.* **57**:639

Sachs, G., Shoemaker, R. L., Blum, A. L., Helander, H. F., Makhlouf, G. M., Hirschowitz, B. I. 1971. Microelectrode studies of gastric mucosa and isolated gastric cells. pp. 257–279. Symp. Med. Hoechst. *In*: Electrophysiology of Epithelial Cells

Shoemaker, R. L., Sachs, G. 1972. Microelectrode studies of *Necturus* gastric mucosa. *In.*: Gastric Secretion. G. Sachs, E. Heinz and K. J. Ullrich, editors. pp. 147–164. Academic Press, New York

Ussing, H. H., Windhager, E. E. 1964. Nature of shunt path and active sodium transport through frog skin epithelium. *Acta Physiol. Scand.* **61**:484

Windhager, E. E., Boulpaep, E. L., Giebisch, G. 1966. Electrophysiological studies on single nephrons. *Proc. 3rd Int. Cong. Nephrol.*, Karger, Basel. Vol. 1, p. 35

Reprinted from
Biochimica et Biophysica Acta
Elsevier Publishing Company
Amsterdam
Printed in The Netherlands

BBA 45593

THE ACTION OF AMYTAL ON FROG GASTRIC MUCOSA

G. SACHS, R. SHOEMAKER AND B. I. HIRSCHOWITZ

Division of Gastroenterology, Department of Medicine, and Department of Physiology, University of Alabama Medical Center, Birmingham, Ala. (U.S.A.)

(Received March 28th, 1967)

SUMMARY

The frog gastric mucosa has been shown to be sensitive to amytal. At 2 mM acid secretion was completely inhibited with a rise of resistance, fall in short-circuit current and no significant change in potential difference. Simultaneously there was 75 % inhibition of O_2 consumption and 50 % depression of ATP levels. Dual-beam spectrophotometric studies of intact mucosa with amytal showed a crossover point between NAD^+ and FAD. The microsomal NADH oxidase ferricyanide reductase has also been shown to be amytal sensitive. Cl^- transport was relatively insensitive to amytal, suggesting a qualitative distinction between the mechanisms underlying the transport of H^+ and Cl^- in the mucosa. This was further brought out by the effects of anoxia in which H^+ transport was inhibited at 5 min but Cl^- transport at minimally 20 min following the onset of anoxia.

INTRODUCTION

Although amytal has been shown to inhibit acid production by the stomach, using a closed-sac technique[1] its effect on other parameters, such as Cl^- transport, potential difference and resistance has not been determined. Moreover a biochemical analysis of its mode of action in this particular tissue, by O_2-consumption measurements, ATP-level determination would establish the type of inhibition occurring in the intact tissue. Of particular importance is the use of dual-beam spectroscopy to localise the action of amytal in the redox chain, to correlate changes in the steady state of redox components with changes in transport.

METHODS

All studies to be reported here were carried out on *Rana pipiens* gastric mucosa. The frogs were obtained from Lemberger and Co., Oshkosh, Wisc., and stored in running water at room temperature for several days prior to use.

Secretion studies

The gastric mucosa was mounted between two lucite chambers as previously described[2]. In this system the potential difference was measured *via* a pair of matched calomel electrodes with renewable KCl junctions, and a vacuum-tube voltmeter

Resistance was calculated from the change in potential difference obtained when a current of 10 μA was sent in either direction through the membrane. Short-circuit current was measured as the amount of current required to reduce the potential difference to zero after sending current for about 30 sec. Acid secretion was measured by the pH stat method of DURBIN AND HEINZ[3]. $^{36}Cl^-$ fluxes were determined in a Nuclear–Chicago scintillation counter, and quench correction was performed using the channels-ratio method as previously outlined[2]. The mucosa was oxygenated with 95 % O_2–5 % CO_2 and in anoxic experiments with 95 % N_2–5 % CO_2. Nutrient solutions contained 118 mM Na^+, 4 mM K^+, 0.8 mM Mg^{2+}, 1.7 mM Ca^{2+}, 18 mM HCO_3^-, 109 mM Cl^- and 10 mM glucose, whereas secretory solutions contained 105 mM Na^+, 4 mM K^+ and 109 mM Cl^-. For Cl^--free conditions Cl^- in bathing media was replaced by SO_4^{2-}. Amytal was added at varying concentrations to the nutrient solution. Fresh sodium amytal solutions were made up daily and all chemicals were reagent grade and solutions made up in glass-distilled water.

O_2-consumption studies

These experiments were performed in a chamber of a design essentially similar to the above, except that magnetic stirring was employed, and the construction material was O_2-impermeable Kel F rather than lucite. Clark O_2 electrodes were used with teflon membranes, and the output of the O_2 amplifier was fed to a scale-expansion system consisting of a bucking voltage and an Esterline Angus recorder. The mucosa was mounted as before, and solutions as above were employed, but were gassed for 30 min with 95 % O_2–5 % CO_2 prior to use. O_2 electrodes were calibrated each day in air, air-equilibrated solutions, and glucose solutions treated with glucose oxidase. At the termination of the experiment 20 mM CN^- was used to reduce the O_2 consumption to zero, to ensure that there were no undetected leaks of O_2 in the system. After an initial period of equilibration, O_2 measurements were performed for 30 min under control conditions. Then amytal was added at 2 mM concentration and O_2 consumption determined for a further 40 min. O_2 consumption was calculated directly from the deflection on the recorder and expressed as μA O_2 used per h per cm^2.

Spectrophotometric studies

These studies were performed in conjunction with Dr. W. S. REHM and Mrs. S. SAUNDERS. Frog mucosa was mounted in a lucite chamber which was designed to fit into the standard cell compartment of an Aminco Chance dual-beam spectrophotometer, and with no current sending agar electrodes, but a clear plastic window on either side of the mucosa. Acid secretion was measured by the usual pH stat method, potential difference *via* calomel electrodes with KCl bridges and circulation maintained by airlift systems. The bathing solutions and gas mixtures were as described above.

The following pairs of wavelengths were used to determine the redox state of each component measured: NAD^+, 374/340 mμ; FAD, 510/465 mμ.

The experimental procedure in each study was to allow the system to come to equilibrium under conditions of oxygenation. After both the rate of H^+ secretion and the absorbance of any one particular redox component had stabilized, anoxia was induced with 95 % N_2–5 % CO_2. The gases used in these experiments were specially prepared and calibrated. Recording of absorbance and acid rate was con-

tinued until acid rate was zero and a stable absorbance had been produced. O_2 was readmitted and acid rate and absorbance allowed to return to control conditions. At this point 2 mM amytal was added to the nutrient side and recording continued to a new steady state. This was followed by a further cycle of anoxia.

In some experiments either before or after adding amytal, uncoupling was induced with dinitrophenol, sodium arsenate or carbonyl cyanide metachlorophenylhydrazone. Following stabilization, an N_2–O_2 cycle was induced and the absorbance recorded as above.

Estimation of ATP levels

Gastric mucosae were incubated with gassing in 95 % O_2–5 % CO_2 in nutrient solutions with varying concentrations of amytal for 30 min at room temperature. The mucosa was chilled, the mucosal cells scraped off with a glass slide, homogenized, heated to 100° for 4 min, and centrifuged. The supernatant was assayed for ATP levels by the luciferin luciferase method with an arsenate buffer according to STREHLER[4]. Recovery of added ATP was better than 90 %, and no interference by ADP could be detected. Protein analysis was carried out on an aliquot of the homogenate by the method of LOWRY *et al.*[5]. Results were expressed as μmoles ATP $\times$ 10^{-2} per mg protein.

Enzyme assays

Gastric mucosal cell suspensions were prepared in ice-cold 5 mM EDTA. Homogenization was carried out in a Waring blender at maximum speed for 30 sec. The homogenate was spun at 1500 $\times$ *g* for 15 min, resuspended and recentrifuged two more times. The final pellet was resuspended in buffer (pH 8.4) to a concentration of about 1 mg protein per ml and homogenised for 20 sec in a Bronwill sonifier. In other preparations frog gastric microsomal preparations were made (*i.e.* 100000 $\times$ *g* precipitate) and ATPase activity was determined as previously detailed[6]. NADH oxidase activity was determined according to MAHLER[7] using ferricyanide as the electron acceptor and a Beckman Model DB recording spectrophotometer. Electron micrographs of the final preparations showed it to be virtually free of nuclei, cell fragments or mitochondrial contamination. Micrographs of the ultrasonic preparation from the EDTA precipitate showed a large preponderance of smooth membrane fragments. Protein analysis was again performed according to the LOWRY method[5] and units of NADH oxidase activity were expressed as Δ 0.001 *A*/min per mg protein.

Summary of methods

The action of amytal on the H^+ and Cl^- transport mechanisms of the frog gastric mucosa was measured with a simultaneous determination of the effect on O_2 consumption, ATP levels and redox systems of this tissue. The microsomal enzyme sensitivity to amytal was also measured. By these methods, the action of amytal in frog mucosa could be compared to its action in other tissue.

RESULTS

Secretion

Acid secretion was inhibited after 30 min by 2 mM amytal. During the decline in acid secretion there was a rise in potential difference and short-circuit current

initially, with little alteration in resistance. The potential difference then fell to about initial values and resistance increased. Measurements of Cl^- flux showed that only the Cl^- associated with H^+ was inhibited at this stage (Fig. 1). The residual potential difference was maintained for about 90 min after the addition of amytal at this level.

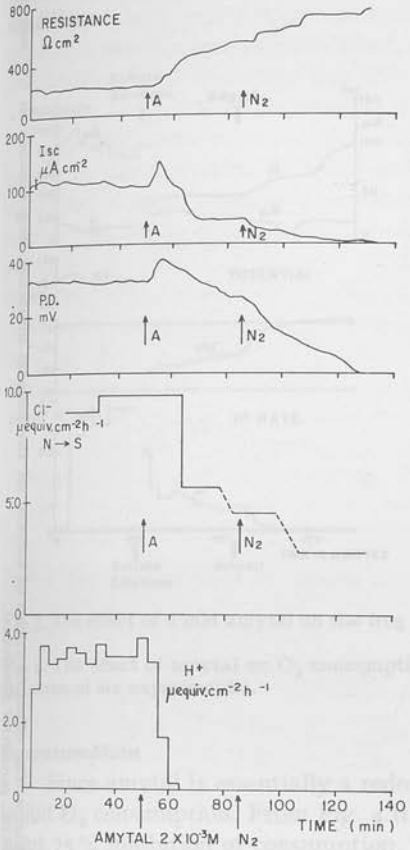

Fig. 1. The effect of 2 mM amytal (A) and anoxia on resistance, short-circuit current (I_{sc}), potential difference (P.D.), Cl^- flux (N → S) and acid rate in the frog mucosa *in vitro* in Cl^- solutions.

At 20 mM amytal, however, there was a rapid fall in Cl^- flux associated with the fall in H^+, and at 0.2 mM there was no significant effect on H^+ or Cl^- transport over 60 min. The data obtained at the 30-min period are summarized in Table I. Since the residual potential could be due to either a Cl^- diffusion or electrogenic potential or a combination of both, the effect of period of anoxia and reoxygenation was studied.

After N_2 was admitted in the amytal-treated mucosa, approx. 40 min were required for the potential difference to be reduced to zero. Upon reoxygenation there was a rise of the potential difference to a stable value after 5 min. During this time there was a rise in the resistance and a fall in net Cl^- flux with anoxia and a fall in resistance and a rise in Cl^- flux upon readmission of O_2 (Fig. 2). These results suggest a functioning Cl^- pump at this concentration of amytal (2 mM) as well as a Cl^-

TABLE I

THE POTENTIAL DIFFERENCE, SHORT-CIRCUIT CURRENT, RESISTANCE, H^+ RATE AND Cl^- FLUX (N → S, S → N) AT 0 min AND AT 30 min FOLLOWING 2 mM AMYTAL

The results given are means of 20 experiments ± S.E. of the mean; ten Cl^- fluxes in either direction.

	H^+ ($\mu equiv \cdot cm^{-2} \cdot h^{-1}$)	*Potential difference* (mV)	*Resistance* ($\Omega \cdot cm^2$)	*Short-circuit current* ($\mu A \cdot cm^{-2}$)	*Cl^- flux* ($\mu equiv \cdot cm^{-2} \cdot h^{-1}$)	
					$N \rightarrow S$	$S \rightarrow N$
Control	3.44 ± 0.2	23.0 ± 2.0	141 ± 24	109 ± 8	10.1 ± 0.49	4.5 ± 0.20
25–30 min after amytal	0.2 ± 0.18	21.5 ± 1.5	331 ± 40	45 ± 7	4.7 ± 0.53	2.6 ± 0.23
Change	−3.1 ± 0.1*	−1.5 ± 1.7	+190 ± 34*	−64 ± 6*	−5.4 ± 0.58*	−1.9 ± 0.22*

* t test significant at 0.01 level.

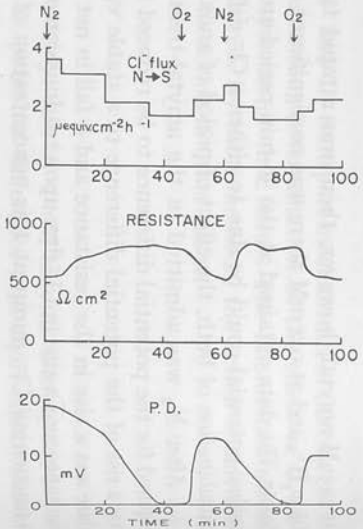

Fig. 2. The effect of cycles of anoxia on the amytal-inhibited frog mucosa in Cl^- solutions (H^+ = 0). P.D., potential difference.

diffusion potential which may account for a considerable fraction of the measured potential difference when H^+ rate is zero.

In mucosae bathed with a non-transported anion (SO_4^{2-}), the inverted potential difference and H^+ rate fell concomitantly to zero upon the addition of amytal (Fig. 3), as demonstrated by REHM AND LEFEVRE[8] for dinitrophenol inhibition under identical conditions.

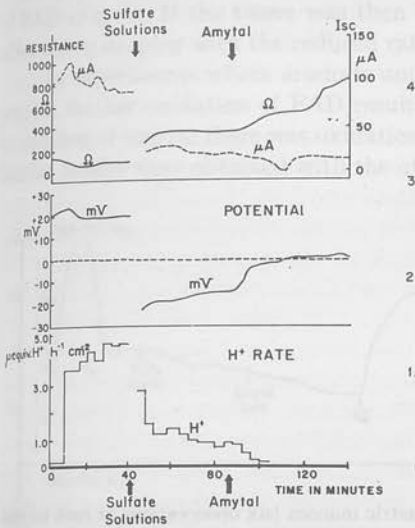

Fig. 3. The effect of 2 mM amytal on the frog mucosa in SO_4^{2-} solutions.

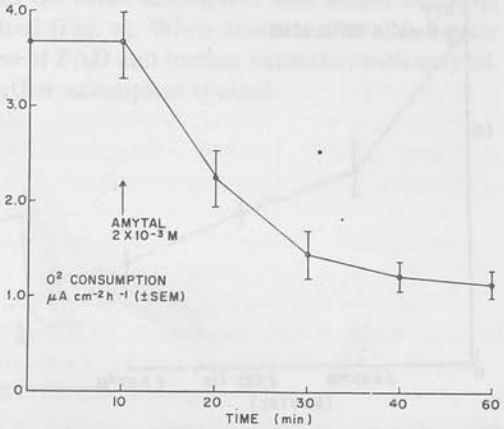

Fig. 4. The effect of amytal on O_2 consumption of the chambered frog mucosa (mean ± S.E. of the mean of six experiments).

O_2 consumption

Since amytal is essentially a redox inhibitor, it would be expected to strongly inhibit O_2 consumption. From Fig. 4 it can be seen that at 2 mM amytal there was about 75 % inhibition of consumption. The calculated $\Delta H^+/\Delta O$ value was 1.6, compatible with a redox theory of secretion.

ATP levels

Concomitant with reduction in electron transfer *via* NAD^+-linked dehydrogenases, the synthesis of ATP would be expected to be markedly depressed. Fig. 5 shows the effect of varying levels of amytal on the frog mucosal ATP level. The maximal drop occurred at 0.2 mM amytal which is not inhibitory to secretion at 30 min. Successive increments progressively decrease ATP levels in the mucosa and at the concentration studied in this paper, namely 2 mM, there was about 50 % residual ATP.

Spectrophotometric studies

In the chambered mucosa, changes in state of NAD^+ (ΔA at 374/340 mμ) were recorded during cycles of deoxygenation and oxygenation. There was a marked

increase in the absorbance with N_2, with an overshoot before the final level was reached with a zero H^+ rate after 5 min (Fig. 6). Upon readmission of O_2 there was a decrease in the ΔA, showing oxidation of NADH. Secretion started after about 3 min following the readmission of O_2 in this type of experiment. After the H^+ rate had stabilized, addition of 2 mM amytal resulted in a slow reduction of NAD^+, which

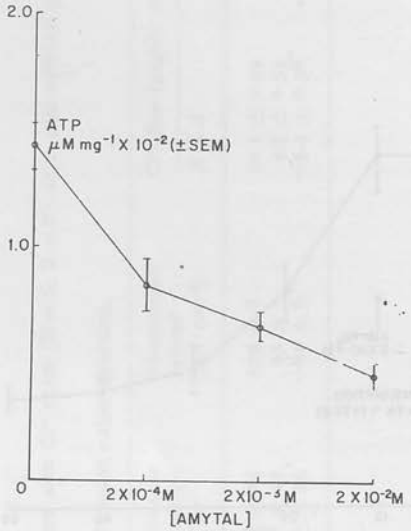

Fig. 5. The effect of amytal on ATP levels in frog gastric mucosa (six observations at each amytal level ± S.E. of the mean).

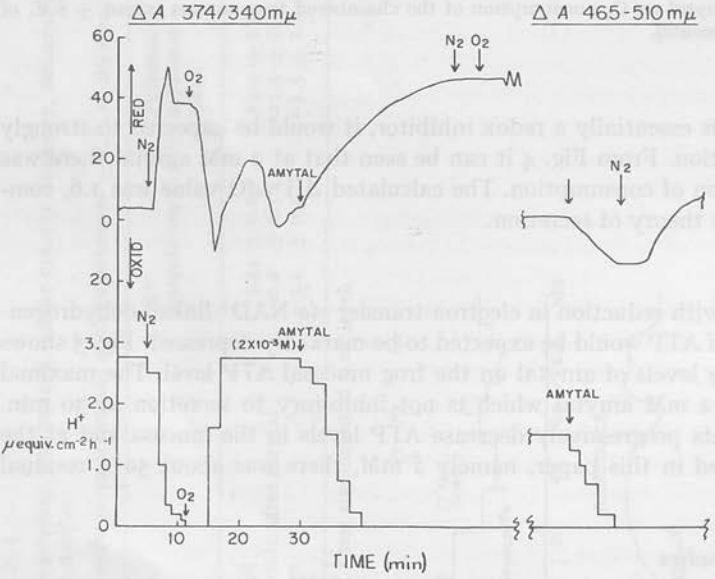

Fig. 6. The effect of anoxia and amytal on the ΔA at 374/340 mμ (NAD^+) and ΔA at 465/510 mμ (FAD) of the frog gastric mucosa in the Aminco Chance dual-beam spectrophotometer.

had not reached a maximum when H^+ was zero. Admission of N_2 followed by O_2 did not alter the observed absorbance. Although the action of amytal was reversible, experiments on the other redox enzymes were usually performed in separate experiments. The state of FAD in the mucosa was determined by ΔA at 510/465 mμ. When the tissue was made anoxic, reduction (*i.e.* decrease in ΔA) occurred as expected, and when O_2 was readmitted there was reoxidation with little evidence of an overshoot. When acid secretion was re-established, 2 mM amytal was added with ensuing oxidation of FAD (Fig. 6). If the tissue was then made anoxic, a slow reduction of FAD was observed in keeping with the reduced rate of electron transfer from NADH.

In experiments where arsenate and the other uncouplers were added following amytal, further oxidation of FAD resulted (Fig. 7). When arsenate was added prior to addition of amytal there was oxidation of FAD and further oxidation with amytal. Similar results were obtained with the other uncouplers studied.

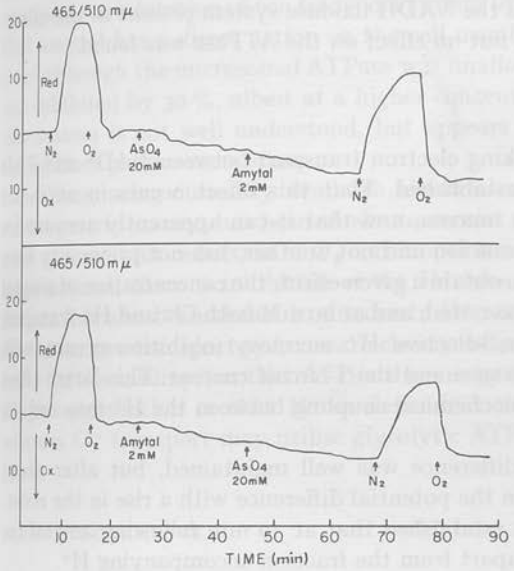

Fig. 7. The effect of sodium arsenate and amytal on the ΔA at 465/510 mμ (FAD) of the frog gastric mucosa. In the top figure arsenate was added before amytal, while the reverse sequence was used in the lower figure.

Enzyme studies

Since the mitochondrial system is not unique in catalysing NADH oxidation, a membrane preparation was studied with respect to the effect of amytal on the NADH oxidase system. In this preparation 2 mM amytal had no detectable effect on the activity, but at 6 mM there was approx. 30 % inhibition. There was also a lag in the onset of inhibition which was not found when amytal was premixed with the enzyme. This membrane preparation also exhibited ATPase activity, which was sensitive to SCN^- (a potent secretory inhibitor) but not to amytal. The NADH oxidase activity, however, was found to be SCN^- insensitive (Table II).

TABLE II

THE EFFECT OF AMYTAL AND SCN^- ON FROG GASTRIC MICROSOMAL NADH OXIDASE AND ATPASE

The results given are means of five experiments ± S.E. of the mean.

	NADH oxidase (Δ 0.001 $A \cdot min^{-1} \cdot mg^{-1}$)	*ATPase* ($\mu moles\ P_i \cdot min^{-1} \cdot mg^{-1}$)
Control	318 ± 31	1.71 ± 0.12
SCN^- (1 mM)	310 ± 26	0.46 ± 0.12
Amytal	216 ± 15	1.73 ± 0.29

Summary of results

Amytal at 2 mM reduced the H^+ secretory rate to zero, with lesser effect on net 'non-acidic' Cl^- flux. At this amytal concentration there was a 50 % depression in ATP levels, a 75 % inhibition of O_2 consumption, with a reduction of NAD^+ and oxidation of FAD. At 6 mM amytal the NADH oxidase system present in the microsomal fraction was 30 % inhibited, but no effect on the ATPase was found.

DISCUSSION

The action of amytal in blocking electron transport between NAD^+ and FAD in mitochondrial systems is well established. That this effect occurs in an intact transporting tissue, such as gastric mucosa, and that it can apparently account for selective inhibition of transport of one ion and not another, has not previously been reported. It appears, that in order to obtain a given effect, the concentration of amytal is critical. At 0.2 mM, little effect was noted, and at 20 mM both Cl^- and H^+ transport were inhibited. At 2 mM, however, selective H^+ secretory inhibition occurs, with an initial rise in the potential difference and short-circuit current. This latter effect is presumably the consequence of biochemical coupling between the H^+ rate and the Cl^- mechanism.

Subsequently the potential difference was well maintained, but after about 60 min there was a steady decline in the potential difference with a rise in the resistance. The measurement of Cl^- flux established that at 30 min following amytal the net Cl^- transport was unchanged, apart from the fraction accompanying H^+.

In SO_4^{2-} solutions, amytal reduced both H^+ secretion and potential difference to zero, since SO_4^{2-} is not transported by *Rana pipiens* gastric mucosa[9].

The maintained potential difference in Cl^- solutions, in the absence of an acid rate with 2 mM amytal could be the result of a residual diffusion potential (cell to lumen) established prior to the amytal inhibition. Anoxia for 40 min resulted in the fall of potential difference to zero, and reoxygenation re-established 60 % of the potential difference within 5 min. This implies that the mechanism for establishing the potential difference is still operative 70 min following amytal addition.

The biochemical changes in the tissue must thus account for the changes in H^+ transport with sparing of the Cl^- mechanism, and might yield some insight into the biochemical dependence of this transport.

Dual-beam studies showed that there was a change in the steady state of NAD^+ towards reduction, and of FAD towards oxidation. The reduction of NAD^+, however, is incomplete at the time that the H^+ rate is zero, whereas with anoxia

there appeared to be simultaneity of inhibition of H^+ and NAD^+ reduction. It can be concluded, however, on the basis of the amytal effect, that there is no simple correlation between NAD^+ metabolism and the H^+ rate.

Since the majority of cellular oxidations traverse the NAD^+ pathway, 70% inhibition of O_2 consumption was observed, coupled with a 50% depression of ATP levels. The measurement of these two parameters appears critical for an evaluation of either a redox or an ATPase theory of secretion. The results obtained here raise difficulties for either theory. The overall $\Delta H^+/\Delta O$ ratio found of 1.6, although compatible with a simple redox theory, is undoubtedly an underestimate since it is highly unlikely that the NAD^+-dependent O_2 consumption is entirely concerned with H^+ production. The ratios previously found depend on the technique used[10]. Since there was 50% residual ATP, an explanation of the action of amytal based on ATP depletion requires some second-order assumptions, the most obvious one being compartmentation of ATP, with depletion of that fraction of the ATP concerned with H^+ transport, or inhibition of the transport system by ADP. Another alternative, namely that amytal has a direct action on the cell membrane, is not excluded by our data, since although the microsomal ATPase was unaffected by amytal, the NADH oxidase was inhibited by 30%, albeit at a higher concentration than 2 mM. The function of this system is not well understood, but appears to be associated with microsomes, rather than plasma membrane.

Thus, using currently available biochemical techniques, the action of amytal on the gastric mucosa has been shown to consist of inhibition of oxidation of NADH with concomitant reduction of O_2 consumption and ATP levels. As a consequence of these actions, there is inhibition of the H^+ rate, with little effect on Cl^- transport. Anoxia has also been shown to dissociate H^+ and Cl^- secretion. It is clear therefore that these two transport systems are clearly differentiated in their metabolic dependence. On the assumption that ATP is the energy source for H^+ and Cl^- secretion, one simple explanation is that H^+ is dependent on mitochondrially generated ATP, whereas Cl^- transport may utilise glycolytic ATP under certain experimental conditions.

ACKNOWLEDGEMENTS

This work was supported by National Institutes of Health Grant No. AM-08541, AM-09260 and National Science Foundation Grant No. GB-3511.

R.S. is a Trainee of U.S. Public Health Service, Grant No. 2A-5286.

REFERENCES

1 W. H. BANNISTER, *J. Physiol. London*, 177 (1965) 440.
2 G. SACHS, R. SHOEMAKER AND B. I. HIRSCHOWITZ, *Am. J. Physiol.*, 209 (1965) 461.
3 R. P. DURBIN AND E. HEINZ, *J. Gen. Physiol.*, 41 (1958) 1035.
4 B. L. STREHLER, in H. U. BERGMEYER, *Methods of Enzymatic Analysis*, Academic, New York, 1963, p. 559.
5 O. H. LOWRY, N. J. ROSEBROUGH, A. L. FARR AND R. J. RANDALL, *J. Biol. Chem.*, 193 (1951) 265.
6 G. SACHS, W. E. MITCH AND B. I. HIRSCHOWITZ, *Proc. Soc. Exptl. Biol. Med.*, 119 (1965) 1023.
7 H. R. MAHLER, in S. P. COLOWICK AND N. O. KAPLAN, *Methods in Enzymology*, Academic, New York, 1957, p. 707.
8 W. S. REHM AND M. E. LEFEVRE, *Am. J. Physiol.*, 208 (1965) 922.
9 S. KANEKO-MOHAMMED AND C. A. M. HOGBEN, *Am. J. Physiol.*, 207 (1964) 1173.
10 J. G. FORTE AND R. E. DAVIES, *Am. J. Physiol.*, 204 (1963) 812.

THE JOURNAL OF BIOLOGICAL CHEMISTRY
Vol. 250, No. 21, Issue of November 10, pp. 8321–8329, 1975
Printed in U.S.A.

Metabolism of Dog Gastric Mucosa

I. NUCLEOTIDE LEVELS IN PARIETAL CELLS*

(Received for publication, April 3, 1975)

HENRY M. SARAU, JAMES FOLEY, GEORGE MOONSAMMY, VIRGIL D. WIEBELHAUS, AND GEORGE SACHS
From the Smith Kline & French Laboratories, Philadelphia, Pennsylvania 19101, and University of Alabama in Birmingham, Birmingham, Alabama 35294

Adenine and pyridine nucleotide levels as well as those of phosphate, phosphocreatine, lactate, pyruvate, β-hydroxybutyrate, acetoacetate, glucose, and glycogen were measured in histologically defined parietal and mucous cell sections of biopsies of dog gastric mucosa at rest, and in various secretory states. As a result of stimulation of secretion, there appeared to be no change in adenine nucleotide levels, or phosphocreatine, but there was a rise in inorganic phosphate and a fall in phosphorylation potential. However, there was a marked increase in NADH, but no change in NADPH with onset of acid secretion. The increase in the lactate to pyruvate ratio showed that the increased NADH level occurred in the cytoplasm and these data are discussed with reference to change in cell pH.

Proton transport is an almost universal phenomenon occurring in subcellular organelles such as mitochondria (1) and chromatophores (2), as well as in unicellular organisms such as *Escherichia coli* (3) or yeast (4), and in plants (5) or animal tissues such as kidney (6), pancreas (7), or stomach (8). The latter tissue is probably the most specialized in this function, the mammalian parietal cells being capable of developing a $10^{6.6}$-fold concentration gradient of H^+. Since it is unlikely that a totally novel mechanism evolved in gastric mucosa, it seems that an understanding of the transport process in this organ would be generally applicable to the problem of H^+ transport in most situations.

Measurement of metabolite levels in gastric mucosa therefore has as its main purpose the determination of the primary energy source for H^+ secretion. Thus, measurement of adenine nucleotide and phosphocreatine levels may be able to answer the question as to whether ATP is the primary energy source, and extension of these measurements to other metabolites should be able to provide information as to the pathway or pathways stimulated to provide the primary energy for transport.

Logically, the tissue metabolites should be studied before and after stimulation, and a comparison of the steady state levels should indicate physiologically significant changes. Two types of measurements have been made. Nondestructive techniques such as dual or split beam spectroscopy (9, 10) have provided information on the steady state changes in the oxidation-reduction components of the mitochondrial respiratory chain, and destructive techniques such as described here have given data on adenine nucleotide levels (11, 12). However, these past experiments have been confined almost exclusively to *in vitro* studies of frog gastric mucosa where the change in H^+ rate is limited, and moreover no distinction has been made between the multiple cell types present in the tissues. The work reported in this and succeeding papers deals with measurements in biopsy samples from an intact mammalian mucosa, in what were determined histologically to be parietal cell regions weighing about 1 μg. The fluorimetric cycling procedures developed by Lowry and his collaborators (13) were used to obtain the necessary sensitivity. This paper reports data obtained for adenine and pyridine nucleotides and metabolites related to the "free" pyridine nucleotide levels in cytosol and mitochondria under resting (*i.e.* nonsecreting), secretory onset, and steady state secretion in dog gastric mucosa.

METHODS

Gastric Preparation—Adult beagle dogs were anesthetised with Nembutal. The abdomen was incised and the gastric mucosa exposed by an incision along the greater curvature. Resting tissue samples were taken at 15 and 30 min after surgery, at which time histamine infusion was started at a rate of 100 μg/kg/hour to give maximal secretion. In some experiments, 100 μg of urecholine were used in addition to histamine to increase secretion further. After 8 to 10 min of infusion, the gastric mucosa reddened, which occurred 1 to 2 min prior to onset of acid. With histamine and urecholine, a faster onset was seen. A sample was taken from the reddened nonsecreting mucosa during this period and labeled "blood flow" sample. Onset of acid secretion was monitored by measuring the fall of pH in 1 ml of saline (0.9% NaCl solution) held on the mucosa by means of a Lashley suction cup (2.27 cm^2) for 3 min. When pH started to fall, tissue samples were taken at that time (HI) and another when the pH stabilized at about 2.0 in the approximately 10-fold diluted sample (HII). H^+ rate was obtained by titration to pH 7.0 (Fig. 1). The acid rate for histamine alone was one-third that found with histamine and urecholine in combination, as known previously.

*This work was supported by National Institutes of Health Grants AM15878 and AM08541, and Grant-in-Aid from Smith Kline & French Laboratories.

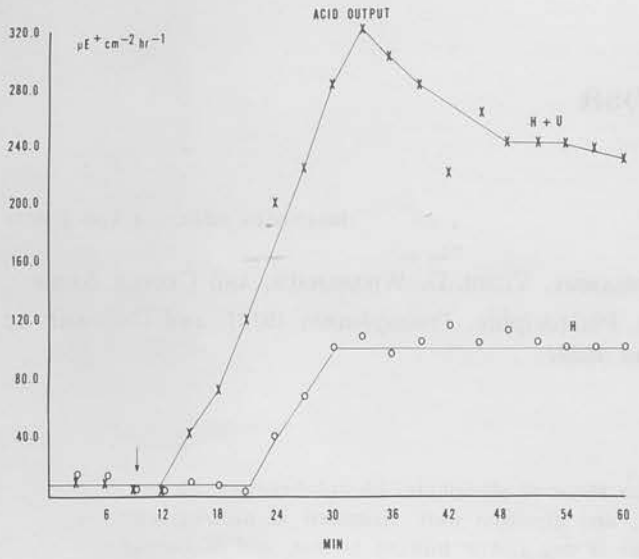

FIG. 1. The stimulation of acid output by histamine, O——O, 100 μg/kg, and histamine + urecholine, ×——×, 100 μg/kg each, in the anesthetized dog. The *arrow* indicates start of infusion.

Precautions were taken to control bleeding, and to keep the mucosa moist and warm at all times. Dogs which showed cyanotic mucosae were rejected as bad experiments.

Sampling Procedure—Samples were taken by precooled rectal biopsy forceps, with scalpel excision of the piece of tissue (~100 mg wet weight). The tissue sample was frozen immediately (<3 s) in liquid nitrogen, and stored at −80° until use. Holding the tissue at room temperature for a period of 30 s did not change the adenine or pyridine nucleotide levels, hence the rapidity of the sampling procedure was deemed adequate. Phosphocreatine decreased and lactate increased in this 30-s procedure, but since no change was found in phosphocreatine in the 3-s sample, this was further evidence for adequately rapid sampling.

Treatment of Samples—The samples were placed in a Harris cryostat at −20° and serially sectioned (20 μm thick) until parietal cell areas were seen, as evidenced by the darker appearance of the tissue. The initial sections consisted exclusively of surface or glandular neck cells. The frozen sections were placed in drilled aluminum blocks at −20° and dried under vacuum at −40°. Every fourth frozen section was transferred to a glass slide and stained for succinic dehydrogenase activity using succinate and nitro blue tetrazolium (14); in this manner the parietal cell area was clearly identifiable (Fig. 2). Adjacent lyophilized sections were trimmed using the stained sections as a guide until only defined parietal cell regions remained. Careful dissection of tissue samples from these areas of the sections were used for the extraction procedures. To ensure that the sections would not absorb atmospheric moisture, freeze-dried sections were maintained at −80° under vacuum for storage and dissected quickly in a specially constructed room maintained at <50% humidity and 18°. In separate experiments, direct extraction of frozen sections gave quantitatively similar data, hence the dissection procedure did not result in metabolite destruction. In some cases, antral tissue was sectioned or the mucous cell sections of fundus were used, and the low level of succinic dehydrogenase staining was used to assess freedom from parietal cells.

Extraction Procedures—Since we are dealing with extremely small samples of tissue (1 μg), the oil well technique (15) was required. A small volume (1.0 to 2.0 μl) of HCl or NaOH is introduced into a specially constructed Teflon rack 10 wells at a time. The sample tissue is then pushed into the droplet of acid or alkali and oil added quickly to avoid evaporation problems. The procedure is performed under a stereo dissecting microscope. The Teflon rack was heated where necessary (generally 20 min, 80°) to destroy endogenous pyridine nucleotide and enzyme activities. Standards dissolved in acid or alkali are treated the same way as the tissue samples following addition to the oil well.

Metabolite Levels—Since several metabolites were measured, tables are presented giving the details of the procedure used for measurement of each metabolite. The sequence of steps is (*a*) extraction of the tissue sample (Table I) and enzymatic assay utilizing the conversion to pyridine nucleotide, oxidized or reduced; (*b*) treatment of sample for cycling (Table II); (*c*) cycling (Tables II and III); (*d*) indicator step (Table IV). Table II also contains the range of substrate standards used and controls are inserted at each stage. References to the methods are on the tables, and a detailed description is given in Ref. 13.

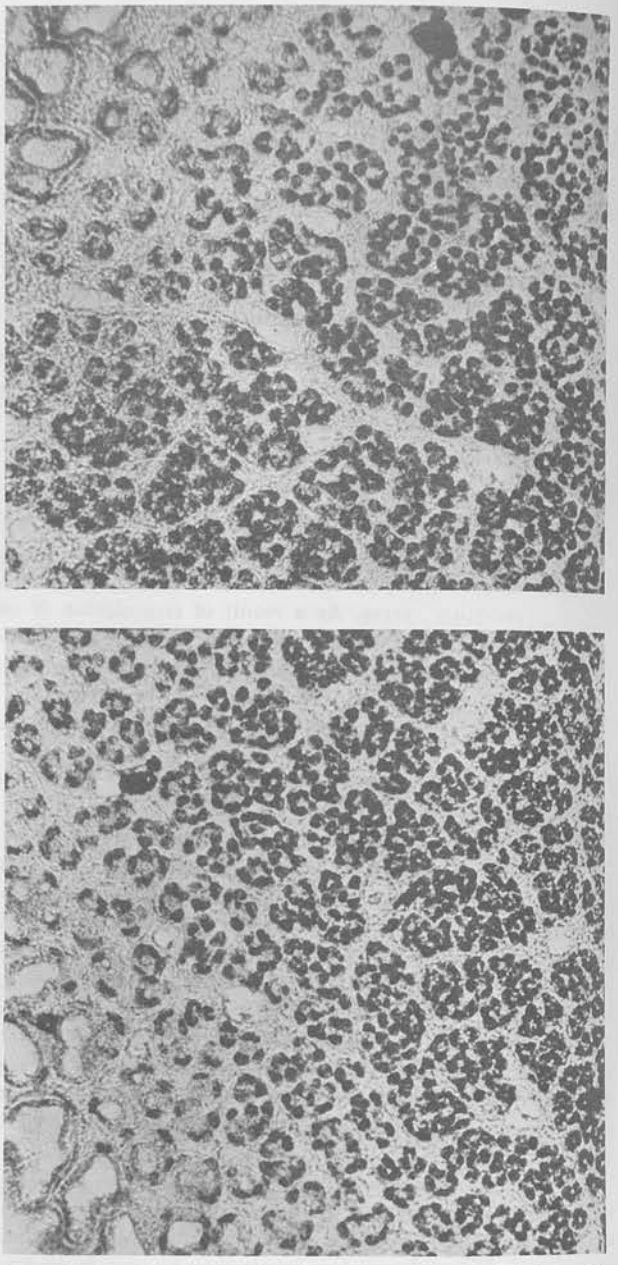

FIG. 2. Sections through dog gastric mucosa stained with nitro blue tetrazolium for succinic dehydrogenase, at rest (*top*) and during secretion (*bottom*). The sections are trimmed for maximal inclusion of stained areas, and exclusion of nonstaining areas, for parietal cells, and the converse for mucous cells.

Cycling Techniques—This varies for NAD^+, NADH, $NADP^+$, and NADPH, and the procedures are detailed in Table III. This is the method used for determination of levels of the pyridine nucleotides, and also for the pyridine nucleotide produced in the other substrate assay methods with, therefore, the omission of the initial step destroying the oxidized or reduced form of the pyridine nucleotide, which step is performed slightly differently for each substrate as detailed in Table I. Also, the amount of cycling enzyme varies for each substrate, as a function of the number of cycles required and this is detailed in Table II. The other reagent levels remain the same.

Indicator Step—In NAD^+ cycle, malate levels were measured as the indicator step by direct fluorimetry using malic dehydrogenase, and for

TABLE I

Substance[a]	Preparation of sample	Volume	Buffer	Enzymes	Other additions	Preparation for cycling
ATP (16)	3 μl of 0.1 N NaOH, 15 min, 75°	To 1 μl add 2 μl reagent, 15 min, R.T.[b]	300 mM Tris, pH 8.0	2 μg/ml yeast hexokinase; 0.25 μg/ml glucose-6-P dehydrogenase	0.05% BSA, 0.5 mM DTT, 5 mM $MgCl_2$, 1 mM glucose, 60 μM TPN	1 μl of 1.2 N NaOH, 20 min, 75°
ADP (13)	3 μl of 0.05 N NaOH + 6 mM H_2O_2, 20 min, 80°	To 1 μl add 3.3 μl reagent, 20 min, R.T.	100 mM imidazole, pH 7.0	Pyruvate kinase, 5 μg/ml; lactic dehydrogenase, 3 μg/ml	0.02% BSA, 2 mM $MgCl_2$, 75 mM KCl, 25 μM PEP, 4 μM NADH	2.1 μl of 0.5 N HCl, 45 min, R.T.
AMP (13)	3 μl of 0.05 N NaOH + 6 mM H_2O_2, 20 min, 80°	To 1 μl add 3 μl reagent, 20 min, R.T.	100 mM imidazole, pH 7.0	Pyruvate kinase, 5 μg/ml; lactic dehydrogenase (BHLDH), 8 μg/ml; myokinase, 2 μg/ml	0.02% BSA, 2 mM $MgCl_2$, 75 mM KCl, 25 μM PEP, 7.5 μM NADH, 5 μM ATP	2 μl of 0.5 N HCl, 30 min, R.T.
PCr (16)	3 μl of 0.1 N NaOH, 15 min, 75°	To 1 μl add 2 μl reagent, 30 min, R.T.	300 mM Tris, pH 8.0	Creatine kinase, 2 mg/ml; hexokinase, 2 μg/ml; glucose-6-P dehydrogenase, 0.25 μg/ml	0.05% BSA, 5 mM $MgCl_2$, 1 mM glucose, 60 μM $NADP^+$, 0.02 mM ADP, 0.5 mM DTT	1 μl of 1.2 N NaOH, 30 min, 75°
Glucose	1 μl of 0.02 N HCl, 20 min, 60°	2 μl reagent, 30 min, R.T.	100 mM Tris, pH 8.0	Yeast, hexokinase, 2 μg/ml; yeast glucose-6-P dehydrogenase, 0.25 μg/ml	10 μM $NADP^+$, 100 μM ATP, 5 mM $MgCl_2$, 0.02% BSA	1 μl of 1.2 N NaOH, 30 min, 80°
Glycogen (17)[c]	7.16 μl of 0.02 N NaOH, 20 min, 60°	To 1 μl add 1 μl 100 mM acetate buffer, pH 4.0, with 2 mg/ml amyloglucosidase, 20 min, 55°, add 1 μl reagent react 30 min, R.T.	300 mM Tris, pH 8.0	20 μg/ml yeast hexokinase, 5 μg/ml yeast glucose-6-P dehydrogenase	100 μM $NaDP^+$, 200 μM ATP, 10 mM $MgCl_2$, 0.04% BSA	1 μl of 1.2 N NaOH, 30 min, 80°
P_i (44)	1 μl of 0.1 N NaOH, 15 min, 65°		0.3 M imidazole, pH 7.0	Phosphorylase 30 μg/ml, phosphoglucomutase 3 μg/ml, glucose-6-P dehydrogenase 1.25 μg/ml	0.02% BSA, 2 mM EDTA, 20 μM 5'-AMP, 60 μM $NADP^+$, 5 mM glycogen	1 μl of 1.2 N NaOH, 15 min, 75°
Lactate (13)	1 μl of 0.02 N NaOH, 20 min, 80°	5 μl reagent, 60 min, R.T.	100 mM AMP,[b] pH 9.75	Beef heart lactic dehydrogenase, 400 μg/ml, glutamate pyruvate transaminase, 50 μg/ml	0.25 mM glutamate, 50 μM NAD^+, 0.02% BSA	5 μl of 0.25 N NaOH, 30 min, 80°
Pyruvate (13)	1 μl of 0.02 N NaOH, 20 min, 80°	2 μl reagent, 20 min, R.T.	50 mM imidazole, pH 7.0	Beef heart lactic dehydrogenase, 0.2 μg/ml	0.02% BSA, 1 μM NADH	1 μl of 0.5 N HCl, 45 min, R.T.
β-Hydroxybutyrate (18)	1 μl of 0.025 N HCl, 20 min, 80°	2 μl reagent, 35 min, R.T.	50 mM Tris hydrazine, pH 8.5	β-Hydroxybutyrate dehydrogenase, 10 μg/ml	100 μM NAD^+, 0.1 mM EDTA, 0.1 mM $MgSO_4$, 0.01% BSA, 1 mM DTT	1 μl of 0.25 N NaOH, 20 min, 80°
Acetoacetate (18)	1 μl of 0.02 N NaOH, 20 min, 80°	2 μl reagent, 90 min, R.T.	200 mM imidazole, pH 7.0	β-Hydroxybutyrate dehydrogenase, 40 μg/ml	2 μM NADH, 2 mM $MgCl_2$, 1 mM EDTA, 0.02% BSA, 30 min, R.T.	1 μl of 0.5 N HCl, 30 min, R.T.

[a] References are given in parentheses.

[b] R. T., room temperature; BSA, bovine serum albumin; DTT, dithiothreitol; $NADP^+$, triphosphopyridine nucleotide; PEP, P-enolpyruvate; BHLDH, beef heart lactate dehydrogenase; PCr, phosphocreatine; NAD^+ diphosphopyridine nucleotide; AMP, 2-amino-2-methyl propanol.

[c] Corrected for glucose blank.

the $NADP^+$ cycle, 6-phosphogluconate was measured directly using 6-phosphogluconate dehydrogenase (Table IV). The sequence of steps is summarized in Fig. 3 for the entire procedure.

Materials—All enzymes were obtained from Boehringer-Mannheim except beef heart lactic dehydrogenase which was purchased from Worthington and further purified with activated charcoal. Substrates were purchased from Sigma Chemical Co., and the Trizma (Tris(hydroxymethyl)aminomethane) buffer from Sigma is treated with Norit before use.

RESULTS

Acid Secretion

As shown in Fig. 1, the dog gastric mucosa initially secretes no measurable acid, zero time on the graph representing 30 min after surgery. Following infusion of histamine there is a 10-min lag, and with histamine and urecholine a 3-min lag. Then reddening of the mucosa is observed consonant with increased

TABLE II

Substance	Aliquot from oil well for cycling	Volume & condition for cycling	Enzymes utilized	Substrate standard utilized ($\times 10^{-12}$ mol)
ATP	1 μl	100 μl, 60 min, 37°	Beef liver glutamic dehydrogenase, 100 μg/ml; glucose-6-P dehydrogenase, 50 μg/ml	4.34–8.68 in 0.1 N NaOH
ADP	1 μl	100 μl, 60 min, 27°	Alcohol dehydrogenase, 120 μg/ml malate dehydrogenase, 17 μg/ml	4.82–9.64 in 0.05 N NaOH
AMP	1 μl	100 μl, 60 min, 27°	60 μg/ml ADH[a]; 10 μg/ml MDH	1.67–3.33 in 0.05 N NaOH
PCr	1 μl	100 μl, 60 min, 37°	54 μg/ml GDH; 27 μg/ml G6PDH	5–10 in 0.1 N NaOH
Glucose	1 μl	100 μl, 60 min, 37°	27 μg/ml GDH; 14 μg/ml G6PDH	2.5–5 in 0.02 N HCl
Glycogen	1 μl	100 μl, 60 min, 37°	27 μg/ml GDH; 13.5 μg/ml G6PDH	7.5–30 in 0.02 N NaOH
Lactate	1 μl	100 μl, 60 min, 27°	60 μg/ml ADH; 10 μg/ml MDH	5–20 in 0.02 N NaOH
Pyruvate	1 μl	100 μl, 60 min, 27°	300 μg/ml ADH; 45 μg/ml MDH	0.96–1.92 in 0.02 N NaOH
β-Hydroxybutyrate	3.3 μl	100 μl, 60 min, 27°	118 μg/ml ADH; 20 μg/ml MDH	0.404–0.808 in 0.025 N HCl
Acetoacetate	3 μl	100 μl, 60 min, 27°	60 μg/ml ADH; 10 μg/ml MDH	1.25–5 in 0.02 N NaOH
P_i	0.535 μl	100 μl, 60 min, 37°	G6PDH 30 μg/ml; GDH 150 μg/ml	9–16 in 0.02 N NaOH

[a] ADH, alcohol dehydrogenase; MDH, malate dehydrogenase; PCr, phosphocreatine; GDH, beef liver glutamic dehydrogenase; G6PDH, glucose-6-P dehydrogenase.

TABLE III

Substance[a]	Cycling reagent	Procedure	Standard range (10^{-12} mol)
$NADP^+$ (19, 20)	100 mM Tris-HCl buffer, pH 8.0 5 mM α-ketoglutarate 1 mM glucose-6-PO_4 25 mM NH_4OAc 100 μg/ml beef liver GDH[b] 25 μg/ml G6PDH	1 μl of 0.025 N HCl with 300 mM ascorbate, 75°, 20 min, cool on ice, 12 μl cycling mixture, incubate 37°, 90 min, stop, 100°, 4 min, cool, 10 μl to 1 ml indicator reagent	0.144–0.228
NADPH (19, 20)	100 mM Tris-HCl buffer, pH 8.0 5 mM α-ketoglutarate 1 mM glucose-6-PO_4 25 mM NH_4OAc 100 μg/ml beef liver GDH 25 μg/ml G6PDH	1 μl of 0.02 N NaOH, 75°, 15 min, cool 12 μl cycling reagent, incubate 37°, 60 min, 100°, 4 min, stop, cool, transfer 10 μl to 1 ml indicator reagent	0.144–0.228
NAD^+ (20, 21)	100 mM Tris-HCl buffer, pH 8.0 300 mM ethanol 2 mM mercaptoethanol 0.02% BSA 2 mM oxalacetate 60 μg yeast ADH 10 μg MDH	1 μl of 0.02 N HCl, 80°, 20 min, cool on ice, 9 μl cycling reagent, 27°, 60 min, stop, 100° for 10 min, 7 μl to 1 ml indicator reagent	1.25–5
NADH (20, 21)	As above, but double enzyme concentration	1 μl of 0.02 N NaOH with 1 mM cysteine, 80°, 20 min, cool on ice, 9 μl cycling reagent, 38°, 1 hr, stop, 100°, 10 min, transfer 7 μl to 1 ml indicator reagent	0.25–1

[a] References are given in parentheses.

[b] GDH, beef liver glutamic dehydrogenase; G6PDH, glucose-6-P dehydrogenase; BSA, bovine serum albumin; ADH, alcohol dehydrogenase; MDH, malate dehydrogenase.

vascular perfusion. Shortly thereafter, measurable secretion starts, and reaches a plateau within 15 min. The combination of stimuli (*e.g.* histamine + urecholine) produced about 2 to 3 times as much acid as histamine alone (Fig. 1).

Adenine Nucleotides

ATP—The levels found in the parietal cells are given in Table V and in the mucous cells in Table VI. The levels found are quite similar to those of other tissues, liver for example (22). The levels in mucous cells are somewhat lower (65%) than those of parietal cells. It is striking, also, that no change is observed with increase of blood flow or acid secretion in the level of this nucleotide.

ADP—Table V shows that the levels of this nucleotide also do not change during the experimental protocol for the parietal cells or the mucous cell layer from the fundus or antrum. Again, the levels found are comparable to those of liver (22). The much greater acid rate obtained with histamine plus urecholine had no effect on the ATP or ADP values, hence all the data are combined.

AMP—The level of AMP increased by about 20% with onset of mucosal perfusion until acid secretion started and stabilized thereafter (Table V). No measurements of this nucleotide were made in the mucous cells. The $ATP \cdot AMP/[ADP]^2$ level suggests an active adenylate kinase.

Total Nucleotides—No significant change was noted in the total adenine nucleotide level found in the parietal cell region as a function of acid secretion (Table V).

Phosphocreatine—A slight, nonsignificant increase was ob-

blood flow, and secreting samples. It should also be pointed out, that in some dogs, although not reflected in the means of the totals, there is a distinct, significant rise in phosphocreatine with onset of acid secretion (Table V). The level in mucous cells is similar to that found in parietal cells (Table VI).

ATP/ADP Ratio—From the data for the individual values, there is no change in the ATP/ADP ratio. Mucous cells show a ATP/ADP ratio of about 1.0 (Table VI), much less than for parietal cell regions, which is about 2.3.

NAD⁺—Table VII shows that there is no significant change in the levels of NAD^+ between rest and secretion. The level in mucous cells is lower by about 30% than those of parietal cells (Table VI).

NADH—In contrast to the constant values obtained for NAD^+ there is a significant (80%) increase in NADH with onset of acid secretion which is maintained during steady state secretion (Table VII). The level in mucous cells is extremely low (Table VI), being only 20% of the parietal cell value.

NAD⁺/NADH Ratio—As can be predicted from the above, there is a significant fall in this ratio, with H^+ secretion in the parietal cells, but even at peak secretion, there is about 3 times as much NAD^+ as NADH. Also it should be noted that with onset of acid there is a slight (8%) increase in the total nicotinamide adenine nucleotide level. The ratio NAD^+/NADH in the mucous cells is about 30, and increases with secretion to 48.

NADP⁺—Table VII shows that with blood flow and onset of acid secretion there is no change in the level of this nucleotide,

TABLE IV

Indicator steps

$NADP^+$/NADPH (19)[a]	20 mM Tris buffer, pH 8.0
	0.02 mM $NADP^+$
	0.01 mM EDTA
	5 μg/ml 6-phosphogluconate dehydrogenase
	1 ml reagent to each tube, react 30 min, 22°, measure NADPH fluorimetrically
	6-PG[b] + $NADP^+$ → R-5-P + NADPH + CO_2
NAD^+/NADH (21)	50 mM 2-amino-2-methyl propanol buffer (AMP), pH 9.9
	0.02 mM NAD^+
	10 mM glutamate
	5 μg/ml MDH
	2 μg/ml GOT
	1 ml reagent to each tube, react 22° for 10 min, measure NADH fluorimetrically
	Malate + NAD^+ → OAA + NADH + H^+
	OAA + glutamate → aspartate + α-KG

[a] References are given in parentheses.

[b] 6-PG, 6-phosphogluconate; R-5-P, ribulose-5-P; MDH, malate dehydrogenase; GOT, glutamate-oxalacetate transaminase; OAA, oxalacetate; α-KG, α-ketoglutarate.

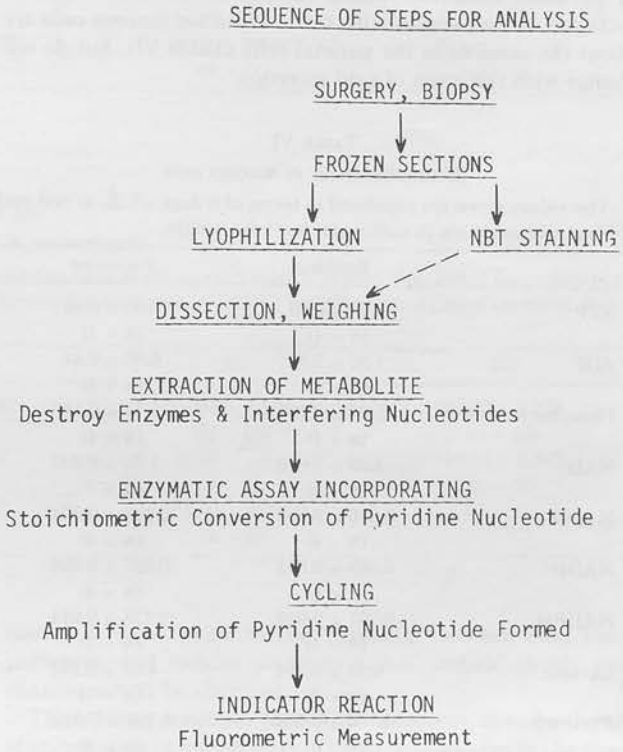

FIG. 3. A schematic representation of the stages used for analysis of cellular levels of metabolites. *NBT*, nitro blue tetrazolium.

TABLE V

Metabolite levels in parietal cells

The values are the means ±S.E. of *n* dogs, at least four measurements having been made on each sample in each dog. Blood flow refers to the state of reddening of the mucosa, HI the sample when acid secretion was detected in that area, and HII a sample at steady state secretion. Values are given, when appropriate, in millimoles kg^{-1} dry weight.

Substance	Resting	Blood flow	HI	HII
ATP	12.438 ± 0.410	12.414 ± 0.627	12.12 ± 0.627	11.959 ± 0.570
	(*n* = 17)	(*n* = 13)	(*n* = 11)	(*n* = 13)
ADP	5.691 ± 0.192	5.741 ± 0.175	5.779 ± 0.269	5.800 ± 0.206
	(*n* = 17)	(*n* = 13)	(*n* = 11)	(*n* = 13)
ATP/ADP	2.267 ± 0.102	2.218 ± 0.133	2.372 ± 0.207	2.216 ± 0.172
	(*n* = 17)	(*n* = 13)	(*n* = 11)	(*n* = 13)
AMP	1.175 ± 0.121	1.383 ± 0.130	1.453 ± 0.122	1.423 ± 0.113
	(*n* = 15)	(*n* = 10)	(*n* = 11)	(*n* = 11)
Total nucleotide	19.30 ± 0.18	19.49 ± 0.23	19.36 ± 0.31	19.18 ± 0.27
	(*n* = 15)	(*n* = 10)	(*n* = 11)	(*n* = 11)
Phosphocreatine	4.149 ± 0.318	4.788 ± 0.434	4.724 ± 0.270	4.812 ± 0.690
	(*n* = 17)	(*n* = 13)	(*n* = 11)	(*n* = 13)
$[ATP][AMP]/[ADP]^2$	0.45	0.52	0.53	0.51

but at steady state secretion there is apparently a decrease in the level of oxidized nucleotide. The level of this nucleotide is lower than in the mucous cells.

NADPH—Corresponding to the values of $NADP^+$ found in the parietal cell region of the mucosa there is no significant change in NADPH levels, during the stages of acid secretion (Table VII). Mucous cells have a slightly lower value of NADPH than parietal cells (Table VI). No change occurs in the mucous cells with secretion.

NADPH/$NADP^+$ Ratio—The value for this ratio does not change during onset of acid secretion, but at the steady state level there is a slight rise in the value, with no change in mucous cells.

Pyruvate—Table VIII shows that there is a progressive rise in pyruvate from the resting sample to blood flow and to secretion in the parietal cells; the levels in the mucous cells are about the same as in the parietal cells (Table VI), but do not change with the onset of acid secretion.

TABLE VI

Metabolite levels in mucous cells

The values given are expressed in terms of n dogs ±S.E. at rest and during acid secretion in millimoles kg^{-1} dry weight.

	Resting	Histamine
ATP	8.13 ± 0.93 (n = 4)	7.66 ± 0.38 (n = 4)
ADP	7.82 ± 0.68 (n = 4)	6.66 ± 0.44 (n = 4)
Phosphocreatine	5.53 ± 0.106 (n = 4)	5.19 ± 0.110 (n = 4)
NAD^+	1.29 ± 0.028 (n = 4)	1.34 ± 0.040 (n = 3)
NADH	0.046 ± 0.008 (n = 4)	0.028 ± 0.004 (n = 4)
$NADP^+$	0.088 ± 0.012 (n = 4)	0.097 ± 0.036 (n = 4)
NADPH	0.161 ± 0.016 (n = 4)	0.178 ± 0.014 (n = 4)
Lactate	4.33 ± 0.254 (n = 3)	4.61 ± 0.252 (n = 3)
Pyruvate	0.766 ± 0.060 (n = 4)	0.768 ± 0.020) (n = 4)

Lactate—Lactate levels double with the onset of acid secretion and are maintained during steady state secretion (Table VII). The lactate level in the mucous cells is similar to that of resting parietal cells and shows no change (Table VI).

Lactate/Pyruvate Ratio—The lactate/pyruvate ratio rises with onset of acid secretion to nearly twice its previous value, but does not change in mucous cells.

Acetoacetate—Table VIII shows that there are no changes observed with this keto acid over the period of observation. The value obtained for gastric mucosa is higher than that observed for control fed rat liver, for example (22), but lower than others have found for fasted liver (23) and higher than in rat brain (24).

β-Hydroxybutyrate—The level of the reduced product of acetoacetate, as was found for lactate, shows an increase with onset of acid secretion, which is maintained with continued secretion (Table VIII). The level found, however, is low compared to levels obtained for fasted liver.

β-Hydryoxybutyrate/Acetoacetate Ratio—There is a progressive rise in this value from onset of acid secretion into the steady state H^+ secretion sample, the final result being an approximate doubling of the ratio found. It should be noted that this ratio is the inverse of what is found in rat liver (22), under either fed or fasted conditions.

Glucose—The level of glucose remained quite constant over the period of observation, showing an insignificant 10% increase (Table IX).

Glycogen—There is a gradual continuing decline in glycogen levels with onset and steady state acid secretion (Table IX), with a net 15% fall.

Inorganic Phosphate—There is a significant rise in levels of inorganic phosphate found in parietal cells with acid secretion, but no change with blood flow (Table IX), the maximal change being about 30%. The rise in this metabolite is unexpected in view of the lack of change of the adenine nucleotides and phosphocreatine, and may be due to entry of phosphate from the blood.

DISCUSSION

Hypotheses as to the energy source for acid secretion have had a major effect on the concepts prevalent in the field. The earliest suggestion postulated that protons could be derived

TABLE VII

Metabolite levels in parietal cells

The values are the means ±S.E. of n dogs, at least four measurements having been made on each sample in each dog. Blood flow refers to the state of reddening of the mucosa, HI the sample when acid secretion was detected in that area, and HII a sample at steady state secretion. Values are given, when appropriate, in millimoles kg^{-1} dry weight.

Substance	Resting	Blood flow	HI	HII
NAD^+	1.970 ± 0.074 (n = 17)	1.962 ± 0.074 (n = 13)	1.882 ± 0.070 (n = 11)	1.933 ± 0.074 (n = 13)
NADH	0.295 ± 0.020 (n = 17)	0.315 ± 0.027 (n = 13)	0.523 ± 0.074[a] (n = 11)	0.507 ± 0.070[a] (n = 13)
NAD^+/NADH	6.68 ± 0.04 (n = 17)	5.91 ± 0.04 (n = 13)	3.60 ± 0.07[a] (n = 11)	3.81 ± 0.07[a] (n = 13)
$NADP^+$	0.069 ± 0.008 (n = 16)	0.069 ± 0.012 (n = 7)	0.064 ± 0.008 (n = 14)	0.046 ± 0.010 (n = 11)
NADPH	0.219 ± 0.012 (n = 20)	0.223 ± 0.014 (n = 14)	0.230 ± 0.013 (n = 12)	0.230 ± 0.072 (n = 14)
NADPH/$NADP^+$	3.17 ± 0.31 (n = 16)	3.23 ± 0.31 (n = 7)	3.59 ± 0.33 (n = 12)	4.78 ± 0.72[b] (n = 17)

[a] $p < 0.001$.
[b] $p < 0.05$.

TABLE VIII

Metabolite levels in parietal cells

The values are the means ±S.E. of *n* dogs, at least four measurements having been made on each sample in each dog. Blood flow refers to the state of reddening of the mucosa, HI the sample when the acid secretion was detected in that area, and HII a sample at steady state secretion. Values are given, when appropriate, in millimoles kg^{-1} dry weight.

Substance	Resting	Blood flow	HI	HII
Lactate	3.909 ± 0.351 (n = 17)	4.679 ± 0.588 (n = 12)	7.823 ± 1.191[a] (n = 11)	7.249 ± 1.020[a] (n = 13)
Pyruvate	0.678 ± 0.032 (n = 15)	0.747 ± 0.046 (n = 12)	0.760 ± 0.074 (n = 11)	0.817 ± 0.080 (n = 13)
Lactate/pyruvate	5.77 ± 0.32 (n = 15)	6.26 ± 0.53 (n = 12)	10.29 ± 1.10[a] (n = 11)	8.87 ± 1.00[b] (n = 13)
Acetoacetate	1.379 ± 0.131 (n = 7)	1.309 ± 0.084 (n = 7)	1.377 ± 0.148 (n = 7)	1.25 ± 0.115 (n = 7)
β-Hydroxybutyrate	0.181 ± 0.013 (n = 7)	0.157 ± 0.021 (n = 7)	0.257 ± 0.024[c] (n = 7)	0.333 ± 0.068[b] (n = 7)
β-Hydroxybutyrate/ acetoacetate	0.140 ± 0.019 (n = 7)	0.135 ± 0.028 (n = 6)	0.211 ± 0.040[c] (n = 7)	0.327 ± 0.113[b] (n = 7)

[a] $p < 0.001$.
[b] $p < 0.01$.
[c] $p < 0.05$.

TABLE IX

Metabolite levels in parietal cells

The values are the means ±S.E. of *n* dogs, at least four measurements having been made on each sample in each dog. Blood flow refers to the state of reddening of the mucosa, HI the sample when acid secretion was detected in that area, and HII a sample at steady state secretion. Values are given, when appropriate, in millimoles kg^{-1} dry weight.

Substance	Resting	Blood flow	HI	HII
Glucose	9.593 ± 0.820 (n = 17)	9.337 ± 0.682 (n = 13)	10.474 ± 1.602 (n = 11)	10.352 ± 1.239 (n = 13)
Glycogen	60.18 ± 3.40 (n = 11)	56.75 ± 4.20 (n = 11)	51.88 ± 3.01 (n = 11)	50.34 ± 3.90[a] (n = 10)
P_i	6.42 ± 0.14 (n = 5)	6.38 ± 0.37 (n = 5)	8.33 ± 1.30[a] (n = 5)	

[a] $p < 0.05$.

directly from oxidation-reduction of a substrate with secretion of H^+ and donation of electrons to an unspecified acceptor (25). This oxidation-reduction hypothesis was amplified further, based on work in yeast (26, 27) and data obtained from dual-split beam spectroscopy (28) have been interpreted as supporting an oxidation-reduction mechanism. On the other hand, measurements showing correlations between ATP levels and acid secretion (29, 30) or results obtained from the use of inhibitors (31, 32) have been interpreted as for (29) or against (30) an ATP-based mechanism. The discovery of ATPase in gastric mucosal membranes, either HCO_3^-- or K^+-stimulated (33, 34) has also been used to support an ATP hypothesis. Measurement of adenine nucleotide and phosphocreatine levels in frog mucosa during onset or increase of acid rate has also implicated ATP as the primary energy source (35).

The conflict of interpretation of the data is reminiscent of the problems in the field of oxidative phosphorylation. Here the proposal of chemiosmotic coupling (36) whereby the breakdown or synthesis of ATP is linked intimately to the generation or dissipation of an H^+ or potential gradient, has in a sense blurred the distinction between ATP- and oxidation-reduction-linked mechanisms.

Since techniques have not been developed for flux measurements of adenine and pyridine nucleotides, steady state levels of these components were measured; the hypothesis was that, because of the large change in energy consumption by the tissue, at some point in the transition between rest, tissue perfusion, and varying secretory states, critical steady state changes would be observed.

The primary reaction, that of H^+ transport, may be the site of stimulation of metabolism. The largest changes in the tissue should be observed in the acid-secreting cells, the parietal cells, and changes in surface epithelial cells should be minimal. The data obtained showed no change in levels of ATP and other adenine nucleotides, as well as no change in phosphocreatine, for either the parietal or the mucous cells. Moreover there was no significant difference in the levels found when the histamine and histamine + urecholine experiments were compared, in spite of the widely differing acid rates.

There is a variety of possible interpretations. The high mitochondrial content of the parietal cells (>32%) suggests that this tissue may well be capable of a rapid response to widely varying energy demands, so that there is little change in ATP or phosphocreatine. In this case, however, since there is no change in total ADP, the primary metabolic stimulus for the increased O_2 consumption (37) must be elsewhere in metabolism or due to changes in intramitochondrial ADP. It may be that mitochondrial metabolism is substrate-limited, rather than ADP-limited, *i.e.* that the mitochondria in gastric mucosa are in State 2 rather than State 4, as has been suggested elsewhere (28).

Compartmentation of the various nucleotides between mito-

chondrion and cytoplasm, also occurs, although this does not apply to phosphocreatine. Thus it is possible to calculate or to measure the phosphorylation potential ATP/ADP·P_i (38). The calculation assumes cytoplasmic localization and equilibrium operation of lactic dehydrogenase, glyceraldehyde-3-PO_4 dehydrogenase, and phosphoglycerate kinase.

The following equation can be shown to hold

$$\frac{\text{ATP}}{\text{ADP}\cdot\text{HPO}_4^{2-}} = \frac{[\text{pyruvate}]\,[\text{glyceraldehyde-3-P}]}{[\text{lactate}]\,[\text{3-P-glycerate}]}\,K$$

where

$$K = \frac{K_{G3P}\,K_{3PGA}}{K_{LDH}} = 53 \times 10^4 \text{ (pH 7.0)}$$

where *G3P* is glyceraldehyde-3-P, *3PGA* is 3-P-glycerate, and *LDH* is lactate dehydrogenase and HPO_4^{2-} is taken as 60% of total P_i. Substituting the data from Table VIII, and the levels of glyceraldehyde-3-PO_4 and 3-phosphoglycerate presented in detail in a subsequent paper and in Ref. 39, the results of Table X are found. It can be seen that the cytoplasmic and total phosphorylation potential fall by 25 to 35%, but that the cytoplasmic potential is twice as large as the total. This may be due to the altered energy state of the mitochondria. A possible artifact to be considered is a change in parietal cell pH, which has often been suggested, but rarely measured (28). Measurements in amphibian mucosa have suggested increases ranging from 0.3 to 1 pH unit.[1] A fall in cell $[H^+]$ will result in activation of phosphofructokinase as well as a decrease in the NAD^+/NADH, hence [pyruvate]/[lactate] ratios. Since pyruvate is the oxidized form, and glyceraldehyde-3-phosphate is the reduced form of the two oxidation-reduction couples involved in calculation of the phosphorylation potential, changes in the ratio of these due to a shift in NAD^+/NADH due to a change of pH will cancel, assuming equilibrium operation.

Data from frog gastric mucosa (35) which show a slight fall in ATP and a rise in ADP may be due to poorer oxygenation of the *in vitro* mucosa, with also slower removal of HCO_3^-, with subsequent hypoxia and alkalinization of the parietal cell, the latter consistent with the effects of increased CO_2 *in vitro* (40). The increase in phosphocreatine observed (35) was explained by the shift in cell pH. Since, however, the equilibrium constant for creatine kinase is 7.2×10^{-9} at pH 7.4, and 2.98×10^{-9} at pH 9.8 (41), the predicted change as a function of pH would be a fall in phosphocreatine, rather than a rise, or a fall in ADP with a rise in ATP. Hence, the constancy, or increase of phosphocreatine is difficult to reconcile with ADP driven metabolic transition. It should be pointed out that constancy in ATP, and ATP/ADP ratios is also found in muscle during a work load (42). However, associated with this, there is a fall in phosphocreatine contrary to what was observed here, and in frog mucosa (35).

Since the ratio $[ATP]\cdot[AMP]/[ADP]^2$ remains fairly constant at about 0.5 and since the equilibrium constant of the reaction, the inverse of the above ratio, is 2.26 at pH 7.4, it can be concluded that gastric parietal cells contain sufficient adenylate kinase to maintain this equilibrium.

In contrast to the constancy of adenine nucleotide level, we observed consistent and significant increases in the NADH level. Although the NAD^+/NADH ratio fell from 6.68 to 3.81, the NAD^+ level was still greater than NADH. Previous work in this area has been confined to spectroscopy where the data show reduction of pyridine nucleotide with stimulation of secretion (10, 28) or at least reduction of the rest of the respiratory chain (39), but some disagreement exists for this finding (9). The spectroscopic data naturally do not distinguish di- or triphosphopyridine nucleotides, nor the cell type or cellular location of the change. $NADP^+$ and NADPH change significantly with acid rate changes, and the NAD^+/NADH ratio doubles in the mucous cell, hence the spectroscopic data probably do indeed relate to the parietal cell (oxyntic cell in amphibia).

It is possible to calculate the NADH/NAD^+ ratio in the cytoplasm and mitochondria (43) on the assumption that (*a*) lactic dehydrogenase and α-glycerophosphate dehydrogenase; β-hydroxybutyrate dehydrogenase and glutamic dehydrogenase are located in the cytoplasm or mitochondria exclusively, (*b*) their activity is sufficient to maintain equilibrium, (*c*) there is no pH gradient between mitochondria and cytoplasm.

The equilibrium constants for lactic dehydrogenase is 1.11×10^{-11} M, and hence from the equation

$$\frac{\text{NAD}^+}{\text{NADH}} = \frac{1}{K_{LDH}}\,\frac{[\text{pyruvate}]\,[\text{H}^+]}{[\text{lactate}]}$$

The cytoplasmic ratio NAD^+/NADH at pH 7.4 is calculated to be 620 and to change to 348 with secretion. The ratio changes of α-glycerophosphate and dihydroxyacetone phosphate are similar to the lactate/pyruvate changes (39), hence the assumption that these dehydrogenases are sufficiently active to maintain equilibrium seems justified (Table XI).

This may well not be so for the β-HO-butyrate in stomach which has low activity in relation to liver. In the liver, the direction of change of acetoacetate/β-hydroxybutyrate and α-ketoglutarate NH_3/glutamate correspond, showing identity of the NAD^+/NADH ratio in mitochondrial membrane and matrix. In the stomach, whereas the acetoacetate/butyrate ratio falls, the α-ketoglutarate ratio increases (39, and subsequent papers) by 50%. This implies that the β-hydroxybutyrate dehydrogenase has too low an activity to maintain equilibrium in parietal cells, and assuming at least no fall in NH_3, that the mitochondrial NAD^+ pool is relatively oxidized with onset of acid secretion. The ratio for cytoplasm is much larger than the measured ratio, presumably due to greater binding of NADH relative to NAD^+ (43).

The influence of pH on this equilibrium is large. Thus, a

TABLE X

Total measured phosphorylation state and calculated "cytoplasmic" phosphorylation state (M^{-1})

Sample	Calculated ATP/ADP·P_i	Measured ATP/ADP·P_i
Resting	4643	2099
Blood flow	5308	2090
HI	3201	1553

TABLE XI

NAD^+/NADH ratio (pH 7.4)

Sample	Calculated NAD^+/NADH Cytosol (pyruvate/lactate)	Total measured NAD^+/NADH
Resting	620	6.68
Blood flow	570	5.91
HI	348	3.60
HII	404	3.81

[1] S. J. Hersey, personal communication.

change of pH from 7.4 to 7.7, as has been suggested to occur in *in vitro* frog mucosa, would be sufficient to induce a 2-fold change in the ratio, as observed here. Since, however, there is no difference between the two maximal secretory rates, where an additional change in cell pH might be expected, and also since there is no change in the $NADP^+/NADPH$ ratio which would be equally pH-sensitive, it may be that *in vivo*, little change in cell pH occurs. Also the rise in mucous cell $NAD^+/NADH$ argues against an alkalinization in this cell type which is coupled electrically to the parietal. Resolution of this problem will have to await direct measurements of pH change *in vivo*, and an attempt to distinguish between cytoplasmic and mitochondrial pH.

In some dogs a sample was taken after prolonged anesthesia and secretion. In those dogs there was a significant fall in ATP and phosphocreatine, as well as a large rise in lactate and NADH. These data could be mimicked by holding the biopsy sample in the forceps for 3 min prior to freezing. Hence anoxia could be a significant factor in these samples. Maintaining anoxia in a biopsy from resting and secreting mucosa did not give significant differences in ATP fall between rest and secretion. Data obtained for rat gastric mucosa (total thickness) show similar changes with hemorrhagic shock (45).

The mucous cells showed little change in any of the metabolites with onset of acid secretion. This shows a lack of effect of histamine on this cell type in the dog.

Acknowledgments—We should like to acknowledge the help and guidance of O. H. Lowry, J. V. Passoneau, and F. Matchinsky in setting up many of our assays.

REFERENCES

1. Mitchell, P., and Moyle, J. (1968) *Eur. J. Biochem.* **4,** 530–539
2. Scholes, P., Mitchell, P., and Moyle, J. (1969) *Eur. J. Biochem.* **8,** 450–454
3. Harold, F. M. (1972) *Bacteriol. Rev.* **36,** 172–230
4. Conway, E. C. (1963) *Biochemistry of Acid Secretion*, Charles C Thomas, Springfield, Ill.
5. Poole, R. J. (1966) *J. Gen. Physiol.* **49,** 551–563
6. Malnic, G., and Giebisch, G. (1972) *Kidney Int.* **1,** 280–296
7. Schulz, I., Strover, F., and Ullrich, K. J. (1971) *Pflugers Arch. Eur. J. Physiol. Ser. B Biol. Sci.* **323,** 121–140
8. Rehm, W. S. (1972) in *Metabolic Pathways* (Hokin, L. E., ed) Academic Press, New York
9. Kidder, G. W., Curran, P. F., and Rehm, W. S. (1971) *Am. J. Physiol.* **211,** 261–277
10. Hersey, S. J. (1971) *Philos. Trans. R. Soc. Lond.* **262,** 261–277
11. Forte, J. G., Adams, P. H., and Davies, R. E. (1965) *Biochim. Biophys. Acta* **104,** 25–38
12. Michelangeli, P. in *Acid Secretion* (Kasbekar, D. K., Rehm, W. S., and Sachs, G., eds) Marcel Dekker, New York, in press
13. Lowry, O. H., and Passoneau, J. V. (1972) *Flexible Method of Enzymatic Analysis*, Academic Press, New York
14. Myren, J., Unihem, O., and Gheruldsen, S. T. (1965) *Scan. J. Clin. Lab. Invest.* **17,** 31–38
15. Lowry, O. H. (1963) *Harvey Lect.* **58,** 1–19
16. Lowry, O. H., Passoneau, J. V., Hasselberger, F. X., and Schulz, D. W. (1964) *J. Biol. Chem.* **239,** 18–30
17. Roehrig, K. L., and Allred, J. B. (1974) *Anal. Biochem.* **58,** 414–421
18. Loewenstein, J. M. (1969) *Methods Enzymol.* **13,** 476–478
19. Lowry, O. H., Passoneau, J. V., Schulz, D. W., and Rock, M. K. (1961) *J. Biol. Chem.* **236,** 2746–2755
20. Matchinsky, F. M. (1968) *J. Neurochem.* **15,** 643–657
21. Kato, T., Berger, S. J., Carter, J. A., and Lowry, O. H. (1973) *Anal. Biochem.* **53,** 86–97
22. Greenbaum, A. L., Gumaa, K. A., and McLean, P. (1971) *Arch. Biochem. Biophys.* **143,** 617–663
23. Hawkins, R. A., Houghton, C. R. S., and Williamson, D. H. (1973) *Biochem. J.* **132,** 19–25
24. Miller, A. L., Hawkins, R. A., and Veech, R. L. (1973) *J. Neurochem.* **20,** 1393–1400
25. Conway, E. J., and Brady, T. G. (1948) *Nature* **162,** 456–457
26. Armstrong, W. McD. (1972) *Transport and Accumulation in Biological Systems*, pp. 407–445, Butterworth, London
27. Seaston, A., Inkson, C., and Eddy, A. A. (1973) *Biochem. J.* **134,** 1031–1043
28. Hersey, S. J. (1974) *Biochim. Biophys. Acta* **344,** 157–203
29. Durbin, R. P. (1968) *J. Gen. Physiol.* **51,** 233–239
30. Sachs, G., Shoemaker, R., and Hirschowitz, B. I. (1967) *Biochim. Biophys. Acta* **143,** 522–531
31. Sachs, G., Collier, R. H., Shoemaker, R. L., and Hirschowitz, B. I. (1968) *Biochim. Biophys. Acta* **162,** 210–219
32. Bannister, W. H. (1966) *J. Physiol. (Lond.)* 88–96
33. Kasbekar, D. K., and Durbin, R. P. (1965) *Biochim. Biophys. Acta* **105,** 472–482
34. Ganser, A. L., and Forte, J. G. (1973) *Biochim. Biophys. Acta* **307,** 169–180
35. Durbin, R. P., Michelangeli, F., and Michel, A. (1974) *Biochim. Biophys. Acta* **367,** 177–189
36. Mitchell, P. (1966) *Biol. Rev. (Camb.)* **41,** 445–488
37. Moody, F. G. (1968) *Am. J. Physiol.* **215,** 127–131
38. Veech, R. L., Raijman, L., and Krebs, H. A. (1970) *Biochem. J.* **117,** 499–503
39. Sachs, G., Rabon, E., Saccomani, G., and Sarau, H. M. *Ann. N. Y. Acad. Sci.*, in press
40. Kidder, G. W. *Am. J. Physiol.*, in press
41. Kuby, S. A., and Noltmann, S. A. (1962) in *The Enzymes* (Boyer, P. D., Lardy, H., and Myrbäck, K., eds) 2nd Ed, Vol. 6, pp. 515–542, Academic Press, New York
42. Williamson, J. R., Illingworth, J. A., Ford, C. L., Kobayashi, K. *Recent Advances in Cardiac Structure and Metabolism*, W. Park Press, in press
43. Williamson, D. H., Lund, P., and Krebs, H. A. (1967) *Biochem. J.* **103,** 514–527
44. Matchinsky, F. M., Passoneau, J. V., and Lowry, O. H. (1968) *J. Histochem. Cytochem.* **16,** 29–39
45. Menguy, R., Desbaillets, L., and Masters, Y. F. (1974) *Gastroenterology* **66,** 46–55

THE JOURNAL OF BIOLOGICAL CHEMISTRY
Vol. 252, No. 23, Issue of December 10, pp. 8572-8581, 1977
Printed in U.S.A.

Metabolism of Dog Gastric Mucosa

LEVELS OF GLYCOLYTIC, CITRIC ACID CYCLE AND OTHER INTERMEDIATES*

(Received for publication, February 7, 1977, and in revised form, July 18, 1977)

HENRY M. SARAU, JAMES J. FOLEY, GEORGE MOONSAMMY, AND GEORGE SACHS

From the Smith, Kline & French Laboratories, Philadelphia, Pennsylvania 19101 and the Laboratory of Membrane Biology, University of Alabama in Birmingham, Birmingham, Alabama 35294

Several metabolites, including those of glycolysis, the citric acid cycle, the hexose monophosphate shunt, glutamate, aspartate, and Coenzyme A were measured in defined parietal cell-enriched freeze-dried sections of dog gastric biopsies derived from nonsecreting and secreting tissue. In addition, NH_3, ribulose 5-phosphate, glycerol, and succinate were measured in perchloric acid extracts of biopsies. The onset of secretion increased the level of glycolytic intermediates including pyruvate and lactate with the most marked increase being in fructose 1,6-diphosphate levels. The level of 6-phosphogluconate and ribulose 5-phosphate also increased, in spite of a constant $NADP^+$/NADPH ratio. The levels of all the citric acid cycle intermediates measured also rose, the most marked rise being in malate and fumarate. The levels of glycerol, acetyl-CoA, and CoA increased, but the ratio of the latter intermediates remained constant. Calculation of the ratio of the oxidized to reduced form of diphosphopyridine nucleotide indicated a fall of the ratio in the cytoplasm and a rise in the mitochondria. From these data, it is concluded that the major energy source for acid secretion is due to an increase in citric acid cycle activity and that glycolysis, and probably also fatty acid oxidation, is stimulated to provide mitochondrial substrate.

In epithelia, such as gastric mucosa, which are capable of large alterations in transport and O_2 consumption with the addition of stimuli such as histamine, metabolic investigations are essential to answer two major questions, the primary energy source for transport, and then the nature of metabolic pathway(s) stimulated to produce the primary energy source. There are classically two means of measuring metabolism, those which measure steady state changes in metabolite levels and those using radioisotopes which measure changes in flux through various pathways. Techniques for the former are now available for most metabolites and are being applied with increasing frequency to a variety of tissues (1, 2). Results from these can demonstrate changes which, when interpreted according to the cross-over theorem (3), show the presence of control points in metabolic pathways. When metabolite levels are combined with studies of the enzymes involved, metabolic activators and inhibitors can be defined, and the metabolic change in turn correlated with the levels of activator or inhibitor.

In most epithelia, the major active function is Na^+ transport with, consequently, ATP as the primary energy source. Gastric mucosa, however, has the active secretion of H^+ and Cl^- as its primary function (4), and there is disagreement as to the primary energy source for transport of either ion (5). Metabolic studies in this tissue have been mainly concerned with changes in adenine nucleotide levels (6) or with spectroscopic measure of oxidation-reduction components (7) and conflicting data have been obtained, especially with the latter technique (8). Delineation of the metabolic pathway involved has largely been indirect and exclusively concerned with the *in vitro* amphibian mucosa (9). Data from such studies have been interpreted as indicating that fatty acid oxidation is a major energy source for acid secretion with some involvement of hexose oxidation (10). Studies in amphibia appear to demonstrate that pyruvate dehydrogenase and pyruvate carboxylase may be rate-limiting (a conclusion derived from alteration of medium lipoate levels) (11). These studies also suggest that this system may not be as critical in mammalian mucosa (12).

Recently, we have completed a study of adenine and pyridine nucleotide levels in defined parietal cell areas of resting and secreting dog mucosa (13) where the change of H^+ rate from rest to secretion is almost 2 orders of magnitude greater than in amphibian mucosa. This paper extends these observations to other metabolites accessible to the microfluorimetric cycling procedures. By necessity for some substrates, such as glycerol, NH_3, succinate, and ribulose 5-phosphate, extracts of canine mucosa were used in place of the usual freeze-dried tissue section in the measurements.

EXPERIMENTAL PROCEDURES

Methods

Surgical Procedures, Biopsy, and Extraction—These have been described in detail in the previous paper of this series (13).

Measurement of Metabolite Levels—Following extraction of the metabolites, they are stoichiometrically reacted to produce one form of pyridine nucleotide which is then measured by insertion into a NAD^+ or $NADP^+$ cycling system followed by fluorimetric measurement of the indicator substrate (14). At each stage of measurement,

* This work was supported by Grant AM 15878 from the National Institutes of Health and Grant GB 31075 from the National Science Foundation. This is the second paper in a series on "Metabolism of Dog Gastric Mucosa." The preceding paper in this series is Ref. 13. The costs of publication of this article were defrayed in part by the payment of page charges. This article must therefore be hereby marked "*advertisement*" in accordance with 18 U.S.C. Section 1734 solely to indicate this fact.

control standards are run, and for each substrate, the linear range of estimate is adjusted appropriate to the level of substrate found in the biopsy extract.

An artifact was found in assays depending on the enzymic conversion of NADH to NAD^+. There appears to be a nonenzymic production of NAD^+ unless ascorbic acid is present in the reagent step. This artifact leads to an overestimate of the levels of ADP, pyruvate, and acetoacetate as reported in the previous paper of this series (13) and in other metabolites whose measurement is dependent on NAD^+ production. We found that this artifact could be corrected by making the reagent 6.7 mM final concentration in ascorbic acid and adding sufficient ascorbic acid during the preparation for cycling to achieve a final level of 50 mM ascorbate. With this procedure, for example, the level of ADP obtained fell by 24% compared to our previously published values. Table I presents the methods used for metabolite measurement.

The procedure for cycling $NADP^+$/NADPH was essentially that of Lowry *et al.* (23) as described in Ref. 13. Each assay utilized 100 μl of a reagent containing 100 mM Tris buffer pH 8.0, 1 mM glucose 6-phosphate, 0.1 mM ADP, 5 mM α-ketoglutarate, and ~25 mM ammonium acetate. The glutamate dehydrogenase and glucose-6-phosphate dehydrogenase levels were varied as shown in Table I to obtain the necessary level of sensitivity for each substrate. Cycling was at 37°.

The procedure for cycling NAD^+/NADH was essentially that of Kato *et al.* (24) as described in Ref. 13. Each assay used 100 μl of cycling reagent containing 100 mM Tris buffer, pH 8.0, 300 mM ethanol, 2 mM mercaptoethanol, 0.02% bovine serum albumin, 2 mM oxalacetate, alcohol dehydrogenase, and malate dehydrogenase as given in Table I. Cycling was at 28°.

The indicator steps for the two cycles were essentially as previously published (23, 24). All metabolites were not measured for every dog due to depletion of some samples for other assay procedures.

Perchloric Acid Extraction Methods – Four substrates, ammonia, ribulose 5-phosphate, succinate, and glycerol were measured in a perchloric acid extract of the frozen biopsy tissue as previously described (25).

NH_3 Assay – One milliliter of a reagent containing 40 mM Tris/HCl pH 8.4, 5 mM α-ketoglutarate, 0.01% bovine serum albumin, 0.1 mM ADP, 200 μg/ml glutamate dehydrogenase in glycerol, and 27.5 μM NADH was added to a 3-ml Pyrex tube and the initial fluorimetric reading taken. Fifty microliters of the above perchloric acid extract was added and the fluorescence read after 10 min incubation at room temperature (25). Standards were run through the entire procedure in perchloric acid blank.

Ribulose 5-Phosphate – Assay of this intermediate was based on the combined action of ribulose-5-phosphate epimerase, transketolase, and glyceraldehyde phosphate dehydrogenase with measurement of the NADH (26). The reagents were as follows: Reagent A contained 100 mM imidazole buffer, pH 7.4, 0.02 mM thiamin pyrophosphate, 2 mM $MgCl_2$, 0.02 mM erythrose-4-PO_4, 60 μM NAD^+, 2 mM Na_2HAsO_4, 2 mM EDTA, 4 mM mercaptoethanol, 0.04% bovine serum albumin, 2 μg/ml of yeast glyceraldehyde phosphate dehydrogenase and 12 μg/ml of transketolase. Reagent B contained, in addition, 18 μg/ml of ribulose-5-phosphate epimerase.

One microliter of perchloric acid extract and 1 μl of H_2O was added to the wells through oil while 1 μl of standard was added to the extract blank in place of the water for standard wells. Two microliters of Reagent A were added to a complete set of blank and tissue wells and 2 μl of Reagent B were added to a second set of wells. The reaction was carried out at room temperature for 20 min and then the NAD^+ destroyed by adding 1 μl of 0.25 N NaOH and heating at 80° for 20 min.

The NADH formed from each reaction was measured by transferring 4-μl aliquots to the standard NADH cycling procedure (100 μl of reagent containing 30 μg of alcohol dehydrogenase and 5 μg of malate dehydrogenase MDH). The indicator step was carried out after 1 h of cycling. The substrate present was calculated from the difference between the fluorimetric readings using Reagent A (blank) and Reagent B.

Succinate – Assay of this intermediate in tissue extract was done using a three-step coupled enzyme reaction (20).

The reagents used were as follows: Reagent A contained 75 mM imidazole buffer, pH 7.5, 4.5 mM phosphoenolpyruvate, 4.5 mM $MgCl_2$, 22.6 mM KCl, 0.6 mM GTP, 0.4 mM CoA, and 40 μg/ml of pyruvate kinase (muscle). Reagent B contains everything in Reagent A plus 180 μg/ml of succinate thiokinase. Reagent C is 200 mM imidazole buffer, pH 7.5, containing 22.5 μM NADH.

In the procedure, two complete sets of disposable glass tubes (10 × 75 mm) were prepared. To one set, 100 μl of Reagent A was added; to the other set, 100 μl of Reagent B. To each sample tube, 50 μl of the tissue extract was added, for blanks and standards, 50 μl of extract reagent blank was added, and for the standard sample tubes, 1 μl of standard was added to make a final level of succinate per assay of 1.25 to 5.0 × 10^{-9} mol. The reaction proceeds to completion in 45 min at room temperature. To each sample, 3 μl of 5 N HCl was added to destroy the NADH oxidase activity in thiokinase preparation. Within 10 min, 1 ml of Reagent C was added and the initial fluorimetric reading made. The final reaction was initiated with 70 μg of Worthington beef heart lactic dehydrogenase and this reaction goes to completion in 20 min at room temperature. The fluorescence was measured and the blank obtained using Reagent A subtracted for each sample from the change in fluorescence obtained with reagent B.

Glycerol – Glycerol was measured in the perchloric acid extracts, in addition to measurement in dried sections, by adding 1 μl of extract to the oil wells followed by the standard reagent and cycling procedures. With lyophilized sections, high values of glycerol were obtained compared to the extract method. Since rat liver values obtained by the extract method were comparable to those previously published, we present the data using the extract. The values for freeze-dried tissue were approximately 10-fold higher for glycerol, but identical for α-glycerol phosphate. It is possible that some lipid breakdown occurred in the lyophilized sections.

Materials

Enzymes were purchased from Boehringer Corp. except for beef heart lactic dehydrogenase which was from Worthington and succinate thiokinase which was obtained from Sigma. The lactic dehydrogenase was purified over activated charcoal. Substrates were from Sigma. Trizma (2-amino-2-hydroxymethyl-1,3-propanediol) base was purified over Norit prior to use.

RESULTS

The values obtained for total pyridine nucleotides, adenine nucleotides, and related metabolites were presented in the first paper of this series (13). The results in this paper are classified into glycogen and glycolysis related intermediates, hexose monophosphate shunt metabolites, Krebs cycle and associated metabolites, and lipid metabolism-related metabolites.

Glycogen and Glycolysis (Table II)

UDP-glucose – The level of this metabolite remained steady during the blood flow transition but commenced to fall with the onset of secretion and continued to fall thereafter. The percentage of change was −12% at HI.

Glucose 6-Phosphate – The level of this metabolite did not change significantly with reddening of the mucosa but increased with the onset of secretion and continued to rise. The change corresponded to an increase of 25% at HI.

Fructose 6-Phosphate – No change was observed in this component with the onset of blood flow, and then there was a rise of 30% with the onset of acid secretion. Next a fall in level occurred with continued secretion (HII).

Fructose 1,6-Diphosphate – This metabolite's level rose slightly with the onset of blood flow, but rose markedly with the onset of secretion. This level was not maintained and fell slightly with continued secretion. The change observed corresponded to an 181% increase at HI.

Glyceraldehyde 3-Phosphate – This did not change with the onset of blood flow, and rose with the onset of acid secretion. The rise was 60% at HI.

Dihydroxyacetone Phosphate – The value of this metabolite rose throughout the period of observation, reaching an increase of 47% at HI.

α-Glycerol Phosphate – No change was observed in this

TABLE I

Measurement methods

Method references are given in parentheses. Methods for glucose, glycogen, β-OH butyrate, lactate, and inorganic phosphate were presented in detail in Ref. 13. The abbreviations used are: Asc, ascorbic acid; DTT, dithiothreitol; EDTA, ethylenediaminetetraacetate; BSA, bovine serum albumin; GDH, glutamic acid dehydrogenase; G-6-PDH, glucose-6-phosphate dehydrogenase; ADH, alcohol dehydrogenase; MDH, malate dehydrogenase.

Substance	Preparation of Sample (Substrate Standard Used)	Reaction I Conditions (Vol., Time, Temp.)	Buffer, Enzymes	Other Addition	Preparation for Cycling	Sample Vol., Time, Enzyme in Cycling
(16) Glucose-6-Phosphate	2.68 µl 0.015 N HCl 20 min, 60°(0.1-1.0 pmoles)	To 1 µl aliquot add 2 µl reagent, react 30 min, R.T.	100 mM Tris, pH 8.0, 0.25 µg/ml G-6-PDH	50 µm $NADP^+$ 100 µM DTT 0.02% BSA	1 µl of 1.2 N NaOH for 20 min, 80°	3 µl, 90 min, 135 µg/ml GDH 68 µg/ml G-6-PDH
(16) Fructose -6-Phosphate	as G-6-P (0.2-0.8 pmoles)	as G-6-P	as G-6-P 0.25 µg/ml G-6-PDH 0.4 µg/ml Phosphoglucoisomerase	as G-6-P	as G-6-P	as G-6-P
(14) Fructose-1,6 diphosphate (FDP)	1 µl of 0.02 N HCl 20 min, 80°C 1 µl of 0.04 N NaOH 5 min, 80° (0.042-0.167 pmoles)	2 µl reagent 60 min, R.T.	100 mM Imidazole, pH 7.5 20 µg/ml Aldolase (rabbit muscle) 2 µg/ml Triose P-Isomerase (rabbit muscle) *100 µg/ml Glyceraldehyde-P dehydrogenase (rabbit muscle)	60 µM NAD^+ 2 mM Na_2HAsO_4 2 mM EDTA 4 mM Mercaptoethanol 0.04% BSA	2 µl of 0.2 N NaOH 20 min, 80°	4 µl, 60 min, 240 µg/ml ADH 40 µg/ml MDH
(14) Dihydroxy acetone Phosphate (DHAP)	1 µl of 0.02 N HCl 20 min, 80° (as FDP)	as FDP	as FDP without the aldolase	as FDP	as FDP	as FDP
(14) Glyceraldehyde-3-Phosphate (GAP)	as DHAP (.025-.100 pmoles)	2 µl reagent 20 min, R.T.	100 mM Imidazole, pH 7.5 *100 µg/ml Glyceraldehyde-P dehydrogenase (rabbit muscle)	as FDP	2 µl of 0.2 N NaOH 30 min, 80°	4 µl, 120 min. 300 µg/ml ADH; 50 µg/ml MDH
(16) 3-Phospho-Glycerate (3-PG)	1 µl of 0.05 N NaOH 20 min, 80° (.25-.75 pmoles)	2 µl reagent 40 min, R.T.	100 mM Imidazole, pH 7.1 2 µg/ml P-Glycerate kinase, 5 µg/ml glyceraldehyde-P dehydrogenase both from rabbit muscle	1 µM NADH 30 µM ATP 1 mM $MgCl_2$ 2 mM Mercaptoethanol 20 mM NaCl 0.02% BSA 10 mM Asc	1 µl of 0.5 N HCl in 200 mM Asc 30 min, R.T.	2 µl, 60 min. as FDP
(16) Phosphoenol pyruvate (PEP)	1 µl 0.02 N NaOH 10 mM hydrazine, 20 min, 80° (.06-.24 pmoles)	2 µl reagent 15 min, R.T.	200 mM Imidazole, pH 7.0 2 µg/ml Pyruvate kinase (rabbit muscle); **5 µg/ml lactic dehydrogenase (beef heart)	1.5 µM NADH 200 µM ADP 2 mM $MgCl_2$ 75 mM KCl 0.02% BSA 10 mM Asc	1 µl of 0.5 N HCl in 200 mM Asc 30 min R.T.	3 µl, 60 min, as GAP
(13) Pyruvate	1 µl 0.02 N NaOH 20 min, 80° (.3-1.2 pmoles)	as GAP	100 mM Imidazole, pH 7.0 1 µg/ml **Lactic dehydrogenase	3 µM NADH 0.02% BSA 10 mM Asc	1 µl of 0.5 N HCl in 200 mM Asc 30 min R.T.	1 µl, 60 min, as GAP
(16) α-Glycerophosphate	1.0 µl, 0.02 N HCl, 20 min, 80° (0.2-0.4 pmoles)	2 µl reagent 30 min, R.T.	400 mM Hydrazine, pH 9.2 10 µg/ml Glycerophosphate dehydrogenase	100 µM NAD^+ 0.02% BSA 2 mM $MgCl_2$ 400 µM EDTA	1 µl of 0.2 N NaOH 20 min, 80°	1 µl, 60 min, as FDP
(22) Glycerol	1 µl PCA extract, 1 µl H_2O (2.5-10.0 pmoles)	as α-glycerol phosphate	400 mM hydrazine, pH 9.2 10 µg/ml glycerophosphate dehydrogenase 5 µg/ml glycerol kinase	200 µM NAD^+ 0.02% BSA 2 mM $MgCl_2$ 400 µM EDTA 200 µM ATP	as α-glycerophosphate	2 µl, 60 min. 60 µg/ml ADH: 10 µg/ml MDH
(20) 6-Phosphogluconate (6-PG)	1 µl, 0.02 N HCl 15 min, 75° (.113-.226 pmoles)	2 µl reagent 30 min, R.T.	100 mM Tris, pH 8.0 2 µg/ml 6-Phosphogluconate dehydrogenase	20 µM $NADP^+$ 0.5 mM DTT 5 mM $MgCl_2$ 1 mM EDTA 30 mM NH_4OAc 0.02% BSA	1 µl of 1.2 N NaOH 15 min, 75°	3 µl, 90 min, 125 µg/ml G-6-PDH 250 µg/ml GDH

TABLE I—*Continued*

Substance	Preparation of Sample (Substrate Standard Used)	Reaction I Conditions (Vol., Time, Temp.)	Buffer, Enzymes	Other Addition	Preparation for Cycling	Sample Vol., Time, Enzyme in Cycling
(17) Uridine-5-diphospho-glucose (UDPG)	1 µl of 0.02 N HCl 20 min, 60° (0.5-2.0 pmoles)	2 µl reagent 40 min, R.T.	100 mM Tris, pH 8.1 15 µg/ml Uridine diphosphate glucose dehydrogenase	200 µM NAD^+ 2 mM $MgCl_2$ 0.01% BSA	1 µl of 0.25 N NaOH 20 min, 80°	3 µl, 60 min, as glycerol
(18) Acetyl CoA	3 µl of 0.025 N HCl 15 min, 80° (.183-.366 pmoles)	to 1 µl aliquot add 2 µl reagent 25 min, R.T.	50 mM Tris, pH 8.1 20 µg/ml α-KG dehydrogenase;**** 0.4 µg/ml carnitine acetyl transferase	100 µM NAD^+ 1 mM DTT 0.01% BSA 0.2 mM α-KG 0.2 mM carnitine	as UDPG	3 µl, 60 min, as GAP
(19) Coenzyme A	3 µl 0.025 N HCl 15 min, 80° (.194-.388 pmoles)	to 1 µl aliquot add 2 µl reagent 20 min, R.T.	50 mM Tris, pH 8.1 2 µg/ml α-KG dehydrogenase	100 µM NAD^+ 1 mM DTT 0.01% BSA 200 µM α-KG	as UDPG	2 µl, 60 min, as GAP
(14) Citrate	1 µl 0.02 N NaOH 20 min, 80° (1.8-3.6 pmoles)	as GAP	200 mM Tris, pH 7.6 1 µg/ml MDH 2 µg/ml citrate lyase	8 µM NADH 40 µM $ZnCl_2$ 0.02% BSA 10 mM Asc	as 3-PG	as Glycerol
(17) α-Ketoglutarate (α-KG)	1 µl of 0.05 N NaOH 20 min, 80° (0.4-1.6 pmoles)	as GAP	200 mM Imidazole acetate, pH 6.9 20 µg/ml GDH	2 µM NADH 50 mM NH_4OAc 200 µM ADP 0.05% BSA 10 mM Asc	as 3-PG	2 µl, 60 min, 210 µg/ml ADH; 35 µg/ml MDH
(14) Malate	3 µl 0.02 N HCl 20 min, 80° (0.125-0.5 pmoles)	To 1 µl aliquot add 2 µl reagent 45 min, R.T.	***100 mM AMP_1, pH 9.9 10 µg/ml Malate dehydrogenase (pig heart) 2 µg/ml glutamic oxalo-acetate transaminase (GOT) (pig heart)	50 µM NAD^+ 500 µM Glutamate 0.02% BSA	1 µl of 0.25 N NaOH 30 min, 80°	3 µl, 60 min, as GAP
(14) Fumarate	as Malate (0.05-0.2 pmoles)	as Malate	as Malate, plus *20 µg/ml fumarase	as Malate	as Malate	as Malate
(14) Glutamate	as DHAP (4.45-7.5 pmoles)	as 6-PG	50 mM Tris-acetate pH 8.4 50 µg/ml GDH (in glycerol)	100 µM NAD^+ 100 µM ADP 0.02% BSA	as UDPG	1 µl, 60 min, 76 µg/ml ADH; 11 µg/ml MDH
(21) Aspartate	1 µl of 0.02 N NaOH 20 min, 80° (1-4 pmoles)	as 6-PG	100 mM Imidazole, pH 7.0 10 µg/ml GOT 2 µg/ml MDH	5 µM NADH 20 µM α-KG 0.01% BSA 10 mM Asc	as 3-PG	2 µl, 60 min, 150 µg/ml ADH; 25 µg/ml MDH
(13) Aceto-acetate	as Aspartate (0.25-1.0 pmoles)	as 6-PG	100 mM Imidazole, pH 7.0 40 µg/ml β-hydroxy butyrate dehydrogenase	2 µM NADH 2 mM $MgCl_2$ 1 mM EDTA 0.02% BSA 10 mM Asc	as 3-PG	3 µl, 60 min, as Aspartate
(14) Isocitrate	1 µl of 0.015 N HCl 20 min, 80°	as GAP	100 mM Tris-HCl, pH 8.1 1 µg/ml Isocitric dehydrogenase	5 µM $NADP^+$ 100 µM $MnCl_2$ 0.02% BSA	1 µl of 1.2 N NaOH 20 min, 80°	3 µl, 60 min, 216 µg/ml GDH 108 µg/ml G-6-PDH

* Remove $(NH_4)_2SO_4$ by centrifugation.

** Purified with charcoal.

*** 2-Amino-2-methyl-1-propanol.

**** α-Ketoglutarate dehydrogenase was prepared by the New England Enzyme Center, Boston, Mass.

metabolite with blood flow, but a sharp rise was found with the onset of secretion which was maintained with continuing secretion. The maximal value occurred at the onset of acid secretion, corresponding to an increase of 117%.

3-Phosphoglycerate—An increase of 42% of this intermediate was found with the onset of blood flow and an increase of 3% obtained with the onset of acid secretion. The level in the nonsecreting mucosa is quite low.

Phosphoenolpyruvate—Level of this metabolite rose with the onset of blood flow which rise was maintained at the onset of acid secretion. The level increased by 171% at HI.

Glycogen, Glucose, Pyruvate, Lactate, P_i—The changes in values for these intermediates have been presented previously (13).

These results are summarized in Table II and Fig. 1. In addition, Fig. 2 shows the percentage of change of measured and calculated phosphorylation potential and of the total and calculated NAD^+/NADH ratios for the cytoplasmic and mitochondrial experiments.

The measured ratios are based on the directly determined values. The calculated phosphorylation potential is derived from the glyceraldehyde 3-phosphate and 3-phosphoglyceroki-

TABLE II

Glycolytic intermediates

The values are the means ± S.E. of n dogs, at least four measurements having been made on each sample in each dog. Blood flow refers to the state of reddening of the mucosa, HI the sample when acid secretion was detected in that area, and HII a sample at steady state secretion. Values are given in millimoles kg^{-1}, dry weight.

	Resting	Blood flow	HI	HII
Glycogen (15)	60.18 ± 3.4 (n = 11)	56.75 ± 4.2 (n = 11)	51.88 ± 3.01[a] (n = 11)	50.35 ± 3.9[a] (n = 10)
UDP-glucose	0.810 ± 0.040 (n = 6)	0.815 ± 0.064 (n = 6)	0.714 ± 0.161 (n = 6)	0.665 ± 0.054[a] (n = 6)
Glucose	9.59 ± 0.82 (n = 17)	9.34 ± 0.68 (n = 13)	10.47 ± 1.60 (n = 11)	10.35 ± 1.24 (n = 10)
Glucose 6-phosphate	0.267 ± 0.039 (n = 14)	0.243 ± 0.024 (n = 12)	0.335 ± 0.031[a] (n = 12)	0.395 ± 0.021[a] (n = 12)
Fructose 6-phosphate	0.094 ± 0.036 (n = 6)	0.092 ± 0.015 (n = 5)	0.122 ± 0.013 (n = 6)	0.072 ± 0.036 (n = 3)
Fructose 1,6-diphosphate	0.033 ± 0.004 (n = 9)	0.044 ± 0.015 (n = 6)	0.093 ± 0.011[b] (n = 6)	0.074 ± 0.025[a] (n = 3)
Glyceraldehyde 3-phosphate	0.015 ± 0.002 (n = 7)	0.017 ± 0.02 (n = 6)	0.024 ± 0.003[a] (n = 7)	
Dihydroxyacetone phosphate	0.045 ± 0.005 (n = 6)	0.053 ± 0.007 (n = 6)	0.066 ± 0.008[a] (n = 6)	
α-Glycerol phosphate	0.219 ± 0.030 (n= 11)	0.220 ± 0.025 (n = 7)	0.475 ± 0.035[b] (n = 7)	0.410 ± 0.072[a] (n = 11)
3-Phosphoglycerate	0.069 ± 0.009 (n = 5)	0.098 ± 0.020 (n = 5)	0.168 ± 0.03 (n = 5)	
Phosphoenolpyruvate	0.014 ± 0.003 (n = 4)	0.024 ± 0.007 (n = 3)	0.038 ± 0.005[a] (n = 4)	
Pyruvate	0.424 ± 0.046 (n = 7)	0.526 ± 0.031 (n = 7)	0.604 ± 0.038[a] (n = 7)	
Lactate	3.41 ± 0.35 (n = 7)	3.68 ± 0.59 (n = 7)	5.93 ± 1.19[c] (n = 7)	
Inorganic phosphate	6.42 ± 0.14 (n = 5)	6.39 ± 0.37 (n = 5)	8.33 ± 1.30[a] (n = 5)	

[a] $p < 0.05$.
[b] $p < 0.001$.
[c] $p < 0.01$.

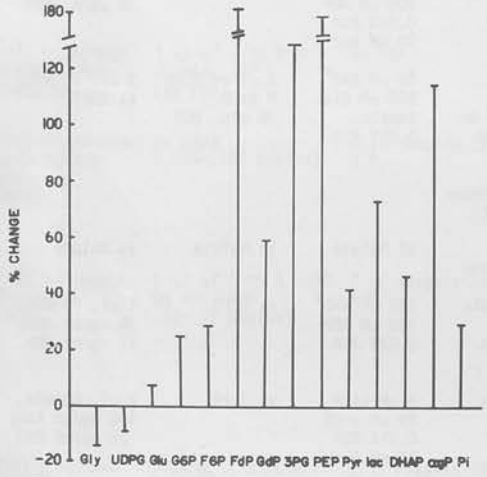

FIG. 1. The percentage of change in levels of glycogen, UDP-glucose, and glycolytic intermediates occurring between rest and secretion (HI) in dog gastric mucosa.

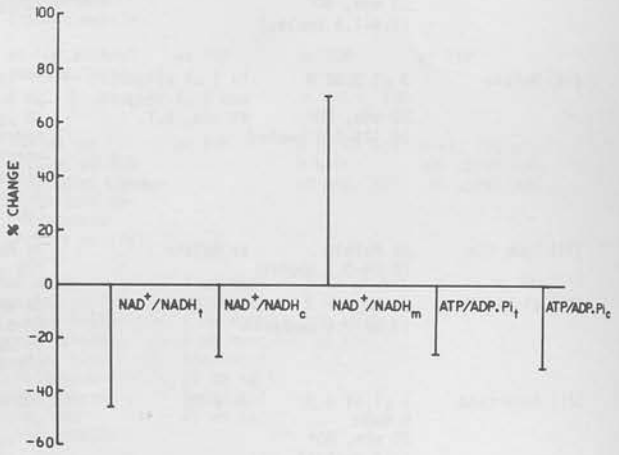

FIG. 2. This shows the percentage of change of the ratio of NAD^+/NADH as measured and as calculated for the cytoplasmic and mitochondrial compartment and of the measured and calculated phosphorylation potential between resting and secreting (HI) in dog gastric mucosa.

nase reactions. Cytoplasmic NAD^+/NADH is derived from the lactic dehydrogenase reaction and the mitochondrial ratio from the glutamic dehydrogenase reaction.

Hexose Monophosphate Shunt (Table III) (Fig. 3)

6-Phosphogluconate – No change was found in this metabolite with blood flow, but an increase was found with the onset of secretion, which was maintained with continued secretion. The value obtained showed an increase of 117%.

Ribulose 5-Phosphate – Due to the low levels and relative insensitivity of this assay, measurements were made in the perchloric acid extract of the tissue, rather than in the freeze-dried section. An increase was observed with blood flow, but a greater increase (by 64%) was observed with acid secretion.

Total $NADP^+$/NADPH Ratio – This was described in the previous publication (13). No change in the levels of either nucleotide was found with acid secretion. The calculated free ratio based on the 6-phosphogluconate dehydrogenase reaction in the cytosol actually decreased slightly.

Krebs Cycle Acids (Table IV) (Fig. 4)

Citrate – The level of citrate rose slightly with blood flow, rose more steeply with the onset of secretion, and even further with continued secretion to 113 and 125% above control levels at HI and HII.

Isocitrate – A small increase at blood flow was followed by a rise of 88% with the onset of acid secretion.

α-Ketoglutarate – The level of this metabolite was only slightly higher with increased perfusion of the mucosa, rose slightly with the onset of secretion, and doubled with continued secretion. At the onset of secretion, the level had increased by 13%.

Succinate – Succinate measured in the perchloric acid extract of the whole tissue increased with the onset of blood flow and reached a level 14% above control with the onset of secretion.

Fumarate – The level of fumarate increases slightly with

TABLE III

Shunt intermediates

The values are the means ± S.E. of n dogs, at least four measurements having been made on each sample in each dog. Blood flow refers to the state of reddening of the mucosa, HI the sample when acid secretion was detected in that area, and HII a sample at steady state secretion. Values are given millimoles kg^{-1}, dry weight, for 6-phosphogluconate and micromoles kg^{-1}, wet weight, for ribulose 5-phosphate.

	Resting	Blood flow	HI	HII
6-Phosphogluconate	0.023 ± 0.003 (n = 11)	0.023 ± 0.003 (n = 4)	0.050 ± 0.004[a] (n = 9)	0.050 ± 0.005[a] (n = 6)
Ribulose 5-phosphate	15.7 ± 1.7 (n = 6)	19.2 ± 1.4 (n = 4)	25.7 ± 4.6[b] (n = 6)	
NADPH/$NADP^+$ (total)	3.17 ± 0.31 (n = 16)	3.28 ± 0.31 (n = 7)	3.59 ± 0.33 (n = 12)	4.78 ± 0.72[b] (n = 17)

[a] $p < 0.001$.
[b] $p < 0.05$.

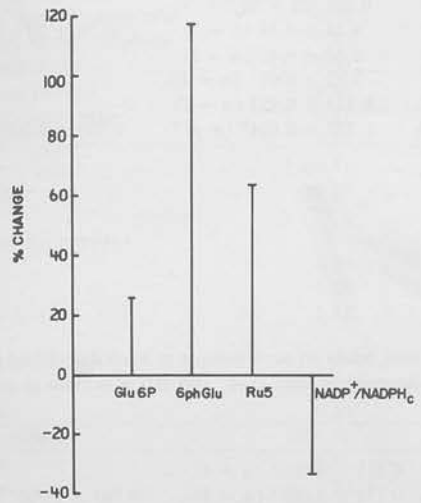

FIG. 3. The percentage of change between rest and secretion (HI) in dog gastric mucosa of the levels of hexose monophosphate shunt associated intermediates as well as the ratio of cytoplasmic $NADP^+$ to NADPH.

increased blood flow and sharply increased with the onset of acid secretion and increased even more with continued secretion. The levels attained were increased by 183% with the onset of secretion (HI).

Malate – Malate increased slightly with the onset of blood flow then rose dramatically with the onset of secretion to 136% above control. The higher malate levels were maintained with continued acid secretion.

Oxaloacetate – The level of calculated oxaloacetate increased by 33% with the onset of secretion.

Other Mitochondrial Metabolites

Glutamate – The level of this amino acid fell with the onset of blood flow, fell slightly more with the onset of secretion, and then rose slightly with continued secretion. The maximum fall was by 23%.

Aspartate – The level of aspartate did not change with the change of blood flow to the mucosa and rose slightly by 7% with the onset of secretion.

NH_3 – This metabolite was measured in tissue extracts since freeze-drying would remove this product. The level of NH_3 increased by 18% with blood flow and this increase was maintained with the onset of acid secretion.

Acetoacetate – The level of acetoacetate increased by 39% with the onset of secretion.

β-OH Butyrate – This keto acid fell slightly with the blood flow sample to 87% of control. With the onset of secretion, the value rose by 42% and then rose further by 84% with continued secretion. It should be noted that the acetoacetate/β-OH butyrate ratio was different from that described for many other tissues. These data are illustrated in Fig. 4 and Table IV).

Lipid-related Metabolites (Table V) (Fig. 5)

Glycerol – The level of this product of triglyceride hydrolysis fell very slightly with blood flow and then rose by 97% with the onset of acid secretion.

CoA – The level of CoA did not change with the onset of blood flow through the mucosal epithelium and then rose by 28% with the onset of secretion. With continued secretion, the value increased further.

Acetyl-CoA – The level of acetyl-CoA rose by 22% with blood flow and then rose further by 34% and continued to rise with continued secretion.

Acetyl-CoA/CoA Ratio – This ratio had a value of 0.36 in the resting mucosa and changed very little (0.37) with the onset of secretion.

Comparison to Liver and Kidney Metabolite Levels

Since this is the first time that the metabolites discussed have been measured in gastric mucosa, and the metabolism of stomach has been relatively unexplored, levels of metabolites found were compared to those of liver. The liver levels were taken from the control values obtained by Greenbaum *et al.* (27).

The level of intermediates of glycolysis was, in general, lower than the corresponding liver levels. The level of phosphoenolpyruvate was especially low, whereas pyruvate and lactate were relatively higher than other intermediates.

Both the hexose monophosphate shunt metabolites, 6-phosphogluconate and ribulose 5-phosphate were lower than control liver values.

The Krebs cycle intermediates in resting mucosa were in general slightly lower than liver. Glutamate and NH_3 were higher and the acetoacetate level was equivalent to that of liver. Aspartate on the other hand was slightly less and β-OH butyrate considerably less than the level found in normal rat liver.

Glycerol, CoA, and acetyl-CoA were all equal or higher than the corresponding liver values (Table VI).

Comparing gastric metabolite levels to those found for kidney (28), the CoA and acetyl-CoA were higher, as was acetoacetate. Glycogen and hexose phosphates were higher in stomach, whereas the rest of the glycolytic intermediates and the Krebs cycle acids in general were lower.

Since stimulation of acid secretion affects mainly mitochondrial metabolites, the level of these approaches the control hepatic and renal values. However, there is no striking anomaly which might suggest a particular feature of parietal cell metabolism.

TABLE IV

Krebs cycle intermediates

The values are the means ± S.E. of n dogs, at least four measurements having been made on each sample in each dog. Blood flow refers to the state of reddening of the mucosa, HI the sample when acid secretion was detected in that area, and HII a sample at steady state secretion. Values are given in millimoles kg^{-1}, dry weight.

	Resting	Blood flow	HI	HII
Citrate	1.06 ± 0.10 (n = 6)	1.28 ± 0.14 (n = 6)	2.26 ± 0.30[a] (n = 9)	2.39 ± 0.33[b] (n = 8)
Isocitrate	0.032 ± 0.011 (n = 3)	0.036 ± 0.01 (n = 3)	0.060 ± 0.01[b] (n = 3)	
α-Ketoglutarate	0.359 ± 0.037 (n = 7)	0.368 ± 0.030 (n = 7)	0.404 ± 0.041 (n = 6)	0.930 ± 0.086[b] (n = 3)
Succinate	2.99 ± 0.29 (n = 5)	3.20 ± 0.24 (n = 5)	3.42 ± 0.48 (n = 5)	
Fumarate	0.075 ± 0.027 (n = 4)	0.108 ± 0.037 (n = 4)	0.212 ± 0.05[b] (n = 4)	0.228 ± 0.054[b] (n = 3)
Malate	0.414 ± 0.030 (n = 11)	0.529 ± 0.069 (n = 11)	0.976 ± 0.139[b] (n = 11)	0.885 ± 0.109[b] (n = 6)
Oxaloacetate[c]	0.018 (7×10^{-5})[c]		0.024 (22×10^{-5})[c]	
Glutamate	12.13 ± 2.04 (n = 7)	9.94 ± 2.68 (n = 7)	9.34 ± 2.38 (n = 7)	10.70 ± 0.79 (n = 3)
Aspartate	2.14 ± 0.16 (n = 6)	2.20 ± 0.11 (n = 7)	2.30 ± 0.45 (n = 7)	
NH_3	1.92 ± 0.06 (n = 10)	2.26 ± 0.08 (n = 8)	2.21 ± 0.07[a] (n = 10)	
Acetoacetate	0.298 ± 0.022 (n = 7)	0.295 ± 0.036 (n = 6)	0.413 ± 0.021 (n = 7)	
β-OH butyrate	0.181 ± 0.013 (n = 7)	0.157 ± 0.027 (n = 7)	0.257 ± 0.024[b] (n = 7)	0.333 ± 0.068[b] (n = 7)

[a] $p < 0.01$.

[b] $p < 0.05$.

[c] Calculated inside parentheses are mitochondrial levels of oxaloacetate.

TABLE V

Lipid related metabolites

The values are the means ± S.E. of n dogs, at least four measurements having been made on each sample in each dog. Blood flow refers to the state of reddening of the mucosa, HI the sample when acid secretion was detected in that area, and HII a sample at steady state secretion. Values are given, when appropriate in millimoles kg^{-1}, dry weight.

	Resting	Blood flow	HI	HII
Glycerol	0.158 ± 0.034 (n = 4)	0.131 ± 0.016 (n = 4)	0.311 ± 0.050[a] (n = 4)	
CoA	0.554 ± 0.065 (n = 8)	0.562 ± 0.048 (n = 4)	0.711 ± 0.086[a] (n = 4)	0.781 ± 0.090[b] (n = 8)
Acetyl-CoA	0.197 ± 0.034 (n = 8)	0.240 ± 0.044 (n = 4)	0.263 ± 0.046 (n = 4)	0.280 ± 0.024[a] (n = 7)

[a] $p < 0.005$.

[b] $p < 0.01$.

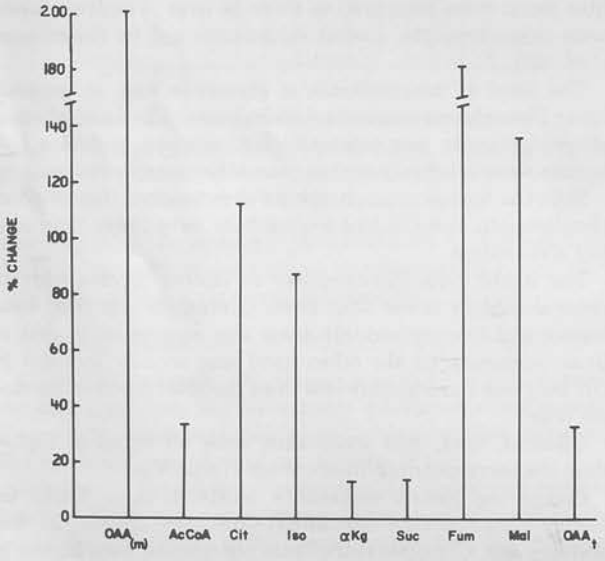

FIG. 4. The percentage of change of the Krebs cycle acids occurring between rest and secretion (HI) in dog gastric mucosa including the calculated change in total and mitochondrial oxaloacetate.

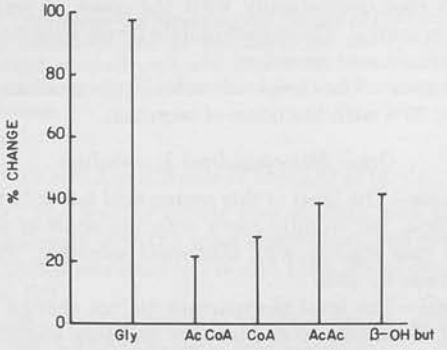

FIG. 5. The percentage of change of certain fatty acid metabolites related intermediates occurring between rest and secretion (HI) in dog gastric mucosa.

TABLE VI

Level of gastric metabolites relative to rat liver and kidney

Values were taken from Refs. 27 and 28. The ratio is gastric level divided by tissue (liver, kidney) level.

	Liver Ratio	Kidney Ratio
Glycolysis		
Glycogen	0.04	7.5
UDP-glucose	0.70	1.13
Glucose	0.35	0.53
Glucose 6-phosphate	0.25	1.3
Fructose 6-phosphate	0.31	1.45
Fructose 1,6-diphosphate	0.57	0.66
Glyceraldehyde 3-phosphate	0.60	
Dihydroxacetone phosphate	0.52	0.6
α-Glycerophosphate	0.33	0.4
3-Phosphoglycerate	0.05	0.16
Phosphoenolpyruvate	0.17	0.3
Pyruvate	1.25	0.9
Lactate	0.81	1.05
Phosphate	0.37	
Lipid-related metabolites		
Glycerol	1.09	
CoA	1.48	1.63
Acetyl-CoA	1.34	2.19
Krebs cycle and others		
Citrate	0.72	0.54
Isocitrate	0.30	
α-Ketoglutarate	0.67	0.65
Succinate	0.81	
Fumarate	0.20	
Malate	0.22	0.18
Oxaloacetate	0.52	
Glutamate	1.07	0.33
Aspartate	0.65	1.1
NH_3	1.07	0.44
Acetoacetate	0.99	1.86
β-Hydroxybutyrate	0.21	0.41
Hexose shunt		
6-Phosphogluconate	0.24	
Ribulose 5-phosphate	0.18	

DISCUSSION

Glycogenolysis – Although a fall in glycogen in amphibian mucosa has been interpreted as due to utilization to support acid secretion (9), phosphorylase activation has not been demonstrated and medium and short chain fatty acids are generally regarded as better substrates than carbohydrates for acid secretion (5).

The decrease observed in the dog mucosa of glycogen and UDP-glucose is consistent with increased utilization and a decrease in glycogenesis from glucose.

Glycolysis – The increased level of glucose, since glucose 6-phosphatase is virtually absent from the stomach[1] is probably due to increased glucose entry. The general trend towards an increase of the glycolytic intermediates may best be interpreted as an increase of flux in this pathway. The mass action ratio of hexokinase indicates that regulation of activity of this enzyme could be effective in regulating glycolytic flux. However, changes in glucose 6-phosphate and the constancy of the ATP/ADP ratio which control enzyme activity (29, 30) do not suggest activation of this enzyme. The coherent rise of the hexose phosphates and fructose 1,6-diphosphate suggests increased glycolytic flux. The fall in phosphorylation potential (13), the increase in NH_3 and in cAMP (31) and the possible rise in cell pH due to HCO_3^- accumulation would tend to activate phosphofructokinase, whereas the increase in citrate would indicate reduction of activity (32). The relatively large increase in the hexose diphosphate indicates that the trend is towards activation of phosphofructokinase (33). Although glyceraldehyde-3-phosphate dehydrogenase may be a regulator of glycolysis (34), in the stomach, the calculated fall in the $NAD^+/NADH$ ratio would reduce enzyme activity. Whereas the rise in phosphoglycerate may reflect the rise in fructose 1,6-diphosphate due to equilibrium operation of glyceraldehyde-3-phosphate dehydrogenase and the glycerate kinase, the rise in phosphoenolpyruvate is more difficult to explain, but the level of this intermediate is quite low relative to liver (27). Although the type of pyruvate kinase present in the stomach is not known, kinases which are regulated are inhibited by ATP and activated by fructose 1,6-diphosphate (35). The rise in both pyruvate and lactate indicates some imbalance between synthesis and utilization. If acetyl-CoA were also being provided from oxidation of fatty acid, a relative decrease could occur in pyruvate dehydrogenase.

The fall in the $NAD^+/NADH$ ratio is reflected in the fall in the pyruvate/lactate ratio and also is atypical of an increase of glycolytic flux. However, a fall in these ratios is seen in tissues with a high rate of fatty acid oxidation.

The rise in phosphate is not due to any loss of measured phosphate, but may be due to hydrolysis of phospholipid or due to increased uptake from the blood.

Hexose Monophosphate Shunt – It has been suggested that in the rat and frog (10) that glucose oxidation forms a major source of energy for the process of acid secretion. The free cytoplasmic $NADP^+/NADPH$ ratio (Table VII) fell when calculated using the equilibria catalyzed by either malic enzyme, isocitrate dehydrogenase, or 6-phosphogluconate dehydrogenase. The mitochondrial ratio apparently increased, perhaps as a result of the fall in intramitochondrial pH due to increased ATP synthesis (36). The increase in the intermediates of this pathway is somewhat surprising in view of the fall in $NADP^+/NADPH$ ratio, indicating that the latter is not the sole regulator of shunt activity.

Krebs Cycle Intermediates – Pyruvate dehydrogenase has been suggested as a major regulatory site in frog gastric mucosa (11). The enzyme is regulated by a phosphorylation-dephosphorylation pathway (37) and levels of acetyl-CoA and NADH (38). The different direction of change of these systems makes it difficult to assess the direction of change of activity

[1] G. Shah and G. Sachs, unpublished observations.

TABLE VII

Distribution of pyridine nucleotide ratio

The value for the cytoplasmic ratio of NAD^+ to NADH was obtained from the lactate pyruvate equilibrium at pH 7.0, and of $NADP^+$ to NADPH for the 6-phosphogluconate dehydrogenase equilibrium. The mitochondrial ratios were calculated using the NAD^+ and $NADP^+$-dependent glutamic dehydrogenase equilibrium. All calculations refer to pH 7.0, ionic strength 0.25. The ratio of the two nucleotide pairs in the cytoplasm approximates 10^5.

Component	Free $NAD^+/NADH$		Free $NADP^+/NADPH$	
	Rest	Secretion	Rest	Secretion
Cytoplasm	1.3×10^3	0.94×10^3[a]	0.016	0.012
Mitochondria	2.94	5.0[a]	4.57	7.75

[a] $p < 0.05$.

of the enzyme. The increase in acetyl-CoA levels indicate increased fatty acid oxidation as well as perhaps increased pyruvate breakdown.

There is a generalized increase in the Krebs cycle acids, which when taken together with the 16-fold increase in O_2 consumption (48) indicates a major increase of activity of this pathway. Although isocitrate dehydrogenase is activated in insect muscle (39) which shows similar oxidation-reduction changes as does the stomach (7) with a work load and citrate synthase is activated in cardiac muscle (40), the changes in the intermediates measured in the stomach indicate activation elsewhere. The major measured changes are in the levels of fumarate and malate, perhaps indications of a rise in succinic dehydrogenase relative to the other enzymes.

Fatty Acid Metabolism—Gastric mucosa contains a soluble triglyceride lipase, but so far no *in vitro* activation of this enzyme has been detected.[2] The rise in glycerol is consistent with increased lipolysis. Equally the concomitant rise in acetyl-CoA and CoA may indicate increased fatty acid oxidation although the ratio would be expected to increase with increased oxidation. Finally, preliminary measurements of β-hydroxyacetyl-CoA dehydrogenase show a 33% rise in activity also indicative of increased fatty acid oxidation.[3]

Oxidation-Reduction Ratios—Table VII presents the calculated changes in levels of oxidized to reduced pyridine nucleotides in the cytoplasm and mitochondria of the parietal cell. The data are similar to those found in liver (27) and only the acetoacetate/β-hydroxybutyrate ratio is anomalous. This is most likely due to the low levels of β-hydroxybutyrate dehydrogenase in the stomach.[3]

Anion Distribution—Although there are various ways of calculating these (21, 27, 41), malate concentration has been shown to be equal between mitochondrion and cytoplasm (42). Assuming no gradient and equilibrium operation of malate dehydrogenase, the cytoplasmic oxaloacetate levels can be calculated. Equivalently, the glutamic dehydrogenase reaction can be used to calculate mitochondrial oxaloacetate. Using a value of 34% for the mitochondrial volume (43), the cytoplasmic oxaloacetate rose from 18 μmol kg^{-1} to 24 μmol kg^{-1} and the mitochondrial level from 70 nmol kg^{-1} to 217 nmol kg^{-1}. From these data, as for liver with the same assumption further calculation of anion distributions results in calculated values exceeding measured values (27).

From the above, it is clear that there is a generalized increase in metabolite levels with onset of acid secretion. In particular, mitochondrial activity would appear to be the major site of activation. This is in agreement with previous suggestions (44) and does not exclude activation of fatty acid oxidation (5). However, previous studies have involved addition of substrates to amphibian mucosa and direct measurements were not attempted. The data in this paper and the previous in the series (13) do not discriminate between an ATP or oxidation-reduction mechanism for acid secretion. Indeed, these data combined with those obtained from spectroscopic observation of amphibian tissue may be interpreted as evidence for a combined ATPase and oxidation-reduction mechanism (45, 46).

The rate of acid secretion (300 μmol cm^{-2}, equivalent to 100 mg, dry weight) and with an H^+/ATP ratio of unity indicates that the content of ATP would turn over in 12 s. Equivalently, an oxidation-reduction substrate would also turn over very rapidly. However, the low mitochondrial NAD^+/NADH ratio argues against reverse electron flow being involved (47).

The pattern of changes observed is not equivalent to liver under various conditions nor to cardiac muscle (27, 49). Indeed, the changes indicate that the gastric parietal cell may well simultaneously increase glycolysis and a fatty acid oxidation as a result of histamine stimulation. Phosphofructokinase would appear to be the major control point in glycolysis, and lipase in the fatty acid pathway. The oxidation-reduction changes observed in mitochondria (7, 46) associated with the mobilization of substrate suggested by the present data also may indicate regulation of substrate entry into the mitochondrial pool.

[2] H. M. Sarau, J. J. Foley, G. Moonsammy, and G. Sachs, unpublished observations.

[3] H. M. Sarau, unpublished observations.

REFERENCES

1. Opie, L. H., Mansford, K. R. L., and Owen, P. (1971) *Biochem. J.* **124**, 475–490
2. Krebs, H. A., and Veech, R. L. (1969) *Energy Level and Metabolic Control in Mitochondria*. (Papa, S. *et al.*, eds) pp. 329–382, Adriatica del' Università, Bari
3. Chance, B., and Williams, G. R. (1955) *J. Biol. Chem.* **217**, 409–427
4. Rehm, W. S. (1972) *Metabolic Pathways* (Hokin, L. E., ed) pp. 187–241, Academic Press, New York
5. Hersey, S. J. (1974) *Biochim. Biophys. Acta* **344**, 157–203
6. Durbin, R. P., Michelangeli, F., and Nickel, A. (1974) *Biochim. Biophys. Acta* **367**, 177–189
7. Hersey, S. J. (1971) *Philos. Trans. R. Soc. Lond. Ser. A Metab. Phys. Sci.* **262**, 261–275
8. Kidder, G. W., Curran, P. F., and Rehm, W. S. (1966) *Am. J. Physiol.* **211**, 153–159
9. Alonso, P., Nigon, K., Door, I., and Harris, J. B. (1967) *Am. J. Physiol.* **212**, 992–1000
10. Sernka, T. J., and Harris, J. B. (1972) *Am. J. Physiol.* **222**, 25–32
11. Harris, J. B., Alonso, D., Park, O. H., Cornfield, D., and Chacin, J. (1975) *Am. J. Physiol.* **228**, 964–971
12. Chacin, J., Park, O. H., Harris, J. B., and Alonso, D. (1976) *Am. J. Physiol.* **231**, 209–215
13. Sarau, H. M., Foley, J., Moonsammy, G., Wiebelhaus, V. D., and Sachs, G. (1975) *J. Biol. Chem.* **250**, 8321–8329
14. Lowry, O. H., and Passonneau, J. V. (1973) *Flexible Methods of Enzymatic Analysis*, Academic Press, New York
15. Roehrig, K. L., and Allred, J. B. (1974) *Anal. Biochem.* **58**, 414–421
16. Lowry, O. H., Passonneau, J. V., Hasselberger, F. X., and Schulz, D. W. (1964) *J. Biol. Chem.* **239**, 18–30
17. Lowry, O. H., Carter, J., Ward, J. B., and Glaser, L. (1971) *J. Biol. Chem.* **246**, 6511–6521
18. Lowenstein, J. M. (1969) *Methods Enzymol.* **13**, 52–53; 508–509
19. Matschinsky, F. M., Kantmann, F. C., and Ellerman, J. E. (1968) *Diabetes* **17**, 475–480
20. Goldberg, N. D., Passonneau, J. V., and Lowry, O. H. (1966) *J. Biol. Chem.* **241**, 3997–4003
21. Lowenstein, J. M. (1969) *Methods Enzymol.* **13**, 473–476
22. Chernick, S. S. (1969) *Methods Enzymol.* **14**, 627–630
23. Lowry, O. H., Passonneau, J. V., Schulz, D. W., and Rock, M. K. (1961) *J. Biol. Chem.* **236**, 2746–2755
24. Kato, T., Berger, J. J., Carter, J. A., and Lowry, O. H. (1973) *Anal. Biochem.* **53**, 86–97
25. Folbergrova, J., Passonneau, J. V., Lowry, O. H., and Schulz, D. W. (1969) *J. Neurochem.* **16**, 191–203
26. Kauffman, F. C., Brown, J. G., Passonneau, J. V., and Lowry, O. H. (1969) *J. Biol. Chem.* **244**, 3647–3653
27. Greenbaum, A. L., Gumaa, K. A., and McLean, P. (1971) *Arch. Biochem. Biophys.* **143**, 617–663
28. Williamson, D. H., and Brosman, J. T. (1974) in *Methods of Enzymatic Analysis* (Bergmeyer, H. U., ed) pp. 2266–2301, Academic Press, New York
29. Crane, R. K., and Sols, A. (1954) *J. Biol. Chem.* **210**, 597–606
30. Knull, H. R., Taylor, W. F., and Wells, W. W. (1975) *J. Biol. Chem.* **248**, 5414–5418
31. Bieck, P. R., Oates, A., Robison, G. A., and Adkins, R. B. (1973) *Am. J. Physiol.* **224**, 158–164
32. Bloxham, D. P., and Lardy, H. A. (1973) in *The Enzymes*

(Boyer, P. D., ed) Vol. 8, pp. 239–278, Academic Press, New York
33. Veech, R. L., Raijman, L., Dalziel, K., and Krebs, H. A. (1969) *Biochem. J.* **115**, 837–842
34. Lowry, O. H., and Passonneau, J. V. (1964) *J. Biol. Chem.* **239**, 31–42
35. Carbonell, J., Feliu, J. E., Marco, R., and Sols, A. (1973) *Eur. J. Biochem.* **37**, 148–156
36. Mitchell, P. (1966) *Biol. Rev. Camb. Philos. Soc.* **41**, 445–502
37. Linn, T. C., Pettit, F. H., and Reed, L. J. (1969) *Proc. Natl. Acad. Sci. U. S. A.* **62**, 234–241
38. Bremer, J. (1969) *Eur. J. Biochem.* **8**, 535–540
39. Hansford, R. G. (1972) *Biochem. J.* **127**, 271–283
40. Randle, P. J., England, P. J., and Denton, R. M. (1970) *Biochem. J.* **117**, 677–695
41. Williamson, J. R. (1969) in *Energy Level and Metabolic Control in Mitochondria* (Papa, S., ed) pp. 385–399, Adriatica del' Università, Bari
42. Elbers, R., Heldt, H. W., Schmucker, P., Soboll, S., and Wiese, M. (1974) *Hoppe-Zeyler Z. Physiol. Chem.* **355**, 378–393
43. Helander, H. F., and Hirschowitz, B. I. (1972) *Gastroenterology* **63**, 951–961
44. Chacín, J., Rincón, R., Inciarte, D., and Cañizales, A. (1976) *Biophys. J.* **16**, 129a
45. Rabon, E., Rehm, W. S., Sarau, H. M., and Sachs, G. (1977) *J. Membr. Biol.* **35**, 189–204
46. Sachs, G., Saccomani, G., Rabon, E., and Sarau, H. M. (1975) *Ann. N. Y. Acad. Sci.* **264**, 456–475
47. Rehm, W. S. (1972) in *Metabolic Pathways* (Hokin, L. E., ed) Vol. 6, pp. 187–241, Academic Press, New York
48. Moody, F. G. (1968) *Am. J. Physiol.* **215**, 127–131
49. Williamson, J. R., Illingworth, J. A., Ford, C. L., and Koboyaski, K. (1976) in *Recent Advances in Cardiac Structure and Metabolism*, University Park Press, Baltimore

J. Membrane Biol. 35, 189–204 (1977)

Redox Involvement in Acid Secretion in the Amphibian Gastric Mucosa

Edd C. Rabon, H.M. Sarau, W.S. Rehm, and G. Sachs

Laboratory of Membrane Biology, University of Alabama in Birmingham, Birmingham, Alabama 35294 and SKF Laboratories, Philadelphia, Pennsylvania

Received 17 September 1976; revised 18 October 1976

Summary. Gastric fundic metabolism was studied by spectroscopic observation in frog mucosa during transitions of secretory status in vitro and by direct measurement of pyridine nucleotides and associated metabolites in biopsies of dog fundic mucosa also during secretory transition. In frog, inhibition of spontaneous secretion by an H_2 antagonist resulted in oxidation of the redox components from flavin adenine dinucleotide (FAD) to cytochrome a_3. Addition of histamine resulted in reduction of these components with onset of secretion by about 50%. In contrast, the effect of apparently, burimamide and subsequently histamine on the ratio of nicotinamide adenine dinucleotide to nicotinamide adenine dinucleotide, reduced (NAD^+/NADH) was relatively slight. Further, the presence of burimamide substantially reduces the effect of amytal on the pyridine nucleotide spectrum and abolishes the effect of amytal on FAD and the cytochromes. Measurements of lactate, pyruvate, α-ketoglutarate, NH_3 and glutamate in the dog showed that whereas the calculated NAD^+/NADH ratio in the cytoplasm declined with onset of secretion, the calculated mitochondrial ratio rose. No change was noted in the nicotinamide adenine dinucleotide phosphate/nicotinamide adenine dinucleotide phosphate, reduced ($NADP^+$/NADPH) ratio. It is concluded that (1) H_2 antagonists act by blocking substrate flow into the mitochondrial respiratory chain, (2) conversely, histamine stimulation acts at the level of substrate mobilization, and (3) there may be a cross-over in the mitochondrial chain between NAD^+ and FAD.

The gastric mucosa is capable of producing a H^+ gradient of one millionfold magnitude as measured by the blood to lumen pH difference. The nature of the primary energy source for this acid secretion, despite much experimentation, remains controversial. Historically, this controversy has settled on two mechanisms [3, 9, 14, 16, 17]. The first mechanism suggests a redox carrier which accepts reducing equivalents from mitochondria presumably supplied by a generalized substrate mobilization and shuttles these to the parietal cell membrane followed by oxidation and secretion of H^+ into the gastric lumen. Presently, it is the absence of information concerning this carrier and the redox reaction in the membrane and of the electron carrier from membrane to mitochondria which limits the development of the 'redox hypothesis'. The second

mechanism proposes that a tissue-specific ATPase provides the pump necessary to move protons across the parietal cell membrane into the gastric lumen.

The strongest argument favoring a direct role for ATP in acid secretion is provided by work with subcellular fractions of the fundic mucosa [5, 15].

Resolution of the problem of the specific participation of the redox and ATPase systems in secretion in the intact mucosa can be approached by two methods which allow measurements of metabolites during secretion. In the first, Lowry enzyme cycling methods may be used to fluorimetrically measure metabolite levels of the parietal cell areas both preceeding and after the establishment of steady-state acid secretion [13, 16]. This technique allows measurement of many metabolites but not FAD or the cytochromes. In the second, the split-beam spectrophotometer with its ability to accommodate samples with large light-scattering properties can be used to monitor cytochrome and pyridine nucleotide levels during changes in the secretory rate of the intact gastric mucosa of frogs [8, 10, 16].

It is the purpose of this paper to compare results with the split-beam spectrophotometer and the cycling methods to characterize the complex redox changes which result from the transition between burimamide-inhibited or resting and histamine-stimulated secretion. This characterization yields information in two ways. First, it allows a comparison to be made between secretion-induced steady-state changes and those of classical mitochondrial activity states. This in turn could indicate the limitation of a specific component vital to the secretory process. Secondly, the existence of a cross-over point induced by the inhibition or stimulation of secretion would indicate the specific locus of interaction of that process with the respiratory system. This identification may be a necessary initial step in the demonstration that the observed changes in mitochondrial electron transport activity induced by the inhibition or stimulation of acid secretion result from the specific involvement of a redox reaction with the secretory mechanism.

Materials and Methods

Spectrophotometric Studies

Bullfrogs (*Rana catesbeiana*) were obtained from the Jacques Wiel Company. Prior to use they were kept in tanks supplied with running tap water and fed daily with crickets. Before each experiment the frogs were decapitated, pithed and the stomachs perfused

with three 20-ml injections of nutrient solution into the dorsal ascending aorta to remove hemoglobin. The stomach was then removed and placed in an aerated nutrient solution where the mucosa was removed by blunt dissection. This mucosa was then stretched on a cork ring and placed in a double segment Plexiglas chamber designed to fit into the Aminco DW-2 spectrophotometer allowing for a control and experimental side. To hold the two parts of the stomach motionless within the Plexiglas chamber, the tissue was pressed secretory surface down against a stainless steel mesh. Inside the chamber, the tissue was bathed with solutions from a four-chambered reservoir. The two serosal reservoirs contained 15 ml of a solution containing (mM): 91 Na^+, 5 K^+, 1.5 Mg^{++}, 1.0 Ca^{++}, 20 HCO_3^-, 1.0 $H_2PO_4^-$, 5.0 glucose and 80 Cl^- at pH 7.4. The mucosal reservoirs held 10 ml of a solution containing (mM): 70 Na^+, 5.0 K^+, 1.5 Mg^{++}, 1.0 Ca^{++} and 80 Cl^-, initially at pH 5.5.

Oxygen tension was maintained by bubbling both mucosal and serosal reservoirs with a mixture of 95–5% O_2/CO_2 while utilizing a 250-ml air trap to avoid mixing solutions through the mucosal or serosal tubes. Uniform flow rate through the optical chambers was maintained by a peristaltic pump connected between the reservoirs and the optical chamber.

For the secreting mucosa, pH was maintained at 4.7 by a Radiometer pH-stat assembly consisting of a PHM 64 Research pH meter, a TTT 60 Titrator, REC 61 Servorecorder equipped with an REA 160 Titrigraph Module and an ABU 12 Autoburette.

Burimamide was supplied by Smith Kline and French, Amytal by Eli Lilly and the remaining reagents by Sigma. Solutions were stored at 4 °C and prepared fresh weekly.

Absorption measurements were made in the Aminco DW-2 Splitbeam Spectrophotometer. The absorption ranges, usually either 0.1 or 0.2 O.D. full scale were calibrated before each experiment. The wavelength accuracy was calibrated by comparison of the instrument settings to the 550 nm absorption peak of reduced cytochrome *c*. The spectral bandwidth was set at 15 nm for each experiment.

The concentrations of the absorbing species were calculated according to the Beer Lambert law: $A = \varepsilon \times b \times c$.

A = absorbance as measured in optical density units ($\log I/I_0$)

b = optical path length (assumed to be the thickness of the tissue, 0.5 mm)

ε = Molar absorptivity ($cm^{-1} \times mM^{-1}$)

c = concentration (mM).

ε values were those calculated by Chance and Williams [2].

Component	Wavelength	E
NADH	340–374 nm	6
FADH I	465–510 nm	11
Cytochrome b_a	564–575 nm	20
Cytochrome $c(c_1)$	540–550 nm	19
Cytochrome a_a	605–630 nm	16
Cytochrome a_3	445–455 nm	60

Absorption changes were monitored continuously after each experimental procedure, but the changes at 30 min were used for the calculations, at which time steady state had been invariably established.

Measurements of Metabolites by Cycling Methods

The experimental details involved in obtaining testing and secreting biopsy samples from anesthetized dogs have been detailed in a previous publication [18]. Briefly, the fasted dog was anesthetized, the abdomen opened, the stomach opened, and several biopsies taken. These were denoted as resting samples by the absence of measurable acid secretion into a Lashley cup. Histamine was then infused and samples taken at reddening of the mucosa and then with onset of acid secretion. Secretion was quantitated by titration of the fluid in the Lashley cup, and ranged from 100–300 μmoles $H^+ cm^{-2} hr^{-1}$.

The biopsy was immediately frozen in liquid N_2 and sectioned at -20 °C. Parietal cell regions were defined by staining for succinic dehydrogenase in every fourth section; the other sections were lyophilized and the metabolites measured under oil wells. The methods used for measurement of the pyridine nucleotides and lactate and pyruvate have been published previously [18].

The principle of the fluorimetric cycling procedure is to convert a metabolite quantitatively to oxidized or reduced pyridine nucleotide, destroying the unwanted form with acid or alkali. The remaining pyridine nucleotide is then measured by a cycling technique, for example, using alcohol, oxaloacetate, alcohol dehydrogenase and malic dehydrogenase. One of the products of the cycling reaction (e.g. malate in the example) is now measured by coupling to the formation of reduced pyridine nucleotide and direct fluorimetric measurement of the latter. In this way levels of about $10^{-12}-10^{-13}$ moles of metabolite are converted to 10^{-9} moles of pyridine nucleotide for the final step [13].

To calculate the ratio of free oxidized and reduced pyridine nucleotide in cytosol and in mitochondria, pairs of metabolites are used on the assumption that firstly, the enzyme interacting with the metabolites is present only in the compartment of interest, and secondly, that it has sufficient activity to maintain reactant equilibrium. For cytoplasmic calculations, the reactions catalyzed by lactic dehydrogenase or α-glycerolphosphate dehydrogenase may be used and give similar data in the stomach. For the mitochondrial compartment the reaction catalyzed by β-hydroxybutyrate dehydrogenase or glutamic dehydrogenase may be used. Measured levels of β-hydroxybutyrate dehydrogenase were sufficiently low so that one could not be sure that adequate quantities of this enzyme were present, hence the levels of α-ketoglutarate, NH_3 and glutamate were used for calculation of the ratios of NAD^+ to NADH in mitochondria. These methods therefore have the advantage of being able to discriminate between changes in NAD^+ and $NADP^+$, as well as discriminate between changes in different cellular compartments and cell types (e.g. mucus as opposed to parietal cells by serial sectioning). Hence, they are complementary to the spectroscopic techniques but being steady-state measurements require a much larger secretory transition than is obtained in the frog, hence necessitating the use of in vivo dog tissue.

α-Ketoglutarate. The sample was treated under oil in specially constructed oil wells with 1 μliter 0.05 N NaOH for 20 min at 80° C. After cooling to room temperature, 2 μliters of a solution containing 200 mM imidazole acetate buffer, pH 6.6, 20 μg/ml glutamate dehydrogenase, 2 μM NADH, 50 mM NH_4OAc, 200 mMADP and 0.05% BSA were added and incubation continued for 30 min. Residual NADH was then destroyed by addition of 1 μliter 0.5 N HCl and incubating for 30 min. One μliter of this reaction mixture was then added to 100 μliters of a solution containing 294 μg/ml alcohol dehydrogenase and 45 μg/ml malic dehydrogenase, with in addition 100 mM Tris HCl buffer, pH 8.0, 300 mM ethanol, 2 mM mercaptoethanol, 0.02% BSA and 2 mM oxaloacetate. After cycling for 60 min at 28 °C, the reaction was stopped by heating to 100 °C for 10 min and 7 μliters were added to 1 ml of indicator reagent.

The latter contained 50 mM 2-amino-2-ethyl propanol buffer, pH 9.9, 0.02 mM NAD^+, 10 mM glutamate, 5 μg/ml malic dehydrogenase, 2 μg/ml glutamate-oxaloacetate transaminase. After 10 min at 22° C, the NADH produced from the oxidation of the malate produced by cycling was measured fluorimetrically [12].

Glutamate. The lyophilized sample was treated with, under oil, 1 μliter of 0.02 N HCl for 20 min at 80 °C to destroy any NADH present. After cooling to room temperature, 2 μliters of a reagent containing 50 mM Tris-acetate, pH 8.4, 50 μg/ml of glutamic dehydrogenase, 100 μM NAD^+, 100 μM ADP and 0.02% BSA was added and the reaction allowed to proceed for 30 min at room temperature. To this 1 μliter of 0.25 M NaOH was added to destroy excess NAD^+ and the mixture heated at 80° C for 20 min. One μliter of this mixture was then added to 100 μliters of cycling reagent as above but containing 76 μg/ml of alcohol dehydrogenase and 11 μg/ml of malic dehydrogenase. Cycling was carried out as above and the indicator step was also the same [12].

NH_3. Since lyophilization would remove NH_3, this metabolite was measured in perchloric acid extracts of the frozen biopsies. The frozen sample was pulverized at −20 °C and 100 μliters of 0.1 N HCl in 99% methanol added. The sample was dispersed and 1 ml of 0.3 M perchloric acid with 1 mM EDTA added in ice. The mixture was centrifuged and the supernatant neutralized by 200 μliters of 1.6 N KOH, 0.4 M imidazole. After a second centrifugation the supernatant was stored at −80 °C [4].

For NH_3 assay 1 ml of a reagent containing 40 mM Tris-Cl, pH 8.4, 5 mM α-ketoglutarate, 0.01% BSA, 0.1 mM ADP, 200 μg/ml glutamic dehydrogenase in glycerol and 27.5 μM NADH was added to a quartz tube and the initial fluorescence measured. Then 50 μliters of the above extract were added and the reading taken after 10 min. The difference was used for NH_3 calculations.

Results

Burimamide Inhibition of Spontaneously Secreting Tissue

Since both the secretory rate and the redox changes produced in the transition from spontaneously secreting to secretagogue-stimulated steady states are very small, the spontaneous secretory rate must initially be reduced to low levels so that a stimulation in secretion will produce a measurable redox change. Burimamide, an H-2 blocker acting at the level of stimulus was added for this purpose [1].

The addition of 3 mM burimamide to the nutrient side of spontaneously secreting tissue reduced secretion from 2.5 μequiv/cm^2/hr to 0 ($n=11$) in a period of approximately 15 min. Thirty minutes after the addition of burimamide during a period of complete inhibition of secretion, a tracing was made between 320 and 640 nm of the absorption changes produced. It should be noted that burimamide had no effect on the absorption of spontaneously resting tissue ($n=5$).

The absorption profile shown in Fig. 1 indicates oxidative shifts in the absorption regions identifying FAD, cytochrome *b*, $c(c_1)$, *a* and a_3. The cytochrome $c(c_1)$ component appeared as a rounded peak with an absorption maximum at 555 nm instead of 550 nm. Cytochrome *b* absorbance was represented by a slight shoulder on the longer wavelength side of the same peak. There appeared to be oxidative changes involving NADH at 340–375 nm. However, since the changes were in general within the noise variation in this area the measurements are omitted.

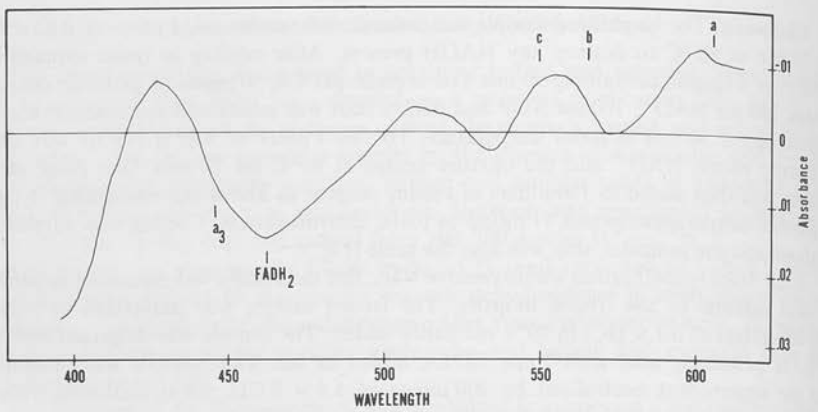

Fig. 1. Absorption spectrum induced by burimamide inhibition of spontaneously secreting frog mucosa: Steady-state absorption changes recorded 30 min after the addition of 3 mM burimamide to the nutrient side of spontaneously secreting frog mucosa. The baseline was drawn with both sides of the mucosa spontaneously secreting. Note that oxidation is upward

The reference wavelengths generally used in mitochondrial studies are a reasonable fit for the baseline drawn through a 575 nm isosbestic point [2]. Using the extinction coefficients measured by Chance, the absorbance changes from five experiments have been converted to concentration changes and recorded in Table 1, row 1. Since uncertainty is introduced into the calculation with the measurement of the pathlength due to light scattering within the tissue and the resolution of unique cytochromes at the measured reference and absorption pairs, these concentrations are only estimates of the true tissue concentration (cf. actual measurements in the dog).

The average of the concentration changes of reduced component relative to cytochrome *a*, shown in Table 1 is: cytochrome *b*, 1.2; cytochrome $c(c_1)$, 1.2; cytochrome *a*, 1.0; cytochrome a_3, 0.7. The variation from unity of this average change found in cytochromes *b* and $c(c_1)$ relative to cytochrome *a* is not experimentally significant due to the large variation between experiments. The ratio of the FAD change relative to cytochrome *a* is 4.3:1. The average values for the oxidative changes induced by the burimamide inhibition of secretion is: FAD -0.017 mM, cytochrome *b* -0.005 mM, cytochrome $c(c_1)-0.005$ mM, cytochrome *a* -0.004 mM, and cytochrome $a_3-0.003$ mM. These concentration changes represent approximately 15% of the total tissue concentration of FAD, cytochromes *b*, $c(c_1)$ and *a* as estimated below. Cytochrome a_3 was slightly

Table 1. Calculated steady-state changes produced by treatment of gastric mucosa (the values given are in mmoles/kg wet weight)

Condition	H^+ (μEquiv cm^{-2} hr^{-1})	Pyridine nucleotide	FAD	cyto *b*	cyto $c(c_1)$	cyto *a*	cyto a_3
Spontaneous to burimamide		–	-0.017 ± 0.005 ($n=5$)	-0.005 ± 0.001 ($n=5$)	-0.005 ± 0.001 ($n=5$)	-0.004 ± 0.001 ($n=5$)	-0.003 ± 0.001 ($n=5$)
Ratio			4.3	1.2	1.2	1.0	0.7
% Total	−2.5	–	15	20	15	14.2	8.8
Burimamide to histamine+ burimamide	+3.5	0.052 ± 0.004 ($n=4$)	0.055 ± 0.018 ($n=5$)	$0.012 + 0.004$ ($n=5$)	0.018 ± 0.005 ($n=5$)	0.013 ± 0.005 ($n=5$)	0.012 ± 0.004 ($n=5$)
Ratio		0.4	4.3	1.0	1.4	1.0	1.0
% Total		3.6	49	54	55	46	42
Burimamide to burimamide+N_2	0	0.141 ± 0.033 ($n=3$)	0.113 ± 0.074 ($n=3$)	0.021 ± 0.002 ($n=3$)	0.029 ± 0.003 ($n=3$)	0.025 ± 0.004 ($n=3$)	0.029 ± 0.004 ($n=3$)
Ratio		5.6	4.5	0.8	1.2	1.0	1.2
% Total		100	100	100	100	100	100
Amytal to N_2+amytal	0	0.122 ± 0.020 ($n=3$)	0.112 ± 0.042 ($n=3$)	0.025 ± 0.011 ($n=3$)	0.034 ± 0.013 ($n=3$)	0.031 ± 0.010 ($n=3$)	0.030 ± 0.007 ($n=3$)
Ratio		4.0	3.8	0.8	1.1	1.0	1.0
% Total		100	100	100	100	100	100

– indicates oxidation.
Ratio indicates ratio of component change to cytochrome *a*.
n is number of experiments ± SEM.

less oxidized with a change accounting for 9% of its total tissue concentration.

From these observations, inhibition of acid secretion at the level of the stimulus apparently interrupts flow of reducing equivalents into the mitochondrial respiratory chain. This effect is also dependent on the presence of secretion since resting tissue does not show any redox changes following burimamide. The relative changes of the redox components also suggest, with the exception of pyridine nucleotides, relatively uniform changes and certainly the absence of a cross-over below FAD.

Histamine Stimulation of Burimamide-Inhibited Tissue

In order to record the redox shifts produced by the transition from a nonsecreting to a secreting steady state, 3 mM histamine was added to the nutrient side of burimamide-inhibited tissue. The addition stimulated secretion from 0 to 3.5 μequiv/cm^2/hr ($n=11$) in approximately 15 min. Thirty minutes after the addition of histamine, during maximal secretion, the absorbance changes were recorded from 300 to 640 nm. The tracing recorded in Fig. 2 indicates a general reduction of all respiratory chain components with the possible exception of pyridine nucleotide.

Cytochrome *a* was a peak measured at 605–630 nm. Cytochrome *b* appears as a shoulder at 564 nm on the absorption peak due to cytochrome *c*. Maximal absorption of cytochrome *c* was recorded at 555 nm. The reason for this shift has not been determined, though contributing factors may be either absorption of c_1 at 554 nm or traces of deoxyhemoglobin not removed by perfusion. The FAD peak occurs at 465 nm. NADH absorption when present appears as a broad peak from 340 to 355 nm.

The concentration changes responsible for these absorbances in five experiments were calculated and recorded in Table 1, row 2. Though there is apparent variation in the concentration of like components between experiments, the average relative change of five experiments for cytochromes *b*, $c(c_1)$, *a* and a_3 is consistently unity. The relative concentration change of FAD is higher, actually about 4.

When compared to the total concentration of tissue components, the histamine-induced reduction accounts for almost 50% of the total tissue concentration of FAD, cytochromes *b*, $c(c_1)$ and *a*. Cytochrome a_3 occupies a slightly more oxidized position with reduction accounting for 42% of its total tissue concentration.

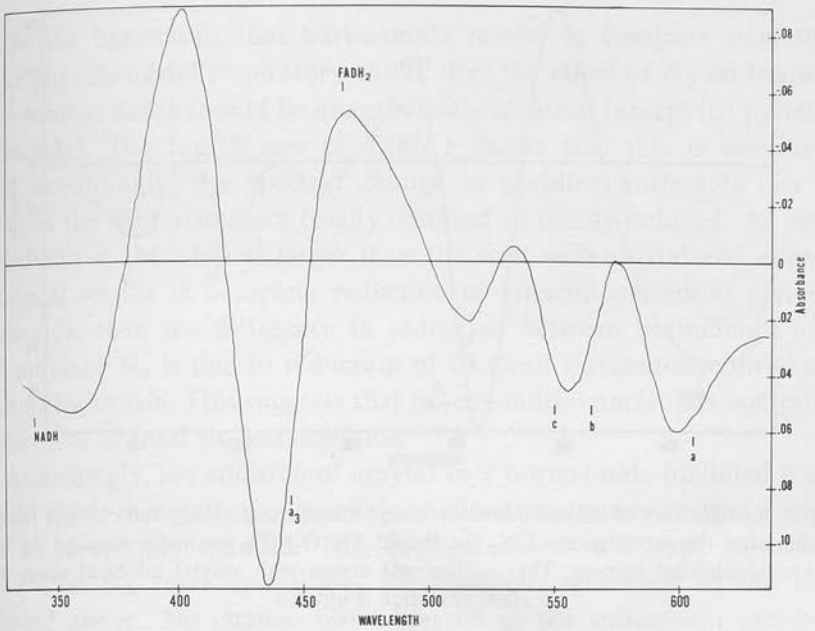

Fig. 2. Absorption spectrum induced by histamine stimulation of burimamide-inhibited frog mucosa: Steady-state absorption changes observed 30 min after the addition of 3 mM histamine to the nutrient side of frog mucosa which had been previously inhibited by the addition of 3 mM burimamide. The baseline was drawn with both sides of the mucosa inhibited with burimamide. Note that oxidation is upward

NADH was more difficult to measure due to a tendency for the 374 nm reference wavelength to shift in some experiments. Unless the 374 nm wavelength was stable, the measurements were omitted in the concentrations recorded in Table 1 (one of five experiments). Measurements indicate that NADH is much less reduced than the other tissue components. Its relative reductive change compared to cytochrome *a* is 0.4. This corresponds to only 3.6% of the total tissue NAD concentration.

These data are similar to those previously published by Hersey and his collaborators [8] in that generalized changes were observed either with stimulation or inhibition of secretion. These are in contrast, however, to reports suggesting only specific changes in cytochrome *c* [11]. A difference between the techniques is the use of CO in the latter experiments. We used 10% CO and in our hands the presence of this gas in the gassing solution did not prevent the general changes observed, hence this gas was not used routinely.

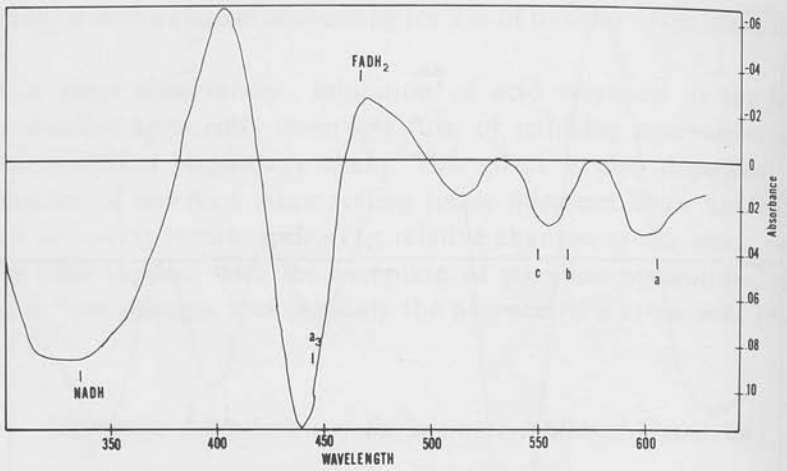

Fig. 3. N_2 reduction of amytal-inhibited tissue: Steady-state absorption changes recorded 20 min after the substitution of N_2 for the 95–5% O_2/CO_2 normally supplied the tissue in amytal-inhibited mucosa. The baseline was drawn with amytal inhibited tissue. Note that oxidation is upward

Interactions of Anoxia and Amytal

If the interpretation of the reciprocal effects of burimamide and histamine are correct, namely that it is substrate mobilization that is affected by stimulus and antagonist, then the presence of antagonist should significantly affect the redox response to amytal.

Fig. 3 shows the effect of N_2 on amytal-inhibited tissue. Since amytal, by blocking electron flow between NAD^+ and FAD results in complete oxidation of all the redox components below NAD^+ and anoxia results in complete reduction, this experiment allows calculation of total tissue concentrations of FAD and the cytochromes.

These data are given in the third row of Table 1. As can be seen there is a characteristic 1:1 shift of the cytochromes relative to cytochrome *a* and a fourfold relative reduction of FAD. Although one would anticipate that mitochondrial pyridine nucleotide is fully reduced, anoxia resulted in a considerable reduction of pyridine nucleotide, although slightly less than anoxic effect on burimamide-inhibited tissue.

This may be interpreted as being due to reduction of extramitochondrial nucleotide. This would put the ratio of extramitochondrial pyridine nucleotide to cytochromes at about 4 and account for the majority of pyridine nucleotide in the tissue.

On the hypothesis that burimamide results in complete oxidation of the mitochondrial respiratory chain, then the effect of N_2 on burimamide-treated tissue should be quantitatively identical (except for pyridine nucleotide). The fourth row of Table 1 shows that this is essentially true. Accordingly, the spectral change in pyridine nucleotide can be taken as the shift also from totally oxidized to totally reduced. As mentioned above, this shift is larger than the shift with amytal and anoxia. If amytal results in complete reduction of intramitochondrial pyridine nucleotide, then the difference in reduction between burimamide + N_2 and amytal + N_2 is due to reduction of oxidized intramitochondrial nucleotide by anoxia. This suggests that mitochondrial nucleotide comprises about 15% of total tissue nucleotide.

Accordingly, the addition of amytal to a burimamide-inhibited tissue should result in a shift of completely oxidized intramitochondrial nucleotide to completely reduced. This corresponds to a change equivalent to 17% of the total nucleotide, a reasonable agreement to the 15% deduced above. No change was observed in the subsequent members of the respiratory chain showing also that there was no electron flow into this portion of the chain with burimamide.

This then raises the question as to why only 3.6% of total nucleotide changed with histamine stimulation of secretion and whether this was due to a change in cytoplasmic or mitochondrial components. This was partially resolved by data derived from studies on dog mucosa.

Levels of Metabolites in Dog Mucosa. The data obtained are shown in Table 2. It can be seen that in terms of total pyridine nucleotide, the change in NADPH is insignificant and can be neglected in predicting the changes likely to be observed spectroscopically. In data published elsewhere [18] the NAD^+ levels in mucous cells were comparable to those of parietal cells, but the NADH levels were only 15% of those in parietal cells. With secretion the latter value actually fell, hence one may also neglect changes in mucous cells as contributing to the data. Thus there is a decline in the measured NAD^+/NADH ratio with onset of secretion in the dog corresponding to an increase of 0.228 mmoles of NADH of a total pyridine nucleotide of 2.265 mmoles. This represents a change of 10% of the total. If this were intramitochondrial nucleotide this would correspond to close to 60% reduction of that compartment based on the considerations discussed in the spectroscopic data. It is therefore essential to calculate the compartmental distribution of the change.

When this is done, it can be seen that there is a 28% fall in the

Table 2. Metabolite levels in dog parietal cell region

	Rest (mmoles/kg dry weight)	Secretion
Lactate	3.41 ± 0.46 ($n=4$)	5.93 ± 1.47^a ($n=4$)
Pyruvate	0.424 ± 0.046 ($n=7$)	0.604 ± 0.038^b ($n=7$)
$NAD^+/NADH$ (cytosol)	1.3×10^3	0.94×10^3
Glutamate	12.13 ± 2.04 ($n=7$)	9.34 ± 2.38 ($n=7$)
α-ketoglutarate	0.359 ± 0.37 ($n=7$)	0.404 ± 0.41 ($n=6$)
NH_3	1.92 ± 0.06 ($n=10$)	2.21 ± 0.07^a ($n=10$)
$NAD^+/NADH$ (mitochondria)	2.94	5.0
NAD^+ (total)	1.97 ± 0.07 ($n=17$)	1.88 ± 0.07 ($n=11$)
NADH (total)	0.295 ± 0.020 ($n=17$)	0.523 ± 0.074^b ($n=11$)
$NAD^+/NADH$ (total)	6.68	3.60
$NADP^+$ (total)	0.069 ± 0.008 ($n=16$)	0.064 ± 0.008 ($n=14$)
NADPH (total)	0.219 ± 0.012 ($n=20$)	0.230 ± 0.012 ($n=12$)
$NADPH/NADP^+$ (total)	3.17	3.59

The values are means ± SEM of four measurements in n dogs. The cytoplasmic $NAD^+/NADH$ ratio was calculated using 1.11×10^{-4} for the LDH equilibrium constant and mitochondrial $NAD^+/NADH$ using 3.87×10^{-6} M for the GDH equilibrium constant. This corresponds to the 'free' nucleotide ratio g since there is significant binding of the reduced form.

[a] $= p < 0.05$.

[b] $= p < 0.01$.

ratio in the cytosolic compartment but a 70% increase in the mitochondrial ratio. From this, the reductive change in the total nucleotide is due entirely to a cytoplasmic change. The mitochondrial change in fact is towards oxidation.

From the spectroscopic calculations 85% of the pyridine nucleotide is extramitochondrial. The reciprocal change in the two compartments is consistent with a net change of 0.30 mmoles/kg dry weight in NADH, close to that actually found.

The total level of 2.3 mmoles/kg dry weight found in the dog can also be compared with the value calculated from the absorption data of 0.141 mmoles/kg wet weight. Since 20% of tissue is dry weight this corresponds to a value of 0.7 mmoles/kg dry weight. The epithelial cell layer comprises only 50% of the mass of the stripped frog mucosa and mucus cells contain only about 2/3 of the tubular (oxyntic) cell content which allows an estimated value of close to 2 mmoles nucleotide per kg dry weight oxyntic cell mass in the frog which is quite comparable to the value found for dog parietal cell regions.

Discussion

From the data presented in the frog and the dog, a consistent picture emerges in terms of what happens to the total pyridine nucleotide with onset of secretion. Thus a small component becomes reduced ranging from about 4% in the frog to about 10% in the dog, measured by quite different techniques.

Moreover, calculation of the cytosolic and mitochondrial distribution of the change in the $NAD^+/NADH$ ratio shows that the reductive change occurred exclusively in the cytoplasm. On the other hand the mitochondrial compartment became relatively oxidized. The ratios calculated are consistent with those found for other tissues [6].

Unfortunately the flavine nucleotides and the cytochromes are not amenable to estimation by the cycling procedures. However, just as the changes in the dog tissue for pyridine nucleotides appear to match these measured spectroscopically in the frog, it seems reasonable to assume that reductive changes occur in FAD and the cytochromes in dog gastric mitochondria with onset of acid secretion.

Since, therefore, the intramitochondrial $NAD^+/NADH$ increases and the $FAD/FADH_2$ decreases, a cross-over occurs between these components of the redox chain.

The oxidation of mitochondrial NADH would be consistent with the fall in the phosphorylation potential, $ATP/ADP \cdot Pi$ as found in both frog and dog [3, 18]. The problem is that the other components of the chain become reduced.

A reduction of NAD and cytochrome *c* in the mitochondrial respiratory chain with work load (muscle contraction) utilizing ATP has been described in insect muscle mitochondria [7]. Here the effect has been explained by a low mitochondrial permeability to metabolic anions and

activation of NADH-dependent isocitrate dehydrogenase. This action, activation of substrate oxidation, supersedes the oxidation of the respiratory chain expected from the decline in phosphorylation potential. It is clear from these data that an anomalous reduction of the respiratory chain does not disprove ATP utilization for work done by a tissue.

A similar situation may exist in part in the stomach. Thus, the largest changes found in metabolite levels in the dog are found in the Krebs cycle intermediates [16]. The effect of burimamide and histamine are also best explained metabolically as being due to substrate mobilization (whether glucose in the dog or additionally fatty acids in the frog) since no electron flow is demonstrable by amytal at FAD and below in the presence of burimamide. This interpretation has been suggested previously [8] and the data are quite similar to those found with theophylline addition to frog mucosa made resting by extensive washing [10].

The involvement of mitochondrial reactions is essential in any mechanism of H^+ secretion. For example, using substrate as a direct H^+ donor we may have

$$\text{lactate} \rightarrow \text{pyruvate} + 2H^+ + 2e.$$

If the protons are secreted and the electrons find their way to O_2, the H^+/O ratio of 2 is obtained provided the pyruvate is excreted and not metabolized. Any direct substrate reaction is subject to the same limitation. If the product of this type of reaction is not excreted but metabolized, the maximal H^+/O ratio is much less than 1, contrary to observation.

Apart from the generation of ATP, mitochondrial metabolism may be directly involved in the reduction of a cytoplasmic H^+ donor and in the reoxidation of a cytoplasmic electron acceptor. The presence of a cross-over between NAD^+ and FAD is not compatible with the utilization of only ATP as a product of mitochondrial metabolism. However, such a finding as well as the reduction of the subsequent redox chain does not exclude ATP utilization.

From the cross-over data it is possible to formulate a specific hypothesis for movement of reducing equivalents into and out of gastric mitochondria. Movement of reducing equivalents out of the mitochondria presents no energetic problem since there is a higher oxidation state of cytoplasmic as opposed to mitochondrial diphosphopyridine nucleotide. Malate would be an appropriate H^+ shuttle, oxidation of malate in the cytoplasm producing cytoplasmic NADH.

This NADH could react with a plasma membrane H^+ transport

system donating H^+ to the lumen, or to a second pump such as the $(H^+ + K^+)$-ATPase [5, 15]. The electrons pass to an acceptor such as dihydroxyacetone phosphate and with $2H^+$ from the cytoplasm, α-glycerol phosphate is formed. This in turn reacts with the flavin linked α-glycerophosphate dehydrogenase as in the α-glycerophosphate cycle [19]. In accord with this possibility there is a rise in malate and α-glycerophosphate with onset of secretion in dog mucosa [16].

This type of reaction sequence may account for a decrease in the cytoplasmic NAD^+/NADH ratio coupled to an increase in mitochondrial NAD^+/NADH ratio associated with a fall in the $FAD^+/FADH_2$ ratio.

In general, therefore, these data suggest the possibility that a reaction may be involved in gastric acid secretion other than, or in addition to, utilization of ATP. Data with isolated vesicles [15] as well as the fall in phosphorylation potential [3, 18] implicate ATP in the process. Thus, the final answer to the problem of H^+ secretion in the stomach may eventually be found in a combined redox and ATP-driven mechanism.

References

1. Black, J.W., Duncan, W.A.M., Durant, C.J., Ganellin, C.R., Parsons, E.M. 1972. Definition and antagonism of histamine H_2 receptors. *Nature* (*London*) **236**:385
2. Chance, B., Williams, G.R. 1955. Respiratory enzymes in oxidative phosphorylation. *J. Biol. Chem.* **217**:395
3. Durbin, R.P., Michelangeli, F., Michel, A. 1974. Active transport and ATP in frog gastric mucosa. *Biochim. Biophys. Acta* **367**:177
4. Folbegrava, J., Passoneau, J.V., Lowry, O.H., Schulz, D.W. 1969. Glycogen, ammonia and related metabolites in the brain during seizures evoked by methionine sulphoximine. *J. Neurochem.* **16**:191
5. Ganser, A.L., Forte, J.G. 1973. K^+-stimulated ATPase in purified microsomes of bullfrog oxyntic cells. *Biochim. Biophys. Acta* **307**:169
6. Greenbaum, A.L., Gumaa, K.A., McLean, P. 1971. The distribution of hepatic metabolites and the control of the pathways of carbohydrate metabolism in animals of different dietary and hormonal status. *Arch. Biochem. Biophys.* **143**:617
7. Hansford, R.G. 1972. Some properties of pyruvate and 2-oxoglutarate oxidation by blowfly flight-muscle mitochondria. *Biochem. J.* **172**:271
8. Hersey, S.J. 1971. The energetic coupling of acid secretion in gastric mucosa. *Phil. Trans. R. Soc. London B* **262**:261
9. Hersey, S.J. 1974. Interactions between oxidative metabolism and acid secretion in gastric mucosa. *Biochim. Biophys. Acta* **344**:157
10. Hersey, S.J., High, W.L. 1971. On the mechanism of acid secretion inhibition by acetazolamide. *Biochim. Biophys. Acta* **233**:604
11. Kidder, G.W., Curran, P.F., Rehm, W.S. 1966. Interactions between cytochrome system and H ion secretion in bullfrog gastric mucosa. *Am. J. Physiol.* **211**:513

12. Loewenstein, J.M. 1969. Aspartate: Determination with glutamate-oxaloacetate transaminase and malate dehydrogenase *In:* Methods in Enzymology. J.M. Loewenstein, editor. Vol. XIII, p. 473. Academic Press Inc., New York
13. Lowry, O.H., Passoneau, J.V. 1972. Flexible Method of Enzymatic Analysis. Academic Press Inc., New York
14. Rehm, W.S. 1972. Proton transport. *In:* Metabolic Pathways. D.M. Greenberg, editor. Vol. 6, p. 187. Academic Press Inc., New York
15. Sachs, G., Chang, H.H., Rabon, E., Schackmann, R., Lewin, M., Saccomani, G. 1977. A non-electronic H^+ pump in plasma membranes of hog stomach. *J. Biol. Chem.* (*in press*)
16. Sachs, G., Rabon, E., Saccomani, G., Sarau, H.M. 1972. Redox and ATP in acid secretion. *Ann. N.Y. Acad. Sci.* **246**:456
17. Sachs, G., Wiebelhaus, V.D., Blum, A.L., Hirschowitz, B.I. 1972. Role of ATP and ATPase in gastric secretion. *In:* Gastric Secretion. G. Sachs, E. Heinz, and K.J. Ullrich, editors. p. 321. Academic Press, New York
18. Sarau, H.M., Foley, J., Moonsamy, G., Wiebelhaus, V.D., Sachs, G. 1975. Metabolism of dog gastric mucosa. *J. Biol. Chem.* **250**:8321
19. Williamson, J.R., Ohkawa, K., Meijer, A.J. 1974. Regulation of ethanol oxidation in isolated rat liver cells. *In:* Alcohol and Aldehyde Metabolizing Systems. R.G. Thurman, T. Yonetani, J.R. Williamson, and B. Chance, editors. p. 365. Academic Press Inc., New York

Rev. Physiol. Biochem. Pharmacol., Vol. 79

H^+ Transport by a Non-Electrogenic Gastric ATPase as a Model for Acid Secretion

G. SACHS*

Contents

* Laboratory of Membrane Biology, University of Alabama in Birmingham, Birmingham, Alabama USA

The primacy of H^+ transport in endergonic and exergonic processes in biolo seems to be becoming part of scientific dogma. One might expect the secreto process of the mammalian perietal cell to be the ultimate expression of the pro transport process and thus to serve as a model for other H^+ translocases.

Accordingly, this review will discuss some recent findings relating to transp by the gastric mucosa, in particular the transport of H^+.

I. Mitochondrial H^+ Transport

Although the role of a proton gradient in chloroplast and mitochondrial phos phorylation and in active transport by bacteria or yeast is well established, w do not have a detailed picture of the structures constituting the H^+ pump. Th original chemiosmotic hypothesis whether correct in detail or not, made the im portant contribution to biological thought that the mode of energy conservatio by mitochondria was in the form of ion gradients [1], especially that of H^+.

Redox reactions catalyze the transfer of H^+ and electrons between donor and acceptors, the terminal acceptor in mitochondria being O_2. A vectori arrangement of such a reaction may be written as:

$$\begin{matrix} AH_2 \\ A \end{matrix} \Big) \quad \Big(\begin{matrix} OH^- \\ 2H^+ \end{matrix}$$

thus an H^+ and OH^- gradient is set up.

Equally the hydrolysis of ATP can be written as:

$$ATP + HOH \rightarrow ADP + Pi.$$

The equilibrium for this reaction can be written as:

$$\frac{ADP \cdot Pi}{ATP \cdot H_2O} = K.$$

If H_2O is reduced to very low levels, then ATP synthesis from ADP and Pi may occur. This was essentially the original core concept of the chemiosmotic hypothesis. However, although in a hydrophobic environment, the $[H_2O]$ can be low, it is very difficult to conceive of a mechanism acting directly to abstract H_2O.

An alternative way of writing the synthesis or breakdown of ATP is:

$$\begin{matrix} H_2O \\ 2H^+ \end{matrix} \Big) \quad \Big(\begin{matrix} ATP + 2H^+ \\ ADP + Pi \end{matrix}$$

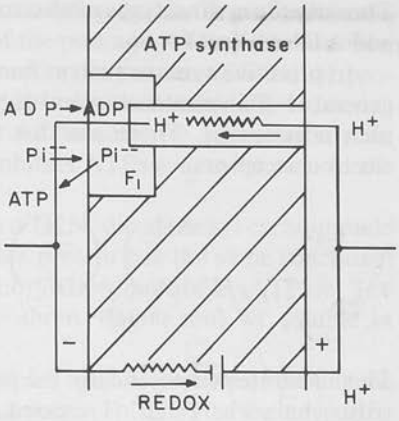

Fig. 1. Schematic representation of the chemiosmotic hypothesis, showing electrogenic redox pump generating an H^+ gradient. Return limb for the H^+ pump is ATP synthase reaction. This involves movement of H^+ across the membrane and reaction with bound ADP and Pi forming ATP

This illustrates the reversible translocation of $2H^+$ with the formation or breakdown of ATP. In this scheme, if the nexus of the arrows is considered to be a phase boundary, such as a membrane, the breakdown of ATP results in the net transfer of $2H^+$ as charged species. Hence, in considering the reversibility of the reaction, the electrochemical gradient of the proton, as well as the phosphorylation potential is significant. This results in:

$$n\left(\frac{RT}{F}\Delta pH - \Delta\psi\right) = \Delta G' = \Delta G^\circ + RT \ln \frac{ATP \cdot H_2O}{ADP \cdot Pi}$$

where R, T, F have their usual meanings, n is number of H^+ transferred, ΔpH is the pH gradient across the membrane, $\Delta\psi$ is the electrical potential difference, $\Delta G'$ is the actual free energy of hydrolysis, ΔG° is the standard free energy of hydrolysis. The term in brackets has been called the proton motive force (pmf). It has been the major contribution of the chemiosmotic hypothesis to recognize the equivalence of the electrochemical gradient of H^+ and the phosphorylation potential [1]. The required value of the pmf for ATP synthesis is, therefore, a function of the phosphorylation potential ATP/ADP · Pi and the value of n. The greater the value of n, the lower the required pmf.

Conversely, at zero potential the maximum gradient of H^+, ΔpH, is determined by the $\Delta G'$. Notably, the ΔG° of ATP is strongly pH-dependent above pH 6.

The critical component, therefore, of an ATP synthetase are a proton conductor across a membrane and a sensor of the H^+ concentration, a reversible ATPase. This is illustrated schematically in Figure 1.

A. Development of H^+ Gradients

It has been amply established that H^+ gradients can drive ATP synthesis [2], or that ATP hydrolysis can produce H^+ gradients [3]. It has also been well documented that redox reactions, or photolytic reactions may generate H^+ gradients [4].

Thus, there are three types of electrogenic mechanisms involved, redox, photolytic and ATP driven.

In primitive systems such as bacteria or mitochondria, in addition to an ATP generator of an electrochemical H^+ potential, there are also redox generators of such a potential. These are due to an oriented transmembrane complex of electron acceptors.

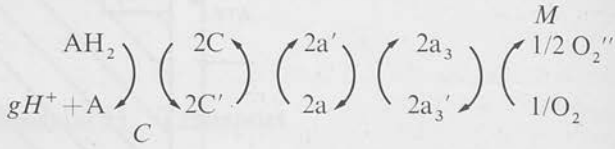

This illustrates schematically the oxidation of a substrate at complex IV of the redox chain where $2H^+$ is released on the cytoplasmic side of the mitochondrial membrane (C) and electrons to O_2 on the matrix side (M). Thus an H^+ gradient is generated electrogenically by such a complex. This is considered to happen at three sites in the mitochondrial redox chain. The disposal of the H^+ electrochemical gradient is by the ATP synthesis complex.

An H^+ gradient may also arise by coupling a proton conductance directly to a generator of potential such as electrogenic anion pump. In this case movement of H^+ is dependent on active movement of another ion.

Finally an electroneutral process may be considered, such as an exchange of H^+ for K^+, both ions participating in the translocation mechanism.

It is intriguing that all these processes must be, and actually have been, considered in the mechanism of H^+ secretion by gastric mucosa.

Because it has been shown that purified mitochondrial ATP synthetase complex may act on its own as an H^+ translocase, and because a gastric ATPase also can translocate H^+ ions, a brief digression into the electrogenic H^+ ATPase is worthwile.

In fact, because of the state of development of knowledge in gastric mucosa, our major concern will not be with the redox involvement in H^+ gradient generation, but with ATP and ATPase mechanisms. The evidence relating to redox involvement has recently been reviewed [5].

B. Electrogenic H^+ ATPase

The ATP synthetase present in mitochondria or chloroplasts contains an ATPase of complex subunit structure (F1) [6]. The function of these subunits is at present not understood. Additional components are associated with the ATPase such as an F_0 complex [7] or oligomycin sensitivity conferring factor (OSCF), a DCCD binding protein and an ATPase inhibitor [8]. Of particular interest is the role of F_0. A suggestion has been made that F_0 is the coupling site for F_1 on the mitochondrial membrane, and that the F_0 complex is responsible for the H^+ conductance of the mitochondrial membrane [9]. Thus, oligomycin or DCCD interacts indirectly with F_0 by combining with other factors inhibiting H^+ movement and in this configuration, (i.e. the combined F_1F_0), the ATPase activity is inhibited. The

coupling between oxidation and phosphorylation being due to the pmf across the membrane, oligomycin prevents interaction of the pmf and ATP synthetase. The F_0 path is not specifically required for respiration hence the addition of protonophores such as DNP or TCS allows respiration to continue [10]. However, H^+ flux through F_0 is specifically required for ATPase activity, since oligomycin, which blocks H^+ conductance through F_0, inhibits ATPase activity even in the presence of uncouplers.

In addition to the oligomycin site, there is a N, N′ dicyclohexyl carbodiimide binding protein [11]. Binding of DCCD to this protein has the same functional result as oligomycin, i.e. inhibition of phosphorylation but not F_1 ATPase. The binding protein is a low M.W. protein of about 10,000 mol wt soluble in chloroform-methanol.

If this type of model is accepted, the F_1 complex must be capable of sensing the change in $[H^+]$ or EMF at the F_0-F_1 interface. This has to be a specific region of proton translocation otherwise uncouplers would be able to reverse the oligomycin or DCCD inhibition of the F_1F_0 complex. It is therefore not adequate to propose a simple proton conducting circuit between F_1 and F_0.

Rather there could be a proton binding site on F_1 and a proton acceptor site on F_0 in the ATPase. Uncouplers would neither be able to accept H^+ from F_1 nor interfere with the translocation of H^+ from F_1 to F_0. H^+ movement across the mitochondrial membrane, in the absence of uncoupler, would then require dissociation of H^+ from the binding site on F_1 and translocation through F_0. ATPase inhibitors such as DCCD or oligomycin would then block either dissociation of H^+ from the binding site on F_0, or translocation from F_1, or translocation of the dissociated H^+ through the F_0 complex. In no case could uncouplers interfere with the reaction. This shielded proton movement implies the existence of channels rather than carriers, as illustrated in Figure 2. Hence, uncouplers will not be able to penetrate the channel region.

The reverse of the process, ATP synthesis by an electrochemical H^+ gradient would then require movement of H^+ through F_0 complex to the binding site and transfer of this H^+ to the acceptor site on F_1. Uncouplers would bypass this process by providing a shunt conductance for H^+ elsewhere in the mitochondrial membrane. Acceleration of ATPase activity with uncouplers then results from the reduction of the back EMF across F_0 complex.

The substantive point of this hypothesis is that there is a chemical group

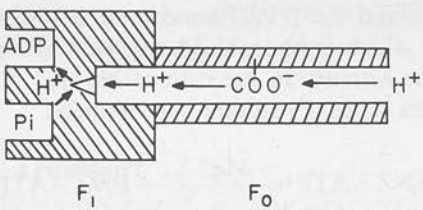

Fig. 2. More detailed representation of electrogenic H^+ ATPase of mitochondria. The representation is in the direction of ATP synthesis. COO^- represents DCCD binding protein F_0 (the H^+ conducting channel). Potential across the membrane is considered to move bound Pi to the H^+ site on F_1, the ATPase complex, and these react with ADP forming ATP. Reverse reaction generates an H^+ gradient and a potential

on F_0 which binds H^+ in response to a gradient (chemical or electrical). This interacts directly with an equivalent group in one of the F_1 subunits resulting in protonation of that subunit. This model has thus translated an ion gradient into a chemical change in F_1, the ATP, ADP and Pi binding complex.

A mechanism must also be present to sense the E.M.F. across the mitochondrial membrane (Fig. 2). If the translocation of Pi through the ATPase is in the charged form, then in the ATP synthetase reaction, direct application of a potential, mitochondrial interior negative, will move phosphate into the H^+ region (the F_0F_1 interface). The reaction at this site could be written [12]:

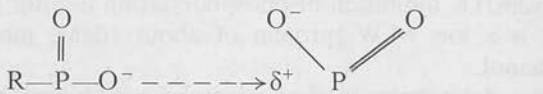

where the protonation of phosphate increases the electrophilic reactivity of the phosphorus. Reaction with O^- of ADP results in transfer of an electron and expulsion of H_2O. The H^+ gradient is responsible for the protonation and the EMF for translocation of the phosphate. Hydrolysis reverses the sequence, also producing a potential and H^+ gradient. The key reactions are therefore H^+ and Pi binding site translocation (Fig. 2).

II. Plasma Membrane Cation Transport

There appear to be two types of cation translocating ATPase. One already discussed is the mitochondrial F_1F_0 complex. No evidence exists for the cation translocation ability of F_1 alone. The other type is exemplified by the $Na^+ + K^+$ ATPase [13] or Ca^{++} ATPase [14] and probably by the $H^+ : K^+$ ATPase [15] of gastric mucosa. These differ in type of subunits and in reaction mechanisms. Thus both the Na^+K^+ and Ca^{++} ATPase contain a 100,000 M_r (relative molecular weight) subunit which is phosphorylated by ATP on a γ-aspartyl group [16, 17] during enzyme activity. In the case of Na^+K^+ ATPase at least, there appears to be a complex series of reaction steps namely:

$$\text{ENZ} + \text{ATP} \xleftarrow{Mg^{++}} \text{ENZ} - \text{ATP} \quad (1)$$

$$\text{ENZ} - \text{ATP} \longleftrightarrow \text{ADP} \cdot \text{ENZ} \cdot \text{Pi} \quad (2)$$

$$\text{ADP} \cdot \text{ENZ} \cdot \text{Pi} \xleftarrow{Na^+} \text{ENZ} \cdot \text{Pi}_1 + \text{ADP} \quad (3)$$

$$ENZ \cdot Pi_I \longleftrightarrow ENZ \cdot Pi_{II} \quad (4)$$

$$ENZ \cdot Pi_{II} \xleftrightarrow{K^+} ENZ_{II} + Pi \quad (5)$$

$$ENZ_{II} \longleftrightarrow ENZ_I \quad (6)$$

These steps have been dissected by the use of inhibitors such as ouabain [18] or N-ethyl maleimide [19], separate addition of Na^+ and K^+ and by ion gradient effects [20]. Kinetics as well as radiation inactivation cross section suggest a dimer form for activity of the enzyme [21]. Although, with the exception of red cell ghosts, vesicles containing this enzyme have been too leaky for transport studies, reconstituted vesicles have recently been described which do transport Na^{++} with ATP addition [22]. Little success has been reported for planar bilayer incorporation of this type of pump, although fragments may have been incorporated [23]. Hence the electrical characteristics of these pumps are not precisely known.

It seems that the isolated sarcoplasmic vesicles containing the Ca^{++} ATPase have a large anionic shunt conductance so that in vitro there is little likelihood of a potential developing with transport [24]. Ion pathways of the NaK ATPase have been measured by flux studies (which do not reveal the electrical characteristics) in red cells, resealed red cell ghosts, and in reconstituted vesicles. There appears to be at least five modes of operation of this pump, or five classes of cation flux. (1) Na^+K^+ exchange, (2) pump reversal, (3) $Na^+ - Na^+$ exchange, (4) K^+K^+ exchange, (5) Na^+ efflux [25]. The explanation for these activities must reside in the location and type of sites responsible for the ion movements.

It should not be considered that there is a fundamental difference in the thermodynamics of this type of ATPase and the electrogenic H^+ ATPase discussed above. Thus, this type of ATPase is also reversible with respect to ion gradients. In red cell ghosts which translocate Na^+ outwards and K^+ in, it was found that loading with K^+ and placing these in high Na^+ medium resulted in net synthesis of ATP. More recently the addition of Na^+ to non-vesicular preparations of $Na^+ + K^+$ ATPase has been shown to result in synthesis of ATP from ADP and Pi. Similarly binding of Ca^{++} can reverse the Ca^{++} ATPase.

The differences between these ATPases and the electrogenic H^+ ATPase may therefore be more apparent than real. That a phosphorylated intermediate is formed may only be coincidental in that a carboxyl group may react with the "activated" phosphate to form an isolatable "intermediate" in the plasma membrane ATPases. In the mitochondrial type a binding site may hold the phosphate for nucleophilic attack by ADP.

III. Photolytic H^+ Transport

The recognition of the proton pump capability of lumirhodopsin [4] has particularly interesting implications about H^+ transport mechanisms. A retinylidene protein (26000 daltons) moves H^+ in response to a light flash. Presumably a

reaction occurs in the retinal to change conformation of the protein. This in turn shifts the pK_a of a group in the protein from a high to low pK_a. This low pK_a form then donates H^+ across the membrane in one or several stages to another low pK_a group which donates H^+ to the medium.

It is not unreasonable to conceive of H^+ translocation to be via a similar mechanism. Thus interaction of a protein with ATP results in phosphate transfer. The acceptor group phosphorylation or binding results in a pK_a shift downward, translocation of H^+ across the membrane, and formation of an H^+ gradient. A similar mechanism with changing cation affinities in a site mobile across the membrane could account for cation translocation as has often been suggested.

IV. Nature of Ion Movement

Two types of structures may be responsible for ion translocation across bilayers. The simplest would be a waterfilled pore of dimensions so that hydrated ions could cross the bilayer (i.e. the cation selectivity sequence would correspond to sequence 1 of Eisenman). The other type involves substitution of water of hydration by binding groups such as polar oxygen and hence would alter the selectivity sequence. This type could be further classified into mobile and fixed sites (i.e. carriers or channels). These can be distinguished readily in a low conductance bilayer since a single channel event can significantly alter the background conductance of a bilayer, the channel "size" being to the order of $10^{-11}\Omega^{-1}$. A carrier binding one or two ions will show smooth conductance changes with incorporation into a low conductance bilayer. With the possible exception of the H^+-K^+ ATPase to be discussed below, no electrical evidence is available to establish whether ion conductance through pumps is by channel or carrier mechanisms.

The mitochondrial H^+ pump discussed above is electrogenic, i.e., the pump is capable of generating a potential or short circuit current across a membrane directly without the presence of diffusion potentials. The reasons for considering a channel mechanism have been discussed.

The rate of pumping (i.e. ATPase activity) will be a function of the gradient and the potential difference across the membrane. Accordingly, an increase of membrane conductance will serve to reduce the potential difference and hence accelerate the pump. The absence of a conductance or return limb will inhibit pump activity. The potential difference generated by a "perfect" electrogenic pump will then be 60 mv for each 10-fold increase in gradient generating capability for a univalent ion. If other conductances are present in the membrane, the potential difference will decrease as a function of the equation:

$$E_M = \frac{g_A E_A}{g_A + g_B}$$

where g_A, E_A are the conductance and E.M.F. of the active pump and g_B is the lumped conductance term for all other conductances. From this if $g_B \gg g_A$, the potential

difference generated by an electrogenic pump could be very small and not necessarily detectable. At $g_B=0$, E_A is 60 mv for a ten-fold gradient developed by the pump.

The alternative to an electrogenic pump is a neutral pump, with forced exchange between cations or anions or forced cotransport of cation and anion. Such a pump could only secondarily generate a potential due to a diffusion potential dependent on the concentration gradients of the ions transported, and the membrane selectivity.

V. Determination of Electrogenicity of Pumps

In intact tissue, the electrogenicity of a pump can be determined in several ways. The measurement of a potential difference in excess of that calculated based on diffusion potentials is perhaps the most direct. Alternatively, demonstration of linear relationships between ion flux and current generated or between potential difference and ion flux seems conclusive. In vesicles the evidence is more indirect, but knowledge of ion gradients across the vesicle membrane is easier to obtain.

In vesicles, measurement of changes in potential difference can be achieved by measuring the distributions of a radioactive or fluorescent lipid permeable cation. Thus,

$$E=\frac{RT}{nF}\ln\frac{A_i}{A_o}$$

where A_i is the internal and A_o is the external concentration of ion. It is often difficult to be exactly sure of A_i (especially in fluorescent studies), hence a calibration technique has been developed whereby the membrane is made K^+ selective by means of valinomycin and then a known K^+ gradient is applied.

An alternative approach in terms of distinguishing neutral and electrogenic pumps is to modify membrane conductance and measure changes in pump rate (i.e. ATPase activity). In general, an electrogenic pump will increase rate with increase in conductance and decrease rate with decrease in membrane conductance. If however, the non-specific conductance g_B is very high as discussed above, it may be very difficult to modify g_B sufficiently to achieve any change in rate or potential. In such vesicles a pump could therefore be effectively non-electrogenic rather than neutral. If however, it can be shown that in vesicles of low conductance, no potential develops and that changes of conductance do not affect pump activity, it may be safe to assume that the pump is neutral.

VI. Measurements of H^+ Gradients

In the special case of H^+ gradient formation by vesicles, it is possible to measure the magnitude of the H^+ gradient in three ways. The simplest is the use of a pH electrode and knowing vesicle volume the pH gradient can be calculated from the

appearance or disappearance of H^+ in the external medium. Alternatively, the trapping of a weak acid or weak base can be used on the supposition that the charged form of these are impermeable and the neutral form is freely permeable. Hence the ΔpH for trapping of a base

$$\Delta pH = \log_{10} \frac{AH^+}{A} = \log_{10} \frac{A_i}{A_o}$$

A technical problem arising is the degree of impermeability. Using a radioactive marker, centrifugation or filtering and washing could result in a considerable underestimate of the gradient if the charged form had finite permeability. Thus, rapid flow dialysis may be the method of choice for estimating uptake of base or acid.

Alternatively, pH indicator dyes can be used with color or fluorescence changes in the appropriate range. The drawbacks in this case are the site of binding of the dye (if bound) and changes in spectrum with binding as well as absorbance changes. Hence, quantitation of the change of pH may be difficult.

These would seem to be the possibilities available and with the measurement of ion movements, the use of potential probes and ionophores, and variation of the conditions of study of transport, a decision as to the type of pump and whether H^+ is transported is in general feasible in isolated vesicles.

With this brief background discussion of a complicated field, we can now approach the problem of H^+ transport in gastric vesicles due to $H^+ + K^+$ ATPase activity.

VII. $H^+ + K^+$ ATPase

The first indication that gastric mucosa might contain a transport ATPase similar to the $Na^+ + K^+$ ATPase was the finding of a K^+ activated p-nitrophenylphosphatase [26] or acetyl phosphatase [27]. The $Na^+ + K^+$ ATPase is capable of catalysing similar partial reactions [28, 29] but in contrast to the gastric phosphatase activity, the $Na^+ + K^+$ partial reaction is ouabain inhibited.

Subsequently a K^+ activated ATPase was shown to be present in rabbit, frog, dog and hog mucosa [15, 30, 31]. In contrast to the $Na^+ + K^+$ ATPase, there was no inhibition by ouabain nor was there any requirement for Na^+.

A. Purification

The K^+ enzyme is localized exclusively in the microsomal fraction of the gastric mucosal homogenate. This microsomal fraction can be further divided into two membranes and one mitochondrial band on density gradient centrifugation using sucrose or ficoll sucrose gradients [32, 33]. At this stage, there is a 10-to 20-fold purification of the ATPase or pNPPase in terms of the original homogenate

Table 1. Purification of vesicles

	μmoles Pi mg^{-1} h^{-1}			
	5′-AMPase	Mg^{++}-ATPase	K^+-ATPase	K^+-ATPase + val
Total homogenate	0.5 ± 0.3	6.2 ± 0.6	2.0 ± 1.0	3.6 ± 1.8
Microsomal fraction	1.5 ± 0.6	15.9 ± 1.5	7.1 ± 4.3	16.7 ± 4.0
Light membrane fraction	4.6 ± 0.1	6.4 ± 1.3	32.5 ± 3.2	62.9 ± 1.7
Electrophoretic fraction I (F1)	0.6 ± 0.2	2.7 ± 0.6	64.1 ± 3.9	87.6 ± 2.5
Electrophoretic fraction II	14.7 ± 1.2	16.6 ± 2.0	17.3 ± 1.2	19.4 ± 1.7

The activity of 5′ AMPase and ATPase in the total homogenate, microsomal fraction (100,000 g precipitate of the post 20,000 g supernatant) the light membrane fraction on the 7.5% ficoll to 37% w/w sucrose gradient and the 2 fractions derived from the latter by free flow electrophoresis. The K^+-ATPase activity is the difference between activity in the presence or absence of K^+. The K^+-ATPase + valinomycin activity is the difference between the activity in the presence of K^+ and valinomycin and in the presence of Mg^{++} alone

Fig. 3. Gel pattern on 10% acrylamide gels of microsomal (*M*) zonal gradient peak (*G*) and free flow electrophoretic fraction (*Fl*) showing progressive reduction of the number of peptides in each fraction and increase in relative amount of the 100,000 peptide region

(Table 1). The two membranous bands differ somewhat in their content of 5′ nucleotidase and considerably in their ion permeability. The material not entering the gradient, i.e., at 7% ficoll is considerably less permeable to H^+. The gel pattern observed is fairly typical of membranes showing a complex pattern with some prominent high mol wt Bands.

Free flow electrophoresis which takes advantage of variations of surface charge separates either membranous band into several fractions. Maximum separation is

obtained in the presence of ATP. The calculated surface charge alteration based on the ATP dependent band displacement is equal to the number of phosphorylation sites per vesicle measured using γ ^{32}P-ATP [33].

This electrophoretic fraction is now 40-fold enriched with respect to $H^+ + K^+$. ATPase and is free of 5′ nucleotidase and Mg^{++} ATPase. Moreover, gel electrophoresis shows that a peptide region of 100,000 mol wt accounts for more than 75% of the protein [33] (Fig. 3). At this stage of purification there is no detectable NADH or NADPH oxidase activity.

B. Properties of the Enzyme

Work on this enzyme has been relatively recent hence details of its action are not nearly as well known as those of the $Na^+ + K^+$ or Ca^{++} ATPase. However, since it bears a remarkable resemblance to these ATPases, rapid progress has been made in defining some of its key features [30].

A phosphorylated intermediate which is acid stable, alkali and NH_2OH labile is formed upon incubation with γ^{32}-ATP and Mg^{++}. A peptide of 100,000 mol wt is phosphoryltated both in the crude membranes and the purified electrophoretic fraction [34]. The pH optimum of phosphorylation is broad, being between 6 and 6.8 (Rabon, unpublished observations). The enzyme also catalyzes an ATP-ADP exchange [35], a characteristic reaction of energy conservation by ion gradients or covalent intermediates [13]. Phosphorylation may be enhanced by inhibitors of the overall reaction such as F^-, Zn^{++} [15] and decreased by inhibitors such as pCMBS and DCCD [35].

The overall ATPase reaction requires the presence of alkali metal cation, as does the pNPPase or acetyl phosphatase. The cation accelerates dephosphorylation of the protein. In our laboratory there is an unexplained anomaly in the relative effectiveness of the various cations in terms of the overall ATPase activity and dephosphorylation. Thus, the selectivity sequence of cations for ATPase activity if K 100; Rb 76; Cs 16; Na 7; Li 4. For dephosphorylation the sequence was found to vary in terms of Cs^+ or Na^+ whereas for pNPPase activity the selectivity sequence was identical to the sequence for ATPase. In contrast to the $Na^+ + K^+$ ATPase, no additional effect is found for combinations of cations. NH_4^+ and TI^+ are also effective stimulating ions, TI^+ being more effective than K^+, and NH_4^+ having about equal activity. The pH optimum for dephosphorylation is 7.4 and the apparent K_A for cation is a function of both pH and temperature. For K^+, at pH 7.4 and 37° C the K_A was found to be 0.5 mM.

The dephosphorylation is not Mg^{++} dependent since CDTA does not block the K^+ enhancement of the reaction. Based on the ATP-ADP exchange and loss of phosphoenzyme with CDTA the first step of the reaction is reversible [35]. The presence of a K^+ gradient allows phosphorylation of the protein from inorganic phosphate, but does not result in an ATP-Pi exchange. This finding implies that there are two forms of the phosphoprotein, a K^+ sensitive form and an ADP sensitive form, as has been suggested for the $Na^+ + K^+$ ATPase [36].

The substrate specificity of the enzyme is ATP 100, GTP 12, CTP 15 ITP 0. β-γ methylene ATP is not hydrolysed by the enzyme, but acts as a competitive

inhibitor for ATP. The K_M for ATP is 10^{-4} M at pH 7.4, 37° C [30, 35]. ATP also is a competitive inhibitor for the pNPPase [30].

From these considerations one may suggest a tentative scheme such as [26, 36] for the $Na^+ + K^+$-ATPase (see above).

$$\mathrm{ATP} + \mathrm{E}_1 \xrightleftharpoons{Mg^{++}} \mathrm{ADP} \cdot \mathrm{E}_1 \cdot \mathrm{Pi}$$

$$\mathrm{ADP} \cdot \mathrm{E}_1 \cdot \mathrm{Pi} \xrightleftharpoons{H^+} \mathrm{E}_1\mathrm{Pi}$$

$$\mathrm{E}_1\mathrm{Pi} \rightleftharpoons \mathrm{E}_2\mathrm{Pi}$$

$$\mathrm{E}_2\mathrm{Pi} \xrightleftharpoons{K^+} \mathrm{E}_2 + \mathrm{Pi}$$

$$\mathrm{E}_2 \rightleftharpoons \mathrm{E}_1$$

This scheme will be discussed later in relation to the possible dimeric structure of the active form of the enzyme.

C. Vesicular Structure of the ATPase Particle

There are several properties of the ATPase which appear to be explained by the vesicular structure in which the ATPase finds itself. Most microsomal preparations from a variety of tissue appear vesicular, but little evidence from $Na^+ + K^+$ ATPase studies suggest that these vesicles are capable of maintaining ion gradients even in the presence of ATP [37].

In contrast, the gastric vesicles seem relatively ion impermeable, as would be expected from the known conductance properties of the mucosal surface of the stomach [38]. A key experiment demonstrated that ATPase activity was enhanced by the addition of ionophores such as valinomycin [39]. Table 2 illustrates the ionophore enhancement of the ATPase activity in a ficoll-gradient preparation from hog mucosa. The stimulation by valinomycin is much less than the stimulation by gramicidin. This can be explained in one of two ways. Valinomycin is K^+ selective and does not transport H^+ and requires an associate conductance path for net K^+ movement. Gramicidin is a channel former which can exchange K^+ for H^+ hence does not require an associate conductance. Hence, the greater stimulation by gramicidin could be due to facilitation of K^+ entry relative to valinomycin or be due to dissipation of a limiting H^+ gradient or both.

Freeze-drying the preparation essentially abolishes the ionophore enhancement of the enzyme. Preincubation with K^+ reduces but does not abolish activation. NH_4^+ stimulation is independent of vesicular form or gramicidin due to the high permeability of NH_3. Protonophores or lipid permeable ions do not stimulate ATPase activity.

Table 2. Effect of ionophores on ATPase mole Pi $mg^{-1}\,h^{-1}$

Mg	K^+	NH_4^+	K^+ valinomycin	K^+ gramicidin	NH_4^+ gramicidin
3.6	5.4	85.6	9.8	96.7	80.1

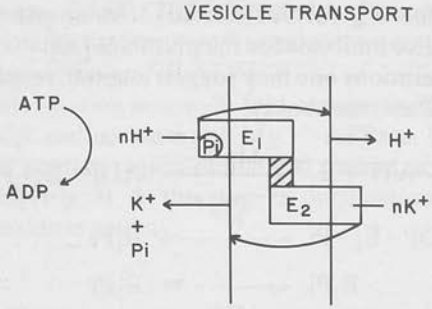

Fig. 4. Scheme illustrating a dimeric model for $H^+ + K^+$ ATPase. Here a H^+ and K^+ site exchange occurs, sites being mobile across the membrane. The movement of H^+ is obligatorily coupled to the E_1 to E_2 conformational change. In turn, because of dimeric nature of the enzyme, this is coupled to the E_2 to E_1 conversion of the other subunit which is K^+ dependent. Irradiation of E_1E_2 form will then inactivate ATPase and H^+ transport whether E_1 or E_2 is destroyed. pNPPase inactivation requires that both E_1 and E_2 are inactivated. Antibody against E_1 will inhibit ATPase, but only partially inhibit pNPPase since both E_1 and E_2 can hydrolyze pNPP but only E_1 can react with ATP

The most reasonable explanation of these findings is that the vesicular permeability to K^+ is low. This explains the K^+ ionophore enhancement of activity. If protonophores or lipid permeable ions also enhanced activity, the explanation could be that there was a potential difference developed which restricted ATPase activity. Since preincubation with K^+ did not abolish but reduced ionophoretic enhancement of activity, the implication is also that K^+ is transported out of the vesicle during ATPase activity.

Accordingly the K^+ site for ATPase, activation is on the opposite side of the membrane compared to the ATP site and K^+ is probably transported during enzyme activity.

In contrast to ATPase activity, pNPP hydrolysis, although K^+ dependent, is insensitive to any of the ionophores. Accordingly, the K^+ site for pNPP hydrolysis is on the external face of the vesicle. Since pNPP hydrolysis is a partial reaction of the ATPase, either the K^+ site for pNPP hydrolysis is different from the ATPase K^+ site, or the site is mobile across the membrane.

The simplest model is, therefore, that the K^+ site is mobile across the membrane (Fig. 4).

D. Active Form of ATPase

The rationale has been given for the involvement of a phosphorylated intermediate in ATPase activity, and for the presence of a mobile K^+ site. The phosphorylated peptide may be the only subunit of the enzyme, or the carbohydrate staining region on the gel may contain a second subunit. Based on the Ca^{++} and $Na^+ + K^+$ ATPase, the 100,000 dalton unit may well be the functional transport unit.

The enzyme may function as a monomer, a dimer, or a higher polymeric form. There are various ways of distinguishing monomer as opposed to functional dimer.

Kinetically, the Hill coefficient for pNPPase activity at a Mg^{++}/pNPP ratio of 1 is 1.8, suggestive of a dimer. With ATP as substrate, the Hill coefficient is 1. This may suggest that for every ATP site on the functional enzyme, there are 2 pNPP sites.

Inactivation of the enzyme by irradiation can be described by:

$$A/A_o = e^{-V \cdot D}$$

where A is activity at time t, A_o is initial activity, V is apparent volume of target and D is dose of radiation. V is obtained from the slope of ln A/A_o against D (in time of irradiation). The ATPase activity is inactivated at twice the rate of the pNPPase. This can be explained if the ATPase is a dimer, with half site reactivity, but either half of the dimer can hydrolyse pNPP.

Recently, it has also been possible to generate antibodies against this ATPase. With this antibody, the inactivation of the ATPase was about twice that of the pNPPase [64]. This may be explained also by half site reactivity, if the antibody is directed against the ATP site (and pNPP site) on half of the enzyme. The pNPP site on the other half of the enzyme is not affected (Fig. 4).

In subsequent sections we shall develop this dimer concept to explain electroneutral H^+ and K^+ exchange.

VIII. H^+ Transport

The addition of ATP to a suspension of dog microsomes [40] or purified hog membrane vesicles [41] results in a transient alkalinisation of the medium (Fig. 5).

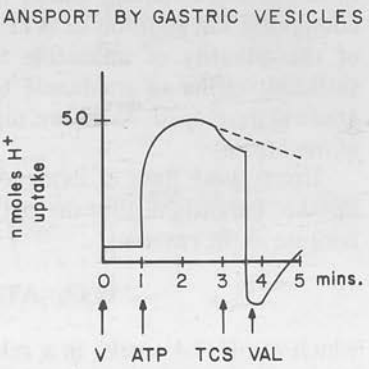

Fig. 5. An experiment where ATP is added to a vesicle suspension in the presence of 150 mM KCl. There is rapid uptake of H^+ which spontaneously dissipates with consumption of ATP. Addition of tetrachlorsalicylanilide (TCS) has only a slight effect. Subsequent addition of valinomycin results in dissipation and overshoot of gradient

A. Detection of H^+ Gradient

This may be done using a pH electrode since the intravesicular space is shielded from the electrode. Disappearance of H^+ may be due to binding, or to uptake into

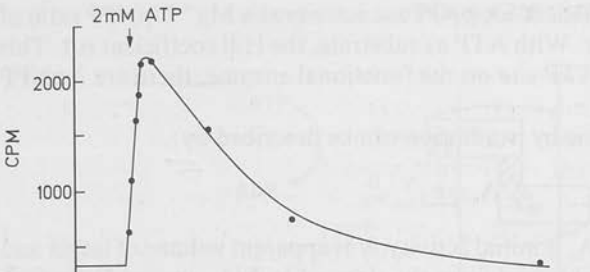

Fig. 6. Effect of ATP on uptake of ^{14}C-imidazole at pH 7.4 and 75 mM RbCl, 125 mM sucrose and 2 mM MgCl with 2 mM MgATP. Wash solution was at pH 6.1 to minimize imidazole efflux and in separate experiments a constant baseline was observed in the absence of ATP additions

an intravesicular space. The effectiveness of ionophores, such as nigericin or a combination of valinomycin and tetrachlorsalicylanilide (TCS) in reducing the alkalinisation, shows that a gradient is probably responsible [40, 41]. The reduction in H^+ uptake obtained by increasing the tonicity of the medium [42] (i.e., decreasing the intravesicular volume) also argues for H^+ uptake.

An alternative method is the use of pH indicator dys and measuring O.D. changes with ATP addition. It is best to use an indicator the color change of which is in the pH range either outside or inside the vesicles and is suitably distributed. This latter point is perhaps the most problematic. The use of such an indicator gives an estimate of the pH range attained in the vesicles. As with the pH electrode techniques, variation in vesicular volume and the use of ionophores allows direct proof that a gradient is produced. A dye which has proved suitable is bromcresol green.

Finally, one may use trapping of a base on the assumption that the charged form is not permeable. The addition of radioactive imidazole at pH 7 followed by filtration and counting allows the distribution ratio to be measured. With this compound the addition of ATP results in a considerable enhancement (35-fold) of the quantity of imidazole trapped (Fig. 6). Unfortunately, there may be sufficient efflux of imidazole to make this a low estimate of the actual pH gradient developed. As before, nigericin prevents the ATP dependent accumulation of imidazole.

From these lines of evidence, gastric vesicles are capable of energized H^+ uptake. Parenthetically, the pH of study of any ATPase reaction is important because of the reaction:

$$H_2O + ATP^{4-} \longrightarrow ADP^{3-} + Pi^{2-} + H^+$$

which at pH 7.4 results in a release of H^+ for every mole ATP hydrolysed. At lower pH, depending on the Mg^{++} concentration [43], one can find a pH at which no H^+ is released upon hydrolysis due to maintained protonation of the products of hydrolysis. Since Mg^{++} affects the pK_a of all the reactants, its concentration is important in determining the pH at which no net change of $[H^+]$ occurs during hydrolysis. Hence, at a pH of around 6.12 for 2 mM Mg^{++}, changes in medium pH are due to transport.

B. Substrate Specificity of H^+ Uptake

Except for ATP no other nucleoside triphosphate gave any indication of H^+ transport [42]. Para nitrophenylphosphate was also inactive in the test system consisting of gastric vesicles suspended in KCl at pH 6.1. Here also there is no net change of pH due to the hydrolytic reaction itself.

Redox substrates such as lactate, NADH, NADPH, ascorbate, reduced cytochrome c and $FADH_2$, were inactive in generating a pH gradient in the purified fraction. These data are in contrast to those obtained in the less purified microsomes where there is a positive change of pH in the medium with the addition of NADH even in the presence of amytal [41] due to H^+ consumption. It would seem, therefore, that the H^+ transport is a property of the ATPase.

C. Cation Requirement

There is an absolute requirement for alkali metal cation in the H^+ transport process. If vesicles which have been prepared directly on the ficoll gradient are added to 150 mM KCl at pH 6.1, there is virtually no H^+ utake with the addition of ATP. After some minutes of incubation, the H^+ uptake is observed following ATP addition. From this it is clear that internal K^+ is required for H^+ uptake. This is futher confirmed by the increased rate and maximal uptake observed with vesicles equilbrated with K^+ or vesicles in an outward K^+ gradient experiment. In fact, the outward gradient results in the largest K^+ uptake.

The cation selectivity of the process is identical to the selectivity of the ATPase. Thus the sequence is, when K^+ is set to 100; K^+ 100; Rb^+ 80; Cs^+ 4.5; Na^+ 0.24; Li^+ 0.1; choline 0.

The requirement for cation is not met by lipid permeable cations, hence is a requirement that is specific and not due to provision of a nonspecific conductance. Accordingly, the cation requirement is for ATPase activation or as a counterion for H^+ uptake or both.

D. Effect of Inhibitors

Various inhibitors of ATPase activity such as Zn^{++}, F^-, pCMBS or DCCD also inhibited H^+ uptake to the same extent as the ATPase.

E. Effect of Ionophores

The use of these agents allows conclusions to be drawn in relation to the inherent membrane conductance as well as to the conductance requirements for transport.

Assuming an outward H^+ gradient is present across the vesicle membrane, generated by ATP and an inward K^+ gradient is present due to the conditions of study (i.e. addition of vesicles to KCl, or generation of a K^+ gradient by ATP),

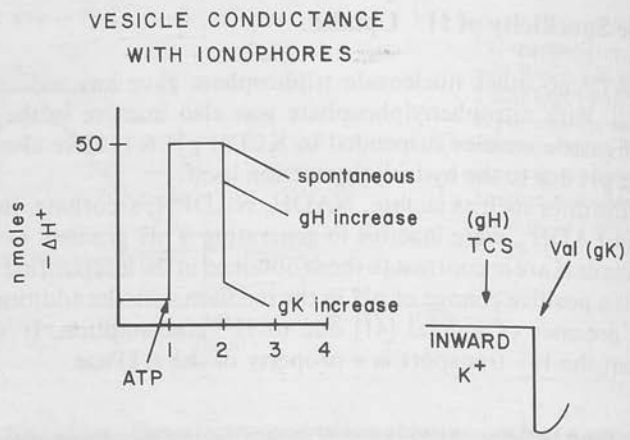

Fig. 7. A schematic representation of the effect of ATP and ionophores on vesicle H^+ gradient. ATP generates an H^+ gradient, and there is a spontaneous decay of the H^+ gradient. Addition of a protonophore rapidly decays gradient by about 20% and then continued decay returns to spontaneous rate (gH increase). Addition of a K^+ ionophore is more effective in dissipating gradient (provided there is an inward K^+ gradient) (gK^+ increase). Second half of figure shows the effect of ionophores on the vesicles in the absence of ATP but with an inward K^+ gradient present. A protonophore has no effect on H^+ gradient. A K^+ ionophore, with or without protonophore, induces an efflux of H^+

then the continued existence of the H^+ gradient is due to a limiting conductance in the membrane, either for H^+, K^+ or Cl^-. If the H^+ conductance is rate limiting, then the addition of an H^+ conductance, as with a protonophore (TCS, CCCP), should effectively dissipate the gradient. If this is not the case, then another conductance may be limiting. The addition of valinomycin which induces a K^+ conductance results in dissipation of a large fraction of the H^+ gradient (Fig. 7). From this we can conclude that the major conductance is for H^+ and not for K^+ (42).

Nigericin which acts as a cation exchange ionophore [44] dissipates either an H^+ or K^+ gradient. In the absence of an initial K^+ gradient, the H^+ gradient is converted to a K^+ gradient with the addition of nigericin. Nigericin dissipates the gradient in gastric vesicles.

The ionophores may also be used to estimate the conductance requirements of the membrane during pump activity. In general, as discussed in relation to the electrogenic H^+ ATPase, increase of membrane conductance will increase pump activity if the pump is electrogenic. No increase in ATPase activity is found with addition of protonophores, nor is there much ($<15\%$) inhibition of H^+ uptake. Valinomycin enhances H^+ uptake with ATP addition under inward K^+ or zero K^+ gradient conditions. This is explained by the requirement of the system for internal K^+, rather than due to any conductance change. Lipid permeable cations do not substitute for K^+ ionophores, which is additional evidence for the specific internal K^+ requirement, rather than K^+ providing a cationic conductance to satisfy an electrogenic H^+ pump.

The major conclusion from this is that the H^+ transport by these vesicles is likely to be non-electrogenic. Accordingly, there is a contransport of anion or

countertransport of cation which is a pump requirement. This can be studied by investigation of the transport of other ions by these gastric vesicles.

F. Stoichiometry of H^+ Uptake

The ratio of H^+ movement for each high energy phosphate in mitochondria and chloroplasts varies between 2 and 4 depending on the conditions of the experiment [45, 46]. Measurement of ATP hydrolyzed at the same time as H^+ uptake gives a ratio of moles H^+ transport per mole ATP hydrolyzed of 4, when only the K^+ activated component of the ATPase is used. From this, since the H^+ gradient achieved by the mucosa is 10^6 or better, the H^+/ATP ratio has to vary from 4 to less than 2 as the H^+ gradient increases. It can be calculated that 9 kcal/mol are required for H^+ transport at a 10^6 gradient. The $\Delta G'$ for ATP hydrolysis is about the same hence the maximal molar ratio of H^+/ATP should be about 1.

IX. Cation and Anion Movement

The uptake of H^+, whether electrogenic or neutral must be accompanied by cotransport of Cl^- or countertransport of K^+, since K Cl is the only added salt. Two types of studies can therefore be performed, uptake and efflux [47].

A. Rb Transport

Using $^{86}Rb^+$ and $^{36}Cl^-$ it was shown that both ions were taken up into an intravesicular space of about 2 μl mg^{-1} protein. The $T_{1/2}$ was temperature sensitive, being several hours at 4°, and 40 min at room temperature. The addition of ATP transiently reduced Rb^+ uptake but had no observable effect on Cl^- uptake.

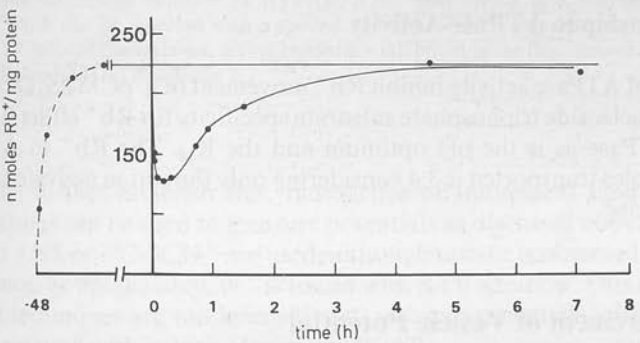

Fig. 8. Efflux of Rb^+: vesicles were preequilibrated for 48 h as detailed in the text and 2 mM ATP added to the suspension at zero time on graph. It can be seen that there is a transient rapid efflux of Rb^+ to about 50% of the measured equilibrium value (horizontal line) and with consumption of the ATP there is reequilibration of the Rb^+

When the vesicles were allowed to equilibrate with either Rb^+ or Cl^-, and ATP added to this suspension, there was a transient efflux of Rb^+, but no effect on Cl^- (Fig. 8). The movement of Rb^+ therefore develops a chemical gradient of Rb^+ and could be due to an energized $H^+ : Rb^+$ exchange, or due to a change of potential across the vesicle membrane, the interior of the vesicle becoming positive with ATP addition.

Two means are available for distinguishing these possibilities, by the use of conductance modifying agents and determining their effects on Rb^+ transport and by the direct measurement of vesicle potential. The latter will be discussed in a subsequent section.

B. Effects of Membrane Active Agents

An ionophore with Rb^+ specificity, such as valinomycin, would be expected to increase the rate of Rb^+ efflux with the Rb^+ movement being due to a potential. In fact no change in Rb^+ efflux was noted in the presence of valinomycin. The reuptake of Rb^+ after ATP had been consumed was accelerated.

Lipid permeable cations, such as triphenylmethyl phosphonium or dimethyl dibenzyl ammonium should, at adequate concentration, substitute for Rb^+ if the movement were due to a potential and reduce Rb^+ efflux as well as themselves show similar efflux characteristics. Neither phenomenon occurs, lipid permeable cations being without any effect on Rb^+ movement and showing no redistribution themselves with ATP addition.

A lipid permeable anion, such as SCN^-, should enter the vesicle in response to a positive internal potential and thereby reduce the potential, and hence reduce Rb^+ movement that is dependent on potential. Again SCN^- is without effect on Rb^+ efflux.

Accordingly, modifying membrane conductance by adding alternate electrogenic pathways does not effect Rb^+ efflux induced by ATP therefore Rb^+ movement is not due to a potential difference across the membrane of the vesicle.

C. Relationship to ATPase Activity

Inhibitors of ATPase activity inhibit Rb^+ movement (e.g. pCMBS, DCCD, Zn^{++}, F^-). The nucleoside triphosphate substrate specificity for Rb^+ efflux is the same as for the ATPase as is the pH optimum and the K_M. The Rb^+ to ATP ratio in terms of moles transported is 3.4 considering only the cation activated component of the ATPase.

X. Measurement of Vesicle Potential

In the previous sections arguments have been put forward that the transport process catalyzed by the ATPase is essentially a nonelectrogenic $H^+ + K^+$

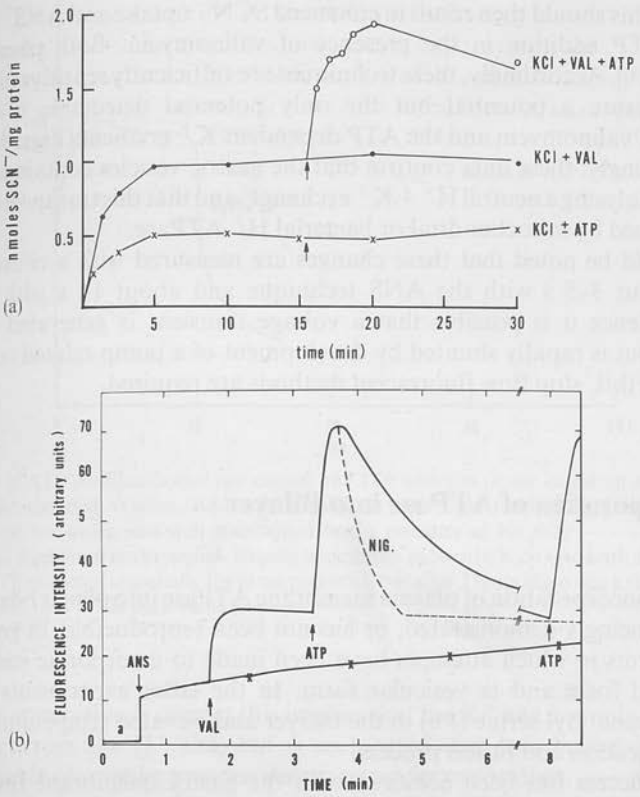

Fig. 9. (a) Uptake of ^{14}C SCN^- with time when added to vesicles alone (*lower* ×——× *curve*) or vesicles in the presence of valinomycin (*upper* ●——● *curve*). ATP was added to both sets of tubes at the time indicated, but enhanced SCN^- uptake only in the presence of valinomycin (○——○). (b) ANS fluorescence events of gastric vesicles. Initial addition is that of membranes to cuvette, followed by ANS. It can be seen that there is an initial rapid rise with ANS addition followed by a slow increase of fluorescence (×——×) which eventually reaches the valinomycin level (not shown). Addition of valinomycin before the plateau results in a further rapid increase in fluorescence, and subsequent addition of ATP (1.7×10^{-5} M) results in a transient fluorescent enhancement, which can be repeated with a second addition of ATP. Also shown is the effect of nigericin on ATP-induced fluorescence, giving immediate inhibition of the fluorescence and inhibition of the effect of subsequent ATP addition

exchange. To further establish this, radioactive or fluorescent lipid permeable anions or cations can be used to measure potentials as discussed above.

Whether ANS or ^{14}C-SCN^- are used, although uptake is observed, no change in fluorescence, or uptake of SCN^- is found with ATP addition. This might be so because the techniques are too insensitive to measure potentials, although these ions have been used with success elsewhere [48, 49].

Since with ATP addition to equilibrated vesicles there is a K^+ gradient developed due to the $K^+ : H^+$ exchange, the presence of valinomycin should theoretically result in the development of a positive internal potential due to the inward K^+

gradient. This should then result in enhanced SCN^- uptake and ANS^- fluorescence with ATP addition in the presence of valinomycin. Both phenomena are found [42, 50]. Accordingly, these techniques are sufficiently sensitive in these vesicles to measure a potential but the only potential detectable is due to the presence of valinomycin and the ATP dependent K^+ gradient (Figs. 9a, b).

Accordingly, these data confirm that the gastric vesicles contain an $H^+ + K^+$ ATPase catalysing a neutral $H^+ + K^+$ exchange, and that this transport differs from that catalyzed by mitochondrial or bacterial H^+ ATPase.

It should be noted that these changes are measured with a considerable lag phase, about 3–5 s with the ANS technique and about 15 s with the $S^{14}CN$ method. Hence it is possible that a voltage transient is generated during this transport but is rapidly shunted by development of a pump related conductance. To exclude this, stop flow fluorescent methods are required.

XI. Incorporation of ATPase into Bilayer

In general, incorporation of plasma membrane ATPase into planar bilayers has not been convincingly demonstrated, or has not been reproducible. In general, there are two forms in which attempts have been made to incorporate such pump, in the purified form and in vesicular form. In the latter experiments Ca^{++}, the use of phosphatidyl serine (PS) in the bilayer and elevated temperatures improve the incorporation and fusion process.

Some success has been achieved with the gastric membrane fractions [51]. The addition of the ATPase enriched fraction to a PS bilayer results in a reproducible conductance increment in the bilayer ranging from one to three orders of magnitude. This conductance is cation selective, with the same selectivity sequence as for the ATPase activation, or for H^+ transport by the vesicles.

In addition, the addition of ATP to the bilayer with the vesicles incorporated results in the development of a sizable P.D. (Fig. 10). Interestingly, the characteristics of the potential response are a function of the cation composition of the medium.

Thus the presence of Na^{++} results in the development of a potential which is little affected by the nature of the anion. Indeed the potential in Cl^- is greater than that in SO_4^{--}. This is similar to the reduced H^+ and Rb^+ movement found with SO_4^{--} as compared to Cl^- but is contrary to what would be expected from the relative bilayer conductance of these anions. Substantial ancillary evidence exists that the bilayer phenomena are pump properties. For example, the reaction is ATP specific and it is blocked by pCMBS, as is the pump in natural vesicles.

In the presence of K^+, the potential develops initially with the same characteristics as with Na^+. In a time-dependent manner however, there is a fall of potential. This time dependence is characteristic of a bilayer thickness dependent phenomenon, as occurs using malonyl digramicidin. It seems reasonable to explain this by postulating a thickness-dependent K^+ conductance developing to shunt the H^+ potential.

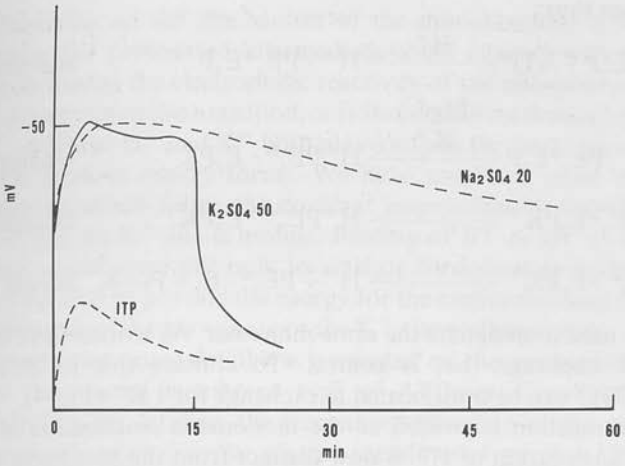

Fig. 10. Effect of ATP addition (*upper two curves*) and ITP addition (*lower curve*) on one side of the bilayer with incorporated vesicles. Addition of ATP at zero time resulted in development of a potential of −50 mv which was well maintained in the presence of Na_2SO_4 (– – – – –). ITP produced only a fraction of the potential. Results of addition of 50 mM K_2SO_4 to both sides of bilayer showed that ATP produced essentially the same potential, but after 15 min there was a sharp decline in potential to about 10% of the peak value (————)

If this interpretation is correct this implies that the K^+ site not only is anatomically distinct from the H^+ site, but is so located that it is buried in a bilayer which is capable of moving protons due to pump incorporation.

In one sense therefore, this may explain the absence of an observed potential in intact vesicles and argues for equal and opposite electrogenicity of the two transport processes, the H^+ and K^+ transport in the vesicles. However, an alternative explanation may be that the form of the pump is different in natural vesicles and in a bilayer. With dilution or change in lipid environment it may be that a dissociation reaction is formed thus:

$$\text{dimer} \longrightarrow \text{monomer}$$

and that monomer transport has different electrical characteristics.

XII. Dimer-Monomer Transport Model

As mentioned above, there is some evidence that the $Na^+ + K^+$-ATPase may function as a dimer, or higher polymer of the catalytic subunit [21, 25]. If one makes the assumption as suggested in a recent review [25] that the functional dimer is composed of two different conformations E_1 and E_2 of the catalytic subunit, i.e., E_1E_2 and does not exist as E_1E_1 or E_2E_2, the reaction sequence

may be written thus:

$$E_1{}^*E_2P + ATP \xrightleftharpoons{H^+} H^+ \cdot PE_1{}^*E_2P \qquad \text{energization}$$

$$H^+ \cdot PE_1{}^*E_2P \xrightleftharpoons[K^+]{Mg^{++}} H^+PE_1{}^* \cdot E_2PK^+ \qquad \text{binding}$$

$$H^+ \cdot PE_1{}^*E_2PK^+ \rightleftharpoons H^+PE_2{}^* \cdot E_1PK^+ \qquad \text{transport}$$

$$HPE_2{}^* \cdot E_1PK^+ \rightleftharpoons H^+ + PE_2{}^* \cdot E_1 + Pi + K^+ \qquad \text{release}$$

Here the * is used to designate the same monomer. As written there is obligatory H^+ and K^+ exchange that is neutral. To convert this to an electrogenic mechanism, $2H^+$ can be translocated in exchange for 1 K^+ (Fig. 4).

When the reaction is written as the monomeric reaction, as in section 7b above, the translocation of H^+ is now distinct from the movement of K^+. The reaction:

$$E_2P \longleftrightarrow E_1P$$

which may occur in the absence of K^+ allows the transport to be electrogenic. The transformation:

$$E_2PK^+ \longleftrightarrow E_1PK^+$$

then represents a K^+ conductance. In the dimer form, this latter transformation depends on the simultaneous:

$$E_1PH^+ \longleftrightarrow E_2PH^+$$

which is energized, and hence cannot formally be represented as a conductance.

XIII. Localisation of the ATPase

Histochemical techniques for ATPase localization are, in general, unsatisfactory. Using a double antibody fluorescent technique, where antibody was raised against the free flow electrophoresis fraction, provided firm evidence that the transport fraction derived exclusively from parietal cells. Moreover, the fluorescence was localized to the apical region of the cytoplasm as would be expected of the localization of the tubulovesicles in the resting parietal cell [64].

General

It appears that the $H^+ + K^+$-ATPase is capable of catalysing a $K^+ : H^+$ exchange and separable H^+ and K^+ conductances are present in the pump mechanism.

The transport mechanism of this ATPase remains obscure as does the mechanism for any other transport ATPase. It seems evident that the mechanism is closely similar to that of the Na^+-K^+ and Ca^{++}-ATPases in that we have a reversible ATPase with a partially electrogenic mechanism and a reaction mechanism operating via a covalent phosphate.

In the discussion on the mechanism of the mitochondrial ATPase, it was pointed out that the protonated intermediate could interact with ADP and Pi binding sites increasing the electrophilic reactivity of the phosphorus. This could result from a direct protonation reaction, or from a conformational change, or both.

In the K^+-ATPase, H^+ and K^+ both play a role in the interconversion of chemical and ion gradient energy forms. We have presented some evidence that the hydrolytic site which forms the covalent intermediate is mobile across the membrane or that the K^+ site is mobile. Binding of K^+ or H^+ at either side of the membrane would serve not only to activate formation or hydrolysis of the intermediate, but also to provide the energy for the conformational change resulting in translocation of the phosphate or the K^+ site on the protein.

In the introduction some detail was presented on the mechanisms of the H^+ ATPase and the plasma membrane type of ATPases. Considering the data available on the gastric ATPase, the mechanism of action of this enzyme seems clearly more closely related to the plasma membrane type of ATPase than the electrogenic H^+ ATPase of mitochondria. This does not mean, that when the molecular mechanism is understood, entirely different reaction paths will be found. For example, if the gastric ATPase functions to transport H^+ by the energized downshift of a group pK_a, this would make an analogy to the photolytic H^+ transport by lumirhodopsin. Mitochondrial FI ATPase may also alter the pK_a of a protonatable group as a function of binding of Pi or ADP. The additional subunit complex of F_1, the F_o with its attendant binding sites which serve to conduct H^+ may be incorporated into the peptide backbone of the gastric ATPase. The nonelectrogenic character of the latter may be determined by the dimeric nature of the transport form, rather than by the characteristics of the ion translocation process itself.

XIV. Relationship of Vesicles to Intact Tissue

In this section, the properties of acid secretion by intact mucosa will be discussed entirely in relationship to the data obtained for hog gastric vesicles. Intact tissue secretion has been well defined only for amphibian mucosa hence the comparison will be between amphibian secretion and mammalian vesicles.

A. Cl^- Transport

As mentioned, gastric vesicles have a low Cl^- permeability, but a Cl^- space equivalent to the cation (Rb^+) space, as well as equivalent uptake rate for Cl^- ($T_{1/2}$=36 min at 22° C). No evidence could be obtained for active Cl^- transport in these vesicles.

The short circuited amphibian mucosa actively transport Cl^- in that there is a net S → M flux of Cl^- under these conditions (52). Removal of Na^+ abolished the Cl^- component as well as the potential difference across the tissue [53]. The addition of amytal inhibits H^+ and Cl^- secretion but adding ascorbate and mena-

dione [51] restores 80% of the ATP level and Cl^- transport, but not H^+ secretion. It would appear that Cl^- transport may therefore be ATP dependent, but complex I is critical for H^+ secretion.

The vesicles discussed above lack the Cl^- transport system. In the absence of Cl^- there is a 80% decline in acid rate if SO_4^{--} is the substituting anion in the medium bathing the mucosa [54]. Removal of Cl^- and addition of SO_4^{--} also reduced H^+ transport and Rb^+ transport in the vesicles but by about 40% (42). Addition of SCN^- did not restore the H^+ uptake in the vesicles, so the reduction in H^+ rate is not due to the development of a potential in SO_4^{--}. This is confirmed by the lack of change of SCN^- uptake or ANS fluorescence with ATP addition in the absence of valinomycin. The reduction by 40% of these parameters in the presence of valinomycin is consistent with the expected fall in the K^+ gradient dependent potential.

Thus, the anion effect in vesicles is reasonably consistent with the data on the intact tissue, but as will be seen later the interpretation has to be different to what has been thought correct for the intact stomach.

B. Metabolic Data

Over the years there has been considerable controversy over the primary energy source for acid secretion, i.e., whether an ATP or directly redox linked process was responsible [5]. The massive quantity of mitochondria in the parietal cell has made a decision particularly difficult. The problem is also complicated by the fact that secretion and metabolism are both stimulated by secretagogues, hence transients that are present due to secretion may be observed by those due to stimulation of metabolism.

The most detailed study of ATP and related nucleotide levels as well as that of phosphocreatine gave only marginal evidence of an ATP-related transport phenomenon [55]. These results in dogs with a large change in secretory rate are in fair agreement with the results in frogs with much smaller changes in secretion [56].

The data obtained by spectroscopic observations of intact frog mucosa [57] have been interpreted as substantiating a redox energy source for acid secretion. As discussed in detail elsewhere, however, [65] this data can be interpreted differently. However, when the observations on metabolite levels made on intact dog mucosa are combined with the spectroscopic data on frogs, it appears that a crossover does occur with onset of secretion between NAD^+ and FAD in the mitochondrial respiratory chain, with reduction of cytoplasmic NAD^+. This suggests that an additional component may be involved in gastric acid secretion other than the $H^+ + K^+$ ATPase.

C. Morphological Data

It seems well established that at rest, the cytoplasm of the parietal cell is filled with tubulo-vesicles the contents of which are not in continuity with the luminal bathing solution [57]. These specialized structures fuse with the apical surface of the cell and vastly increase its surface area upon stimulation of secretion [58]

and then revert to the cytoplasmic form with cessation of secretion. This provides a rationale for two of the major findings discussed above; first a unique and simple structure present in fractions of this tissue and second a degree of ion impermeability usually found only in preformed vesicles. It would seem intuitively obvious, althoug not proven, that the vesicular structures contain a component essential for H^+ secretion, as for example the $H^+ + K^+$ ATPase.

It is therefore possible to develop the hypothesis that at least part of transport regulation by gastric mucosa is due to incorporation of the pump into the plasma membrane of the cell. As such, this is a relatively unique means of transport regulation.

D. The Requirement for K^+

That H^+ secretion had a requirement for K^+ in the bathing solution was shown almost 20 years ago [59]. Removal of K^+ rapidly inhibited secretion, at a time when tissue K^+ had only been slightly reduced [60]. Addition of K^+ to the mucosal solution rapidly restored secretion [60]. Hence, it would appear that a small K^+ compartment is essential for secretion. This was confirmed in experiments using Rb^+ to restore insulin inhibited secretion in the dog [61]. Moreover, the K_M for K^+ is much less than the acid rate [62]. This finding is consistent with a recycling mechanism for K^+ if involved in $K^+ : H^+$ exchange. As for the vesicles, Rb^+ and Cs^+ can partially substitute for K^+, but not Na^+ or Li^+.

The data for the vesicles are therefore quite compatible with the findings on intact mucosa.

E. Electrogenicity of H^+ Secretion

One of the most striking results in amphibian mucosa is the finding that while acid secretion continues in SO_4^{--} containing, Cl^- free solutions, the P.D. across the mucosa is inverted, i.e., the lumen is positive [54]. Moreover, the P.D. is linearly related to the acid rate [63]. This has been interpreted as compelling evidence for electrogenic H^+ secretion. In Cl^- solutions, the data are much less convincing. Based on this, one would anticipate that, at least in SO_4^{--} solutions, evidence would have been obtained for electrogenic H^+ uptake in vesicles.

However, an alternative interpretation of the SO_4^{--} effect on acid secretion may be proposed. In SO_4^{--} solutions, in contrast to Cl^- solutions, the mucosal surface of the tissue demonstrate a K^+ selective conductance [38].

If the inverted potential is then due to a K^+ diffusion potential across the mucosal surface of the tissue, then the magnitude of the potential will be a function of the concentration of K^+ at the luminal surface.

In the presence of an $H^+ + K^+$ exchange that is non-electrogenic, the K^+ concentration at this surface will be reduced in proportion to the acid rate, hence the potential will also be proportional to the acid rate.

Thus, although electrogenic H^+ secretion may be the correct interpretation of data from the intact mucosa, alternate explanations may be correct (Fig. 11). Such explanations are certainly necessary to reconcile vesicle data with those of intact organs.

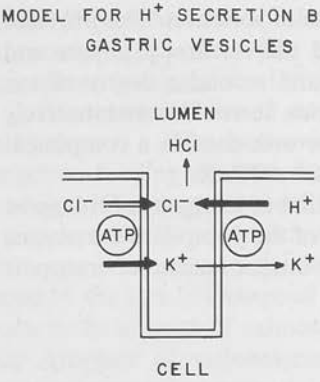

Fig. 11. Schematic representation of secretory surface of parietal cell. H^+ secretion is visualized as being due to the $H^+ + K^+$ ATPase, here due to an $H^+ + K^+$ exchange. K^+ is visualized as diffusing into the lumen accompanying electrogenic active Cl^- transport that is also ATP dependent. Site of energization of Cl^- transport may not be at the apical membrane

XV. Summary

It would appear, therefore, that hog gastric mucosa contains a particularly interesting system which in many respects is compatible with a model for H^+ secretion. It is quite different, at current levels of analysis, from the H^+ ATPase of mitochondria. Indeed the stomach appears to have developed a unique method of developing H^+ gradients. The magnitude of this gradient is such that perhaps this ATPase is only partially responsible, and that a second pump, in series with the one discussed in some detail here, is required for the complete process.

References

1. Mitchell, P.: Coupling of phosphorylation to electron and hydrogen transfer by a chemiosmotic type of mechanism. Nature (Lond.) **191,** 144–148 (1961)
2. Jagendorf, A. T., Uribe, E.: ATP formation caused by acid-base transition of spinach chloroplasts. Proc. nat. Acad. Sci (Wash.) **55,** 170–177 (1966)
3. Kagawa, Y., Racker, E.: Partial resolution of the enzymes catalyzing oxidative phosphorylation. XXV. Reconstitution of vesicles catalyzing ^{32}Pi-ATP exchange J. biol. Chem. **246,** 5477-5487 (1971)
4. Racker, E., Stoeckenius, W.: Reconstitution of purple membrane vesicles catalyzing light driven H^+ uptake and ATP formation. J. biol. Chem. **249,** 662–666 (1974)
5. Hersey, S. J.: Interaction between oxidative metabolism and acid secretion in gastric mucosa. Biochim. biophys. Acta **244,** 157–203 (1974)
6. Senior, A. E.: The structure of mitochondrial ATPase. Biochim. biohys. Acta **301,** 249–277 (1973)
7. MacLennan, D. H., Tzagoloff, A.: Studies on the mitochondrial adenosine triphosphatase system. IV. Purification and characterization of the oligomycin sensitivity conferring protein. Biochemistry **7,** 1603–1609 (1968)
8. Pullman, H. W., Monroy, G. C.: A naturally occurring inhibitor of mitochondiral ATPase. J. biol. Chem. **238,** 2762–2769 (1963)
9. Hinkle, P. C., Horstman, L. L.: Respiration driven proton transport in submitochondrial particles. J. biol. Chem. **246,** 6024–6028 (1971)
10. Mitchell, P., Moyle, J.: Mechanism of proton translocation in reversible proton translocating ATPases. Biochemistry **4,** 91–111 (1974)
11. Holloway, C. T., Roberton, A. M., Knight, I. G., Beechey, R. B.: The binding of [^{14}C] dicyclohexylcarbodiimide to mitochondrial fractions. Biochem. J. **100,** 79 (1966)

12. Kroman, E. F., McLick, J.: ATP synthesis in oxidative phosphorylation: A direct-union stereochemical reaction mechanism. J. Bioenerg. **3,** 147–158 (1972)
13. Skou, J. C.: Enzymatic basis for active transport of Na^+ and K^+ across cell membrane. Physiol. Rev. **45,** 596–617 (1965)
14. Martonosi, A.: Transport of calcium by the sarcoplasmic reticulum. In: Metabolic Transport. Hokin, L. E. (ed.). New York: Academic Press, 1972, Vol VI, p. 317–349
15. Ganser, A. L., Forte, J. G.: K^+ stimulated ATPase in purified microsomes of bullfrog oxyntic cells. Biochim. biophys. Acta **307,** 169–180 (1973)
16. Degani, G., Boyer, P. D.: A borohydride reduction method for characterization of the acyl phosphate linkage in proteins and its application to sarcoplasmic reticulum ATPase. J. biol. Chem. **248,** 8222–8226 (1973)
17. Nishigaki, T., Chen, F. T., Hokin, L. E.: Studies on Na+K ATPase. XV. Direct chemical characterization of acyl phosphate in the enzyme as β-aspartyl phosphate. J. biol. Chem. **249,** 4911–4916 (1974)
18. Post, R. L., Merritt, C. R., Kinsolving, C. R., Albright, C. D.: Membrane adenosine triphosphatase as a participant in the active transport of sodium and potassium in the human erythrocyte. J. biol. Chem. **235,** 1796–1802 (1960)
19. Fahn, S., Hurley, J. R., Koral, G. J., Albers, R. W.: Sodium potassium activated adenosine triphosphatase of electrophoresis electric organ. J. biol. Chem. **241,** 1890–1895 (1966)
20. Taniguchi, K., Post, R. L.: Synthesis of ATP and exchange between Pi and ATP in $Na^+ + K^+$ ATPase. J. biol. Chem. **250,** 3010–3018 (1973)
21. Kepner, G. R., Macey, R. I.: Membrane enzyme systems. Biochim. biophys. Acta **163,** 188–203 (1968)
22. Goldin, S. N., Tong, J. W.: Reconstitution of active ion transport by the Na+K ATPase J. biol. Chem. **249,** 5902–5915 (1975)
23. Shamoo, A. E., Ryan, T. E.: Isolation of ionophores from ion transport systems. Ann. N. Y. Acad. Sci. **264,** 83–97 (1975)
24. Racker, E., Knowles, A. F., Eytan, E.: Resolution and reconstitution of ion transport system. Ann. N. Y. Acad. Sci. **264,** 17–33 (1975)
25. Glynn, I. M., Karlish, J. D.: Different approaches to the mechanism of the sodium pump. In: *Energy Transformation in Biological System*, 205–224 (1975) Ciba Geigy
26. Forte, J. G., Forte, G. M., Saltman, P.: K^+ stimulated phosphatase of microsomes from gastric mucosa. J. cell. comp. Physiol. **69,** 293–304 (1967)
27. Sachs, G., Rose, J. D., Shoemaker, R. I., Hirschowitz, B. I.: Phosphatase reactions of transport ATPase. Physiologist, **9,** 281 (1966)
28. Sachs, G., Rose, J. D., Hirschowitz, B. I.: Acetyl phosphatase in rat brain microsomes. Arch. Biochem. **119,** 277–281 (1967)
29. Albers, R. W., Arnaiz, G. R. L., De Robertis, E.: Sodium-potassium-activated ATPase and potassium-activated p-nitrophenylphosphatase: A comparison of their subcellular localizations in rat brain. Proc. nat Acad. Sci. (Wash.) **53,** 557–564 (1965)
30. Ganser, A. L., Tanisawa, A. S., Forte, J. G.: The K^+-stimulated ATPase system of microsomal membranes from gastric oxyntic cells. Ann. N. Y. Acad. Sci. **242,** 255–267 (1974)
31. Forte, J. G., Ganser, A., Beesly, R., Forte, T. M.: Unique enzymes of purified microsomes from pig fundic mucosa. Gastroenterology **69,** 175–189 (1975)
32. Spenney, J. G., Saccomani, G., Spitzer, H. L., Sachs, G.: Characterization of gastric mucosal membranes. Arch. Biochem. biophys. Acta **161,** 456–471 (1974)
33. Saccomani, G., Stewar, H.B., Shaw, D., Lewin, M., Sachs, G. Fractionation and purification of K^+ ATPase containing vesicles. Biochim. biophys. Acta **465,** 311–330 (1977)
34. Saccomani, G., Shah, G., Spenney, J. G., Sachs, G.: Localization of peptides by iodination and phosphorylation. J. biol. Chem. **250,** 4802–4809 (1975)
35. Saccomani, G., Rabon, E., Sachs, E.: In preparation.
36. Sachs, G., Hirschowitz, B. I.: (1968) Secretion by in vitro amphibian mucosa IN: Physiology of Gastric Secretion. Myren, J. (ed.). Oslo: Oslo University Press, 1968, pp. 186–202
37. Jarnefelt, J., Stedingk, L. V. von: Some properties of the ATP dependent Na binding system of rat brain microsomes. Acta physiol. scand **57:** 328–338 (1963)
38. Sachs, G., Shoemaker, R. L., Blum, A. L., Helander, H. F., Makhlouf, G. M., Hirschowitz, B. I.: (1971) Microelectrode studies of gastric mucosa. IN: Electrophysiology of Epithelial Cells. Giebisch, G. (ed.) pp. 257–279

39. Ganser, A. L., Forte, J. G.: Ionophoretic stimulation of K^+ ATPase of oxyntic cell microsomes. Biochem. Biophys. Res. Comm. **54,** 690–696 (1973)
40. Lee, J., Simpson, E., Scholes, P.: Changes of outer pH in suspension of membrane vesicles accompanying ATP hydrolysis. Biochem. Biophys. Res. Commun. **60,** 825–834 (1974)
41. Sachs, G., Rabon, E., Saccomani, G., Sarau, H. M.: Redox and ATP in acid secretion. Ann. N. Y. Acad. Sci. **264,** 456–475 (1975)
42. Sachs, G., Hung, H., Rabon, E., Schackmann, R., Lewin, M., Saccomani, G. A non-electrogenic H^+ pump in plasma membranes of hog stomach. J. biol. Chem. **251**, 7690–7698 (1976)
43. Alberty, R. A.: Standard Gibbs free energy, enthalpy and entropy changes as a function of pH and pMg for several reactions involving adenosine phosphates. J. biol. Chem. **244,** 3290–3302 (1969)
44. Martin, V. S., Sokolov, J. S., Boguslavsky, L. I., Janskinsky, L. S.: Nigericin induced charge transfer across membranes. J. Membr. Biol. **25,** 23–46 (1973)
45. Witt, T. H.: Primary acts of energy conservation in the functional membrane of photosynthesis. (1974) Ann. N. Y. Acad. Sci. **227,** 203–206 (1974)
46. Brand, M. D., Reynafarje, B., Lehninger, A. L.: Stoichiometric relationship between H^+ and electron transport. Proc. nat. Acad. Sci. (Wash.) **73,** 437–441 (1976)
47. Schackmann, R., Schwartz, A., Saccomani, G., Sachs, G.: Cation transport by gastric $H^+ + K^+$ ATPase. J. Membr. Biol. **32**, 361–381 (1977)
48. Scarborough, G. A.: The neurospora plasma membrane ATPase is an electrogenic pump. Proc. nat. Acad. Sci. **73,** 1485–1488 (1976)
49. Azzi, A., Gheradini, P., Santato, P.: Flurochrome interaction with the mitochondrial membrane. J. biol. Chem. **246,** 2035–2042 (1971)
50. Lewin, M., Saccomani, G., Schackmann, R., Sachs, G.: Use of ANS as a probe of gastric vesicle transport. J. Membr. Biol. in press **32**, 301–318 (1977)
51. Goodall, M. C., Sachs, G.: Reconstitution of a proton pump. J. Membr. Biol. in press (1977)
52. Hogben, C.A.M.: The Cl^- transport system of gastric mucosa. Proc. nat. Acad. Sci. **37,** 343–395 (1951)
53. Sachs, G., Shoemaker, R. L., Hirschowitz, B. I.: Effect of Na removal from in vitro frog gastric mucosa. Proc. Soc. exp. Biol. (N. Y.) **123,** 47–52 (1966)
54. Heinz, E., Durbin, R. P.: Evidence for an independent H^+ ion pump in the stomach. Biochim. biophys. Acta **31,** 246–247 (1959)
55. Sarau, H. M., Foley, J., Moonsamy, G., Wiebelhaus, V. D., Sachs, G.: Metabolism of dog gastric mucosa. J. biol. Chem. **250,** 8321–8329 (1975)
56. Durbin, R. P., Michelangeli, F., Michel, A.: Active transport and ATP in frog gastric mucosa. Biochim. biophys. Acta **357,** 177–189 (1974)
57. Sedar, A. W.: Fine structure of the stimulated oxyntic cell. Fed. Proc. **24,** 1360–1367 (1965)
58. Helander, H. F., Hirschowitz, B. I.: Quantitative ultrastructural studies on gastric parietal cells. Gastroenterology **63,** 951–961 (1972)
59. Harris, J. B., Frank, H., Edelman, I. S.: Effect of K^+ on ion transport and biolectric potentials of frog gastric mucosa. Amer. J. Physiol. **195,** 499–504 (1958)
60. Rehm, W. S., Sanders, S. S., Rutledge, J. R., David, T. L., Kurfee, J. F., Keesee, D. C., Bajandas, F. J.: Effect of removal of external K^+ on frog stomach in Cl^- free solutions. Amer. J. Physiol. **210,** 689–693 (1966)
61. Hirschowitz, B. I., Sachs, G.: Insulin inhibition of gastric secretion reversal by Rb^+. Amer. J. Physiol. **213,** 1401–1405 (1967)
62. Sachs, G., Collier, R. H., Pacifico, A., Hirschowitz, B. I.: Action of SCN^- on gastric mucosa in vitro. Biochim. biophys. Acta **173,** 504–507 (1969)
63. Rehm, W. S.: Electrophysiology of gastric mucosa in Cl^- free solutions. Fed. Proc. **24,** 1387–1395 (1965)
64. Sachs, G., Mihas, A., Crago, S., Saccomani, G.: Localization of a gastric H^+ pump component. Gastroenterology Abstr. **72**, 1125 (1977)
65. Rabon, E.C., Sarau, H.M., Rehm, W.S., Sachs, G.: Redox involvement in acid secretion in the amphibian gastric mucosa. J. Membr. Biol. in press (1977)

THE JOURNAL OF BIOLOGICAL CHEMISTRY
Vol. 250, No. 12, Issue of June 25, pp. 4802–4809, 1975
Printed in U.S.A.

Characterization of Gastric Mucosal Membranes

VIII. THE LOCALIZATION OF PEPTIDES BY IODINATION AND PHOSPHORYLATION*

(Received for publication, November 22, 1974)

GAETANO SACCOMANI, GING SHAH, JERRY G. SPENNEY, AND GEORGE SACHS‡

From the Laboratory of Membrane Biology, Division of Gastroenterology, University of Alabama in Birmingham, and Veterans Administration Hospital, Birmingham, Alabama 35294

SUMMARY

Two fractions of gastric mucosal membranes obtained by Ficoll-sucrose density gradient centrifugation were studied by a variety of techniques to localize the polypeptides. Gel electrophoresis showed the presence of five major polypeptides and several minor ones. Only one of these, 82,000 daltons, was available for iodination in the intact tissue. The two membrane fractions differed in their accessibility to peroxidase. The denser fraction showed two major defined iodination peaks at 82,000 and 102,000 daltons. Freeze-thawing and iodinating with ^{131}I produced additional labeling of peaks as well as relabeling the 82,000-dalton component, showing it was accessible from both sides of the membrane. The two major components were also sensitive to cross-linking, the 102,000 polypeptide being especially sensitive to -SH oxidation. Proteolysis with trypsin removed both components in the denser membrane fraction, in addition to inhibiting the K^+-ATPase and K^+-*p*-nitrophenylphosphatase of that fraction. Phosphorylation with [γ-^{32}P]ATP labeled the 102,000-dalton component and K^+, HCO_3^- and *p*-nitrophenylphosphate reduced the level of labeling. Hence the 102,000 region contains a subunit of the ATPase, is readily iodinated in inside-out vesicles, and is the most available for interpeptide S—S cross-linking.

Topographical knowledge of lipid and peptide arrangement in natural membranes forms an integral part of an understanding of membrane function. Peptide localization depends on the use of a variety of labeling techniques, using nonpenetrating reagents. Peroxidase-dependent iodination (1), the formation of a Schiff base using pyridoxal phosphate followed by borotritide reduction (2), and formyl methionyl sulfone acylation (3) are among the many reactions used. Another approach has been the use of proteolytic enzymes to remove surface groups (4). Localization of enzymes is in part determined by consideration of the probable localization of substrate; hence phosphorylation of the larger polypeptide of ($Na^+ + K^+$)-ATPase is taken as evidence for the internal localization of that polypeptide (5). Use of an inhibitor such as ouabain, known to be effective on only one side of the membrane, shows that the same peptide is labeled by ouabain (6), hence must also be available on the outside surface.

Other techniques, especially double labeling with ^{125}I and ^{131}I (7) can be used to determine whether a peptide traverses the membrane. In general all of these techniques have been applied to isolated cell suspensions, such as the red cell (8), platelets (9), fat cells (10), HeLa cells (11), and ascites tumor cells (12). The sidedness of membranes of subcellular organelles such as mitochondria (13) and microsomes (14) has also been investigated using iodination techniques assuming maintenance of restricted permeability during preparation. A refinement of this localization technique investigates potential peptide interaction in the membrane by the use of cross-linking reagents or reactions (15) on the assumption that cross-linking will occur only between closely associated peptides.

Although iodination of an epithelium has been described (16), to our knowledge no investigation of peptide localization in such tissue has been published. The gastric mucosa has certain distinct advantages in such a study. The apical membrane of the acid secreting cell contains a HCO_3^--stimulated ATPase (17) and a K^+-stimulated ATPase (18) which form a phosphorylated intermediate similar to the ($Na^+ + K^+$)-ATPase (19), allowing functional localization and identification of that peptide. Moreover, this cell in the resting and nonsecreting state contains apical vesicles which upon stimulation fuse with the plasma membrane (20) in such a way that they evert, hence are "inside-out" in the intact cell (21). Recently, a method has been described using zonal rotors for large scale purification of this membrane fraction enriched in HCO_3^- or K^+-ATPase (22, 23) and the membrane polypeptides characterized (24).

In this study we report data on localization of certain of the polypeptides of intact and fractionated membranes of gastric mucosa and the functional identification of one of these.

EXPERIMENTAL PROCEDURE

Materials

ATP, AMP, *p*-nitrophenylphosphate (Ditris salt), phenylmethanesulfonyl fluoride, lactoperoxidase (40 to 50 units/mg),

* This research was supported by National Institutes of Health Grants AM15878, CA13158, and HL11310 and National Science Foundation Grant GB31075. Credit is given to Projects 8059-01 and 8059-02, Veterans Administration Hospital, Birmingham, Alabama.

‡ To whom communications regarding this paper should be addressed at: Laboratory of Membrane Biology, University of Alabama in Birmingham, University Station, Birmingham, Alabama 35294.

benanthroline, trypsin, α-chymotrypsin, and soybean trypsin ibitor were obtained from Sigma. Glucose oxidase (110 units/) was obtained from Worthington. Glutaraldehyde (8% solu-) came from Fisher Scientific Corp. γ-Globulin (human), ine serum albumin, ovalbumin, chymotrypsinogen A (beef reas), and myoglobin (sperm whale) were purchased from warz/Mann. Na ^{125}I and Na ^{131}I were purchased from Inter- ional Chemical and Nuclear Corp., Cleveland, Ohio. [γ-^{32}P]- P was purchased from New England Nuclear. All of the chemi- were reagent grade.

Methods

paration of Gastric Membranes

The technique used has been previously described (25). Briefly, dog gastric mucosa is stripped from the underlying connective sue, homogenized in 0.25 M sucrose-20 mM Tris-HCl (pH 7.4) the post 20,000 × *g* supernatant centrifuged at 100,000 × *g* 60 min. The precipitate is then distributed by zonal centrif- tion using a continuous density gradient made from 7.5% w) Ficoll-0.25 M sucrose and 37% (w/w) sucrose in 20 mM Tris- l buffer as described (22).

Membranes collected at 11.5% sucrose (Peak I) and 23% su- se (Peak II) were then diluted with 20 mM Tris-HCl (pH 7.4) less than 10% sucrose and centrifuged at 100,000 × *g* for 60 to obtain purified gastric cell membrane pellets from either ve. The amount of protein in both fractions was determined rding to Lowry *et al.* (26).

ymatic Assays

The ATPase and AMPase activity was assayed in a medium taining 3 mM ATP or AMP, 3 mM $MgCl_2$, 100 mM Tris-HCl H 7.4) in the presence or absence of 20 mM $NaHCO_3$ and 20 mM l. The phosphate released was measured by the method of kin and Yoda (27) following incubation at 37° for 15 min.

N-Ph-Pase[1] activity was assayed in a medium containing 6 *p*-nitrophenylphosphate, 6 mM $MgCl_2$, 20 mM Tris-acetate H 7.5) in the presence or absence of 20 mM KCl. The *p*-nitro- nol liberated was measured by the method of Torriani (28).

teolytic Digestion

Suspensions of isolated gastric membranes in 20 mM Tris-HCl H 7.4) were treated with varying concentrations of trypsin and ymotrypsin for different periods of time.

n a typical experiment, 1 mg/ml of membrane protein was in- ated at 37° and the digestion was initiated by the addition of g of proteolytic enzymes preincubated at the same tempera- e. The suspensions were incubated for 10 min at 37° in a shaker h. To terminate the reactions, 250 μg of soybean trypsin in- itor (type I-S) were added to the trypsin sample and 0.1 ml mM $PhCH_2SO_2F$ were added to the α-chymotrypsin sample. suspensions were cooled to 0–4° and centrifuged. The pellets e washed three times in 20 mM Tris-HCl buffer and then sub- ed to electrophoresis, following Na dodecyl-SO_4-β-mercapto- nol solubilization.

The degree of proteolytic digestion was assessed by comparing Lowry-reactive material in the treated and the native mem- nes.

n other experiments, membrane particles were incubated in ia for measurement of ATPase, K^+-ATPase and HCO_3^-- Pase, AMPase, pN-Ph-Pase and K^+-pN-Ph-Pase with and out the addition of the proteases. Samples of the incubation ium were taken at different times and assayed for substrate rolyzed. Alternatively the washed pellet as treated above was yed for residual enzyme activity.

nation Procedure

Plasma Membrane Fractions—The iodination technique used a modification of the Reichstein-Blostein method (29). Mem- nes were suspended in 20 mM Tris-HCl (pH 7.4) and the sample g/ml) was incubated in a shaking water bath at 37° for 15 min in a medium consisting of 10^{-6} M NaI containing 25 μCi of carrier-free Na ^{125}I or Na ^{131}I, 40 μg/ml of peroxidase, 20 μg/ml of glucose oxidase, and 1 mg/ml of glucose.

The labeling reactions were stopped by the addition of ice-cold 10^{-5} M $Na_2S_2O_3$ (final concentration) followed by washing the suspension with a large excess of cold Tris-HCl buffer three times before solubilization in Na dodecyl-SO_4. Membranes treated similarly, but without peroxidase, contained no incorporated label, nor was there an incorporated label when ^{125}I was added subsequent to solubilization. In some experiments the membrane fractions were freeze thawed at least five times and reiodinated with ^{131}I under the same conditions.

In pilot experiments, the concentration of NaI and incubation times were varied, and it was determined that saturation of labeling was achieved at the above concentration and incubation times.

Intact Gastric Mucosa—Fresh dog gastric fundus was washed with cold 0.25 M sucrose-20 mM Tris-HCl (pH 7.4) and opened. It was placed in a glass container with 10 ml of sucrose buffer solution containing 1 mCi Na ^{125}I carrier-free, 0.4 mg of peroxidase, 0.2 mg of glucose oxidase, and 10 mg of glucose. The mixture was bubbled with O_2-CO_2 (95:5, v/v) for 20 min at room temperature. The tissue was then scraped and fractionated as described earlier.

One milliliter of the final 100,000 × *g* pellet suspension was layered on a linear density gradient made from 7.5% (w/w) Ficoll-0.25 M sucrose and 37% (w/w) sucrose and centrifuged for 16 hours at 23,500 rpm in a Spinco SW 25 rotor. Each protein fraction (Peak I and II) was pooled, diluted, and centrifuged at 100,000 × *g* for 60 min.

The relabeling reaction with Na ^{131}I was performed on each gastric membrane fraction as described above. Gel electrophoresis was carried out on the pellets after Na dodecyl-SO_4 solubilization.

Phosphorylation Procedure

[γ-^{32}P]ATP with a specific activity of 16.4 Ci/mM was used to label the gastric ATPase. Thirty micrograms of membrane protein were incubated at 4° for 30 s in a solution containing 20 mM Tris-HCl (pH 7.4), 1 mM $MgCl_2$, 2 μM ATP containing 0.2 μCi of [γ-^{32}P]ATP in the presence or absence of 20 mM KCl and 20 mM choline bicarbonate, in a total volume of 0.1 ml. The reaction was stopped by the addition of 1 ml of ice-cold 5% $HClO_4$ containing 1 mM P_i and 0.1 mM ATP as carriers to reduce nonenzymatic labeling. The time course of the reaction showed that at 30 s steady state labeling had been achieved. In some experiments, varying concentrations of pN-Ph-P were added.

The samples were filtered through Millipore filters type HA25 (Millipore Corporation) and washed four times with the cold stop solution. Dried filters were placed in glass scintillation vials and counted in a Nuclear-Chicago liquid scintillation counter using 10 ml of Aquasol (New England Nuclear) as scintillation fluid. For samples which were to undergo electrophoresis, the labeling reaction was stopped with 1% Na dodecyl-SO_4-5% mercaptoethanol and electrophoresis performed at 4°.

Cross-Linking Reactions

Gastric membrane pellet from Peaks I and II was resuspended in 20 mM Tris-HCl buffer (pH 7.4) to approximately 2 mg of protein/ml. A suspension of 50 μl was mixed with an equal volume of reagent dissolved in the same buffer. Concentrations of glutaraldehyde ranging from 0.1 mM to 3 mM and concentrations of *o*-phenanthroline/$CuSO_4$ at micromolar levels of 50/10, 25/50, 100/20 were used. Samples were incubated at room temperature for fixed intervals of time varying from 10 to 60 min. The reactions were stopped by the addition of 50 μl of 5% Na dodecyl-SO_4. In some experiments membrane suspensions treated with glutaraldehyde or *o*-phenanthroline were solubilized in 5% Na dodecyl-SO_4-0.16 M β-mercaptoethanol. The optimal conditions were determined to be 60 min incubation time at 3 mM glutaraldehyde and 50 μM *o*-phenanthroline.

Polyacrylamide Gel Electrophoresis in Na Dodecyl-SO_4

Membrane protein was solubilized by incubating for 15 min at 37° in 20 mM Tris-HCl buffer (pH 7.4), containing 1% Na dodecyl-SO_4-5% β-mercaptoethanol. Samples (50 to 100 μg of protein) were applied to the gels (6.0 mm × 80 mm) containing 0.1% detergent. A 3.5% stacking gel was prepared in 0.1 M Tris-HCl (pH 6.8) by polymerization using dimethylaminoproprionitrile (1

[1] The abbreviations used are: pN-Ph-Pase, *p*-nitrophenylphosphatase; pN-Ph-P, *p*-nitrophenolphosphate; $PhCH_2SO_2F$, phenylmethanesulfonyl fluoride; Na dodecyl-SO_4, sodium dodecyl sul-

μl/ml of gel solution). Separating gels were 10% acrylamide prepared in 0.4 M Tris-HCl (pH 8.6). In each gel 2.5% of the acrylamide was *N,N'*-methylenebisacrylamide. Reservoir buffer was 0.19 M glycine adjusted to pH 8.6 with solid Tris-base. Electrophoresis was performed at constant current of 1 ma/gel until the buffer front had entered the running gel and the current was then increased to 2.5 ma/gel. The gels were stained for protein with Coomassie blue as described by Fairbanks *et al.* (30) and for carbohydrates by a periodic acid-Schiff procedure according to Korn and Wright (31).

For destaining, the gels were treated as previously described (24). Gel densitometry was carried out using a Gilford 2400 spectrophotometer equipped with a gel scanner at 1.0 cm/min using a slit width of 0.05 mm. Gels were scanned at 550 nm for Coomassie blue and at 560 nm for Schiff reagent.

The radioactive iodide distribution within the gels was determined by slicing the gels into sections of approximately 1.5-mm thickness and the γ emissions of each slice were counted directly in a Nuclear Chicago γ-spectrometer.

Gels run with ^{32}P-labeled membranes were sliced immediately after electrophoresis and each 1.5-mm slice incubated in 0.2 ml of 50% hydrogen peroxide at 60° overnight. The radioactivity was counted in 10 ml of Aquasol scintillation fluid in a Nuclear Chicago Isopac 300 liquid scintillation counter.

Molecular weight estimations were made on gels using γ-globulin (M_r = 160,000), bovine serum albumin (M_r = 67,000), ovalbumin (M_r = 45,000), chymotrypsinogen A (M_r = 25,000), and myoglobin (M_r = 17,800) as standards for proteins in absence of β-mercaptoethanol.

RESULTS

Electrophoretic Fractionation—Fig. 1, *A* and *B*, shows the polypeptide pattern from the two membrane fractions obtained from zonal density gradient centrifugation of the "microsomal" fraction of dog gastric mucosal homogenate. Excluding the band running at the dye front, there are 5 major bands in Peak I membranes out of a total of 30, and 4 major bands in Peak II out of a total of 31. Noteworthy is a prominent 150,000-dalton band in Peak II absent in Peak I. There are also two carbohydrate bands in each fraction, one running ahead of the dye front, a similar band being visible in red blood cell (31), human platelet membrane (32), and Hela cell membrane (33). It should be noted the M_r = 102,000 band is more prominent in Peak I.

Labeling of Intact Stomach—When the mucosal surface of intact dog stomach was labeled with ^{125}I and fractionated Ficoll-sucrose gradients as described under "Methods," Peak I and Peak II were labeled, but the mitochondrial peak not, showing the absence of intracellular label. Since, based enzyme assay, there is considerable cross contamination in t of both 5'-nucleotidase and K^+ pN-Ph-Pase (22, 23), label of both peaks is not unexpected. Gel electrophoresis of e fraction, shown in Fig. 2*A* and *B*, gave three labeling peaks which did not enter the running gel, a peak at M_r = 82,000 a peak at the dye front. The polypeptides of Peak II had al twice the labeling of those in Peak I.

Relabeling these membrane fractions with ^{131}I gave seve additional peaks, as well as labeling the high molecular we region of Peak I, the M_r = 82,000 polypeptides and low m

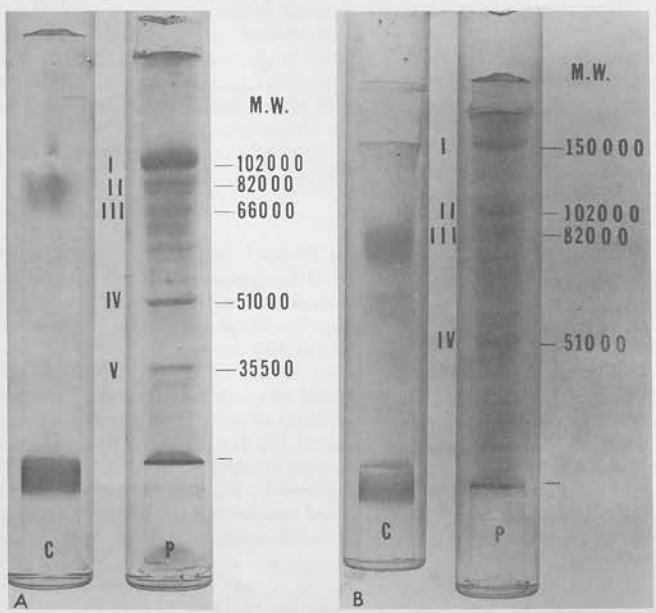

FIG. 1. *A*, Na dodecyl-SO_4-polyacrylamide gel electrophoretic patterns of Peak I stained with Coomassie blue for protein (*P*) and periodic acid-Schiff for carbohydrate (*C*). *B*, Na dodecyl-SO_4-polyacrylamide gel electrophoretic patterns of Peak II stained with Coomassie blue for protein (*P*) and periodic acid-Schiff for carbohydrate (*C*).

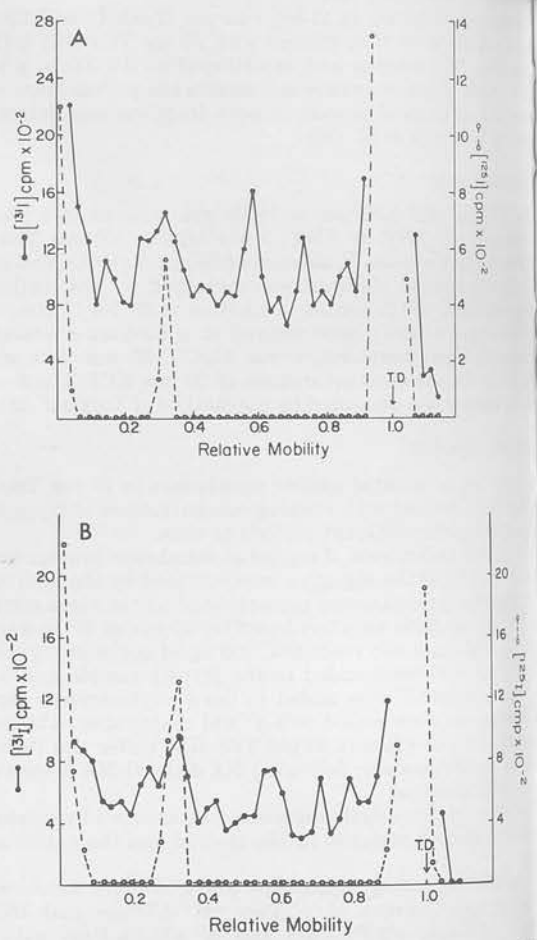

FIG. 2. *A*, Distribution of ^{125}I and ^{131}I in polypeptides of Pea I membrane after electrophoresis in Na dodecyl-SO_4 gels of 10 acrylamide. Intact dog gastric mucosa was labeled with ^{131} Peak I membrane fraction subjected to electrophoresis (O- - -O Same membranes were freeze-thawed and relabeled with (●——●). The maximum counts in the low M_r region (*brok peak*) were 1,800 cpm for ^{125}I and 25,000 cpm for ^{131}I labeling. shows the position of the tracking dye. *B*, distribution of ^{131} ^{131}I in polypeptides of Peak II membrane after electrophoresi Na dodecyl-SO_4 gels of 10% acrylamide. Intact dog gastric cosa was labeled with ^{125}I and Peak II membrane fraction s jected to electrophoresis (O- - -O). Same membranes were free thawed and relabeled with ^{131}I (●——●). The maximum cou in the low M_r region (*broken peak*) were 680 cpm for ^{125}I and 6,0 cpm for ^{131}I labeling. *T.D.* shows the position of the tracking d

ular weight regions of both Peaks I and II. The M_r = 82,000 d 51,000 regions were the most significantly labeled with ^{131}I. he pattern obtained was quite consistent, so that even the minor beling was quite reproducible. Both peaks had more ^{131}I counts the low molecular weight region than ^{125}I.

Labeling of Membrane Fractions—In this series of experiments membrane fractions were treated with ^{125}I, washed several mes, relabeled with ^{131}I after freeze-thawing, washed, dissolved, d subjected to electrophoresis. It was hoped that Peak II, ich was largely vesicular on electron microscopy, would demstrate restricted access to the peroxidase-I complex. The patrns observed were essentially identical in three separate experients, so that even minor labeling peaks occurred reproducibly. terms of the counts that entered the running gel, the heaviest beling occurred at the dye front, followed by labeling at M_r = ,000 and 102,000, in terms of both Peak I and Peak II. After eze-thawing, the low and high molecular weight polypeptides both fractions labeled with ^{131}I. Peak I showed equal relabeling of the M_r = 102,000 and 82,000 bands and a sharper labeling of M_r = 51,000 polypeptide. In contrast Peak II showed relabeling of the M_r = 82,000 polypeptide with ^{131}I to a greater extent than the M_r = 102,000 polypeptide, and relabeling of three other polypeptides to a relatively higher level than with the initial labeling, at M_r = 64,000, 51,000, and 31,500. The 51,000-dalton peak of ^{131}I corresponded to a broad region of initial labeling with ^{125}I (Fig. 3, *A* and *B*).

Cross-Linking Studies—Glutaraldehyde treatment of both Peak I and Peak II resulted in an alteration of polypeptide pattern, not reversed by β-mercaptoethanol, suggesting that since glutaraldehyde can react with both —SH and amino groups (34) the effects observed are due to $—NH_2$ cross-linking. Peak I shows a significant reduction in almost all of the peptides, with an increase of staining in the high molecular weight region whereas the effect of glutaraldehyde on Peak II is very slight with some increase of stain intensity in that region.

—SH oxidation of Peak I shows a reduction of intensity of several peaks, most notably those associated with the 102,000-dalton region. Peak II, however, shows some slight alteration in the intensity of the 33,500- and 31,500-dalton polypeptide, but most striking is the almost complete disappearance of the 102,000-dalton region, changes which are reversed by β-mercaptoethanol (Fig. 4).

Susceptibility to Proteolysis—When the gastric membrane fractions were treated with trypsin or α-chymotrypsin, there was a reduction in the intensity of many bands, particularly in the high molecular weight region, and an intensification of the low molecular weight region. All of the iodinated bands disappeared and ^{125}I increased at the dye front in both Peaks I and II (Fig. 5).

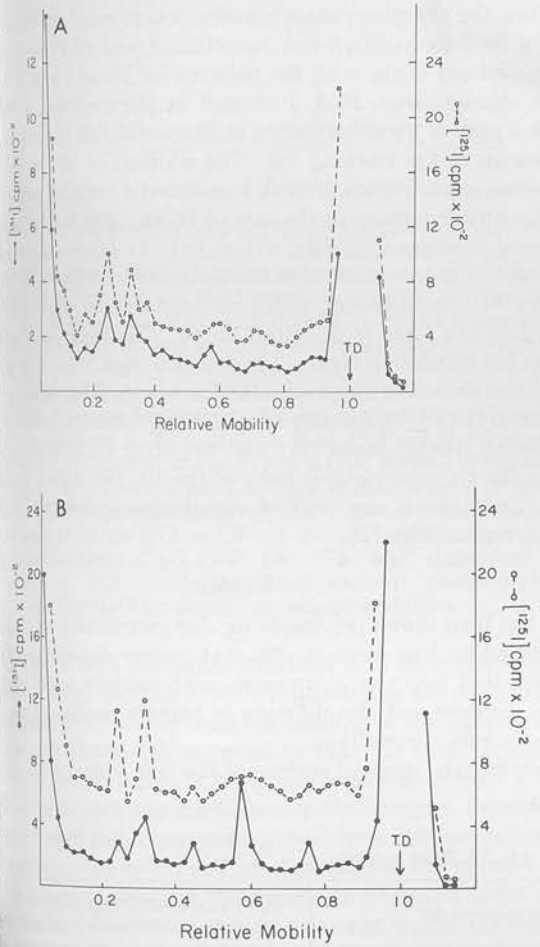

Fig. 3. *A*, Distribution of ^{125}I and ^{131}I of double labeled Peak I tric membrane following Na dodecyl-SO_4-electrophoresis in acrylamide gel. The membrane fraction was labeled with ^{125}I --O) and after freeze thaw relabeled with ^{131}I (●——●). maximum counts in the low M_r region (*broken peak*) were 0 cpm for ^{125}I and 21,000 cpm for ^{131}I labeling. *T.D.* shows position of the tracking dye. *B*, distribution of ^{125}I and ^{131}I ouble labeled Peak II gastric membrane, following Na do-SO_4 electrophoresis in 10% acrylamide gel. The membrane ion was labeled with ^{125}I (○- - -○) and after freeze-thaw, eled with ^{131}I (●___●). The maximum counts in the low gion (*broken peak*) were 13,000 cpm for ^{125}I and 11,000 cpm I labeling. *T.D.* shows the position of the tracking dye.

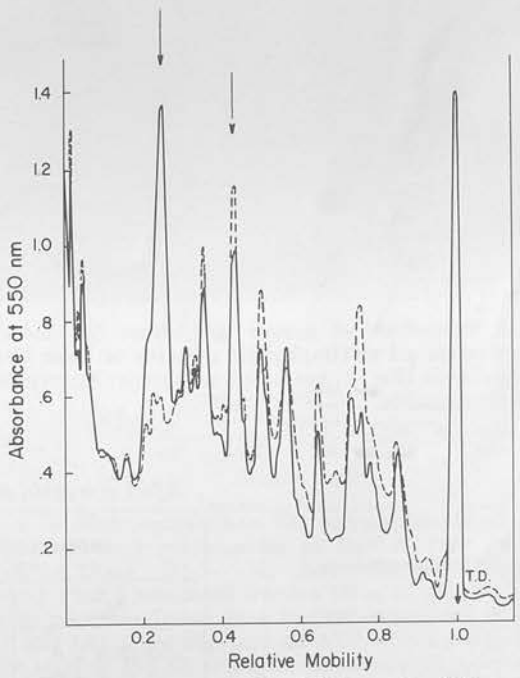

Fig. 4. Effect of *o*-phenanthroline/$CuSO_4$ on Peak II membrane fraction. Mixture of gastric membrane (1 mg protein/ml) and 50 μM *o*-phenanthroline/10 μM $CuSO_4$ was incubated for 60 min. After solubilization of the sample in 1% Na dodecyl-SO_4 lacking β-mercaptoethanol, electrophoresis was performed in 10% acrylamide. Gels were stained and scanned at 550 nm. (——) untreated membrane; (- - -) treated membrane; (→) designates the 102,000- and 82,000-dalton polypeptides. *T.D.* shows the position of the tracking dye.

Effects of Proteolysis on Membrane Enzymes—With evidence that selective peptide labeling occurred and the suggestion that freeze thawing altered the labeling patterns of Peak II, some of the functional properties of the membrane peptides were examined. The effect of proteolysis on several membrane enzymes was determined (Table I). There is a 2-fold stimulation of the ATPase by K^+ in both Peak I and Peak II, a 33% stimulation by HCO_3^- in Peak I, and a 50% stimulation in Peak II. Treatment with trypsin abolished the K^+ stimulation, but did not significantly affect the HCO_3^- stimulation, nor was the basal Mg^{2+}-ATPase activity reduced. Freeze thawing results in inhibition of the HCO_3^--ATPase activity by trypsin.

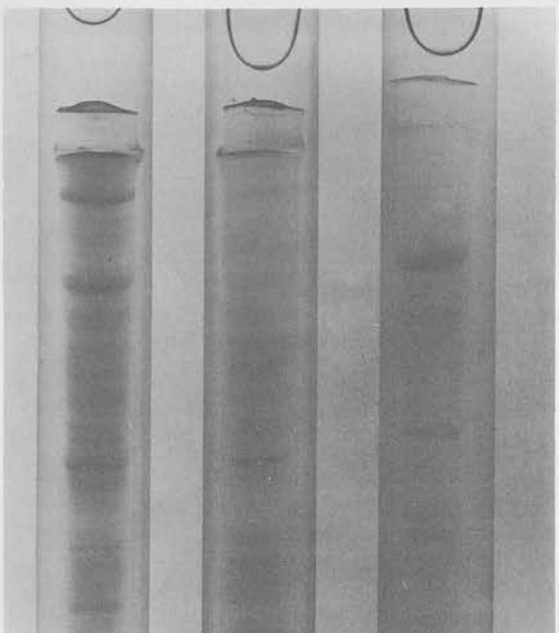

FIG. 5. Proteolysis of gastric membrane: Na dodecyl-SO_4-polyacrylamide gel electrophoretic patterns of Peak II stained with Coomassie blue. *A*, untreated membrane; *B*, trypsin; *C*, α-chymotrypsin.

K^+-pN-Ph-Pase activity is about three times higher in Peak II than in Peak I and is sharply reduced by tryptic hydrolysis. α-Chymotrypsin had the same effect, although the M_r 102,000 band is less affected.

Membrane Phosphorylation—Since it has been shown that gastric ATPase has what could be a phosphorylated intermediate (18, 19), some of the properties of this reaction were determined in Peaks I and II. Varying the K^+ or HCO_3^- concentration, measuring the degree of phosphorylation on a Millipore filter showed little effect on Peak I. Peak II, on the other hand, showed a concentration-dependent decrease in phosphorylation level with K^+ or choline bicarbonate, K^+ being the more effective ion (Fig. 6*A*). These latter effects were not additive, and choline Cl was without effect. The addition of pN-Ph-P to the phosphorylating mixture reduced the acid precipitable counts slightly in Peak I, and by about 50% in Peak II. There was a slight effect on the level of phosphorylation in the presence of K^+ or HCO_3^-. The K_I for pN-Ph-P was 0.5 mM, at a pN-Ph-P:ATP ratio of 250:1 (Fig. 6*B*).

When the phosphorylation reaction was stopped by the addition of Na dodecyl-SO_4 β-mercaptoethanol, and gel electrophoresis carried out in the cold, the patterns for Peaks I and II were quite characteristic. Peak I showed in the presence of Mg^{2+} alone a peak of phosphorylation at M_r = 102,000 and counts in the region of the tracking dye. The addition of K^+ or HCO_3^- preceding solubilization of Peak I produced a complex pattern of counts with five peaks in the case of HCO_3^- and K^+ but not in identical positions (Fig. 7*A*).

Peak II, however, showed one sharp band with a 20 times greater ^{32}P incorporation, which corresponded to the counts retained on the filter as described above. This band was located in the 102,000-dalton region. The addition of K^+ virtually abolished the counts in this region and a new peak of labeling appeared in the 64,000-dalton region. HCO_3^- addition in the form of choline HCO_3^- (since Na^+ and the other alkali cations also affect the phosphorylation) reduced the 102,000-dalton peak by 80%, and again a new peak of counts appeared at the 64,000-dalton region (Fig. 7*B*).

DISCUSSION

It has been shown previously for dog gastric mucosa (22) and confirmed for frog stomach (35) that gastric membranes can be fractionated into two components with relative enrichment of some enzymes and also differing in peptide pattern, lipid, and carbohydrate composition.

Labeling the mucosal surface of the dog stomach resulted

TABLE I

Effect of trypsin on ATPase and pN-Ph-Pase activity

Membrane fractions	ATPase activity in μmol of P_i/mg of protein/hr[a]			pN-Ph-Pase activity in μmol of pNP/mg of protein/hr[b]	
	Mg^{2+}	$Mg^{2+}K^+$	$Mg^{2+}HCO_3^-$	Mg^{2+}	$Mg^{2+}K^+$
Peak I	25.0 ± 2.6	46.2 ± 7.8	34.1 ± 2.7	1.9 ± 0.9	6.8 ± 1.6
Peak I + trypsin[c]	25.0 ± 1.0	28.2 ± 1.0	33.8 ± 1.8	1.4 ± 0.5	2.1 ± 0.8
Peak II	18.7 ± 2.6	37.4 ± 8.9	27.2 ± 3.3	2.5 ± 0.6	14.9 ± 4.2
Peak II + trypsin	17.2 ± 0.6	19.2 ± 0.4	25.2 ± 1.3	1.6 ± 0.5	3.5 ± 0.5

[a] The ATPase activity was measured at 37° in the presence of the following where appropriate: 3 mM ATP, 3 mM $MgCl_2$, 20 mM KCl, and 20 mM $NaHCO_3$.

[b] The pN-Ph-Pase activity was measured at 37° in the presence of the following where appropriate: 6 mM pN-Ph-P, 6 mM $MgCl_2$ and 20 mM KCl.

[c] Concentration of trypsin used was 25 μg per mg of membrane protein.

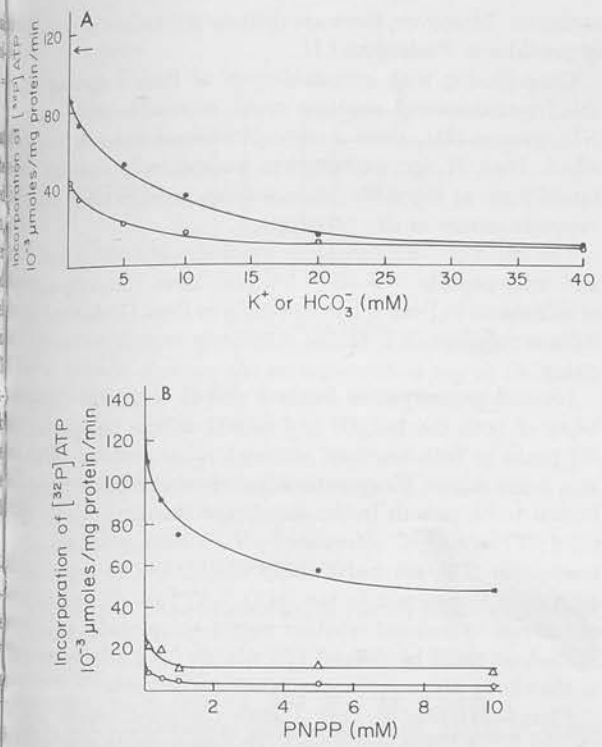

FIG. 6. *A*, the effect of varying concentrations of KCl or choline bicarbonate (from 0.1 to 20 mM) on the phosphorylated intermediate ATPase at 4°. Peak II (30 μg of protein) was incubated at 4° for 30 s in a final volume of 0.1 ml containing 100 mM Tris-Cl, pH 7.4, 1 mM $MgCl_2$, 2 μM ATP with 0.2 μCi [γ-^{32}P]ATP (specific activity 16.4 Ci/mmol) and various concentrations of K^+ (○——○) or HCO_3^- (●——●). (→) designates the amount of $E \sim {}^{32}P$ in the presence of Mg^{2+} alone. *B*, the effect of various concentrations of pN-Ph-P on the Mg^{2+}, Mg^{2+}-K^+ and Mg^{2+}-HCO_3^- phosphorylated intermediate ATPase of Peak II at 4°. Peak II (30 μg of protein) was incubated at 4° for 30 s in a final volume of 0.1 ml containing 100 mM Tris-Cl, pH 7.4, 1 mM $MgCl_2$, 2 μM ATP with 0.2 μCi [γ-^{32}P]ATP (specific activity 16.4 Ci/mmol) in the presence or absence of 20 mM KCl and 20 mM choline bicarbonate and varying concentrations of pN-Ph-P. (●——●) Mg^{2+}-dependent phosphorylation; (○——○) $Mg^{2+}K^+$-dependent phosphorylation; (△—△) $Mg^{2+}HCO_3^-$-dependent phosphorylation.

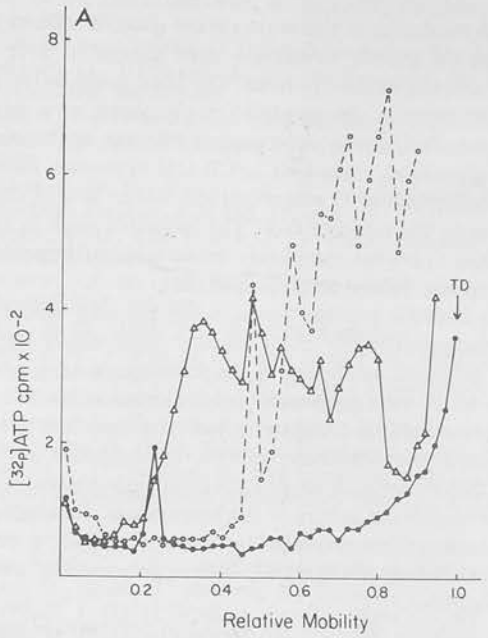

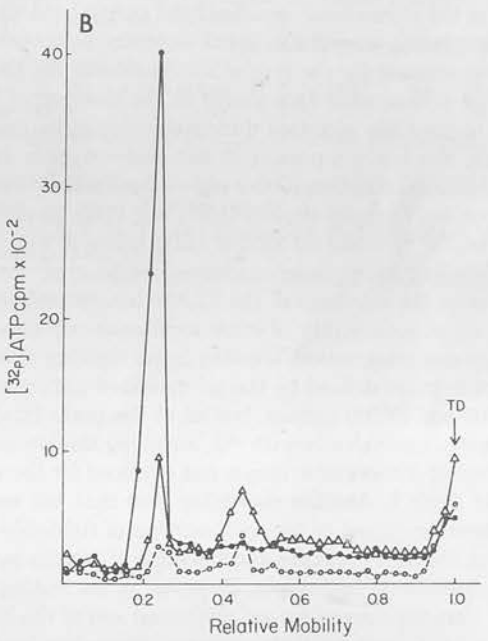

FIG. 7. *A*, Electrophoresis on 10% polyacrylamide gel of phosphorylated Peak I polypeptides of Mg^{2+}-ATPase (●——●), (Mg^{2+}-K^+)-ATPase (○- - -○), and (Mg^{2+}-HCO_3^-)-ATPase (△——△). Peak I membrane fraction (30 μg of protein) was subjected to phosphorylation in a medium consisting of 100 mM Tris-Cl (pH 7.4), 1 mM $MgCl_2$, 2 μM ATP with 2 μCi [γ-^{32}P]ATP (specific activity 16.4 Ci/mmol) in the absence or presence of 20 mM KCl or 20 mM choline bicarbonate. *T.D.* shows the position of the tracking dye. *B*, electrophoresis on 10% polyacrylamide gel of phosphorylated Peak II polypeptides of Mg^{2+}-ATPase (●——●), (Mg^{2+}-K^+)-ATPase (○- - -○), and (Mg^{2+}-HCO_3^-)-ATPase (△——△). Peak II membrane fraction (30 μg of protein) was subjected to phosphorylation in a medium consisting of 100 mM Tris-Cl (pH 7.4), 1 mM $MgCl_2$, 2 μM ATP with 2 μCi [γ-^{32}P]ATP (specific activity 16.4 Ci/mmol) in the absence or presence of 20 mM KCl or 20 mM choline bicarbonate. *T.D.* shows the position of the tracking dye.

fractionation of both membrane fractions, with apparently a higher specific activity in Peak I; but when activities are determined on polyacrylamide gel, there is twice the labeling of the high molecular weight and 82,000-dalton region in Peak II. However, the low molecular weight region is more heavily labeled in Peak I. These data suggest that the fractionation discriminates between different types of membrane such as those from different cells rather than between the apical and basal surfaces of the tissue.

The labeling pattern of the membrane iodinated in the intact tissue shows the presence of high molecular weight material not associated by Na dodecyl-SO_4-β-mercaptoethanol, and we have not defined this further. Thus it could be undissociated material corresponding to the other peaks or be entirely different. Iodination of low molecular weight material has been described before. In a study using Hela cells (33) it was shown that this material was not iodinated, and was more strongly iodinated following fractionation. Reiodination of the ^{125}I-labeled membranes resulted in increased labeling in the low molecular weight region with Peak I, as would be predicted from the Hela cell studies. However, in those studies the counts were clearly associated with a peak corresponding for carbohydrate and lipid which ran ahead of the tracking dye, a similar band being present in the gastric membranes.

Although resolution in this region is not good, it seemed that the counts in the gastric membrane were associated with a band running actually at the dye front. The band could be low molecular weight peptide, glycopeptide, or glycolipid, or a mixture of all of these. Preliminary data suggest that the iodination is partially in glycolipid, since $CHCl_3/CH_3OH$ extraction followed by saponification and ether extraction resulted in 50% of the counts appearing in the ether extract. The iodinated peak in Hela cell membranes appeared completely extractable with alcohol-ether and hence was defined as glycolipid (33).

Of the multiple peptide bands in the gel, only one, at 82,000 daltons iodinated in the intact mucosa. Since steady state labeling was achieved, relabeling of the membranes gave labeling in peptides which were not accessible to external iodination. Freeze-thawing was used to disrupt any vesicular structure that might be present in the membrane fraction, in preference to more disruptive techniques such as solubilization since we wished to preserve the membrane nature of the preparation. Relabeling under these circumstances produced several new labeling peaks, as well as relabeling of the 82,000-dalton polypeptide, which was most prominent.

This suggested that the 82,000-dalton polypeptide was accessible from both sides of the membrane. Relabeling without freeze-thawing also labeled the 82,000-dalton polypeptide; thus the results were not due to freeze-thawing exposing new groups on this peptide. However, homogenization, or the presence of this peptide in the intracellular vesicles of the parietal cell which fuse with the plasma membrane upon secretory stimulation (20) could well account for the results. Iodination of the histamine-stimulated mucosa gave data similar to the above since it is not feasible to maintain secretion during our iodination conditions. Moreover, the low pH present in the gastric tubule (<pH 1) would preclude iodination in this region during secretion.

Electron micrographs showed that Peak II in particular contained largely vesicular structures (22); hence it was felt that double labeling under these conditions might give some information as to the sidedness of the 82,000-daltons polypeptide as well as to the accessibility of other membrane peptides. Peak I iodination and reiodination following freeze thawing showed that two peptide peaks defined by the gel iodinated particularly well at 102,000 and 82,000 daltons, but all of the peaks labeled with ^{125}I iodinated equivalently with ^{131}I, including the low molecular weight region. Hence, no evidence was obtained for the vesicular nature of Peak I. Another possibility was that the vesicles in Peak I were composed on an equal number of right-side out and inside-out vesicles. Breakage and resealing of plasma membrane produces vesicles of both types. However, in the resting parietal cell, the intracellular vesicles are preformed and of the inside-out variety with respect to their ultimate orientation on the cell surface (21). Iodination of Peak II gave data suggesting that this fraction was vesicular, restricting peroxidase access and also was composed mainly of vesicles in one orientation (inside-out). Initial iodination produced two major defined peaks, at 102,000 and 82,000 daltons, and reiodination labeled the 82,000-dalton peak significantly more than the 102,000-dalton peak, as well as what would appear to be a new peptide at M_r = 51,000. The latter could be a peptide inside the vesicles, or one structurally exposed by freeze-thawing. Hence these data suggest that two peptides in the membrane fractions are particularly accessible to iodination in the fresh preparation, and that the 82,000-dalton peptide may indeed traverse the bilayer. In addition, of the 30 or so peptides defined by this fractionation, only 5 are iodinatable under these conditions, hence are located in a defined membrane structure. Moreover, there are definite differences in accessibility of peptides in Peaks I and II.

Cross-linking with glutaraldehyde of Peak I showed that in this fraction several peptides could be readily cross-linked via NH_2 groups (34), since β-mercaptoethanol did not reverse the effect. Peak II, in contrast, was unexpectedly resistant to glutaraldehyde at the same concentration, perhaps again due to the vesicular nature of this preparation.

The effect of —SH oxidation which would result in both intra- and inter-peptide —S—S— bridging gave the somewhat surprising result in Peak I, but especially in Peak II, that the 102,000 daltons polypeptide is almost selectively cross-linked by this procedure.

Limited proteolysis of Peaks I and II confirmed the accessibility of both the 102,000 and 82,000 daltons polypeptides and ^{125}I peaks in both fractions although other peptides are affected to a lesser degree. Enzymatic assay showed that of the enzymes known to be present in the membrane fractions, the K^+ stimulated ATPase and K^+ stimulated pN-Ph-Pase, which are ouabain-insensitive (19) are particularly susceptible to proteolytic inactivation in contrast to the HCO_3^--ATPase. It was, therefore, of interest to find out whether any of the peptides accessible to iodination could be defined functionally as a component of one of the above enzymes if indeed they are distinct.

Phosphorylation of Peak I gave confusing results. Thus although K^+-ATPase and K^+-pN-Ph-Pase activity were present in this fraction, little K^+-dependent dephosphorylation was observed. Moreover, although a single peak of phosphorylation was observed with Mg^{2+} alone, at M_r = 102,000 a complex labeling of peptide was found in the presence of K^+ or HCO_3^-. This finding explained the lack of dephosphorylation found by the Millipore filtration technique, but its significance is not known.

In contrast, phosphorylation of Peak II was quite sensitive to the presence of K^+ or choline bicarbonate. Various cations, but not choline, can substitute for K^+ with varying degrees of effectiveness, hence apparently HCO_3^- can also dephosphorylate the enzyme. pN-Ph-P competes with ATP in terms of phosphorylation, but even a large excess of pN-Ph-P does not reduce phosphorylation to the K^+ or HCO_3^- level. One explanation might be that pN-Ph-P is capable only of interacting with the K^+ enzyme since HCO_3^- does not stimulate pN-Ph-Pase activity. The data for Peak II thus correlate with the higher level of K^+-pN-Ph-Pase activity found in this fraction, rather than the K^+-ATPase which is similar in Peaks I and II (Table I).

Resolution of the phosphorylated peptide on Peak II showed that a single peak of phosphorylation was present at 102,000 daltons, and that K^+, and HCO_3^- to a lesser degree, reduced the peak height, and labeling was found in a new peptide of M_r = 64,000, which was, incidentally, slightly labeled by iodination. Again, the significance of this second labeling peak is not understood but may be involved in the enzyme mechanism. The data show that since the 102,000-dalton polypeptide is an ATPase component, this peptide is located on the inner face of the cell membrane.

Thus, in the gastric mucosa, it would appear that a peptide of M_r = 102,000 is particularly susceptible to iodination or proteolysis and —SH cross-linking and is also a component of the ion-sensitive ATPase of the gastric membrane. Another peptide of M_r = 82,000 is iodinatable in the intact tissue and is also readily available for iodination in the membrane fraction, and we have tentative evidence that this peptide perhaps spans the bilayer. In addition only 5 of the 30 peptides iodinate, and a 51,000-dalton polypeptide also showed a structural dependence

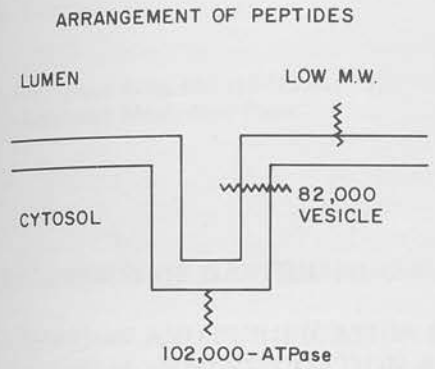

FIG. 8. A model showing the arrangement of two of the major polypeptide regions of gastric mucosal membranes.

of labeling. Fig. 8 shows a tentative model of the locations proposed.

REFERENCES

1. PHILLIPS, D. R., AND MORRISON, M. (1970) *Biochem. Biophys. Res. Commun.* **40**, 284–289
2. RIFKIN, D. B., COMPANS, R. W., AND REICH, E. (1972) *J. Biol. Chem.* **247**, 6432–6437
3. BRETSCHER, M. S. (1971) *J. Mol. Biol.* **58**, 775–781
4. STECK, I. L., FAIRBANKS, G., AND WALLACH, D. H. F. (1971) *Biochemistry* **10**, 2617–2624
5. HOKIN, L. E., DAHL, J. L., DEUPREE, J. D., DIXON, J. F., HACKNEY, J. F., AND PERDUE, J. F. (1973) *J. Biol. Chem.* **248**, 2593–2605
6. RUSHO, A., AND KYTE, J. (1974) *Proc. Natl. Acad. Sci. U. S. A.* **71**, 2352–2356
7. BRETSCHER, M. S. (1971) *J. Mol. Biol.* **59**, 351–357
8. PHILLIPS, D. R., AND MORRISON, M. (1971) *Biochemistry* **10**, 1766–1771
9. PHILLIPS, D. R. (1972) *Biochemistry* **11**, 4582–4588
10. CZECH, M. P., AND LYNN W. S. (1973) *Biochemistry* **12**, 3597–3601
11. TSAI, C.-M., HUANG, C.-C, AND CANELLAKIS, E. S. (1973) *Biochim. Biophys. Acta* **332**, 47–58
12. SHIN, B. C., AND CARRAWAY, K. L. (1973) *Biochim. Biophys. Acta* **330**, 254–268
13. ASTLE, L., AND COOPER, C. (1974) *Biochemistry* **13**, 154–160
14. KREIBICH, G., HUBBARD, A. L., AND SABATINI, D. D. (1974) *J. Cell Biol.* **60**, 616–627
15. STECK, T. L. (1972) *J. Mol. Biol.* **66**, 295–305
16. STRUM, J. M., AND EDELMAN, I. S. (1973) *J. Membr. Biol.* **14**, 17–32
17. KASBEKAR, D. K., DURBIN, R. P., AND LINDLEY, D. (1965) *Biochim. Biophys. Acta* **102**, 472–482
18. GANSER, A. L., AND FORTE, J. G. (1973) *Biochim. Biophys. Acta* **307**, 169–180
19. TANISAWA, A. S., AND FORTE, J. G. (1971) *Arch. Biochim. Biophys.* **147**, 165–175
20. SEDAR, A. W. (1965) *Fed. Proc.* **24**, 1360–1367
21. FORTE, J. G., FORTE, G. M., AND RAY, T. K. (1972) in *Gastric Secretion* (SACHS, G., HEINZ, E., AND ULLRICH, K. J., eds) pp. 37–68, Academic Press, New York
22. SPENNEY, J. G., STRYCH, A., PRICE, A. H., HELANDER, H. F., AND SACHS, G. (1973) *Biochim. Biophys. Acta* **311**, 545–564
23. SPENNEY, J. G., STRYCH, A., AND SACHS, G. (1974) in *Methodological Developments in Biochemistry* (BIRNIE, A. D., ed) in press
24. SPENNEY, J. G., SACCOMANI, G., SPITZER, H. L., TOMANA, M., AND SACHS, G. (1974) *Arch. Biochem. Biophys.* **161**, 456–471
25. SACHS, G., SHAH, G., STRYCH, A., CLINE, G., AND HIRSCHOWITZ, B. I. (1972) *Biochim. Biophys. Acta* **266**, 625–638
26. LOWRY, O. H., ROSEBROUGH, N. J., FARR, A. L., AND RANDALL, R. J. (1951) *J. Biol. Chem.* **193**, 265–275
27. YODA, A., AND HOKIN, L. E. (1970) *Biochim. Biophys. Res. Commun.* **40**, 880–884
28. TORRIANI, A. (1968) *Methods Enzymol.* **12B**, 212–215
29. REICHSTEIN, E., AND BLOSTEIN, R. (1973) *Biochem. Biophys. Res. Commun.* **54**, 494–500
30. FAIRBANKS, G., STECK, T. L., AND WALLACH, D. F. H. (1971) *Biochemistry* **10**, 2606–2617
31. KORN, E. D., AND WRIGHT, P. L. (1973) *J. Biol. Chem.* **248**, 439–447
32. NACHMAN, R. L., AND FERRIS, B. (1970) *Biochemistry* **9**, 200–205
33. HUANG, C.-C., TSAI, C.-M., AND CANELLAKIS, E. S. (1973) *Biochim. Biophys. Acta* **332**, 59–68
34. HABEEB, A. F. S. A., AND HIRAMOTO, R. (1968) *Arch. Biochem. Biophys.* **126**, 16–26
35. RAY, T. K., AND FORTE, J. G. (1974) *Biochim. Biophys. Acta* **363**, 320–339

rinted from

himica et Biophysica Acta, 465 (1977) 311—330
sevier/North-Holland Biomedical Press

77633

ARACTERIZATION OF GASTRIC MUCOSAL MEMBRANES

FRACTIONATION AND PURIFICATION OF K^+-ATPase-CONTAINING SICLES BY ZONAL CENTRIFUGATION AND FREE-FLOW ELECTRO-DRESIS TECHNIQUE

ACCOMANI, H.B. STEWART, D. SHAW, M. LEWIN and G. SACHS *

oratory of Membrane Biology, University of Alabama in Birmingham, Birmingham, Ala. 4 (U.S.A.)

ceived June 15th, 1976)

mmary

Methods are described for purification of a vesicular membrane fraction of g gastric mucosa using differential centrifugation, density gradient separation zonal rotors and free-flow electrophoresis. As a result a fraction is obtained iched 40-fold in terms of K^+-ATPase and free of any other enzyme marker er than K^+-activated *p*-nitrophenyl phosphatase.

he 5'-nucleotidase and basal Mg^{2+}-ATPase are clearly separated from the er enzymes.

smotic shock, Triton X-100 treatment or K^+ ionophores increased the K^+-ase activity in isotonic conditions, but K^+-*p*-nitrophenyl phosphatase is not cted by these treatments, nor is the ATPase activity in the presence of NH_4^+. results suggest that the electrophoretic fraction contains a major popula-of tight vesicles, whose permeability to K^+ is rate limiting for the ATPase ity but not for the *p*-nitrophenyl phosphatase activity. It is concluded that ite for the ATPase is internal whereas the K^+ site for the *p*-nitrophenyl sphatase is external, hence, the K^+ site must be mobile across the mem-ne.

oduction

he gastric mucosa is a complex heterocellular epithelium containing as r cell types the surface cell, the mucus neck cell, the parietal cell and the

* To whom correspondence should be addressed.

Abbreviations: HEPES, *N*-2-hydroxyethylpiperazine-*N'*-2-ethanasulfonic acid; SDS, sodium dodecyl sulfate.

chief of peptic cell. Current interest centers on the properties of the parietal acid secreting cell, and fractionation of gastric homogenate has been aimed producing purified preparations of the parietal cell's apical membrane as which H^+ transport occurs. Plasma membranes of gastric fundic mucosa h been prepared by a variety of techniques in species such as frog [1], nectu [2], dog [3], rabbit [4] and recently, in hog [5]. Perhaps the most purif membrane fractions were obtained using Ficoll sucrose density gradients zonal rotors, as applied to the dog [3]. Similar techniques applied to the hog produced fractions of equivalent purity, but various manipulations of gradi composition and shape, as well as rate rather than isopycnic centrifugation, not improve the purity. Recently, free-flow electrophoresis technique has b used to successfully separate the basal and apical membranes of rat kidn tubule cells [6]. In the present work this technique was used to increase purity of gastric membrane fractions, and optimum electrophoretic separati conditions as well as some morphological and biochemical studies of the lated fractions are described.

Materials and Methods

Fresh hog stomachs were obtained from the local slaughterhouse. Af washing free of contents in tap water, the fundic mucosa surface was flood with a saturated solution of NaCl, and the surface mucus and most of superficial cells removed by vigorous wiping with paper towels, leaving mos parietal and peptic cells. The fundic mucosa was then scraped from the under ing muscular layer and suspended in (approx. 10% tissue, w/w) cold solution 0.25 M sucrose, 20 mM Tris · HCl buffer at pH 7.4. Homogenization was ca ried out in a tight-fitting teflon-glass homogenizer (Potter-Elvehjem) with up-down strokes at 2000 rev./min.

Differential centrifugation. The resulting homogenate was centrifuged 20 000 × *g* for 30 min in a Sorvall RC-2 centrifuge. The pellet was washed once, and the combined supernatants were centrifuged at 78 000 × *g* * for 6 min in a Beckman L-2 ultracentrifuge with a No. 30 rotor to yield the cru microsomal pellet. The remaining material was termed the final supernat

Zonal centrifugation. The technique used has been previously described [3 The 78 000 × *g* pellet was resuspended in 0.25 M sucrose 20 mM Tris · HCl (p 7.4) and after homogenization was distributed by zonal centrifugation using continuous density gradient made from 7.5% (w/w) Ficoll 0.25 M sucrose an 37% (w/w) sucrose in 20 mM Tris · HCl at pH 7.4.

Absorbance at 280 nm was used to estimate protein peaks in gradient fra tions, while the Lowry method [7] was used in all other instances. Sucrose con centration was measured with an Abbe refractometer. Fractions collected between a density of 1.04 and 1.06 (GI), between 1.06 and 1.08 (GI–GII between 1.08 and 1.12 (GII), between 1.12 and 1.15 (GII—GIII) and betwe 1.15 and 1.26 (GIII) were diluted with 20 mM Tris · HCl (pH 7.4) to less th 1.04 density and centrifuged at 78 000 × *g* for 60 min to obtain pellets.

Free-flow electrophoresis. Further fractionation of GI and GII fracti

* *g* value at R_{max} = 105 500.

tained from zonal separation was accomplished on the FF5 electrophoresis paratus developed by Hannig [8] (Biomedical Instruments, N.Y.). The elec-phoresis buffer (or the separation buffer) was 8 mM Trizma-base, 8 mM etic acid and 0.25 M sucrose adjusted to pH 7.4 by 2 M NaOH, containing 1 mM MgATP. The electrode buffer consisted of 100 mM Trizma-base and 0 mM acetic acid adjusted to pH 7.4 by 2 M NaOH.

Prior to electrophoresis, GI and GII fractions were washed twice in separa-on buffer and suspended to a final protein concentration of 8 mg/ml. Sample ection rate was 1 ml/h, and 90 fractions were collected at 4° C. The condi-ns of the runs were as follows: 120 ± 10% V/cm, 147 mA, temperature 7.4 ± 2° C and electrophoresis buffer flow 4 ml per fraction per h.

Mobility measurement. The total deflections of individual bands of particles thin the separation chamber were recorded photographically. The lateral dis-cement of particles was made up of one component due to the electro-oretic velocity of the particles and a second component due to the electro-motic velocity of the separation buffer. To correct for the electro-osmotic locity of the separation buffer, a zero mobility marker (separation buffer ntaining 0.4 M sucrose) was injected into the chamber. The angle of deflec-on of the bands due to electrophoretic velocity of the particles was measured the difference between the angles of total deflection of the individual bands d the angle of deflection of the marker. The volume flow rate of the separa-on buffer was measured directly by collecting of the output of the electro-oretic chamber for measured time intervals. The maximum vertical velocity the separation buffer was calculated from the volume flow rate and the ometry of the chamber. The separation buffer was assumed to exhibit lami-r flow, with a parabolic velocity profile across the narrowest dimension of e chamber.

The mobility of a given band of particles was calculated using the formula:

$$u = \frac{v}{E}(\tan \alpha - \tan \alpha_o)$$

ere u = electrophoretic mobility, v = maximum velocity of the buffer solu-n, E = electric field within the chamber, α = the angle of deflection of the rticles bands, and α_o = the angle of deflection of the zero mobility marker.

Electron microscopy. Zonal and free-flow electrophoresis fractions were n down at 100 000 × g for 1 h. The pellets were fixed with 3% glutaralde-de for 1 h. After removing the glutaraldehyde by washing with 50 mM Tris · Cl (pH 7.4), the samples were fixed with cold 1% OsO_4 buffered with 50 mM codylate (pH 7.4) for 1 h. The pellets were then washed in buffer and dehy-ated in increasing concentrations of ethanol. The pellets were placed in pro-lene oxide for 30 min and then in a mixture of propylene oxide and Epon : 1, v/v) for 12 h. Thereafter the pellets were embedded in pure Epon, lymerized for 40 h at 60° C. Thin sections were studied in a Phillips EM 300 ctron microscope.

Enzymatic assays. Substrates used for the biochemical assays were obtained m Sigma Chemical Co. All of the chemicals were reagent grade.

5'-Nucleotidase was measured in a medium containing 3 mM $MgCl_2$, 3 mM IP and 40 mM HEPES Tris buffer at pH 7.4. ATPase activity was assayed in

a medium containing 2 mM $MgCl_2$, 20 mM KCl or 20 mM $NaHCO_3$, 2 mM ATP (disodium salt), 40 mM Tris · HCl buffer at pH 7.4. Valinomycin was added in 10 µl methanol to give a final concentration of 10^{-5} M, and the effect compared to controls with only 10 µl methanol added. The term "basal ATPase" refers to the activity observed when the only activating ion present was Mg^{2+}. The phosphate released was measured by the method of Yoda and Hokin [9] following incubation at 37°C. K^+-stimulated *p*-nitrophenyl phosphatase was assayed using a medium containing 6 mM $MgCl_2$, 6 mM *p*-nitrophenyl phosphate (ditris salt) and 50 mM Tris/acetate (pH 7.5). The *p*-nitrophenol liberated was measured by the method of Torriani [10]. 5—50 µg of protein was used for the above assays depending on the specific activity of the sample. Other experimental variables are indicated in the figures and tables.

Cytochrome *c* oxidase was measured by the procedure of Cooperstein and Lazarow [11] and succinate dehydrogenase by the method of King [12]. Monoamine oxidase was estimated by a modification of the method of Tabor et al. [13] by following the formation of benzaldehyde spectrophotometrically at 250 nm at 37°C in a medium containing 2.5 mM benzylamine and 50 mM phosphate buffer at pH 7.6, using a Gilford 2400 recording spectrophotometer. RNA was determined according to Munro and Fleck [14] while DNA was assayed by the method of Burton [15].

$^{86}Rb^+$ uptake. For uptake experiments, gastric membrane fractions at a final protein concentration ranging from 0.75 to 2.10 mg/ml were incubated for 72 h at 4°C in a medium containing 40 mM Tris/acetate, 75 mM RbCl with 1 µCi/ml $^{86}Rb^+$, 125 mM sucrose and 2 mM $MgCl_2$ at pH 6.1, the optimum pH for H^+ transport [16]. Separation of the Rb^+-containing vesicles from the incubation medium was achieved by Millipore filtration as previously reported [16]. $^{86}Rb^+$ uptake under these conditions has been demonstrated to reach equilibrium.

Polyacrylamide gel electrophoresis in SDS. Electrophoresis was carried out following the method previously described [3]. Solubilized membranes were fractionated on 6.1 × 80 mm polyacrylamide gels.

A 3.5% stacking gel was prepared in 0.1 M Tris · HCl (pH 6.8). Separation gels were 10% acrylamide prepared in 0.4 M Tris · HCl (pH 8.6). In both cases 2.5% of the acrylamide was *N,N'*-ethylenebisacrylamide. Reservoir buffer was 0.19 M glycine/Tris base at pH 8.6. Gels and reservoir buffer contained 0.1% SDS. Samples applied contained approx. 50 µg of protein. Gels were stained for protein by Coomassie Blue. Molecular weight estimations were made on gels using standard proteins as described earlier [3].

Results

(1) Differential centrifugation. The distribution of the various marker enzymes tested in this work is plotted in Fig. 1 according to the classical method of de Duve [17] and is similar to that found by Forte et al. [5] for the preparation of hog gastric microsomes; it is presented in terms of the 20 000 *g* (M), 100 000 × *g* (P), and supernatant (S) fractions. In this representation the specific activity of all the constituents in the homogenate is set at 1; the height of the blocks gives the relative purification achieved over the homo-

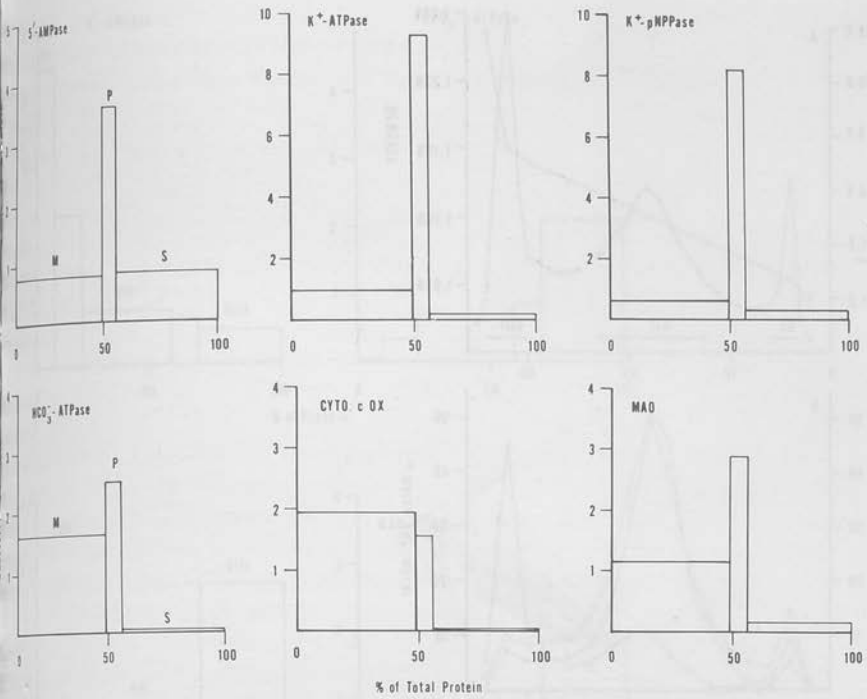

Fig. 1. Differential fractionation of hog gastric mucosa. The subcellular patterns are standardized. ATPase was estimated in presence of 2 mM ATP, 2 mM $MgCl_2$ with 20 mM KCl or $NaHCO_3$, in 40 mM Tris · HCl buffer pH 7.4. Other assay procedures were as described in Materials and Methods. Fraction M, (20 000 × *g*); fraction P (100 000 × *g*); fraction S (supernatant). pNPPase, *p*-nitrophenyl phosphatase; CYTO c Ox, cytochrome *c* oxidase; MAO, monoamine oxidase.

...te and the surface area of the blocks (relative specific activity × % protein) is ...e percentage of the constituent recovered in the corresponding fraction. Two characteristic distributions are obtained at this stage. 5′-Nucleotidase, ...-ATPase and *p*-nitrophenyl phosphatase are localised in the microsomal fraction, while cytochrome *c* oxidase is associated with the mitochondrial fraction, ...good agreement with data reported for gastric mucosa of other species [1,3], ...cluding hog [5]. Monoamine oxidase, HCO_3^--stimulated ATPase and Mg^{2+}-...Pase showed a distribution somewhat different from the above markers; ...hough the major portion of these three enzymes were found in the mito...ondrial fraction, all showed a relative enrichment in the microsomal pellet. ...e microsomal fraction accounted for 8.5% of the protein, 31% of the RNA ...d 0.3% of the DNA of the total homogenate.

(2) Density gradient separation. Separation of the microsomal fraction on ...nsity gradients was trimodal, as shown in Fig. 2A, with peaks of protein at ...nsities of 1.05 (GI), 1.11 (GII), and 1.16 (GIII). Material was also detected ...tween the fractions, (GI—GII and GII—GIII).

Mg^{2+}-ATPase and HCO_3^--ATPase showed very similar distributions with max...al enrichment in GIII, but significant activity was detected in GII (28% for HCO_3^--ATPase). The markers for inner mitochondrial membranes, cytochrome ...oxidase and succinate dehydrogenase, exhibited greater than 90% of their

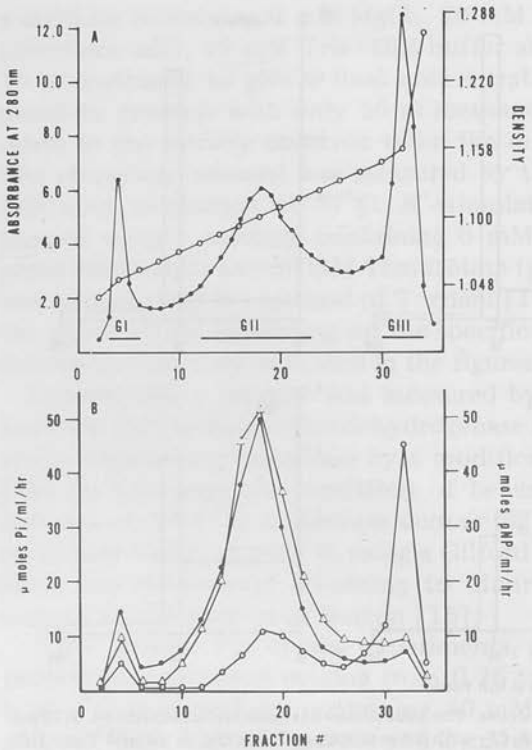

Fig. 2.(A) Fractionation of gastric cell membranes (microsomal pellet) by isopycnic zonal centrifugation on 7.5% Ficoll/0.25 M sucrose and 37% sucrose in 20 mM Tris · HCl at pH 7.4. ●———●, protein distribution; ○———○, sucrose density. (B) Enzymes fractionation by zonal centrifugation. ATPase and *p*-nitrophenyl phosphatase activities are given as μmol of P_i and *p*-nitrophenyl (pNP) released per ml per ○———○, Mg^{2+}-ATPase; △———△, K^+-ATPase; ●———●, K^+-*p*-nitrophenyl phosphatase.

activity in GIII, with very little activity in GII and none in GI. Monoamine oxidase showed essentially the same distribution as these mitochondrial markers in contrast to the Mg^{2+}- or HCO_3^--ATPase. On the other hand, the K^+-*p*-nitrophenyl phosphatase or K^+-ATPase showed a characteristically different distribution; both enzymes exhibited maximal activity and percent distribution in GII also showing significant activity in GI, but minimal in GIII. 5′-Nucleotidase had a different distribution from the above enzymes, with its activity peak in GI and decreasing thereafter (Figs. 2B and 3). These results are comparable to those reported for rat fundus [18] and other species [1,3].

(3) Free-flow electrophoresis separation. The indication that the GII gastric membrane fraction was enriched almost 19-fold in K^+-ATPase when compared with the starting homogenate, suggested that further purification of the enzyme from others (such as Mg^{2+}-ATPase and 5′-AMPase) could be achieved using the free-flow electrophoresis technique.

In order to preserve the structural and morphological integrity of the membranes, an isotonic isolation and separation medium was used. In the standard moving curtain buffer (8 mM Tris or triethanolamine/acetate at pH 7.4), the GII fraction separated in two poorly resolved major bands. Addition of 0.1 mM

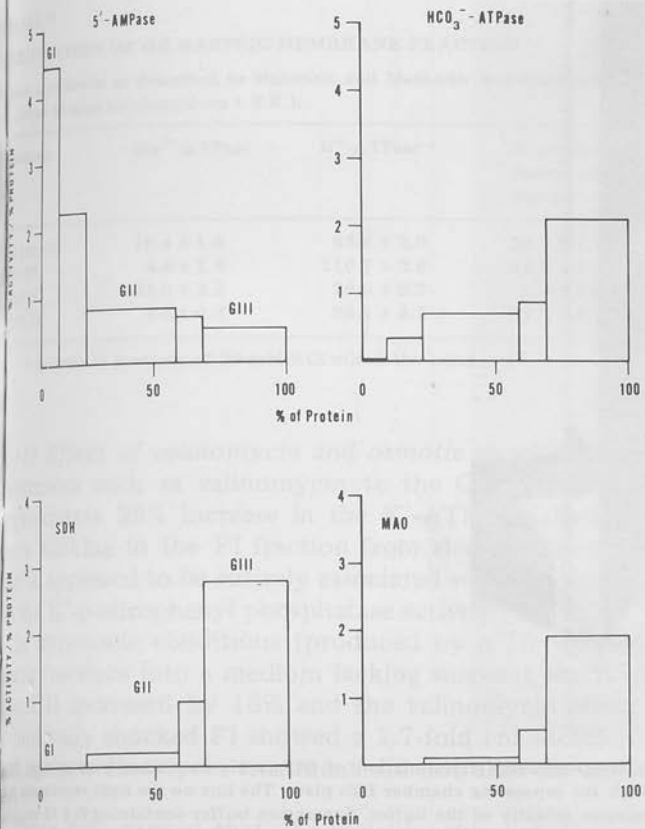

Fig. 3. The distribution of enzymes among the gastric membrane fractions derived from zonal centrifugation. Assay procedures were as described in Materials and Methods. SDH, succinate dehydrogenase; MAO, monoamine oxidase.

MgATP resulted in a much sharper separation into three bands, the first (FI) being displaced towards the anode by ATP, the second (FII) remained stationary. An additional minor peak (FIII) appeared which had the lowest electrophoretic mobility.

Fig. 4 shows a photograph taken during a typical electrophoretic separation of GII gastric membrane preparation. The mobilities of each band were calculated from the angles of deflection, from the observed flow rate of the separation buffer, and from the field strength within the chamber (Table I). The zeta potentials of the three fractions were calculated from the mobility data and buffer characteristic by application of Henry's equation [19]. The method and tabulated data of Loeb and Wiersema [20] were used to determine the surface charge density of FI only since FII and FIII were not closed spheres.

Protein and enzyme profiles of the fractions collected are shown in Fig. 5. K^+-ATPase and *p*-nitrophenyl phosphatase activities are almost entirely associated with FI, although activity is found in FIII, while Mg^{2+}-ATPase and 5′-AMPase are clearly separated from the other enzymes and confined to FII. This purification produced a further 2-fold enrichment in K^+-ATPase with respect to

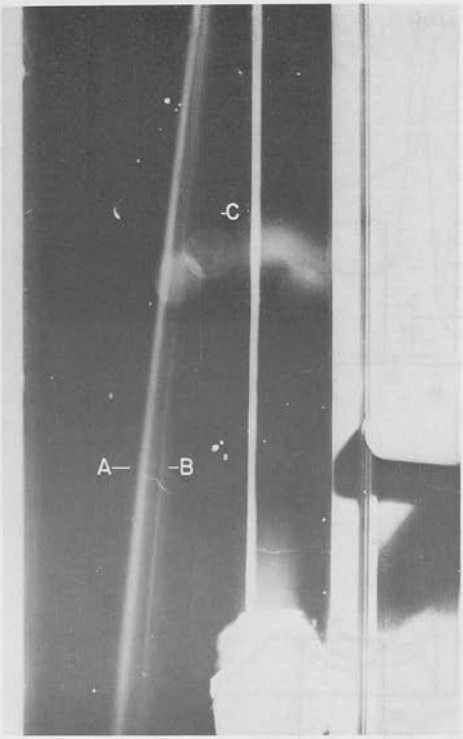

Fig. 4. Bands produced by the electrophoretic fractionation of GII gastric membrane preparation. The bands were photographed through the separating chamber face plate. The line on the right represents the deflection due to the electro-osmotic velocity of the buffer. Separation buffer containing 0.4 M sucrose was injected into the standard separation buffer which contained 0.25 M sucrose. A white thread was superimposed to allow a photographic record. The oblique line (A) is FI band; (B) and (C) indicate FII and FIII bands, respectively.

the original GII zonal fraction (Table II). HCO_3^--stimulated ATPase appeared to be equally distributed in all three protein peaks, the percent of stimulation however, increasing in FI due to the fall in the Mg^{2+}-ATPase level.

TABLE I

ELECTRICAL CHARACTERISTIC OF GASTRIC MEMBRANE FRACTIONS FROM FREE-FLOW ELECTROPHORESIS

Values shown indicate mean of five electrophoretic separation ± S.E.

Fractions	Mobility ($cm^2 \times 10^4/V \cdot s$)	Zeta potential (mV)	Surface charge density ($\mu C/cm^2$)
GII—FI	1.34 ± 0.04	—50.7 ± 1.0	—3.89 ± 0.01
	(1.12 ± 0.02) *	(—42.2 ± 0.5)	(—3.03 ± 0.03)
GII—FII **	1.06 ± 0.02	—40.1 ± 1.7	—
GII—FIII	0.52 ± 0.01	—19.7 ± 0.9	—

* In between parenthesis are represented values where free-flow electrophoresis was carried out in absence of 0.1 mM MgATP into the separation buffer.

** The surface charge density for FII and FIII fractions were not calculated since these fractions appeared to be in non-vesicular form.

TABLE II

PURIFICATION OF GII GASTRIC MEMBRANE FRACTION

Assay conditions as described in Materials and Methods. Activities are expressed in μmol/mg protein per h (mean of nine fractionations ± S.E.).

Fractions	Mg^{2+}-ATPase	K^+-ATPase *	K^+-*p*-nitrophenyl phosphatase	5′-AMPase
GII (zonal)	19.4 ± 1.8	63.6 ± 2.0	61.2 ± 4.2	2.2 ± 0.3
GII–FI	4.4 ± 1.0	110.7 ± 2.6	68.0 ± 2.5	0.3 ± 0.06
GII-FII	31.0 ± 3.1	20.0 ± 0.7	9.4 ± 1.0	5.4 ± 1.0
GII-FIII	2.8 ± 0.4	50.1 ± 3.2	31.0 ± 2.2	0.1 ± 0.1

* Activity in presence of 20 mM KCl minus the basal rate.

(4) Effect of valinomycin and osmotic shock. Addition of K^+-ionophoretic substances such as valinomycin to the GII membrane fraction produced an approximate 25% increase in the K^+-ATPase activity. Stimulation was much more striking in the FI fraction from electrophoretic separation (about 85%) and it appeared to be entirely associated with this peak. No effect was detected on the K^+-p-nitrophenyl phosphatase activity [28].

In hypotonic conditions (produced by a 10—30-fold dilution of the membrane fractions into a medium lacking sucrose), the K^+-ATPase activity of fraction GII increased by 18% and the valinomycin effect was almost abolished. Osmotically shocked FI showed a 1.7-fold enhancement of K^+-ATPase activity and again, valinomycin treatment did not alter the activity significantly (Table III).

These data suggest that, if a vesicular structure is present in the gastric membranes, the GII vesicle might be more permeable to K^+, and FI vesicles less permeable to the same ion. The K^+ site is therefore on the interior of the vesicle. A final concentration of 0.003% (w/v) Triton X-100 stimulated the K^+-ATPase in GII and FI fractions to the level reached in hypotonic medium and now valinomycin was without effect. Higher concentrations of Triton X-100 inhibited the K^+-ATPase activity. When K^+ was replaced with NH_4^+, since NH_3 appears to be freely permeable across cell membranes [21], in isotonic conditions, an increase in ATPase activity was observed, but valinomycin and osmotic shock were without effect (Table III). Hence the effect of ionophores is indeed due to limited K^+ penetration of the vesicle. It is important to point out that K^+-*p*-nitrophenyl phosphatase, 5′-AMPase and basal Mg^{2+} activities were not affected by osmotic shock.

(5) Electron microscopy. An electron micrograph of GII membrane fraction is shown in Fig. 6. This fraction consists almost entirely of smooth-surfaced vesicular particles, 0.1—0.2 μm in diameter. Many of the vesicles in this fraction are present in double membrane forms, which often appeared to be two fused membranes. Spherical particles (500 Å), probably mitochondrial fragments, are also seen. Micrographs of thin sections of the FI electrophoretic fraction also exhibited a double membrane structure with occasional granular content. No other cell particles could be detected (Fig. 7). Freeze-fracture confirmed the double membrane structure and also showed the presence of intercalated

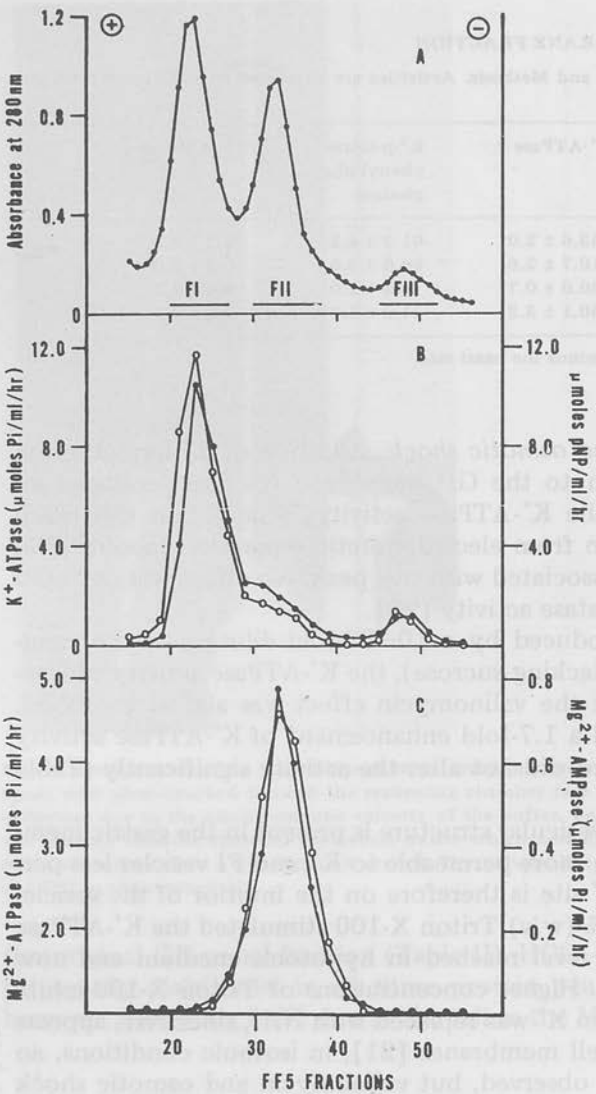

Fig. 5. Separation of GII membrane fraction by free-flow electrophoresis. A, protein distribution in the fractions collected; B, distribution of K^+-ATPase activity (○———○), and K^+-*p*-nitrophenyl phosphatase activity (●———●); C, distribution of Mg^{2+}-ATPase (●———●), and 5′-AMPase (○———○). Separation was carried out using 2 mM Tris/acetate as chamber buffer, containing 0.1 mM Mg^{2+}-ATP at pH 7.4. (See Materials and Methods). pNP, *p*-nitrophenyl

200 Å particles. Fractions FII and FIII showed the presence of both open and closed membrane forms (Fig. 8 and 9) and some contaminating material.

(6) $^{86}Rb^+$ uptake. Table IV shows the equilibrium levels of $^{86}Rb^+$ uptake. The total uptake of the original GII fraction was approximately equal to the sum of the relative uptakes (relative uptake = % uptake/% protein) of each free-flow electrophoretic fraction.

FI and FII exhibited $^{86}Rb^+$ uptake, while fraction FIII showed very little

TABLE III

EFFECT OF ISOTONICITY AND OSMOTIC SHOCK ON THE K^+-ATPase ACTIVITY OF GASTRIC MEMBRANE VESICLES

Activity in presence of the following where appropriate: 2 mM ATP, 2 mM $MgCl_2$, 20 mM KCl, 10^{-5} M valinomycin, 0.003% (w/v), Triton X-100, 0.25 M sucrose in 40 mM Tris · HCl. Activities are expressed in μmol/mg protein per h. (mean of six experiments ± S.E.)

Fractions	Isotonic		Isotonic+Triton X-100	Hypotonic	
	K^+-ATPase	K^+-ATPase + valinomycin	K^+-ATPase	K^+-ATPase	K^+-ATPase + valinomycin
GII (zonal)	52.7 ± 2.2 (66.9 ± 1.5) *	68.3 ± 3.3 (64.4 ± 2.3)	67.4 ± 1.3	63.6 ± 2.0	66.3 ± 1.0
GII—FI	63.7 ± 2.1 (86.4 ± 1.5)	101.5 ± 2.4 (95.6 ± 2.8)	102.2 ± 1.7	110.7 ± 2.6	112.4 ± 1.4
GII—FII	21.2 ± 1.1 (22.7 ± 0.5)	21.4 ± 0.7 (20.4 ± 1.3)	18.6 ± 2.3	20.0 ± 0.7	19.8 ± 2.1
GII—FIII	50.4 ± 3.0 (51.7 ± 1.4)	50.2 ± 2.8 (51.0 ± 2.7)	47.4 ± 3.0	50.1 ± 3.2	51.3 ± 1.7

* Values in between parentheses indicate the ATPase activity when K^+ was replaced with 20 mM, NH_4^+ minus the basal rate.

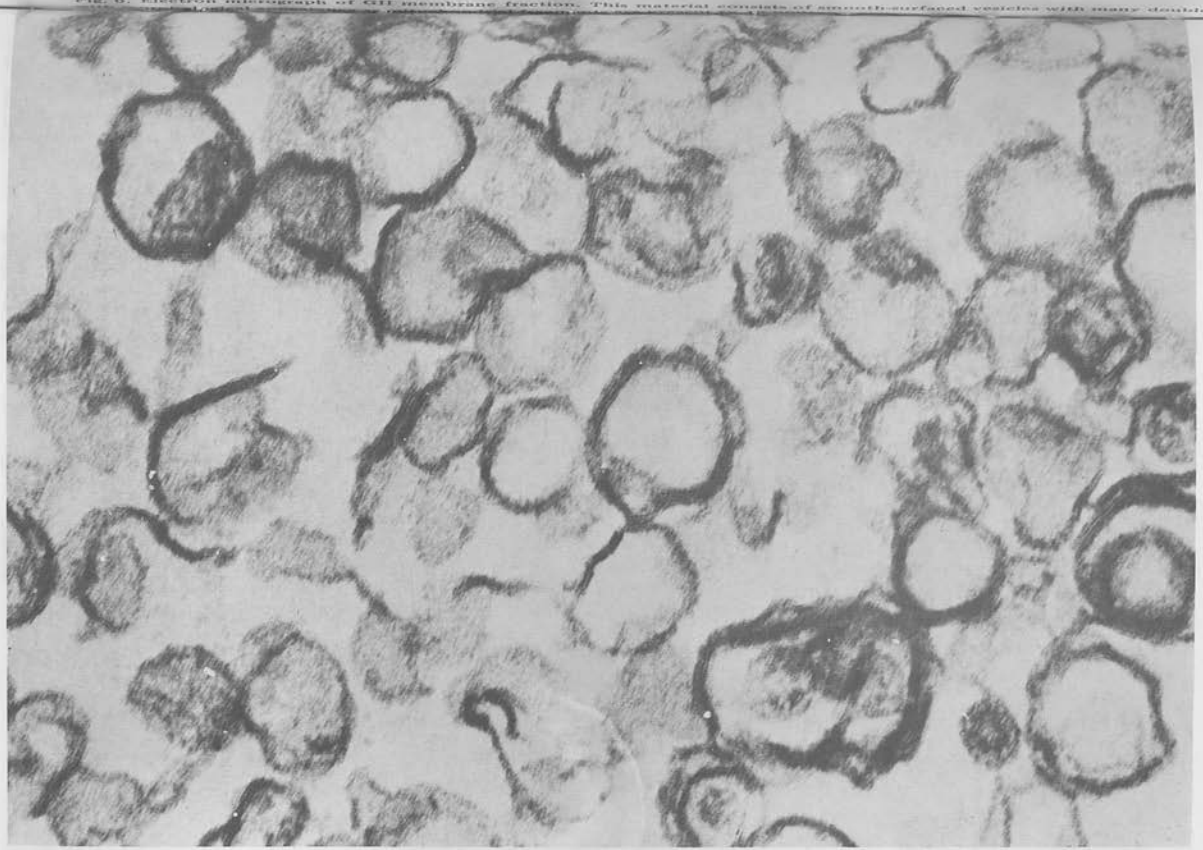

Fig. 7. Electron micrograph of FI electrophoretic fraction. The morphology is similar to that of GII fraction. Contaminations by other cell particles are quite absent (× 96 000).

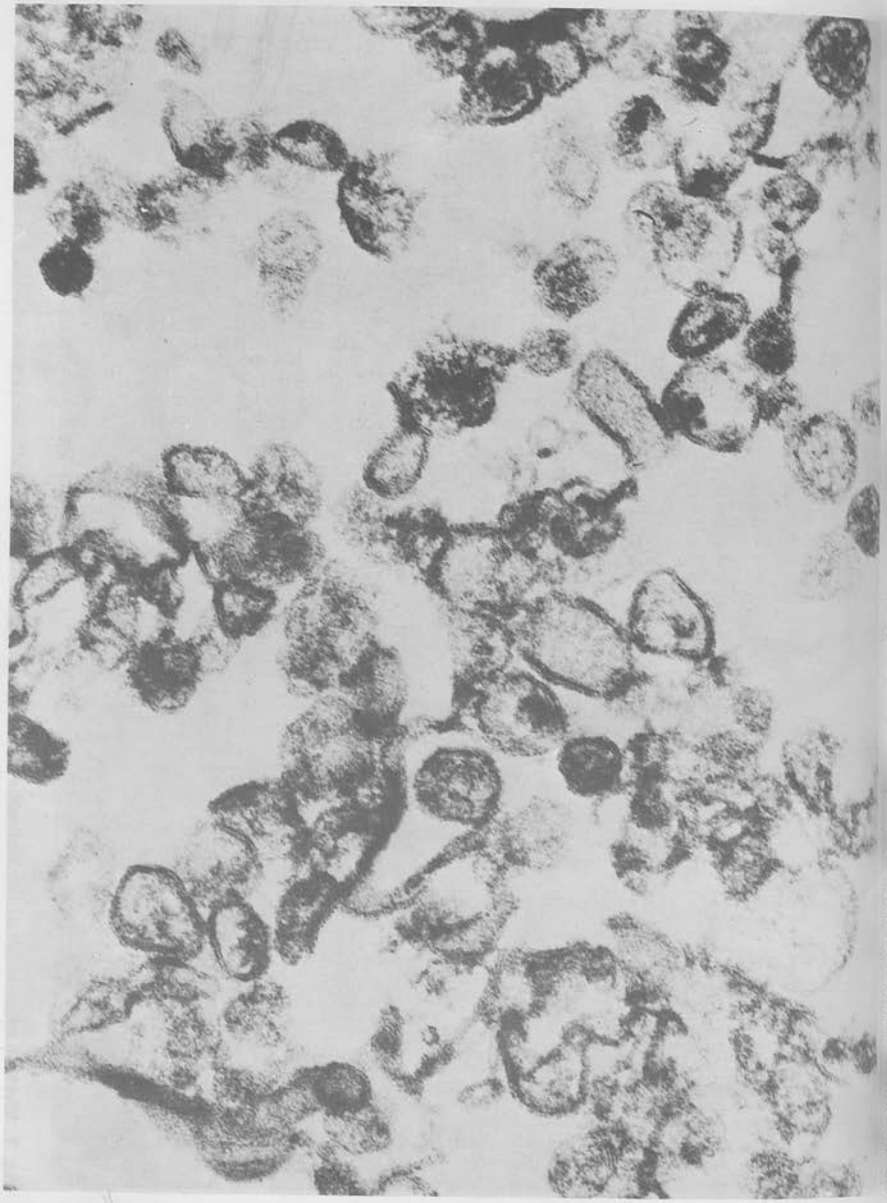

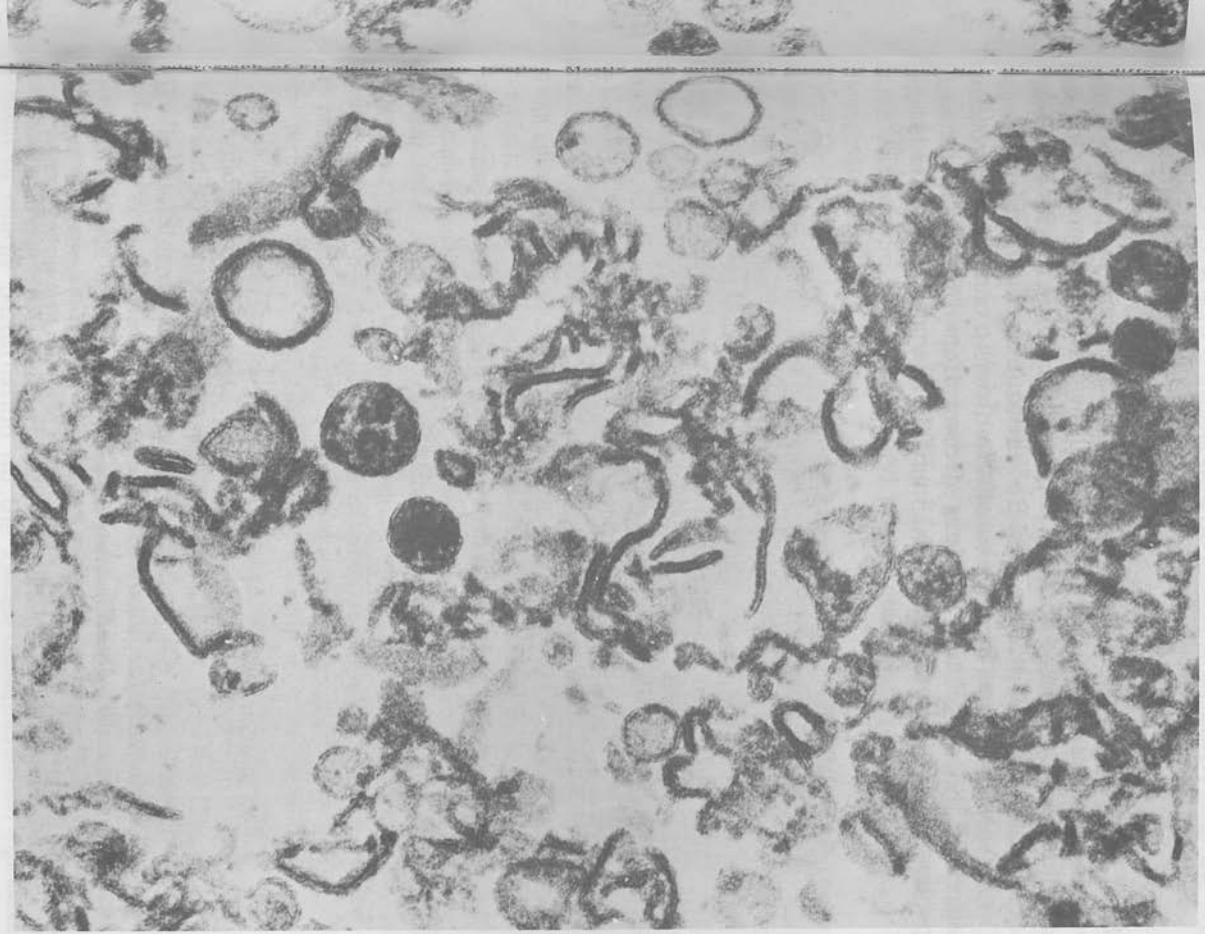

Fig. 9. Electron micrograph of FIII electrophoretic fraction. A mixture of open and closed membranes can be seen (× 16 000).

TABLE IV

$^{86}Rb^{+}$ UPTAKE AND EFFLUX OF GASTRIC MEMBRANE FRACTIONS

Values shown indicate a mean of four determinations.

Fractions	nmol $^{86}Rb^{+}$ uptake/mg protein	nmol $^{86}Rb^{+}$ efflux mg/protein *
GII (zonal)	160	60
GII—FI	235	125
GII—FII	195	8
GII—FIII	75	0

* $^{86}Rb^{+}$ efflux experiments were carried out in the presence of 2 mM ATP, under conditions described in Materials and Methods.

spite of its K^{+}-ATPase activity. For GII and FI fractions, the presence of valinomycin increased the rate, but not the final level, of $^{86}Rb^{+}$ uptake. It appeared that valinomycin enhanced the Rb^{+} permeability of the vesicles [16]. Addition of ATP stimulated H^{+} uptake and Rb^{+} efflux only in the FI fraction [16].

(7) Polyacrylamide gel electrophoresis. In order to compare the peptide composition of the subcellular fractions derived from hog gastric mucosa, the respective fractions were solubilized in SDS-β-mercaptoethanol and subjected

Fig. 10. SDS-polyacrylamide gel electrophoresis patterns of various gastric membrane fractions stained with Coomassie blue. The microsomal fraction P, obtained by differential centrifugation is shown and compared with fractions GII, FI, FII, FIII. Approx. 50 μg of protein were applied to each gel. Molecular weight was estimated by calibration of identical gels with standard protein. Note the increasing purification of the M_r = 100 000 polypeptide region.

acrylamide gel electrophoresis. Gels stained for protein (Fig. 10) revealed nsiderable simplification on the polypeptide pattern between the microsomal ction (P) and the electrophoretic gel purified fraction (FI). It can be seen t, consistent with the enzymatic data presented above, a major polypeptide ion of M_r = 100 000 accounts for 23% of the total protein stain in the micro- nal fraction and for 75% of the FI fraction. This polypeptide was phos- orylated by [γ-^{32}P]ATP and dephosphorylated in the presence of K^+ [3,5]. the other hand, FII electrophoretic pattern shows mainly the remaining otides of the original GII fraction.

Of interest is fraction FIII which shows the presence of a M_r = 100 000 poly- tide region in quite large amounts.

cussion

Previous studies on purification of gastric microsomal membranes [1,4,5] e used methods similar to those described here, with the exception of zonal pycnic centrifugation in a Ficoll/sucrose continuous gradient. This technique arates two classes of membranes: GI at density of 1.05 which is relatively iched in 5′-nucleotidase, and GII at density of 1.11 which is enriched 19- ld in K^+-ATPase and K^+-*p*-nitrophenyl phosphatase with respect to the origi- l homogenate.

The HCO_3^--stimulated ATPase, which has been the subject of much work in gastric membrane [3,4,18] seemed at first to be located in the denser ion of the sucrose gradient where mitochondrial and ribosomal markers were high activity [5,18]. However, detailed analysis of its distribution indicated t 28% of its activity was still located in GII where only 10% of mitochon- al markers activity was found.

The fractionation procedure described above yielded a satisfactory separa- n between 5′-AMPase, which is probably associated with other plasma mem- nes, and K^+-ATPase (or *p*-nitrophenyl phosphate), which is probably associ- d with apical membrane of the parietal cell surface and the tubulovesicular tem [1,5]. Yet it also indicates that densities of the membranes in which se two clases of enzymes are located are perhaps not different enough to w a complete separation by gradient centrifugation.

In recent investigations [6,23,24] it has been shown that the preparative e-flow electrophoresis technique is capable of effecting separation not pos- le by other methods. One important conditions for a successful application this relatively new technique is a difference in the electrical behavior of the terial to be purified. In the case of separations of biological membranes, refore, it is necessary that the membranes have unique electrical surface rges. In most cases, this varying surface charge appears to be related to a ctional and morphological difference.

Our initial attempt at the further purification of the K^+-ATPase in GII mem- ne fraction by free-flow electrophoresis under standard conditions gave fferent results, probably because of an insufficient difference in charge of particles involved. However, enzymatic analysis of the fractions collected icated that some degree of separation had been obtained. It seemed that the ucement of charge perturbation on the system could increase the electro-

phoretic resolution. Since it has been shown that the gastric ATPase can be phosphorylated in absence of cation such as K^+ [22], from the level of phosphorylation (approx. 10^{-9} mol of phosphate/mg protein) and the vesicular volume (2 μl/mg protein) of the membranes, it was possible to calculate a probable increase of 500 negative charges per vesicle. Based on this observation, MgATP was added to the electrophoretic separation medium.

The subsequent change in electrophoretic mobility of the membrane particles, produced by an increase in the negative charge density, resulted in a distinct separation of K^+-ATPase and *p*-nitrophenyl phosphatase from Mg^{2+}-ATPase and 5′-nucleotidase-carrying membrane. However, HCO_3 stimulation of ATPase was present in all the fractions. From the surface charge densities calculated for the FI fraction by the mobility measurements, in presence and absence of MgATP into the separation buffer, it was found that the change in negative charges per vesicle was in good agreement (approx. 600) with the value obtained from phosphorylation experiments.

The morphological appearance of the GII membrane fraction before electrophoretic separation, as seen in the electron microscope was not altered by this technique. The vesicular structure and the double membrane forms observed in GII fraction were also found in FI. On the other hand, the contamination present in GII was clearly separated and primarily confined to FII. Along with the enzymatic data and the electron microscope appearance, the gel pattern of membrane proteins separated by acrylamide electrophoresis tend to confirm the actual fractionation and purification of the gastric K^+-ATPase. The progressive increase in M_r = 100 000 region containing the phosphorylated peptide subunits of the K^+-ATPase and the considerably simplified polypeptide pattern in FI demonstrate the purification produced, when compared to GII and FIII fractions.

The free-flow electrophoresis technique appeared also to separate K^+-ATPase present in "tight" vesicles, from K^+-ATPase localised in open membrane fragments. The findings that ionophores such as valinomycin, in isotonic conditions, increase the K^+-ATPase activity of the membrane preparation, suggest that this ionophore enhanced the penetration of K^+ into the interior of the vesicles, eliminating the permeability barrier. This effect appeared significantly larger in fraction FI when compared to GII and it was not observed in fractions FII and FIII.

Based on those data, treatments designed to disrupt membrane vesicles should also be effective. Osmotic shock induced by hypotonic lysis and Triton X-100 treatment [25] were used to alter the tightness of the vesicles. In both cases the K^+-dependent ATPase activity was increased nearly to the valinomycin-expressed rate. It should be noted that increasing the concentration of Triton X-100 increased the ATPase activity up to a maximum and thereafter decreased. These treatments did not affect fractions FII and FIII. $^{86}Rb^+$ uptake studies confirmed the different degree of permeability of the vesicles. The high level of $^{86}Rb^+$ uptake in FI might be explained considering that this fraction could either contain a large percentage of vesicular material per mg of protein or vesicles less permeable to the ion involved, when compared to the original GII. On the other hand fractions FII and FIII showed less $^{86}Rb^+$ uptake. If the K^+-ATPase was in vesicular form, Rb^+ efflux should occur with ATP addition

16] as occurs in FI. The lack of efflux in FII and FIII implies either the absence of functional vesicles or vesicles highly permeable to Rb^+.

The results presented so far in this paper indicate that K^+ permeability is a limiting factor in the vesicular gastric ATPase activity. The data obtained by replacing K^+ with NH_4^+ in isotonic conditions supports this point of view. Again, analysis of the kinetics of activation both by K^+ and additional activation by ionophore(s) lead to the same conclusion [22]. The fact that K^+ stimulates both the ATPase and the phosphatase of gastric microsomal membranes raises the question of the relationship between those two enzymes. As for Ca^{2+}-ATPase and $(Na^+ + K^+)$-ATPase [26,27] there is considerable evidence that the phosphatase activity is a property of the ATPase complex. For example, in terms of purification, cation selectivity and action of inhibitors [4,5,16], it would seem that phosphatase and ATPase activity reside on the same enzyme.

The insensitivity to ionophores and to vesicle rupture of the *p*-nitrophenyl phosphatase activity suggests that K^+ penetration is not rate limiting for the activity of this enzyme, in contrast to the ATPase. Rb^+ transport does not occur with *p*-nitrophenyl phosphatase or acetyl phosphate as substrate, hence it is likely that the K^+ site for *p*-nitrophenyl phosphatase activity is readily available to external K^+, whereas the K^+ site for ATPase is internal. Since K^+ is transported by the vesicle and both an internal and external K^+ site are present, the site must be mobile across the membrane.

The double or multilayered structure of many of the membrane forms in GII and FI would suggest that a change in specific enzyme activity might also occur with rupture of the vesicles if the inner vesicle also contained K^+-ATPase. The action of ionophores in achieving maximal activity and the insensitivity of *p*-nitrophenyl phosphatase to loss of vesicle integrity suggests that either ATP or *p*-nitrophenyl phosphate has free access to the inner vesicle, or that this inner vesicle has a different peptide composition from the outer vesicle.

Acknowledgments

The authors wish to express their gratitude to Dr. G. Shah and D. Dailey for the excellent technical assistance and to Dr. R. Schackmann for the $^{86}Rb^+$ experiments and for the stimulating discussion. Supported by N.I.H. grant AM 5878 and N.S.F. grant GB31075.

References

Ganser, A. and Forte, J.G. (1973) Biochim. Biophys. Acta 307, 169—180
Wiebelhaus, V.D., Sung, H.P., Helander, H.F., Shah, G., Blum, A.L. and Sachs, G. (1971) Biochim. Biophys. Acta 241, 49—56
Saccomani, G., Shah, G., Spenny, J.G. and Sachs, G. (1975) J. Biol. Chem. 250, 4802—4809
Forte, J.G., Forte, G.M. and Saltman, P. (1967) J. Cell. Physiol. 69, 293—304
Forte, J.G., Ganser, A., Beesley, R. and Forte, G.M. (1975) Gastroenterology 69, 175—189
Heidrich, J.G., Kinne, R., Kinne-Saffran, E. and Hannig, K. (1972) J. Cell Biol. 54, 232—245
Lowry, O.H., Rosebrough, N.J., Farr, A.L. and Randall, R.J. (1951) J. Biol. Chem. 193, 265—275
Hannig, K. (1972) in Techniques of Biochemical and Biophysical Morphology (Glick, D. and Rosenbaun, R.M., eds.), Vol. 1, pp. 191—232, Wiley, J. and Sons, New York
Yoda, A. and Hokin, L.E. (1970) Biochem. Biophys. Res. Commun. 40, 880—884
Torriani, A. (1968) Methods Enzymol. 12B, 212—215
Cooperstein, S.J. and Lazarow, A. (1951) J. Biol. Chem. 208, 645—661
King, T.E. (1967) Methods Enzymol. 10, 322—331

12 Tabor, C.W., Tabor, H. and Rosenthal, S.M. (1954) J. Biol. Chem. 208, 645—661
14 Munro, H.N. and Fleck, A. (1966) Methods Biochem. Anal. 14, 113—176
15 Burton, K. (1956) Biochem. J. 62, 315—323
16 Sachs, G., Changh, H.H., Rabon, E., Schackman, R., Lewin, M. and Saccomani, G. (1976) J. Biol. Chem. 251, 7690—7698
17 De Duve, C. (1971) J. Cell Biol. 50, 20D—55D
18 Soumarmon, A., Lewin, M., Cheret, A.M. and Bonfils, S. (1974) Biochim. Biophys. Acta 339, 403—414
19 Henry, D.C. (1931) Proc. R. Soc. Lond. Ser. A. 133, 106—140
20 Loeb, A.L. and Wiersema, P.H. (1961) The Electric Double Layer around a Spherical Colloid Particle, The M.I.T. Press, Cambridge, Mass.
21 Jacobs, M.H. and Stewart, D.R. (1947) J. Cell. Comp. Physiol. 30, 79—103
22 Saccomani, G., Rabon, E. and Sachs, G. (1977) J. Biol. Chem., submitted
23 Ryan, K.J., Kalent, H. and Llewellyn, T.E. (1971) J. Cell. Biol. 49, 235—246
24 Stahn, R., Maier, K.P. and Hannig, K. (1970) J. Cell. Biol. 46, 576—591
25 Walter, H. (1975) Eur. J. Biochem. 58, 595—601
26 De Meis, L. (1969) J. Biol. Chem. 244, 3733—3739
27 Rose, J.D., Hirschowitz, B.I. and Sachs, G. (1967) Arch. Biochem. Biophys. 119, 277—281
28 Gauser, A.L. and Forte, J.G. (1973) Biochem. Biophys. Res. Commun. 54, 690—696

THE JOURNAL OF BIOLOGICAL CHEMISTRY
Vol. 251, No. 23, Issue of December 10, pp. 7690–7698, 1976
Printed in U.S.A.

A Nonelectrogenic H^+ Pump in Plasma Membranes of Hog Stomach*

(Received for publication, October 28, 1975, and in revised form, April 12, 1976)

GEORGE SACHS,‡ HSUAN HUNG CHANG, EDD RABON, ROBERT SCHACKMAN, MIGUEL LEWIN, AND GAETANO SACCOMANI

From the Laboratory of Membrane Biology, University of Alabama Medical Center, Birmingham, Alabama 35294

Differential and density gradient centrifugation were used to prepare a vesicular membrane fraction from hog gastric mucosa enriched 17-fold with respect to cation-activated ATPase and 5′-AMPase. Fractionation of the gradient material by free flow electrophoresis resulted in a fraction 35-fold enriched in cation-activated ATPase and essentially free of 5′-AMPase and Mg^{2+}ATPase. The addition of ATP to either fraction resulted in H^+ uptake and Rb^+ efflux. The ionophoric and osmotic sensitivity showed that these ion movements were due to transport rather than binding. The cation selectivity sequences, substrate specificities and action of inhibitors indicated that the transport was a function of K^+ATPase activity. The characteristics of the ATP-dependent enhancement of SCN^- uptake and 8-anilinonapthalene-1-sulfonate fluorescence in the presence of valinomycin and the action of ionophores and lipid-permeable ions suggested that the energy dependent K^+:H^+ exchange was effectively nonelectrogenic. Thus these vesicles contain a nonelectrogenic (H^+ + K^+)-ATPase, hence acid secretion by the stomach is probably due to an ATP-dependent H^+ + K^+ exchange.

Hydrogen ion transport systems have been demonstrated in several microorganisms (1) in organelles such as *Escherichia coli* membrane vesicles (2), mitochondria (3), and chloroplasts (4). Hydrogen ion transport has also been shown in artificial vesicles containing oxidation-reduction enzymes (5) or mitochondrial ATPase with F_0 (6). In all these cases the pump appears to be primarily electrogenic (7) and the hydrogen ion gradient to be of major importance in energy transduction and solute transport (8).

The gastric proton pump is the longest studied, the most potent and, so far, the most elusive. Work on the intact amphibian mucosa has suggested that this proton pump, like all the others, is electrogenic (9). In addition, studies of the intact tissue have not been decisive in terms of an ATP or oxidation-reduction-driven proton pump in the stomach (10). Studies of a microsomal fraction have shown the presence of an ATP-dependent H^+ uptake (11).

In the present study we describe the preparation of membrane fraction from the stomach that carries out an ATP-dependent electroneutral H^+:K^+ exchange. It would appear therefore, that the gastric proton pump contains an ATP-driven component which is nonelectrogenic.

MATERIALS AND METHODS

Vesicle Preparation—Stomachs were obtained from freshly slaughtered hogs. The fundic mucosal surfaces were flooded with saturated NaCl and wiped dry to remove mucus cells. The gastric mucosa was then scraped from underlying connective tissue and homogenized in a 10% suspension (w/w) in 0.25 M sucrose, using a Teflon-glass homogenizer. The microsomal fraction was obtained by centrifugating the post-20,000 × *g* supernatant at 100,000 × *g* for 60 min. The pellet was resuspended in 0.25 M sucrose and was separated on a step gradient consisting of a layer of 7% (w/w) Ficoll in 0.25 M sucrose on top of a 30% (w/w) sucrose layer in a Beckman Z60 rotor by centrifuging for 2 h at 59,000 rpm. The membranes (GI) banding at the top of the gradient were more active than the second membrane fraction (GII) in the transport studies. The lighter fraction was used in the studies unless otherwise indicated. As described in detail elsewhere (12), the lighter fraction was shown to have undetectable levels of mitochondrial markers such as succinic dehydrogenase, monamine oxidase, or cytochrome oxidase and to be 17-fold enriched with respect to the total homogenate in terms of K^+ATPase and 5′-AMPase activity. This fraction was further separated by free flow electrophoresis on a Hannig FF5 free flow machine (Biomedical Instruments, New York) using 8 mM Tris[1] base, 8 mM acetic acid, and 250 mM sucrose, adjusted with 2 N NaOH at pH 7.4, in the presence of 0.1 mM MgATP as curtain buffer with a voltage gradient of 100 V/cm and a flow rate of 180 ml/h at 7.5°. This divides the gradient preparation into K^+ATPase (FI) and 5′-AMPase (FII) enriched fractions.

Sodium dodecyl sulfate gel electrophoresis was carried out as previously described (13).

Enzyme Assay—ATPase activity was measured in a medium containing approximately 10 μg of protein, 2 mM $MgCl_2$, 2 mM ATP in 40 mM Tris/acetate buffer with or without 20 mM KCl or other salts at pH 7.4 in a final volume of 1 ml. In some assays 0.25 M sucrose was present in addition to the other constituents. In some experiments

* This work is supported by National Institutes of Health Grant AM 15878 and National Science Foundation Grant GB31075.

‡ To whom correspondence should be addressed.

[1] The abbreviations used are: Tris, tris(hydroxymethyl)-methylamine; *p*NPP, *p*-nitrophenyl phosphate; ANS, 8-anilinonaphthalene-1-sulfonate; CCCP, *m*-chloro(carbonyl cyanide)phenylhydrazone; DCCD, *N,N′*-dicyclohexylcarboniimide; *p*CMBS, *p*-chloromercuribenzenesulfonate.

ATP hydrolysis was measured during transport studies after 10-s incubation but at a 20-fold greater protein concentration. Ionophores were added in 10 μl of methanol with appropriate methanol controls. Incubation was carried out for usually 15 min at 37°. Phosphate release was measured by the method of Yoda and Hokin (14). Protein was measured according to Lowry et al. (15).

p-Nitrophenyl phosphate hydrolysis was measured as previously described (16) in a medium containing 10 μg of protein, 6 mM $MgCl_2$, 6 mM *p*-nitrophenyl phosphate (*p*NPP) and 40 mM Tris/acetate buffer (pH 7.5) with or without 20 mM KCl. 5′-AMPase was measured as previously described (16).

H^+ Transport – Proton uptake was measured using a pH electrode placed in a magnetically stirred vessel at room temperature. Membranes (about 1 mg of protein) suspended in 1 ml of 0.25 M sucrose were added to 6 ml of a medium containing 5 mM glycylglycine buffer (pH 6.11), 150 mM salt (usually KCl), and 2 mM $MgCl_2$. After a 3-min preincubation, ATP or other substrates were then added to give final concentrations between 1.5×10^{-7} and 3×10^{-4} M. In some experiments the nature and concentration of the alkali metal chloride was varied both in the external medium and the intravesicular water. Preincubation of the vesicles in the alkali metal salt and adding these vesicles to a medium containing the identical salt concentration gave conditions of zero cation gradient with varying cation concentration. Adding the preincubated vesicles in 1 ml to 5 ml of medium containing choline chloride in place of the metal chloride gave a constant outward gradient with varying internal cation concentration. Preincubation of the vesicles for 48 h at 4° as above in choline chloride and adding to varying concentrations of cation gave varying external cation concentrations and varying initial inward cation gradients. This procedure allowed the effects of varying cation concentration and varying cation gradient to be assessed.

In some experiments samples of the medium were taken for phosphate analysis 10 s after ATP addition and the quantity of H^+ transported at this time measured. Ionophores such as valinomycin (1.5×10^{-6} M), nigericin (1 μg/ml), and tetrachlorsalicylanilide (9×10^{-7} M) (final concentrations) were added in 10 μl of methanol. Kinetic analyses were performed using the initial 6 s of measurement (initial rate).

The measurement of pH change was carried out using a Radiometer pHM 64 pH meter coupled to a servorecorder with a REA 112 amplifier. One centimeter chart width corresponded to a change of .008 pH unit. The H^+ concentration change was measured in each experiment by back titration with 10^{-3} M HCl which allowed for buffering artifacts.

$^{86}Rb^+$ Transport – For uptake experiments a 200-μl vesicle suspension (2.5 to 4 mg/ml) was mixed with an equal volume of a solution containing 150 mM RbCl with 10 μCi/ml of $^{86}Rb^+$, 10 mM glycylglycine (pH 6.12), and 4 mM $MgCl_2$. At various times 20 μl of the incubation solution were transferred to 1 ml of a solution at 0–5° containing 150 mM choline chloride, 5 mM glycylglycine, and 2 mM $MgCl_2$ at pH 6.12. This was blended on a Vortex mixer and filtered on a Millipore type HA filter (0.45 μ pore size) and washed four times with 2 ml of the ice-cold choline chloride solution. All samples were run in duplicate. Adding 1% Triton X-100 to the stop solution reduced trapped radioactivity to 5% of the radioactivity obtained without detergent and treating the vesicles with distilled water prior to the experiment reduced radioactivity to less than 15% of control treated in the usual way.

Efflux experiments were carried out from equilibrated vesicles. Forty-eight hours of incubation at 4° was required for equilibration. After incubation in the uptake medium 2 mM ATP was added directly to the solution so that efflux in the presence of ATP was measured in the absence of any initial gradient of Rb^+ or $^{86}Rb^+$. Efflux of $^{86}Rb^+$ under these conditions would be against a concentration gradient. Sampling was carried out as above. The amount of $^{86}RB^+$ on the filter was expressed as nanomoles of mg protein^{-1}.

$^{36}Cl^-$ Transport – Movement of Cl^+ across the vesicle membrane was studied essentially in the same way as Rb^+ movement. Uptake studies were performed as above, except that the solutions contained 150 mM KCl with 10 μCi/ml of $^{36}Cl^-$ and choline or lithium sulfate solutions were used as stop solutions. Experiments were also carried out using equilibrated vesicles as for Rb^+, with again the use of SO_4^{2-} instead of Cl^- as the anion in the washing solutions to reduce anion exchange efflux.

Uptake of $S^{14}CN$ – Thiocyanate was used as a lipid-permeable anion (17), since dipicrylamine inhibited ATPase and tetraphenylborate precipitates K^+. Uptake of SCN^- was studied by adding 200 μl of vesicles as in the cation uptake studies to 200 μl of a solution containing 150 mM KCl, 1.82 mM $NaS^{14}CN$ (4 μCi), 80 mM Tris/acetate buffer at pH 6.1, and 2 mM $MgCl_2$. In addition one set of tubes contained 10^{-6} M valinomycin in 4 μl of methanol After sampling for 15 min, 2 mM ATP was added to half of both sets of tubes and sampling continued for another 15 min. The 20-μl samples were added to 1 ml of ice-cold 120 mM Li_2SO_4 solution, filtered, and washed once with 4 ml of the Li_2SO_4 solution. The filters were dried and counted as before.

Fluorescence of 8-Anilinonapthalene-1-sulfonate – Fluorescence of ANS was measured at 27° in an Aminco Bowman spectrofluorimeter with an excitation wavelength of 375 nm and emission wavelength of 480 nm. Standard conditions were the addition of 100 μl of the membrane suspension (5 mg of protein/ml) to a quartz cuvette containing 2 ml of 150 mM KCl and 40 mM Tris/acetate buffer (pH 6.1). ANS was added in 10 μl of methanol usually at 2.5×10^{-6} M, followed by valinomycin 5×10^{-6} M also in methanol, and then MgATP, usually at 5×10^{-5} M. Other additions such as nigericin (1 μg/ml) or *m*-chloro(carbonyl cyanide)phenylhydrazone (CCCP) (10^{-5} M) were in 10 μl of methanol. ATP analogs were added at the same final concentration as ATP, and dicyclohexylcarbodiimide was added at 10^{-3} M, final concentration.

Chemicals – ATP and its analogs were purchased from Sigma Chemicals, radioactive substances from ICN, and ANS from Eastman Kodak. Ionophores were purchased commercially or obtained as gifts from Dr. H. A. Lardy. Hog stomachs were donated by Lumberjack Meats, Inc.

RESULTS

Nature of Active Fraction – Active H^+ transport is an unusual property of cell plasma membranes but clearly must be present in gastric mucosa. H^+ transport is also a property of mitochondria and perhaps lysosomes. It is necessary therefore to clearly separate the H^+ transport particle from any other cell component. This was achieved by density gradient and electrophoretic separation. The lighter of the two membrane fractions (density = 1.05) was more active in terms of H^+ uptake. Electron microscopy showed it to be composed of smooth surfaced vesicles with an occasional inclusion of a second vesicle (Fig. 1). Compared either to the total homogenate or to the microsomal fraction, the vesicles were enriched with respect to both K^+ATPase and 5′-AMPase. The peptide pattern on sodium dodecyl sulfate gels was quite complex although simpler than the original microsomes (Fig. 2). Further resolution of the gradient peak was achieved by free flow electrophoresis. The anodic fraction (FI) (Fig. 3) was enriched in terms of K^+ATPase giving a final 35-fold purification and was depleted of Mg^{2+}ATPase and 5′-AMPase (Table I). The valinomycin sensitivity of the K^+ATPase was also present only in FI (12). The sodium dodecyl sulfate gel pattern of FI is considerably simplified compared to the density gradient fraction, and contained two peptide regions, of M_r = 100,000 and M_r = 84,000 and a minor band at the dye front (Fig. 2). The major peptide region (>75% of protein) of M_r = 100,000 was phosphorylated by [γ-^{32}P]ATP and dephosphorylated in the presence of K^+. No oxidation of NADH or NADPH by this preparation was observed.

Following free flow electrophoresis, only FI responded to ATP addition by H^+ uptake or Rb^+ extrusion. Therefore, these properties are associated with a membrane whose peptide composition is relatively simple. Due to yield and ease of preparation GI was used in most of the transport studies to be described.

K^+ATPase Properties – Since cation-activated ouabain-insensitive ATPase or *p*-nitrophenyl phosphate hydrolysis were the only enzyme activities of those measured associated with the active fraction, some of the properties of this enzyme were measured to enable a correlation to be made between transport and enzyme activity. ATP was the most active substrate

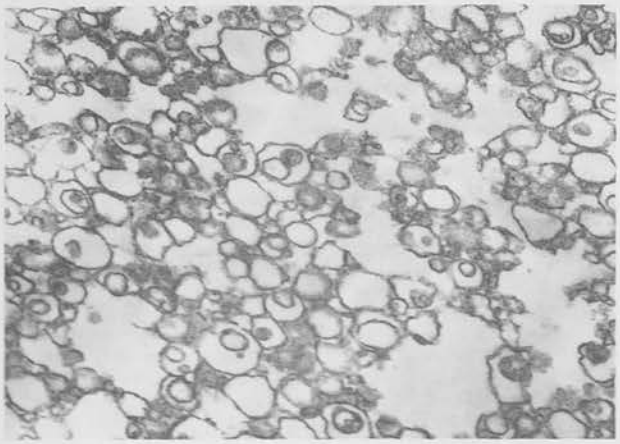

FIG. 1. Electron micrograph of the light membrane fraction used in these studies (× 40,000). Most of the membranes are single layered and smooth surfaced. Some have electron dense material associated and some appear to contain a second vesicular structure.

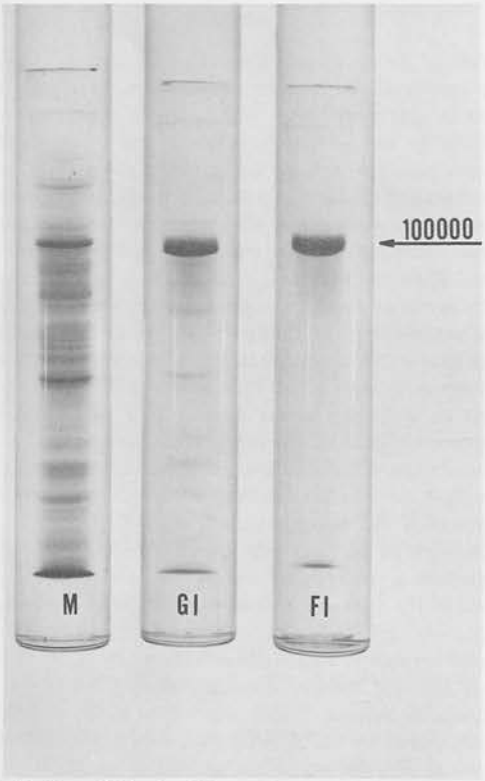

FIG. 2. Sodium dodecyl sulfate gel patterns of the microsomal fraction, the gradient fraction and the electrophoretic fraction showing the increasing purification of the M_r = 100,000 band.

for the ATPase. K^+-stimulated hydrolysis occurred (ATP activity is set to 100) in the sequence ATP 100:GTP 12:CTP 15:ITP 0:ADP 0.7. No hydrolysis of β,γ-methylene ATP was observed, although this compound did act as a competitive inhibitor of the ATPase.

Since H^+ uptake was cation dependent and selective, the cation selectivity of the ATPase was measured to obtain a correlation between activity and transport. The cation selectivity was (where the activity with K^+ is given the value 100)

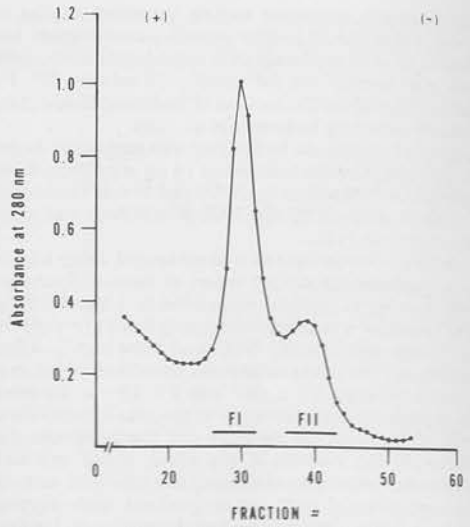

FIG. 3. Protein profile of the electrophoretic fractionation of the density gradient peak showing 2 major bands, the larger being closer to the anode.

TABLE I

Purification of vesicles

The activity of 5′-AMPase and ATPase in the total homogenate, microsomal fraction (100,000 × *g* precipitates of the post 20,000 × g supernatant) the light membrane fraction on the 7% Ficoll to 30% w/w sucrose gradient and the 2 fractions derived from the latter by free flow electrophoresis. The K^+ATPase activity is the difference between activity in the presence and absence of K^+. The K^+ATPase + valinomycin activity is the difference between the activity in the presence of K^+ and valinomycin and in the presence of Mg^{2+} alone.

	5′-AMPase	Mg^{2+}ATPase	K^+ATPase	K^+ATPase + valinomycin
		$\mu mol\ P_i\ mg^{-1}\ h^{-1}$		
Total homogenate	0.5 ± 0.3	6.2 ± 0.6	2.0 ± 1.0	3.6 ± 1.8
Microsomal fraction	1.5 ± 0.6	15.9 ± 1.5	7.1 ± 4.3	16.7 ± 4.0
Light membrane fraction (GI)	4.6 ± 0.1	6.4 ± 1.3	32.5 ± 3.2	62.9 ± 1.7
Electrophoretic fraction (FI)	0.6 ± 0.2	2.7 ± 0.6	64.1 ± 3.9	87.6 ± 2.5
Electrophoretic fraction (FII)	14.7 ± 1.2	16.6 ± 2.0	17.3 ± 1.2	19.4 ± 1.7

K^+ 100:Rb^+ 76:Cs^+ 16:Na^+ 7:Li^+ 4:choline 0, and this was the same relative sequence as for *p*-nitrophenylphosphate hydrolysis (Table IV).

In analyzing the transport function of an enzyme present in the membrane of ion-impermeable vesicles, the effect of ionophores or lipid-permeable ions on ATPase activity gives insight into the electrical characteristics of transport. Thus increase of activity with both classes of compound suggests that conductance plays a role in pump action *i.e.* that the pump is electrogenic. An increase in activity due to a K^+ selective ionophore but no increase of activity with lipid-permeable ions suggests a requirement for K^+ inside the vesicle but is not consistent with a change in pump activity simply due to a conductance change in the membrane, as would be expected of an electrogenic mechanism. A larger increase with K^+ ionophores and a smaller increase of activity with lipid-permeable ions would suggest both an electrogenic mechanism and a K^+ requirement in the vesicle interior.

The addition of 10^{-5} M valinomycin stimulated ATPase ac-

tivity by 78% in the density gradient fraction and by 40% in the free flow FI fraction (Table I), but had no effect on *p*-nitrophenyl phosphate hydrolysis. Protonophores such as CCCP or 3,3′,4,5′-tetrachlorosalicylanilide at 10^{-5} M did not affect ATPase activity and had no additional effect on the valinomycin stimulation. Lipid-permeable ions such as triphenylmethyl phosphonium or dimethyldibenzyl ammonium did not increase ATPase activity at 10^{-3} M even in the presence of SCN^-.

Dipicrylamine, Zn^{2+}, F^-, pCMBS, and DCCD all inhibited the K^+ATPase activity (Table II), but SCN^- and dimethyldibenzyl ammonium were without effect on enzyme activity.

H^+ Uptake—The presence of an ATPase in these vesicles and the absence of any detectable oxidation-reduction activity such as oxidation of NADH or NADPH suggested that ATP was probably the required substrate for transport.

The addition of ATP did indeed produce a rapid but transient alkalinization of the medium (Fig. 4). The reversal of the alkalinization was due to the consumption of the added ATP (1.7×10^{-5} M) followed by leaks of the accumulated H^+ back into the medium. The dissipation of the gradient was accelerated by ionophores such as valinomycin or nigericin but only transiently accelerated by protonophores such as tetrachlorosalicylanilide.

The effect of ionophores is strong evidence for the presence of a gradient of H^+ across the vesicle membrane. This was further established by the effect of varying the vesicle volume which would be expected to affect uptake but not binding. Fig. 5 shows that the H^+ uptake (maximum uptake) was a function of the medium osmolarity. This also allowed assessment of the amount of H^+ bound due to ATP addition. Extrapolation to infinite osmolarity showed that binding was quantitatively small in relation to transport of H^+.

To relate uptake to ATPase activity, various experiments were performed. Uptake of H^+ occurred only with ATP and not with GTP, CTP, ITP, TTP, or ADP. β,γ-Methylene ATP was also inactive and *p*-nitrophenyl phosphate up to 10 mM had no effect on H^+ distribution. ATPase inhibitors such as Zn^{2+}, F^-, DCCD, and *p*CMBS inhibited H^+ uptake at 1 mM. Alkali cation was required for H^+ uptake and different rates of H^+ uptake were obtained with different cations. The sequence of effectiveness found (with K^+ set to 100) was K^+ 100:Rb^+ 60:Cs^+ 45:Na^+ 0.24:Li^+ 0.1:choline 0 (Table IV). All these data were consistent with the hypothesis that ATPase activity was required for the H^+ uptake.

Measurement of the H^+ uptake and ATP hydrolysis over the initial 10 s following addition of the vesicles to the uptake medium allowed calculation of the ratio of moles of H^+ transport to moles of ATP hydrolyzed. Considering only the K^+ activated component of the ATPase, the value for this ratio was 4.1 ± 0.2 ($n = 10$). Using a value of 2 μl mg^{-1} for vesicular volume, the minimal pH inside the vesicles based on the quantity of H^+ disappearing was 1.7. The actual value is probably higher due to the buffer present as well as due to the intrinsic buffering capacity of the inside surface of the vesicles.

The electrical characterisitcs of H^+ transport were investigated using ionophores and lipid-permeable ions. The finding that the H^+ gradient could dissipate spontaneously and that this dissipation could be accelerated by valinomycin in the presence of an inward K^+ gradient suggested the presence of an H^+ conductance in the vesicle membrane (Fig. 4). The relative ineffectiveness of a protonophore such as tetrachlorosalicylanilide, in the absence of an added K^+ conductance argues for a low inherent K^+ conductance or indeed anion

TABLE II

Effect of inhibitors on K⁺ATPase

The action of various inhibitors on K^+ATPase activity. ATPase was assayed as described in the text.

	Inhibition
	%
*p*CMBS (10^{-5} M)	72
DCCD (10^{-3} M)	82
F^- (10^{-2} M)	80
Zn^{2+} (10^{-3} M)	90
Dimethyldibenzyl ammonium (10^{-3} M)	0
SCN^- (10^{-2} M)	0
Dipicrylamine (10^{-3} M)	100

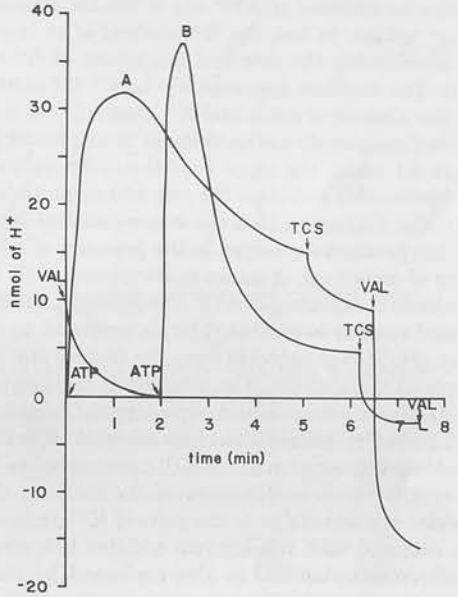

FIG. 4. H^+ uptake by the vesicles. *Curve A*, vesicles were added to a solution of 150 mM KCl with additions as in text followed by 1.7×10^{-5} M ATP. At times indicated tetrachlorsalicylanilide (*TCS*) and valinomycin (*VAL*) were added. *Curve B*, valinomycin was added immediately after the addition of the vesicles from the same preparation, then ATP at 1.7×10^{-5} M was added.

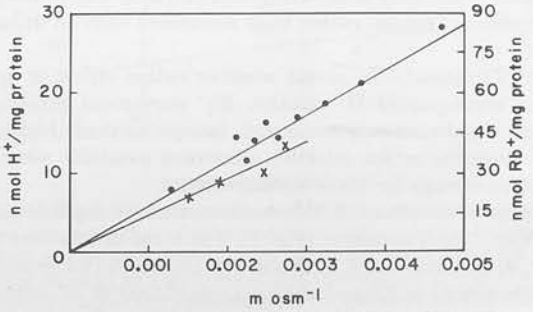

FIG. 5. The effect of vesicular volume on H^+ and Rb^+ uptake. The vesicles were added to a solution containing 90 mM KCl with appropriate addition of mannitol to vary the osmolarity and other additions as detailed in text. ATP (1.7×10^{-5} M) was added, and the H^+ uptake measured (●——●). $^{86}Rb^+$ uptake was measured by adding the vesicles to a medium containing 75 mM RbCl with mannitol added to vary the osmolarity and other additions as detailed in the text (×——×).

conductance. This finding also suggests that K^+ conductance or penetration may be rate limiting for H^+ uptake. This was confirmed by the finding that valinomycin added before ATP increased the uptake rate of H^+ (Fig. 4). This effect is not due to a nonspecific conductance increase in the membrane resulting in shunting of a potential due to electrogenic H^+ transport. This is shown by the finding that a lipid-permeable cation such as dimethyldibenzyl ammonium did not influence H^+ uptake at concentrations as high as 10^{-3} M. SCN^- inhibited H^+ uptake by 40% at 10^{-2} M but this appeared to be due to a more rapid dissipation of the gradient since the efflux of H^+ was accelerated. Other lipid-permeable ions such as $TPMP^+$ or dipicrylamine inhibited H^+ uptake but also inhibited ATPase activity by the same amount.

The effect of valinomycin is therefore due to the specific effect of increasing the K^+ penetration into the vesicle. This is substantiated by the finding that preincubation of the vesicles in KCl prior to addition of ATP has a similar accelerating effect on H^+ uptake. In fact, the K^+ gradient is an important factor in determining the rate and magnitude of H^+ uptake (Table III). The smallest apparent K_A for K^+ (32 mM) is obtained in the absence of an initial K^+ gradient and is of the same order of magnitude as the value of 20 mM found for the ATP at pH 6.1 under the same conditions. An outward K^+ gradient considerably increases the rate and magnitude of the H^+ uptake also suggesting that the cation gradient is related to the H^+ ion gradient developed in the presence of ATP.

Coupling of movement of cation to movement of H^+ can be obtained also in the absence of ATP. For example, adding KCl preincubated vesicles to choline chloride produced no change in medium pH. This is expected from the finding of a low K^+ conductance in the vesicles. The addition of valinomycin, or more effectively valinomycin and tetrachlorosalicylanilide but not tetrachlorosalicylanilide alone induces an H^+ uptake. Conversely, adding valinomycin to the KCl medium before vesicle addition results in an acidification of the medium (Fig. 4) when vesicles are added due to the inward K^+ gradient. The overshoot obtained with valinomycin addition following ATP and tetrachlorosalicylanilide is also explained by electrical coupling of the inward K^+ movement to H^+ efflux. Since tetrachlorosalicylanilide alone does not induce H^+ movement in response to a K^+ gradient this confirms what was suggested above, namely, that the intrinsic H^+ conductance of the vesicles is larger than the intrinsic K^+ conductance.

These data then suggest that H^+ uptake is a function of the ATPase, is probably nonelectrogenic, and may well be coupled to an efflux of cation, rather than associated with an influx of anion.

Rb^+ Transport—To assess whether cation efflux or anion influx accompanied H^+ uptake, Rb^+ movement across the vesicle membrane was measured. Isotope methods had to be used since the cation selective electrodes available were not sensitive enough for these measurements.

The passive uptake of Rb^+ was temperature dependent and also osmotically sensitive (Fig. 5). The $t_{1/2}$ of uptake was 12 h at 4°, 40 min at 22°, and 10 min at 37°. Incubation for prolonged periods of time at 22° and short periods of time at 37° damaged the vesicles as assessed by the maximal H^+ gradient obtained. ATP transiently reduced influx presumably due to acceleration of efflux. To study this further the vesicles were therefore preloaded with $^{86}Rb^+$ before ATP addition for the efflux studies.

Incubation at 4° resulted in equilibration in terms of trapped radioactivity by 48 h. The quantity trapped allowed calculation of the intravesicular volume with the value found being 2.0 ± 0.3 μl mg^{-1} ($n = 23$).

Although efflux could be measured by diluting the vesicles into nonradioactive medium, the conditions of zero gradient were more appropriate for determining the effect of ATP on Rb^+ efflux. Thus if there is a decreased trapped radioactivity found with ATP addition directly to the preincubation medium followed by re-equilibration to the previous value after the ATP is hydrolyzed, this can be taken as evidence for active cation extrusion.

As shown in Fig. 6, the addition of ATP to the Rb^+-loaded vesicles did indeed result in rapid cation extrusion followed by a slow re-uptake. The re-uptake rate had a similar $t_{1/2}$ to uptake found in the experiments where the vesicles were added to the radioactive medium.

The relationship of this phenomenon to ATPase activity was established by the inhibition of Rb^+ efflux by 1 mM concentrations of F^-, Zn^{2+}, DCCD, and *p*CMBS.

If Rb^+ efflux were due to movement of Rb^+ in response to a potential generated by an electrogenic H^+ pump, then the distribution ratio of Rb^+ between vesicle and medium would allow calculation of the potential. The vesicles lose $44 \pm 7\%$ ($n = 16$) of their radioactivity with ATP addition. This would correspond to a potential of 18 mV vesicle interior positive. However, this interpretation is in conflict with the data previously presented on ATPase activity and H^+ uptake which were

TABLE III

Effect of K^+ gradient and concentration on H^+ uptake

The preincubation conditions were as detailed in the text and the ionic concentrations were varied from 1 to 150 mM, mannitol being used to maintain isotonicity. The initial gradient was kept constant under two conditions (*i.e.* outward and zero) and only the i ic concentrations were varied allowing calculation of apparent K_A f m a best fit Lineweaver Burk plot.

$[K^+]_{in}/[K^+]_{out}$	Initial velocity	V_{max}	K_A
	nmol H^+ mg^{-1} min^{-1}	*nmol H^+ mg^{-1} min^{-1}*	*mM*
0.006[a]	130	216	62
1.0	163	218	32
6.0	563	1,370	182

[a] With the inward gradient, the gradient varied due to the conditions used. The value of 0.006 was the gradient under standard conditions, since a value of 1 mM K^+ was found in the vesicle preparation before addition of K^+. The data above are obtained following a 3-min preincubation, hence the magnitude of the inward gradient is only an estimate. All the experiments were carried out on the same preparation.

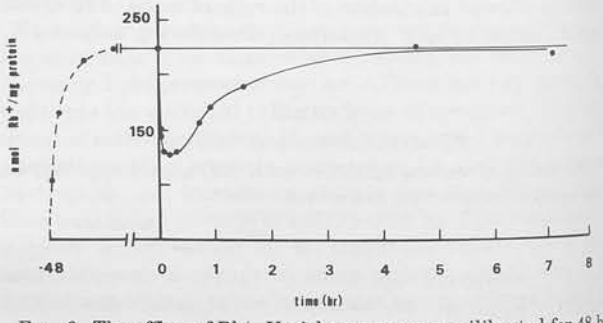

FIG. 6. The efflux of Rb^+. Vesicles were pre-equilibrated for 48 h as detailed in the text and 2 mM ATP added to the suspension at zero time on the graph. It can be seen that there is a transient rapid efflux of Rb^+ to about 50% of the measured equilibrium value (*horizontal line*) and with consumption of the ATP there is re-equilibration of the Rb^+.

interpreted as excluding a significant K^+ conductance.

If indeed movement of Rb^+ were due to a potential, then adding lipid-permeable cations would reduce Rb^+ movement since the cation would efflux instead of the Rb^+. Adding a Rb^+ ionophore such as valinomycin would accelerate Rb^+ movement since the Rb^+ conductance of the membrane would be increased. In fact neither dimethyldibenzyl ammonium, a lipid-permeable cation (even in the presence of SCN^- to increase its lipid solubility), nor valinomycin had any effect on Rb^+ efflux. Valinomycin did increase the re-uptake rate of Rb^+.

Accordingly, it is unlikely that cation efflux is coupled to a potential but more likely that cation efflux is directly related to ATPase activity.

Measurement of the ratio between moles of Rb^+ transported and ATP hydrolyzed gave a value of 3.5 ± 0.4 ($n = 4$) using only the cation-stimulated component of the ATPase activity.

Cl^- Transport – Although from the studies on cation efflux it would seem unlikely that Cl^- uptake accompanied H^+ uptake, the efflux studies were performed on equilibrated vesicles. It was possible that under conditions of an inward K^+ gradient, Cl^- uptake occurred with addition of ATP.

Cl^- uptake had similar characteristics to passive uptake of Rb^+. The $t_{1/2}$ of Cl^- at room temperature was 36 min as compared to the $t_{1/2}$ of 40 min for Rb^+. The equilibrium uptake volume was also 2.0 μl mg^{-1} of protein. The addition of ATP, however, was without any effect on the uptake rate. Moreover, there was no effect of ATP on the Cl^- distribution after the vesicles had equilibrated with $^{36}Cl^-$ in contrast to the data found with Rb^+. The addition of valinomycin had no effect on Cl^- uptake in the presence of a K^+ gradient or following ATP addition showing that these vesicles had minimal Cl^- conductance. This had already been concluded from the effect of ionophores on the H^+ gradient.

Thus data on H^+, Rb^+, and Cl^- movement across the vesicle membrane argue against the development of a potential during transport.

Uptake of $S^{14}CN^-$ – To determine whether the above indirect arguments excluding the development of a potential difference were correct, the effect of ATP on the distribution of a lipid-permeable anion, SCN^-, was determined.

Thiocyanate is taken up in a time-dependent fashion (Fig. 7) into an osmotically sensitive space. The $t_{1/2}$ of 2 min is very much less than the $t_{1/2}$ for Cl^- or Rb^+ confirming the SCN^- enters vesicles by an additional path presumably due to its lipid permeability. The apparent uptake of SCN^- in the presence of valinomycin is increased. This increased uptake requires the presence of K^+. Presumably this is due to increased binding of SCN^- in the hydrophobic phase due to the formation of the lipid-soluble valinomycin $K^+ \cdot SCN^-$ complex (Fig. 7) since preincubation of vesicles in KCl does not inhibit the valinomycin enhancement. This valinomycin increment is not osmotically sensitive confirming that this effect is on binding.

The addition of ATP has no effect on the distribution of SCN^- between vesicles and medium in the absence of valinomycin. This suggests that no potential develops under these conditions. From Rb^+ efflux studies a K^+ gradient would develop with the addition of ATP and this K^+ gradient would result in a potential difference only in the presence of valinomycin. The enhanced uptake of SCN^- obtained by ATP addition in the presence of valinomycin is consistent with the development of a potential in the presence of valinomycin. This increased uptake is osmotically sensitive.

Fluorescence of ANS – Radioactive isotope distribution may have too long a lag phase to detect a transient potential. For example, an electrogenic H^+ transport would result in development of an interior positive potential. This potential could result in the development of a K^+ conductance and current which would then shunt the potential. Hence, a fluorescent probe of potential, ANS, was used on the assumption that optical detection would have a more rapid response time than trapping of radioactivity.

The sequential addition of membranes ANS and ATP results in the fluorescence changes shown in Fig. 8. The addition of ANS results in rapid increase in fluorescence with a $t_{1/2}$ too rapid to measure with our instrumentation. This rapid fluorescence increase is followed by a second slow rise to a plateau after 30 min. The addition of ATP at any time under these conditions results in no change in fluorescence. Accordingly, if ANS is acting as a probe of potential, no potential change occurs.

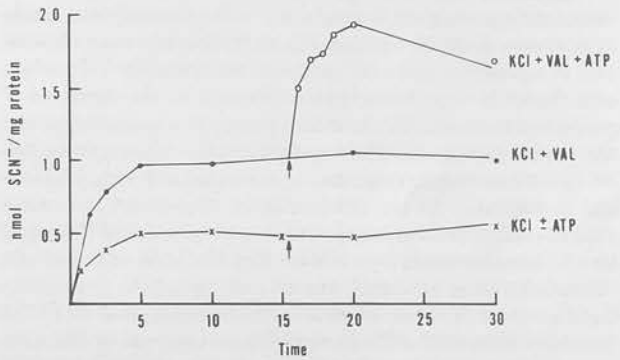

FIG. 7. The uptake of $S^{14}CN^-$ with time when added to vesicles alone (×——×) or vesicles in the presence of valinomycin (●——●). ATP was added to both sets of tubes at the time indicated, but enhanced SCN^- uptake only in the presence of valinomycin (○——○).

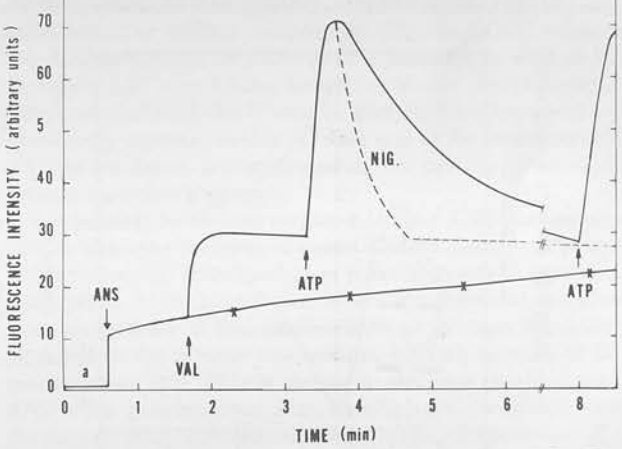

FIG. 8. The ANS fluorescence events of the gastric vesicles. The initial addition is that of the membranes to the cuvette, followed by ANS. It can be seen that there is an initial rapid rise with ANS addition followed by a slow increase of fluorescence (×——×) which eventually reaches the valinomycin level (not shown). The addition of valinomycin (*VAL*) before the plateau results in a further rapid increase in fluorescence, and the subsequent addition of ATP (1.7×10^{-5} M) results in a transient fluorescent enhancement, which can be repeated with a second addition of ATP. Also shown is the effect of nigericin (*NIG*) on the ATP induced fluorescence, giving immediate inhibition of the fluorescence and inhibition of the effect of subsequent ATP addition.

Quite different data are obtained in the presence of valinomycin. The addition of valinomycin after the initial fluorescence increment produces a rapid rise in fluorescence to the same level as occurs without valinomycin after 30 min. This increase in fluorescence requires the presence of K^+ and the magnitude is a function of the concentration of K^+, but not the K^+ gradient. Hence this fluorescence change is due to the increased binding of ANS in the membrane because of the increased solubility of the ANS · valinomycin · K^+ complex in the hydrophobic phase of the membrane. The presence of a positive interior potential as would occur with an inward K^+ gradient in the presence of valinomycin is therefore insufficient to produce a large enough change in fluorescence to obscure the fluorescence increase due to increased penetration of ANS. It should also be noted that an inward K^+ gradient in the presence of valinomycin would produce an alkalinization of the vesicle interior.

Addition of ATP in the presence of valinomycin produces a transient increase in fluorescence with precisely the same time course as the H^+ uptake (Fig. 9). This is due to a combination of a potential and a H^+ gradient. From the Rb^+ efflux data and the SCN^- uptake, a cation gradient in the presence of valinomycin results in the development of a potential across the vesicle membrane. The requirement for valinomycin to see an ANS fluorescence response suggests that a change of potential is necessary for the effect. Fig. 10 shows that the initial rate of change of fluorescence is a linear function of the log of the K^+ concentration ($r = 0.992$). This would be expected of a Nernst diffusion potential due to a K^+ gradient provided a fixed internal [K^+] was reached with the addition of ATP. If a potential difference were the only factor involved in the ANS response in the presence of valinomycin then dissipation of the H^+ gradient by nigericin which is a neutral exchange ionophore would not be expected to abolish or completely inhibit development of the fluorescence. In fact, both nigericin and carbonyl cyanide *p*-trifluoromethoxyphenylhydrazone inhibit or abolish the response (Fig. 8). Moreover, if ANS was responsive only to a potential in this system, then valinomycin alone should enhance the fluorescence of ANS as a function of the K^+ gradient, not the K^+ concentration. ANS appears capable of rapidly responding to a potential difference and an H^+ gradient in these vesicles. The lack of response in the absence of valinomycin is therefore reasonable evidence for the absence of a potential during transport by the gastric vesicles. The cation selectivity sequence is shown in Table IV which also shows the effectiveness of the cations in acid secretion.

Effect of Cl^- Removal – One of the more significant approaches to the problem of electrogenic transport by the intact amphibian stomach has been the removal of Cl^- and the substitution of SO_4^{2-} in the bathing solutions. Under these conditions, there is a linear relationship between development of a potential difference and acid rate (9). Accordingly, the effect of Cl^- removal and SO_4^{2-} substitution was determined on the ATPase, H^+ uptake, cation efflux, and SCN^- and ANS-related properties of the vesicles.

If in the absence of a Cl^- conductance, the electrogenicity of H^+ uptake was unmasked due to the slow diffusion rate of SO_4^{2-} as opposed to Cl^-, then effects of potential on the various parameters should be detectable. For example, ATPase activity should decrease unless the potential is shunted by some other permeable ion. H^+ uptake should decrease (if H^+ movement is the electrogenic component) and Rb^+ efflux increase (if Rb^+ movement is compensating for a potential generated by the H^+ pump). Changes in ANS fluorescence and SCN^- distribution should occur in the absence of valinomycin. In fact ATPase activity was not affected by Cl^- removal and SO_4^{2-} substitution. H^+ uptake and Rb^+ efflux were each reduced by 40% and the valinomycin requirement for detection of a potential difference was still present. Moreover, the magnitude of

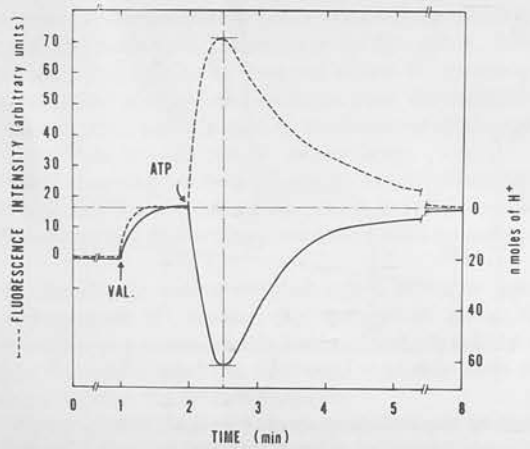

FIG. 9. The time course of ANS fluorescence and H^+ uptake was measured on the same preparation under identical conditions. 100 μl of vesicles (*c* 50 μg of protein) were added to 2 ml of a medium containing 150 mM KCl and 5 mM glycylglycine (pH 6.1) followed by 2.5×10^{-6} M ANS and 5×10^{-6} M valinomycin (*VAL*). ATP (5×10^{-5} M) was then added and the pH change and fluorescence change monitored as detailed in the text. It can be seen that the time course of the change in fluorescence has virtually an identical time course to the H^+ uptake showing the close relationship of the two effects of ATP addition.

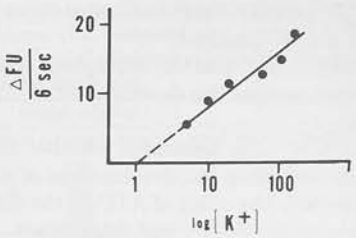

FIG. 10. The relationship of the initial rate of change of ANS fluorescence with the addition of ATP to the log of the K^+ concentration. The rate of change of fluorescence (arbitrary units in the first 6 s) is plotted against the log of the K^+ concentration present in the medium to which the vesicles are added. The concentrations of ANS, valinomycin, and ATP added to the vesicles were 2.5×10^{-6} M, 5×10^{-6} M, and 5×10^{-5} M, respectively, and the concentration of KCl was varied between 5 and 150 mM.

TABLE IV

Cation selectivity of vesicle function and H^+ secretion

This shows the relative effectiveness of the alkali metal cations and choline in stimulating ATPase and *p*NPP hydrolysis, H^+ uptake, and ATP-enhanced ANS fluorescence in gastric membrane vesicles with the effectiveness of K^+ set to 100. These values are compared to the effectiveness of these cations and choline in supporting H^+ secretion by the intact frog mucosa mounted in an Ussing chamber.

	ATPase/*p*NPP hydrolysis	H^+	ANS	H^+ Secretion
K^+	100	100	100	100
Rb^+	76	60	90	90
Cs^+	16	4.5	30	3.4
Na^+	7	.24	1	0
Li^+	4	.1	1	0
$Choline^+$	0	0	0	0

the potential difference was reduced by 40% as would be expected from the diminished cation efflux. Accordingly, Cl^- removal and SO_4^{2-} substitution results in reduction of transport activity of the ATPase but does not result in electrogenic transport by the ATPase.

DISCUSSION

To date, two types of transport ATPase have been described. One type is exemplified by mitochondrial ATPase and catalyzes an electrogenic H^+ translocation. Examples of the other type are $(Na^+ + K^+)$-ATPase and Ca^{2+}-ATPase which catalyze cation translocation that is nonelectrogenic or partially electrogenic. In this work we have described a translocation of H^+ by a plasma membrane ATPase from gastric mucosa that appears to be nonelectrogenic and to have a mechanism similar to that of Ca^{2+} or $(Na^+ + K^+)$-ATPase.

This statement can be justified by comparing the characteristics of H^+ translocation by mitochondrial ATPase as typical of one class of ATPase on one hand and by the gastric $(H^+ + K^+)$-ATPase on the other.

Historically one of the key features of coupling between respiration and phosphorylation was the absence of an identifiable covalently linked phosphorylated intermediate (8). It is now clear that the coupling between respiration and phosphorylation depends on the generation of an electromotive force and an H^+ gradient across the mitochondrial membrane (8). In contrast, plasma membrane ATPases (18) and the gastric $(H^+ + K^+)$-ATPase (16, 19) form isolatable phosphorylated intermediates.

The transport of the hydrogen ion by mitochondrial ATPase is electrogenic. Membranes containing this type of ATPase develop both a potential and an H^+ gradient (20, 21) and the ATPase is reversible with respect to both parameters. Accordingly, alteration of membrane conductance by ionophores or protonophores increases ATPase activity and abolishes the potential induced by the ATPase. The change of potential can be shown directly by measuring the distribution of lipid-permeable ions or by measuring changes in ANS fluorescence (20, 22).

In contrast gastric $(H^+ + K^+)$-ATPase activity in the vesicles shows no stimulation by increments in membrane conductance such as induced by protonophores or lipid-permeable ions.

Measurement of the moles of H^+ transported per high energy phosphate bond has given data between 2 and 4 (8, 23, 24) for the electrogenic type of H^+ ATPase. Our measurements using the initial rate gave values close to 4, and it would appear that 2 Ca^{2+} are transported per ATP hydrolyzed by the Ca^{2+} ATPase, *i.e.* 4 charges per ATP. From our data however, it is not possible to conclude that the ratio is fixed and the value of 4 may apply only under the specific conditions of study.

There have been suggestions that an H^+:K^+ exchange may occur in mitochondrial phosphorylation (3) but in reconstituted vesicles (21) no specific cation requirement for H^+ gradient formation by the mitochondrial ATPase has been established.

It is evident from the data presented that gastric vesicle H^+ transport is cation-requiring, similar to Na^+ transport by $(Na^+ + K^+)$-ATPase (18).

Valinomycin and other ionophores are capable of uncoupling mitochondrial respiration, or stimulating mitochondrial ATPase activity in coupled particles. In a sense similar data are found for gastric vesicles (Table I, and Refs. 19 and 25) in that ATPase activity is stimulated by K^+ ionophores. This stimulation is reduced by K^+ preincubation, K^+ is required in the interior of the vesicles for H^+ uptake and K^+ dephosphorylates the protein (16, 19). Stimulation by NH_4^+ is not increased by gramicidin[2] which increases membrane conductance to NH_4^+. This would be expected if NH_4^+ was required in the vesicle interior and the permeability of NH_3 was already very high. Since NH_3 movement is nonconducting, gramicidin would stimulate NH_4^+-dependent ATPase activity if a potential developed which would be reduced by the shunt conductance provided by gramicidin. The effect of K^+ ionophores is therefore not due to the provision of a shunt conductance for an H^+ or K^+ battery but is due to an increase of intravesicular K^+ required for H^+:K^+ exchange and ATPase activity.

Concomitant with the H^+ uptake there is cation efflux. Lipid-permeable ions do not substitute for the alkali metal cation nor do they inhibit cation efflux or H^+ uptake (in the absence of ATPase inhibition). This is in contrast to their inhibitory action on oxidation-reduction-dependent transport by bacterial vesicles (2). Thus, in contrast to the electrogenic H^+ transport systems cation transport is a specific accompaniment of H^+ transport by gastric $(H^+ + K^+)$-ATPase.

There are also considerable differences in the subunit complexity of the mitochondrial ATPase and the gastric ATPase transport system. The F_1ATPase of mitochondria is a complex multisubunit structure (26) and on its own does not act as an H^+ translocator. Other factors such as F_0 (27) are required before H^+ transport across a membrane can occur. The interaction between the F_1ATPase and the membrane H^+ conducting proteins is, however, specific in that DCCD or oligomycin block ATPase activity only of the intact complex (28). This is assumed to be due to inhibition of H^+ translocation through F_0, since F_1ATPase by itself is not affected by these inhibitors. This ATPase inhibition cannot be overcome by protonophores (*i.e.* uncouplers) hence the H^+ ion exchange between F_1ATPase and the F_0-transporting subunit is direct and provision of alternate H^+ pathways is not sufficient to bypass the blockade of H^+ movement through F_0.

The gastric H^+-transporting system is considerably less complicated in subunit composition (Fig. 2). DCCD inhibits the ATPase activity of these gastric particles as well as H^+ transport and also blocks formation of the phosphorylated intermediate.[2] Both the H^+ and K^+ component of transport are specifically required in this ATPase and as for mitochondrial ATPase transport, protonophores do not provide effective alternate transport pathways.

It is possible by various means, including ANS fluorescence (22), to show the presence of potentials and changes of potential in untreated mitochondria or submitochondrial particles. Changes in ANS fluorescence in submitochondrial particles show an increase in fluorescence with an increase of positive potential in the interior concomitant with an increase of H^+ concentration (22). This is similar to the data obtained with ANS in the gastric system (Fig. 7), which also correlated with the data on SCN^- distribution (Fig. 8). The interpretation of a change of potential and H^+ distribution accounting for these findings is consistent therefore with data on mitochondria. However, for this potential to occur in the gastric vesicles valinomycin was required. This showed that the methods used were sufficiently sensitive to detect a potential but that the unmodified gastric ATPase particle did not develop a potential during transport activity. Ca^{2+}ATPase particles also show changes in ANS fluorescence with ATP addition (29) which are interpreted as being due to increased Ca^{2+} binding.

[2] Unpublished observations.

From these considerations, although gastric ATPase translocated H^+ as do the electrogenic H^+ATPases of mitochondria, chloroplasts, and bacteria, the gastric ATPase at least at this stage of analysis is similar to the plasma membrane type of ATPases as exemplified by the $(Na^+ + K^+)$- and Ca^{2+}ATPases (30).

It should be possible to correlate the properties of the vesicles described above and the properties of the H^+ secretory process of the intact gastric mucosa. For example, acid secretion should be K^+-requiring and ATP-dependent. The electrical conductance of the luminal (acid secretory) membrane to K^+ or Cl^- should be low and the process of H^+ secretion should be nonelectrogenic.

Most of the data on the electrical characteristics of acid secretion by the intact mucosa have been obtained on the amphibian stomach mounted in an Ussing chamber (9). K^+ is required for the process (31) and addition of mucosal K^+ more rapidly restores acid secretion after K^+ has been removed from both sides of the tissue. Analysis of tissue K^+ content after K^+ removal from the bathing solutions showed that H^+ secretion stopped when only a small amount of tissue K^+ had been lost (32). The concept of a small K^+ compartment involved in acid secretion was confirmed in experiments on intact dog (33). Flux studies show that the K^+ flux from serosa to mucosa is only a fraction (*c* 10%) of the H^+ flux (34). This, however, would be compatible with a small K^+ compartment that did not readily exchange with the bulk of tissue K^+. Measurement of change of transmucosal potential or change of potential across the luminal membrane (35) in response to changes in K^+ and Cl^- concentrations in luminal bathing solutions showed that the electrical conductance of the luminal membrane to K^+ or Cl^- was indeed low. Thus, the data from the vesicles are quite compatible with the data summarized above for the intact mucosa.

The role of ATP in acid secretion by the stomach has been difficult to establish by direct approaches (10). Measurement of metabolites in the resting and secreting dog stomach (36) gave data which were difficult to interpret as being due to stimulation of a simple ATPase mechanism. However, the large quantities of mitochondria in the parietal cell (*c* 40% of cell volume) may maintain steady state ATP levels in spite of large changes in work load.

Perhaps the major problem in accepting the vesicles as isolated as totally representative of the secretory apparatus of the intact stomach is the question of electrogenicity. It seems well established that in Cl^- free, SO_4^{2-}-containing solutions, H^+ secretion by amphibian mucosa is electrogenic (9). Moreover under these SO_4^{2-} conditions a K^+ conductance is present on the luminal surface of the tissue (35). In the vesicles, although SO_4^{2-} substitution reduced both H^+ and Rb^+ flux by 40% this effect was not overcome by ionophores or lipid-permeable ions, suggesting that the effect was not due to unmasking of the electrogenicity of the H^+ pump. Moreover, SO_4^{2-} reduced the valinomycin-dependent ANS effect, but did not remove the valinomycin requirement, hence no evidence for a potential in the vesicles in SO_4^{2-} media was observed.

Perhaps the effect of Cl^- removal and SO_4^{2-} substitution in the intact mucosa is not due to unmasking of an electrogenic H^+ pump, but due to development of a K^+ conductance on the luminal surface which can be shown to be present in SO_4^{2-} solutions (35). The potential across this surface will then depend on the log of the concentration ratio of K^+ cell to lumen. In turn the luminal concentration of K^+ will depend on the activity of the $(H^+ + K^+)$-ATPase *i.e.* on acid rate. The lower the activity, the lower the potential, as is found (9).

A model for acid secretion by the intact mucosa then requires a functional $(H^+ + K^+)$-ATPase, and the presence of luminal K^+. This K^+ diffuses into the lumen accompanying the active Cl^- transport present in the tissue, and is exchanged for H^+, resulting in the net secretion of HCl.

Acknowledgments – Thanks are due to the excellent technical assistance of B. Stewart, D. Shaw, and D. Dailey.

REFERENCES

1. Maloney, P. D., Kashket, E. R., and Wilson, T. H. (1974) *Proc. Natl. Acad. Sci. U. S. A.* **71**, 3896–3900
2. Kaback, H. R. (1974) *Science* **186**, 882–892
3. Azzone, G. F., Massari, S., Colonna, R., Dell Antone, P., and Frigert, L. (1974) *Ann. N.Y. Acad. Sci.* **227**, 337–347
4. Jagendorf, A. T., and Uribe, E. (1966) *Proc. Natl. Acad. Sci. U. S. A.* **55**, 170–177
5. Hinkle, P. C., Kim, J. J., and Racker, E. (1972) *J. Biol. Chem.* **247**, 1338–1339
6. Kagawa, Y., Kaudrach, A., and Racker, E. (1973) *J. Biol. Chem.* **248**, 676–684
7. Harold, F. M. (1974) *Ann. N.Y. Acad. Sci.* **227**, 297–331
8. Mitchell, P. (1966) *Biol. Rev.* **41**, 445–502
9. Rehm, W. S. (1965) *Fed. Proc.* **24**, 1387–1395
10. Hersey, S. J. (1974) *Biochim. Biophys. Acta* **344**, 157–203
11. Lee, J., Simpson, G., and Scholes, P. (1974) *Biochem. Biophys. Res. Commun.* **60**, 825–832
12. Saccomani, G., Stewart, H. B., Shaw, D., Lewin, M., and Sachs, G. (1976) *Biochim. Biophys. Acta,* in press
13. Spenney, J. G., Saccomani, G., Spitzer, H. L., Tomana, M., and Sachs, G. (1974) *Arch. Biochem. Biophys.* **161**, 456–471
14. Yoda, A., and Hokin, L. E. (1970) *Biochem. Biophys. Res. Commun.* **40**, 880–886
15. Lowry, O. H., Rosebrough, N. J., Farr, A. L., and Randall, R. J. (1951) *J. Biol. Chem.* **193**, 265–275
16. Saccomani, G., Shah, G., Spenney, J. G., and Sachs, G. (1975) *J. Biol. Chem.* **250**, 4802–4809
17. Scarborough, G. A. (1976) *Proc. Natl. Acad. Sci. U. S. A.* **73**, 1485–1488
18. Skou, J. C. (1965) *Physiol. Rev.* **45**, 596–617
19. Forte, J. G., Ganser, A. L., and Tanisawa, A. S. (1974) *Ann. N.Y. Acad. Sci.* **242**, 255–267
20. Kagawa, Y., and Racker, E. (1971) *J. Biol. Chem.* **246**, 5477–5487
21. Skulachev, V. P. (1976) in *Energy Transducing Mechanisms* (Racker, E., ed) pp. 31–74, Butterworths, London
22. Azzi, A. P., Gherardini, P., and Santato, M. (1971) *J. Biol. Chem.* **246**, 2035–2042
23. Brand, H. P., Reynafarje, B., and Lehinger, A. L. (1976) *Proc. Natl. Acad. Sci. U. S. A.* **73**, 437–441
24. Witt, T. H. (1974) *Ann. N.Y. Acad. Sci.* **227**, 203–206
25. Sachs, G., Rabon, E., Saccomani, G., and Sarau, H. M. (1976) *Ann. N.Y. Acad. Sci.* **264**, 456–475
26. Senior, A. E. (1973) *Biochim. Biophys. Acta* **301**, 249–277
27. Mitchell, P., and Moyle, J. (1974) in *Membrane ATPase and Transport Processes* (Bronk, J. R., ed) pp. 91–112, Biochemical Society, London
28. Tzagoloff, A., and Meagher, P. (1971) *J. Biol. Chem.* **247**, 594–603
29. Vanderkooi, J., and Martonosi, A. (1971) *Arch. Biochem. Biophys.* **144**, 87–98
30. Martonosi, A. (1972) in *Metabolic Transport* (Hokin, L. E., ed) pp. 317–350, Academic Press, New York
31. Harris, J. B., and Edelman, I. S. (1964) *Am. J. Physiol.* **206**, 769–782
32. Davies, T. L., Rutledge, J. R., Kease, D. C., Bajandas, F. J., and Rehm, W. S. (1965) *Am. J. Physiol.* **209**, 146–152
33. Hirschowitz, B. I., and Sachs, G. (1967) *Am. J. Physiol.* **213**, 1401–1405
34. Sachs, G., Collier, R. H., Pacifico, A., Shoemaker, R. L., and Hirschowitz, B. I. (1969) *Biochim. Biophys. Acta* **173**, 509–517
35. Sachs, G., Shoemaker, R. L., Blum, A. L., Helander, H. F., and Makhlouf, G. M. (1971) in *Electrophysiology of Epithelial Cells* (Giebisch, G., ed) pp. 257–279, Schattauer, Stuttgart
36. Sarau, H. M., Foley, J., Moonsammy, G., Wiebelhaus, V. D., and Sachs, G. (1975) *J. Biol. Chem.* **250**, 8321–8329

Reprinted from

Biochimica et Biophysica Acta, 464 (1977) 313—327

BBA 77580

PROTON TRANSPORT BY GASTRIC MEMBRANE VESICLES

H. CHANG, G. SACCOMANI, E. RABON, R. SCHACKMANN and G. SACHS *

Laboratory of Membrane Biology, University of Alabama in Birmingham, Birmingham, Ala. 35294 (U.S.A.)

(Received May 31st, 1976)

Summary

A highly purified membrane fraction was derived from hog gastric mucosa by a combination of differential and density gradient centrifugation and free flow electrophoresis. This final fraction was 35-fold enriched with respect to cation activated ouabain-insensitive ATPase. Antibody against this fraction was shown to be bound to the luminal surface of the gastric glands. The addition of ATP to this fraction or the density gradient fraction resulted in H^+ uptake into an osmotically sensitive space. The apparent K_m for ATP was $1.7 \cdot 10^{-4}$ M in the absence of a K^+ gradient similar to that found for ATPase activity. The reaction is specific for ATP and requires cation in the sequence $K^+ > Rb^+ > Cs^+ > Na^+ > Li^+$ and is inhibited by ATPase inhibitors such as *N,N'*-dicylclohexylcarbodiimide. Maximal H^+ uptake occurs with an outward K^+ gradient but the minimal apparent K_A is found in the absence of a K^+ gradient. The pH optimum for H^+ uptake is between 5.8 and 6.2 which corresponds to the pH range for phosphorylation of the enzyme, but is considerably less than the pH maximum of the K^+ dependent dephosphorylation. In the presence of an inward K^+ gradient, protonophores such as tetrachlorsalicylanilide only partially abolish the H^+ gradient but valinomycin dissipates 75% of the gradient, and nigericin abolishes the gradient. The vesicles therefore have a low K^+ conductance but a measurable H^+ conductance, hence a K^+ gradient can produce an H^+ gradient in the presence of valinomycin. The uptake and spontaneous leak of H^+ are temperature sensitive with a similar transition temperature. Ultraviolet irradiation inactivates ATPase and proton transport at the same rate, approximately at twice the rate of *p*-nitrophenylphosphatase inactivation. It is concluded that H^+ uptake by these vesicles is probably due to a dimeric $(H^+ + K^+)$-ATPase and is probably non-electrogenic.

* To whom correspondence should be addressed.
Abbreviation: DCCD, *N,N'*-dicyclohexylcarbodiimide.

Introduction

The generation and utilization of proton gradients by bacteria [1], bacterial vesicles [2], chloroplasts [3] and mitochondria [4] have now assumed primary importance in understanding coupling of ion gradients to chemical synthesis or solute transport. In all these systems one is dealing in general with a complex series of redox reactions, a multi-subunit ATPase and a large number of putative ion and organic solute carriers. The parietal cell of gastric fundic mucosa at rest contains a large number of smooth surfaced closed vesicular structures in the apical cytoplasm which fuse with the intracellular canalicular membrane during secretion forming a complex microtubular system [5]. In this state the cell is capable of generating a better than 10^6 : 1 H^+ gradient.

There are many indications that the purified membrane fractions of gastric mucosa are vesicular apart from the H^+ transport studies to be reported. Thus the K^+ ATPase activity [6] is enhanced in fresh preparations by the addition of ionphores such as valinomycin [7] and electron micrographs show the preparations to be vesicular, often with a double membrane appearance [8]. Using a lactoperoxidase method, it has also been shown that only certain peptides can be iodinated in fresh preparations from dog mucosa and that additional peptides iodinate in frozen thawed fractions [9]. Recently, it has been shown that a crude microsomal fraction from dog stomach is capable of transiently alkalinising the medium at pH 6.1 with the addition of ATP, the alkalinisation being reversed only by adding both valinomycin and protonophore [10]. The importance of this finding to proton secretion by the stomach and to studies relating proton gradients to ATP turnover makes it necessary to define the characteristics of this gradient, such as its magnitude, location, ion requirements, substrate specificity, electrogenicity and relationship to ATPase activity.

Materials and Methods

1. Vesicle preparation. Scrapings of hog gastric mucosa, after flooding with 3 M NaCl to remove mucus and large numbers of surface cells [11], were homogenized in unbuffered 0.25 M sucrose and the crude microsomal pellet prepared by centrifuging the post 20 000 × *g* supernatant at 78 000 × *g* (mean value) for 1 h. The pellet was resuspended at a concentration of 25 mg/ml protein again in 0.25 M sucrose, layered on top of a discontinuous gradient of 7% (w/v) ficoll and 30% sucrose, and centrifuged in a Z60 zonal rotor for 2 h at 59 000 rev/min. Three particulate fractions were obtained, one at the 0.25 M sucrose-7% ficoll interface, one at the interface between 7% ficoll-30% sucrose layers and one at the bottom of the gradient. Similar procedures applied to the hog antrum (with the exception that polytron (Brinkmann Instruments) homogenization was required) produced only two fractions, that at the sucrose ficoll interface, the other at the bottom of the tube.

The fraction at the sucrose ficoll interface (GI) was used in most of the experiments. The step gradient produced a sufficiently concentrated fraction to allow use without further centrifugation. Ficoll was found to be superior to sucrose in producing vesicles of low permeability.

In addition GI fraction was subjected to free flow electrophoresis on a Hanning FF5 free flow machine (Biomedical Instruments, New York) using 8 mM

Tris/acetate in 250 mM sucrose adjusted to pH 7.4 with 2 M NaOH with the addition of 0.1 mM MgATP in the curtain buffer with a voltage gradient of 100 V per cm and a flow rate of 180 ml/h at 7.5° C. This procedure separates the gradient fraction into an FI and FII fraction. Both of these were studied for H^+ uptake.

Gel electrophoresis was carried out in sodium dodecyl sulphate as previously described [9].

2. *H^+ uptake.* The experiments were carried out in a magnetically stirred vessel and the change of pH measured by a Radiometer pHM 64 pH meter with a servorecorder coupled to a REA 112 high sensitivity module. The amplification was so arranged that a deflection of 1 cm corresponded to a change of pH of 0.01 units.

The pH of all solutions was adjusted to the exact pH of the experiment prior to mixing any of the solutions and in general was adjusted to pH 6.11. The quantity of membranes added gave a final concentration of 0.17 mg/ml in 6 ml volume. The standard buffer was 5 mM glycyl glycine. KCl (or other salt) was added at 150 mM with 2 mM $MgCl_2$ to maintain osmolarity. Nucleotide or other substrate was added usually at $1.7 \cdot 10^{-5}$ M. For experiments in which osmolarity was varied, salt concentration was reduced to 90 mM and mannitol was added to the solution at various concentrations. Ionophores such as valinomycin (10^{-6} M) tetrachlorsalicylanilide (10^{-6} M) nigericin (1.7 μg/ml) were added in 10 μl methanol to the final volume of the solution of 6 ml. The internal medium of the vesicles was controlled by preincubating the vesicles for 48 h at 4° C in appropriate medium such as 150 mM KCl or other cation chloride. The time to reach equilibrium was determined in separate experiments using radioactive tracers such as $^{86}Rb^+$ [12], which technique also allows an estimate of the intravesicular volume.

Control experiments in the absence of vesicles showed that the addition of ATP did not change the pH. Rupture of the vesicles or the presence of nigericin abolished the pH changes showing that these changes were not due to proton release by breakdown of ATP. The pH of 6.11 was chosen to prevent any artefact due to this phenomenon [13].

In experiments to determine the H^+/ATP ratio, 150 mM K^+ equilibrated vesicles had 0.3 mM ATP added and the data obtained at 10 s were used. For inactivation comparison, $6 \cdot 10^{-5}$ M ATP and 111 μg ml^{-1} protein was used for H^+ uptake and 2 mM ATP and 20 μg ml^{-1} protein was used for hydrolysis measurements.

The change in pH was converted to nmol H^+ absorbed by the vesicles by back titration with 10^{-3} M HCl under each experimental condition.

3. *Enzyme assays.* ATPase activity was measured in a medium containing approximately 10 μg protein, 2 mM MgCl, 2 mM ATP in 40 mM Tris/acetate with or without 20 mM KCl at pH 7.4, following incubation at 37° C in a final volume of 1 ml. In some experiments pH 6.1 and room temperature was used. Phosphate released was measured as described elsewhere [14]. In others the concentration of MgATP was varied.

p-Nitrophenylphosphatase was measured in a medium containing 10 μg protein, 6 mM $MgCl_2$ and 6 mM *p*-nitrophenyl phosphate in 40 mM Tris/acetate buffer, pH 7.4 following incubation at 37° C [8].

Protein was measured by the method of Lowry et al. [15] and all chemicals used were the highest purity grade available.

4. Irradiation experiments. A vesicular suspension at a protein concentration of about 2 mg/ml was diluted in 0.25 M sucrose to give a final concentration of 400 μg/ml. The sample was shielded with aluminum foil and kept in an ice bath at a constant temperature of 4° C. The mercury lamp, used as the ultraviolet light source, was placed 2.0 cm above the sample suspension. At 30-s intervals the ultraviolet lamp was turned off and 1.2 ml aliquots were removed for H^+ uptake, ATPase and *p*-nitrophenyl phosphatase activity measurements.

The data were interpreted based on the equation

$$a = a_0 \, e^{-VD}$$

where a is activity at time t, a_0 is initial activity, V is volume of target and D is dose of irradiation which was taken as proportional to the time of irradiation.

5. Localization of the active fraction. Antibody against the gastric K^+-ATPase was produced in rabbits by injection of the frozen dried free flow FI fraction at concentration of 0.5 mg/ml, suspended in Freund's adjuvant. The cation activated ATPase was shown to be inhibited by this antibody in studies described in detail elsewhere (Saccomani, G., Sachs, G., Shaw, D. and Mihas, A., in preparation).

Immunofluorescence experiments were carried out using the method of indirect staining [16]. Small pieces (about 1 cm^2) of hog gastric mucosa from both fundus and antrum were fixed in 95% ethanol for 24 h at 4° C, dehydrated and embedded in paraffin. Cryostat section measuring 6—8 μm were cut after paraffin was removed by xylene, and incubated with the antibody for 1 h at 25°. After washing in 0.1 M phosphate buffer containing 0.15 M NaCl at pH 7.8, the sections were treated with fluorescein-isothiocyanate conjugated goat anti-rabbit γ-globulin. Following three more washes in phosphate-saline buffer, the sections were covered under buffered glycerine, sealed with nail polish and examined in a Leitz fluorescence microscope. The specificity of the staining was determined by using "pre-immune" rabbit serum and anti-IgG, anti-IgA and anti-IgM non-specific antibodies as controls.

Results

1. Purification of vesicles. H^+ uptake dependent upon the addition of ATP occurred in the microsomal fraction, the lighter density gradient fraction (GI) and in only the anodic peak of the free flow fractionation (FI).

In accord with the H^+ uptake activity, there was enrichment of cation activated ATPase in these fractions associated with the cation activated phosphatase (Table I). At the same time there is a progressive enrichment of the 100 000 M_r peptide on the acrylamide gels (Fig. 1) so that the final free flow fraction contains more than 75% of its peptide at the 100 000 M_r location. This peptide region is phosphorylated by [γ-^{32}P]ATP and dephosphorylated in the presence of K^+ [9]. The fractionation technique is described in detail elsewhere [8]. Antral membrane fractions contained neither the cation activated ATPase or H^+ uptake properties with ATP addition. Fundic vesicles were stable up to 5 days after preparation.

TABLE I

PURIFICATION OF VESICLES

Assay conditions as described in Materials and Methods. The K^+-ATPase activity is the difference between activity in presence and absence of 20 mM K^+ (mean of 10 fractionations ± S.E.).

	Protein in mg	5'-AMPase	Mg^{2+}-ATPase (μmol · P_i mg^{-1} · h^{-1})	K^+-ATPase	K^+-pNNPase (μmol pNP · mg^{-1} · h^{-1})
Total homogenate	4800	0.5 ± 0.3	6.2 ± 0.6	2.0 ± 1.0	3.1 ± 0.5
Microsomal fraction	360	1.5 ± 0.6	15.9 ± 1.5	7.1 ± 4.3	22.7 ± 3.9
Light membrane fraction (GI)	31	4.6 ± 0.1	6.4 ± 1.3	32.5 ± 3.2	51.6 ± 3.6
Electrophoretic fraction (FI)	16	0.6 ± 0.2	2.7 ± 0.6	64.1 ± 3.9	54.0 ± 4.0
Electrophoretic fraction (FII)	7	14.7 ± 1.2	16.6 ± 2.0	17.3 ±1.2	18.8 ± 2.4

2. Localization of active fraction. Using the immunofluorescence technique, was possible to show fluorescence present in hog fundic sections, but not ntral sections. The fluorescence appears to have mainly a supranuclei and api- surface localization which corresponds to the region of the tubulovesicles or icrovilli of the parietal cell [5] (Fig. 2). Fluorescence was not obtained when on-immunized rabbit γ-globulin was used. Longitudinal sections showed that he majority of the fluorescence was in the middle third of the gastric glands, hich is the region of the majority of parietal cells.

3. Uptake of H^+. No change of pH was observed with the addition of ATP to he medium alone. Moreover, freeze drying the vesicles abolished more than 0% of the pH change normally observed. Sonication of the vesicles progres- ely reduced H^+ uptake with a much more rapid decline of H^+ uptake than of TPase activity (Fig. 3).

Ionophores also reversed the H^+ gradient and all these data suggest that the isappearance of H^+ was due to uptake rather than binding of H^+. To quantitate he contribution of these two processes, the medium osmolarity was varied and he effect of this on H^+ uptake measured. Plotting H^+ uptake as a function of he reciprocal of osmolarity showed a good fit to a straight line ($r = 0.992$) and trapolation of the line to infinite osmolarity gave a zero intercept on the H^+ otake axis (Fig. 4). These data show that, under the conditions of study, inding of H^+ does not contribute significantly to the H^+ disappearance.

4. Characteristics of ATP effect. The addition of vesicles to the KCl medium sulted in no change of pH until the addition of ATP (Fig. 5). With addition of TP there is a rapid uptake of H^+, followed by release of H^+ when the ATP is nsumed. The addition of tetrachlorsalicylanilide results in a rapid but small lease of H^+. Valinomycin alone results in a larger release of H^+ under the con- tions of an inward K^+ gradient. This suggests that the K^+ conductance of the sicle is lower than that of H^+. If valinomycin is added before ATP to the vesi- es, then there is initially a slight acidification due to the K^+ gradient exchanging for H^+. If ATP is added under these conditions there is a more rapid uptake d more rapid release of H^+. From the above, it seems that ion gradients as ll as ATP can produce H^+ gradients in these vesicles. This is confirmed incubating the vesicles in 1 M KCl and diluting into equimolar choline loride thus creating an outward K^+ gradient. There is no change of pH as

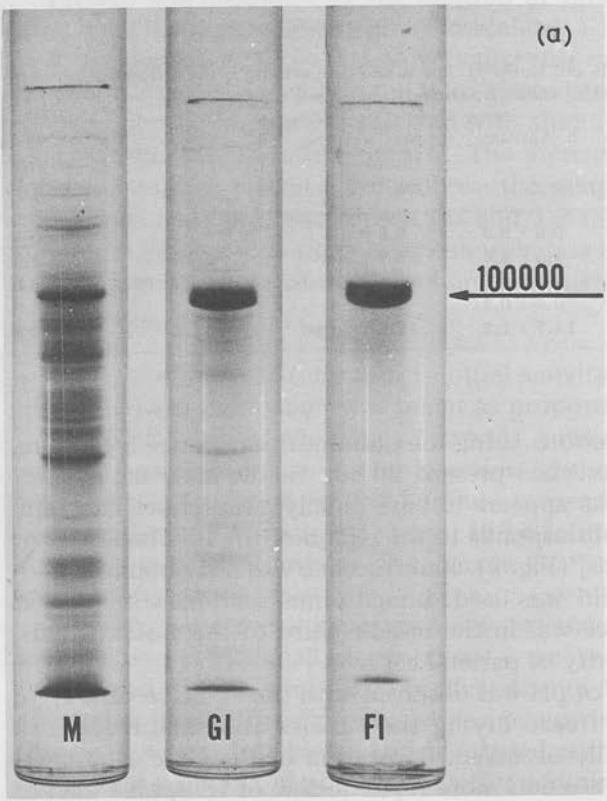

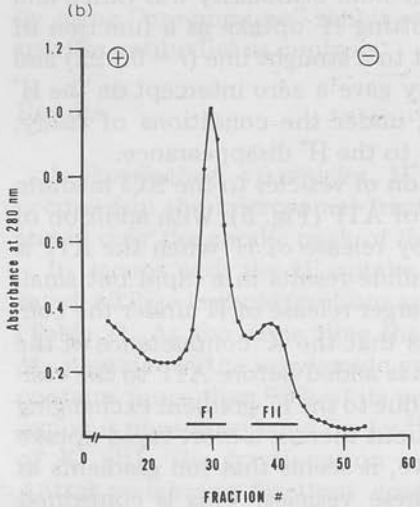

Fig. 1. (a) Sodium dodecyl sulphate gel patterns of the microsomal fraction, the gradient fraction and the electrophoretic fraction showing the increasing purification of the 100 000 M_r band. (b) The free flow profile of the gradient fraction.

ig. 2. The appearance of a section of gastric gland from hog fundus following treatment with rabbit anti-erum to FI fraction of the free flow electrophoresis and the staining with fluorescein conjugated goat nti-rabbit gamma globulin (X 176).

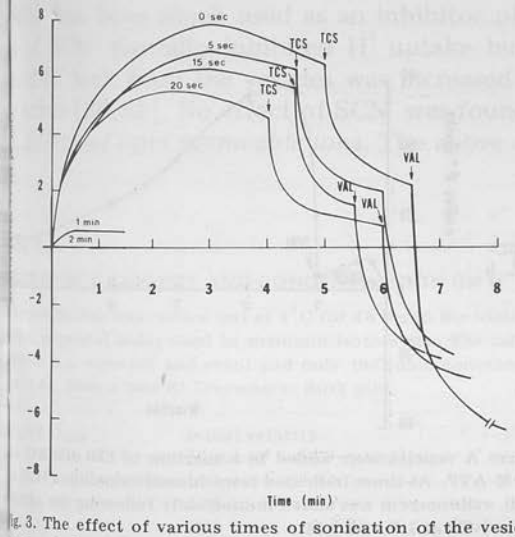

ig. 3. The effect of various times of sonication of the vesicles prior to addition to the standard uptake edium using a Labsonic microtip sonifier. This demonstrates progressive loss of H^+ uptake and at 1 min here 75% residual ATPase activity is found actually no H^+ uptake is seen. Again, tetrachlorsalicylanilide CS) only partially dissipates the gradient, and the subsequent addition of valinomycin (VAL) results in acid overshoot since these experiments were performed in the presence of an inward KCl gradient.

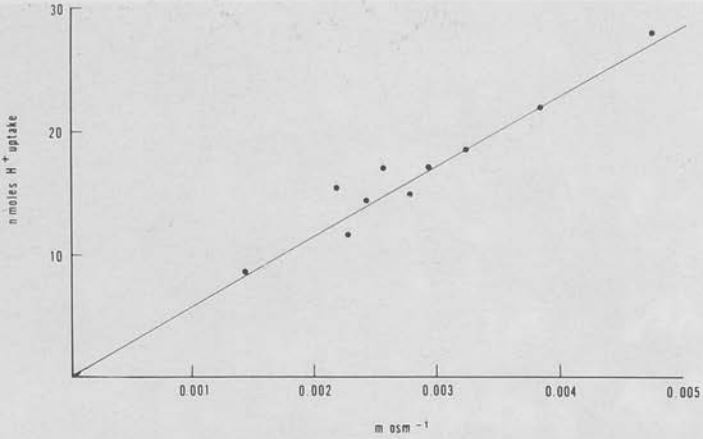

Fig. 4. The effect of vesicular volume on H^+ uptake. The vesicles were added to a solution containing 150 mM KCl with appropriate addition of mannitol to vary the osmolarity and other additions as in text. ATP $1.7 \cdot 10^{-5}$ M was added, and the H^+ uptake measured.

would be predicted from the low K^+ conductance inferred above. The addition of a protonophore, *m*-chlorocyano carbonyl phenylhydrazone produces only a slight alkalinisation showing that H^+ or Cl^- conductance are not limiting. The addition of valinomycin produces a transient alkalinisation (Fig. 6).

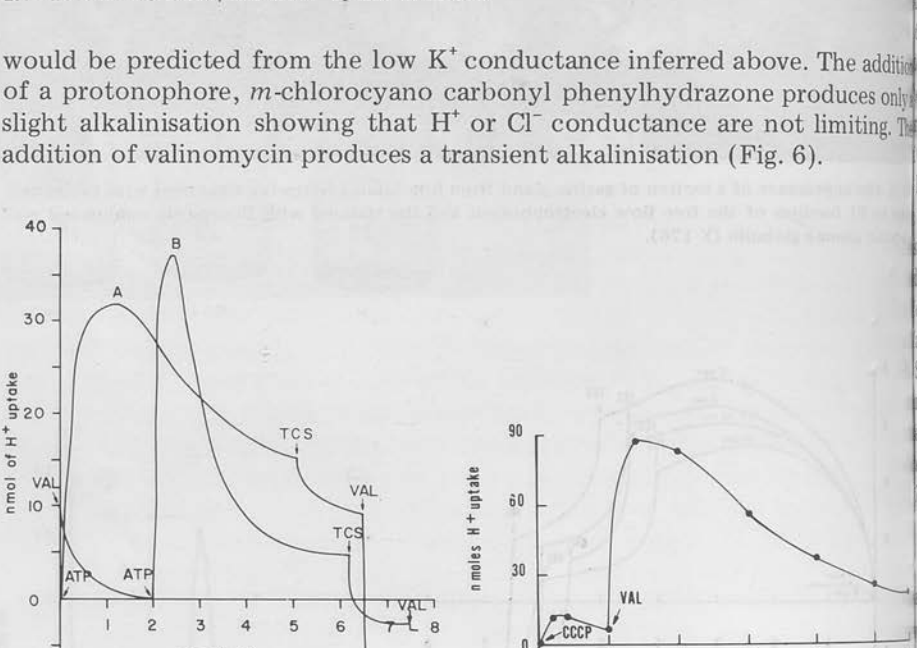

Fig. 5. H^+ uptake by the vesicles: In the curve A vesicles were added to a solution of 150 mM KCl with additions as in text, followed by $1.7 \cdot 10^{-5}$ M ATP. At times indicated tetrachlorsalicylanilide (TCS) and valinomycinin (VAL) were added. In curve B, valinomycin was added immediately following the addition of the vesicles from the same preparation, then ATP at $1.7 \cdot 10^{-5}$ M.

Fig. 6. The effect of preincubating the vesicles in 1 M KCl and then diluting into equimolar choline solution (●——●) with the addition of 10^{-5} M CCCP and then 10^{-6} M valinomycin showing the development of an H^+ gradient in the absence of ATP.

5. Effect of cations. Since the cation conductance of the vesicles is low, the ect of varying the nature and distribution of the cations was determined. th the rate and maximal uptake of H^+ was a function of the nature of the ion. The sequence was $K^+ > Rb^+ > Cs^+ > Na^+ > Li^+$, using initial rate values. is is the same sequence of activation as for the ATPase or *p*-nitrophenyl phosatase [17].

The rate of uptake of H^+ was increased by preincubating the vesicles in KCl d the apparent K_A for K^+ was reduced from 62 to 32 mM. However, the K_A the ATPase was about 7 mM under identical conditions. The maximum take and fastest rate was obtained with an outward K^+ gradient i.e. when the sicles were diluted into choline chloride. This suggests that when ATP is ded, the outward K^+ gradient can contribute to the uptake of H^+. This can be plained by the development of a K^+ limitation due to efflux of K^+ with the dition of ATP [12], and development of a K^+ gradient even with preequilited vesicles. The outward K^+ gradient would reduce the gradient limitation ble II). These data suggest that H^+ uptake is accompanied by cation efflux as tailed elsewhere [12].

6. Effect of anions. The conclusion that cation and cation movement is obligory for H^+ uptake suggests that anion is not required for the process. e removal of Cl^- and substitution by other anions gives a selectivity sequence anions of $Cl^- > Br^- > I^- > F^-$. The latter anion is inhibitory in the presence Cl^- since the ATPase is also inhibited [6].

It has been demonstrated that H^+ secretion by gastric mucosa is electrogenic the presence of SO_4^{2-} as a substitute for Cl^-. Under SO_4^{2-} conditions in the sicles H^+ uptake was reduced by 40% even after preincubation. SO_4^{2-} also uced cation uptake [12] and hence the inhibition might be due to reduction cation in the intravesicular medium. No evidence was found for development a potential in the presence of SO_4^{2-}.

SCN^- has been much used as an inhibitor of acid secretion [19]. The addin of SCN^- partially inhibited H^+ uptake but the results were variable. The e of H^+ leak from the vesicles was increased by SCN^- which is a lipid permee anion [20,22]. No effect of SCN^- was found on ATPase activity.

7. Effect of lipid permeable ions. The above data strongly suggest a non-elec-

BLE II

ECT OF K^+ GRADIENT AND CONCENTRATION ON H^+ UPTAKE

preincubation was carried out at 4° C for 48 h and the ionic concentrations were varied from 1 mM to mM, mannitol being used to maintain isotonicity. The initial gradient was kept constant under two itions (i.e. outward and zero) and only the ionic concentrations were varied allowing calculation of rent K_A from a best fit Lineweaver Burk plot.

$[K^+]_{in}/[K^+]_{out}$	Initial velocity (nmol $H^+ \cdot mg^{-1} \cdot min^{-1}$)	V (nmol $H^+ \cdot mg^{-1} \cdot min^{-1}$)	K_A (mM)
6 *	130	216	62
	163	218	32
	563	1370	182

* With the inward gradient this varied due to the conditions used. The value of 0.006 was the gradient under standard conditions.

trogenic $H^+ : K^+$ exchange. If electrical coupling does play a role in this phenomenon, then modification of membrane conductance by the addition of a permeable cation or anion should increase H^+ uptake. Dimethyldibenzylammonium and SCN^- at 1 mM concentration had no effect on H^+ uptake. These data suggest that development of a potential does not limit H^+ uptake under these conditions, contrary to what would be predicted for electrogenic H^+ uptake.

8. Relationship to ATPase activity. The uptake of H^+ was a saturable function of the ATP concentration and was specific for ATP. The apparent K_m in the absence of a K^+ gradient was $1.7 \cdot 10^{-4}$ M with a V of 154 μmol $H^+ \cdot mg^{-1}$ protein per h^{-1}.

The molar ratio of H^+ uptake to ATP hydrolyzed measured in the first 10 under standard conditions was 3.1 ± 0.4 ($n = 10$) if the total ATPase activity was used and 4.1 ± 0.2 ($n = 10$) if only the cation activated component of the ATPase was used in the calculation. Those ratios are to be compared to the value of 4 obtained for H^+ transport per high energy bond for chloroplasts [3] or mitochondria [4].

The pH of the luminal solution of intact mucosa at maximal secretion is less than 1. From this, it can be calculated that transport of 1 mol of H^+ would require about 9 kcal. From values for the energy available from ATP this would suggest a ratio of 1 mol H^+ transported per mol ATP hydrolyzed. In the intact mucosa this discrepancy with the vesicle data may be explained by a variable coupling ratio of the enzyme as a function of the gradient.

From the quantity of H^+ taken up, and the vesicular volume 2 μl mg protein), an internal pH of 1.7 can be calculated giving a ΔpH of 4 or so. The actual value is probably less due to buffering inside the vesicles.

The optimum pH of H^+ uptake was found to be between 5.8 and 6.2, correcting for the change in H^+ released by the ATPase reaction. This corresponds generally to the pH optimum of phosphorylation of the enzyme by [γ-^{32}P]ATP not to the pH optimum of dephosphorylation. The correction at a pH 7.0 and above due to H^+ release by the ATPase is larger than the observed uptake. To establish that an H^+ gradient is indeed present, the uptake of [^{14}C] imidazole was measured, at pH 7.4. This depends on the assumption that the protonated form of imidazole (pK 6.8) is charged and hence reactively impermeable, and thus the neutral form equilibrates across the vesicle membrane. The increment of imidazole inside the vesicles is shown in Fig. 7. This allows calculation of a pH difference of 1.5 at this pH. The molar ratio of H^+ taken up to ATP hydrolyzed would be much less at pH 7.4 than at 6.1. However, the imidazole technique is much slower in response than the pH electrode, and is also less sensitive and quantitation depends on the impermeability of the charged form.

Thus a pH gradient is developed across a broad range of pH but seems most closely related to the phosphorylation stage of the overall ATPase reaction, namely:

$$ATP + H^+ + ENZ \rightarrow P\text{-}ENZ\text{-}H^+ + ADP$$

$$P\text{-}ENZ\text{-}H^+ + K^+ \rightarrow P\text{-}ENZ\text{-}K^+ + H^+$$

9. Effect of temperature. The availability of a plasma membrane derived

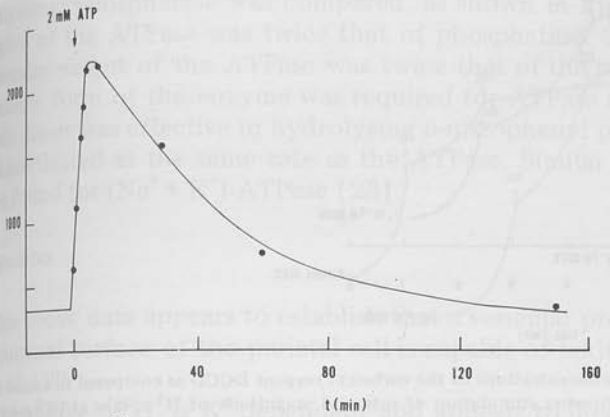

7. The uptake of ^{14}C-labelled imidazole as a function of addition of 2 mM ATP. The vesicles were ibrated using 0.1 mM imidazole as determined by radioactivity trapped on a Millipore HAWP filter ATP added at zero time on the graph. There was a transient uptake as shown, which decayed over a d of two and a half hours due to the large quantity of ATP used.

icle with low permeability and active transport properties made the effect of mperature on transport and ionophore action of interest. Fig. 8 shows the ct of increasing temperature on H^+ uptake as a function of initial rate of ximal uptake under zero K^+ gradient conditions. Both parameters are tem- ature sensitive, but the rate of uptake is more sensitive with a temperature imum of 37° C, as for the ATPase activity. When the data for initial rate of ake and leak of H^+ were plotted as an Arrhenius plot a transition temper- re of 22° C was found, with an activation energy of 3.0 kcal/mol above the

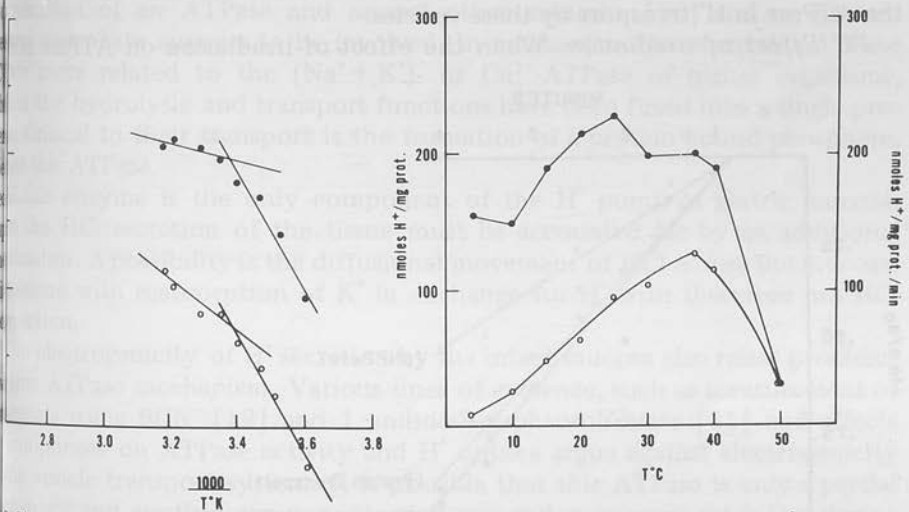

8. The effect of temperature on H^+ uptake by gastric vesicles with the addition of $1 \cdot 10^{-4}$ M ATP in bsence of a K^+ gradient with 150 mM KCl. The left hand side of the figure shows the Arrhenius plot e initial rate (nmol $H^+ min^{-1}$) with ATP addition (●——●) and the leak (nmol $H^+ min^{-1}$) (○——○). ight hand side shows the maximal H^+ uptake observed (●——●) and the initial rate (○——○) as ction of temperature.

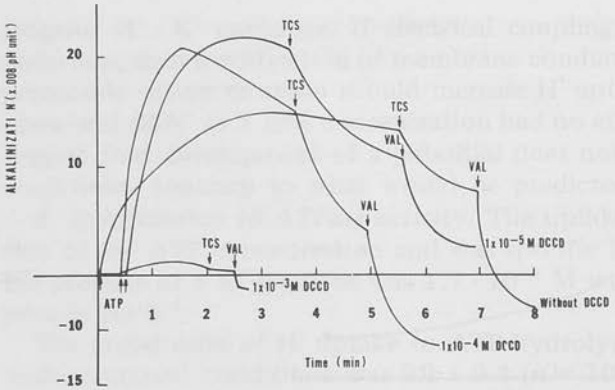

Fig. 9. The effect of various concentrations of the carboxyl reagent DCCD as compared to control on H^+ uptake induced by ATP showing stimulation of rate and magnitude of H^+ uptake at 10^{-5} and 10^{-4} and inhibition of 10^{-3} M. TCS, tetrachlorsalicylanilide; VAL, valinomycin.

transition temperature and 18.1 kcal/mol below that temperature for H^+ uptake. The leak rate had a higher activation energy of 8.7 kcal/mol above the transition temperature and a similar 19.4 kcal below.

The action of valinomycin disappeared below 20° C but nigericin was still effective in dissipating the gradient at 4° C.

10. Effect of ATPase inhibitors. Inhibitors of ATPase activity, such as Zn^{++}, F^- and *p*-chloromercuribenzoate, inhibited H^+ uptake. The action of *N,N'*-dicyclohexylcarbodiimide (DCCD) was investigated in more detail since this reagent also inhibits proton translocation in intact mitochondria [22]. Fig. 9 shows that low concentrations of DCCD apparently increase the rate and maximum of H^+ uptake, whereas at concentrations which inhibit the ATPase, DCCD inhibits H^+ transport.

The action of this inhibitor is therefore complex, but confirms the role of the ATPase in H^+ transport by these vesicles.

11. Effect of irradiation. When the effect of irradiation on ATPase and

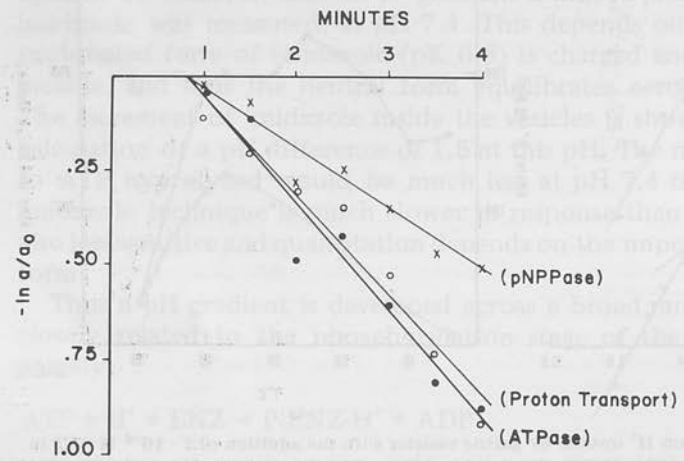

Fig. 10. The effect of irradiation of the vesicles on H^+ uptake (○———○) ATPase (●———●), and *p*-nitrophenyl phosphate (X———X) activities plotted as ln a/a_0 against time of irradiation where a is activity at time t and a_0 is initial activity.

trophenyl phosphatase was compared, as shown in Fig. 10, the rate of inac-vation of the ATPase was twice that of phosphatase. This suggested that the olecular weight of the ATPase was twice that of the phosphatase, hence that dimeric form of the enzyme was required for ATPase activity, but either half f the dimer was effective in hydrolysing *p*-nitrophenyl phosphate. H^+ transport s inactivated at the same rate as the ATPase. Similar inactivation data have een found for $(Na^+ + K^+)$-ATPase [23].

iscussion

The above data appears to establish that a vesicular preparation derived from e luminal surface of the parietal cell is capable of taking up H^+ with the addi-n of ATP.

The uptake of H^+ is K^+ dependent and appears to involve a $K^+ : H^+$ exchange established above and by direct measurement of cation and anion movement 2].

Measurement of metabolite levels in resting and secreting mucosa of frog 4] and dog mucosa [25] showed a decline in phosphorylation potential. In dition the intramitochondrial pyridine nucleotide became relatively oxidized th onset of acid secretion [26]. These data are compatible with an ATP based chanism of H^+ secretion, as are data using inhibitors [27].

It has also been known for some time that K^+ is required for H^+ secretion 8] and that this K^+ is only a minor component of the total cellular K^+ [29]. These data derived from the intact mucosa are therefore compatible with a $^+$: H^+ exchange ATPase being responsible for H^+ secretion.

This H^+ transport mechanism, occurring in the plasma membrane of a eukar-tic cell appears quite distinct from the H^+ transport process of lower life rms [1]. These latter are clearly electrogenic, do not require cation, involve operation of an ATPase and several other subunits [30] and no protein und phosphate appears to be involved. In mechanism therefore this ATPase ems more related to the $(Na^+ + K^+)$- or Ca^{2+}-ATPase of higher organisms, ere the hydrolytic and transport functions have been fused into a single pro-n. Critical to their transport is the formation of a protein bound phosphate, for this ATPase.

If this enzyme is the only component of the H^+ pump of gastric mucosa, en the HCl secretion of the tissue must be accounted for by an additional chanism. A possibility is the diffusional movement of KCl across the mucosal mbrane with reabsorption of K^+ in exchange for H^+ with therefore net HCl duction.

The electrogenicity of H^+ secretion by the intact mucosa also raises problems this ATPase mechanism. Various lines of evidence, such as measurement of tentials using SCN^- [12] and 1 anilino-8-naphtosulfonate [31] and effects ionophores on ATPase activity and H^+ uptake argue against electrogenicity the vesicle transport system. It is possible that this ATPase is only a partial chanism and another component, such as a redox component is lost during ification. Another possibility is that the conductance of the pump changes stically at pH 7.4.

It is interesting also that the ATPase functions in its transport mode as a

dimer. The monomeric *p*-nitrophenylphosphatase reaction does not catalyze transport. On this basis, as for the $(Na^+ + K^+)$-ATPase [32] it can be argued that the enzyme exists as a dimer of unlike conformation E_1E_2 rather than E_1E_1 or E_2E_2. Either E_1 or E_2 can react with *p*-nitrophenylphosphate.

If only E_1 can bind and react with ATP and as a result bind H^+ and E_2P react with K^+ and release H^+ and then transport K^+, the transport reaction may be written as

$$H^+E_1P \cdot E_2PK^+ \rightarrow H^+E_2P \cdot E_1PK^+$$

with release of H^+ in the interior of the vesicle and K^+ and P_i on the exterior with reformation of E_1. In this model therefore the translocation of H^+ and K^+ are strictly coupled. The electrogenicity is thus a function of the pump stoichiometry as for the $(Na^+ + K^+)$-ATPase [33].

Further evidence for the role of this ATPase will depend on the development of specific inhibitors such as ouabain. The enzyme is not a component of other cell membranes which catalyze the development of pH gradients such as the pancreas or the distal tubule of the kidney [34] and thus represents a gastric specialization for H^+ secretion, if indeed it is the H^+ pump of the stomach.

Acknowledgements

Thanks are due to the excellent technical assistance of B. Stewart, D Shaw and D. Dailey and to Dr. A. Mihas and S. Goodson for collaboration in the antibody localization studies. This work was supported by NIH grant AM 15878, CVRTC HL 11310 and NSF grant GB31075.

References

1 Maloney, P.D., Kashket, E.R. and Wilson, T.H. (1974) Proc. Natl. Acad. Sci. 71, 3896–3900
2 Kaback, H.R. (1974) Science 186, 882–892
3 Witt, T.H. (1971) Ann. N.Y. Acad. Sci. 227, 203–206
4 Brand, M.D., Reynafarje, B. and Lehninger, A.L. (1976) Proc. Natl. Acad. Sci. U.S. 73, 437–441
5 Sedar, A.W. (1965) Fed. Proc. 24, 1360–1367
6 Ganser, A.L. and Forte, J.G. (1973) Biochim. Biophys. Acta 387, 169–180
7 Ganser, A.L. and Forte, J.G. (1973) Biochem. Biophys. Res. Commun. 54, 690–696
8 Saccomani, G., Shaw, D., Stewart, H.B., Lewin, M. and Sachs, G. (1976) Biochim. Biophys. Acta, submitted
9 Saccomani, G., Shah, G., Spenney, J.G., Sachs, G. (1975) J. Biol. Chem. 250, 4802–4809
10 Lee, J., Simpson, G. and Scholes, P. (1974) Biochem. Biophys. Res. Commun. 60, 825–832
11 Forte, J.G. and Ray, T.K. (1972) J. Appl. Physiol. 32, 714–717
12 Schackmann, R., Schwartz, A., Saccomani, G. and Sachs, G. (1976) J. Membrane Biol., in the press
13 Alberty, R.P. (1969) J. Biol. Chem. 244, 3290–3302
14 Yoda, A. and Hokin, L.E. (1970) Biochem. Biophys. Res. Commun. 40, 880–884
15 Lowry, O.H., Rosebrough, M.J., Farr, A.L. and Randall, R.I. (1951) J. Biol. Chem. 193, 265–275
16 Coons, A.H., Leduc, E.H. and Connolly, J. (1955) J. Exp. Med. 102, 49–60
17 Forte, J.G., Tanisawa, A. and Ganser, A.L. (1974) Ann. N.Y. Acad. Sci. 242, 255–267
18 Rehm, W.S. (1965) Fed. Proc. 24, 1387–1395
19 Davenport, H.W. (1940) Am. J. Physiol. 129, 505–514
20 Scarborough, G.A. (1976) Proc. Natl. Acad. Sci. 73, 1485–1489
21 Sachs, G., Chang, H.H., Rabon, E., Schackmann, R., Lewin, M. and Saccomani, G. (1976) J. Biol. Chem., in the press
22 Beechey, R.B., Robertson, O.N., Holloway, C.L. and Knight, I.G. (1967) Biochemistry 6, 3867–3879
23 Kepner, G.R. and Macey, R.I. (1968) Biochim. Biophys. Acta 163, 188–203
24 Durbin, R.P., Michelangeli, F. and Michel, A. (1974) Biochim. Biophys. Acta 367, 177–189

Sarau, H.M., Foley, J., Moonsamy, G., Wiebelhaus, V.D. and Sachs, G. (1975) J. Biol. Chem. 250, 8321–8329
Sachs, G., Rabon, E., Saccomani, G. and Sarau, H.M. (1976) Ann. N.Y. Acad. Sci. 264, 456—475
Sachs, G., Collier, R.H., Shoemaker, R.L. and Hirschowitz, B.I. (1968) Biochim. Biophys. Acta 162, 210–219
Harris, J.B. and Edelman, I.S. (1964) Am. J. Physiol. 206, 769—782
Rehm, W.S., Sanders, J.S., Rutledge, J.R., Davies, T.L., Kurfees, J.F., Keesee, D.C. and Bajandas, F.J. (1966) Am. J. Physiol. 210, 689—693
Catterall, W.A. and Pedersen, P.L. (1974) Biochem. Soc. Spec. Publ. 4, 63—90
Lewin, M., Saccomani, G., Schackmann, R. and Sachs, G. (1976) J. Membrane Biol., in the press
Glynn, I.M. and Karlish, J.D. (1975) Energy Transformations in Biological Systems, pp. 205—224, Ciba Press
Sen, A.K. and Post, R.L. (1964) J. Biol. Chem. 239, 345—352
Schwartz, I.L., Shaltz, L.J., Kinne-Saffran, E. and Kinne, R. (1974) Proc. Natl. Acad. Sci. U.S. 71, 2595–2649

J. Membrane Biol. 32, 361–381 (1977)

Cation Transport by Gastric $H^+ : K^+$ ATPase

R. Schackmann, A. Schwartz, G. Saccomani, and G. Sachs*

Laboratory of Membrane Biology, University of Alabama in Birmingham, Birmingham, Alabama 35294, and Department of Cell Biophysics, Baylor University, Houston, Texas

Received 13 May 1976; revised 2 September 1976

Summary. A vesicular microsomal fraction isolated from hog fundic mucosa demonstrates the capacity to take up equal amounts of RB^+ and Cl^-. The amount of the Rb^+ uptake is sensitive to the extravesicular osmolarity, and rate of uptake is sensitive to temperature. $^{86}Rb^+$ efflux is dependent upon the cation composition of the diluting solution. ATP, but not β-γ methylene ATP, induces a reversible efflux of $^{86}Rb^+$ from loaded vesicles, and this is dependent upon a functional K^+-ATPase. The ATP induced efflux is not affected by CCCP (carbonyl cyanide *m*-chlorophenylhydrazone) or TCS (tetrachlorosalicylanilide) nor by lipid soluble ions or valinomycin. Nigericin inhibits the efflux by 40%. Uptake of the lipid soluble ion $^{14}C\text{-}SCN^-$ has been demonstrated and is enhanced by ATP only in the presence of valinomycin. The results are consistent with a neutral or isopotential exchange of H^+ for Rb^+ mediated by K^+-ATPase.

The availability of a vesicular preparation from hog gastric mucosa has allowed an experimental approach to the role of K^+ in gastric acid secretion due to the capacity of the vesicles to take up H^+ in the presence of ATP, in a K^+ dependent fashion.

Work on the intact amphibian mucosa has shown that K^+ is essential for acid secretion (Davis *et al.*, 1965). Rb^+ and Cs^+, but not Na^+ or Li^+, can partially substitute for K^+ (Forte, Forte & Saltman, 1967). In K^+-free solutions with complete inhibition of the acid rate, the intracellular K^+ content remains high, falling only by 10 to 20% (Davis *et al.*, 1965). This has been interpreted as evidence for a K^+ compartment necessary for H^+ secretion. In intact dog stomach, insulin inhibition is also reversed by injection of K^+ or Rb^+, and results of flux studies have also been interpreted as providing evidence for a K^+ compartment (Hirschowitz & Sachs, 1967). In contrast, high K^+ levels in the serosal solution of frog mucosa reduce active Cl^- secretion significantly (Hogben, 1968). Measurement of K^+ movement across gastric mucosa showed that the unidirectional K^+ flux is considerably less than the H^+ rate

* *To whom correspondence should be addressed.*

(Sachs *et al.*, 1969) and this K^+ flux was inhibitied by SCN^- as was the H^+ rate. In Cl^- free, SO_4^{2-} containing solutions, high mucosal $[K^+]$ results in a significant increase in H^+ rate as well as in an inversion of the potential difference from mucosal positive to mucosal negative (Davis, Rutledge & Rehm, 1963). Passage of current to produce the same P.D. change as produced by K^+ in SO_4^{2-} solutions also stimulates H^+ secretion.

The discovery of a K^+ *p*-nitrophenyl phosphatase (Forte *et al.*, 1967) K^+-acetyl phosphatase and K^+-ATPase activity (Forte *et al.*, 1975; Sachs *et al.*, 1966; Saccomani *et al.*, 1975) in fundic mucosa of various species suggested that the role of K^+ might be as an activator of a proton transporting ATPase (Sachs & Hirschowitz, 1968). The demonstration of H^+ transport by dog microsomes (Lee, Simpson & Scholes 1974) or hog gastric membrane fractions (Sachs *et al.*, 1975, 1976) allowed a direct test of the transport functions of these preparations and the K^+-ATPase in particular. It was established that K^+ (or Rb^+ and Cs^+) was necessary for H^+ uptake (Sachs *et al.*, 1976). In this work we establish that the role of K^+ in the vesicle is not only as an activator of the K^+-ATPase but that K^+ (or Rb^+) is transported in exchange for H^+ by the K^+-ATPase.

Materials and Methods

Preparation of Vesicles

The method has been described in detail elsewhere (Saccomani *et al.*, 1977). Fundic mucosa is homogenized in 0.25 M sucrose and centrifuged for 40 min at $26000 \times g$ and the supernatant is centrifuged for 60 min at $100,000 \times g$ to provide the microsomal pellet. This fraction was further separated on a discontinuous gradient of 7% ficoll and 20% ficoll both in 250 mM sucrose in a Beckman Z60 zonal rotor at 60,000 rpm for 2 hr. The fraction at the 7% ficoll interface was free of mitochondrial markers such as succinic dehydrogenase, monamine oxidase or cytochrome oxidase and was 20-fold enriched in K^+-ATPase, K^+-pNPPase and 5′-AMPase activity. Further purification of this fraction was obtained by free flow electrophoresis using 8 mM tris-acetate buffer at pH 7.4, 0.1 mM MgATP in 0.25 M sucrose as curtain buffer and 100 mM tris-acetate pH 7.4 as electrode buffer. The separation was carried out at 7.5 °C with a voltage gradient of 120 v/cm and a flow rate of 180 ml/hr distributed through 90 tubes. This fractionation produced a fraction 35-fold enriched in K^+-ATPase (*F1*) and another fraction enriched in 5′-AMPase (*F11*). The *F1* fraction was essentially free of 5′-AMPase or Mg^{2+}-ATPase and contained essentially only 1 peptide region of 100,000 M_r on SDS gel electrophoresis. The zonal gradient or *F1* fractions were used for the studied outlined as specified in the text (Table 1), but the majority of transport studies were carried out on the gradient fraction.

ATPase Assay

ATPase assays were performed in the same incubation medium as the Rb^+ efflux studies. The incubation contained in 1 ml: ca. 170 μg protein, 75 mM RbCl, 50 mM tris-

Table 1. Purification of gastric membranes

	μmole Pi mg^{-1} hr^{-1}		
	Mg^{2+}-ATPase	K^+-ATPase[a]	5′-nucleotidase
Total homogenate	6.2±0.6	2.0±1.0	0.5±0.3
Microsomal fraction	15.9±1.5	7.1±4.4	1.5±0.6
Gradient fraction (*G1*)	6.4±1.3	32.5±3.2	4.6±0.1
Electrophoretic fraction *F1*	2.7±0.6	64.1±3.9	0.6±0.2
Electrophoretic fraction *F11*	16.6±2.0	17.3±1.2	14.7±1.2

(n=5)

[a] The K^+-ATPase activity is the difference between activity is presence and absence of K^+.

acetate or 5 mM glycylglycine buffer, pH 6.1, 125 mM sucrose, 2 mM $MgCl_2$ and 2 mM ATP. The reaction was carried out at room temperature for varying times between 10 sec and 15 min. The phosphate liberated was measured by butyl acetate extraction of the phosphomolybdrate complex (Yoda & Hokin, 1970) and protein by Lowry's method (Lowry *et al.*, 1951).

Transport Studies

Uptake. For uptake studies vesicles obtained from the gradient at a concentration of 2–6 mg/ml protein were added to an equal volume of a medium containing 150 mM RbCl containing 10 μCi $^{86}Rb^+$, 80 mM tris-acetate or 10 mM glycylglycine buffer pH 6.12 and 4 mM $MgCl_2$, to give a final volume of 400 μl. The pH of 6.12 was chosen so as to be able to compare the data with those of H^+ uptake. Incubation was carried out at varying temperature and 20 μl samples were taken and added to 1 ml of ice-cold "stop" solution containing 150 mM choline chloride and 40 mM tris-acetate buffer (or 5 mM glycylglycine) buffer pH 6.12. After vortexing the sample was filtered on a Millipore HAWP filter (0.45 μ). The filter was washed twice with 4 ml of the stop solution, dried and the radioactivity measured in a LKB 8100 scintillation counter. As necessary osmolarity was varied by adding mannitol to the incubation medium.

Efflux. Efflux studies were performed on vesicles which had been equilibrated with radioisotope by incubating for 48 hr at 4 °C in the uptake conditions just described. This incubation time was necessary to achieve equilibrium at that temperature. High temperatures of preincubation even for times as short as 2 hr at 37 °C resulted in vesicular damage. Two types of efflux study were performed: efflux with a gradient of Rb^+ or $^{86}Rb^+$, and efflux induced by the addition of ATP with no initial gradient present.

For efflux with a gradient the preloaded vesicles were diluted into a medium containing different external cation such as choline, K^+, Rb^+, Cs^+, Na^+ or Li^+ as chloride salts at 150 mM with other constituents the same as in the equilibration solution. Sampling and washing were carried out as for the uptake studies. These efflux studies allowed measurement of the cation selectivity of the exchange efflux pathway. Ionophores such as valinomycin, 10^{-6} M, nigericin, 1 mg/ml, tetrachlorsalicylanilide (TCS), 10^{-5} or 10^{-6} M, or carbonyl cyanide *m*-chlorophenylhydrazone (CCCP), 10^{-4} or 10^{-5} M, were added in 4 µl methanol.

Efflux in the equilibrium situation was assessed by adding ATP at pH 6.12 at varying concentrations directly to the vesicles in the equilibrated medium and sampling as usual. Ionophores as above or lipid permeable ions such as dimethyl dibenzyl ammonium (DDDA), dipicrylamine (DPA), or SNC^- were added as necessary at 1 or 10 mM concentrations.

Control experiments to determine binding of isotope to the filters were performed by solubilizing the vesicles with 1% triton X-100 in the stop solution, or by diluting the vesicles into H_2O, rather than stop solution before filtration. The former procedure reduced the radioactivity by 95% and the latter by 85% in terms of the activity usually trapped on the filter.

On occasion $^{22}Na^+$ or $^{137}Cs^+$ were used; and the experiments were performed as for $^{86}Rb^+$. In other experiments $^{36}Cl^-$ or ^{14}C-SCN^- were used, and with these 120 mM Li_2SO_4 was used as stop solution instead of choline chloride. For experiments in which SO_4^{2-} replaced Cl^-, 75 mM Rb_2SO_4 replaced the 150 mM RbCl solutions. Sucrose was used to adjust the SO_4^{2-} medium to maintain isotonicity.

H^+ Uptake Studies. Vesicles preincubated in 150 mM salt as above were added to a medium containing 150 mM salt and 5 mM glycylglycine pH 6.12 in a stirred vessel at room temperature. The change of pH was measured by a combination pH and calomel electrode connected to a pHM64 pH meter and a Radiometer Servorecorder, with a sensitivity of 1 cm per 0.01 pH units. 0.3 mM ATP was added to initiate the reaction and ionophores were added as above in methanol.

Results

Uptake of Cations

Kinetics. Uptake of Rb^+, Cs^+ or Na^+ was temperature and time dependent. Little difference was noted in uptake rate between the different

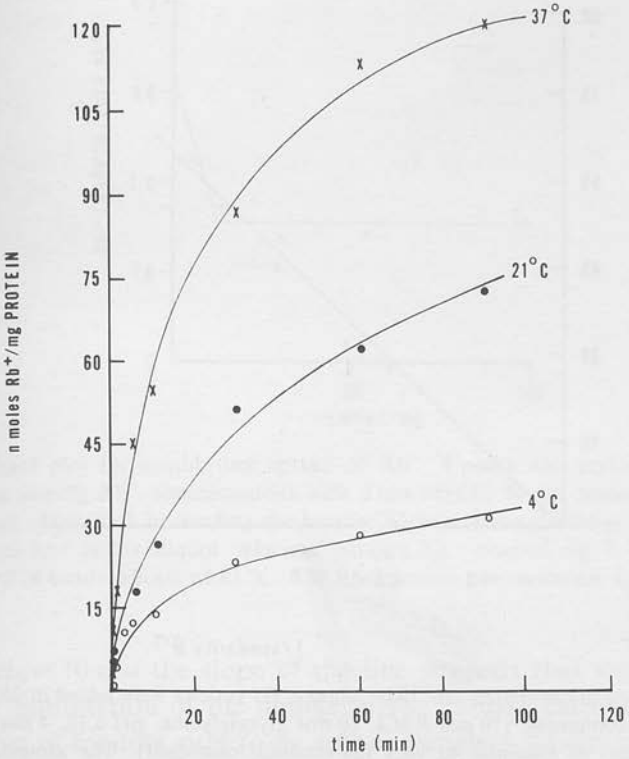

Fig. 1. Uptake of Rb^+ at three temperatures. *G1* vesicles in 250 mM sucrose, 200 µl, were mixed with 200 µl of a solution containing 150 mM RbCl, 10 mM glycylglycine, pH 6.12, 4 mM $MgCl_2$, ×—×, 37 °C; ●—●, 21 °C; ○—○, 4 °C. Sampling was performed in triplicate at times longer than 5 min and in duplicate up to five min. The final protein concentration was 1.9 mg/ml and the final levels of uptake were equal after 48 hr further incubation

cations, and the final level reached was identical for the three cations studied.

The uptake of $^{86}Rb^+$ with time is shown in Fig. 1 for the same preparation at 3 different temperatures. It can be seen that the process is time and temperature dependent. At 37 °C, the uptake curve is fitted to a single exponential with a $t_{1/2}$ of 16.5 min ($r=0.991$). At room temperature, the equilibrium value is not reached except after several hours incubation, and this value is lower than that reached at 37 °C in 2 hr, suggesting that some impairment of vesicular impermeability has occurred. This is substantiated by the finding that H^+ uptake is reduced and a greater leak of the ATP induced H^+ gradient is observed. The $t_{1/2}$ using the actual equilibrium value obtained at room temperature had a range of 28 to 51 min with a mean of 40 ± 9 min ($n=5$). The

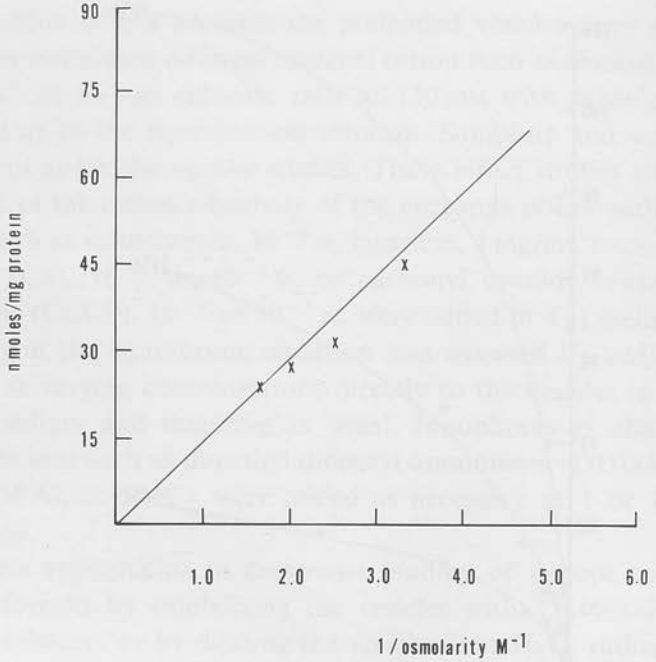

Fig. 2. Variation of osmolarity on $^{86}Rb^+$ uptake. *G1* vesicles were added in 250 mM sucrose to a medium containing 150 mM RbCl, 10 mM glycylglycine, pH 6.12, 4 mM $MgCl_2$ with varying amounts of mannitol to vary the medium osmolarity. The samples were taken in triplicate 10 min after mixing. The uptake was performed at 21 °C and the final protein concentration was 2.9 mg/ml

variation from preparation to preparation is presumably due to a varying degree of permeability of the vesicles as they are prepared. Maximal final uptake was observed by incubating the vesicles at 4 °C for 48 hr, which procedure had the least effect on H^+ uptake; hence, this procedure was used to load the vesicles with cations. The equilibrium level at this temperature allowed calculation of an intravesicular volume of 2.0 ± 0.3 µl per mg protein ($n = 23$).

Binding. Variation of medium osmolarity results in alteration of Rb^+ uptake as shown in Fig. 2. It can be seen that there is minimal binding of Rb^+, since there is no apparent uptake predicted at infinite osmolarity. The mannitol used as a nonpermeant species does, however, slowly penetrate the vesicles ($t_{1/2} > 2$ hr), hence only short exposures to the mannitol medium were used.

A Scatchard plot of the Rb^+ taken up at varying initial Rb^+ concentrations (Fig. 3) showed that above 10 mM a zero slope was observed as would be expected of uptake into a nonsaturating intravesicular

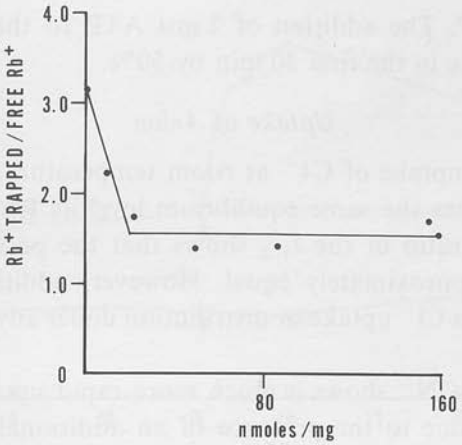

Fig. 3. Scatchard plot for equilibrium uptake of Rb^+. Uptake was performed at 4 °C for 72 hr with varying Rb^+ concentrations with 2 mM $MgCl_2$, 40 mM trisacetate, pH 6.1. Isotonicity was maintained by varying the sucrose concentration. *Ordinate:* nmoles Rb^+ trapped/nmoles Rb^+ in the aliquot. *Abscissa:* nmoles Rb^+ trapped mg^{-1}. The sampling was performed in quadruplicate at 21 °C. The final protein concentration was 0.82 mg/ml

volume. Below 10 mM the slope of the line suggests that some binding may occur. Subtraction of the uptake of Rb^+ allows calculation of the total number of binding sites to be approximately 5 nmoles/mg protein. This value may be neglected when dealing with the usual uptake of 150 nmoles or so.

Nature of Vesicle. Uptake of Rb^+ into the *F1* and *F11* fractions showed similar levels compared to the *G1* fraction (Table 2). The combined uptake of Rb^+ in *F1* and *F11* in this experiment was 191 nmoles/mg based on 72% of *G1* as *F1* and 28% *F11* (Saccomani *et al.*, 1977). This level compares within experimental error to the 181 nmoles/mg uptake by the *G1* fraction implying that during free flow electrophoresis little vesicular damage occurs.

Table 2. $^{86}Rb^+$ uptake and ATP-stimulated efflux from *G1* and *G1* free-flow electrophoresis

Fraction	Percentage of *G1* as protein	Equilibrium uptake nmole/mg protein	ATP (2 mM) induced efflux nmole/mg protein
G1	100	181	79
G1–F1	72	199	115
G1–F11	28	171	15

Efflux was measured 10 min after the addition of ATP

Effect of ATP. The addition of 2 mM ATP to the uptake medium reduces the uptake in the first 30 min by 50%.

Uptake of Anion

Chloride. The uptake of Cl^- at room temperature is similar to that of Rb^+ and reaches the same equilibrium level as Rb^+. The mean $t_{1/2}$ was 36 min. The ratio of the $t_{1/2}$ shows that the permeability ratio of Rb^+ to Cl^- is approximately equal. However, addition of nucleotide is without effect on Cl^- uptake or distribution under any of the conditions of study.

Thiocyanate. SCN^- shows a much more rapid uptake ($t_{1/2}=2$ min). This is probably due to the presence of an additional uptake path for SCN^-, i.e., a lipophilic route (Scarborough, 1976). In the presence of valinomycin the uptake is further increased. This enhancement of uptake is independent of the initial K^+ gradient.

The presence of valinomycin and a K^+ gradient would be expected to induce a potential which would increase SCN^- uptake and result in a potential-dependent SCN^- concentration gradient. This gradient would then dissipate at the same rate as the K^+ gradient. This expectation is contrary to the experimental findings. Thus the enhanced uptake in the presence of valinomycin is present even in vesicles equilibrated in KCl prior to $S^{14}CN^-$ addition. The interpretation of the increase uptake of SCN^- in the presence of valinomycin is problematic. It could be due to binding of SCN^- to the membrane that is dependent on the presence of the lipophilic valinomycin-K^+ complex. ANS shows a similar enhanced binding (Lewin *et al.*, 1977). This binding could then obscure a transient due to the K^+ gradient dependent potential. Alternatively, the combination of a lipophilic anion and the lipophilic valinomycin K^+ complex could result in rapid equilibration of K^+.

The addition of ATP has no effect on the equilibrium level of SCN^- in the absence of valinomycin, as for $^{36}Cl^-$. In contrast to Cl^- however, in the presence of a valinomycin there is an enhanced SCN^- uptake (Fig. 4). From the data presented below, there is a K^+ gradient induced by ATP, which in the presence of valinomycin would induce a positive potential inside the vesicles. This is the simplest interpretation of the ATP induced redistribution. The ATP dependent SCN^- uptake is osmotically sensitive, hence is not due to binding. Since the fraction of transporting vesicles is not known, calculation of the potential difference gives a minimal value, assuming all vesicles are transporting equally (i.e., have an identical K^+ gradient), of approximately 18 mV.

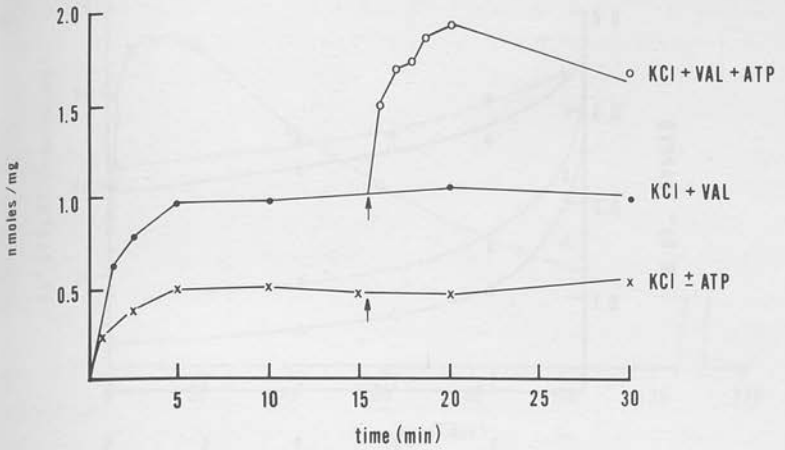

Fig. 4. Uptake of $S^{14}CN^-$. *Gl* vesicles in 250 mM sucrose, 200 ml were mixed with 200 µl of a solution containing 150 mM KCl, 80 mM tris-acetate, 4 mM $MgCl_2$, and 1.8 mM NaSCN (4 µCi ^{14}C). Valinomycin was added in 4 µl methanol to give 10^{-6} M. ATP was added (arrows) to give a final concentration of 2 mM. ×—×, $-S^{14}CN$ uptake with or without ATP; ●—● $-S^{14}CN$ uptake with valinomycin; ○—○ $-S^{14}CN$ uptake with valinomycin and ATP added after 15 min

Efflux of Cation

Dilution Efflux

This was performed as detailed in *Materials and Methods*. The rate of efflux of $^{86}Rb^+$ was influenced by the cation composition of the external medium. The sequence of effectiveness of various cations (Table 3) in terms of the inverse of the $t_{1/2}$ of efflux was, with the rate in the presence of K^+ set arbitrarily at 100, K^+ 100; Rb^+ 82; Cs^+ 64; Na^+ 20; Li^+ 11; choline 2. This efflux seems to be due, therefore,

Table 3. Exchange efflux of $^{86}Rb^+$

External cation	$t_{1/2}$ (min)
K^+	1.8
Rb^+	2.2
Cs^+	2.8
Na^+	9
Li^+	16
Choline	80

The mean of three experiments.

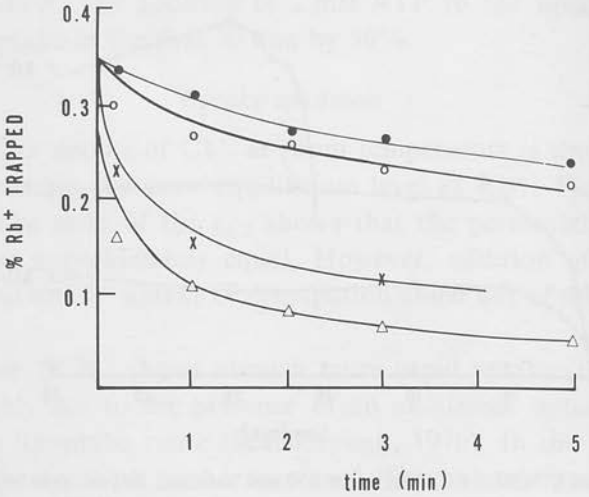

Fig. 5. Exchange efflux of $^{86}Rb^+$ in the presence of ionophores. Vesicles were equilibrated with $^{86}Rb^+$ in 75 mM RbCl, 125 mM sucrose, 2 mM $MgCl_2$, 5 mM glycylglycine, pH 6.12 for 72 hr at 4 °C. The efflux of $^{86}Rb^+$ was initiated by diluting 200 µl of the vesicles into 800 µl of solutions containing 150 mM MCl, 2 mM $MgCl_2$, 5 mM glycylglycine, pH 6.12. ●—●, M = Na^+; ○—○, M = Na^+ with 10^{-6} M valinomycin; ×—×, M = Na^+ with 1 µg/ml nigericin; △—△, M = Rb^+ with 10^{-6} M valinomycin. The experiment was performed at 21 °C and the final protein concentration was 2 mg/ml

to a cation/cation exchange process, the selectivity of this exchange corresponding to the sequence of activation of the ATPase or H^+ uptake (Sachs *et al.*, 1976). It seems possible, therefore, that the pathway is due to pump sites.

Addition of ionophores affects the dilution efflux according to their known selectivities. Thus valinomycin (Fig. 5) enhances efflux of Rb^+ with Rb^+ or K^+ as external cation, but does not affect efflux with Na^+ as external cation. Nigericin also stimulates efflux in the presence of Na^+. The permeability in uptake studies was calculated to be 10^{-9} cm sec^{-1} and for efflux with external K^+, 2×10^{-8} cm sec^{-1} at RT.

Equilibrium Efflux

Effect of ATP. Most of the studies were performed on efflux from an equilibrium situation. This transport may be primary active, but could be secondary active due to coupling to a potential of an electrogenic pump or due to contraction of the vesicles. The filtration technique can detect a transient efflux due to various possibilities. First, the treatment with ATP could result in a sudden increase in Rb^+ permeability.

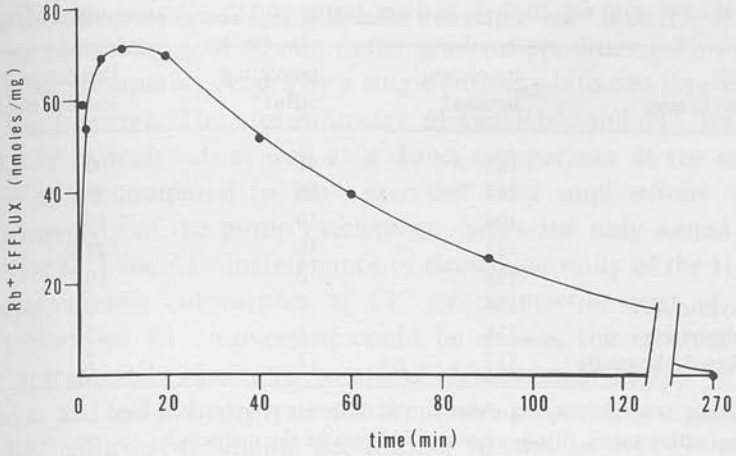

Fig. 6. Typical ATP stimulated efflux of Rb^+ from equilibrated vesicles. *G1* vesicles were incubated in 75 mM RbCl, 125 mM sucrose, 2 mM $MgCl_2$, 5 mM glycylglycine, pH 6.12 for 48 hr at 4 °C. ATP (2 mM) was added in 6.5 µl to initiate the efflux at 21 °C. Sampling was performed in triplicate at times over five min. and in duplicate up to five min

Such vesicles placed in the stop solution would lose Rb^+ more than untreated controls. However, there are several findings which exclude this possibility. Proton uptake studies show that the vesicles do not become extremely permeable to either H^+ or K^+. With the addition of ATP Rb^+ uptake is decreased by ATP. The effect of valinomycin on SCN^- uptake and ANS fluorescence engendered by ATP can be most easily explained by the development of a K^+ gradient (Lewin *et al.*, 1977). $^{36}Cl^-$ efflux or $S^{14}CN^-$ efflux would be expected with an increased leakiness and is not observed. Contraction of the vesicles would likewise enhance Cl^- or SCN^- efflux. A reduction of ATP induced efflux in the presence of nigericin occurs and this would not be expected of an increased wash out phenomenon.

Alternatively, an actual concentration gradient develops in the solution to which the ATP is added, and with loss of ATP due to hydrolysis, the previous equilibrium is reestablished. Fig. 6 shows the typical time course of the Rb^+ efflux and reequilibration with ATP addition to the *G1* fraction.

Kinetics. The efflux produced by ATP is rapid and the maximum efflux obtained is a function of the ATP concentration used. The K_M calculated from the Eadie-Hofstee plot was 2.5×10^{-4} M. This value is similar to the K_M for the ATPase and H^+ uptake activities of the vesicles (Sachs *et al.*, 1976).

Table 4. $^{86}Rb^+$ Efflux as a function of high energy phosphates

Nucleoside phosphate (2 mM)	nmole/mg uptake[a]	nmole/mg efflux[b]	Percentage of ATP induced efflux[c]
ATP	187	91	100
CTP	168	56	87
GTP	194	10	17
ITP	182	16	28
UTP	198	0	0
β-γ methylene ATP	134	0	0
Acetyl phosphate	118	8	15
pNitrophenyl phosphate	117	1	2

[a] Differences in uptake levels are due to the different preparations used.
[b] Maximal efflux taken 10 min after the addition of the nucleotide.
[c] Percentages were based on the average ATP induced effluxes for the preparations used.

Varying the ATP concentration also changes the initial rate of Rb^+ efflux, but with the filtration technique used, the initial 15 sec values are close together and could not be adequately analyzed.

The maximal efflux observed is a function of passive influx and passive efflux as well as of active efflux. The finding of a correspondence between the K_M of the efflux process with respect to ATP and the H^+ uptake and ATPase activity suggests that the active efflux is predominant. The long $t_{1/2}$ values for both efflux and influx as compared to the ATP effect substantiates this suggestion.

With increasing ATP the gradient is maintained for longer periods of time, as would be expected. The H^+ gradient is similarly affected (Sachs *et al.*, 1976).

The efflux of Rb^+ was relatively specific for ATP. Of the other nucleoside triphosphates tested (GIP, UTP, TTP, CTP) only CTP was capable of inducing Rb^+ efflux, but at a slower rate (Table 4). β-γ methylene ATP shows no transport activity though known to compete with ATP for the hydrolysis site (Saccomani *et al.*, 1977). pNPP also shows no transport though hydrolyzed by the enzyme in the presence of K^+. The average maximum efflux obtained for the *G1* fraction was $44 \pm 7\%$ of the initial level of Rb^+. The pH curve from 6.0 to 7.4 of the maximum transported Rb^+ activity corresponded to the K^+-ATPase curve. Inhibitors of K^+-ATPase activity such as Zn^{++}, F^- (Forte *et al.*, 1975) and DCCD at 1 mM (Sachs *et al.*, 1976) completely inhibited Rb^+ efflux.

Following efflux there is reuptake of Rb^+ to the same level as found before ATP addition to the equilibrated vesicles. The reuptake can be

described by a single exponential with a $t_{1/2}$ of 53 min which is to be compared to the $t_{1/2}$ of 40 min under gradient conditions. This reuptake therefore presumably occurs by a single pathway into one type of vesicle.

Stoichiometry. The stoichiometry of the Rb^+ and H^+ transported and ATP hydrolyzed, as well as a direct comparison of the moles H^+ taken up as compared to Rb^+ extruded have implications as to the electrogenicity of the pump mechanism. Since the only added ions are Rb^+ (or K^+) and Cl^- maintenance of electroneutrality of the H^+ uptake process requires cotransport of Cl^- or countertransport of Rb^+ (or K^+). Since no Cl^- movement could be shown, the ratio of H^+ and Rb^+ transported is likely to be unity. Measurement of Rb^+ efflux, H^+ uptake, and ATP hydrolysis on the same preparations gave a value for Rb^+ efflux of 6.5 μmole per mg per hr and an ATPase activity of 3.6 μmole Pi per mg per hr in the presence of Rb^+ and 1.8 μmole Pi per mg per hr in the absence of Rb^+. The calculated ratio of Rb^+ transported to ATP hydrolyzed is therefore 1.6 ± 0.2 using total ATPase activity and 3.5 ± 0.4 ($n = 4$) using only the cation activated component. These studies were done at room temperature at pH 6.1, and this accounts for the relatively large contribution of "basal" ATPase activity. The same conditions, using the cation activated ATPase activity for the calculation, the H^+ transported to ATP hydrolyzed ratio was 4.1 ± 0.2 ($n = 10$) (Sachs *et al.*, 1976). It should be noted however, that the H^+ measurement is electrometric, as compared to the filtration method for Rb^+. The relative ratio obtained is reasonably close to one, as was predicted. This does not prove that the pump is nonelectrogenic. As discussed in more detail elsewhere, however (Sachs, *et al.*, 1976; Lewin *et al.*, 1977), the results with ionophores and probes of vesicle potential strongly suggest that the transport mechanism is different from the H^+ ATPase of mitochondria or neurospora, for example (Scarborough, 1976).

Effects of Ionophores. Ionophores have variable effects on ATP induced Rb^+ efflux from preloaded vesicles (Table 5). Valinomycin and TCS did not affect Rb^+ efflux but valinomycin accelerated the reuptake phase of Rb^+ movement. Nigericin reduced Rb^+ efflux by 40% at 1 μg/ml. Lipid permeable ions such as DDA, DPA or SCN^- had no effect on the level of Rb^+ efflux at concentrations up to 10 mM, alone or in combination.

Effect of Rb^+ Concentration. Variation of Rb^+ concentration does not alter the steady state ratio of Rb^+ between vesicles and medium achieved by the addition of ATP. Moreover, it appears that the quantity of Rb^+ transported is a linear function of the Rb^+ concentration below

75 mM (Fig. 7). In contrast, ATPase activity is a saturable function of cation concentration, the apparent K_A for Rb^+ being 15 mM at pH 6.1 at room temperature.

Two interpretations may be suggested for these data. If the Rb^+ movement were in response to electrogenic H^+ uptake, then the final ratio would be independent of Rb^+ concentration, and also the quantity

Table 5. $^{86}Rb^+$ Efflux in the presence of ATPase inhibitors and ionophores[a]

Efflux stimulus and concentration	Total nmole/mg uptake	nmole efflux	% ATP stimulated efflux[b]
ATP + TCS (0.9×10^{-6} M)	154	72	98%
ATP + valinomycin (10^{-6} M)	152	70	92%
ATP + SCN (10 mM)	155	66	106%
ATP + nigericin (1 g/ml)	151	39	63%
ATP + F^- (1 mM)	162	3	5%
ATP + Zn^{2+} (1 mM)	161	1	1%
ATP + DCCD (1 mM)	159	0	0%
ATP + 10 mM DDA + 1 mM NaSCN	152	75	90%
ATP + 10 mM DDA + 10 mM NaSCN	192	117	127%
ATP + 10^{-5} M DPA	146	75	77%
ATP + 1 mM NaSCN + 1 mM DDA	174	85	88%

[a] Efflux measured 10 min after the addition of ATP.
[b] Based on ATP stimulated effluxes for same preparation.

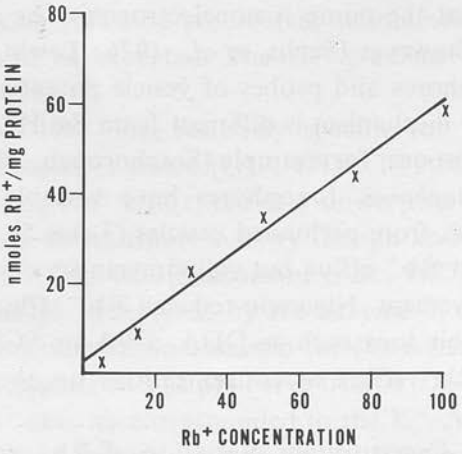

Fig. 7. ATP stimulated Rb^+ efflux as a function of Rb^+ concentration *G1* vesicles were incubated at 4 °C for 48 hr in X mM RbCl, 125 mM sucrose, 2 mM $MgCl_2$ 5 mM glycylglycine, pH 6.12 and (75-X) mM choline chloride. Efflux was initiated at room temperature with 2 mM ATP and measured ten min after ATP addition. Samples were taken in triplicate

transported would be a linear function of Rb^+ concentration. The distribution ratio would then suggest a value of 18 mV for the vesicular potential.

However, there are many suggestive lines of evidence that argue against the idea that Rb^+ is acting as a passive counterion for an electrogenic H^+ ATPase. Thus increasing the conductance of the vesicular membrane to Rb^+, by the addition of valinomycin would be predicted to increase Rb^+ efflux rate, which does not happen. The provision of alternate conductance paths, such as with lipid permeable cations and anions such as DDA^+ and SCN^- should reduce Rb^+ efflux, which again does not occur (Table 5). If a potential does develop during ATP hydrolysis, then ATP hydrolysis should be stimulated by increasing membrane conductance. In general this does not occur, unless K^+ selective ionophores are used (Ganser & Forte, 1973*b*). The activation of K^+ stimulated ATPase by these ionophores is due to increased levels of intravesicular K^+, since vesicular disruption abolishes the ionophore effect and NH_4^+ activation is not enhanced by valinomycin (NH_3 being highly permeable) (Saccomani *et al.*, 1977).

An alternative interpretation of the final steady state ratio is that only a fraction of the vesicles transport as a function of the addition of ATP. This fraction then achieves a similar internal level of Rb^+ independent of the initial level of ATP. Separation of the density gradient fraction by free flow electrophoresis produced two vesicular fractions which trap approximately the same quantity of Rb^+ (Table 1). However, only the anodic fraction demonstrates Rb^+ efflux with ATP addition, and a higher level of efflux (58%) is obtained as compared to the original zonal fraction (44%). If there is a random orientation of the ATPase in the fraction, only half of this fraction will actually transport. Hence the approximate 3:1 steady state ratio achieved may be misleading. When ANS was used as a probe of intravesicular potential, the initial rate of change of fluorescence with the addition of ATP in the presence of valinomycin was a linear function of the log of the added K^+ concentration (Sachs *et al.*, 1976; Lewin *et al.*, 1977). This implies that the internal cation reaches a fixed value. Hence the Rb^+ ratio of the fraction of the vesicles transporting is likely to be greater than 3:1.

H^+ Uptake: Fig. 8 shows the H^+ uptake induced with the addition of 0.3 mM ATP in vesicles equilibrated with RbCl as for the Rb^+ transport studies. The addition of a protonophore such as tetrachlorsalicylanilide (TCS) only partially dissipates the H^+ gradient and the further addition of valinomycin is required. This suggests the apparent absence of

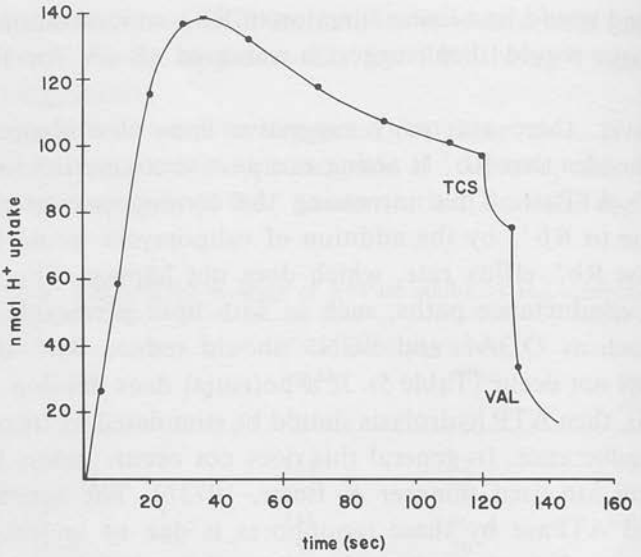

Fig. 8. The uptake of H^+ when 0.3 mM ATP was added to vesicles equilibrated with RbCl in 5 mM glycylglycine buffer pH 6.1 and the effect of addition of tetrachlorsalicylanilide (TCS) and valinomycin (val)

sufficient K^+ or Cl^- conductance to adequately dissipate the gradient even with an added H^+ conductance. This is further evidence against potential dependent redistribution of Rb^+. In this particular experiment the initial 10 sec uptake rate of H^+ was equivalent to 21.2 μmole per mg per hr, and the initial hydrolysis rate corresponded to 8.16 μmole Pi per mg per hr giving a ratio of H^+ transported to ATP hydrolyzed of 2.9. Correcting for basal ATPase activity in this particular experiment gave a ratio of 4.2 μmole H^+ transported per mole ATP hydrolyzed. The sensitivity of H^+ uptake to ATPase inhibitors is identical to that of the Rb^+ efflux.

It should be noted that the maximal H^+ gradient is developed at about 30 sec under these equilibrated conditions as compared to about 5 min for the Rb^+ efflux. At 1 min, directly comparing H^+ uptake and Rb^+ efflux, approximately a 2:1 ratio is obtained whereas the ratio approaches 1:1 at longer time intervals. The interpretation of this result is made difficult since the measurement of H^+ uptake electrometrically is more sensitive than the filtration technique used for Rb^+ efflux. Cation electrodes are insufficiently sensitive for cation efflux studies with these preparations. However, these data as compared to the calculated stoichiometry based on ATP hydrolysis suggest that the latter must be viewed with caution.

Discussion

From the data presented above, it has been possible to prepare, from hog gastric mucosa, a vesicular fraction which contains a cation activated ATPase (Ganser & Forte, 1973*a*). This preparation contains vesicles of low ion permeability and this low permeability is maintained during the fractionation procedures including free flow electrophoresis. If these vesicles derive from the tubulo-vesicular system of the parietal cell, this implies that they are preformed in the cell and are not actually vesiculated by homogenization as would be necessary for plasma membranes of other cell types. The tubulovesicles fuse with the apical plasma membrane of the acid secreting cell with formation of microvilli (Sedar, 1965) and presumably contain the acid secreting system. It is therefore striking that these vesicles contain few peptides revealed on SDS gel electrophoresis, more than 75% being accounted for in the 100,000 M_r region (Sachs *et al.*, 1976).

The vesicles, either the zonal gradient or the free flow fraction, take up H^+ with addition of ATP as previously established for dog microsomes (Lee *et al.*, 1974). Since both a proton and a cation conductance were required to dissipate the H^+ gradient (Lee *et al.*, 1974; Sachs *et al.*, 1975, 1976) it was suggested that the uptake was nonelectrogenic. Since changes in membrane conductance such as those induced by lipid permeable ions or protonophores did not affect ATPase activity (Sachs *et al.*, 1976) and since no potential was detected during transport (Fig. 4 and Lewin *et al.*, 1977) also using lipid permeable ions it was likely that the mechanism of H^+ uptake was not by a mechanism similar to the electrogenic H^+-ATPase (Mitchell, 1966). Since cation and chloride ion were the only additions to the H^+ uptake medium which could satisfy the ionic requirements for the uptake process, pathways for these ions were presumed to be present in this vesicular preparation.

Both cation and chloride were taken up by this preparation into an osmotically sensitive space at about the same rate. The low interactionic selectivity of uptake is typical of channels such as gramicidin (Goodall, 1973) or of noninteractive sites such as large diameter waterfilled pores. Both of these structures have a high H^+ permeability, and if present in these vesicles must be few in number.

Efflux of Rb^+ into choline solutions was very slow as would be expected from the slow uptake observed, but external cation stimulated efflux considerably and selectively although the discrimination between K^+ and Na^+ was less than that for H^+ uptake or ATPase activity (Sachs

et al., 1976). Carriers of the valinomycin type are more selective and conductive whereas nigericin is less selective and essentially neutral (Henderson, McGiven & Chappell, 1969). The selectivity of this exchange process suggests that it is distinct from the nonselective uptake pathway revealed by the influx studies. It is also likely to be neutral since cation gradients do not result in H^+ movement across the vesicle membrane even in the presence of a proton conductance (i.e., in the presence of TCS).

From both these types of studies the cation permeability and conductance of the unenergized membrane preparation is low as is the anion permeability.

The addition of ATP significantly affects cation but not anion movements in the untreated membranes. Thus influx is apparently reduced and efflux stimulated. Studies of Rb^+ movement following equilibration showed that Rb^+ was transported uphill following ATP addition. The cation requirement for H^+ uptake and the identical effects of inhibitors on ATPase, H^+ uptake, and Rb^+ movement suggested that these processes were interlinked. Indeed, the absence of Cl^- redistribution under identical conditions implied that countertransport of cation was probably obligatory for H^+ uptake and that the ratio of cation efflux to H^+ uptake would therefore have to be 1:1. Studies on H^+ uptake showed that intravesicular cation was required (Sachs *et al.*, 1976) and the evidence against electrogenicity of H^+ uptake or ATPase activity and against a cation conductance path made it likely that cation transport was due to direct coupling to the pump rather than due to indirect coupling by a potential due to electrogenic H^+ transport. This was substantiated in these studies by the finding that shunt conductances (e.g., lipid permeable ions) added to the vesicles did not affect Rb^+ efflux; and that SCN^- did not detect a positive interior potential with the addition of ATP.

However, the final steady state ratio achieved by the vesicles for the gradient fraction ($\bar{c}$2:1 and 3:1 for the electrophoretic fraction) could be interpreted as evidence for an 18–25 mV potential gradient. The data derived for the stoichiometry of the pump showed close to a 1:1 ratio if the ratio relative to ATP hydrolysis was used. A discrepancy did exist comparing pH measurements directly to Rb^+ movement at short time intervals, which might be due to the lower sensitivity and longer response time of the filtration technique.

Thus the ATPase of these vesicles simultaneously translocates H^+ and cation in a directly coupled reaction.

From other studies cations dephosphorylate the ATPase as they do the $Na^+ + K^+$ ATPase (Tanisawa & Forte, 1971). This ATPase therefore can be classified as an $H^+:K^+$ ATPase in analogy to the $Na^+ + K^+$ or Ca^{++} ATPases (Skou & Hilberg, 1969; Martonosi, 1969). A major difference between the preparation described here, and similar preparations of the other enzymes is the ion tightness of the vesicle. Ca^{++}-ATPase containing vesicles have a high anion permeability (Duggan & Martonosi, 1970) making it very difficult to determine the electrical characteristics of the pump. With this enzyme analogs such as carbamyl phosphate energize transport in contrast to the $H^+:K^+$ ATPase. Most preparations of $Na^+ + K^+$ ATPase are too leaky for transport studies, and this enzyme is usually present in membranes of a more complex peptide composition than the $H^+:K^+$ ATPase (Walter, 1975). Reconstituted vesicles containing this enzyme do exhibit Na^+ and K^+ transport (Hilden & Hokin, 1975).

Although from these studies it would appear that the $H^+:K^+$ ATPase catalyzes a transmembranal neutral $K^+:H^+$ exchange, results with frog gastric mucosa in SO_4^{2-} solutions are compatible only with an electrogenic process in the gastric mucosa (Davis *et al.*, 1963). Metabolic data in dog gastric mucosa (Sarau *et al.*, 1975) and spectroscopic observations (Hersey, 1974) are also not incompatible with a redox energy source for secretion. On the other hand, based on antibody studies (Saccomani, *unpublished observations*) it is clear that this $H^+:K^+$-ATPase is a specific component of the parietal cell and is a transport enzyme requiring K^+, which cation is essential for acid secretion (Davis *et al.*, 1965). One might suggest that the electrogenic properties of the intact tissue reside in the Cl^- pump (Hogben, 1951) and perhaps in another membrane associated component removed by our isolation procedures or absent from the plasma membrane in nonsecreting tissue.

The authors are grateful for the assistance and discussion given by Dr. E. Rabon, Ms. H. Hung Chang and Mr. H.B. Stewart.

This work was supported by grants NIH AM 15878; NSF Gb31075; CA 16877 and CA 16722 (G.S.) and HL07906 and contract HV52998 (A.S.).

References

Davis, F.L., Rutledge, J.R., Keesee, D.C., Bajandas, F.J., Rehm, W.S. 1965. Acid secretion, potential and resistance of frog stomach in K^+-free solutions. *Am. J. Physiol.* **209**:146

Davis, F.L., Rutledge, J.R., Rehm, W.S. 1963. Effect of potassium on secretion and potential of frog's gastric mucosa in Cl^- free solutions. *Am. J. Physiol.* **205**:873

Duggan, P.F., Martonosi, A. 1970. Sarcoplasmic reticulum. IX. The permeability of sarcoplasmic reticulum membranes. *J. Gen. Physiol.* **56**:147

Forte, J.G., Forte, G.M., Saltman, P. 1967. K^+-stimulated phosphatase of microsomes from gastric mucosa. *J. Cell Physiol.* **69**:293

Forte, J.G., Ganser, A., Beesley, R., Forte, T.M. 1975. Unique enzymes of purified microsomes from pig fundic mucosa. K^+-stimulated adenosine triphosphatase and K^+-stimulated pNPPase. *Gastroenterology* **69**:175

Ganser, A., Forte, J.G. 1973*a*. K^+-stimulated adenosine triphosphatase in purified microsomes of frog oxyntic cells. *Biochim. Biophys. Acta* **307**:169

Ganser, A.L., Forte, J.G. 1973*b*. Ionophoretic stimulation of K^+-ATPase of oxyntic cell microsomes. *Biochem. Biophys. Res. Commun.* **54**:690

Goodall, M.C. 1973. Action of two classes of channel forming synthetic peptides in lipid bilayers. *Arch. Biochem. Biophys.* **157**:514

Henderson, P.J.F., McGivan, J.D., Chappell, J.B. 1969. The action of certain antibiotics on mitochondrial, erythrocyte, and artificial phospholipid membranes. The role of induced proton permeability. *Biochem. J.* **111**:521

Hersey, S.J. 1974. Interaction between oxidative metabolism and acid secretion in gastric mucosa. *Biochim. Biophys. Acta* **344**:157

Hilden, S., Hokin, L.E. 1975. Active potassium transport coupled to active sodium transport in vesicles reconstituted from purified sodium and potassium ion-activated adenosine triphosphatase from the rectal gland of *squalus acanthias*. *J. Biol. Chem.* **250**:6296

Hirschowitz, B.I., Sachs, G. 1967. Insulin inhibition of gastric secretion and reversal by rubidium. *Am. J. Physiol.* **213**:1401

Hogben, C.A.M. 1951. The chloride transport system of the gastric mucosa. *Proc. Nat. Acad. Sci. USA* **37**:393

Hogben, C.A.M. 1968. Observations on ionic movement through the gastric mucosa. *J. Gen. Physiol.* **51**:2405

Lee, J., Simpson, G., Scholes, L. 1974. An ATPase from dog gastric mucosa: Changes of outer pH in suspensions of membrane vesicles accompanying ATP hydrolysis. *Biochem. Biophys. Res. Commun.* **60**:825

Lewin, M., Saccomani, G., Schackmann, R., Sachs, G. 1977. The use of ANS as a probe of gastric vesicle transport *J. Membrane Biol.* **32**:301

Lowry, O.H., Rosebrough, N.J., Farr, A.L., Randall, R.J. 1951. Protein measurement with the folin phenol reagent. *J. Biol. Chem.* **193**:265

Martonosi, A. 1969. Sarcoplasmic reticulum VII. Properties of a phosphoprotein intermediated implicated in calcium transport. *J. Biol. Chem.* **244**:613

Mitchell, P. 1966. Chemiosmotic coupling in oxidative and photosynthetic phosphorolation. *Biol. Rev.* **44**:445

Saccomani, G., Shah, G., Spenney, J.G., Sachs, G. 1975. Characterization of gastric mucosal membranes. VIII. The localization of peptides by iodination and phosphorylation. *J. Biol. Chem.* **250**:4802

Saccomani, G., Stewart, H.B., Shaw, D., Lewin, M., Sachs, G. 1977. Characterization of gastric mucosal membranes. X. Fractionation and purification of K^+-ATPase containing vesicles by zonal centrifugation and free-flow electrophoresis technique. *Biochim. Biophys. Acta (in press)*

Sachs, G., Collier, R.H., Pacifico, A., Shoemaker, R.l., Zweig, R.A., Hirschowitz, B.I. 1969. Action of thiocyanate on gastric mucosa in vitro. *Biochim. Biophys. Acta* **173**:509

Sachs, G., Hirschowitz, B.I. 1968. Secretion by in vitro amphibian gastric mucosa. *In:* The physiology of Gastric Secretion. L.S. Semb and J. Myren, editors. Vol. 186, p. 202. Universitetsforlaget, Oslo

Sachs, G., Chang, H., Rabon, E., Schackmann, R., Lewin, M., Saccomani, G. 1976. A non-electrogenic H^+ pump in plasma membranes of hog stomach. *J. Biol. Chem.* **251**:7690

Sachs, G., Rabon, E., Saccomani, G., Sarau, H.M. 1975. Redox and ATP in acid secretion. *Ann. N.Y. Acad. Sci.* **264**:456

Sachs, G., Rose, J.A., Shoemaker, R.L., Hirschowitz, B.I. 1966. Phosphatase reactions of transport ATPases. *Physiologist* **9**:281

Sarau, H.M., Foley, J., Moonsamy, G., Wiebelhaus, V.D., Sachs, G. 1975. Metabolism of dog gastric mucosa. I. Nucleotide levels in parietal cells. *J. Biol. Chem.* **250**:8321

Scarborough, G.A. 1976. The neurospora plasma membrane ATPase in an electrogenic pump. *Proc. Nat. Acad. Sci. USA* **73**:1485

Sedar, A.W. 1965. Fine structure of the stimulated oxyntic cell. *Fed. Proc.* **24**:1360

Skou, J.C., Hilberg, C. 1969. The effects of cations, *g*-strophanthin and oligomycin on the labeling from [^{32}P] ATP of the ($Na^+ + K^+$)-activated enzyme system and the effect of cations and *g*-strophanthine on the labeling from [^{32}P] ITP and ^{32}Pi. *Biochim. Biophys. Acta* **185**:198

Tanisawa, A.S., Forte, J.G. 1971. Phosphorylated intermediate of microsomal ATPase from rabbit mucosa. *Arch. Biochem. Biophys.* **147**:165

Walter, H. 1975. Tightness and orientation of vesicles from guinea pig kidney estimated from reactions of adenosine triphosphatase dependent on sodium and potassium ions. *Eur. J. Biochem.* **58**:595

Yoda, A., Hokin, L.E. 1970. On the reversibility of binding of cardiotonic steroids to a partially purified ($Na^+ + K^+$) activated adenosine triphosphatase from beef brain. *Biochem. Biophys. Res. Commun.* **40**:880

mbrane Biol. 32, 301–318 (1977)
Springer-Verlag New York Inc. 1977

Use of 1-Anilino-8-Naphthalene-Sulfonate as a Probe of Gastric Vesicle Transport

M. Lewin, G. Saccomani, R. Schackmann, and G. Sachs*

atory of Membrane Biology, University of Alabama in Birmingham, Birmingham, Alabama 35294

Received 8 April 1976; revised 7 June 1976; revised again 16 August 1976

ummary. The interaction of 1-anilino-8-naphthalene-sulfonate (ANS) with vesicles d from hog fundic mucosa was studied in the presence of valinomycin and with dition of ATP. Evidence was found for two classes of sites, those rapidly accessible NS with a K_D of 7.5 μM and those slowly accessible, but rapidly accessed in the ce of valinomycin with a K_D of 2.5 μM. ATP transiently increases the quantum f the latter ANS binding sites only in the presence of valinomycin, but does not he number of K_D of those sites. The time course of this increase correlates with ake and Rb^+ extrusion by those vesicles and H^+ carriers such as tetrachlorsalicylanil- nigericin abolish the ATP response. With ATP addition in the presence of $SC^{14}N$ alinomycin there is transient uptake of SCN^-. It is concluded that ANS is acting obe of a structural change dependent on a potential and H^+ gradient.

he vesicular membrane fraction isolated from hog gastric mucosa een characterized in some detail (Forte, Ganser, Beesley & Forte, and further subfractionated using ficoll-sucrose or ficoll-ficoll den- radients (Sachs, Rabon, Chang, Schackmann, Lewin & Saccomani, . It has been shown in several species (Ganser & Forte, 1974*a*; , Ganser & Tanisawa, 1974; Spenney, Strych, Price, Helander & , 1974*b*) that the membrane fractions isolated from gastric fundus in a cation or K^+-stimulated ATPase which is insensitive to oua- but is also capable of forming a phosphorylated intermediate sensi- K^+ (Tanisawa & Forte, 1971). The ATPase activity is also en- d by valinomycin, gramicidin or nigericin (Ganser & Forte, 1973*b*) ore recently it has been claimed that a proton gradient is generated the addition of ATP (Lee, Simpson & Scholes, 1974) in a dog somal preparation.

e unique capacity of the gastric mucosa to generate a H^+ gradient :1, across the membrane of the parietal cell in the mammal,

m correspondence should be addressed.

combined with the observations outlined above, make this membrane fraction a particularly interesting model because of the apparent lack of the complex redox system associated with other H^+ transport vesicles. Since it has also recently been shown that these smooth membrane fractions are probably randomly oriented and are also, in the case of hog fractions, capable of absorbing H^+ and ejecting Rb^+ (Sachs, Saccomani, Rabon & Sarau, 1975; Sachs *et al.*, 1976) with the addition of ATP, it seems important to approach the problem of the membrane changes or energization induced by ATP. Some years ago, it was shown that ATP produced conformational changes in membrane fraction derived from dog mucosa by the use of corrected CD spectra (Masotti, Long, Sachs & Urry, 1972).

1-anilino-8-naphthalene-sulfonate (ANS) is a fluorescent membrane probe which has two major properties of interest for this study. First, fluorescent enhancement and a bathochromic shift occur with change of the environment from high to low dielectric constant which enables assessment of the change of hydrophobicity of the ANS environment (Stryer, 1965); and second, being negatively charged, the movement of ANS is sensitive to the alteration of potential gradients across a vesicular membrane such as mitochondria (Azzi, Chance, Radda & Lee, 1969*a*, Chance & Lee, 1969) everted submitochondrial particles (Azzi *et al.*, 1969*a*) or single layer liposomes (Bakker & Van Dam, 1974). It has also been suggested that site protonation may account for increased ANS binding (Chance, 1970).

In this paper we report significant effects on ANS fluorescence induced by ATP, that appear to be dependent on H^+ and potential gradients across the membrane and correlate these effects with the properties described elsewhere of H^+ and Rb^+ transport induced by ATP.

Materials and Methods

Smooth surface gastric vesicles (SGV) were prepared from hog gastric mucosa as described in detail elsewhere (Spenney, Saccomani, Spitzer, Tomana & Sachs, 1974*a*; Saccomani, Shah, Spenney & Sachs, 1975) but with the modification of teflon-glass homogenization. Using a 7–20% ficoll density step gradient (15 hr, SW 25, 23,000 rpm), the microsomal fraction was separated into three fractions, GI, GII and GIII (Saccomani, Stewart, Shaw, Lewin & Sachs, 1977), GI being the band obtained at the 7% ficoll interface. The rationale for using the GI fraction and the avoidance of sucrose in the gradient is that GI is more active in terms of H^+ transport (Sachs *et al.*, 1976) and Rb^+ efflux, and is also more active when prepared with pure ficoll gradients as compared to ficoll/sucrose gradients.

This GI fraction has been shown to contain a 20-fold enrichment of K^+ *p*-nitrophenyl phatase (*p*NPPase) or K^+-ATPase (Sachs *et al.*, 1976) and to contain less than 5% e microsomal content of RNA, succinic dehydrogenase, monamine axidase or cyto-me *c* oxidase. Electronmicrographs showed it to be a smooth-surfaced vesicular fraction. s stored in the refrigerator until use.

The fluorescence of ANS was measured in an Aminco Bowman spectrofluorimeter hermostatted cuvette at an excitation wavelength of 375 nm and an emission wavelength 0 nm. Under each experimental condition repetitive scans were carried out to ensure ity of the scatter and emission peaks. Fluorescence was measured at a sensitivity g of 30, and expressed as arbitrary units (FU).

The standard conditions were the addition successively of 100 µl of GI suspension aining 5 mg protein/ml) to a quartz cuvette containing 2 ml of a solution of 150 mM, 50 mM, Tris acetate buffer, pH 6.1 at 27 °C. ANS was added in 10 µl methanol chieve a final concentration of 2.5×10^{-6} M, followed by valinomycin (10 µl solution ve a final concentration of 5×10^{-6} M) and Mg ATP (10 µl solution to give a final ntration of Mg ATP of 5×10^{-5} M). In some experiments the concentration of each e constituents was varied independently as was the pH of the suspending medium. n the protein concentration was varied at a fixed ANS concentration (Fig. 7), the scence calculated at infinite protein concentration was assumed to be the fluorescence e total quantity of ANS added. This allowed calculations of the quantity of ANS d under conditions of varying ANS concentration and hence the free ANS from ifference between total added and amount bound. "Aging" of the SGV preparation carried out at refrigerator temperature for a period of five days. Other additions as nigericin (1 µg/ml), *m*-chlorocyanocarbonylphenylhydrazone (CCCP) (10^{-5} M), tet-orsalicylanilide (TCS) (10^{-6} M) were dissolved in 10 µl methanol before addition to uvette. Ten µl methanol alone was without any action. Analogs of ATP were used same final concentration as ATP and dicyclohexylcarbodiimide (DCCD) was added oncentration of 10^{-3} M also in 10 µl of methanol.

With ethidium bromide, a positively charged fluorescent marker, all the conditions he same, except that 10^{-6} M ethidium bromide was used and 530 nm was the excitation 90 nm was the emission wavelength. No effect of K^+, valinomycin, or ATP was ved.

The generation of a proton gradient was measured as described elsewhere (Sachs 1975).

The distribution of SCN^- between vesicles and medium was assessed by adding 200 µl sicle suspension to 200 µl of a solution containing 150 mM KCl, 80 mM tris-acetate 1, 2 mM $MgCl_2$ and 1.82 mM $S^{14}CN$ (4 µCi) at room temperature. At the start of the iment to one set of tubes in a final volume of 400 µl, valinomycin was added in ethanol at 10^{-6} M.

After incubation and sampling for 15 min, ATP was added to both sets of tubes ampling (20 µl) continued. The samples taken at various times before and after ATP on were injected into 1 ml of a 120 mM Li_2SO_4 solution at pH 6.1 and 0 °C. The re was filtered on a Millipore HAWP 0.45 microfilter, washed once with 4 ml Li_2SO_4 on, the filters were dried and counted in an LKB 81,000 scintillation counter. In experiments $^{36}Cl^-$ was used instead of SCN^-.

All chemicals were the highest purity available; nigericin was a gift from Eli Lilly any. ANS was obtained from Eastman Kodak. Hog stomachs were obtained fresh slaughterhouse through the courtesy of Lumberjack Meat Company and the fractions ed on the day of the slaughter.

Results

Initial Observations

Prior to ANS addition, the SGV suspension had negligible emission at 480 nm (Fig. 1). The addition of ANS at a final concentration of 2.5×10^{-6}M resulted in an increase of 12 FU rapidly ($t_{1/2}$ too small to measure with our technique) followed by a second slow phase which reached a plateau after 20 min (Fig. 1) at 22 FU. Omission of membranes gave, with addition of ANS, an emission at 575 nm.

Valinomycin added at 1 min after the addition of membranes resulted in an increase of fluorescence to 29 FU (Fig. 1). Without membranes at the standard concentration of valinomycin (5×10^{-6}M) no change in FU was observed, but at higher concentrations (5×10^{-5}M) a change of 5 FU was found, as has previously been described for several ionophores such as valinomycin or nigericin (Feinstein & Felsenfeld, 1971).

Subsequent addition of ATP produced a large transient increase in fluorescence (Fig. 1), 69 ± 2 FU, $n=8$ being the mean $\pm$ SEM for a given

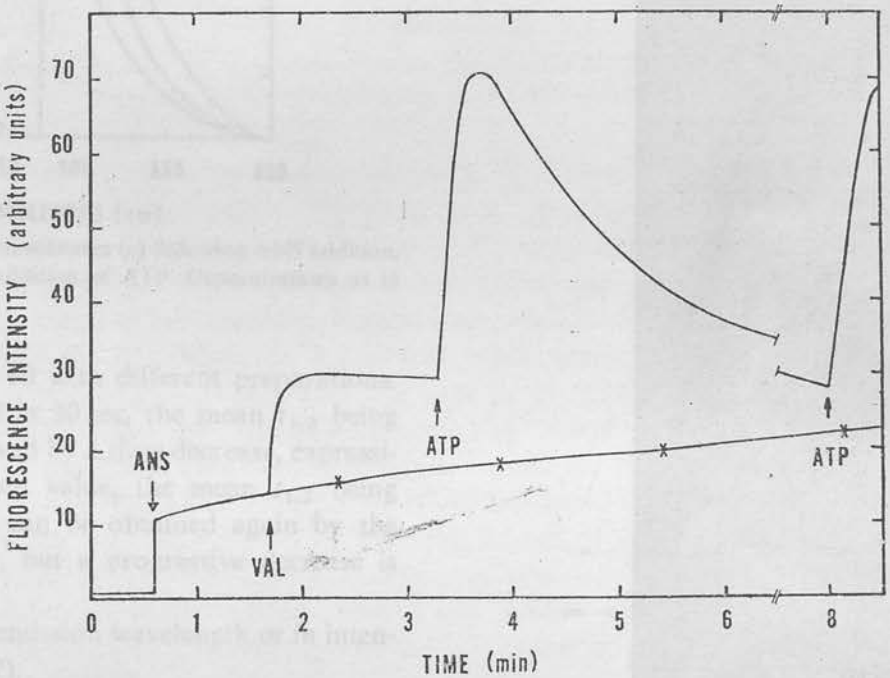

Fig. 1. The effect of addition of ANS to gastric vesicles on fluorescence at 480 nm showing an initial rapid rise followed by a slow increment. The addition of valinomycin prior to the slow rise results in rapid attainment of the final level. Addition of ATP only in the presence of valinomycin results in a transient fluorescent enhancement

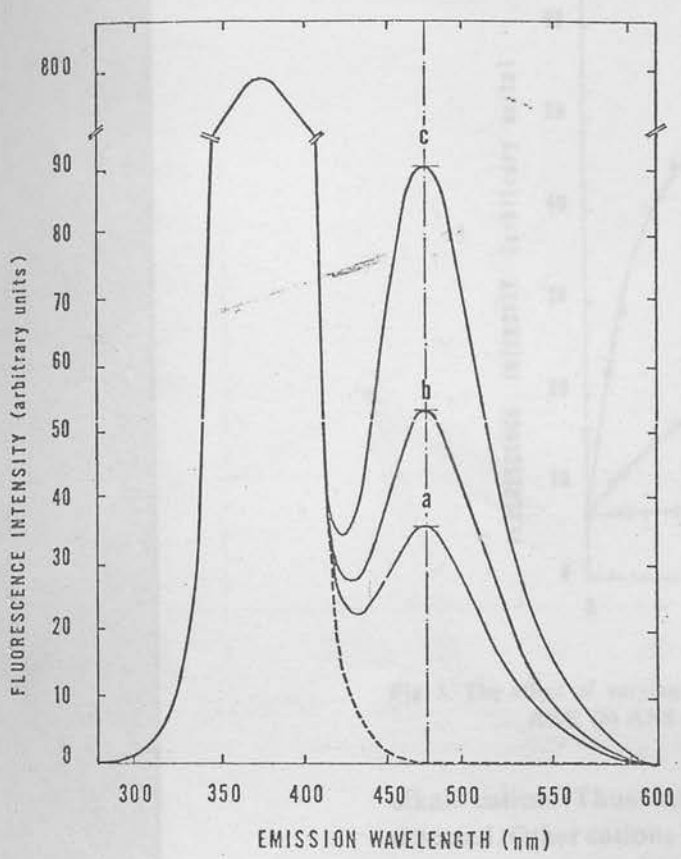

2. An emission scan of fluorescence of gastric membranes (*a*) following ANS addition, llowing valinomycin addition, (*c*) with the addition of ATP. Concentrations as in text

preparation and ranged from 45 to 90 with different preparations. maximum fluorescence was reached in 30 sec, the mean $t_{1/2}$ being c±1.2 ($n=8$). The maximum is followed by a slow decrease, expressi- as a simple exponential, to the basal value, the mean $t_{1/2}$ being sec. The fluorescence enhancement can be obtained again by the dition of ATP following the decay, but a progressive decrease is d with successive additions of ATP.

Under these conditions, no change in emission wavelength or in inten- of the scatter peak was found (Fig. 2).

K^+ *Valinomycin Requirement*

The ΔFU obtained with the addition of ATP was absolutely depen- on the presence of valinomycin, of the ionophores tested and on

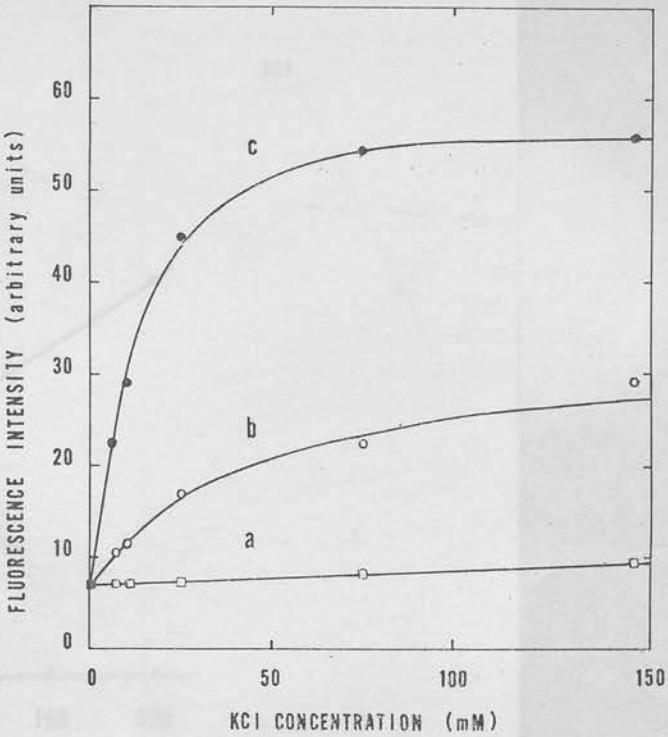

Fig. 3. The effect of varying the KCl concentration on (*a*) the fluorescence induced by ANS, (*b*) ANS + valinomycin, and (*c*) ANS-valinomycin + ATP

alkali cation. Thus with valinomycin in choline media no effect was detected. Other cations substituted for K^+ in the sequence K^+ (100) > Rb (90) > Cs (30) > Na, Li (1). The lipophilic cation triphenylmethylphosphonium ($TPMP^+$) was able to partially (50%) substitute for valinomycin, in terms of the valinomycin dependent ANS fluorescence enhancement, but did not substitute in the ATP effect where valinomycin was still required. Preincubation of the vesicles in KCl did not remove the requirement for valinomycin, and other ionophores such as nigericin or gramicidin also were unable to substitute for valinomycin.

Since there were two phases of ANS-induced fluorescence, the possibility that the addition of valinomycin served to accelerate the slow phase of ANS binding was examined by adding valinomycin after 20 min following ANS addition. Indeed this resulted in a 90% reduction in the effect of valinomycin, but the ionophore was still required for the ATP effect.

The effect of variation of KCl concentration was examined in some detail. The effect of valinomycin was sensitive to KCl concentration.

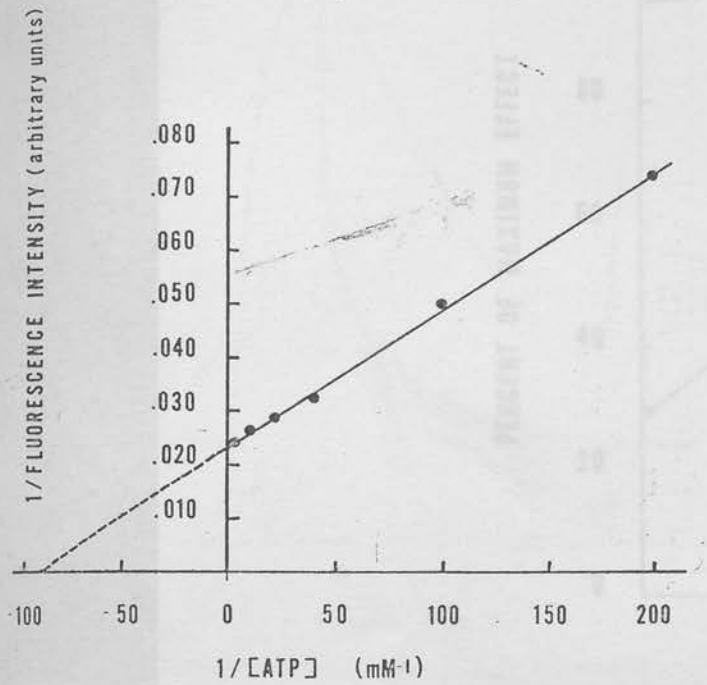

4. A Lineweaver Burk plot of the effect of varying the ATP concentration of the maximal fluorescence obtained

ever, varying the K^+ gradient by preincubating the vesicles in KCl adding the vesicles to equimoiar KCl or choline chloride instead Cl did not alter the fluorescence obtained when KCl was present ally only on the exterior of the vesicles. The apparent K_A for valino-in-induced fluorescence was 5×10^{-2}M (Fig. 3).

Variation of KCl also affected the ATP-induced ANS fluorescence ncement. Two effects were noted. The maximal fluorescence as plot-in Fig. 3 gave a good fit to Michaelis-Menten kinetics ($r=0.996$) an apparent K_A of 1.5×10^{-2}M. However, K^+ also affected the decreasing the $t_{1/2}$ of excitation and decay. If the initial rate of rescence change was used the data did not conform to Michaelis-ten kinetics but instead the change in fluorescence was linearly re-to the log of the K^+ concentration ($r=0.992$) and the zero fluores-e intercept corresponded to 1 mM K^+. The slope corresponded to FU for a 10-fold change in K^+ concentration. In the ATP situation, direction of the initial gradient had slight, variable effects on the rescence obtained.

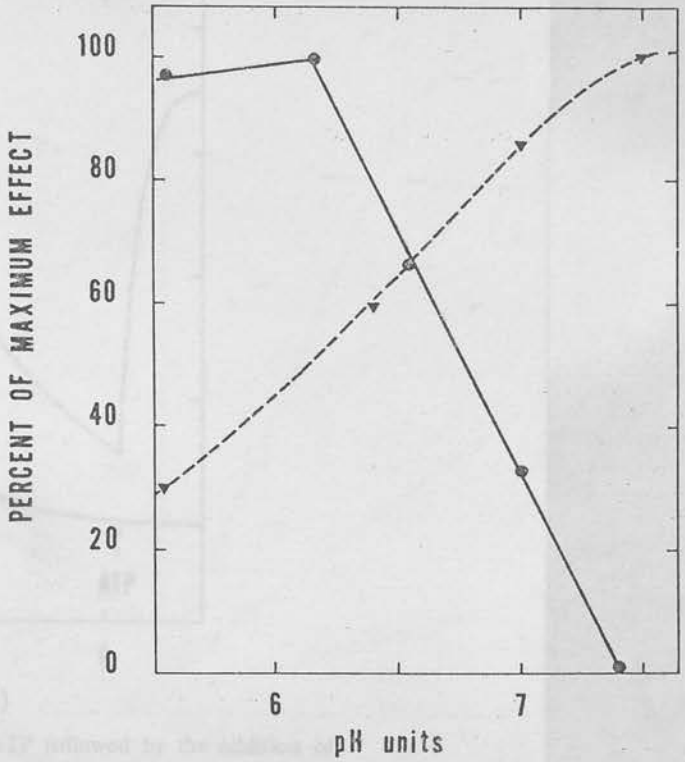

Fig. 5. The variation of maximal fluorescence obtained with ATP addition as a function of medium pH (●——●). Superimposed is the K^+-ATPase activity as a function of pH under identical conditions

Substrate Specificity

At various concentrations GTP, UPT, ITP, TTP, ADP, acetylphosphate, and *p*NPP were all shown to be ineffective in promoting a fluorescence enhancement.

Variation of ATP concentration had significant effects on the time course and maximum fluorescence obtained. A double reciprocal plot of the effect of ATP on maximal fluorescence is shown in Fig. 4, giving an apparent K_M of 1.1×10^{-5}M and a calculated maximal FU of 46.5 for this preparation. A change of fluorescence could readily be detected with concentrations of ATP as low as 5×10^{-6}M.

Dependence on K^+-ATPase Activity

The effect of pH is shown in Fig. 5 where it can be seen that there is a linear decrease of ATP-induced ΔFU from pH 6.1 to pH 7.4, whereas

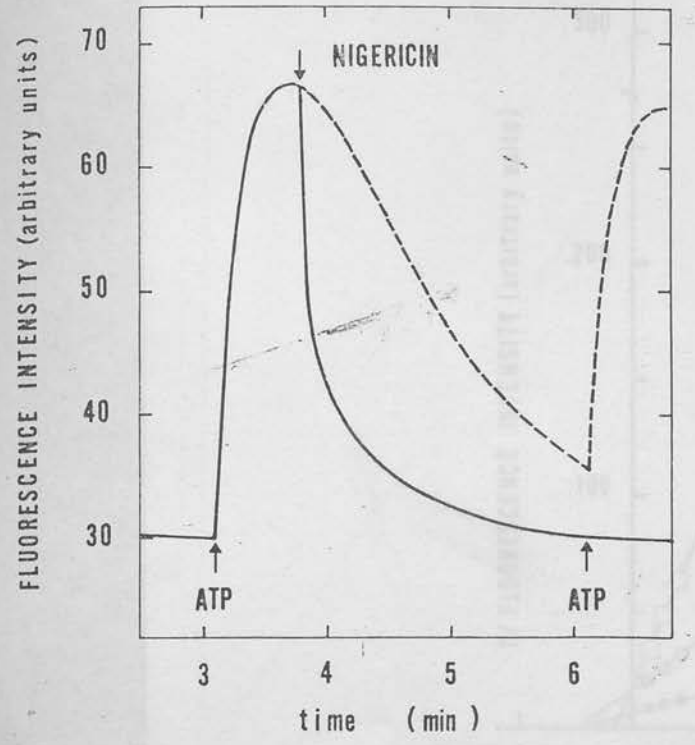

g. 6. The effect on fluorescence of the addition of ATP followed by the addition of gericin at the peak of fluorescence, and also showing the lack of effect of a subsequent TP addition. The dotted line shows the decay and reexcitation of fluorescence in an identical control preparation

TPase activity increased over this range, being optimal at pH 7.4, where e ΔFU is not detected. β-γ methylene ATP, a nonhydrolyzable analog ATP did not produce a ΔFU. DCCD blocked the ANS response d also inhibited the K^+-ATPase activity.

Effect of Ionophores

Fig. 6 shows the effect of the addition of nigericin which is similar the effect of addition of CCCP (10^{-5}M) or TCS (10^{-6}M). Thus, prior dition of nigericin blocks the response to ATP, or addition of nigericin the peak of fluorescence rapidly collapses the ΔFU observed (Fig. 6). ramicidin also inhibited the fluorescence, due to the H^+/K^+ exchange aracteristics of this ionophore.

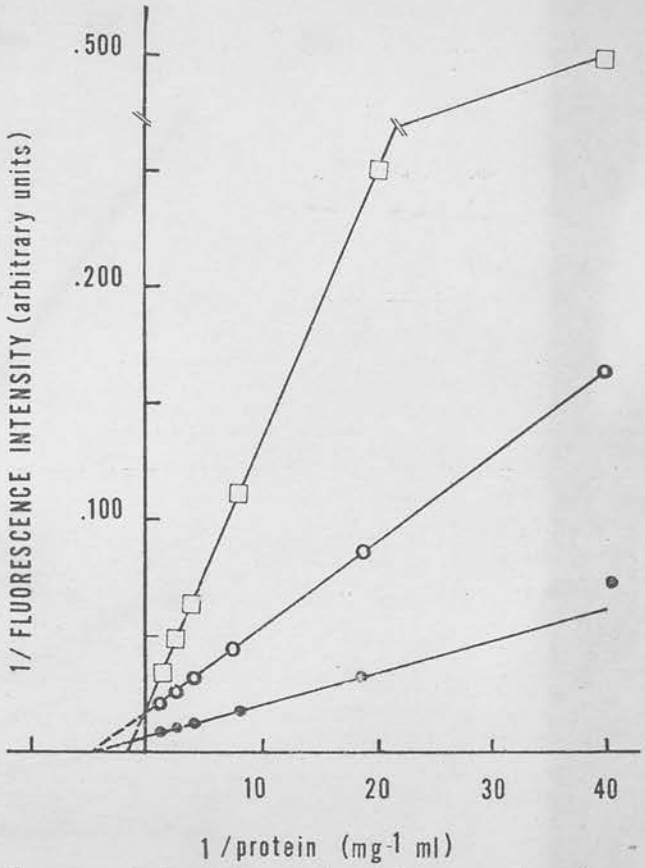

Fig. 7. A double reciprocal plot of the variation of fluorescence intensity at a fixed ANS concentration with alteration in membrane concentration: □—□ ANS alone; ○—○ ANS+valinomycin; ●—● ANS+valinomycin+ATP

Effect of Vesicle Integrity

Aging the vesicles by maintaining them at refrigerator temperature results in gradual loss of response to ATP, but does not significantly change the response to valinomycin. Two cycles of freeze thawing also sharply reduced the response to ATP, but again not the valinomycin effect.

Effect of Protein Concentration

At a fixed concentration of ANS (5×10^{-6} M), increasing the protein concentration resulted in a fluorescence that was a hyperbolic function of protein concentration under all conditions studied: ANS, ANS+valinomycin and ANS+valinomycin+ATP. Fig. 7 shows this finding in

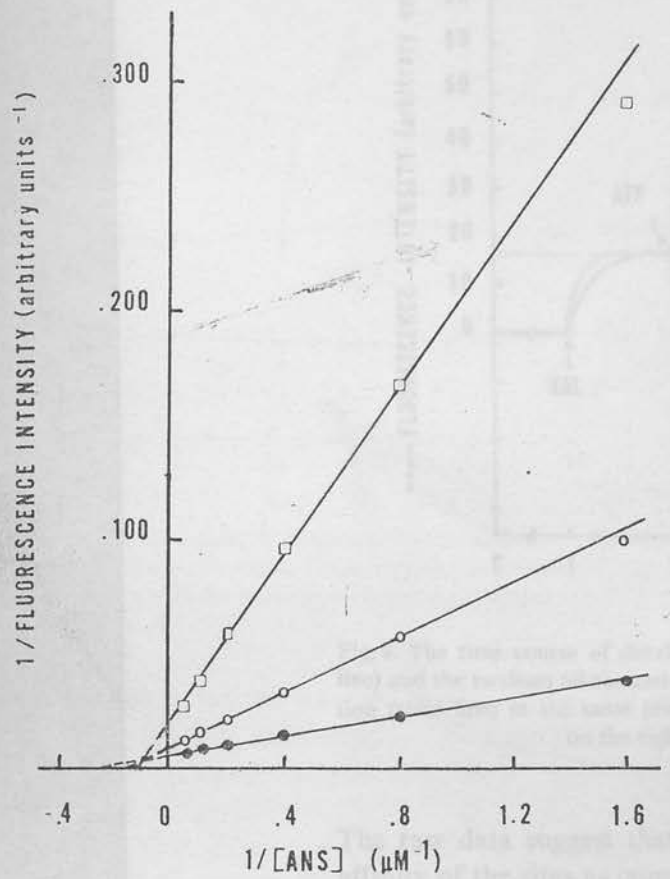

Fig. 8. A Lineweaver Burk plot of the variation in fluorescence produced by a variation in ANS concentration: □——□ ANS alone; ○——○ ANS + valinomycin; ●——● ANS + valinomycin + ATP

ouble reciprocal form, from which it can be calculated that at infinite rotein concentration, since all the ANS can be assumed to be bound, NS or ANS + valinomycin show the same maximal fluorescence (50 FU) ut the addition of ATP increased the maximal fluorescence for the me quantity of ANS to 125 FU, i.e., increased the quantum yield r ANS by a factor of 2.5 (Brocklehurst, Freedman, Hancock & Radda, 970).

Effect of ANS Concentration

The effect of varying the ANS concentration on the total fluorescence tained with the membranes alone, the membranes with valinomycin d with, in addition, ATP is shown in double reciprocal form in Fig. 8.

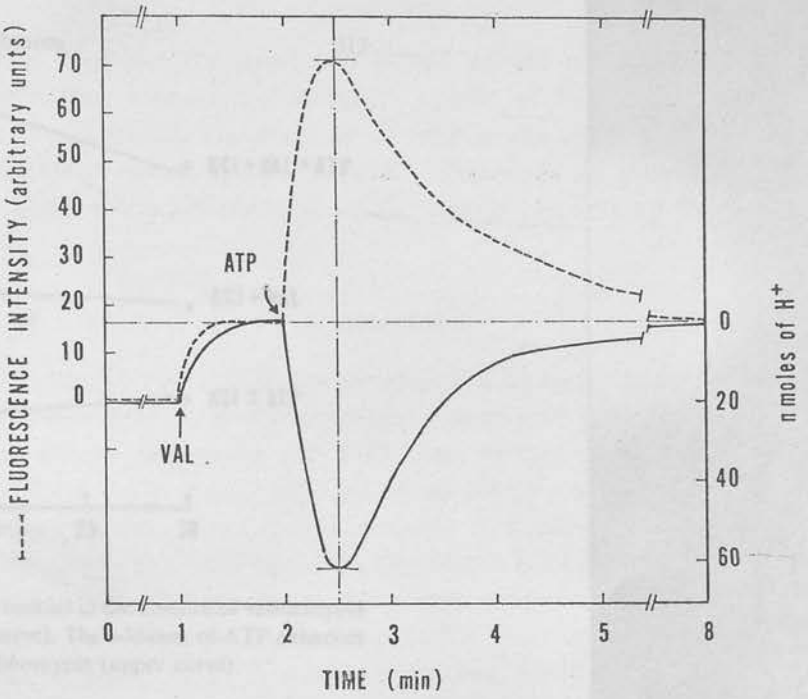

Fig. 9. The time course of development of the ANS response to ATP addition (dotted line) and the medium alkalinization developed in response to an identical ATP concentration (solid line) in the same preparation under otherwise identical conditions. The bar on the right corresponds to 10 nmoles of H^+

The raw data suggest that there is little effect of valinomycin on the affinity of the sites as compared to ANS alone, but there is an apparent increase in the number of sites. ATP apparently augments the number and affinity of these sites.

It has been suggested, based on nanosecond decay studies, that saturation of membrane "sites" by ANS is only apparent, and that the saturation observed is due to electrostatic shielding preventing ANS access (Fortes, 1976). If correct, and also for the gastric vesicles, calculation of the number and affinity of the ANS "sites" based on the above data will underestimate the true values. However, one may assume that there are two types of sites—one type, superficial, binding ANS rapidly and the other type binding ANS slowly to which access is increased by valinomycin. Considering these as independent and noninteracting, it is possible to consider the fluorescence of each site independently by subtracting the basal ANS fluorescence from the valinomycin-induced fluorescence. If this is done, it can be concluded that the number of

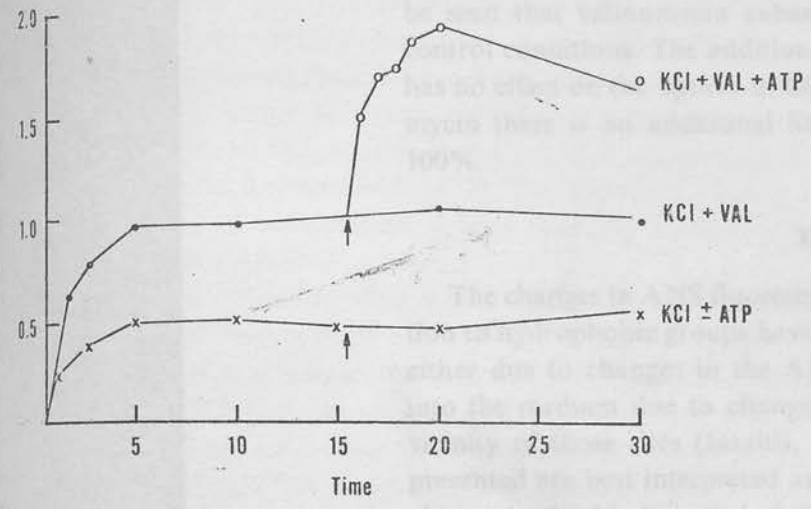

10. The time course of SCN^- uptake by the gastric vesicles in the absence of valinomycin er curve) and the presence of valinomycin (upper curve). The addition of ATP enhances SCN^- uptake only in the presence of valinomycin (upper curve)

rficial sites is the same as the number of sites dependent on lipid neable cation, such as K^+ valinomycin. The superficial sites have apparent affinity of 7.5×10^{-6} M and the "slow" sites an affinity $.5 \times 10^{-6}$ M.

Further, since the ATP effect is to increase the quantum yield of ANS bound, and if the assumption is also made that ATP has no ct on the superficial sites, it is possible to calculate corrected values the ATP-induced fluorescence. Such a plot is curvilinear (concave ards) on the double reciprocal plot at high ANS concentrations, ch may be due to ANS inhibition of the ATPase ($K_I = 75$ μM) or use ATP also affects the superficial sites. As a first approximation, ever, this manipulation of the data suggests that ATP does not ct the number or affinity of the valinomycin-dependent sites but ly increases the quantum yield of the ANS bound at those sites.

Relation to H^+ Gradient

Where the uptake of H^+ was measured under identical conditions he same preparation on the same day, and compared to the fluores- e change induced by ATP, the curves of Fig. 9 were obtained. It be seen that the time course is very similar and that the decline uorescence corresponded to the decline of the H^+ gradient.

SCN^- Uptake

Fig. 10 shows the uptake of SCN^- by the gastric vesicles. It can be seen that valinomycin enhances uptake of SCN^- as compared to control conditions. The addition of ATP in the absence of valinomycin has no effect on the uptake of SCN^-, whereas in the presence of valinomycin there is an additional SCN^- uptake, increasing the uptake by 100%.

Discussion

The changes in ANS fluorescence following the primary binding reaction to hydrophobic groups have been interpreted generally in two ways, either due to changes in the ANS sites, or due to movement of ANS into the medium due to changes of an electrochemical gradient in the vicinity of those sites (Jasaitis, Kuliene & Skulachev, 1971). The data presented are best interpreted as due to the former, namely a character change in the binding site of the gastric membranes, an interpretation which is now more generally accepted for other systems as well.

As in other work (Friedman & Radda, 1969) there are two phases of ANS binding, most likely due to two classes of sites. The rapid binding sites are likely to be on the external face of the membrane, whereas the slower sites are either within the membrane, or located on the inner face of the membrane. At varying concentrations of ANS after prolonged incubation, the binding achieved was almost the same as that in the presence of valinomycin, and the effect of the ionophore was apparently to increase the rate of ANS binding. Calculation also showed that the affinity of the valinomycin-dependent sites was greater than the affinity of the initial ANS sites and that the affinity of the "slow" sites was similar to the valinomycin "sites". At high protein concentrations there was also an overshoot of fluorescence with the addition of valinomycin, which may be a function of the K^+ gradient present upon adding the vesicles.

On the other hand, the quantum yield was not changed by the addition of valinomycin, hence it may be concluded that the action of valinomycin-K^+ complex is to allow a more rapid access of ANS to restricted, higher affinity sites located within the membrane or within the vesicle.

The effect of valinomycin may be due to several factors. The presence of a lipophilic cation, the valinomycin-K^+ complex, may facilitate the transport of the anionic ANS. Clearly, neither gramicidin nor nigericin could then substitute and this explanation is substantiated by the finding

t $TPMP^+$ can mimic the effect of valinomycin when added to the xture of ANS and membranes. Moreover, a mixture of ANS and alone results in enhanced fluorescence when valinomycin is added, hough quantitatively much less than the effect in the presence of mbranes, and this shows the possible formation of a valinomycin-K^+ S complex (Feinstein & Felsenfeld, 1971). The increased binding of N^- in the presence of valinomycin is then formally similar to the ct of valinomycin on ANS.

An important point which has often been considered is the movement ANS due to the development of a membrane potential. Under the ndard conditions of our assay, the prevailing K^+ gradient would lt in a potential such that the vesicle interior was positive with the portant reservation that a K^+-selective conductance has to be present. Since protonophores do not dissipate a preformed pH gradient nor uce a pH gradient in the presence of K^+ gradients it is reasonable conclude that a cation-selective conductance is not present in the reated gastric membranes. However, even in the presence of valinomy- varying the direction of the K^+ gradient does not affect the valinomy- component of the fluorescence; hence this component is not depen- t on potential. At 27 °C, in the presence of valinomycin, the initial ard K^+ gradient would dissipate rapidly ($t_{1/2}=2.5$ min) so that at time of ATP addition only a small residual gradient would be present. have shown (Sachs *et al.*, 1976) that addition of ATP under these ditions (i.e., cationic equilibrium) generates a gradient (medium to cle) of cations such as K^+ or Rb^+.

The cationic enhancement of ANS fluorescence has been described nany authors in other systems (Rubalcava, deMunoz & Gitler, 1969) has been interpreted as being due to charge redistribution within mbranes or hydrophobic regions. The effect is not restricted to the li metal cations, Ca^{2+} being more effective than K^+, for example balcava *et al.*, 1969). With the gastric membranes cation alone is sufficient, but a lipophilic cation is required due to, perhaps, the icted permeability of these particles. The fluorescent enhancement ed by valinomycin is a function of the K^+ concentrations (as shown ig. 3 with an apparent K_A of 50 mM) but not of the K^+ gradient. lthough, as discussed above, the stimulation of ANS fluorescence alinomycin appears independent of the potential gradient, this is he case with the ATP effect. Indeed both a potential gradient and ncreased vesicular H^+ concentration appear to be required.

he rate of change of fluorescence with the addition of ATP is a

function of the log $[K^+]$, as would be expected of a Nernst diffusion potential due to the K^+ electrode characteristics of the valinomycin-treated vesicle and the appearance of a K^+ gradient due to ATP. Using radioactive SCN^-, the only evidence for development of a potential was obtained in the presence of both valinomycin and ATP. Studies of cation efflux (Sachs *et al.*, 1976) have shown that a cation gradient develops in these vesicles with ATP addition. Studies of dissipation of a preformed H^+ gradient have shown that these vesicles have a low K^+ conductance in the absence of valinomycin (Sachs *et al.*, 1976). It is reasonable, therefore, to consider that only in the presence of valinomycin would a potential develop across the vesicle membrane due to the ATP-induced K^+ gradient.

Since the fluorescence enhancement due to valinomycin alone does not seem to be sensitive to a potential an additional factor is required. The H^+ gradient generated by ATP would seem the most likely candidate. It can be calculated that a pH of less than 2 may be achieved inside the vesicle with the addition of ATP (Sachs *et al.*, 1976). Nigericin would dissipate a H^+ gradient without necessarily affecting the K^+ diffusion potential (Markin, Sokolov, Boguslavsky & Taguzhinsky, 1975) and nigericin inhibits the ATP effect. The fluorescence of ANS is increased by addition of H^+ to the vesicle in the presence of valinomycin.

Hence, it is proposed that the valinomycin and ATP-dependent ANS fluorescence enhancement is due to the establishment under these conditions of a simultaneous H^+ and potential gradient. Both of these are required for the fluorescent shift, and this results in an alteration in the ANS site giving an enhanced quantum yield which accounts for most of the fluorescence increase.

A similar change in ANS fluorescence is observed in mitochondria and submitochondrial particles (Azzi, Gherardini & Santato, 1971) which also appears to depend on at least the development of a change in potential across the membrane. On the other hand, a change in ANS fluorescence is also obtained with the addition of ATP to sarcoplasmic reticulum vesicles in the presence of Ca^{2+} (Vanderkooi & Martonosi, 1971). The anionic shunt conductance of these membranes is such that a development of a potential is unlikely. Hence, this latter phenomenon has been explained as due to increased binding of ANS by the internally accumulated Ca^{2+}.

The increase of quantum yield of ANS would imply a shift of binding to a more hydrophobic region. This could be due to a change in conformation dependent on the proton concentration at the inner surface as well as on the membrane potential.

This work was supported by NSF GB 31075, NIH ATPase AM 15878, NIH CA 977 and a grant in aid from Smith, Kline and French Laboratories.

References

zi, A., Chance, B., Radda, G.K., Lee, C.P. 1969*a*. A fluorescence probe of energy dependent structure changes in fragmented membranes. *Proc. Nat. Acad. Sci. USA* **62**:612

zi, A., Gherardini, P., Santato, P. 1971. Fluorochrome interaction with the mitochondrial membrane; the effect of energy conservation. *J. Biol. Chem.* **246**:2035

zi, A., Fleischer, S., Chance, B. 1969*b*. Cytochrome *c* phospholipid interaction: Structural transitions associated with valency changes. *Biochem. Biophys. Res. Commun.* **36**:322

ker, E.P., Van Dam, K. 1974. The influence of diffusion potentials across liposomal membranes on the fluorescence intensity of 1-anilino-naphthalene-8-sulphonate. *Biochim. Biophys. Acta* **339**:157

cklehurst, J.R., Freedman, R.B., Hancock, D.J., Radda, G.K. 1970. Membrane studies with polarity-dependent and excimer-forming fluorescent probes. *Biochem. J.* **116**:721

ance, B. 1970. Fluorescent probe environment and the structural and charge changes in energy coupling of mitochondrial membranes. *Proc. Nat. Acad. Sci. USA* **67**:560

ance. B., Lee, C. 1969. Comparison of fluorescence probe and light-scattering readout of structural states of mitochondrial membrane fragments. *FEBS Lett.* **4**:181

nstein, M.B., Felsenfeld, H. 1971. The detection of ionophorous antibiotic-cation complexes in water with fluorescent probes. *Proc. Nat. Acad. Sci. USA* **68**:2037

te, J.G., Ganser, A., Beesley, R., Forte, T.M. 1975. Unique enzymes of purified microsomes from pig fundic mucosa; K^+-stimulated adenosine triphosphate and K^+-stimulated pNPPase. *Gastroenterology* **69**:175

te, J.G., Ganser, A.L., Tanisawa, A.S. 1974. The K^+-stimulated ATPase system of microsomal membranes from gastric oxyntic cells. *Ann. N.Y. Acad. Sci.* **242**:255

es, P.A.G. 1976. Nanosecond fluorescence spectroscopy of biological membranes. *In:* Mitochondria: Bioenergetics, Biogenesis and Membrane Structure. Packer and Gomez-Puyou, editors. Academic Press, N.Y. pp. 327–348

dman, R.B., Radda, G.K. 1969. The interaction of 1-anilino-8-naphthalene sulfonate with erythrocyte membranes. *FEBS Lett.* **3**:150

ser, A.L., Forte, J.G. 1973*a*. K^+ stimulated ATPase in purified microsomes of bullfrog oxyntic cells. *Biochim. Biophys. Acta* **307**:169

ser, A.L., Forte, J.G. 1973*b*. Ionophoretic stimulation of K^+-ATPase of oxyntic cell microsomes. *Biochem. Biophys. Res. Commun.* **54**:690

itis, A.A., Kuliene, V.V., Skulachev, V.P. 1971. Anilinonaphthalenesulfonate fluorescence changes induced by non-enzymatic generation of membrane potential in mitochondria and submitochondrial particles. *Biochim. Biophys. Acta* **234**:177

J., Simpson, G., Scholes, P. 1974. An ATPase from dog gastric mucosa: Changes of outer pH in suspensions of membrane vesicles accompanying ATP hydrolysis. *Biochem. Biophys. Res. Commun.* **60**:825

kin, V.S., Sokolov, V.S., Boguslavsky, L.I., Jaguzhinsky, L.S. 1975. Nigericin-induced charge transfer across membranes. *J. Membrane Biol.* **25**:23

otti, L.F., Long, M.M., Sachs, G., Urry, D.W. 1972. The effect of ATP on the CD spectrum of membrane fraction from oxyntic cells. *Biochim. Biophys. Acta* **255**:420

ulcava, B., deMunoz, D.M., Gitler, C. 1969. Interaction of fluorescent probes with membranes. I. Effect of ions on erythrocyte membranes. *Biochemistry* **8**:2742

omani, G., Stewart, H.B., Shaw, D., Lewin, M., Sachs, G. 1977. Fractionation and purification of K^+ ATPase containing vesicles by zonal centrifugation and free flow electrophoresis technique. *Biochim. Biophys. Acta* (*In press*)

Saccomani, G., Shah, G., Spenney, J.G., Sachs, G. 1975. Characterization of gastric mucosal membranes. VIII. The localisation of peptides by iodination and phosphorylation. *J. Biol. Chem.* **250**:4802

Sachs, G., Rabon, E., Chang, H., Schackmann, R., Lewin, M., Saccomani, G. 1976. A nonelectrogenic H^+ pump in plasma membranes of hog stomach. *J. Biol. Chem.* **251**:7690

Sachs, G., Saccomani, G., Rabon, E., Sarau, H.M. 1975. Redox and ATP in acid secretion. *Ann. N.Y. Acad. Sci.* **264**:456

Spenney, J.G., Saccomani, G., Spitzer, H.L., Tomana, M., Sachs, G. 1974*a*. Characterization of gastric mucosal membranes; composition of gastric cell membranes and polypeptide fractionation using ionic and nonionic detergents. *Arch. Biochem. Biophys.* **161**:456

Spenney, J.G., Strych, A., Price, A.H., Helander, H.F., Sachs, G. 1974*b*. Preparation of gastric cell membranes by zonal density gradient centrifugation. *Method. Dev. Biochem.* **4**:309

Stryer, L. 1965. The interaction of a naphthalene dye with apomyoglobin and apohemoglobin; a fluorescent probe of non-polar binding sites. *J. Molec. Biol.* **13**:482

Tanisawa, A.S., Forte, J.G. 1971. Phosphorylated-intermediate of microsomal ATPase from rabbit gastric mucosa. *Arch. Biochem. Biophys.* **147**:165

Vanderkooi, J.M., Martonosi, A. 1971. Sarcoplasmic reticulum. XII. The interaction of 8-anilino-1-naphthalene sulfonate with skeletal muscle microsomes. *Arch. Biochem. Biophys.* **144**:87

J. Membrane Biol. 35, 285–301 (1977)

Reconstitution of a Proton Pump from Gastric Mucosa

M. C. Goodall and G. Sachs*

Laboratory of Membrane Biology, University of Alabama in Birmingham, Birmingham, Alabama 35294

Received 19 July 1976

Summary. Purified vesicular fractions from hog gastric mucosa have been incorporated into phosphatidyl serine bilayers. In the presence of MgATP on one side and symmetrical Na_2SO_4 solutions, a short circuit current (SCC) away from that side is observed increasing exponentially with time, while the corresponding open circuit potential (OCP) is maintained constant for > 30 min. In K_2SO_4 solutions the SCC time course is essentially unchanged, but the OCP falls to almost zero after 15–20 min. In Na – K gradient there is a similar SCC away from the K-side whose exponential rate is increased by ATP added to both sides. The time course of these events depends only on the time from the formation of the black film. These results are interpreted as showing: (1) There is an ATP-driven proton pump generating a constant potential E_H in series with a time dependent conductance $g_H \propto e^{kt}$. (2) There is a shunting K-conductance $g_K \propto e^{k't}$. (3) In the presence of ATP $k' > k$. (4) This time dependence is due to thickness changes in the bilayer. A model relates these results to those obtained with the intact vesicles.

The microsomal or plasma membrane fraction of dog or hog gastric mucosal homogenates take up H^+ into an intravesicular space with the addition of ATP (Lee, Simpson & Scholes, 1974; Sachs *et al.*, 1976*a*, *b*). Redox substrates are neither oxidized by the purified membrane fraction nor show any observable effects on ion distributions (Sachs *et al.*, 1976*b*). The uptake of H^+ and simultaneous efflux of K^+ (Sachs *et al.*, 1976*a*) seems to be a property of the K^+-ATPase (Ganser & Forte, 1973) which is 40-fold enriched in the purified membranes. Much of the evidence relating to this H^+/cation exchange suggests that the pump mechanism is neutral or, if electrogenic, then isopotential (Lee *et al.*, 1974; Sachs *et al.*, 1976*a*, *b*). Although techniques are available for potential measurements in vesicles and for short circuiting vesicles using a combination of ionophores or lipid permeable ions (Skulachev, 1976), measurements of conductance in vesicles is considerably more difficult. Data using ionophores to dissipate H^+ gradients or to alter rates of H^+ uptake or K^+

* To whom correspondence should be addressed.

efflux suggested that proton conductance was predominant in these membranes and that the inherent K^+ or Cl^- conductance was low. Cation exchange efflux studies provided evidence for a cation-selective path corresponding to sequence *V* (Eisenman, 1961) in the nonenergized membrane. A similar selectivity was obtained for H^+ uptake dependent on ATP and for ATPase activity and these data suggest the possibility of a cation conductance pathway, although from the above, of low magnitude. The low conductance of artificial bilayers may allow a more exact analysis of these properties.

This work reports on the conductance properties of planar bilayers following incorporation of the gastric vesicles and on the electrical events associated with ATP-induced transport in the artificial system.

Materials and Methods

Hog gastric membrane vesicles were prepared as described in detail elsewhere (Saccomani *et al.*, 1976). Briefly, this involved separation of the vesicular fraction of the gastric homogenate on a ficoll-sucrose density gradient (Fig. 1) and the lighter of the 2 membrane peaks was used in these studies. The anodic peak from free flow electrophoretic fractionation of this peak (Fig. 2) contains the highest activity of the K^+-ATPase (Saccomani *et al.*, 1976) and was used on occasion (Table 1). The fractions were used either on the day of preparation or following freezing and storage at −84 °C. The suspension was added to one side of the bilayer chamber at a final concentration of approximately 10–25 μg protein ml^{-1} after formation of the bilayer, with an activity of 60–90 μmole Pi mg^{-1} protein hr^{-1}.

The electrical properties of the bilayer were measured as described previously (Goodall, 1973). Open circuit potential difference or short circuit current were recorded under conditions of constant stirring from the time of film formation. Thus there is a 1/2 to 2-min period before the appearance of the black bilayer region and this is completed within 1–3 min. In view of the thickness dependence of the phenomena to be described, the time course in all records is measured from the initial formation. The outside chamber was connected to ground through the current amplifier and is referred to as "trans" with the sign conventions corresponding. The acceptable limit for bilayer background conductance was $2\text{–}3 \times 10^{-9}\ \Omega^{-1}\ cm^{-2}$. Thinning of the bilayer was monitored visually to the black stage (1–3 min) and thereafter by the current voltage ($I-V$) curve plotted on an $X-Y$ recorder (Esterline Angus 2411 TB) using a triangular wave form from a battery operated function generator (Krohn-Hite 5600). This showed a continuous and approximately linear increase of capacity to 50% at 20 min.

Bionic potentials were measured with 100 mM SO_4^{--} salts of alkali metal cation pairs present on either side of the bilayer. For thallous ion 10 mM concentrations were used because of solubility limitations. Solutions were buffered with 2 mM tris acetate pH 7.4. For cation/anion selectivity a 10:1 concentration gradient of the Na salt was used.

For studies of ATP-dependent transport 10 mM Na_2SO_4 buffered with 2 mM tris acetate pH 7.4 was present on both sides of the bilayer and MgATP or other nucleotide buffered to the same pH was added at a final concentration of 0.75 mM to the "cis" side, i.e., the side containing the vesicles. Inhibitors such as *p*-chloromer curibenzoate (*p*CMBS) (10^{-4} M) were also added to this side. 50 mM K_2SO_4 was added to both

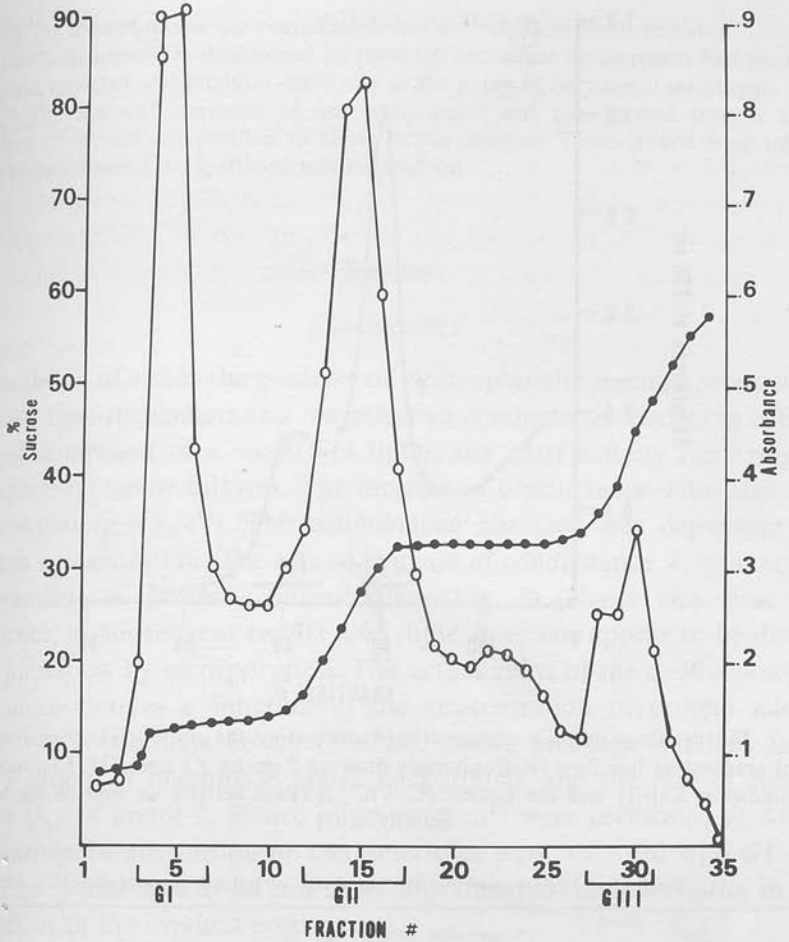

Fig. 1. The profile of protein obtained by fractionating the microsomal pellet of hog gastric mucosal homogenate on a step gradient in a Z60 zonal rotor. *G*1 corresponds to a step between 0.25 M sucrose and 7 % ficoll in 0.25 M sucrose, *G*11 is a step between 7 % ficoll in 0.25 M sucrose and 31 % sucrose and *G*111 between 31 and 60 % sucrose

solutions as necessary in the presence of ATP. The temperature of study was 34 °C and the lipid used was bovine phosphatidyl serine (chromatographically pure, Applied Science Labs) at 3–5 mg/ml in decane (Eastman Kodak).

Apart from the difficulty of incorporation, a major problem has been the sensitivity of the low conductance bilayer to artifacts of various types. The following pragmatic criteria of successful incorporation were used in this study:

(1) A low conductance membrane with only H^+ permeability and virtually no permeability to anions or cations was used throughout.

(2) With incorporation the increment in conductance was smooth or otherwise well characterized rather than the irregular noise which often occurs with contaminated bilayers prior to breakage.

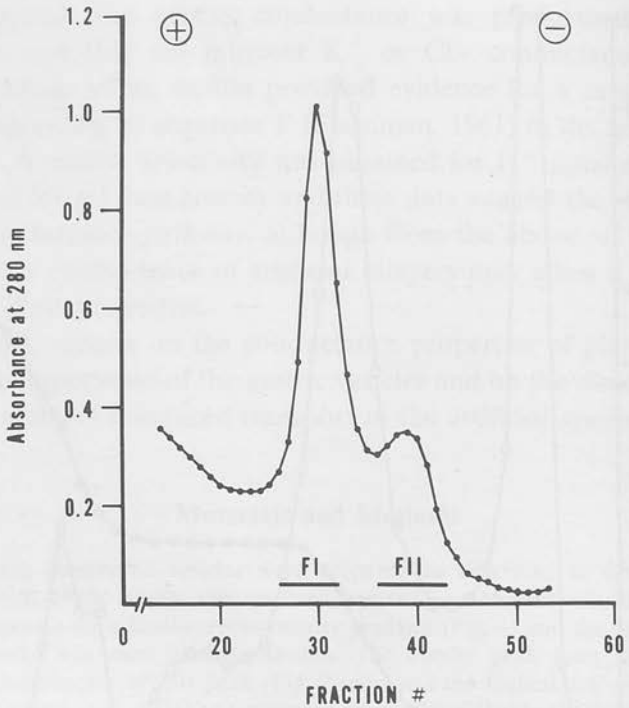

Fig. 2. The profile of protein obtained by fractionating the initial ($G1$) peak from the zonal gradient by free flow electrophoresis showing 2 peaks, $F1$ and $F11$, $F1$ containing the transport activity and the highest $H^+ + K^+$ ATPase activity as well as the bilayer activity of $G1$

Table 1. AMPase and ATPase activity of gastric membranes

	μmoles Pi mg^{-1} hr^{-1}		
	ATPase		AMPase
	Mg^{++}	K^+	
Total homogenate	6.2±0.6	2.0±1.0	0.5±0.3
Microsomal pellet	15.9±1.5	7.1±4.3	1.5±0.6
GI Fraction	6.8±1.1	35.8±2.2	8.8±0.2
FI Fraction	2.7±0.6	66.8±1.4	0.8±0.2

(3) The bilayer was generally stable for at least 30 min after or during incorporation.

(4) The increment in conductance was at least two or more orders of magnitude and was dependent on the concentration of material added.

(5) The denaturation of the protein resulted in an inactive preparation.

(6) The conductance modification corresponded in selectivity to the conductance selectivity of the natural membrane.

(7) The incorporation was reproducible qualitatively from batch to batch.
(8) Pump activity as determined by potential or current development had the same substrate, activator and inhibitor selectivity as the pump in the natural membrane.
(9) The material consisted of few components and was derived from a single structure of defined composition to allow further analysis. These criteria were met by fresh preparations of the gastric membrane fraction.

Results

Conductance

Addition of either the gradient or electrophoretic fraction produced a smooth, time-dependent and ion-selective conductance change in a lipid bilayer composed of a variety of lipids, the most activity occurring in phosphatidyl serine bilayers. The increase of conductance with time was exponential ($g_t = g_0\, e^{kt}$). The conductance obtained was dependent on protein concentration. The rate of increase of conductance, k, was largely independent of protein concentration (Fig. 3). Hence this time dependence, as subsequent results also show, does not appear to be due to rate limitation by incorporation. The actual value of the conductance at any given time is a function of the concentration of protein added, typically the conductance level reached before breakage was between 2 and 3 orders of magnitude above background, and the rate of change had a Q_{10} of about 2. Hence all experiments were performed at 34 °C. The incorporation and pump characteristics were obtained with *G*1 and *F*1 (Figs. 1 and 2). *F*2 did not show any transport characteristics in the bilayer or in the original preparation.

The selectivity sequence of the specific conductances (Table 2) was determined to be $H^+ > K^+ > Rb^+ > Cs^+ > Na$, $Li > Tl^+ > Cl^-$. This sequence corresponds to that found for H^+ uptake and for K^+-ATPase activity with the exception of Tl^+ which is the most active cation for the latter process. The relative intracationic activity for the different vesicular transport (i.e., H^+, K^+ and ANS) processes and bilayer conductance is also consistent with the supposition that the same groups are involved in the natural and artificial membrane.

Transport

Results using the intact vesicles (Sachs *et al.*, 1976*a*) indicated the possibility that the addition of ATP resulted in a K^+:H^+ exchange by the vesicle fraction. Of the different alkali cations tested Na^+ was only

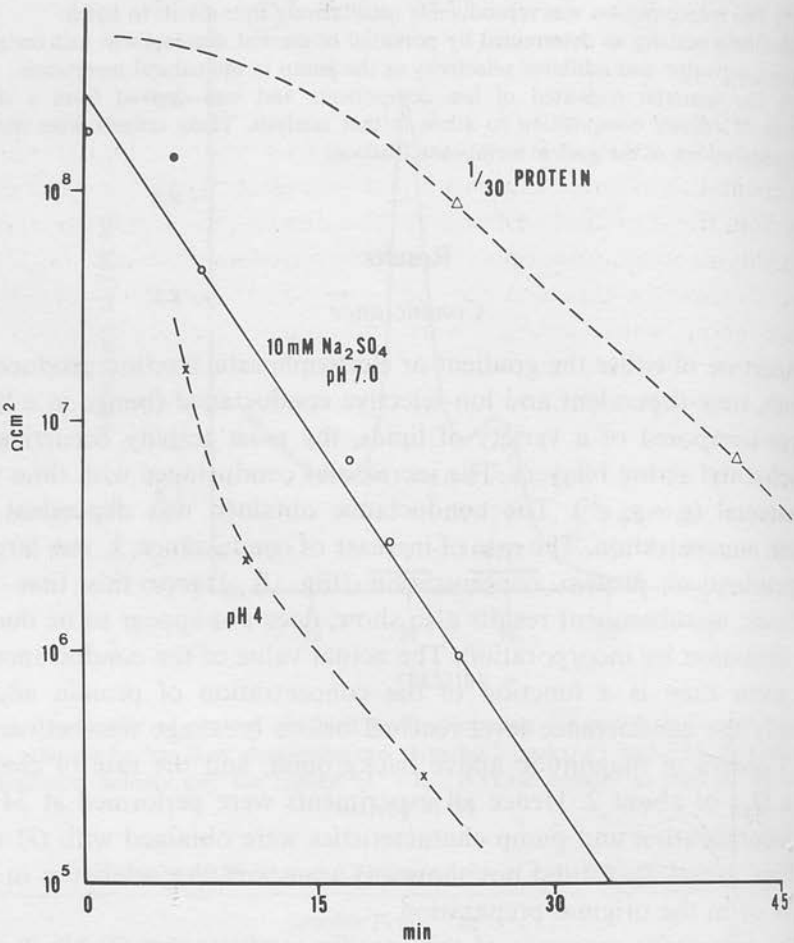

Fig. 3. The effect of addition of *G*1 fraction on the development of conductance in the bilayer. In the absence of addition no change in conductance was observed. At pH 7, in the presence of 10 mM Na_2SO_4 an exponential increase in conductance with time was observed ○——○. Altering the protein concentration △------△ altered the conductance level but had a much lesser effect on the time course of the conductance change. Lowering the pH ×------× increased the conductance but again had a relatively slight effect on the time course

Table 2

	H	NH_4	K	Rb	Cs	Na	Li	Tl	Cl
Specific conductance (relative)	10^6	24	10	8	6	1	1	0.75	0.35
ATPase	–	14	14	11	2.3	1	0.56	>19	–

1% as effective as K^+ in the vesicles, hence Na_2SO_4 solutions were used for the bilayer experiments in the ATP studies to possibly unmask an electrogenic H^+ pump.

The addition of 0.25 mM ATP to the cis side of the phosphatidyl serine bilayer resulted in the development of a negative potential (Fig. 4). This orientation is compatible with a proton electrogenic pump directed away from the ATP and vesicle side. The dissipation of the potential by the addition of a protonophore such as tetrachlorsalicylanilide (TCS) would therefore be expected but the conductance increment induced by the ionophore would serve to shunt the potential whether due to H^+ transport or not. The magnitude of the potential was a function of the nature of the lipid. The mean potential obtained with phosphatidyl serine was 33.4 ± 4.7 mV ($n = 17$). The effect of ATP may be due to two factors, the effect of ATP on the pump and the effect of adsorption of ATP on the bilayer surface. $\beta-\gamma$ methylene ATP and ITP also adsorb on the bilayer and produce a transient potential corresponding to 20% of the ATP-dependent potential. The addition of ATP in addition to $\beta-\gamma$

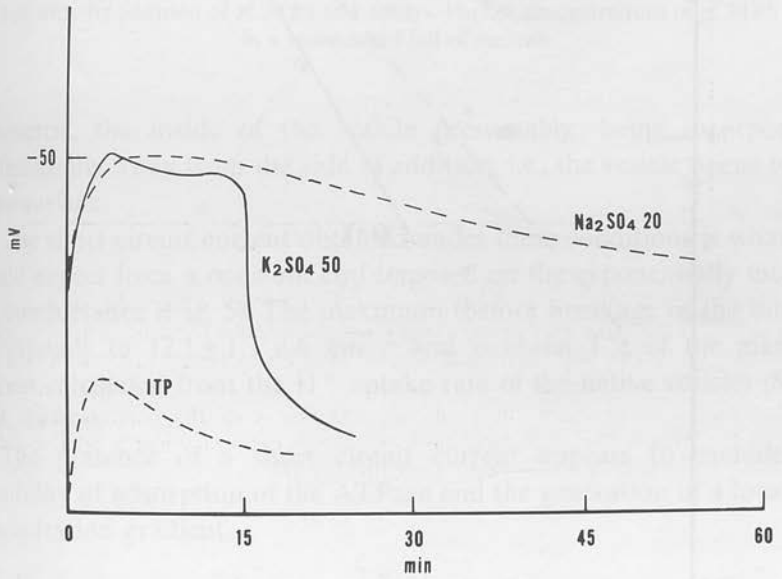

Fig. 4. The effect of ATP addition (upper 3 curves) and ITP addition (lower curve) on one side of the bilayer with incorporated *G*1. The addition of ATP at 0 time resulted in development of a potential of -50 mV which was well maintained in the presence of Na_2SO_4 (------). ITP produced only a fraction of the potential. The results of addition of 50 mM K_2SO_4 to both sides of the bilayer showed that ATP produced essentially the same potential, but after 15 min there was a sharp decline in the potential to about 10% of the peak value (——)

methylene ATP produces a normal ATP response. An inhibitor of the ATPase, *p*CMBS markedly reduces the potential obtained to about 20% of the initial value, but does not reduce the prevailing conductance (Fig. 6). Addition of ATP to the trans side produces a potential of opposite orientation, though of lesser magnitude (*see* Fig. 8 below), showing that although the orientation of the current flow is determined by the sidedness of ATP the incorporation of the protein is not completely

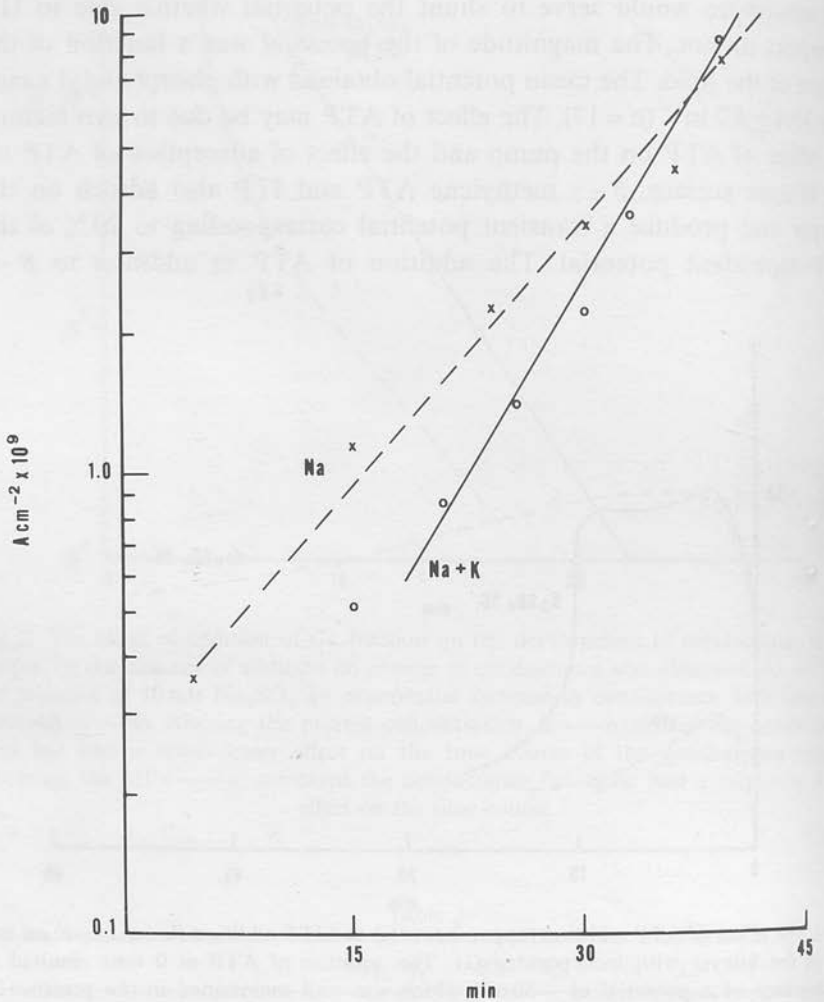

Fig. 5. The increase of short circuit current with time in the presence of Na (×------×) or $Na^+ + K^+$ (○——○). Zero time is the appearance of the initial black region. It should be noted that the presence of K^+ allows a similar exponential current increase which argues against an E_K^+ being present

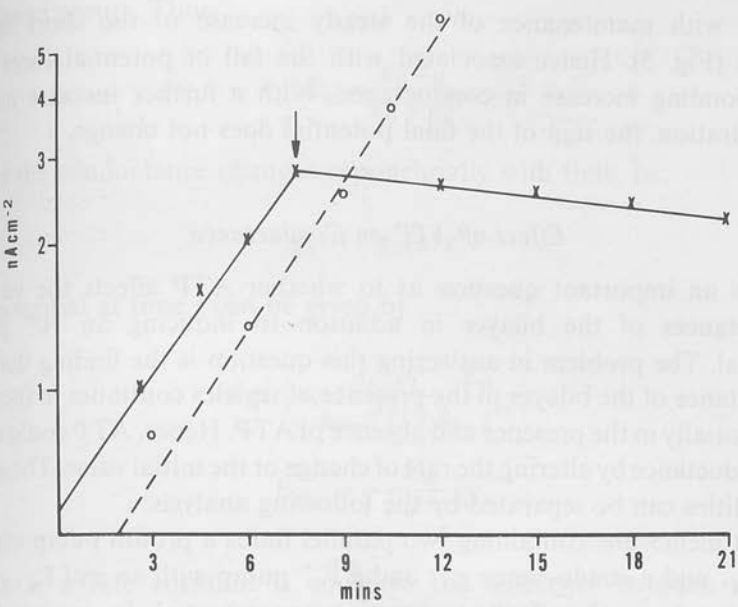

Fig. 6. The effect of 4×10^{-4} M *p*CMBS on short circuit current. The current in the absence of *p*CMBS is shown on the dashed line (o------o). The increase of current is blocked with the addition of *p*CMBS and decays. Higher concentrations of *p*CMBS result in a more rapid fall of current

symmetric, the inside of the vesicle presumably being incorporated preferentially away from the side of addition, i.e., the vesicle opens to the trans surface.

The short circuit current obtained under these conditions is what one would expect from a constant emf imposed on the exponentially increasing conductance (Fig. 5). The maximum (before breakage of the bilayer) corresponds to 12.1 ± 1.7 nA cm^{-2} and is about 1% of the maximal current calculated from the H^+ uptake rate of the native vesicles (Sachs *et al.*, 1976*a*).

The presence of a short circuit current appears to exclude the possibility of adsorption of the ATPase and the generation of a local H^+ concentration gradient.

Effect of K^+

The presence of K^+ symmetrically in both solutions characteristically alters the ATP response. Thus initially with the addition of ATP a potential is obtained similar in magnitude to that observed with Na^+. After some 15 min there is a fall in the potential to 7 ± 3 mV ($n = 10$) (Fig.

4), but with maintenance of the steady increase of the short circuit current (Fig. 5). Hence associated with the fall of potential there is a corresponding increase in conductance. With a further increase in K^+ concentration, the sign of the final potential does not change.

Effect of ATP on Conductance

It is an important question as to whether ATP affects the various conductances of the bilayer in addition to inducing an H^+ pump potential. The problem in answering this question is the finding that the conductance of the bilayer in the presence of vesicles continues to increase exponentially in the presence and absence of ATP. Hence, ATP could effect the conductance by altering the rate of change or the initial value. These two possibilities can be separated by the following analysis.

In a membrane containing two parallel limbs a proton pump with an emf, E_{H^+} and a conductance g_{H^+} and a K^+ pump with an emf E_{K^+} and a conductance g_{K^+} (Fig. 7) the transmembrane potential, E_M is given by

$$E_M = \frac{g_H E_H - g_K E_K}{g_H + g_K}. \tag{1}$$

This equation can be simplified based on the observation that varying the K^+ concentration does not change the final potential and that the short circuit current which would be given by the equation

$$I_{sc} = I_H - I_K$$

does not fall as would be predicted by the presence of an I_K. From these it would appear that E_K is very small, or that $\Delta I_H = \Delta I_K$, i.e., a neutral

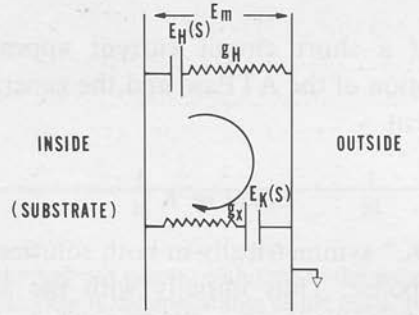

Fig. 7. An equivalent circuit illustrating a possible model for the pump which consists of 2 parallel patterns for K^+ and H^+ with their corresponding emfs and resistances

exchange occurs. Thus

$$E_M = \frac{g_H E_H}{g_H + g_K}. \tag{2}$$

Since the conductance changes exponentially with time, i.e.,

$$g_X(t) = g_X(o)\, e^{kt} \tag{3}$$

the potential at time t can be given by

$$E_M(t) = \frac{g_{H_0}\, e^{k_H t} \cdot E_H}{g_{H_0}\, e^{k_H t} + g_{K_0}\, e^{k_K t}}; \tag{4}$$

$$E_{M_{(t)}} = \frac{E_H}{1 + e^{k(t - t_0)}}, \tag{5}$$

where k, a rate constant is equal to the difference between the rate constants for the change in K^+ and H^+ conductances namely

$$k = k_K - k_H$$

and

$$kt_0 = -\ln g_{K_0}/g_{H_0}$$

where g_{K_0}, g_{H_0} are the initial conductances.

Fitting Eq. (5) to the data for open circuit potential in the presence of ATP we find $k = 0.002$ sec^{-1} and $g_{H_0}/g_{K_0} = 6.5$. Assuming a constant E_H with the appearance of a K^+ conductance, $k_H = 0.004$ sec^{-1} and thus $k_K = 0.006$ sec^{-1}. These data are obtained in the presence of ATP.

It is also possible to derive the rate constant for change of K^+ conductance from other experiments. Addition of ATP to symmetric solutions and on both sides of the bilayer results in only a small change of potential, i.e., there is only a small H^+ emf. Assuming that the H^+ emf can be neglected when ATP is added to both sides of a membrane in the presence of a $K^+ - Na^+$ trans-cis gradient, then current flow under these conditions is due to K^+ movement from trans to cis. The exponential rise of current without ATP gave $k_K = 0.0044$ sec^{-1} increasing to $k_K = 0.010$ sec^{-1} on the addition of ATP (Fig. 8) in fair agreement with the above value.

In the absence of ATP $k_K = 0.002$ sec^{-1} and $g_{H_0}/g_{K_0} \sim 10$ (pH 7.4, 50 mequiv K^+). Thus ATP increases the rate constant for changes of K^+ conductance but has little effect on the value of either K_H or g_{H_0}.

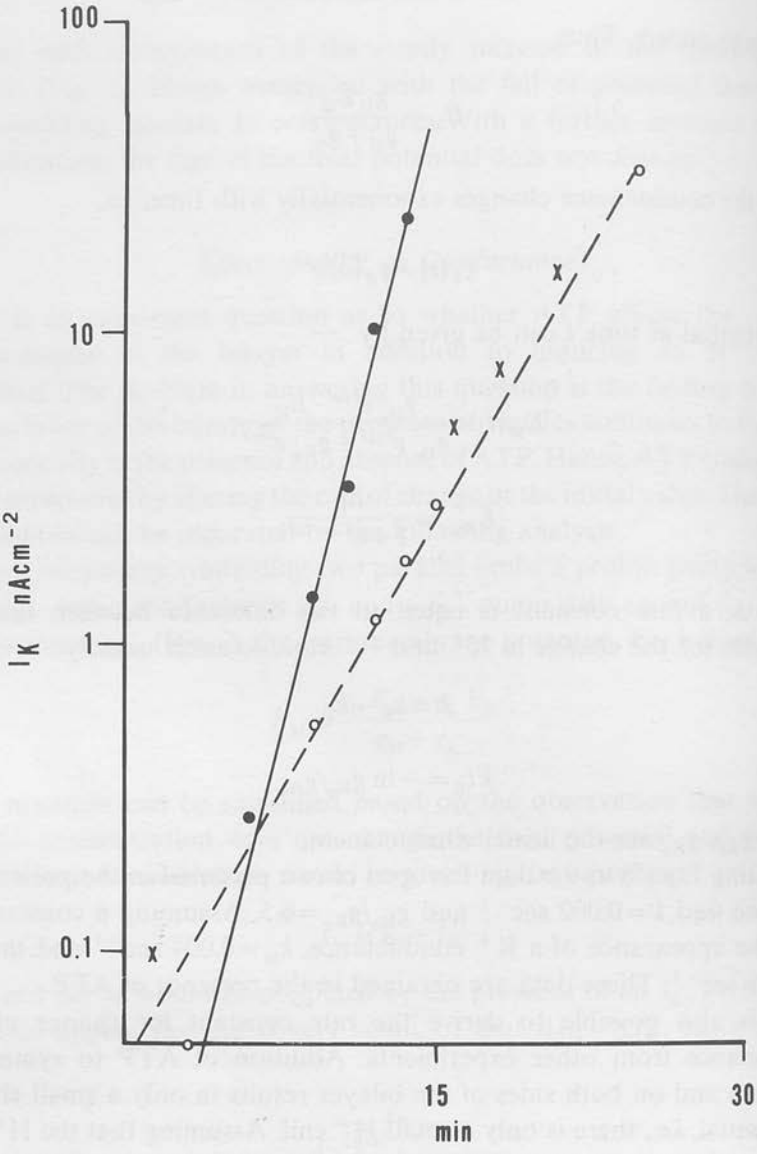

Fig. 8. The rate of change of K^+ current (due to a K^+/Na^+ gradient across the bilayer) as a function of the addition of ATP. This figure compares the K^+ current (inward) in the absence of ATP (o------o) to the current in the presence of ATP on both sides (●——●). It can be seen that ATP increases the magnitude of the current, and the rate of increase of the current

Effect of Bilayer Thickness

Fig. 9 shows that the rate-limiting factor for transport is not incorporation of vesicles but rather something which takes place in the

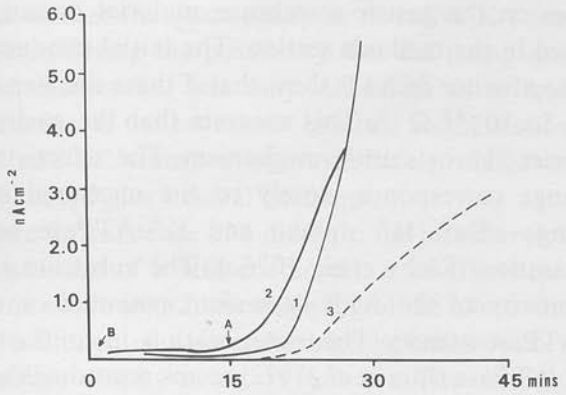

Fig. 9. The effect of bilayer status and sidedness of *G*1 and ATP on short circuit current. In curve *1*, in the presence of ATP, the bilayer was formed at zero time and *G*1 added at the arrow *A*. It can be seen that there is less than a 5-min lag before development of current. In curve *2* *G*1 and ATP are both present, arrow *B*, from the time of formation of the bilayer. It can be seen that there is a 15-min lag before development of current. Curve *3* shows the effect of adding *G*1 to the side opposite to that of ATP (arrow *B*) showing a lower current hence an asymmetry of the ATP site in the original preparation, as well as an even longer lag phase, indicating an additional restriction of incorporation of the ATP site in this configuration

bilayer prior to their addition. When ATP is present it is the time from the formation of the bilayer that is the determining factor in development of short circuit current. The analogous experiment with gramicidin is shown in Fig. 5 in Goodall, 1971. Also shown in Fig. 9 curve *3* is the SCC when the vesicles are added on the opposite side to ATP.

Discussion

Incorporation of membrane located pumps into synthetic membrane has been successfully achieved in many instances using liposomes (Kagawa, Kandrach & Racker, 1973; Hilden, Rhee & Hokin, 1974). In these instances the transport and electrical characteristics of the pump processes have been ascertained by the use of ionophores, lipid permeable ions, and ion flux measurements which, although informative, lack the sensitivity and resolution of direct electrical measurement. The suitability of the planar bilayer for electrical rather than chemical probing of transport events has led to much effort being expended in attempts to incorporate pumps into planar membranes. For various reasons connected with the criteria listed under *Materials and Methods*, success has been limited (Jain *et al.*, 1972).

Our studies on the gastric membrane material essentially fulfill the criteria as listed in the methods section. The initial conductance changes obtained in the absence of ATP show that if there are step changes these are less than $5 \times 10^{-13}\ \Omega^{-1}$. This suggests that the gastric membranes contain a carrier-like or shuttle mechanism. The selectivity of the conductance change corresponds closely to the measured selectivities of cation exchange efflux, H^+ uptake and K^+-ATPase activity in the original preparation (Sachs *et al.*, 1976*a*). The substrate selectivity and inhibitor sensitivity of the ATP dependent potential or current is the same as for ATPase activity. The incorporation, in contrast to the report on $Na^+ + K^+$ ATPase (Jain *et al.*, 1972) seems reproducible to the extent that in fresh preparations 80% of the experiments are successful. The most important factor found in this study is the freshness of the microsomes. The best results obtained here were with microsomes at 16 hr from slaughter. Aging at 0 °C resulted in loss of ability to modify bilayer conductance after about 48 hr. The material that is used for the incorporation experiments is usually density gradient purified fraction. This has been purified further by free flow electrophoresis and this material incorporates with the same characteristics as the density gradient fraction. The highly purified material has 75% of the Coomassie Blue staining material associated with the 100,000 dalton region of SDS polyacrylamide gels (Sachs *et al.*, 1976*a*).

Previous work on reconstitution of pumps in artificial membranes has been confined largely to reconstitution in liposomes. Reconstitution of the electrogenic ATPase of mitochondria results in retention of the electrogenic properties of that ATPase. The electrogenic properties of $Na^+ + K^+$ and Ca^{++} ATPases are more doubtful in the intact biological membrane. That a property change does occur on reconstitution of this type of ATPase is shown by the high anion permeability of the native *SR* vesicles and the low anion permeability of the reconstituted pump vesicles.

The evidence for nonelectrogenicity of the $H^+ + K^+$ ATPase in the isolated mature vesicles is convincing by the techniques used, namely effects of change of conductance of the membranes and redistribution of lipid permeable ions (Sachs *et al.*, 1976*a*). The most striking features of the bilayer reconstituted system on the other hand are (a) the presence of an electrogenic H^+ pump and the nonexistence of active K^+ transport, i.e., $E_K \sim 0$; (b) the exponential increase of all conductances with time; and (c) the increase of the exponential rate k_K in the presence of ATP.

It seems to us that the discrepancy as to active K^+ transport can be explained by considering the possibility that the pump exists as a dimer in the natural membrane, but may dissociate to a monomer in the artificial membrane. If the monomer has two configurations E_1 and E_2, which are H^+ and K^+ transporting, respectively, obligatory coupling in the form $E_1 E_2$ could give neutral exchange.

The evidence for existence of a dimer in the intact vesicles depends on (1) the demonstration of a Hill coefficient, n, of 1.8 when *p*-nitrophenyl phosphate is the substrate, (2) the doubling of the effectiveness of ATP as a competitive inhibitor of *p*-nitrophenylphosphatase with rupture of the vesicular structure (Sachs *et al.*, 1976*a*), (3) The twofold more rapid inactivation of ATPase and H^+ transport compared to inactivation of *p*NPPase (Hung *et al.*, 1976).

Evidence for E_1 and E_2, i.e., 2 sites or forms of the enzyme in the bilayer, comes from the different behavior of the exponential increases in g_H and g_K in presence and absence of ATP. Previous results obtained with gramicidin A (Goodall, 1971) show a similar exponential increase where it seems that the effect is due to a further thinning of the bilayer from 50 Å, at the initial collapse to the bilayer state, to 27 Å after a period of 10–20 min. The activation energy for gramicidin dimer formation, i.e., the conducting state, depends on thickness and is about kT/Å. In the present case one can suppose the ion transporting sites require an activation energy to reach the bilayer surface. Then the results for g_K show that the dependence of this activation energy on thickness (1/4 kT/Å) is increased (t_0 1/2 kT/Å) in the presence of ATP.

Our model assumes that only the $E_1 E_2$ form exists in the dimer. As pointed out elsewhere, (Glynn & Karlish, 1976) this implies that only half the sites are reactive with ATP and that H^+ and K^+ binding sites coexist. The transport sequence can then be written, where the asterisk identifies the same subunit:

$H_2O + E_1^* \cdot E_2$	$\leftrightarrow H^+ P \cdot E_1^* E_2 P + ADP$	H^+ binding
$H^+ P \cdot E_1^* E_2 P + K^+$	$\leftrightarrow H^+ P \cdot E_1^* E_2 PK^+$	K^+ binding
$H^+ P \cdot E_1^* E_2 PK^+$	$\leftrightarrow H^+ P E_2^* E_1 PK^+$	translocation
$H^+ P E_2^* E_1 PK^+$	$\leftrightarrow H^+ + P E_2^* \cdot E_1 + Pi + K^+$	dissociation

As written, this is an obligatory neutral exchange pump.

At the pH of 6.1 the actual ratio of H^+ or Rb^+ exchanged per mole ATP hydrolyzed seems to be 4 (Sachs *et al.*, 1976*a*). As the intracation stoichiometry varies so will the degree of electrogenicity. However, it may be simpler to develop a scheme for the transition between nonelec-

trogenic transport in the vesicle to electrogenic transport in the planar bilayer when we consider dissociation of the imer to the monomeric form. In this case the transport reactions may be written

$H_2O + E_1 + ATP$	$\leftrightarrow H^+ E_1 P$	phosphorylation
$H^+ E_1 P$	$\leftrightarrow H^+ E_2 P$	H^+-translocation
$H^+ E_2 P$	$\leftrightarrow H^+ + E_2 P$	dissociation
$E_2 P + K^+$	$\leftrightarrow K^+ E_2 P$	association
$K^+ E_2 P$	$\leftrightarrow K^+ E_1 P$	K^+-translocation
$K^+ E_1 P$	$\leftrightarrow K^+ + E_1 + P$	dissociation/dephosphorylation

From this scheme the movement of H^+ is now dissociated from the movement of K^+, provided an additional thickness dependent reaction

$$E_2 P \rightleftharpoons E_1 P \quad \text{(thickness increasing} \rightharpoonup\text{)}$$

is allowed; whereas in the dimer situation, this transformation can occur only during the H^+ and K^+ exchange. K^+ serves to accelerate this interconversion hence the K^+ conductance will increase as a function of phosphorylation. In the absence of K^+, in the presence of Na^+, for example, H^+ transport will result in a potential. K^+, due to the conductance of the reaction $K^+ E_2 P \rightharpoonup K^+ E_1 P$ will serve to shunt the H^+ emf but will not produce a K^+ emf. Hence there will not be a drop in the short circuit current associated with the presence of K^+. Also in the monomer, H^+ and K^+ sites sequentially, not simultaneously.

This work was supported by U.S. Public Health Service grants NIH NS12279, NIH ATPase AM15878, and NSF GB31075.

References

Eisenman, G. 1961. Cation selective glass electrodes and their mode of operation. *Biophys. J.* **2(2):**259

Ganser, A., Forte, J.G. 1973. K^+-stimulated ATPase in purified microsomes. *Biochim. Biophys. Acta* **307:**169

Glynn, I.M., Karlish, S.J.D. 1975. Different approaches to the mechanism of the sodium pump. *In:* Energy Transformation in Biological Systems. Ciba Foundation Symposium. p.31. London

Goodall, M.C. 1971. Thickness dependence in the action of gramicidin A on lipid bilayers. *Arch. Biochem. Biophys.* **147:**129

Goodall, M.C. 1973. Action of two classes of channel forming synthetic peptides on lipid bilayers. *Arch. Biochem. Biophys.* **157:**814

Hilden, S., Rhee, H.M., Hokin, L.E. 1974. Na^+ transport by phospholipid vesicles containing purified $Na^+ + K^+$ ATPase. *J. Biol. Chem.* **249:**7342

Hung, H.H., Saccomani, G., Rabon, E., Schackmann, R., Sachs, G. 1977. H^+ transport by gastric membrane vesicles. *Biochim. Biophys. Acta* **464**:313

Jain, M.K., White, F.P., Strickholm, A., Williams, E., Cordes, E.H. 1972. Studies concerning the possible reconstitution of an active cation pump across an artificial membrane. *J. Membrane Biol.* **8**:363

Kagawa, Y., Kandrach, A., Racker, E. 1973. Partial resolution of the enzymes catalyzing phosphorylation. *J. Biol. Chem.* **248**:676

Lee, J., Simpson, G., Scholes, P. 1974. An ATPase from dog gastric mucosa. Change of pH in membrane vesicles accompanying ATP hydrolysis. *Biochem. Biophys. Res. Commun.* **60**:825

Saccomani, G., Stewart, H.B., Shaw, D., Lewin, M., Sachs, G. 1977. Fractionation of hog gastric mucosa. *Biochim. Biophys. Acta* **465**:311

Sachs, G., Hung, H., Rabon, E., Schackmann, R., Lewin, M., Saccomani, G. 1976a. A non-electrogenic H^+ pump in plasma membranes of hog stomach. *J. Biol. Chem.* **251**:7690

Sachs, G., Rabon, E., Saccomani, G., Sarau, H.M. 1976*b*. ATP and redox in acid secretion. *Ann. N.Y. Acad. Sci.* **264**:456

GASTROENTEROLOGY 73:931–940, 1977

Vol. 73, No. 4, Part 2
Printed in U.S.A.

METABOLIC AND MEMBRANE ASPECTS OF GASTRIC H^+ TRANSPORT

G. SACHS, M.B., CH.B., H. CHANG, M.A., E. RABON, PH.D., R. SHACKMAN, PH.D., H. M. SARAU, PH.D., AND G. SACCOMANI, PH.D.

Laboratory of Membrane Biology, University of Alabama in Birmingham, Birmingham, Alabama

Metabolic properties of dog gastric mucosa, investigated by substrate level measurements, implicate the Krebs cycle as the major energy-yielding metabolic pathway but are equivocal in terms of an ATP-based H^+ secretion. Purification of gastric membranes by centrifugation and free flow electrophoresis results in a class of membrane vesicles enriched in K^+-ATPase and capable of ATP-energized H^+ uptake. Immunohistochemistry shows these to be derived from the parietal cell. H^+ uptake by the vesicles is accompanied by K^+ efflux, and movement of either ion is not potential-coupled. The simplest interpretation of these transport studies is uptake of KCl by the vesicles by passive diffusion followed by active H^+:K^+ exchange. In some respects, however, this model fails to conform to the expectations from in vitro studies. It may be, therefore, that another pump (i.e., redox) or another membrane component (i.e., Cl^- conductance) is lost during purification. The properties of the vesicles are such, however, as to establish their role in H^+ secretion by the stomach.

Gastric secretion of H^+ is caused by the reaction of the parietal cell to stimuli. Of these, histamine, gastrin and acetylcholine are the ones most frequently considered as being primary. There is considerable dispute as to the nature of interaction between these stimuli as well as to their action on the parietal cell. In this paper we are concerned with the response of the cell to changes of second messengers, whether Ca^{2+}, cAMP, or some unknown component.

The response of the parietal cell can be divided into three components: a metabolic response, a possible membrane fusion reaction, and H^+ secretion accompanied by Cl^-.

Metabolic Response

The changes in metabolite pattern occurring in the parietal cell between rest and secretion were determined in histological sections of parietal cell regions of dog gastric mucosa by comparing the steady state levels of glycolytic, glucose oxidative, lipolytic, and Krebs cycle intermediates.[1–3]

Glycolysis. There were significant changes in parietal cell levels of intermediates of this pathway. There was no crossover in levels of any of these, but the relative changes of fructose-6-phosphate and fructose 1,6-diphosphate imply activation of phosphofructokinase. The rise in pyruvate and lactate also implies some regulation at the pyruvate dehydrogenase reaction, as suggested by studies of the effect of lipoate on acid secretion by frog mucosa.[4] The small change in glycogen indicates that glycogenolysis is not a major energy source in this mammalian tissue. The increase of glycolysis must then be attributable to increased glucose entry into the cell, presumably Na^+ gradient-controlled. The rise in phosphoenol pyruvate was also large but the level of phosphoenol pyruvate was very low.

Glucose oxidation. The measured intermediates of this metabolic chain increased with onset of secretion. However, the total $NADP^+$:NADPH ratio did not change and the calculated cytoplasmic ratio fell. This suggests that a major activation of this pathway does not occur and that moreover, because there is an increase of intermediates, control of this pathway may be elsewhere than in the triphosphopyridine ratio.

Lipolytic and other intermediates. There was a marked rise of glycerol with onset of secretion, supporting the concept that there might be some activation of triglyceride lipase. There was also a rise in acetyl coenzyme A (CoA), CoA acetoacetate, and β-hydroxy butyrate, indicative of some increase in fatty acid oxidation.

Krebs cycle and related intermediates. From the data in figure 1 it seems fairly clear that the onset of acid secretion is associated with a large increase in the steady state levels of most of the citric acid cycle intermediates. The increase in citrate suggests an increase in citrate synthetase activity, attributable to the increase in oxaloacetate and acetyl CoA rather than to an activation of the enzyme per se. The large rise in fumarate and malate relative to succinate implies activation of succinic dehydrogenase.

Summary of metabolic pathways. Clear evidence has been obtained for the activation of glycolysis and mitochondrial metabolism owing to stimulation of acid secretion. Partial evidence is available that fatty acid oxidation may also be implicated. However, only the phosphofructokinase and succinic dehydrogenase reaction intermediates show sufficient change to suggest

Address requests for reprints to: Dr. George Sachs, Laboratory of Membrane Biology, University of Alabama Medical School, University Station, Birmingham, Alabama 35294.

This study was supported by Grants AM 15878 and CA 16722 from the National Institutes of Health.

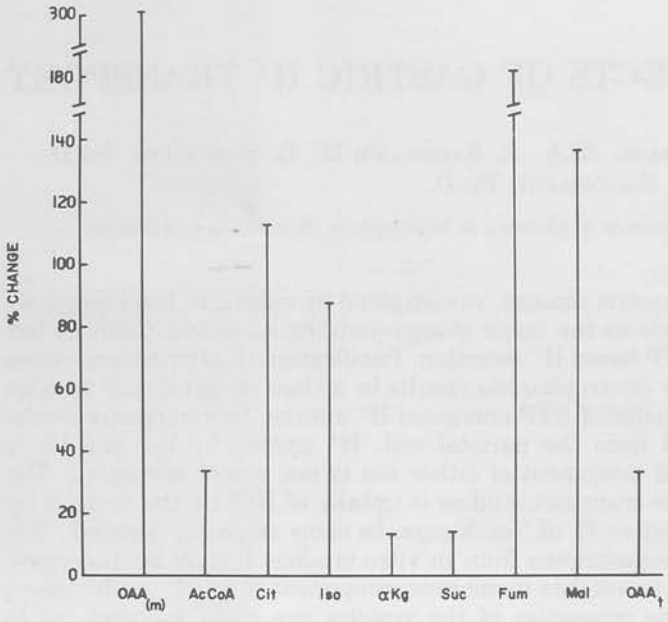

FIG. 1. The percentage change observed in Krebs cycle and related intermediates in parietal cell regions of dog gastric mucosa.

primary activation at those sites. One may speculate, based on these data, and on observations of the redox changes found in the chambered amphibian mucosa,[5–7] that gastric mitochondria may be defective in one or several of the metabolic anion transport systems.[8] This would not be unique to gastric mitochondria, because it is also found in insect muscle[9] and heart muscle[8] mitochondria. Control of mitochondrial metabolism may therefore be exerted at the entry step of substrate, fatty acetyl CoA, or at pyruvate transport, for example.

Changes in pyridine nucleotides. Spectroscopic observations have suggested that there is a generalized reduction of the observable components of the redox chain.[6, 7, 10, 11] There may, however, be a relative sparing of the pyridine nucleotide component.[7] This may implicate the reactions of complex I of the mitochondrial respiratory chain in acid secretion.[12] Direct measurement of NAD^+ and NADH levels in the parietal cell area during the transition from rest to full secretion showed a fall in the total ratio of NAD:NADH, as would be predicted from spectroscopic studies. Assuming equilibrium operation of lactic dehydrogenase in the cytoplasm and glutamic dehydrogenase in the mitochondria, one can calculate the ratio in these two compartments. There was a fall in the cytoplasmic ratio and an increase in the mitochondrial ratio, implying a flow of reducing equivalents into the cytoplasmic compartment. This flow is in the energetically favorable direction and may be interpreted as evidence for utilization of these reducing equivalents for the process of H^+ secretion.

Changes in adenine nucleotides and phosphocreatine. There was a fall in the phosphorylation potential ($ATP:ADP \cdot P_i$), but this was due usually to an increase in inorganic phosphate. The levels of ATP, ADP, and phosphocreatine changed very little. This finding is somewhat unexpected if the sole mechanism of H^+ secretion is dependent on ATP and the metabolic stimulus resulting in the large increase in O_2 consumption[13] is a fall in the phosphorylation potential. Moreover, the source of the increase of P_i is obscure. Perhaps there is a large change in phospholipids such as phosphatidyl inositides associated with secretory stimulus.

An alternative explanation for the constancy of the high energy phosphate pool is that although the total adenine nucleotides do not change, the mitochondrial compartment changes very differently from the cytoplasmic pool. However, calculation of the change in phosphorylation potential using the glyceraldehyde phosphate equilibrium in the cytoplasm provides data quantitatively identical to the change found by calculation using measured nucleotide levels.

Summary of Metabolic Response

A combination of the data from spectroscopic and metabolite measurements in the gastric mucosa does not give a resolved picture of either the metabolic pathway(s) or the energy source for H^+ transport in the mucosa. It may therefore be suggested that both ATP and a redox substrate are involved. To resolve this question further, one can consider the membranes involved in gastric proton transport. Before describing the compositional and transport features of the secretory membrane, we shall digress briefly into an anatomical description of the morphology of the parietal cell.

Morphological Changes

It appears that the resting parietal cell contains large quantities of cytoplasmic membranes named tubulovesicles. With stimulation of secretion, these fuse with the apical membrane of the cell, producing amplification of the secretory surface, which persists during secretion. This process is reversed with cessation of stimulus. The alteration seems quite complex[14] in that there are double membrane forms (hexa- and pentalaminar) observed both in the intact tissue[15] and in isolated membrane fractions.[14] These double membrane forms are an unexpected feature of a simple fusion membrane-recycling system.

Isolation and Composition of Gastric Plasma Membranes

As in any other tissue, purification of the plasma membrane fraction is not entirely straightforward. Classically, the procedure involves separation of a smooth membrane fraction from other cellular particulate material by differences in mass and density, and defining markers (enzymic, receptor, and compositional) for this membrane fraction. In the case of heterocellular epithelia, the problem is complicated by heterogeneous plasma membranes both with respect to cell type and cell surface, the apical, basal, and lateral surfaces subserving different functions. Gastric mucosa contains four major cell types; surface, neck, parietal, and peptic cells. Flooding the cell surface with hypertonic NaCl results in selective removal of most of the surface and neck cells, leaving the parietal and peptic

cells. Homogenization and differential centrifugation of the homogenate results in a microsomal pellet. This can be fractionated further by density gradient centrifugation in a zonal rotor using sucrose or Ficoll sucrose gradients, resulting in two fractions consisting of smooth surface membrane vesicles uncontaminated by mitochondrial markers and a third fraction containing mitochondrial markers and RNA.

As previously described,[14] there is enrichment of 5′-nucleotidase (5′-AMPase), a K^+-activated ATPase that is ouabain-insensitive,[16] and Mg^{2+} ATPase in both smooth membrane fractions. A HCO_3^- activation of a Mg^{2+} ATPase is also present in both membrane fractions.[17]

Further fractionation of these membranes is possible using free flow electrophoresis producing two and three membrane fractions from the lighter and heavier material, respectively. As shown in figure 2 and table 1, this fractionation provides a separation between the K^+-ATPase on one hand and the Mg^{2+} ATPase and 5′-AMPase on the other. Two other activities of interest are the presence of cytochromes and HCO_3^- activation of ATPase activity.

With respect to cytochrome, there is, in the presence of dithionite, the appearance of an absorbance at 431, 520, and 561 nm, with an additional shoulder at 555 nm (fig. 3). The similarity to complex III and to the cytochrome b_{561} present in chromaffin granules[18] is striking. However, the cytochrome b_{561} component is separated from the K^+-ATPase by free flow electrophoresis.

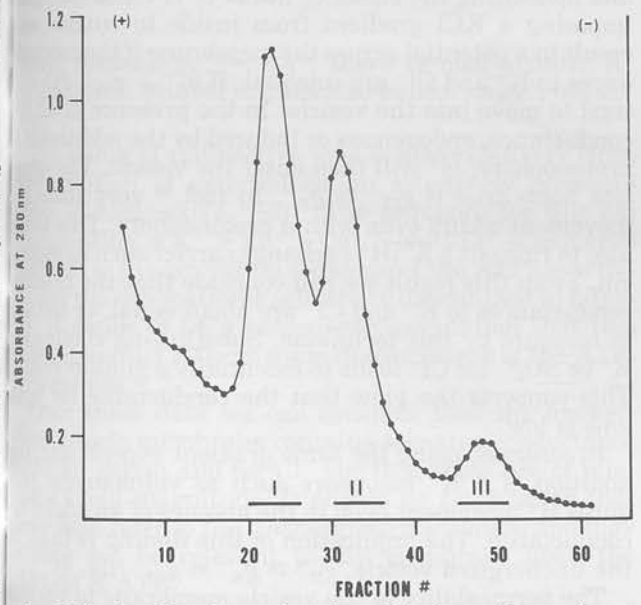

FIG. 2. The free flow electrophoresis profile of a gastric membrane fraction showing the optical density at 280 nm K^+ ATPase:pNPPase activity is associated with FI and Mg ATPase and AMPase activity are associated with FII. FIII contains some K^+ ATPase activity. (Reproduced from Biochim Biophys Acta 465:311–330, 1977, with permission.)

HCO_3^- activation of the ATPase is present in the K^+-ATPase fraction. This activity is insensitive to the presence of mitochondrial ATPase inhibitor, in contrast to the HCO_3^- activation of the mitochondrial ATPase, which is highly sensitive to the inhibitor.

The significance of this activation by HCO_3^- is not known. Surveying the occurrence of HCO_3^- activation of a Mg^{2+} ATPase that is nonmitochondrial, such as in colon[19] or distal tubule[20, 21] of kidney, it is tempting to assign a role for this enzyme in Cl^- or Na^+ transport across the apical membrane of the cell. There seems to be some question as to whether Cl^- transport occurs actively across the cell membrane, or down an electrochemical concentration gradient from an accumulated Cl^- cellular pool.[22] If so, it is possible that the HCO_3^- activation reflects a role of this enzyme in Cl^- transport as originally suggested.[17]

The major emphasis is on the presence and purification achieved of the K^+-activated ATPase.[14, 16] Associated with about a 50-fold increase in specific activity of the ATPase as compared to the original homogenate is a purification of the 100,000 mol wt region of the peptides present in sodium dodecyl sulfate-polyacrylamide gel electrophoresis (SDS-PAGE) (fig. 4). From this it can be seen that the membrane fraction labeled contains at least 80% of the peptide in this 100,000 mol wt region. It is this region that is phosphorylated by γ-[^{32}P]ATP.[23]

There are several characteristics which distinguish this enzyme from the other plasma membrane ATPases which have been previously described, such as the Ca^{2+} ATPase[27] and $Na^+ + K^+$ ATPase[24] as well as similarities.

Thus Na^+ is not required for activity, Ca^{2+} is inhibitory to the enzyme, and ouabain is without effect on enzyme activity, as examples of differences.

All three enzymes contain a major peptide of 100,000 mol wt as the catalytic subunit,[14, 24, 27] as well as, in the case of the Na + K ATPase, a glycoprotein of about 55,000 mol wt.

All three enzymes show a complex pattern using isoelectric focusing, and their patterns differ characteristically. The significance of this complexity is unclear, but may represent postsynthetic modification of the transport protein.

The gastric ATPase occurs in vesicles with transport characteristics, which makes their study a particularly relevant area in investigating acid secretion.

TABLE 1. *Purification of GII gastric membrane fraction*[a]

Fractions	Mg^{2+} ATPase	K^+ ATPase[b]	K^+ *p*-nitrophenyl phosphatase	5′-AMPase
GII (zonal)	19.4 ± 1.8	63.6 ± 2.0	61.2 ± 4.2	2.2 ± 0.3
GII-FI	4.4 ± 1.0	110.7 ± 2.6	68.0 ± 2.5	0.3 ± 0.06
GII-FII	31.0 ± 3.1	20.0 ± 0.7	9.4 ± 1.0	5.4 ± 1.0
GII-FIII	2.8 ± 0.4	50.1 ± 3.2	31.0 ± 2.2	0.1 ± 0.1

[a] Activities are expressed in micromoles per milligram of protein per hour (mean of nine fractionations ± SE).
[b] Activity in presence of 20 mM KCl minus the basal rate.

Origin of Fraction FI Vesicles

Injection of fraction FI into rabbits provided an antiserum which had the properties of (1) giving a single precipitation line on immunodiffusion plates against Triton X-100 solubilized microsomal or FI membrane protein, (2) inhibiting both the K^+-activated ATPase and *p*-nitrophenylphosphatase, and (3) inhibiting H^+ transport by gastric vesicles.

Staining of gastric antral and fundic sections with this antibody, as compared to staining with nonimmunized serum, showed that it was specifically an antiparietal cell antibody and probably bound more firmly to the supranuclear region of the cell. This would be expected of an antibody against the apical tubulovesicular system (fig. 5).

Transport by Gastric Vesicles

In a medium containing only KCl and $MgCl_2$ with no or minimal buffering capacity, gastric vesicles (fraction GI or FI) take up H^+ from the medium[25] with ATP addition (fig. 6).

From this observation one can predict a series of possibilities relating to the proton transport mechanism. For example, the pump could be electrogenic K^+ outward or electrogenic Cl^- inward, resulting in H^+ movement in response to a potential. Alternatively, an electrogenic H^+ pump could be present, moving Cl^- inward or K^+ outward through a membrane K^+ conductance. The pump could also be a coupled HCl inward, or KCl could enter passively followed by an H^+:K^+ exchange (fig. 7).

It is possible, using ionophores to change membrane conductance and then follow passive and active ion movements, or ATPase activity in nonleaky vesicles, to decide between most of these models. Moreover, using radioactive or fluorescent lipid-permeable ions, it is possible to obtain an estimate of potential difference changes across vesicle membranes.

ATPase. Considering first the information obtainable using ATPase activity, we can provisionally exclude many of these models. A model requiring a Cl^- pathway as a conductance or a pump component would then predict that ATPase activity would change when Cl^- is substituted for by a less permanent anion such as SO_4^{2-} or glucuronate. This does not happen; thus, models 2, 3, and 6 of figure 7 are unlikely. An electrogenic H^+ ATPase of the mitochondrial type would be uncoupled by the addition of an H^+ conductance by a protonophore such as tetrachlorsalicylanilide (TCS); hence, ATPase activity would increase. Because this does not happen, models 3 and 4 are not favored. An electrogenic K^+ pump with a limiting H^+ conductance should also increase activity with the addition of an H^+ conductance, unless there is a high Cl^- conductance. In this case, the sensitivity to TCS should increase in SO_4^{2-} solutions, and it does not. An H^+:K^+ exchange pump with a passive KCl limb should increase in activity when the internal K^+ of the vesicles is maintained, because after a time the vesicles become depleted of K^+. This seems to be borne out by the finding[26] that K^+ ionophores, in contrast to lipid-permeable ions, increase ATPase activity if the enzyme is present in vesicular form. The internal K^+ requirement suggested by these data is not fully satisfied by preincubation in K^+ medium. Hence, just from these data, one might suggest that K^+ efflux occurs from the vesicles with the addition of ATP.

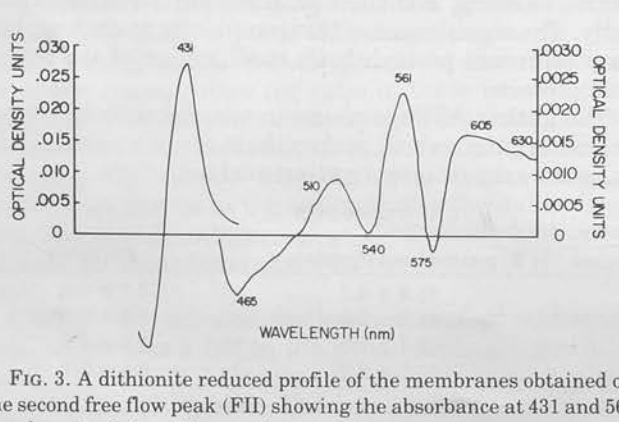

FIG. 3. A dithionite reduced profile of the membranes obtained on the second free flow peak (FII) showing the absorbance at 431 and 561 nm characteristic of the membranes.

Conductance of the vesicle membrane. The relative conductances of the vesicle membrane can be assessed by imposing ion gradients across the vesicle membrane and measuring the efflux or influx of H^+. For example, imposing a KCl gradient from inside to outside will result in a potential across the membrane if the conductances to K^+ and Cl^- are unequal. If $g_{K^+} > g_{Cl^-}$, H^+ will tend to move into the vesicle. In the presence of an H^+ conductance, endogenous or induced by the addition of a protonophore, H^+ will then enter the vesicle. The opposite holds true if $g_{Cl^-} > g_{K^+}$. In fact,[22] very little H^+ movement occurs even with a protonophore. This tends also to rule out a K^+:H^+ exchange carrier such as nigericin. From this result we can conclude that the relative conductances to K^+ and Cl^- are about equal, or too low to measure by this technique. Substituting choline for K^+ or SO_4^{2-} for Cl^- leads to essentially a similar result. This supports the view that the conductance for both ions is low.

In contrast, using the same gradient experiment, the addition of a K^+ ionophore such as valinomycin produces H^+ movement even in the absence of an added H^+ conductance. The implication of this finding is that, in the unenergized vesicle, $g_{H^+} > g_{K^+} \approx g_{Cl^-}$ (fig. 8).

The permeability of the vesicle membrane to various anions and cations can also be estimated by measuring uptake or efflux of radioactive ions.

From the formula

$$p = (0.693/t_{1/2})\, r$$

the permeability in centimeters per second can be estimated, where r is the radius of the vesicle and $t_{1/2}$ is the half-time. As described previously,[28] the net uptake rate of Rb^+, Cs^+, Na^+, and Cl^- are about equal, with a $t_{1/2}$ of the order of 40 min, giving $p \approx 10^{-8}$ cm sec^{-1}.

The addition of a K^+ ionophore accelerates the uptake of cation such as Rb^+ and is due to both an increased entry of Cl^- and an increased efflux of H^+. This result shows that there is a finite Cl^- conductance; hence, from

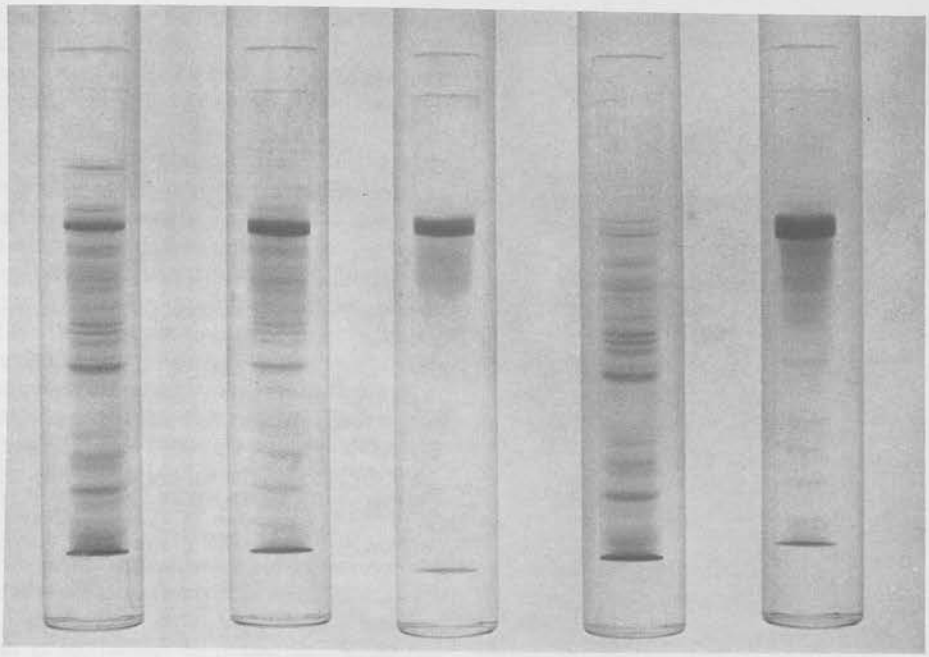

FIG. 4. SDS-PAGE gels of, from *left* to *right*, the gastric microsomes, the deeper gradient band, and the three free flow electrophoresis peaks, FI, FII, and FIII. FI is active in H^+ uptake and was used for immunization. (Reproduced from Biochim Biophys Acta 465:311–330, 1977, with permission.)

above, because $g_{K^+} \approx g_{Cl^-}$, there is also a finite K^+ conductance. Bilayer studies also indicate a g_{K^+}, but $g_{K^+} > g_{Cl^-}$.[29]

The efflux of radioactive ions is also relatively slow. The addition of external cation selectively increases efflux of radioactive $^{86}Rb^+$. The sequence for this exchange efflux is $K^+ > Rb^+ > Cs^+ > Na^+, Li^+$, a sequence identical to the activation sequence of the ATPase activity and the intracationic selectivity determined in bilayers. It seems to be a reasonable speculation that this exchange efflux reflects some characteristic of the ATPase peptides.[28]

From these data we can conclude that the unenergized vesicle membrane contains selective conductance paths for cation and for Cl^- but that these are of relatively small magnitude. It should be emphasized that these data refer to the unenergized membrane and may or may not be relevant to the membrane upon the addition of ATP.

H^+ uptake. The uptake of H^+ due to the addition of ATP clearly reflects the function of the K^+ ATPase.[22, 30] The uptake observed by a *p*H electrode (i.e., the disappearance of H^+ from the medium) can be due to (1) binding of H^+, (2) H^+ movement into an intramembranal region, or (3) uptake of H^+ into intravesicular water. Classically, the way to distinguish these has been the demonstration that either ionophores can reverse or inhibit the phenomenon or the uptake is sensitive to vesicular volume, i.e., medium osmolarity. H^+ uptake is dissipated by ionophores, and apparently there is zero H^+ uptake at infinite osmolarity.[22] However, this latter experiment must be interpreted with caution if a K^+:H^+ exchange is taking place. Then the effect of vesicular volume is to reduce the quantity of intravesicular K^+; hence, the effect on H^+ uptake is secondary. Otherwise, with intravesicular buffer present, the buffer concentration would also increase with declining volume and the H^+ uptake would stabilize. With 5 mM buffer present in the medium, 10 nmoles would be present in 2 μl of vesicle volume, and this should be detected as a finite intercept on the line relating uptake to the reciprocal of the osmolarity.

The effect of ionophores can be studied in three phases of the experiment, addition before ATP, during the action of ATP, and after the ATP is utilized and an H^+ gradient is slowly dissipating due to the endogenous H^+ leak of the membranes. In the latter case, nigericin, which acts mainly but not exclusively as a neutral cationic exchange ionophore, rapidly dissipates the gradient, presumably exchanging H^+ for K^+. Both a protonophore (TCS) and a K^+ ionophore are required to dissipate the gradient. If a high Cl^- conductance were present, a protonophore alone would dissipate the gradient; this would be equally true of a high K^+ conductance. The action of TCS is less than the action of valinomycin and exhibits the peculiar feature that there is only a transient increase in the dissipation rate. This is difficult to interpret on the basis of a single compartment of H^+ with a uniform K^+ or Cl^- conductance because this would produce an exponential decline of the gradient.

If the vesicle conductance to K^+ or Cl^- were dependent on the intravesicular *p*H, a low *p*H increasing conductance to one of these ions, and at a certain *p*H the conductance suddenly fell, then the effect of TCS would be different depending on the magnitude of Cl^- as compared to H^+ conductance.

Protonation of the membrane would tend to increase Cl^- conductance, and because the K^+ conductance is

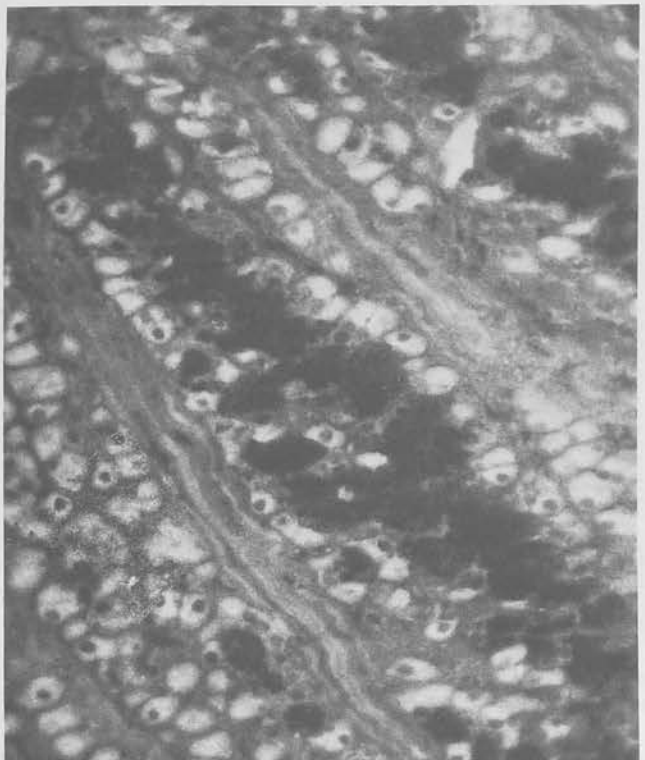

FIG. 5. The immunofluorescence of a gastric section after treatment of an alcohol-fixed paraffin-embedded longitudinal section of hog fundic mucosa with anti-FI antibody and fluorescein-conjugated anti-rabbit γ-globulin. The parietal cell fluorescence shown is not obtained in antral sections or with nonimmunized serum.

low, the initial efflux of H^+-TCS would be associated with Cl^- efflux. At higher *p*H, the Cl^- conductance would fall, and the movement of H^+-TCS would return to the rate limited by conductance of other ions.

The effect of valinomycin alone, after consumption of the ATP, is larger than that of TCS, and depends on the H^+ conductance of the vesicle membrane. Because this is relatively high compared to Cl^- and K^+ in the resting membrane (see above), considerable dissipation of the gradient occurs.

Gramicidin, a channel-inducing ionophore, consistently shows a slower effect on the H^+ gradient than valinomycin, valinomycin and TCS, or nigericin. This is in sharp contrast to its effectiveness in stimulating ATPase activity, where it is considerably more effective than a combination of valinomycin and TCS.

Amphotericin B is without measurable effect on H^+ leaks in these vesicles.

As a class, lipid-permeable cations such as dimethyl dibenzyl ammonium have variable effects. They are considerably less effective than valinomycin, even at 10 mM concentration, but do appear to increase the leak of

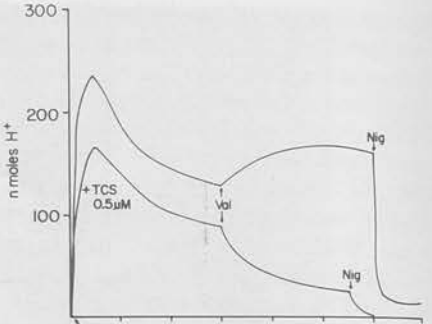

FIG. 6. The *upper curve* shows H^+ disappearance (or OH^- extrusion) from the vesicle medium with the addition of 0.3 mM ATP. The subsequent addition of valinomycin results in a second increase in H^+ uptake. This effect is not produced by lipid-permeable cations. The *lower curve* shows partial inhibition by tetrachlorsalicylanilide (TCS). In the presence of TCS, valinomycin now dissipates the gradient, as does nigericin in the first experiment.

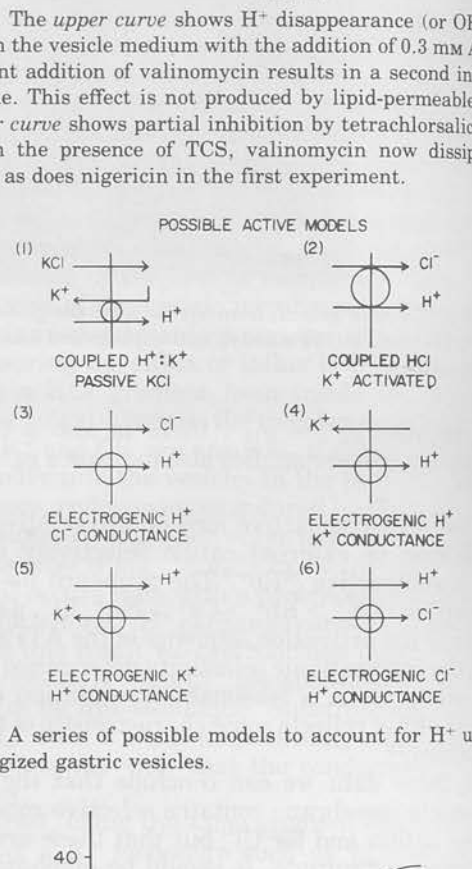

FIG. 7. A series of possible models to account for H^+ uptake by ATP-energized gastric vesicles.

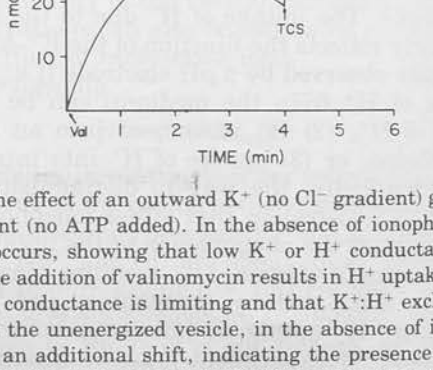

FIG. 8. The effect of an outward K^+ (no Cl^- gradient) gradient on H^+ movement (no ATP added). In the absence of ionophores no H^+ movement occurs, showing that low K^+ or H^+ conductance is rate limiting. The addition of valinomycin results in H^+ uptake, showing that the K^+ conductance is limiting and that K^+:H^+ exchange does not occur in the unenergized vesicle, in the absence of ionophores. TCS causes an additional shift, indicating the presence of another H^+ compartment, perhaps due to another class of vesicles or an intramembranal site, for example.

H^+; the increased leak tends to have the same time course as the protonophore effect.

Lipid-permeable anions such as SCN^- (up to 20 mM) also appear to increase the leak of H^+ in some, but not all, experiments.

The variability of some of these data implies that there are tissue or preparative variations in the passive conductance properties of the vesicles. Because the presence of the pump is invariant, the variation is therefore not due to the properties of the pump itself.

Addition of ionophores or lipid-permeable ions before the addition of ATP allows some deductions to be made about the characteristics of the pump.

Pretreatment with valinomycin when a K^+ gradient out to in is present increases the rate and magnitude of H^+ uptake and dissipation. This may be due to the provision of a shunt conductance for an electrogenic H^+ pump or to an increased supply of K^+ to external sites. If the former is the case, a lipid-permeable cation should have the same effect. Dimethyl dibenzlyammonium at 1 mM or 10 mM has no effect in some preparations and inhibits in others. This can be explained on the basis of a g_{H^+} varying from preparation to preparation, or the magnitude of the H^+ gradient induced by ATP varying. However, the rate and magnitude of H^+ uptake are not increased. Hence, the action of valinomycin is not due to the provision of a cationic shunt conductance, in contrast to bacterial vesicles.[31]

Preincubation of the vesicles in KCl allowing the internal K^+ to accumulate markedly accelerates H^+ uptake (fig. 9). This indicates that internal (vesicular space or intramembranal sites) K^+ is required for H^+ uptake. Adding valinomycin before ATP under these conditions has less effect on H^+ uptake, which can be explained by the increased leak of H^+ induced by valinomycin balancing the removal of the K^+ movement restriction. H^+ uptake is only slightly increased by valinomycin under these conditions.

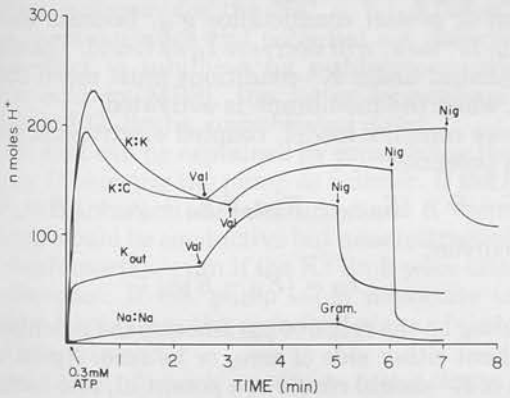

FIG. 9. The effect of varying the intravesicular K^+ on ATP-induced H^+ uptake, and the effect of Na^+ substitution. The *lowest* curve shows H^+ uptake in the presence of equal concentrations of Na^+ inside and outside the vesicles. This small H^+ gradient is dissipated by gramicidin. In the presence of K^+ initially only on the outside of the vesicles, H^+ is taken up with no overshoot. With K^+ initially present in the vesicle interior, there is a much increased H^+ uptake and an overshoot. In all three cases, valinomycin increases H^+ uptake in the continuing presence of ATP, suggesting that either K^+ has been transported out of the vesicle or H^+ uptake is potential restricted. Because lipid-permeable cations do not mimic valinomycin, the former possibility is indicated.

On this basis, valinomycin thus increases access of K^+ to critical sites, and its action argues against the presence of an outward electrogenic K^+ pump.

If the H^+ pump were electrogenic, then the addition of protonophores before the addition of ATP should result in a reduction of the H^+ transport, which does occur by up to 40%, but the magnitude of the inhibition varies from preparation to preparation (fig. 6). Because TCS does increase the dissipation of the gradient, presumably owing to efflux along with Cl^-, the partial inhibition is not unexpected. This, taken along with the ATPase data, argues against a simple electrogenic pump for H^+.

Addition of ionophores during pump activity may also be informative. Thus, as shown in figures 6 and 9, valinomycin added during the presence of ATP, whether the vesicles were preequilibrated with K^+ or not, results in an increased H^+ uptake. Lipid permeable cations do not do this; hence again, the simplest interpretation is increased access of K^+ to intravesicular sites.

Anions clearly play a critical role in secretion by the intact mucosa. As shown in figure 10, monovalent anions are excellent substitutes for Cl^-. SO_4^{2-} restricts H^+ movement, and this effect is independent of K^+ in the vesicle interior. However, subsequent entry of K^+ might be restricted. The addition of valinomycin would in this case accelerate K^+ entry only as far as the reduced anion conductance would allow. There is indeed a stimulation of H^+ uptake with valinomycin addition. Also shown in this figure is the inhibitory action of 150 mM SCN. As pointed out before, the effect of SCN^- varies from preparation to preparation. In some cases virtually no inhibition is seen. In others, 20 mM results in significant inhibition. In no case, however, is there inhibition of the ATPase.

Cation efflux. As discussed in detail elsewhere,[28] it can be shown that Rb^+ efflux accompanies H^+ uptake at *p*H 6.1 and follows the *p*H profile of the enzyme's activity (fig. 11). Rb^+ efflux is inevitable whether the pump is electrogenic H^+ or not, provided that g_{Cl^-} is not much greater than g_{Rb^+}. Evidently, if g_{Cl^-} is zero, the H^+:Rb^+ ratio will approach unity.

However, one would expect valinomycin to increase Rb^+ efflux if g_{Cl^-} were finite, and lipid-permeable cations to decrease efflux if this efflux were dependent on a cation path elsewhere in the membrane. Neither event happens; hence, not only must g_{Cl^-} be close to zero, but also the g_{cation} must be high. Probably neither of these is true, based on the data already discussed; hence, the cation movement must be through specific pump pathways, i.e., the pump is a truly H^+:K^+ coupled pump at *p*H 6.1. Modeling this pump electrically is considered in the following section.

This concept also explains the greater H^+ transport in the presence of K^+ in the vesicle. Figure 9 shows that the rate of H^+ uptake is much higher with no K^+ gradient than with an inward K^+ gradient. In this figure

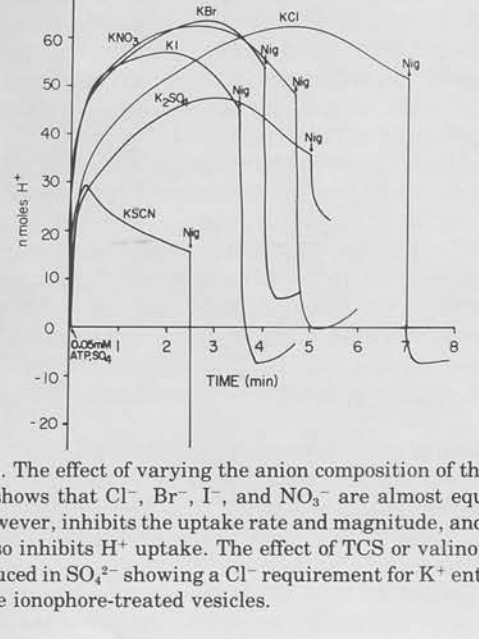

FIG. 10. The effect of varying the anion composition of the vesicle medium shows that Cl^-, Br^-, I^-, and NO_3^- are almost equivalent. SO_4^{2-}, however, inhibits the uptake rate and magnitude, and 150 mM KSCN also inhibits H^+ uptake. The effect of TCS or valinomycin is much reduced in SO_4^{2-} showing a Cl^- requirement for K^+ entry or H^+ exit in the ionophore-treated vesicles.

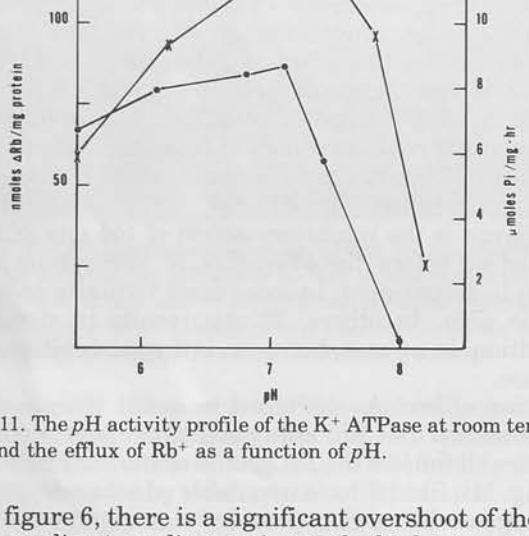

FIG. 11. The *p*H activity profile of the K^+ ATPase at room temperature and the efflux of Rb^+ as a function of *p*H.

and in figure 6, there is a significant overshoot of the H^+ (no K^+ gradient) gradient owing to the biphasic action of ATP. Thus the initial effect is to remove the intravesicular K^+ resulting in a rapid H^+ uptake. At this point, the ATPase reaction is rate limited by KCl influx, and the H^+ leak and the new H^+ uptake balance at a lower steady state. As shown in Figure 9, when the vesicles are not preequilibrated with KCl no overshoot is observed.

Vesicle potential. This can be measured by lipid-permeable ions, either fluorescent or radioactive.[28, 32] The distribution of these ions does not appear to change at *p*H 6.1 with the addition of ATP unless valinomycin is also present. This argues against the development of a large potential. Because Cl^- removal and SO_4^{2-} substitution does not alter this conclusion at *p*H 7.4, the absence of a potential does not appear to be due to a large g_{Cl^-}. The use of lipid-permeable ions, especially the highly soluble aromatic types such as anilinonaphthosulfonic acid or acridine orange, alters the properties of the membrane; thus, the cationic shunt conductance increases, and if the dye binds, induction of surface charge may also alter the ion permeability of the membrane. This may be particularly important when dealing with a membrane of low permeability, as appears to be the case with gastric vesicles.

Taken altogether, there is no evidence for a potential or conductance limitation for this H^+ transport phenomenon. One can consider two electrogenic explanations: an electrogenic H^+ pump with an inherent K^+ conductance, or coupled electrogenic H^+ and K^+ pumps.

General consideration of vesicle studies. In the former case the potential across the vesicle membrane would be given by

$$E = E_H g_H/(g_H + g_K + g_X)$$

where E_H is the electromotive force of the proton pump, and g_H and g_K are specific pump conductances, and g_X is all other conductances. In the absence of K^+, the potential across the membrane would be given by E_H. The rate of the pump is considerably slowed in the presence of Na^+. Increasing membrane conductance should then increase pump rate and H^+ uptake. As shown in figure 9, the addition of gramicidin, which activates ATPase but only slowly dissipates the gradient, does not result in increased uptake, but the gradient is dissipated. Measurements of vesicle potential using $S^{14}CN$ or 8-anilino-1-naphthosulfonic acid do not provide evidence for the development of a potential when Na^+ is substituted for K^+[28, 32] at *p*H 6.1.

Current flow in this model is given by

$$I_H = (E \cdot g_X)$$

Adding a g'_K (increase g_X) will increase I_H as found. An addition of proton conductance g'_H, because this will result in H^+ leak, will decrease I_H as found. The absence of a potential under K^+ conditions must mean that $g_{K^+} > g_{H^+}$, when the membrane is activated.

A more complex model, coupled electrogenic pumps, gives a potential

$$E = (E_H g_H - E_K g_K)/(g_H + g_K + g_X)$$

and a current

$$I_H = (E_H - E)g_H$$

Depending on the relative parameters the potential may vary about either side of zero, or be zero. Again, elimination of K^+ should result in a potential, and increasing g_X by any maneuver, provided that H^+ conductance is not increased, should increase current flow. Removal of a component of g_X (i.e., SO_4^{2-} for Cl^-) will reduce I_H or ATPase activity.

Many more examples could be taken, and although some data fit these types of model many do not. Accordingly, from these data, one has to consider the nonelectrogenic H^+:K^+ exchange model with a passive KCl entry into the vesicle. As illustrated in Figure 12, this pump requires K^+ in the vesicle interior and there are shunt pathways for K^+ and Cl^- in the membrane.

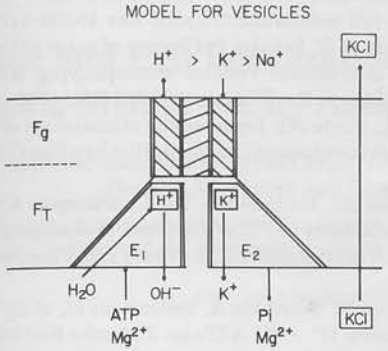

FIG. 12. A conceptual model of the ATPase, illustrated as a transducing unit $F_T(E_1E_2)$ and associated conductances F_g. The F_T form transports H^+ to the conductance unit, converting to E_2, and K^+ moves through another conductance to allow conversion of E_2 back to E_1. KCl enters the vesicle by other pathways.

Bilayer studies as detailed elsewhere provide a clue as to what might cause some of the difficulties with the vesicle studies.[29]

In the presence of K^+, the addition of ATP generates a potential when pump is incorporated into a planar bilayer. This potential decays in a thickness-dependent fashion, so that when the bilayer is thin, only a small potential develops. The continuing increase of current during this voltage decay suggests the model of an electrogenic H^+ limb with a specific pump conductance for K^+ which exceeds the H^+ conductance during pump activity.

Bilayer studies using a novel technique of forming the bilayer from the vesicle membranes themselves for the gastric ATPase and purified $Na^+ + K^+$ ATPase (kindly provided by Drs. Lois Lane and A. Schwartz) show different results. Here for the gastric K^+ ATPase an increase of conductance is produced, but no change in potential; however, for the $Na^+ + K^+$ ATPase, an increase in conductance and potential are observed. The former effect is inhibited by *p*-chloromercuribenzene sulfonic acid (pCMBS), the latter by ouabain (M.C. Goodall and G. Sachs, *unpublished data*).

These data can be explained by considering the model in figure 12 showing the pump as a dimer. If the E_1 to E_2 and E_2 to E_1 conversion were linked and K^+ dependent, the pump would be conductive but nonelectrogenic, with a 1:1 stoichiometry, even if the K^+ limb were essentially a conductance. If the pump could dissociate into the monomer form, then the standard planar bilayer data would be explained.

Relationship of vesicle studies to intact tissue. Calculations of the H^+ flux rate across the vesicle membranes gives a figure of about 5×10^5 molecules sec^{-1} μ^{-2}, similar to calculations made for the intact rat stomach.[33] K^+ is a known requirement for acid secretion.[34] Cl^-, however, plays a critical role, and as discussed, the metabolic data suggest the involvement of a component other than ATP.[12] In SO_4^{2-}, H^+ secretion appears to be electrogenic[35] and an H^+:ATP ratio of 4 exceeds thermodynamic possibility.

The two evident defects in the vesicle picture are the role of Cl^- and the role of the redox systems. The former could have what might be regarded as a trivial explanation. With onset of acid secretion, there is a fall in *p*H of the cell surface. Groups on this surface (glycocalyx) protonate, thereby increasing the surface positive charge. This restricts the movement of K^+ away from the surface and allows Cl^- to move away. This will facilitate K^+:H^+ exchange. At onset of secretion, before a large change in *p*H occurs, the initial secretion will therefore contain higher quantities of K^+ than later. There are many other possible explanations, such as the presence of a dissociable Cl^- conductance.

The evidence against a pure ATPase scheme is fairly formidable. Perhaps the most cogent is the finding that menadione can reverse amytal inhibition of Cl^- secretion by elevation of ATP levels, but not amytal inhibition of H^+ secretion.[11] The maximum ΔpH we have been able to observe in the vesicles using aminoacridine as an indicator is about 3. Perhaps a second pump in series is necessary to achieve the 10^6 H^+ gradient.

Studies on vesicles isolated from secreting tissue are needed to evaluate some of these possibilities. However, at worst, it seems clear that in these vesicles we are studying a critical component of the acid secretory mechanism; at best, it is the gastric proton pump.

REFERENCES

1. Sarau HM, Foley J, Moonsamy G, et al: Metabolism of dog gastric mucosa. 1. Nucleotide levels in parietal cell. J Biol Chem 250:8321–8329, 1975
2. Sarau HM, Foley J, Moonsamy G, et al: Metabolism of dog gastric mucosa. II. Levels of glycolytic and other intermediates. J Biol Chem (in press) 1977
3. Sachs G, Rabon E, Saccomani G, et al: Redox and ATP in acid secretion. Ann NY Acad Sci 264:456–475, 1976
4. Harris JB, Alonso D, Post OH, et al: Lipoate effect on carbohydrate and lipid metabolism and gastric H^+ secretion. Am J Physiol 228:964–971, 1976
5. Kidder GW, Curran PF, Rehm WS: Interactions between cytochrome system and H ion secretion in bullfrog gastric mucosa. Am J Physiol 211:153–159, 1966
6. Hersey SJ, Jobsis FF: Redox changes in the respiratory chain related to acid secretion by intact gastric mucosa. Biochem Biophys Res Commun 36:243–250, 1969
7. Rabon EC, Sarau HM, Rehm WS, et al: Redox involvement in acid secretion in the amphibian gastric mucosa. J Membr Biol (in press) 1977
8. Williamson JR: Mitochondrial metabolism and cell regulation. *In* Mitochondria Bioenergetic Biogenesis and Membrane Structure. Edited by L Packer, A Gomez-Puyon. New York, Academic Press, 1976, p 79–107
9. Hansford RG: Some properties of pyruvate and 2 oxoglutarate oxidation by blowfly plight muscle mitochondria. Biochem J 127:271–283, 1972
10. Kidder GW: Cytochrome c as a site of action of thiocyanate in frog gastric mucosa. Am J Physiol 219:645–648, 1970
11. Hersey SJ: Influence of amytal and menadione on high energy phosphates and acid secretion in frog gastric mucosa. Biochim Biophys Acta 496:359–366, 1977
12. Hersey SJ: Interactions between oxidation metabolism and acid secretion in gastric mucosa. Biochim Biophys Acta 244:157–203, 1975
13. Moody FG: Oxygen consumption during thiocyanate inhibition of gastric acid secretion in dogs. Am J Physiol 215:127–131, 1968
14. Saccomani G, Stewart HB, Shaw D, et al: Characterization of

gastric mucosal membranes. IX. Fractionation and purification of K^+ ATPase containing vesicles by zonal centrifugation and free flow electrophoresis technique. Biochim Biophys Acta 465:311–330, 1977.

15. Forte TM, Machen TE, Forte JG: Ultrastructural changes in oxyntic cells associated with secretory function: a membrane-recycling hypothesis. Gastroenterology 73:941–955, 1977
16. Ganser AL, Forte JG: K^+ stimulated ATPase in purified microsomes of bullfrog oxyntic cells. Biochim Biophys Acta 307:169–180, 1973
17. Kasbekar DK, Durbin RP: An adenosine triphosphatase from frog gastric mucosa. Biochim Biophys Acta 105:472–488, 1965
18. Flatmark T, Terland O: Cytochrome b_{561} of the bovine adrenal chromaffin granules. A high potential b type cytochrome. Biochim Biophys Acta 253:487–491, 1971
19. Jackson R, Stewart HB, Sachs G: Plasma membranes from normal and neoplastic colon. Cancer (in press) 1977
20. Schwartz IL, Schlatz LJ, Kinne-Saffran E, et al: Target cell polarity and membrane phosphorylation in relation to the mechanism of action of ADH. Proc Natl Acad Sci USA 71:2592–2599, 1974
21. Iyengar R, Mailman D, Sachs G: Separation of apical and basal-lateral membranes from renal medulla. Am J Physiol (in press) 1977
22. Sachs G, Chang H, Rabon EC, et al: A non-electrogenic H^+ pump in plasma membrane of hog stomach. J Biol Chem 251:7690–7698, 1976
23. Saccomani G, Shah G, Spenney JG, et al: Characterization of gastric mucosal membranes. VIII. Localization of peptides by iodination and phosphorylation. J Biol Chem 250:4802–4809, 1975
24. Skou JC: The enzymatic basis for active transport of Na^+ and K^+ across the cell membrane. Physiol Rev 45:596–617, 1965
25. Lee J, Simpson E, Scholes P: Change of outer pH in suspensions of gastric microsomal vesicles accompanying ATP hydrolysis. Biochem Biophys Res Commun 60:825–834, 1974
26. Ganser AL, Forte JG: Ionophoretic stimulation of K^+ ATPase of oxyntic cell membranes. Biochem Biophys Res Commun 54:690–696, 1973
27. MacLennan DH, Holland PC: The Ca transport ATPase of sarcoplasmic reticulum. *In* The Enzymes of Biological Membranes. Edited by A Martonosi. Vol. 3. New York, Plenum Press, 1976, p 221–260
28. Schackmann R, Schwartz A, Saccomani G, et al: Cation transport by gastric $H^+ + K^+$ ATPase. J Membr Biol 32:361–381, 1977
29. Goodall MC, Sachs G: Reconstitution of a proton pump from gastric vesicles. J Membr Biol (in press) 1977
30. Chang H, Saccomani G, Rabon E, et al: Proton transport by gastric membrane vesicles. Biochim Biophys Acta 464:313–327, 1977
31. Ramos S, Kaback HR: The relationship between the electrochemical proton gradient and active transport in *E. coli* membrane vesicles. Biochemistry 16:854–859, 1977
32. Lewin M, Schackmann R, Saccomani G, et al: The use of ANS as a probe of vesicle transport. J Membr Biol 32:301–318, 1977
33. Helander HF: An attempt to correlate functional and morphological data for the gastric parietal cells. Gastroenterology 73:956–957, 1977
34. Harris JB, Edelman IS: Transport of potassium by gastric mucosa of frog. Am J Physiol 198:280–284, 1960
35. Rehm WS: Electrophysiology of gastric mucosa in Cl^- free solutions. Fed Proc 24:1387–1395, 1965

Proc. Symp. Gastric Ion Transport, Uppsala 1977

Tissue and Cell Localization of Hog Gastric Plasma Membrane by Antibody Technique

Gaetano Saccomani, Silvia Crago, Anastasios A. Mihas, Douglas W. Dailey and George Sachs

From the Laboratory of Membrane Biology, University of Alabama in Birmingham, Birmingham, Alabama 35294, U.S.A.

Received 4 October 1977

STRACT: Antibodies have been obtained which specifically interact with e transport enzyme ($H^+ + K^+$)-ATPase. The antigen used was a highly tive gastric plasma membrane preparation from hog fundic mucosa purified homogeneity as judged by polyacrylamide gel electrophoresis. Gamma obulin from immunized animals, but not from control animals or pre-munesera, inhibited the K^+-ATPase activity up to a maximum of 80%. In-bation of alcohol fixed, parafin embedded section of hog fundus and trum with immune and preimmunesera as well as isolated rat parietal lls, followed by fluorescein conjugated anti-rabbit γ-globulin showed ecific binding of the latter (1) only following immunesera, (2) only the fundus, (3) only in the parietal cells, (4) mainly in the apical gion. These data confirm that the site of origin of the ($H^+ + K^+$)-Pase vesicles derives from the gastric parietal cell and is compatible th a role of this system in gastric H^+ secretion.

Over the past several years the complex mechanism of gastric acid se-etion by the gastric mucosa has been the subject of much research rough electrophysiological (1, 2, 3), metabolic (4, 5, 6) and ultra-ructural studies (7, 8, 9, 10) of this heterocellular epithelium.

To date it seems well established that the acid secretory cell of the stric mucosa contains an elaborate system of smooth membranes (tubulo-sicles) which are abundant in the apical region of the parietal cell d are directly involved in the secretory process (11, 12, 13).

Evidence has previously been presented to support the suggestion that e tubulo-vesicular membranes are isolated with a purified gastric

microsomal fraction derivated from fundic homogenate either from amphibian or mammalian tissue (14, 15, 16, 17).

Such purified microsomes possess an ATP hydrolyzing system, perhaps unique for the gastric tissue, which is cation dependent and is capable of catalyzing a K^+:H^+ exchange across the vesicle membranes and to act as an electroneutral proton pump (18, 19).

Based on these findings, it is important to define the cell type and the region of the cell from which the active fraction originates. In the present work immunological techniques were used for this purpose.

MATERIALS AND METHODS:

1. Membrane Isolation: Gastric membranes from hog fundic mucosa were prepared as previously described (17) by differential centrifugation, density gradient separation on zonal rotor and free-flow electrophoresis.

The final three fractions designated FI (vesicular structure associated with K^+-ATPase and K^+-pNPPase activities), FII (membranes containing the basal Mg^{2+}-ATPase and 5'-nucleotidase), and FIII (essentially membrane fragments containing K^+-ATPase and pNPPase activities) were routinely lyophilized and stored at -80°C prior to use for antibody study.

2. Preparation of antisera to membrane protein: New Zealand white rabbits were pre-bled and sera were obtained after clotting at r.t. for 1 hour and overnight at 4°C, then centrifuged at 3,000 x g for 15 minutes.

Two weeks after pre-bleeding, the rabbits were immunized using 1 mg of FI membrane protein fraction suspended in 1 ml of 0.9% NaCl solution and mixed with an equal volume of Freund's complete adjuvant.

Subsequent injections were administered bi-weekly for eight weeks and five days after the second injection the rabbits were bled and sera prepared as described above. Thereafter, rabbits were bled weekly and sera tested for immunreactivity towards the respective antigen (membrane pro-

by double immunodiffusion (20).

Fractionation and purification of antisera: Preparation of γ- globulins from preimmunesera as well as antisera were carried out by dropwise addition at 4°C of a volume of saturated $(NH_4)_2SO_4$ solution equal to the volume of the sera. After centrifugation at 10,000 x g for 30 minutes, the precipitate was resuspended in a volume of deionized water equal to 50% of the original volume of the sera. The precipitation and resolubilization cycle was repeated three times.

The final γ-globulin fractions were dialyzed against 150 mM Tris-Cl buffer (pH 7.4) at 4°C for a period of 72 hours.

In all experiments the antibody fractions were further purified by absorption on insoluble antigens (21). Antibodies and preimmunesera aliquots of about 0.5 ml each were stored at -20°C until use.

Chemical determination: Protein was determined by the method of Lowry, et al, (22). ATPase, 5'-nucleotidase, and pNPPase were analyzed as previously described (17).

For experiments in which the effect of antibodies on enzyme activities was studied, antigens either fresh or lyophilized, were pre-incubated at 37°C for 30 minutes with the purified antibodies and preimmunesera as controls, in the assay medium before substrate addition.

Cell isolation from rat fundic mucosa: Cell isolation and separation was performed following the method of Lewin et al., (23). Separation of parietal cells from other cell types was achieved by a serial centrifugation technique carried out at 100 x g for 45 seconds (24).

Parietal cells were identified by the dark blue granules after succinic dehydrogenase stain, using nitrotetrazolium blue (25).

Immunohistochemical studies: Immunofluorescence technique was carried out using the method of Sainte-Marie (26). Fifty to 100 µl of

antibodies (1.5 to 3.0 mg of protein) were applied to 5 - 6μ thick sections and incubated in moist atmosphere at r.t. for 45 minutes.

After washing in phosphate-buffered saline, the sections were stained by 'indirect method' (27) and fluorescein-isothiocyanate conjugated goat anti-rabbit γ-globulin (Hyland Lab., Los Angeles, CA.) reconstituted in 1.0 ml of sterile distilled water, using 50 - 100 μl of a 1/10 dilute solution.

Following incubation at r.t. for 45 minutes, the sections were washed overnight and mounted in buffered ethanol. Stained sections were examined with a Leitz fluorescence microscope and photographed. The specificity of the staining was determined by using the preimmunesera and rabbit anti-IgG, IgA, and IgM as controls.

For the immunofluorescence study, enriched preparations of rat parietal cells were washed twice in phosphate-buffered saline containing 1% bovine serum albumin and 0.03% Na azide. Two hundred μl of cell suspension containing about 1-5 x 10^6 cells were incubated at r.t. for 1 hour with 100 μl of antibodies or γ-globulin from non-immunized rabbit.

After being spun down at 100 x g for 5 minutes, the sediment was washed twice. The pellet was resuspended in 200 μl of phosphate-buffered saline and 100 μl of 1/10 dilute fluorescein conjugated goat, anti-rabbit γ-globulin were added. After 30 minutes incubation at r.t., the cells were washed and the final pellet dispersed in a few drops of buffer. The suspension was examined under the fluorescence microscope.

7. Polyacrylamide gel electrophoresis: Gel electrophoresis was performed with 5.6% acrylamide (28) in 0.1% SDS. Samples were solubilized in 1.0% SDS - 1.0% β-mercaptoethanol and 10 - 15 μg of protein were applied to each gel. Staining and distaining for protein and carbohydrates were carried out as previously described (16).

RESULTS AND DISCUSSION:

The gastric K^+-ATPase is a membrane-bound enzyme composed of about 95% of one glycoprotein of 105,000 M.W. It has been purified from hog fundic mucosa (17) using differential centrifugation, density gradient separation, and free-flow electrophoresis. The fractionation procedure yielded a distinct separation between membranes carrying Mg^{2+}-ATPase and 5'-AMPase and membranes containing K^+-ATPase (or p-nitrophenyl phosphatase)(Table I).

TABLE I

PURIFICATION OF GII GASTRIC MEMBRANE FRACTION
Activities are expressed in μmoles Pi and pNP/mg protein/hr

Fractions		5'-AMPase	Mg^{2+}-ATPase	K^+-ATPase*	K^+-pNPPase
GII	(zonal)	2.2 ± 0.3	19.4 ± 1.8	63.6 ± 2.0	61.2 ± 4.2
GII-FI	(FFE)	0.3 ± 0.06	4.4 ± 1.0	110.7 ± 2.6	68.0 ± 2.5
GII-FII	(FFE)	5.4 ± 1.0	31.0 ± 3.1	20.0 ± 0.7	9.4 ± 1.0
GII-FIII	(FFE)	0.1 ± 0.1	2.8 ± 0.4	50.1 ± 3.2	31.0 ± 2.2

*Activity in presence of 20 mM KCl minus the basal rate.

Along with the 40-fold enrichment in K^+-ATPase activity (17), this vesicular fraction FI responded to ATP addition in terms of H^+ uptake and K^+ extrusion (18, 19).

Although ultrastructural evidence indicates that the parietal cell contains an abundant intracytoplasmic vesicular system (11, 12) and H^+ transport is a property of the isolated FI vesicles (18, 19), direct evidence that these vesicles derive from the acid secretory region of the parietal cell has been lacking.

Since enzyme-specific antibodies have proven to be sensitive and powerful probes for the purpose of elucidating structural and functional characteristics of certain enzymes (29, 30, 31) as well as their locali-

zation into the particular biological system from which they derive (32), we used immunochemical studies directed to determine the tissue and cell origin of the purified K^+-ATPase membrane fraction.

Antibodies were obtained from the serum of rabbits injected with several preparations of purified and highly active native enzyme. The γ-globulin obtained from anti-serum was purified by adsorption to and elution from the enzyme in the native membrane fraction and the antigen-antibody reaction was tested by double diffusion technique.

Immunodiffusion of purified anti K^+-ATPase γ-globulin (FI AB) against Triton X-100 solubilized enzyme (FI Ag) gave single precipitation band, while no immunoreactivity was detected when FII and FIII membrane fractions were used (Fig. 1). Serum and γ-globulin from non-immunized rabbits did not give any precipitation bands.

These results indicate that specific complex formation is only obtained between FI Ag and FI AB.

It is known that antibodies may produce inhibition or stimulation of enzyme activity, may alter certain physical characteristics, or may react with the enzyme without causing detectable changes in enzymatic activity (31).

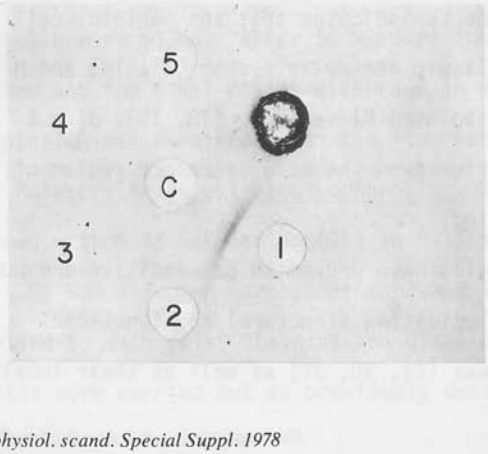

Fig. 1. Double diffusion gel precipitation. Well C contains FI AB. Peripheral wells contain: (1) FI Ag; (2) FII Ag; (3) FIII Ag; (4) control globulin; (5) control globulin. Antigens were solubilized in 1% Triton X-10

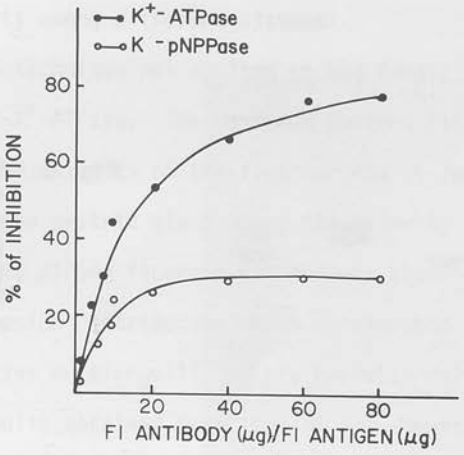

Fig. 2. Inhibitory effects of varying concentration of FI AB preparation on K^+-ATPase and pNPPase activities. In these studies, 5 μg of enzyme were used.

Fig. 2 shows the effects of varying concentration of the purified anti-K^+-ATPase γ-globulin obtained from two different rabbits, on K^+-ATPase and pNPPase activities of the native enzyme. It is evident from the results that the degree of inhibition of enzyme activities was proportional to the increasing amounts of antibody with maximal inhibition of about 80% for the K^+-stimulated ATPase and approximately 30% for the K^+-activated pNPPase. The control γ-globulin fraction from non-immunized rabbit did not inhibit the enzyme activities. Since no inhibition of the basal Mg^{2+}-ATPase' was detected, this antibody is specific for the K^+ activation step, consistent with its effect on the phosphatase.

However, antibodies obtained from two other rabbits did not affect the enzyme activities, although showing immunreactivity when tested by double-diffusion technique against solubilized FI Ag.

Since in this case the antibodies did not inactivate the enzyme activity, it was necessary to provide convincing evidence that they were bound specifically to the enzyme and not to impurities. For this purpose, FI Ag in native form was incubated with different concentrations of FI AB at 37°C for 30 min. The mixtures were allowed to stand at 4°C

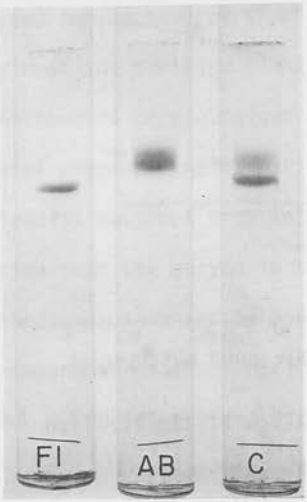

Fig. 3. SDS-polyacrylamide gel electrophoresis. (FI), purified K^+-ATPase membrane fraction; (AB), FI specific antibody; (C) FI Ag- FI AB complex. Experiments were carried out as described in the text.

overnight and were then centrifuged at 100,000 x g for 60 min. After the pellets were washed by resuspension in water followed by centrifugation for three times, the final immunoprecipitates were dissociated in 1% SDS and electrophoresed as described (28).

Fig. 3 shows the gel pattern obtained from a typical experiment. It can be seen that the immunoprecipitate contains only two polypeptides corresponding to FI Ag and FI AB, indicating a specific non-covalent binding between the two proteins. When FII membrane fraction was incubated with FI AB and experiments carried out as described above, the gel pattern of the immunoprecipitate showed only the presence of FII polypeptides pattern indicating once more that FI AB was specifically produced against FI Ag. This is in agreement with the fact that greater than 95% of the protein in the immunizing FI Ag was K^+-ATPase.

The availability of antibody specifically directed against the membrane-bound K^+-ATPase made it possible for us to determine the localization of

is antigen and its specificity among different tissues.

Indirect immunofluorescence technique was applied on hog fundic sec-ions, using the purified anti-K^+-ATPase. The staining pattern illu-rated in Fig. 4 shows that the majority of the fluorescence is localized the middle third region of the gastric gland where the majority of arietal cells is present. This strong fluorescence appears also to have ainly a supranuclear apical region distribution which corresponds to e region of the tubulo-vesicles or microvilli of the parietal cell. Sections treated with γ-globulin obtained from sera of non-immunized bbits were uniformly negative. Antrum sections as well as sections om ten other different tissues did not show any positive fluorescence aining confirming the specificity of the FI AB only for the fundic cosa.

It is often difficult to determine with accuracy the cell type and cell egion from which a particular antigen derives just by fluorescent tissue ections, especially when it is a complex system like the gastric mucosa. munofluorescence studies performed on isolated and separated cells from ndic mucosa could be more informative.

When suspensions of isolated cells from rat stomach were treated with

ig. 4. Indirect immunofluorescent staining of hog fundic mucosa gland in the middle third region, with FI AB (x270).

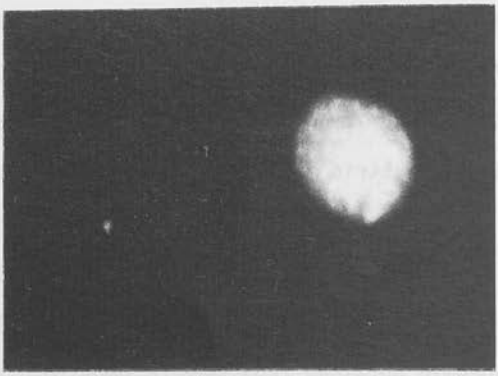

Fig. 5. Staining pattern observed in rabbit isolated parietal (right) and chief (left) cells with FI AB (x775).

purified anti-K^+-ATPase antibody and goat anti-rabbit γ-globulin fluorescent reagent, only the parietal cells shows a strong positive staining (Fig. 5). On some parietal cells of the same preparation, fluorescence was distributed on the entire surface, while on most of them a more regular perimeter membrane staining was observed. The intensity of the stain was quite pronounced in one region of the cell, probably the apical surface (Fig. 6). Suspensions treated with γ-globulin from non-immunized rabbit were uniformly negative.

In conclusion, we have demonstrated that antibody raised against and

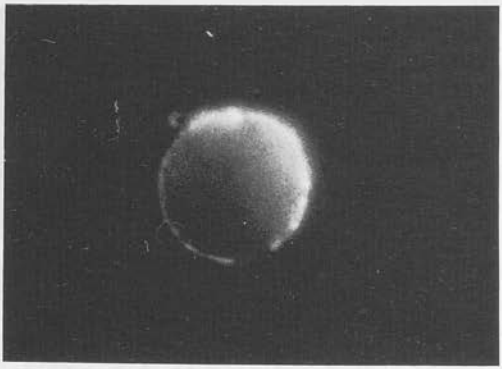

Fig. 6. Immunofluorescent staining of an isolated rat parietal cell with FI anti-K^+-ATPase (x775).

ecific for a gastric K^+-ATPase membrane system, stains by immunofluore-
ence cells derived from fundic epithelium and does not stain cells
riginating from other tissues. Thus, this antibody appears to be organ-
ecific.

In addition, the antibody may well be cell-type-specific because it
oes not stain cells other than parietal. The antigen detected by the
nti-K^+-ATPase antibody is located on the parietal cell surface as demon-
trated by the perimeter-type of immunofluorescence staining.

Because viable, intact cells were used in the present experiments rather
han fixed cells, the possibility that the surface antigen detected by
nti-K^+-ATPase is also present in the intracytoplasmic vesicular system
annot be ruled out.

The recent technique of ultracryotomy (33) for locating antigens and
etermining their distributions within cells ultrastructural intact, by
taining them with ferritin-conjugated antibodies, will definitely prove
his point. Such studies are presently in progress.

ACKNOWLEDGMENT:

This work was supported in part by grants NIH AM 15878 and NSF
PCM-77-18951.

REFERENCES:

1. Rehm, W.S. (1965) Fed. Proc. 24: 1387.
2. Harris, J.B. and Edelman, I.S. (1964) Am. J. Physiol. 206: 769.
3. Heinz, E. and Durbin, R.P. (1959) Biochim. Biophys. Acta 31: 246.
4. Hersey, S.J. (1974) Biochim. Biophys. Acta 344: 157.
5. Durbin, R.P. (1973) Curr. Top. Mem. Transport 4: 305.
6. Sarau, H.M., Foley, J., Moonsamy, G., Wiebelhaus, V.D., Sachs, G. (1975) J. Biol. Chem. 250: 8321.
7. Sedar, A.W. (1961) J. Biophys. Biochem. Cytol. 10: 47.
8. Helander, H.F. (1964) J. Ultrastruct. Res. 10: 160.
9. Ito, S. (1961) J. Biophys. Biochem. Cytol. 11: 333.
10. Sedar, A.W. and Wiebelhaus, V.D. (1972) Am. J. Physiol. 233: 1088.
11. Helander, H.F. and Hirschowitz, B.I. (1972) Gastroenterology 63: 951.
12. Forte, T.M., Machen, T.E. and Forte, J.G. (1975) Gastroenterology 69: 1208.
13. Forte, J.G., Forte, T.M. and Ray, T.K. (1972) IN: Gastric Secretion (Sachs, G., ed), pp. 37, Academic Press, N.Y.
14. Ganser, A. and Forte, J.G. (1973) Biochim. Biophys. Acta 307: 169.
15. Forte, J.G., Forte, T.M. and Saltman, P. (1967) J. Cell. Physiol. 69: 293.
16. Saccomani, G., Shah, G., Spenney, J.G. and Sachs, G. (1975) J. Biol. Chem. 250: 4802.
17. Saccomani, G., Stewart, H.B., Shaw, D., Lewin, M. and Sachs, G. (1977) Biochim. Biophys. Acta 465: 311.
18. Sachs, G., Chang, H.H., Rabon, E., Schackmann, R., Lewin, M. and Saccomani, G. (1976) J. Biol. Chem. 251: 7690.
19. Chang, H.H., Saccomani, G., Rabon, E., Schackmann, R. and Sachs, G.

(1977) Biochim. Biophys. Acta 464: 313.

Ouchterlony, O. (1948) Acta Pathol. Microbiol. Scand. 25: 186.

McCans, J.L., Lane, L.K., Lindenmayer, G.E., Butler, V.P. and Schwartz, A. (1974) Proc. Nat. Acad. Sci. 71: 2449.

Lowry, O.H., Rosebrough, N.J., Farr, A.L. and Randall, R.J. (1951) J. Biol. Chem. 193: 265.

Lewin, M., Cheret, A.M., Soumarmon, A. and Girodet, J. (1974) Biol. Gastroenterol. 7: 139.

Soumarmon, A., Cheret, A.M. and Lewin, M. (1977) Gastroenterology (in press).

Blum, A.L., Shah, G., Wiebelhaus, V.D., Brennan, F.T., Helander, H.F., Ceballos, R. and Sachs, G. (1971) Gastroenterology 62: 189.

Sainte-Marie, G. (1962) J. Histochem. Cytochem. 10: 250.

Winchester, R.J. IN: In Vitro Methods in Cell Mediated and Tumor Immunity (1976) (Bloom, B.R., ed), pp. 171, Academic Press, N.Y.

Fairbanks, G., Steck, T.L. and Wallach, D.F.H. (1971) Biochem. 10: 2606.

Martonosi, A. and Fortier, F. (1974) Biochem. Biophys. Res. Comm. 60: 382.

Jean, D.H., Albers, R.W. and Koval, G.J. (1975) J. Biol. Chem. 250: 1035.

Celada, F. and Strom, R. (1972) Quart. Rev. Biophys. 5: 395.

Kyte, J. (1974) J. Biol. Chem. 249: 3652.

Tokuyasu, K.T. (1973) J. Cell. Biol. 57: 551.

Proc. Symp. Gastric Ion Transport, Uppsala 1977

Transport Parameters of Gastric Vesicles

Edwin Rabon, Hsuan Hung Chang, Gaetano Saccomani
and George Sachs

From the Laboratory of Membrane Biology, University of Alabama in Birmingham, University Station, Birmingham, Alabama 35294 U.S.A.

Received 4 October 1977

BSTRACT: Studies are reported using the effects of osmolarity on astric vesicle uptake of H^+, indicating that an exchange of H^+ for K^+ r a symport of K^+ with OH^-, is the major mechanism of H^+ ion uptake. sing carbocyanine dyes and other techniques the only potentials detected n the vesicles are those due to secondary diffusion potentials. Studies ith 9 amino-acridine show that there is a discrepancy in the ΔpH by this ethod as compared to electrode or imidazole uptake measurements. The ction of SCN^- appears to be inhibition of a forward reaction in the ransport, rather than increase of leak paths, and there is a discrepancy sing acridine orange both quantitatively with ΔpH measurements and with espect to SCN^- action, in that the AO signal is more sensitive to SCN^- han ΔpH.

ASIC OBSERVATIONS: In the last few years, the study of the enzyme eactions and transport properties of gastric vesicles has become a major rontier in an attempt to understand H^+ transport by the stomach (1, 2, 3, 4, 5). The key observations are illustrated in Fig. 1 where it is seen hat the addition of ATP (at pH 6.1) results in alkalinization of the edium. After the ATP has been utilized, a combination of a protonophore (tetrachlorsalicylanilide, TCS) and a K^+ ionophore (valinomycin) are required to dissipate the formed H^+ gradient. Alternatively, nigericin, a neutral exchange cation ionophore abolishes the gradient. Since two conductance pathways must be provided, it is tempting to conclude that H^+ uptake by the vesicles is non-electrogenic. It must be emphasized

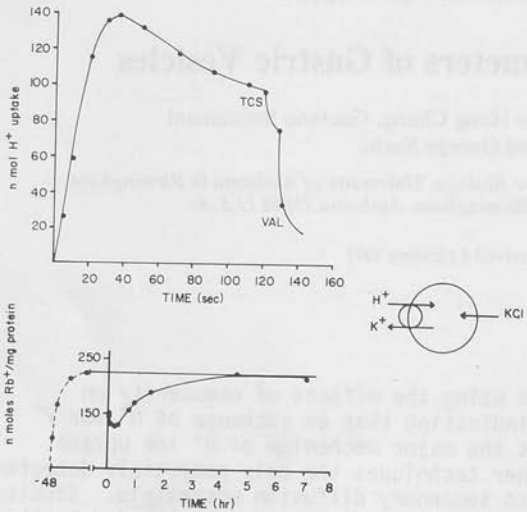

Fig.1 The upper part of the figure shows that with the addition of 1.7×10^{-5}M ATP, H^+ disappears from the medium and both TCS and valinomycin are required to dissipate the gradient. The lower part of the figure shows that $^{86}Rb^+$ is extracted from pre-equilibrated vesicles with the addition of ATP.

that this assumes the addition of ATP does not change the conductance properties of the vesicles which, based on bilayer studies, is not correct (6), since ATP increases the K^+ conductance.

Also in fig.1, the efflux of $^{86}Rb^+$ is measured, from an equilibrium situation with ATP addition, showing that efflux of cation accompanies uptake of H^+ (or appearance of OH^-). Again, on this basis, we may conclude that an H^+:K^+ exchange occurs with the addition of ATP. However, if the pump were electrogenic, driving H^+ into the vesicle, and the only conductance were K^+, an efflux of K^+(Rb^+)would be associated with the H^+ uptake. Alternatively, the H^+:K^+ countertransport could be a direct result of an H^+:K^+ exchange pump similar in principle to the $Na^+ + K^+$ ATPase. Since it has been shown that Rb^+ efflux is insensitive to protonophores, valinomycin, buffer strength or lipid permeable cations, the latter conclusion was made more likely (3,5) but not definite. Moreover, the existence of an H^+:K^+ exchange does not determine whether the exchange is electrogenic or neutral.

TRANSPORT MODELS: Considering that the ion movements are observed with

e sole addition of KCl to the medium, the possible mechanisms are classified in fig.2. The simplest type of pump would be an H^+ uniport(electrogenic H^+) with the electrical requirements satisfied by a Cl^- or K^+ onductance. In this situation there is net flux of ions independent of e initial ion content of the vesicles. Hence, osmotic sensitivity of ptake is always independent of the time of KCl equilibration. A Cl^- niport associated with a H^+ conductance would give the observed H^+ upake. Osmotic sensitivity would also not be altered by KCl preincubation. e above two uniports, however, would be readily distingusihed by the use

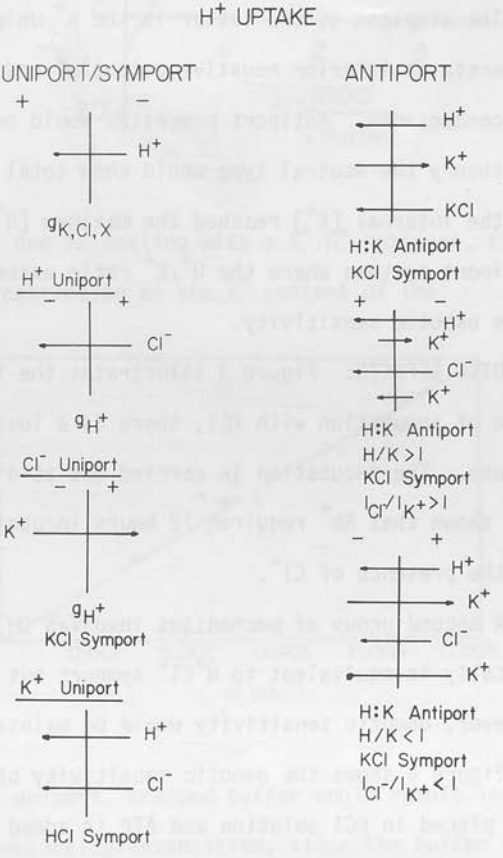

Fig.2 A series of conceptual models illustrating the possible ways in which H^+ uptake occurs due to the ATPase with only KCl added to the medium. For brevity OH^- mechanisms are not illustrated

of ionophores prior to, or in the presence of ATP, as well as a different sign of the vesicle potential. An HCl symport would also provide H^+ uptake and show maintained osmotic sensitivity, but would not result in the development of a vesicle potential. Not illustrated is coupled H^+ and Cl^- uniport. These would show identical properties to the HCl symport, except that with the absence of anion pumping, the vesicle would develop an internal positive potential.

All of these mechanisms would maintain osmotic sensitivity in spite of internal KCl. The next group of mechanisms would show progressive loss of osmotic sensitivity as the vesicles equilibrate with medium K^+.

The simplest of the latter is the K^+ uniport mechanism which would generate an interior negative potential and H^+ uptake due to an associated H^+ conductance. Antiport processes would be neutral or electrogenic. In theory the neutral type would show total loss of osmotic sensitivity as the internal $[K^+]$ reached the maximum $[H^+]$ achievable. Electrogenic antiport systems where the H^+/K^+ ratio exceeded unity would only partially lose osmotic sensitivity.

OSMOTIC EFFECTS: Figure 3 illustrates the finding that with progressive time of incubation with KCl, there is a loss of osmotic sensitivity of H^+ uptake. The incubation is carried out at 4°C, and in previous work it was shown that Rb^+ requires 72 hours incubation to reach equilibrium (5), in the presence of Cl^-.

A second group of mechanisms involves OH^-/Cl^- antiport which experimentally is equivalent to H^+Cl^- symport but is conceptually different. However, osmotic sensitivity would be maintained with this mechanism.

Figure 4 shows the osmotic sensitivity of H^+ uptake where vesicles are placed in KCl solution and ATP is added two minutes later. It can be seen that uptake is completely sensitive to vesicle volume and apparently

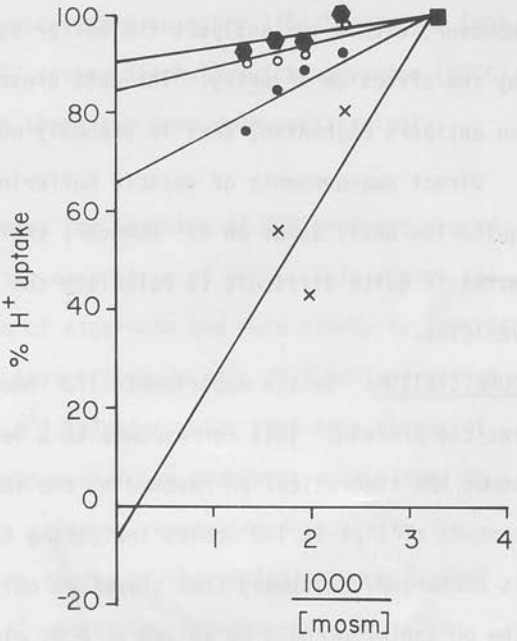

Fig. 3. The osmotic sensitivity of H^+ uptake with progressive preincubation times in KCl: x—x 5 min., ●—● 24 hrs., o—o 48 hrs, ■—■ 72 hrs. Medium osmolarity was varied with mannitol.

o binding occurs. However, if one is dealing with a K^+:H^+ antiport, the smotic sensitivity is due to restriction on the K^+ content of the

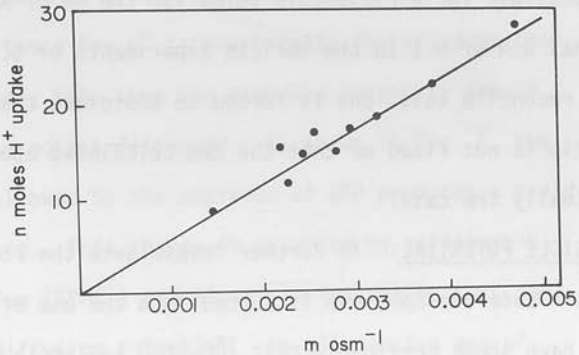

Fig. 4. The osmotic sensitivity of H^+ uptake following only 2 min. preequilibration with KCl.

esicles. With a reversible H^+ uniport, trapped buffer would result in a fraction of the uptake being osmotically insensitive, since the buffer

content would remain the same although vesicle volume is decreasing. However, with K^+:H^+ antiport the buffering capacity would be obscured by the effect on K^+ entry. The data presented here are consistent with an antiport mechanism, that is probably non-electrogenic.

Direct measurements of vesicle buffering capacity indicates that it is quite low until about pH 2. However, the possible buffering capacity makes it quite difficult to calculate the internal pH reached by the vesicles.

QUANTITATION: In six experiments 173 nmoles H^+ were taken up by 1 mg vesicle protein. This corresponds to a vesicular volume of 2 µl and hence the theoretical pH reached by the vesicle is 1.06. The initial K^+ content of 1 µl is 150 nmoles indicating that only about half of the K^+ is exchanged. Assuming that therefore only half of the vesicles transport, the pH achieved could be as low as 0.8, close to the maximum attainable by mammalian mucosa.

Measurement of the initial stoichiometry of the H^+ uptake showed that the H^+/ATP ratio was close to 4 (3). This rate is thermodynamically impossible for a reasonable value for the ΔG of ATP hydrolysis, at a final ΔpH of 5.3 in the vesicle experiments or 6.6 in the intact mucosa. To reconcile this, one is forced to postulate that either the H^+/ATP ratio is not fixed or that the ΔpH calculated above is much higher than actually the case.

VESICLE POTENTIAL: To further investigate the role of potentials or to quantitate the ΔpH, one is forced into the use of lipid permeable ions. We have shown previously that ^{14}C-SCN^- redistributes across the vesicle membrane only in the presence of valinomycin and ATP (3, 5). Similar data were obtained for 8-anilino-napthalene-1-sulfonate (7). This was interpreted as showing that the only potential generated by the vesicles

as a secondary K^+ diffusion potential in the presence of valinomycin. However, our observations were extended to other lipid permeable ions such as the carbocyanine dyes (8) either diethyloxadicarbocyanine (DOCC) or di-$SC_{(3)}$-5. The results with these two dyes were qualitatively identical.

In the absence of any ionophore, the addition of ATP produces a gradual ($t_{1/2}$ > 60 sec) decline in the absorption of DOCC. This change is rapidly reversed by the addition of nigericin and more slowly by lowering external pH. On the assumption that nigericin acts as a neutral cation exchange ionophore (i.e. K^+ for H^+) this indicates that this change of DOCC absorption is due to the presence of ion gradients established by the ATPase, rather than due to a potential generated directly by the pump (Fig. 5). However, the time course of the optical change is much slower than the time course of H^+ uptake (or disappearance from the medium) and would suggest that the ratio of g_{H^+}/g_{K^+} is increasing over the time of change of DOCC absorbance. Since DOCC is a lipid permeable cation, the vesicle interior is apparently becoming negative. Alternatively, the vesicles could be developing a Cl^- conductance.

If the membrane conductance for H^+ is drastically increased by the addition of a protonophore, TCS, then the membrane potential should directly reflect the H^+ gradient developed. As shown in Fig. 6, the prior addition of TCS followed by the addition of ATP produces a rapid decline in DOCC absorbance. This change is reversed by valinomycin, triphenylmethylphosphonium ($TPMP^+$) and nigericin indicating that the change is due to an H^+ diffusion potential. An alternative way of showing that changes are due to secondary diffusion potentials, rather than primary pump potentials is to use, in the case of H^+, penetrating buffers such as imidazole. As in Fig. 6, increasing imidazole inhibits

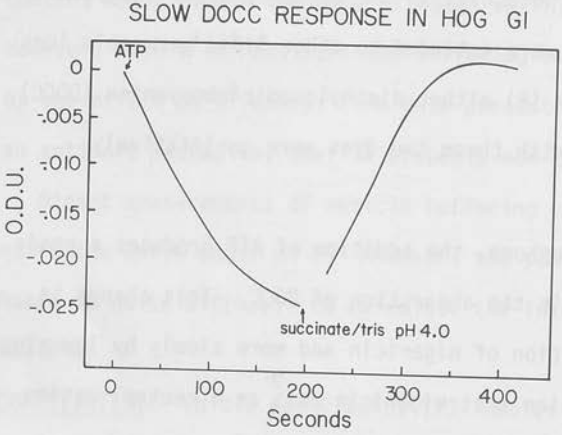

Fig. 5. The slow absorbance change induced by ATP with the dye DOCC, showing reversal by altering medium pH.

the DOCC signal. Since imidazole does not inhibit the ATPase, the simplest explanation is that, with the unprotonated form being freely permeable, imidazole reduces the ΔpH across the vesicle membrane. Accordingly, if the vesicles possessed a reversible electrogenic H^+ pump, potential would be maximized as ΔpH minimized since (9)

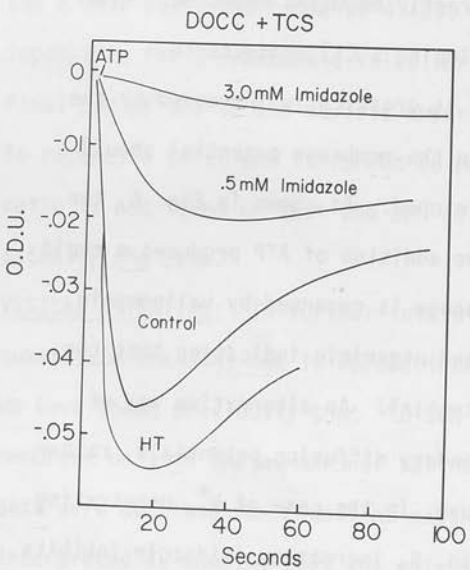

Fig. 6. The effect of ATP on DOCC absorbance in the presence of TCS, varying concentrations of imidazole and in the presence of hypertonic mannitol.

$$\Delta\bar{\mu}_H = \Delta\Psi - \frac{RT}{F}\Delta pH$$

Imidazole would maximize the potential if we were dealing with an electrogenic H^+ pump. The additional assumption for this conclusion is that the protonated form of imidazole is very much less permeable than the neutral form and therefore imidazole does not act as a good uncoupler of the system. Since imidazole in the absence of TCS does not mimic TCS, this assumption is probably correct.

The data, therefore, with ANS as a liphophilic anion and DOCC as a liphophilic cation indicate that although secondary diffusion potentials can be generated by the H:K ATPase, the enzyme present in hog gastric vesicles does not of itself generate a potential across the vesicle membrane upon energization.

It is also possible to use the TCS dependent H^+ diffusion potential to test the effect of osmolarity on the H^+ gradient. If it is true that increasing vesicular volume by osmole addition fixes K^+ content, but increases K^+ concentration and thereby increases the $[K^+]$ driving the H^+ exchange, then, with the quantity of H^+ uptake being constant, the H^+ gradient will increase. According to this picture, increasing the osmolarity will increase the H^+ diffusion potential in the presence of TCS, and, if this dominates the picture, will increase the DOCC signal. As shown in Fig. 6, this appears to be the case.

VESICLE pH: Fluorescent dyes or pH indicator dyes may also be used in an attempt to quantitate the intravesicular pH.

One of the dyes most frequently used is 9-amino acridine (9 A.A.] (10). The following equation is used

$$\frac{H^+_i}{H^+_o} = \frac{Q}{1-Q} \cdot v^{-1}$$

where H^+_i/H^+_o is the H^+ concentration ratio, Q is the fractional quench,

and v^{-1} is the reciprocal of the fraction of total volume that is intravesicular space. The use of this equation rests on several assumptions, such as that the dye which enters the vesicle in response to an H^+ gradient is free and not bound; that all the intravesicular dye is quenched; that entry of the dye does not change intravesicular volume and that the dye does not act as an uncoupler.

A typical 9 A.A. response is shown in Fig. 7. The action of inhibitors, ionophores and imidazole shows that the 9 A.A. is responding to a ΔpH. Quantitatively, this corresponds to a ΔpH of 3 units, i.e. an uptake of 1 nmole $H^+ \mu l^{-1}$ vesicle space. This low value could be due to intravesicular buffering capacity or because some of the above assumptions are incorrect. In separate experiments it was shown that the signal was only partially osmotically sensitive and the degree of osmotic sensitivity was critically dependent on 9 A.A. concentration. Accordingly, there are binding sites for 9 A.A. induced by ATP addition. At concentra-

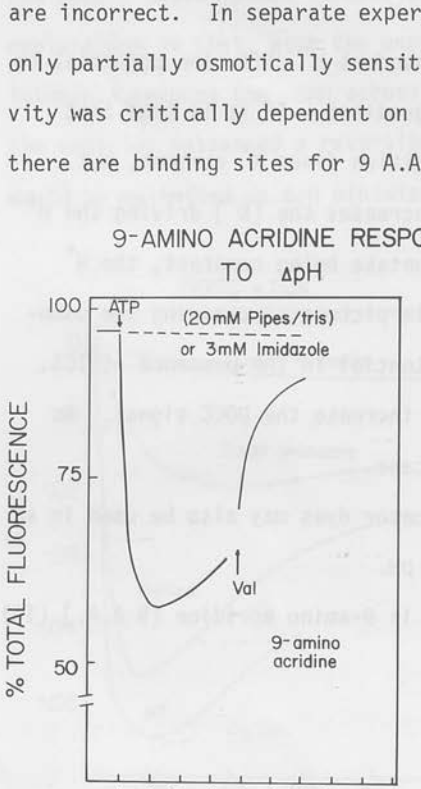

Fig. 7. The response of 9-amino acridine fluorescence to ATP addition, followed by the addition of valinomycin, or in the presence of imidazole or strong buffer.

ions of 9 A.A. such as 10 μM, where binding makes a less significant contribution, the ΔpH as measured by the pH electrode technique decreases. This shows that another problem exists, since the efflux of H^+

$$J^{H^+}_{out} = k_1[H^+] + k_2[AH^+]$$

where k_1 is the H^+ permeability and k_2 is the permeability of protonated base (eg. 9 A.A.). Even if $k_2 << k_1$, as $[AH^+]$ increases, the second term can become significant. The loss of pH signal provides evidence, therefore, that 9 A.A. at concentrations adequate to obscure binding, can partially uncouple these vesicles. It is therefore questionable whether we can accept that ΔpH of 3 as being true of the situation in the absence of 9 A.A.

Use of the weak base ^{14}C imidazole, and measuring trapping by filtration gave data in our best experiments showing uptake of better than 20 nmoles H^+ from calculation of the buffering capacity of imidazole and from the equation

$$\frac{I_i}{I_o} = \frac{K_A + H^+_i}{K_A + H^+_o}$$

where I refers to imidazole concentration (11). This is less than that found by direct ΔpH measurements, but considerably more than that found by the 9 A.A. technique.

VESICLE DYE BINDING: Membrane changes can also be monitored by binding of a dye such as acridine orange (AO). This has been shown to undergo binding dependent quench of fluorescence in various vesicle preparations (12) including hog gastric vesicles and frog gastric vesicles (13). There are several noteworthy features about these reactions. Since acridine orange is positively charged, binding is to negative sites induced by the addition of ATP. The signal reproduces many of the proper-

ties already established by the pH electrode i.e., K^+ dependent, enhanced by internal K^+, dissipated by nigericin and other ionophores (Fig. 8). It depends on intact vesicles but is not quantitatively related to the amount of H^+ uptake. Thus, although hog vesicles take up about 20 times more H^+ than frog, the AO signal is approximately the same. Another feature of the AO response is that it is partially osmotically sensitive, indicating that not all the response is due to binding.

AO thus senses the development of negative binding sites in the vesicle membrane that are related, but not quantitatively, to H^+ (or OH^-) movement across the vesicle membrane. The site, being sensitive to buffer, is in the outside region of the membranes.

ACTION OF SCN^-: SCN^- action has been a constant problem in gastric physiology for more than 30 years. The use of gastric vesicles perhaps might be expected to solve the mechanism of action of this compound. When vesicles are placed in a KCl medium and ATP is added, based on the K^+:H^+ antiport (or K^+:OH^- symport) hypothesis, prior to proton gradient develop-

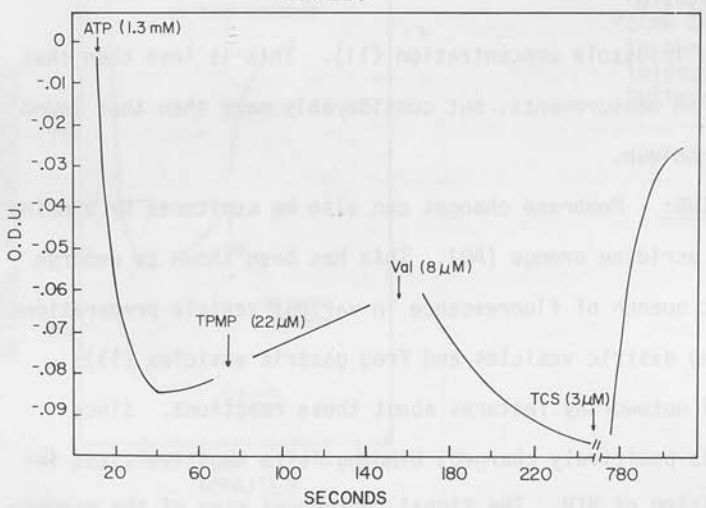

Fig. 8. The effect of ATP on acridine orange absorbance, showing that whereas $TPMP^+$ has little effect, valinomycin increases the response, which is subsequently dissipated by TCS.

ent, KCl has to enter the vesicle. A considerable amount of evidence as accumulated that in the absence of ATP, vesicle conductance to either $^+$ or Cl^- is low. This suggests that a KCl symport pathway is involved ted K^+ uptake for the transport reaction.

20 Accordingly, inhibition of transport by the vesicles could occur (a) her by inhibition of the ATPase, (b) by increasing the H^+ leak and (c) by e, inhibition of the KCl symport. When vesicles are placed in KCl solution cle for a short time and then ATP is added, H^+ uptake occurs in two phases, nt as shown in Fig. 9 with two clearly different rate constants.

n As shown in Fig. 9, SCN^- does not affect the fast uptake, but blocks the slow uptake phase. SCN^- added subsequent to the development of an H^+ gradient does not increase the leak of H^+, nor does SCN^- inhibit the ht ATPase of hog gastric vesicles. Thus, SCN^- interferes with the KCl sym- port step in some manner. The AO signal is also sensitive to SCN^-, being completely abolished if 30 mM SCN^- is added prior to the addition of ATP.

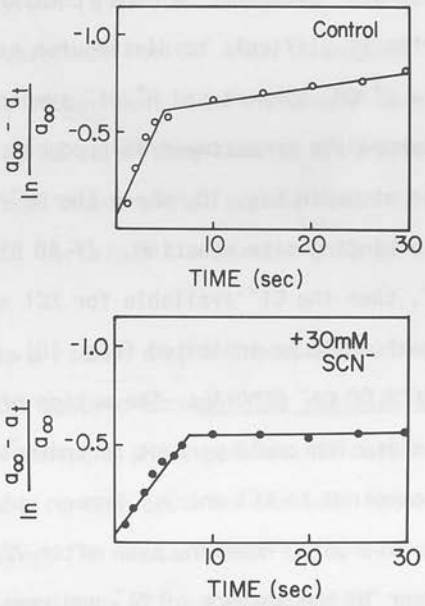

Fig. 9. An exponential analysis of H^+ uptake by non-equilibrated vesicles, showing two kinetic constants. The slower of these is blocked by SCN^-.

If the SCN^- is added subsequent to the signal, the decay of the signal is somewhat faster than usual, but not as fast as is obtained with ionophores. This indicates that SCN^- inhibits a forward step in the transport process, but does not induce sufficient leak to account for the inhibition.

SCN^- has been shown to inhibit mitochondrial F_1 ATPase at concentrations which also inhibit gastric secretion. There is also considerable dispute as to whether all the HCO_3^- activated SCN^- inhibitable ATPase present in gastric mucosa is localized to mitochondrial fractions or is also present in the plasma membrane.

The action of SCN^- in inhibiting the AO response, reducing the KCl entry dependent component of H^+ uptake and the sensitivity of the AO response to external buffer indicates that the simple H^+:K^+ antiport model might require elaboration.

In the intact mucosa another component might be required for activating an OH^-/Cl^- antiport. A model consisting of an OH^-/Cl^-, K^+/H^+ antiports in series is difficult to distinguish experimentally from a model consisting of a K^+/OH^- symport and H^+/Cl^- symport in series. In these models, an intermediate compartment is produced. A condensed version of these is also shown in Fig. 10, where the OH^-/Cl^- exchange component is visualized as a binding site reaction. If AO binds to the OH^-, and SCN^- displaces OH^-, then the Cl^- available for KCl symport would be reduced, and the AO signal would be inhibited (Fig. 10).

EFFECT OF Cl^- REMOVAL: The action of Cl^- removal and $SO_4^{"}$ or isethionate substitution could perhaps be understood by restriction of K_2SO_4 entry as compared to KCl entry. Tracer uptake measurements show that this is the case (5). However, even after 72 hrs. incubation, H^+ uptake is still slower in the absence of Cl^- and remains osmotically sensitive. Fig. 11

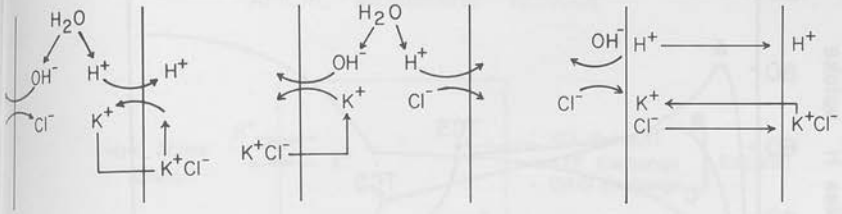

ig. 10. Possible models involving intransmembranal compartments of H^+, OH^- or K^+ classified as series models, or a model involving an OH^-/Cl^- exchange site on the membrane surface.

ompares control conditions where KCl is present on both sides of the membrane to the situation where $SO_4^{"}$ is internal and Cl^- external, showing a eduction in rate and magnitude of H^+ uptake. Also, in this figure, the resence of $SO_4^{"}$ only on both sides of the membrane shows a slower 'uptake' f H^+. The addition of Cl^- in the presence of ATP increases uptake. The uptake' is difficult to dissipate with protonophores, valinomycin or igericin, but is dissipated by tributyltin (a Cl^-/OH^- antiport). In the eries type of model, $SO_4^{"}$ would not substitute for Cl^- with consequent ccumulation of OH^- or H^+ in a membrane compartment. In the single model $SO_4^{"}$ would reduce the cycling of K^+. It is surprising that an H^+ gradient is found in the vesicle preparation since intact piglet mucosa does not ecrete H^+ in the presence of $SO_4^{"}$ (14). Certainly the permeability of the embrane vesicles to K_2SO_4 is very low.

ELL MODEL: It is possible to provide a rather simple conceptual scheme or transport in hog vesicles and piglet gastric mucosa. The vesicles are isualized as containing an active $K^+:H^+$ antiport and a passive KCl symport. In the intact parietal cell, the basal surface contains the well known $a^+ + K^+$ ATPase, with 3:2 $Na^+:K^+$ coupling. An neutral NaCl symport on the ame cell surface allows the cell to accumulate KCl. The excess Cl^- moves

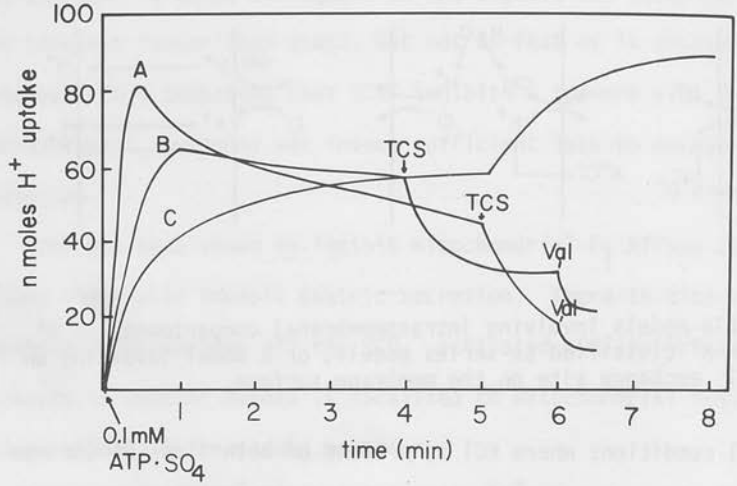

Fig. 11. The H^+ uptake of hog vesicles in the KCl equilibrated condition (A), K_2SO_4 inside KCl outside (B) and with K_2SO_4 on both sides of the membrane (C).

across the luminal membrane by a Cl^- uniport, the circuit being completed by Na^+ moving across the paracellular shunt. This predicts that 'active' Cl^- transport is ouabain sensitive and Na^+ dependent; the former being true of piglet (14), the latter of frog (15).

The accumulated KCl is used for the K^+:H^+ exchange by having the KCl symport present on the luminal surface allowing KCl exit, followed by K^+:H^+ exchange (Fig. 12).

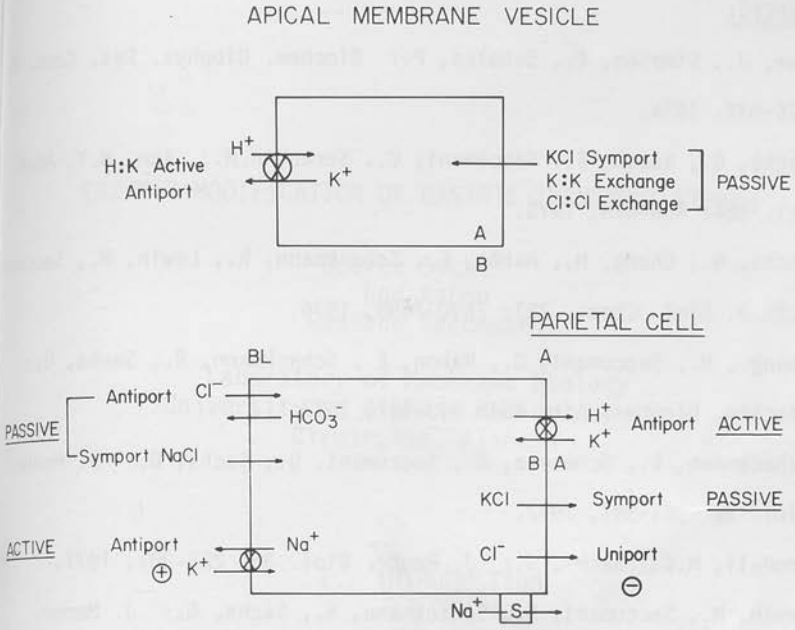

Fig. 12. A general model for gastric vesicles and the gastric parietal cell using the H^+:K^+ and Na^+:K^+ ATPases to drive all the known transport processes.

REFERENCES:

1. Lee, J., Simpson, E., Scholes, P.: Biochem. Biophys. Res. Comm. 60: 825-834, 1974.
2. Sachs, G., Rabon, E., Saccomani, G., Sarau, H.M.: Ann. N.Y. Acad. Sci. 264: 456-475, 1975.
3. Sachs, G., Chang, H., Rabon, E., Schackmann, R., Lewin, M., Saccomani, G.: J. Biol. Chem. 251: 7690-7698, 1976.
4. Chang , H., Saccomani, G., Rabon, E., Schackmann, R., Sachs, G.: Biochim. Biophys. Acta 464: 313-327, 1977.
5. Schackmann, R., Schwartz, A., Saccomani, G., Sachs, G.: J. Membr. Biol. 32: 361-381, 1977.
6. Goodall, M.C., Sachs, G.: J. Membr. Biol. 35: 285-301, 1977.
7. Lewin, M., Saccomani, G., Schackmann, R., Sachs, G.: J. Membr. Biol. 32: 301-318, 1977.
8. Waggoner, A.J., Wang, C.H., Tolles, R.L.: J. Membr. Biol. 33: 109-140, 1977.
9. Mitchell, P.: Biol. Rev. 41: 445-502, 1966.
10. Fiolet, J.W.T., Bakker, E.P., van Dam, K.: Biochim. Biophys. Acta 368: 432-445, 1974.
11. Pick, U., Armon, M.: Eur. J. Biochem. 70: 569-576, 1976.
12. Dett'Antone, P., Colonna, R., Azzone, G.F.: Eur. J. Biochem. 24: 553-576, 1972.
13. Lee, H.C., Qunitanilha, A.T., Forte, J.G.: Biochem. Biophys. Res. Comm. 72: 1179-1186, 1976.
14. Forte, J.G., Machen, T.E.: J. Physiol. (Lond) 244: 33-51, 1975.
15. Sachs, G., Shoemaker, R.L., Hirschowitz, B.I.: Proc. Soc. Exptl. Biol. Med. 123: 47-52, 1966.

ENZYMIC MODIFICATION OF GASTRIC TRANSPORT ATPase

George Sachs[1]
Edd Rabon
Gaetano Saccomani

Laboratory of Membrane Biology
University of Alabama Medical Center
Birmingham, Alabama

I. INTRODUCTION

Gastric ATPase purified either partially by differential and zonal density gradient centrifugation or more extensively by free flow electrophoresis (1) has been shown to accumulate H^+ (2-4) and extrude K^+ (5) with addition of ATP. The use of ionophores (6), dye probes such as carbocyanine dyes (7), oxonols (unpublished observations) or ANS (8) seems to indicate a non-electrogenic H^+ for K^+ exchange as the transport mechanism of this enzyme. The K_A for activation by K^+ however is at least an order of magnitude lower than the K_A for the K^+ requirement for H^+ transport. Further, the reconstitution of the enzyme into planar bilayer shows the presence of a thickness dependent K^+ conductance (9). The H^+ gradient developed by the vesicles is in the range of 3-4 units at pH 6.1 or 7.4 respectively (7) assuming equal transport by all the vesicles, less than the 6.6 achieved by the intact stomach. Also, the H^+ disappearance from the medium is less than the H^+ appearance internally (7), although the enzyme-containing membrane is localized to the apical surface of the parietal cell (10).

The enzyme seems to be at least a dimer present in 105,000 M_r group of peptides (1,4). A phosphorylated 'intermediate' is formed (11,12) in the presence of ATP, discharged by K^+ and a

[1]Supported by NIH grants AM15878 and AM21588; NSF grant PCM 77-18951.

ISBN 0-12-225401-5

reaction mechanism similar to the $Na^+ + K^+$ ATPase has been suggested (6,9,11).

In this investigation, a correlation of structure and function is initiated using tryptic modification of the enzyme.

II. MATERIALS AND METHODS

Vesicles from hog gastric mucosa were purified by previously published methods (1,7). For studies of transport, the gradient fractions were incubated for two hours at room temperature as described previously (7) and either acridine orange or diethyl oxocarbodicyanine (DOCC) dye with or without tetrachlorsalicylanilide (TCS) used to measure pH gradients. Either 75 mM K_2SO_4 or 150 mM KCl in 2 mM PIPES-Tris, pH 7.4 were used for the preincubation. Transport was initiated by the addition of MgATP and measurement of dye signal was carried out in an Aminco DW2 dual beam spectrophotometer (7). Nigericin was added in 10 µl methanol at 1 µg/ml to dissipate the pH gradient. For studies of tryptic modification of the enzyme, the vesicles, as above, were incubated with trypsin (Sigma or Worthington, high purity grade) at a protein to trypsin ratio between 60 and 480. Incubation was carried out at 22°C for 20 minutes and the reaction terminated by adding a 30-fold weight excess of trypsin inhibitor and the addition of MgATP followed. The protein was always 0.3 mg ml^{-1}. For studies of enzyme activity, the electrophoretically purified material (1) was incubated for various times at 30°C at a 100/1 ratio, inhibitor added, washed and resuspended for assay of ATPase and pNPPase activity by previously published methods (1). Phosphorylation was carried out using [γ-^{32}P]-ATP and SDS-β-mercaptoethanol gel electrophoresis was carried out as in reference 1. In some experiments the vesicles were preincubated for 5 minutes with 2 mM ATP, ADP, TTP or 100 mM KCl or NaCl before trypsin addition. Control studies showed that addition of trypsin inhibitor before trypsin was completely effective in blocking proteolysis, loss of transport signal or enzyme activity.

III. RESULTS

1. Transport: Under control conditions, in fresh vesicles, H^+ transport in the presence of KCl always exceeded the rate and maximum achievable with K_2SO_4. This has previously been interpreted as due to low permeability to the K_2SO_4 (13). The acridine orange signal was more resistant to trypsin than the signal of the cyanine dye in the presence of TCS (Figure 1),

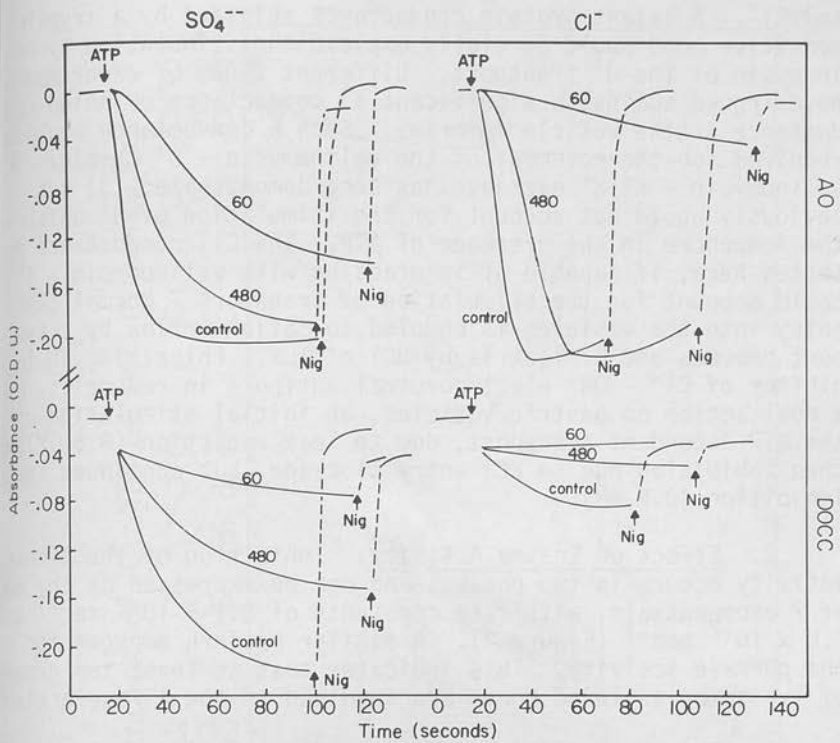

FIGURE 1. The effect of varying trypsin/protein ratios on the acridine orange (upper) or DOCC + TCS signal (lower) generated by ATP in KCl (right) and K_2SO_4 (left). Lower 1/2 of figure was aged vesicles.

although with increasing trypsin both signals eventually fell to zero. The relative sensitivity of the two signals was explained by two further experiments. The addition of TCS to the acridine orange protocol was without significant effect on the leak rate (dissipation of the signal) unless trypsinization had been carried out. This would suggest that trypsinization induced a conductance leak eg. OH^-, Cl^-, K^+ to compensate for the charged translocation of TCS - H^+. In the presence of K_2SO_4, both signals (DOCC or AO ± TCS) increased and became more like the normal KCl signal in fresh untrypsinized vesicles. This substantiates the conductance hypothesis and indicates further that Cl^- conductance is the basis for this discriminatory effect of trypsin or aging. The appearance of this conductance correlates with the breakdown of the ATPase peptide.

It is difficult to decide whether this conductance reflects a specific property of the membrane embedded protein or a non-specific leak, since liposomes also discriminate between SO_4^{--}

and Cl^-. A latent protein conductance shielded by a trypsin sensitive bond would partially explain the stimulation by valinomycin of the H^+ transport. Different types of experiments have argued against a significant K^+ conductance or anion conductance in the vesicle membrane. Such a conductance would be required for the movement of the valinomycin - K^+ complex. A valinomycin - K^+:H^+ exchange has been demonstrated (3) but obviously would not account for the stimulation of H^+ uptake by the ionophore in the presence of ATP. The Cl^- conductance detected here, if capable of interacting with valinomycin - K^+, could account for the stimulation of transport. Normal Cl^- entry into the vesicles is coupled to cation influx by a symport process and H^+ leak is by HCl efflux. Phlorizin, an inhibitor of Cl^- - OH^- electroneutral antiport in red cells, has a dual action on gastric vesicles, an initial stimulation of the ATP dependent transport, due to leak reduction (8.5 μM) and then inhibition due to KCl entry blockade, but continued leak inhibition (0.5 mM).

2. Effect on Enzyme Activity: Inhibition of the ATPase activity occurs in two phases, and can be expressed as the sum of 2 exponentials, with rate constants of 0.1×10^{-2} sec^{-1} and 1.8×10^{-2} sec^{-1} (Figure 2). A similar pattern emerges for the pNPPase activity. This indicates that at least two groups of lysine or arginine bonds are involved in the ATPase activity.

3. Effect on Peptide Pattern: The purified gastric vesicles show a single peptide region of 105,000 M_r on SDS-β-mercaptoethanol PAGE. Treatment with trypsin for varying times produces a complex series of peptides ranging from 87,000 M_r to 47,000 M_r, with the major peptide being 78,000 M_r (Figure 3). At 15 minutes when essentially complete inhibition of ATPase is observed, and continuing largely unchanged to 30 minutes, 40% of the 105,000 M_r glycopeptide remains, showing that region is inhomogeneous. From phosphorylation studies, assuming 1 Pi group incorporated per 2 mol 105,000 M_r and given a maximum phosphorylation of 1500 pmol Pi mg^{-1} protein (unpublished observations), we would anticipate ca. 50% of the peptide to be the ATPase catalytic peptide.

With increasing time of incubation, the peptides produced initially also are hydrolyzed to peptides of very small M_r which are not detected in the gel.

4. Effect on Phosphorylation: In contrast to the initial rapid inhibition of ATPase or pNPPase activity, the level of phosphoprotein obtained from [γ-^{32}P]-ATP increased following trypsin treatment and then declined, but remained higher than control. Figure 4 shows the level of acid precipitated phosphoprotein. This would suggest that one of the steps

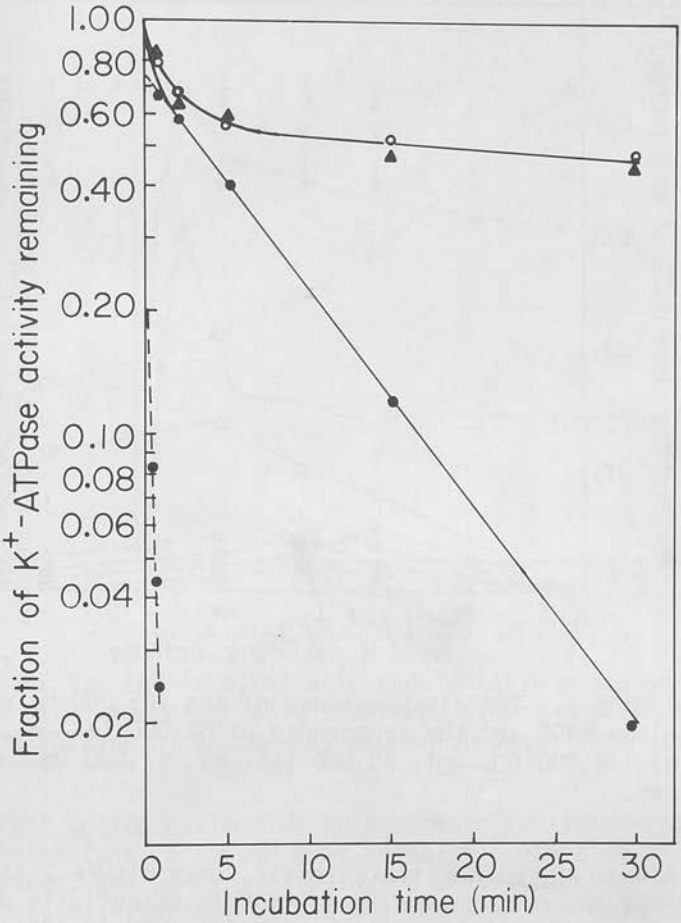

FIGURE 2. The % inhibition of ATPase with time of trypsin treatment at a protein/trypsin ratio of 100/1 (●——●) and in presence of ATP (o——o) and ADP (▲——▲).

leading to dephosphorylation is blocked by the initial action of the proteolytic enzyme. K^+-dependent dephosphorylation remains relatively fixed in terms of nmole Pi discharged but a K^+-insensitive EP form is produced. An interpretation consistent with the above data would be that the initial action of the enzyme is to interfere with the interconversion of 2 phosphorylated forms of the enzyme (see below).

5. Effects of Ligands:

a. Enzyme activity: If the vesicles are preincubated

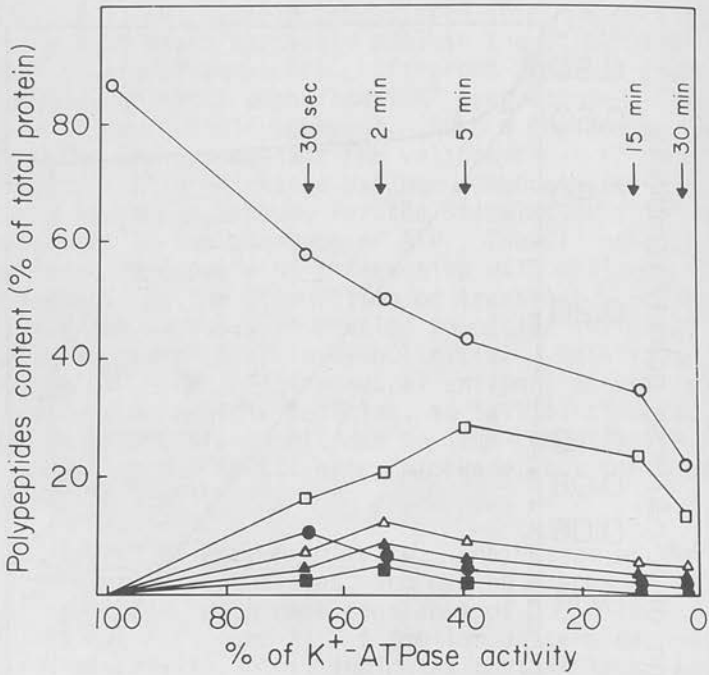

FIGURE 3. The disappearance of the 105,000 M_r region (o—o) on PAGE and the appearance of 87,000 (●—●), 84,000 (△—△), 78,000 (□—□), 65,000 (▲—▲), 47,000 (■—■) M_r peptides.

with ATP or ADP at substrate levels, then figure 2 shows that the first phase of enzyme inhibition is essentially unaffected, whereas the slower phase is abolished. pNPPase activity is also protected by these ligands. In contrast to ATP or ADP, TTP, AMP, β-γ methylene ATP or pNPP exert virtually no protective effect on the enzyme. From these data one can conclude that not only are there specific sites for ATP or ADP, but that although ATP and pNPP binding sites interact, a conclusion based on the mutual competition by these substrates they are non-identical in that pNPP exerts no protective effect. The overall enzyme reaction can thus be written

$$\text{ENZ} + \text{ATP} \xleftrightarrow{Mg^{++}} \text{ENZ} - \text{ATP}$$
$$\text{ENZ} - \text{ATP} \longleftrightarrow \text{ADP} - \text{ENZ} - \text{Pi}$$
$$\text{ADP} - \text{ENZ} - \text{Pi} \longleftrightarrow \text{ENZ} - \text{Pi}_I + \text{ADP}$$
$$\text{ENZ} - \text{Pi}_I \xleftrightarrow{H^+} \text{ENZ} - \text{Pi}_{II}$$
$$\text{ENZ} - \text{Pi}_{II} \xleftrightarrow{K^+} \text{ENZ} + \text{Pi}$$

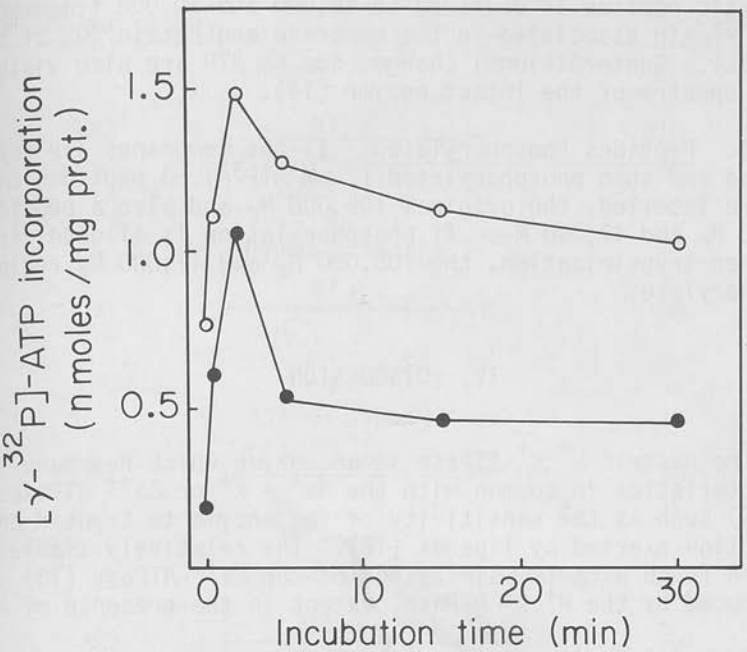

FIGURE 4. The level of acid precipitable phosphoprotein obtained with time of trypsin treatment (100:1 protein/trypsin ratio) in absence of K^+ (o——o) and in presence of K^+ (●——●).

In contrast to the nucleotide or phosphate substrate specificities, the cations, although they are also protective of the second phase, are non-specific in the sense that both Na^+ and K^+ protect, high concentrations are required and peptide patterns do not change.

b. Peptide pattern: The peptides produced by trypsin, in the presence of ATP or ADP, are changed. Only two peptides are present on the gel, at 78,000 M_r and 30,000 M_r. At 5' loss of the 105,000 M_r peptide is maximal and corresponds to a loss of about 40% of this region. CHO staining indicates little change in the 105,000 M_r band. Accumulation of the two fragments account for about 36% of the original 105,000 M_r band. At this point, 60% of the initial ATPase activity remains. Two interpretations may be suggested. Firstly, that ligands protect the 105,000 M_r component of the ATPase against degradation, and hence the 78,000 and 30,000 fragments are generated from a non-ATPase peptide. Alternatively, and consonant with the 40% inhibition of activity found, the residual 105,000 M_r peptide is not the catalytic protein of the ATPase, but the

catalytic peptide is degraded to 78,000 and 30,000 fragments which remain associated in the membrane and retain 60% of the activity. Conformational changes due to ATP are also visible in CD spectra of the intact enzyme (14).

6. Peptides Phosphorylated: If the membranes are trypsinized and then phosphorylated (2 μM ATP^{32}), 3 peptides on the gel are labelled, the original 105,000 M_r and also a peptide at 87,000 M_r and 47,000 M_r. If phosphorylation is allowed first and then trypsinization, the 105,000 M_r and 47,000 M_r regions phosphorylate.

IV. DISCUSSION

The gastric H^+:K^+ ATPase is an enzyme which has many characteristics in common with the $Na^+ + K^+$ or Ca^{++} ATPases (15,16) such as the sensitivity of the enzyme to trypsin and protection exerted by ligands (17). The relatively simple pattern found with trypsinization of the Ca^{++}-ATPase (18) is not reproduced by the H^+:K^+ ATPase, except in the presence of ATP or ADP.

Associated with conformational changes, transport reactions occur within the protein resulting in electroneutral H^+ for K^+ exchange. Presumably, the binding of ATP or ADP converts the enzyme into a transport active form which is followed by the phosphorylation-dephosphorylation cycle. The changes occur within an individual subunit of the enzyme complex. A previously undetected Cl^- conductance appears, which may play a physiological role. This can also be obtained by aging vesicles.

Two transport components are known in the stomach, that of HCl, which may be accounted for by KCl symport (passive) and active H^+:K^+ antiport, pathways clearly present in the vesicles and that of NaCl, driven by the $Na^+ + K^+$ ATPase in the basal-lateral membranes conjugated with an apical Cl^- conductance and a paracellular Na^+ shunt. It may be this latter conductance that is revealed by proteolysis.

Evidence for this can be obtained directly in rabbit gastric glands (19). Here ouabain reduces the potential, based on ^{3}H-TPMP distribution, and inhibits acid secretion. This latter effect is reversed by increasing medium K^+. This can be interpreted as the $Na^+ + K^+$ ATPase being (a) electrogenic, (b) required for intracellular K^+, (c) this K^+ is in turn required for H^+ secretion, (d) the electrogenic component is required for 'pseudoactive' or rheotrophic Cl^- transport.

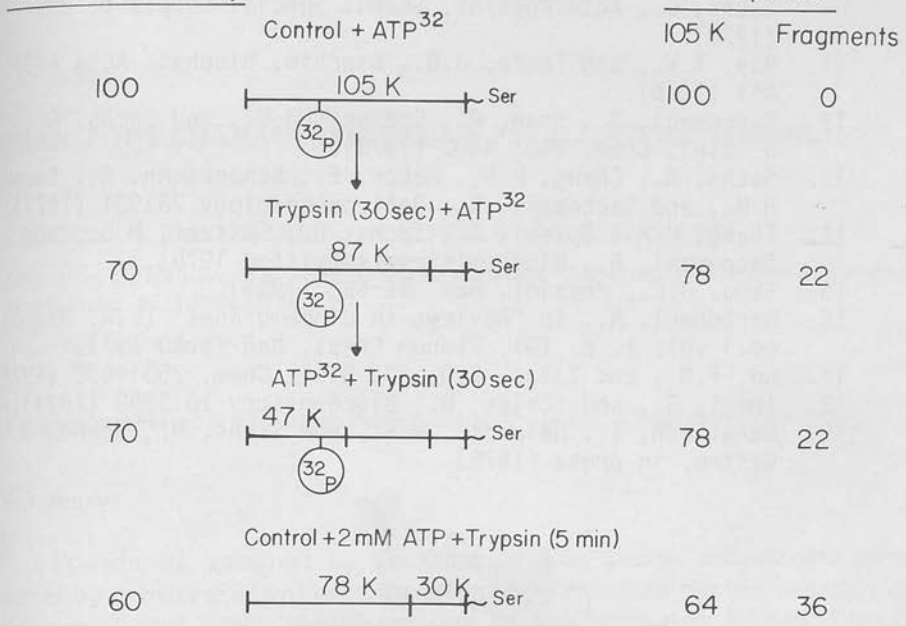

FIGURE 5. A tentative model of the trypsin sensitive sites on the enzyme, with and without protective ligands.

REFERENCES

1. Saccomani, G., Stewart, H.B., Shaw, D., Lewin, M. and Sachs, G., Biochim. Biophys. Acta 465:311 (1977).
2. Lee, J.E., Simpson, G., and Scholes, P., Biochem. Biophys. Res. Comm. 60:825 (1974).
3. Sachs, G., Chang, H.H., Rabon, E., Schackmann, R., Lewin, M., and Saccomani, G., J. Biol. Chem. 251:7690 (1976).
4. Chang, H.H., Saccomani, G., Rabon, E., Schackmann, R., and Sachs, G., Biochim. Biophys. Acta 464:313 (1977).
5. Schackmann, R., Schwartz, A., Saccomani, G., and Sachs, G., J. Membr. Biol. 32:361 (1977).
6. Sachs, G., Rev. Physiol. Biochem. Pharmacol. 79:133 (1977).
7. Rabon, E., Chang, H.H., and Sachs, G., Biochemistry in press (1978).
8. Lewin, M., Saccomani, G., Schackmann, R., and Sachs, G., J. Membr. Biol. 32:301 (1977).
9. Goodall, M.C., and Sachs, G., J. Membr. Biol. 35: 285 (1977).

10. Saccomani, G., Crago, S., Mihas, A.A., Dailey, D.W., and Sachs, G., Acta Physiol. Scand. Special Suppl. p. 293 (1978).
11. Ray, T.K., and Forte, J.G., Biochim. Biophys. Acta 443: 451 (1976).
12. Saccomani, G., Shah, G., Spenney, J.G., and Sachs, G., J. Biol. Chem. 250: 4802 (1975).
13. Sachs, G., Chang, H.H., Rabon, E., Schackmann, R., Sarau, H.M., and Saccomani, G., Gastroenterology 73:931 (1977).
14. Chang, H.H., Spisni, A., Sachs, G., Spitzer, H.L., and Saccomani, G., Biochemistry (submitted 1978).
15. Skou, J.C., Physiol. Rev. 45:596 (1965).
16. Martonosi, A., in "Reviews in Biomembranes" (L.A. Manson, ed.) vol. 1, p. 191. Plenum Press, New York, 1971.
17. Lo, T.N., and Titus, E.O., J. Biol. Chem. 253:4432 (1978).
18. Inesi, G., and Scales, D., Biochemistry 16:3298 (1974).
19. Berglindh, T., Helander, H.F., and Sachs, G., Scand. J. Gastro. in press (1978).

Biochimica et Biophysica Acta, 551 (1979) 432—447

BBA 78298

TRANSPORT CHARACTERISTICS OF FROG GASTRIC MEMBRANES

E. RABON , G. SACCOMANI, D.K. KASBEKAR * and G. SACHS **

Laboratory of Membrane Biology, University Station, University of Alabama in Birmingham, Birmingham, AL 35294 (U.S.A.)

(Received July 4th, 1978)

Key words: Transport properties; Proton pump; Cl^- pump; (Frog gastric membrane)

Summary

ATP-induced transport by fractions of frog gastric microsomes prepared either by density gradient centrifugation or by free flow electrophoresis were K^+ dependent and hence considered due to a K^+-activated ATPase. Significant activity of this enzyme was, however, only found in the anodic peak of the free flow electrophoretic separation, which in addition to separating transporting from non-transporting particles, also separated membranes containing a phosphorylatable peptide (M_r = 105 000) region as the major peptide on SDS-polyacrylamide gel electrophoresis from those containing a peptide (M_r = 44 000) on SDS-polyacrylamide gel electrophoresis. H^+ uptake, measured either by acridine orange or 3,3′-diethyloxadicarbocyanine + tetrachlorosalicylanilide absorbance changes was dependent on K^+ intravesicularly. Using $^{86}Rb^+$, active extrusion of the cation followed ATP addition. SCN^-, an inhibitor of acid secretion did not affect the latter, but blocked signals due to H^+ uptake, in contrast to mammalian preparations.

Introduction

Frog gastric mucosa is the best studied in vitro model of acid secretion [1—4]. Several conclusions have been drawn from observations of the functioning gastric mucosal sheet and metabolite assays of parietal cell regions. These findings may be summarized as follows: (a) the H^+ pump may be electrogenic [1]; (b) an independent Cl^- pump is present [1,5]; (c) H^+ secretion is abso-

* Present address: Department of Physiology, Georgetown University, Washington, DC
** To whom correspondence should be addressed.
Abbreviations: TCS, tetrachlorosalicylanilide; DOCC, 3,3′-diethyloxacarbodicyanine; $DiBac_4(5)$, bis-[1,3-dibutyl-barbituric acid-(5)]pentamethinoxonol; Pipes, piperazine-*N*,*N*′-bis(2-ethanesulfonic acid).

lately O_2 dependent and while changes in the redox state of mitochondria preceed the onset of acid secretion these component changes do not indicate an ATP-dependent pump [4,5]; (d) changes in high energy phosphates are not in favor of such a pump [7]; (e) microsomal fractions contain a K^+-activated ATPase [8].

Although analysis of metabolite profiles in the dog [9] also do not provide direct evidence for an ATP-driven H^+ pump, studies of mammalian gastric membranes show the presence of an electroneutral ATP-dependent H^+ for K^+ exchange in membrane vesicles, clearly implicating an ATP-driven H^+ pump [10,11]. This pump is present in dog [12,13] rabbit [14], hog [15,16] and man [17].

Characterization of the frog microsomal system which indicates the existence of K^+-sensitive ATPase, has previously been described [8,14]. Since the K^+-ATPase of gastric mucosa in other species exhibits transport properties, membranes isolated by centrifugal and electrophoretic techniques have been studied. Significant similarities and differences exist between preparations of mammalian and amphibian membranes.

Materials and Methods

Preparation. Following the 3 M NaCl lysis of surface cells [18] the deeper cell layers from the gastric fundic mucosa of seven large bullfrogs (*Rana catesbina*) were removed by scraping with a microscope slide. These scrapings were homogenized with 10 strokes at 2000 rev./min in a teflon-glass homogenizer in cold 0.3 M sucrose, 5 mM Tris-HCl, pH 7.4. Differential centrifugation of this homogenate included spins of 10 min at 800 × *g*, 15 min at 10 000 × *g* and 1 h at 100 000 × *g*.

Free flow electrophoresis. The crude microsomal pellet was resuspended in 0.3 M sucrose, 8 mM acetic acid and 8 mM Tris-HCl, pH 7.4, spun down once for 1 h at 100 000 × *g* and resuspended in the same buffer. This suspension was loaded on the FF5 free flow electrophoresis unit developed by Hannig et al. [19] (Biochemical Instruments, NY) and separation was carried out as previously described [16]. The sample which was injected at 1 ml/h was separated into 90 fractions which were collected at 4°C. Electrophoresis was interrupted every 30 min to remove mucous build-up at the curtain entry port. Conditions in the run were: 120 ± 10% V/cm, 147 mA, temperature 7.4 ± 0.2°C and electrophoresis buffer flow 4 ml/fraction per h. The resolved protein peaks, monitored as 280 nm absorption profiles were pooled, spun down for 1 h at 100 000 × *g* and resuspended in 0.3 M sucrose, 2 mM piperazine-*N*,*N*'-bis(2-ethane sulfonic acid) (Pipes)/Tris, pH 7.4.

Density gradient centrifugation. In other experiments, 2 ml of the microsomal fraction was loaded onto step gradients consisting of successive 5-ml steps of 7% Ficoll (w/w) in 0.3 M sucrose, 22% sucrose and 30% sucrose (w/w). Centrifugation was carried out in a Sorvall AH-627 swinnging bucket rotor spun at 25 000 rev./min for 14 h. The bands were removed by Pasteur pipette. Protein was determined by the method of Lowry et al. [20].

Phosphorylation. 20 μg of membrane protein was added at 4°C to 0.5 ml of a mixture containing 150 mM choline chloride, 5 μM ATP containing 0.2 μCi

[γ-^{32}P]ATP, 10 μM $MgCl_2$ and 5 mM Pipes/Tris (pH 7.4) with or without 20 mM KCl. After a 15 s incubation, 0.5 ml of ice-cold 12% trichloroacetic acid containing 0.1 mM P_i and 1.0 mM ATP was added to stop the reaction. The precipitate was then filtered on HAWP (0.45 μm) millipores and washed three times with 3.0 ml of 150 mM choline chloride, 10 μM $MgCl_2$ and 5 mM Pipes/Tris, pH 7.4. Radioactivity was measured by an LKB 81000 liquid scintillation counter. For gel electrophoresis, 20 μg of membrane protein was added at 4°C to 80 μl total volume containing 0.1 μM ATP, 2.0 μCi [γ-^{32}P]ATP, 10 μM $MgCl_2$ and 20 mM Tris/HCl (pH 7.4) with or without 20 mM KCl. Following a 15 s incubation at 4°C, the membranes were solubilized with 80 μl of 2.0% SDS/2.0% β-mercaptoethanol and gel electrophoresis carried out immediately at 4°C.

Polyacrylamide gel electrophoresis. Gel electrophoresis was performed as previously described [13]. Briefly, in this procedure 20 μg of solubilized membrane protein (80 μl) was layered on a a 1.0 cm stacking gel system consisting of 3.5% polyacrylamide, pH 6.8, layered on top of 10% polyacrylamide, pH 8.6. A current of 1 mA/gel was applied for 1 h to run the sample through the stacking gel. Afterwards, the current was increased to 2.5 mA/gel, until the completion of the gel run. At this point, the ^{32}P-labelled gels were sliced into 1.5-mm sections and incubated in 200 μl of 50% H_2O_2 overnight at 60°C. In the morning the samples were cooled, diluted in 10 ml of Aquasol and counted in the LKB 81000 liquid scintillation counter. The gels to be stained with Coomassie blue were washed overnight in a solution of 7.5% acetic acid and 30% methanol and then stained with 0.25% Coomassie blue in 7.5% acetic acid/30% methanol for 6 h. After 48 h of destaining, the gels were scanned at 550 nm in a Gilford 2400 Spectrophotometer equipped with a gel scanner at 1.0 cm/min scan rate using a slit width of 0.05 mm.

ATPase assay. ATPase activity was assayed in 1 ml of medium containing 10 μg membrane protein, 40 mM Tris-HCl, pH 7.4, 2 mM $MgCl_2$ and 2 mM ATP (disodium salt). Optional additions to the assay included 20 mM KCl, 20 mM Na^+ or $KHCO_3$, 20 mM NaSCN and 10 μg of oligomycin. NaSCN and oligomycin were incubated with the membrane protein for 10 min at room temperature before the start of the assay. After incubation at 37°C for 15 min, the inorganic phosphate released was measured either by the method of Yoda and Hokin [21]or Fiske-Subarrow [22]. The term 'basal ATPase' refers to the activity observed when the only activating ion present was Mg^{2+}.

Dithionite-reduced spectrum. 0.5 mM sodium dithionite ($Na_2S_2O_4$) was added to a 350 μl sample in a microcuvette containing 1 mg/ml membrane protein suspended in 20 mM Tris-HCl, pH 7.4. After manually deriving a baseline for reference and sample cuvettes, solid $Na_2S_2O_4$ was added to the sample cuvette to a final concentration of 0.5 mM. The absorption difference between this and an untreated reference membrane sample was scanned from 400 to 650 nm in the Aminco DW-2 split-beam spectrophotometer. Wavelength pairs and extinction coefficients used in the calculation of pigment concentration were those published by Chance and Williams [23].

Transport activity. Proton gradient formation was assessed by measurement of the absorbance change of 5 μM acridine orange and potential difference was assessed by the absorbance changes of 4 μM 3,3′-diethyloxadicarbocyanine

iodide (DOCC) or the oxonol dye bis-[1,3-dibutyl-barbituric acid-(5)]pentamethinoxonol ($diBAC_4(5)$) following ATP addition. The addition of a protonophore in the presence of DOCC and ATP induced H^+ diffusion potential resulting in dye absorbance changes quantitatively related to the H^+ gradient. As previously described [24], the membrane material was suspended in 150 mM KCl, 2 mM $MgCl_2$ and 2 mM Pipes/Tris (pH 7.4) to 0.3 mg/ml final concentration. For chloride-free experiments, K_2SO_4 and $MgSO_4$ were substituted for KCl and $MgCl_2$, respectively. After 2 h room temperature preincubation, either 5 μM acridine orange, 4 μM DOCC ± 6 μM tetrachlorsalicylanilide (TCS) or 4 μM $diBAC_4(5)$ was added to 350 μl of the suspension. Either $MgCl_2$/ATP (pH 7.4) or $MgSO_4$/ATP (pH 7.4) (0.6 mM final concentration) was added and absorbance changes monitored at the appropriate wavelength pairs (i.e. acridine orange, 496 to 446 nm; DOCC, 588—636 nm; $diBAC_4(5)$, 600—640 nm).

$^{86}Rb^+$ efflux. The membrane fractions were suspended in a solution consisting of 75 mM RbCl, 2 mM $MgCl_2$, 2 mM Pipes/Tris, pH 6.1, 6.6 μCi $^{86}Rb^+$ at a final protein concentration of 1 mg/ml. In some experiments 75 mM KCl was used. After a 2 h room temperature preincubation, total uptake of $^{86}Rb^+$ was measured by placing duplicate 20-μl aliquots in a stop solution consisting of 500 μl of ice-cold 75 mM choline chloride, 2 mM $MgSO_4$, 0.135 M sucrose and 2 mM Pipes/Tris, pH 6.1. This suspension was filtered on HAWP millipore filters (0.45 μm) and washed four times with 2.5 ml ice-cold stop solution. Following the addition of 2 mM MgATP, pH 6.1, further 20-μl aliquots were removed and filtered as above at different times. For some experiments, a 10 min 23°C incubation with 20 mM NaSCN preceded the addition of ATP. After drying, the filters were placed in 10 ml of Amersham ACS counting fluid and counted on an LKB 81000 liquid scintillation counter.

Materials. 3,3′-Diethyloxadicarbocyanine (DOCC) iodide was purchased from Eastman. $diBAC_4(5)$ was a gift from Dr. A. Waggoner, acridine orange was a gift from Dr. J. Mentor. $^{86}RbCl$ was purchased from New England Nuclear. Bullfrogs were purchased by Animal Services from Jaques Wiel Co. Chemicals used in biochemical assays were obtained from Sigma. All chemicals were of reagent grade.

Results

Resolution of microsomal membranes

Free flow electrophoresis. The amphibian microsomal pellet, prepared as outlined in Materials and Methods, was a heterogeneous material containing what appeared to be both clear and pigmented membranes. Fig. 1 indicates that this material, when washed and resuspended in isotonic, Tris/acetate buffer, pH 7.4, could be resolved by the free flow electrophoresis procedure into two separate protein peaks with some additional material between these peaks. This resolution was characteristic of every amphibian microsomal sample tested. Preparational variations were restricted to changes in the proportions of these two major peaks.

Discontinuous sucrose gradient. Membrane material designated GI (Ficoll-sucrose), GII (20% sucrose) or GIII (29% sucrose) was found at each interface on the step gradient. The lightest band (GI) produced the smallest yield of

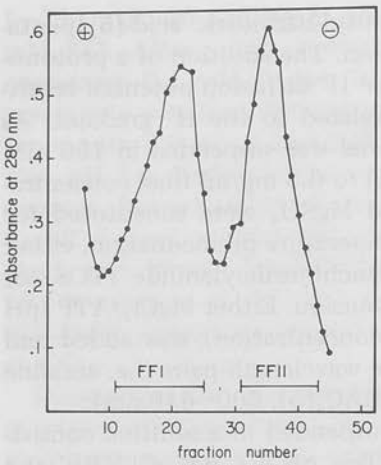

Fig. 1. Electrophoretic resolution of membrane-bound proteins utilizing the Hannig model 5, free flow electrophoresis apparatus. Material from the two major 280 nm absorbance peaks, FFI (tubes 11—25) and FFII (tubes 31—43) was pooled and prepared as detailed in Materials and Methods.

materials. This membrane fraction, trapped on the top of the Ficoll-sucrose interface was cleanly separated from the heavier material. The GII material was trapped at the sucrose-ficoll-22% sucrose interface. Like the GI material, the quantity of this material was low in comparison to the GIII fraction. The 22% sucrose layer contained a diffuse cloud of membrane material concentrating in the 29% sucrose interface. The material at the 29% interface (GIII) was the predominant band on the discontinuous gradient. The 30% sucrose layer also contained a diffuse cloud of material. A pellet was formed at the bottom of the tube.

There appeared to be little color in the ficoll-sucrose band. However, pigmentation progressively increased in the heavier gradient bands. The pellet under the 30% sucrose was heavily pigmented.

Dithionite-reduced spectrum. Fig. 2 shows a dithionite-reduced spectrum for each of the electrophoretically separated fractions (i.e. FFI and FFII). Characteristic absorption peaks identify flavoprotein, cytochromes *b*, $c + c_1$, *a* and a_3. The components identified by those spectra are listed in Table I. This comparison indicated a substantial mitochondrial contamination within the crude microsomal material which was enriched in the second peak. This enrichment in the second fraction was greater for complex IV (i.e. cytochromes *a* and a_3) whose average values increased 3.4-fold over the anodic peak (FFI). For complex III (i.e. cytochromes *b* and c_1) the average increase was 1.8-fold. Absorption peaks characteristic of other microsomal redox systems were not detected in either FFI and FFII.

ATPase activity. Basal Mg^{2+}-ATPase activity was present in every microsomal membrane fraction isolated. The large variations in this activity indicated the presence of a heterogenous population of ATPases. Table II lists this basal Mg^{2+}-ATPase as well as the activity in the presence of the stimulating ions K^+ and HCO_3^- for both free flow and discontinuous sucrose gradient procedures.

Comparison of the basal Mg^{2+}-ATPase activity in the sucrose gradient

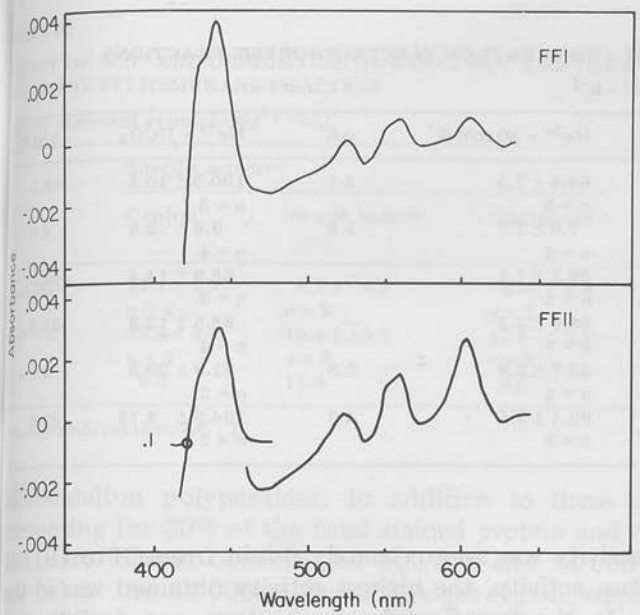

Fig. 2. Comparison of the $Na_2S_2O_4$-reduced spectrum of FFI and FFII. See Materials and Methods for details of procedure. For both FFI and FFII membranes, full scale absorbance on the Aminoc DW-2 split beam system was set at 0.02 absorbance unit. The first bands (shorter wavelengths) in the FFII membrane system were recorded with full scale absorbance sensitivity decreased to 0.1 absorbance unit.

fractions (i.e. GI, GII, GIII) showed that the basal Mg^{2+}-ATPase activity was enriched in the membrane fractions which equilibrated in progressively denser sucrose. Table II shows that the membranes at the 29% sucrose (i.e. GII) interface had an 11-fold increase in activity over the material equilibrated at the sucrose-ficoll interface (i.e. GI). This separation of basal Mg^{2+}-ATPase into fractions with either low or high activity (i.e. GI or GIII) was also achieved by free flow fractionation. At 92.1 $\mu mol \cdot mg^{-1} \cdot h^{-1}$, the Mg^{2+}-ATPase activity of the FII membranes was the highest obtained by either purification procedure.

Enrichment of the HCO_3^--stimulated component of the ATPase activity coincided with that of the basal Mg^{2+}-ATPase. Within the density gradient

TABLE I

IDENTIFICATION OF REDOX COMPONENTS REDUCED BY $Na_2S_2O_4$

Values are given as μmol/mg membrane protein. Wavelength pairs and extinction coefficients used were those determined by Chance and Williams [23].

	Flavo-protein	Cytochrome			
		b	$c + c_1$	*a*	a_3
Microsomal	0.304	0.151	0.132	0.296	0.289
FFI	0.204	0.098	0.074	0.112	0.078
FFII	0.296	0.141	0.158	0.311	0.309

TABLE II

ATPase ACTIVITY IN GRADIENT AND FREE FLOW ELECTROPHORESIS FRACTIONS

Values are expressed as $\mu mol \cdot mg^{-1} \cdot h^{-1}$.

Fraction	Basal Mg^{2+}	Mg^{2+} + 20 mM K^+	ΔK^+	Mg^{2+} + HCO_3^-	ΔHCO_3^-
Microsomal	62.3 ± 6.2 $n = 5$	64.4 ± 7.5 $n = 5$	2.1	100.5 ± 10.3 $n = 3$	38.2
GI	5.2 ± 1.2 $n = 6$	7.0 ± 1.7 $n = 6$	1.8	9.8 ± 2.6 $n = 4$	4.6
GII	42.4 ± 10.8 $n = 4$	39.2 ± 7.1 $n = 4$	—	68.9 ± 14.4 $n = 3$	26.5
GIII	58.2 ± 5.94 $n = 7$	56.6 ± 4.2 $n = 7$	—	83.5 ± 12.8 $n = 4$	25.3
FI	18.0 ± 5.3 $n = 4$	23.7 ± 5.9 $n = 4$	5.8	21.9 ± 20.3 $n = 2$	3.9
FII	92.1 ± 6.2 $n = 5$	96.4 ± 9.5 $n = 3$	4.3	124.9 ± 4.75 $n = 2$	32.8

material this increase in activity was approximately 6-fold from GI to GII. As with the basal Mg^{2+}-ATPase activity, the highest activity obtained was in the free flow fraction, FFII. In the free flow fractions, there was depletion of HCO_3^- stimulation in the FFI fraction with concomitant enrichment in the FFII membranes.

The results of an experiment which assayed the sensitivity of the components of the ATPase reaction to the mitochondrial inhibitor protein are displayed in Table IV. Clearly, most of the activity in the GIII fraction, regardless of the stimulating ion, is sensitive to the mitochondrial inhibitor protein. The GI fraction differs somewhat from the inhibitory pattern observed with the GIII material. In the GI fraction, that component of the ATPase reaction which is stimulated by $KHCO_3$ is partially insensitive to the mitochondrial inhibitor protein. Only 40% of the $KHCO_3$ stimulation is lost by incubation with the mitochondrial inhibitor protein.

K^+-stimulated ATPase activity was highest in the membrane fraction FFI isolated by free flow electrophoresis. In the FFI fraction the K^+-stimulated activity was approximately 6 $\mu mol \cdot mg^{-1} \cdot h^{-1}$. This exceeded that observed in any of the sucrose gradient fractions. In membranes isolated by sucrose gradient fractionation, a slight K^+ stimulation is present in the lightest fraction, but was smaller than that of the FFI. K^+-stimulation does not appear present in the 20% and 29% sucrose fractions, but a small activation could be obscured by the high basal Mg^{2+} activities of these fractions.

The K^+-stimulated ATPase of the FFI fraction was insensitive to both 20 mM NaSCN and oligomycin (2.8 : 1). Table III emphasizes the disparity between Mg^{2+}- and K^+-ATPase sensitivities. The basal Mg^{2+}-ATPase activity was 89% inhibited by oligomycin and 62% by 20 mM NaSCN. This was in contrast to an apparent 16% stimulation of the K^+ component by oligomycin and 36% stimulation by SCN^- of this activity.

Polypeptide pattern. Fig. 3 shows the complex polypeptide pattern of the membrane fractions resolved by free flow electrophoresis. In the microsomal fraction there were two major polypeptide peaks representing 100 000- and

TABLE III

EFFECT OF SCN^- AND OLIGOMYCIN ON BASAL Mg^{2+} AND THE K^+-STIMULATED ATPase ACTIVITY OF THE FFI MEMBRANE FRACTION

Activity expressed as $\mu mol \cdot mg^{-1} \cdot h^{-1}$

	Specific activity			% sensitivity	
	Control	20 mM NaSCN	Oligomycin *	20 mM NaSCN	Oligomycin
Basal Mg^{2+}	21.1 ± 2.7 $n = 4$	8.1 ± 4.2 $n = 2$	2.35 ± 0.8 $n = 3$	−61.6	−88.9
$Mg^{2+} + K^+$	29.4 ± 3.4 $n = 3$	19.4 ± 10.2 $n = 2$	11.9 ± 1.9 $n = 2$	−34.0	−59.5
ΔK^+	8.3	11.3	9.6	+36.1	+15.6

* Oligomycin/protein, 2.8 : 1.

44 000-dalton polypeptides. In addition to these major peaks, four bands accounting for 30% of the total stained protein and five bands accounting for 25% were located between the 100 000 and 44 000 molecular weight region and below the 44 000 molecular weight region, respectively. The first anodic peak (FFI) was enriched both in the 100 000 molecular weight region and in the region between 44 000 and 100 000. In this fraction the 100 000 molecular weight region accounted for approximately 53% of total stained protein. Together with the peptides of molecular weight range 44 000 and 100 000, they accounted for approximately 86% of the Coomassie blue-stained protein in this fraction. The major protein peak of the FFII fraction, the 44 000 molecular weight peak, was 35% of the protein in the FFII membrane fraction. Gradient fractionation showed only poor resolution of those peptides.

Membrane phosphorylation. Incubation of the anodic free flow fraction with [γ-^{32}P]ATP, labelled a component of the trichloroacetic acid precipitate of this material. In FFI, 226 pmol/mg of membrane protein were labelled with ^{32}P. As indicated in Table V, this label was partially sensitive to 20 mM KCl. 46% of the ^{32}P-label was lost if the membranes were phosphorylated in the presence of 20 mM KCl. In contrast to the FFI material, there was little phosphorylation in the FFII fraction. Table V indicates formation of a K^+-insensitive component of only 16 pmol/mg.

The 10% polyacrylamide gel peptide pattern of the 1% SDS/1% β-mercapto-

TABLE IV

ATPase SENSITIVITY OF SUCROSE GRADIENT FRACTIONS TO MITOCHONDRIAL INHIBITOR PROTEIN (MIP)

Activity expressed as $\mu mol \cdot mg^{-1} \cdot h^{-1}$.

		Untreated	MIP-treated
Basal Mg^{2+}	GI	0.14	0
	GIII	84.6	0
$Mg^{2+} + KHCO_3$	GI	6.4	3.8
	GIII	138.0	1.7

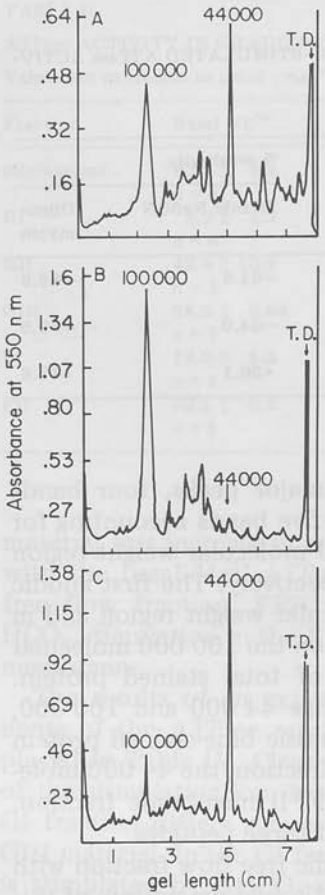

Fig. 3. Polypeptide pattern resulting from 1% SDS/1% β-mercaptoethanol solubilization of the crude microsomal, FFI and FFII membrane systems. See Materials and Methods for details. Molecular weight determinations were calculated by relative mobility in comparison to a series of standards of known molecular weight. (A) Represents the crude microsomal material; (B) the FFI membrane fraction and (C) the FFII membrane fraction (T.D. = tracking dye).

ethanol-solubilized phosphorylated FFI system is presented in Fig. 4. Two areas of the gel were heavily labelled. The first was the 100 000 molecular weight peptide region. From the counts recorded in Fig. 4 in this region 57% of this phosphoprotein was sensitive to 20 mM KCl. The second region was at the end of the gel and did not correspond to an area of peptide stain. These counts are due to free inorganic ^{32}P and low molecular weight glycolipids which are labelled at alkaline pH [13,25].

Transport experiments

Acridine orange. Absorbance signals consistent with the generation of a proton gradient are dependent on previous incubation of the anodic material (FFI) with KCl. The KCl requirement can be fulfilled by prolonged incubations at 4°C, 2 h room temperature incubations or the addition of valinomycin to non-equilibrated material. Under these conditions, ATP addition to the vesicles

TABLE V

[γ-^{32}P]ATP PHOSPHORYLATION OF MEMBRANE FRACTIONS SEPARATED BY FREE FLOW ELECTROPHORESIS

^{32}P-labelled protein is expressed as pmol Pi/mg membrane protein.

^{32}P-labelled protein	Mg^{2+} only	Mg^{2+} + 20 mM K^+	% K^+ sensitive
FFI	266	144	46
FFII	16	19	—

in the presence of 5 μM acridine orange resulted in the absorption changes shown in Fig. 5. This nigericin and tributyltin-sensitive signal (latter results not shown) exhibited an 80 s t_{max} followed by a slow decay to baseline. 10 min equilibration with SCN^- reduced the magnitude of the absorbance change by 86%. The same equilibration procedure with 10 μg of oligomycin (10 μg oligomycin/105 μg protein) reduced the acridine orange signal by 47%. In the presence of oligomycin, the t_{max} was shifted to 140 s. Acridine orange changes were not observed in FFII.

The development of an acridine orange response to the ATP-dependent

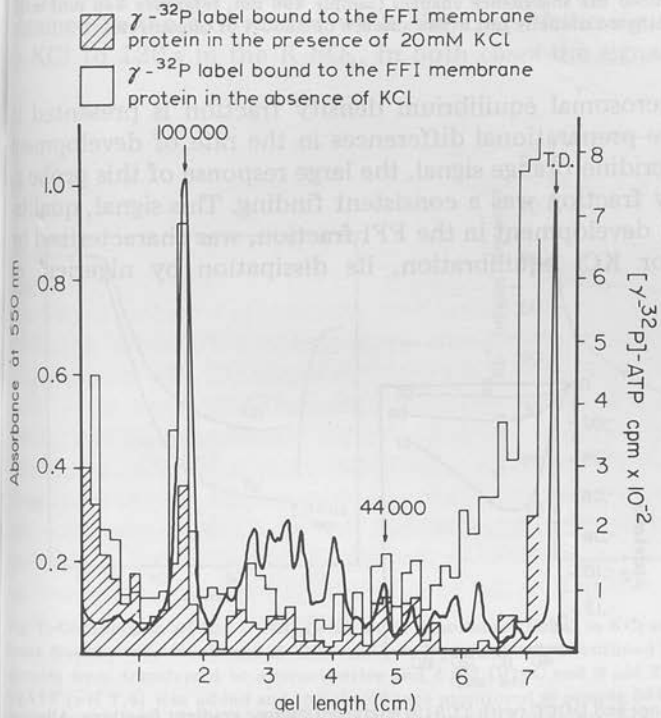

Fig. 4. [γ-^{32}P]ATP phosphorylation pattern of the FFI membrane system. 40 μg of FFI protein was added at 4°C to an 80 μl total volume containing 0.1 μM ATP, 2.0 μCi [γ-^{32}P]ATP, 10 mM $MgCl_2$ and 20 mM Tris-HCl, pH 7.4, with or without 20 mM KCl. After a 15 s incubation at 4°C, the membranes were solubilized in 1.0% SDS/1% β-mercaptoethanol and this material applied to the gel system detailed in Materials and Methods. Absorbance of the Coomassie blue-stained proteins was measured at 550 nm.

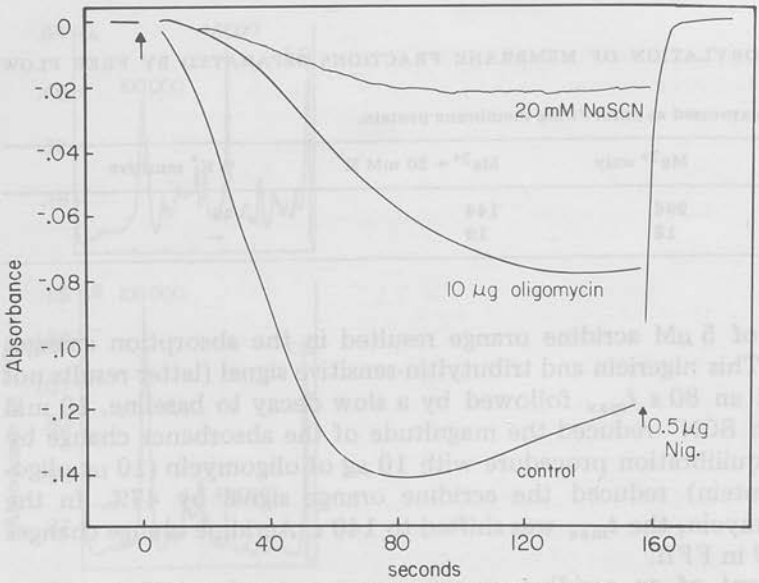

Fig. 5. Absorbance of acridine orange in energized FFI. Following the preloading procedure detailed in Materials and Methods, a 350 μl aliquot was transferred to a microcuvette to begin a 10 min incubation in either 20 mM NaSCN or 10 μg oligomycin. 5 μM acridine orange was added and at zero time, 0.8 mM MgATP, pH 7.4, addition produced the absorbance changes (sample 496 nm, reference 446 nm) monitored. The control signal was incubated similarly but in the absence of NaSCN or oligomycin.

energization in each microsomal equilibrium density fraction is presented in Fig. 6a. While there were preparational differences in the rate of development and magnitude of the acridine orange signal, the large response of this probe in each equilibrium density fraction was a consistent finding. This signal, qualitatively identical to signal development in the FFI fraction, was characterized by its dependence on prior KCl equilibration, its dissipation by nigericin or

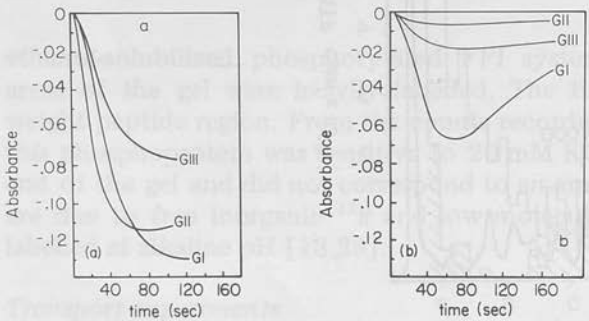

Fig. 6. Absorbance of acridine orange and DOCC (with TCS) in energized sucrose gradient fractions. Aliquots of each membrane fraction were prepared as detailed in Materials and Methods. (a) 5 μM acridine orange was added to each fraction. At zero time, 0.8 mM ATP, pH 7.4, addition produced the absorbance changes monitored at, sample 496 nm, reference 446 nm. (b) The procedure was identical as in (a) except that 4 μM DOCC and 6 μM TCS were substituted for acridine orange. DOCC absorbance was measured at sample 588 nm, reference 636 nm. GI, GII and GIII are the membrane fractions designated in the text.

ributyltin and its enhancement when valinomycin was added before ATP depletion.

Diethyloxadicarbocyanine. The DOCC + TCS measurement of the ability of each fraction to generate a potential upon ATP addition is recorded in part b of Fig. 6. In contrast to the activity observed with acridine orange in each fraction, the DOCC + TCS measured potential did show a gradient resolved enhancement. As shown in Fig. 6b, the largest DOCC + TCS absorbance changes were generated in the lightest fraction. The inverse relationship between DOCC + TCS signal development and the equilibrium density of the fractions was a consistent observation between preparations and could be accounted for by a progressive increase in other conductances with density. As noted for dog vesicles [24] this signal development was dependent upon the inclusion of TCS in the reaction media and prior equilibration with KCl. In the absence of 6 μM TCS, the ATP-dependent absorption changes of DOCC were of small magnitude and slow in development (results not shown). This signal was reversed by the addition of valinomycin or nigericin.

The TCS-dependent DOCC response was also present in the anodic free flow peak. In this fraction, the magnitude of the DOCC + TCS signal was small in comparison to the acridine orange response of the same material. Fig. 7 compares the ATP-dependent signal in the anodic peak after substitution of K_2SO_4 for KCl. In K_2SO_4 media the absorbance maximum increases 28% over that obtained in the KCl media, while the t_{max} of the signal was delayed from 80 s in KCl to 120 s in the K_2SO_4. In both cases the signal was nigericin sensitive.

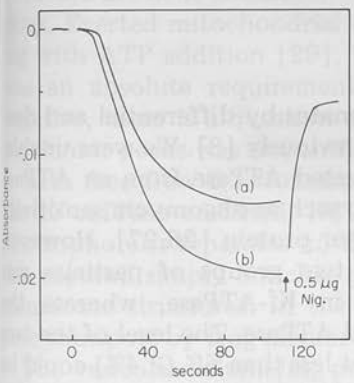

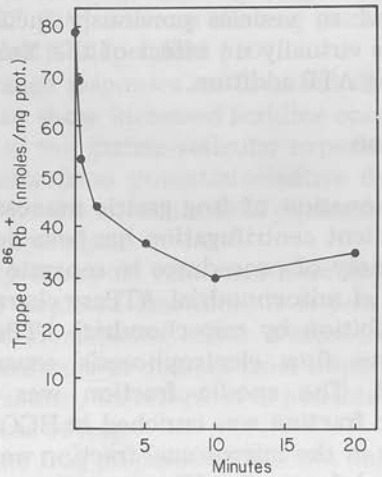

Fig. 7. Comparison of the DOCC (with TCS) absorbance signal in KCl and K_2SO_4 media. The FFI membrane fraction was incubated in either KCl or K_2SO_4 media as outlined in Materials and Methods. 350-μl aliquots were transferred to microcuvettes and 4 μM DOCC and 6 μM TCS added. At zero time, 0.8 mM MgATP (pH 7.4) was added and the absorbance monitored at sample 598 nm, reference 636 nm. Curve a, the absorbance signal of the FFI material incubated in KCl media; curve b, material incubated in K_2SO_4 media.

Fig. 8. 2 mM MgATP (pH 6.1) was added at zero time to the FFI membrane fraction previously incubated with $^{86}Rb^+$ as detailed in Materials and Methods. Each point, representing the amount of trapped $^{86}Rb^+$ remaining at that time, is the average of two experiments.

TABLE VI

NaSCN SENSITIVITY OF $^{86}Rb^+$ EFFLUX

FFI membranes	Trapped $^{86}Rb^+$ following ATP addition (nmol)		
	0	90 s	10 min
Control	105	80.7	56.5
+20 mM NaSCN	105	79.1	53.6

With a 10 min incubation, 20 mM SCN^- inhibited the DOCC + TCS signal by greater than 90%.

K^+ efflux. The identification of K^+ as a transported ion was observed as the ATP-dependent loss of trapped $^{86}Rb^+$ from vesicles previously incubated in $^{86}RbCl$. Preincubation of the material for 2 h at room temperature was used for equilibration of the isotope within the membrane-bound space. Calculation of the counts trapped by the FFI material at this time gave an apparent volume of 1.3 μl/mg. The addition of 2 mM Mg^{2+}-ATP caused a rapid loss of trapped $^{86}Rb^+$ which accounted for 62% of the initial equilibrated $^{86}Rb^+$. The kinetics of this $^{86}Rb^+$ disappearance from the anodic material are shown in Fig. 8. 71% of the total counts sensitive to ATP were lost within the first 90 s. A slow loss during the subsequent 8.5 min accounted for the remaining efflux. After 10 min (ATP depletion occurs about this time) there is a slow re-equilibration of the $^{86}Rb^+$). Similar data were obtained when $^{86}RbCl$ was used in the presence of KCl.

In another preparation, the normal ATP-dependent loss of trapped $^{86}Rb^+$ was compared to vesicles previously incubated with 20 mM NaSCN. Table VI indicates virtually no effect of the NaSCN on either the 90 s or 10 min values following ATP addition.

Discussion

Fractionation of frog gastric mucosal homogenates by differential and density gradient centrifugation has been described previously [8]. We were unable, by a variety of procedures to separate a K^+-activated ATPase from an ATPase which had mitochondrial ATPase characteristics, such as oligomycin sensitivity and inhibition by mitochondrial ATPase inhibitor protein [26,27]. However, using free flow electrophoresis, separation of two groups of particles was achieved. The anodic fraction was enriched in K^+-ATPase, whereas the cathodic fraction was enriched in HCO_3^--activated ATPase. The level of the two ATPases in the microsomal fraction was such that less than 5% (3.4%) could be accounted for as the K^+-activated component, whereas in the anodic fraction 32.0% was due to the K^+ component. This K^+-component insensitivity to 20 mM SCN^- and oligomycin was similar to hog enzyme [10]. Spectral analysis of the two fractions showed the continued presence of mitochondrial redox components, but significant depletion in the anodic fraction compared to the cathodic fraction. A more striking segregation of markers was found using polyacrylamide gel electrophoresis in SDS. The 100 000 dalton peptides, which characterizes the K^+-ATPase of dog [12,13], hog [15,16], rabbit [14] or man

[17] was found exclusively in the anodic fraction, whereas the cathodic fraction had a 44 000 dalton peptide as its major component. The expected subunit pattern of the mitochondrial F_1 ATPase, however, was not observed. In accordance with expectation, the phosphorylation of membrane peptide by [γ-^{32}P]ATP occurred in the anodic fraction. The level found, 266 pmol/mg ^{32}P is one fifth of that found in hog enzyme [31], but only 46% of the phosphorylation is discharged by K^+. Thus, the above data indicate, that in contrast to centrifugation methods, in our hands, free flow electrophoresis is capable of partially resolving ATPase activities of frog microsomes.

Both particulate fractions isolated by free electrophoresis are vesicular, in that, based on $^{86}Rb^+$ uptake, an equilibrium volume of 1.3 μl/mg is found. As for hog, Rb^+ loss dependent on the presence of ATP occurs only in the anodic fraction [11]. This loss occurs in two phases, a rapid phase accounting for 71% of total loss occurring within 90 s, and a slower phase lasting until the depletion of ATP. The efflux was insensitive to SCN^- and thus these data corresponded in large measure to those already described for hog [10,11]. Accordingly, frog gastric vesicles are capable of generating K^+ gradients in the presence of ATP.

There are several means of measuring proton gradients in vesicles such as electrometric techniques, potential dye probes, binding dyes such as acridine orange and weak bases such as 9-aminoacridine. Except for the potential dye probes, these techniques do not in general discriminate between plasma membrane or everted mitochondrial vesicles since both types could be expected to generate a ΔpH with the addition of ATP. However, in the case of the mitochondrial ATPase the pump mechanism is electrogenic and gradient or potential development is independent of added K^+ [28] whereas the hog gastric plasma membrane ATPase transport is neutral and K^+ dependent [10].

In the gradient fractions, acridine orange responses are found in all the fractions. Everted mitochondrial vesicles also show increased acridine orange binding with ATP addition [29], but since in the gastric vesicular experiments, K^+ was an absolute requirement and results from potential-sensitive dyes were negative, there is a question as to whether the mitochondrial contamination of the denser peaks was responsible for the dye signal.

With free flow fractionation, the only transport responses were observed in the K^+-ATPase enriched, HCO_3^--ATPase depleted fractions. It is possible that electrophoresis separates normally fused membranes, but it is more likely that this method simply enriches plasma membrane as distinct from other vesicular membrane structures. In the anodic fraction, therefore, it is possible to compare transport by frog membranes to those of hog.

The vesicular volume/mg protein of the frog preparation is about half of that of the hog. Using FFI membrane material and the pH electrode the change in external pH corresponds to an uptake, in equilibrated vesicles, of 19 nmol/μl, considerably less (1/5) than an average hog preparation. However, the Rb^+ efflux is close to that of the hog in terms of nmol/μl transported.

The presence of an HCl leak path and the absence of a large Rb^+ leak could account for the discrepancy, the H^+ being exchanged for Rb^+ by the pump and HCl leaking by an unspecified pathway. A back leak of OH^- in exchange for Cl^- would also result in this discrepancy.

The signal generated by the addition of ATP in the presence of acridine orange was similar in magnitude compared to that found in hog [24] in spite of the lower proton uptake values. The acridine orange signal is due to binding of the dye to negative sites induced by a pH gradient. The number of those sites could be a function of the phospholipid composition of the membrane (e.g. the per cent and orientation of phosphatidylserine residues) and hence quantitative correlation may not be anticipated betweeen species. The time of formation of the maximum dye signal was considerably delayed compared to the hog, but correlated with the fast Rb^+ efflux phase. This, coupled with the Rb^+ efflux found, would lead to the conclusion, as for the hog, that a K^+ for H^+ exchange is the transport mechanism.

An unequal stoichiometry, in the absence of shunting conductances would result in development of a potential difference. Positively or negatively charged dyes, such as DOCC or $diBAC_4(5)$ (oxonol) would then show a response to ATP addition. This was not the case, but as for the hog, the addition of a protonophore to the DOCC experiment, resulted in the development of a potential difference, interior negative, explained as due to H^+ diffusion potential across the protonophonic conductance [24]. This indicates the development of a H^+ gradient, and also the absence of a large enough shunting conductance to short circuit the H^+ diffusion potential.

The in vitro frog mucosa, in the absence of Cl^-, but in the presence of SO_4^{2-}, shows an inverted potential difference interpreted as due to the electrogenic H^+ pump [1]. In hog vesicles, replacement of Cl^- by SO_4^{2-} reduced the rate of development and magnitude of all the transport signals [10], unless the vesicles had been aged or treated with trypsin or chymotrypsin [30]. In this case, partial restoration of the signals could be achieved by Cl^- removal and SO_4^{2-} substitution. In the case of frog free flow fraction I, the signal generated by DOCC in the presence of TCS was increased by the SO_4^{2-} substitution. This is explained as being due to removal of a Cl^- conductance which, in the presence of a TCS-induced H^+ conductance, partially shunts the H^+ diffusion potential. Thus, frog vesicles may contain a significant Cl^- conductance perhaps contributing to the discrepancy between H^+ and Rb^+ fluxes, as noted above. The absence of Cl^- however, did not result in a response of the negatively charged $diBAC_4(5)$ which would have occurred had an electrogenic pump been unmasked.

Another difference between hog and frog, qualitative rather than quantitative, was the abolition of the acridine orange and DOCC + TCS response by 20 mM SCN^-. Since the K^+-ATPase hydrolytic activity was insensitive to this ion it seems reasonable that the action of SCN^- influences the coupling of ATP turnover to H^+ or Rb^+ transport. As Rb^+ transport was unaffected, SCN^- apparently uncouples H^+ from Rb^+ transport in frog vesicles. The simplest interpretation is that SCN^- provides an anion conductance path allowing H^+ to leak across the whole membrane, or uncouples an intramembranal transport compartment of bound H^+. Since SCN^- addition after the signal had developed was less effective than a 10 min incubation with SCN^- before ATP addition, we favor an uncoupling action at an intramembranal site, rather than induction of a transmembranal leak. Indeed the latter would require an associated large H^+ conductance, and although the H^+ conductance exceeds the K^+ conductance, it

is still too small to be detected by DOCC alone. A series pump model, using components (e.g. $\alpha_2\,\beta_2$) of the mitochondrial F_1 ATPase and the specific gastric $H^+ + K^+$)-ATPase would show many of the above properties.

Thus, frog mucosa, as for hog, contains a membrane which is capable of H^+ and K^+ transport, as well as having an associated K^+-ATPase activity and a phosphorylatable M_r 100 000 peptide. Differences between hog and frog membrane properties are both quantitative and qualitative, but the general aspects of the transport phenomena are similar.

Acknowledgement

This work was supported in part by grants NIH AM15878 and AM21588 and NSF PCM 77-18951.

References

1 Rehm, W.S. (1972) Metabolic Transport (Hokin, L.E., ed.), pp. 187—241, Academic Press
2 Sachs, G., Spenney, J.R. and Lewin, M. (1978) Physiol. Rev. 58, 106—173
3 Forte, J.G. and Solberg, L.A. (1973) International Encyclopedia of Pharmacology and Therapeutics (Holton, P., ed.), pp. 195—260, Permagon Press
4 Hersey, S.J. (1974) Biochim. Biophys. Acta 344, 157—203
5 Rehm, W.S. (1965) Fed. Proc. 24, 1387—1395
6 Rabon, E.C., Sarau, H.M., Rehm, W.S. and Sachs, G. (1977) J. Membrane Biol. 35, 189—204
7 Durbin, R.P., Michelangeli, F. and Michel, A. (1974) Biochim. Biophys. Acta 367, 177—189
8 Ganser, A.L. and Forte, J.G. (1973) (Biochim. Biophys. Acta 307, 169—180
9 Sarau, H.M., Foley, J., Moonsamy, G., Wiebelhaus, V.D. and Sachs, G. (1975) J. Biol. Chem. 250, 8321—8329
10 Sachs, G., Chang, H.H., Rabon, E., Schakmann, R., Lewin, M. and Saccomani, G. (1976) J. Biol. Chem. 251, 7690—7698
11 Schackmann, R., Schwartz, A., Saccomani, G. and Sachs, G. (1977) J. Membrane Biol. 32, 361—381
12 Lee, J.E., Simpson, ●,● and Scholes, P. (1974) Biochem. Biophys. Res. Commun. 60, 825—834
13 Saccomani, G., Shah, G., Spenney, J.G. and Sachs, G. (1975) J. Biol. Chem. 250, 4802—4809
14 Forte, J.G., Ganser, A.L. and Tanisawa, A.S. (1974) Ann. N.Y. Acad. Sci. 242, 255—267
15 Forte, J.G., Ganser, A., Beesly, R. and Forte, T.M. (1975) Gastroenterology 69, 175—189
16 Saccomani, G., Stewart, H.B., Shaw, D., Lewin, M. and Sachs, G. (1977) Biochim. Biophys. Acta 465, 311—330
17 Saccomani, G., Chang, H.H., Crago, S., Mihas, A.A. and Sachs, G. (1978) J. Clin. Invest., in press
18 Forte, J.G., Ray, T.K. and Poulter, J.L. (1972) J. Appl. Physiol. 32, 714—717
19 Hannig, K., Glick, D. and Rosenbaum, R.M. (1972) Techniques of Biochemical and Biophysical Morphology, p. 191, J. Wiley and Sons
20 Lowry, O.H., Rosebrough, N.J., Farr, A.L. and Randall, R.J. (1951) J. Biol. Chem. 193, 265—275
21 Yoda, A., and Hokin, L.E. (1970) Biochem. Biophys. Res. Commun. 40, 880—884
22 Fiske, C.H. Subbarow, Y. (1925) J. Biol. Chem. 66, 375—400
23 Chance, B. and Williams, G.A. (1955) J. Biol. Chem. 217, 395—407
24 Rabon, E., Chang, H.H. and Sachs, G. (1978) Biochemistry 17, 3345—3353
25 Avruch, J. and Fairbanks, G. (1972) Proc. Natl. Acad. Sci. U.S. 69, 1216—1220
26 Hortsman, L.L. and Racker, E. (1970) J. Biol. Chem. 245, 1336—1344
27 Kagawa, Y. and Racker, E. (1966) J. Biol. Chem. 241, 2461—2466
28 Azzone, G.F. and Massari, S. (1973) Biochim. Biophys. Acta 301, 195—226
29 Dell'Antone, P., Colonna, R. and Azzone, G.F. (1971) Biochim. Biophys. Acta 234, 541—544
30 Rabon, E., Kajdos, I. and Sachs, G. (1978) Biochim. Biophys. Acta submitted
31 Sach, G., Rabon, E. and Saccomani, G. (1978) International Symposium on Bioenergetics, Kobe, Japan, Academic Press, in press

[Reprinted from Biochemistry, (1978) 17, 3345.]

Quantitation of Hydrogen Ion and Potential Gradients in Gastric Plasma Membrane Vesicles

E. Rabon, H. Chang, and G. Sachs

Quantitation of Hydrogen Ion and Potential Gradients in Gastric Plasma Membrane Vesicles†

E. Rabon, H. Chang, and G. Sachs*

ABSTRACT: The ATP-dependent uptake of H^+ by hog gastric parietal cell vesicles was quantitated by using the pH indicator dyes bromcresol green and malachite green, the weak bases, aminopyrine and 9-aminoacridine, and the pH electrode. A K^+-dependent H^+ uptake was found, with a significant difference between the quantity of H^+ disappearing from the medium (ΔH_o) and the quantity appearing inside the vesicle (ΔH_i). 9-Aminoacridine gave a lower value for the ΔH_i than any of the other probes. Probes of potential such as diethyloxadicarbocyanine or oxonol dyes showed that only secondary diffusion potentials occurred during H^+ uptake and that the cationic dyes in the presence of protonophores could also be used to quantitate H^+ uptake. The potential in the presence of protonophore indicated a ΔH_i greater than that found with the other probes. Binding sites for acridine orange were generated either by ATP or an artificial pH gradient and corresponded to the ΔH_i indicated by aminopyrine. SCN^- (30 mM) only partially inhibited the H^+ gradient, and this, coupled with the failure to detect the physiological ΔpH of 6.6, indicated that these vesicles may be an incomplete model of gastric acid secretion.

Purified hog gastric vesicles derived from the acid secreting (parietal) cell of gastric epithelium (Saccomani et al., 1978) contain as a major protein a K^+-activated ATPase (Forte et al., 1974; Sachs et al., 1976) distinct from the $Na^+ + K^+$ ATPase (Skou, 1965). These vesicles, due to the ATPase, are capable of simultaneously translocating H^+ and K^+ (Sachs et al., 1976) apparently by an electroneutral exchange (Schackmann et al., 1977; Lewin et al., 1977). These vesicles are oriented so that the cytoplasmic side faces the external medium (Saccomani et al., 1977). In the absence of ATP the vesicles have a low permeability to K^+ and Cl^- and a low, but measurable H^+ conductance (Chang et al., 1977).

Since these vesicles provide a unique opportunity to study the transport activity of a plasma membrane ATPase of a eukaryotic cell, a variety of probes were used in order to quantitate the pH gradient and any primary or secondary potentials generated by the transport process.

Osmotic gradient experiments have proved useful in distinguishing uptake and binding (Kinne et al., 1975) and are also helpful in discriminating between net uptake and exchange mechanism. 9-Aminoacridine has been used extensively in detection and quantitation of H^+ trapped in vesicles (Schuldiner et al., 1972; Fiolet et al., 1974). pH indicator dyes are useful in discriminating pH changes in the medium or in the vesicle space (Chance, 1975). Uptake of a weak base or weak acid has been employed for studies of pH gradients in gastric glands (Berglindh, 1977) and in vesicles (Ramos & Kaback, 1977). Carbocyanine dyes as probes of potential have been applied to intact tissue such as cornea (Graves et al., 1978), squid axon (Waggoner, 1976) or chromatophores (Pick & Avron, 1976), red cells (Sims et al., 1974), and mitochondria (Laris et al., 1973) and appear to be useful probes of potentials across membranes. Acridine orange appears to alter its binding characteristics in mitochondria (Dell'Antone et al., 1972) and gastric vesicles (Lee et al., 1976) as a function of what has been termed energization, or more probably H^+ gradients. All of these probes may act as ATPase inhibitors, or as uncouplers; thus optical measurements are combined with measurement of enzyme activity and measurement of ΔH_o using the pH electrode.

The application of these techniques to gastric vesicles, as described herein, indicates that a quantitative discrepancy may exist between the amount of H^+ disappearing from the medium and the quantity of H^+ appearing inside the vesicle with different probes. As concluded previously, the H^+ pump appears to have nonelectrogenic characteristics. SCN^- did not inhibit transport by these vesicles to the extent expected from its action in the intact tissue.

Materials and Methods

A. Vesicle Preparation

The purified gastric vesicles were obtained as detailed elsewhere (Chang et al., 1977). The fraction used was obtained at the sucrose–ficoll interface in a Beckman Z60 rotor.

For studies of transport parameters, the vesicles were routinely incubated in a suspension at a final concentration of 150 mM KCl, 2 mM $MgCl_2$ and 1–20 mM buffer (pH 6.1 or 7.4) for 2 h at room temperature. The suspension was then placed on ice and used within 3 h. Longer times of incubation at room temperature resulted in increased leak by the vesicles. On occasion vesicles were used which had not been KCl equilibrated. Ionophores were added as described and SCN^-, when used, was present at 30 mM final concentration. Vesicle protein was set to a final concentration of 0.25 to 0.3 mg/mL, corresponding to 0.50 to 0.66 μL of vesicle volume mL^{-1}. Protein was measured according to Lowry et al. (1951) and ATPase as previously described (Saccomani et al., 1977). The probes were added at concentrations identical with those used in the optical experiments.

B. Measurements

1. *Proton Uptake Measurements.* Proton uptake with a pH electrode was measured as described elsewhere (Chang et al., 1977), using a Radiometer pHM 64 meter. Proton uptake was measured in the presence of each probe used under conditions identical with those chosen for the optical assays, at pH 6.1.

For measurement of the effects of osmolarity on proton

† From the University of Alabama in Birmingham, Laboratory of Membrane Biology, Birmingham, Alabama 35204. *Received January 11, 1978.* Supported by National Institutes of Health Grant No. AM 15878 and National Science Foundation Grant No. PCM 77-18951.

uptake, two conditions were chosen. In one set of experiments vesicles were added to 150 mM KCl in 5 mM glycylglycine buffer containing increasing concentrations of mannitol giving an osmolarity range of 310 mosM to 770 mosM. Since ΔH_o was measured in these experiments, a weak buffer was used in the medium. ATP (0.6 mM) was added 2 min later. Alternatively, vesicles were preequilibrated in 150 mM KCl at 4 °C for 24, 48, and 72 h before the addition of the mannitol and ATP. At 4 °C the vesicles were virtually equilibrated between 48- and 72-h incubation (Schackmann et al., 1977). The 4 °C temperature was chosen in order to maintain vesicle function over the prolonged period required to achieve equilibration of KCl. In each case the maximum transport was measured and plotted as a function of the reciprocal of the osmolarity.

Calibration of the pH signal was carried out in all experiments by measuring the deflection caused by the addition of 10 nmol of HCl in 10 μL to the final mixtures, or by returning the external pH to the initial value, by successive additions of 10 nmol of HCl in 10 μL volumes.

2. *Measurements Using Bromcresol Green.* Absorbance changes of this dye were measured in the Aminco DW2 spectrophotometer in the dual beam mode set at 617 and 680 nm. The reaction mixture consisted of 1.0 mg/mL vesicle suspension incubated for 2 h in 150 mM KCl, 2 mM $MgCl_2$, and 5 mM glycylglycine buffer (since external pH is being monitored), pH 6.1, also containing bromcresol green at 15 μM. ATP was added to a final concentration of 0.6 mM to initiate the reaction and ionophores were added in 4 μL of methanol. Calibration was carried out using additions of 10-μL aliquots of 10^{-3} M HCl and measuring the absorbance change, since this dye monitored extravesicular pH.

3. *Aminoacridine.* Fluorescent quenching of 9-aminoacridine was measured in a Perkin-Elmer MPF 44 scanning fluorometer with 398-nm excitation and 430-nm emission wavelengths. The standard experimental sample consisted of a 500-μL aliquot of vesicles (0.25–0.3 mg mL^{-1}) equilibrated in 150 mM KCl, 2 mM $MgCl_2$, and 2 mM Pipes[1]–Tris (pH 6.1 or 7.4); then 3.5 μL of aqueous 1 mM 9-aminoacridine was added and 7 μL of 30 mM Mg ATP at identical pH was added to initiate the reaction. Ionophores such as nigericin, valinomycin, or tetrachlorosalicylanilide (TCS) were added in 3.5 μL of methanol. Control experiments showed that this quantity of methanol was without effect. In experiments designed to shrink the preequilibrated vesicles, the volume of the initial suspension, with concentrations as above, except for twice the protein, was 200 μL to which was added 200 μL of a solution containing 150 mM KCl, 2 mM $MgCl_2$, 2 mM Pipes–Tris (pH 6.1 or 7.4) and 67–333 mM mannitol, the mannitol being added to vary the osmolarity. Subsequent additions were as above. In nonequilibrated experiments, only 15 min exposure to the KCl solution was allowed before ATP addition.

For direct calibration of the ATP-induced signal since this was due to a change in intravesicular pH, the vesicles were incubated in 0.25 M sucrose containing 5 mM sodium succinate (pH 5.5) for 30 min at room temperature. The succinate was used to increase the proton capacity of the intravesicular space. At this point 100 μL of 100 mM Pipes–Tris buffer adjusted to pH 6, 6.5, or 7 and 100 mM Tris buffer adjusted to pH 8, 8.5, 9, 9.5, or 10 was added to 350 μL of this suspension giving a final protein concentration of 0.3 mg mL^{-1}. The pulse-generated change in fluorescence was recorded. Varying sucrose concentrations were used with each pulse to maintain constant osmotic pressure and a plot made of the log of fluorescence quenching ratio against the change of pH. Parallel experiments with appropriate volume increments were used to measure the exact pH change induced by buffer addition, using the pH meter. The principles of this method have been worked out for other subcellular particles (Schuldiner et al., 1972).

4. *Measurements Using [^{14}C]Aminopyrine.* Twenty micrograms of the vesicles was suspended to a final volume of 450 μL in 150 mM KCl, 2 mM $MgCl_2$, 5 mM glycylglycine (pH 6.1) or 5 mM Pipes–Tris (pH 7.4) for 24 h at 4 °C. This time was chosen since an equivalent KCl equilibration occurred as compared with the 2 h at room temperature used with the other probes. After warm up to room temperature, the reaction was initiated by addition of 50 μL of ATP and [^{14}C]aminopyrine giving a final concentration of 2 mM ATP and 5 μM aminopyrine with 100 000 cpm mL^{-1}. At timed intervals, the suspension was placed directly on a Millipore filter (HAWP, 0.45 μm) and immediately washed with 10 mL of 150 mM KCl, 2 mM $MgCl_2$, and 5 mM glycylglycine (pH 6.1) or 5 mM Pipes–Tris (pH 7.4) at 0 °C. Each time point was repeated in triplicate; the filters were dried and suspended in 10 mL of Aquasol. An LKB 81000 scintillation counter was used to measure radioactivity remaining on the filters. The ΔH_i was calculated from the equation, ratio in/out = $1 + 10^{pK-pH_i}/1 + 10^{pK-pH_o}$. This distribution ratio method has been used, for example, in bacterial vesicles (Ramos & Kaback, 1977).

5. *Measurements Using Malachite Green.* The experiments were carried out, also with the dual beam spectrophotometer set at 623 and 680 nm. Vesicles at 0.3 mg mL^{-1} were incubated with 15 μM malachite green, 150 mM KCl, 2 mM $MgCl_2$, and 2 mM Pipes–Tris buffer at pH 6.1 and 7.4 for 2 h at room temperature. ATP was added to a final concentration of 0.6 mM to initiate the reaction. Ionophores were added as usual in 3.5 μL of methanol.

6. *Potential Measurements.* Absorbance of 3,3′-diethyloxadicarbocyanine iodide (DOCC) and di-S-C_3-(5) was monitored in the Aminco DW 2 scanning spectrophotometer. Absorbance changes were measured at 598–636 nm for DOCC and 661–714 nm for di-S-C_3-(5). The reaction suspension consisted of vesicles (0.3 mg mL^{-1}; incubated for 2 h) in 150 mM KCl, 2 mM $MgCl_2$, and 2 mM Pipes–Tris at pH 6.1 and 7.4. Dye additions (4 μM) were made from a 400 μM solution in MeOH. ATP, 0.6 mM (adjusted to pH), was added at zero time to a 350-μL aliquot of the reaction suspension with or without 6 μM tetrachlorosalicylanilide (TCS).

For osmotic experiments, 386 mM mannitol was added immediately before the ATP. Calibration of the cyanine dye signal due to a change in intravesicular pH was carried out by suspending the vesicles (0.3 mg mL^{-1}) in a solution of 5 mM sodium succinate (pH 5.5) in 238 mM sucrose with 4 μM dye and adding 100 μL of 100 mM Pipes–Tris buffer adjusted to pH 6, 6.5, or 7 and at 100 mM Tris buffer adjusted to pH 8, 8.5, 9, 9.5 to 350 μL of the suspension. Absorbance was recorded for 20 s and then 6 μM TCS was added and absorbance recorded for a further 40 s. The actual change of pH was measured on a pH meter with the volume of reaction mixture scaled up to 2.0 mL. The standard curve was generated from a plot of the total absorbance change at each pH increment. The principle of these experiments was the same as used elsewhere, except that valinomycin–K^+ gradients have been more generally used for calibration (Waggoner, 1976).

7. *Measurements Using Acridine Orange.* Absorbance changes of acridine orange were measured in the DW2 spectrophotometer in the dual beam mode set at 446 and 496 nm.

[1] Abbreviations used: TCS, tetrachlorosalicylanilide; DOCC, 3,3′-dimethyloxadicarbocyanine iodide; di-S-C_3-(5), 3,3′-dipropyl-2,2′-thiodicarbocyanide iodide; Pipes, piperazine-*N*,*N*′-bis(2-ethanesulfonic acid); Ans, 8-anilino-1-naphthalenesulfonate.

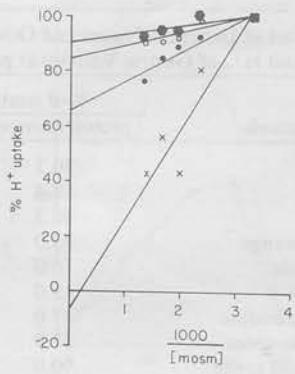

FIGURE 1: Vesicles were incubated with 150 mM KCl, 5 mM glycylglycine, 2 mM $MgCl_2$ at 4 °C for varying lengths of time [(X—X) 2 min; (●—●) 24 h; (O—O) 48 h; (●—●) 72 h], and 0.6 mM ATP was added with varying concentrations of mannitol. The maximal H^+ uptake measured by the pH electrode (calculated as % of control) was plotted as a function of the reciprocal of total medium osmolarity.

To 350 μL of a vesicle suspension (0.3 mg mL^{-1}) incubated for 2 h with 150 mM KCl, 2 mM $MgCl_2$, and 2 mM Pipes–Tris buffer (pH 6.1 or 7.4), ATP at identical pH to the incubation buffer was added to give a final concentration of 0.6 mM. Acridine orange was present at 5 μM final concentration. Ionophores were added in 3.5 μL of methanol before or after ATP addition.

Two methods were used to calibrate the absorbance change. Again, since the change was due to an increase in H^+_i, vesicles were incubated in 250 mM sucrose containing 5 mM sodium succinate at pH 5.5, 6, 6.5, 7, 7.5, 8, 8.5, and 9 and the pH was increased abruptly by addition of 100 μL of 100 mM Pipes–Tris buffer adjusted to 1 pH unit greater than the 350 μL of the vesicle suspension containing 5 μM dye. Alternatively, 350-μL vesicles (0.3 mg mL^{-1}) equilibrated with 238 mM sucrose containing 5 mM sodium succinate at pH 5.5 were pulsed with 100 μL of Pipes–Tris buffer at pH 6.0 and 6.5 or 100 mM Tris buffer adjusted to pH 7, 7.5, 8, 8.5, 9, and 9.5. Again, varying sucrose concentrations were used to maintain isoosmotic conditions. The exact pH gradient was calibrated in a volume of 2.0 mL using a pH meter as before. The methods used were similar to those previously applied (Lee et al., 1976; Dell'Antone et al., 1972).

8. *ATPase.* ATPase was measured as previously described (Saccomani et al., 1977). The conditions in the measurement of P_i release were 40 mM Tris-Cl (pH 7.4), 2 mM $MgCl_2$, 2 mM ATP, and 10 μg of enzyme per tube. The material was incubated for 15 min at 37 °C in 1 mL total volume. Probe additions were added at concentrations identical with those used in the optical experiments. In the presence of SCN^- the conditions were 50 mM Tris–acetate (pH 7.4), 2 mM $MgCl_2$, 2 mM ATP, and 20 g of enzyme per tube and incubation time was increased to 30 min at 37 °C.

C. Chemicals

ATP was purchased from Sigma, 3,3′-diethyloxadicarbocyanine iodide from Eastman, and 9-aminoacridine from Aldrich. Di-S-C_3-(5) was a gift from Dr. A. Waggoner. Acridine orange was a gift from Dr. J. M. Menter. Malachite green was a gift from Dr. T. Christian. Ionophores were purchased from Sigma Chemical Co. or obtained as gifts from Dr. H. A. Lardy. Tributyltin was purchased from K & K Lab, Inc. All other chemicals were the highest purity grade available. Hog stomachs were donated by R. L. Zeigler Meats, Tuscaloosa, Ala.

TABLE I: A Comparison of the ΔpH Obtained Using Various Probes of pH Inside or Outside the Vesicles at pH 6.1 or 7.4.

transport measurement	pH 6.1	pH 7.4
pH electrode	4.92	[c]
fluorescent quench 9-aminoacridine	2.2[a], 1.9[b]	2.8[a], 2.8[b]
[^{14}C]aminopyrine accumulation	3.37	4.41
absorption of (DOCC + TCS)	3.7	5.9
absorption of acridine orange	3.2	4.6
absorption of bromcresol green	4.89	[c]

[a] This value was calculated from the equation in text. [b] This value was obtained from the standard curve. The values given here were obtained on the same vesicle population for which the calibration curves were generated but reflect the average signal obtained in several experiments. [c] Not measurable at this pH. The values of ΔpH were obtained directly from the calibration curves as shown in the figures and are typical of the different probes used.

Results

A. Probes of pH

(a) *External.* Here two methods, the pH electrode and bromcresol green, were used.

1. pH Electrode. Under the standard conditions (2-h incubation, room temperature) the addition of 0.6 mM ATP resulted in a change of pH of the external medium equivalent to the uptake of 69 nmol of H^+ μL^{-1} vesicle space (Table I). These data have been detailed elsewhere (Chang et al., 1977).

The osmotic sensitivity of vesicular transport may be used to distinguish various aspects of uptake. It was previously shown that uptake of ^{86}Rb was time and temperature dependent, and 48 h or more at 4 °C was required for equilibration in the presence of Cl^- (Schackmann et al., 1977) but considerably longer was necessary in the presence of SO_4^-. As shown in Figure 1, the time of equilibration with KCl has marked effects on osmotic sensitivity. With only 2-min incubation, at infinite osmolarity, zero H^+ uptake is predicted. As the vesicles approach equilibrium, osmotic sensitivity is progressively reduced, and essentially disappears after 72-h incubation. If K_2SO_4 was used, even after 72 h, partial osmotic sensitivity was retained. The addition of lipid permeable ions did not reduce the osmotic sensitivity in SO_4^{2-} solutions (data not shown), suggesting the presence of a KCl symport pathway, rather than a coupled K^+ and Cl^- conductance.

2. Bromcresol Green. The addition of ATP to the preincubated vesicles resulted in a rapid shift of the dye absorbance (Figure 2). Calibration of this dye signal showed that the change of pH indicated by this dye corresponded almost exactly to the change measured by the pH electrode, that is, a change of 4.89 at pH 6.1 (Table I). Partial inhibition of ATPase activity occurred with this dye, which probably accounts for the small inhibition of H^+ uptake seen using the pH electrode in the presence of this dye. The OD change shown by bromcresol green was reversed by nigericin or a combination of valinomycin and TCS. Addition of a stronger buffer to the medium (10 mM Pipes–Tris) abolished the OD response.

(b) *Internal.* 1. 9-Aminoacridine. ATP addition to incubated vesicles in the presence of 9-aminoacridine resulted in quenching of the fluorescence as would be predicted from the development of intravesicular acidity (Schuldiner et al., 1972) and hence trapping of the dye. Nigericin reversed the change of fluorescence (Figure 3) and, after exhaustion of ATP, the addition of valinomycin also reversed the signal. In contrast to the enhancement obtained with the pH electrode (Sachs et al., 1977) the addition of valinomycin in the presence of ATP

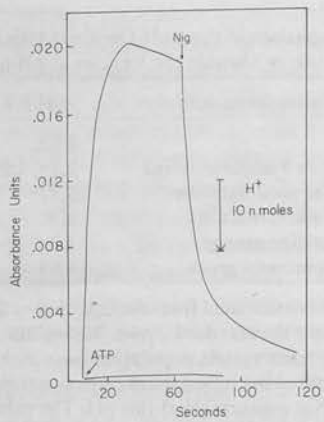

FIGURE 2: Change in absorbance of 15 μM bromcresol green resulting from addition of 0.6 mM Mg–ATP to 350 μL of incubation medium. As in text, incubation medium consisted of 150 mM KCl, 2 mM $MgCl_2$, 5 mM glycyglycine (pH 6.1) incubated for 2 h at room temperature with GI at a final protein concentration of 1 mg mL^{-1}. The OD difference between 680 and 617 nm was monitored. The calibration signal corresponds to the addition of 10 nmol of HCl. The lower curve shows the optical change in the presence of 10 mM Pipes–Tris buffer (pH 6.1).

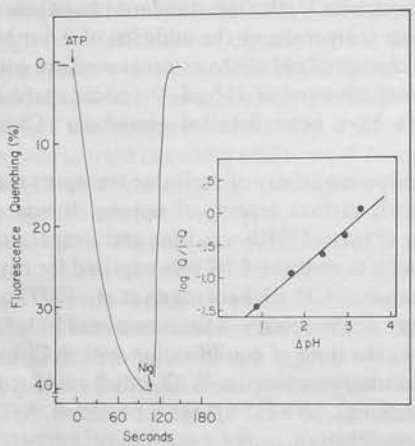

FIGURE 3: The vesicles were incubated with 150 mM KCl, 2 mM $MgCl_2$, and 2 mM Pipes–Tris buffer (pH 7.4) for 2 h at room temperature. Following 9-aminoacridine addition to a 250-μL aliquot of the incubated material, 0.6 mM Mg–ATP was added and the reaction followed in a fluorimeter set at excitation 398 nm, emission 430 nm. Nigericin (1 μg mL^{-1}) was added at the point of maximal fluorescent quenching. The insert shows the plot of log of quench ratio as a function of an applied pH gradient by addition of external base, the initial pH being 5.5. When the ratio is unity, the vesicular volume is calculated as 1.9 μL mg^{-1}.

resulted in a slight reduction of the signal. This dye has a slightly larger effect on the quantity of H^+ transport as compared with the inhibition of ATPase activity (Table II).

The response to 9-aminoacridine was maximal in 90 s, in contrast to the 30-s maximum given by the pH electrode, bromcresol green, and acridine orange. However, the rate of reversal by nigericin was as fast as with the other methods. Imidazole at 0.3 mM reduced the signal observed, without an effect on ATPase activity, but with a reduction in H^+ uptake as also measured by the pH electrode (Table II).

SCN^- (30 mM) partially inhibited the dye signal (Table III) in contrast to the complete inhibition of H^+ transport observed in the intact mucosa (Rehm, 1972) and isolated glands (Berglindh, 1976).

The magnitude of the signal was linearly dependent on protein concentration in the range of 0.125–0.5 mg of protein at 10 μM aminoacridine. Above that concentration, the degree of quench was reduced.

TABLE II: The Effect of Different Probes and Other Additions on ATPase Activity and H^+_o of Gastric Vesicles at pH 6.1.[a]

additions to controls	% of control activity: proton transport	% of control activity: K^+-ATPase
6 μM TCS	70.3	77.5
50 μM $TPMP^+$	68.4	77.5
4 μM DOCC	80.2	83.0
4 μM acridine orange	73.0	97.6
0.3 mM imidazole	76.0	95.3
3 mM imidazole	19.0	97.0
10 μM 9-aminoacridine	87.0	94.0
15 μM malachite green	87.3	85.0
15 μM bromcresol green	90.0	84.5
0.5 μM tributyltin	10.0	46.0
5 μM aminopyrine	94.5	101.4

[a] The concentrations of material used were the same as used in the experiments in the text. Proton transport was measured using the pH electrode with vesicles preincubated with KCl for 2 h at room temperature, and the compounds of interest were added before ATP. ATPase activity was measured at 37 °C and reflects the effect of the compounds on the K^+ increment of activity.

TABLE III: The Effect of SCN^- (30 mM) on the Transport Parameters of Gastric Vesicles at pH 6.1 and 7.4.

transport measurement	% inhibition with 30 mM SCN^-: pH 6.1	% inhibition with 30 mM SCN^-: pH 7.4
10 μM 9-aminoacridine	39.7	40.0
4 μM DOCC (+TCS)	77.5	73.3
4 μM acridine orange	7.9	29.0
5 μM aminopyrine	36.8	30.7
pH electrode	48.8	*a*

[a] Could not be measured at this pH. These experiments were done on a single preparation of vesicles but are generally representative of the effects found, following addition of SCN^- before the addition of ATP. The inhibitory action of SCN^- on ATPase under these conditions was minimal.

Osmotic sensitivity of the dye signal, using 10 M dye, was measured under conditions where ΔH_o was osmotically sensitive. The signal was partially osmotically sensitive, the intercept at zero vesicular volume corresponding to the bound component, constituting about 20% of the total signal. With preincubated vesicles, no effect on the signal was observed due to an osmotic gradient showing that the decrease in trapping volume was exactly balanced by the increase in $[H^+_i]$.

From the equation

$$\frac{A_i}{A_o} = \frac{[H^+_i]}{[H^+_o]} = \frac{Q}{100 - Q}\frac{V}{v}$$

(where A_i and A_o are internal and external aminoacridine concentrations, $[H^+_i]$ and $[H^+_o]$ are internal and external H^+ concentrations, Q is the % quench, V is medium volume, and v is vesicle volume), the ΔH_i can be calculated (Table I). Equivalently, the ΔH_i can be obtained directly from the calibration curve of aminoacridine (Table I). It can be seen that, although the maximum pH gradient was observed at pH 7.4, more than two orders of magnitude difference was obtained with this technique comparing ΔH_i and ΔH_o at pH 6.1. In part, this may be due to uncoupling by the dye (Table II) or due to internal buffering capacity of the vesicles or other H^+ binding sites.

2. Aminopyrine Uptake. Since the data using aminoacridine did not agree quantitatively with the pH electrode observations,

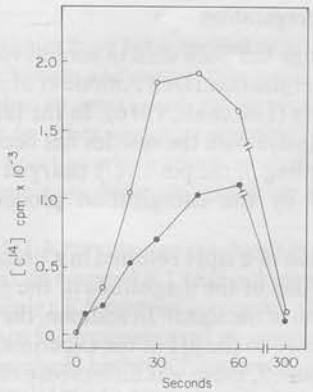

FIGURE 4: Vesicles were incubated 24 h at 4 °C in 150 mM KCl, 2 mM $MgCl_2$, and either 5 mM glycylglycine (pH 6.2) or 2 mM Pipes–Tris (pH 7.4); protein concentration was 44 μg mL^{-1}. For each point, a 450-μL aliquot was removed and equilibrated to 23 °C. At zero time, 50 μL of solution containing 20 mM Mg–ATP (pH 6.1) and 50 μM aminopyrine (with 100 000 dpm) was added to the incubated vesicles. At the indicated time intervals, the reaction mixture at pH 6.1 (O—O) or pH 7.4 (●—●) was placed directly on a HAWP (0.45 μm) Millipore filter and washed, dried, and counted as detailed in the text.

uptake of [^{14}C]aminopyrine was measured under identical conditions. As shown in Figure 4, this base was rapidly accumulated by the vesicles at pH 6.1 or 7.4 with an accumulation ratio of 209 and 160, respectively, upon the addition of ATP. Aminopyrine did not affect ATPase activity and slightly inhibits H^+ uptake at these concentrations (Table II). Again, as shown in Table I, the ΔH_i calculated from the distribution ratio was considerably less than that found using the pH electrode; this corresponds to a ΔpH of 3.37 units, larger than that calculated with 9-aminoacridine.

3. Malachite Green. This dye was chosen because of its low pK (0.8–1.2) and because it was shown to rapidly bind to the vesicles (95% within 10 min, 22 °C). As shown in Figure 5, the addition of ATP produced an acid shift of the dye absorbance, which was reversed by nigericin. At the concentration necessary for an observable optical signal, the dye showed partial inhibition of ATPase and H^+ transport activity (Table II). The response time of the dye, either at pH 6.1 or 7.4, was considerably slower than the pH electrode response. While the signal was reversed by nigericin, the rate of reversal was slow compared with the effects of nigericin using other probes. This slow effect was also produced by acid or base pulses or valinomycin addition at the point of maximum absorbance shift. This could be due to a slow displacement of the dye from membrane binding sites into intravesicular space or slow conformational changes in the vesicle membrane. Slow responses of malachite green have also been observed in squid axon (Cohen et al., 1974), explained as due to scattering changes.

B. Probes of Potential

It was shown previously that uptake of lipid permeable anions such as [^{14}C]SCN (Schackmann et al., 1977) or changes in fluorescence of 8-anilino-1-naphthalenesulfonate (Ans) were dependent on the presence of both ATP and valinomycin (Lewin et al., 1977). Moreover, in the case of Ans a sharp pH optimum was found at 6.1 in contrast to the transport of H^+ or Rb^+. Because Ans responses are highly pH dependent and certain ambiguities exist in the interpretation of the Ans signal (Aiuchi et al., 1977; Williams et al., 1977), carbocyanine dyes (Waggoner, 1976) were used in this study. Essentially identical data were obtained using either diethyl oxadicarbocyanine (DOCC) or Di S-C_3-(5); hence we will only describe the results using DOCC.

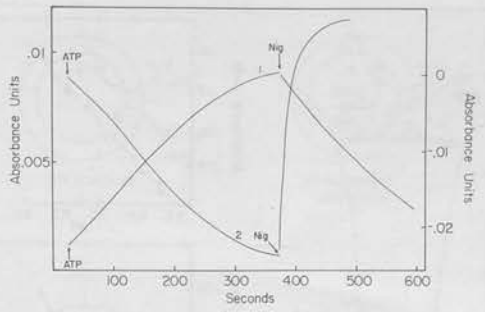

FIGURE 5: The vesicles (0.3 mg mL^{-1}) were incubated in 150 mM KCl, 2 mM $MgCl_2$, and 2 mM Pipes–Tris (pH 7.4) for 2 h at room temperature. Following a 10-min incubation of 350 μL of this material with either 15 μM malachite green or 4 μM DOCC, 0.6 mM Mg–ATP was added. Absorbance was monitored at 623–680 nm for malachite green (left-hand axis) and 588–636 nm for DOCC (right-hand axis). Curve 1 shows the change of OD of malachite green upon addition of Mg–ATP. The shift corresponds to an acid shift of the dye. Curve 2 shows the slow DOCC signal resulting from Mg–ATP addition. Nigericin (1 μg mL^{-1}) addition in both curves was at the point of the maximum absorbance shift.

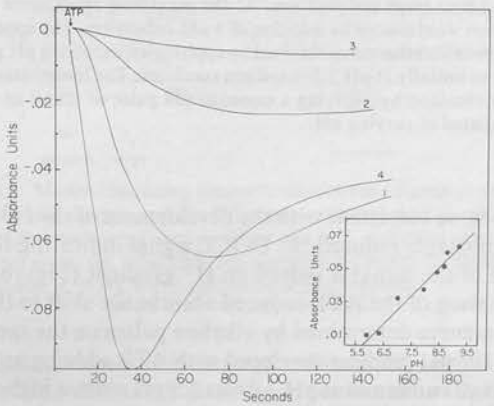

FIGURE 6: GI vesicles (0.3 mg mL^{-1}) were incubated in 150 mM KCl, 2 mM $MgCl_2$, and 2 mM Pipes–Tris (pH 7.4) for 2 h at room temperature. For each experiment, 4 μM DOCC and 6 μM TCS were added to 350-μL aliquots of the incubated material. Following addition of 0.6 mM Mg–ATP, the absorbance change at 588–636 nm was monitored. (Curve 1) Control signal for DOCC and TCS; (curve 2) 10-min incubation with 0.3 mM imidazole before addition of Mg–ATP; (curve 3) 10-min incubation with 50 μM $TPMP^+$ before addition of Mg–ATP; (curve 4) addition of Mg–ATP immediately after addition of 286 nM mannitol. According to details in the text, the insert shows a calibration curve obtained with the vesicles by adding a pulse of base to vesicles preincubated at pH 5.5 in sodium succinate.

(1) *Slow Changes.* Whether a ΔpH is applied chemically in the absence of a K^+ gradient, or ATP added to preincubated vesicles, a slow change in the absorbance of DOCC occurred which was rapidly dissipated by nigericin. The time course of the slow change, as shown in Figure 5, was slower than that observed under the same conditions with 9-aminoacridine, bromcresol green, or the pH electrode, but similar to that of malachite green.

No transient increase of absorbance was seen, and the development of this slow change, antagonized by nigericin, argues against an electrogenic H^+ pump. Moreover, oxonol dyes were altogether unresponsive to ATP addition arguing against development of a positive potential (data not shown) due to pump activity.

(2) *Fast Changes.* The addition of a proton conductance, in the form of TCS, drastically altered the time course of the reduction of DOCC absorbance and increased its magnitude (Figure 6). Under these conditions, the addition of ATP, or a pulse of base, produced a rapid change of absorbance, with a

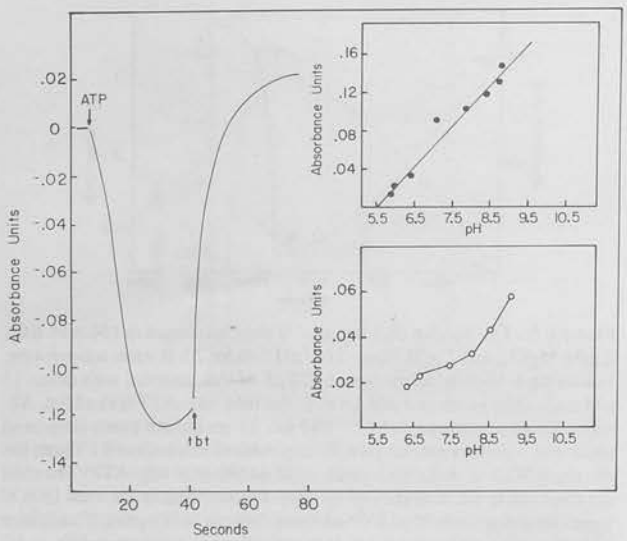

FIGURE 7: The change in acridine orange absorbance following the addition of 0.6 mM Mg-ATP to vesicles preincubated as in the text at pH 6.1 for 2 h at room temperature. At the maximum absorbance change dissipation was induced by addition of 5 μM tributyltin. The upper insert shows the calibration curve obtained by applying an increasing pH gradient to vesicles initially at pH 5.5 in sodium succinate. The lower insert shows a curve obtained by applying a constant pH pulse of 1 unit to vesicles preincubated at varying pH.

time course consistent with the development of the H^+ gradient. Imidazole reduced the DOCC signal indicating that the source of the signal is indeed an H^+ gradient (Figure 6). By comparison of the ATP-induced absorbance shift to the calibration curve determined by alkaline pulses on the same material, the pH gradient developed with ATP addition at pH 6.1 was 4.1 pH units and at pH 7.4 was 5.9 pH units, a higher value than observed with other probes.

When the vesicles are equilibrated with KCl, approximately doubling the osmotic gradient would transiently double the H^+ ion concentration inside the vesicles given an electroneutral H^+:K^+ exchange. This would result in an increase of the diffusion potential by a factor of 58 log 2, i.e., 17 mV, and a corresponding doubling of the dye concentration inside the vesicle, which would balance the decline in volume if dye uptake were the sole mechanism for potential sensitivity of this probe. Accordingly, as for 9-aminoacridine, no net change in signal would be expected. But, as shown in Figure 6, there is a more rapid and a larger change in absorbance.

$TPMP^+$ abolished the signal when added before ATP, as expected of a lipid permeable cation dissipating the potential in preference to the dye. This cation did not, under these conditions, abolish the H^+ gradient (Table II). Valinomycin (10^{-6} M) in the presence of TCS prevented or abolished the pH electrode response (Chang et al., 1977) and the dye signal. Imidazole also reduced the signal as with the pH electrode (Figure 6 and Table II). The dye reduced ATPase activity by 17% at 4 μM (Table II). SCN^- significantly reduced the signal, both at pH 6.1 and 7.4. Apparently, the action of SCN^- was additive to the action of TCS on H^+ uptake (48% + 30%) (Table III). Hence, the direct action of SCN^- on the H^+ gradient sensed by DOCC was similar to that found with other probes.

Substitution of K^+ with Na^+ abolished the response, and of Cl^- by SO_4^{2-} reduced the response, as observed previously with the pH electrode and all the other probes. In aged vesicles, the substitution of Cl^- by SO_4^{2-} increased the response slightly and reduced the leak rate of the gradient.

C. Probes of Energization

Acridine orange has been used in several vesicular systems as a probe of energization (Dell'Antone et al., 1972) and also in gastric vesicles (Lee et al., 1976). In the latter system, the interaction of the dye with the vesicles has been interpreted as being due to binding of the positively charged dye to negative sites generated by the energization process (Lee et al., 1976).

The application of a ΔpH resulted in a linear change of the signal as a function of the magnitude of the pH gradient, allowing calibration of the signal. In addition, the acridine orange signal was sensitive to the pH of the experiment. As shown in the insert in Figure 7, there was an increase of the signal with increase of pH, at a constant H^+ gradient. The two types of signal were reversible with nigericin, but not with TCS indicating the absence of an endogenous conductance other than that for H^+ in nonenergized vesicles.

The addition of ATP produced a rapid metachromatic shift of acridine orange as shown in Figure 7. Calibration of this response by comparison of the shifts produced by standard pH pulses of the same vesicle material indicated a ΔH_i of 3.2 units at pH 6.1. As with pH electrodes and other probes of pH, K^+ was required in the vesicle interior for the ATP dependent signal. Valinomycin with TCS, or nigericin alone, dissipated the signal. The effect of valinomycin was to increase the absorption change if added prior to the addition of ATP or in the presence of ATP. This effect was not given by $TPMP^+$ and, as before, the action of valinomycin (Sachs et al., 1976; Rabon et al., 1978) was interpreted as due to increased access of K^+ to the exchange sites. The signal under conditions where ΔH_o was osmotically sensitive was also osmotically sensitive.

SCN^- had a more variable effect on this dye than on any other signal studied. At pH 7.4, depending on the preparation, inhibition with 30 mM SCN^- ranged from 13 to 78%. Addition of SCN^- before ATP addition was required for the inhibition. Added after ATP, no effect was observed. It was also noted that in some preparations the relative size of the signal did not correlate with the pH electrode measured transport capacity of the vesicles, i.e., ΔH_o. Signals of similar magnitude could be obtained with vesicles transporting 10 or 50 nmol μL^{-1}, as indicated by the pH electrode.

D. Probes of OH^-:Cl^- Exchange

There are few anion selective ionophores known. Tributyltin, however, has been shown to be an OH^-:Cl^- exchange ionophore in mitochondria (Dawson et al., 1972). In the gastric vesicle, this compound had a dual action. It was a potent inhibitor of the ATPase apparently binding irreversibly (Kasbekar et al., in preparation) (Table II), but, in addition to inhibiting the ATPase, it was also capable of dissipating the H^+ (or OH^-) gradient when added after exhaustion of the ATP. Its action was also more rapid in abolishing the ΔpH than expected of an ATPase inhibitor (Figure 7), the rate being comparable to that of nigericin. Tributyltin also rapidly reversed the signals obtained with DOCC or acridine orange, as well as with the pH electrode. As expected of an OH^-:Cl^- antiport, replacement of Cl^- with SO_4^{2-} prevented the action of tributyltin.

E. Summary

Figure 8 summarizes our current concepts of the modes of action of the ATPase, ionophores, and the probes used in this work.

Discussion

Various techniques have been applied to attempt to further describe the mechanism and quantitative aspects of H^+ uptake by gastric vesicles. In most cases, the approaches have been used previously in other vesicular systems, but the gastric vesicles have properties which result in modifications of the use of, for example, osmotic shrinkage or potential probe dyes.

Based on an H^+:K^+ exchange mechanism for H^+ uptake, and a slow efflux of trapped K^+ (Schackmann et al., 1977), then as the vesicular K^+ content increases, shrinking the intravesicular space by application of an osmotic gradient will result in a progressively higher K^+ content being available for exchange. This will lead to a progressive loss in osmotic sensitivity, as was found. The finding of complete osmotic sensitivity in nonpreincubated (2 min) vesicles may therefore not be interpreted as showing absence of binding or nonpermeant buffers, but rather as evidence of K^+ entry being necessary for H^+ uptake. The absence of osmotic sensitivity at KCl equilibration (ca. 72 h at 4 °C) supports an exchange mechanism, which would be osmotically insensitive, rather than net uptake of HCl. The sensitivity of the technique does not allow distinction between equal or unequal exchange stoichiometrics.

These osmotic data also allow predictions to be made about dye responses to changes in vesicular volume. For a dye that is trapped by partition between vesicle water space and the medium due to a pH gradient, osmotic sensitivity of dye uptake should be observed in nonequilibrated vesicles, where osmotic sensitivity of H^+ uptake persists. Partial osmotic sensitivity of the 9-aminoacridine signal was found indicating some binding (ca. 20%) of the dye. In equilibrated vesicles no osmotic sensitivity of this signal would be predicted and was not found.

As the K^+ content of the vesicles increases, although the number of protons taken up will increase, this is into a progressively smaller intravesicular volume. The pH gradient should increase in exact proportion to the change of volume; hence no change in signal would be found with a dye such as 9-aminoacridine in preincubated vesicles. This is not the case however, for a potential sensitive probe such as DOCC. Although some of the signal generated by this dye may be due to diffusion of the dye from bulk aqueous phase into intravesicular water, driven by the H^+ diffusion potential in the presence of TCS, a considerable fraction of the signal is due to dye moving from the hydrophobic phase to the membrane surface in response to a potential difference (Waggoner, 1976). This latter component will be volume independent, and hence a larger pH gradient which will generate a larger potential will give an increased response. Since this was found (Figure 6), this further substantiates the concept of an H^+:K^+ exchange in these vesicles, and also shows that the pH gradient can be elevated above control levels by the osmotic gradient. The leak rate is also increased, showing that the steady-state gradient capacity of the vesicles is in part leak-rate limited.

The use of any probes in transport studies requires a careful analysis of their mechanism in a given system, before mechanistic or quantitative conclusions can be drawn.

The pH electrode has a relatively slow response, due to the mechanical stirring system used and only measures changes in medium pH. The actual H^+ gradient formed is unknown. Often, an optical probe of changes of external pH is convenient, especially for rapid kinetics. In the case of gastric vesicles, bromcresol green was shown to monitor exclusively the external pH. Inhibition of transport activity by this dye correlated with inhibition of ATPase activity.

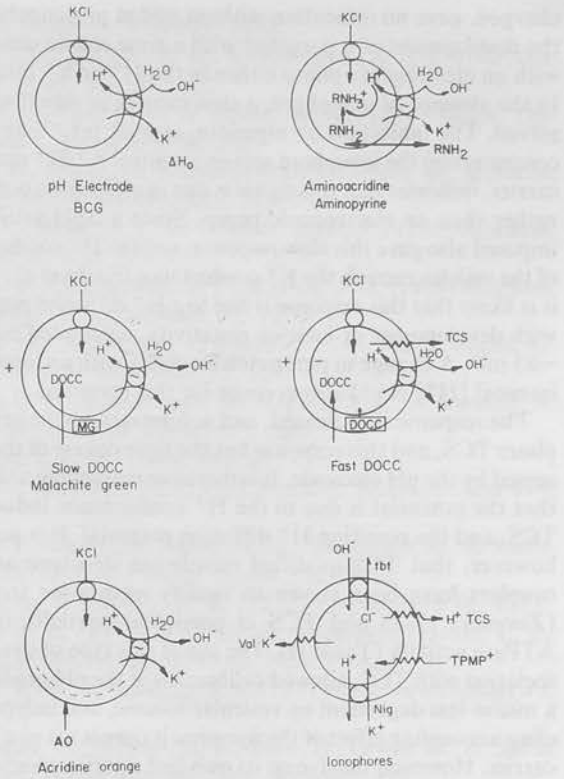

FIGURE 8: Models illustrating the mechanism of the different probes used to monitor pH changes and the different ionophores used to modify the signals. Abbreviations not used elsewhere are: MG, malachite green; BCG, bromcresol green; tbt, tributyltin; nig, nigericin; ⊖, pump; O, carrier; (〰) conductance; R, NH_2, 9-aminoacridine or aminopyrine.

For measurement of changes of internal pH, several probe types are available: weak bases which accumulate in the vesicle space, potential probe dyes used in the presence of protonophores and dyes which bind to the membrane as a function of the presence of a pH gradient.

The weak base, 9-aminoacridine, gives a rate of response significantly slower than the pH electrode. The rate of response is a function of the pump rate, the efflux of H^+, and the rate of penetration of the neutral form of the dye. The latter is excluded as rate limiting by the rapid dissipation of the signal by nigericin. Thus, given the greater reduction of the proton transport signal as compared with ATPase activity, this probe appears to act as an uncoupler of H^+ transport due to significant permeability of the protonated form. This is also shown by the reduction of the signal by valinomycin in the presence of ATP. Imidazole antagonizes the signal, due in part to the buffering effect of the accumulated imidazole, and at higher concentrations due again to the permeability of the protonated imidazole. Although we had previously used uptake of [^{14}C]imidazole as our index of intravesicular pH, these data showed that it was unsuitable (Rabon et al., 1978).

[^{14}C]Aminopyrine, on the other hand, accumulated in the vesicles with the addition of ATP and at the concentrations used showed slight uncoupling activity. As such, it was therefore more suitable than imidazole as a probe of internal pH.

Malachite green gave a slow acid shift with the addition of ATP, which was slowly dissipated by ionophores. Given the almost complete binding of the dye, and its low pK, it may be that this dye responds to a region of intramembranal acidity. However, it did not appear possible to calibrate this signal with pH pulses.

The probes of potential, DOCC or di-S-C_3-(5), which are positively charged, or oxonol dyes which are negatively

charged, gave no indication without added protonophore, of the development of a potential with a time course consistent with an electrogenic pump either in the H^+ or K^+ direction. In the absence of ionophore, a slow change in signal was observed. The inhibition by nigericin, at 1 $\mu g\ mL^{-1}$, at which concentration the ionophore acts as a neutral K^+:H^+ exchange carrier, indicates that this signal is due to a diffusion potential, rather than an electrogenic pump. Since a ΔpH artificially imposed also gave this slow response, and the H^+ conductance of the vesicles exceeds the K^+ conductance (Sachs et al., 1976), it is likely that this response is due to a H^+ diffusion potential, with development of interior negativity, calculated equal to −85 mV. A change in pump stoichiometry with an increase in internal $[H^+]$ could also account for this potential.

The response is increased, and accelerated by the protonophore TCS, and this response has the time course of the ΔpH sensed by the pH electrode. It is therefore reasonable to assume that the potential is due to the H^+ conductance induced by TCS, and the resulting H^+ diffusion potential. It is possible, however, that TCS-modified membrane structure and uncouplers have been shown to modify membrane structure (Zimmer, 1977) and TCS in particular partially inhibits ATPase activity (Table II). The use of this type of dye, in association with TCS, allowed calibration of the pH gradient by a means less dependent on vesicular volume, and independent of an uncoupling effect of the dye since it cannot act as a proton carrier. However, the dye on its own had significant effects on ATPase activity and H^+ transport and, hence, as in other systems (Waggoner, 1976) affects the membrane to which it binds.

Acridine orange has been shown to bind to gastric vesicles with development of an H^+ gradient (Lee et al., 1976). With a change of external pH, at a fixed pH, the increase of signal shows that deprotonation of a membrane group increases binding of this dye. Since both ATP and a ΔpH induce these binding sites, it suggests that these binding sites for acridine orange are in some way related to the transport activity of the membrane. In a given vesicle preparation, the size of the signal is quantitatively related to the magnitude of the H^+ gradient. It should be pointed out, however, that if the DOCC + TCS signal is compared with the acridine orange signal, different results may be obtained since the former signal is more sensitive to the presence of, for example, a Cl^- conductance. Also, since the latter signal depends on the presence of binding sites, such as phosphatidylserine, variation in content of this phospholipid from species to species, or preparation to preparation will alter the ratio of the acridine orange signal as compared with other probes.

An anion-exchange ionophore, such as tributyltin, has two apparently independent actions on the gastric vesicles, inhibition of ATPase activity, and a true ionophore effect that is Cl^- dependent. Hence, this compound can be used in this system to detect an active Cl^-:OH^- antiport which may coexist with the H^+:K^+ antiport.

Previous conclusions about the neutrality of the pump contained reservations since, if the addition of ATP activated a K^+ conductance, the vesicle potential would be given by, neglecting all other conductances:

$$PD = \frac{E_H g_H}{g_H + g_K}$$

where E_H is the EMF of the H^+ limb of the ATPase, and g_H and g_K are the specific conductances for H^+ and K^+, respectively. Thus, if $g_K > g_H$, a low potential would be observed as the g_K increased. Thus, perhaps only a transient would be observed. The absence of such a transient with either type of charged cyanine dye argues against this possibility. The removal of Cl^-, and substitution by SO_4^{2-}, an impermeant anion, also does not elicit a cyanine dye measurable potential. The experiments shown here are therefore not consistent with an electrogenic mechanism.

The electrochemical gradient obtained from an H^+ pump can be defined as (Mitchell, 1966)

$$\Delta\bar{\mu}_{H^+} = \Delta\Psi - 2.3\frac{RT}{F}\Delta pH$$

The intact mammalian stomach generates a pH of 0.8 and a potential difference (correcting for diffusion potentials) of about 60 mV lumen negative, due to Na^+K^+ ATPase dependent Cl^- transport (Rabon et al., 1978). Thus, the $\Delta\bar{\mu}_{H^+}$ anticipated from the isolated gastric H^+ pump is 333 mV, or a ΔpH of 5.74 units.

At pH 6.1, since no H^+ is released from the ATPase reaction, it is possible to compare directly the change of H^+ in the medium and in the vesicles. The loss of H^+ from the medium was calibrated with the pH electrode or the absorbance change of bromcresol green. The data indicate a possible pH change of 5 units in the intravesicular space, on the assumption that all vesicles transport H^+ equally and that there is no significant buffering capacity. However, when probes of internal pH are used, such as weak bases (9-aminoacridine and aminopyrine) or probes of H^+ gradient dependent sites (acridine orange), the change in internal pH is in the range of 2.2 to 3.7 units giving a final internal pH of about 2 to 4. This discrepancy between ΔH_i and ΔH_o may be explained by intravesicular buffer. If the gastric ATPase were capable of generating a ΔpH of 5 units, intravesicular buffering would result in an increase in ΔH_o but a final $[H^+_i]$ still equivalent to the gradient capacity of the pump. Thus, it must be concluded that the maximal gradient capacity of the vesicles is 3.7 units, almost two orders of magnitude less than expected. Another explanation is the presence of membranal bindings sites for H^+. Since the majority (ca. 90%) of membrane protein (Saccomani et al., 1977) has a subunit M_r of 105 000 containing 25% carbohydrate (Saccomani et al., in preparation), this would correspond to 10 mol of H^+ bound mol^{-1} protein. Alternatively, a leak pathway may be responsible but this would not account for the discrepancy between ΔH_o and ΔH_i.

At pH 7.4, although ΔH^+_o cannot be calibrated, the ΔpH found with the probes ranged from 3 to 4.5 (with the exception of DOCC + TCS), giving the same internal pH as at 6.1. This constancy of $[H^+_i]$ with varying $[H^+_o]$ could be interpreted as due to a buffering component at that pH or a pH dependent leak pathway fixing the internal pH. The application of an osmotic gradient in equilibrated vesicles increased the ΔpH showing that the gradient capacity of the vesicles was not limited by the leak path for H^+. Since the vesicles were preincubated with 150 mM KCl in these experiments, the initial uptake was not K^+ limited.

Of all the probe methodologies, only DOCC in the presence of TCS generated a large enough signal to approach the ΔH_o and even the predicted gastric H^+ pump gradient at pH 7.4. Although a probe of potential, it was converted to a probe of pH by the addition of a protonophore, TCS. The protonophore may provide a conductance across the whole vesicle membrane and perhaps also between a compartment of H^+ and the vesicle exterior. In this model, however, since the vesicle can be represented as two EMF's in parallel, no additional potential will be found, other than that expected from the pH gradient probed by the weak bases. This probe may also be pH sensitive at pH <2.

Considering the various probes, it seems that, at the least,

the expected ΔpH of 5.3 at pH 6.1 is not achieved and a discrepancy of about two orders of magnitude is found, when measuring intravesicular pH (Table I). In general the same is true at pH 7.4, although the ΔpH increases by one unit. This may indicate that the vesicles may not contain the complete system.

Another line of evidence which leads to caution in accepting the $H^+ + K^+$ ATPase as a complete model of the parietal cell proton pump is the lower effectiveness of SCN^- in blocking H^+ transport in these vesicles. Thus, although 30 mM SCN^- has a significant inhibitory action when added before, but not after ATP, the inhibition is not complete in contrast to the action of this compound in the intact tissue (Rehm & Sanders, 1977) or gastric gland (Berglindh, 1976). Moreover, imidazole can reverse the action of SCN^- on the intact tissue (Rehm & Sanders, 1977) which does not occur in the vesicles.

In conclusion, probes of pH and potential show that, in contrast to data obtained for intact frog mucosa (Rehm, 1972), no evidence can be obtained for an electrogenic H^+ pump in these vesicles and that the gradient achieved by the ATPase is less than expected based on the gradient capacity of the intact organ. This H^+ pump mechanism therefore is in contrast to the better known electrogenic H^+ pumps of mitochondria and chloroplasts (Mitchell, 1968).

References

Aiuchi, T., Kamo, N., Karihara, K., & Kabatake, K. (1977) *Biochemistry 16,* 1620.

Berglindh, T. (1976) *Acta Physiol. Scand. 97,* 401.

Berglindh, T. (1977) *Biochim. Biophys. Acta 464,* 217.

Chance, B. (1975) *MTP Int. Rev. Sci.: Biochem. 3,* 1.

Chang, H., Saccomani, G., Rabon, E., Schackmann, R., & Sachs, G. (1977) *Biochim. Biophys. Acta 464,* 313.

Cohen, L. B., Salzberg, B. M., Davila, H. V., Ross, W. N., Landowne, D., Waggoner, A. S., & Wang, C. H. (1974) *J. Membr. Biol. 19,* 1.

Dawson, A. P., & Selwyn, M. J. (1972) *Biochem. J. 152,* 333.

Dell'Antone, P., Colonna, R., & Azzone, G. F. (1972) *Eur. J. Biochem. 24,* 553.

Fiolet, J. W. T., Bakker, F. P., & Van Dam, K. (1974) *Biochim. Biophys. Acta 348,* 1432.

Forte, J. G., Ganser, A. L., & Tanisawa, A. S. (1974) *Ann. N.Y. Acad. Sci. 242,* 255.

Graves, C., Sachs, G., & Rehm, W. S. (1978) *Invest. Opthalmol. Visual Sci. 50,* 278.

Kinne, R., Murer, H., Kinne-Saffran, E., Thees, M., & Sachs, G. (1975) *J. Membr. Biol. 21,* 375.

Laris, P., Bahr, D. P., & Chaffee, R. R. J. (1975) *Biochim. Biophys. Acta 376,* 415.

Lee, H. C., Quintanilha, A. T., & Forte, J. G. (1976) *Biochem. Biophys. Res. Commun. 72,* 1179.

Lewin, M., Saccomani, G., Schackmann, R., & Sachs, G. (1977) *J. Membr. Biol. 32,* 301.

Lowry, O. H., Rosebrough, M. J., Farr, A. L., & Randall, R. I. (1951) *J. Biol. Chem. 193,* 265.

Mitchell, P. (1966) *Biol. Rev. 41,* 455.

Pick, U., & Avron, M. (1976) *Biochim. Biophys. Acta 440,* 189.

Rabon, E., Chang, H., Sarau, H. M., Saccomani, G., & Sachs, G. (1978) *Acta Physiol. Scand.* (in press).

Ramos, S., & Kaback, H. R. (1977) *Biochemisry 16,* 4271.

Rehm, W. S. (1972) in *Metabolic Transport* (Hokin, L. E., Ed.), p 187, Academic Press, New York, N. Y.

Rehm, W. S., & Sanders, S. S. (1977) *Gastroenterology 73,* 959.

Saccomani, G., Stewart, H. B., Shaw, D., Lewin, M., & Sachs, G. (1977) *Biochim. Biophys. Acta 465,* 311.

Saccomani, G., Crago, S., Mihas, A., Dailey, D., & Sachs, G. (1978) *Acta Physiol. Scand. Suppl.* 409.

Sachs, G., Chang, H., Rabon, E., Schackmann, R., Lewin, M., & Saccomani, G. (1976) *J. Biol. Chem. 251,* 7690.

Schackmann, R., Schwartz, A., Saccomani, G., & Sachs, G. (1977) *J. Membr. Biol. 32,* 361.

Schuldiner, S., Rottenberg, H., & Avron, M. (1972) *Eur. J. Biochem. 25,* 64.

Sims, P. J., Waggoner, A. S., Wang, C. H., & Hoffman, J. F. (1974) *Biochemistry 13,* 3315.

Skou, J. C. (1965) *Phys. Rev. 45,* 596.

Waggoner, A. S. (1976) *J. Membr. Biol. 27,* 317.

Williams, P. W., Layton, D. G., & Johnston, C. (1977) *J. Membr. Biol. 33,* 21.

Zimmer, G. (1977) *Arch. Biochem. Biophys. 181,* 26.

SUMMARY

Much evidence has been accumulated that gastric ATPase is critically involved in acid secretion by the stomach. As an H^+ pump this enzyme appears to be unique in that it is cation requiring and exchanges K^+ for H^+ without development of a potential. As such, this appears to be the first non-electrogenic H^+ ATPase described. Since it contained a 100,000 M_r subunit which is phosphorylated, it appears to belong to the class of ATPases containing the $Na^+ + K^+$ and Ca^{++} ATPases. However, it has not been established that this ATPase is the complete gastric proton pump and some of the data would indicate the contrary. The availability of this type of ATPase in non-leaky vesicle preparation free of any other major contamination is an exciting prospect for structure function studies of this type of pump.

This is to certify that the work described in this thesis was done under my direction as the director of the Membrane Biology Laboratory at the University of Alabama in Birmingham, Birmingham, Alabama U.S.A.

11

Date

George Sachs